

REPORT SERIES IN AEROSOL SCIENCE  
N:o 142 (2013)

**Proceedings of FCoE in 'Physics, Chemistry, Biology and Meteorology of  
Atmospheric Composition and Climate Change' Annual Meeting 2013**

Editors: Markku Kulmala, Hanna K. Lappalainen,  
Magdalena Brus and Jenni Kontkanen

Helsinki 2013

ISSN 0784-3496

ISBN 978-952-5822-75-5 (electronic publication)

Aerosolitutkimusseura ry – Finnish Association for Aerosol Research FAAR

<http://www.atm.helsinki.fi/FAAR/>

# TABLE OF CONTENTS

## OVERVIEW

M. Kulmala, H. K. Lappalainen, J. Bäck, A. Laaksonen, E. Nikinmaa, M.-L. Riekkola, T. Vesala, Y. Viisanen, M. Boy, M. Dal Maso, H. Hakola, P. Hari, K. Hartonen, V.-M. Kerminen, A. Lauri, T. Laurila, H. Lihavainen, T. Petäjä, J. Rinne, A. Virtanen, S. Romakkaniemi, S. Sorvari, H. Vehkamäki + the FCoE teams Finnish CoE in Physics, Chemistry, Biology and Meteorology of Atmospheric Composition and Climate Change: General overview of the results and activities in 2008-2013	19
---	----

## TEAM OVERVIEWS

M. Boy, N. Babkovskaia, R. Gierens, K.V. Gopalkrishnan, L. Liao, D. Ogersen, A. Rusanen, S. Smolander, L. Zhou, P. Zhou Activities in the Atmosphere Modelling Group: 2011-2013	32
--	----

J. Bäck, E. Nikinmaa, F. Berninger, P. Hari, T. Hölttä, E. Juurola, P. Kolari, A. Mäkelä, A. Porcar-Castell Ecosystem processes – overview of 2007-2013 activities	38
---	----

H. Hakola, H. Hellén, U. Makkonen, M. Vestenius, M. Hemmilä In situ measurements of volatile organic compounds and inorganic gases and particles	48
---	----

V.-M. Kerminen, N. L. Prisle, P. Paasonen, A. Asmi, J. Hong, J. Kontkanen, E.-M. Kyrö, H. Lappalainen, R. Makkonen, T. Nieminen, M. Paramonov, O. Peräkylä, L. Riuttanen, S.-L. Sihto, M. Vogt, H. Vuollekoski, T. Yli-Juuti, T. Petäjä, M. Dal Maso, and M. Kulmala An overview of the activities by Aerosol-Cloud-Climate Interactions Group of the University of Helsinki	55
---	----

A. Laaksonen, S. Romakkaniemi, J. Joutsensaari, A. Hamed, J. Malila, I. Ahmad, E. Baranizadeh, L. Hao, A. Jaatinen, H. Keskinen, T. Korhola, A. Kortelainen, T. Kühn, Z. Maalick, P. Miettinen, S. Mikkonen, A. Pajunoja, J. N. Smith, P. Vaattovaara, P. Yli-Pirilä, A. Virtanen Overview of the studies conducted by the UEF Aerosol Physics Group	63
---	----

H. Lihavainen, T. Anttila, E. Asmi, D. Brus, A. Hirsikko, R. Hooda, A. Hyvärinen, N. Kivekäs, J. Leppä, K. Neitola, E. O’connor, T. Raatikainen, J. Svensson, O. Tolonen-Kivimäki, V. Vakkari and T. Viskari Overview about activities in Aerosols and Climate group	70
J. Pumpanen, J. Heinosalo, M. Pihlatie, H. Aaltonen, F. Berninger, J. Bäck, P. Hari, A.-J. Kieloaho, J.F.J. Korhonen, K. Köster, A. Lindén, L. Kulmala, M. Kulmala, E. Nikinmaa, A. Ojala, T. Rasilo, and T. Vesala Rhizosphere processes play an important role in soil organic matter; Decomposition and greenhouse gas fluxes in boreal landscape; Summary of soil research carried out at FCoE during the second FCoE period (2009-2013)	76
M.-L. Riekkola, K. Hartonen, J. Parshintsev, T. Laitinen, M. Jussila, H. Junninen, L. Feijó Barreira, T. Petäjä, and M. Kulmala Atmospheric aerosols and gases: study of chemical composition and determination of physicochemical properties of individual compounds	86
J. Rinne, M.K. Kajos, J. Patokoski, P. Rantala, R. Taipale, S. Haapanala, T.M. Ruuskanen Biosphere-atmosphere exchange and atmospheric concentrations of volatile organic compounds	93
H. Vehkamäki, N. Bork, H. Henschel, O. Kupiainen-Määttä, T. Kurtén, V. Loukonen, T. Olenius, I. Ortega, K. Ruusuvuori, and N. Tsona Tchinda An overview of University of Helsinki Computational Aerosol Physics Group activities in 2011-2013	97
T. Vesala, I. Mammarella, L. Järvi, P. Alekseychik, S. Dengel, S. Haapanala, J. Heiskanen, P. Keronen, A. Nordbo, O. Peltola, M. Pihlatie, A. Praplan, M. Raivonen, J. Rinne, S. Smolander, M.-K. Tu, P. Kolari, T. Aalto, T. Laurila, A. Ojala, E.-S. Tuittila, J. Levula, J. Pumpanen, E. Nikinmaa, J. Bäck Biosphere-atmosphere interactions	104

---

K. Hämeri, T. Hussein, B. Molgaard, V. Dos Santos-Juusela, J. Koivisto, A.-K. Viitanen, A. S. Godinho, G. Ripamonti, L. Järvi, A. Nordbo, A. Maragkidou, M. Repo An overview of University of Helsinki Urban and Indoor Aerosols Group activities in 2012-2013 .....	111
H.E. Manninen, K. Lehtipalo, P.P. Aalto, J. Backman, X. Chen, J. Duplissy, A. Franchin, N. Kalivitis, J. Kangasluoma, F. Korhonen, R. Krecji, J. Lampilahti, K. Leino, G. Steiner, R. Wagner, D. Wimmer, R. Väänänen, T. Petäjä, And M. Kulmala Recent advances in ion and aerosol measurements .....	115
M. Sipilä, M. Ehn, H. Junninen, T. Jokinen, S. Schobesberger, N. Sarnela, A. Praplan, A. Adamov, J. Kangasluoma, R. Taipale, M. P. Rissanen, T. Laitinen, G. Lönn, V.-M. Sundell, M. Äijälä, and T. Petäjä An overview of University of Helsinki Mass Spectrometry Group activities in 2012-2013 .....	118
 INFRASTRUCTURE AND LARGE RESEARCH INITIATIVES	
M. Kaukolehto, E. Juurola, S. Sorvari, T. Laurila, S. Haapanala, P. Keronen, P. Kolari, I. Mammarella, M. Komppula, K. Lehtinen, J. Levula, T. Aalto, M. Aurela, L. Laakso, J. Hatakka, A. Lohila, T. Mäkelä, A. Nordbo, Y. Viisanen and T. Vesala ICOS RI, towards a European research infrastructure .....	123
H.K. Lappalainen, T. Petäjä, J. Kujansuu, T. Suni, T. Ruuskanen, Vm Kerminen, Y. Viisanen, V. Kotlyakov, N. Kasimov, V. Bondur, G. Matvienko, S. Zilitinkevich and M. Kulmala Pan-Eurasian Experiment (PEEX) initiative .....	126
T. Petäjä, H.K. Lappalainen, S. Sorvari, and M. Kulmala ACTRIS RI – Research infrastructure for aerosols, clouds and trace gases .....	130
S. Siitonen, J. Bäck and the AnaEE team AnaEE – A European infrastructure for ecosystem research .....	133
S. Sorvari, A. Asmi, J. Bäck, T. Petäjä, M. Kulmala Restructuring the FCoE research infrastructures - Integrated Atmospheric and Earth System Science Research Infrastructure (INAR RI) .....	136

## RESEARCH ABSTRACTS

Aalto, J., Kolari, P., Porcar-Castell, A., Bäck, J.

Springtime monoterpene emission bursts from Scots pine in the light of photosynthesis recovery dynamics

.....144

T. Aalto, J. Hatakka, R. Kouznetsov and K. Stanislawska

Background MBL signal in atmospheric CO<sub>2</sub> mixing ratios observed at Pallas station: comparison of two models for tracing air mass history

.....148

H. Aaltonen, H. Hakola, A. Ojala, L. Klemedtsson, J. Pumpanen, E. Peltomaa and J. Bäck

Emissions of volatile organic compounds from boreal humic lakes

.....152

I. Ahmad, S. Mikkonen, T. Kühn, and S. Romakkaniemi

Aerosol first indirect effect from Puijo measurement station: implications to climate studies

.....155

P. Alekseychik, A. Korrensalo, E.-S. Tuittila, J. Rinne and T. Vesala

Northern bog surface heterogeneity: implications for the ecosystem-atmosphere interactions

.....159

T. Anttila, J. Leppä, E. Asmi and H. Lihavainen

Estimating the growth rate of a newly formed aerosol mode

.....164

E. Asmi, D. Brus, S. Carbone, J. Hatakka, R. Hillamo, A. Hirsikko, T. Laurila, H. Lihavainen, E. Rouhe, S. Saarikoski and Y. Viisanen

Airborne measurements of aerosol particles and greenhouse gases in Southern Finland

.....166

K. Atlaskina, J. Pulliainen, K. Luojus, M. Takala, J. Ikonen, M. Kulmala, G. De Leeuw

Intercomparison and validation of snow cover fraction parameterizations in climate models

.....170

N. Babkovskaia, M. Boy, S. Smolander, S. Romakkaniemi, M. Kulmala

A study of aerosol production at the cloud edge with DNS

.....173

J. Backman, A. Virkkula, , V. Vakkari, J.P. Beukes, P.G. Van Zyl, M. Josipovic, S. Piketh, P. Tiitta, K. Chiloane, J.J. Pienaar, A. Wiedensohler, T. Tuch, T. Petäjä, M. Kulmala and L. Laakso Non-standard measurement method of particle soot absorption photometer for absorption Ångström exponents	176
E. Baranizadeh, A. Arola, A. Hamed, T. Nieminen, A. Virtanen, M. Kulmala and A. Laaksonen The effect of cloudiness on new particle formation: investigation of radiation levels	179
A.M. Batenburg, C. Gaston, J.A. Thornton and A. Virtanen Effects of organic coatings on the reactivity of aerosol particles	184
D. Brus, E. Asmi, T. Raatikainen, K. Neitola, M. Aurela, U. Makkonen, J. Svensson, A.-P. Hyvärinen, A. Hirsikko, H. Hakola, R. Hillamo, and H. Lihavainen Ground-based observations of aerosol and cloud properties at sub-arctic Pallas GAW-station, Pallas cloud experiment (PACE 2012)	187
S. Carbone, S. Saarikoski, D.R. Worsnop, and R. Hillamo Detection of trace metals with the soot-particle aerosol mass spectrometer	192
T. Chan, T. Hölttä, F. Berninger, E. Nikinmaa Seasonal dynamics of stem CO <sub>2</sub> efflux and stem diameter growth	196
X. Chen, H. E. Manninen, A. Franchin, P. Aalto, P. Keronen, A. Mäkelä, T. Petäjä, M. Kulmala Variations in ion concentrations and the possible effect of lightning and ozone	202
J. Duplissy, J. Merikanto, D. Wimmer, L. Rondo, H. Vuollekoski, S. Schobesberger, A. Franchin, K. Lehtipalo, A. Kuerten, G. Tsagkogeorgas, F. Riccobono, F. Bianchi, A. Praplan, G. Steiner, J. Kangasluoma, H. Junninen, T. Nieminen, M. Breitenlechner, D., S. Ehrhart, R. Sitals, A. Amorin, A. Tome, A. Määttänen, A. Kupc, H. Vehkamäki, M. Kulmala and CLOUD collaboration Effect of ions on sulphuric acid-water binary nucleation: experimental data and comparison with improved classical nucleation theory	208
A. Franchin, J. Kangasluoma, T. Nieminen, K. Lehtipalo, A. Downard, J. Duplissy, the CLOUD collaboration, T. Petäjä, R. Flagan, and M. Kulmala Improving the size resolution of air ion measurements in the 1-6 nm range	211

R. Gierens, D. Mogensen, L.Zhou, V. Vakkari, L. Laakso, J.P. Beukes, P.G. Van Zyl and M. Boy Year-round modelling study on particle formation on a South African Savannah .....	214
J. Hakala, J. Kangasluoma and T. Petäjä Hygroscopicity of sub-6 nm sodium chloride and ammonium bisulfate particles .....	217
L.Q. Hao, S. Romakkaniemi, A. Kortelainen, A. Jaatinen, H. Portin, P. Miettinen, M. Komppula, A. Leskinen, J.N. Smith, D. Sueper, D.R. Worsnop, K. Lehtinen, A. Laaksonen, and A. Virtanen Observation of atmospheric organic nitrate aerosols and application in clouds by aerosol mass spectrometry .....	221
J. Heinonsalo, A.-J. Kieloaho, K. Bäcklund, M. Kulmala, M. Pihlatie, J. Pumpanen, M.-L. Riekkola, T. Vesala and J. Parshintsev Forest soil amines -ectomycorrhizal fungi is significant reservoir but is it also a source of volatile amines? .....	226
H. Henschel, O. Kupiainen-Määttä, T. Olenius, I. K. Ortega, T. Kurtén and H. Vehkamäki Insights into the impact of hydration on sulphuric acid/base mediated particle formation .....	228
T. Hölttä and E. Nikinmaa A whole tree level approach to explain stomatal control of transpiration and photosynthesis .....	231
J. Hong, S. A. K. Häkkinen, M. Äijälä, J. Hakala, J. Mikkilä, M. Paramonov and T. Petäjä, M. Kulmala Hygroscopic, CCN and volatility properties of submicron atmospheric aerosol in a boreal forest environment during the summer of 2010 .....	237
A. Jaatinen, S. Romakkaniemi, A. Laaksonen, and A. Virtanen The evaporation of ammonium nitrate in the DMT-CCN counter .....	241
L. Järvi, C.S.B. Grimmond, A. Nordbo, I. Strachan, M. Taka and H. Setälä Modelling of surface energy and water balance in high latitude cities – impact of snow .....	244

J. Joensuu, A.-J. Kieloaho, M. Raivonen, N. Altimir, P. Kolari, T. Sarjala, J. Bäck, P. Keronen, T. Vesala and E. Nikinmaa The effect of nitrogen fertilization on shoot NO fluxes	249
T. Jokinen, T. Berndt, M. Sipilä, M. Ehn, H. Junninen, H. Herrmann and M. Kulmala Oxidation product study from three different monoterpenes	254
E. Juurola, J.F. Korhonen, U. Taipale and J. Levula Novel viewpoints for the transactions of forests and atmosphere -art/science residence at Hyytiälä 2013-2014	257
K. Kabiri Koupaei, E. Nikinmaa and P. Hari Formation of crown structure in Scots pine trees	259
M.K. Kajos, M. Hill, H. Hellén, P. Rantala, J. Patokoski, R. Taipale, C. C. Hoerger, S. Reimann, H. Hakola, T. Petäjä and T.M. Ruuskanen Concentrations of oxidized VOCs and aromatic VOCs at a boreal forest	262
V., Kasurinen, P., Kolari, K., Alfredsen, I., Mammarella, P., Alekseychick, T., Vesala, F., Berninger Modeling latent heat exchange in boreal and arctic biomes	264
J. Kim, H. Keskinen, P. Vaattovaara, P. Miettinen, J. Joutsensaari, A. Virtanen, and CLOUD collaboration Hygroscopic properties of nucleated nanoparticles in the presence of sulfuric acid and organics during CLOUD 7	273
G.V. Kokkatil, H. Vuollekoski, V. Sinclair, A. Hellsten, M. Kulmala and M. Boy FLAMO - flexible atmospheric model: a new high-resolution 3d regional model to study atmospheric processes in the planetary boundary layer	276
P. Kolari, M. Dominguez, E. Juurola, S. Juntila, J. Bäck and E. Nikinmaa Photosynthesis and nitrogen in different needle age classes in Scots pine	279

J. Kontkanen, K. Lehtipalo, J. Kangasluoma, H. E. Manninen, E. Järvinen, J. Hakala, A. Hamad, A. Laaksonen, C. Rose, K. Sellegri, E. Asmi, T. Petäjä, and M. Kulmala Observations of sub 3-nm atmospheric clusters and particles in different environments .....	283
T. Korhola, H. Kokkola, H. Korhonen, S. Romakkaniemi Comparison of cloud droplet activation between sectional and modal aerosol models .....	287
J.F.J. Korhonen, J. Pumpanen and M. Pihlatie A new way to assess the systematic errors in static chamber measurements .....	290
A. Kortelainen, J. Joutsensaari, P. Tiitta, A. Jaatinen, P. Miettinen, L. Hao, J. Leskinen, O. Sippula, T. Torvela, J. Tissari, J. Jokiniemi, D. R. Worsnop, A. Laaksonen, and A. Virtanen HR-ToF-AMS measurements of particulate emissions from woodchip combustion .....	295
K. Köster, J. Heinosalo, J. Pumpanen, E. Koster, F. Berninger Changes in soil enzyme activities and litter decomposition across the chronosequence of forest fires in Värriö strict nature reserve, Eastern Lapland .....	299
T. K. Uhn, H. Kokkola, S. Romakkaniemi, and A. Laaksonen Black carbon in global climate modelling .....	302
L. Kulmala, P. Schiestl-Aalto, H. Mäkinen, A. Mäkelä Physiological growth model CASSIA predicts carbon allocation and wood formation of Scots pine .....	305
L. Kulmala, J. Aalto, H.-S. Helmisaari, K. Kabiri, P. Kolari, J.F.J. Korhonen, J. Levula, J. Leppälammi-Kujansuu, H. Mäkinen, P. Schiestl-Aalto, P. Hari, J. Bäck, A. Mäkelä, E. Nikinmaa Tree growth measurements at SMEAR II .....	310
O. Kupiainen-Määttä, T. Olenius and H. Vehkamäki Assessing the validity of the nucleation theorem for measured data .....	316
N. Kuusinen, E. Tomppo, F. Berninger Estimating the effect of stand age on forest albedo .....	319

E.-M. Kyrö, R. Väänänen, V.-M. Kerminen, A. Virkkula, A. Asmi, T. Nieminen, M. Dal Maso, T. Petäjä, P. Keronen, P. P. Aalto, I. Riipinen, K. Lehtipalo, P. Hari and M. Kulmala Long-term aerosol and trace gas measurements in Eastern Lapland, Finland: the impact of Kola air pollution to new particle formation and potential CCN	320
J. Lampilahti, H.E. Manninen <sup>1</sup> T. Nieminen <sup>1</sup> S. Mirme, I. Pullinen, T. Yli-Juuti, S. Schobesberger, J. Kangasluoma, K. Lehtipalo <sup>1</sup> , T.F. Mentel, T. Petäjä and M. Kulmala Investigations on the spatiotemporal properties of new particle formation events in a boreal forest environment	324
K. Lehtipalo, A. Franchin, J. Kontkanen, J. Mikkilä, J. Vanhanen, J. Kangasluoma, T. Petäjä, and M. Kulmala A10 PSM: A new version of the particle size magnifier for detection of atmospheric clusters and particles as small as 1 nm	330
K. Leino, T. Nieminen, L. Riuttanen, R. Väänänen, T. Petäjä, L. Järvi, P. Keronen, A. Virkkula, T. Pohja, P.P. Aalto, and M. Kulmala Observations of Russian wild fire smoke in Finland in summer 2010	333
L. Liao, V. M. Kerminen, M. Boy, M. Kulmala and M. D. Maso Temperature influence on natural aerosol production potentials over boreal forests	336
L. Lindfors, T. Hölttä, A. Lintunen, A. Porcar-Castell, E. Nikinmaa, E. Juurola Freezing associated depression of photosynthesis of Scots pine seedlings	339
M. Linkosalmi, C. Biasi, J. Pumpanen, J. Heinonsalo, A. Linden and A. Lohila The impact of possible priming effect on different CO <sub>2</sub> balance in two forestry-drained peat soils	343
A. Lintunen, L. Lindfors, P. Kolari, E. Nikinmaa, E. Juurola and T. Hölttä Gas bursts during freezing help trees to avoid winter embolism	345
A. Lohila, T. Penttilä and T. Laurila CH <sub>4</sub> and N <sub>2</sub> O fluxes in a spruce forest in Northern Finland	348

V. Loukonen, N. Bork and H. Vehkamäki Insights into atmospherically relevant molecular collisions from first-principles molecular dynamics .....	353
Z. Maalick, H. Korhonen, H. Kokkola, A. Laaksonen, and S. Romakkaniemi Cloud resolving model simulations of marine stratocumulus cloud by sea salt injections .....	357
K. Macháčová, M. Pihlatie, A. Vanhatalo, E. Halmeenmäki, H. Aaltonen, P. Kolari, J. Aalto, J. Pumpanen, M. Pavelka, M. Acosta, O. Urban, J. Bäck Can pine trees act as sources for nitrous oxide (N <sub>2</sub> O) and methane (CH <sub>4</sub> )? .....	362
R. Makkonen, Ø. Seland, A. Kirkevåg, T. Iversen, and J.E. Kristjansson Secondary aerosol formation in a changing environment .....	367
U. Makkonen and A. Virkkula NH, HNO and HONO diurnal cycles in the summer of 2010 and 2012 .....	374
J. Malila, A. Pajunoja, L.Q. Hao, J. Joutsensaari, A. Laaksonen, K.E.J. Lehtinen, and A. Virtanen Estimating the viscosity range of secondary organic material from particle coalescence times .....	377
I. Mammarella, K.-M. Erkkilä, S. Haapanala, J. Heiskanen, A. Ojala, T. Vesala Long term measurements of carbon dioxide and methane fluxes over a small boreal lake in Southern Finland .....	381
T. Markkanen, T. Thum, J. Susiluoto, J. Kaurola and T. Aalto Assessing regional forcing for land surface schemes in carbon cycle studies .....	386
J. Merikanto, J. Duplissy, A. Määttänen, H. Vehkamäki, and M. Kulmala Charged and neutral nucleation of sulfuric acid and water: from experiments to theory and to atmospheric modeling .....	391
P. Miettinen, A. Jaatinen and A. Laaksonen Vertical particle flux at Lake Pyhäselkä .....	395

D. Mogensen, M. K. Kajos, J. Aalto, J. Bäck, M. Kulmala, S. Schallhart, S. Smolander, R. Taipale, L. Zhou, and M. Boy The lesser studied isoprenoids in Hyytiälä	397
B. Mølgaard, J. Ondráček, P. Štávová, L. Džumbová, M. Barták, T. Hussein, and J. Smolík Evaluation of the multi-compartment size-resolved indoor aerosol model	401
B. Mølgaard, W. Birmili, Sam Clifford, Andreas Massling, K. Eleftheriadis, M. Norman, S. Vratolis, B. Wehner, J. Corander, K. Hämeri, and T. Hussein Urban particle number concentration forecast model evaluation	403
B. Mølgaard, A.J. Koivisto, T. Hussein, and K. Hämeri Clean air delivery rate test of five portable air cleaners	405
K. Neitola, D. Brus, U. Makkonen, M. Sipilä, T. Jokinen, K. Kyllönen, H. Lihavainen and M. Kulmala Sulphuric acid monomer vs. total sulphate in nucleation studies	407
T. Nieminen, T. Yli-Juuti, H. E. Manninen, V.-M. Kerminen and M. Kulmala Forecasting NPF events during Pegasos-Zeppelin Northern mission 2013 in Hyytiälä, Finland	412
A. Nikandrova, A-M. Sundström, V-M. Kerminen And M. Kulmala Climate feedbacks linking atmospheric CO <sub>2</sub> concentration, BVOC emissions and aerosols in forest ecosystems derived from satellite data	416
E. Nikinmaa, R. Sievänen and T. Hölttä Simulated interaction between tree structure and xylem and phloem transport in 3d tree crowns using model LIGNUM	418
A. Nordbo and L. Järvi Urban surface cover determined using airborne lidar in Helsinki	423

A. Ojala, J. Pumpanen, T. Rasilo, H. Miettinen, M. Rantakari, J. Heiskanen, I. Mammarella, J. Huotari, P. Kankaala, J. Levula, J. Bäck, P. Hari and T. Vesala Evidence of lateral transport of carbon gases of terrestrial origin in boreal aquatic ecosystems	429
B. Olascoaga and A. Porcar-Castell The relationship between fluorescence yield and photochemical yield in the presence of photoinhibition of reaction centres	433
I.K. Ortega, N.M. Donahue and H. Vehkamäki Can highly oxidized organics contribute to new particle formation?	437
P. Paasonen, K. Kupiainen, M. Amann and M. Kulmala Estimating the number and sizes of particles from anthropogenic emissions – now and in future	441
A. Pajunoja, M. R. Alfarra, A. Buchholz, W.T. Hesson, G.B. Mcfiggans, A. Virtanen Investigation of the effects of chemical and physical factors on the phase state of SOA particles	446
M. Paramonov, M. Äijälä, P.P. Aalto, A. Asmi, N. Prisle, T. Nieminen, U. Makkonen, H. Hakola, M. Kajos, J. Patokoski, R. Taipale, T. Ruuskanen, J. Rinne, V.-M. Kerminen M. Kulmala and T. Petäjä Long-term size-segregated Cloud Condensation Nuclei Counter (CCNC) measurements in a boreal environment and its implications for aerosol-cloud interactions	448
J. Patokoski, T.M. Ruuskanen, M.K. Kajos, R. Taipale, P. Rantala, J. Aalto, H. Hakola and J. Rinne Long-term source analysis of VOCs in boreal forest during years 2006-2011	452
O. Peltola, A. Hensen, C. Helfter, L. Beleggi Marchesini, S. Haapanala, F. Bosveld, W. C. M. Van Den Bulk, T. Röckmann, T. Laurila, A. Vermeulen, E. Nemitz and I. Mammarella Measurements of methane emissions on multiple scales in an agricultural landscape	454
O. Peräkylä, M. Vogt, T. Petäjä, J. Aalto, M.K. Kajos, P.A. Rantala, H. Aaltonen, T. Nieminen, R. Taipale, P. Kolari, P. Keronen, H.K. Lappalainen, T.M. Ruuskanen, J. Rinne, V.-M. Kerminen, T. Vesala, I. Mammarella, M. Kulmala, J. Bäck Oxidation capacity and rate of monoterpenes over a boreal forest: temporal variation and connection to new particle formation events	458

A. Porcar-Castell, B. Olascoaga, J. Atherton, F. Berninger and P. Kolari, Interpretation of temporal dynamics in leaf-level chlorophyll fluorescence: a mechanistic model .....	461
H. Portin, A. Leskinen, L. Hao, A. Kortelainen, P. Miettinen, A. Jaatinen, S. Romakkaniemi, A. Laaksonen, K.E.J. Lehtinen, and M. Komppula Effect of local pollutant sources on aerosol-cloud interactions at Puijo tower measurement station .....	464
N.L. Prisle, J. Koskinen, B. Molgaard, T. Raatikainen, T.B Kristensen, T. Ylijuuti, and A.-P. Hyvärinen Surfactants in microscopic droplets .....	467
T. Raatikainen, D. Brus, A.-P. Hyvärinen, J. Svensson and H. Lihavainen Black carbon concentrations and coating thickness at Pallas, Finland .....	471
M. Raivonen, S. Smolander, M. Tomasic, T. Hölttä, J. Susiluoto, T. Aalto, E-S. Tuittila, J. Rinne, S. Haapanala, A. Valdebenito, R.J. Schuldt, V. Brovkin, C. Reick, T. Kleinen and T. Vesala A model of methane emissions from boreal peatlands .....	475
P. Rantala, S. Haapanala, M.K. Kajos, J. Patokoski, L. Järvi, R. Taipale, J. Rinne and T.M. Ruuskanen VOC measurements with PTR-MS at urban background site in Helsinki .....	479
L. Riuttanen, A.-M. Sundström, J. Räisänen and M. Bister Sensitivity of radiative forcing to changes in upper tropospheric humidity associated with aerosols .....	482
A. Rusanen, M. Boy, S. Smolander, D. Mogensen, P. Roldin, and E. Hermansson Multicomponent aerosol modelling with specific chemical species .....	485
K. Ruusuvuori, P. Hietala, O. Kupiainen, T. Kurtén and H. Vehkamäki The charging properties of protonated acetone and acetone clusters .....	489
M. Santalahti, H. Sun, A.-J. Kieloaho, F. Asiegbo, F. Berninger, K. Koster, J. Pumpanen and J. Heinonsalo The interactions between soil fungal communities and soil organic nitrogen (SON) transformation in boreal forests – the effects of season, geographical location and natural disturbances .....	491

S. Schallhart, P. Rantala, R. Taipale, E. Nemitz, R. Tillmann, T.F. Mentel, T. Ruuskanen and J. Rinne VOC exchange measurements at Bosco Fontana (IT) and Hyytiälä (FI)	494
S. Schobesberger, H. Junninen, A. Franchin, F. Bianchi, J. Dommen, N.M. Donahue, J. Duplissy, M. Ehn, K. Lehtipalo, G. Lönn, T. Nieminen, I.K. Ortega, M. Sipilä, the CLOUD collaboration, T. Petäjä, M. Kulmala and D.R. Worsnop Measurements of cluster composition in new particle formation from sulphuric acid, small bases, and oxidised organics	496
L. Šigut, I. Mammarella, P. Kolari and P. Sedlák, New tool for CO <sub>2</sub> flux gap-filling and flux separation	500
S. Smolander, A. Arneth and T. Vesala Global vegetation simulations with isoprene and monoterpenes emissions for past 8000 years	502
G.Steiner, M. Breitenlechner, A. Hansel, T. Petäjä, M. Kulmala A portable cluster calibration unit	507
A.-M. Sundström, A. Arola, P. Kolmonen, and G. De Leeuw, On the use of satellite remote sensing based approach to determine aerosol direct radiative effect over land	512
A.-M. Sundström, A. Nikandrova, K. Atlaskina, T. Nieminen, V. Vakkari, L.Laakso, J.P. Beukes, P.G. Van Zyl, M. Josipovic, A.D. Venter, K. Jaars, J.J. Pienaar, S. Piketh, A. Wiedensohler, E.K. Chiloane, G. De Leeuw, and M. Kulmala Estimating the concentration of nucleation mode particles over South Africa using satellite remote sensing measurements	516
R. Taipale, N. Sarnela, M. Rissanen, H. Junninen, F. Korhonen, E. Siivola, M. Kulmala, R. L. Mauldin III, T. Petäjä and M. Sipilä A new instrument for measuring atmospheric concentrations of non-OH oxidants of SO <sub>2</sub>	521

T. Thum, T. Markkanen, T. Aalto, T. Laurila, N. Carvalhais, S. Zaehle, C. Reick, M. Törmä and S. Hagemann The effect of temperature and precipitation on carbon calances in Finland according to the JSBACH model	525
N.T. Tsona, N. Bork, And H. Vehkamäki Computational studies of ion-induced oxidation of SO <sub>2</sub>	531
S. M. Tu, A. Nordbo, A. Hellsten, J. Rinne and T. Vesala Large eddy simulations for forest canopy	534
B. Ľupek, K. Minkkinen, T. Vesala, and E. Nikinmaa CH <sub>4</sub> and N <sub>2</sub> O fluxes of boreal forest mire transitions	538
R. Väänänen, R. Krejci, P.P. Aalto, T. Pohja, L. Zhou, V. Hemmilä, H. Manninen, T. Yli-Juuti, T. Nieminen, T. Petäjä, M. Kulmala Airborne aerosol measurements performed during the Pegasos spring 2013 campaign	541
V. Vakkari, V.-M. Kerminen, J.P. Beukes, P. Tiitta, P.G. Van Zyl, M. Josipovic, A.D. Venter, K. Jaars, M. Kulmala and L. Laakso, Significant increase in CCN yield in fresh biomass burning plumes in Southern Africa	543
A. Vanhatalo, T. Chan, J. Aalto, J. Korhonen, P. Kolari, K. Rissanen, H. Hakola, T. Hölttä, E. Nikinmaa and J. Bäck, Dynamic relationship between the VOC emissions from a Scots pine stem and the tree water relations	546
D. Wimmer, K. Lehtipalo, T. Petäjä, M. Kulmala, J. Curtius and the CLOUD collaboration. Sub3-nm growth rates in the CLOUD experiment	550
A. Virkkula, A. Aarva, O. Järvinen, J. Svensson, N. Kivekäs, O. Meinander, A. Hyvärinen, K. Neitola, H. Lihavainen, H.-R. Hannula, A. Kontu, K. Anttila, J. Peltoniemi, M. Gritsevich, T. Hakala, H. Karttinen, P. Lahtinen, A. Raaterova, R. Väänänen, P. Dagsson-Waldhauserova, R.E. Bichell and G. De Leeuw Experimental studies on the effects of black carbon on snow albedo	554

A. Virkkula	
Effective particle size estimated from total scattering coefficient and total number concentration	557
M. Vogt, H. Vuollekoski, T. Petäjä, M. Sipilä, H. Lappalainen, J. Ahokas, A. Korpela, H. Mikkola and M. Kulmala	
Surfaces for water harvesting	563
H. Vuollekoski, R. Makkonen, A. Asmi, R. Hillamo, T. Petäjä and M. Kulmala	
Climate and biofuels in Brazil	565
H. Vuollekoski, A. Rusanen and M. Kulmala	
A brief glance at PUMA: Pythonic Unified Model of Aerosols	569
T. Yli-Juuti, K. Barsanti, L. Hildebrant Ruiz, A.-J. Kieloaho, U. Makkonen, T. Petäjä, T. Ruuskanen, M. Kulmala and I. Riipinen	
Nanoparticle growth and particle phase acid-base chemistry – a modeling study	572
L. Zhou, M. Boy, T. Nieminen, D. Mogensen, S. Smolander and M. Kulmala	
Long term modelling of new particle formation event in a boreal forest	575
P. Zhou, M. Boy, S. Smolander, K. Oswald and Ü. Rannik	
Large-eddy simulation of canopy effects on spatial distribution of chemicals and aerosols	577
M. Äijälä, H. Junninen, M. Ehn, T. Petäjä, M. Kajos, R. Väänänen, F. Canonaco, J. Slowik, A. Prévôt, P. Aalto, M. Kulmala and D. Worsnop	
Identifying the chemical fingerprints of aerosol sources at a rural background site	582

**FINNISH CoE IN PHYSICS, CHEMISTRY, BIOLOGY AND METEOROLOGY OF  
ATMOSPHERIC COMPOSITION AND CLIMATE CHANGE  
GENERAL OVERVIEW OF THE RESULTS AND ACTIVITIES IN 2008-2013**

MARKKU KULMALA<sup>1</sup>, HANNA K. LAPPALAINEN<sup>1,3</sup>, JAANA BÄCK<sup>1,2</sup>, ARI LAAKSONEN<sup>3,4</sup>,  
EERO NIKINMAA<sup>2</sup>, MARJA-LIISA RIEKKOLA<sup>5</sup>, TIMO VESALA<sup>1</sup>, YRJÖ VIISANEN<sup>3</sup>, MICHAEL  
BOY<sup>1</sup>, MIKKO DAL MASO<sup>1</sup>, HANNELE HAKOLA<sup>3</sup>, PERTTI HARI<sup>2</sup>, KARI HARTONEN<sup>5</sup>, VELI-  
MATTI KERMINEN<sup>1,3</sup>, ANTTI LAURI<sup>1</sup>, TUOMAS LAURILA<sup>3</sup>, HEIKKI LIHAVAINEN<sup>3</sup>, TUUKKA  
PETÄJÄ<sup>1</sup>, JANNE RINNE<sup>1</sup>, ANNELE VIRTANEN<sup>4</sup>, SAMI ROMA KANIEMI<sup>4</sup>, SANNA  
SORVARI<sup>1,3</sup>, HANNA VEHKAMÄKI<sup>1</sup> + the FCoE TEAMS

<sup>1</sup>Department of Physics, University of Helsinki, Finland

<sup>2</sup>Department of Forest Sciences, University of Helsinki, Finland

<sup>3</sup>Finnish Meteorological Institute, Finland

<sup>4</sup>Department of Physics, University of Eastern Finland, Kuopio Unit, Finland

<sup>5</sup>Department of Chemistry, University of Helsinki, Finland

**BACKGROUND AND SCOPE**

The Finnish Center of Excellence (FCoE) in *Physics, Chemistry, Biology and Meteorology of Atmospheric Composition and Climate Change* (2008-2013) is completing its research activity by the end of this year. This moment can be considered as a turning point summarizing scientific results of a long-term approach that started already in 2002 when the first Center of Excellence (2002-2007) was established.

The backbone of the scientific approach has been the supra-disciplinary research work by different teams from Departments of Physics, Chemistry and Forest Sciences at the University of Helsinki, Finnish Meteorological Institute and Department of Physics at the University of Eastern Finland. In the begin of the 2<sup>nd</sup> period of FCoE, in 2008, the FCoE set the following objectives: “Our main objective is to contribute *to the reduction of scientific uncertainties concerning global climate change issues, particularly those related to aerosols and clouds*. We aim at creating a *deep understanding on the dynamics of aerosol particles and ion and neutral clusters in the lower atmosphere, with the emphasis of biogenic formation mechanisms and their linkage to biosphere-atmosphere interaction processes, biogeochemical cycles and trace gases*. The relevance and usage of the results in the context of global scale modelling, and the development and utilization of the newest measurement techniques are addressed. The cores of activities are a) in continuous measurements and database of atmospheric and ecological mass fluxes and aerosol precursors and CO<sub>2</sub>/aerosol/trace gas interactions in SMEAR field stations and GAW station and b) in focused experiments and modelling to understand the observed patterns.”

These objectives emphasized the new understanding of role of biogenic formation mechanisms and their linkage to biosphere-atmosphere interaction processes, biogeochemical cycles and trace gases. During the last three years the scientific scope of the FCoE has moved from a new understanding of the phenomena towards so called all scale concept. In practice this means that the relevance and usage of the scientific outcome starting from the molecular scale can be applied and upscaled in the context of a global-scale phenomena such as prediction of climate change. Today the scientific orientation of the FCoE research community is called “*Atmospheric Science – From Molecular and Biological processes to The Global Climate*” (ATM), which will be also the name of the new, the 3<sup>rd</sup> FCoE, targeted for the years 2014-2019.

This abstract presents an overview of our scientific approach, including the main results and scientific highlights and the identification of the most important methodological developments and data pools. Furthermore, we introduce the main research collaboration and training and public outreach activities of the last three years. The FCoE scientific work has also initiated the development state-of-the-art research infrastructures, increased the volume of education activities and opened opportunities for innovation and climate policy making both national and international levels. We present here the overall organization of

there activities. At the end, we will outline the scientific approach of the new FCoE starting in January 2014, for next six years.

## SCIENTIFIC APPROACH

Here we summarize the research activities and scientific highlights especially for the last three years (2011-2013) of the FCoE<sub>2</sub>. The research work has been carried out by 12 main teams (Fig 1.) and 2 supporting teams with a focus on specific research areas of the land – atmosphere interactions in a boreal forest domain; for a detailed description of results see the Chapter of Team overview abstracts. The FCoE teams cover several critical parts needed for a holistic understanding of land-atmosphere interactions. The main themes of the FCoE science scope on main objectives, have been: (i) Aerosol physics and chemistry (Teams: Vehkämäki, Petäjä, DalMasó/Kerminen, Riekkola), (ii) Aerosol-cloud-climate interactions (Teams: Laaksonen, Lihavainen, Kerminen), (iii) Biosphere-Atmosphere interactions (Teams: Vesala, Bäck, Pumpanen, Rinne, Laurila, Hakola), (iv) Modelling approaches bridging the gaps from process level via mesoscale and reaching up to global scales (Teams: Boy, Laaksonen, Kerminen) and (v) Development of analytical methods in the laboratory (Riekkola, Hakola, Petäjä).

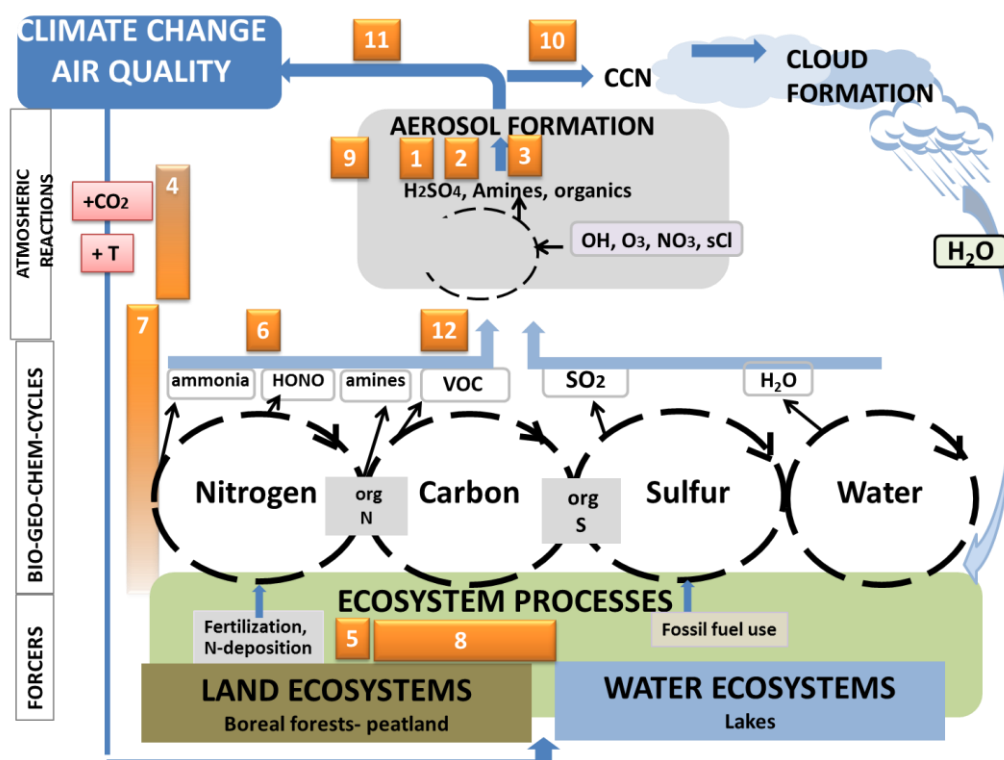


Fig. 1. FCoE main teams and team leaders and their research focus area: 1) Computational aerosol physics; H.Vehkamäki, 2) Aerosol measurements; T.Petäjä, 3) Aerosol phenomenology; M.Dal Maso/VM Kerminen, 4) Atmosphere modelling; M.Boy, 5) Soil dynamics, J.Pumpanen, 6) Biogenic hydrocarbon fluxes; J.Rinne, 7) Micrometeorology; T.Vesala, 8) Ecosystem processes; J.Bäck, 9) Sophisticated instrumental analytical techniques; M-L. Riekkola, 10) Atmospheric aerosols and aerosol cloud interactions; A.Laaksonen, 11) Aerosols and climate; H.Lihavainen, 12) Organic chemistry of the atmosphere; H Hakola.

## AEROSOL PHYSICS AND CHEMISTRY

**The aerosol physics and chemistry** group has made crucial advances in understanding the initial steps of aerosol formation and addressed the relative roles of condensing vapors on the nucleation and growth. The work includes both detailed laboratory experiments as well as a wide variety of intensive field campaigns around the world in different environmental conditions (Team Petäjä). Based on the experimental evidence, we have formulated the atmospheric aerosol formation as a two-step process involving atmospheric chemistry (oxidation), clustering (acid-base chemistry) and multi-component condensation. The key results have been published by Kulmala et al. (2013). The conceptual methodology for measuring and analyzing atmospheric aerosol formation is presented in Kulmala et al. (2012).

In more detail, we have studied several base compounds and their role in the aerosol formation process by combining theoretical approaches, field studies, process analysis and development of new laboratory techniques on aerosol composition (Teams Vehkamäki, Petäjä, Dalmaso/Kerminen). We have studied the nucleating molecules and atoms aimed to understand how and why a certain group of molecules eventually forms a cluster that has the potential to grow towards climatically important sizes. See Manninen et al. and Sipilä et al., this issue, for more details.

The main focus in the theoretical group (Team Vehkamäki) during the last three has been on extent of the computational task to develop the Atmospheric Cluster Dynamics Code (ACDC) and to perform related quantum chemical calculations and to build a methodology for and starting novel molecular dynamic simulations of atmospheric cluster formation. The ACDC has now been validated and used the model to assess the role of the critical cluster concept in atmospheric particle formation. Despite the fact that the model can not accurately simulate the atmospheric particle formation, we can now test the feasibility of the different particle formation mechanisms (Vehkamäki et al., this issue).

In the second approach we have used complementary information from state-of-the-art laboratory and long-term field experiments in order i) to comprehensively characterize the physical, chemical and optical properties of atmospheric aerosol particles in various environments, ii) to identify the compounds participating in atmospheric new particle formation, iii) to investigate gas phase precursors, ions and their interactions leading to new particle formation, iv) to explore anthropogenic and biogenic influences on the atmospheric aerosol population and their connections to the global change, and v) to develop the instruments. We have also been focused on process studies of the formation, evolution and transportation of aerosols and associated trace gases in the following focus areas: i) characterization of physical, chemical and dynamical parameters from aerosol field measurements; ii) aerosol dynamics model studies to develop tools for the parameterization of the evolution of aerosol particle populations; iii) transportation and dispersion studies of atmospheric trace elements, especially aerosols and other air pollutants; and iv) multivariate methods for analysis of atmospheric field observations (Team Petäjä). As an example, the teams have made a comprehensive analysis of the diurnal – seasonal and annual behavior of BVOC emissions and linked these patterns to the initial steps of atmospheric nucleation. This work has been enabled by the measurement tools developed to detect the particles in the sub-3 nm diameter size range.

A facility for studying the formation of secondary organic aerosol from real plant emissions as a means of studying realistic atmospheric processes under controlled conditions has been developed (Virtanen). The laboratory and field observations have been used interactively for studying a variety of atmospheric models from process level to global scale.

The scientific approach by the Teams Petäjä, Dal Maso, Kerminen and Vehkamäki combines several outstanding results on the wide spectrum of the aerosols formation- characteristics and links between aerosols and biosphere and clouds. The approach has expanded into even to a wider scale compared with the original objectives set for the teams. In other words, the aerosol formation as a phenomenon could be connected to the ecosystem-atmosphere interactions as a whole, as this sensitive process is tightly regulated by the gas phase concentrations, biosphere and anthropogenic emissions. The hypothesis is that

by resolving the chemical composition of initially forming aerosol particles we are able to probe the coupled carbon-water-nitrogen-sulfur cycles (Fig.1).

## **AEROSOLS, CLOUDS, CLIMATE AND AIR QUALITY**

The research on aerosol-cloud-climate interactions has covered studies on cloud condensation nuclei (CCN), clouds and aerosol-cloud interactions, as well as integration of these results into large-scale applications (Teams, Laaksonen, Kerminen, Lihavainen). The main interest has been in characterizing the physical and chemical properties of atmospheric aerosol, especially particles that form from nucleation, and understanding the role of aerosols as CCN. The work has included the development unique instruments that measure aerosol chemical composition both directly and indirectly, and deploy these in intensive field studies in Puijo, Finland as well as throughout the world. Process and cloud models have been developed and better parameterizations to describe aerosol-cloud interactions in global models have been produced (Laaksonen et al. this issue).

The connections between atmospheric aerosols, climate and air quality have been investigated in various environments. The approach has been based on continuous (the SMEAR-station network in Värriö, Hyytiälä, Helsinki and Puijo, the Pallas-Sodankylä Global Atmospheric Watch (GAW) station, the Utö Atmospheric and Marine Research Station and Virolahti measurement station) and campaign-type (India, Tiksi in Siberia, Saudi Arabia, and Marambio in Antarctica) measurements, laboratory experiments and modeling. The observational data contributes to model development and provides a solid basis for the result integration and synthesis. Examples of the conducted work include comprehensive analyses of observation data from the recent field campaigns, interpreting results from the lab experiments investigating the growth of nano-sized sulphuric acid particles, interpreting results from single particle soot photometer (SP2) and climate modeling, and investigating the possibilities to mitigate warming of Arctic climate by black carbon (BC) emissions reduction at mid-latitudes, especially in Europe ([www.maceb.fi](http://www.maceb.fi)). The impact of the current air quality and climate relevant legislation in the northern hemisphere on BC emissions, their transport to the Arctic, and eventually Arctic warming has been investigated as well (Lihavainen et al. this issue).

## **BIOSPHERE-ATMOSPHERE INTERACTIONS**

The interdisciplinary teams (Teams Vesala, Laurila, Bäck, Pumpanen, Rinne) of forest, peatland and freshwater ecologists and atmospheric physicists and chemists within FCoE have been concentration on the biosphere – atmosphere interaction processes. The bio-atm interactions approach has addressed the process understanding of various types of energy flows between the biosphere and atmosphere. The approach has covered different environments such as forest canopies, soil and lake. The large-scale research interest has been focused on vegetation control vs. ecosystem biogeochemical cycles, vegetation affect vs. exchange of greenhouse gases and BVOCs and the analysis of mechanisms involved in the control. The research question are also addressing, how do the biogeochemical cycles and atmospheric processes and forest development affect vegetation (Bäck et al., this issue, Vesala et al. 2013, this issue). The main data pool for the modeling approach have been GHG flux and concentration measurements (Teams Vesala, Laurila) together with BVOC concentration and emission data (Teams Rinne, Hakola, Bäck). For more details, see Bäck et al., this issue, Vesala et al., this issue, Laurila et al. this issue).

The forest canopy has been the long-term research focus areas of the bio-atm teams, however the role of lakes and soil research has increased during the later period of FCoE. Soils play an important and active role in controlling the greenhouse gas balance in the atmosphere and it also affects indirectly the radiative forcing of the atmosphere through various feedback effects (Pumpanen et al. this issue). The flux studies over lakes are scarce: there are only seven articles reporting eddy-covariance EC measurements of CO<sub>2</sub> fluxes over, and none over rivers, and the lengths of the records are rather short.

The Vesala and Bäck teams have made major progress in tree related physiological analysis, measuring aquatic ecosystem gas exchange, peatland methane emissions and detecting biogenic VOC (amines, sesquiterpenes) compounds in field conditions. Overview of the methods developed is provided by Kulmala et al. 2012.

## **MODELLING APPROACH FROM MESOSCALE TO GLOBAL SCALE**

The understanding of the whole process of formation of secondary aerosols, starting from the emissions of precursors from the canopy up to their activation to form cloud droplets is in the core of the models simulating the behavior of the climate system (Teams Boy, Laaksonen, Kerminen).

The mesoscale modeling approach is bridging the gap between the most novel instrumentations operated at our SMEAR stations and the global modeling community by detailed process-oriented studies in the lower part of the troposphere. Special focus is to achieve a comprehensive picture of the climate change by models from nanometer to global scale and from seconds to centuries. This includes investigating the mechanism related to the formation of secondary organic aerosols (SOA), the role of vertical mixing in photochemistry and SOA formation, and future trends in the formation of new particles with resulting impacts on climate through direct and indirect aerosol effects. During the last three major part of the meso scale modeling has been concentrating to improve the following models: MALTE-BOX, a zero-dimensional model: both chemical and aerosol dynamical processes; SOSAA, a one-dimensional chemistry-transport mode gas-phase chemistry and aerosol dynamics; ASA, a Large-Eddy-Simulation model; MEGAN, a canopy module and the emission module; a PENCIL-CLOUD, a model of hydrodynamic flows; and FLAMO, a regional meteorological model (Boy et al., this issue).

Global-scale analyses have been made using the global aerosol-climate model ECHAM5-HAM(2) (Teams Laaksonen, Kerminen). For example, we have investigated the impact of the increasing aerosol emissions in China and India between 1996 and 2010 on global climate. The warming contribution of black carbon concentrations above clouds nearly cancels the cooling effect of sulfate aerosols, thus making it unlikely that the increase in aerosol emissions in China and India has caused the "hiatus" in global warming during the last decade. Recent work has been done to produce faster aerosol modules capable of presenting all relevant aerosol processes (sectional aerosol module SALSA tested). More detailed evaluation showed that currently commonly used modal representation of aerosol in large scale models suffers several issues in describing aerosol-cloud interactions (Laaksonen et al., this issue). In order to improve the BVOC-aerosol-climate interactions, several processes that couple organic vapours to particle formation and growth in ECHAM5.5-HAM2 has been implemented. Five different nucleation mechanisms were introduced to the model, including nucleation rate formulations with organic gases (Kerminen et al, this issue).

## **DEVELOPMENT OF ANALYTICAL METHODS**

Intensive development of analytical methods have been made concerning (i) in situ measurements of volatile organic compounds and inorganic gases and particles (Hakola et al., this issues) and (ii) measurement of the chemical composition and physicochemical properties of individual compounds in the gas phase and atmospheric aerosol particles (Sipilä et al., this issue, Riekkola et al this issue).

Various chemical ionization methods have been tested and developed during the FCoE. These include implementation of nitrate ion source for acidic cluster detection (Sipilä et al., this issue, Jokinen et al. 2012, ACP) as well as a bi-sulphate ion source for bases (Sipilä et al., this issue). These techniques have been applied both to field and chamber studies (Schobesberger et al. 2013, in press) revealing the concentrations of key precursors in sub-ppt concentration levels as well as the temporal evolution of the cluster composition during nucleation (Kulmala et al. 2013).

The development work of volatile organic compounds and inorganic gases and particles have included the developed of an inlet for in-situ GC measurements enabling mono- and sesquiterpene measurements. The system was conducted for the first time in-situ biogenic VOC measurements, including sesquiterpenes, in a boreal forest covering the whole year. Furthermore the team has made in-situ measurements of inorganic gases and aerosols in urban and rural air and studied the chemical composition of organic aerosols and measured for the first time, for example, caryophyllenic acid concentrations in ambient particles (Hakola et al., this issues).

One part of the aerosol physics and chemistry approach has been the development of new laboratory techniques for analyzing the atmospheric aerosol particle composition to cover the identification of organic compounds in different size atmospheric aerosol particles as well as determination of aliphatic and aromatic amines in atmospheric aerosol particles and vapor pressures of several atmospherically relevant compounds. During the last yeas a novel gas chromatographic methodology for the determination of vapour pressures of compounds in mixtures has been developed and utilized in aerosol studies. Vapor pressures of several atmospherically relevant compounds were determined for the first time. The method proved to be superior over all the existing techniques in terms of time, sensitivity, precision and sample preparation (Riekkola et al., this issue).

### SCIENTIFIC HIGHLIGHTS

In years 2011 – 2013 we have published altogether **10** papers in Nature, Nature Geosciences, Nature Protocols or Science. The total number of all peer reviewed publications by members of the FCoE in 2011–2013 (until Sep 30<sup>th</sup>) is more than 200. In 2011–2013 our most important scientific results are on the new sights on the atmospheric new particle formation (Kirkby et al. 2011; Kulmala et al. 2013) and growth (Riipinen et al. 2012), atmospheric oxidation (Mauldin et al. 2012), linkages and processes in the land- atmosphere interface (Kulmala and Petäjä 2011, Yvon-Durocher et al. 2012), and biosphere-atmosphere feedbacks (Paasonen et al., 2013). We have also attributed the hot spot of the current climate policy debate on the role of black carbon in the climate system by presenting results on absorption features of and mixing state of black carbon (Cappa et al. 2012)

One of the key strength of the FCoE<sub>2</sub> approach has been a successful combination of new methods, instrument development, and comprehensive measurements, which have been used to improve fundamental process understanding and to develop parameterizations to various models. As a synthesis of a long-span instrument development on aerosol measurements, the team published a scientific protocol on the measurement of the nucleation of atmospheric aerosol particles in Nature Protocols (Kulmala et al. 2012). The protocol describes the procedures for identifying new-particle-formation (NPF) events, and the methods for determining the nucleation, formation and growth rates during such events under atmospheric conditions. Also the descriptions of the present instrumentation, best practices and other tools used to investigate the atmospheric nucleation and the NPF at a certain mobility diameter (1.5, 2.0 or 3.0 nm) are addressed. Furthermore, the reliability of the methods used and requirements for the proper measurements and data analysis are discussed (Kulmala et al. 2012). This work provides a summary of methodology development within the FCOE<sub>2</sub> during the last two decades. It will be used as a benchmark, to which future research on the experimental nanoparticle formation in the atmosphere will be compared

The latest research highlight is presented in Kulmala et al. (2013) we gave an improved insight on atmospheric new particle formation and cluster dynamics. Atmospheric nucleation is the dominant source of aerosol particles in the global atmosphere and an important player in aerosol climatic effects. The key steps of this process occur in the sub-2 nm size range, in which direct size-segregated observations have not been possible until very recently. In Kulmala et al. (2013) we presented detailed observations of atmospheric nanoparticles and clusters down to 1 nm mobility diameter. We identified three separate size regimes below 2 nm diameter that build up a physically, chemically and dynamically consistent framework on atmospheric nucleation, more specifically aerosol formation via neutral pathways. Our findings emphasize the important role of organic compounds in atmospheric aerosol formation,

subsequent aerosol growth, radiative forcing and associated feedbacks between biogenic emissions, clouds and climate.

The results indicates clearly how simultaneous use of particle Size Magnifier, ions spectrometers and mass spectrometers allows us to find out physic and chemistry of new particle formation in the atmosphere.

**List of FCoE Nature / Nature Geosciences / Nature Protocols and Science papers published in 2011-2013:**

1. Kirkby, J., Curtius, J. Almeida, J. Dunne, E., Duplissy, J., Ehrhart, S., Franchin, A., Gagné, S., Ickes, L., Kürten, A., Kupc, A., Metzger, M., Riccobono, F., Rondo, L., Schobesberger, S., Tsagkogeorgas, G., Wimmer, D., Amorim, A., Bianchi, F., Breitenlechner, M., David, A., Dommen, J., Downard, A., Ehn, M., Flagan, R. C., Haider, S., Hansel, A., Hauser, D., Jud, W., Junninen, H., Kreissl, F., Kvashin, A., Laaksonen, A., Lehtipalo, K., Lima, J., Lovejoy, E. R., Makhmutov, V., Mathot, S., Mikkilä, J., Minginette, P., Mogo, S., Nieminen, T., Onnela, A., Pereira, P., Petäjä, T., Schnitzhofer, R., Seinfeld, J. H., Sipilä, M., Stozhkov, Y., Stratmann, F., Tomé, A., Vanhanen, J., Viisanen, Y., Vrtala, A., Wagner, P. E., Walther, H., Weingartner, E., Wex, H., Winkler, P. M., Carslaw, K. S., Worsnop, D. R., Baltensperger, U. and Kulmala, M.: **The role of sulfuric acid, ammonia and galactic cosmic rays in atmospheric aerosol nucleation**, Nature, 476, 429-433, doi:10.1038/nature10343, 2011.
2. Kulmala, M. and Petäjä, T.: Soil nitrites influence atmospheric chemistry, Science, 333, 1586-1587, doi:10.1126/science.1211872, 2011.
3. R.L. Mauldin III, T. Berndt, M. Sipilä, P. Paasonen, T. Petäjä, S. Kim, T. Kurtén, F. Stratmann, V.-M. Kerminen and M. Kulmala: **A new atmospherically relevant oxidant of sulphur dioxide**. 2 0 1 2 4 8 8 | 1 9 3- 197. doi:10.1038/nature11278
4. Yvon-Durocher G., Caffrey J.M, Cescatti A., Dossena M., del Giorgio P., Gasol J.M, Montoya J.M, Pumpanen J., Staehr P.A, Trimmer M., Woodward G. & Andrew A.P.: **Reconciling the temperature dependence of respiration across timescales and ecosystem types**. doi:10.1038/nature11205
5. Riipinen I., Yli-Juuti T., Pierce J.R, Petäjä T., Worsnop D.R., Kulmala, M. & Donahue N.M.: **The contribution of organics to atmospheric nanoparticle growth**. Nature Geoscience 5, 453-458 (2012) doi:10.1038/ngeo1499
6. Cappa, C.D., Onasch, T.B., Massoli, P., Bates, T.S., Gaston, C.J., Hakala, J., Petäjä, T., Hayden, K., Kolesar, K.R., Lack, D.A., Mellon, D., Li, S.-M., Nuaaman, I., Prather, K.A., Quinn, P.K., Song, C., Subramanian, R., Vlasenko, A., Worsnop, D.R. and Zaveri, R.A., **Radiative Absorption Enhancements Due to the Mixing State of Atmospheric Black Carbon**, Science, 337, 1078-1081 DOI: 10.1126/science.1223447
7. Kulmala, M., Petäjä, T., Nieminen, T., Sipilä, M., Manninen, H.E., Lehtipalo, K., Dal Maso, M., Aalto, P.P., Junninen, H., Paasonen, P., Riipinen, I., Lehtinen, K.E.J., Laaksonen, A. and Kerminen V.-M. (2012) **Measurement of the nucleation of atmospheric aerosol particles**, Nature Protocols 7, 1651-1667, doi:10.1038/nprot.2012.091.
8. Markku Kulmala, Jenni Kontkanen, Heikki Junninen, et al. (2013) **Direct Observations of Atmospheric Aerosol Nucleation**. Science 22: 943-946. [DOI:10.1126/science.1227385]
9. Cappa, C.D., Onasch, T.B., Massoli, P., Worsnop, D.R., Bates, T.S., Cross, E.S., Davidovits, P., Hakala, J., Hayden, K., Jobson, B.T., Kolesar, K.R., Lack, D.A., Lerner, B.M., Li, S.-M., Mellon, D., Nuaaman, I., Olfert, J.S., Petäjä, T., Quinn, P.K., Song, C., Subramanian, R., Williams, E.J. and Zaveri, R.A. (2012) **Response to Comment on “Radiative Absorption Enhancements Due to the Mixing State of Atmospheric Black Carbon”**, Science 339, 393c.
10. Paasonen, P., Asmi, A., Petäjä, T., Kajos, M.K., Äijälä, M., Junninen, H., Holst, T., Abbatt, J.P.D., Arneth, A., Birmili, W., Denier van den Gon, H., Hamed, A., Hoffer, A., Laaksonen, A., Laakso, L., Leaitch, R., Plass-Dülmer, C., Pryor, S.C., Räisänen, P., Swietlicki, E., Wiedensohler, A., Worsnop, D.R., Kerminen, V.-M. and Kulmala, M. (2012) **Warming-induced increase in aerosol number concentration likely to moderate climate change**, Nature Geosci., doi: 10.1038/NGEO1800.

## **PARTICIPATION IN LARGE SCALE, INTEGRATED FIELD AND LABORATORY EXPERIMENTS**

The backbones of our research activities have been data products from our SMEAR and GAW station network. The access to global and European scale aerosol and other climate data pools have been attained by the active coordination or participation to European Union FP6 projects such as EUCAARI (European Integrated project on aerosol, cloud, climate and air quality interactions) (Kulmala et al. 2011) and Integrated Infrastructures Initiatives project EUSAAR (European Supersites for Atmospheric Aerosol Research). In order to ensure the access to best data pools in the field of atmospheric sciences and biosphere–atmosphere interface the FCoE teams have continued active participation to the ongoing European FP7 research and infrastructure projects. The most crucial projects here are the four-year projects FP7-ACTRIS-I3 (Aerosols, Clouds, and Trace gases Research InfraStructure Network (Petäjä et al. this issue) and FP7-PEGASOS (The Pan-European Gas-AeroSols Climate Interaction Study (Manninen et al. this issue), FP7- EXPEER-I3 (Experimentation in Ecosystem Research), and the recently concluded FP7-MarieCurie-ITN-CLOUD representing a leading edge laboratory experiments at CERN. The data analysis of these activities is ongoing. For example we have started the extensive analysis and compared the computational results with CLOUD experiments and Hyytiälä field data. The work is aimed to provide theoretical support for experiments and instrument development and seek to improve and test our model by comparing to a wide selection of experiments (Vehkamäki et al., this issue). We have also made a major scientific outcome of the CLOUD experiment on formation of aerosol particles both via neutral and ion induced pathways.

One of the most extensive field campaigns conducted by our teams so far took place in May – June 2012 when the Zeppelin lights over Hyytiälä, Southern Finland. The measurements of the vertical and the horizontal extension of NPF events were performed using an instrumented airship, Zeppelin. The vertical profile measurements represent the particle and gas concentrations in the lower parts of the atmosphere. At the same time, the ground based measurements records present conditions in the surface layer. Horizontal, almost Lagrangian, experiments were possible as the airship drifted with the air mass (Manninen et al. this issue).

Participation in the European large-scale projects has provided standardized and quality-controlled data products, in addition to which it has brought good visibility and active use of the SMEAR- data products. To ensure the continuous development of national data products and the research infrastructures used by the FCoE teams, the data product development has been networked to the ongoing EU-FP7-projects: FP7-ENVRI-project “Common Operations of Environmental Research Infrastructures” in Europe and FP7-COOPEUS-project “Transatlantic cooperation in the field of environmental research infrastructures” between Europe and USA. The aim of these research infrastructure projects is the identification of next generation user friendly data structures and formats (Sorvari et al. this issue).

As a summary FCoE research community has worked towards building internationally leading, multidisciplinary research environment for atmospheric and Earth system science to study biosphere-aerosol-cloud-climate-air quality interactions. This work has included establishment of Super sites (SMEAR stations, Pallas, several experimental field sites and laboratories, process and climate/Earth system components, and databases to store and distribute the data. So far these different types of infrastructures have been operated separately and managed by the FCoE partners individually. The future aim is to establish an Integrated Atmospheric and Earth System Science Research Infrastructure – INAR RI to increase the coordination, management, interoperability and interworkability of the research infrastructure components (Sorvari et al. this issue).

## RESEARCH TRAINING

In 2011-2013 FCoE has continued the collaboration among Nordic centers of excellence CRAICC (Cryosphere-Atmosphere Interactions in a Changing Arctic Climate), DEFROST and SVALI, appointed by NordForsk. In 2011-2013 FCoE researchers have participated in Earth System Modelling - CRAICC-SVALI-DEFROST workshop in June 2012 at the University of Helsinki, Finland, Black Carbon workshop June 2012 at the Lund University, Sweden, the Ice Nucleation workshops in February 2012 at ETHZ, Zurich, Switzerland, the Eddy covariance flux workshop in January 2013 in Helsinki, as well as the annual workshops of the Nordic centers.

Altogether over 50 MSc's and 36 PhD's finalized their theses within the FCoE during 2011-2013 (until August 31<sup>st</sup> 2013). Until the end of 2013, the education and knowledge transfer of the Centre of Excellence has been formalized in the National ACCC Doctoral Programme (Atmospheric Composition and Climate Change: From Molecular Processes to Global Observations and Models), involving more than 200 doctoral students. However, the funding scheme is changing in 2013. The Academy of Finland doctoral programmes will cease to exist, and the funding will be transferred to the budget funding of the Finnish universities. Both University of Helsinki and University of Eastern Finland have started their local programmes directly related to FCoE (University of Helsinki: Doctoral Programme in Atmospheric Sciences; University of Eastern Finland: Doctoral Programme in Aerosol Science). ACCC will remain as a national network, but without own funding. As a recognition of the scientific excellence of the FCoE work, M. Kulmala and S. Zilitinkevich were granted the ERC-Advanced Grants, and H. Vehkamäki and I. Riipinen the ERC-Starting Grants.

Between last three year period the FCoE units organized a total of 14 intensive graduate courses. In total, more than 300 students participated in these courses. The intensive courses were usually organized in collaboration with several international projects and programmes, e.g. iLEAPS, CLOUD-ITN, CLOUD-TRAIN, the Nordic Master's Degree Programme ABS, and the Nordic Centres of Excellence CRAICC, DEFROST and SVALI.

In order to maintain the good working atmosphere and to support the equal career opportunities between men and women, an Equality task group was established at the Division of Atmospheric Sciences (Univ of Helsinki) in 2011. The group works towards identifying and prevention of any kind of inequality or discrimination of the personnel. The task group executed an Equality Questionnaire in summer 2012, and the results were presented in autumn 2012. The questionnaire was aimed at screening the work atmosphere and attitudes, and it gathered up over 100 replies.

## OUTREACH

The non-scientific end-users of the data are informed using distributed written material and press conferences, which generates interviews and articles in popular science magazines and in domestic and international newspapers as well as in the television and radio. FCoE teams are also been active players in several platforms for outreach: (1) Hiukkastieto ([www.hiukkastieto.fi/](http://www.hiukkastieto.fi/)) for aerosol information, (2) Hiilipuu ([www.hiilipuu.fi](http://www.hiilipuu.fi/)) for illustration of CO<sub>2</sub> fluxes of boreal tree and (3) Ympäristötiedon foorumi ([www.ymparistotiedonfoorumi.fi](http://www.ymparistotiedonfoorumi.fi/)), which is a collaborative network of actors in environmental science to promote dialogue between scientists and decision makers at different levels. One more example of a modern approach to get the public attention to science was launched by Helsinki University in 2011. FCoE research was presented at the "Think Corner"—science cafe, as a part of the Helsinki Design year activities (<http://blogs.helsinki.fi/wdc-2012/think-corner/>). During one week in June 2012, the FCoE researchers gave 15 presentations to public audience, and a scientific exhibition showing e.g. measurement tools and the interactive Carbon tree software were included in the program of the week. All the presentations and discussions were recorded for a wider audience via the "Think Wall" facebook site (<http://www.helsinki.fi/thinkwall/>).

## **RESEACH INFRASTRUCTURES, EDUCATION, INNOVATION AND POLICY MAKING ACTIVITIES INITATED BY THE SCIENTIFIC APPROACH**

The scientific approach of the FCoE has been the primus motor for expanding the scientific outcome into the wider context and for the use of the international research community and society. The FCoE , presently the ATM, approach in has awaked new actions in a national, Nordic, European and global scale and has provided critical mass and scientific mandate for the FCoE partners to take leadership role in several sectors related to science approach in Europe and to promote atmospheric sciences globally and to make a climate policy impact.

In the national scale one of the core stones of the FCoE-ATM has been the continuing development of SMEAR stations infrastructure. SMEAR stations data pools have been the main material for several in situ first-observations and scientific breakthrough of the FCoE. The FCoE teams (Teams Petäjä, Lihavainen) have been intensively involved with a super-site concept development in Europe and outside Europe. In spring 2012, the Chinese research bodies introduced a SMEAR-type station near Nanjing. In addition, the co-operation to establish atmospheric measurement stations in Estonia, South Africa and Saudi Arabia is on the way. We are also involved in a collaboration to establish a state of the art, long term measurement station to Siberia (Tiksi) in Russia, especially to attain year-round observations of important climate forcing agents within the Russian side of the Arctic (Lihavainen et al., this issue). These collaborations are a direct consequence of the FCoE<sub>2</sub> activities.

Active development of the SMEAR station concept including instrument and methodological innovations, data products, data delivery and storage systems has provided a strong international role for the FCoE partners, Univ.Helsinki and FMI to contribute the European Research Area initiatives. Today FCoE partners are central players in ESFRI infrastructures (European Strategy Forum on Research Infrastructures) via ICOS, the Integrated Carbon Observation System leading the ICOS headquarters in Helsinki (Kaukolehto et al., this issue), ANAEE, the Infrastructure for Analysis and Experimentation on Ecosystems (Siitonen et al, this issue.) and via strategic planning of European aerosol and atmospheric chemistry infrastructure (ACTRIS-I3) (Petäjä et al. this issue). In 2012 it was decided that ICOS headquarters will be established in Helsinki.

In the global scale the most important large scale initiative is just recently established Pan Eurasian Experiment (PEEX), which is the first of the kind bottom up –top down (co-design) organized initiative in a global scale. PEEX geographical domain covers one on the most curial regions of the Earth in terms of the Global change. PEEX domain covers Siberian boreal forests region being the curial source for the bvoc emissions in a global scale. Furthermore, the domain is covering extensive areas of fast thawing permafrost regions of the Northern Pan Eurasian region, regions of Arctic sea and deals with the air quality problematic of Moscow and Peking, the megacities. PEEX is in a phase of consolidating it's position in the global scale research –research infrastructure-education initiative landscape. In practice this means the finalization of PEEX Science Plan and giving the frames and structure the PEEX implementation. Also the commitment of PEEX partners and collaborators in Europe, Russia and China is ongoing. First steps towards implementation has just been taken by selecting the core stations the development of a coherent coordinated atmospheric-ecosystem measurements in Pan Eurasian region (Lappalainen et al. of this issue).

The main channels for the European and global climate policy impact for the FCoE activities are the IGBP iLEAPS, Integrated Land Ecosystem – Atmosphere Processes Study and participation to the IPCC panels (Sun et al. this issue). Helsinki University is hosting the iLEAPS international project office at Helsinki and prof. Kulmala was a co-chair of the iLEAPS Scientific Steering Committee in 2010-2012. Futhermore, FCoE PIs prof. V-M-Kerminen and prof. T. Vesala are participating in the IPCC Fifth Assessment Report (AR5, years 2010–2014) processes and future developments of the global research programmes (IGBP/WCRP). Prof. Kerminen is a lead author of the chapter “Cloud and Aerosols” in

Working Group 1 (WG1) of AR5, and Prof. Vesala is a Review Editor of the chapter “Carbon and other biogeochemical cycles” in WG1 of AR5.

The Finnish Ministry of Environment established a national Climate Panel in December 2011 and nominated Prof. Kulmala as the chair of the panel for the period 1.12.2011 – 31.12.2013. As a chair of the Climate Panel Prof. Kulmala has given a great number of TV and radio interviews providing publicity and visibility also to the FCoE research. The national climate panel is collating climate change research for politicians. The panel consists of 13 members, who are senior scientists in the fields of natural sciences, economics and other social sciences, engineering and international politics. One of the first tasks of the national Climate Panel has been to mediate the insights of the science community for the preparation process of Climate Act for Finland. The preparation work Climate Act is one examples demonstrating the policy impact.

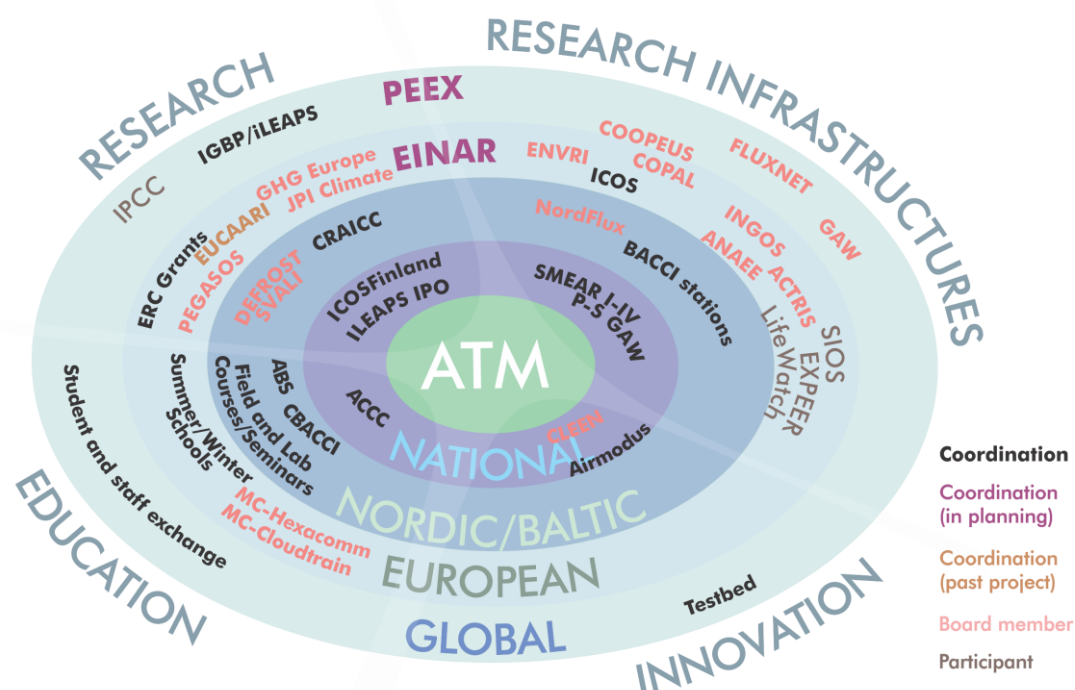


**Fig. 2.** Research infrastructure, research, education and innovation activities of the ATM community.

Abbreviations: ABS=Atmosphere-Biosphere Studies; ACTRIS=European aerosol and atmospheric chemistry infrastructure; ANAEE=Analysis and Experimentation on Ecosystems; BACCI=Biosphere-Aerosol-Cloud-Climate Interactions; CBACCI=Carbon- Biosphere-Atmosphere-Cloud-Climate-Interactions; CLOUD=Cosmics Leaving Outdoor Droplets; COPAL=Community heavy-PAYload Long endurance Instrumented Aircraft for Tropospheric Research in Environmental and Geo-Sciences; CRAICC=Cryosphere-Atmosphere Interactions in a Changing Arctic Climate; DEFROST=A changing cryosphere-depicting ecosystem-climate feedbacks as affected by permafrost, snow and ice; EINAR=European Institute of Atmospheric Sciences and Earth System Research; EUCAARI=European Integrated Project on Aerosol-Cloud- Climate-Air Quality Interactions; EXPEER=Distributed Infrastructure for EXPErimentation in Ecosystem Research; FCoE=Finnish Centre of Excellence in Physics, Chemistry, Biology and Meteorology of Atmospheric Composition and Climate Change; FLUXNET=Integrated CO<sub>2</sub> flux measurement network; GHGEurope=Greenhouse gas management in European land use system GAW=Global Atmospheric Watch; IAGOS=In-service Aircraft for Global Observing System; ICOS=Integrated Carbon Observation System; IGBP=International Geosphere-Biosphere Program; iLEAPS=integrated Land Ecosystem Atmosphere Processes Study; IPCC=Intergovernmental Panel for Climate Change; LifeWatch=e-science and technology infrastructure for biodiversity data and observatories; MC=Marie Curie Initial Training Network; NordFlux=A Nordic research network for greenhouse gas exchange from northern ecosystems; P-S GAW=Pallas-Sodankylä Global Atmosphere Watch Station; PEEX=PanEurasian Experiment; PEGASOS=Pan-European Gas-Aerosols-climate interaction Study; SIOS=Svalbard Integrated Arctic Earth Observing System; SMEAR=Station for Measuring Ecosystem-Atmosphere Relations; SVALI=Stability and Variations of Arctic Land Ice.

### FUTURE PROSPECTS AND the 3<sup>rd</sup> FCoE

During last six years FCoE has taken the world leading position in building up scientific understanding related to the dynamics of aerosols, ions, and neutral clusters in the lower atmosphere and their links to biosphere-atmosphere interaction processes, biogeochemical cycles and trace gases. Current knowledge on formation and growth mechanisms of atmospheric aerosols, aerosol and air ion dynamics, the effect of secondary biogenic aerosols on global aerosol load, aerosol-cloud-climate interactions, air pollution-climate interactions and the relationships between the atmosphere and different ecosystems, particularly boreal forest is largely based on scientific approach by the FCoE<sub>1</sub> and the ending FCoE<sub>2</sub>.

However, in spite of the improved understanding on the aerosol formation process and related dynamics, there is still a great challenge in the assessment and prediction of climate change and especially upgrading processes understanding into a global scale. In June 2013 the ATM research community was granted for a new center-of-excellence-period for the years 2014-2019 and to mobilize a group of 200 scientists to study, solve and quantify the feedbacks of the so called COntinental Biosphere-Aerosol-Cloud-Climate (COBACC) hypothesis. Kulmala et al. (2004) has suggested a negative climate feedback mechanism whereby higher temperatures and CO<sub>2</sub>-levels boost continental biomass production, leading to increased biogenic secondary organic aerosol (BSOA) and cloud condensation nuclei (CCN) concentrations, tending to cause cooling. The COBACC feedback can be considered as a broad framework which connects the human activities, the continental biosphere, and the changing climate conditions. The COBACC (COntinental Biosphere-Aerosol-Cloud-Climate) feedback is similar to the so-called CLAW-hypothesis by Charlson et al. (1987) which connects the ocean biochemistry and climate via a negative feedback loop involving CCN production due to sulfur emissions from plankton (e.g. Quinn & Bates, 2011). In general the future ATM-FCoE vision is based on a solution oriented approach, which will provide reliable prediction tools for the society to cope with environmental impacts of climate change. Refer to Fig.1 the understanding of the feedback and link of biogeochem cycles will be brought to the next level in the becoming FCoE. Study domain will be removed from boreal forest scale to global scale and via the “all scale approach” the new knowledge will be integrated into EMS.

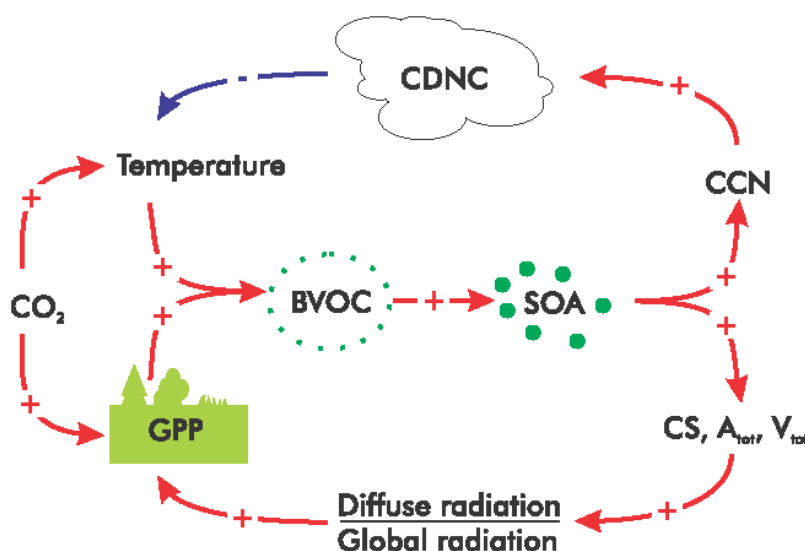


**Fig. 3.** The two feedback loops associated with the COBACC feedback. BVOC=biogenic volatile organic compounds, SOA=secondary organic aerosol, CS=the condensation sink,  $A_{tot}$ =total aerosol surface area,  $V_{tot}$ =total aerosol volume, CCN=cloud condensation nuclei, CDNC=cloud droplet number concentration, and GPP=Gross Primary Productivity, which is a measure of ecosystem-scale photosynthesis.

## ACKNOWLEDGEMENTS

The FCoE work is supported by the Academy of Finland Center of Excellence program (project number 1118615), ERC ATM-NUCLE (project number 227463), Nordic Centre of Excellence CRAICC and several EU-FP7 projects: ICOS, ACTRIS and PEGASOS.

## REFERENCES

- Boy et al. this issue: Activities in the atmosphere modelling group: 2011-2013
- Bäck et al. this issue: Ecosystem processes – overview of 2007-2013 activities.
- Charlson, R. J. et al. Nature 326, 655 1987.
- Hakola et al. this issue: In situ measurements of volatile organic compounds and inorganic gases and particles.
- Hämeri et al. this issue: An overview of university of Helsinki urban and indoor aerosols group activities in 2012-2013.
- Jokinen, T. et al. Atmos. Chem. Phys. 12, 4117-4125, 2012.
- Kaukolehto et al. this issue: ICOS RI, Towards a European research infrastructure.
- Kerminen et al. this issue: An overview of the activities by aerosol-cloud-climate interactions group of the University of Helsinki.
- Kulmala, M. et al. Atmos. Chem. Phys. 557, 2004.
- Kulmala, M. et al., Atmos. Chem. Phys., 11, 13061, 2011a.
- Kulmala, M et al. Report series in Aerosol Science N:o 134 (2012)
- Kulmala, M., et al. Nature Protocols 7, 1651-1667, doi:10.1038/nprot.2012.091
- Laaksonen et al. this issue: Overview of the studies conducted by the UEF Aerosol Physics Group
- Lappalainen et al. this issue: Pan-Eurasian Experiment (PEEX) initiative.
- Laurila et al. this issue: Activities on the greenhouse gases research.
- Lihavainen et al. this issue: Overview about activities in aerosols and climate group.
- Manninen et al. this issue: Recent advances in ion and aerosol measurements.
- Paasonen, P. et al. Nature Geosci., doi: 10.1038/NGEO1800
- Petäjä et al. this issue: ACTRIS RI – research infrastructure for aerosols, clouds and trace gases
- Pumpanen et al. this issue: Rhizosphere processes play an important role in soil organic matter decomposition and greenhouse gas fluxes in boreal landscape; summary of soil research carried out at fcoe during the second fcoe period (2009-2013).
- Riekkola et al. this issue: Atmospheric aerosols and gases: study of chemical composition and determination of physicochemical properties of individual compounds.
- Rinne et al. this issue: Biosphere-Atmosphere exchange and atmospheric concentrations of volatile organic compounds.
- Siitonen et al. this issue: AnaEE – A European infrastructure for ecosystem research.
- Sipilä et al., this issue: An overview of University of Helsinki Mass Spectrometry Group activities in 2012-2013.
- Sorvari et al. this issue: Restructuring the FCoE research infrastructures - integrated atmospheric and earth system science research infrastructure (INAR RI)
- Vehkamäki et al. this issue: An overview of university of helsinki computational aerosol physics group activities in 2011-2013.
- Vesala et al. this issue: Biosphere-atmosphere interactions.
- Quinn, P. K. & Bates, T. S., Nature, 480, 51–56, 2011.

## ACTIVITIES IN THE ATMOSPHERE MODELLING GROUP: 2011-2013

M. BOY, N. BABKOVSKAIA, R. GIERENS, K.V. GOPALKRISHNAN, L. LIAO, D. MOGENSEN, A. RUSANEN, S. SMOLANDER, L. ZHOU, P. ZHOU

Department of Physics, University of Helsinki, P.O. Box 64, FI-00014 University of Helsinki, Finland

Keywords: ATMOSPHERE MODELLING, VOC'S, AEROSOLS, TURBULENCE, CLOUDS

### INTRODUCTION

Climate change is currently one of the central scientific issues in the world and affects the life of billions of people in many ways. For making political decisions, it is crucial to achieve a reliable understanding of the climate system. The effects of long-lived greenhouse gases like carbon dioxide or methane are fairly well known, whereas the impacts of radiative forcing through aerosols are still very uncertain. Aerosols may also have adverse effects on human health and visibility.

### OBJECTIVES

The Atmosphere Modelling Group in the Division of Atmospheric Sciences at the University of Helsinki was established in the beginning of 2009. In average 6 to 8 under- and graduated students and two post-docs have worked in the group during the last three years. The main scientific focuses are to quantify seasonal and vertical distributions of organic compounds, and their reaction products, including organic nitrates from the forest canopy and the soil. To pinpoint where the formation and growth of particles happen inside the PBL including the effect of turbulent flow, and to predict the below- and in-cloud activation of CCNs. Further the group investigates how the new developed mechanisms will affect the ecosystem-atmosphere interactions under future climate conditions. In this way the group is bridging the gap between the most novel instrumentations operated at our SMEAR stations and the global modelling community by detailed process-oriented studies in the lower part of the troposphere.

### METHODS

Our scientific activities combine detailed chemistry, aerosol and cloud microphysics from zero-dimensional modelling up to high-resolution 3-dimensional chemistry-transport models. These outstanding computational experiments are not concentrate on single mechanisms but aim for comprehensive understanding of the forest-atmosphere interrelations by including turbulence explicitly. In total five different models (explained in more detail below and in Figure 1), which were fully or partly developed by the group are used to contribute to the main scientific aims of our Finnish Centre of Excellence.

MALTE-BOX is a zero-dimensional model and includes modules for the simulation of both chemical and aerosol dynamical processes. SOSAA is a one-dimensional chemistry-transport model and includes the same modules for gas-phase chemistry and aerosol dynamics as MALTE-BOX. It is a parallelized model operating on a high-performance super cluster to investigate different atmospheric processes for longer periods with high vertical resolution. ASAM is a Large-Eddy-Simulation model and implements the moist compressible Euler equation set in its dynamic core. A canopy module and the emission module MEGAN were implemented in order to parameterize and simulate the turbulent flow of organic compounds above and within the canopy. PENCIL-CLOUD model is a high order finite difference code for compressible hydrodynamic flows. A detailed chemistry module, including an accurate description of all necessary quantities, and an aerosol module have been implemented. FLAMO is a regional model using offline

meteorological input from the Weather Research and Forecasting Model (WRF). The emission module MEGAN has been implemented and next step is the implementation of a chemistry module. A more detailed description with references from all models used inside the group is available at the group website: [http://www.physics.helsinki.fi/tutkimus/atm/english/research/atmosphere\\_modelling.html](http://www.physics.helsinki.fi/tutkimus/atm/english/research/atmosphere_modelling.html).

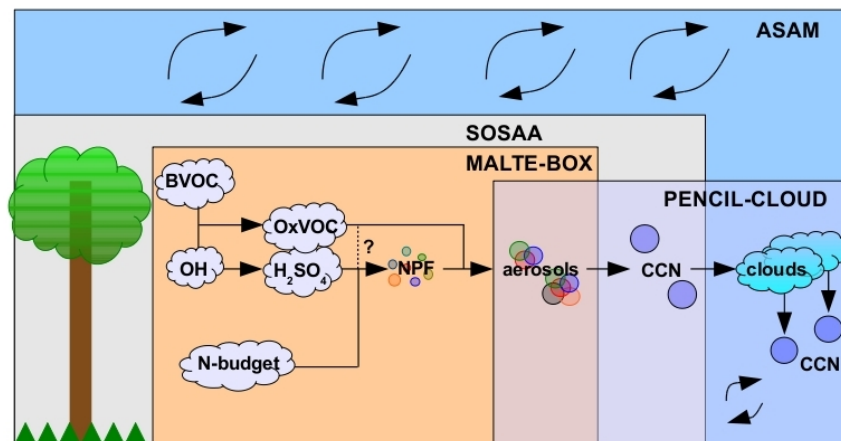


Figure 1: The scientific concept of our computational tools without the regional model FLAMO

## RESULTS

All students and post-docs from the group will submit their own abstract about their newest findings. On the following I, as a group leader will present certain selected results which demonstrate the wide-spread activities of the Atmosphere Modelling Group on different topics crucial for increasing our understanding on the forest-atmosphere system.

### Emissions of VOC's

In a recently submitted publication by Smolander and co-workers (2013) we describe three monoterpene emission models (G97 – original version of MEGAN, MEGAN-new, SIM-BIM) and used these, together with the chemistry-transport model SOSA (Boy et al., 2011, Mogensen et al., 2011), to model monoterpene concentrations in the air at different heights in the canopy, and compared the simulations to the measured concentrations over the year in and above the boreal pine forest stand at the SMEAR II station in Hyytiälä. All three models agreed fairly well with the measurements upon the seasonal emission patterns (especially in the midsummer period), although the theoretical bases of the models were quite different.

The new MEGAN brought the estimates closer to SIM-BIM approach with the introduction of the preceding temperature and a leaf age factor. Monoterpenes emitted from conifers were identified as specific storage in resin canals, or resin ducts, and the emissions did continue during the night. Available forest floor emission data were included in the model for several months as well, and we found that the high forest floor emission seasons were spring and autumn with active microbes and increased litterfall. The modelled dominant compounds of monoterpene composition were  $\alpha$ -pinene, followed by  $\Delta^3$ -carene and  $\beta$ -pinene, which is compatible with the measurements. The model as well as the observations reported prominent seasonal variations with the highest concentrations in summer and small cycles throughout the year. The diurnal maximum monoterpene emissions appeared during the afternoon hours, whereas the monoterpene concentrations in ambient air were small at daytime. The vertical concentrations were found at very low values near ground but to reach their maximum in canopy region and then to decrease with height.

To investigate the impact of chemodiversity pattern inside the pine forest stand at the SMEAR II station in Hyytiälä on the atmospheric chemistry we performed simulations with the model SOSA. The results showed that the modelled monoterpene concentrations and distribution at the site were significantly influenced and hence the chemical reactions in the atmosphere (Bäck et al., 2012).

### Atmospheric chemistry

According to several studies (e.g. Sipilä et al., 2010; Lauros et al., 2011) sulphuric acid is one of the initial or required molecules in the atmospheric nucleation mechanism(s). In order to quantify future atmospheric sulphuric acid concentrations a complete understanding of the sink and source terms is crucial. Although the precursors for sulphuric acid (at least some of them), as well as the main sink term (condensation on atmospheric aerosols) have been measured in several places, the closure between measured and calculated sulphuric acid concentrations has rarely been investigated (e.g. Boy et al., 2005).

The effect of increased reaction rates of stabilized Criegee intermediates (sCIs) with SO<sub>2</sub> to produce sulphuric acid was investigated using data from two different locations, SMEAR II, Hyytiälä, Finland, and Hohenpeissenberg, Germany. Results from MALTE, a zero-dimensional model, showed that using previous values for the rate coefficients of sCI + SO<sub>2</sub>, the model underestimates gas phase H<sub>2</sub>SO<sub>4</sub> by up to a factor of two when compared to measurements. Using the rate coefficients published by Mauldin et al. (2012) increases sulphuric acid by 30–40 %. Increasing the rate coefficient for formaldehyde oxide (CH<sub>2</sub>OO) with SO<sub>2</sub> according to the values recommended by Welz et al. (2012) increases the H<sub>2</sub>SO<sub>4</sub> yield by 3–6 %. Taken together, these increases lead to the conclusion that, depending on their concentrations, the reaction of stabilized Criegee intermediates with SO<sub>2</sub> could contribute as much as 33–46 % to atmospheric sulphuric acid gas phase concentrations at ground level. Using the SMEAR II data, results from SOSA, a one-dimensional model, show that the contribution from sCI reactions to sulphuric acid production is most important in the canopy, where the concentrations of organic compounds are the highest, but can have significant effects on sulphuric acid concentrations up to 100 m. The recent findings that the reaction of sCI + SO<sub>2</sub> is much faster than previously thought together with these results show that the inclusion of this new oxidation mechanism could be crucial in regional as well as global models, especially when comparing modelled and measured sulphuric acid values at ground level.

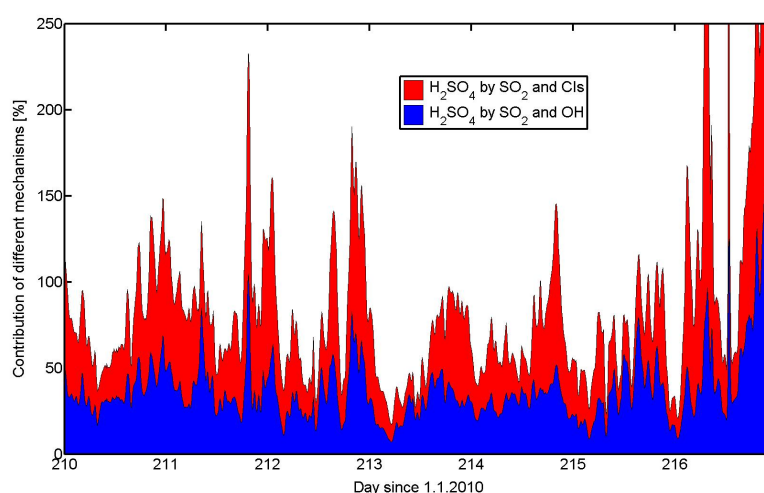


Figure 2: Cumulative percentage contribution of the different SO<sub>2</sub> oxidation mechanisms for Hyytiälä

### Atmospheric aerosols – formation and growth

Biogenic volatile organic carbon (BVOC) compounds, such as  $\alpha$ -pinene, are emitted by the vegetation and oxidized in the atmosphere to form less volatile compounds. These compounds can take part in the

formation and growth of secondary organic aerosols (SOA). We have modelled the formation and growth of secondary particles along an air mass trajectory over the northern European boreal forest and compared the results with size distribution measurements from three stations the air mass passes close to (Abisko, Pallas and Värriö). The models used is an updated version of the aerosol dynamic and particle phase chemistry module ADCHEM model (Roldin et al 2011) and MALTE-BOX (Boy et al., 2013), both coupled with the Master Chemical Mechanism version 3.2. The emission of BVOC (represented by  $\alpha$ -pinene in our model) is estimated using a method described in Tunved et al (2006). The model then considers the gas-to-particle partitioning of all oxidation products. Liquid saturation vapour pressures of each oxidation product are decided by using the method proposed by Nannoolal et al (2008).

During the first 54 hours of the trajectory, the air mass is over the Atlantic Ocean, while it spends the remaining hours over land where the particle mass starts increasing. The modelled growth is mainly caused by organic gas-to-particle conversion and seems to be a bit slower than the measured growth. Despite this, the model seems to be able to handle SOA formation relatively well at realistic BVOC-emissions and low primary particle concentration (Figure 3).

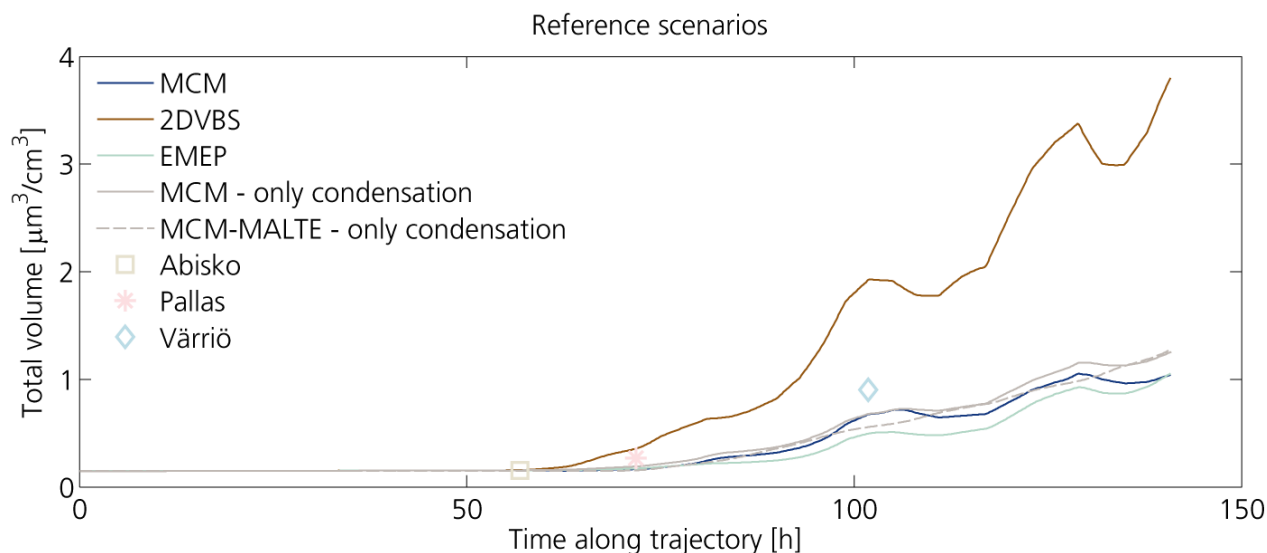


Figure 3: Three “reference” gas-phase scenarios coupled to ADCHEM are shown (2DVBS refers to Jimenez et al., 2009 and EMEP refers to Simpson et al., 2012). Also two runs with only condensation: MCM – only condensation (coupled to ADCHEM) and MCM-MALTE – only condensation (coupled to MALTE-BOX).

### Activation of CCN

Direct numerical simulations (DNS) were used to study the structure of the cloud edge area. In this study we used the direct numerical simulation high-order public domain finite-difference PENCIL Code for compressible hydrodynamic flows. This code is widely documented in the literature and used for many different applications (e.g. W. Dobler et al., 2006). A detailed chemistry module has been implemented, including an accurate description of all necessary quantities, such as diffusion coefficients, thermal conductivity, reaction rates etc. (Babkovskaia et al., 2011). The new developed aerosol-module coupled to the PENCIL Code was used to calculate evaporation and condensation processes of aerosol particles, which consists of a solid core covered by liquid water.

In the first study (Babkovskaia et al., 2013) we checked how crucial is the Smagorinski approximation for calculation of activation and evaporation of aerosol particles. We compare the results of 2D and 3D simulations for 4, 2, 1 and 0.5 cm cell size (Fig 4). We conclude that the results of 2D and 3D simulations

differ much smaller than the results of 2D simulations with different cell sizes. We suppose that for studying of particle activation 2D model is appropriate, and therefore, 2D simulations with high resolution give more realistic results than low resolved 3D simulations. Next we studied the effect of aerosol dynamics on the temperature of air. We conclude that activation of particles decreases the air temperature by about 0.03 K, and evaporation of particles increases the temperature by about 0.26 K. Further we investigated the effect of initially generated turbulence on the air temperature (with included aerosol dynamics). We see that the turbulent friction increases/decreases the air temperature by about 2.5K. This is much larger than the effect of aerosol dynamics on the air temperature, and therefore, air dynamics. We inspected the influence of turbulent motion on aerosol dynamics and vice versa. We find that aerosol dynamics increases the supersaturation in the most part of the domain on 16 %, and in some places up to 46 %.

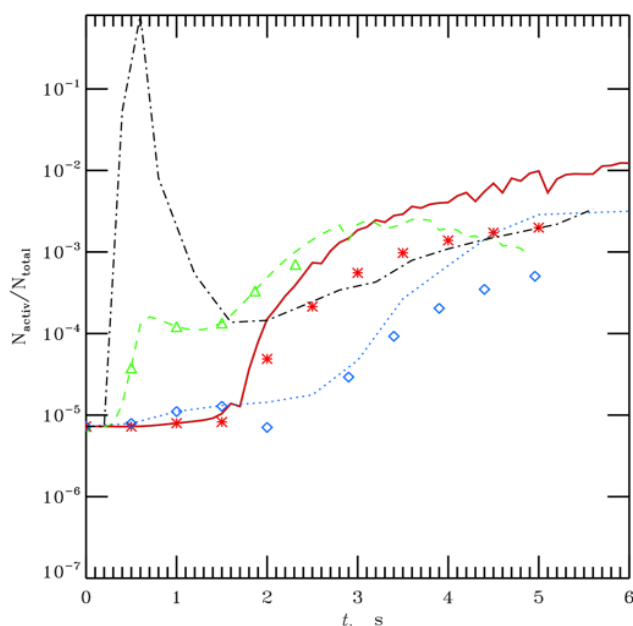


Figure 4: A ratio of a number of activated particles to the total number as a function of time for 2D model runs with grid cell of 4 cm (red solid curve), 2 cm (blue dotted curve), 1 cm (green dashed curve) and 0.5 cm (black dotted-dashed curve); and for 3D model runs with grid cell of 4 cm (red asterisks), 2 cm (blue diamonds) and 1 cm (green triangles)

## SUMMARY AND OUTLOOK

During the last three years about half of the time inside the group was used for new and further model development. As a model is ‘never’ in his final state we will continue to improve our tools and update them with the newest findings in the different scientific areas. One important target for next year is to implement in our aerosol dynamic module the particle phase chemistry module (which considers acid catalyzed oligomerization, heterogeneous oxidation reactions in the particle phase and non-ideal interactions between organic compounds, water and inorganic ions) and a kinetic multilayer module for diffusion limited transport of compounds between the gas phase, particle surface and particle bulk phase. These modules were developed by Dr Pondus Roldin at Lund University who will join the group for two years post-doc in the beginning of 2014.

## ACKNOWLEDGEMENTS

This work was supported by the Helsinki University Centre for Environment (HENVI). The financial support by the Academy of Finland Centre of Excellence program (project no 1118615) is gratefully

acknowledged. This work was also supported by the Nordic Centre of Excellence CRAICC and the Maj ja Tor Nessling foundation.

## REFERENCES

- Babkovskaia, N., Haugen, N., Brandenburg, A.: A high-order public domain code for direct numerical simulations of turbulent combustion, *J. of Computational Physics*, 230, 1, 2011.
- Babkovskaia, N., Boy, M., Smolander, S., Romakkaniemi, S. and Kulmala, M.: A study of aerosol production at the cloud edge with direct numerical simulations, *Atmospheric Research*, submitted 09/2013.
- Boy, M., Kulmala, M., Ruuskanen, T. M., Pihlatie, M., Reissell, A., Aalto, P. P., Keronen, P., Dal Maso, M., Hellen, H., Hakola, H., Jansson, R., Hanke, M. and Arnold, F.: Sulphuric acid closure and contribution to nucleation mode particle Growth, *Atmos. Chem. Phys.*, 5, 863–878, 2005.
- Boy, M., Sogachev, A., Lauros, J., Zhou, L., Guenther, A. and Smolander, S.: SOSA - a new model to simulate the concentrations of organic vapours and sulphuric acid inside the ABL - Part I: Model description and initial evaluation, *Atmos. Chem. Phys.* 11, 43-51, 2011.
- Boy, M., Mogensen, D., Smolander, S., Zhou, L., Nieminen, T., Paasonen, P., Plass-Dülmer, C., Sipilä, M., Petäjä, T., Mauldin, L., Berresheim, H. and Kulmala, M.: Oxidation of SO<sub>2</sub> by stabilized Criegee intermediate (sCI) radicals as a crucial source for atmospheric sulfuric acid concentrations, *Atmos. Chem. Phys.*, 13, 3865-3879, 2013.
- Bäck, J., Aalto, J., Henriksson, M., Hakola, H., He, Q. and Boy, M.: Chemodiversity in terpene emissions at a boreal Scots pine stand, *Biogeosciences*, 9, 689-702, 2012.
- Dobler W., Stix M., Brandenburg, A.: Magnetic field generation in fully convective rotating spheres *Astrophys. J.*, 638, 336, 2006.
- Lauros, J., Sogachev, A., Smolander, S., Vuollekoski, H., Sihto, S.-L., Laakso, L., Mammarella, I., Rannik, U. and Boy, M.: Particle concentration and flux dynamics in the atmospheric boundary layer as the indicator of formation mechanism, *Atmos. Chem. Phys.* 11, 5591-5601, 2011.
- Mauldin III, R.L., Berndt, T., Sipilä, M., Paasonen, P., Petäjä, T., Kim, S., Kurtén, T., Stratmann, F., Kerminen, V.-M. and Kulmala, M.: A new atmospherically relevant oxidant, *Nature*, 488, 193, 2012.
- Mogensen, D., Smolander, S., Sogachev, A., Zhou, L., Sinha, V., Guenther, A., Williams, J., Nieminen, T., Kajos, M., Rinne, J., Kulmala, M. and Boy, M.: Modelling atmospheric OH-reactivity in a boreal forest ecosystem, *Atmos. Chem. Phys.*, 11, 9709-9719, 2011.
- Nannoolal, Y., Rarey, J. and Ramjugermath, D.: *Fluid Phase Equilibria* 269, 117-133, 2008.
- Roldin, P., Swietlicki, E., Schurgers, G., Arneth, A., Lehtinen, K. E. J., Boy, M. and Kulmala, M.: Development and evaluation of the aerosol dynamics and gas phase chemistry model ADCHEM, *Atmos. Chem. Phys.*, 11, 5867-5896, 2011.
- Sipilä, M., Berndt, T., Petäjä, T., Brus, D., Vanhanen, J., Stratmann, F., Patokoski, J., Mauldin III, R. L., Hyvärinen, H., Lihavainen, H., and Kulmala, M.: The Role of Sulphuric Acid in Atmospheric Nucleation, *Science*, 327, 1243–1246, 2010.
- Smolander, S., He, Q., Mogensen, D., Zhou, L., Bäck, J., Ruuskanen, A., Noe, S., Guenther, A., Kulmala, M. and Boy, M.: Modelling monoterpene emissions from boreal pine forest in Southern Finland, *Biogeosciences*, submitted 9/2013.
- Tunved, P., Hansson, H.C., Kerminen, V.M., Ström, J., Dal Maso, M., Lihavainen, H., Viisanen, Y., Aalto, P.P., Komppula, M. and Kulmala, M.: *Science* 312, 261-263, 2006.
- Welz, O., Savee, J.D., Osborn, D.L., Vasu, S.S., Percival, C. J., Shallcross, D. E. and Taatjes, C. A.: Direct kinetic measurements of Criegee Intermediate (CH<sub>2</sub>OO) formed by reaction of CH<sub>2</sub>I with O<sub>2</sub>, *Science*, 335, 204-207, 2012.

## ECOSYSTEM PROCESSES – OVERVIEW OF 2007-2013 ACTIVITIES

J. BÄCK<sup>1,2</sup>, E. NIKINMAA<sup>1</sup>, F. BERNINGER<sup>1</sup>, P. HARI<sup>1</sup>, T. HÖLTTÄ<sup>1</sup>, E. JUUROLA<sup>1,2</sup>, P. KOLARI<sup>1,2</sup>,  
A. MÄKELÄ<sup>1</sup>, A. PORCAR-CASTELL<sup>1</sup> et al.

<sup>1</sup>Dept. of Forest Sciences, P. O. Box 27, 00014 University of Helsinki, Finland

<sup>2</sup>Dept. of Physics, P.O. Box 64, FI-00014 University of Helsinki, Finland.

### INTRODUCTION

The Ecosystem processes –team in the Center of Excellence has concentrated on analyzing the structure and functioning of boreal forest ecosystems in changing climate. Our main aim has been to develop a comprehensive understanding of the feedbacks and linkages between different compartments in the ecosystem and the environment. We have approached this from several viewpoints, on the one hand from the properties and functions of ecosystem itself, and on the other hand from the environmental drivers that are reflected in the functions or influenced by them. Simultaneous and continuous high quality and high time resolution measurements of the various complex processes in a forest ecosystem and plant individuals are crucial for achieving this aim.

Our main activities have concentrated on a) the exchange of CO<sub>2</sub> and water vapor between soil, vegetation and atmosphere, and on how this depends on driving variables (irradiation, temperature and humidity); b) how the physiological state of the vegetation explains variation in the exchange responses to the driving atmospheric variables; c) how the physiological and environmental variation is reflected to plant level volatile organic compound (VOC) synthesis and emissions; d) how forest composition and management activities influence these interactions.

A significant achievement of our team - jointly with the whole FCoE - during the 2008-2013 funding period was the publication of two Springer volumes: ‘Boreal Forest and Climate Change’ (ed. by P. Hari & L. Kulmala, 2008) and ‘Physical and Physiological Plant Ecology’ (ed. by P. Hari, K. Heliövaara and L. Kulmala, 2013). These books outline our research philosophy, utilizing the intensive, systematic, long-term measurements in boreal environments, and present the applications in a global climate change context. The books provide detailed, schematically illustrated insights into both conceptual and mechanistic process models describing associated processes, their interactions, and scale dependencies.

Below we summarize some highlights during the second FCoE funding period, 2008-2013.

#### 1)- HOW DOES VEGETATION CONTROL ECOSYSTEM BIOGEOCHEMICAL CYCLES BY ALTERING MATERIAL AND ENERGY FLOWS?

At SMEAR stations one of our main goals is to understand how vegetation controls the carbon and water fluxes. We quantified the forest stand carbon balance with different methods (Ilvesniemi et al. 2009, Kolari et al. 2009). The interannual variability of EC-based and modelled stand GPP was in the order of 10% of the annual GPP (Ilvesniemi et al. 2009, Kolari et al. 2009). The annual NEE varied relatively more, approximately  $\pm 25\%$ . The interannual variability of NEE can be largely explained by tree growth (Ilvesniemi et al. 2009) which matched flux-based productivity estimates well. Annual net uptake of carbon was highest the earlier was the onset of the growing season (Kolari et al. 2009) while warm autumns resulted in increased respiration (Vesala et al. 2010).

Quantification of respiration components has long been a major deficiency in ecosystem carbon exchange models. We analyzed this using detailed gas exchange measurements from major contributing sources over several years. The contribution of stem respiration to the ecosystem respiration was about 10% (Kolari et al. 2009). The variability was connected to temperature in a delayed fashion which can be explained by slowness in diffusion of CO<sub>2</sub> out of the stem. The temporal dynamics and vertical variability were also strongly modified by diffusion of CO<sub>2</sub> transported by sapflow upstream of the sites of CO<sub>2</sub> production. We constructed a novel dynamic model of stem CO<sub>2</sub> efflux that incorporates the vertical transport of CO<sub>2</sub> in sapflow (Hölttä and Kolari 2009). The model can explain well the spatial and temporal variability in stem CO<sub>2</sub> effluxes. We have also developed method to use simultaneous observations of xylem and bark diameters to predict the sugar transport in phloem (Mencuccini et al. 2013). This ability will further allow us to better estimate above and below carbon allocation and the role of different processes in ecosystem respiration.

The annual cycles of photosynthesis and respiratory fluxes were similar. Respiration in standard temperature showed higher values during spring recovery and onset of growth than in autumn. Respiration also responded in a similar way to drought as photosynthesis which manifests the close linkage of respiration to photosynthetic productivity (Kolari et al. 2009). Our stand modelling framework SPP developed during the long-term ecophysiological research in our group (Mäkelä et al. 2006, Duursma et al. 2008, Kolari et al. 2009) proved successful in predicting the seasonality and the drought response of photosynthetic production (Kolari et al. 2009). Also the interannual variability could be predicted relatively well. Further analysis of the roles of different environmental factors in the seasonality of photosynthesis and transpiration revealed also a strong effect of low soil temperature on spring recovery (Wu et al. 2012).

In a closed-canopy pine stand, trees contribute to almost 90% of ecosystem GPP (Ilvesniemi et al. 2009). The role of ground vegetation in the photosynthetic productivity at different-aged stands was further assessed in a modelling study by Kulmala et al. (2011). GPP peaked couple of years after clear felling at approximately one third of total GPP of a closed canopy forest stand. The age-related dynamics of GPP in the ground vegetation was consistent with the development of ground vegetation biomass and species composition from grasses and forbs towards less productive dwarf shrubs and mosses and the increasing shading by tree canopy.

We analysed the annual cycle of gas exchange with a network of 12 eddy covariance stations from the evergreen coniferous forest. To each site we fit a simple phenomenological model of gas exchange based on Mäkelä et al. (2004). The inclusion of an annual cycle model of gas exchange, assuming that photosynthetic capacity reacts to the running mean average temperature, improved the fit for all sites, except the warmest and very maritime Douglas-fir sites. There was a certain dependence of the summer time maximum photosynthetic capacity on the NDVI. The phenology, i.e. the transition of photosynthesis from the winter state to the summer state does not seem to differ between species, but sites in cold climates did change more slowly from winter to summer states (Gea et al. 2010).

We also analysed the evapotranspiration of different boreal ecosystems using a network of 65 eddy covariance towers in the boreal and arctic domain. Parameters of the physically based Penman-Monteith equation were estimated for all sites assuming a stomatal conductance model and assuming that there are temperature dependent differences in winter and summer transpiration. Wintertime stomatal resistances were smaller in all vegetation types but coastal Douglas fir. A temperature driven transition from winter to summer state improved usually the fit of the models. Evapotranspiration was usually higher for forests, due to a quite high canopy conductance and high aerodynamic conductances.

In a satellite based study we used land cover maps and the satellite derived MODIS albedo product to evaluate the effects of land use on albedo. We developed a linear unmixing method to attribute albedo values

to land cover types (Kuusinen et al. 2012a). The results can be used to estimate unbiased albedo estimates for large landscapes. We analysed also the annual variation of canopy albedo at the SMEAR 2 station in Hyytiälä. We found that the summer albedo was rather constant, but that the variation of the winter albedo could be attributed to snow or frost cover of the forest canopy (Kuusinen et al. 2012b). This snow cover was important during the early winter (when radiative fluxes were low) but decreased during late winter (late February, March, April) when radiative fluxes were higher. The reason seems that the global radiation warms the canopy and drops the snow from the trees. The research shows that care has to be used for the use of albedo models in the boreal region.

We checked experimentally the effect of changes in snow cover on the leaf development and gas exchange of black spruce and trembling aspen in Canada. Snow was either removed prematurely or we tried to prolonged soil frost and snow cover by removing snow during the mid-winter and returning more snow in early spring to ensure a deeper soil penetration of frost. Other treatments were removal of mosses and adding Sphagnum to the plants. We followed the yield of photosynthesis of aspen and black spruce. Contrary to our expectations the negative effects of snow and moss removal dominated, while negative effects of snow addition were not detectable. We believe that the protective role of snow and moss, which insulate the soil from late frosts might be more important than previously thought (Frechette et al. 2011).

We tested to what extend trees at the treeline were sink limited using a series of manipulation experiments. Removal of sinks (buds) resulted into a larger growth of the remaining buds while there were no indications of a downregulation of sapflow. We think, therefore, that sink limitation are not dominant at the treeline of Scots pine in Värriö (Susiluoto et al. 2010)

## 2)- HOW DOES VEGETATION AFFECT THE EXCHANGE OF GREENHOUSE GASES AND BVOCS?

Field measurements on BVOC exchange between ecosystems and atmosphere have been conducted for over 10 years at the SMEAR II forest, and they have provided us novel understanding on which processes are playing key roles, on what are the critical periods for this exchange, and on how the boundary layer atmospheric chemistry is influenced by vegetation.

The atmospherically most significant group of biogenic VOCs in boreal coniferous forests is terpenoids, most importantly mono- and sesquiterpenes. Based on enclosure measurements, the two most abundant compounds in pine emissions at SMEAR II are  $\alpha$ -pinene and  $\Delta^3$  carene, followed by  $\beta$ -pinene, myrcene and camphene, and several minor compounds (Tarvainen et al 2005, Hakola et al 2006). However, unlike previously thought, there is huge variation in the VOC blend that is emitted by trees of the same species in a seemingly homogeneous stand (Bäck et al., 2012, Yassaa et al., 2012). This has important implications for emission models, which are normally parameterized using information from one tree individual only (Bäck et al 2012, Smolander et al., ms submitted to BGD). The most abundant sesquiterpenes in pine emissions are  $\beta$ -caryophyllene and  $\alpha$ -farnesene (Hakola et al., 2006, Yassaa et al., 2012). In recent years, with the novel online measurement technique PTR-MS (proton-transfer reaction mass spectrometer), also significant fluxes of other volatile compounds have been measured from boreal forests (Lappalainen et al., 2009, 2012, Aaltonen et al 2011). These include short-chained alcohols, aldehydes and ketones such as methanol, ethanol, acetaldehyde and acetone. Also one larger alcohol, methyl butenol (MBO) was detected in Scots pine emissions (Tarvainen et al 2005, Hakola et al 2006).

Estimates of the above-canopy fluxes of VOCs are needed for quantitative Earth system studies and assessments of past, present and future air quality and climate. The main short-term drivers for emissions are temperature and irradiation, which control the volatilization and synthesis of compounds, respectively. Emission estimates are traditionally obtained for mature leaves under standard (constant) conditions to yield

standard emission potential values ('Guenther approach'), which then are used as model parameters (e.g. Guenther et al 2006). However, seasonality (aside from the direct temperature effect) has been recognized to strongly influence isoprene and monoterpene emission rates as well as the emission capacity (e.g. Tarvainen et al 2005, Hakola et al 2006). A particular feature in boreal regions is that evergreen vegetation is dormant in winter, but recovers from dormancy when temperatures rise in spring. Surprisingly, the maximum emission rates for monoterpenes are observed before growth even starts. Our measurements showed that the new biomass growth processes induce high emissions of VOCs from buds and shoots (Aalto et al 2013 ms submitted). New shoots make up a small biomass in the beginning, but their absolute contribution to the emissions from foliage is 50-75% for monoterpenes, 25-50% for methanol, 25% for acetone and 25-50% for MBO.

The dynamic enclosure system (Kolari et al., 2012) in SMEAR II enables detailed measurements of environmental and physiological factors driving the trace gas exchange under field conditions, and permits the analysis of simultaneous contributing processes. The setup is used for measurements of VOC emission rates with good accuracy, while at the same time minimizing the disturbance caused by the enclosure to the object being measured. The system slightly underestimates the isoprene, monoterpene and oxygenated VOC fluxes (5-30%), mainly due to the enclosure itself, whereas the measurement design with >60 m Teflon tubing seems to contribute only little to the actual measured flux. The systematic error is higher at high relative humidity than in drier conditions, which suggests that the thickness of the water film adsorbed on the chamber inner surfaces (and thus transpiration) contributes to the VOC loss rate in the chamber.

In addition to emissions from green tissues, VOCs are also originating from other sources in boreal ecosystems. The below-canopy compartments, both the ground vegetation, decaying litter, and soil processes, are important sources for VOCs in particular during spring and fall, when fresh litter is dropping down to the ground and decomposing (Aaltonen et al., 2011, 2012b). The forest floor plays a substantial role (from a few per cents to several tens of per cents, depending on the season) in the total VOC emissions of the boreal forest ecosystem. Somewhat surprisingly, the wintertime fluxes within the snowpack can be equal to those from the soil during warmer periods, especially after strong winter storms when large amounts of litter and other residues are accumulating in the snow (Aaltonen et al., 2012a). The common species of soil fungi are also potent contributors for the soil VOC fluxes, especially emitting the oxygenated compounds (methanol and acetone) (Bäck et al., 2010).

Although significant advancements have been made in quantifying the role of forest vegetation to atmospheric reactivity in recent years, we still need to improve our understanding on the processes contributing to emissions from the whole ecosystem and the driving factors over short and long time scales. The next steps are to analyze the role and regulation of non-foliage sources in canopy scale flux and their links to main physiological processes (e.g. water and sugar transport, growth and resource allocation). Although Scots pine is covering 50% of coniferous forests in Finland, we still are lacking emission measurements from other important boreal tree species. We have initiated measurements of pine stem resin flow and VOC emissions (Vanhatalo et al and Rissanen et al, this issue). We are also measuring VOC exchange between the lake and atmosphere (Ojala et al this issue) and the effect of tree roots and forest floor vegetation on soil VOC exchange (Heinonsalo et al this issue).

### 3)- WHAT MECHANISMS ARE INVOLVED IN THE CONTROL, AND HOW?

With our continuous and comprehensive measurement strategy, we can analyze the processes and linkages between processes over time and in different structural elements. The overall conclusion is that in order to understand the ecosystem scale phenomena, very often a more detailed understanding of the smaller scale processes are needed. Best example of such linking is provided by our long term analysis of factors

influencing tree gas exchange. We have shown that by using evolutionary optimization principle in leaf stomatal control, it is possible to predict very accurately the tree gas exchange (e.g. Hari et al. 2009). This approach requires determination of marginal cost of water in terms of carbon. This variable can be determined from quite limited number of field observations and subsequently used to predict the gas exchange (Hari et al. 2009). Recently we showed that stomata regulate leaf gas exchange in a manner that maximizes assimilate transport from leaves to carbohydrate sinks, such as growing tissue (Nikinmaa et al. 2013). This approach yields identical behavior to the previously described optimality approach, but as it is based on the mechanistic description of water and sugar transport and the sugar source and sink processes in trees, it opens a new avenue to derive, how the stomatal behavior could depend on tree structure, growth activity or soil conditions.

The above approach forms a framework to connect various localized metabolic processes to whole tree level response to environment. Structural development is the major sink of carbon in trees and has feedback to carbon fluxes. One of the key issues is the contradictory demands that high water conductivity and safety against spreading of air-bubbles, i.e. cavitation, is achieved in tree stems. Larger water conduits are more efficient at conducting water, but also more susceptible to cavitation Lintunen et al. (2013). Lintunen et al. (2013) found that large water conduits also more susceptible to freezing nucleation, i.e. they freeze at temperatures closer to zero. Spreading of air bubbles has a dual role since if it only takes place in a moderate degree, it can help the tree to use water stored in stem to overcome transitory lack of water and allow leaves to continue photosynthesizing, but in ample scale will cause a collapse of the whole transport system (Hölttä et al. 2009). We showed that an optimal solution for structural properties at cellular, tissue and the whole tree level can be found (Hölttä et al. 2011). Regularities stem in structures can be expected as the water transport and associated water tension gradient set strong boundary conditions for the growth of new xylem cells (Hölttä et al. 2010). This approach automatically emphasizes the role of tree size for stem growth and the resulting fine structure of wood but the position of growing shoots also influences their growth dynamics (Schiestl-Aalto et al. 2013). Environmental factors that influence photosynthesis influence growth also because of the linking with sugar concentration and water potential that directly influence growth (Hölttä et al. 2010). In addition both current temperature and the previous year's temperature particularly during the formation of new buds influence the growth (Schiestl-Aalto 2013)

In addition to the short term immediate drivers such as temperature and irradiation, BVOC emissions are responsive to medium-term changes in growth conditions, which may affect the emission capacity, the shape of the light response as well as the temperature optimum of emission (Arneth et al., 2007, Lappalainen et al., 2012). Branch scale BVOC emissions follow closely plant biological activity most of the time in summer, but in stressful periods (e.g. drought), the emissions are decoupled from physiological parameters (Porcar-Castell et al 2009, Yassaa et al 2012). During the most active growth period, the emissions from growing shoots originate mainly from growth processes (Aalto et al ms submitted to BGD).

Photosynthetic activity can be estimated using optical data. Chlorophyll fluorescence (ChlF) and spectral reflectance have been widely used to infer the dynamics of photosynthesis at the diurnal scale (seconds-day), but the processes that control the signals still remain unclear at the seasonal scale. Understanding the link between optical data and photosynthesis at the seasonal-scale is a pre-requisite to implement remote sensing to the study of photosynthesis. There is probably linkage between the activity of light reactions and above described source – sink relations as excess photosynthetic activity relative to sugar transport and utilization leads to photosynthetic down regulation (Nikinmaa et al. 2013). During the last three years we have substantially advanced in this field by developing theoretical and methodological tools to study the seasonal dynamics of photosynthesis using spectral reflectance and ChlF:

We presented the first annual time series of leaf-level ChlF, and a theoretical framework to interpret the data (Porcar-Castell 2011). This study opened a number of research questions that will be especially relevant for the remote sensing of ChlF and its use in interpreting regional gross primary production (GPP). The new challenges are the subject of a review currently under preparation (Porcar-Castell et al. In prep). Diurnal variation in the photochemical reflectance index (PRI) is known to be controlled by the operation of the xanthophyll-cycle, but the seasonal controls remained untested. Further, we presented the first annual-level analysis of the physiological controls behind leaf level PRI and validated the hypothesis that PRI is controlled by the slow acclimation of carotenoid and chlorophyll contents at the seasonal scale in addition to other conformational arrangements of the thylakoid membrane (Porcar-Castell et al. 2012). We have also identified and characterized a new dynamic process that interacts with the seasonal variation in leaf level light absorption, i.e. the dynamics in reflectance properties of epicuticular waxes (Olascoaga et al. submitted manuscript). Leaf-level measurements of ChlF are conducted with active methods that involve the supply of a pulse of saturating light. The saturating pulse induces a transient peak in the fluorescence emission and the information is used to derive the light use efficiency of photochemistry. However, the approach cannot be exported to the remote sensing of ChlF, and modeling tools are still needed to bypass this limitation. We have been evaluating two potential model alternatives:

The potential of the PRI as a seasonal proxy of variations in thermal energy dissipation (NPQ) in the photosystems has been assessed. We found that although PRI and NPQ are strongly correlated in needles of Scots pine during the year the signals decouple during early spring due to differences in controlling factors (Porcar-castell et al. 2012). These differences challenge the use of the PRI as a proxy of NPQ as well as the integration of PRI and ChlF data.

We have also characterized the seasonal relationship between leaf-level fluorescence yield and photochemical yield both in the field and in the lab with controlled experiments (Olascoaga & Porcar-Castell, in prep). We recognized three different phases linking ChlF yield and photochemical yield: photochemical phase (PQ) under low light, non-photochemical phase (NPQ) under high light, and Photoinhibitory Phase (PI) under severe stress and high light (see Olascoaga & Porcar-Castell in this issue). These novel findings have implications in the detection of stress using remotely sensed data because NPQ and PI phases overlap with each other. To solve this conundrum we have developed a mechanistic model (Porcar-Castell et al. In prep; see also Abstract by Porcar-Castell et al.). The model is also coupled to a leaf-level radiative transfer model so that it can be used to interpret variations in ChlF obtained either with active or passive fluorescence methods (Atherton et al., In prep).

#### 4)- HOW DO THE BIOGEOCHEMICAL CYCLES AND ATMOSPHERIC PROCESSES AFFECT VEGETATION AND THE DEVELOPMENT OF A FOREST?

Plant responses to global changes in carbon dioxide (CO<sub>2</sub>), nitrogen, and water availability are critical to future atmospheric CO<sub>2</sub> concentrations, hydrology, and hence climate. Our understanding of those responses is incomplete, however. Multiple-resource manipulation experiments and empirical observations have revealed a diversity of responses, as well as some consistent patterns. But vegetation models—currently dominated by complex numerical simulation models—have yet to achieve a consensus among their predicted responses, let alone offer a coherent explanation of the observed ones. We have proposed an alternative approach based on relatively simple optimization models (OMs) and used this approach to derive growth as a function of carbon and nitrogen availabilities to boreal pine and spruce stands (Mäkelä et al. 2009, Mäkelä and Valentine 2012). The method and results were further highlighted in a summary paper on the results of three recent forest OMs, which together explain a remarkable range of observed forest responses to altered resource availability (Dewar et al. 2009). We concluded that OMs now offer a simple yet powerful approach

to predicting the responses of forests—and, potentially, other plant types—to global change. We recommended ways in which OMs could be developed further in this direction (Dewar et al. 2009).

We have developed novel methods for utilising eco-physiological information for predicting material flux rates and forest growth in large geographical areas. The objective of this work has been to develop models with inputs that are readily available in the regional scale, so as to reduce the input uncertainties of the results. These models also apply results from the above OM approach. We have developed and tested models for daily canopy processes (Mäkelä et al. 2008, Peltoniemi et al. 2010, Duursma et al. 2008, 2009, Gea-Izquierdo et al. 2010) and canopy structure (Duursma et al. 2010, Valentine et al. 2013) and applied these successfully in regional growth predictions (Härkönen et al. 2010) and gas exchange estimations (Härkönen et al. 2011, 2013). The long term growth analysis seems to emphasize the faith of nitrogen in changing climate in the ecosystem (Hari, Heliövaara and Kulmala 2013) as the boreal forest ecosystems are far from being nitrogen saturated despite of the relatively abundant nitrogen deposition from atmosphere (Korhonen et al. 2013). However, simulations would suggest that during the next decades the growth response is dominated by the age structure dynamics resulting from forest management and only after 2050 would the climate impact start to be clear (Forsius et al. 2013)

We used data from the international tree ring data base to analyse the growth of Scots pine in Eurasia north of 60 °N. While we initially searched for a growth increase caused by CO<sub>2</sub>, we found that actually most of the sites decreased their growth. When we further analysed the growth decrease we found that the decrease was correlated with the sulphur deposition. Both the proportion of trees which decreased growth and the diameter growth decreased when sulphur deposition increased. Also, we found that sulphur deposition increased the sensitivity of tree growth to drought. (Savva and Berninger 2010).

#### ACKNOWLEDGEMENTS

The team consists of >40 members, including ca. 25 post-graduate students, 12 post docs and 7 senior researchers. Funding was received from Academy of Finland (CoE grant, project grants and several fellowship grants), University of Helsinki (HENVI), the EU-FP7 projects EXPEER, ANAEE, ICOS, IMECC and BRIDGE; the Doctoral programme in ‘Atmospheric Composition and Climate Change: From molecular processes to global observations and models’ (ACCC); Nordforsk NCoE CRAICC; the Finnish Cultural Foundation, Maj and Tor Nessling Foundation, and Ella and Georg Ehrnroth Foundation. An indication of our interdisciplinary approach is that most research themes overlap with themes studied by other teams in the FCoE. This has resulted e.g. in large numbers of joint publications and presentations, common field campaigns and joint doctoral training, and is highly acknowledged.

#### REFERENCES

- Aaltonen, H., Aalto, J., Kolari, P., Pihlatie, M., Pumpanen, J., Kulmala, M., Nikinmaa, E., Vesala, T. & Bäck, J. (2012b) Continuous VOC flux measurements on boreal forest floor. *Plant and Soil* 369: 241–256 DOI 10.1007/s11104-012-1553-4.
- Aaltonen H., Pumpanen J., Hakola H., Vesala T., Rasmus S. & Bäck J. (2012a). Snowpack concentrations and estimated fluxes of volatile organic compounds in a boreal forest. *Biogeosciences* 9: 2033–2044
- Aaltonen H., Pumpanen J., Pihlatie M., Hakola H., Hellén H., Kulmala L., Vesala T. & Bäck J. (2011) Boreal pine forest floor biogenic volatile organic compound emissions peak in early summer and autumn. *Agricultural and Forest Meteorology* 151: 682-691
- Arneth A., Niinemets Ü., Pressley S., Bäck J., Hari P., Karl T., Noe S., Prentice IC., Serça D., Hickler T., Wolf A. & Smith B. (2007) Process-based estimates of terrestrial ecosystem isoprene emissions: incorporating the effects of a direct CO<sub>2</sub>-isoprene interaction. *Atmospheric Chemistry and Physics* 7, 31-53.

- Bäck J., Aalto J., Henriksson M., Hakola H., He, Q. & Boy, M. (2012) Chemodiversity of a Scots pine stand and implications for terpene air concentrations. *Biogeosciences* 9: 689–702.
- Bäck J., Aaltonen H., Hellén H., Kajos M., Patokoski J., Taipale R., Pumpanen J. & Heinonsalo J. (2010) Variable emissions of microbial volatile organic compounds (MVOCs) from root-associated fungi isolated from Scots pine. *Atmospheric Environment* 44: 3651-3659.
- Duursma R.A., Kolari P., Perämäki M., Nikinmaa E., Hari P., Delzon S., Loustau D., Ilvesniemi H., Pumpanen J., Mäkelä A. (2008). Predicting the decline in daily maximum transpiration rate of two pine stands during drought based on constant minimum leaf water potential and plant hydraulic conductance. *Tree Physiology* 28, 265-276.
- Duursma, R. A., Kolari, P., Perämäki, M., Pulkkinen, M., Mäkelä, A., Nikinmaa, E., Hari, P., Aurela, M., Berbigier, P., Bernhofer, Ch., Grunwald, T., Loustau, D., Molder, M., Verbeeck, H., Vesala, T. (2009). Contributions of climate, leaf area index and leaf physiology to variation in gross primary production of six coniferous forests across Europe: a model-based analysis. *Tree Phys.* 29: 621-639.
- Duursma, R.A., Mäkelä, A., Reid, D.E.B., Jokela, E.J., Porté, A., Roberts, S.D. (2010). Self-shading affects allometric scaling in trees. *Functional Ecology* 24:723-730.
- Dewar R.C., Franklin O., Mäkelä A., McMurtrie R.E., Valentine H.T. (2009). Optimal function explains forest responses to global change. *Bioscience* 59:127-139.
- Forsius, M., Anttila, S., Arvola, L., Bergström, I., Hakola, H., Heikkinen, H.I., Helenius, J., Hyvärinen, M., Jylhä, K., Karjalainen, J., Keskinen, T., Laine, K., Nikinmaa, E., Peltonen-Sainio, P., Rankinen, K., Reinikainen, M., Setälä, H., & Vuorenmaa, J. (2013). Impacts and adaptation options of climate change on ecosystem services in Finland: A model based study. *Current Opinion in Environmental Sustainability*, 5 (1), pp. 26-40.
- Fréchette, E., Ensminger, I., Bergeron, Y., Gessler, A., Berninger, F. (2011), Will changes in root-zone temperature in boreal spring affect recovery of photosynthesis in *Picea mariana* and *Populus tremuloides* in a future climate? *Tree Physiology*, 31:1204-1216.
- Gea-Izquierdo G., Mäkelä A., Margolis H., Bergeron Y., Black A.T., Dunn A., Hadley J., Pa U K.T., Falk M., Wharon S. Monson R., Hollinger D.Y., Laurila T., Aurela M., McCaughey H., Bourque C., Vesala T. and Berninger F. (2010). Modeling acclimation of photosynthesis to temperature in evergreen conifer forests. *New Phytologist*. 188:175-186.
- Hakola H., Tarvainen V., Bäck J., Ranta H., Bonn B., Rinne J. & Kulmala M. (2006). Seasonal variation of mono- and sesquiterpene emission rates of Scots pine. *Biogeosciences* 3: 93-101.
- Hari, P., Heliövaara, K. & Kulmala, L. (eds) (2013) *Physical and physiological Forest Ecology*. Springer Verlag.
- Hari, P., H. Hänninen, F. Berninger, P. Kolari, E. Nikinmaa & A. Mäkelä. (2009). Predicting Boreal Conifer Photosynthesis in Field Conditions. *Boreal Env. Res* 14:19-28.
- Hari, P. & Kulmala, L. (eds) (2008) *Boreal forest and Climate Change*. *Advances in Global Change Research*, Vol. 34, Springer Verlag.
- Härkönen, S., Lehtonen, A., Eerikäinen, K., Peltoniemi, M., Mäkelä, A. (2011). Estimating carbon fluxes for large regions in Finland based on process-based modeling, NFI data and Landsat satellite images. *Forest Ecology and Management* 262:2364-2377.
- Härkönen S., Pulkkinen M., Duursma R.A., Mäkelä A. (2010). Estimating annual GPP, NPP and stem growth in Finland using summary models. *For. Ecol. Manage.* 259: 524-533.
- Härkönen S., Tokola T., Packalen P., Korhonen L. and Mäkelä A. (2013). Predicting forest growth based on airborne light detection and ranging data, climate data, and a simplified process-based model. *Canadian Journal of Forest Research* 43:354-375.
- Hölttä, T., Cochard, H., Nikinmaa, E. and M. Mencuccini. (2009). Capacitive effect of cavitation in xylem conduits: results from a dynamic model. *PCE* 32(1):10-21.

- Hölttä, T., Mäkinen, H., Nöjd, P., Kolari, P., Mäkelä, A. & E. Nikinmaa (2010). A Physiological model of softwood cambial growth. *Tree Physiology*.
- Hölttä, T., Mencuccini, M. & E. Nikinmaa.(2011). An optimality model explains the structure of plant vascular systems. *Plant Cell and Environment* 34: 1819–1834
- Ilvesniemi H, Levula J, Ojansuu R, Kolari P, Kulmala L, Pumpanen J, Launiainen S, Vesala T, Nikinmaa E (2009). Long-term measurements of the carbon balance of a boreal Scots pine dominated forest ecosystem. *Boreal Environment Research* 14, 731–753.
- Ilvesniemi H, Pumpanen J, Duursma R, Hari P, Keronen P, Kolari P, Kulmala M, Mammarella I, Nikinmaa E, Rannik Ü, Pohja T, Siivola E, Vesala T (2010). Water balance of a boreal Scots pine forest. *Boreal Env. Res.* 15, 375-396.
- Kolari P., Bäck J., Taipale R., Ruuskanen T.M., Kajos M.K., Rinne J., Kulmala M. & Hari P. (2012) Evaluation of accuracy in measurements of VOC emissions with dynamic chamber system. *Atmospheric Environment* 62: 344-351
- Kolari P, Kulmala L, Pumpanen J, Launiainen S, Ilvesniemi H, Hari P, Nikinmaa E (2009). CO<sub>2</sub> exchange and component CO<sub>2</sub> fluxes of a boreal Scots pine forest. *Boreal Environment Research* 14, 761-783.
- Korhonen, J.F.J., Pihlatie, M., Pumpanen, J., Aaltonen, H., Hari, P., Levula, J., Kieloaho, A.-J., Nikinmaa, E., Vesala, T., & Ilvesniemi, H. (2013). Nitrogen balance of a boreal Scots pine forest. *Biogeosciences*, 10. 1083-1095.
- Kulmala L, Pumpanen J, Kolari P, Muukkonen P, Hari P, Vesala T (2011). Photosynthetic production of ground vegetation in different aged Scots pine forests. *Canadian Journal of Forest Research* 41, 2020-2030.
- Kuusinen, N., Kolari, P., Levula, J., Porcar-Castell, A., Stenberg, P., & Berninger, F. (2012a). Seasonal variation in boreal pine forest albedo and effects of canopy snow on forest reflectance. *Agricultural and Forest Meteorology*, 164, 53-60.
- Kuusinen, N., Tomppo, E. & Berninger, F. (2012b), Linear unmixing of MODIS albedo composites to infer subpixel land cover type albedos, *ITC Journal*, .
- Lappalainen H.K., Sevanto S., Bäck J., Ruuskanen T.M., Kolari P., Taipale R., Rinne J., Kulmala M. & Hari P. (2009) Day-time concentrations of biogenic volatile organic compounds in a boreal forest canopy and their relation to environmental and biological factors. - *Atmospheric Chemistry and Physics* 9: 5447-5459.
- Lappalainen H.K., Sevanto S., Dal Maso M., Taipale R., Kajos M., Kolari P. & Bäck J. (2013) A source orientated approach for estimating day-time concentrations of biogenic volatile organic compounds in an upper layer of a boreal forest canopy. *Boreal Environment Research* 18: 127–144.
- Lintunen, A., Hölttä, T., & Kulmala, M. (2013). Anatomical regulation of ice nucleation and cavitation helps trees to survive freezing and drought stress. *Scientific Reports*, 3.
- Mäkelä A, Kolari P, Karimäki J, Nikinmaa E, Perämäki M, Hari P. (2006). Modelling five years of weather-driven variation of GPP in a boreal forest. *Agricultural and Forest Meteorology* 139, 382-398.
- Mäkelä A., Pulkkinen M., Kolari P., Lagergren F., Berbigier B., Lindroth A., Loustau D., Nikinmaa E., Vesala T., Hari P. (2008). Developing an empirical model of stand GPP with the LUE approach: analysis of eddy covariance data at five contrasting conifer sites in Europe. *Global Change Biology* 14: 98- 108.
- Mäkelä A., Valentine H., Helmisaari H.-S. (2008). Optimal co-allocation of carbon and nitrogen in a forest stand at steady state. *New Phytologist* 180:114-123.
- Mencuccini, M., Hölttä, T., Sevanto, S., & Nikinmaa, E. (2013). Concurrent measurements of change in the bark and xylem diameters of trees reveal a phloem-generated turgor signal. *New Phytologist* 198, 1143-1154
- Nikinmaa, E., Hölttä T., Hari P., Kolari P., Mäkelä A., Sevanto S. & Vesala T. (2013). Assimilate transport in phloem sets conditions for leaf gas exchange. *Plant Cell and Environment* 36:655-659.
- Olascoaga B, Juurola E, Pinho P, Halonen L, Nikinmaa E, Bäck J, Porcar-Castell A (Submitted Manuscript) Seasonal variation in the reflectance of photosynthetically active radiation from epicuticular waxes of Scots pine (*Pinus sylvestris* L.) needles.

- Peltoniemi M., Pulkkinen M., Kolari, P., Duursma, R., Montagnani, L., Wharton, S., Lagergren, F., Takagi, K., Verbeeck, H., Christensen, T., Vesala, T., Falk, M., Loustau, D., Mäkelä, A. (2012). Does canopy mean N concentration explain differences in light use efficiencies of canopies in 14 contrasting forest sites? *Tree Physiology* 32: 200-218
- Porcar-Castell A (2011) A high-resolution portrait of the annual dynamics of photochemical and non-photochemical quenching in needles of *Pinus sylvestris*. *Physiologia Plantarum* 143:139-153.
- Porcar-Castell A, Garcia-Plazaola JI, Nichol CJ, Kolari P, Olascoaga B, Kuusinen N, Fernández-Marín B, Pulkkinen M, Juurola E, Nikinmaa E (2012) Physiology of the seasonal relationship between the photochemical reflectance index and photosynthetic light use efficiency. *Oecologia* 170:313-323.
- Porcar-Castell A., Peñuelas J., Owen S. M., Llusà J., Munné-Bosch S. & Bäck J. (2009) Leaf carotenoid concentrations and monoterpene emission capacity under acclimation of the light reactions of photosynthesis. *Boreal Environment Research* 14: 794-806.
- Savva Y, Berninger F (2010) Sulphur deposition causes a large-scale growth decline in boreal forests in Eurasia. *Global Biogeochemical Cycles*. doi:10.1029/2009GB003749,
- Tarvainen V., Hakola H., Hellen H., Bäck J., Hari P. & Kulmala M. (2005). Temperature and light dependence of the VOC emissions of Scots pine. *Atmospheric Chemistry and Physics* 5: 6691-6718
- Shiestl-Aalto P., Nikinmaa E. and Mäkelä A. 2013. Duration of shoot elongation in Scots pine varies within the crown and between years. *Annals of Botany*. doi:10.1093/aob/mct180
- Susiluoto S., Hiltavuori E., Berninger F., (2010) Testing the growth limitation hypothesis for subarctic Scots pine. *Journal of Ecology* doi: 10.1111/j.1365-2745.2010.01684.x
- Valentine H.T., Amateis R.L., Gove H., Mäkelä A. (2013). Crown rise and crown-length dynamics: application to loblolly pine. *Forestry*. 86:371-375
- Valentine H.T, Mäkelä, A. (2012). Modeling forest stand dynamics from optimal balances of carbon and nitrogen. *New Phytologist*. 194: 961–971
- Vesala T, Launiainen S, Kolari P, Pumpanen J, Sevanto S, Hari P, Nikinmaa E, Kaski P, Mannila H, Ukkonen E, Piao S, Ciais P (2010). Autumn temperature and carbon balance of a boreal Scots pine forest in Southern Finland. *Biogeosciences* 7, 163-176.
- Wu SH, Jansson, P-E, Kolari P (2012). The role of air and soil temperature in the seasonality of photosynthesis and transpiration in a boreal Scots pine ecosystem. *Agricultural and Forest Meteorology* 156, 85-103.
- Yassaa N., Song W., Vanhatalo A., Bäck J., Williams J. (2012) Diel cycles of isoprenoids in the emissions of Norway spruce, four Scots pine chemotypes, and in Boreal forest ambient air during HUMPPA-COPEC-2010. *Atmospheric Chemistry and Physics*, 12, 7215–7229.

# IN SITU MEASUREMENTS OF VOLATILE ORGANIC COMPOUNDS AND INORGANIC GASES AND PARTICLES

H. HAKOLA, H. HELLÉN, U. MAKKONEN, M. VESTENIUS, M. HEMMILÄ

Finnish Meteorological Institute, PL 503, 00101 Helsinki, Finland

Keywords: VOC, monoterpene, sesquiterpene, nitrous acid, nitric acid, ammonia, on-line GC, on-line IC

## INTRODUCTION

The overall research themes of the chemical analytical research are the short-term variability of organic and inorganic gases using chromatographic techniques, and the chemical characterization of fine particles. Our recent achievements have been the following. (i) We have developed an inlet for in-situ GC measurements, enabling mono- and sesquiterpene measurements, and conducted for the first time in-situ biogenic VOC measurements, including sesquiterpenes, in a boreal forest covering the whole year. (ii) We have conducted in-situ measurements of inorganic gases and aerosols in urban and rural air. (iii) We have studied the chemical composition of organic aerosols and measured for the first time, for example, caryophyllenic acid concentrations in ambient air.

### 1.- INLET DEVELOPMENT FOR MONO- AND SESQUITERPENE MEASUREMENTS

We optimized the heated, stainless steel inlet for the ozone removal and for the measurements of mono- and sesquiterpenes in ambient air (Hellén et al., 2012a). Five different inlets were used with different flows, temperatures and ozone and biogenic volatile organic compound (BVOC) concentrations. Both ozone removal capacities and recoveries of BVOCs were determined. Recovery tests of BVOCs were conducted both with zero air and with ozone rich air. Inlets were optimized especially for online GC and adsorbent tube measurements of mono- and sesquiterpenes.

Study shows that it was possible to remove ozone without removing most VOCs with this set up. Setting the temperature, stainless steel grade and flow correctly for different inlet lengths was shown to have a crucial role. Results show that ozone removal capacity increases with increasing temperature and inlet length. Stainless steel grade 316 was shown to be more efficient than grade 304. Based only on ozone removal capacity longest possible stainless steel inlet with heating would be the optimum solution. Of the tested set ups 3 m inlet ( $\frac{1}{4}$  in. grade 304) heated to 120°C with the flow of 1 or 2 l min<sup>-1</sup> was showing the best results with the respect of the ozone removal efficiency and compound recovery.

### 2.- THE MEASUREMENTS OF VOCs IN URBAN AIR

Sources, concentration levels and effects of isoprene and monoterpenes on local atmospheric chemistry were studied in urban background air in Helsinki (Hellén et al., 2012b). Ambient air concentration measurements were conducted using an in-situ gas chromatograph with a mass spectrometer at an urban background station during different seasons in 2011.

Highest concentrations of isoprene and monoterpenes were measured in summer ( $990 \text{ ng m}^{-3}$ ), but concentrations were clearly above detection limit also in winter ( $230 \text{ ng m}^{-3}$ ). The concentrations of aromatic hydrocarbons were higher during all seasons, but reactivity scaled concentrations showed that also isoprene and monoterpenes have a strong influence on local atmospheric chemistry also in urban air. In winter and spring the urban background concentrations were higher than in a forested site in Finland indicating anthropogenic sources of isoprene and monoterpenes. Source estimates obtained by Unmix multivariate receptor model showed that traffic and wood combustion are main local contributors to the measured concentration levels in winter, spring and November, but in July and October biogenic sources are dominating.

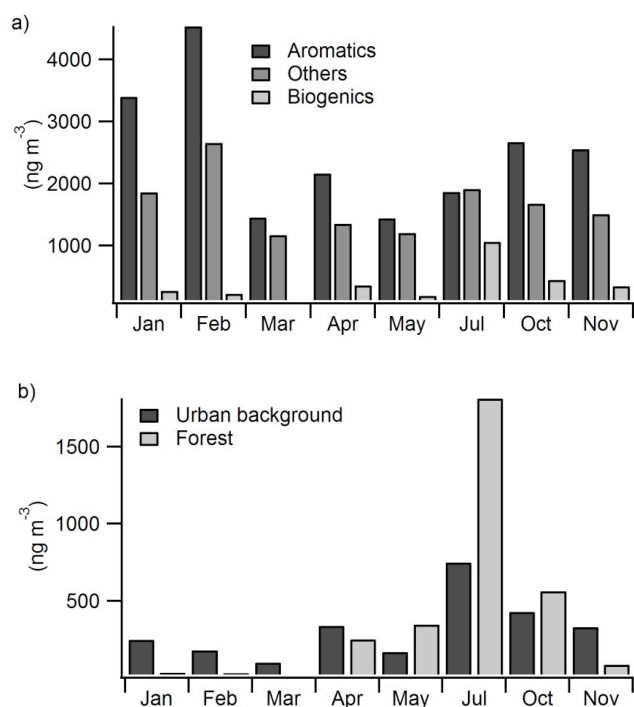


Figure 1. a) Concentrations of measured VOCs during different seasons at urban background site Helsinki in 2011 and b) monoterpene concentrations at the urban background site and in a forest 220 km North from Helsinki in 2011 (Hakola et al. 2012).

### 3.- THE MEASUREMENTS OF VOCs IN FORESTED AREA

We conducted VOC measurements over the period October 2010-October 2011 in Hyytiälä, at least one week every month (Hakola et al., 2012). Isoprene, mono- and sesquiterpene and aromatic hydrocarbon mixing ratios were measured in a boreal pine forest using an in situ gas chromatograph mass-spectrometer. The measurements covered the whole year, at least one week every month. To our knowledge there are no earlier species-speciated semi-continuous BVOC data also covering dormant periods. During the winter months, and still in March, the mixing ratios of all biogenic compounds were very low, most of the time below detection limits. Occasionally, the mixing ratios of monoterpenes, particularly camphene and p-cymene, increased together with  $\text{NO}_x$  mixing ratios, implying an anthropogenic source. These episodes lasted from a few hours to few days and were originated from nearby sawmills or the city of Tampere.

The monoterpene mixing ratios increased in April and started to show diurnal variability, with maximum mixing ratios at night and minima during the day as expected, since Scots pine VOC emissions are only temperature-dependent. The diurnal variability continued until October, after which the mixing ratios decreased, with only occasional episodes taking place. The diurnal variability during summer is shown in Figure 2. The diurnal variation was affected by the friction velocity, high mixing ratios being found with low friction velocities and low mixing ratios being observed high friction velocities. Sesquiterpenes diurnal curve was measured for the first time in boreal areas and was similar as that of monoterpenes, but only in August. The main sesquiterpenes were longifolene and isolongifolene. The diurnal variation of isoprene was opposite to the mono- and sesquiterpene diurnal curve, due to its totally light-dependent emissions. Due to its daytime maximum mixing ratios, isoprene also dominated hydroxyl radical reactivity in summer even though our isoprene measurements are underestimates due to breakthrough in a cold trap.

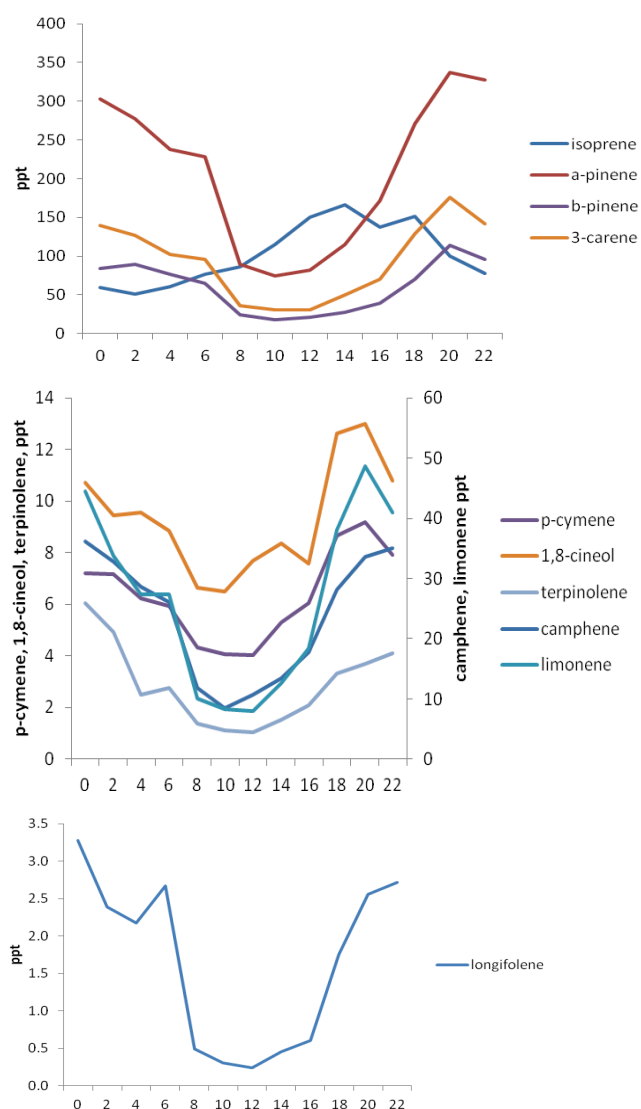


Figure 2: The mean diurnal variability of monoterpenes, longifolene and isoprene in summer (Jun, July, Aug). Longifolene data is from August only. Isoprene concentrations are underestimates due to breakthrough of the cold trap.

#### 4.- THE MEASUREMENTS OF INORGANIC GASES AND AEROSOLS IN URBAN AIR

We measured concentrations of 5 gases (HCl, HNO<sub>3</sub>, HONO, NH<sub>3</sub>, SO<sub>2</sub>) and 8 major inorganic ions in particles (Cl<sup>-</sup>, NO<sub>3</sub><sup>-</sup>, SO<sub>4</sub><sup>2-</sup>, NH<sub>4</sub><sup>+</sup>, Na<sup>+</sup>, K<sup>+</sup>, Mg<sup>2+</sup>, Ca<sup>2+</sup>) with an online monitor MARGA 2S in two size ranges,  $D_p < 2.5 \mu\text{m}$  and  $D_p < 10 \mu\text{m}$ , in Helsinki, Finland from November 2009 to May 2010 (Makkonen U. et al., 2011). There were clear seasonal cycles in the concentrations of the nitrogen-containing gases: the median concentrations of HNO<sub>3</sub>, HONO, and NH<sub>3</sub> were 0.09 ppb, 0.37 ppb, and 0.01 ppb in winter, respectively, and 0.15, 0.15, and 0.14 in spring, respectively. The gas-phase fraction of nitrogen decreased roughly with decreasing temperature so that in the coldest period from January to February the median contribution was 28 % but in April to May 53%. There were also large fractionation variations that temperature alone cannot explain. HONO correlated well with NO<sub>x</sub> but a large fraction of the HONO-to-NO<sub>x</sub> ratios were larger than published ratios in a road traffic tunnel suggesting that a large amount of HONO had other sources than vehicle exhaust. Aerosol acidity was estimated by calculating ion equivalent ratios. The sources of acidic aerosols were studied with trajectory statistics that showed that continental aerosol is mainly neutralized and marine aerosol acidic.

#### 5.- THE MEASUREMENTS OF INORGANIC GASES AND AEROSOLS IN HYYTIÄLÄ

We measured concentrations of gases (HCl, HNO<sub>3</sub>, HONO, NH<sub>3</sub>, SO<sub>2</sub>) and inorganic ions (Cl<sup>-</sup>, NO<sub>3</sub><sup>-</sup>, SO<sub>4</sub><sup>2-</sup>, NH<sub>4</sub><sup>+</sup>, Na<sup>+</sup>, K<sup>+</sup>, Mg<sup>2+</sup>, Ca<sup>2+</sup>) in PM<sub>10</sub> and PM<sub>2.5</sub> particles with an online ion chromatograph MARGA 2S in boreal forest environment in Hyytiälä (SMEAR II station), Finland from 21 June 2010 to 31 April 2011. As part of the quality control laboratory tests, NO<sub>2</sub> in the sample was found to produce artifacts on HONO and HNO<sub>3</sub> after the wet rotating denuder. From the laboratory tests a correction function was derived and it was applied to the field data. The MARGA data were compared with those of the filter samples and the on-line aerosol chemical composition determined by Aerosol Mass Spectrometer. Linear-regression slopes derived from MARGA against the filter data were 0.98, 1.08 and 0.83 for SO<sub>2</sub>, SO<sub>4</sub><sup>2-</sup> and HNO<sub>3</sub>+NO<sub>3</sub>, respectively. The respective correlation coefficients ( $r^2$ ) were 0.89, 0.90 and 0.87. After installing the concentration column improved cation slopes were 1.19, 0.88, 1.00, 0.73 and 0.89 for NH<sub>4</sub>+NH<sub>3</sub>, Na<sup>+</sup>, K<sup>+</sup>, Mg<sup>2+</sup>, and Ca<sup>2+</sup>, respectively. The corresponding correlation coefficients ( $r^2$ ) were: 0.83, 0.95, 0.90, 0.85 and 0.62. According to these results traditional filter collection can be replaced with the MARGA instrument at background sites, if a concentration column is used at least for the cations. This would improve the temporal resolution of the observations. The average concentrations of nitrogen-containing gases were the highest in summer (NH<sub>3</sub>: 0.47 ppb, HNO<sub>3</sub>: 0.10 ppb and HONO: 0.10 ppb) and the lowest in winter (0.05, 0.03 and 0.04 ppb), which can be explained by the fact that agriculture- and soil-related sources are low when the ground is frozen and covered with snow and also photo-chemical reactions are limited during the dark period. In the summer clear diurnal cycles were found in all N-containing gases, but in winter the concentrations remained low and no diurnal cycles were observed (Fig. 3). Concentration of ammonia was found to depend exponentially on the prevailing temperature and the increase with temperature was the strongest in dry conditions.

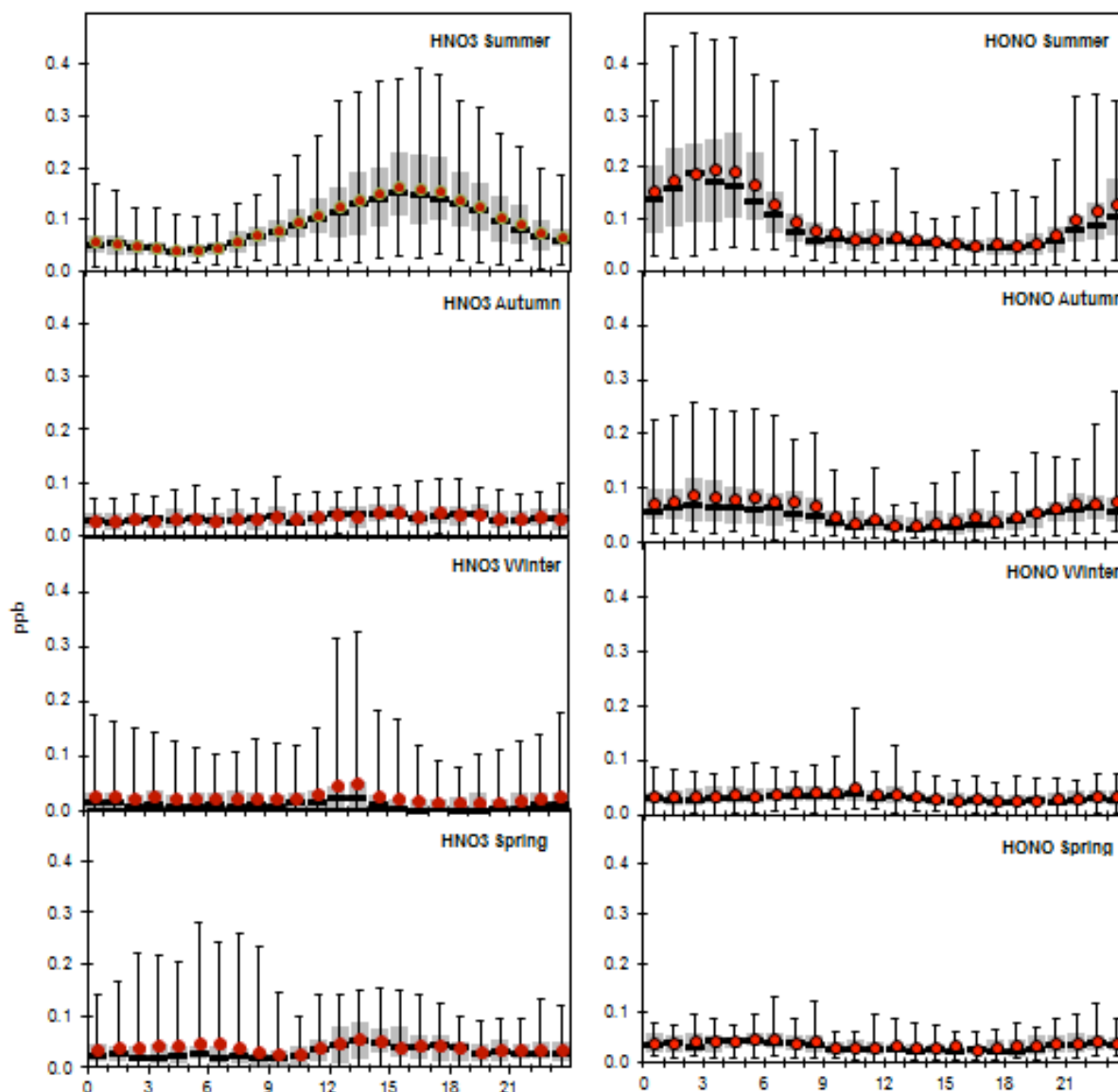


Figure 3. Diurnal cycle of nitrous and nitric acid during different seasons.

## 6.- THE MEASUREMENTS OF BIOGENIC ACIDS

There are studies on concentrations of pinonic and pinic acids in real atmospheres but very little on concentrations of other biogenic acids mainly due to the lack of authentic standards. Especially products of fast sesquiterpenes are of interest since the parent compounds are often too reactive to be measured in ambient air.  $\beta$ -Caryophyllene has been found to be the main sesquiterpene in many emission studies in boreal forests but it has never been detected in the ambient air due its high reactivity. The organic laboratory of Helsinki University synthesized the  $\beta$ -caryophyllinic acid, limonic acid and carenic acid for us and we analyzed these and commercially available pinic and pinonic acids from filter samples collected from Hyytiälä from October 2010 to October 2011.

The highest biogenic acid concentrations were measured in summer (Fig. 4) concomitant with the parent mono- and sesquiterpene mixing ratios. Pinonic and  $\beta$ -caryophyllinic acids were the most abundant acids in summer. The  $\beta$ -caryophyllinic acid contribution was higher than expected on the basis of emission calculations implicating that  $\beta$ -caryophyllene emissions are underestimated. Limonic acid concentration peaked already in spring. This is in accordance with the measured spruce emissions that also reach their maximum in spring. Pinonic and limonic acids had quite high concentrations in winter too. These winter concentrations can be of anthropogenic origin. The  $\beta$ -caryophyllinic and caric acids were correlated with the accumulation mode particle number concentrations implicating they participate in the particle growth process (Fig. 5).

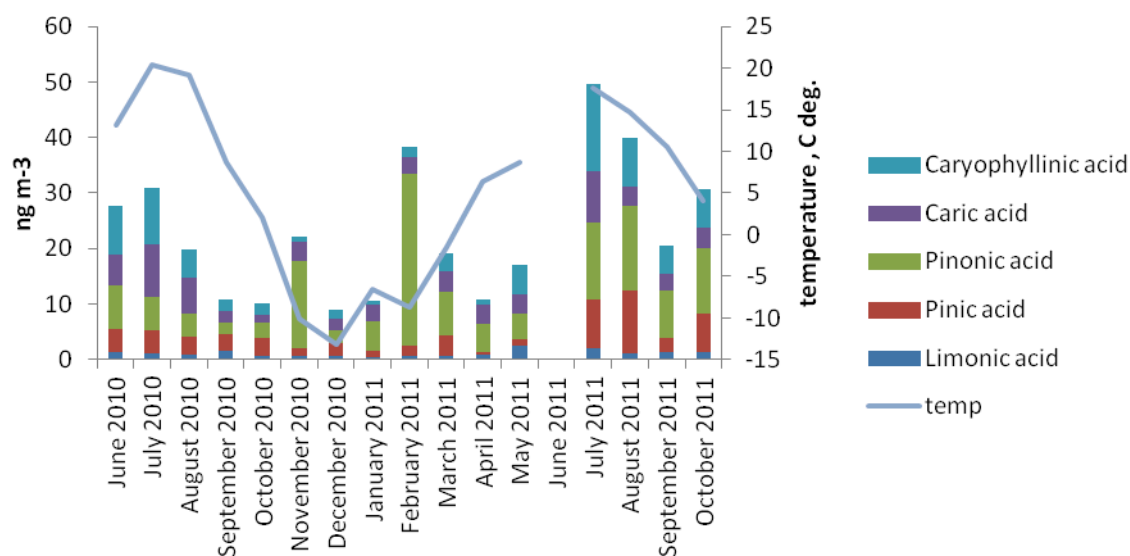
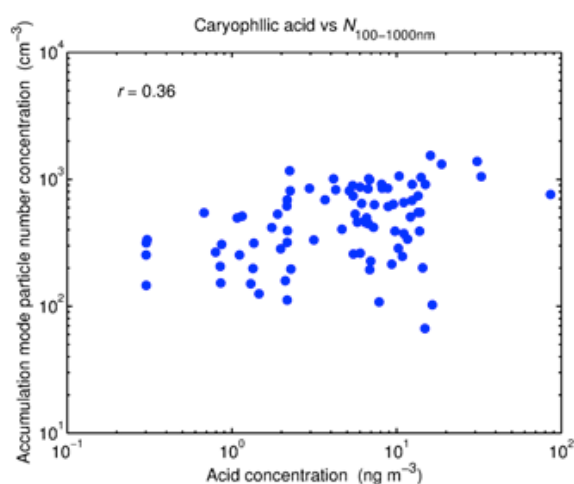


Figure 4: Monthly means of biogenic acid concentrations in PM<sub>2.5</sub> fraction and mean temperature at a time of the measurements.



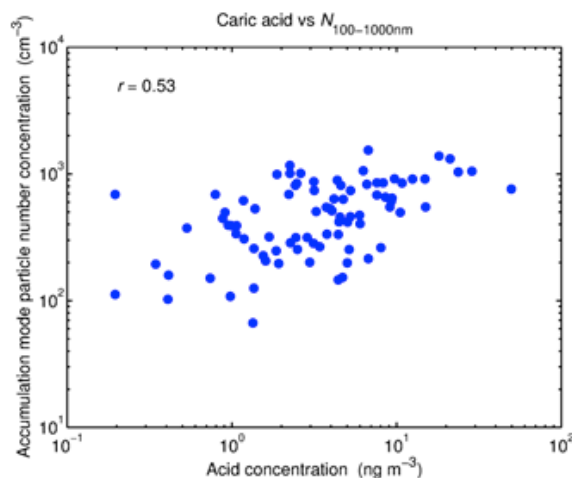


Fig.5 Correlations between  $\beta$ -caryophyllinic and caric acids and the accumulation mode particle number concentrations.

#### ACKNOWLEDGEMENTS

The financial support by the Academy of Finland Centre of Excellence program (project no 1118615) is gratefully acknowledged.

#### REFERENCES

- Hakola H., Hellén H., Henriksson M., Rinne J. and Kulmala M., 2012. In situ measurements of volatile organic compounds in a boreal forest. *Atmos. Chem. Phys.*, 12, 11665-11678.
- Hellén, H., Kuronen, P., Hakola, H.: Heated stainless steel tube for ozone removal in the ambient air measurements of mono- and sesquiterpenes. *Atmospheric Environment* 57 35-40, 2012a
- Hellén H., Tykkä T., and Hakola H, 2012. Importance of monoterpenes and isoprene in urban air in Northern Europe. *Atmospheric Environment* 57 35-40, 2012b
- Makkonen U., Virkkula A., Mäntykenttä J., Hakola H., Keronen P., Vakkari V., and P. Aalto 2012. Semi-continuous gas and inorganic aerosols measurements at a Finnish urban site: comparisons with filters, nitrogen in aerosol and gas phases, and aerosol acidity *Atmos. Chem. Phys.*, 12, 5617-5631, 2012
- Makkonen U., A. Virkkula, H. Hellen, M. Hemmilä, J. Mäntykenttä, M. Äijälä, M. Ehn, H. Junninen, P. Keronen, T. Petäjä, D.R. Worsnop, M. Kulmala, and H. Hakola, 2013. Semi-continuous gas and inorganic aerosol measurements at a boreal forest site: seasonal and diurnal cycles of NH<sub>3</sub>, HONO and HNO<sub>3</sub>. manuscript
- Vestenius M., Hellén H., Levula J., Kuronen P., Helminen K.J., Nieminen T., Kulmala M. and Hakola H. Acidic reaction products of mono- and sesquiterpenes in atmospheric fine particles in a boreal forest, manuscript.

# AN OVERVIEW OF THE ACTIVITIES BY AEROSOL-CLOUD-CLIMATE INTERACTIONS GROUP OF THE UNIVERSITY OF HELSINKI

V.-M. KERMINEN, N. L. PRISLE, P. PAASONEN, A. ASMI, J. HONG, J. KONTKANEN, E.-M. KYRÖ, H. LAPPALAINEN, R. MAKKONEN, T. NIEMINEN, M. PARAMONOV, O. PERÄKYLÄ, L. RIUTTANEN, S.-L. SIHTO, M. VOGT,  
H. VUOLLEKOSKI, T. YLI-JUUTI, T. PETÄJÄ, M. DAL MASO, and M. KULMALA

Department of Physics, 00014 University of Helsinki, Finland

## INTRODUCTION

Concentrations of greenhouse gases, aerosol particles and reactive trace gases are tightly connected with each other via physical, chemical and biological processes occurring in the atmosphere, biosphere and at their interface (Hallquist et al. 2009, Arneth et al. 2010, Carslaw et al. 2010, Mahowald 2011). The continental biosphere plays an important role in the climate system by affecting the accumulation of carbon dioxide and other greenhouse gases to the atmosphere (e.g. Heimann and Reichstein, 2008), and by acting as a major source of natural aerosol particles and their precursors (e.g. Pöschl 2005, Guenther et al. 2012).

Kulmala et al. (2004) suggested a negative climate feedback mechanism whereby higher temperatures and CO<sub>2</sub>-levels boost continental biomass production and volatile organic compound (VOC) emissions, leading to increased biogenic secondary organic aerosol (SOA) and cloud condensation nuclei (CCN) concentrations, and by that way tending to cause cooling in a manner similar to the CLAW-hypothesis that linked climate change with the ocean biochemistry (Charlson et al. 1987, Quinn and Bates 2011). Kulmala et al. (2013a) extended the idea of the continental biosphere-aerosol-cloud-climate (COBACC) feedback further by adding the connection between aerosol particles, radiation and gross primary production (GPP) which is a measure of ecosystem-scale photosynthesis. In this extended view, the COBACC feedback mechanism has two major overlapping feedback loops, both initiated by increased CO<sub>2</sub> concentrations and acting toward suppressing global warming (Fig. 1).

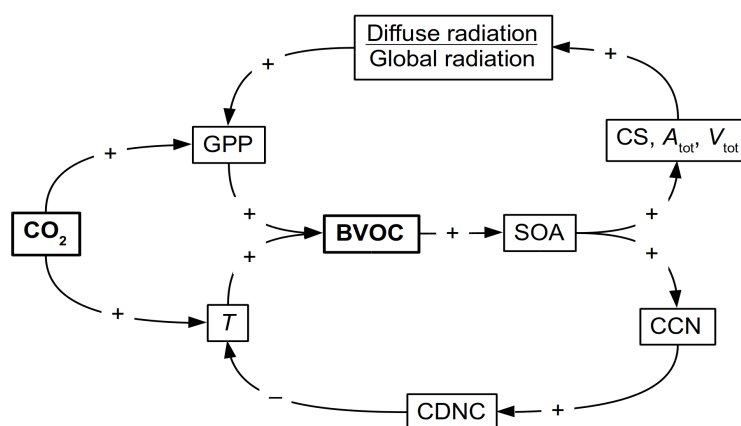


**Figure 1.** The feedback loops associated with the COBACC feedback (Kulmala et al., 2013a). Here GPP is gross-primary production, BVOC and SOA refer to biogenic volatile organic compounds and secondary organic aerosol, respectively, CS is the condensation sink,  $A_{\text{tot}}$  and  $V_{\text{tot}}$  are the total aerosol surface area and volume concentrations, respectively, CCN refers to cloud condensation nuclei, and CDNC is the cloud droplet number concentration.

Most of the work made within the aerosol-cloud-climate interactions group can be tied to the lower branch of the COBACC feedback mechanism that connects biogenic VOC emissions, atmospheric new-particle

formation and growth, CCN formation, interaction of aerosols with clouds, indirect radiative effects, and the ambient temperature. Below we will summarize the current status of this work.

## ADVANCES IN UNDERSTANDING AND HIGHLIGHTS OF THE RESULTS

### **Biogenic volatile organic compounds: emissions, concentrations and chemistry**

Volatile organic compounds (VOCs) originating from bio- or anthropogenic sources play a significant role in atmospheric chemistry and physics. Recent studies have shown the potential of VOCs to influence the climate on both local and global scales through aerosol and cloud condensation nuclei formation as well as direct and indirect greenhouse effects. Despite the global climate effects, BVOCs have multiple impacts on the atmospheric composition, including enhanced ozone formation rates, decreased oxidizing capacity and substantial contribution to tropospheric aerosol abundances.

We have investigated the seasonal and diurnal variations of the mixing ratios of nine volatile organic compounds. In general, BVOCs show the highest mixing ratios during summertime, most likely due to higher emissions during that period, whereas anthropogenic VOC mixing ratios peaked in wintertime. Diurnal patterns can be seen for all the investigated compounds. The features of the diurnal pattern may be explained by sink or dilution processes (e.g. boundary layer evolution). We have also investigated the oxidation capacity and rate of monoterpenes over a boreal forest in Finland and its connection to new particle formation (Peräkylä et al., abstract in this collection).

### **Initial steps of atmospheric nucleation**

The progress in this subject area includes improved understanding of atmospheric nucleation mechanisms and refinement of semi-empirical nucleation rate parameterizations for large-scale modeling frameworks. Crucial factors in the progress have been the development of new measurement tools in the sub-3 nm diameter size range and systematically combining data from field and laboratory measurement with theoretical understanding and modeling activities.

As an overall summary of our work on initial steps of atmospheric nucleation, Kulmala et al. (2013b) provide an observational-based framework on atmospheric aerosol formation. This framework identifies three size regimes below 2 nm diameter and combines in a consistent way i) molecules, small atmospheric clusters and growing nanoparticles, ii) sulphuric acid, strong bases and organic vapours, and iii) various dynamical processes. The framework confirms that atmospheric aerosol formation is essentially a two-step process. In the first step taking place in the second size regime, atmospheric nucleation or the formation of stabilized clusters will occur. The second step, characterized by enhanced cluster growth rates due to the activation of the growing clusters by organic vapours, is initiated in the third size regime just below 2 nm. This second step determines the formation rate of 3 nm particles and is efficient only during periods of active aerosol formation.

Our findings emphasize the important role of organic compounds in atmospheric new particle formation and the usual dominance of neutral nucleation pathways in the lower troposphere. The next step is to investigate whether, and to which extent, these findings can be generalized to different atmospheric environments. A work toward this goal has been initiated (e.g. Kontkanen et al., abstract in this collection).

In terms of parameterizing atmospheric nucleation, Paasonen et al. (2010) generated, and compared with observations, several nucleation parameterizations involving sulphuric acid and low-volatility organic vapours. The concentrations of low-volatility organic compounds were determined from growth rates of 2–4 nm particles. Including organic compounds as nucleating vapours enhanced the predictability of the nucleation rate, especially between different sites, as compared with parameterizations involving only sulphuric acid.

## Atmospheric new particle formation and growth

In this subject area, we have been involved in plenty of new field observations, related theoretical studies, model development, and in developing new parameterizations.

As examples of atmospheric observations, Kyrö et al. (2013) provided the first evidence of Antarctic new particle formation from biogenic precursors originating from melt-water ponds in continental Antarctica, and Järvinen et al. (2013) showed that Antarctic new particle formation may also take place during dark winter conditions. Kyrö et al. (manuscript in preparation) investigated long-term trends in new particle formation in Eastern Lapland and demonstrated that the frequency of atmospheric new particle formation has been influenced by decreasing sulphur emissions from Kola Peninsula area since the late 1990s. Nieminen et al. (2013, manuscript in preparation) analysed long-term changes in the character of new particle formation events at the SMEAR II station in Hyytiälä, Southern Finland, representing the longest field data set on this phenomenon.

Kulmala et al. (2012) compiled a detailed protocol for making atmospheric nucleation measurements, and for analysing atmospheric nucleation events. Nieminen et al. (abstract in this collection) developed a tool to forecast new particle formation at the SMEAR II station in Hyytiälä, Finland, extending to the next 5-day period from the beginning of the forecast.

Considerable progress has been made in understanding and modelling the growth of both neutral and charged newly-formed particles. Yli-Juuti et al. (2011) made a comprehensive analysis of the growth rates of nucleation mode particles at the SMEAR II station, and completed this work by developing a new aerosol dynamical model (Yli-Juuti et al., 2013). Häkkinen et al. (2013) derived a new parameterization for size-dependent nanoparticle growth in continental environments and tested this parameterization in a global modelling framework. Leppä et al. (2011) investigated the role of charged particles and electric interactions on nanoparticle dynamics and found that the presence of charges may significantly affect nuclei self-coagulation and coagulation scavenging. Leppä et al. (2013) analysed the validity of various methods used commonly to determine either nanoparticle growth rates or the contribution of ion-induced nucleation from field measurement data.

## Cloud condensation nuclei

Sihto et al. (2011) investigated the seasonal variation of CCN concentrations and aerosol activation properties at the SMEAR II station. One of the main results of this paper was a clear, observed contribution of atmospheric new particle formation to measured CCN concentrations.

Paramonov et al. (2013) presented a long-term multi-year Cloud Condensation Nuclei Counter (CCNC) dataset obtained at the SMEAR II station. They reported a seasonal pattern of aerosol hygroscopicity  $\kappa$  for particles of ~150 nm in diameter, with a maximum in February and a minimum in July. The hygroscopicity of particles grown to CCN sizes from freshly-nucleated particles was found to be indistinguishable from that of already existing particles of the same size. Due to the  $\kappa$  distributions being different for different particle sizes, the paper calls for a careful reconsideration of the use of a single value of  $\kappa$  when describing the hygroscopicity of an ambient aerosol population.

Hong et al. (abstract in this collection) demonstrated the benefit of combining information on aerosol hygroscopicity and volatility behaviour when investigating their CCN properties.

Prisle et al. (2011) proposed a simple representation of the overall effect of surface activity on organic aerosol CCN activation and tested it against comprehensive thermodynamic model calculations, as well as laboratory measurements of CCN activity for binary organic-inorganic particle mixtures, comprising 4 different organic surfactants (3 atmospheric fatty acid salts and model surfactant sodium dodecyl sulfate)

mixed with sodium chloride in different ratios. For these mixtures, the simple representation gave close agreement with both detailed model and measurements.

### **Clouds and aerosol-cloud interactions**

Aerosol effect on shallow clouds has been studied widely in recent decades, deep convective clouds getting much less attention. Bister and Kulmala (2011) propose that aerosol effect on microphysics of deep convective clouds may increase upper tropospheric humidity in convectively active areas. Water vapor in the upper troposphere affects radiation balance strongly and therefore even small increases have a strong positive radiative forcing (Riuttanen et al, 2013, abstract in this collection).

Kyrö et al. (2009) parameterized aerosol snow scavenging during light, continuous snowfall. The parameterization was based on field observations from Hyytiälä and was further tested with the University of Helsinki Multicomponent Aerosol Model (UHMA).

### **Integration and large-scale applications**

Asmi et al. (2011) studied the phenomenology of submicron aerosol number size distributions in Europe by collecting and consistently analysing data from 24 EUSAAR network stations. The results gave a comprehensive overview of the European near surface aerosol particle number concentrations and number size distributions between 30 and 500 nm of dry particle diameter and analysed the spatial and temporal distribution of aerosols in the particle sizes most important for climate applications. Asmi et al. (2013) investigated long-term trends of total aerosol particle number concentrations from stations located in Europe, North America, Antarctica and Pacific Ocean islands. The majority of the sites showed clear decreasing trends. The most likely cause of many northern hemisphere trends was found to be decreases in the anthropogenic emissions of primary particles, sulphur dioxide, or some co-emitted species.

Kerminen et al. (2012) made a synthesis of existing knowledge about atmospheric CCN formation associated with atmospheric nucleation, including field observations, theory and large-scale modeling. The paper concludes that in order to better quantify the role of atmospheric nucleation in CCN formation and Earth System behaviour, more information is needed on i) the factors controlling atmospheric CCN production and ii) the properties of both primary and secondary CCN and their interconnections. In future investigations on this subject, more emphasis should be put on combining field measurements with regional and large-scale model studies.

Prisle et al. (2012) implemented the simple representation of the overall effect of surface activity on organic aerosol CCN activation in the global model framework of ECHAM-HAM, together with another recent surfactant representation taking surface partitioning into account (Topping et al, GMD 2010) as well as a framework where surfactants are included according to bulk properties. This analysis showed that the difference in predicted cloud droplet number concentrations and radiative forcing, from the base case of not including surfactant effect, but simply treating surface active organic aerosol as a regular and fully soluble solute, is highly significant if macroscopic properties are assumed, and only minor when using representations based on comprehensive thermodynamics. In the absence of global data for comparison, we can not say conclusively that the partitioning-based representations more closely resemble conditions in the real atmosphere, but we do show quite clearly that if you consider surfactant effects of organic aerosol, then it makes a significant difference on a global scale, how this is done.

Makkonen et al. (2012a) investigated BVOC-aerosol-climate interactions in ECHAM5.5-HAM2 by implementing several processes that couple organic vapours to particle formation and growth. Five different nucleation mechanisms were introduced to the model, including nucleation rate formulations with organic gases (Paasonen et al., 2010). Two mechanistically different BVOC emission datasets were tested, namely MEGAN2 and LPJ-GUESS. Although the sensitivity tests produces some variance in CN

and CCN concentrations with different nucleation and BVOC emission schemes, these effects were significantly smaller than e.g. the effects of anthropogenic emission change until year 2100.

Paasonen et al. (2013) demonstrated for the first time that the lower branch of the COBACC feedback takes place continental size scale. The analysis was based partly on long-term field observations (the relation between temperature, BVOC, SOA and CCN) and partly on existing parameterizations (the relation between CCN, CDNC and temperature relation) (see Fig. 1). The paper pointed out the prominent role of the boundary layer height on the climate effects of biogenic and anthropogenic formation of CCN sized particles.

Work is currently in progress in investigating the climatic effects of biofuel adoption with focus on Brazil (Vuollekoski et al, abstract in this collection) and in deriving particle number emission inventories for both present day and future conditions (Paasonen et al., abstract in this collection).

## OUTLOOK

During the last few years, our overall understanding on biosphere-atmosphere interaction has been increased, and even more so when considering some specific processes like atmospheric new particle formation and growth. Future progress in this area requires dedicated field, laboratory and modeling activities on one hand, and more integrative work on the other hand. The latter includes versatile use of continuous and comprehensive in situ observations from multiple measurement sites, active utilization of various remote sensing techniques, developing new model parameterizations, and improving large-scale modeling frameworks.

One example of new activities integrating different approaches is the BAECC (Biogenic Aerosols: Effects on Clouds and Climate) project that will start operational phase in January 2014. In BAECC, versatile cloud observations with ground-based remote sensing will be combined with in situ measurements at the SMEAR II station. This, along with application of hierarchy of models and satellite observations, aim to getting better understanding on the impact of biogenic aerosol formation on cloud properties and climate.

Finally, it is important to point out that most of the natural feedback mechanisms involving the biosphere and atmosphere are somehow tied with human and societal actions, including the emission policy, forest management and land use change (Arneth et al. 2009, Makkonen et al. 2012b, Shindell et al. 2012). As a result, the COBACC feedback illustrated in Figure 1 can be considered as a broad framework which connects the human activities, the continental biosphere, and the changing climate conditions.

## ACKNOWLEDGEMENTS

The Academy of Finland Center of Excellence program (project no. 1118615), several other projects by the Academy of Finland, and Maj and Tor Nessling Foundation are acknowledged for funding.

## REFERENCES

- Arneth, A., Unger, N., Kulmala, M., and Andreae M. O.: Clean the air, heat the planet (2009) *Science*, 326, 672–673.
- Arneth, A., Harrison, S. P., Zaehle, S., Tsigaridis, K., Menon, S., Bartlein, P. J., Feichter, J., Korhola, A., Kulmala, M., O'Donnell, D., Shurgers, G., Sorvari, S., and Vesala, T. (2010) Terrestrial biogeochemical feedbacks in the climate system. *Nat. Geosci.*, 3, 525–532.

Asmi, A. et al. (2011) Number size distributions and seasonality of submicron particles in Europe 2008–2009. *Atmos. Chem. Phys.*, 11, 5505–5538.

Asmi, A. et al. (2013) Aerosol decadal trends – Part 2: In-situ aerosol particle number concentrations at GAW and ACTRIS stations. *Atmos. Chem. Phys.*, 13, 895–916.

Bister, M. and Kulmala, M. (2011) Anthropogenic aerosols may have increased upper tropospheric humidity in the 20th century. *Atmos. Chem. Phys.*, 11, 4577–4586.

Carslaw, K. S., Boucher, O., Spracklen, D. V., Mann, G. W., Rae, J. G. L., Woodward, S., and Kulmala, M.: A review of natural aerosol interactions and feedbacks within the Earth system (2010) *Atmos. Chem. Phys.*, 10, 1701–1737.

Charlson, R. J., Lovelock, J. E., Andreae, M. O., Warren, S. G. (1987) Oceanic phytoplankton, atmospheric sulphur, cloud albedo and climate. *Nature*, 326, 655–661.

Guenther, A. B., Jiang, X., Heald, C. L., Sakulyanontvittaya, T., Duhl, T., Emmons, L. K., and Wang, X. (2012) The Model of Emissions of Gases and Aerosols from Nature version 2.1 (MEGAN2.1): an extended and updated framework for modeling biogenic emissions. *Geosci. Model Dev.*, 5, 1471–1492.

Heimann, M. and Reichstein, M. (2008) Terrestrial ecosystem carbon dynamics and climate feedbacks. *Nature*, 451, 289–292.

Hallquist, M. et al. (2009) The formation, properties and impact of secondary organic aerosol: current and emerging issues. *Atmos. Chem. Phys.*, 9, 5155–5236.

Häkkinen, S. A. K., Manninen, H. E., Yli-Juuti, T., Merikanto, J., Kajos, M. K., Nieminen, T., D’Andreae, S. D., Asmi, A., Pierce, J. R., Kulmala, M., and Riipinen, I. (2013) Semi-empirical parameterization of size-dependent atmospheric nanoparticle growth in continental environments. *Atmos. Chem. Phys.*, 13, 7665–7682.

Järvinen, E., Virkkula, A., Nieminen, T., Aalto, P. P., Asmi, E., Lanconelli, C., Busetto, M., Lupi, A., Schioppa, R., Vitale, V., Mazzola, M., Petäjä, T., Kerminen, V.-M., and Kulmala, M. (2013) Seasonal cycle and modal structure of particle number size distribution at Dome C, Antarctica. *Atmos. Chem. Phys.*, 13, 7473–7487.

Kerminen, V.-M., Paramonov, M., Anttila, T., Riipinen, I., Fountoukis, C., Korhonen, H., Asmi, E., Laakso, L., Lihavainen, H., Swietlicki, E., Svenningsson, B., Asmi, A., Pandis, S. N., Kulmala, M. and Petäjä, T. (2012) Cloud condensation nuclei production associated with atmospheric nucleation: a synthesis based on existing literature and new results. *Atmos. Chem. Phys.*, 12, 12037–12059.

Kulmala, M., Suni, T., Lehtinen, K. E. J., Dal Maso, M., Boy, M., Reissell, A., Rannik, U., Aalto, P., Keronen, P., Hakola, H., Back, J. B., Hoffmann, T., Vesala, T., and Hari, P.: A new feedback mechanism linking forests, aerosols, and climate (2004) *Atmos. Chem. Phys.*, 4, 557–562.

Kulmala, M., Petäjä, T., Nieminen, T., Sipilä, M., Manninen, H. E., Lehtipalo, K., Dal Maso, M., Aalto, P. P., Junninen, H., Paasonen, P., Riipinen, I., Lehtinen, K. E. J., Laaksonen, A., and Kerminen, V.-M. (2012) Measurement of the nucleation of atmospheric aerosol particles. *Nat. Protoc.*, 7, 1651–1667.

Kulmala, M., Nieminen, T., Chellapermal, R., Makkonen, R., Bäck, J., and Kerminen, V.-M. (2013a) Climate feedbacks linking the increasing atmospheric CO<sub>2</sub> concentration, BVOC emissions, aerosols and clouds in forest ecosystems. In Niinemets, Ü, and Monson, R. K. (eds.), *Biology, Controls and Model Tree Volatile Organics Compound Emissions*, Springer, Dordrecht, pp. 489–508.

- Kulmala M. et al. (2013b) Direct observations of atmospheric aerosol nucleation. *Science*, 339, 943–946.
- Kyrö, E.-M., Grönholm, T., Vuollekoski, H., Virkkula, A., Kulmala, M., and Laakso, L. (2009) Snow scavenging of ultrafine particles: field measurements and parameterization. *Boreal Environ. Res.*, 14, 527–538.
- Kyrö, E.-M., Kerminen, V.-M., Virkkula, A., Dal Maso, M., Parshintsev, J., Ruiz-Jimenez, J., Forsström, L., Manninen, H. E., Riekkola, M.-L., Heinonen, P., and Kulmala, M. (2013) Antarctic new particle formation from continental biogenic precursors. *Atmos. Chem. Phys.*, 13, 3527–3546.
- Leppä, J., Anttila, T., Kerminen, V.-M., Kulmala, M., and Lehtinen, K. E. J. (2011) Atmospheric new particle formation: real and apparent growth of neutral and charged particles. *Atmos. Chem. Phys.*, 11, 4939–4955.
- Leppä, J., Gagne, S., Laakso, L., Manninen, H. E., Lehtinen, K. E. J., Kulmala, M., and Kerminen, V.-M. (2013) Using measurements of the aerosol charging state in determination of the particle growth rate and the proportion of ion-induced nucleation. *Atmos. Chem. Phys.*, 12, 463–486.
- Mahowald, N. (2011) Aerosol indirect effect on biogeochemical cycles and climate. *Science*, 334, 794–796.
- Makkonen, R., Asmi, A., Kerminen, V.-M., Boy, M., Arneth, A., Guenther, A., and Kulmala, M. (2012a) BVOC-aerosol-climate interactions in the global aerosol-climate model ECHAM5.5-HAM2. *Atmos. Chem. Phys.*, 12, 10077–10096.
- Makkonen, R., Asmi, A., Kerminen, V.-M., Boy, M., Arneth, A., Hari, P. and Kulmala, M. (2012b) Air pollution control and decreasing new particle formation lead to strong climate warming. *Atmos. Chem. Phys.*, 12, 1515–1524.
- Paasonen, P., Asmi, A., Petäjä, T., Kajos, M. K., Äijälä, M., Junninen, H., Holst, T., Abbatt, J. P. D., Arneth, A., Birmili, W., Denier van der Gon, H., Hamed, A., Hoffer, A., Laakso, L., Laaksonen, A., Leaitch, W. R., Plass-Dulmer, C., Pryor, S. C., Räisänen, P., Swietlicki, E., Wiedensohler, A., Worsnop, D. R., Kerminen, V.-M., and Kulmala, M. (2013) Warming-induced increase in aerosol number concentration likely to moderate climate change, *Nature Geosci.*, 6, 438–442.
- Paramonov, M., Aalto, P. P., Asmi, A., Prisle, N., Kerminen, V.-M., Kulmala, M., and Petäjä, T. (2013) The analysis of size-segregated cloud condensation nuclei counter (CCNC) data and its implications for aerosol-cloud interactions. *Atmos. Chem. Phys. Discuss.*, 13, 9681–9731.
- Prisle, N. L., Dal Maso, M., and Kokkola, H. (2011) A simple representation of surface active organic aerosol in cloud droplet formation. *Atmos. Chem. Phys.*, 11, 4073–4083.
- Prisle, N. L. et al. (2012) Surfactant effects in global simulations of cloud droplet activation, *Geophys. Res. Lett.*, 39, L05802, doi:10.1029/2011GL050467.
- Pöschl, U. (2005) Atmospheric aerosols: Composition, transformation, climate and health effects. *Angew. Chem. Int. Ed.*, 44, 7520–7540.
- Quinn, P. K. and Bates T. S. (2011) The case against climate regulation via oceanic phytoplankton sulphur emissions. *Nature*, 480, 51–56.

Shindell, D., et al (2012) Simultaneously mitigating near-term climate change and improving human health and food security. *Science*, 335, 183–188.

Sihto, S.-L., Mikkilä, J., Vanhanen, J., Ehn, M., Liao, L., Lehtipalo, K., Aalto, P. P., Duplissy, J., Petäjä, T., Kerminen, V.-M., Boy, M., and Kulmala, M. (2011) Seasonal variation of CCN concentrations and aerosol activation properties in boreal forest. *Atmos. Chem. Phys.*, 11, 13269–13285.

Yli-Juuti, T., Nieminen, T., Hirsikko, A., Aalto, P. P., Asmi, E., Horrak, U., Manninen, H., Patokoski, J., Dal Maso, M., Petäjä, T., Rinne, J., Kulmala, M., and Riipinen, I. (2011). Growth rates of nucleation mode particles in Hyytiälä during 2003–2009: variation with particle size, season, data analysis method and ambient conditions. *Atmos. Chem. Phys.*, 11, 12865–12886.

Yli-Juuti, T., Barsanti, K., Hildebrandt Ruiz, L., Kieloaho, A.-J., Makkonen, U., Petäjä, T., Ruuskanen, T., Kulmala, M., and Riipinen, I. (2013) Model for acid-base chemistry in nanoparticle growth (MABNAG). *Atmos. Chem. Phys. Discuss.*, 13, 7175–7222.

## OVERVIEW OF THE STUDIES CONDUCTED BY THE UEF AEROSOL PHYSICS GROUP

A. LAAKSONEN<sup>1,2</sup>, S. ROMAkkANIEMI<sup>1</sup>, J. JOUTSENSAARI<sup>1</sup>, A. HAMED<sup>1</sup>, J. MALILA<sup>1</sup>, I. AHMAD<sup>1</sup>, E. BARANIZADEH<sup>1</sup>, L. HAO<sup>1</sup>, A. JAATINEN<sup>1</sup>, H. KESKINEN<sup>1</sup>, T. KORHOLA<sup>1</sup>, A. KORTELAINE<sup>1</sup>, T. KÜHN<sup>1</sup>, Z. MAALICK<sup>1</sup>, P. MIETTINEN<sup>1</sup>, S. MIKKONEN<sup>1</sup>, A. PAJUNOJA<sup>1</sup>, J. N. SMITH<sup>1,3</sup>, P. VAATTOVAARA<sup>1</sup>, P. YLI-PIRILÄ<sup>1</sup>, A. VIRTANEN<sup>1</sup>

<sup>1</sup>University of Eastern Finland, Department of Applied Physics, Kuopio, Finland

<sup>2</sup>Finnish Meteorological Institute, Helsinki, Finland

<sup>3</sup>National Centre for Atmospheric Research, Boulder, CO 80305, USA

Keywords: aerosols, clouds

## INTRODUCTION

Our main interests lie in characterizing the physical and chemical properties of atmospheric aerosol, especially particles that form from nucleation, and understanding the role of aerosols as cloud condensation nuclei (CCN). We develop unique instruments that measure aerosol chemical composition both directly and indirectly, and deploy these in intensive field studies throughout the world. Together with FMI we maintain a long term measurement station, the SMEAR IV station at the top of the 75m Puijo Tower in Kuopio, for studying aerosol properties and aerosol-cloud interactions. In the laboratory, we have developed a facility for studying the formation of secondary organic aerosol from real plant emissions as a means of studying realistic atmospheric processes under controlled conditions. We interpret our laboratory and field observations using a variety of atmospheric models from process level to global scale. In the group we are also developing both process and cloud resolving models to produce better parameterizations to describe aerosol-cloud interactions in global models.

## AEROSOL-CLOUD-CLIMATE INTERACTIONS

UEF aerosol physics group is mainly working on the field of aerosol-cloud microphysics by developing theories and modelling tools, and conducting both experimental and modelling studies. The main activities during 2011-2013 can be summarized as:

- Measurements at Puijo station show that there are differences in partitioning of different chemical compounds between interstitial particles and cloud droplets due to both activation kinetic as well as transfer of semivolatile components through gas phase in the cloud (Hao et al. 2013).
- The sizedependent information on aerosol composition is needed in order to correctly estimate the CCN-concentration of aerosol population. In the experiment conducted at Pallas measurement station it was shown that using the bulk composition from AMS can cause overestimation in aerosol hygroscopicity leading to overestimation of CCN concentration estimates (Jaatinen et al. 2013).
- The aerosol effect on cloud droplet concentration can be saturated already at relatively low ( $\sim 250\text{cm}^{-3}$ ) droplet concentrations. This was seen both with in situ measurements conducted at Puijo station and in MODIS retrieved data (Ahmad et al. 2013). In more polluted conditions this effect is even more evident and thus using aerosol concentration or AOD as a proxy for cloud droplet concentration is not recommended as it can cause overestimation of the first aerosol indirect effect (Romakkaniemi et al. 2012).

- Nitric acid effect on global radiation through indirect aerosol effect was taken to global models, and it was found that the nitric acid contribution to the present-day cloud albedo effect was  $-0.32 \pm 0.01 \text{ Wm}^{-2}$ , and to the total indirect effect  $-0.46 \pm 0.25 \text{ Wm}^{-2}$  (compared to a nitric acid free atmosphere) (Makkonen et al. 2013). Related to topic, the first experimental setup to quantify the effects of semi-volatiles on CCN-activity was introduced (Romakkaniemi et al. 2013).
- In several studies the surface active compounds have been speculated to affect the cloud droplet formation, although theory of surface partitioning does not support these findings (Sorjamaa et al. 2005). Now we performed modelling studies showing that even in the case of semi-volatile surfactants the effect on CCN activity is very small (Romakkaniemi et al. 2011) and in the global scale the effect on global radiation budget is negligible if surfactants are represented with state of the art methods (Prisle et al. 2012).
- Using the ECHAM5-HAM2, we investigated the impact of the increasing aerosol emissions in China and India between 1996 and 2010 to global climate. The warming contribution of black carbon concentrations above clouds nearly cancels the cooling effect of sulfate aerosols, thus making it unlikely that the increase in aerosol emissions in China and India has caused the "hiatus" in global warming during the last decade. (Kuhn et al. 2013).
- The change in mean temperature in Finland was investigated with Dynamic Linear Models (DLM) in order to define magnitude of the trend in the temperature time series within the last 165 years. The mean temperature has risen by a total of  $2.7^\circ\text{C}$  in the years 1847-2012, which amounts to  $0.16 \pm 0.03^\circ\text{C/decade}$ . After year 1968, the trend rate has been as high as  $0.27 \pm 0.01^\circ\text{C/decade}$ . The observed warming is somewhat higher than the global trend, which confirms the assumption that warming is stronger in higher latitudes. (Mikkonen et al. 2013).
- Recently the group has focused more on production of faster aerosol modules that are still capable of presenting all relevant aerosol processes. Bergman et al. (2012) presented the model development study where sectional aerosol module SALSA was tested and evaluated in atmospheric model ECHAM5.5. More detailed evaluation study by Korhola et al. (2013) shows that currently commonly used modal representation of aerosol in large scale models suffers several issues in describing aerosol-cloud interactions. We have been also developing new methodologies to correct approximation errors due to coarse representation of aerosol in the models (Lipponen et al. 2013).
- There is no trend visible towards decreasing greenhouse gas emissions so researchers have started to plan optional methods to counteract the global warming. Partanen et al. (2012) found that by artificial emission of sea salt particles on persistent stratocumulus regions  $-0.8 \text{ Wm}^{-2}$  radiative flux perturbation can be achieved, making the technique promising candidate. This study is continued with more detailed models on cloud resolving scale (Maallick et al 2013). In Laakso et al. (2012) the possibility to use passenger aircrafts to increase the amount of particles in the stratosphere was studied, but this method was found inefficient with the radiative flux perturbation being only  $-0.1 \text{ Wm}^{-2}$  even with highly elevated sulfur emissions as compared to current fuels used.

## ORGANIC AEROSOL PROPERTIES

Our recent plant chamber and field results show that atmospheric SOA particles from biogenic origin can be amorphous solid in their physical phase (Virtanen et al., 2010). The phase state of SOA particles has important implications for a number of atmospheric processes because the phase of particles may influence the partitioning of volatile compounds, reduce the rate of heterogeneous chemical reactions, affect the particles' ability to accommodate water and act as cloud condensation or ice nuclei, and change the atmospheric lifetime of the particle. During years 2012-2013 there has been significant increase in the understanding of the occurrence of solid phase of SOA particles and implications of the finding.

The main activities on the field of organic aerosols properties during the years 2011-2013 are:

- To study phase state of aerosol particles, a novel method based on impaction and subsequent counting of bounced particles by a condensation particle counter have been developed (Saukko et al., 2012a) and applied to study the effect of humidity on physical state of the particles (Saukko et al., 2012b). All the studied SOA systems, both from biogenic and anthropogenic precursors were amorphous solid or semi-solid in their physical state at RH <50 % and showed full or partial deliquescence when the humidity increased up to 65%.
- We have estimated the viscosity of SOA from pine emitted VOCs based on SEM images revealing agglomerated particles. According to coalescence time analysis, the viscosity of the particles is close to the viscosity of glasses ( $10^{12}$  Pas). (Pajunoja et al., 2013a)
- The particle hygroscopic properties and phase were studied in detail in Boston College flow tube reactor. We saw a clear correlation between the particle O:C ratio and precursor molar mass both on hygroscopic behaviour and phase: particles with low O:C and with high precursor molar mass were less hygroscopic and also remained in solid phase even at high humidities. The hygroscopic behaviour of particles in sub-saturation conditions implies also, that there are clear kinetic limitations of molecules in particle bulk. (Pajunoja et al., 2013b)
- We have further studied the physical and chemical factors affecting the SOA particle phase in chamber studies in Univ. Manchester. According to our results the aging of SOA particles from anthropogenic and biogenic mixtures increases the O:C ratio of the particles modestly. Also a slight increase in hygroscopicity was detected. Interestingly, the particle liquefaction humidity of the particles clearly decreased with age. We also studied the effect of evaporation on phase: after thermodenuder treatment particles remained in solid phase at higher humidities implying that the fraction of oligomers increased in particle phase after the thermodenuder treatment. (Pajunoja et al., 2013c)
- Recently, we have studied the role of low volatile organics on secondary organic aerosol formation based on VOC partitioning using chamber experiments and model calculations (Kokkola et al. 2013). The results showed that the underestimation of SOA yields in large-scale atmospheric models can partly be explained by wall-losses of SOA forming compounds during chamber experiments.
- We have also studied the effect of biotic stress (i.e. insect herbivory) on SOA formation and aerosol forcing of climate (Joutsensaari et al., 2013). The results from field and laboratory experiments, global modelling (GLOMAP), and satellite observations suggest that more frequent insect outbreaks in a warming climate could result in ample increase in biogenic SOA formation in the boreal zone and affect both aerosol forcing of climate at regional scales.
- Finally, we have developed methods to analyse VOC and HONO concentrations (dynamic flow-through chamber) as well as to study particle formation (UV flow reactor) from soils and plants emissions. Our results showed that drainage of pristine peatlands enhances their HONO production in northern acidic soils (Maljanen et al. 2013) as earlier reported for the N<sub>2</sub>O and NO.
- In addition to SOA studies described above, we have also studied the chemical composition of particles from wood combustion by using High Resolution Aerosol Mass Spectrometer (HR-AMS). A positive matrix factorization method was used for the first time to analyse combustion aerosols emitted from the burner. Results show that particulate emissions from wood combustion can be varied significantly when combustion conditions are changed, even for very short periods. The overall PAH emissions can be entirely dominated by short disturbances of the combustion process and, thus, formation of PAH formation can be reduced efficiently when keeping combustion conditions stable. (Kortelainen et al., 2013)

## ATMOSPHERIC NEW PARTICLE FORMATION

New particle formation (NPF) events have been observed frequently almost everywhere globally (*Kulmala et al., 2004* and references therein). However, the fundamental processes causing nucleation and subsequent growth into the size-range of a few nanometres are still not well understood. Most likely there is not just one mechanism that controls atmospheric nucleation processes. To improve the understanding

of atmospheric NPF, we have performed numerous field measurements, laboratory experiments and theoretical and model studies. During 2011-2013 the main results are:

- Statistical proxies for  $\text{H}_2\text{SO}_4$  concentrations were formulated by Mikkonen et al. (2011). For the EUCAARI sites, Mikkonen et al. concluded that the best predictive proxy of  $\text{H}_2\text{SO}_4$  at different European sites was achieved by multiplying combinations of global solar radiation,  $\text{SO}_2$  concentration, condensation sink and relative humidity
- Hamed et al. (2011) considered the reasons for the apparent correlation found between atmospheric NPF events and relative humidity. It was concluded that High RH is correlated with cloudiness, and therefore with decreased UV radiation levels, which in turn causes lower OH concentrations and diminished  $\text{H}_2\text{SO}_4$  production. NPF events therefore tend to occur easier at low RH. Additionally, RH often exhibits a diurnal minimum close to midday, when OH concentrations and  $\text{H}_2\text{SO}_4$  production are peaking, which causes an anticorrelation between RH levels and NPF rates.
- New particle growth in the CLOUD experiments conducted at CERN was analyzed by Keskinen et al. (2013). The main result was that in experiments of NPF from sulfuric acid, ammonia, and organics (oxidation products of pinanediol), the organic volume fraction in the particles increased with increasing particle size.
- Measurement data from the San Pietro Capofiume station was employed by Westervelt et al. (2013) in a study comparing modelled CCN production in NPF events to observations from different measurement stations. It was found that the global aerosol microphysics model GEOS-Chem-TOMAS underestimates the CCN production by up to a few tens of percents.
- Simultaneous NPF events measured at San Pietro Capofiume and Bologna measurement sites situated some 40 km apart were studied by Laaksonen et al. (2013). In the studied cases, the first new particles appeared 1-2 hours earlier in SPC than in Bologna. This appears to be associated with the morning boundary layer development (start of vertical mixing) that starts earlier in SPC. In order to characterize the boundary layer evolution during the morning, the mixed layer height was modelled using the high-resolution weather model HARMONIE. The reason for the delayed onset of the boundary layer evolution in Bologna was found to be the urban heat island effect.
- To extract further information on the nucleation process behind observed NPF, the first nucleation theorem has been routinely used. This theorem links together the number of molecules in so-called critical nucleus, presenting bottleneck for vapour-to-particle transition, the rate of NPF and concentration of condensing species (e.g. sulphuric acid). Recently, we have demonstrated for a model systems that coagulation losses of clusters smaller than the critical size distort the results of this analysis (Malila et al., 2013a) towards larger sizes, while cluster-cluster interactions (Vehkamäki et al., 2012) have dominantly an opposite effect. Work to extend these results for atmospherically relevant systems is in progress (Malila et al., 2013b).
- The 3nm particle formation rate ( $J_3$ ) and the nucleation rate ( $J_1$ ) are central quantities for nucleation and NPF analysis. The estimation of  $J_1$  is usually extrapolated from the apparent formation rate of 3 nm particles ( $J_3$ ), which is obtained from measured particle size distributions. Many of uncertainties around this issue were discussed lately in many publications (e.g. Korhonen et al., 2011). Lehtinen et al. (2013) are developing a new method for estimating the nucleation rates from apparent particle formation rates and vice versa, taking into account the effect of size dependent growth rates as was recommended by latest study of Kuang et al., (2011).

## REFERENCES

Ahmad, I., T. Mielonen, H. Portin, A. Arola, A. Leskinen, M. Komppula, K.E.J Lehtinen, A. Laaksonen, S. Romakkaniemi: Long term measurements of cloud droplet concentrations and aerosol-cloud interactions in continental boundary layer clouds, accepted to Tellus B, 2013

- Bergman, T., Kerminen, V.-M., Korhonen, H., Lehtinen, K. J., Makkonen, R., Arola, A., Mielonen, T., Romakkaniemi, S., Kulmala, M., and Kokkola, H. (2012). Evaluation of the sectional aerosol microphysics module SALSA implementation in ECHAM5-HAM aerosol-climate model, *Geosci. Model Dev.*, 5, 845-868
- Hamed, A., H. Korhonen, S.-L. Sihto, J. Joutsensaari, H. Jarvinen, T. Petaja, F. Arnold, T. Nieminen, M. Kulmala, J. N. Smith, K. E.J. Lehtinen, and A. Laaksonen (2011) The role of relative humidity in continental new particle formation. *J. Geophys. Res.* 116, D03202, 12 PP.. doi:10.1029/2010JD014186
- Hao, L. Q., Romakkaniemi, S., Yli-Pirilä, P., Joutsensaari, J., Kortelainen, A., Kroll, J. H., Miettinen, P., Vaattovaara, P., Tiitta, P., Jaatinen, A., Kajos, M. K., Holopainen, J. K., Heijari, J., Rinne, J., Kulmala, M., Worsnop, D. R., Smith, J. N., and Laaksonen, A. (2011). Mass yields of secondary organic aerosols from the oxidation of alpha-pinene and real plant emissions. *Atmos. Chem. Phys.*, 11, 1367-1378
- Hao, L.Q., S. Romakkaniemi, A. Kortelainen, A. Jaatinen, H. Portin, P. Miettinen, M. Komppula, A. Leskinen, A. Virtanen, J.N. Smith, D.R. Worsnop, K.E.J. Lehtinen, and A. Laaksonen: Aerosol Chemical Composition in Cloud Events by High Resolution Time-of-Flight Aerosol Mass Spectrometry, *Environ. Sci. Technol.*, 47, 2645–2653, doi: 10.1021/es302889w, 2013.
- Joutsensaari J., P. Yli-Pirilä, H. Korhonen, A. Arola, J. D. Blande, J. Heijari, M. Kivimäenpää, L. Hao, P. Miettinen, P. Lyytikäinen- Saarenmaa, A. Laaksonen, J. K. Holopainen (2013). Biotic stress accelerates formation of climate-relevant aerosols in boreal forests. *Nature Climate Change*, submitted
- Jaatinen, A., S. Romakkaniemi, T. Anttila, A.-P. Hyvärinen, L. Hao, A. Kortelainen, P. Miettinen, J.N. Smith, A. Virtanen and A. Laaksonen: The 3rd Pallas Cloud Experiment: consistency between the hygroscopic growth and CCN activity parameterisations, submitted to *Boreal Environ. Research*. (2013).
- Keskinen H., S. Romakkaniemi, A. Jaatinen, P. Miettinen, E. Saukko, J. Joutsensaari, J. M. Mäkelä, A. Virtanen, J. N. Smith, and A. Laaksonen (2011) On-Line Characterization of Morphology and Water Adsorption on Fumed Silica Nanoparticles. *Aerosol Science and Technology*, Vol. 45, Iss. 12, 1441-1447.
- Keskinen, H., Virtanen, A., Joutsensaari, J., Tsagkogeorgas, G., Duplissy, J., Schobesberger, S., Gysel, M., Riccobono, F., Slowik, J. G., Bianchi, F., Yli-Juuti, T., Lehtipalo, K., Rondo, L., Breitenlechner, M., Kupc, A., Almeida, J., Amorim, A., Dunne, E. M., Downard, A. J., Ehrhart, S., Franchin, A., Kajos, M.K., Kirkby, J., Kürten, A., Nieminen, T., Makhmutov, V., Mathot, S., Miettinen, P., Onnela, A., Petäjä, T., Praplan, A., Santos, F. D., Schallhart, S., Sipilä, M., Stozhkov, Y., Tomé, A., Vaattovaara, P., Wimmer, D., Prevot, A., Dommen, J., Donahue, N. M., Flagan, R.C., Weingartner, E., Viisanen, Y., Riipinen, I., Hansel, A., Curtius, J., Kulmala, M., Worsnop, D. R., Baltensperger, U., Wex, H., Stratmann, F., and Laaksonen, A.: Evolution of particle composition in CLOUD nucleation experiments, *Atmos. Chem. Phys.*, 13, 5587-5600, doi:10.5194/acp-13-5587-2013, 2013.
- Kokkola, H., Yli-Pirilä, P., Vesterinen, M., Korhonen, H., Keskinen, H., Romakkaniemi, S., Hao, L., Kortelainen, A., Joutsensaari, J., Worsnop, D. R., Virtanen, A., and Lehtinen, K. E. J.: The role of low volatile organics on secondary organic aerosol formation, *Atmos. Chem. Phys. Discuss.*, 13, 14613-14635, doi:10.5194/acpd-13-14613-2013, 2013.
- Korhola T., H. Kokkola, H. Korhonen, A.-I. Partanen, A. Laaksonen, and S. Romakkaniemi: Reallocation in modal aerosol models: impacts on predicting aerosol radiative effects, *Geosci. Model Dev. Discuss.*, 6, 4207-4242, 2013.
- Korhonen, H., Sihto, S.-L. , Kerminen, V.-M. and Lehtinen, K. (2011): Evaluation of the accuracy of analysis tools for atmospheric new particle formation. *Atmos. Chem. Phys.*, 11, 3051-3066, 2011
- Kortelainen, A., Joutsensaari, J., Tiitta, P., Jaatinen, A., Miettinen, P., Hao, L., Leskinen, J., Sippula, O., Torvela, T., Tissari, J., Jokiniemi, J., Worsnop, D.R., Laaksonen, A., and Virtanen, A. Real-time Chemical Composition Analysis of Particle Emissions from Woodchip Combustion. Submitted to *Environ. Sci. Tech.*, September 2013.
- Kuang, C., Chen, M., Zhao, J., Smith, J., McMurry, P.H., and Wang, J.(2012): Size and time-resolved growth rate measurements of 1 to 5 nm freshly formed atmospheric nuclei. *Atmos. Chem. Phys.*, 12, 3573-3589, 2012

Kulmala, M., Vehkamäki, H., Petäjä, T., Dal Maso, M. Lauri, A., Kerminen, V.-M. W., Birmili, W., and McMurry, P. H.: Formation and growth rates of ultrafine atmospheric particles: a review of observations, *J. Aerosol Sci.*, 35, 143–176, 2004.

Kühn T., A-I Partanen, A Laakso, Z Lu, T Bergman, S Mikkonen, H Kokkola, H Korhonen, P Räisänen, D G Streets, S Romakkaniemi, and A Laaksonen (2013): Climate impacts of changing aerosol emissions since 1996. *Nature Geosci.*, in review

Laakso A., A.-I. Partanen, H. Kokkola, A. Laaksonen, K.E.J. Lehtinen, H. Korhonen (2012). Stratospheric passenger flights likely an inefficient geoengineering strategy. *Environ. Res. Lett.*, in press.

Laaksonen Ari, Amar Hamed, Sami Niemelä, Larisa Sogacheva, Federico Angelini, Gian Paolo Gobbi, Stefano Decesari, Jorma Joutsensaari, Vanes Poluzzi<sup>5</sup>, M. Cristina Facchini (2013): The urban heat island effect, boundary layer evolution, and triggering of new particle formation: A case study from Bologna, Italy Manuscript in preparation.

Lehtinen, K., Kerminen, V.M, and Korhonen, H (2013): Estimating nucleation rates from apparent particle formation rates and vice versa 2: effect of size dependent growth rates. Manuscript under preparation

Leskinen, A., Arola, A., Komppula, M., Portin, H., Tiitta, P., Miettinen, P., Romakkaniemi, S., Laaksonen, A., and Lehtinen, K. E. J. (2012). Seasonal cycle and source analyses of aerosol optical properties in a semi-urban environment at Puijo station in Eastern Finland. *Atmos. Chem. Phys.*, 12, 5647-5659.

Lipponen A., V. Kolehmainen, S. Romakkaniemi and H. Kokkola: Correction of approximation errors with random forest applied to modeling of aerosol first indirect effect, *Geosci. Model Dev. Discuss.*, 6, 2551-2583, 2013.

Maalick Z., H. Korhonen, H. Kokkola, A. Laaksonen, and S. Romakkaniemi: Large eddy simulations of marine stratocumulus geoengineering, This issue.

Makkonen, R., Romakkaniemi, S., Kokkola, H., Stier, P., Räisänen, P., Rast, S., Feichter, J., Kulmala, M., and Laaksonen, A. (2012). Brightening of the global cloud field by nitric acid and the associated radiative forcing, *Atmos. Chem. Phys.*, 12, 7625-7633.

Malila, J., R. McGraw, A. Laaksonen and K. E. J. Lehtinen (2013a). Losses of precritical clusters and the first nucleation theorem. Manuscript in preparation.

Malila, J., R. McGraw, A. Laaksonen and K. E. J. Lehtinen (2013b). Precritical cluster scavenging and nucleation theorems for binary H<sub>2</sub>SO<sub>4</sub>-H<sub>2</sub>O nucleation. Submitted to FCoE, 2012. Hyytiälä, September 19-21, 2012.

Maljanen, M.E., P. Yli-Pirilä, J. Hytönen, J. Joutsensaari and P.J. Martikainen (2013) Acidic northern soils as sources of atmospheric nitrous acid (HONO). *Soil Biology & Biochemistry*, accepted.

Mikkonen, S., Romakkaniemi, S., Smith, J. N., Korhonen, H., Petäjä, T., Plass-Duelmer, C., Boy, M., McMurry, P. H., Lehtinen, K. E. J., Joutsensaari, J., Hamed, A., Mauldin III, R. L., Birmili, W., Spindler, G., Arnold, F., Kulmala, M., and Laaksonen, A. (2011). A statistical proxy for sulphuric acid concentration. *Atmos. Chem. Phys.*, 11, 11319-11334

Mikkonen, S., M. Laine, H. Tietäväinen, H. Gregow, H. Tuomenvirta, M. Lahtinen, A. Laaksonen: Trends in the average temperature in Finland 1847-2012, Submitted to Stochastic Environmental Research and Risk Assessment 2013.

Pajunoja, A., Malila, J., Hao L., Joutsensaari, J., Lehtinen, K. E. J. and Virtanen, A. Estimating the Viscosity Range of SOA Particles Based on Coalescence Times, Submitted to *Aerosol Sci. Tech.*, April 2013a.

Pajunoja, A., et al. Hygroscopic growth of SOA particles is restricted by their amorphous solid phase. Manuscript in preparation, 2013b

- Pajunoja A, M. R. Alfarra, A. Buchholz, W.T. Hesson, G.B. McFiggans, A. Virtanen (2013c): Investigation of the effects of chemical and physical factors on the phase state of SOA particles. Abstract, European Aerosol Conference, 2013
- Partanen, A.-I., H. Kokkola, S. Romakkaniemi, V.-M. Kerminen, K. E.J. Lehtinen, T. Bergman, A. Arola, and H. Korhonen (2012). Direct and indirect effects of sea spray geoengineering and the role of injected particle size, *J. Geophys. Res.*, 117, D2
- Portin, H. , T. Mielonen, A. Leskinen, A. Arola, E. Pärjälä, S. Romakkaniemi, A. Laaksonen, K.E.J. Lehtinen, M. Komppula (2012). Biomass burning aerosols observed in Eastern Finland during the Russian wildfires in summer 2010 – Part 1: In-situ aerosol characterization. *Atmos. Environ.* 47, 269-278
- Prisle, N. L., Asmi, A., Topping, D., Partanen, A.-I., Romakkaniemi, S., Dal Maso, M., Kulmala, M., Laaksonen, A., Lehtinen, K.E.J., McFiggans, G. and Kokkola, H. (2012) Surfactant effects in global simulations of cloud droplet activation, *Geophys. Res. Lett.*, vol 39, L05802, doi:10.1029/2011GL050467
- Romakkaniemi S., Kokkola H. and Laaksonen A. : Parameterization of the nitric acid effect on CCN activation. *Atmos Chem Phys* 5 879-885, 2005.
- Romakkaniemi S., H. Kokkola, J.N. Smith, N.L. Prisle, A.N. Schwier, V.F. McNeill, A. Laaksonen: Partitioning of semivolatile surface active compounds between bulk, surface and gas phase, *Geophys. Res. Lett.*, 38, L03807, doi:10.1029/2010GL046147, 2011
- Romakkaniemi, S., A. Arola, H. Kokkola, W. Birmili, T. M. Tuch, V.-M. Kerminen, P. Räisänen, J. Smith, H. Korhonen, and A. Laaksonen (2012) Effect of aerosol size distribution changes on AOD, CCN and cloud droplet number concentration: case studies from Erfurt and Melpitz, Germany *J. Geophys. Res.*, 117, D07202, 8 PP., doi:10.1029/2011JD017091
- Romakkaniemi, S., A. Laaksonen and T. Raatikainen: : Effect of phase partitioning of semivolatile aerosol compounds on particles CCN-activity, submitted to *Atmos. Meas. Tech.*, 2013
- Saukko, E., Kuuluvainen, H., and Virtanen, A. (2012a) A method to resolve the phase state of aerosol particles, *Atmos. Meas. Tech.*, 5, 259-265, doi:10.5194/amt-5-259-2012
- Saukko, E., Lambe, A. T., Massoli, P., Koop, T., Wright, J. P., Croasdale, D. R., Pedernera, D. A., Onasch, T. B., Laaksonen, A., Davidovits, P., Worsnop, D. R., and Virtanen, A. (2012b) Humidity-dependent phase state of SOA particles from biogenic and anthropogenic precursors, *Atmos. Chem. Phys.*, 12, 7517-7529
- Sorjamaa, R. and Laaksonen A. (2007) The effect of H<sub>2</sub>O adsorption on cloud-drop activation of insoluble particles: a theoretical framework. *Atmos Chem Phys* 7 6175-6180.
- Vehkamäki, H., M. J. McGrath, T. Kurtén, J. Julin, K. E. J. Lehtinen and M. Kulmala (2012). Rethinking the application of the first nucleation theorem to particle formation. *J. Chem. Phys.*, 136, 094107.
- Virtanen, A., Joutsensaari, J., Koop, T., Kannosto, J., Yli-Pirilä, P., Leskinen, J., Mäkelä, J.M., Holopainen, J.K., Pöschl, U, Kulmala, M, Worsnop D.R. and Laaksonen, A. (2010). An amorphous solid state of biogenic secondary organic aerosol particles. *Nature* 467 824–827
- Westervelt, D. M., Pierce, J. R., Riipinen, I., Trivitayanurak, W., Hamed, A., Kulmala, M., Laaksonen, A., Decesari, S., and Adams, P. J. (2013) Formation and growth of nucleated particles into cloud condensation nuclei: model–measurement comparison. *Atmos. Chem. Phys.*, 13, 7645-7663

## OVERVIEW ABOUT ACTIVITIES IN AEROSOLS AND CLIMATE GROUP

H. LIHAVAINEN, T. ANTILA, E. ASMI, D. BRUS, A. HIRSIKKO, R. HOODA, A. HYVÄRINEN, N. KIVEKÄS, J. LEPPÄ, K. NEITOLA, E. O'CONNOR, T. RAATIKAINEN, J. SVENSSON, O. TOLONEN-KIVIMÄKI, V. VAKKARI and T. VISKARI

Finnish Meteorological Institute, Helsinki, PO.Box 503, 00101 Finland.

Keywords: Aerosol, Climate, Measurements, Modelling.

### INTRODUCTION

Aerosol and climate research group carry out research on properties, processes and influences of aerosols to climate in the atmosphere, especially at northern latitudes. The research is based on continuous and campaign type measurements, laboratory experiments and modelling. The objective of the research is to answer following questions:

- what is the direct radiative forcing in our environment ?
- how does pollution in the atmosphere affect to the properties of clouds and indirect radiative forcing in northern latitudes ?
- what is the ratio between direct and indirect forcing in our environment ?
- what is the role of human activities to the radiative forcing by aerosols in our environment

Here we report some of the group's recent activities.

### METHODS

The activities of the group can be divided into four categories: continuous in situ field measurements, modelling and data analysis, laboratory experiments and instrument development and campaign based measurements. In the following a more detailed insight to recent activities is given.

#### 1. Continuous field measurements

Continuous field measurements of aerosol physical and optical properties are conducted in three different stations in Finland: In Pallas-Sodankylä Global Atmosphere Watch (GAW) station, Utö Atmospheric and Marine Research Station, and Virolahti measurement station. Utö and Virolahti are part of European Monitoring and Evaluation Programme (EMEP). In Pallas-Sodankylä GAW station we have studied aerosol long term properties, for example, time series of new particle formation events (Asmi et al., 2011) and long term trends of aerosol properties (Collaud Coen et al. 2012 , Asmi et al., 2012). Data from all above mentioned three stations, along with two other stations, Hyytiälä and Kuopio, have been used to characterize black carbon aerosol properties in Finland, a gateway to Arctic (Hyvärinen et. al. 2011a).

Group is also involved in several long term measurement programs abroad; India, Tiksi in Siberia, Saudi Arabia, and Marambio in Antarctica. The purpose is to study how aerosols in these very different environments affect to climate and air quality, what is the relationship between the effects of anthropogenic and natural aerosol sources.

In India we have established a continuous measurement station, which has been operational since 2006. We have characterized the basic properties of aerosol, the effect of monsoon on aerosols properties (e.g Hyvärinen et al, 2011b, Hyvärinen et al., 2011c, Panwar et el. 2012) and new particle formation in rural background environment in northern India (Neitola et al., 2011).

In collaboration with Russian Roshydromet and NOAA from USA, FMI has established a state of the art long term measurement station in Tiksi, Siberia , since direct year-round observations of important

climate forcing agents have been inadequate within the Russian side of the Arctic. Since summer 2010, aerosol number size distributions of  $>7$  nm particles have been measured in Arctic Russia, Tiksi. These aerosol measurements program was updated in summer 2013, and additional measurements of e.g. aerosol scattering and absorption, as well as ultrafine ( $>3$  nm) particle numbers were started. New particle formation has been frequently observed in Tiksi, peaking in spring and summer months and is generally connected with clean, Arctic air masses (Asmi et al., 2013).

A new aerosol in situ measurement station was established to Marambio in Antarctic peninsula in January 2013 in co-operation with SNMA (Servicio Meteorologico Nacional Argentina). Measurements in Marambio include aerosol number size distribution, aerosol scattering and absorption coefficients, aerosol chemistry with impactors,  $\text{CO}_2$ ,  $\text{CH}_4$ ,  $\text{H}_2\text{O}$  and albedo. Aerosol concentrations are typically as low in Pallas in winter time ( $\sim 100 \text{ cm}^{-3}$ ). New particle formation events are observed during local summer.

The Finnish Meteorological Institute, together with the King Abdulaziz University (KAU) and the University of Helsinki, has established a background measurement station to study aerosols in the Western Saudi Arabia (Hyvärinen et al., 2013). The object of this study is to evaluate the quantities and properties of both natural and anthropogenic aerosols in the area, and their effect on climate change and air quality. The measurements were started in October 2012 with a projected length of three years. To our knowledge, this is the first effort to measure the size distribution, scattering and absorption properties of sub-micron particles with in situ methods in the region. In addition, the project includes upgrading the KAU air quality stations in Jeddah and knowledge transfer in the matters of climate change and air quality.

Building of Finland's remote sensing network has been accomplished. The aims for the network include monitoring and investigating aerosol, clouds and boundary layer wind and dynamics for weather forecast, air quality, aviation safety and climate change assessment purposes. The sites in the network represent different environments and climate conditions from southern to northern Finland : 1) Helsinki, urban environment with marine influence, 2) Utö island, part of the Finnish archipelago, 3) Hyytiälä, continental background site, 4) Kuopio, continental urban site and 5) Sodankylä, arctic continental site. Doppler lidar (HALO Photonics) is one of the key instruments of the infrastructure (Wood et al., 2013). Therefore, performances of six Doppler lidars were investigated by carrying out two inter-comparison campaigns (Hirsikko et al, 2013).

## 2. Modeling and data analysis

Recent modelling activities of the group cover the following topics: 1) developing a method to determine the growth rate of a newly-formed particle mode, 2) analysis of the results from the recent field campaigns conducted at the Pallas GAW- and Hyytiälä SMEAR station, 3) interpreting results from the laboratory experiments investigating the growth of nano-sized sulphuric acid particles, 4) interpreting results from single particle soot photometer (SP2) and 5) and climate modelling.

The growth rate of newly-formed particles (GR) is an important parameter with regard to the climatic impact of the resulting CCN, but determining the GR of a growing particle mode from field measurements poses a formidable problem. We have approached the issue by developing an algorithm that 1) calculates the “representative” diameter of the mode, 2) calculates the derivative of the resulting diameter to obtain GR, and 3) applies another algorithm to smooth the data series of GR in order to eliminate possible noise present in the data. The developed algorithm has been successfully tested against new particle formation events generated with a numerical model and against events observed at the GAW Pallas station (Anttila et al., 2013a).

The CCN activity of particles was calculated on the basis of H-TDMA and AMS measurements and compared to the measured CCN activity for the 3<sup>rd</sup> Pallas cloud campaign (Anttila et al., 2012). The aim of these studies was to assess if information provided by these instruments can be used to predict the particle CCN activation properties accurately. Also, a series of sensitivity studies were performed to investigate if

simplified representation of the particle chemical composition can be used when parameterizing the cloud droplet formation in large scale models. The results show that results 1) calculations based on the H-TDMA provided more accurate results compared to those obtained from the AMS data, and 2) simplified representations increased the discrepancy between calculations and measurements to some degree.

We have also studied aerosol cloud activation capacity by means of CCN and HTDMA measurements and chemical composition was measurements by an aerosol mass spectrometer at Hyytiälä, Finland, during spring 2007 (Cerully et al., 2011). For a fixed aerosol size, CCN activity depends on hygroscopicity which describes the ability of particles to absorb water. Ideally, hygroscopicity can be calculated when aerosol chemical composition and the properties of the species are known. The aerosol organic fraction is a complex mixture of hundreds of compounds, but by applying a factorization algorithm to the mass spectrometer data, two different organic groups were identified. One group contains more oxidized hygroscopic organic species and the other group contains the less oxidized and less hygroscopic species. Aerosol composition was further examined by analyzing filter samples with nuclear magnetic resonance (NMR) spectroscopy (Finessi et al., 2012) and the spectra were again analyzed by the factorization algorithms. The more and less oxidized organic groups were also identified with the NMR method, which gives additional information about structures of the molecules in each group.

The Hyytiälä 2007 CCN data set was representing Boreal forests in study examining droplet growth kinetics at different environments (Raatikainen et al., 2013a). For example, an organic surface film could decrease water vapor condensation rates during cloud formation and this would increase the total number of cloud droplet, but the average size would be smaller. However, the study showed that such kinetic limitations are not common in atmospheres or at least their effect on droplet size is negligible.

Growth rate of nanoparticles produced by homogenous nucleation of  $\text{H}_2\text{SO}_4$  and water were measured in a laminar flow tube (Škrabalová et al., 2013). The measured growth rates were compared against calculations performed with a condensational growth rate model. The results imply that the wall losses of gaseous  $\text{H}_2\text{SO}_4$  in such systems can be smaller than previously thought and that the generated particles were probably neutralized by ammonium to some degree during the experiments.

Single particle soot photometer (SP2) can measure both soot mass and scattering size for 100-500 nm particles, which can be used to calculate the fraction of particles containing soot, soot particle size distributions and total mass and number, and coating thickness for soot particles. For example, soot aerosol optical properties and CCN activity depend on the coating thickness. The work at the FMI includes development of the SP2 data analysis method, especially the method to calculate coating thickness, and both laboratory and field measurements. For example, measurements at Pallas, Finland, have showed that soot concentrations are low and practically all particles are thickly coated (Raatikainen et al., 2013b).

We have studied the approach to mitigate warming of Arctic climate by black carbon (BC) emissions reduction at mid-latitudes, especially in Europe ([www.maceb.fi](http://www.maceb.fi)). The impact of the current air quality and climate relevant legislation in the northern hemisphere on BC emissions, their transport to the Arctic, and eventually Arctic warming was investigated. We used the combination of emission data from both global (GAINS) and national (Finland, FRES) emission models; global (ECHAM5-HAM) and regional (REMO) atmospheric climate models; and measurements of BC concentrations in surface air and snow. Finally, the objective of the project is to transfer action procedures and experiences to assess and mitigate BC emissions from most important source sectors, e.g. small-scale wood burning.

### 3. Laboratory experiments and instrument development

In laboratory we have mainly studied nucleation, both unary and multicomponent nucleation. To the best of our knowledge, this is the first experimental work providing temperature dependent nucleation rate

measurements using a high efficiency particle counter with a cutoff- size of 1.5 nm together with direct measurements of gas phase sulfuric acid concentration (Brus et al., 2011).

The influence of total pressure on homogeneous nucleation was investigated in cooperation with researchers from University of Cologne, Germany. The results fit well to previously published data of pressure effect measurements in alcohols series and also agree with theoretical predictions (Görke et al, 2010).

The growth of nanoparticles produced by homogenous nucleation of H<sub>2</sub>SO<sub>4</sub> and water was studied in a laminar flow tube at wide range of temperatures 283-303 K, under dry (a relative humidity of 1%) and wet conditions (relative humidity of 30%) and residence times between 30 and 90 s. Results of this study are summarized in Škrabalová et al. (2013)

In instrument development we have found an undercounting feature of black carbon in Multi Angle Absorption Photometer (MAAP). This was found during field experiments in polluted areas and occurs with high concentration. This was quantified with laboratory experiments and a method to correct for this has been proposed (Hyvärinen et al., 2013).

#### 4. Field campaigns

We have been conducting a series of cloud campaigns in Pallas-Sodankylä Global GAW station. The first Pallas Cloud Experiment (PaCE) was held in 2004, second in 2005, third one in 2009 and fourth in 2012. The wide range of instrumentation used in this campaign allowed us to investigate in deep the physico-chemical properties of aerosol, cloud droplet activation and hygroscopicity of aerosol particles and also directly the cloud particle phase. The results of this campaign has been partly analysed (Brus et al., 2013a) and presented also here (Brus et al., 2013b). The group also participated in an international cloud campaign held in January and February 2013 at Cézeaux –Opme-puy-de-Dôme (CO-PDD), Clermont-Ferrand, France.

The group started flight measurements using a modified short SC7 skyvan airplane in summer 2012. Several vertical profiles of aerosol and CCN numbers, aerosol chemistry and scattering, as well as GHG and trace gases have been measured during summer 2012 and winter and spring 2013. This data have been used to study e.g. nitrate partitioning in aerosol phase at higher altitudes, as well as the occurrence of layers of small particles (Asmi et al., 2013). In spring 2013 flights were organized together with an EU-pegasos project, to fly simultaneously using different platforms and complementing instrumentation. In winter and spring 2013, particulate and gaseous emissions from ships were measured using two different airplanes and a helicopter (Lihavainen et al., 2013).

The group has been active also in finding out the effects of black carbon to snow properties. For example the spatial and temporal dynamics of black carbon in the snowpack has been investigated. An example of this was the spatial variability of elemental carbon (a proxy of black carbon) that was addressed in surface snow on a metre scale (Svensson et al., 2013). Snow samples were collected at a clean site (Pallas, northern Finland) and a polluted site (Stockholm, Sweden) during winter and spring for comparison. The results showed metre scale horizontal variability in concentration, and that the relative variability in Pallas was much greater than in Stockholm despite the fact that Stockholm is closer to the black carbon sources. Post depositional processes in the snow (such as wind drift) are proposed to explain this feature. This study emphasize the importance of carefully choosing sampling sites and the importance of collecting multiple snow samples to obtain representative black carbon concentrations in an investigation area.

#### CONCLUSIONS

An overview has been presented of the group's recent activities. These supports the objectives of the group mentioned in the introduction, the collaborating universities and institutes and the goals of the

Finnish Center of Excellence 'Physics, Chemistry, Biology and Meteorology of Atmospheric Composition and Climate Change' program. Our work contributes to achieve the objectives in Work Packages 1, 2, 3 and 4.

## ACKNOWLEDGEMENTS

This research was supported by the Academy of Finland Center of Excellence program (project number 1118615), Academy of Finland project A4, LASTU, AERODA and COOL, EU LIFE + program, Ministry of Foreign Affairs of Finland, Nordic research and innovation initiative CRAICC (Cryosphere-atmosphere interactions in a changing Arctic climate) and Maj and Thor Nessling foundation.

## REFERENCES

- Anttila, T., D. Brus, A. Jaatinen, A.-P. Hyvärinen, N. Kivekäs, S. Romakkaniemi, M. Komppula, and H. Lihavainen (2012): Relationships between particles, cloud condensation nuclei and cloud droplet activation during the third Pallas Cloud Experiment. *Atmospheric Chemistry and Physics*, 12, 11435-11450.
- Anttila, T., J. Leppä, and H. Lihavainen (2013a) A novel method to determine the growth rate of a growing particle mode. Conference abstract, abstracts of EAC 2013
- Asmi, A., et al., (2012a) Aerosol decadal trends – Part 2: In-situ aerosol particle number concentrations at GAW and ACTRIS stations, *Atmos. Chem. Phys. Discuss.*, 12, 20849-20899
- Asmi E., V. Kondratyev, D. Brus, H. Lihavainen, T. Laurila, M. Aurela, T. Uttal, V. Ivakhov and A. Makshtas: Secondary particle formation in Arctic Russia, abstracts of EAC 2013.
- Asmi E., D. Brus, S. Carbone, R. Hillamo, J. Hatakka, T. Laurila, H. Lihavainen, E. Rouhe, S. Saarikoski and Y. Viisanen: Airborne measurements of aerosol particle physical, optical and chemical properties in Finland, abstracts of EAC 2013
- Asmi E., N. Kivekäs, V.M. Kerminen, M. Komppula, A. Hyvärinen, J. Hatakka, Y. Viisanen, and H. Lihavainen (2011) Secondary new particle formation in Northern Finland Pallas site between the years 2000 and 2010, *Atmos. Chem. Phys.*, 11, 12959-12972
- Brus, D., K. Neitola, A.-P. Hyvärinen, T. Petäjä, J. Vanhanen, M. Sipilä, P. Paasonen, M. Kulmala, and H. Lihavainen (2011) Homogenous nucleation of sulfuric acid and water at close to atmospherically relevant conditions, *Atmos. Chem. Phys.*, 11, 5277-5287, doi:10.5194/acp-11-5277-2011
- Brus D., E. Asmi, T. Raatikainen, K. Neitola, M. Aurela, U. Makkonen, J. Svensson, A.-P. Hyvärinen, A. Hirsikko, H. Hakola, R. Hillamo, and H. Lihavainen: Ground-based observations of aerosol and cloud properties at sub-arctic Pallas GAW-station, Pallas Cloud Experiment (PaCE 2012); *this issue*.
- Brus D., K. Neitola, E. Asmi, M. Aurela, U. Makkonen, J. Svensson, A.-P. Hyvärinen, A. Hirsikko, H. Hakola, R. Hillamo, and H. Lihavainen: Pallas cloud experiment, PaCE 2012, 19th International Conference: NUCLEATION AND ATMOSPHERIC AEROSOLS, 23–28 June 2013, Fort Collins, Colorado, USA, AIP Conf. Proc. 1527, pp. 964-967; doi: <http://dx.doi.org/10.1063/1.4803433>
- Cerully K. M., T. Raatikainen, S. Lance, D. Tkacik, P. Tiitta, T. Petäjä, M. Ehn, M. Kulmala, D. R. Worsnop, A. Laaksonen, J. N. Smith, and A. Nenes. Aerosol hygroscopicity and CCN activation kinetics in a boreal forest environment during the 2007 EUCAARI campaign, *Atmos. Chem. Phys.*, 11, 12369–12386, 2011
- Collaud Coen, M., et al (2012), Aerosol decadal trends – Part 1: In-situ optical measurements at GAW and IMPROVE stations, *Atmos. Chem. Phys. Discuss.*, 12, 20785-20848
- Finessi E., S. Decesari, M. Paglione, L. Giulianelli, C. Carbone, S. Gilardoni, S. Fuzzi, S. Saarikoski, T. Raatikainen, R. Hillamo, J. Allan, Th. F. Mentel, P. Tiitta, A. Laaksonen, T. Petäjä, M. Kulmala, D. R. Worsnop, and M. C. Facchini. Determination of the biogenic secondary organic aerosol fraction in the boreal forest by NMR spectroscopy, *Atmos. Chem. Phys.*, 12, 941–959, 2012
- Görke H., Neitola K., Brus D., Hyvärinen A.-P., Wölk J., Strey R.: Influence of the carrier gas pressure of

- homogeneous nucleation of n-propanol measured in a laminar flow diffusion chamber, Abstract Book of the International Aerosol Conference 2010, Abstract 6D1, Helsinki, Finland (2010).
- Hirsikko, et al., Y.: Observing wind, aerosol particles, cloud and precipitation: Finland's new ground-based remote-sensing network, *Atmos. Meas. Tech. Discuss.*, 6, 7251-7313, doi:10.5194/amtd-6-7251-2013, 2013.
- Hyvärinen, A.-P., P. Kolmonen, V.-M. Kerminen, A. Virkkula, A. Leskinen, M. Komppula, J. Hatakka, J. Burkhardt, A. Stohl, P. Aalto, M. Kulmala, K. E. J. Lehtinen, Y. Viisanen, and H. Lihavainen (2011a) Aerosol black carbon at five background measurement sites over Finland, a gateway to the Arctic, *Atmospheric Environment*, 45, 24, 4042-4050, doi:10.1016/j.atmosenv.2011.04.026. 2011a.
- Hyvärinen, A.-P., Raatikainen, T., Brus, D., Komppula, M., Panwar, T. S., Hooda, R. K., Sharma, V. P., and Lihavainen, H.: Effect of the summer monsoon on aerosols at two measurement stations in Northern India – Part 1: PM and BC concentrations, *Atmos. Chem. Phys.*, 11, 8271-8282, doi:10.5194/acp-11-8271-2011, 2011b.
- Hyvärinen, A.-P., Raatikainen, T., Komppula, M., Mielonen, T., Sundström, A.-M., Brus, D., Panwar, T. S., Hooda, R. K., Sharma, V. P., de Leeuw, G., and Lihavainen, H.: Effect of the summer monsoon on aerosols at two measurement stations in Northern India – Part 2: Physical and optical properties, *Atmos. Chem. Phys.*, 11, 8283-8294, doi:10.5194/acp-11-8283-2011, 2011c.
- Hyvärinen A.-P., H. Al-Jeelani, M. Alghamdi, T. Hussein, M. Khodeir, H. Lihavainen, M. Kulmala, and A. Laaksonen: Particle size distribution measurements at Hada Al Sham, Western Saudi Arabia, *19th International Conference Nucleation and Atmospheric Aerosols, Book of Abstracts*, pp. 602-603, Fort Collins, CO, USA, 23-28 June (2013).
- Hyvärinen, A.-P., Vakkari, V., Laakso, L., Hooda, R. K., Sharma, V. P., Panwar, T. S., Beukes, J. P., van Zyl, P. G., Josipovic, M., Garland, R. M., Andreae, M. O., Pöschl, U., and Petzold, A.: Correction for a measurement artifact of the Multi-Angle Absorption Photometer (MAAP) at high black carbon mass concentration levels, *Atmos. Meas. Tech.*, 6, 81-90, doi:10.5194/amt-6-81-2013, 2013.
- Lihavainen H., E. Asmi, J.-P. Jalkanen, A. Hyvärinen, T. Laurila, J. Walden and R. Hillamo; Airborne measurements of ship emissions, abstracts of EAC 2013.
- Neitola, K., E. Asmi, M. Komppula, A.-P. Hyvärinen, T. Raatikainen, T.S. Panwar, V.P. Sharma, and H. Lihavainen., 2011, New particle formation infrequently observed in western Himalayas – why?, *Atmos. Chem. Phys.*, 11, 8447-8458, doi:10.5194/acp-11-8447-2011
- Panwar T.S., R.K. Hooda, H. Lihavainen, A.-P. Hyvärinen, V.P. Sharma, and Y. Viisanen, Atmospheric aerosols at a regional background Himalayan site – Mukteshwar, India, *Environmental Monitoring and Assessment*, 10.1007/s10661-012-2902-8, 2012
- Raatikainen T., A. Nenes, J.H. Seinfeld, R. Morales, R.H. Moore, T.L. Latham, S. Lance, L.T. Padró, J.J. Lin, K.M. Cerully, A. Bougiatioti, J. Cozic, C.R. Ruehl, P.Y. Chuang, B.E. Anderson, R.C. Flagan, H. Jonsson, N. Mihalopoulos, and J.N. Smith. Worldwide data sets constrain the water vapor uptake coefficient in cloud formation, *P. Nat. Acad. Sci. USA*, 110 (10) 3760-3764, 2013a
- Raatikainen T., et al. (2013b), Black carbon concentrations and coating thickness at Pallas, Finland, *This issue*
- Škrabalová, L., D. Brus, T. Antilla, V. Ždímal, and H. Lihavainen (2013). Growth of sulphuric acid nanoparticles under wet and dry conditions. *Atmospheric Chemistry and Physics Discussions*, accepted.
- Svensson, J., Ström, J., Hansson, M., Lihavainen, H., Kerminen, V.-M.: Observed metre scale horizontal variability of elemental carbon in surface snow. *Environmental Research Letters*, 8, 034012, doi:10.1088/1748-9326/8/3/034012.
- Wood, CR, Järvi, L, Kouznetsov, RD, Nordbo, A, Joffre, S, Drebs, A, Vihma, T, Hirsikko, A, Suomi, I, Fortelius, C, O'Connor, E, Moiseev, D, Haapanala, S, Moilanen, J, Kangas, M, Karppinen, A, Vesala, T, Kukkonen, J: An overview on the Urban Boundary-layer Atmosphere Network in Helsinki, accepted to BAMS, doi: 10.1175/BAMS-D-12-00146.1, 2013.

**RHIZOSPHERE PROCESSES PLAY AN IMPORTANT ROLE IN SOIL ORGANIC MATTER  
DECOMPOSITION AND GREENHOUSE GAS FLUXES IN BOREAL LANDSCAPE; SUMMARY OF SOIL  
RESEARCH CARRIED OUT AT FCoE DURING THE SECOND FCoE PERIOD (2009-2013)**

J. PUMPANEN<sup>1</sup>, J. HEINOSALO<sup>2</sup>, M. PIHLATIE<sup>3</sup>, H. AALTONEN<sup>4</sup>, F. BERNINGER<sup>1</sup>, J. BÄCK<sup>1</sup>,  
P. HARI<sup>1</sup>, A.-J. KIELOAHO<sup>2</sup>, J.F.J. KORHONEN<sup>3</sup>, K. KÖSTER<sup>1</sup>, A. LINDÉN<sup>1</sup>, L. KULMALA<sup>1</sup>, M.  
KULMALA<sup>3</sup>, E. NIKINMAA<sup>1</sup>, A. OJALA<sup>4</sup>, T. RASILO<sup>5</sup> and T. VESALA<sup>3</sup>

<sup>1</sup>Department of Forest Sciences,  
P.O. Box 27, FIN-00014 University of Helsinki, Finland

<sup>2</sup>Department of Food and Environmental Sciences,  
P.O. BOX 56, FIN-00014 University of Helsinki, Finland

<sup>3</sup>Department of Physics, Division of Atmospheric Sciences,  
P.O. BOX 48, FIN-00014 University of Helsinki, Finland

<sup>4</sup>Department of Environmental Sciences, University of Helsinki, Lahti, Finland

<sup>5</sup>Département des sciences biologiques  
Université du Québec à Montréal, C.P. 8888, Succursale centre-ville  
Montréal QC H3C 3P8, Canada

**OVERVIEW OF THE PERSONNEL DEVELOPMENT DURING THE 2<sup>ND</sup> FCoE**

In 2009-2013 soil research at FCoE was expanding rapidly. We opened up new research areas such as the emissions of biogenic volatile compounds (BVOCs) from soil, lateral carbon transport and its importance for landscape scale carbon balance and the effect of easily decomposable carbon on the decomposition of soil organic matter (SOM) and the effect of disturbances on soil carbon cycle. Due to growing number of research topics, the number of personnel working on soil related studies increased rapidly. We got two Academy Researcher fellowships (Jukka Pumpanen and Jussi Heinonsalo) and 2 post-doctoral fellowships (Mari Pihlatie from Academy of Finland and Kajar Köster from Estonian Science Foundation and Academy of Finland) and several PhD student grants from different foundations (e.g. Janne Korhonen, Hermann Aaltonen and Antti-Jussi Kieloaho). Funding from Academy of Finland also helped us to recruit new PhD students (Aki Lindén, Minna Santalahti and Heli Miettinen) and several MSc students. During the second FCoE period 3 PhD theses related to soil and forest floor greenhouse gas fluxes were completed (Liisa Kulmala 2011 'Photosynthesis of ground vegetation in boreal Scots pine forests', Hermann Aaltonen 2012 'Boreal forest soil as a source of BVOC emissions' and Terhi Rasilo 'Connecting silvan and lacustrine ecosystems: transport of carbon from forests to adjacent water bodies' 2013).

**SCIENTIFIC REVIEW OF THE TOPICS RELATED TO SOIL RESEARCH IN THE 2<sup>ND</sup> FCoE BETWEEN 2009-  
2013**

The research was focused on interactions of soil processes with atmosphere and the greenhouse gas fluxes (CO<sub>2</sub>, CH<sub>4</sub>, N<sub>2</sub>O, Biogenic volatile organic compounds BVOCs and volatile organic nitrogen compounds VONs) between the soil and the atmosphere and the underlying processes. The response of forest soil to rising atmospheric CO<sub>2</sub> concentration and rising temperature, and their feedback effects on greenhouse gases and aerosols in the atmosphere, and thus to the radiative forcing of the atmosphere, are key questions when predicting the future climate.

Plant growth and carbon allocation in boreal forest ecosystems depend on the supply of recycled nutrients within the forest ecosystem, because the external inputs in the form of atmospheric

deposition and weathering are very low compared to the total requirement. Recent studies have shown that plants emit root exudates rich in carbohydrates which sustain mycorrhizal fungal symbionts, but also other groups of specialized micro-organisms (Högberg and Read, 2006, Pumpanen et al., 2009; Heinonsalo et al., 2010, Pumpanen et al. 2012). In microcosm experiment, we observed that the amount of carbon allocated to root and rhizosphere respiration was about 9–26%, and the amount of carbon allocated to root and ectomycorrhizal biomass about 13–21% of the total assimilated CO<sub>2</sub> (Pumpanen et al., 2009, Heinonsalo et al., 2010). The flux of carbon belowground stimulates the decomposition of SOM and nitrogen uptake of trees (Drake et al., 2011, Phillips et al., 2011). It has been suggested that root exudates and other easily decomposable carbon could enhance the decomposition of old SOM (Fontaine et al., 2007, Kuzyakov 2010) and turnover rates of nitrogen in the rhizosphere with possible growth enhancing feedback in vegetation (Phillips et al. 2011). In our ongoing studies, we have also observed that the root exudates and other easily decomposable carbon increase mineralization of old recalcitrant SOM. This was shown both in the age of respired CO<sub>2</sub> from the soil and <sup>15</sup>N isotopic signal of the trees (Lindén et al., 2013 submitted manuscript).

In coupled climate-carbon cycle models, biological activity of soils is usually driven by abiotic factors such as temperature and moisture (Conant et al., 2011). However, in nature the effects of temperature are coupled with other environmental factors such as irradiation, and allocation of carbon belowground (Reichstein et al., 2005), which are seasonally and geographically highly variable. Plant growth and carbon allocation in boreal forest ecosystems depends on the supply of recycled nutrients within the forest ecosystem, because the external inputs in the form of atmospheric deposition are very low. In nitrogen limited boreal forest ecosystems the biologically available nitrogen (NH<sub>4</sub> and NO<sub>3</sub>) is in short supply although the amount of N bound to SOM may be large (Korhonen et al. 2013). Upon the decomposition of lignocellulose, the proportion of compounds with higher nitrogen content increases while the proportion of compounds containing carbohydrates (hemicellulose and cellulose) decreases. Therefore, there is a large pool of immobilized nitrogen in the slowly decomposing SOM pool (Hättenschwiler and Vitousek 2000).

Nitrogen balance of boreal forests and peat lands have been one of the focal points of the soil research conducted in the FCoE. Korhonen et al. (2013) showed that in the boreal forest stand at SMEARII station nitrogen uptake and retranslocation were of same importance as sources of N for plant growth. Most of the nitrogen taken up originated from decomposition of organic matter, and the fraction of nitrogen that could originate directly from deposition was about 30%. Dry deposition and organic nitrogen in wet deposition contributed over half of the input in deposition. Total output of nitrogen from the site was only 0.4 kg N ha<sup>-1</sup> yr<sup>-1</sup>, the most important outputs being atmospheric N<sub>2</sub>O emission and organic nitrogen flux in drainage flow. Kieloaho et al. (2013 in press) observed seasonal cycle in amine concentrations in air samples collected from the forest canopy at SMEARII station. The amine concentrations seem to be linked with vegetation, soil activity, and litterfall, rather than to other trace gases in the atmosphere. Due to the large pool of organic nitrogen soil can also be a substantial source of organic amine compounds. This is because the most common form of N in soils is amino acid N (20–50% of the total N as amino N) (Senwo and Tabatabai, 1998). Recently, we carried out a mesocosm experiment where amine formation in forest soil was induced with different enzyme treatments and artificial glucose amendments. The preliminary results show that amine formation is closely linked with root system and its processes. In more detailed laboratory conditions, the main pool of amines in soil seem to be certain ectomycorrhizal fungi that also have high proteolytic activities (Heinonsalo et al. unpublished).

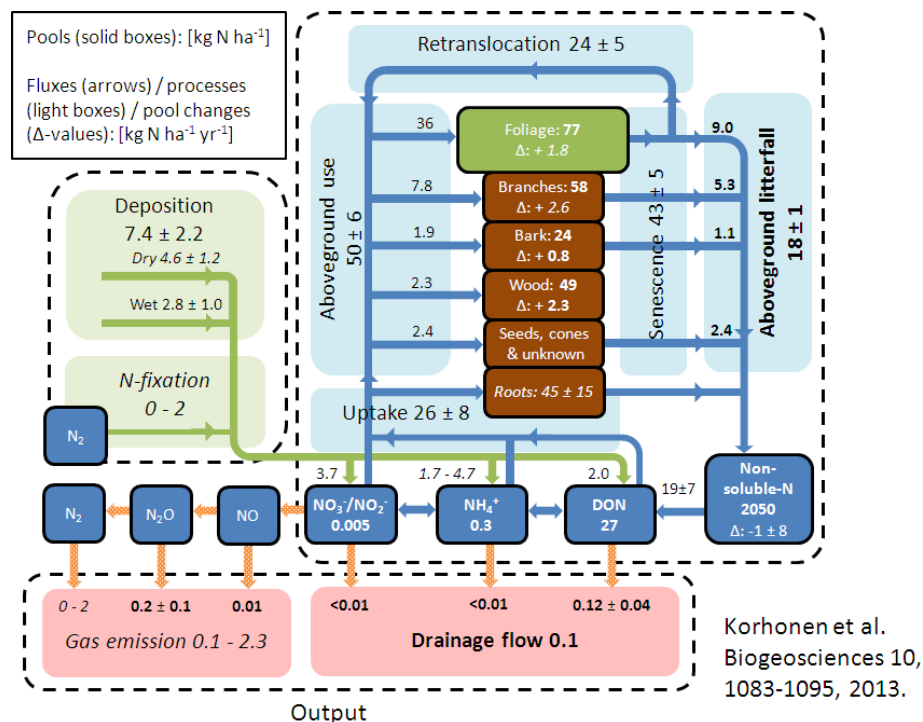


Figure. 1 Nitrogen balance of a boreal Scots pine stand at SMEARII (Korhonen et al. 2013).

Recent studies have shown that the nitrogen mineralization is stimulated by increases in the flux of carbon belowground resulting in feedbacks to nitrogen cycling and nitrogen uptake of the trees (Drake *et al.*, 2011 and Phillips *et al.*, 2011). This may further increase net primary productivity of the forest ecosystem (Hari and Kulmala, 2008). However, the feedback mechanisms are poorly known and not quantified so that they could be incorporated in coupled climate-carbon cycle models (Arneeth *et al.*, 2010, Drake *et al.*, 2011, Conant *et al.*, 2011). We are studying the processes underlying nitrogen acquisition of trees and ground vegetation from old recalcitrant SOM by using stable isotopes (<sup>15</sup>N, <sup>13</sup>C), radiocarbon dating, mesocosm and field experiment as well as process modeling. According to our results, the amount of easily decomposable carbon (glucose) affects the source of nitrogen of *Pinus sylvestris* (Lindén *et al.*, 2013 submitted). We have also observed that the activity of belowground carbon sink is reflected to the aboveground photosynthesis in the common boreal tree species (Pumpanen *et al.*, 2012). The photosynthetic rate decreased in low soil temperatures (7–12°C) and increased at higher temperatures (12–15°C and 16–22°C). The net CO<sub>2</sub> exchange and seedling biomass did not increase with increasing temperature due to a concomitant increase in carbon assimilation and respiration rates. Biomass accumulation was highest in the medium temperature (12–15°C).

Fire and storm are the most important natural disturbances in the boreal zone greatly influencing the structure, composition and functioning of forests. Although less than 1 % of the boreal forests burn each year, it is a significant land area since boreal forests cover 15% of the Earth's land area. It is expected that with future climate change the fires in boreal forests will become more frequent as a result of long droughts. Already now, large forest fires are common in Russia and Canada in summer. During a fire, SOM, mostly carbon, is released from the forest biomass rapidly to the atmosphere through combustion, and simultaneously the mineralized N is released in the soil in the form of NO<sub>3</sub><sup>-</sup> and NH<sub>4</sub><sup>+</sup> favoring the re-establishment of vegetation during the first years of succession. However, the long term consequences of fire on the carbon and nitrogen cycle are largely unknown. For instance, we do not know how the turnover rate of the remaining SOM will change as a result of changes in the fire interval. In 2010, we established a chronosequence study at SMEAR I station and its surrounding forests in Värriö Strict Nature Reserve for studying the processes underlying carbon and nitrogen cycle at taiga forests exposed to fire. Until now, we have conducted soil CO<sub>2</sub> efflux measurements as well as above and below ground carbon and nitrogen pool inventories. We observed

that in the fire chronosequence fungal biomass determines the turnover rate of SOM (Köster *et al.*, 2013 submitted). We also noticed that the SOM turnover rate was higher the older the forest stand was, and we assume that this was related to the increased below ground carbon allocation needed for nutrient acquisition from recalcitrant SOM. Currently, we are studying how the decomposition activity in the soil is related to the activity of enzymes and microbial population structure. This work is based on molecular biological methods such as high-throughput pyrosequencing.

The chronosequence approach was also used when studying the role of ground vegetation in the carbon exchange of boreal forest ecosystems (Kulmala *et al.* 2011a,b). A process model for estimating the gross primary productivity (GPP) of the most common shrub species was developed by Kulmala *et al.* (2011a), and used for determining the GPP of a chronosequence of clear-cut sites around Hyytiälä (Fig. Kulmala *et al.*, 2011b). In boreal forests ground vegetation plays an important role in the carbon exchange; its contribution to total annual GPP was highest in 6 to 9-year-old forest sites (about 350 g C m<sup>-2</sup>) and decreased during the forest succession.

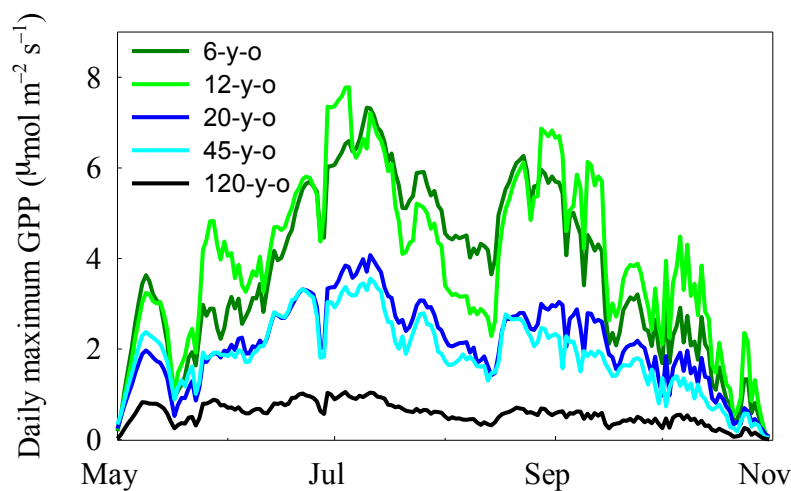


Figure 2. Kulmala *et al.* 2011 Daily maximum rates of photosynthesis of ground vegetation at different aged Scots pine forests in Southern Finland (Kulmala *et al.* 2011b)

The role of aquatic systems as a net sink or a source for atmospheric CO<sub>2</sub> is presently under debate. In a recent Nature paper (Yvon-Durocher *et al.*, 2012), we showed that the annual ecosystem respiration in aquatic ecosystems shows a substantially greater temperature response compared to terrestrial ecosystems. This can be due to differences in the importance of other variables such as primary production and allochthonous/terrestrial carbon inputs to the aquatic systems. When precipitation or other processes push large volumes of organic matter from the land into nearby lakes, this carbon effectively disappears from the terrestrial carbon budget if - as usual - lacustrine fluxes are ignored. We tracked the flow of carbon into and out of a lake in Southern Finland over five years and found that the lake was a net source of carbon, emitting from 70 and 100 g C m<sup>-2</sup> each year. When compared against the surrounding old growth forest, which was a net carbon sink, the lacustrine emissions were enough to offset about 10% of the forest's annual carbon sequestration (Huotari *et al.*, 2011). It is obvious that aquatic carbon fluxes must be accounted for when estimating carbon fluxes at landscape and regional level. This is especially true in the boreal zone where lakes are abundant (Hanson *et al.*, 2004; Wetzel, 2001). The CO<sub>2</sub> which is transported from aquatic ecosystems to the atmosphere originates from the surrounding soils and wetlands, from mineralization of organic carbon and from respiration of roots and mycorrhiza. Thus, the biological processes in the terrestrial ecosystem (e.g. photosynthesis, respiration and decomposition) are linked with the aquatic processes. In our recent studies, we observed that CO<sub>2</sub> concentrations in stream and lake are indeed controlled by the water flushing from the surrounding forest soil through the riparian zone during and after heavy rain events (Rasilo *et al.*, 2012).

For monitoring the CO<sub>2</sub> concentrations in the aquatic systems and in the soil profile, we developed a novel method using non-dispersive infrared CO<sub>2</sub> sensors (Hari *et al.*, 2008). The system has been successfully used in our group for measuring photosynthesis and respiration of planktonic algae (Hari *et al.*, 2008), vertical distribution of respiration in the soil profile and the seasonal pattern of root and rhizosphere respiration (Pumpanen *et al.*, 2008) and changes in the CO<sub>2</sub> concentrations in the soil, riparian zone, stream and lake continuum following rain events (Rasilo *et al.*, 2012).

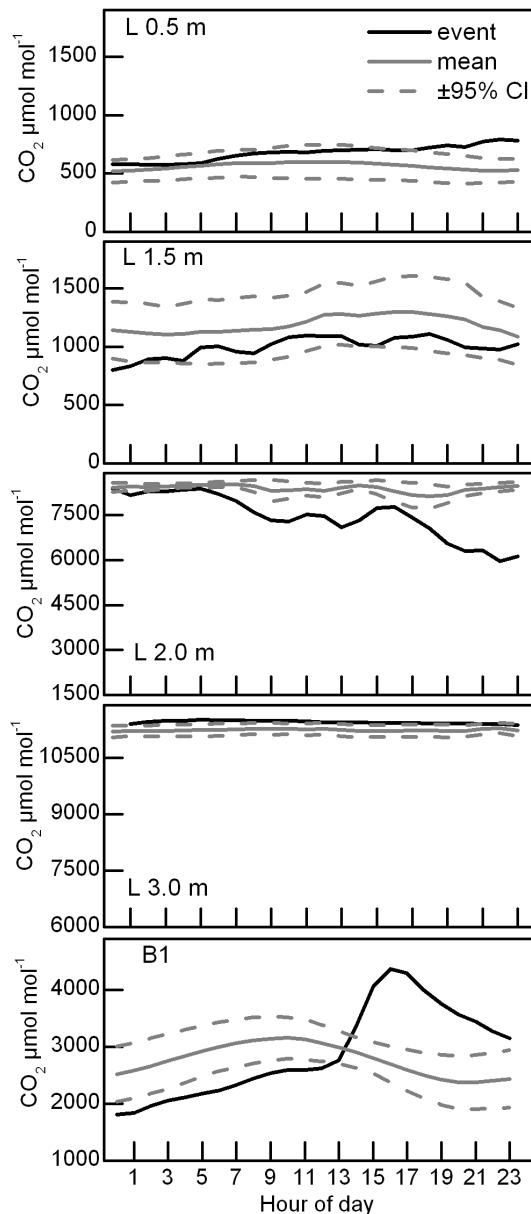


Figure 3. Time lags in CO<sub>2</sub> concentration following rain event at 0.5, 1.5, 2.0 and 3.0 m depth in the lake and in outlet stream 150 m downs stream from the lake. The gray lines denote 24 h average CO<sub>2</sub> concentrations over a 7 day period prior to the rain event and the black line is the CO<sub>2</sub> concentration after the rain event (Rasilo *et al.* 2012).

Riparian zone, i.e. the interface between terrestrial and aquatic ecosystems is an important hotspot area having important implications both in the lateral transport of carbon and nitrogen and as a source

of the important greenhouse gases CO<sub>2</sub>, CH<sub>4</sub>, N<sub>2</sub>O and also BVOCs. In lakes greenhouse gases (CO<sub>2</sub>, CH<sub>4</sub>, N<sub>2</sub>O) accumulate under the ice during winter and are released rapidly after ice out. The proportion of aromatic compounds in the water percolating through the soil profile increases as it passes through the riparian zone (Rasilo *et al.*, manuscript 2013) indicating that the riparian zone also acts as a source of aromatic and volatile compounds. However, the processes affecting the water quality in the pathway from the terrestrial to the aquatic ecosystems are still poorly known.

Forest floor is also a significant source of BVOCs (Aaltonen *et al.* 2011, Bäck *et al.* 2010), and a potential source of volatile organic nitrogen compounds (VON) (Kieloaho *et al.*, 2013). Emissions of most common BVOCs  $\alpha$ -pinene,  $\Delta^3$ -carene and camphene,  $\beta$ -pinene, limonene, isoprene and sesquiterpenes were highest in spring and autumn (Aaltonen *et al.*, 2011). The most abundant BVOCs were monoterpenes  $\alpha$ -pinene,  $\Delta^3$ -carene and camphene which contributed over 90% of the soil BVOC emissions. Monoterpene emissions were  $5.04 \mu\text{g m}^{-2} \text{h}^{-1}$ . Important steps forward in soil BVOC and VON research in the FCoE were the development of automated continuous chambers for BVOC measurements (Aaltonen *et al.*, 2013) and a sampling system for atmospheric VON measurements (Kieloaho *et al.*, 2013). The BVOC chambers were connected to a proton transfer reaction mass spectrometer (PTR-MS) which enabled continuous online measurements of molecular masses of the BVOCs. The continuous measurements provided first information on the relationship between soil surface BVOC emissions, relative humidity (RH), temperature, photosynthetically active radiation (PAR) and net CO<sub>2</sub> exchange of forest floor. The automated chamber measurements revealed a clear diurnal variation in BVOC fluxes, a positive correlation between air temperature and BVOC emissions and a negative correlation between RH and BVOC emissions, but no clear correlations with PAR and net CO<sub>2</sub> exchange of the forest floor (Aaltonen *et al.*, 2013). The results suggest that to forest floor BVOC fluxes forest floor vegetation may be more important than soil itself. We developed and tested at SMEAR II station a measuring systems for atmospheric VON compounds (amines), and the first measurements revealed a clear seasonal variation in the VON concentrations, and similarly to BVOCs, the results suggest that many of the atmospheric amines could originate from the forest floor (Kieloaho *et al.*, 2013). In future, this measurement system will be adapted to measurements of VON fluxes from the forest floor. During the second FCoE period, we also developed a method to measure the BVOC concentrations in the snow pack *in situ* and calculated the winter time BVOC production and consumption in the snow pack using the concentration gradient method (Aaltonen *et al.*, 2012). We measured 20 VOCs from the snowpack, monoterpenes being the most abundant group with concentrations varying from 0.11 to  $16 \mu\text{g m}^{-3}$ . Sesquiterpenes and oxygen containing monoterpenes were also detected. Inside the pristine snowpack, the concentrations of terpenoids decreased from soil surface towards the surface of the snow, suggesting soil as the source for terpenoids. Our results from winter time BVOC measurements also showed that soil processes are active and efficient VOC sources also during winter, and that natural or human disturbance can increase forest floor VOC concentrations substantially.

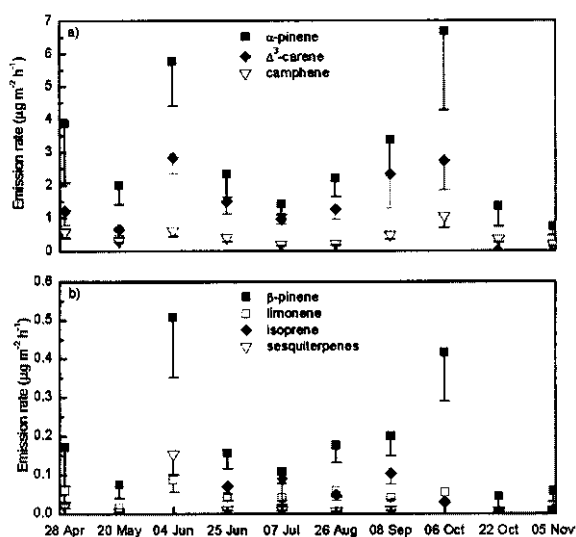


Figure 3. Seasonal pattern of BVOC emissions with manual chamber measurements (Aaltonen *et al.* 2011)

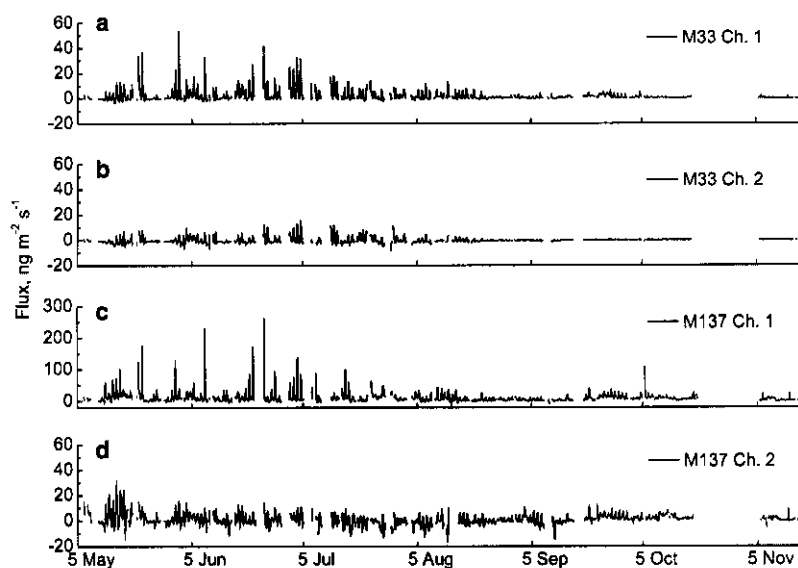


Figure 4. Seasonal pattern of BVOC emissions with automated continuous chamber measurements (Aaltonen et al. 2013).

## CONCLUSIONS

To sum it up, soil plays an important and active role in controlling the greenhouse gas balance in the atmosphere and it also affects indirectly the radiative forcing of the atmosphere through various feedback effects. In the future, we will emphasize the process understanding in our studies by planning field and laboratory experiments for studying the connection between above and below ground parts of the forest ecosystem. We will also continue studying the role of lateral transport of greenhouse gases between the ecosystems e.g. the connection between aquatic and terrestrial systems. Incorporation of the feedback mechanisms of belowground carbon allocation, in particular the role of root exudates and ectomycorrhizal fungi, and mineralization of soil organic matter into the soil carbon decomposition models e.g. YASSO, will also be an important part of the research activity of the soil group in the next FCoE period. We will also study the role of disturbance and weather extremes such as drought events and fires on the biogeochemical processes in the forest ecosystems, because the frequency of disturbance events is expected to increase in the future as a result of climate change. Finally, last but not least we will strengthen our already strong methodological skills in greenhouse gas flux measurements (Pumpanen et al. 2004, Pihlatie et al. 2013) by organizing a new campaign to quantify errors related to N<sub>2</sub>O flux chamber measurements in 2014.

## ACKNOWLEDGEMENTS

This work was supported by Academy of Finland Research grants 218094, 263858, 259217, 138575, 21309, European Social Fund and Estonian Science Foundation “Mobilitas” grant MJD94 and Academy of Finland Centre of Excellence program (project no 1118615). We are grateful for the staff of Lammi Biological Station and Hyytiälä Forestry Field Station.

## REFERENCES

- Aaltonen, H., Aalto, J., Kolari, P., Pihlatie, M., Pumpanen, J., Kulmala M., Nikinmaa, E., Vesala, T. and Bäck, J. (2013) Continuous VOC flux measurements on boreal forest floor. **Plant and Soil** DOI 10.1007/s11104-012-1553-4.
- Aaltonen, H., Pumpanen, J., Hakola, H., Vesala, T., Rasmus, S. and Bäck, J. (2012b). Snowpack concentrations and estimated fluxes of volatile organic compounds in a boreal forest. – *Biogeosciences* **9**: 2033–2044
- Aaltonen, H., Pumpanen, J., Pihlatie, M., Hakola, H., Hellén, H., Kulmala, L., Vesala, T. and Bäck, J. (2011) Boreal pine forest floor biogenic volatile organic compound emissions peak in early summer and autumn. - *Agricultural and Forest Meteorology* **151**, 682-691
- Arneth, A., Harrison, S.P., Zaehle, S. et al. 2010. Terrestrial biogeochemical feedbacks in the climate system. *Nat. Geosci.* **3**(8),525-532.
- Bäck, J., Aaltonen, H., Hellén, H., Kajos, M., Patokoski, J., Taipale, R., Pumpanen, J. and Heinonsalo, J. (2010) Variable emissions of microbial volatile organic compounds (MVOCs) from root-associated fungi isolated from Scots pine. - *Atmospheric Environment* **44**, 3651-3659.
- Conant, R.T., Ryan, M.G., Ågren, G.I. et al.. 2011. Temperature and soil organic matter decomposition rates – synthesis of current knowledge and a way forward. *Glob. Change Biol.* **17**, 3392 – 3404.
- Drake, J.E. Gallet-Budynek, A., Hofmockel, K.S. et al. 2011. Increases in the flux of carbon belowground stimulate nitrogen uptake and sustain the long-term enhancement of forest productivity under elevated CO<sub>2</sub>. *Ecol. Lett.* **14**, 349-357.
- Fontaine, S., Barot, S., Barré, P. et al. 2007. Stability of organic carbon in deep soil layers controlled by fresh carbon supply. *Nature* **450**(8), 277-280.
- Hanson, P. C., Pollard, A. I., Bade, D. L., Predick, K., Carpenter, S. R. and Foley, J. A. 2004. A model of carbon evasion and sedimentation in temperate lakes. *Glob. Change Biol.* **10**, 1285-1298.
- Hari, P., Pumpanen, J., Huotari, J., Kolari, P., Grace, J., Vesala, T. and Ojala, A. 2008. High-frequency measurements of productivity of planktonic algae using rugged nondispersive infrared carbon dioxide probes. *Limnology and Oceanography: Methods* **6**: 347-354.
- Heinonsalo, J., Pumpanen, J., Rasilo, T., Hurme, K.-R. and Ilvesniemi, H. 2010. Carbon partitioning in ectomycorrhizal Scots pine seedlings. *Soil Biol. & Biochem.* **42** (9), 1614-1623
- Huotari, J., Ojala, A., Peltomaa, E., Nordbo, A., Launiainen, S., Pumpanen, J., Rasilo, T., Hari, P. and Vesala, T. 2011. Long-term direct CO<sub>2</sub> flux measurements over a boreal lake: Five years of eddy covariance data. *Geophys. Res. Lett.* doi: 10.1029/2011GL048753
- Hättenschwiler, S. and Vitousek, P.M. 2000. The role of polyphenols in terrestrial ecosystem nutrient cycling. *Tree* **15**(6), 238-243.
- Högberg, P. and Read, D.J. 2006. Towards a more plant physiological perspective on soil ecology. *Trends in Ecol. and Evol.* **21** (10),548-554.
- Kieloaho, A.-J., Hellén H., Hakola H., Manninen H.E., Nieminen T., Kulmala M. and Pihlatie M. 2013. Gas-phase alkylamines in a boreal Scots pine forest air. accepted to *Atmospheric Environment*

- Korhonen, J.F.J., Pihlatie, M., Pumpanen, J., Aaltonen, H., Hari, P., Levula, J., Kieloaho, A.-J., Nikinmaa, E., Vesala, T. and Ilvesniemi, H. 2013. Nitrogen balance of a boreal Scots pine forest. *Biogosciences* **10**, 1083-1095.
- Kulmala, L., Pumpanen, J., Hari, P., and Vesala, T. 2011. Photosynthesis of ground vegetation in different aged pine forests: Photosynthesis of ground vegetation in different aged pine forests: Effect of environmental factors predicted with a process-based model. *Journal of Vegetation Science* **22**, 96-110.
- Kulmala, L., Pumpanen, J., Kolari, P., Muukkonen, P., Hari, P. and Vesala, T. 2011. Photosynthetic production of ground vegetation in different aged Scots pine forests. *Canadian Journal of Forest Research* **41(10)**, 2020-2030, 10.1139/x11-121
- Kuzyakov, Y. 2010. Priming effects: Interactions between living and dead organic matter. *Soil Biol. & Biochem.* **42**, 1363-1371.
- Köster, K., Berninger, F., Lindén, A. and Pumpanen, J. 2013. Increases of fungal biomass drive Soil organic matter turnover in Boreal fire chronosequence. Submitted to *Ecosystems*.
- Lindén, A., Heinonsalo, J., Buchmann, N., Oinonen, M., Sonninen, E., Hiltavuori, E and Pumpanen, J. 2013. Contrasting effects of increased carbon input on SOM decomposition in boreal soil with and without living root system of *P. sylvestris*. Submitted to *Plant and Soil*.
- Phillips, R.P., Finzi, A.C. and Bernhardt, E.S. 2011. Enhanced root exudation induces microbial feedbacks to N cycling in a pine forest under long-term CO<sub>2</sub> fumigation. *Ecol. Lett.* **14**, 187-194
- Pihlatie, M., Christiansen, J.-R., Aaltonen, H., et al.. 2013. Comparison of static chambers to measure CH<sub>4</sub> emissions from soils. *Agricultural and Forest Meteorology* **(171– 172)**, 124– 136.
- Pumpanen, J., Kolari, P., Ilvesniemi, H. et al. 2004. Comparison of different chamber techniques for measuring soil CO<sub>2</sub> efflux. *Agricultural and Forest Meteorology* **123**, 159-176.
- Pumpanen, J., Ilvesniemi, H., Kulmala, L., et al. 2008. Respiration in boreal forest soil as determined from carbon dioxide concentration profile. *Soil Science Society of America Journal*. **72(5)**, 1187-1196.
- Pumpanen, J.S., Heinonsalo, J., Rasilo, T., Hurme, K. –R. and Ilvesniemi, H. 2009. Carbon balance and allocation of assimilated CO<sub>2</sub> in Scots pine, Norway spruce and Silver birch seedlings determined with gas exchange measurements and <sup>14</sup>C pulse labelling in laboratory conditions. *Trees-Structure and Function* **23**, 611-621.
- Pumpanen, J., Heinonsalo, J., Rasilo, T. and Ilvesniemi, H. 2012. The Effects of soil and air temperature on CO<sub>2</sub> exchange and net biomass accumulation in Norway spruce, Scots pine and Silver birch seedlings. *Tree Physiology* **32(6)**, 724-736.
- Rasilo, T., Ojala, A., Huotari, J. and Pumpanen, J. 2012. Rain induced changes in CO<sub>2</sub> concentrations in the soil – lake – brook continuum of a boreal forested catchment. *Vadose Zone Journal*. doi:10.2136/vzj2011.0039.
- Rasilo, T., Ojala, A., Huotari, J., Starr, M. and Pumpanen, J. 2013 Concentrations and quality of DOC along a boreal forested terrestrial-aquatic continuum. Submitted to *Journal of Fresh Water Science*.
- Reichstein, M., Falge, E., Baldocchi, D. et al. 2005. On the separation of net ecosystem exchange into assimilation and ecosystem respiration: review and improved algorithm. *Glob. Change Biol.* **11**, 1-16.
- Senwo, Z.N. and Tabatabai, M.A.1998. Amino acid composition of soil organic matter. *Biol. Fertil. Soils* **26(3)**, 235-242.

Wetzel, R. G. 2001. *Limnology, Lake and River Ecosystems*, Academic, 443 San Diego, Calif.

Yassaa, N., Song, W., Vanhatalo, A., Bäck, J. and Williams, J. (2012) Diel cycles of isoprenoids in the emissions of Norway spruce, four Scots pine chemotypes, and in Boreal forest ambient air during HUMPPA-COPEC-2010. - *Atmospheric Chemistry and Physics*, **12**, 7215–7229.

Yvon-Durocher, G., Caffrey, J.M., Cescatti, A., Dossena, M., del Giorgio, P., Gasol, J.M. , Montoya, J.M., Pumpanen J., Staehr, P.A., Trimmer, M., Woodward, G. and Allen, A.P. 2012. Reconciling differences in the temperature-dependence of ecosystem respiration across time scales and ecosystem types. *Nature*. **7408 (vol.487)**, 472-476

# ATMOSPHERIC AEROSOLS AND GASES: STUDY OF CHEMICAL COMPOSITION AND DETERMINATION OF PHYSICOCHEMICAL PROPERTIES OF INDIVIDUAL COMPOUNDS

M.-L. RIEKKOLA<sup>1</sup>, K. HARTONEN<sup>1</sup>, J. PARSHINTSEV<sup>1</sup>, T. LAITINEN<sup>1,2</sup>, M. JUSSILA<sup>1</sup>, H. JUNNINEN<sup>2</sup>, L. FEIJÓ BARREIRA<sup>1</sup>, T. PETÄJÄ<sup>2</sup>, and M. KULMALA<sup>2</sup>

<sup>1</sup>Laboratory of Analytical Chemistry, Department of Chemistry, P.O. Box 55, FI-00014, University of Helsinki, Finland

<sup>2</sup>Division of Atmospheric Sciences, Department of Physics, P.O. Box 64, FI-00014, University of Helsinki, Finland

Keywords: ATMOSPHERIC AEROSOLS, PRECURSOR GASES, SAMPLING, CARBON CLUSTERS

## INTRODUCTION

Secondary organic aerosol formation is one of the key issues in the atmospheric chemistry. In order to understand it thoroughly, information on chemical composition of atmospheric aerosols and gas phase compounds is needed. Aerosol chemical composition can be determined either, for example, on-line using mass spectrometric techniques or off-line by analysing filter samples. The same principles are applied for the gas phase composition, where mass spectrometry (proton transfer) is used for on-line analysis and e.g., denuders or traps- for off-line. Distribution of compounds between these two phases can be predicted theoretically with models utilizing vapour pressures, for example. All these techniques, however, suffer from disadvantages. On-line techniques do not separate compounds prior detection producing mixed spectrum and thus, isobaric ions are quantified as sum. Low time resolution is a main drawback of the off-line techniques. In addition, theoretical calculations for environmental modelling need numerous experimentally derived physicochemical constants of compounds to be determined. It is clear, that there is a need for new developments in this field.

Here we present several novel approaches for determination of aerosol and gas phase chemical composition. Solid phase microextraction (SPME) coupled to portable gas chromatograph-mass spectrometer (GC-MS) offers a new semi-online approach to determine gas phase composition with good time resolution. Technique is based on equilibrium, which may reveal some new facts about the behaviour of gaseous compounds. Portable analytical device reduces error associated with sample logistics. Absence of sample treatment increases the quality of the results due to authenticity of the samples, avoidance of solvent background, etc.

Since aerosol chemical composition depends e.g. on size, all-sized aerosol samples do not provide enough information. In this study, we utilized differential mobility analyser (DMA)- separated samples (Parshintsev et al. 2011) in order to determine chemical composition of ultrafine aerosol particles (20- and 30-nm). We focused on organosulfates in order to study their importance for the aerosol formation and growth. Samples were analysed by ultra-performance liquid chromatography- quadrupole- time-of-flight mass spectrometry (UPLC-q-TOFMS) and compounds which give sulphuric acid fragment in MS<sup>2</sup> experiment were detected.

As one of the key value for atmospheric chemistry, vapour pressure must be known for the majority of relevant compounds. Theoretically derived values are often incorrect and conventional experimental techniques are time consuming, laborious and require high quantities of pure compounds. Method based on comprehensive two-dimensional gas chromatography-time-of-flight mass spectrometry (GCxGC-TOFMS) offers a new, fast, cheap and easy way to determine vapour pressures of numerous compounds in complicated matrices simultaneously. Here, the method was developed and applied for the atmospheric aerosol samples.

One of the hot topics in aerosol science is soot. It may refer to black carbon, elemental carbon or carbon clusters depending on a measurement technique. Carbon clusters are often determined by mass spectrometric methods (Baumgardner, Popovicheva et al. 2012). The aerosol particles that contains significant amount of soot, affect local and global climate by changing the radiation balance of the Earth, cloud formation, and visibility. However, the soot measurement techniques today do not provide real quantitative data due to lack of reference materials. Here we demonstrate how the reference materials can be produced from 50 nm graphite particles suspended in toluene and used for the quantitative analysis of urban air 50 nm aerosol particles with laser AMS.

## METHODS

### *Solid-phase microextraction coupled to portable gas chromatograph-mass spectrometer for the determination of gas phase compounds*

To study gas phase composition simultaneously with aerosol filter sampling at SMEARII station, SMPE-GC-MS was utilized. The sampling set-up which was built in our laboratory is presented in Figure 1.

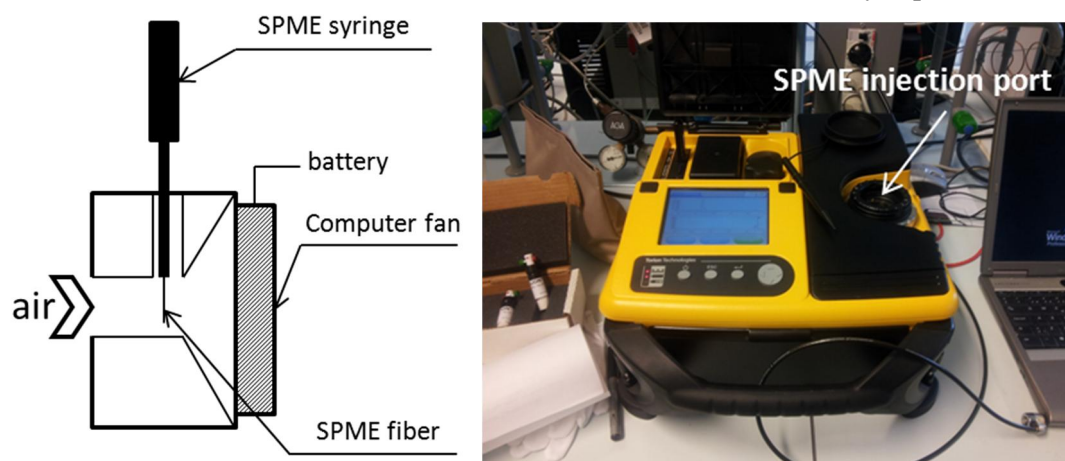


Figure 1. Scheme of the SPME sampling set-up (left) and portable GC-MS system (right).

Briefly, three orifices were made into polyoxymethylene (POM) holder: one for the sample air, one (gas tight) for the SMPE needle and one for the suction fan. The fan was needed to increase the sampling efficiency and it was operated using 12V battery which had to be recharged every second day. Polydimethylsiloxane-divinylbenzene (PDMS-DVB) fibers were used in SPME and collection time varied from one to four hours. During optimization step, several sampling sites were tested. Finally, two hour sampling near the main cottage of SMEARII station was selected. Samples were collected, and analysed immediately during five days from June 10<sup>th</sup> to 15<sup>th</sup>, 2013. Agilent ChemStation software was employed for the data analysis.

For the evaluation of the performance of the portable SPME-GC-MS system, four carefully selected compounds were used: 3-carene,  $\alpha$ -pinene, pinonaldehyde and *cis*-pinonic acid. Peaks of these model compounds were integrated and cross checked for correlations. As can be seen from Figure 2A, 3-carene and  $\alpha$ -pinene correlated well ( $r^2=0.837$ ). The result is in agreement with the literature for the measurement site (Hakola et al. 2000). However, if we assume that responses of these two terpenes are the same, 3-carene concentration was higher than that of  $\alpha$ -pinene. This can happen in Hyytiälä sometimes (Janson et al. 2001). Figure 2B demonstrates the correlation between  $\alpha$ -pinene and pinonaldehyde. Since the latter compound is produced solely from  $\alpha$ -pinene, this correlation is logical. Absence of correlation between  $\alpha$ -pinene and *cis*-pinonic acid is understandable, since acid can be produced by different reaction routes, either directly from  $\alpha$ -pinene or by oxidation of pinonaldehyde, for example (Fig. 2C) resulting in weak correlation as seen between pinonaldehyde and pinonic acid (Fig. 2D).

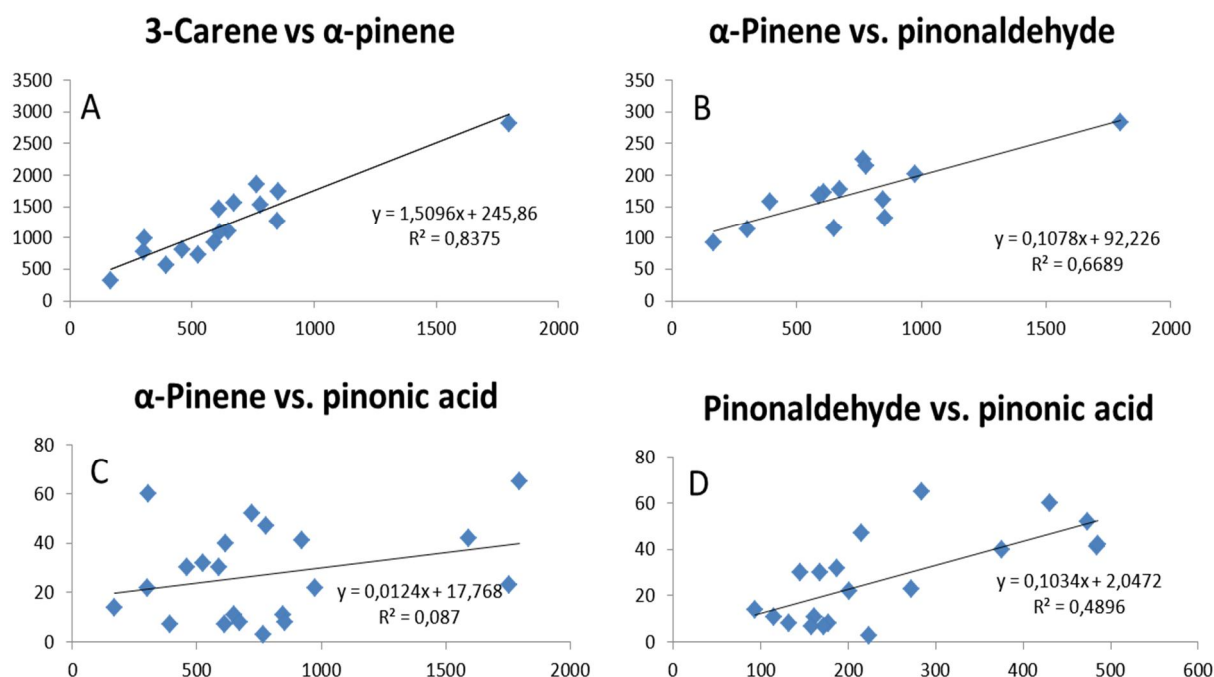


Figure 2. Correlation plots of peak areas of compounds determined by portable SPME-GC-MS.

### *Organosulfates in ultrafine particles*

Size segregated aerosol samples together with gas phase samples were collected at SMEARII station in spring-summer 2013. Samples from the first week (April 29<sup>th</sup>- May 10<sup>th</sup>) were analysed for the presence of organosulfates in the Laboratory of Aerosol Chemistry in the University of Århus, Denmark. UPLC-QTOFMS was used in all the experiments with parameters optimized for organosulfate analysis. Compounds producing sulphuric acid fragments in collision cell of the instrument were found in all the samples, however, abundances differed significantly. The highest peaks were found for 20-nm samples. 30-nm and gas phase samples contained only traces of organosulfates. Due to different DMA assisted collection systems designed for 20 and 30 nm, the sample flow rate was almost 7 times higher for 20 nm samples than for 30 nm samples. This partially explains the difference in abundances shown in Figure 3. The highest peak (around 16 min) was tentatively identified as organosulfate of pinonaldehyde (or any monoterpenealdehyde). The majority of other peaks were tentatively identified as organosulphates of  $\alpha$ -pinene oxidation products and isoprene with the help of study by Surratt et al. 2008. Since organosulfates represent a large fraction in the chromatogram of aerosol sample, their importance is obvious. However, due to absence of reference materials, determination of these compounds is still challenging.

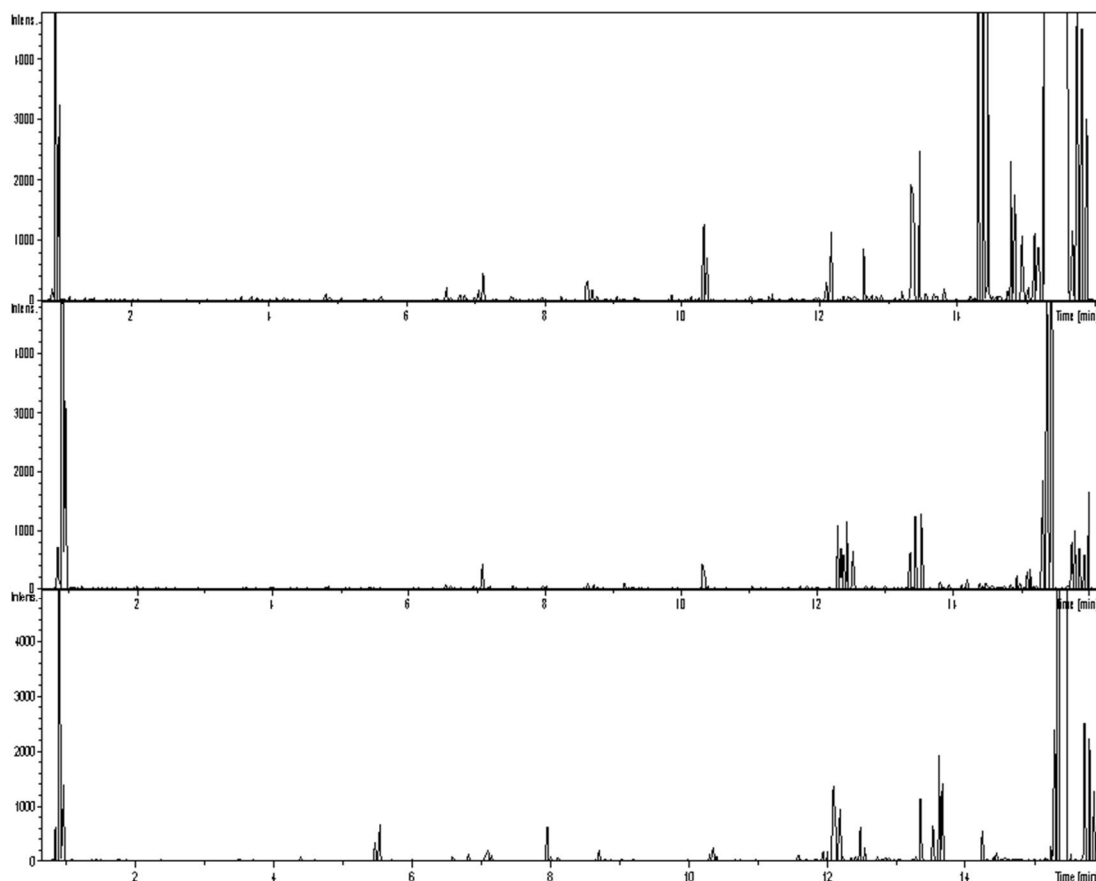


Figure 3. Extracted ion chromatograms ( $MS^2$ , displayed ion 96.96) from 20 nm particle sample (upper), 30 nm particle sample (middle) and gas phase sample (lower) collected at the SMEARII station on April 24<sup>th</sup>, 2013.

*A new way to determine vapor pressures of compounds in multicomponent systems by comprehensive two-dimensional gas chromatography coupled to time-of-flight mass spectrometry*

Vapor pressures of the oxidation products of terpenes (pinonaldehyde, caryophyllene aldehydes, pinic and *cis*-pinonic acids) were first determined by conventional GC-MS with a temperature gradient program and compared with vapor pressures determined by retention index method (Hartonen et al. 2013). A solution containing analytes and all the reference compounds of the study (51 compounds) was then analyzed by GCxGC-TOFMS, and the vapor pressure values achieved were compared with those obtained by our optimized GC-MS method, the retention index method (isothermal), and literature values. The method was then applied to atmospheric aerosol samples, and finally the feasibility of the method was evaluated for derivatized (silylated) compounds (Parshintsev et al. 2013). All-sized aerosol sample was collected on quartz filter at the SMEARII station on March 31<sup>st</sup>, 2011.

The subcooled liquid vapor pressure of an analyte was determined from the known vapor pressures of the reference compounds eluting immediately before and after the analyte (eq. 1, Donovan et al. 1996).

$$\log P^\circ = \frac{(\log P_1^\circ - \log P_2^\circ)t_R + t_1 \log P_2^\circ - t_2 \log P_1^\circ}{t_1 - t_2} \quad (1)$$

$P^\circ$  and  $t_r$  are the vapor pressure and retention time of the unknown compound, and  $P_1$ ,  $P_2$ ,  $t_1$  and  $t_2$  are the vapor pressures and retention times of the known reference compounds.

The laser AMS instrument collects charged and size-selected aerosol particles by electrostatic deposition on a stainless steel collection surface at atmospheric pressure (Laitinen, Hartonen et al. 2009). The collected particle sample from the collection surface is introduced to the high vacuum side of the mass spectrometer with a rotating sampling valve. Also, liquid samples can be used in the system (standards) by applying the sample directly to the collection surface resulting in rapid analysis. In MS side, the sample is desorbed from the collection surface with an IR laser (1064 nm wavelength) and ionized with a UV laser (193 nm wavelength). The formed ions are then guided with ion lenses to the orthogonal time-of-flight mass spectrometer (TOF-MS) and detected according to their flight times on MCP detector.

Usually the instrument operation is optimized for ions produced by the ionization laser, but in this experiment the ions produced by the desorption laser were used for the quantitative analysis of carbon clusters, making the technique highly selective, and also sensitive for carbon clusters. For each sample, a combined mass spectrum was calculated from applied laser shots, normalized to total ion count and mass calibrated with common background peaks. Then a unit mass resolution stick spectrum was calculated and used for further analysis. The processing of mass spectra was done with the tofTools software package.

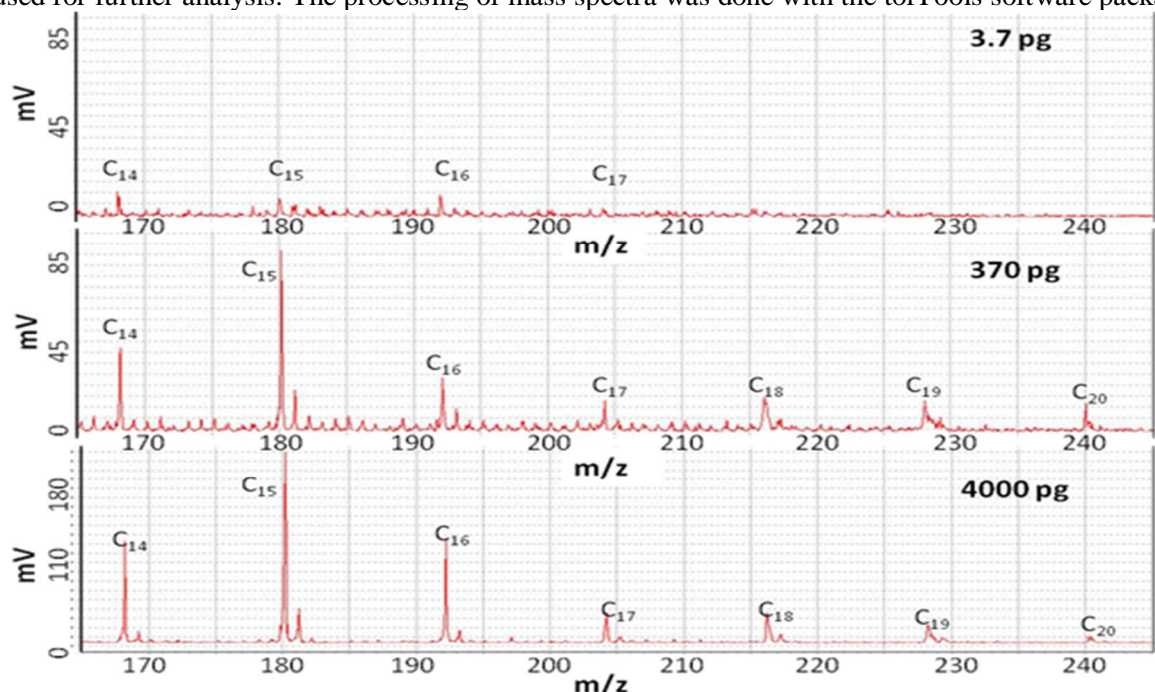


Figure 4. Mass spectra of standard sample of one laser shot of 50 nm graphite particle toluene suspension with sample amounts (3.7 pg, 370 pg, and 4000 pg).

Measurements of urban air (20 samples) were conducted between October 1<sup>st</sup> and December 17<sup>th</sup>, 2012 on the third floor in the Department of Chemistry, University of Helsinki, Kumpula Campus, Finland. A differential mobility analyzer (DMA) with a closed loop arrangement for the sheath air flow with particle size of 50 nm was used for ambient air studies. Particles were charged with a unipolar charger (<sup>241</sup>Am) before entering to the DMA. The sheath air flow of the DMA was set to 10 lpm while the aerosol flow was 3 lpm. Particle concentrations during the experiments were measured with a condensation particle counter (CPC, Model 3025, TSI Inc., MN, USA).

Several standard materials and methods were tested suitable for quantitative carbon cluster analysis from 50 nm urban air aerosols. The tests included colloidal solution of 200  $\mu$ m graphite particles, fullerene C<sub>60</sub> dissolved in toluene, and toluene suspensions of stove soot, and 200  $\mu$ m and 50 nm graphite particles. As the final result the 50 nm graphite particle toluene suspension after 72 hours of high power sonication produced suitable standard suspension that was usable to quantify the carbon clusters from the ambient

aerosol samples. Additionally, fullerene demonstrated its potential for further aerosol studies: it could be used in the laser AMS to quantify the fullerene in the ambient samples at urban areas. Figure 4 demonstrates the mass spectra of standard samples with detected carbon clusters in the range  $C_{14}$  to  $C_{19}$ . The sample amounts were 3.7 pg, 370 pg, and 4000 pg.

In our previous studies, the laser AMS detected carbon clusters in 10 to 50 nm aerosol particles at rural area (Laitinen, Ehn et al. 2011). These studies encouraged us to continue measurements in urban area. In these measurements, carbon clusters from  $C_{14}$  to  $C_{19}$  were used for the quantification as the standards. Our aim was to collect samples with highest particle concentrations, but the results revealed that the amount of carbon clusters in the samples ranged from 0.01 up to 30 percent (average of 7.2%) and was independent of the time of day. Figure 5 shows a typical mass spectrum of the carbon clusters in 50 nm urban air particles collected in Helsinki and analyzed by laser AMS.

Our results indicated that the carbon cluster concentration in the 50 nm particles during the measurements were more or less constant over a 24-hour period, except for a minor decrease at night and weekends. Also, minor or moderate snowing did not have any impact on the carbon cluster concentrations. One additional feature that was noticed during the measurements was that fullerenes were present in low concentrations in some samples starting from about  $C_{50}$  up to  $C_{100}$ . The highest signal was provided by  $C_{60}$ . It was not our aim to study the fullerenes, but it might be an interesting task to quantify fullerenes in the future.

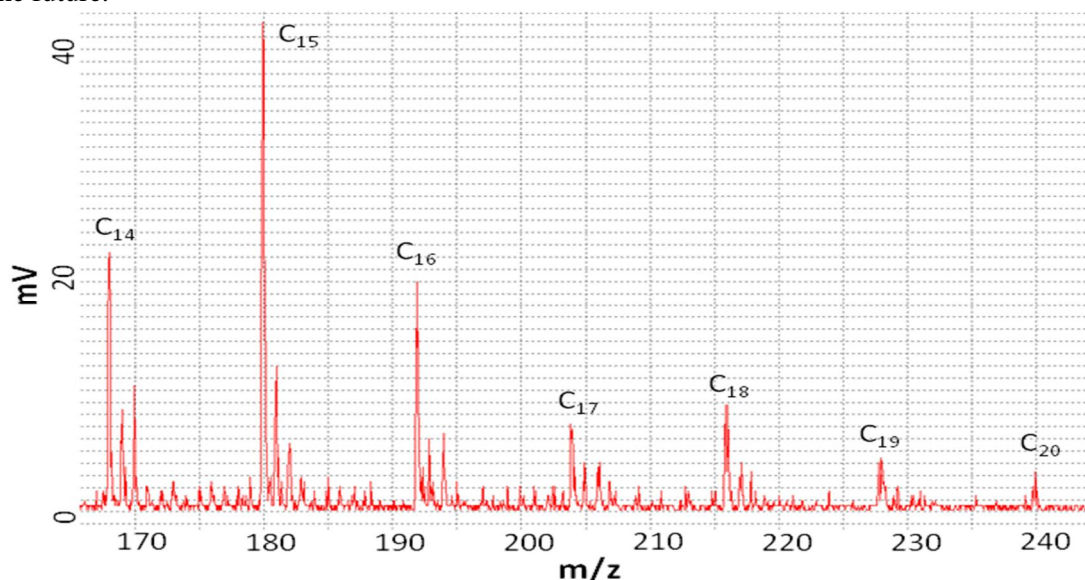


Figure 5. Carbon clusters detected from 50 nm urban air aerosol particles by laser AMS (one laser shot) on December 2<sup>nd</sup>, 2012 at Helsinki, Finland.

## CONCLUSIONS

SPME combined with portable GC-MS proved its applicability for the determination of gas phase chemical composition in the atmosphere with good time resolution. Opposite to existing on-line techniques, gas chromatographic separation allows the quantitative analysis of individual compounds. On the other hand, higher sampling efficiencies can be achieved with existing off-line techniques. In addition, they are more reliable and fully quantitative. However, their sampling time resolution is, unfortunately much lower, and the methods can be laborious and costly. A high potential of the developed SPME-GC-MS technique should be utilized in the future. Together with other determination methods it is useful as complimentary method for the understanding of gas to particle phase partitioning.

Organosulfates were found for the first time in ultrafine 20 and 30 nm aerosol particles with the help of UPLC-QTOFMS. The high flow rate DMA assisted collection device was shown to be effective for the sampling of ultrafine particles.

The application of GCxGC-TOFMS was expanded to determine vapor pressures of compounds in atmospheric aerosols. The lowest vapor pressure value determined was  $6 \times 10^{-3}$  Pa for tetrahydroaraucarolone in atmospheric aerosol sample. However, values down to  $10^{-6}$  Pa can easily be determined with the described setup. Smaller values would require higher temperatures in GC and more stable columns. Derivatization appears not to influence the determination, and could extend the applicability of the method to low vapor pressure compounds. In comparison with existing approaches, our method is far more superior in terms of simplicity, time consuming and cost, and requires only picograms of compounds in sample mixtures.

Suspensions from 50 nm graphite particles in toluene after 72 hours of high power sonication were used as standards for quantitative carbon cluster analysis by laser AMS from 50 nm urban air particles in winter 2012 at Helsinki, Finland. The lowest measurable concentration of the 50 nm graphite standard suspension was 3.7 pg of C<sub>14</sub> to C<sub>19</sub> carbon clusters at average relative content of 7.2% per sample. Laser AMS was also found to be suitable for the detection of fullerenes in 50 nm particles from C<sub>50</sub> up to C<sub>100</sub>.

#### ACKNOWLEDGEMENTS

This research was supported by the Academy of Finland Center of Excellence program (project number 1118615). Pasi Aalto, Mikael Tilli, Quentin Alverdi and Niina Kärkkäinen are acknowledged for the help in the laboratory and SMEAR II station. Financial support was also provided by the Emil Aaltonen and Otto A. Malm Foundations.

#### REFERENCES

- Baumgardner, D., Popovicheva, O., et al. (2012). "Soot reference materials for instrument calibration and intercomparisons: a workshop summary with recommendations", *Atmospheric Measurement Techniques* 5(8): 1869-1887.
- Hakola, H., Laurila, T. et al. (2000). "The ambient concentrations of biogenic hydrocarbons at a northern European, boreal site", *Atmospheric Environment* 34: 4971-4982.
- Hartonen, K., Parshintsev, J. (2013) "Gas chromatographic vapour pressure determination of atmospherically relevant oxidation products of  $\beta$ -caryophyllene and  $\alpha$ -pinene", submitted to *Atmos. Environ.*
- Janson, R., de Serves, C. (2001). "Acetone and monoterpene emissions from the boreal forest in northern Europe" *Atmospheric Environment* 35: 4629-4637.
- Laitinen, T., Ehn M., et al. (2011). "Characterization of organic compounds in 10-to 50-nm aerosol particles in boreal forest with laser desorption-ionization aerosol mass spectrometer and comparison with other techniques", *Atmospheric Environment* 45(22): 3711-3719.
- Laitinen, T., Hartonen K., et al. (2009). "Aerosol time-of-flight mass spectrometer for measuring ultrafine aerosol particles", *Boreal Environment Research* 14(4): 539-549.
- Surratt, J.D., Gomez-Gonzalez, Y. et al. (2008). "Organosulfate formation in biogenic secondary organic aerosol", *J. Physical Chemistry A* 112: 8345-8378.
- Parshintsev, J., Ruiz-Jimenez, J. et al. (2011) "Comparison of quartz and Teflon filters for simultaneous collection of size-separated ultrafine aerosol particles and gas-phase zero samples". *Anal. Bioanal. Chem.* 400: 3527-3535
- Parshintsev, J., Lai, C.-K. et al. (2013) "A new way to determine vapor pressures of compounds in multicomponent systems by comprehensive two-dimensional gas chromatography coupled to time-of-flight mass spectrometry", submitted to *Analytical Chemistry*.

## BIOSPHERE-ATMOSPHERE EXCHANGE AND ATMOSPHERIC CONCENTRATIONS OF VOLATILE ORGANIC COMPOUNDS

J. RINNE<sup>1</sup>, M.K. KAJOS<sup>1</sup>, J. PATOKOSKI<sup>1</sup>, P. RANTALA<sup>1</sup>, R. TAIPALE<sup>1</sup>, S. HAAPANALA<sup>1</sup>, T.M. RUUSKANEN<sup>1</sup>

<sup>1</sup>Department of Physics, University of Helsinki, Finland.

Keywords: HYDROCARBON, EMISSION.

### INTRODUCTION

The volatile organic compounds (VOC) are a diverse group of compounds having an important influence on e.g. aerosol particle growth, tropospheric ozone formation and atmospheric hydroxyl radical levels. VOCs originate from both human activities and nature, mostly vegetation. Globally the biogenic source has been estimated to be an order of magnitude higher than the anthropogenic source.

The aim of the Biogenic VOC flux group is to understand the biosphere-atmosphere exchange of VOCs and their atmospheric behavior, especially in the boreal regions. Thus we have conducted measurements of VOC fluxes and atmospheric concentrations in various ecosystems to analyze the dynamics of the biological and atmospheric processes.

### ECOSYSTEM SCALE VOC EMISSION

We have measured ecosystem scale VOC emission from pine forest ecosystem at SMEAR II (Rinne et al., 2007; Taipale et al., 2011), clear-cut pine forest (Haapanala et al., 2012), semi-urban area at SMEAR III in Helsinki (Rantala et al., 2013), and Mediterranean oak forest (Schallhart et al., 2013). We have also conducted enclosure measurements of VOC emissions from mature larch trees in a remote Siberian site (Kajos et al., 2013). In order to estimate the effect of atmospheric chemistry has on the measured VOC fluxes we have developed a model (SLTC) combining stochastic Lagrangian transport model and a simple representation of VOC lifetimes in the atmosphere (Rinne et al., 2012).

The measurements conducted above pine forest ecosystem have corroborated the parallel emission pathway model of monoterpene emissions, in which part of the emission originates directly from synthesis while the other part comes from large storage reservoirs. The model is supported by the stable isotope labeling experiments conducted earlier in laboratory (Ghirardo et al., 2010). The measurements of monoterpene emissions from a clear-cut forest indicate that the monoterpene release from cutting residue is locally much higher than the emission from intact forest and can be significant part of the regional scale monoterpene emission. The VOC emission measurements from Siberian larch forest confirm the important role of these forests as a source of monoterpenes into the northern continental atmosphere (Kajos et al., 2013).

In addition to terpenoid emissions the forests generally emit also other VOC species such as methanol and acetone (Rinne et al., 2007). The measurements conducted at semi-urban location revealed considerable emissions of methanol and ethanol, presumably from automobile exhaust (Rantala et al., 2013).

We participated in an ECLAIRE intensive measurement campaign 2012 in Bosco Fontana natural reserve in the Po valley, Lombardia (Schallhart et al., 2013). The aim of the campaign was to investigate the in-canopy processes on net biosphere - atmosphere exchange fluxes. In cooperation with the Forschungszentrum Juelich, the Division of Atmospheric sciences was measuring fluxes of VOCs with a PTR-ToF-MS as well as aerosol particle number-size distributions with a DMPS. The data will be used to model how climate change alters the threat of air pollution on European land ecosystems including soils (ECLAIRE 2011).

Using the SLTC model and oxidant data ( $O_3$ , OH,  $NO_3$ ) obtained during COPEC-HUMPPA-2010 campaign in Hyytiälä (Williams et al., 2011), we estimated the effect of atmospheric chemistry on above canopy fluxes of isoprene and most monoterpenes to be minimal while the effect on more reactive sesquiterpenes is considerable (Rinne et al., 2012).

We have continued long-term VOC flux measurements with PTR-QMS using the surface-layer gradient technique (SLG) at SMEAR II during 2011–2013. Our aim has been to develop a reliable and feasible method to measure ecosystem scale VOC emissions by micrometeorological methods and the SLG has many functional advantages for that purpose, such as effortless data processing.

In summer 2011 we organised an intercomparison campaign between the disjunct eddy covariance method (DEC) and the SLG. As a main result of the preliminary analysis, the SLG was proven to be reliable method for continuous flux measurements and in low flux conditions (e.g. isoprene emissions) and gave even more robust realistic values than the DEC.

We collaborated in new method development to determine eddy covariant VOC fluxes with a PTR-ToF and determining above a temperate mountain grassland site in Stubai (Ruuskanen et al., 2011) and above a boreal forest site in Hyytiälä (Ruuskanen et al., 2013). The collaboration has revealed the influence of ambient concentration on the deposition of monoterpenes (Bamberger et al., 2012) and acetaldehyde (Hörtnaegl et al., 2013).

We have also collaborated in developing new VOC emission models, such as the photosynthesis based isoprene emission model (Unger et al., 2013) and in the estimation of the robustness of monoterpene emission models coupled with the atmospheric chemistry and gas concentrations model SOSA (Smolander et al., 2013).

## ATMOSPHERIC VOC CONCENTRATIONS

Atmospheric nucleation is influenced by organic compounds and our atmospheric VOC concentration measurements have led to descriptions of atmospheric nucleation and growth of aerosol formation processes (Kulmala et al., 2013). Our collaboration has given further insight on the molecular composition of boreal forest aerosol (Kourtchev et al., 2013)

While fluxes are the key in determining the local exchange of VOCs, ambient concentrations are essential for the study of processes on larger temporal and spatial scale. The analysis of atmospheric concentrations of VOCs has revealed that although monoterpene emissions result from the release of them from the forest, even in SMEAR II there is anthropogenic contribution to monoterpene concentrations (Liao et al., 2011; Patokoski et al., 2013a). This is slightly surprising since the lifetimes of monoterpenes are considered short, within hours, during the summertime. However, oxidized volatile organic compounds (OVOCs) such as acetaldehyde and acetone and aromatic VOCs such as benzene and toluene originate from various natural and anthropogenic sources. These compounds have relatively long lifetime, varying from hundreds of days in the winter to a few days in summer and thus they are effectively transported.

In addition to the measurement of ambient VOC concentrations at SMEAR II for several years, we have datasets for shorter periods at semi-urban SMEAR III and the datasets are used to determine e.g. VOC sources and atmospheric processes such as aerosol particle formation and growth (Liao et al., 2011; Yli-Juuti et al., 2011, 2013, Patokoski et al., 2013a; 2013b).

We have characterized that in semi-urban SMEAR III in Helsinki, concentrations of VOCs are typically higher, and their diurnal variations more pronounced than at the rural SMEAR II site in Hyytiälä. Aromatic hydrocarbons, such as benzene and toluene, originate from traffic at SMEAR III while also distant sources contribute at SMEAR II. At the Helsinki site OVOCs originate from traffic during the

winter, while in the spring and at in Hyytiälä most OVOCs originate from distant sources (Patokoski et al., 2013a).

In April-May 2012 we had a measurement campaign at SMEAR II site to study the ambient concentrations of acetaldehyde, acetone, benzene and toluene. The measurements were done with two different methods; Gas Chromatography-Mass Spectrometry (GC-MS) and Proton Transfer Reaction-Mass Spectrometry (PTR-MS). The aim of our study was to compare the performance of two different methods for measuring the volume mixing ratios of aromatic and oxidized VOCs in the ambient air of a boreal forest and preliminary results show promising agreement between the different methods (Kajos et al., 2013).

#### ACKNOWLEDGEMENTS

We acknowledge the funding from the Academy of Finland (139656, 120434, 125238), Academy of Finland Center of Excellence (project no 1118615) and the Nordic Center of Excellence CRAICC.

#### REFERENCES

- Bamberger, I., L. Hörtnagl, T. M. Ruuskanen, R. Schnitzhofer, M. Müller, M. Graus, T. Karl, G. Wohlfahrt, and A. Hansel (2011), Deposition fluxes of terpenes over grassland, *J. Geophys. Res.*, **116**, D14305.
- Ghirardo, A., K. Koch, R. Taipale, I. Zimmer, J.-P. Schnitzler & J. Rinne, (2010). Determination of de novo and pool emissions of terpenes from four common boreal/alpine trees by  $^{13}\text{CO}_2$  labeling and PTR-MS analysis. *Plant, Cell & Environment*, **33**, 781-792.
- Haapanala, S., H. Hakola, H. Hellén, M. Vestenius, J. Levula, & J. Rinne, (2012). Is forest management a significant source of monoterpenes into the boreal atmosphere? *Biogeosciences*, **9**, 1291-1300.
- Hörtnagl, L., I. Bamberger, M. Graus, T.M. Ruuskanen, R. Schnitzhofer, M. Walser, A. Unterberger, A. Hansel, G. Wohlfahrt (2013). Acetaldehyde exchange above a managed temperate mountain grassland, submitted to ACP.
- Kajos, M.K., H. Hakola, T. Holst, T. Nieminen, V. Tarvainen, T. Maximov, T. Petäjä, A. Arneth & J. Rinne, 2013a: Terpenoid emissions from fully grown east Siberian *Larix cajanderi* trees, *Biogeosciences*, **10**, 4705-4719.
- Kajos M.K., M. Hill, H. Hellén, P. Rantala, J. Patokoski, R. Taipale, C. C Hoerger, S. Reinmann, H. Hakola, T. Petäjä and T.M. Ruuskanen (2013). Concentrations of oxidized VOCs and aromatic VOCs at a boreal forest. FCoE2013.
- Kourtchev, I., S., Fuller, J., Aalto, T.M., Ruuskanen, M. W., McLeod, W., Maenhaut, R., Jones, M., Kulmala and M. Kalberer (2013). Molecular composition of boreal forest aerosol from Hyytiälä, Finland, using ultrahigh resolution mass spectrometry, *Environmental Science & Technology*, 03/2013; DOI:10.1021/es3051636.
- Kulmala, M., J., Kontkanen, H., Junninen, K., Lehtipalo, H.E., Manninen, T., Nieminen, T., Petäjä, M., Sipilä, S., Schobesberger, P. Rantala, A. Franchin, T. Jokinen, E. Järvinen, M. Äijälä, J., Kangasluoma, J., Hakala, P.P., Aalto, P., Paasonen, J., Mikkilä, J., Vanhanen, J., Aalto, H., Hakola, U., Makkonen, T., Ruuskanen, R.L. Mauldin III, J., Duplissy, H., Vehkamäki, J., Bäck, A. Kortelainen, I., Riipinen, T., Kurten, M.V., Johnston, J.N., Smith, M., Ehn, T.F., Mentel, K.E.J., Lehtinen, A., Laaksonen, V.-M., Kerminen, and D.R. Worsnop (2013). Direct observations of atmospheric nucleation, *Science*, **339**, 943.
- Liao, L., M. Dal Maso, R. Taipale, J. Rinne, M. Ehn, H. Junninen, M. Äijälä, T. Nieminen, P. Alekseychik, M. Hulkkonen, D.R. Worsnop, V.-M. Kerminen, & M. Kulmala, (2011). Monoterpene pollution episodes in a forest environment: indication of anthropogenic origin and association with aerosol particles. *Boreal Environment Research*, **16**, 288–303.
- Patokoski, P., T.M. Ruuskanen, H. Hellén, R. Taipale, T. Grönholm, M.K. Kajos, T. Petäjä, H. Hakola, M. Kulmala & J. Rinne, (2013a). Winter to spring transition and diurnal variation of VOCs in Finland in an urban background and a rural location. *Boreal Environment Research*. In press.

- Patokoski, J., T.M. Ruuskanen, M.K. Kajos, R. Taipale, P. Rantala, J. Aalto, H. Hakola & J. Rinne, (2013). Long-term source analysis of VOCs in boreal forest during years 2006-2011. FCoE2013
- Rantala P., S. Haapanala, M.K. Kajos, J. Patokoski, L. Järvi, R. Taipale, J. Rinne & T.M. Ruuskanen, (2013). VOC measurements with PTR-MS at urban background site in Helsinki. FCoE2013
- Rinne, J., T. Markkanen, T.M. Ruuskanen, T. Petäjä, P. Keronen, M.J. Tang, J.N. Crowley, Ü. Rannik & T. Vesala, (2012). Effect of chemical degradation on fluxes of reactive compounds – a study with a stochastic Lagrangian transport model. *Atmospheric Chemistry and Physics*, **12**, 4843–4854.
- Ruuskanen, T.M., M. Müller, R. Schnitzhofer, T. Karl, M. Graus, I. Bambergerl, L. Hörtnagl, F. Brilli, G. Wohlfahrt, and A. Hansel (2011) Eddy covariance VOC flux emission and deposition above grassland. *Atmos. Chem. Phys.*, **11**, 611-625.
- Ruuskanen et al., (2013) Determination of eddy covariance VOC emission and deposition fluxes using PTR-TOF-MS, conference abstract for Analytix – 2013.
- Schallhart, S., P. Rantala, R. Taipale, E. Nemitz, R. Tillmann, T.F. Mentel, T. Ruuskanen & J. Rinne, (2013) VOC exchange measurements at Bosco Fontana (IT) and Hyytiälä (FI). FCoE 2013.
- Smolander, S., Q. He, D. Mogensen, L. Zhou, J. Bäck, T. Ruuskanen, S. Noe, A. Guenther, H. Aaltonen, M. Kulmala, and M. Boy (2013). Improved models for monoterpene emissions and air chemistry in a boreal forest, submitted to Biogeoscience.
- Taipale, R., M.K. Kajos, J. Patokoski, P. Rantala, T.M. Ruuskanen, & J. Rinne, (2011). Role of de novo biosynthesis in ecosystem scale monoterpene emissions from a boreal Scots pine forest. *Biogeosciences*, **8**, 2247-2255.
- Unger, N., K. Harper, Y. Zheng, N.Y. Kiang, I. Aleinov, A. Arneth, G. Schurgers, C. Amelynck, A. Goldstein, A. Guenther, B. Heinesch, C.N. Hewitt, T. Karl, Q. Laffineur, B. Langford, K.A. McKinney, P. Misztal, M. Potosnak, J. Rinne, S. Pressley, N. Schoon, and D. Serca, (2013). Photosynthesis-dependent isoprene emission from leaf to planet in a global carbon-chemistry-climate model. *Atmospheric Chemistry and Physics Discussion*, **13**, 17717-17791.
- Williams, J., J. Crowley, H. Fischer, H. Harder, M. Martinez, T. Petäjä, J. Rinne, J. Bäck, M. Boy, M. Dal Maso, J. Hakala, M. Kajos, P. Keronen, P. Rantala, J. Aalto, H. Aaltonen, J. Paatero, T. Vesala, H. Hakola, J. Levula, T. Pohja, F. Herrmann, J. Auld, E. Mesarchaki, W. Song, N. Yassaa, A. Nölscher, A. M. Johnson, T. Custer, V. Sinha, J. Thieser, N. Pouvesle, D. Taraborrelli, M. J. Tang, H. Bozem, Z. Hosaynali-Beygi, R. Axinte, R. Oswald, A. Novelli, D. Kubistin, K. Hens, U. Javed, K. Trawny, C. Breitenberger, P. J. Hidalgo, C. J. Ebben, F. M. Geiger, A. L. Corrigan, L. M. Russell, H. G. Ouwersloot, J. Vilà-Guerau de Arellano, L. Ganzeveld, A. Vogel, M. Beck, A. Bayerle, C. J. Kampf, M. Bertelmann, F. Köllner, T. Hoffmann, J. Valverde, D. González, M.-L. Riekkola, M. Kulmala, and J. Lelieveld, (2011). The summertime Boreal forest field measurement intensive (HUMPPA-COPEC-2010): an overview of meteorological and chemical influences. *Atmospheric Chemistry and Physics*, **11**, 10599-10618.
- Yli-Juuti, T., T. Nieminen, A. Hirsikko, P.P. Aalto, E. Asmi, U. Hörrak, H.E. Manninen, J. Patokoski, M. Dal Maso, T. Petäjä, J. Rinne, M. Kulmala, and I. Riipinen, (2011). Growth rates of nucleation mode particles in Hyytiälä during 2003–2009: variation with particle size, season, data analysis method and ambient conditions. *Atmospheric Chemistry and Physics*, **11**, 12865-12886.
- Yli-Juuti, T., K. Barsanti, L. Hildebrandt Ruiz, A.-J. Kieloaho, U. Makkonen, T. Petäjä, T. Ruuskanen, M. Kulmala and I. Riipinen. Model for acid-base chemistry in nanoparticle growth (MABNAG), *Atmospheric Chemistry and Physics Discussion*, **13**, 7175-7222.

## AN OVERVIEW OF UNIVERSITY OF HELSINKI COMPUTATIONAL AEROSOL PHYSICS GROUP ACTIVITIES IN 2011-2013

H. VEHKAMÄKI, N. BORK, H. HENSCHER, O. KUPIAINEN-MÄÄTTÄ, T. KURTÉN, V. LOUKONEN, T. OLENIUS, I. ORTEGA, K. RUUSUVUORI, AND N. TSONA TCHINDA

Department of Physics, FI-00014 University of Helsinki, Finland

Keywords: PARTICLE FORMATION, MOLECULAR CLUSTERS, SULPHURIC ACID

### INTRODUCTION

During the period 2011-2013 the main activities of the group have been developing the Atmospheric Cluster Dynamics Code (ACDC) and performing related quantum chemical calculations, as well as building methodology for and starting novel molecular dynamic simulations of atmospheric cluster formation. We have validated ACDC by comparing its predictions to mass spectrometric cluster size distribution studies, and used the model to assess the role of the critical cluster concept in atmospheric particle formation, understanding chemical ionization mass spectrometry and atmospheric particle formation. We have worked on improving the theoretical picture of ion induced nucleation together with experimentalists.

This synthesis is based mainly on the work published within years 2011-2013, with references to also some recently submitted articles.

### ATMOSPHERIC CLUSTER DYNAMICS CODE DEVELOPED

We have developed Atmospheric Cluster Dynamics Code (ACDC) to study the first steps of atmospheric new particle formation by examining the formation of molecular clusters from atmospherically relevant molecules. The program models the cluster kinetics by explicit solution of the birth–death equations, using an efficient computer script for their generation and alternatively a MATLAB (McGrath *et al.* 2011) or Fortran routine for their solution. The molecule-cluster and cluster-cluster collision rates are taken from the kinetic gas theory, while the evaporation rate coefficients are derived from formation free energies calculated by quantum chemical methods. We have mainly applied the model for studying atmospherically relevant clusters containing sulphuric acid and dimethylamine and/or ammonia (Ortega *et al.* 2012a and 2013). The development of ACDC has involved assessing and validating the accuracy computationally affordable methods that might be used for the calculation of the binding energies of larger clusters for atmospheric modelling (Leverentz *et al.* 2013). The extent of the computational task is illustrated by the fact that performing the quantum chemical calculations for the set clusters now incorporated into ACDC was started six years ago, and several researchers have been involved, albeit not 100% of their working time.

### BENCHMARKING COMPARISONS TO MASS SPECTROMETRIC STUDIES

To validate our modelling approach, we have applied ACDC to laboratory experiments. We have concentrated on mass spectrometric data which reports distributions of small charged clusters. First, the model was used to study the kinetics of the substitution of ammonia by DMA (Kupiainen *et al.* 2012). In the charged case, we found a very good agreement between our results and experimental observations of positive clusters by Bzdek *et al.* (2010) obtained using a Fourier transform ion cyclotron resonance mass spectrometer. Our results show that there are some major differences between the charged and undetected neutral clusters. Collisions between neutral clusters or molecules occur less frequently, but on the other

hand the clusters are not as strongly bound and evaporate faster. The composition of the most stable clusters is different in the two cases. Both ammonia and DMA stabilize sulphuric acid clusters significantly, but the effect is even stronger for DMA. The concentration of atmospheric ammonia is typically a few orders of magnitude larger than that of DMA, and sulphuric acid therefore collides more frequently with ammonia. Due to the extremely effective substitution of DMA for ammonia, the vast majority of sub-nanometer sulphuric acid clusters in the atmosphere are, however, likely to contain DMA. Second, we modelled the steady-state concentrations of neutral clusters and negative cluster ions measured with the state-of-the-art Atmospheric Pressure interface Time-Of-Flight mass spectrometer (APi-TOF) in the CLOUD chamber experiments at CERN (Kirkby *et al.* 2011). The behaviour of the concentrations of negative clusters with respect to variations in the acid and ammonia concentrations is well predicted by the model, although there are some discrepancies between the measured and modelled absolute cluster concentrations. The discrepancies are consistent with still poorly understood cluster fragmentation inside the mass spectrometer. The model correctly predicts that the smallest negative ammonia-containing clusters have four acid molecules. The comparison of measured and modelled ammonia content of the clusters suggest that evaporation of ammonia inside the instrument may occur. Also in this case the model was used to obtain information on neutral clusters which cannot be directly observed with the mass spectrometers (Olenius *et al.* 2013a).

We also compared the predictions of the quantum chemical methods we use for pyridine-containing water cluster ions and their reactions with ammonia, studied experimentally using a quadrupole-time-of-flight mass spectrometer. Our model results are consistent with the observed pattern of magic numbers, suggesting that  $\text{H}^+(\text{NH}_3)(\text{pyridine})(\text{H}_2\text{O})_n$  have structures consisting of a  $\text{NH}_4^+(\text{H}_2\text{O})_n$  core with the pyridine molecule hydrogen-bonded to the surface of the core. (Ryding *et al.* 2012)

## UNDERSTANDING CHEMICAL IONIZATION MASS SPECTROMETRY

Chemical ionization mass spectrometry (CIMS) based on nitrate reagent ions is the state-of-the art method for measuring atmospheric gas-phase sulphuric acid. We have assessed effect of the sulphuric acid molecules forming clusters with base molecules on CIMS measurements using quantum chemical calculations. A significant fraction of the gas-phase sulphuric acid molecules are very likely clustered with dimethylamine  $(\text{CH}_3)_2\text{NH}$  if the amine concentration is around or above a few ppt, but the CIMS instruments will charge all but a small fraction (less than 10%) of these acid-amine clusters. The amine molecules will evaporate practically immediately after charging, and will thus not be detected in the mass spectrometer (Kurtén *et al.* 2011). In further study, we show that the  $\text{H}_2\text{SO}_4 \cdot (\text{CH}_3)_2\text{NH}$  cluster gets ionized, and as the cluster has a much higher dipole moment than the pure  $\text{H}_2\text{SO}_4$  molecule, it also has a higher collision rate with charger ions. Clustering of sulphuric acid with bases may therefore actually increase its detection probability in the CIMS. Comparison of different quantum chemical methods shows some uncertainty on how tightly dimethylamine binds with sulphuric acid, and no experimental data is available for comparison. Based on the different charging efficiencies of the monomer and the cluster, we thus propose a method for determining experimentally the binding energies of sulphuric acid-base clusters by measuring the extent of cluster formation as a function of base concentration (Kupiainen-Määttä *et al.* 2013). We have assisted in the interpretation of laminar flow tube experiments on sulphuric acid dimerization, and concluded that even in ultraclean conditions trace gases, whose concentration are below current detection limits, stabilize sulphuric acid cluster formation significantly more effectively than water. Amines are promising candidates for the stabilizing substance (Petäjä *et al.* 2011). We have also helped to rule out significant participation to particle formation of some oxidation products of sulphur dioxide other than sulphuric acid (Toivola *et al.* 2011).

## MODELLING ATMOSPHERIC PARTICLE FORMATION

In the atmosphere, the mixture of clustering molecules is much more diverse than in laboratory experiments, and some of the key compounds may not have been detected yet. Meteorology, as well as spacial and temporal variations in the trace gas concentrations, also complicate the picture. Thus, we

cannot claim that our model can accurately simulate the atmospheric particle formation. We can however, test feasibility of particle formation mechanisms. Although compounds actually forming particles may not be exactly the ones in our model, using certain molecules as representative examples can bring light to the nature of real processes. A tutorial review (Vehkamäki and Riipinen, 2012a) summarizes current key questions in atmospheric particle formation. ACDC was used to demonstrate that in cases where small thermodynamically stable clusters are abundant, and cluster-cluster collisions can not be ignored, application of the commonly used nucleation theorem may lead to erroneous interpretations concerning existence or the size of the critical cluster (Vehkamäki *et al.* 2012b). ACDC predicts that particle formation involving dimethylamine and sulphuric acid is most often barrierless, and thus critical cluster does not exist (Olenius *et al.* 2013b).

Our quantum chemical data was utilised to model the formation rate of clusters containing sulphuric acid and amine molecules at varying atmospherically relevant conditions as a function of concentrations of sulphuric acid, dimethylamine and trimethylamine, temperature and relative humidity. The model was tested against observations conducted at seven locations spread around Europe, America and Asia. The results suggest that the formation rate of clusters with at least two sulphuric acid and two amine (or amine-like) molecules could be the rate-limiting step for atmospheric particle formation (Paasonen *et al.* 2012). We also assisted in interpretation of novel atmospheric measurements of neutral clusters with diameters between one and two nanometers, combined with the mass-spectrometric information of the charged fraction of these clusters. We concluded that the observations are consistent with barrierless sulphuric acid-amine cluster formation (Kulmala *et al.*, 2013).

There are indications that, besides sulphuric acid and nitrogen-containing base molecules, highly oxidized organic compounds are involved in new particle formation. We participated an experimental study where new particle formation potential of three different monoterpens were tested (Ortega *et al.* 2012b). We found that alpha-pinene and especially limonene were able to induce new particle formation events even in dark conditions. We concluded that the oxidation products of those monoterpenes were the responsible for the observed events. Recently we have thus focused our quantum chemical calculations in the study of clusters of sulphuric acid and alpha-pinene oxidation products. The results confirm that high O:C ratio compounds are able to form stable clusters with sulphuric acid, and therefore may be involved in new particle formation from the first steps (Donahue *et al.* 2013).

## ADVANCES IN UNDERSTANDING ION-INDUCED NUCLEATION

As it is clear that the molecular level approach can not be extended to clusters with tens or hundreds of molecules, we aim to improve also the coarse-grained models, such as classical nucleation theory, so that a realistic picture of cluster formation and growth could be obtained with a reasonable computational effort. The ACDC model suggests that if ions are present, charged clusters contribute significantly to particle formation in the sulphuric acid-ammonia system, whereas in the sulphuric acid-dimethylamine system the role of ions is minor (Olenius *et al.* 2013b). Thus, ion induced particle formation may be significant in some parts of the lower atmosphere, depending both on types of trace gases present and their concentrations, and improved theory of ion-induced nucleation is needed. Comparison of experiments involving the activation of single ion molecules in a supersaturated *n*-propanol vapour to classical ion-induced nucleation theory revealed the activation of molecules into droplets to happen via formation of critical clusters substantially larger than the seed molecule. The critical clusters sizes were found to be reasonably well predicted by the classical Kelvin-Thomson relation (Winkler *et al.* 2012). To understand the deviations between the experiments and theory, we have participated in the development of refined ion-induced nucleation theory. The currently available model for ion-induced nucleation assumes complete spherical symmetry of the system, implying that the seed ion is immediately surrounded by the condensing liquid from all sides. The new theoretical framework takes a step further and treats more realistic geometries, where a cap-shaped liquid cluster forms on the surface of the seed particle (Noppel *et*

*al.* 2013a and 2013b). We also performed quantum chemical calculations to shed light in the interactions between tungsten oxide seeds and *n*-propanol vapour (Ruusuvaori *et al.* 2011).

## MOLECULAR DYNAMIC STUDIES

Atmospheric cluster formation from vapour is essentially a dynamic non-equilibrium process. Most of the models currently used, ranging from classical nucleation theory to the use of quantum chemistry in ACDC, rely on using the properties of equilibrium clusters to describe this process. In the past, the use of molecular dynamics to study cluster formation in the atmospherically relevant systems, has been computationally too demanding. For these systems quantum chemical (i.e. *ab initio*) interactions, as opposed to classical force fields, are required to capture the proton transfer occurring as a key part of the cluster formation. We have assessed the validity of the equilibrium picture when describing nucleation in the case of Lennard-Jones argon, a simple model substance (Napari and Vehkamäki, 2013). The development of computers and algorithms are now starting to make truly dynamic studies of atmospheric clusters feasible.

We started our *ab initio* molecular dynamic studies by investigating two reactions of atmospheric sulphur containing compounds. First case is the oxidation of  $\text{SO}_2$  to  $\text{SO}_3^-$  by  $\text{O}_3^-(\text{H}_2\text{O})_n$ . We found that not all the collisions led to sticking, and even when sticking occurred, in some cases chemical reaction did not follow. Steric effects were found to be significant: most of the  $\text{SO}_2\text{--O}_3^-$  hits lead to rapid  $\text{SO}_3^-$  formation, while most of the  $\text{SO--H}_2\text{O}$  hits lead to a non-sticking collision (Bork *et al.* 2013a). Second, we studied the reaction of  $\text{O}_2\text{SO}_3^-(\text{H}_2\text{O})_{0-1}$  with  $\text{O}_3$ . The likely reaction path is altered by the presence or absence of the water molecule, but in general decomposition to  $\text{SO}_3$ ,  $\text{O}_2$  and  $\text{O}_3^-$  is the most likely outcome. The previously unknown origin of both  $\text{O}_2\text{SO}_3^-$  and  $\text{SO}_4^-$ , seen in several experiments and field studies, is explained through this mechanism (Bork *et al.* 2013b).

We have then proceeded to perform first-principles molecular dynamics simulations probing the stability and dynamics of electrically neutral sulphuric acid-ammonia and sulphuric acid-dimethylamine clusters with 2-4 acid molecules and a varying number of base molecules. In simulations corresponding to 300 K temperature the clusters exhibited pronounced thermal motion including rotations of the molecules within the clusters, but stayed bound together. The dipole moments of the clusters were found to be sensitive to the thermal motion and thus large fluctuations were observed. In addition, the vibrational spectra indicate that the observed thermal motion differs from purely harmonic motion (Loukonen *et al.* 2013a).

In a subsequent study, we studied collisions of a sulphuric acid monomer or a sulphuric acid – water cluster with dimethylamine. The simulations indicate that the interaction between the molecules is strong enough to overcome the possible initial non-optimal collision orientations, and thus the sticking factor in the collisions is unity. Furthermore, no post-collisional cluster break up is observed. A proton transfer reaction takes place in each of the collision simulations, and the clusters show very dynamic ion pair structure. This behaviour is different from what is predicted by both the static structure optimization calculations and the equilibrium first-principles molecular dynamics simulations. In general, the water allocates a fraction of the released clustering energy stabilizing thus the cluster, and acts in some simulation runs as a proton bridge

## OUTLOOK

The Atmospheric Cluster Dynamic Code (ACDC) has reached a mature stage where it can be applied to study systems with sulphuric acid, ammonia and dimethylamine forming both electrically neutral and charged clusters. We are currently in the process of including the effect of water molecules, inevitably colliding and attaching to the clusters in the atmosphere. Most of the quantum chemical calculations required for the water inclusion have been completed. Based on the same quantum chemical data we also study adequacy and limits of using a thermodynamic model for the description of these hydrated clusters,

aiming to build a bridge from the molecular to thermodynamic description. We plan to further test and develop the model by applying it to various experimental setups, comparing the cluster size distributions to mass spectrometric results whenever possible. We will continue our molecular dynamics studies, aiming to understand the limitations of using equilibrium-based statistical physics in describing cluster formation. We work on developing concepts of meta-dynamics and thermodynamics that would allow inserting information on the entropy changes in the clustering process, derived from truly dynamic simulations, to computationally more affordable schemes such as ACDC. We are especially interested in studying the fate of clusters inside mass spectrometers, their fragmentation and evaporation of molecules, and charging probabilities in cases where the neutral clusters and molecules in the sample are charged in connection with the measurement. Understanding non-equilibrium processes is vital for this task.

## ACKNOWLEDGEMENTS

This work was supported by Academy of Finland (Center of Excellence program project number 1118615, LASTU program project number 135054), ERC Starting Grant 257360-MOCAPAF, the Maj and Tor Nessling Foundation (project number 2011200), Vilho, Yrjö and Kalle Väisälä Foundation and the Nordic Center of Excellence CRAICC. We thank CSC – IT Center for Science in Espoo, Finland, for computing time.

## REFERENCES

- Bork, Nicolai, Theo Kurtén and Hanna Vehkamäki (2013b) Exploring the atmospheric chemistry of  $\text{O}_2\text{SO}_3^-$  and assessing the maximum turnover number of ion catalysed  $\text{H}_2\text{SO}_4$  formation *Atmospheric Chemistry and Physics*, 13, 3695.
- Bork, Nicolai, Ville Loukonen and Hanna Vehkamäki (2013a). Reactions and Reaction Rates of Atmospheric  $\text{SO}_2$  and  $\text{O}_3^-(\text{H}_2\text{O})_n$  Collisions via Molecular Dynamics Simulations. *Journal of Physical Chemistry A*, 117,3143.
- Bzdek, B. R., D. P. Ridge, and M. V Johnston (2010). Amine exchange into ammonium bisulfate and ammonium nitrate nuclei. *Atmospheric chemistry and physics* 10, 3495.
- Donahue, Neil M., Ismael K. Ortega, Wayne Chuang, Ilona Riipinen, Francesco Riccobono, Siegfried Schobesberger, Josef Dommen, Markku Kulmala, Douglas Worsnop, and Hanna Vehkamäki, (2013). How Do Organic Vapors Contribute to New-Particle Formation?. *Faraday Discussions*, DOI: 10.1039/C3FD00046J
- Kirkby, Jaspert et al. (2011). Role of sulphuric acid, ammonia and galactic cosmic rays in atmospheric aerosol nucleation. *Nature* 476, 429.
- Kulmala, Markku, Jenni Kontkanen, Heikki Junninen, Katrianne Lehtipalo, Hanna E. Manninen, Tuomo Nieminen, Tuukka Petäjä, Mikko Sipilä, Siegfried Schobesberger, Pekka Rantala, Alessandro Franchin, Tuija Jokinen, Emma Järvinen, Mikko Äijälä, Juha Kangasluoma, Jani Hakala, Pasi P. Aalto, Pauli Paasonen, Jyri Mikkilä, Joonas Vanhanen, Juho Aalto, Hannele Hakola, Ulla Makkonen, Taina Ruuskanen, Roy L. Mauldin III, Jonathan Duplissy, Hanna Vehkamäki, Jaana Bäck, Aki Kortelainen, Ilona Riipinen, Theo Kurtén, Murray V. Johnston, James N. Smith, Mikael Ehn, Thomas. F. Mentel, Kari E.J. Lehtinen, Ari Laaksonen, Veli-Matti Kerminen, and Douglas R. Worsnop (2013). Direct observations of atmospheric nucleation. *Science*, 339.
- Kupiainen, Oona, Ismael K. Ortega, Theo Kurtén, and Hanna Vehkamäki (2012). Amine substitution into sulfuric acid - ammonia clusters. *Atmospheric Chemistry and Physics*, 12, 3591.
- Kupiainen-Määttä, Oona, Tinja Olenius, Theo Kurtén, and Hanna Vehkamäki (2013). CIMS sulfuric acid detection efficiency enhanced by amines due to higher dipole moments – a computational study. *Submitted to Journal of Physical Chemistry A*.
- Kurtén, Theo, Tuukka Petäjä, James Smith, Ismael Kenneth Ortega, Mikko Sipilä, Heikki Junninen, Mikael Ehn, Hanna Vehkamäki, Lee Mauldin, Douglas R. Worsnop, and Markku Kulmala (2011). The effect of  $\text{H}_2\text{SO}_4$  – amine clustering on chemical ionization mass spectrometry (CIMS)

- measurements of gas-phase sulfuric acid. *Atmospheric Chemistry and Physics*, 11, 3007.
- Leverentz, Hannah, Ilja Siepmann, Donald Truhlar, Ville Loukonen and Hanna Vehkamäki (2013). Energetics of Atmospherically Implicated Clusters Made of Sulfuric Acid, Ammonia, and Dimethyl Amine. *Journal of Physical Chemistry A*, 117, 3819.
- Loukonen, Ville, I-F. William Kuo, Matthew J. McGrath, and Hanna Vehkamäki (2013a). On the Stability and Dynamics of (sulfuric acid)(ammonia) and (sulfuric acid)(dimethylamine) clusters: a first-principles molecular dynamics investigation. *Submitted to Physical Chemistry Chemical Physics*.
- Loukonen, Ville, Nicolai Bork, and Hanna Vehkamäki (2013b). From collisions to clusters: first steps of sulfuric acid nanocluster dynamics. *Submitted to Physical Review A*.
- Napari, Ismo and Hanna Vehkamäki (2013). On the similarity of equilibrium and critical clusters in atomic vapors. *Journal of Chemical Physics*, 138, 104504.
- Noppel, Madis, Hanna Vehkamäki, Paul Winkler, Markku Kulmala, and Paul Wagner (2013a). Heterogeneous nucleation in multi-component vapor on a partially wettable charged conducting particle. I. Formulation of general equations. Electrical surface and line excess quantities. *Accepted for publication in Journal of Chemical Physics*.
- Noppel, Madis, Hanna Vehkamäki, Paul Winkler, Markku Kulmala, and Paul Wagner (2013b). Heterogeneous nucleation in multi-component vapor on a partially wettable charged conducting particle. II. The generalized Laplace, Gibbs-Kelvin and Young equations and application to nucleation. *Submitted to Journal of Chemical Physics*.
- McGrath, Matthew J., Tinja Olenius, Ismael K. Ortega, Ville Loukonen, Pauli Paasonen, Theo Kurtén, Markku Kulmala, and Hanna Vehkamäki (2012). Atmospheric Cluster Dynamics Code: a flexible method for solution of the birth-death equations. *Atmospheric Chemistry and Physics*, 12, 2345.
- Olenius, Tinja, Siegfried Schobesberger, Oona Kupiainen, Alessandro Franchin, Heikki Junninen, Ismael K. Ortega, Theo Kurtén, Ville Loukonen, Doug Worsnop, Markku Kulmala and Hanna Vehkamäki (2013a) Comparing simulated and experimental molecular cluster distributions *Faraday Discussions*, DOI: 10.1039/C3FD00031A.
- Olenius, Tinja, Oona Kupiainen, Ismael Ortega, Theo Kurtén, and Hanna Vehkamäki (2013b). Free energy barrier in the growth of sulfuric acid-ammonia and sulfuric acid-dimethylamine clusters. *Accepted for publication in Journal of Chemical Physics*
- Ortega, Ismael K. , Oona Kupiainen, Theo Kurtén, Tinja Olenius, Olli Wilkman, Matthew J. McGrath, Ville Loukonen, and Hanna Vehkamäki (2012a). From quantum chemical formation free energies to evaporation rates. *Atmospheric Chemistry and Physics*, 12, 225.
- Ortega, Ismael K., Tanja Suni, Michael Boy, Tiia Grönholm, Hanna E. Manninen, Tuomo Nieminen, Mikael Ehn, Heikki Junninen, Hannele Hakola, Heidi Hellén, Tuomas Valmari, Hannu Arvela, Steve Segelin, Dale Hughes, Mark Kitchen, Helen Cleugh, Douglas R. Worsnop, Markku Kulmala, and Veli-Matti Kerminen (2012b). New insights into nocturnal nucleation. *Atmos. Chem. Phys.*, 12, 4297
- Ortega, Ismael K. , Oona Kupiainen, Theo Kurtén, Tinja Olenius, Olli Wilkman, Matthew J. McGrath, Ville Loukonen, and Hanna Vehkamäki (2013). Corrigendum to "From quantum chemical formation free energies to evaporation rates" published in *Atmos. Chem. Phys.*, 12, 225–235. *Atmospheric Chemistry and Physics*, 13, 3321.
- Paasonen, Pauli, Tinja Olenius, Oona Kupiainen, Theo Kurtén, Tuukka Petäjä, Wolfram Birmili, Amar Hamed, Min Hu, L. Gregory Huey, Christian Plass-Duelmer, James N. Smith, Alfred Wiedensohler, Ville Loukonen, Matthew J. McGrath, Ismael K. Ortega, Ari Laaksonen, Hanna Vehkamäki, Veli-Matti Kerminen, and Markku Kulmala (2012). On the formation of sulphuric acid - amine clusters in varying atmospheric conditions and its influence on atmospheric new particle formation. *Atmospheric Chemistry and Physics*, 12, 9113.
- Petäjä, Tuukka, Mikko Sipilä, Pauli Paasonen, Tuomo Nieminen, Theo Kurtén, Ismael K. Ortega, Frank Stratmann, Hanna Vehkamäki, Torsten Berndt and Markku Kulmala (2011). Experimental observation of strongly bound dimers of sulphuric acid nucleating in the atmosphere. *Physical Review Letters* 106, 228302.
- Ruusuvuori, Kai, Theo Kurtén, Ismael K. Ortega, Hanna Vehkamäki, Ville Loukonen, Martta Toivola,

- Markku Kulmala (2011). Density-functional study of the sign preference of the binding of 1-propanol to tungsten oxide seed particles. *Computational and Theoretical Chemistry*, 966, 322, 2011.
- Ryding, Mauritz, Kai Ruusuvaori, Patrik Andersson, Alexey Zatula, Matthew McGrath, Theo Kurtén, Ismael Ortega Colomer, Hanna Vehkamäki and Einar Uggerud (2012). Structural Rearrangements and Magic Numbers in Reactions between Pyridine-containing Water Clusters and Ammonia. *Journal of Physical Chemistry A*, 116, 4902.
- Toivola, Martta, Theo Kurtén, Ismael K. Ortega, Markku Sundberg, Agilio Padova, Hanna Vehkamäki (2011). Quantum chemical studies on peroxodisulfuric acid-sulfuric acid-water clusters. *Computational and Theoretical Chemistry*, 967, 219.
- Vehkamäki, Hanna, Matthew McGrath, Theo Kurtén, Jan Julin, Kari E. J. Lehtinen, and Markku Kulmala (2012b). Rethinking the application of the first nucleation theorem to particle formation. *Journal of Chemical Physics*, 136, 09410.
- Vehkamäki, Hanna and Ilona Riipinen, (2012a) Thermodynamics and kinetics of atmospheric aerosol particle formation and growth. *Chemical Society Reviews* 41, 5160.
- Winkler, Paul M., Aron Vrtala, Gerhard Steiner, Daniela Wimmer, Hanna Vehkamäki, Kari E. J. Lehtinen, Georg P. Reischl, Markku Kulmala and Paul E. Wagner (2012). Quantitative characterization of critical nanoclusters nucleated on large single molecules. *Physical Review Letters*, 108, 085701.

## BIOSPHERE-ATMOSPHERE INTERACTIONS

T. VESALA<sup>1</sup>, I. MAMMARELLA<sup>1</sup>, L. JÄRVI<sup>1</sup>, P. ALEKSEYCHIK<sup>1</sup>, S. DENGEL<sup>1</sup>, S. HAAPANALA<sup>1</sup>, J. HEISKANEN<sup>1</sup>, P. KERONEN<sup>1</sup>, A. NORDBO<sup>1</sup>, O. PELTOLA<sup>1</sup>, M. PIHLATIE<sup>1</sup>, A. PRAPLAN<sup>1</sup>, M. RAIVONEN<sup>1</sup>, J. RINNE<sup>1</sup>, S. SMOLANDER<sup>1</sup>, M.-K. TU<sup>1</sup>, P. KOLARI<sup>1,2</sup>, T. AALTO<sup>3</sup>, T. LAURILA<sup>3</sup>, A. OJALA<sup>4</sup>, E.-S. TUUTTILA<sup>5</sup>, J. LEVULA<sup>6</sup>, J. PUMPANEN<sup>2</sup>, E. NIKINMAA<sup>2</sup>, J. BÄCK<sup>2</sup>

<sup>1</sup>Department of Physics, University of Helsinki

<sup>2</sup>Department of Forest Sciences, University of Helsinki

<sup>3</sup>Finnish Meteorological Institute, Helsinki

<sup>4</sup>Department of Ecological and Environmental Sciences, University of Helsinki

<sup>5</sup>University of Eastern Finland, Kuopio, Finland

<sup>6</sup>Hyttiälä Forestry Field Station, Finland

**Keywords:** Greenhouse gases, carbon cycle, water cycle, nitrogen cycle, ozone, carbonyl sulphide, aerosol fluxes, boreal forest, lakes, urban surface, eddy covariance, Earth systems

## INTRODUCTION

We present recent developments and results on biosphere-atmosphere interactions processes. In many cases the related work was initiated in the first period of FCoE. The work is stemming from the close co-operation between forest, peatland and freshwater ecologists and atmospheric physicists within FCoE. We focus on the results related to data processing and methodological developments of the eddy covariance technique, fluxes of greenhouse gases, ozone, carbonyl sulfide and aerosol particles over forest, lake and urban surfaces, and process modeling of methane and BVOC emissions. Beside the report activities, two new flux towers have been recently established: above-canopy and sub-canopy fluxes at Värriö, SMEAR I sub-arctic pine forest and bog at Siikaneva wetland.

## EDDY-COVARIANCE METHOD DEVELOPMENTS

### *Data processing*

The eddy-covariance flux-measurement technique (EC) has been recognized as the standard means of measuring surface—atmosphere interactions (Aubinet *et al.*, 2012). Yet, the raw-data post-processing methodology has not entirely converged: different choices in processing steps may lead to discrepancies of tens of percent in final flux values (Nordbo *et al.*, 2012). To this end, flux-data post-processing software, EddyUH, has been developed at the University of Helsinki ([www.atm.helsinki.fi/Eddy\\_Covariance](http://www.atm.helsinki.fi/Eddy_Covariance)).

Probably the most challenging step in post processing of flux data is spectral corrections, performed in order to account for lost fluctuations in data, caused especially by signal dampening in tubes. Two new correction methods have been developed: (i) an approach to correct any raw data point-by-point using Wavelets (Nordbo and Katul 2013), and (ii) an approach that corrects for dampening based on a sorption model, which describes physically the processes that water vapor undergoes with tube walls (Nordbo *et al.*, 2013).

### *Night-time decoupling*

It is well known that during night-time stable conditions the storage corrected EC CO<sub>2</sub> flux frequently underestimates the net ecosystem exchange over tall forest ecosystems (Aubinet *et al.*, 2012). In such condition, beside the systematic and random errors of EC flux measurements, other mechanisms are responsible for carbon dioxide depletion during night-time. Because of the difficulties to determine the other transport processes and related uncertainties, on routine basis in most of the micrometeorological sites, NEE (net ecosystem CO<sub>2</sub> exchange) estimations under low night-time turbulence conditions are filtered out (filtering approach) and replaced with NEE values modelled as a function of soil/air temperature. However, when the air flows above and below canopy are decoupled, the friction velocity measured above the canopy (at the same level of EC flux) fails to represent the degree of turbulent mixing within the canopy.

Recently, we have studied the occurrence of night-time decoupling situations occurring in the canopy layer at Hyytiälä forest, and we proposed the use of alternative decoupling indicators (Alekseychik et al., 2013). Night-time decoupling conditions were found in at least 30% of summer night periods, when drainage flow was detected close to ground. Finally, by using within canopy measurements of temperature and wind speed profiles, we found the depth of the decoupled layer related to variations of atmospheric stability, and explained to some extent the fraction of night-time respiration not detected by the above canopy EC system.

## FLUX STUDIES

### *Lakes and carbon dioxide*

Lakes differ drastically from other types of terrestrial land in terms of surface—atmosphere interactions. The CO<sub>2</sub> dynamics are driven both by biological processes, and physical processes due to turbulence in the lake and in the atmosphere. A boreal lake can be a source of CO<sub>2</sub>, which compares to about 10% of the TER production in the surrounding forest (Huotari et al., 2011). The energy budget is governed by the large thermal inertia of water, which enables nocturnal evaporation (Nordbo et al., 2011). Thus, one consequence is that lakes should be treated separately as a different tile in numerical weather prediction models (Manrique-Suñén et al., 2013). The recent review article by Reignier et al. (2013) on global scale carbon fluxes from land to ocean stresses the need for more direct flux measurements over inland waters.

### *Urban surface and carbon dioxide*

The long term variability of CO<sub>2</sub> net exchange was analysed at the urban measurements station SMEAR III. In addition, the gap filling methods (neural network with and without traffic as one of the independent variables and median diurnal cycles) to calculate annual CO<sub>2</sub> fluxes (Järvi et al. 2012). The measured fluxes were highly dependent on the prevailing wind direction with the highest fluxes downwind from a large road and lowest downwind from the area of high fraction of vegetation cover. On an annual level, the area of the road emitted 3500 g C m<sup>-2</sup> whereas the area of high fraction of vegetation cover emitted only 870 g C m<sup>-2</sup>. Seasonal differences in the CO<sub>2</sub> exchange downwind from the road were mainly caused by reduced traffic rates in summer, whereas in other directions seasonality was more determined by vegetation activity. Differences between the gap filling methods were small, but slightly better (0.6 μmol m<sup>-2</sup> s<sup>-1</sup> smaller RMSE) results were obtained when the artificial neural network with traffic counts was used instead of the one without traffic network and method based on median diurnal cycles. The measurement site was a net carbon source with average annual emissions of 1760 g C m<sup>-2</sup>, with a biased error of 6.1 g C m<sup>-2</sup> caused by the gap filling. The annual CO<sub>2</sub> emission obtained in this study was combined with annual estimates from other cities and these were compared to the natural surface cover ( $f_n$ ) (Nordbo et al. 2012).  $f_n$  seems to be a good proxy for the annual CO<sub>2</sub> emissions in urban areas and can further be used to get regional CO<sub>2</sub> emission estimated for urban areas. Fig. 1 presents the comparison between fluxes for four different surfaces.

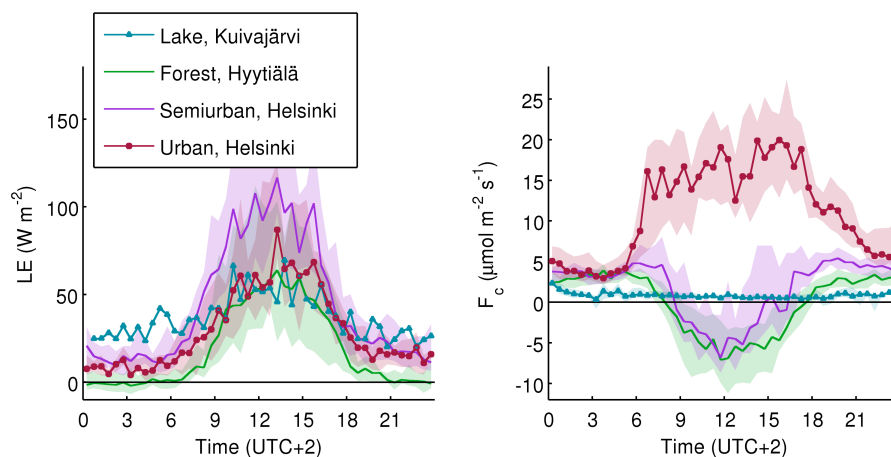


Fig. 1. The monthly-average diurnal variation of the latent heat flux (evapo-transpiration; LE) and CO<sub>2</sub> flux ( $F_c$ ) over lake, forest, semiurban and urban surface. The median and 25 and 75% quartiles are presented. The data is collected over September 2012.

#### *Methane gradient-based flux measurements over forest*

Methane and carbon dioxide concentration profile are measured at Hyytiälä tall tower (16, 67 and 125 m) since Nov 2011. These measurements were initialized as the ICOS (Integrated Carbon Observation System) tall tower activity. Ecosystem scale fluxes of CH<sub>4</sub> are estimated by using the modified Bowen ratio (MBR). by using MBR the eddy diffusivity is not parameterized, but it is directly derived from measurements. The eddy diffusivity coefficient is estimated by using simultaneous measurements of CO<sub>2</sub> flux (by EC) and concentration gradient from the same tower. First results from SMEAR II tall tower look interesting, showing, on average, a CH<sub>4</sub> uptake during winter and CH<sub>4</sub> emission during the growing season. CH<sub>4</sub> flux measurements at forest floor (performed by chambers in 2002 and 2003) show an average uptake value of -50 µg m<sup>-2</sup> h<sup>-1</sup> (Pihlatie et al., 2008). Possible reasons for the emission measured at the tower are: 1) oxic production of CH<sub>4</sub> by the canopy; 2) anoxic production of CH<sub>4</sub> in small ponds at forest floor; 3) anoxic production of CH<sub>4</sub> in wetlands & lakes inside the tall tower footprint. The analysis is under progress.

#### *Urban surface and nitrous oxide*

Besides, in summer – fall 2012 we had a measurement campaign for N<sub>2</sub>O fluxes using the eddy covariance technique. These represent second of their kind in urban areas (Famulari et al. 2010). The measurements lasted from 21 June to 27 November 2012 and measurement setup consisted of the same ultrasonic anemometer (USA-1, Metek GmbH, Germany) as used in the other flux observations and a TDL spectrometer (TGA-100A, Campbell Scientific Inc.) to observe the N<sub>2</sub>O concentrations. The preliminary results show a weak dependency on local traffic with clear morning and afternoon peaks following those of the CO<sub>2</sub> fluxes. The net N<sub>2</sub>O emissions are highest from the direction of the high vegetation cover fraction when compared to other directions, build and road, with higher emissions from the University Botanical Garden, where intense fertilization is done, than in the allotment garden, where only natural fertilization is allowed.

#### *Forest and ozone*

In a recent study by Rannik et al. (2012) we analyzed the canopy-level ozone fluxes, measured at Hyytiälä Scots Pine forest, for deposition characteristics and partitioning into stomatal and non-stomatal fractions, with the main focus on growing season day-time data. Ten years of measurements enabled the analysis of ozone deposition variation at different time-scales, including daily to inter-annual variation as well as the dependence on environmental variables and concentration of biogenic volatile organic compounds. It was found that the O<sub>3</sub> day-time total and stomatal conductance evolved throughout the growing season being the highest during the peak of the growing season. The non-stomatal fraction of conductance increased and achieved maximum in the end of the growing season. While seasonal changes in total O<sub>3</sub> deposition were mostly correlated with photosynthetic capacity, PAR, VPD and monoterpene concentration, these same environmental variables did not explain inter-annual differences of O<sub>3</sub> deposition.

#### *Forest and carbonyl sulphide*

In April 2013 we started EC flux measurements of carbonyl sulfide (COS) over the Hyytiälä forest. COS is the new compound measured at Hyytiälä and number of the direct COS flux measurements worldwide is very small. As the uptake of COS and CO<sub>2</sub> by vegetation is closely coupled during photosynthesis, we aim to use concurrent COS and CO<sub>2</sub> measurements to separately quantify the photosynthesis (GPP) and respiration (TER) at ecosystem scales. The first results look promising, showing clear uptake of COS by trees during daytime similar to results by Asaf et al. (2013). Fig. 2 shows the COS flux for the Hyytiälä forest. The data-processing and further analysis is under progress.

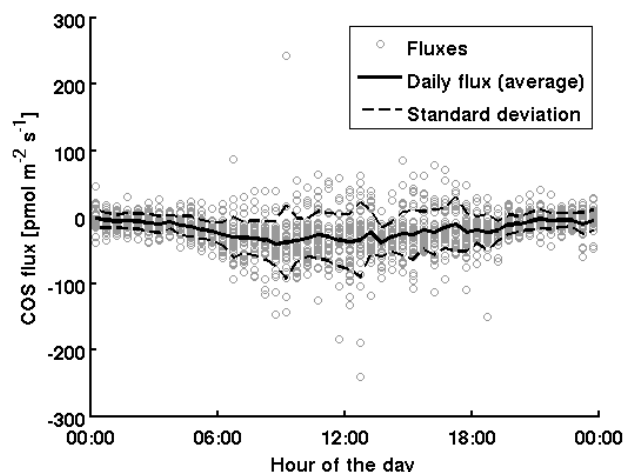


Fig. 2. The monthly-averaged diurnal flux of carbonyl sulfide and single  $\frac{1}{2}$  h fluxes for June 2013 at Hyytiälä forest.

#### *Urban surface and aerosol particles*

Three years (2008 - 2010) of aerosol particles fluxes together with aerosol particle concentrations and size distributions were examined (Ripamonti *et al.* 2013) over the urban surface in Helsinki. Traffic emissions were identified as the most important source of particles by both concentrations and fluxes. Considering the differences in the flux and concentration footprints, the effect of local or distance sources on the measured particle number concentration and size distributions was shown. Combining the measured particle fluxes and footprints calculated using the Korman and Meixner model (Korman and Meixner 2001) we were able to estimate emission factors for the mixed fleet traffic passing by the road next to the measurement tower. The emission factors increase with decreasing temperature. The increased particle number emissions at low temperatures have been associated with increased new particle formation in vehicle exhaust and the enhanced nucleation and condensation of emitted condensable compounds.

## PROCESS MODELLING

#### *Modelling methane emissions from wetlands*

We have been developing a process model of  $\text{CH}_4$  transport and oxidation in boreal peatlands. The model is aiming to be a part of the CBALANCE carbon tool of the JSBACH (Jena Scheme for Biosphere-Atmosphere Coupling in Hamburg), land component of the MPI (Max Planck Institute) Earth System Model. Carbon uptake and soil respiration in peatlands were modeled by the group at MPI (Schuldt *et al.*, 2013). Our part of the peatland model simulates production of  $\text{CH}_4$  as a proportion of anoxic soil respiration, transport of  $\text{CH}_4$  and oxygen between the soil and the atmosphere via diffusion in aerenchymatous plants and peat,  $\text{CH}_4$  ebullition, and oxidation of  $\text{CH}_4$ . The model is based on the methane emission model of Wania *et al.* (2010); however, we have improved several parts.

The model takes as input the anoxic respiration rates in two soil compartments, intermittently oxic acrotelm and constantly anoxic catotelm. The processes are simulated for a peat column that has an adjustable layer structure and total thickness. In the development phase, we have used 7 to 9 soil layers, with thinner layers at the top. The transport model is forced with water table depth, soil temperature, and relative coverage of gas-transporting plants. Rate of  $\text{CH}_4$  oxidation depends on the oxygen concentration. At the moment, the model development is finished and we are about to start validating it against observational data of measured  $\text{CH}_4$  fluxes.

#### *Modelling of BVOC emissions including dynamic vegetation*

Estimates of past atmospheric concentration of biogenic volatile organic compounds (BVOCs) are important for both their contribution to the formation of secondary organic aerosols (SOAs) in part atmospheres, and

for the role they play in the oxidative capacity of the atmosphere. The hydroxyl radical (OH) is the main atmospheric sink for methane, and BVOCs compete with methane for being oxidized by OH. We have run global dynamic vegetation simulations, with a vegetation BVOC emission model included, for the past 8000 years to estimate past levels of isoprene and monoterpenes emissions for both preindustrial and pre-agriculture times. We also used two different scenarios of the extent of past human land use to provide a high and a low estimate of its effect.

Simulations were run with LPJ-GUESS (Smith et al. 2001, Sitch et al. 2003), a process-based dynamic vegetation model. It uses climate inputs as physical drivers (temperature, precipitation, sunlight, ambient CO<sub>2</sub> concentration, soil type) to simulate ecosystem processes, such as photosynthesis, evapotranspiration, vegetation and soil respiration, decomposition in the soil, and also BVOC emissions. Vegetation is represented as 11 different plant function types (PFTs), which differ in physiological characteristics and bioclimatic limits. The BVOC emission model (Arneth et al. 2007, Schurgers et al. 2009) links BVOC production to the electron transfer rate of the photosynthesis model. The two different estimates of the time evolution of human land use during the last 8000 years were by Kaplan et al. (2010) and by Klein Goldewijk et al. (2011). These two reconstructions present quite different estimates of area under human land use before modern times.

#### ACKNOWLEDGMENTS

Academy of Finland Center of Excellence (project no 1118615), the Nordic Center of Excellence DEFROST, ICOS, ICOS-Finland and InGOS EU project are acknowledged.

#### REFERENCES

- Alekseychik, P., I. Mammarella, S. Launiainen, Ü. Rannik and T. Vesala. Evolution of the nocturnal decoupled layer in the pine forest canopy. *Agric. Forest Meteorol.* (in press)
- Arneth, A., Niinemets, Ü., Pressley, S., Bäck, J., Hari, P., Karl, T., Noe, S., Prentice, I. C., Serça, D., Hickler, T., Wolf, A. and Smith, B. (2007). Process-based estimates of terrestrial ecosystem isoprene emissions: incorporating the effects of a direct CO<sub>2</sub> isoprene interaction. *Atmos. Chem. Phys.*, 7: 31-53.
- Aubinet, M., T. Vesala and D. Papale (2012). *Eddy Covariance - A Practical Guide to Measurement and Data Analysis*, Springer atmospheric sciences, 438.
- Famulari D., Nemitz E., Di Marco C., Phillips G.J., Thomas R., House E. and Fowler D. (2010). Eddy Covariance measurements of nitrous oxide fluxes above a city. *Agricultural and Forest Meteorology* 150, 786 – 793.
- Huotari, J., A. Ojala, E. Peltomaa, A. Nordbo, S. Launiainen, J. Pumpanen, T. Rasilo, P. Hari and T. Vesala. (2011). Long-term direct CO<sub>2</sub> flux measurements over a boreal lake: Five years of eddy covariance data, *Geophys. Res. Lett.*, 38, L18401.
- Järvi L., Nordbo A., Junninen H., Riikonen A., Moilanen J., Nikinmaa E. and Vesala T. (2012). Seasonal and annual variation of carbon dioxide surface fluxes in Helsinki, Finland, in 2006-2010. *Atmospheric Chemistry and Physics* 12, 8475 – 8489.
- Kaplan, J. O., Krumhardt, K. M., Ellis, E. C., Ruddiman, W. F., Lemmen, C., and Goldewijk, K. K. (2011). Holocene carbon emissions as a result of anthropogenic land cover change. *The Holocene*, 21(5), 775-791.
- Klein Goldewijk, K., Beusen, A., Van Dreht, G., and De Vos, M. (2011). The HYDE 3.1 spatially explicit database of human-induced global land-use change over the past 12,000 years. *Global Ecology and Biogeography*, 20(1), 73-86.
- Korman, R. and Meixner, F. (2001). An analytical footprint model for non-neutral stratification. *Boundary Layer Meteorology* 99, 207 – 224.

- Manrique-Suñén, A., A. Nordbo, G. Balsamo, A. Beljaars and I. Mammarella. (2013). Representing Land Surface Heterogeneity: Offline Analysis of the Tiling Method, *J. Hydrometeorol.*, 14, 850-867.
- Nordbo, A., S. Launiainen, I. Mammarella, M. Leppäranta, J. Huotari, A. Ojala and T. Vesala. (2011). Long-term energy flux measurements and energy balance over a small boreal lake using eddy covariance technique, *J. Geophys. res.*, 116, 1-17.
- Nordbo A., Järvi L., Haapanala S., Wood C. and Vesala T. (2012). Fraction of natural area as main predictor of net CO<sub>2</sub> emissions from cities. *Geophysical Research Letters*. 39, L20802, doi:10.1029/2012GL053087.
- Nordbo, A., L. Järvi and T. Vesala. (2012). Revised eddy covariance flux calculation methodologies - effect on urban energy balance, *Tellus Ser. B-Chem. Phys. Meteorol.*, 64, 18184.
- Nordbo, A., P. Kekäläinen, E. Siivola, R. Lehto, T. Vesala and J. Timonen. (2013). Tube transport of water vapor with condensation and desorption, *Applied Physics Letters*, 102
- Nordbo, A. and G. Katul. (2013). A Wavelet-Based Correction Method for Eddy-Covariance High-Frequency Losses in Scalar Concentration Measurements, *Bound. -Layer Meteorol.*, 146, 81-102.
- Pihlatie, M., A. Simojoki, J. Pumpanen and P. Hari, In: Hari, P., Kulmala, L. (Eds.) *Boreal Forest and Climate Change*. Springer, 582 pp., 2008.
- Rannik, Ü., N. Altimir, I. Mammarella, J. Bäck, J. Rinne, T. M. Ruuskanen, P. Hari, T. Vesala and M. Kulmala (2012). Ozone deposition into a boreal forest over a decade of observations: evaluating deposition partitioning and driving variables. *Atmos. Chem. Phys.* 12, 12165-12182.
- Reignier P. et al. (2013). Anthropogenic perturbation of the carbon fluxes from land to ocean. *Nature Geosci.* 6, 597-607.
- Ripamonti G., Järvi L., Mølgaard B., Hussein T., Nordbo A. and Hämeri K. (2013). The effect of local sources on aerosol particle number size distribution, concentrations and fluxes in Helsinki, Finland. *Tellus B* 65, <http://dx.doi.org/10.3402/tellusb.v65i0.19786>.
- Asaf, D., E. Rotenberg, F. Tatarinov, U. Dicken, S.A. Montzka and D. Yakir (2013). Ecosystem photosynthesis inferred from measurements of carbonyl sulphide flux. *Nature Geosci.* 6, 186-190.
- Schuldt, R. J., Brovkin, V., Kleinen, T., and J. Winderlich (2013). Modelling Holocene carbon accumulation and methane emissions of boreal wetlands – an Earth system model approach. *Biogeosciences*, 10, 1659-1674.
- Schurgers, G., Arneth, A., Holzinger, R., and Goldstein, A. H. (2009). Process-based modelling of biogenic monoterpene emissions combining production and release from storage. *Atmos. Chem. Phys.* 9(10), 3409-3423.
- Sitch, S., Smith, B., Prentice, I. C., Arneth, A., Bondeau, A., Cramer, W., Kaplan, J. O., Levis, S., Lucht, W., Sykes, M. T., Thonicke, K., and Venevsky, S.: Evaluation of ecosystem dynamics, plant geography and terrestrial carbon cycling in the LPJ dynamic global vegetation model, *Global Change Biol.*, 9, 161– 185, 2003.
- Smith, B., Prentice, I. C., and Sykes, M. T.: Representation of vegetation dynamics in the modelling of terrestrial ecosystems: comparing two contrasting approaches within European climate space, *Glob. Ecol. Biogeosci.*, 10, 621–637, 2001.

Wania, R., I. Ross and I.C. Prentice (2010). Implementation and evaluation of a new methane model within a dynamic global vegetation model: LPJ-WHyMe v1.3.1. *Geoscientific Model Development* 3: 565-584.

## AN OVERVIEW OF UNIVERSITY OF HELSINKI URBAN AND INDOOR AEROSOLS GROUP ACTIVITIES IN 2012-2013

K.HÄMERI<sup>1</sup>, T. HUSSEIN<sup>1</sup>, B. MOLGAARD<sup>1</sup>, V. DOS SANTOS-JUUSELA<sup>1</sup>, J. KOIVISTO<sup>2</sup>, A.-K. VIITANEN<sup>2</sup>, A. S. GODINHO<sup>1,2</sup>, G. RIPAMONTI<sup>1</sup>, L. JÄRVI<sup>1</sup>, A. NORDBO<sup>1</sup>, A. MARAGKIDOU<sup>1</sup>, M. REPO<sup>1</sup>

<sup>1</sup>Department of Physics, FI-00014 University of Helsinki, Finland.

<sup>2</sup>Finnish Institute of Occupational Health, FI-00250 Helsinki, Finland.

Keywords: URBAN AEROSOLS, INDOOR AEROSOLS, WORKPLACE AEROSOLS, NANOTECHNOLOGY, EXPOSURE ASSESSMENT, and HEALTH EFFECTS

### INTRODUCTION

During the last years the activities of the urban and indoor aerosol group of Division of Atmospheric Science, University of Helsinki has been strongly increasing. We have been developing several models to describe the aerosol behaviour indoors and outdoors in urban areas. The indoor aerosols model MC-SIAM has been under continuous evaluation and validation with experimental databases that emerge from our, and also our collaborators', measurement campaigns. This aerosol model is also capable of determining and quantifying indoor emissions that accompany inhabitants' activities. On the other hand, we have recently developed a statistical model (M-FUAQ) to predict the fine particle number concentrations in the urban background atmosphere. With the MC-SIAM, M-FUAQ can be utilized as a tool to investigate the exposure of humans in the future by forecasting the aerosol particles indoors and outdoors. Very recently, we developed a simple model (DOSE) to estimate the deposited fraction of aerosol particles in the respiratory system. The combined modelling approach including DOSE, MC-SIAM, and F-UAQ was recently utilized for a group of subjects living in the Helsinki Metropolitan Region.

Our research is not limited to the abovementioned perspective; we also continuously develop tools and models to be shared with our partners as applications. For instance, we developed a first-principle model to estimate the dry deposition of aerosol particles on any type of surface. This model was tested for deposition of fungi spores inside canopies. This model is foreseen to have a wide range of applications starting from small-scale models to large models utilized in climate models.

The presented short synthesis is based mainly on the work published within years 2011-2013. Furthermore, some on going research activities are introduced shortly by refereeing to relevant extended abstracts in this issue of FCoE proceedings and to already published works in the scientific literature.

### ADVANCES IN AEROSOL MODELLING

We have developed a statistical model for forecasts of urban particle number concentrations. It relates particle concentrations to weather conditions and traffic intensity. Recently the model was tested with data from five cities and it performed well in locations in which local emissions contribute substantially to the particle concentration.

### ADVANCES IN LABORATORY EXPERIMENTS

We tested five air cleaners in a room size chamber, and quantified their performance in terms of the Clean Air Delivery Rate (CADR), which is a standard measure of air cleaner performance. The three filter based air cleaners performed best (CADR > 100 m<sup>3</sup>/h) and an electrostatic precipitator had CADR of around 70

m<sup>3</sup>/h. An ion generator had CADR clearly below 50 m<sup>3</sup>/h for particle sizes above 100 nm, but it performed better for ultrafine particles.

#### ADVANCES IN URBAN NANOPARTICLE STUDIES

Understanding the spatial – temporal variability of UFP is crucial for realistically estimating exposure levels in urban areas. We aimed to evaluate the contrast and correlation of particle number concentrations (PNC) between a hotspot and an urban background of Helsinki. For this purpose, we measured PNC in a busy, poorly ventilated street (urban hotspot) and an urban background (3 km away) continuously for about six months. In addition, we also investigated the association between PNC and PM<sub>2.5</sub>, PM<sub>10</sub> and BC, and the effects of temperature, wind speed and wind direction on PNC at the street. Our results show that although concentrations correlated well between the sites ( $r = 0.70$ ), median PNC at the street was about 3.5 times higher than the background levels (1-h means). PNC were inversely proportional to wind speed and temperature, and highly dependent on wind direction. Moreover, PNC were highly correlated to BC, moderately correlated to PM<sub>2.5</sub> and weakly correlated to PM<sub>10</sub>, indicating that regulations based solely on PM mass measurements may be inadequate to prevent harmful exposure to UFP in urban areas.

#### ADVANCES IN URBAN SIZE DISTRIBUTION AND FLUX STUDIES

Three years of aerosol particle number concentrations, size distributions, and vertical particle fluxes measured at the semi-urban SMEAR III station in Helsinki, Finland, were studied. The purpose was to study the local emission sources and their effect on particle concentrations and size distributions. By means of cluster analysis, six representative size distributions were identified. Their occurrence together with particle concentrations and fluxes were found to vary significantly with wind direction. Lower particle concentrations and fluxes were measured downwind from vegetated and residential areas compared to directions where the measurement site is downwind from roads passing near the measurement site. For these directions contribution of the local sources on the measured particle concentrations and size distributions were evident. In particular, size distributions with a mode in the size range 20-40 nm were found to be more affected by local traffic emissions whereas the mode shifted towards larger sizes when contribution from distant sources was more evident. Using flux footprint functions, mixed vehicle fleet emission factors (EF) were derived from the particle flux measurements.

#### ADVANCES IN NANOPARTICLE EXPOSURE STUDIES

We have developed methods to discriminate process specific concentrations from background particles. Inhaled dose of the concentrations can be estimated with lung deposit models which further can be used to estimate acute health effects for certain toxicological endpoints when the biological dose responses are known. We have developed exposure setups to study health effects of engineered nanomaterials (ENMs) in vitro. There were used to study inflammatory genotoxicity of metal oxide nanoparticles and carbon nanotubes.

We have assessed process specific ENM exposures in four different workplaces using following processes: synthesis of metaloxides, Packing of TiO<sub>2</sub> nanomaterial, handling of nanodiamonds, and synthesis of carbon nanotubes. Workers risk to suffer inflammatory and genotoxic health effects was low in TiO<sub>2</sub> synthesis and packing. According to our preliminary tests to estimate inflammatory dose response from in vivo showed a minor risk in handling of nanodiamonds.

We monitored over eight consecutive days, gases concentration, particulate matter (PM) and transmission electron microscope (TEM) samples continuously during transparent films CNTs production. This study revealed that workers' exposure to CNTs during operation could not be easily distinguished based on these particle measurements. However, during the work days, elevated particle number, mass and CO concentrations up to  $2.7 \times 10^4$  cm<sup>-3</sup> and  $3.2 \times 10^2$  µg m<sup>-3</sup> and  $6.3 \times 10^5$  µg m<sup>-3</sup> respectively were

observed and revealed that CNTs exposure did occur. Additionally, TEM images confirmed the presence of CNTs in the room air.

## ACKNOWLEDGEMENTS

The funding from the Academy of Finland Center of Excellence program and The Finnish Work Environment Fund are acknowledged.

## REFERENCES

- Hussein T, Löndahl J, Paasonen P, Koivisto AJ, Petäjä T, Hämeri K, Kulmala M. Modeling Regional Deposited Dose of Submicron Aerosol Particles. *Science of the Total Environment* 2013, 458–460: 140–149.
- Hussein T, Norros V, Hakala J, Petäjä T, Aalto PP, Rannik Ü, Vesala T, Ovaskainen O. Species Traits and Inertial Deposition of Fungal Spores. *Journal of Aerosol Science* 2013, 61: 81–98.
- Hussein T, Paasonen P, Kulmala M. Activity pattern of a selected group of school occupants and their family members in Helsinki – Finland. *Science of the Total Environment* 2012, 425: 289–292.
- Hussein T, Smolik J, Kerminen V-M, Kulmala M. Modeling dry deposition of aerosol particles onto rough surfaces. *Aerosol Science and Technology* 2012, 46: 44–59.
- Hämeri K., Lähde T., Hussein T., Koivisto J., and Savolainen K. (2009). Facing the key workplace challenge: Assessing and preventing exposure to nanoparticles at source. *Inhalation Toxicology* 21, 17–24.
- Dos Santos-Juusela V., Petäjä T., Kousa A., and Hämeri K. (2013) Spatial - temporal variations of particle number concentrations between a busy street and the urban background, *Atmospheric Environment*, 324–333 DOI 10.1016/j.atmosenv.2013.05.077
- Koivisto, A.J., Palomäki, J.E., Viitanen, A.-K.K., Kanerva, T.S., Alenius, H.T., Hussein, T., Hämeri K. (2013). A risk assessment of Nanodiamonds showed low risk of toxic effects in industrial settings. Submitted to *Nanotoxicology*.
- Koivisto, A.J. (2013). Source specific risk assessment of indoor aerosol particles. Report Series In *Aerosol Science* 140.
- Koivisto, A.J., Aromaa, M., Mäkelä, J.M., Pasanen, P., Hussein, T., Hämeri, K. (2012). Concept to estimate regional inhalation dose of industrially synthesized nanoparticles. *ACS Nano* 6 1195–1203.
- Koivisto, A.J., Yu, M., Hämeri, K., Seipenbusch, M. (2012). Size resolved particle emission rates from an evolving indoor aerosol system. *Journal of Aerosol Science* 47:58–69.
- Koivisto, A.J., Lyyränen, J., Auvinen, A., Vanhala, E., Hämeri, K., Tuomi, T., Jokiniemi J. (2012). Industrial worker exposure to airborne particles during the packing of pigment and nanoscale titanium dioxide. *Inhalation Toxicology* 24:839–849.
- Koivisto A.J., Mäkinen M., Rossi E.M., Lindberg H.K., Miettinen M., Falck G.C.-M., Norppa H., Alenius H., Korpi A., Riikonen J., Vanhala E., Vippola M., Pasanen P., Lehto V.-P., Savolainen K., Jokiniemi J., and Hämeri K. (2011). Aerosol characterization and lung deposition of synthesized TiO<sub>2</sub> nanoparticles for murine inhalation studies. *Journal of Nanoparticle Research* 13:2949–2961.

Leskinen, J., Joutsensaari, J., Lyyrinen, J., Koivisto, J., Ruusunen, J., Järvelä, M., Tuomi, T., Hämeri, K., Auvinen, A., Jokiniemi, J., (2012). Comparison of nanoparticle measurement instruments for occupational health applications. *Journal of Nanoparticle Research* 14:718.

Lindberg, H.K., Falck, G. C.-M., Catalán, J., Koivisto, A.J., Suhonen, S., Järventaus, H., Rossi, E.M., Nykäsenoja, H., Peltonen, Y., Morenoc, C., Alenius, H., Tuomi, T., Savolainen, K.M., Norppa, H. (2012) Genotoxicity of inhaled nanosized TiO<sub>2</sub> in mice. *Mutation Research* 745:58-64.

Mølgaard B, Ondráček J, Šťávoň P, Džumbová L, Barták M, Hussein T, Smolík J. Migration of Aerosol Particles inside a Two-Zone Apartment with Natural Ventilation: a Multi-Zone Validation of the MC-SIAM. *Indoor and Built Environment* 2013 (Available on-line DOI: 10.1177/1420326X13481484).

Mølgaard B, Hussein T, Corander J, Hämeri K. Forecasting Size-Fractionated Particle Number Concentrations in the Urban Atmosphere. *Atmospheric Environment* 2012, 46: 155–163.

Ripamonti G., Järvi L., Mølgaard B., Hussein T., Nordbo A. and Hämeri K. (2013) The effect of local sources on aerosol particle number size distribution, concentrations and fluxes in Helsinki, Finland, *Tellus*, in press.

Rossi E.M., Pylkkänen L., Koivisto A.J., Nykäsenoja H., Wolf H., Savolainen K., and Alenius H. (2010). Inhalation exposure to nanosized and fine TiO<sub>2</sub> particles inhibits features of allergic asthma in a murine model. *Particle and Fibre Toxicology*, 7:35.

Rossi E.M., Pylkkänen L., Koivisto A.J., Vippola M., Jensen K.A., Miettinen M., Sirola K., Nykäsenoja H., Karisola P., Stjernvall T., Vanhala E., Kiilunen M., Pasanen P., Mäkinen M., Hämeri K., Joutsensaari J., Tuomi T., Jokiniemi J., Wolf H., Savolainen K., Matikainen S., and Alenius H. (2009). Airway Exposure to Silica-Coated TiO<sub>2</sub> Nanoparticles Induces Pulmonary Neutrophilia in Mice. *Toxicological Sciences* 113:422-433.

Rydman E, Ilves M, Koivisto J, Kinaret P, Fortino V, Savinko T, Lehto M, Pulkkinen V, Vippola MM, Hämeri K, Matikainen S, Wolff H, Savolainen K, Greco D, Alenius H. (2013). Inhalation of rod-like carbon nanotubes causes unconventional asthma. Submitted to *Nature Nanotechnology*.

## RECENT ADVANCES IN ION AND AEROSOL MEASUREMENTS

H.E. MANNINEN, K. LEHTIPALO, P.P. AALTO, J. BACKMAN, X. CHEN, J. DUPLISSY, A. FRANCHIN, N. KALIVITIS, J. KANGASLUOMA, F. KORHONEN, R. KRECJI, J. LAMPILAHTI, K. LEINO, G. STEINER, R. WAGNER, D. WIMMER, R. VÄÄNÄNEN, T. PETÄJÄ, and M. KULMALA

Aerosol and Ion Group, Division of Atmospheric Sciences, Department of Physics, University of Helsinki,  
P.O. Box 64, 00014, Helsinki, Finland.

Keywords: Atmospheric aerosol particles, long-term measurements, PBL, laboratory studies.

### INTRODUCTION

Aerosol and Ion group at University of Helsinki has a comprehensive long-term experience of ground-level aerosol measurements. Measurements of ambient aerosol size distributions were started at the SMEAR II station at Hyytiälä, Finland, in January 1996, and have been on-going since then. We are especially interested in these size distribution data to characterize and parameterize periods of new particle formation and growth. Secondary formation of atmospheric aerosol particles, so-called new particle formation (NPF), is believed to be the dominant source of aerosol particles in the atmosphere. Nucleation is a process of gas-to-particle conversion, beginning with a few gas molecules colliding to form a cluster of 1-2 nm in diameter (Kulmala *et al.*, 2013). This first step of NPF is followed by the growth of the newly formed particles. NPF is a frequent phenomenon in the lower atmosphere. Recent development in the aerosol instrumentation to measure the critical particle size below 3 nm in size has enabled the direct detection of the newly formed particles connecting the gas and particle phases (Kulmala *et al.*, 2012).

At this moment, the mechanisms of particle formation and the vapours participating in this process are not truly understood. Especially, in which part of the atmosphere the NPF takes place, is still an open question. Until now, there exists only a few atmospheric dataset measured in lower troposphere over the Northern boreal forests. Our aim is to supplement the on-ground measurements with airborne measurements to cover the cryosphere-aerosol-cloud-climate interactions within the planetary boundary layer (PBL). The PBL is chemically and physically the most dynamic part of the atmosphere as it has high loading of aerosol particles and their gaseous precursors.

### ADVANCES IN UNDERSTANDING ATMOSPHERIC FORMATION AND GROWTH IN THE LOWER ATMOSPHERE

We measured the chemical and physical processes within the PBL to detect directly the very first steps of NPF in the atmosphere. These measurements of the vertical and the horizontal extension of NPF events were performed using an instrumented airship, Zeppelin. The vertical profile measurements (altitudes up to 1 km) represent the particle and gas concentrations in the lower parts of the atmosphere: the residual layer, the nocturnal boundary layer, and the PBL. At the same time, the ground based measurements records present conditions in the surface layer. Horizontal, almost Lagrangian, experiments are possible as the airship drifts with the air mass. The main nucleation campaigns were performed in Po Valley, Northern Italy (summer 2012), and Hyytiälä, Southern Finland (spring 2013).

The key instruments on-board Zeppelin to measure the onset of NPF were Atmospheric Pressure interface Time-Of-Flight mass spectrometer (APi-TOF), a Particle Size Magnifier (PSM), and a Neutral cluster and Air Ion Spectrometer (NAIS). Instruments are described in more detailed in Kulmala *et al.* (2013) and reference therein. These instruments are able to measure particles at the size range ~1-2 nm where atmospheric nucleation and cluster activation takes place. The high time resolution of the instruments allowed us to observe the starting time, location and altitude of the NPF. These measurements are part of

the PEGASOS project which aims to quantify the magnitude of regional to global feedbacks between the atmospheric chemistry and physics, and thus quantify the changing climate. The Zeppelin flights are observing radicals, trace gases, and aerosols inside the lower troposphere over Europe.

We use also a small Cessna 172 one-engine aircraft with slow velocity (air velocity around 130 km/h) operating between altitudes of 300 m and 3.5 km (Schobesberger *et al.*, 2013). The Cessna flight campaigns have been on-going since spring 2010. We measured vertical profiles up to 3.5 km above the countryside of Southern Finland which is patched with boreal forests of different ages, mires, small lakes, and cultivated land. The aircraft carries comprehensive instrumentation to measure aerosol particle and trace gas properties, and meteorological parameters. The Cessna is able to fly much higher altitudes and cover wide areas, whereas Zeppelin is able to stay over fixed location and fly very low altitudes. The Cessna can easily reach the free troposphere conditions even when the PBL is fully thermally mixed and fly close to cloud deck to study aerosol-cloud interactions, whereas Zeppelin scans the air from first 1000 meters.

## ADVANCES IN INSTRUMENTAL DEVELOPMENT AND LABORATORY STUDIES

In the atmosphere, the mechanisms and vapours contributing to the initial aerosol growth after the cluster formation are not completely understood, which is partly because of the lack of instruments capable of measuring atmospheric clusters and particles between 1 and 3 nm. The break-through to measure neutral particles in sub-3 nm size range was made with the PSM (Airmodus A09, Vanhanen *et al.* 2011) which measures particles down to the mobility diameter of about 1 nm. The PSM is a mixing-type CPC, in which the aerosol is turbulently mixed with air saturated with diethylene glycol. The 50% activation diameter of the instrument can be varied between about 1–2 nm in mobility diameter by changing the mixing ratio of the saturator and sample flows.

In addition to the PSM's capabilities, to measure the sub-7 nm growth rates and get the first indirect measurements of the particle chemical composition between 2 and 3 nm, we built a nano Condensation Particle Counter Battery (nano-CPCB, Kangasluoma *et al.*, 2013) which consists of four CPCs optimized for the detection of sub-3 nm particles, using diethylene glycol, water, and butanol as the CPC working fluids. The nano-CPCB was calibrated with seven different test aerosols, and the size, charge and composition dependent response was obtained for each CPC. From the ambient relevant test aerosols, ammonium sulphate and sodium chloride showed a clear preference to water activation, whereas organics showed preference to butanol activation, which is the foundation of obtaining indirect information from atmospheric aerosols. After the calibration, a TSI nano-DMA was integrated to the nano-CPCB, which was then deployed in an intensive field campaign in Hyytiälä in spring 2013.

On the other hand, laboratory experiments in the CLOUD-chamber (Kirkby *et al.*, 2011) can be also used to study the cryosphere-aerosol-cloud interactions. In the forthcoming CLOUD8 (October-December 2013), 46 instruments from 14 institutes will be deployed around the CLOUD-chamber at CERN to study the effect of the charges on aerosol activation to ice and droplet for temperature condition varying from -65C to +20C. The aerosol will consist of a control mixture of monodisperse aerosol produced in an evaporator and flush inside the chamber. In order to create a cloud inside the chamber, the chamber wall is first coated with ice, creating a saturated relative humidity over ice of 100% inside the chamber. The activation of the cloud is then created by a precisely control adiabatic expansion. The NAIS measuring the ions and neutral cluster concentration has been rebuilt to support such pressure changes. In addition, the NAIS will operate at temperature below 0C, when needed, in a temperature control environment, reducing possible artefact due to ions evaporation. To complete the setup, a SMPS (Scanning Mobility Particle Sizer) and possibly a PSM with fast response time to allow measurement of coagulation between droplet and inactivated aerosol (interstitial).

## ADVANCES IN CONNECTING ATMOSPHERIC ELECTRICITY AND AEROSOL-CLOUD INTERACTIONS

Small ions are part of the atmospheric aerosol spectrum, and in atmospheric sciences study of ion-aerosol interactions is essential. Small ions are small molecular clusters carrying a net electric charge. They are produced by ionisation of molecules in the air. Ion-induced NPF is limited by the ion production rate. The results indicate that particle formation seems to dominate over ion-mediated mechanisms, at least in the boreal forest conditions.

Atmospheric ions play an important role in the fair weather electricity. Atmosphere's fair weather condition concerns the electric field and the electric current in the air as well as the air conductivity. On the other hand, atmospheric ions are important for Earth's climate, due to their potential role in secondary aerosol formation. This can lead to increased number of cloud condensation nuclei (CCN), which in turn can change the cloud properties. Our aim is to quantify the connections between these two important roles of air ions based on field observations and existing data archives. We studied the interactions between atmospheric electricity (air conductivity, electric field, and ambient concentration of small ions), aerosol particles, and cloud properties. In other words, the correlations and trends in atmospheric ionization, electricity, aerosols, and CCN properties were studied.

## OUTLOOK

Within our group, the recent advances have been obtained after collaborative research efforts between laboratory experiments and comprehensive field observations. Thus, the long-term field observations and detailed laboratory and field campaigns are both needed in the future to characterize the cryosphere-aerosol-cloud-climate interactions. The air quality and climate interactions are not neglected. And our measurements are part of international measurement networks e.g. SMEAR, WMO-GAW, NOAA and ACTRIS.

## ACKNOWLEDGEMENTS

This research is supported by European Commission under the Framework Programme 7 (FP7-ENV-2010-265148), the Academy of Finland Centre of Excellence program (project no. 1118615), Academy of Finland Project (139656), the Nordic Centers of Excellence CRAICC, Maj and Tor Nessling Foundation, and Nordic Centre of Excellence CRAICC (CRYosphere-Atmosphere Interactions in Changing Climate). International team of scientists and technicians working with Zeppelin are all acknowledged. The support by the Finnish Cultural Foundation is gratefully acknowledged. In addition, we acknowledge the CLOUD collaboration (FP7 215072).

## REFERENCES

- Kangasluoma, J. et al. (2013) Sub 3 nm Particle Size and Composition Dependent Response of a Nano-CPC Battery, submitted to Atmos. Meas. Tech.
- Kirkby, J. et al. (2011) Role of sulphuric acid, ammonia and galactic cosmic rays in atmospheric aerosol nucleation, *Nature*, 476, 429-U477, 10.1038/nature10343.
- Kulmala, M. et al. (2012) Measurement of the nucleation of atmospheric aerosol particles, *Nature Protocols* 7, 1651-1667, doi:10.1038/nprot.2012.091.
- Kulmala M. et al. (2013) Direct observations of atmospheric aerosol nucleation, *Science* 339, 943-946.
- Schobesberger, S. et al. (2013): Airborne measurements over the boreal forest of southern Finland during new particle formation events in 2009 and 2010. *Boreal Env. Res.* 18: 145-163.
- Vanhanen et al. (2011) Particle size magnifier for nano-CN detection. *Aerosol Sci. Technol.* 45, 533.

## AN OVERVIEW OF UNIVERSITY OF HELSINKI MASS SPECTROMETRY GROUP ACTIVITIES IN 2012-2013

M. SIPILÄ<sup>1</sup>, M. EHN<sup>1,2</sup>, H. JUNNINEN<sup>1</sup>, T. JOKINEN<sup>1,3</sup>, S. SCHOBESBERGER<sup>1</sup>, N. SARNELA<sup>1</sup>, A. PRAPLAN<sup>1</sup>, A. ADAMOV<sup>1</sup>, J. KANGASLUOMA<sup>1</sup>, R. TAIPALE<sup>1</sup>, M. P. RISSANEN<sup>1</sup>, T. LAITINEN, G. LÖNN<sup>1</sup>, V.-M. SUNDELL<sup>1</sup>, M. ÄIJÄLÄ<sup>1</sup>, AND T. PETÄJÄ<sup>1</sup>

<sup>1</sup>Department of Physics, FI-00014 University of Helsinki, Finland

<sup>2</sup>Research Center Jülich (IEK-8), Jülich, Germany

<sup>3</sup>Institute for tropospheric research (Tropos), Leipzig, Germany

Keywords:

ATMOSPHERIC AEROSOL PARTICLES, LABORATORY AND FIELD MEASUREMENTS, MASS SPECTROMETRY, INSTRUMENT DEVELOPMENT.

### INTRODUCTION

The last years have been active for the mass spectrometry group of Division of Atmospheric Science, University of Helsinki. Scientific achievements include breakthroughs in atmospheric oxidation (Mauldin et al. 2012, Berndt et al. 2012), in nanoparticle and cluster formation (Kulmala et al. 2013, Sipilä et al. 2010, Ehn et al. 2012, Petäjä et al. 2011, Kirkby et al. 2011, Kulmala et al. 2012, Almeida et al., 2013 Nature Accepted), in aerosol growth (Riipinen et al. 2012), all published within the last few years in a scientific collaboration with external partners as well as within the Finnish Center of Excellence.

The presented short synthesis is based mainly on the work published within years 2012-2013 including a short overview of ongoing research activities. A broader outlook is given at the end.

### ADVANCES IN UNDERSTANDING ATMOSPHERIC OXIDATION

Sulphuric acid has been a long time one of the favourite molecules connected to atmospheric aerosol formation (Weber et al. 1996, Petäjä et al. 2009, Sipilä et al. 2010). A recent laboratory study by Wetz et al. (2012) showed that also stabilized Criegee Intermediates (sCI) can oxidize SO<sub>2</sub> with a reaction rate orders of magnitude higher than assumed previously (Johnson, et al., 2001).

In the atmosphere, the sCI radicals originate from ozonolysis of alkenes. Ozone attacks the double bond of alkenes producing an energy-rich primary ozonide, which decomposes very rapidly forming the so-called Criegee Intermediate, CI that can be collisionally stabilized by the gaseous medium. This sCI can decompose via unimolecular reactions. However, besides this reaction, the sCIs can react with several atmospheric constituents (Wetz, et al., 2012, Taatjes et al., 2012). Simultaneously with the laboratory findings by Wetz et al. (2012) we discovered a non-OH oxidant, potentially sCI, from the Boreal forest and in our laboratory experiments (Mauldin et al., 2012, Berndt et al., 2012). We demonstrated that the oxidation of SO<sub>2</sub> by the newly found oxidant can account for a significant fraction of sulphuric acid production (up to even 50%) at the surface layer in forested environment (Mauldin et al., 2012). This new pathway can potentially contribute to the atmospheric oxidation and budgets of various other compounds. This can have consequences for current knowledge on atmospheric oxidation capacity as well as new particle formation.

### ADVANCES IN UNDERSTANDING ATMOSPHERIC NUCLEATION

The atmospheric new particle formation is a complicated problem. Sometimes laboratory studies in controlled surroundings can resolve some of the complexities. A detailed study by Kirkby et al. (2011) in the CLOUD chamber shed light into the formation of aerosol particles both via neutral and ion induced pathways. One of the main outcomes of this study was that the sulphuric acid – water system is not capable of reproducing observed atmospheric particle formation rates in the boundary layer. The role of ammonia at concentrations less than 100 pptv crucially enhanced the nucleation rate considerably.

Ammonia is not the only atmospheric base capable of stabilizing highly acidic sulphuric acid clusters. For example, amines (Ge et al. 2011) have been identified as potential candidates for this stabilization (Kurtén et al. 2008). In order to explain our surprisingly high formation rates of sulphuric acid dimers (Petäjä et al. 2011) in a laminar flow tube setup in IFT, Leipzig, we proposed that amines are present even in ultra-clean laboratory experiments. The presence of the stabilizing compound prevented the dimer evaporation. Our results are in line with recent data obtained from the CLOUD chamber. In subsequent studies we have investigated the role of amines in nucleation process further.

The key to observations in the laboratory and field were made possible by the Atmospheric Pressure interface Time-of-Flight mass spectrometer (APi-TOF, Junninen et al. 2010, Ehn et al. 2010). This instrument is sensitive enough to resolve the nucleating clusters and follow their growth molecule by molecule, given that the process occurs at the measurement site. Schobesberger et al. 2013 shows ion cluster evolution in experiments with sulphuric acid, ammonia, amines and pinanediol during the initial steps of nucleation and cluster formation in the CLOUD chamber. These observations indicate that gas phase oxidation can rapidly produce also low volatile organic compounds.

The Chemical Ionization APi-TOF utilizing nitrate ions to charge the ambient sample was introduced in Jokinen et al. (2012). This CI-APi-TOF is capable of detecting virtually all the neutral gas phase compounds that are relevant for atmospheric new particle formation. These compounds include, e.g. sulphuric acid and highly oxidized, extremely low vapour pressure organics (Ehn et al 2013, submitted; Jokinen et al 2013, in prep.), and, if operated in a bisulphate-cluster-ion mode also bases such as ammonia and amines. The sensitivity of the instrument is reaching levels of few thousands of molecules per cc (Sipilä et al., 2013, in prep.).

## ADVANCES IN UNDERSTANDING NANOPARTICLE GROWTH

Organic vapours are thought to be responsible for a large fraction of the aerosol growth (Riipinen et al. 2012) as it cannot be typically explained with sulphuric acid alone. Riipinen et al. (2012) illustrated that a coherent picture can be drawn from the net effect of the organic condensation to nanoparticle growth for example in Hyytiälä. The results indicated that already at sizes around 5 nm more than half of the aerosol mass fraction is organic. The exact nature of these condensing organic vapours is unknown, however the majority needs to have extremely low vapour pressures, such that they condense near-irreversibly onto the particles (Riipinen et al., 2011).

Laboratory study at a Teflon chamber at Paul Scherrer Institute, Switzerland revealed also the importance of organic condensable vapours to nucleation and growth. The results indicated that the organics contribute to the process already at 2 nm (Riccobono et al. 2012). Extremely oxidized organic molecules and their importance in the clustering process and aerosol formation was examined in Ehn et al. (2012). Based on this work we estimated concentration of these organic vapours in Hyytiälä to be in the range of 0.1-1 pptv, and these may constitute a large fraction of the required, nearly non-volatile, organics required (Riipinen et al., 2011) to explain nanoparticle growth in forested regions.

## ADVANCES IN METHODOLOGIES AND TECHNOLOGICAL DEVELOPMENT

Kulmala et al. 2012 presents a complete methodology to characterize regional new particle formation events. This work was mainly done in collaboration with the FCoE. In Kulmala et al. 2012 we explain

how formation, nucleation and growth rates of atmospheric nanoparticles can be determined from state-of-the-art observational data. We introduce the relevant technologies for detecting these particles, explain needed data analysis techniques, provide the best practices to a wider community and even give troubleshooting advice. Furthermore, we underline the need for a long-term commitment of measurements, which is needed in order to resolve regional new particle formation and its consequences in various atmospheric environments.

Instrument development during the last few years has been productive. A crucial step in the development is building up an instrument characterization setup. Kangasluoma (2012) and Kangasluoma et al. (2013, this issue) describes a calibration and instrument verification setup capable of generating ions, clusters and charged particles from molecular standards, inorganic salts, metals and even fullerene in the size range 1-5 nm in a controlled and clean manner. The purity of the system has proven to be crucial in the success of instrument verification and development in the sizes below 3 nm.

The generation setup is important for ongoing development of chemical ionization methods for mass spectrometers (Adamov and Sipilä, 2013, this issue; Jokinen et al. 2013b, this issue) as a sample can be prepared with the same and known chemical composition increasing the repeatability and representativeness of the laboratory verifications (Lehtipalo et al. 2012, Hakala et al. 2013, this issue). The setup can also be used for transmission and fragmentation studies inside the mass spectrometers.

## OUTLOOK

Our scientific understanding on the atmospheric nucleation, growth and aerosol effects on climate have expanded and strengthened during the last few years. The main findings have been obtained after teaming up with various research groups. The added value of the FCoE comes with the collaborative research. Excellent example is e.g. use of quantum chemical considerations to understand better chemical ionization processes (Kurtén et al. 2011). Breaking free from the methodological boundaries will evolve in a wider scientific understanding of the physical and chemical processes leading to secondary aerosol formation. The upcoming years are likely to see a wide range of high-level publications on all the topics discussed in this abstract, with the focus shifting more and more to the study of oxidized organics.

The role of organic vapours in the initial steps and in the subsequent growth needs to be addressed. This requires detailed laboratory experiments both in laminar flow tubes and in static chambers. The laboratory experiments need to be connected to the atmosphere by performing field campaigns in different environments. The oxidative capacity of the atmosphere needs to be resolved in more detail and in the near future, observational capacity in the atmospheric oxidants need to be improved, including the hydroxyl radicals as well as peroxy radicals and stabilized Criegee intermediates.

Together we can tackle grand challenges that are arising. In the atmospheric – surface interface the cycles of carbon, nitrogen, sulphur, water and energy are interconnected. These issues can only be solved jointly in a large group, utilizing all the tools available in an open and coordinated research effort.

## ACKNOWLEDGEMENTS

The Academy of Finland Center of Excellence program (project no. 1118615), Academy of Finland Project (139656) and Nordic Center of Excellence CRAICC.

## REFERENCES

Berndt, T., Jokinen, T., Mauldin III, R.L., Petäjä, T., Herrmann, H., Junninen, H., Paasonen, P., Worsnop, D.R. and Sipilä, M. (2012) Gas-phase ozonolysis of selected olefins: the yield of stabilized criegee intermediate and the reactivity toward SO<sub>2</sub>, *J. Phys. Chem. Lett.*, 3 (19), pp 2892–2896  
DOI: 10.1021/jz301158u

Ehn, M., Junninen, H., Petäjä, T., Kurtén, T., Kerminen, V.-M., Schobesberger, S., Manninen, H.E., Ortega, I.K., Vehkamäki, H., Kulmala, M. and Worsnop, D.R. (2010) Composition and temporal behavior of ambient ions in the boreal forest. *Atmos. Chem. Phys.* 10, pp. 8513-8530.

Ehn, M., Kleist, E., Junninen, H., Petäjä, T., Lönn, G., Schobesberger, S., Dal Maso, M., Trimborn, A., Kulmala, M., Worsnop, D.R., Wahner, A., Wildt, J. and Mentel, Th.F. (2012) Gas phase formation of extremely oxidized pinene reaction products in chamber and ambient air, *Atmos. Chem. Phys.* 12, 5113-5127.

Ge, X., Wexler, A.S. and Clegg, S.L. (2011) Atmospheric amines – Part I, a review, *Atmos. Environ.* 45, 524-546.

Johnson, D., Lewin, A. G. & Marston, G. (2001) The effect of Criegee-intermediate scavengers on the OH yield from the reaction of ozone with 2-methylbut-2-ene. *J. Phys. Chem. A* 105, 2933–2935.

Jokinen, T., Sipilä, M., Junninen, H., Ehn, M., Lönn, G., Hakala, J., Petäjä, T., Mauldin III, R.L., Kulmala, M. and Worsnop, D.R. (2012) Atmospheric sulphuric acid and neutral cluster measurements using CI-API-TOF, *Atmos. Chem. Phys.* 12, 4117-4125.

Junninen, H., Ehn, M., Petäjä, T., Luosujärvi, L., Kotiaho, T., Kostianen, R., Rohner, U., Gonin, M., Fuhrer, K., Kulmala, M. and Worsnop, D.R. (2010) API-ToFMS: a tool to analyze composition of ambient small ions. *Atmos. Meas. Technol.*, 3, pp. 1039-1053.

Kangasluoma, J., H. Junninen, K. Lehtipalo, J. Mikkilä, J. Vanhanen, M. Attoui, M. Sipilä, D. Worsnop, M. Kulmala, and T. Petaja (2013), Remarks on Ion Generation for CPC Detection Efficiency Studies in Sub-3-nm Size Range, *Aerosol Sci Tech*, 47(5), 556-563, doi:Doi 10.1080/02786826.2013.773393.

Kerminen, V.-M., Paramonov, M., Anttila, T., Riipinen, I., Fountoukis, C., Korhonen, H., Asmi, E., Laakso, L., Lihavainen, H., Swietlicki, E., Svenningsson, B., Asmi, A., Pandis, S.N., Kulmala, M. and Petäjä, T. (2012) Cloud condensation nuclei production associated with atmospheric nucleation: a synthesis based on existing literature and new results, *Atmos. Chem. Phys. Discuss.* 12, 22139-22198.

Kirkby, J., Curtius, J., Almeida, J., Dunne, E., Duplissy, J., Ehrhart, S., Franchin, A., Gagné, S., Ickes, L., Kürten, A., Kupc, A., Metzger, A., Riccobono, F., Rondo, L., Schobesberger, S., Tsagkogeorgas, G., Wimmer, D., Amorim, A., Bianchi, F., Breitenlechner, M., David, A., Dommen, J., Downard, A., Ehn, M., Flagan, R.C., Haider, S., Hansel, A., Hauser, D., Jud, W., Junninen, H., Kreissl, F., Kvashin, A., Laaksonen, A., Lehtipalo, K., Lima, J., Lovejoy, E.R., Makhutov, V., Mathot, S., Mikkilä, J., Minginette, P., Mogo, S., Nieminen, T., Onnela, A., Pereira, A., Petäjä, T., Schnitzhofer, R., Seinfeld, J.H., Sipilä, M., Stozhkov, Y., Stratmann, F., Tome, A., Vanhanen, J., Viisanen Y., Vrtala, A., Wagner, P.E., Walther, H., Weingartner, E., Wex, H., Winkler, P.M., Carslaw, K.S., Worsnop, D.R., Baltensperger, U. and Kulmala, M. (2011) The role of sulphuric acid, ammonia and galactic cosmic rays in atmospheric aerosol nucleation, *Nature*, 476, pp. 429-433, doi:10.1038/nature10343.

Kulmala, M., Petäjä, T., Nieminen, T., Sipilä, M., Manninen, H.E., Lehtipalo, K., Dal Maso, M., Aalto, P.P., Junninen, H., Paasonen, P., Riipinen, I., Lehtinen, K.E.J., Laaksonen, A. and Kulmala, M. (2012) Measurement of the nucleation of atmospheric aerosol particles, *Nature Protocols* 7, 1651-1667, doi:10.1038/nprot.2012.091.

Kurtén, T., Loukonen, V., Vehkamäki, H., and Kulmala, M. (2008) Amines are likely to enhance neutral and ion-induced sulphuric acid-water nucleation in the atmosphere more effectively than ammonia, *Atmos. Chem. Phys.*, 8, 4095-4103.

Kurtén, T., Petäjä, T., Smith, J., Ortega, I. K., Sipilä, M., Junninen, H., Ehn, M., Vehkamäki, H., Mauldin, L., Worsnop, D. R., and Kulmala, M. (2011) The effect of H<sub>2</sub>SO<sub>4</sub> - amine clustering on chemical ionization mass spectrometry (CIMS) measurements of gas-phase sulphuric acid, *Atmos. Chem. Phys.*, 11, 3007-3019.

Lehtipalo, K., Vahanen, J., Toivola, T., Mikkilä, J., Petäjä, T. and Kulmala, M. (2012) Characterization of the Airmodus A20 Condensation Particle Counter, this issue.

Mauldin III, R.L., Berndt, T., Sipilä, M., Paasonen, P., Petäjä, T., Kim, S. Kurtén, T., Stratmann, F., Kerminen, V.-M. and Kulmala, M. (2011) New atmospherically relevant oxidant, *Nature*, 488, 193-197, doi:10.1038/nature11278.

Petäjä, T., Sipilä, M., Paasonen, P., Nieminen, T., Kurtén, T., Stratmann, F., Vehkamäki, H., Berndt, T. and Kulmala, M. (2011) Experimental observation of strongly bound dimers of sulphuric acid: application to nucleation in the atmosphere. *Phys. Rev. Lett.* 106, 228302.

Riccobono, F., Rondo, L., Sipilä, M., Barmet, P., Curtius, J., Dommen, J., Ehn, M., Ehrhart, S., Kulmala, M., Kürten, A., Mikkilä, J., Petäjä, T., Weingartner, E. and Baltensperger, U. (2012) Contribution of sulphuric acid and oxidized organic compounds to particle formation and growth, *Atmos. Chem. Phys. Discuss.* 12, 11351-11389.

Riipinen, I., Pierce, J. R., Yli-Juuti, T., Nieminen, T., Häkkinen, S., Ehn, M., Junninen, H., Lehtipalo, K., Petäjä, T., Slowik, J., Chang, R., Shantz, N. C., Abbatt, J., Leaitch, W. R., Kerminen, V.-M., Worsnop, D. R., Pandis, S. N., Donahue, N. M., and Kulmala, M.: Organic condensation: a vital link connecting aerosol formation to cloud condensation nuclei (CCN) concentrations, *Atmos. Chem. Phys.*, 11, 3865-3878, doi:10.5194/acp-11-3865-2011, 2011

Riipinen, I., Yli-Juuti, T., Pierce, J.R., Petäjä, T., Worsnop, D.R., Kulmala, M. and Donahue, N.M. (2012) The contribution of organics to atmospheric nanoparticle growth, *Nat. Geo. Sci.* 5, 453-458, doi: 10.1038/ngeo1499.

Sipilä, M., Berndt, T., Petäjä, T., Brus, D., Vanhanen, J., Stratmann, F., Patokoski, J., Mauldin III, R.L., Hyvärinen, A.-P., Lihavainen, H. and Kulmala, M. (2010) The Role of sulphuric acid in atmospheric nucleation *Science*, 327, pp. 1243-1246.

Taatjes, C. A., Welz, O., Eskola, A. J., Savee, J. D., Osborn, D. L., Lee, E P. F., Dyke, J. M., Mok, D.W. K., Shallcross, D. E. and Percival, C. J. (2012) Direct measurement of Criegee intermediate (CH<sub>2</sub>OO) reactions with acetone, acetaldehyde, and hexafluoroacetone, *Phys. Chem. Chem. Phys.*, 14, 10391-10400.

Weber, R. J., Marti, J. J., McMurry, P. H., Eisele, F. L., Tanner, D. J, and Jefferson A.: Measured atmospheric new particle formation rates: Implications for nucleation mechanisms, *Chem. Eng. Commun.*, 151, 53-64, 1996.

Welz, O., Savee, J.D., Osborn, D.L., Vasu, S.S., Percival, C.J., Shallcross, D.E. and Taatjes, C.A. (2012). Direct kinetic measurements of Criegee intermediate (CH<sub>2</sub>OO) formed by reaction of CH<sub>2</sub>I with O<sub>2</sub>. *Science* 335, 204-207.

## ICOS RI, TOWARDS A EUROPEAN RESEARCH INFRASTRUCTURE

M. KAUKOLEHTO<sup>1</sup>, E. JUUROLA<sup>1,3</sup>, S. SORVARI<sup>2</sup>, T. LAURILA<sup>2</sup>, S. HAAPANALA<sup>1</sup>, P. KERONEN<sup>1</sup>, P. KOLARI<sup>1,3</sup>, I. MAMMARELLA<sup>1</sup>, M. KOMPPULA<sup>4</sup>, K. LEHTINEN<sup>4</sup>, J. LEVULA<sup>5</sup>, T. AALTO<sup>2</sup>, M. AURELA<sup>2</sup>, L. LAAKSO<sup>2</sup>, J. HATAKKA<sup>2</sup>, A. LOHILA<sup>2</sup>, T. MÄKELÄ<sup>2</sup>, A. NORDBO<sup>1</sup>, Y. VIISANEN<sup>2</sup> and T. VESALA<sup>1</sup>

<sup>1</sup>Department of Physics, PL 48, FIN-00014, University of Helsinki, Finland.

<sup>2</sup>Finnish Meteorological Institute, Helsinki, Finland.

<sup>3</sup>Department of Forest Sciences, University of Helsinki, Finland.

<sup>4</sup>University of Eastern Finland, Kuopio, Finland.

<sup>5</sup>Hyttiälä Forestry Field Station, Finland

Keywords: Greenhouse gases, long term observations, climate change, distributed research infrastructure

### BACKGROUND

Climate change is one of the most challenging problems that mankind will have to cope with in the coming decades. The driving force of current and future climate change is the increasing greenhouse gases in the atmosphere, driven by man-made emissions that overtake the natural cycles of carbon dioxide (CO<sub>2</sub>), methane (CH<sub>4</sub>) and nitrous oxide (N<sub>2</sub>O). The concentrations of CO<sub>2</sub> and CH<sub>4</sub> in the atmosphere are at their highest in the past 25 million years. Current levels of CO<sub>2</sub> have increased by 30% from pre-industrial times and they continue to rise, as fossil fuel emissions are climbing up. Current levels of CH<sub>4</sub> are nearly triple the pre-industrial value.

The primary agents of change in greenhouse gas concentrations are fossil fuel combustion and modifications of global vegetation through land use change, in particular deforestation. The natural carbon cycle offers a discount of 50% on the Earth greenhouse effect by absorbing half of the anthropogenic emissions. At the current atmospheric level of CH<sub>4</sub>, the natural oxidizing power cleans up almost all the CH<sub>4</sub> injected by human and natural sources but expected increases of emissions will further raise the CH<sub>4</sub> mixing ratios.

Deeper understanding of the driving forces of climate change requires full quantification of the greenhouse gas emissions and sinks and their dynamics. These can be assessed by long term, high precision observations in the atmosphere and at the ocean and land surface. ICOS will provide the long-term observations required to understand the present state and predict future behaviour of the global carbon cycle and greenhouse gas emissions.

### DISTRIBUTED RESEARCH INFRASTRUCTURE

The legal structure to coordinate and integrate ICOS Research Infrastructure is ERIC (European Research Infrastructure Consortium), set by the European Commission 2009 (Council Regulation n° 723/2009). ERIC is a specific legal form designed to facilitate the joint establishment and operation of research infrastructures of European interest. ICOS ERIC is planned to be established early 2014.

The three tier ICOS RI structure include: 1) Organized ICOS National Networks, 2) ICOS Central Facilities and 3) European legal entity, ICOS ERIC, including the Head Office (HO) and Carbon Portal (CP).

The backbone of ICOS RI is formed by the national measurement stations. *Atmospheric stations* are established to measure continuously the greenhouse gas (CO<sub>2</sub>, CH<sub>4</sub>, N<sub>2</sub>O) concentration variability due to regional and global fluxes. *Ecosystem Stations* are built for monitoring the functioning of land ecosystems and the exchange of energy and greenhouse gases between the ecosystems and the atmosphere. *Marine ICOS* will provide the long-term oceanic observations required to understand the present state and predict future behaviour of the global carbon cycle and climate-relevant gas emissions. A network of ships and fixed stations will be monitoring carbon exchange between the surface ocean and the atmosphere, acidification of oceans, surface temperature, salinity and other variables. Initially there will be more than 80 ICOS observation stations. The ICOS National Networks will gradually extend as more stations are integrated into ICOS RI.

*ICOS Central Facilities* include Atmospheric Thematic Centre (ATC), Ecosystem Thematic Centre (ETC), Ocean Thematic Centre (OTC) and Central Analytical Laboratory (CAL).

ATC is responsible for continuous and discontinuous air sampling, instrument development/servicing, data processing and storage. A central place is needed to ensure that all data are treated with the same algorithms and properly archived for the long term, that the ICOS atmospheric stations can receive permanent support for optimal operation during their lifetime, and that new sensors can be smoothly implemented in the network in the future.

CAL ensures the accuracy of observational data, thorough quality control and routine testing of air sampling material. It provides reference gases for calibration of in-situ measurements performed at the continuous monitoring stations. It also analyses air samples collected at the monitoring stations.

ETC coordinates the ICOS Ecosystem Network providing assistance with instruments and methods, testing and developing new measurement techniques and associated processing algorithms. It also ensures a high level of data standardization, uncertainty analysis and database services in coordination with the ICOS Carbon Portal.

OTC will be coordinating measuring the carbon cycle in oceans within ICOS. It will provide support to the ICOS marine network in the form of information and technical backup on the state of the art instrumentation and analytical methods. It will provide data storage and processing techniques, quality control, and network-wide integration of data to into useful products, such as maps of CO<sub>2</sub> fluxes, carbon transport, and the assessment of ocean acidification.

*The Carbon Portal* shall provide a "one-stop shop" for ICOS data products. It is envisioned as a place where all data produced within ICOS station network can be discovered and accessed and where the scientific community can post elaborated data products that are obtained from ICOS data. The Carbon Portal will provide easily accessible and understandable science and education products.

## THE ROLE OF FINLAND

Finland is leading the implementation and establishment of ICOS organisation. The legal seat and the head office of the ICOS RI will be located in Helsinki, Finland, with secondary node in France. ICOS ERIC is the first ESFRI organisation, of which statutory seat will be located in Finland.

Finland has also a role as a Nordic Hub and mobile laboratory operator of the Atmospheric Thematic Centre (ATC), led by France. Finnish contribution to ATC includes the testing of the instruments and related training under cold Northern conditions, and the operation of the mobile laboratory for the quality assurance of the atmospheric concentration measurements. The ATC-related work has already started and the construction of the mobile lab is almost finished.

The ICOS-Finland is established by three national partners: University of Helsinki (UH), Finnish Meteorological Institute (FMI), and University of Eastern Finland (UEF). ICOS-Finland will operate 14 ICOS measurement stations: four Class 1 atmospheric measurement sites; two Class 1 ecosystem measurement sites; one Class 2 ecosystem measurement site; and seven associate ecosystem measurement sites.

#### RECENT PROGRESS

ICOS community agreed on the statutes and the financial plan in May 2013 and ICOS ERIC application has been submitted by the Finland's permanent representation to the EU to the Commission for step 1 evaluation in 21.6.2013.

In May 2013 ICOS community decided that the Carbon Portal will be coordinated and hosted by Sweden together with The Netherlands. The hosting countries have started the development and construction period. Carbon Portal will be fully operative in 2015.

The ICOS OTC evaluation for the science case has been positively concluded within the ICOS Community. The financial and management case is yet to be evaluated. OTC will be hosted by Norway and the United Kingdom.

The preparatory phase project for ICOS ended in March 2013, and the Transitional Head Office was officially established in Helsinki.

#### ACKNOWLEDGEMENTS

The financial support by EU projects ICOS and IMECC and the Academy of Finland Centre of Excellence program (project no 1118615) and the Academy project "ICOS" (project no 17352) are gratefully acknowledged. The Ministry of Education and Culture, and the Ministry of Transport and Communications have supported the ICOS work in Finland in 2010-2013.

#### WWW –LINKS

<http://www.icos-infrastructure-transition.eu>

<http://www.icos-infrastructure.fi/>

## PAN-EURASIAN EXPERIMENT (PEEX) INITIATIVE

H.K. LAPPALAINEN<sup>1,2</sup>, T. PETÄJÄ<sup>1</sup>, J. KUJANSUU<sup>1</sup>, T. SUNI<sup>1</sup>, T. RUUSKANEN<sup>1</sup>, VM Kerminen<sup>1</sup>,  
Y. VIISANEN<sup>2</sup>, V. KOTLYAKOV<sup>3</sup>, N. KASIMOV<sup>4</sup>, V. BONDUR<sup>5</sup>, G. MATVIENKO<sup>6</sup>, S.  
ZILITINKEVICH<sup>2</sup> and M. KULMALA<sup>1</sup>

<sup>1</sup>Dept. of Physics, P.O. Box 64, FI-00014 University of Helsinki, Finland.

<sup>2</sup>Finnish Meteorological Institute, P.O. Box 503, FI-00101 Helsinki, Finland

<sup>3</sup>The Institute of Geography RAS, 119017, Staromonetny pereulok 29, Moscow, Russia

<sup>4</sup>Moscow State University, Moskovskij Gosudarstvennyj Universitet im. M.V. Lomonosova, Leninskie  
Gory, Moscow 119992, Russia

<sup>5</sup>AEROCOSMOS, 4, Gorokhovskiy lane, Moscow, 105064, Russia

<sup>6</sup>Inst. of Atmospheric Optics SB RAS, Academician Zuev square, Novosibirsk, Novosibirsk reg., 634021  
Russia

Keywords: climate change, biogeochemical cycles, atmospheric aerosols, atmospheric boundary layer, ,  
Siberian ecosystems, Arctic Ocean, research infrastructures, remote sensing, PhD education programmes,  
socio-economic research

## INTRODUCTION

Pan-Eurasian Experiment (PEEX) is a multidisciplinary research –research infrastructure – education initiative aiming at resolving the major uncertainties in the Earth system science and global sustainability questions in the Arctic and boreal Pan-Eurasian regions. PEEX mission is to be a next generation natural sciences and socio-economic research initiative having a major impact on the future environmental, socio-economic and demography development of the Arctic and boreal regions and to be a science community building novel infrastructures in the Northern Pan-Eurasian region. PEEX agenda is built on a initiative by several European, Russian and Chinese research organizations and institutes. The promoter institutes here have been University of Helsinki, Finnish Meteorological Institute in Finland and Institute of Geography, Moscow State University, Aerocosmos and Institute of Atmospheric Optics Siberian Branch, RAS, in Russia. The first PEEX meeting was held in Helsinki in October 2012, followed by the second meeting in Moscow in February 2013 and the third meeting in Hyytiälä in August 2013. PEEX currently involves ca 40 research institutes. From European perspective PEEX experiment can be considered as a crucial part of the strategic aims of several European and national roadmaps for climate change research and the development of next generation research infrastructures.

The PEEX agenda is divided into four focus areas: F-1 Research Agenda, F-2 Infrastructures, F-3 Society Dimension and F-4 Knowledge Transfer. F-1 Research Agenda will use an integrated observational and modeling framework to identify different forcing and feedback mechanisms in the northern parts of the Earth system, and therefore enable more reliable predictions of future regional and global climate. The strategic focus of the F-2 Infrastructures is to ensure the long-term continuation of advanced measurements in the land-atmosphere-ocean continuum in northern Eurasian area. The F-3 Society Dimension, is aimed to provide fast-track assessments of global environmental change issues for climate policy-making and mitigation and adaptation strategies for the northern Pan-Eurasian region. F-4 Knowledge transfer will provide education programmes for the next generation scientists, instrument specialists and data engineers. It will distribute information for general public to build the awareness of climate change and human impact on different scales of the climate problematic and increase visibility of the PEEX activities in Europe, Russian and China. Part of the F-4 PEEX will engage the larger international scientific communities also by collaborating with, utilizing, and advancing major observation

infrastructures such as the SMEAR, ICOS (Kaukolehto et al., this issue), ACTRIS (Petäjä et al., this issue), and ANAEE (Siitonen et al., this issue) networks in addition to building its own in the Northern Pan-Eurasian region. PEEEX will promote standard methods and best practices in creating long-term, comprehensive, multidisciplinary observation data sets and coordinate model and data comparisons and development

The PEEEX domain covers natural and urban environments of Northern Pan-Eurasian region. The natural environments include boreal coniferous and deciduous forests, steppe, wetlands and aquatic ecosystems including marshes, large river systems and freshwater bodies as well as the marine ecosystems, mountains and sub-arctic tundra ecosystems. Siberia and the Arctic Ocean is the core geographical region of the PEEEX domain. The majority of the PEEEX geographical domain is situation in the territory of Russia and China.

## APPROACH

The implementation of PEEEX agenda is based on three components (C-1) Coordination and facilitation of existing activities (projects, infrastructures, education), (C-2) Establishing new PEEEX activities; new research project and (C-3) Collaboration with international organization and networks. PEEEX research philosophy is designed as a research chain that aims to advance our understanding of climate and air quality through a series of connected activities beginning at the molecular scale and extending to the regional and global scale (Kulmala et al. 2011).

One of the first activities of C-1 will be establishing the process towards Northern Pan-Eurasian Observation Networks based on SMEAR-typed integrated land-atmosphere observation system (Fig.1). These RIs will include ground-based, aircraft and satellite observations as well as multi-scale modelling. The PEEEX labeled stations network will be designed co-operate with several EC and ESA funded activities aimed to develop next generation research infrastructures and data products such as EU-FP7-ACTRIS-I3-project (Aerosols, Clouds, and Trace gases Research InfraStructure Network-project 2011-2015), ICOS a research infrastructure to decipher the greenhouse gas balance of Europe and adjacent regions and EU-FP-7 e-infra ENVRI “Common Operations of Environmental Research Infrastructures” project. The works starts with analyzing (i) the existing measurements and stations, (ii) detailed parameter lists in coordination with the contributing networks and modelers, (iii) contribution networks responsible for harmonization of measurements and data analysis (QA/QC), (iv) the existing recommendations and calibration centers of different networks such as GAW and ACTRIS and (v) socio-economic data collection, data archives.



**Fig1.** Preliminary list of PEEEX Observation network sites/stations: SMEAR-I-II-III-IV-stations in Finland, SMEAR-Estonia, SMEAR-Nanjing, China ecosystem network (CERN), Yakutsk, Nizni Novgorod-Moscow-Borok, Tomsk, Kola Arctic / White Sea, Tiksi,, Zotino (Institute of Forest, Krasnojarsk, MPI Jena), Tjumin, Baikal - Irkutsk – Ulan Ude region.

Part of the first PEEEX activities in addition to establishing the Northern Pan Eurasian observation network is to take first steps towards the PEEEX Education Programme. In practice this means a web based education portal as a part of the PEEEX webpages (<http://www.atm.helsinki.fi/peex/>) offering information PEEEX involved institutes already existing courses for PEEEX members as well as first PEEEX benchmark courses on key topics such data processing and radar measurement techniques. The education portal will be opened in October 2013.

Three large-scale options to strengthen PEEEX initiative via initiating connections between scientific communities and existing observational networks and organizations have already been specified. At first The Pan-Eurasian Experiment will be acting as a most significant research program in an Arctic and boreal regional and apply a regional node status in a frame of Future Earth. Furthermore, PEEEX has also great potential to be one of international programs enhance the Arctic Data/Information coordination for Cold Regions by international programs (SAON, SIOS, PEEX, INTERACT, ABDS-ABA/CAFF, Cryoclim) part of the Building on Global Earth Observation System and Systems (GEOSS):GEO Cold Regions. Thirdly, the role of the Pan-Eurasian initiative in the global framework of the Global Atmosphere Watch Programme could be established by (a) Establish the collaboration with “non-atmospheric” domains on a regional level (e.g. with biospheric community) to better evaluate feedbacks in the Earth system (e.g. connections between climate change and atmospheric composition), (b) Extension of the atmospheric observational network in PEEEX region using GAW QA principles, (c) Involvement of GAW experts from non-PEEX geographical domain (d) Involvement of academic research in GAW activities and (e) Opportunities for specialized training, capacity building and outreach.

## FUTURE PROSPECTS

PEEX will integrate a new Earth system research community in the Pan-Eurasian region by opening its research and modeling infrastructure and inviting international partners and organizations to share in its development and use. PEEX initiative will be a major factor integrating the socioeconomic and natural science communities to working together towards solving the major challenges influencing the wellbeing of humans, societies, and ecosystems in the PEEX region. The first PEEX funding application will take place in autumn 2013. PEEX research community is currently finalizing the Science Plan which will be ready in spring 2014. The next PEEX-3 meeting will take place in St.Petersburg, Russia in March, 2014. PEEX aims to be operational starting from 2014.

## REFERENCES

Kaukolehto et al of this issue

Kulmala M., Alekseychik P., Paramonov M., Laurila T., Asmi E., Arneth A., Zilitinkevich S. & Kerminen V.-M. (2011). On measurements of aerosol particles and greenhouse gases in Siberia and future research needs. *Boreal Env. Res.* 16: 337-362.

Kulmala et al.( 2011). General overview: European Integrated project on Aerosol Cloud, Climate and Air Quality interactions (EUCAARI) – integrating aerosol research from nano to global scales. *Atmos. Chem. Phys.* 11: 13061–13143.

Pan Eurasian Experiment (PEEX) Science Plan, draft version 0.5 . <http://www.atm.helsinki.fi/peex/>

Petäjä et al. of this issue.

Siitonen et al of this issue.

## **ACTRIS RI – RESEARCH INFRASTRUCTURE FOR AEROSOLS, CLOUDS AND TRACE GASES**

T. PETÄJÄ<sup>1</sup>, H.K. LAPPALAINEN<sup>1,2</sup>, S. SORVARI<sup>2</sup>, and M. KULMALA<sup>1</sup>

<sup>1</sup>Dept. of Physics, P.O. Box 64, FI-00014 University of Helsinki, Finland.

<sup>2</sup>Finnish Meteorological Institute, P.O. Box 503, FI-00101 Helsinki, Finland

**Keywords:** research infrastructure, atmospheric aerosols, trace gases, clouds, climate change, biogeochemical cycles,

### **INTRODUCTION**

The new organization of the European research infrastructures (RI) towards world class research facilities and data services is under way. The European Union has set the roadmap, how the European research communities should organize and project their research facilities, data collection and services for a long-term, high-quality operative activity. As a part of building the European Union research area and to ensure Europe's competitiveness in "frontier" research EU is listing the European world class research infrastructures in the European Strategy Forum on Research Infrastructures (ESFRI) roadmap. The ESFRI's Roadmap identifies and determines the pan-European Research Infrastructures (RIs) and their services for European research communities for the next 10 to 20 years. The successful ESFRI projects will construct their services towards operational systems in a process, which will go on for four to five years. To step in the process towards European world class infrastructure requires a well established observation network with harmonized services in the research area of interest. The successful completion of the EU-FP-7 Infrastructure Projects demonstrates the type of readiness for the RI process (I3-project ACTIS Roadmap).

One of the key areas of European interest in the ESFRI process is the Environment segment including climate and air quality monitoring. The development of the greenhouse gases research infrastructure, the integrated carbon observations (ICOS) is already in the end of its preparatory phase and will soon establish its long-term operational observation and services system. However, at present the roadmap is lacking a coordinated European RI to sustain simultaneous observation of aerosol and their interaction with the other atmospheric constituents, the trace gases and clouds. Aerosols, clouds, greenhouse and trace gases are the key atmospheric components related to processes and feedback mechanisms of Earth radiation balance, climate change and air quality. Contrary to greenhouse gases, radiative forcing by short-lived trace gases and aerosol particles, in particular, is still very uncertain. The scientific understanding and research of these processes relies on high quality and harmonized datasets. The need for long-term observation of these atmospheric variables has been unambiguously asserted in the latest IPCC Fourth Assessment Report (IPCC 2007) and in the recent revision of the Thematic Strategy on air pollution of the EU. ACTRIS Aerosols, Clouds, and Trace gases Research Infrastructure Network -project (FP7-ACTRIS-I3, No 262254) is the current European level activity towards a long-term coordinated European research infrastructure of the key climate components. EU-FP7-ACTRIS-I3 is an outstanding research infrastructure launched in 2011 and active until 2015. ACTRIS will, for the first time, provide pan-European coordinated observations of the major atmospheric variables. The ACTRIS-I3 data and data products on aerosols, trace gases and clouds will fill in the gap of European SLCF research related atmospheric processes of global climate and air quality (I3-project ACTIS Roadmap).

## APPROACH

The current core activity for establishing a long-term ACTRIS RI in Europe is the EU-FP7-ACTRIS-I3 “Aerosols, Clouds, and Trace gases Research InfraStructure Network” project (No 262254). The ACTRIS-I3 “Aerosols, Clouds, and Trace gases Research InfraStructure Network” project is an European Commission FP-7-Project aiming at integrating European ground-based stations equipped with advanced atmospheric probing instrumentation for aerosols, clouds, and short-lived gas-phase species. ACTRIS will be active for a period of 4 years, from 1st April 2011 to 30th March 2015. The project is coordinated by CNR (Italy) and CNRS (France) and has 29 partners. ACTRIS consortium represents 35 infrastructures in 24 European countries; furthermore, more than 60 sites are reporting ACTRIS labelled data.

The ACTRIS-I3-project is an essential pillar of the EU ground-based observing system that provides the long-term observations information required to understand current variability of the atmospheric aerosol components and better predict their impact on climate and air quality in a changing climate. ACTRIS provides the key information required to develop the proper level of understanding on the evolution of the aerosol cycle, including attribution of sources and sinks, assessment of climate forcing and possible climate feedbacks. ACTRIS is developed in support of the EU research initiatives and designed and operated as an essential support of operational networks for long-term air quality monitoring and of the on-going development of atmospheric services within GMES. ACTRIS RI is supporting and complementing aircraft and satellite observations and has the important role in validation, integration, full exploitation of remote sensing data. The ACTRIS infrastructure will deliver critical long-term datasets for the climate and air quality research including evaluation of weather forecast and climate models (I3-project ACTIS Roadmap).

The ACTRIS-I3-project will establish a new infrastructure for the continuous, comprehensive advanced aerosol, trace gas and cloud measurements. ACTRIS is a step forward in merging of already existing measurements of critical climate factors and in delivering a near-real time data products. After 2015 the European ACTRIS stations network will consist of prototyped ACTRIS core stations with aerosol *in-situ* observations, concentrations of reactive trace gases and aerosol and cloud active remote sensing. Furthermore, ACTRIS RI provides integration of vertical aerosol and cloud profiles with comprehensive *in-situ* surface measurements.

The ACTRIS RI delivers critical long-term datasets for the climate and air quality research used to evaluate weather forecast and climate models. It will also facilitate the data access across complementary aerosol, trace gas and cloud data and to combined, value added, *in-situ* and vertical profiling observations. University of Helsinki is a full partner of the ACTRIS-I3 and the Finnish Meteorological Institute is an associated partner. University of Helsinki has a central role in the projects and have the leading responsibility of the strategic Work Package (WP6) aimed for providing the steps of ACTRIS RI towards ESFRI Process and towards a joint long-term European Atmospheric Research Infrastructure for advanced measurements of aerosols, clouds and reactive trace gases. Univ. Helsinki and FMI are also key actors in ACTRIS-I3 to prepare the ACTRIS prototype stations and RI stations in Finland will be equipped in the future with the standardized ACTRIS sensors, instruments and data handling protocols.

## FUTURE PROSPECTS

The ESFRI's (European Strategy Forum on Research Infrastructures) Roadmap is currently identifying the pan-European Research Infrastructures (RIs) and their services for European research communities for the next 10 to 20 years. ACTRIS-I3-project RI aims to be listed under the European world class research infrastructures in the ESFRI (Environment cluster) roadmap. Via ESFRI status, ACTRIS will be part of the environmental ESFRI RI landscape and provide important atmospheric data and knowledge for the

whole environment cluster. As a part of the process towards a long-term, world class European RI, the ACTRIS RI needs to be listed also in the National research infrastructures Roadmaps. National RI status is needed for earmarking of national budgets for participating in a common pan-European effort. After having ESFRI and national RI status the ACTRIS RI is targeted for the FP preparatory phase project (4 yrs) to prepare and construct the future ACTRIS RI and to set-up the ACTRIS legal entity, most possible under the model of an ERIC - European Research Infrastructure Consortium. The estimated schedule of the process from the ACTRIS-I3 project to ACTRIS world-class European RI in operation would be in 8 years. 1) EU-FP-7-ACTRIS-I3 years 2011-2015, 2) National ACTRIS Roadmap Statuses established by 2015, 3) ACTRIS-ESFRI-Roadmap-proposal submission and status in the next ESFRI Roadmap update process (approx. 2014/15), followed 4) ACTRIS-RI pan-European Infrastructure Preparatory Phase, 4 years with last two years for RI construction, and 5) Start of operation in 2019 (I3-ACTRIS Roadmap).

## REFERENCES

I3-ACTRIS-Roadmap document by Lappalainen HK., Pappalardo G., Sorvari S. Kulmala M. + ACTRIS I3-WP-leaders.

Kaukolehto et al of this issue

Kulmala et al.( 2011). General overview: European Integrated project on Aerosol Cloud, Climate and Air Quality interactions (EUCAARI) – integrating aerosol research from nano to global scales. Atmos. Chem. Phys. 11: 13061–13143.

Lappalainen et al., this issue

Petäjä et al., this issue.

Siitonen et al., this issue.

## **AnaEE – A EUROPEAN INFRASTRUCTURE FOR ECOSYSTEM RESEARCH**

S. SIITONEN<sup>1</sup>, J. BÄCK<sup>1,2</sup> and the AnaEE team

<sup>1</sup>Department of Forest Sciences, University of Helsinki, FINLAND

<sup>2</sup>Department of Physics, University of Helsinki, FINLAND

Keywords: ESFRI, EUROPEAN RESEARCH AREA, CLIMATE CHANGE IMPACTS

### **INTRODUCTION**

During the course of this century an unprecedented combination of change in climate and other human-induced drivers is compromising the natural adaptation ability of many ecosystems. Exposure to substantially higher CO<sub>2</sub> levels and temperatures and to changing disturbance regimes such as wildfires, insects, droughts and floods is likely to alter the structure, reduce biodiversity and perturb the functioning of many terrestrial and aquatic ecosystems. Further, over-exploitation of resources, landscape fragmentation, land-use change and pollution as outgrowth of increasing human population are causing additional ecological impairments. As policy makers have to balance between the needs of a growing human population and the long-term sustainability of the ecosystems to provide goods and services, there is a strong motivation to invest in understanding and quantifying the full range of climate change impacts. Motivation is enhanced by the fact that we know that some of the ecosystem impacts feed back to the climate change; the greenhouse gases (CO<sub>2</sub>, CH<sub>4</sub>, N<sub>2</sub>O, and tropospheric O<sub>3</sub>) and other climate feedbacks (albedo, clouds and aerosols) have potentially both global and local influences.

While advances in experimental science, analytics and ecosystem modelling are offering new insights and measurable predictions of biosphere changes, the nature and the global scope of the problem requires a transdisciplinary and an international solution. Bringing the multitude of research across Europe engaged with ecosystem functioning under one umbrella will support broad community access to a range of data and services for the benefit of everyone.

### **THE INFRASTRUCTURE FOR ANALYSIS AND EXPERIMENTATION ON ECOSYSTEMS – AnaEE**

The Research Infrastructures having pan-European relevance and contributing to the enhancement of the European Research Area (ERA) have been identified by the European Strategy Forum for Research Infrastructures (ESFRI) and rounded up on ESFRI roadmap since 2006. ESFRI is a strategic instrument to develop the scientific integration of Europe and to strengthen its international outreach. AnaEE was listed on the ESFRI roadmap in 2010. With funding from the EU 7<sup>th</sup> Framework Programme AnaEE entered its Preparatory Phase in 2012 aiming for stronger integration of the long-term experimental ecosystem research across Europe. By providing Europe with a coordinated set of platforms to analyse and predict the effects of environmental and land use changes on the major continental ecosystems, AnaEE also provides integrated services to different stakeholders, not limited to scientists, and enables cross-disciplinary science to serve society and promote innovation (Figure 1.).

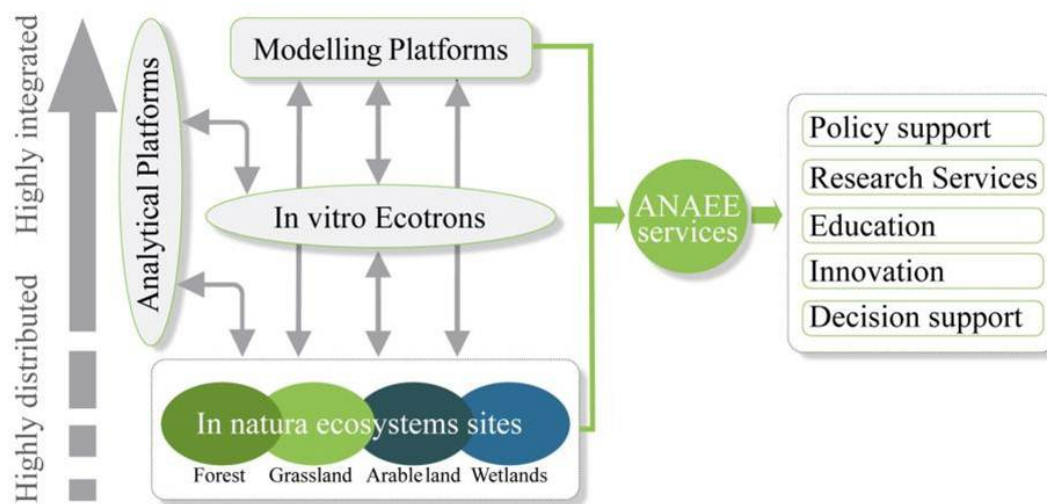


Figure 1. AnaEE architecture illustrating the functional relationships between its four complementary components and the various services they offer.

AnaEE will consist of a distributed network of *in natura* and *in vitro* experimental platforms and facilities equipped with the latest technology. They will be associated with analytical and modelling platforms and will be linked to networks of instrumented observation sites that will provide indispensable calibration and validation datasets. AnaEE will combine the development of new sites (*in vitro* and *in natura*) and platforms (analytical and modelling) with the upgrade of existing sites.

*In natura* Long term Experimental Platforms will be distributed across the main types of environments (arable land, grassland, forest, wetlands) covering large gradients in climate and nature in Europe. Main experimental treatments will refer to land management, climate and biodiversity changes. *In vitro* experiments in highly-instrumented Ecotrons will allow a better understanding of interacting processes by testing specific combinations of forcing variables in enclosed, environmentally controlled chambers, and their impact on living organisms and ecosystems. Analytical Platforms at the cutting edge of technological development will be used to analyse samples of soil, water, organisms or air to help better understand and quantify the complex interactions between the different bio-geochemical cycles, ecological states, fluxes and compartments. Databases, models and a European Modelling Platform will complete the AnaEE infrastructure. This Platform will consist of a toolbox of numerical models, sharing concepts between disciplines, which will evaluate and predict the effects of climate and land use changes on ecosystem processes.

AnaEE keenly supports the EC's plans for responding to the global challenges for new services to science. AnaEE will contribute structuring the currently fragmented research community on terrestrial and aquatic ecosystems within the European Research Area and enhance the attractiveness of the EU for scientist by offering cutting edge experimental ecosystem research facilities. One of the big challenges is to train and create capacity of using infrastructures and services across disciplines, not only by providing access to wealth of data, but also understanding the data products in order to offer intelligible integrated processing. AnaEE will also play a crucial role in the implementation of the forthcoming European Joint

Programming Initiative on Agriculture, Food Security and Climate Change (JPI FACCE), which is setting out its strategic priorities for transdisciplinary research. The JPIs will help identify the range of services to be offered by the AnaEE research infrastructure and associated access rules for different user types. AnaEE recognises a clear need to work with JPIs as early as possible on defining these services.

By establishing interoperable services in experimental ecosystem sciences on a European scale, Europe can play a leading role within a global scale. Platform provided by AnaEE will promote the EU and its Member States' research and innovation credentials, aimed at securing European global competitiveness, in line with the objectives of the Horizon 2020 programme. On a global scale, AnaEE will help decision makers to better understand how ecological systems respond to global changes-related perturbations, to take appropriate measures for sustainable policies and to test sustainable land use and innovative green technologies in order to address societal challenges. AnaEE aims to be the reference point for the rigorous assessment of ecosystem services, providing answers to key questions surrounding the emerging European Green economy alongside other important political and environmental concerns.

## IMPLEMENTATION AND NEXT STEPS

AnaEE Preparatory Phase is in the beginning of setting-up the organizational, legal and financial framework for efficient coordination, open access and sustainable funding of the future AnaEE. Integration of existing national Research Infrastructures in terms of access to facilities and data, harmonization of protocols, methods and instruments, is a major undertaking and requires a great deal of coordination.

The workplan of the AnaEE Preparatory Phase has been built around the development of the AnaEE Strategic Roadmap (WP2) which will be the backbone and key deliverable of the Preparatory Phase project. This Roadmap (for the construction and implementation phase) will be developed in an iterative process through the tasks of WPs 3 to 7 supported by a strong coordination (WP1), communication and dialogue with stakeholders (WP8) to ensure that they are involved in the process from day 1 and thus contribute directly to the development and validation of the AnaEE Roadmap. WP3 will deliver the technical plan for the construction phase based on end-user needs and long-term scientific considerations. A data and access policy will be elaborated by WP4 based on the expected offer (WP3) and taking into consideration the needs and innovative developments of private and public bodies (WP5). Definition of the pricing policy and funding model (WP7) will ensure the financial feasibility and sustainability of the roll-out of AnaEE. WP6 will provide the governance and legal framework for this roll-out phase. These activities will be conducted in close collaboration with national stakeholders (WP8) to ensure the necessary commitments are in place at project end (2016).

## ACKNOWLEDGEMENTS

The financial support by the Academy of Finland Centre of Excellence program (FCoE in Physics, Chemistry, Biology and Meteorology of Atmospheric Composition and Climate Change) and by the European Commission's 7<sup>th</sup> Framework Programme (DG Research & Innovation) are greatly acknowledged.

# **RESTRUCTURING THE FCoE RESEARCH INFRASTRUCTURES - INTERGRATED ATMOSPHERIC AND EARTH SYSTEM SCIENCE RESEARCH INFRASTRUCTURE (INAR RI)**

S. SORVARI<sup>1</sup>, A. ASMI<sup>2</sup>, J. BÄCK<sup>3</sup>, T. PETÄJÄ<sup>2</sup>, M. KULMALA<sup>2</sup>

<sup>1</sup>Finnish Meteorological Institute (FMI), Helsinki, Finland

<sup>2</sup>Department of Physics, University of Helsinki, Finland

<sup>3</sup>Department of Forest Sciences, University of Helsinki, Finland

**Keywords:** RESEARCH INFRASTRUCTURES, SMEAR, PALLAS-SODANKYLÄ, ICOS, ANAEE, ACTRIS, OBSERVATIONS, EXPERIMENTS, MODELLING, E-INFRASTRUCTURE

## **BACKGROUND**

During the last decades, Finnish atmospheric and Earth system scientists have been systematically working towards building internationally leading, multidisciplinary research environment for atmospheric and Earth system science to study biosphere-aerosol-cloud-climate-air quality interactions. This work has included establishment of 1) a set of high-standard atmospheric and environmental observation stations, such as the four SMEAR-stations (Stations for Measuring Ecosystem and Atmosphere relations) and Pallas-Sodankylä Super site, 2) several experimental field sites and laboratories, 3) process and climate/Earth system components, and 4) creating databases to store and distribute the data. Until now, most of the stations, research facilities, modelling components and databases have been operated separately and managed by the FCoE partners individually. The aim is to establish an Integrated Atmospheric and Earth System Science Research Infrastructure – INAR RI to increase the coordination, management, interoperability and interworkability of the research infrastructure components.

## **INAR RI OBJECTIVES**

The objectives of the INAR RI are i) to fully integrate the existing RI components and further development of the sensors, instruments, RI platforms and interoperable e-infrastructure solutions to enable the production and integration of versatile measurement data, ii) to explore and study material and energy flows between atmosphere and biosphere (from its various ecosystem components), iii) to simulate and model the complex interactions and feedbacks and parameterize the processes to the climate and Earth system models, and iv) to provide state-of-the-art, long-term, continuous data series for researchers and other interested end-users.

INAR RI will provide data and RI access to the researchers both nationally and internationally to work toward the following topics that are most plausible topic areas for the future scientific breakthroughs: 1) Atmospheric oxidation and its connection with emissions of biogenic volatile organic compounds (BVOCs); 2) Composition and dynamics of neutral and charged clusters and aerosol particles in the atmosphere; 3) Formation and properties of cloud condensation nuclei, cloud microphysics, ice nucleation and precipitation formation in warm, mixed-phase and ice clouds; 4)

Synthesis of BVOCs and organic nitrogen compounds in various ecosystems and their association with ecosystem properties and functions; 5) Atmospheric turbulence and boundary layer dynamics, and their influences on the biosphere-atmosphere exchange and aerosol-cloud interactions; 6) Biogeochemical cycling of carbon, sulphur, nitrogen, phosphorus and water, and the associated feedback loops in a variety of natural, managed and urban ecosystems; and 7) Global importance of the feedback loops and climate-air quality interactions now and in changing future conditions.

The capability of INAR RI in creating new scientific breakthroughs in the future is tight firmly to its forefront position as an internationally leading RI. This can be only achieved by systematically developing the RI and by fostering the deeper integration of its RI components. With these efforts, INAR RI will be able to attract the best international scientists to work at its RI locations and to use the INAR RI data. Figure 1 describes the structure of INAR RI, its' supporting projects and the position of the INAR RI in the wider societal and scientific environment.

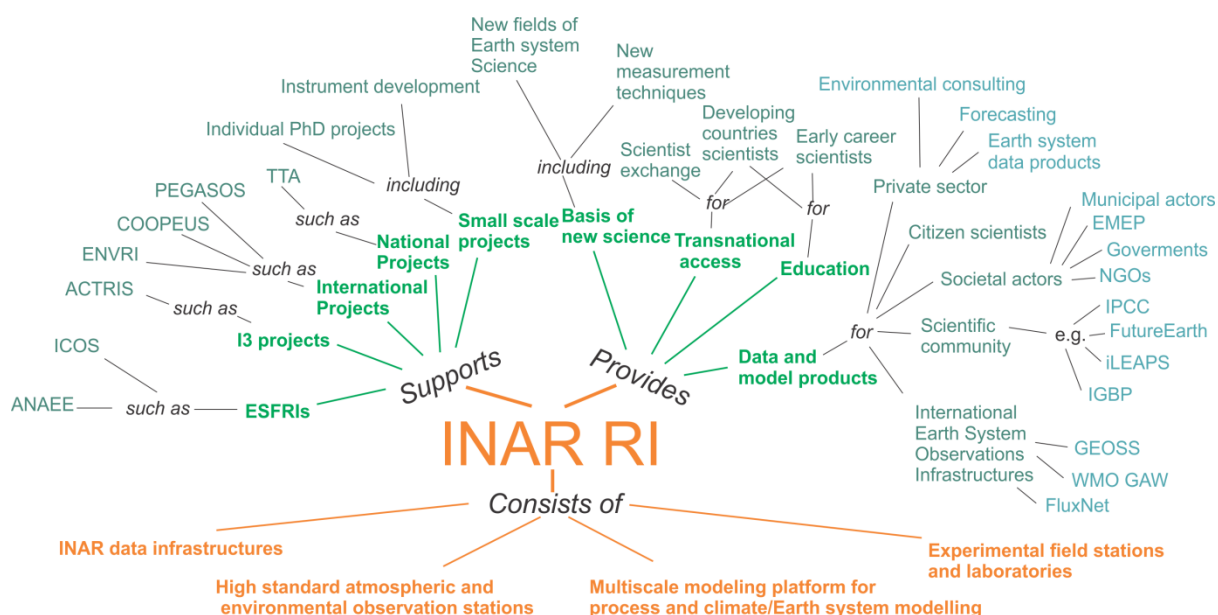


Figure 1. INAR RI in a nutshell.

The National Survey of Research Infrastructures in Finland in 2009 placed the INAR RI (previously called *Environmental and Atmospheric Sciences RI*) on the list of nationally important research infrastructures and on the priority list of Finnish RI roadmap. Many components of the INAR RI are important parts of the European level ESFRIs (European Strategy Forum on Research Infrastructures) or other similar research infrastructures and networks. INAR RI is a part of European ICOS (Integrated Carbon Observation System) RI, ANAEE ESFRI (Infrastructure for Analysis and Experimentation on Ecosystems) platform, ACTRIS (Aerosols, Clouds, and Trace gases Research InfraStructure Network) RI. INAR RI also contributes to LifeWatch, SIOS (Svalbard Integrated Observation System), InGOS (Integrated Non-CO<sub>2</sub> Greenhouse Gas Observing System), EXPEER (Distributed infrastructure for EXperimentation in Ecosystem Research), and RI cluster projects ENVRI and COOPEUS. In addition, INAR RI observation stations feed data in many international Earth observation systems and networks, such as to EMEP, WMO GAW, FluxNet, AERONET, SolRad-Net and EARLINET.

## INAR RI STRUCTURE

The aim of the INAR RI is to build an integrated, comprehensive atmospheric and environmental research infrastructure that consists of i) continuous and multi-disciplinary observation stations located in different environments/ecosystems providing ground- and complemented by satellite-based measurements, ii) experimental field sites and laboratories providing experimental platforms for atmospheric and ecological research, iii) multiscale modelling platform to combine current models and modelling environments into one functional RI platform, and iv) INAR RI databases and data portal enabling the data access for scientists and other end-users as well as the data achieving.

The INAR RI composes of the following components:

*1. High-standard atmospheric and environmental observation stations* (incl. ground-based, airborne and remote sensing)

INAR RI operates currently five field stations in Finland: The Pallas-Sodankylä super site and the four SMEAR (Station for Measuring Forest Ecosystem Atmosphere Relations) stations. SMEAR II is the world leading station due to its comprehensive research program and due to its unique time series of aerosol formation and biogeochemical fluxes (Hari & Kulmala, 2005). In addition, INAR RI is constructing novel atmosphere-marine observation station in Utö, Baltic Sea (Utö marine station). *In-situ* measurements from SMEAR stations, Pallas-Sodankylä and Utö marine station are complemented by advanced aerosol, trace gas and cloud measurements from remote sensing and airborne techniques (lidars, radars, aircrafts and satellites) enabling integration of vertical, boundary-layer aerosol and cloud profiles. Sodankylä is one of European main receiving sites for environmental satellite data and its Very Fast Delivery (VFD) data receiving and processing technics enables the immediate data production from satellite data. The *in-situ* measurements from observation stations have important role in validation, integration, and full exploitation of environmental (e.g. greenhouse gases, aerosol) remote sensing data.

The SMEAR-station concept will also be utilized in developing new comprehensive measurement sites from the experimental infrastructures, such as the Viikki Agricultural Production Laboratory for managed land-atmosphere studies.

The atmospheric and environmental observation stations:

- SMEAR I-III Stations (UHEL/Kulmala, Petäjä, Bäck)
- SMEAR IV (UEF/Virtanen, Lehtinen)
- Pallas-Sodankylä Super site, incl. satellite and remote sensing centre (FMI/Viisanen)
- Utö Atmospheric and Marine Research Station (FMI/Viisanen, Laakso)
- Aircraft Cessna 172, update to Cessna 185 (UHEL/Petäjä)
- SC7 Skyvan turboprop aircraft (instrumentation FMI/Viisanen, aircraft Aalto Univ.)

*2. Experimental field stations and laboratories*

Experimental research methods are utilized in detailed process studies, and for testing and parameterizing models describing the atmosphere-ecosystem exchange. INAR operates several high-quality experimental facilities, both in laboratory and field conditions.

- Experimental ecosystem field sites: SMEAR I-IV (UHEL & UEF), Pallas-Sodankylä (FMI) and FMI field stations - Lettosuo, Lompolojänkki, Kaamanen, Kenttäröva, Siikajoki, Lakkasuo (FMI/Viisanen, Lohila; UEF/Tuittila), Viikki Agricultural Production Laboratory (VAPL; UHEL/Alakukku)
- Ecophysiological laboratories, indoor/outdoor plant exposure facilities and growth chambers, rhizotrons/dasotrons (UHEL/Bäck, METLA/Finer, UEF/Tuittila, Holopainen, Virtanen)
- Kumpula Radar Meteorology Laboratory (FMI/Viisanen and UHEL/Moiseev)
- Aerosol laboratories: Helsinki Aerosol Particle Laboratory (UHEL/Kulmala, Petäjä); Helsinki Analytical Chemistry Laboratory (UHEL/Hartonen, Riekkola); Kuopio Aerosol Physics Laboratory (UEF/Lehtinen); FMI Aerosol Experimental Laboratory (FMI/Viisanen)
- TUT Mobile Aerosol Measurement Unit (TUT/Keskinen, dal Maso)
- Field and laboratory test beds for sensor, instrument and methodology development (in SMEAR II and Pallas-Sodankylä stations)

### 3. Multiscale modeling platform for process and climate/Earth system modeling

Multiscale modelling platform from quantum chemistry to Earth System Models provides improved conceptual understanding over the relevant spatial and temporal scales. The multiscale modelling platforms consists of:

- FMI process and Earth System Modeling Platform (FMI/Laaksonen)
- UHEL Process and Earth System Modeling Platform (incl. zero and one dimensional process model, Large Eddy Simulation models, Regional transport models, Global vegetation models, Global climate models, Earth System models) with computing resources, including user support and software applications (UHEL/Kulmala)
- Integrated Aerosol Dynamics Modeling and Data Analysis Platform (TUT/Keskinen, dal Maso)
- CSC high-performance computing (HPC) and cloud computing services (CSC/Pursula)

### 4. INAR RI database and data portal

The diverse data obtained from the measurement and experimental infrastructure parts requires e-infrastructure to ensure data interoperability and high throughput from measurement to modeling. Advanced data structures are essential for ensuring the distribution and access to the data as well as for data archiving. Quality checked INAR RI data products are currently distributed with the SMART-SMEAR database web interface <http://www.atm.helsinki.fi/~junninen/> (Junninen et al. 2009). As a part of the Finnish Ministry of Education and Culture's national multidisciplinary project "Tutkimuksen Tietojärjestelmät" (TTA), a pilot data infrastructure on storing environmental research data from SMEAR stations has been initiated in 2012 (SMEAR-DATA), and the first version of INAR RI database web interface – data portal – will be constructed and made operational by the end of 2013. INAR RI will also continue to collaborate with TTA, which is aiming to build a national information infrastructure including for example a storage service for research data (IDA -Intelligent Data Agent) and a data catalogue service. Based on the outcomes of the mentioned pilot projects, the construction of INAR RI database and data portal are planned for the years 2014 - 2016 aiming to launch the fully operational INAR RI database and web interface covering most of the INAR RI data and data flows in years 2017-2018.

- SMEAR-DATA pilot prototype (UHEL/Kulmala, Asmi, CSC/Pursula)
- TTA IDA data storage and access (UHEL/Kulmala, Asmi, CSC/Pursula)

- INAR data base and data portal (UHEL/Kulmala, FMI/Viisanen, UEF/Lehtinen, TUT/dal Maso, CSC/Pursula)

## INAR RI OPERATIONS AND SERVICES

### *Data access management*

INAR RI is pioneering in comprehensive continuous observations, experimental networks, model development, and in production of modelled data. The aim is to build a data system where material and data operates under a common data management infrastructure and with a common user experience throughout the INAR RI: raw data, data analysis, different datasets and publications are stored and shared via a common data platform, including the necessary metadata for context. The “research data systems” project (TTA) of the Finnish Ministry of Education and Culture provides the necessary infrastructure for the planning of the INAR RI material storage, with key design criteria of data long-term storage, accessibility, citability and openness. Finnish IT Centre for Science (CSC) permanent storage platform ensures the long-term security of the datasets, including version control and secure backups. The methodologies, work flow and storage of the SMEAR-data project for all the data streams will be used in a joint manner for the INAR RI data, and all the climate relevant parameters defined by IPCC. All remote sensing data and products provide by INAR RI are freely available for the external researchers and research groups. Modelling and simulation data from all scales will be stored locally on a data archive where it will be made available for researchers within the next years when the INAR RI data portal is fully operational.

The INAR RI datasets will be made publicly available after quality control, with the aim of having most of the observational data submitted as near real time data. By 2016, most of the INAR RI data (including the earlier datasets) will be available in similar format and stored permanently in national IDA (Intelligent Data Agent) storage archive maintained by CSC and made available for the global GEOSS initiative and other stakeholder groups. All final evaluated model results will be stored in the archive permanently and will be available for scientific use for the research communities. Parameterizations will be published under an open access license and will be available to the community. Intellectual Property Rights, in case needed, will be agreed upon in the Consortium Agreement between INAR RI partners.

### *RI access management*

In addition to the data access (open data distribution via INAR RI data portal) INAR RI also provides RI platform access. In other words, INAR RI observation stations, experimental field sites and laboratories, and modelling platforms offer *in-situ* access to the researchers to visit and perform their own research at the sites. This RI access will be managed and monitored from the integrated management systems (to be constructed, currently under planning). For time being, the stations and laboratories are providing individually RI access and/or via EC I3-projects such as InGOS, ACTRIS, EXPEER in the form of Transnational Access (TNA). The coordinated INAR RI access will be based on the evaluation of the applicants and scientific excellence of the proposed projects.

## INAR RI CONTRIBUTION TO THE ENVIRONMENTAL ESFRI PROJECTS

INAR RI is a vital part of the European ESFRI or related RIs, especially being vital part of ICOS, ACTRIS, and ANAEE.

### *ICOS RI – Integrated Carbon Observation System*

Finland has participated in the preparation and building of the European ICOS RI over the last four years. The INAR RI observation stations have been under extensive building and deployment of new GHG instruments and supporting infrastructure to reach the ICOS standards. During the construction

phase in 2011-2012, many INAR RI stations were upgraded to fulfil the ICOS Ecosystem and ICOS Atmosphere sites in respect to their GHG measurements. In total, INAR RI hosts in the form of ICOS-Finland now 14 operational ICOS approved GHG sites in its stations around the country (see Figure 2). In the future, the upgrades of INAR RI GHG measurements will be done in the ICOS framework.

In addition to the ICOS-Finland measurement sites, INAR RI partners are leading the establishment of the ICOS ERIC legal entity. The ICOS ERIC Head Office (HO) will be located in Helsinki with the secondary node in Paris. ICOS ERIC is the first ESFRI organisation, of which statutory seat will be located in Finland. ICOS-Finland participates also in the operation of Atmospheric Thematic Centre (ATC), led by France. Finnish ATC contribution includes the testing of the instruments and related training under cold Northern conditions (testing done at the INAR RI stations), and the operation of the mobile laboratory for the quality assurance of the atmospheric concentration measurements. The ATC-related work has already started and the construction of the mobile lab is almost finished.

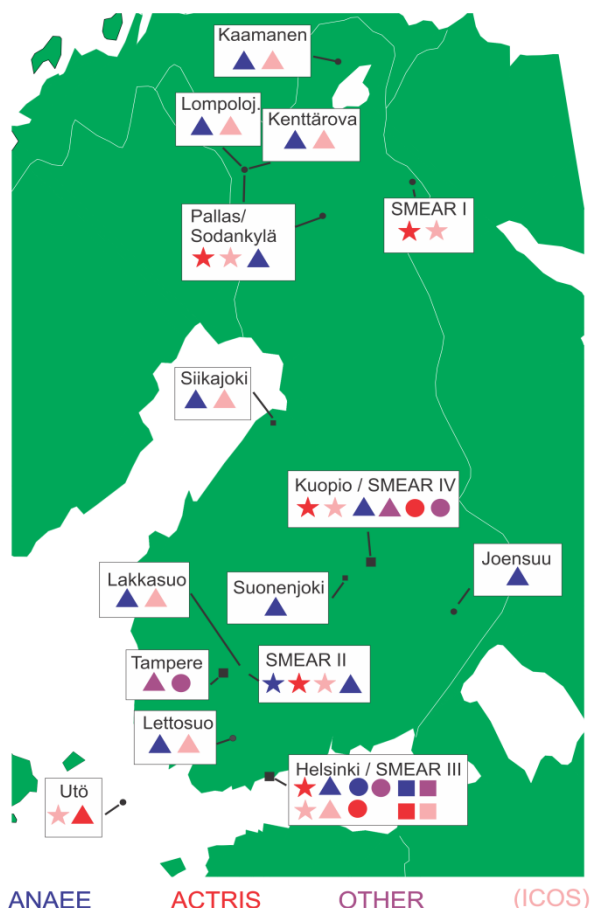


Figure 2. Map of INAR sites and their connection to ANAEE, ACTRIS and ICOS infrastructures.

have the leading responsibility of the strategic Work Package (WP6) aimed for providing the steps of ACTRIS RI towards ESFRI Process and towards a joint long-term European Atmospheric Research Infrastructure for advanced measurements of aerosols, clouds and reactive trace gases. INAR RI partners are also key actors in ACTRIS-I3 to prepare the ACTRIS prototype stations and INAR RI stations will be equipped in the future with the standardized ACTRIS sensors, instruments and data handling protocols. The future INAR RI developments and upgrades related to aerosols, cloud observations and trace gases will be done in the ACTRIS framework.

### *ACTRIS RI – Research Infrastructure for Aerosols, Clouds and Trace gases*

INAR RI/University of Helsinki is a full partner of the ACTRIS-I3 and the Finnish Meteorological Institute is an associated partner. INAR RI partners have a central role in the projects and

### *ANAEE ESFRI- Analysis and Experimentation on Ecosystems*

The ANAEE component in INAR RI develops the expertise in field stations and laboratories under a coordinated framework, combining the atmospheric and ecosystem research. UHEL is a core partner in ANAEE PP, aiming at a European scale ESFRI in ecosystem research. ANAEE RI will consist of long-term, well-designed experimental facilities with up-to-date technology, innovative sensors, measurements, and experiments. It will combine the well-equipped, comprehensive experimental field sites with modern *in vitro* plant growth and exposure systems and molecular biological and analytical facilities. INAR RI laboratories, experimental facilities and field stations will be following the standardized ANAEE ESFRI protocols regarding ecosystem experimentation, instrumentation and data structures. The developments of the ecosystem experiments of INAR RI will be done under the ANAEE framework.

### ORGANIZATION OF INARI RI

The INAR RI is led and coordinated by Institute of Atmospheric Research and Earth System Science (INAR), which is a joint organization of University of Helsinki, Finnish Meteorological Institute, University of Eastern Finland and Tampere University of Technology in the field of atmospheric and environmental sciences. INAR was established in January 2013. The INAR RI board together with INAR coordination office oversees the integration and completion of the set objectives, tasks, and is responsible for 1) defining, dividing and developing the tasks; 2) supervising the progress of the work; 3) coordinating the research initiatives; 4) coordinating the preparation of the reports (technical, financial, etc.); and 5) permitting and facilitating exchange of information between the partners. The partner organizations hosting INAR RI components are responsible for implementing decisions of the INAR RI Board and providing the required RI and data access for the users.

### INAR RI WORK PLAN FOR 2014 – 2019

The main future INAR RI development needs include:

- upgrading of observing stations to fulfil ICOS and ACTRIS instrumentation, standards, data processing, workflows, and RI and data access
- upgrading of experimental laboratories and field sites to fulfil ANAEE instrumentation, standards, data processing, and RI and data access
- developing and testing new sensors, instruments, methods and techniques for observing stations and experimental sites to actively participate in planning and constructing also other future atmospheric and environmental RI initiatives at the national and European level
- combining of GHG, trace gas and aerosol satellite data to *in-situ* observations and inverse modelling
- improving modelling platform collaboration via common technical support personnel, software development procedures, run-time environments in CSC computing facilities and developing joint work flows
- creating a national level INAR RI database with web interface for data management, distribution and access, data processing and database archiving system (based on SMEAR-DATA, TTA IDA pilots)
- establishing a national level INAR RI coordination and management tools for monitoring and reporting the INAR RI access and user levels

## CONCLUSIONS

INAR RI aims to be a leading atmospheric and environmental infrastructure in the world. It will benchmark procedures on how to plan, construct and operate continuous, comprehensive observation stations, experimental laboratories and field stations, multi-scale modelling platforms as well as how to establish an e-infrastructure enabling the wide and efficient use of the research infrastructure.

# SPRINGTIME MONOTERPENE EMISSION BURSTS FROM SCOTS PINE IN THE LIGHT OF PHOTOSYNTHESIS RECOVERY DYNAMICS

AALTO, J., KOLARI, P., PORCAR-CASTELL, A., BÄCK, J.

Department of Forest Sciences, University of Helsinki, Finland

Keywords: VOC emissions, photosynthesis, new particle formation

## INTRODUCTION

In boreal regions, both the emission potential of terpenoids acting as aerosol precursors and atmospheric new particle formation events are peaking in springtime (Tarvainen *et al.* 2005, Dal Maso *et al.* 2007). Springtime is characterized by rather fast shift from cold winter to moderate summer conditions within a few weeks. During this shift extreme differences between daily maximum and minimum temperatures are common, as well as large fluctuations in daily mean temperatures. In high latitudes also the theoretical maximum irradiance increases substantially during spring months. The full release of dormancy takes place in stages at about the same time when daily mean temperatures rise above zero (Kolari *et al.* 2007).

## MATERIAL AND METHODS

We measured the gas exchange and monoterpene emissions of a boreal Scots pine (*Pinus sylvestris* L.) shoots using an automated gas exchange measurement system, based on dynamic enclosures, coupled with PTR-QMS (proton transfer reaction – quadruple mass spectrometer) during years 2009, 2010 and 2012 in Hyytiälä SMEAR II station (Station for Measuring forest Ecosystem – Atmosphere Relations), southern Finland. (Kolari *et al.* 2012, Taipale *et al.* 2008)

The photosynthesis parameters were determined separately for each half day period applying Michaelis-Menten kinetics to irradiance-carbon assimilation relationship. The photosynthetic light use efficiency (LUE) was defined as ability of needles to photosynthesize in the forenoon maximum irradiance compared to the summertime photosynthesis in same light conditions. The daily total and de novo monoterpene emission potentials were obtained using the hybrid model formulation (Taipale *et al.* 2011), where emissions are originating both from recent biosynthesis (de novo emissions) and storage pools, and depend on both light and temperature levels.

## RESULTS

We discovered several types of monoterpene emission burst events (MEB events) every spring, typically in April (Fig. 1). The MEB events lasted from a couple of hours to one week. The events were characterized by high monoterpene emission potential, at least two times higher when compared to median springtime emission potential.

No straightforward causes to or correlations with MEB events were found; identical ambient conditions could produce totally different kind of emission responses (Fig. 2). However, most of the MEB events coincided with the early stages of photosynthesis recovery, i.e. they occurred at the time when the light use efficiency was around 20 %. It seems that the MEB events were preceded by either:

- I. Extremely rapid period of photosynthesis recovery due to sudden rise in temperature, or
- II. Temporary photosynthesis downregulation, caused by a transient colder period combined with high PAR levels, and followed by a warmer period.

Either way, the fluctuation in photosynthesis recovery seems to be a prerequisite for a MEB event. Based on the modeled emission sources, most of the monoterpene emissions originated directly from

synthesis during the MEB events (Fig. 3). This suggests that the enhanced emissions were induced by high levels of photosynthetically active radiation, and weren't primarily driven by temperature.

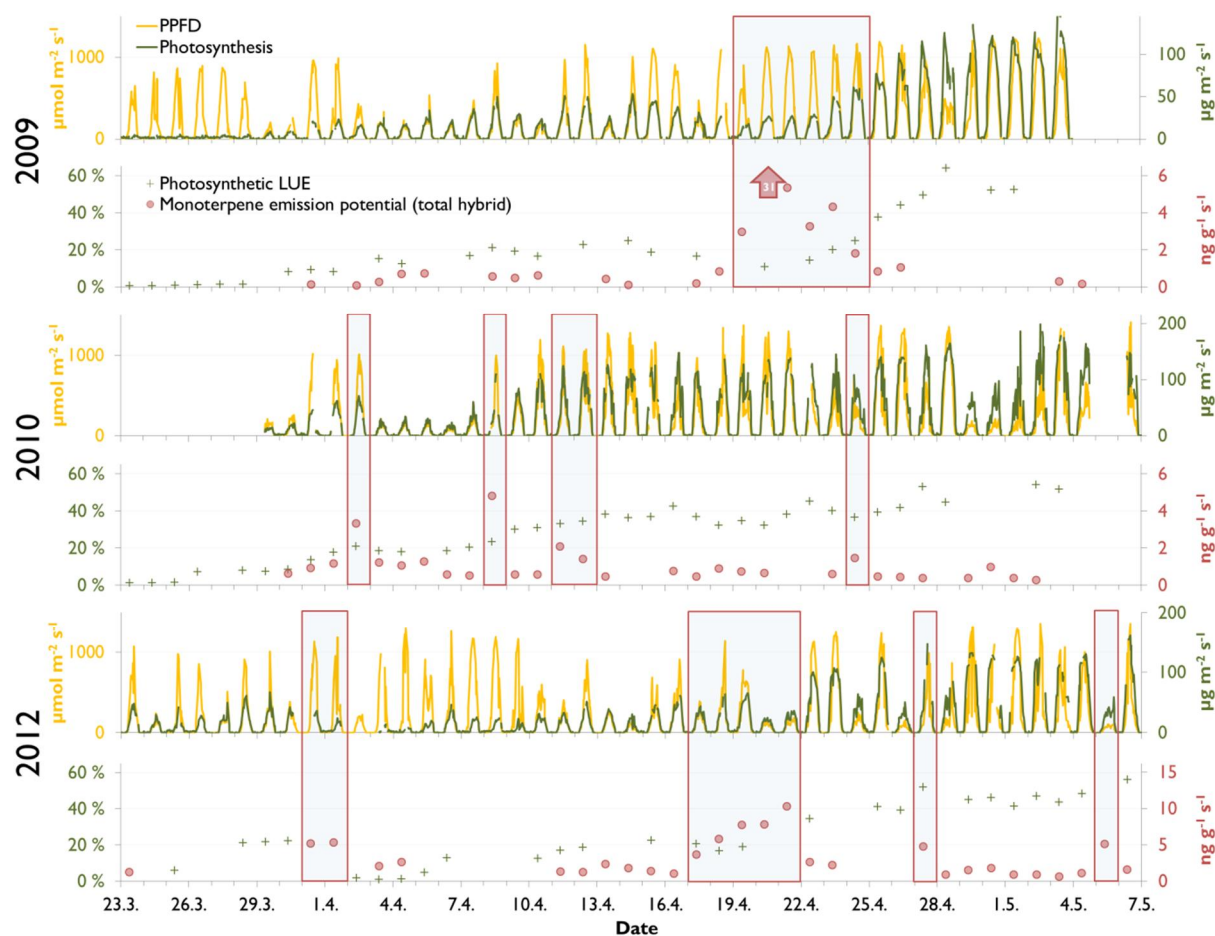


Figure 1. The MEB-events during springs 2009, 2010 and 2012. Photosynthetically active radiation, photosynthesis, relative photosynthetic LUE and total monoterpene emission potential (obtained using hybrid model as tool) during three springs. The MEB events marked with rectangles.

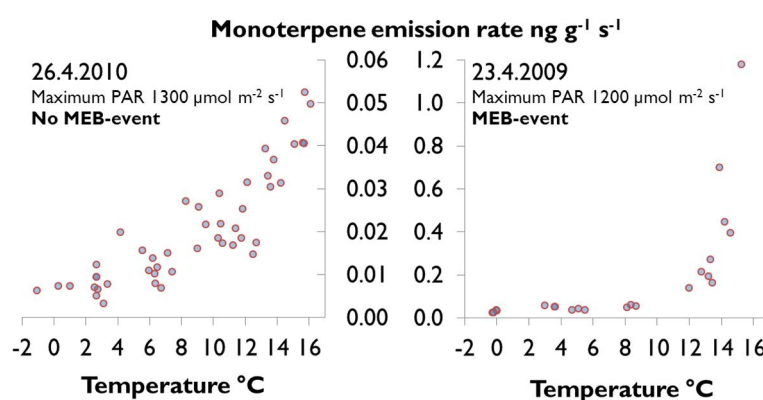


Figure 2. The monoterpene emission response to temperature during a selected non-MEB-event day and a MEB event day. NOTE: The y-axis of the figures are different due to magnitude difference in emission rates.

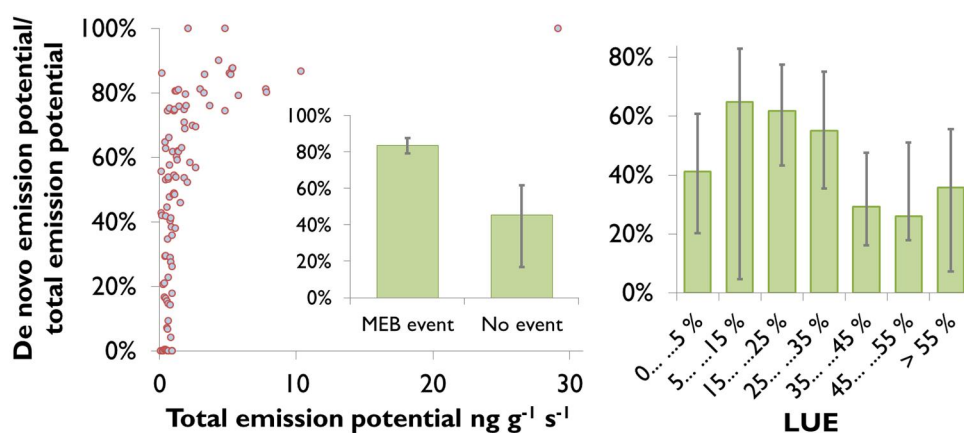


Figure 3. The contribution of modeled de novo emissions from the total emitted monoterpenes in relation to total emission potential, MEB events and photosynthetic light use efficiency. The scatter plot represents individual days. The bar plots represent median values, and error bars represent lower and upper quartiles.

## CONCLUSIONS

High springtime monoterpene emissions from boreal Scots pine forests are reported earlier by Tarvainen *et al.* (2005) and Hakola *et al.* (2006). Lappalainen *et al.* (2013) noticed very high monoterpene concentrations at shoot scale in April. Those are evidently sign of high monoterpene emissions from pine shoots. Our findings considering MEB-events are consistent with those earlier findings, but at the first time we are able to give a more detailed explanation for the high monoterpene emission rates during spring period.

The prerequisites for MEB events are consistent with two long-debated hypothesis behind monoterpene emission:

- I. The “safety-valve” role during the critical period of spring recovery of photosynthesis (Peñuelas & Munne-Bosch 2005), and
- II. The opportunistic emission of monoterpenes along with the synthesis of carotenoids (Owen & Peñuelas 2005, Porcar-Castell *et al.* 2009).

The photosynthetic machinery in boreal evergreens is highly downregulated during winter. Along with the increasing temperature a shift takes place in the type of protective mechanism used by foliage: from highly efficient but sustained (locked) mechanisms, to less efficient but more dynamic. Additional protection is thus needed during this critical period when late cold spells combined with high irradiance could photodamage the photosynthetic machinery. Our results suggest that this additional protection could be attained not only through the transitory peak in the pools of carotenoids (Porcar-Castell *et al.* 2012), but perhaps also by opening the monoterpene safety valve. Our observations give evidence of an intricate link between the acclimation of photosynthesis and the dynamics of terpenoid emission potential during spring recovery, a link that might help us to understand the peaking atmospheric new particle formation events in spring.

## ACKNOWLEDGEMENTS

The work was supported by the Academy of Finland Centre of Excellence program (project no 1118615), and the graduate school in Physics, Chemistry and Meteorology of Atmospheric Composition and Climate Change.

## REFERENCES

- Dal Maso, M. & P. Hari (2007). Aerosol size distribution measurements at four Nordic field stations: identification, analysis and trajectory analysis of new particle formation bursts. *Tellus* **59B**, 350-361.
- Hakola, H., V. Tarvainen, J. Bäck, H. Ranta, B. Bonn, J. Rinne & M. Kulmala (2006). Seasonal variation of mono- and sesquiterpene emission rates of Scots pine. *Biogeosciences* **3**: 93-101.
- Kolari, P., H. K. Lappalainen, H. Hänninen & P. Hari (2007). Relationship between temperature and the seasonal course of photosynthesis in Scots pine at northern timberline and in southern boreal zone. *Tellus* **59B**: 542-552.
- Kolari, P., J. Bäck, R. Taipale, T. M. Ruuskanen, M. K. Kajos, J. Rinne, M. Kulmala & P. Hari (2012). Evaluation of accuracy in measurements of VOC emissions with dynamic chamber system. *Atmos. Environ.* **62**: 344-351.
- Lappalainen, H. K., S. Sevanto, M. Dal Maso, R. Taipale, M. Kajos, P. Kolari, & J. Bäck (2013). A source-orientated approach for estimating daytime concentrations of biogenic volatile organic compounds in an upper layer of a boreal forest canopy. *Boreal Environ. Res.* **18**: 127-144.
- Owen, S. & J. Peñuelas (2005). Opportunistic emissions of volatile isoprenoids. *Trends Plant Sci.* **10**: 420-426.
- Peñuelas, J. & S. Munne-Bosch (2005). Isoprenoids: an evolutionary pool for photoprotection. *Trends Plant Sci.* **10**: 166-169.
- Porcar-Castell, A., J. Peñuelas, S. M. Owen, J. Llusia, S. Munne-Bosch & J. Bäck (2009). Leaf carotenoid concentrations and monoterpene emission capacity under acclimation of the light reactions of photosynthesis. *Bor. Env. Res.* **14**: 794-806.
- Porcar-Castell, A., J. I. Garcia-Plazaola, C. J. Nichol, P. Kolari, B. Olascoaga, N. Kuusinen, B. Fernández-Marín, M. Pulkkinen & E. Nikinmaa (2012). Physiology of the seasonal relationship between the photochemical reflectance index and photosynthetic light use efficiency. *Oecologia* **170**: 313-323.
- Taipale, R., T. M. Ruuskanen, J. Rinne, M. K. Kajos, H. Hakola, T. Pohja & M. Kulmala (2008). Technical note: Quantitative long-term measurements of VOC concentrations by PTR-MS – measurement, calibration, and volume mixing ratio calculation methods. *Atmos. Chem. Phys.* **8**: 6681-6698.
- Taipale, R., M. K. Kajos, J. Patokoski, P. Rantala, T. M. Ruuskanen & J. Rinne (2011). Role of de novo biosynthesis in ecosystem scale monoterpene emissions from a boreal Scots pine forest. *Biogeosciences* **8**: 2247-2255.
- Tarvainen, V., H. Hakola, H. Hellén, J. Bäck, P. Hari & M. Kulmala (2005). Temperature and light dependence of the VOC emissions of Scots pine. *Atmos. Chem. Phys.* **5**: 989-998.

# BACKGROUND MBL SIGNAL IN ATMOSPHERIC CO<sub>2</sub> MIXING RATIOS OBSERVED AT PALLAS STATION: COMPARISON OF TWO MODELS FOR TRACING AIR MASS HISTORY

T. AALTO, J. HATAKKA, R. KOUZNETSOV and K. STANISLAWSKA

Finnish Meteorological Institute, P.O.Box 503, FI-00101 Helsinki, Finland.

Keywords: trajectory, dispersion, influence region, marine boundary layer.

## INTRODUCTION

Global baseline CO<sub>2</sub> mixing ratio is increasing year by year. This increase is monitored by numerous stations around the globe. The ground-based stations are situated in various locations ranging from marine to mountainous environments. The aim is to measure air samples that are representative to a large volume of atmosphere, and far from large point emission sources. Thus measurements are being selected for well-mixed air using e.g. wind speed and hourly standard deviation. Even if the station is remote, atmospheric circulation can occasionally bring in air masses that are affected by large emissions and thus are elevated in CO<sub>2</sub>. These episodes also need to be tracked. Air mass back-trajectories and footprints are useful in finding explanations for the observed CO<sub>2</sub> level. If air masses have been transported in low altitude over continental populated regions before arrival to measurement station, we can expect higher CO<sub>2</sub> levels than after transport above marine region. There are different methods to trace the history of air masses. Traditionally a Lagrangian trajectory model can be used, which gives only one back-trajectory path related to one observation time and place. However, in a dispersion model an ensemble of particles can be released relating to one observation time and place, and these particle paths can be used to construct a footprint map depicting the probable source regions. Accurate evaluation of a footprint requires a very large number of trajectories. Alternatively, an Eulerian dispersion model can be run to evaluate the footprints directly. In this work, Lagrangian trajectory model FLEXTRA and Eulerian dispersion model SILAM are compared from a perspective of selecting Pallas CO<sub>2</sub> observations according to different source regions. The results are evaluated against NOAA marine boundary layer (MBL) reference, describing the CO<sub>2</sub> background according to global observation network.

## SITE AND METHODS

Pallas site is located in the Pallas-Yllästunturi National Park in Northern Finland (Hatakka *et al.*, 2003, Aalto *et al.*, 2002). The main station, Sammaltunturi, is located on the treeless top of an arctic hill (67°58'24''N, 24°06'58''E, 565 m a.s.l.). The terrain around the site is characterized by patches of boreal forests, wetlands and lakes. CO<sub>2</sub> is continuously monitored at the site. The current measurement configuration is based on cavity ring down spectroscopy (CRDS) instrumentation (Picarro G1301, G2401), which is capable to high precision and frequency measurements of the sample air. Working standard cylinders are measured alternately with the sample air, and in addition a target cylinder is used for independent quality check. The measurements are calibrated against a set of WMO/CCL primary mixing ratio standards once in every two or three months.

In order to remove periods with weak atmospheric mixing and thus significant local influences, the hours with low wind speed and high mixing ratio variation were excluded from the CO<sub>2</sub> data set. Based on wind statistics, during January the limit was 4 m/s. The limit for one standard deviation in hourly mixing ratios was 0.3 ppm in winter. In addition for MBL data set, exceptionally high and low values were removed by using distance to fit. All data further than 2.0 standard deviations from the curve fitted through the data was rejected. In order to separate the different origins of long range transported signals, Pallas surroundings were divided into five characteristic air mass source regions (Local, Arctic, East, West,

South) as described in Aalto *et al.* (2002). Arctic and West are mainly marine, East and South are continental. Local includes continental northern Finland, Sweden and Norway.

Trajectories were utilized in analysis of long-range transport of carbon dioxide. They were calculated five days backwards using a three-dimensional kinematic FLEXTRA trajectory model (e.g. Stohl and Seibert, 1998), using numerical meteorological data from the European Centre for Medium-Range Weather Forecasts (ECMWF) for years 1998 - 2010. Footprints, i.e. compilation of cases when air parcels touched ground before arrival at Pallas, were simulated with SILAM regional chemical weather assessment and forecasting model (e.g. Sofiev *et al.*, 2006) for years 2010 - 2012. The footprints were aggregated from Eulerian mode simulations extending five days backwards and using arrival window of three hours. The meteorological information was taken from the ECMWF operational forecast archive. As a result, there was a footprint or trajectory connected to all observations at Pallas. Each hour of observation was assigned to multiple influence regions (Local, Arctic, East, South, West) according to percentage of the total footprint or length of trajectory spent over the corresponding region.

NOAA MBL reference was used for comparison and validation of Pallas MBL data. NOAA MBL reference is a data product derived directly from CO<sub>2</sub> measurements of weekly air samples, predominantly of well-mixed marine boundary layer (MBL) air representative of a large volume of the atmosphere. It is based on measurements from a subset of sites from the NOAA Cooperative Global Air Sampling Network (GLOBALVIEW-CO<sub>2</sub>, 2012, Masarie, K.A. and P.P. Tans, 1995).

## RESULTS AND CONCLUSIONS

FLEXTRA and SILAM produce similar synoptic scale features regarding air mass transport to Pallas during January 2010, but there are also differences which affect the classification of each observation to a specific CO<sub>2</sub> influence region. FLEXTRA tends to favour West and East as an influence region and SILAM South and Arctic. Local region gets larger contributions from SILAM, which is expectable since in FLEXTRA trajectories all points are counted and in a straight line trajectory there are only a couple of points close to site, whereas in SILAM surface point clouds there are always more points in the vicinity of the site. Only results for January 2010 are shown here for shortness and clarity, and because the deviations from background due to anthropogenic emissions are more clearly seen in CO<sub>2</sub> mixing ratios during winter.

Mixing ratio of CO<sub>2</sub> is shown together with SILAM and FLEXTRA influence regions in Fig. 1 for January 2010. SILAM shows a rather clear distinction between continental and marine influence regions. High contributions (>40%) from Arctic and West influence regions are often connected with low CO<sub>2</sub> observations and high East and South contributions are connected with elevated CO<sub>2</sub>. Some of the high East and South contributions also indicate low CO<sub>2</sub>, but high Arctic and West are never connected with elevated CO<sub>2</sub>, which is promising considering extraction of the MBL signal. The results by FLEXTRA are more mixed. Some of the high West contributions are connected with elevated CO<sub>2</sub>, and high East is more evenly spread over the CO<sub>2</sub> scale. This may be due to the fact that SILAM only accounts for cases when the transported air mass was close to the surface and thus reflects the actual vertical exchange. Also, as FLEXTRA favours East & West, some South elevated CO<sub>2</sub> cases have been mistakenly attributed to West. However, also FLEXTRA correctly indicates very low CO<sub>2</sub> from Arctic influence region.

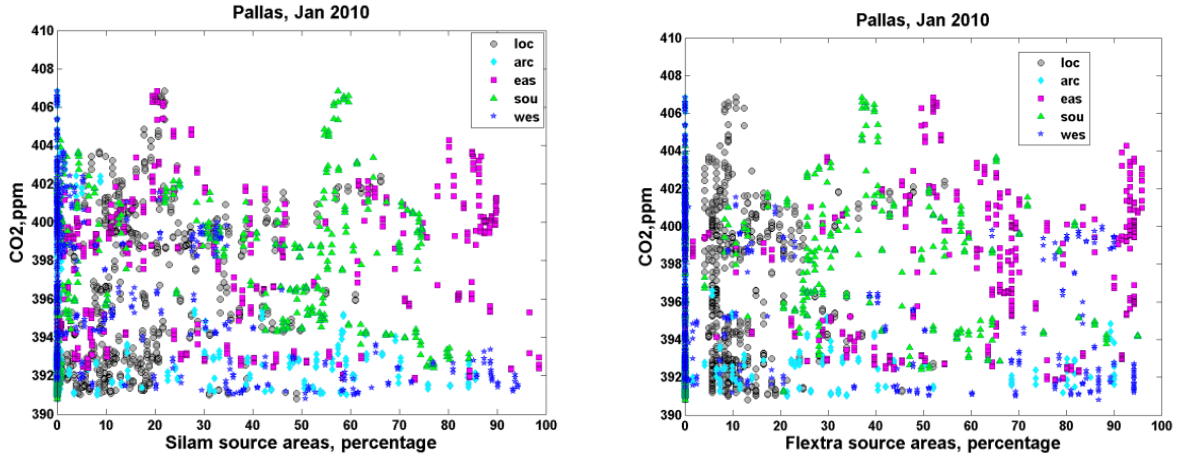


Fig. 1. Hourly mean mixing ratio of CO<sub>2</sub> observed at Pallas and percentage of a) SILAM footprint and b) FLEXTRA trajectory length coming from different influence regions.

Based on SILAM results, the CO<sub>2</sub> observations were selected for MBL signal by limiting the Local influence region contribution to < 20 % and South and West to < 1 %. This is in agreement with earlier classification by FLEXTRA. In comparison to NOAA MBL reference, both FLEXTRA and SILAM perform well, though differences between NOAA MBL reference and SILAM were smaller. The monthly averages of MBL signal selected according to FLEXTRA and SILAM are shown in Fig. 2 together with the reference for year 2010. It has to be noted, that only one year of data is too little to evaluate the differences, but the results look promising. Also an independent evaluation of longer data sets for FLEXTRA period (1998 - 2010) and SILAM period (2010 - 2012) confirms the result. Thus, as SILAM results were consistent with FLEXTRA and in a good quantitative agreement with NOAA MBL reference, it will serve as a new primary tool for on-line estimation of the influence regions and MBL signal at Pallas.

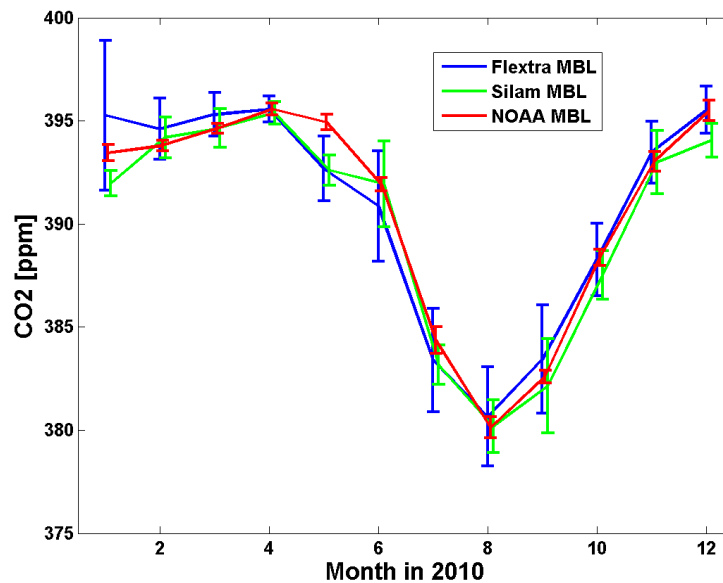


Fig. 2. Monthly mean mixing ratio of CO<sub>2</sub> observations selected for MBL signal at Pallas according to SILAM and FLEXTRA models, and NOAA MBL reference for year 2010.

## ACKNOWLEDGEMENTS

This work was supported by Academy of Finland Center of Excellence (project no 1118615) and the Nordic Center of Excellence DEFROST.

## REFERENCES

- Aalto, T., J. Hatakka, J. Paatero, J.-P. Tuovinen, M. Aurela, T. Laurila, K. Holmen, N. Trivett and Y. Viisanen (2002). Tropospheric carbon dioxide concentrations at a northern boreal site in Finland: Basic variations and source areas. *Tellus* **54B**, 110-126.
- GLOBALVIEW- CO<sub>2</sub> (2012): Cooperative Atmospheric Data Integration Project - Carbon Dioxide. CD-ROM, NOAA ESRL, Boulder, Colorado [Also available on Internet via anonymous FTP to ftp.cmdl.noaa.gov, Path: ccg/co2/GLOBALVIEW]. See version history (www.esrl.noaa.gov/gmd/ccgg/globalview/co2/co2\_version.html).
- Hatakka, J., T. Aalto, V. Aaltonen, M. Aurela, H. Hakola, M. Komppula, T. Laurila, H. Lihavainen, J. Paatero, K. Salminen and Y. Viisanen (2003). Overview of atmospheric research activities and results at Pallas GAW station. *Boreal Environment Research* **8**, 365-384.
- Masarie, K.A. and P.P. Tans (1995). Extension and Integration of Atmospheric Carbon Dioxide Data into a Globally Consistent Measurement Record, *Journal of Geophysical Research* **100**, 11593-11610.
- Sofiev, M., P. Siljamo, I. Valkama, M. Ilvonen and J. Kukkonen (2006) A dispersion modelling system SILAM and its evaluation against ETEX data. *Atmospheric Environment* **40**, 674-685, DOI:10.1016/j.atmosenv.2005.09.069.
- Stohl, A. and P. Seibert (1998). Accuracy of trajectories as determined from the conservation of meteorological tracers. *Quarterly Journal of the Royal Meteorological Society* **124**, 1465–1484.

# EMISSIONS OF VOLATILE ORGANIC COMPOUNDS FROM BOREAL HUMIC LAKES

H. AALTONEN<sup>1</sup>, H. HAKOLA<sup>2</sup>, A. OJALA<sup>3</sup>, L. KLEMEDTSSON<sup>4</sup>, J. PUMPANEN<sup>1</sup>, E. PELTOMAA<sup>3</sup>  
and J. BÄCK<sup>1,5</sup>

<sup>1</sup>Department of Forest Sciences, University of Helsinki, Finland.

<sup>2</sup>Finnish Meteorological Institute, Helsinki, Finland.

<sup>3</sup>Department of Environmental Sciences, University of Helsinki, Finland.

<sup>4</sup>Department of Biological and Environmental Sciences, University of Gothenburg, Sweden.

<sup>5</sup>Department of Physics, University of Helsinki, Finland

Keywords: VOCs, BOREAL LAKE, CLIMATE CHANGE.

## INTRODUCTION

Biological sources of VOCs in aquatic ecosystems are related to algal and microbial functions, which have been reported to produce significant quantities of volatile compounds, e.g. dimethyl sulphide, isoprene and monoterpenes (Colomb *et al.*, 2008; Yassaa *et al.*, 2008) especially during the algal bloom periods. Oceans have proven to be significant sources of aerosol precursor gases, but in inland lakes also algae and bacteria may produce VOCs in quantities comparable to those of terrestrial soil and forest floor vegetation (Bäck *et al.*, manuscript in preparation). The diurnal pattern observed in freshwater VOC emissions suggests a significant contribution of biological (both bacterial and algae) processes on the production of VOCs.

Aquatic VOC emissions have mostly been measured during the ice-free period when the biological activity is greatest. However, the ice cover does not inhibit bacterial metabolism, which is independent on light. Since also algal photosynthesis begins already below the ice cover after snow has disappeared and saturates at very low PAR levels (Tulonen *et al.*, 1994; Ojala, pers. comm.), it is anticipated that biologically produced VOCs could accumulate beneath the ice cover, and released to the air during the ice melt period. In freezing marine ecosystems the VOCs may also be accumulated in the brine pockets. In this project we conducted springtime VOC measurements on boreal lakes hypothesizing that:

- 1) ice cover does not restrain VOC production in boreal lakes, and
- 2) melting of ice may lead to a burst of accumulated VOCs from the top layers of the water column

## METHODS

The springtime emissions of terpenoids were measured from two boreal lakes: on the Lake Kuivajärvi, in southern Finland and on Lake Erssjön, in southern Sweden (Figure 1). Measurements were conducted with floating flow-through chambers and the samples were taken from air entering and leaving the enclosure to adsorbent tubes (Tenax TA-Carbopack B). Samplings were performed with three campaigns, starting at the time of ice melt. Earlier at the winter, background samples were taken from a chamber placed above a small hole in the ice cover. Terpenoid analyses from adsorbent tubes were performed at the Finnish Meteorological Institute with thermodesorption-gas chromatograph-mass spectrometer (TD-GC-MS).

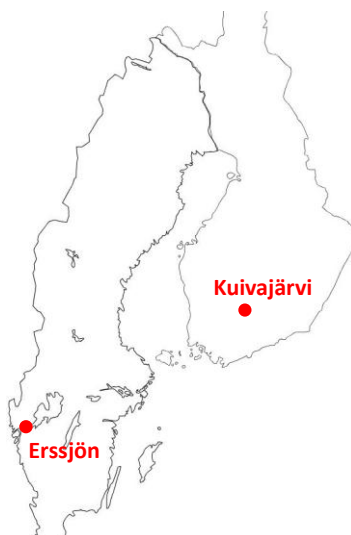


Figure 1. Map of the measurement lakes in Sweden and Finland.

In addition to the VOC emission measurements, terpenoid and short-chained hydrocarbon concentrations were measured parallel on the Lake Kuivajärvi with on-line TD-GC-MS, and these measurements are still on-going. The concentrations were measured about 50 cm above water surface and the sampling inlet was coupled with 3D ultrasonic anemometer.

The VOC emission measurements were combined with those of air temperature, solar radiation, chlorophyll, and phytoplankton populations. Phytoplankton samples will be analysed later in the laboratory under microscope as well as phytobiomass using chlorophyll determination with a spectrophotometer. At the Lake Kuivajärvi, measurement raft provides plenty of data about physical parameters and gas concentrations ( $O_2$ ,  $CO_2$ ,  $CH_4$ ) in the lake and gas fluxes from the lake. In both the lakes, water balance as well as carbon input and output were continuously monitored.

## RESULTS AND CONCLUSIONS

The preliminary data shows measurable terpenoid emissions from boreal lakes and the emissions consist on several mono- and sesquiterpenes. However, the absolute springtime emissions seem to be quite low in both the lakes, and a burst in the emission during/after ice melt was not observable. The emissions seem to increase during the spring with higher temperatures. The data on terpenoid and short-chained carbohydrate concentrations from the Lake Kuivajärvi are not yet available.

The three most abundant compounds in aquatic terpenoid emissions were monoterpenes  $\alpha$ -pinene,  $\Delta^3$ -carene and  $\beta$ -pinene, same compounds that are abundant also in VOC fluxes from boreal forest floor (Aaltonen *et al.*, 2011). Several sesquiterpenes (most abundantly longifolene) were also seen in the emissions, although generally their emission rates were very low. The oxygenated terpenoids linalool and bornyl acetate were emitted in notable amounts.

## ACKNOWLEDGEMENTS

This work was supported by a fellowship from the Nordic Centre of Excellence CRAICC and the Academy of Finland Centre of Excellence program.

## REFERENCES

- Aaltonen, H., Pumpanen, J., Pihlatie, M., Hakola, H., Hellen, H., Kulmala, L., Vesala, T. and J. Bäck (2011). Boreal pine forest floor biogenic volatile organic compound emissions peak in early summer and autumn, *Agr. Forest Meteorol.* **151**, 682–691.
- Colomb, A., Yassaa, N., Williams, J., Peeken, I. and K. Lochte (2008). Screening volatile organic compounds (VOCs) emissions from five marine phytoplankton species by head space gas chromatography/mass spectrometry (HS-GC/MS), *J. Environ. Monit.* **10**, 325–330.
- Tulonen, T., Kankaala, P., Ojala, A. and L. Arvola (1994). Factors controlling production of phytoplankton and bacteria under ice in a humic, boreal lake, *J. Plankton Res.* **16**, 1411–1432.
- Yassaa, N., Peeken, I., Zöllner, E., Bluhm, K., Arnold, S., Spracklen, D. and J. Williams (2008). Evidence for marine production of monoterpenes, *Environ. Chem.* **5**, 391–401.

# AEROSOL FIRST INDIRECT EFFECT FROM PUIJO MEASUREMENT STATION: IMPLICATIONS TO CLIMATE STUDIES

I. AHMAD, S. MIKKONEN, T. KÜHN, and S. ROMAkkANIEMI

Department of Applied Physics, University of Eastern Finland, Kuopio (Finland)

Keywords: AEROSOL, CLOUD DROPLET, LIQUID WATER CONTENT, DROPLET NUMBER CONCENTRATION.

## INTRODUCTION

Atmospheric aerosol is significantly affecting earth's radiation budget through their direct effect (extinction), as well as by changing clouds optical and microphysical properties [IPCC 2007]. The radiative properties of low level continental boundary layer clouds depend on their liquid water profile, droplet effective radius ( $R_{eff}$ ), cloud droplet number concentration ( $N_d$ ), droplet size distribution and meteorological parameters. Cloud's thickness and vertical profile of liquid water content are mainly determined by the meteorology.  $N_d$  depends on aerosol concentration ( $N_{acc}$ ), chemical composition of aerosols, temperature, and on the updraft wind at the cloud base [McFiggans et al., 2006]. An increase in Cloud Condensation Nuclei (CCN) results in an increased cloud droplet concentration and decreased cloud droplet size, which together enhance the reflection of solar radiation back to space (first Aerosol Indirect Effect (1st AIE)) [Twomey 1977].

To study the interaction between aerosol and clouds, we need both measurements and model simulation. Models can easily be extended to all kinds of atmospheric conditions, but their results must be compared against measurements to evaluate their performance. In this study we analyse the cloud droplet number concentration  $N_d$  from ground based in situ measurements, with special interest in how much aerosol and altitude inside the cloud are affecting the measured  $N_d$ .

## METHODS

In this study we have used Puijo measurement station (62°54'34" N, 27°39'19" E), Kuopio (Finland) for analyzing aerosol cloud interaction. Cloud droplet properties are measured using an optical instrument, Cloud Droplet Probe (CDP). Aerosol properties are measured using a Differential Mobility Particle Sizer (DPMS) [Leskinen et al, 2009, Portin et al, 2009]. Puijo tower (Puijo station) is equipped with different instruments for the measurements of aerosol, cloud, atmospheric gases, and meteorological parameters. This site is a unique and good place for the observation of aerosol-cloud-interactions as the tower is approximately 15% of the days inside clouds. Because of its height it can provides promising observations for analysing air masses coming from different aerosol sources.

We studied the aerosol-cloud-interaction (ACI, Eq. 1) and CDP instrument data quality using data collected during 2012 campaign (Oct–Nov, 2012). The CDP at Puijo station measures cloud droplet concentration in 30 different bins ranging from 3  $\mu\text{m}$  to 50  $\mu\text{m}$  in diameter. The used CDP data from 2012 campaign is the best resolution data (1 Hz, 1 second data) available allowing to capture even small scale variability in cloud droplet properties. However, when using only short measurement times, the instrumental uncertainty increases. We thus have used statistical methods to remove random noise. The filtering was done using "Time series decomposition using eigenvector filtering" EVF. An example of the original data, filtered  $N_d$  and the residual are shown in Fig. 1. On average the residual  $N_d$  is 2.3  $\text{cm}^{-3}$ . This data is compared against the aerosol size distribution data available in 12 minutes time resolution from the DMPS system.

$$ACI = \frac{1}{3} \frac{d \ln(N_d)}{d \ln(N_{acc})} \quad (1)$$

## RESULTS

During the campaign the average droplet number concentration was  $214 \text{ cm}^{-3}$ , liquid water content was  $0.11 \text{ g/m}^3$ , and droplet effective radius was  $3.5 \text{ }\mu\text{m}$ . As we are measuring boundary layer clouds, it can be expected that LWC has a vertical profile which increases from bottom to top more or less adiabatically, while  $N_d$  should be constant. However, when we plot  $N_d$  as a function of both  $N_{acc}$  and LWC, we see clear trends. This is shown in Fig. 2, where the measurement data is organized according to these parameters, and probability density distributions for  $N_d$  are plotted. In Fig. 2,  $N_{acc}$  is increasing vertically in each row keeping LWC constant to represent the Twomey effect (1<sup>st</sup> aerosol indirect effect), while LWC is increasing from left (subplot) to right (subplot). It is evident that the peaks of  $N_d$  are shifting toward higher values in Fig. 2. However, also the LWC is clearly affecting  $N_d$ , the reason for this behaviour can only be speculated upon. It may be that closer to cloud base the descending air parcel already experienced lot of droplet evaporation causing bimodal shape for droplet concentrations as can be seen from top right panels in Fig. 2. Also the cloud thickness might be different, with thinner clouds having lower  $N_d$  values. To confirm this, however, we would need information on the cloud thickness.

**Table. 1:** List of LWC,  $N_{acc}$ , and the corresponding ACI values and mean values of  $N_d$  (filtered).

LWC ( $\text{g/m}^3$ )	$N_{acc}$ ( $\text{cm}^{-3}$ )	Mean $N_d$ ( $\text{cm}^{-3}$ )	ACI
0.02-0.04	100-200	104	0.2606
	200-300	172	
	300-400	214	
	400-1000	249	
0.04-0.06	100-200	132	0.2631
	200-300	214	
	300-400	268	
	400-1000	315	
0.06-0.08	100-200	150	0.2714
	200-300	236	
	300-400	284	
	400-1000	367	
0.08>	100-200	150	0.3110
	200-300	251	
	300-400	322	
	400-1000	413	

To further analyse how the LWC value is affecting the aerosol cloud interactions we used the same data classification and calculated the value of ACI (Eq. 1) parameter. These are presented in Table 1.

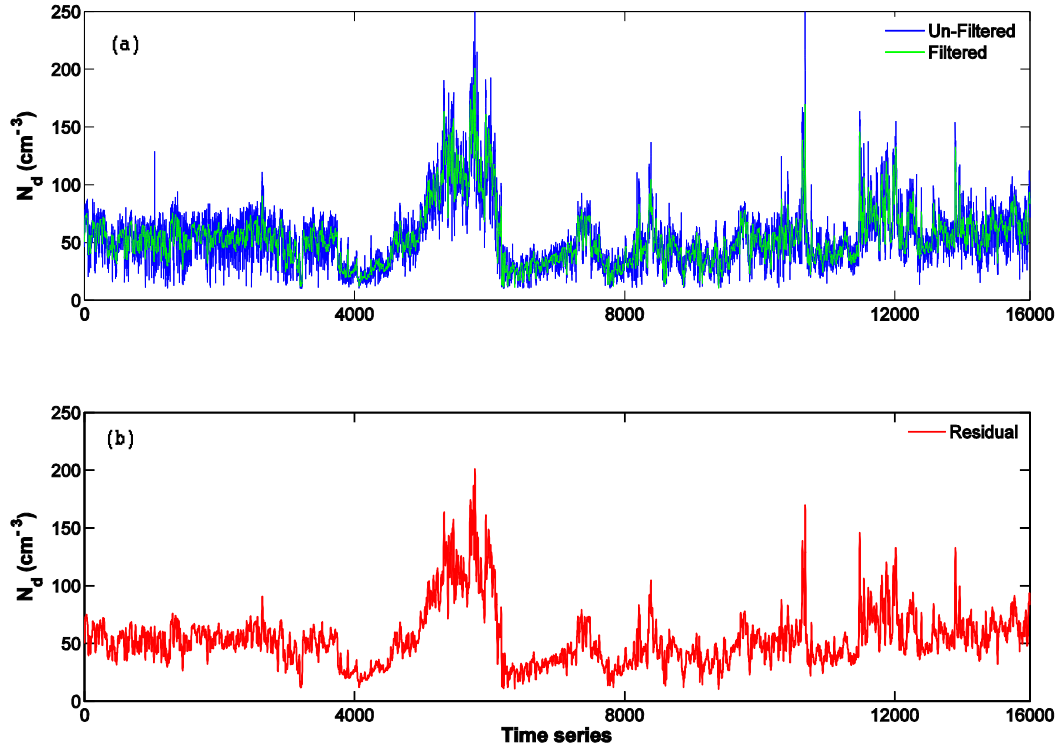


Fig. 1: (a).Time series of Un-filtered (blue) and filtered (green) cloud droplet number concentrations data from 26<sup>th</sup> Nov, 2012. Panel (b) shows the residual of the filtered data.

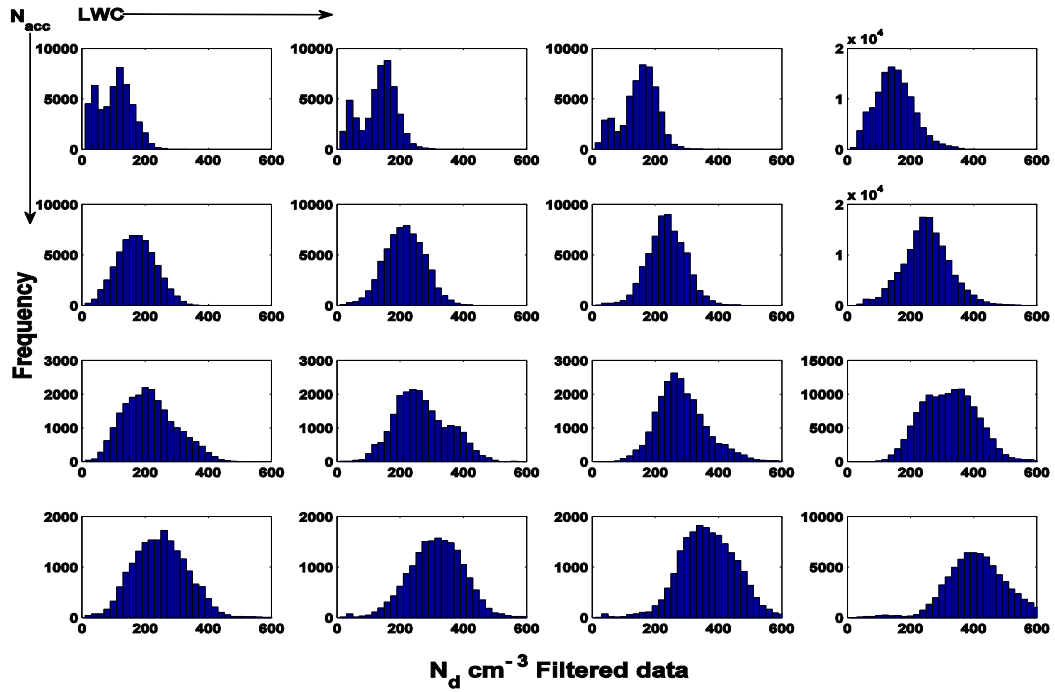


Fig. 1: Filtered data – Effect of aerosol on cloud droplet number concentration keeping LWC and aerosol number concentration constant in each column and row, respectively. LWC values increase from left to right and aerosol concentrations increase from top to bottom.

## ACKNOWLEDGEMENTS

This work was supported by Maj and Tor Nessling Foundation, the Academy of Finland Center of Excellence program (project number 1118615) and by the strategic funding of the University of Eastern Finland.

## REFERENCES

- Intergovernmental Panel on Climate Change. (Eds S Solomon, D Qin, M Manning, Z Chen, M Marquis, KB Averyt, M Tignor, HL Miller), *Cambridge University Press, Cambridge*, UK and New York, NY, USA, 996 pp.
- Leskinen, A., H., Portin, M. Komppula, P., Miettinen, A. Arola, H., Lihavainen, J. Hataka, A., Laaksonen, and K. E. J., Lehtinen., Overview of the research activities and results at the Puijo semi-urban measurement station, *Boreal Env. Res.*, 14, 576-590, 2009
- McFiggans, G., P. Artaxo, U. Baltensperger, H., Coe, M. C. Facchini, G., Feingold, S. Fuzzi, M. Gysel, A. Laaksonen, U. Lohmann, T. F. Mentel, D. M. Murphy, C. D., O'Dowd, J. R. Snider, and E. Weingartner., The effect of physical and chemical aerosol properties on warm cloud droplet activation, *Atmos. Chem. Phys.*, 6, 2593–2649, doi:10.5194/acp-6-2593-2006.
- Portin, J. H., M. Komppula, A.P. Leskinen, S. Romakkaniemi, A. Laaksonen, and K. E. J. Lehtinen., Overview of the aerosol-cloud interaction at the Puijo semi-urban measurement station, *Boreal Env. Res.*, 14: 641-653, 2009.
- Twomey, S. 1977. The influence of pollution on the shortwave albedo of clouds. *J. Atmos. Sci.*, 34, 1149–1152.

# NORTHERN BOG SURFACE HETEROGENEITY: IMPLICATIONS FOR THE ECOSYSTEM-ATMOSPHERE INTERACTIONS

P. ALEKSEYCHIK<sup>1</sup>, A. KORRENSALO<sup>2</sup>, E.-S. TUUTTILA<sup>2</sup>, J. RINNE<sup>1</sup> and T. VESALA<sup>1</sup>

<sup>1</sup> Department of Physics, University of Helsinki, Helsinki, Finland

<sup>2</sup> University of Eastern Finland, Kuopio, Finland

Keywords: wetlands, microsites, carbon cycle, energy cycle.

## INTRODUCTION

Boreal peatlands are known to be a massive storage of soil carbon, making up to about 20% of the world terrestrial carbon reserves. The carbon storage in peatlands has played a crucial role in the climate development since the last glacial period. Nowadays, however, the changing climate has been exerting a pressure on boreal peatlands under which their carbon reserves are becoming unstable. Massive evidence suggests that the expected climate shifts may destabilize the peatlands enough for the major fraction of their organic carbon to be emitted into the atmosphere in the form of greenhouse gases, mainly as CO<sub>2</sub> and CH<sub>4</sub>. At the same time, the peat accumulation zone may progress northwards as the arctic climate changes (Charman *et al.*, 2013).

Besides that, however, peatlands have the potential to alter the climate through the energy exchange with the atmosphere. This process bears importance on many scales. At the scale of 1 to 10 m<sup>2</sup>, it is responsible for the heating of peat, which directly controls the production of GHG; at the scale of 10 to 100 km<sup>2</sup>, the Bowen ratio largely determines the local and regional climate. On an even larger scale, the conversion between the open peatlands and forested areas, occurring both naturally and through management, feeds back to the global climate.

Specific features of boreal climate have led the peatlands to develop distinctive microtopography with the associated differences in the vegetation communities, peat characteristics and hydraulics (Bridgham *et al.*, 1996). Those differences have been shown to create steep gradients in the mass and energy exchange in wetlands. This implies that ecosystem-scale exchange processes at wetlands cannot be modelled correctly without account of the differences in microsite dynamics.

Siikaneva, the biggest wetland to remain in its natural state in Southern Finland, is a perfect polygon for the examination of the peatland microsite heterogeneity. This important aspect of the wetland biogeochemistry is addressed at the bog part of the wetland, the site known as Siikaneva-2.

## METHODS AND AIMS

The bog area of Siikaneva has been the site of various multi-scale experiments brought out by the collaboration of the University of Helsinki, University of Eastern Finland and the Finnish Meteorological Institute. The work that has been brought out at the site during the three field seasons of 2011-2013, and is to be continued, includes:

- 1) Eddy-covariance measurements. The EC setup in Siikaneva-2 provides the ecosystem-scale estimates of CO<sub>2</sub>, CH<sub>4</sub>, sensible and latent heat fluxes. The EC-derived wetland-atmosphere exchange rates provide twofold information that may be hard to interpret because of the source heterogeneity. In the first few tens of meters near the EC mast, the primary source area of the turbulent fluxes may have the size comparable with the sizes of individual microsites. Farther away,

the microsite mosaic is less important, since the turbulent fluxes effectively become spatially averaged at larger distances from the EC sensor.

- 2) Manual chamber measurements. The chamber measurements are performed at 6 microsites; each microsite is sampled 3 times for better representativeness. The microforms currently measured are: high hummock, hummock, high lawn, lawn, hollow and mud bottom. Additionally, floating chambers are used to estimate the ebullition flux from mud bottoms / pond surfaces.
- 3) Gas concentration sampling. Dissolved gas collection points are equipped with the tubes reaching down to 2m depths in all representative microsites. Through these measurements, we hope to obtain new evidence of the greenhouse gas production across the bog microtopography gradient.
- 4) Vegetation sampling. Examination of the vegetation composition has been brought out within the 99% contribution area of EC fluxes (200m radius around the EC mast). A total of 354 plots have been sampled, with the additional sampling in the maximum EC contribution zone to follow. Derived quantities include leaf area index, biomass and species composition.
- 5) LIDAR and aerial photography. Completed in spring 2013, this remote sensing campaign has provided a high-resolution view of the area around the site, which will be used to construct the source mosaic map, in coordination with the vegetation map.
- 6) Net radiation and temperature monitoring. 4 pairs of  $R_{\text{net}}$  sensors and  $T_{\text{peat}}$  profiles (down to 0.3m depth) have been installed at representative microsites, since we expect different with respect to the net radiation flux and the soil heat conduction. These are tightly linked with e.g. microsite-specific surface cover, peat structure and water content.
- 7) Collection of peat cores and peat depth measurements along transects. Done throughout the extent of the wetland, these data will help reconstruct the peatland development in the past and may be used to forecast the state of the wetland under future climate conditions.

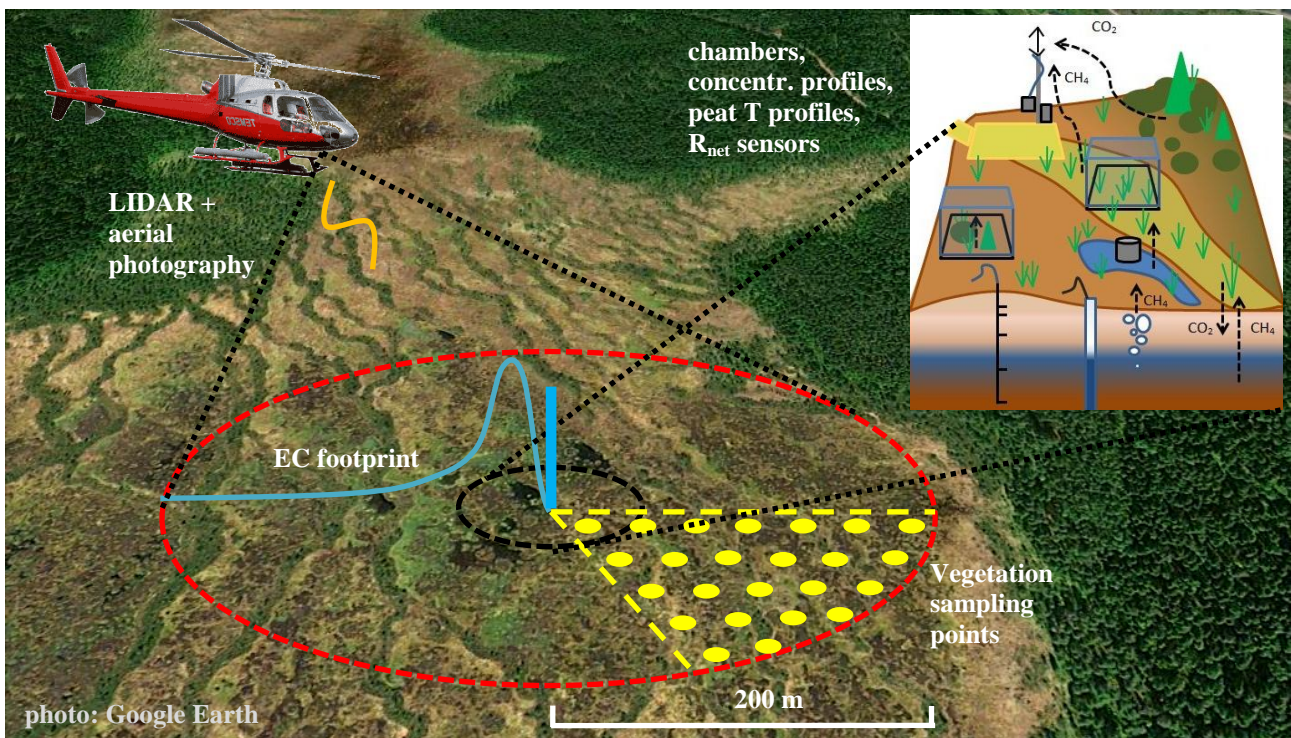


Figure 1. Organization of measurements and campaigns at the Siikaneva-2 site. Due to the larger spatial scale of the work, the peat cores are not included. Vegetation sampling points are uniformly distributed over the EC footprint zone.

Our ultimate purpose is to draw clear distinction between the responses of different microsites to the main environmental drivers such as interannual weather fluctuations or peatland management, and their individual contributions to the local and regional carbon and energy balances.

## RESULTS

Already the first results suggest give an indication of large differences between the energy and mass exchange processes between the different microsites at our site. Figure 2 demonstrates the significant offsets between the net and ground heat fluxes at the original (“old”) measurements and the new microsite-specific measurements, based on 2 weeks of measurements in August 2013. Keep in mind that just the average systematic offsets are seen in Figure 2, while the site-specific fluxes at 30 minute resolution may deviate still much more. The net and ground heat flux offsets are expectedly of different sign and partly compensate each other. The differences we observe are of similar scale to those in the study of a prairie wetland by Burba *et al.* 1999.

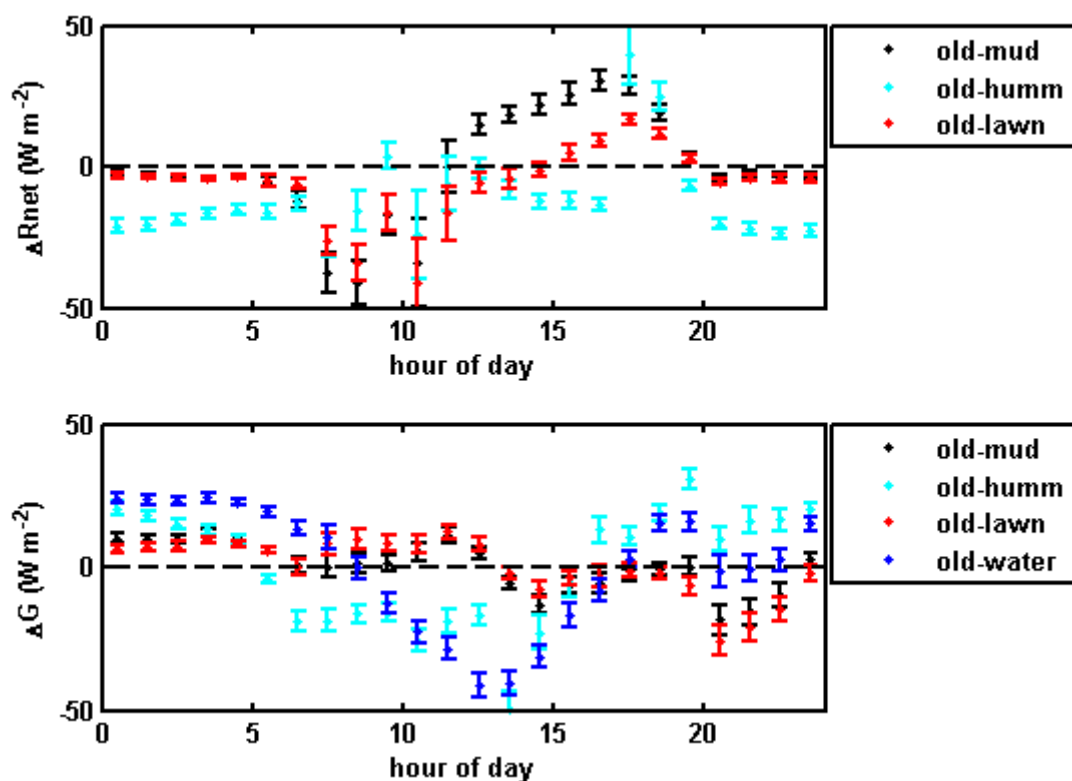


Figure 2. Two-week average diurnal course of the offsets between the net and ground heat fluxes in the original and new site-specific measurements. The “old” measurements are best described as representative of mixed hollow-lawn community with a small contribution of open water surface.

Regarding the GHG fluxes measured at all representative microsites with the manual chamber technique, the differences are just as big (Figure 3). The  $CH_4$  fluxes range between almost zero and about  $150 mg CH_4 m^{-2} d^{-1}$ , apparently being controlled by the type of vegetation community, water table level and availability of nutrients in peat. Importance of microsite segregation in GHG flux analyses is perfectly expressed by the difference between the  $CH_4$  flux at the hollows and the mud bottoms, which represent the two extremes in emission while having almost identical relative surface height and WTD; the presence of vegetation in the hollows seems to be a crucial factor for the local methane production and/or emission.

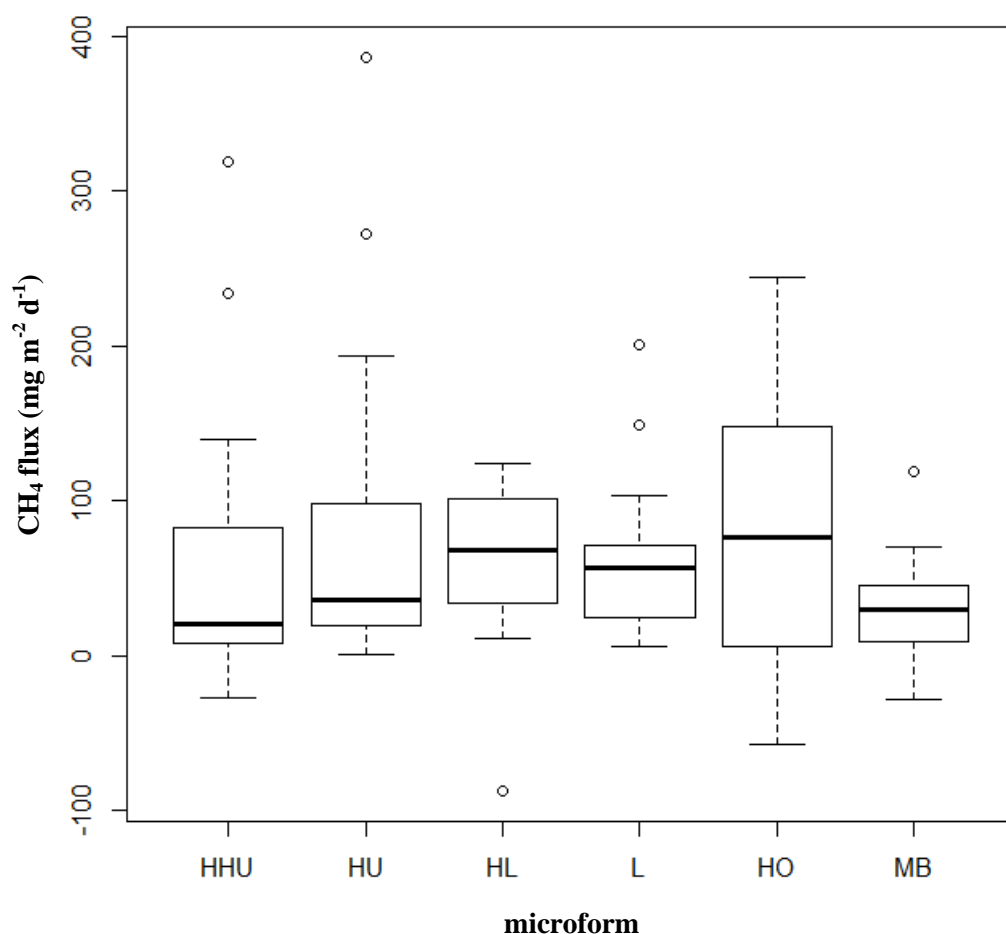


Figure 3. CH<sub>4</sub> fluxes in different microforms at Siikaneva bog site.

## CONCLUSIONS

Confirming the expectation, the energy and mass exchange at the Siikaneva bog site has a strongly local character. The exchange processes observed at the 6 types of surface cover were significantly different, rendering the use of single “average” values senseless. We intend to develop this approach with a more detailed and varied system of field observations. These efforts will aid constructing the process-based models, improve the treatment of peatlands in the global models and reconcile the chamber and EC measurement techniques.

## ACKNOWLEDGEMENTS

We gratefully acknowledge the support from several projects: Academy of Finland Center of Excellence Program (project No. 1118615), Finnish National Doctoral Programme “Atmospheric Composition and Climate Change: From Molecular Processes to Global Observations and Models” (ACCC), Nordic Centre of Excellence DEFROST, ICOS and GHG-Europe.

## REFERENCES

Bridgman S., Pastor J., Janssens J., Chapin C. and Malterer Th. (1996). Multiple limiting gradients in peatlands: a call for a new paradigm, *Wetlands* **16**, 45-65.

Burba G., Verma S., Kim J. (1999). A comparative study of surface energy fluxes of three communities (*Phragmites Australis*, *Scirpus Accutus*, and open water) in a prairie wetland ecosystem. *Wetlands* **19**, 451-457.

Charman D. J., Beilman D.W., Blaauw M., Booth R. K., Brewer S., Chambers F. M., Christen J. A., Gallego-Sala A., Harrison S. P., Hughes P. D. M., Jackson S. T., Korhola A., Mauquoy D., Mitchell F. J. G., Prentice I. C., van der Linden M., De Vleeschouwer F., Yu Z. C., Alm J., Bauer I. E., Corish Y. M. C, Garneau M., Hohl V., Huang Y., Karofeld E., Le Roux G., Loise J., Moschen R., Nichols J. E., Nieminen T. M., MacDonald G. M., Phadtare N. R., Rausch N., Sillasoo Ü., Swindles G. T., Tuittila E.-S., Ukonmaanaho L., Väliranta M., van Bellen S., van Geel B., Vitt D. H., and Zhao Y. (2013). Climate-related changes in peatland carbon accumulation during the last millennium, *Biogeosciences* **10**, 929–944.

# ESTIMATING THE GROWTH RATE OF A NEWLY FORMED AEROSOL MODE

T. ANTTILA<sup>1</sup>, J. LEPPÄ<sup>1,2</sup>, E. ASMI<sup>1</sup> and H. LIHAVAINEN<sup>1</sup>

<sup>1</sup>Finnish Meteorological Institute, P.O. Box 503, 00101 Helsinki, Finland

<sup>2</sup>Departments of Chemical Engineering and Environmental Science and Engineering,  
California Institute of Technology, Pasadena, California

Keywords: AEROSOL DYNAMICS, NEW PARTICLE FORMATION

## INTRODUCTION

Atmospheric new particle formation (NPF) events are characterized by appearance of particles at the lowest measured diameter range and subsequent emergence of a growing mode which can often be visualized as a “banana” (Fig. 1). These events have atmospheric relevance as they provide a potentially large source of particles that act as seeds for cloud droplets. A key parameter associated with this phenomenon is the growth rate (GR) of a newly-formed aerosol mode as it contains information on the mechanisms underlying atmospheric NPF events and provides constraints for numerical models simulating NPF (Yli-Juuti *et al.*, 2011). Several methods for determining GR have been developed, but obtaining accurate size- and time-resolved data on GR can still be challenging with the current methods. Here we propose a complimentary method to determine GR of a growing aerosol mode.

## METHODS

Here we propose a method for determining the growth that is based on calculating the count mean diameter CMD over a certain size interval  $[d_{\min}(t), d_{\max}(t)]$ , and using the following relation:

$$GR(t) = \frac{d}{dt} CMD(t) = \frac{d}{dt} \left( \frac{\int_{d_{\min}(t)}^{d_{\max}(t)} n(d_p) d_p dd_p}{\int_{d_{\min}(t)}^{d_{\max}(t)} n(d_p) dd_p} \right) \quad (1)$$

where  $d_p$  is the particle diameter and  $n(d_p)$  is the particle number size distribution. In practice, GR is obtained through numerical differentiation and integrals are replaced by sums.

Two main challenges in applying equation (1) are: how to determine parameters  $d_{\min}$  and  $d_{\max}$ , and how to eliminate “noise” that arises from numerical differentiation of CMD together with “noise” in the original size distribution data? We approached the former issue by first calculating the diameter corresponding to the peak concentration in the growing mode as a function of time,  $d_{peak}(t)$ . A log-normal fit was then performed around  $d_{peak}$  which yields the geometric standard deviation of the mode as a function of time,  $\sigma_g(t)$ . Finally, the following relations were used:  $d_{\min}(t) = d_{peak}(t)/(\sigma_g(t) \times \alpha)$ , and  $d_{\max}(t) = d_{peak}(t) \times (\sigma_g(t) \times \alpha)$ . Here  $\alpha$  is a free dimensionless parameter that, together with  $\sigma_g$ , determines the size range over which CMD is calculated. Regarding the latter issue, GR was calculated numerically with finite differences, and the resulting time series was then smoothed using an algorithm described by Stickel (2010).

## EVALUATION OF THE METHOD

The approach was evaluated against NPF events generated with an aerosol dynamic model (Anttila *et al.*, 2010), where GR was held constant. To imitate atmospheric data, particle concentrations were perturbed

by  $\pm 10\%$ . Such a comparison is illustrated in Figures 1 and 2. As can be seen, after a growing mode has emerged, the smoothed GR tracks the correct GR accurately despite the fact that non-smoothed GR contains significant amount of noise. The simulated and estimated GR were also compared in a series of Monte Carlo simulations. Based on a large number of simulations, it can be concluded that the estimated GR agree well with each other if: 1) the size resolution is sufficiently high, 2) the emerging mode contains considerable amount of particles compared to the background particle population, and 3) the time series of the size distribution does not contain too much noise.

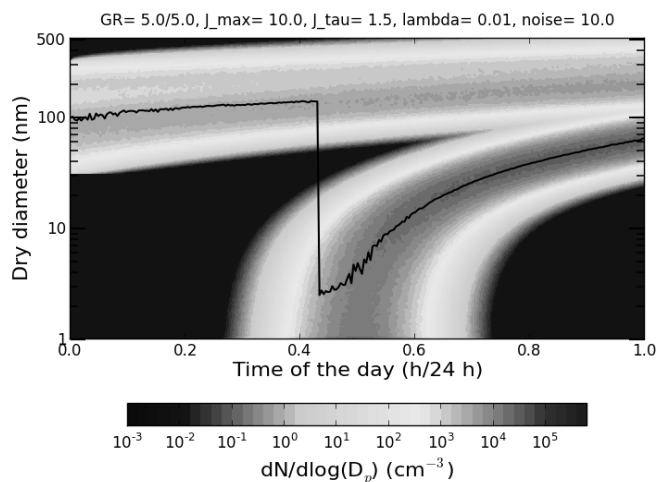


Figure 1. Time evolution of the simulated particle size distribution and CMD (black line).

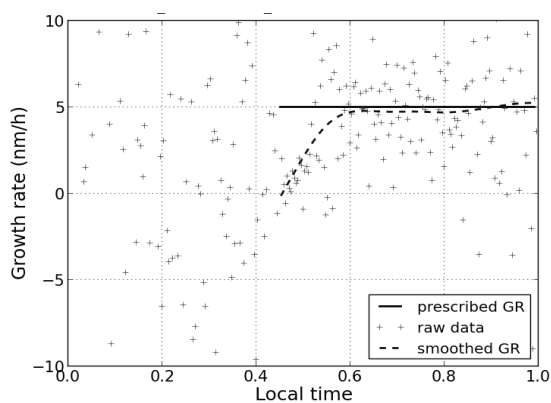


Figure 2. Various growth rates (see legend) during the simulation depicted in Figure 1.

#### ACKNOWLEDGEMENTS

This work was supported by the Academy of Finland Center of Excellence program (project number 1118615) and by the Nordic Center of Excellence CRAICC.

#### REFERENCES

- Anttila, T., Kerminen, V.-M., and Lehtinen, K. (2010). *J. Aerosol Sci.* **41**, 621-636.
- Stickel, J. (2010). *Comp. Chem. Eng.* **34**, 467-475

# AIRBORNE MEASUREMENTS OF AEROSOL PARTICLES AND GREENHOUSE GASES IN SOUTHERN FINLAND

E. ASMI<sup>1</sup>, D. BRUS<sup>1</sup>, S. CARBONE<sup>1</sup>, J. HATAKKA<sup>1</sup>, R. HILLAMO<sup>1</sup>, A. HIRSIKKO<sup>1</sup>, T. LAURILA<sup>1</sup>,  
H. LIHAVAINEN<sup>1</sup>, E. ROUHE<sup>2</sup>, S. SAARIKOSKI<sup>1</sup> and Y. VIISANEN<sup>1</sup>

<sup>1</sup>Finnish Meteorological Institute, Erik Palménin aukio 1, P.O. Box 503, FI-00101, Helsinki, Finland.

<sup>2</sup>Department of Radio Science and Engineering, Aalto University, P.O. Box 13000, FI-00076 Aalto, Finland

Keywords: AIRPLANE MEASUREMENTS, VERTICAL PROFILES, AEROSOL CHEMISTRY, GHG.

## INTRODUCTION

The largest anthropogenic climate forcings are caused by atmospheric aerosol particles and by greenhouse gases (GHGs). Currently, the surface heating effect of increasing atmospheric GHG concentrations is nearly counterbalanced by the cooling from aerosols. The impact of aerosol particles on climate is poorly understood, which is further reflected in uncertainties in climate sensitivity to different forcings. Because the climate effects depend on the composition and quantities of the whole atmospheric column, there is a strong demand for vertical measurements of the important climate forcings, such as aerosol particles and greenhouse gases.

For this purpose, a new measurement platform for airborne studies was constructed and tested in Finland. The concept includes extensive measurements of aerosol particle properties, greenhouse gases and trace gases among the important meteorological parameters. In future, the platform will be used to study: 1) mixing and transformation processes, 2) the cloud processes, and 3) air quality and emissions. On the first flights over southern Finland, profiles were measured over land and sea, and these results were compared with stationary boundary layer measurements.

## METHODS

A modified Short Skyvan SC-7 research airplane, operated by Radio Science and Engineering Department of Earth observation group at Aalto University, was further updated by Finnish Meteorological Institute (FMI) to meet the measurement needs. The airplane is a non-pressurized twin-engine turbo-propeller aircraft with a maximum operating distance of 1370 km. It is equipped with the MIDG II INS/GPS, an Inertial Navigation System with Global Positioning System for recording of precise position and speed.

Onboard on first flights were instruments for aerosol chemical and physical characterization: a Soot Particle-Aerosol Mass Spectrometer (SP-AMS, Aerodyne Research Inc., USA) for fast high resolution particle chemical characterization (DeCarlo et al., 2006), a 3-wavelength nephelometer model 3563 (TSI Inc., St. Paul, Minnesota, USA) for particle scattering measurements, a continuous-flow stream wise thermal-gradient cloud condensation nuclei counter (DMT-CCNC) model CCN-100 (Droplet Measurement Technologies, Inc., DMT, USA) for CCN total number measurements at fixed supersaturation of 0.34 % (Roberts and Nenes 2005) and two condensation particle counters (CNC) model 3010 (TSI Inc., St. Paul, Minnesota, USA). The CCN, one CNC, and SP-AMS were operated behind the Constant Pressure Inlet (CPI, DMT, USA) set to 650 mbar. Concentrations of carbon dioxide (CO<sub>2</sub>), methane (CH<sub>4</sub>) and water vapour (H<sub>2</sub>O) were measured using a Picarro G1301-m (Picarro, Inc. Sunnyvale, CA USA), using near-infrared lasers and Cavity Ring-Down Spectroscopy, and specifically designed for airplane measurements (Crosson, 2008; Chen et al., 2010).

All the onboard instruments were connected to a BMI Isokinetic Inlet System (Model 1200, Brechtel Manufacturing Inc., USA). The inlet system is fully automated, with a transmission efficiency of > 90% for particles with aerodynamic diameters < 10  $\mu\text{m}$ . It is equipped with anti-icing system, Pitot tube, and temperature and pressure sensors.

The data presented are corrected to STP (273.15 K; 1013 mbar). Nephelometer data are also corrected for truncation as suggested by Anderson and Ogren 1998, and effect of pressure on CCN supersaturation is corrected with laboratory calibration results at 650 mbar.

Two flights, taking place on 30 and 31 July, 2012, were performed over the southern Finland and the Baltic Sea (Fig. 1). Weather during flights was warm (around 20-25 °C at ground level), with mild winds from south or south-west, and broken sky with occasional cumulus clouds. Flight routes can be seen on the map (Fig. 1), and the normal cruising altitudes were about 200-300 m (boundary layer) and about 3000 m (free troposphere). Two vertical profiles over land were done on the first flight and four vertical profiles: one over land and three over sea near the island of Utö, were done on the second flight. Results presented here discuss solely on the second flight, and focus mainly on the first profile measured over the land.

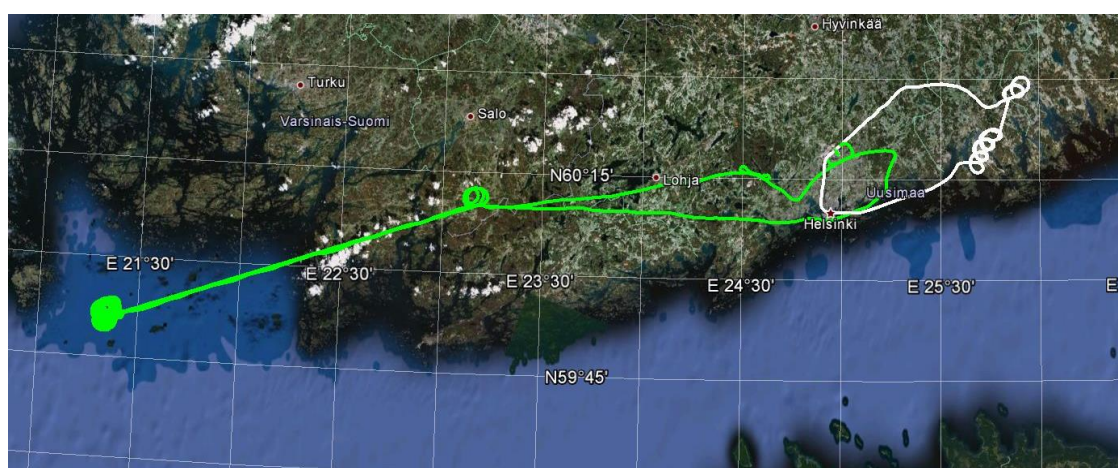


Figure 1. The flight route on July 30 (white) and July 31 (green) left from Helsinki-Vantaa airport to east (1st flight) and to west (2nd flight) over the island of Utö. The spirals present the vertical ascents from about 200 m up to about 3000 m.

## CONCLUSIONS

Total particle concentration in the boundary layer was around 2000  $\text{cm}^{-3}$  and decreased down to around 1000  $\text{cm}^{-3}$  higher in the free troposphere. There was no clear gradient between land and sea concentrations at neither of the altitudes, but above 2500 m some very concentrated (> 3000  $\text{cm}^{-3}$ ) regions indicating secondary formation of particles were observed (see e.g. Fig. 2a). At these concentrated regions, aerosol scattering was typically low, indicating a low sink for vapors and small particles, possibly favoring the particle formation (Fig. 2b).

Cloud condensation nuclei concentrations above the land surface (measured at 0.34 % supersaturation) were at their maximum at 600 m altitude, after which they decreased gradually to close to 100  $\text{cm}^{-3}$  at 3000 m. Particle scattering coefficient decreased with altitude up to about 1800 m, after which a second layer of aerosols, consisting mainly of larger particles, was detected (Fig. 2b). At this layer, concentrations of aerosol nitrate and ammonia increased, accompanied with an increase of  $\text{CO}_2$ . Back trajectories showed south-westerly transported air masses from central and Western Europe. Simultaneous decrease of temperature and relative humidity (Fig. 2c) favors the partitioning of nitrate in the aerosol phase, which is likely a partial explanation for the high nitrate concentration (e.g. Morino et al., 2006). Instead, sulfate and organic concentrations were not elevated in this layer.

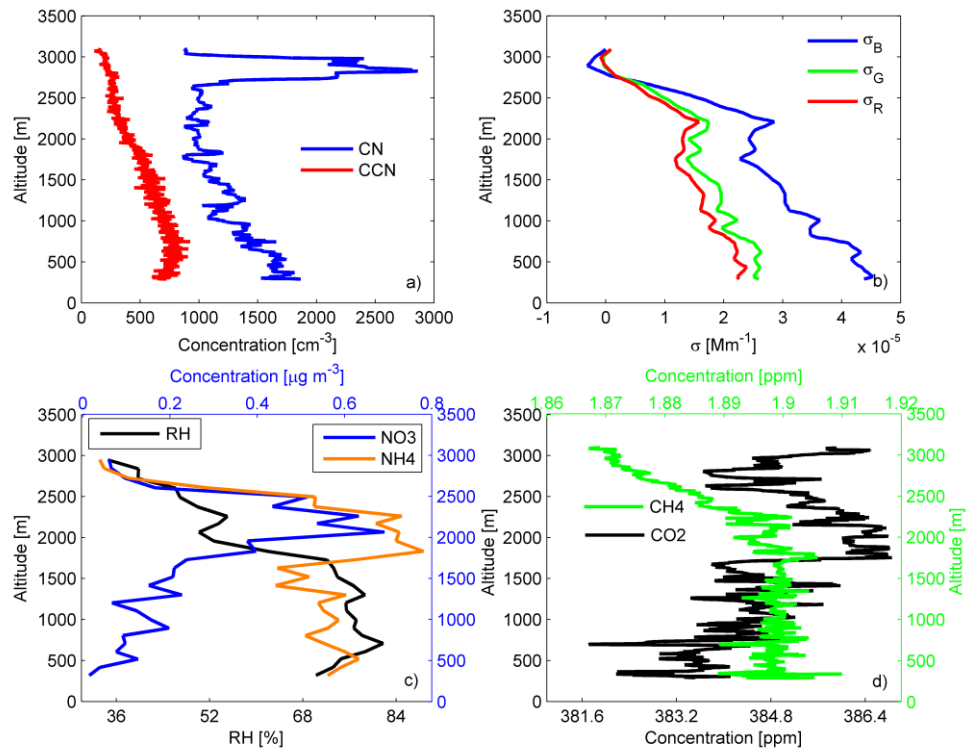


Figure 2. a) Total (CN) and CCN particle number concentration, b) aerosol scattering coefficients at 450 nm (blue), 550 nm (green) and 700 nm (red) wavelengths, c) relative humidity (black) and nitrate (blue) and ammonia (orange) concentrations, and d) carbon dioxide (black) and methane (green) concentrations, all measured during the first ascent over land with altitude presented in y-axis.

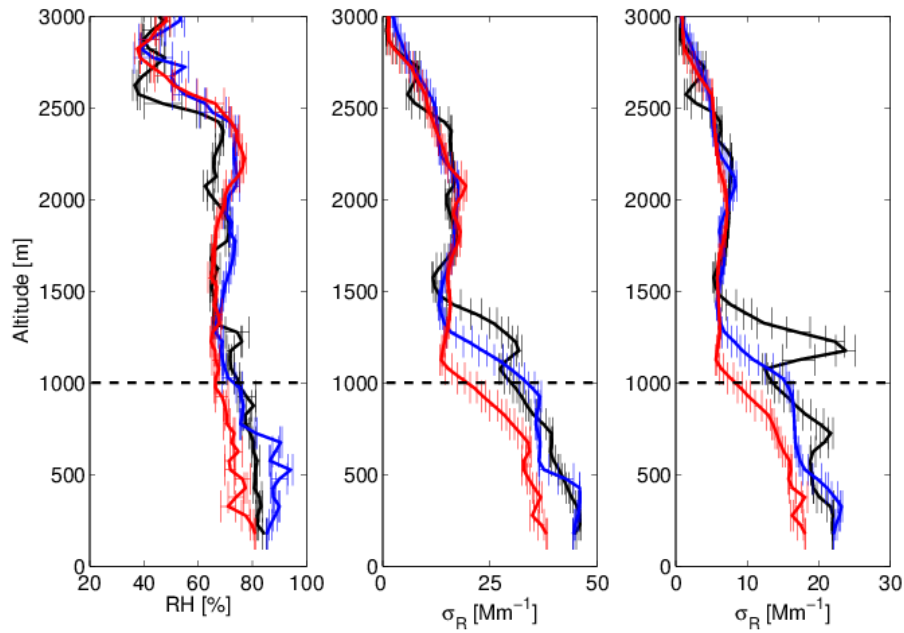


Figure 3. Vertical profiles of RH (left), scattering coefficient at 450 nm (middle) and scattering coefficient at 700 nm (right) during the first (black), second (blue) and third (red) vertical profile with an airplane over the island of Utö.

The measurements on board the airplane were also compared with stationary measurements performed at the island of Utö. Over Utö, three vertical profiles were measured and as an example we show a comparison of measured vertical profiles of scattering by aerosol particles (Fig. 3) as compared with the backscattering signal seen with the Doppler-lidar (Fig. 4). In both of these data, a decreasing signal of scattering with time is visible and an intense layer of scattering is observed during the first profile measurement. With Doppler-lidar, the layers of clouds can also be observed from the data (Fig 4).

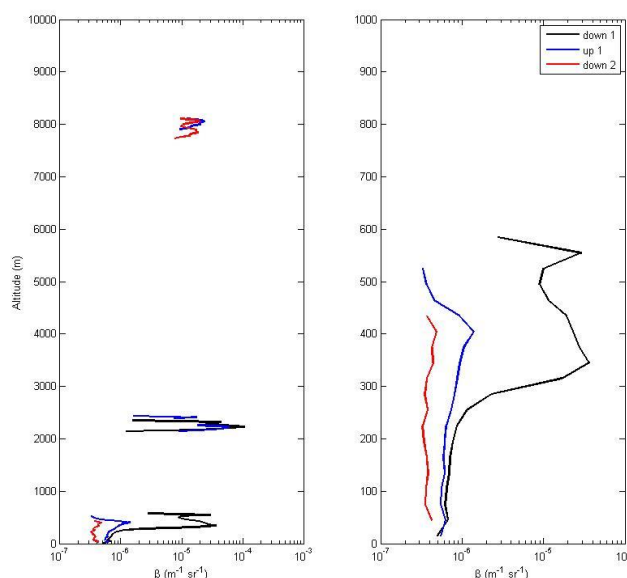


Figure 4. Vertical profiles of aerosol backscatter signal measured with HALO Doppler-lidar on the island of Utö during the first (black), second (blue) and third (red) vertical profile with an airplane.

## ACKNOWLEDGEMENTS

This work was supported by the Measurement, Monitoring and Environmental Assessment (MMEA) and by the Academy of Finland Center of Excellence (project number 1118615) programs.

## REFERENCES

- Anderson, T.L. and Ogren, J.A. (1998). Determining aerosol radiative properties using the TSI 3563 integrating nephelometer. *Aerosol Sci. and Technol.* **29**, 57-69.
- Morino, Y., Kondo, Y., Takegawa, N., Miyazaki, Y., Kita, K., Komazaki, Y., Fukuda, M., Miyakawa, T., Moteki, N. and Worsnop, D.R. (2006). Partitioning of  $\text{NH}_4\text{NO}_3$  and particulate nitrate over Tokyo: Effect of vertical mixing, *J. Geophys. Res.* **111**, D15215, doi:10.1029/2005JD006887.

# INTERCOMPARISON AND VALIDATION OF SNOW COVER FRACTION PARAMETERIZATIONS IN CLIMATE MODELS

K. ATLASKINA<sup>1</sup>, J. PULLIAINEN<sup>2</sup>, K. LUOJUS<sup>2</sup>, M. TAKALA<sup>2</sup>, J. IKONEN<sup>2</sup>, M. KULMALA<sup>1</sup>, G.  
DE LEEUW<sup>1,2</sup>

<sup>1</sup>Department of Physics, University of Helsinki, Finland

<sup>2</sup>Finnish Meteorological Institute, Helsinki, Finland

Keywords: SNOW COVER FRACTION, SNOW MASS, CLIMATE MODELLING, SATELLITE  
DATA.

## INTRODUCTION

The seasonal snow cover governs the terrestrial surface albedo and radiation balance of the climate system at high latitudes. Changes in the atmosphere circulation patterns, air temperature, or, for instance deposition of black carbon, may cause changes of snow albedo and snow mass. A decrease of snow mass and snow albedo can lead to an increase of absorbed solar radiation resulting in a rise of temperature, triggering positive feedbacks to climate change. Changes of snow cover extent and snow mass also affect the hydrological balance through soil moisture, runoff, evaporation and precipitation alteration.

Global climate models (GCM) predict the future state of the climate system on regional and global scales. One of the sources of errors in models' output lays within the way different processes are parameterized. Usually in GCM's snow cover fraction (SCF), which is a function of the snow water equivalent (SWE), is a prognostic variable and its parameterization is simplified. This leads to significant errors in albedo estimation, especially during the melting season (Pedersen and Winther, 2005). The SWE dataset which was recently developed as part of the European Space Agency (ESA) GlobSnow project (Takala *et al.*, 2011) can be used as a reliable data input into the SCF models to facilitate evaluation the performance of parameterizations during the last decades.

In this study we present the modelled snow cover fraction in the northern hemisphere (NH), north from 50° N latitude for the years 2000-2011, in the spring season (March-May) and validate these against the snow cover fraction retrieved from satellite data from Moderate Resolution Imaging Spectroradiometer (MODIS) sensors.

## METHODS

The GlobSnow SWE dataset is constructed with an assimilation approach utilizing satellite passive microwave radiometry measurements, in situ snow depth observations and forward model simulations of brightness temperature. A recent study (Hancock *et al.*, 2013) shows that the GlobSnow SWE is superior to pure earth observation products. The GlobSnow SWE has been used in this study as input to five SCF model parameterizations:

1. Joint UK Land Environment Simulator (JULES)
2. Community Land Model (CLM) – two formulations
3. Best Approximation of Surface Exchange (BASE)
4. Simplified Simple Biosphere (SSiB)
5. Max Plank Institute general circulation model (ECHAM-5)

Some of these models are participating into the fifth phase of Coupled Models Intercomparison Project (CMIP5) (Taylor *et al.*, 2012). Several other CMIP5 models will later be included in the study.

For some parameterizations SWE had to be converted to the snow depth. To do so we used the Global Seasonal Snow Classification System (Sturm *et al.*, 1995) that defines for six different snow cover classes, each of which with its own snow density (assumed constant for each class). Five of these snow cover classes were used in this study: tundra, taiga, maritime, prairie and alpine.

MODIS data used in this study was available with spatial resolution of 5 km and temporal resolution of 8 days. To facilitate direct comparison of the datasets, MODIS SCF data fields were reprojected, resampled and aggregated in space to match the GlobSnow 25 km spatial resolution in EASE-grid.

## RESULTS

Preliminary results show that no preferable parameterization can be unambiguously rated as the best (Figure 1).

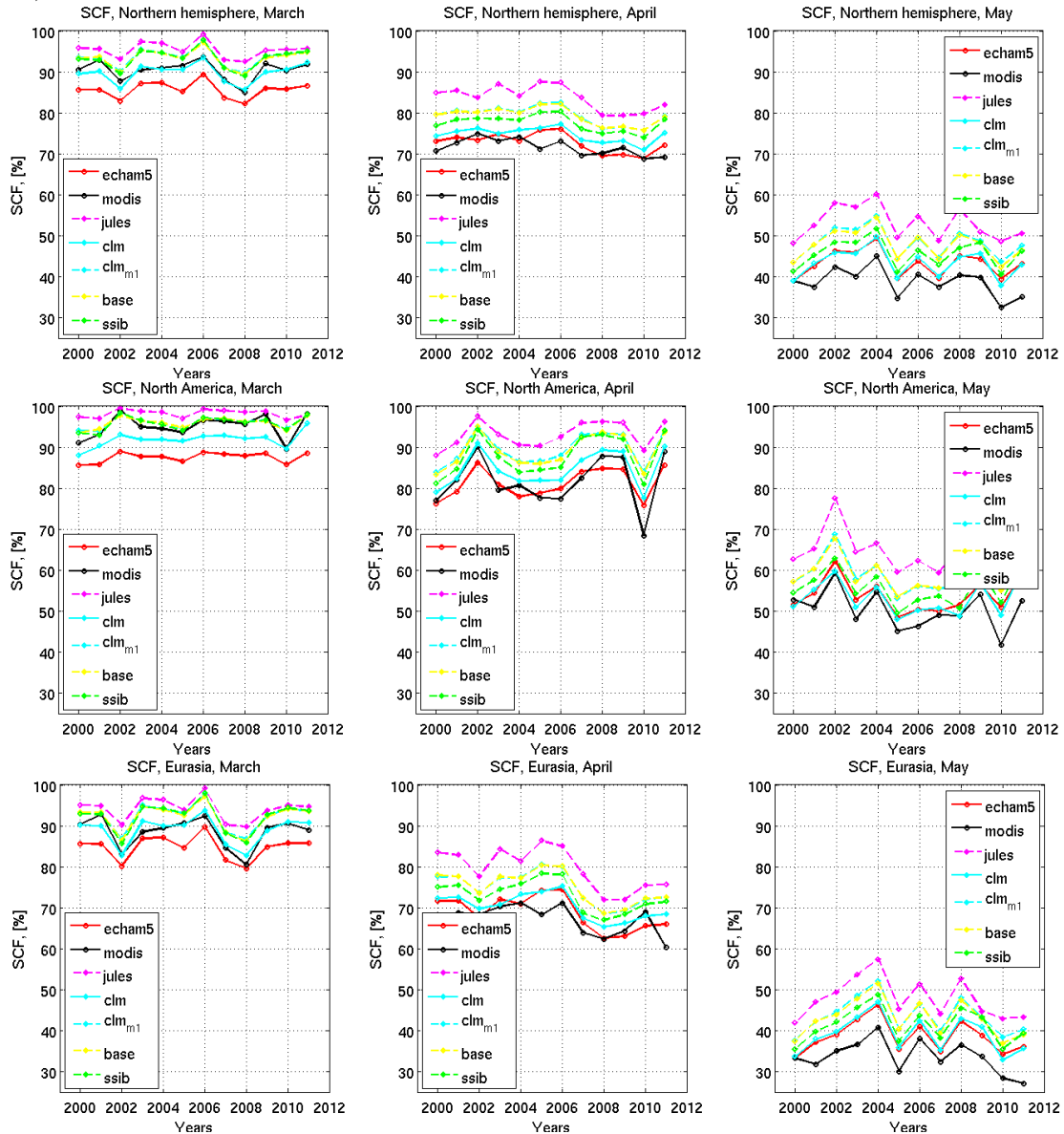


Figure 1. Timeseries of the modelled and MODIS SCF for the NH (upper panel), for North America (middle panel) and for Eurasia (bottom panel), for the years 2000-2011.

CLM performs best of all in March (left panel), ECHAM-5 in April (central panel). In May ECHAM-5 and CLM both show the closest to MODIS SCF, but with bias up to 7 percent (right panel). JULES, BASE and one of CLM schemes significantly overestimate observed SCF in every month, while in general all models show highest overestimation in May. None of the models were able to reproduce the decrease in the SCF in Eurasia in April and May 2011, though all of them follow year-to-year changes well (all panels).

## ACKNOWLEDGEMENTS

This work was supported Academy of Finland Center of Excellence (project number 1118615) and the Nordic Center of Excellence Cryosphere-Atmosphere interaction in a changing Arctic climate (CRAICC).

## REFERENCES

- Hancock, S., Baxter, R., Evans, J., & Huntley, B. (2013). Evaluating global snow water equivalent products for testing land surface models. *Remote Sensing of Environment*, **128**, 107–117.
- Pedersen, C., & Winther, J.-G. (2005). Intercomparison and validation of snow albedo parameterization schemes in climate models. *Climate Dynamics*, **25**(4), 351–362.
- Sturm, M., J. Holmgren and G. E. Liston. (1995). A seasonal snow cover classification system for local to global applications. *Journal of Climate*, **8**(5), 1261–1283.
- Takala, M., Luojus, K., Pulliainen, J., Derksen, C., Lemmetyinen, J., Kaernaes, J., Bojkov, B. (2011). Estimating northern hemisphere snow water equivalent for climate research through assimilation of space-borne radiometer data and ground-based measurements. *Remote Sensing of Environment*, **115**(12), 3517–3529.
- Taylor, K.E., R.J. Stouffer, G.A. Meehl (2012). An Overview of CMIP5 and the experiment design. *Bull. Amer. Meteor. Soc.*, **93**, 485–498.

# A STUDY OF AEROSOL PRODUCTION AT THE CLOUD EDGE WITH DNS

N. BABKOVSKAIA, M. BOY, S. SMOLANDER, S. ROMAkkANIEMI, M. KULMALA

<sup>1</sup> Division of Atmospheric Sciences, Department of Physics, University of Helsinki PO Box 48,  
Erik Palmenin aukio, 1, 00014 University of Helsinki, Finland.

<sup>2</sup>Department of Applied Physics, University of Eastern Finland, P.O.Box 1627, 70211 Kuopio,  
Finland.

Keywords: cloud physics, DNS, aerosol dynamics

## INTRODUCTION

Atmospheric aerosol particles are affecting the Earth's radiative balance both by scattering solar radiation and by acting as cloud condensation nuclei (CCN). CCNs are a subset of all particles that are able to form cloud droplets in specific atmospheric conditions. Cloud is a dynamic system with spatially and temporally varying properties. More cloud droplets may form due to in-cloud activation or due to entrainment of air from the cloud edges that might lead to formation of fresh cloud droplets. On the other hand, cloud droplets may evaporate because of mixing at the cloud boundaries or in-cloud dynamics. The latter of these can be important in stratus type clouds with long in-cloud residence time of the air parcel. The mixing at cloud boundaries takes place in all clouds, and the type of mixing is dependent on the meteorological conditions and mixing time scales. Different phenomena related to aerosol cloud interactions and cloud dynamics involve large range of scales. Microphysics of aerosol-cloud interactions can be studied by process models, or so called box models, which are mainly used to study how and which aerosol particles are able to form cloud droplets. On the other end of scales are global models, which are needed to assess how changes in cloud properties affect the global radiation budget.

We use direct numerical simulation (DNS) to study for example cloud boundaries in the scales from a few centimetres up to a few meters at most. Recently, in order to study the activation process at the cloud edge, the following model was proposed by our research group (Babkovskaia et al., 2012). In this model the gas is compressible; thermal conductivity and diffusion coefficients of every species and of a mixture are described by the accurate expressions (Babkovskaia et al., 2011); thermal flux, change of energy by evaporation/condensation and viscous heating are included in the energy equation, and the solute effect is taken into account. To study the activation of aerosol particles, we take 80 size classes of the cloud droplets with the droplet size logarithmically distributed in a range from 0.08 to 10  $\mu\text{m}$ .

## METHODS

We will use the direct numerical simulation high-order public domain finite-difference PENCIL Code for compressible hydrodynamic flows. The code advances the equations in a non-conservative form. The degree of conservation of mass, momentum and energy can then be used to assess the accuracy of the solution. The code uses six-order centered finite differences. For turbulence calculation we normally use the RK3- 2N scheme for the time advancement. This scheme is of Runge-Kutta type, third order. On a typical processor, the cache memory between the CPU and the RAM is not big enough to hold full three-dimensional data arrays. Therefore, the Pencil Code has been designed to evaluate first all the terms on the right-hand sides of the evolution equations along a one-dimensional subset (pencil) before going to the next pencil. This implies that all derived quantities exist only along pencils. Only in exceptional cases do we allocate full 3-dimensional arrays to keep derived quantities in memory. The code is highly modular and comes with a large selection of physics modules. It is widely documented in the literature and used for many different application (Dobler et al., 2006; <http://pencil-code.googlecode.com> and references therein).

## CONCLUSIONS

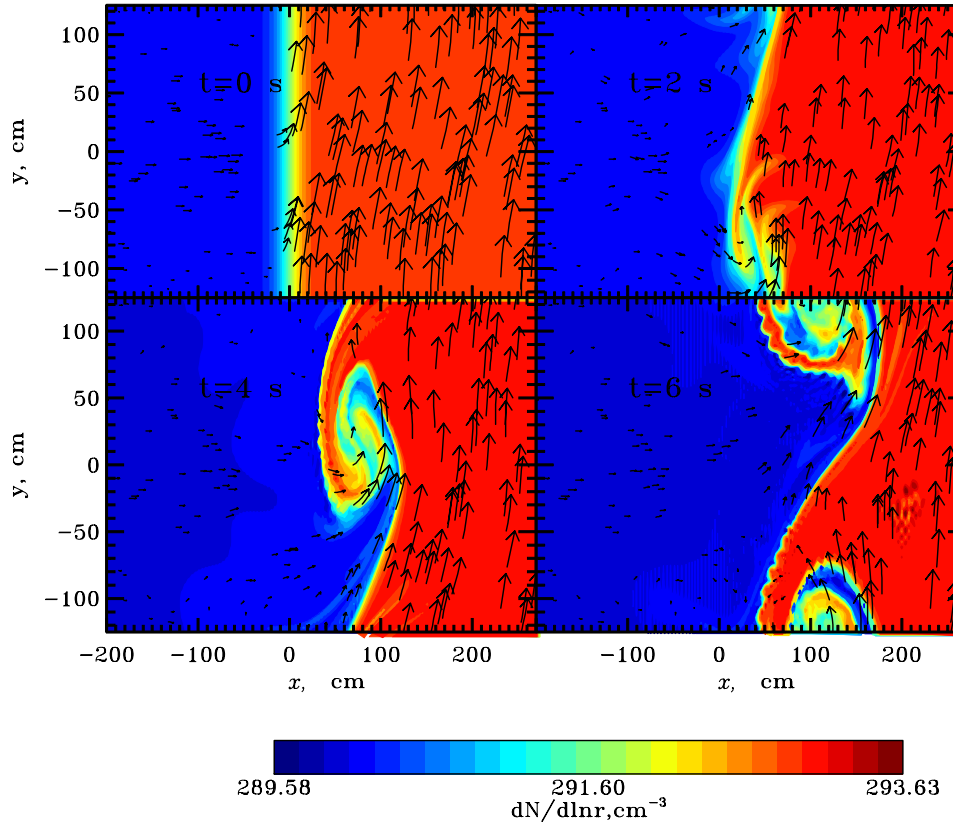


Figure 1. Velocity and temperature fields in the 2D calculated.

We consider a 3D domain of the size of 500 cm x 250 cm x 250cm. The dry and cold air flux comes with velocity of 30 cm/s through the right boundary and interacts with a vertical wind with velocity of 100 cm/s. To study the effect of turbulence on aerosol dynamics we generate the turbulent motion at the beginning of simulations with randomly directed external force, see Fig.1. The estimated Kolmogorov scale is of  $O(1)$  mm. For the model runs with the larger cell size we use the Smagorinski subgrid scale modelling with the parameter for turbulent viscosity  $C_s = 0.15$  (Haugen et al., 2006, Kleissl et al., 2006).

One of the purpose of this paper is to check how crucial is the Smagorinski approximation for calculation of activation/evaporation of aerosol particles. We compare the results of 2D and 3D simulations for 4 cm, for 2 cm cell size, for 1 cm cell size, and for 0.5 cm cell size. We conclude that the results of 2D and 3D simulations differ much smaller than the results of 2D simulations with different cell sizes. We suppose that for studying of particle activation 2D model is appropriate, and therefore, 2D simulations with high resolution give more realistic results than low resolved 3D simulations. It allows ones to save many CPU hours to study the aerosol dynamics and carry out different numerical experiments for more detailed understanding of the cloud edge structure.

Also, we study the effect of aerosol dynamics on the temperature of air. Analyzing simultaneously the temperature distribution and temperature difference, we conclude that activation of particles decreases the air temperature by about 0.03 K, and evaporation of particles increases the temperature by about 0.26 K. Additionally, we study the effect of initially generated turbulence on the air temperature. We see that the turbulent friction increases/decreases the air temperature by about 2.5 K. This is much larger than the effect of aerosol dynamics on the air temperature, and therefore, air dynamics. In turn, since the aerosol evaporation/activation is extremely sensitive to the air temperature, the correct description of the air dynamics appears to be extremely important for the accurate description of aerosol production. At last, we inspect the influence of turbulent motion on aerosol dynamics, and vice versa. We find that aerosol

dynamics increases the supersaturation in the most part of the domain on 16 %, and in some places it is up to 46 %.

## ACKNOWLEDGEMENTS

We thank the Helsinki University Centre for Environment (HENVI), the Academy of Finland (251427, 139656) and computational resources from CSC TAY IT Center for Science Ltd are all gratefully acknowledged. The financial support by the Academy of Finland Centre of Excellence program (project no. 1118615).

## REFERENCES

- Andrejczuk, M., Grabowski, W., Malinowski, S., Smolarkiewicz, P. (2006). Numerical simulations of Cloud-clear air interfacial mixing: Effects on cloud microphysics. *J. of Atmospheric Sciences*, 63, 3204-3225.
- Babkovskaia, N., Haugen, N., Brandenburg, A. (2011). A high-order public domain code for direct numerical simulations of turbulent combustion. *J. of Computational Physics*, 230, 1-12.
- Brenguier, J.-L., W. W. Grabowski, (1993). Cumulus entrainment and cloud droplet spectra: A numerical model within a two-dimensional dynamical framework. *J. Atmos. Sci.*, 50, 120-136.
- Dobler W., Stix M., Brandenburg, A. (2006). Magnetic field generation in fully convective rotating spheres *Astrophys. J.*, 638, 336-343.
- Haugen N. E., Brandenburg, A. (2006). Hydrodynamic and hydro-magnetic energy spectra from large eddy simulations *Phys. Fluids* , 18, 1-7.
- [Pencil Code, 2001] The PENCIL Code, <http://pencil-code.googlecode.com>, (2001).
- Seinfeld, J. H. and Pandis S. N., (2006). *Atmospheric chemistry and physics: From Air pollution to Climate Change*. (John Wiley & Sons, Inc)
- Twomey, S. (1977). The Influence of Pollution on the Shortwave Albedo of Clouds. *J. of Atmospheric Sciences*, 34, 1149-1152.

# NON-STANDARD MEASUREMENT METHOD OF PARTICLE SOOT ABSORPTION PHOTOMETER FOR ABSORPTION ANGSTROM EXPONENTS

J. BACKMAN<sup>1</sup>, A. VIRKKULA<sup>1,2</sup>, V. VAKKARI<sup>2</sup>, J.P. BEUKES<sup>3</sup>, P.G. VAN ZYL<sup>3</sup>, M. JOSIPOVIC<sup>3</sup>, S. PIKETH<sup>3</sup>, P. TIITTA<sup>3,4</sup>, K. CHILOANE<sup>5</sup>, J.J. PIENAAR<sup>3</sup>, A. WIEDENSOHLER<sup>6</sup>, T. TUCH<sup>6</sup>, T. PETÄJÄ<sup>1</sup>, M. KULMALA<sup>1</sup> and L. LAAKSO<sup>2,3</sup>

<sup>1</sup>Department of Physics, University of Helsinki, Helsinki, Finland

<sup>2</sup>Finnish Meteorological Institute, Helsinki, Finland

<sup>3</sup>Environmental Sciences and Management, North-West University, Potchefstroom, Republic of South Africa

<sup>4</sup>University of Eastern Finland, Kuopio, Finland

<sup>5</sup>ESKOM, Sustainability and Innovation, Environmental Sciences Department, South Africa

<sup>6</sup>Leibniz Institute for Tropospheric Research, Leipzig, Germany

Keywords: soot, absorption, measurements, filter-based.

## INTRODUCTION

Aerosols affect the climate in a variety of different ways. Increasing attention has revealed the climatic effects of the absorber of insolation named black carbon (BC). Research suggests BC to be the second most prominent radiative forcer. In brief, BC is considered to be soot carbon that originates from incomplete combustion that absorbs visible light, which is inversely proportional to the wavelength of light ( $\lambda^{-1}$ ). However, particulate organic carbon (OC) is a strong absorber of light in the ultraviolet (UV) region (Kirchstetter and Thatcher, 2012). The spectral dependence of light absorbing OC differs from that of BC. Light absorption by OC in the UV and near-UV tend to be brownish in color; which invoked the term brown carbon (BrC) (e.g. Andreae and Gelencser, 2006).

Atmospheric absorbers will reduce the insolation at the surface. Thus, energy gets vertically redistributed throughout the atmosphere. In polluted regions, with high concentrations of atmospheric BC and BrC, the aerosol layer heats up the air thus reducing the vertical temperature gradient between the surface layer and the air-mass aloft and can inhibit cloud formation. Research suggest BrC to be a significant specie for atmospheric UV absorption and thus mitigate UV photochemistry (Albuquerque *et al.*, 2005).

## METHODS

The filter-based absorption measurements techniques are economical; therefore, widely used for determining particulate atmospheric absorption. Among others, the Particle Soot Absorption Photometer (PSAP) is widely used to retrieve light-absorption coefficients ( $\sigma_{AP}$ ), at three wavelengths. In brief, the deposition of light-absorbing species onto a filter-matrix will reduce the amount of light transmitted through the filter. Light absorption by the particles can then be calculated by measuring the attenuation of light through the filter-matrix. The aerosol accumulates onto the fibre filter which changes how the instrument responds to the sample.

However, there are artefacts associated with the technique; they need to be taken into account using a correction algorithm. The purpose of correction algorithms is to compensate for the change in the radiative transfer of light through a fibre-filter as it gets loaded with aerosol particles. The instrument response to the sample will decrease with the decrease of the filter transmittance. Eventually, the aerosol-laden filter need to be changed to a new one. The interval by which the filter needs to be changed can be increased by diluting the sample. Sample air dilution calls for post-processing of the data acquired at concentrations lower than the detection limit of the instrument, which cannot efficiently be done by standard boxcar

averaging (Springston and Sedlacek, 2007). If such post-processing can be done successfully, the applicability of the multi-wavelength instruments requiring manually-changed filters can be extended to calculate the spectral dependence of the absorbing aerosol. The comparison between a diluted sample for a particle soot absorption photometer (PSAP) and a non-diluted multi angle absorption photometer (MAAP) provides a means of assessing the method.

The data comprise of 23 months of measurements conducted on the Mpumalanga Highveld in South Africa, from February 2009 to January 2011.

## CONCLUSIONS

Figure 1 show that the method is in agreement with the reference method with a slope of 1.17 and a correlation coefficient ( $R^2$ ) of 0.819, with 60 minute averages. The method, however, requires a data post processing for calculating  $\sigma_{AP}$ , described in detail by Virkkula *et al.* (2005).

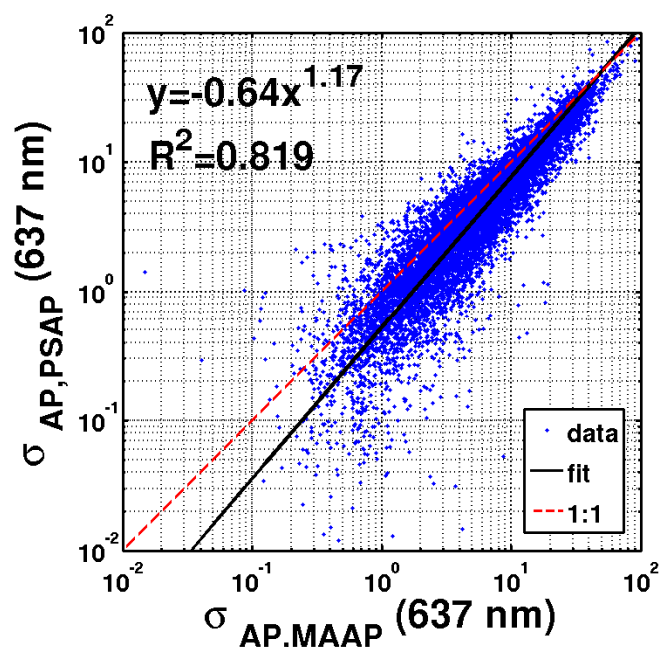


Figure 1. Scatterplot and regression of the light absorption coefficients  $\sigma_{AP}$  measured by the reference instrument (MAAP) and the PSAP,  $\sigma_{AP,MAAP}$  and  $\sigma_{AP,PSAP}$  respectively.

The three wavelength  $\sigma_{AP}$  data could then be used to calculate the spectral dependence of the light absorption, i.e., the Ångström exponent ( $\alpha_{AP}$ ) as  $\ln(\sigma_i(\lambda_i)) = -\alpha \ln(\lambda_i) + C$ . The monthly variations  $\alpha_{AP}$  is shown in Figure 2.

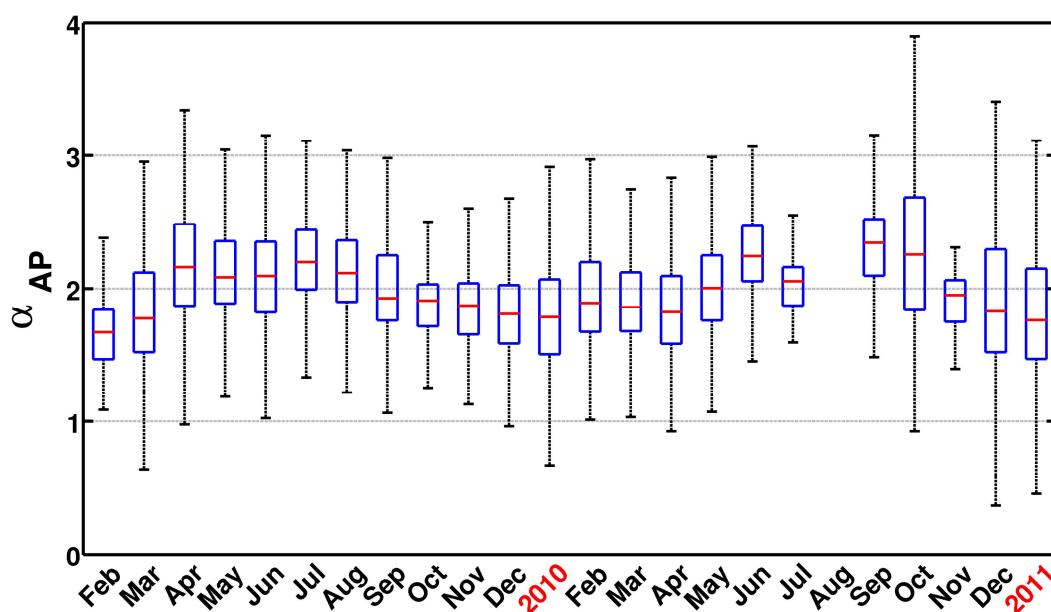


Figure 2. The monthly variations of the light-absorption Ångström exponents ( $\alpha_{AP}$ ). The blue boxes represent the 25th to 75th percentile range whereas the red line represents the monthly median values. The black whiskers represent the statistical edges of the monthly variations.

#### ACKNOWLEDGEMENTS

This research was supported by the Academy of Finland Center of Excellence program (project number 1118615).

#### REFERENCES

- Albuquerque, L.M.M., K.M. Longo, S.R. Freitas, T. Tarasova, A. Plana Fattori, C. Nobre and L.V. Gatti (2005). Sensitivity studies on the photolysis rates calculation in Amazonian atmospheric chemistry – Part I: The impact of the direct radiative effect of biomass burning aerosol particles, *Atmos. Chem. Phys. Discuss.*, **5**, 9325-9353, 10.5194/acpd-5-9325-2005.
- Andreae, M.O. and A. Gelencser (2006). Black carbon or brown carbon? The nature of light-absorbing carbonaceous aerosols, *Atmos. Chem. Phys.*, **6**, 3131-3148, 10.5194/acp-6-3131-2006.
- Kirchstetter, T.W. and T.L. Thatcher (2012). Contribution of organic carbon to wood smoke particulate matter absorption of solar radiation, *Atmos. Chem. Phys. Discuss.*, **12**, 5803-5816, 10.5194/acpd-12-5803-2012.
- Springston, S.R. and A.J.III Sedlacek (2007). Noise characteristics of an instrumental particle absorbance technique, *Aerosol. Sci. Technol.*, **41**, 1110-1116, 10.1080/02786820701777457.
- Virkkula, A., N.C. Ahlquist, D.S. Covert, W.P. Arnott, P.J. Sheridan, P.K. Quinn and D.J. Coffman (2005). Modification, calibration and a field test of an instrument for measuring light absorption by particles, *Aerosol. Sci. Technol.*, **39**, 68-83, 10.1080/027868290901963.

# THE EFFECT OF CLOUDINESS ON NEW PARTICLE FORMATION: INVESTIGATION OF RADIATION LEVELS

E. BARANIZADEH<sup>1</sup>, A. AROLA<sup>2</sup>, A. HAMED<sup>1</sup>, T. NIEMINEN<sup>3</sup>, A. VIRTANEN<sup>1</sup>, M. KULMALA<sup>3</sup> and A. LAAKSONEN<sup>1,4</sup>

<sup>1</sup>Department of Applied Physics, University of Eastern Finland, Kuopio, Finland

<sup>2</sup>Finnish Meteorological Institute, Kuopio Unit, Kuopio, Finland

<sup>3</sup>Department of Physics, University of Helsinki, Helsinki, Finland

<sup>4</sup>Finnish Meteorological Institute, Climate Change Unit, Helsinki, Finland

Keywords: CLOUDINESS, NEW PARTICLE FORMATION, RADIATION, NUCLEATION.

## INTRODUCTION

Atmospheric New particle formation events (NPF), i.e. nucleation and the growth of the newly formed particles have been well documented in many different environments all around the world (Kulmala et al., 2004 and references therein). Boy and Kulmala (2002) suggested that low atmospheric water vapor content, low condensation sink, and high solar radiation, in particular the UV-A component, create favorable circumstances for NPF. They showed that appearance of clouds during the events did sometimes stop the nucleation, and sometimes nucleation continued after the disappearance of clouds. Moreover, they concluded that the radiation level required for the appearance of the smallest detectable 3 nm particles is more than one third of daily maximum radiation and that nucleation stops when the radiation decreases below the same value. Sogacheva et al., (2008) showed that NPF events either turn into less clearer events or even never takes places by cloudiness higher than 4 octas. They also concluded that the frontal cloudiness cuts off the growth of particle and slows down the formation rate of new particles. Pirjola (1999) applied a sectional model (AEROFOR) to find out the impact of UV-B radiation on formation of new particles by a binary nucleation mechanism of H<sub>2</sub>SO<sub>4</sub>-H<sub>2</sub>O. She concluded that the increased UV-B increases the number concentration of newly nucleated particles linearly (e.g. the number concentration of particles becomes 2.5 fold by 50% increase in the UV-B radiation). She also investigated the combined effect of increasing both UV-B levels and the concentrations of biogenic volatile organic compounds (BVOC) and concluded that when the increased BVOC effect is dominant the number concentration of freshly formed particles decreases and vice versa. The importance of solar radiation as a driver of new particle formation has been firmly confirmed in the literature. However, seasonal cloud effects on NPF-events and radiation levels during nucleation have not been systematically investigated. In this research, we study the cloud effects on NPF using a relative radiation intensity parameter as an indicator of cloudiness level.

## METHODS

This research has been carried out for two stations: 1- SMEAR II characterized by boreal coniferous forest, located in Hyytiälä (61° 51' N, 24° 17' E, 181 m asl), Southern Finland. 2- San Pietro Capofiume (SPC) measurement station (44° 39' N, 11° 37' E) located northeast of the city of Bologna, Po Valley, a high population area and the largest industrial, trading and agricultural area in Italy. The particle size distribution measurements in diameter size ranges 3-500 nm and 3-600 nm for Hyytiälä and SPC stations, respectively, are carried out by Differential Mobility Particle Sizer (DMPS) systems. We calculated the relative radiation intensity (hereafter ratio) defined as the ratio of measured global radiation  $I$  (W m<sup>-2</sup>) at a given time divided by the clear-sky global radiation  $I_{\max}$  (W m<sup>-2</sup>) at the same time for all days during 2002-2012. However, we only analyzed the ratio  $I/I_{\max}$  for the duration between nucleation start and end times (i.e. the times when 3nm particle production starts and ends, respectively -hereafter 3nm-time-window) for NPF event days, and from one hour after sunrise until noon for Non-events and undefined days. The 3nm-time-window was defined visually from the so called banana plots. The global radiation ( $I$ ) was measured

at the SMEAR II station in half-hour average time resolution during 2002-2012. Radiation data collected from SPC station are hourly average data from the period March 2002- April 2005. The  $I_{\max}$  data are modelled clear sky data downloaded from the AERONET website (<http://aeronet.gsfc.nasa.gov/>) for both sites. Note that this data was not available for SPC station. However, since there was no significant difference in  $I_{\max}$  data between close sites regarding the fact that aerosol and cloud effects are left out, we used Modena (44°39'N, 10°56'E) data located on the south side of the Po Valley. The SPC  $I_{\max}$  data were converted to hourly averages to be consistent with the time resolution of actual global radiation data. We classified the NPF event days as “quantifiable” and “non-quantifiable” according the criterion introduced by Dal Maso et al (2005) which is whether or not the event is homogeneous enough to quantify the basic characteristics such as formation rate and growth rate. We left out the days where the DMPS instrument had broken resulting in days from which the aerosol size distribution data was either completely missing or corrupted. Therefore, our data pool consists of event (E), non-event (NE) and undefined days, the latter being days during which the evolution of the size distribution is too unclear for definitive determination of whether or not NPF has been occurring. Due to missing measurement radiation data especially in SPC station the ratio  $I/I_{\max}$  data is not computable for all days. Figure 1 shows the seasonal number of E, NE and undefined days of this study for which the ratio  $I/I_{\max}$  data is available.

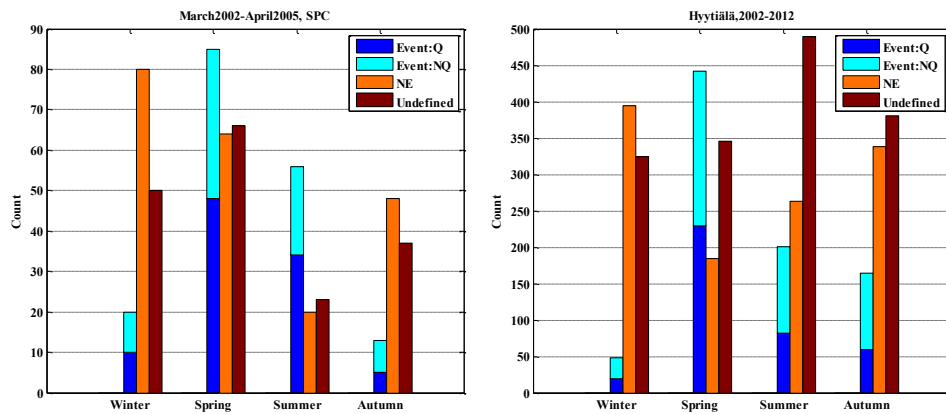


Figure. 1. Seasonal number of events including Quantifiable Events (Q) and Non-Quantifiable events (NQ), Non-Events (NE) and undefined days in seasons winter (Dec-Jan-Feb), spring (Mar-Apr-May), summer (Jun-Jul-Aug) and autumn (Sep-Oct-Nov), recorded in (right) Hyytiälä during period 2002-2012 and (left) SPC during March 2002-April 2005.

## CONCLUSIONS

The ratio  $I/I_{\max}$  values have been averaged (average ratio) over the 3nm- and NE-time-windows for each single E and NE day, respectively. The average ratio values are between 0-1, as it is expected. We defined 20 average ratio ranges with the width interval and the spacing set to 0.05 (x- axis of Figure 2). Then we calculated the fraction (%) of days (out of E+NE + undefined) which are event (hereafter we call it  $\Delta_E$ ) or non-event (hereafter we call it  $\Delta_{NE}$ ) in the each given ratio range (y-axis of Figure 2). General speaking, the higher (lower) the average  $I/I_{\max}$  ranges, the higher (lower)  $\Delta_E$  ( $\Delta_{NE}$ ) values. For example, values of  $\Delta_E$  for Hyytiälä are 53%, 70% and 71% while the values of  $\Delta_{NE}$  are 13%, 6% and 7% in the average ratio ranges of 0.85-0.9, 0.9-0.95 and 0.95-1, respectively. The corresponding percentages for SPC are 25%, 42% and 60% for  $\Delta_E$  values and 30%, 24% and 17% for  $\Delta_{NE}$  values, respectively. The  $\Delta_E$  values in the average ratio ranges lower than 0.95 is much less than Hyytiälä, indicating that occurrence of a NPF-event in SPC is highly likely only at close to clear sky conditions. On the other hand, Figure 2 shows that  $\Delta_E$  values in the low ratio ranges (i.e. indicating the presence of cloud) in Hyytiälä is higher than SPC. For example values of  $\Delta_E$  in the ranges 0.4-0.45, 0.45-0.5 and 0.55-0.6 are 11, 14 and 18% in Hyytiälä and 4, 3 and 5% in SPC, respectively. The corresponding percentages for  $\Delta_{NE}$  values are 45, 39 and 31 in Hyytiälä

and 53, 54 and 51% in SPC. Note that the sum of  $\Delta_E$ ,  $\Delta_{NE}$  and  $\Delta_{Undefined}$  in each average ratio  $I/I_{max}$  range is 100 % in Figure 2.

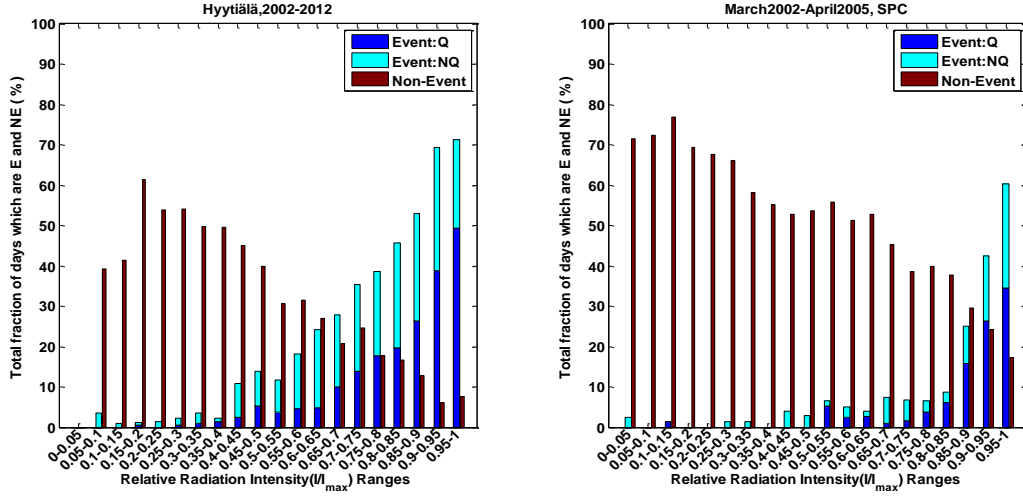


Figure 2. Total fraction (%) of days which are Event ( $\Delta_E$ ) and Non-event ( $\Delta_{NE}$ ) in each given average ratio (i.e. ratio values over are averaged over defined time-windows for each single E and NE)  $I/I_{max}$  range in (Left) Hyytiälä during period 2002-2012 and (Right) SPC during March 2002-April 2005. Note that the remained fraction in each given ratio range is related to undefined days. Q=Quantifiable event, NQ=non-Quantifiable event.

To investigate the seasonal cloudiness effect on E, the same fractions (%) as Figure 2 including  $\Delta_E$ ,  $\Delta_{NE}$  and  $\Delta_{Undefined}$  has been extracted but for different seasons separately (see Figure 3). This has been done only for Hyytiälä because the seasonal number of days in SPC is not statistically reliable due to missing ratio data. The  $\Delta_E$  values in the average  $I/I_{max}$  range 0.95-1 is 26%, 92%, 57% and 57% in winter, spring, summer and autumn respectively. The corresponding percentages for  $\Delta_{NE}$  are 26%, 1%, 13% and 0%, respectively. This means that occurrence of E at clear sky conditions is much more probable in spring than other seasons. The same holds for the statistics in the other high  $I/I_{max}$  ranges 0.75-0.95 and 0.7-0.9. Interestingly,  $\Delta_E$  statistics in the ranges with interval widths 0.05 limited to 0.5-0.9, in the autumn is much higher than the summer. Note that previous studies (Dal Maso et al., 2005; Kulmala et al., 2004) have found a summer minimum and secondary autumn maximum for Hyytiälä seasonal event frequency but as seen from the Figure 1 this is not the case here. For example, the values of  $\Delta_E$  are 24%, 23% and 33% in summer and 44%, 58% and 56% in autumn in ranges 0.7-0.75, 0.75-0.8 and 0.8-0.85, respectively. Generally speaking, an increasing trend of  $\Delta_E$  values with increasing ratio ranges is observed in all seasons. However, the  $\Delta_E$  values have almost plateaued in the ranges with the intervals widths 0.05 limited to [0.65-0.8] in summer (201 E days), in contrast to spring (442 E days) and autumn (164 E days) where an increasing trend for mentioned quantity is observed. A few event days in low  $I/I_{max}$  ranges (i.e. presence of during the 3nm-time-window) in all seasons (e.g. in the range 0.05-0.2: 22-Feb-2008, 20-Apr-2012, 21-Jul-2011, 09-Sep-2010) is seen which are mostly weak events. In addition, some fraction of days with maximum values in winter is NE ( $\Delta_{NE}$ ) in the high  $I/I_{max}$  ranges. Such days (i.e. events (non-events) with low (high)  $I/I_{max}$ ) will be considered as anomalous days and will be investigated in later sections by looking into other variables which affect NPF event.

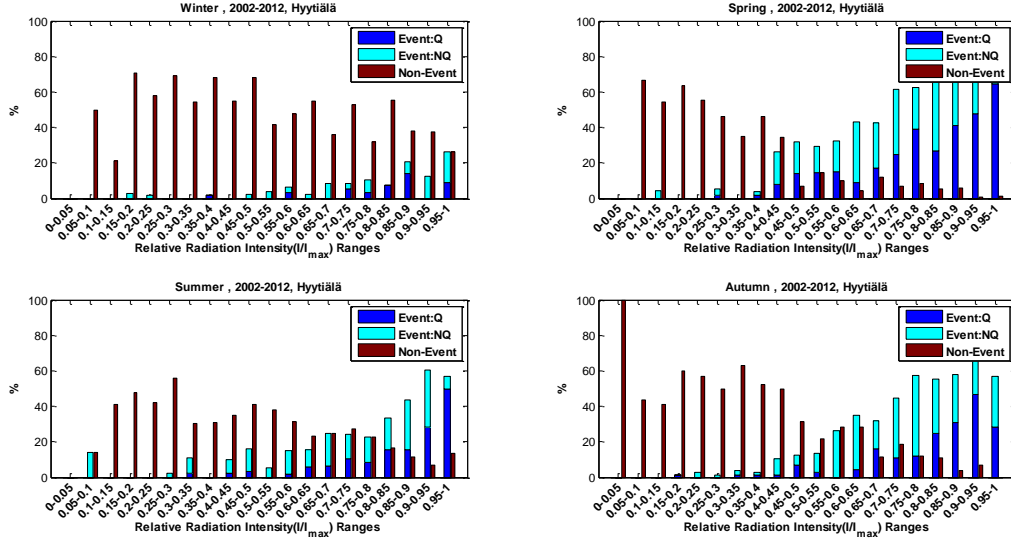


Figure 3. The same as the Figure 2 but for different seasons separately.

We have also investigated the values of relative radiation intensity  $I/I_{\max}$  in the start and end of 3nm-time-window of the NPF events (see Figure 4). The total number of events for which the ratio  $I/I_{\max}$  data is available, is 855 and 174 (see Fig. 1) in Hyytiälä and SPC, respectively. Figure 4 shows that, overall, 35% and only 17% of Es have been started in the  $I/I_{\max}$  values below 0.8 in Hyytiälä and SPC, respectively (top panels-Figure 4). Specifically, about 9% (40%) and 7% (56%) of events in Hyytiälä and SPC, respectively, have started in  $I/I_{\max}$  values below 0.5 (above 0.9). Note that the Figure 4 has been extracted using only the start and end data points of events separately. Mentioned statistics reveals that starting the nucleation event under cloudy sky condition in Hyytiälä is more probable than SPC. Interestingly, fraction statistics related to end time of Es has almost the same trend as start time statistics (bottom panels-Figure 4). For example, 9% (28%) of Es in Hyytiälä and 10 % (53%) of Es in SPC have been stopped (bottom plots in the Figure 4) in the  $I/I_{\max}$  values below 0.5 (higher than 0.9). According to the mentioned statistics stopping the nucleation by cloudiness is much more probable in Hyytiälä than SPC.

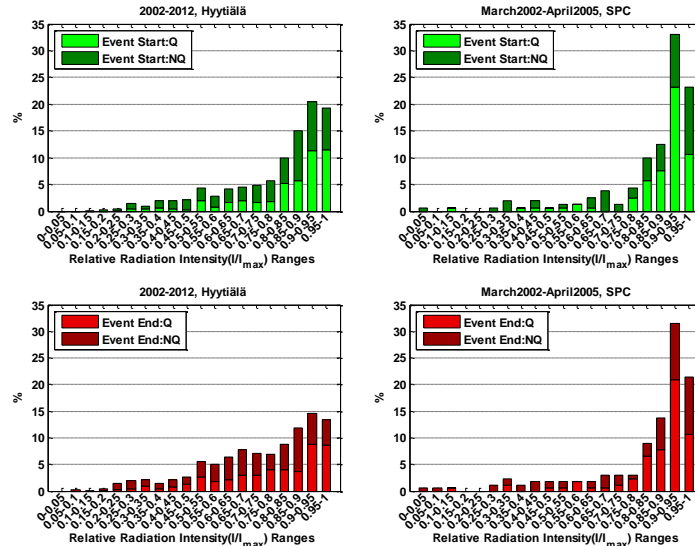


Figure 4. Fraction (%) of events in different given ratio  $I/I_{\max}$  ranges corresponding to the value of ratio  $I/I_{\max}$  in the start (dark and light green colors) and end (dark and light red colors) of 3nm-time-window in (left panels) Hyytiälä during period 2002-2012 and (right panels) SPC during March 2002-April 2005. Q=Quantifiable event, NQ=Non-Quantifiable event.

NPF event (NE) days in which sky is cloudy (clear) during the whole or a substantial part (i.e. at least one hour) of the 3nm-time-window (time window of one hour after sunrise till noon) have been considered as anomalous days. Values of  $I/I_{\max} < 0.5$  and  $I/I_{\max} > 0.8$  have been assumed as cloudy and clear sky hours, respectively. We found about 126 and 26 event days in Hyytiälä and SPC, respectively, having the described condition (Table 1). We have looked into the auxiliary parameters including Condensation Sink (CS), Relative Humidity (RH %),  $\text{SO}_2$  (ppb),  $\text{O}_3$  (ppb),  $\text{NO}_2$  (ppb) and  $\text{H}_2\text{O}$  (ppth) to get insight into atmospheric conditions which could favour NPF despite the cloudiness. Results show that low condensation sink and high level of  $\text{SO}_2$  are the most important parameters which favor the nucleation despite the cloudiness. We observed that, in many nucleation events  $\text{SO}_2$  (source) and CS (sink) values compensate the unfavorable change of each other during cloudy hours and favored the nucleation. Moreover, we found that Es in which sky is cloudy for the duration of nucleation start and times are mostly weak events with very low concentration of ultrafine particles. Also, in some of Es appearance of cloud within 3nm-time-window interrupts or decreases dramatically the production of 3nm particles and start to reproduce after sky clears. Therefore, cloudiness can decrease the clarity of an E and converts it to non-quantifiable class. This is in agreement with Sogacheva et al., (2008) who concluded that cloudiness causes an NPF event to become type Ia or II (i.e. non-quantifiable) instead of Ia (i.e. quantifiable). There are some NE days in clear sky condition (i.e. high  $I/I_{\max}$  values). Investigation of such NEs reveals that, very high CS values in both sites with average values  $5.3 \times 10^{-3} \text{ s}^{-1}$  and  $19.2 \times 10^{-3} \text{ s}^{-1}$  in Hyytiälä and SPC, respectively, has prevented the occurrence of nucleation event. In addition, high amounts of  $\text{H}_2\text{O}$  in Hyytiälä and high  $\text{NO}_2$  values in SPC explain the non-occurrence of nucleation event under clear sky condition.

#### ACKNOWLEDGEMENTS

This work was funded by Cryosphere-atmosphere interactions in a changing Arctic climate project (CRAICC).

#### REFERENCES

- Kulmala, M., Vehkamäki, H., Petäjä, T., Dal Maso, M., Lauri, A., Kerminen, V.-M., Birmili, W., and McMurry, P. (2004). Formation and growth rates of ultrafine atmospheric particles: a review of observations, *J. Aerosol Sci.*, 35, 143–176.
- Boy, M., & Kulmala, M. (2002). Nucleation events in the continental boundary layer: Influence of physical and meteorological parameters. *Atmospheric Chemistry and Physics*, 2(1), 1-16.
- Dal Maso, M. , Kulmala, M. , Riipinen, I. , Wagner, R. , Hussein, T. , Aalto, P. P. & Lehtinen, K. E. J. (2005). Formation and growth of fresh atmospheric aerosols: eight years of aerosol size distribution data from SMEAR II, Hyytiälä, Finland, *Boreal Environment Research*. 10, 5, p. 323-336. 14 p.
- Pirjola, L. (1999). Effects of the increased UV radiation and biogenic VOC emissions on ultrafine sulphate aerosol formation, *J. Aerosol Sci.*, 30, 355–367.
- Sogacheva, L., Saukkonen, L., Nilsson, E. D., Dal Maso, M., Schultz, D. M., De Leeuw, G., and Kulmala, M. (2008) New aerosol particle formation in different synoptic situations at Hyytiälä, Southern Finland, *Tellus*, 60(4), 485–494.

# EFFECTS OF ORGANIC COATINGS ON THE REACTIVITY OF AEROSOL PARTICLES

A.M. BATENBURG<sup>1</sup>, C. GASTON<sup>2</sup>, J.A. THORNTON<sup>2</sup> and A. VIRTANEN<sup>1</sup>

<sup>1</sup>Aerosol Physics Group, Department of Applied Physics, University of Eastern Finland, Kuopio, Finland.

<sup>2</sup>Department of Atmospheric Sciences, University of Washington, Seattle, USA.

Keywords: heterogeneous reactions, aerosol aging, flow tube experiments, organics.

## INTRODUCTION

Heterogeneous reactions on aerosol particles play a significant role in the cycles of various atmospheric trace gases, most famously in the stratosphere, but also in the troposphere (Ravishankara, 1997). On the other hand, heterogeneous reactions can change the properties of the aerosol particles (Jimenez et al., 2009). An important (but not the only) property that “chemical aging” by atmospheric oxidation can change is the hygroscopicity of the particles, which in turn alters their optical and cloud forming properties with important implications for the climate.

A large part of the total global aerosol matter is composed of organic compounds. These can adopt liquid or amorphous (semi)solid physical phase states (Virtanen *et al.*, 2010). According to the Stokes-Einstein equation, the diffusivity of gas molecules into the aerosol particles is inversely proportional to the viscosity of the aerosol material, which varies over many orders of magnitude between liquid and solid states. Shiraiwa *et al.* (2011) and Zhou *et al.* (2012) showed that heterogeneous reactions with ozone (O<sub>3</sub>) can be limited by bulk diffusion in semisolid or solid material, extending the lifetime of the organics. It is highly likely that the uptake of water is similarly limited. Conversely, since water can act as a “plasticizer” and decrease the viscosity of the organic material, the magnitude of the decrease in gas-particle interactions due to diffusion limitations may depend on the surrounding humidity.

An additional complication is that organic coatings alter how the surface of the particles interacts with gas molecules. A monolayer of organic surfactant can already decrease the reactivity with N<sub>2</sub>O<sub>5</sub> three- to fourfold (Thornton and Abbatt, 2005).

The goal of this project is to better understand and quantify how the viscosity and phase state of organic aerosol matter affect gas-particle interactions. As a model system to work with, we have chosen the reaction of O<sub>3</sub> with particles composed of a potassium iodide (KI) core and an organic coating of varying thickness and composition. While primarily chosen for its convenient experimental properties, this system is not without relevance of its own. Iodide is naturally present in marine aerosol, and plays a role in ozone destruction in the marine boundary layer (Rouvière *et al.*, 2010).

## METHODS

In this project, the reactions of interest are studied in an aerosol flow reactor. An aerosol flow reactor usually consists of a vertical flow tube with dimensions chosen to ensure laminar flow over the largest part of its length, and a movable, axial injector for the injection of the reactive gas under study. The air containing the aerosol is inserted at the top of the tube. By moving the injector, the interaction length, and therefore the interaction time, between the particles and the reactive gas can be varied. Alternatively, the production of aerosol particles can be switched on and off. The remaining concentration of the reactive gas is monitored from the bottom of the tube. If the loss of reactive gas X is described as a first-order process, as

$$\frac{d[X]}{dt} = -k[X]$$

the reaction rate  $k$  can be determined from the measurements, which is related to the reactive uptake coefficient  $\gamma$  as

$$k = \frac{S\omega\gamma}{4}$$

with  $S$  the aerosol surface area per volume of gas, and  $\omega$  the mean molecular velocity of the reactive gas.

The aerosol flow reactor system that will be used in Kuopio is not built yet, but exploratory experiments with KI particles coated with polyethylene glycol (PEG) have been performed at the University of Washington (UW). A schematic of the setup used there is shown in Figure 1. The flow tube used was a 90 cm long pyrex glass tube with an inner diameter of 6 cm, coated with halocarbon wax. The  $O_3$  was injected through 1/8" PTFE tubing within an axial stainless steel injection rod of which the position could be varied. The upper and lower 20 cm of the tube were not used for injection to avoid effects of non-laminar flow conditions.

Aerosol particles were generated in an atomizer filled with solutions with varying concentrations of KI and PEG. The particle flow was then diluted with a flow of nitrogen or zero air with controlled humidity and inserted at the top of the flow tube. Excess flow was vented before that, so the flow tube operated under atmospheric pressure.

$O_3$  and particle concentrations were monitored with an  $O_3$  monitor and an SMPS system at the lower end of the flow tube. Together, these instruments pulled a flow of 2,6 L/min through the tube. Most of the experiments performed were particle modulation experiments with the injector at 60 cm height, leading to an estimated particle/ $O_3$  interaction time of 47 s. A TeFlo filter had to be inserted before the  $O_3$  monitor to prevent the particles from interfering with the optical  $O_3$  detection method. It proved necessary to also insert a nafion dryer before this filter to effloresce the KI particles and keep them from reacting with  $O_3$  on the filter. This method worked well for uncoated KI particles, but large  $O_3$  losses were observed on the filter after PEG-coated particles were used. Other particle separation methods are currently being investigated.

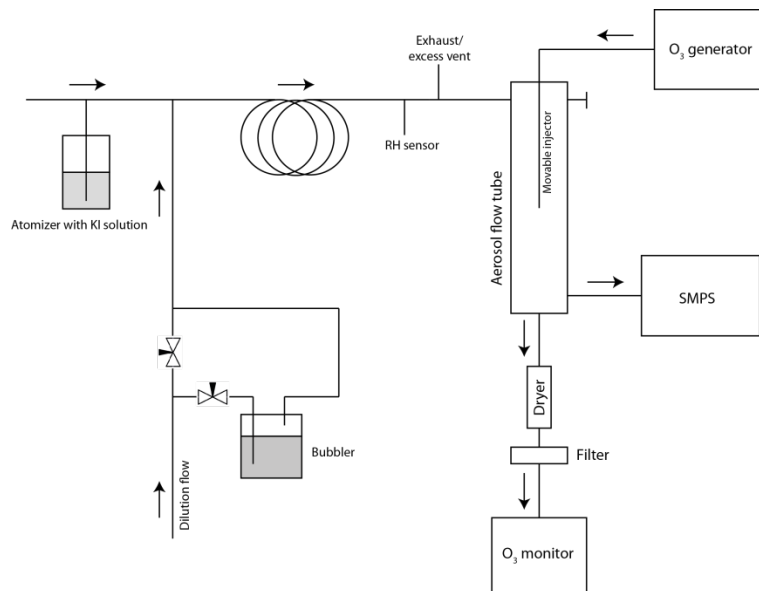


Figure 1. Schematic of the setup used for exploratory experiments at the University of Washington

## RESULTS/PROJECT STATUS

The large O<sub>3</sub> losses on the TeFlo filter limited the precision of the  $\gamma$ -determinations with PEG-coated particles at UW. Nevertheless, it was observed that already a thin ( $\approx 5$  nm) coating sufficed to significantly reduce the observed  $\gamma$  with respect to the  $1.1 \times 10^{-2}$  that was determined by Rouvière *et al.* (2010) for uncoated deliquesced KI particles.

We will build an improved setup in the Aerosol Physics lab in Kuopio this autumn and conduct follow-up experiments.

## ACKNOWLEDGEMENTS

This work was supported by the Academy of Finland Center of Excellence (project no 1118615) and the Nordic Center of Excellence CRAICC.

## REFERENCES

- Jimenez, J. L., Canagaratna, M. R., Donahue, N. M., Prevot, A. S. H., Zhang, Q., Kroll, J. H., ... (2009), Evolution of Organic Aerosols in the Atmosphere, *Science*, 326:1525-1529
- Ravishankara, A. R. (1997), Heterogeneous and Multiphase Chemistry in the Troposphere, *Science*, 276:1058-1065
- Rouvière, A., Sosedova, Y. and Ammann, M. (2010), Uptake of Ozone to Deliquesced KI and Mixed KI/NaCl Aerosol Particles, *J. Phys. Chem.*, 114:7085-7093
- Shiraiwa, M., Ammann, M., Koop, T. and Pöschl, U. (2011), Gas uptake and chemical aging of semisolid organic aerosol particles, *PNAS*, 108:11003-11008
- Thornton, J.A. and Abbatt, J.P.D. (2005), N<sub>2</sub>O<sub>5</sub> Reaction on Submicron Sea Salt Aerosol: Kinetics, Products, and the Effect of Surface Active Organics, *J. Phys. Chem.*, 109: 10004-10012
- Virtanen, A., Joutsensaari, J., Koop, T., Kannosto, J., Yli-Pirilä, P., Leskinen, J., ... (2010), An amorphous solid state of biogenic organic aerosol particles, *Nature*, 467:824-827
- Zhou, S., Lee, A. K. Y., McWhinney, R. D. and Abbatt, J. P. D. (2012), Burial Effects of Organic Coatings on the Heterogeneous Reactivity of Particle-Borne Benzo[a]pyrene (BaP) toward Ozone, *J. Phys. Chem.*, 116:7050-7056

## GROUND-BASED OBSERVATIONS OF AEROSOL AND CLOUD PROPERTIES AT SUB-ARCTIC PALLAS GAW-STATION, PALLAS CLOUD EXPERIMENT (PACE 2012)

D. BRUS, E. ASMI, T. RAATIKAINEN, K. NEITOLA, M. AURELA, U. MAKKONEN,  
J. SVENSSON, A.-P. HYVÄRINEN, A. HIRSIKKO, H. HAKOLA, R. HILLAMO, AND  
H. LIHAVAINEN

Finnish Meteorological Institute, Erik Palménin aukio 1, P.O.Box 503, FI-00101, Helsinki, Finland

Keywords: aerosol, cloud droplets, hygroscopicity, black carbon, CCNC, HTDMA, ACSM, MARGA

### INTRODUCTION

Clouds constitute perhaps the largest source of uncertainty in predicting the behaviour of the Earth's climate system. Vulnerable Arctic region is slowly heading towards a new climatic state with substantially decreased permanent ice cover. However, due to poorly understood feedback mechanisms, the rate of Arctic climate response to changes is very hard to predict with current global models. Arctic clouds are supposed to have central role in these feedback processes (Vavrus, 2004). Many of the climatically important cloud properties, including the reflectivity, lifetime and precipitation patterns of clouds, depend strongly on atmospheric aerosol particle properties, like chemical composition or number concentration. The essential cloud microphysical parameters in studying aerosol-cloud-climate interactions are the total number concentration and effective radius of cloud droplets, cloud liquid water content and the relative dispersion of a cloud droplet population (Komppula *et al.*, 2005; Lihavainen *et al.*, 2008).

### METHODS AND RESULTS

The 4<sup>th</sup> Pallas cloud experiment was carried out six weeks, between September 17<sup>th</sup> and October 30<sup>th</sup> 2012, at Finnish Meteorological Institute's Pallas-Sodankylä Global Atmosphere Watch (GAW) station in northern Finland (Hatakka *et al.*, 2003). The measuring site - Sammaltunturi station (67°58'N, 24°07'E) - resides on a top of the second southernmost fjeld, a round topped treeless hill, in a 50-km-long north and south chain of fjelds at an elevation of 565 m a.s.l. Sammaltunturi station is, due to topography of the surrounding terrain, a great place for ground-based observations of orographic clouds. Thus providing an opportunity to investigate not only the cloud droplet activation of aerosol particles but also directly the cloud particle phase (Komppula *et al.*, 2005; Antila *et al.*, 2009; Kivekas *et al.*, 2009; Antila *et al.*, 2012).

In autumn, probability the station to be inside cloud is high. During the campaign the station was inside cloud (visibility below 1000 m) 50 % of time. The maximum and minimum temperatures were between 8 and -13 °C during the campaign. The temperature was below 0 °C during half of time. The winds were mostly western and north-eastern with average wind speed of 6.5 m/s (1 m/s to 15.4 m/s). The ambient RH was measured with Vaisala HUMICAP sensor, and visibility and temperature were measured with Vaisala FD12P weather sensor.

Particle hygroscopicity was measured with a HTDMA (Hygroscopicity Tandem Differential Mobility Analyzer). The HTDMA is constructed to meet the EUSAAR standards for continuous measurements of the aerosol hygroscopicity at a fixed RH. The proper operation of the HTDMA is verified with dry calibrations (by-passing the humidifier) and with ammonium sulfate on regular basis. The Cloud Condensation Nuclei Counter (CCNC, DMT model CCN-100) connected to total air inlet was operated at a total flow rate of 0.5 l/min and at five different supersaturations (0.1, 0.15, 0.2, 0.6 and 1.0 %), each set for 10 min. The CCNC was switching between total and size resolved CCN every hour. Time series of CN and CCN concentrations together with values of corresponding kappa ( $\kappa$ ) and growth factor ( $GF$ ) properties measured during the PaCE 2012 campaign are presented in Fig. 1.

Two differential mobility particle sizers (DMPS) were used to measure the aerosol number size distribution. One DMPS was attached to a total air inlet, which lets in all particles including cloud droplets. After drying cloud droplets, dry cloud condensing nuclei were measured among the non-activated particles. The other DMPS was attached to a PM 2.5  $\mu\text{m}$  inlet which prevented the cloud droplets from entering the system and hence the DMPS measured only the non-activated particles. Each of the DMPS instruments measured the dry diameter range 7–500 nm in 30 discrete size fractions. The whole size range was scanned in approximately five minutes by each DMPS (Komppula *et al.*, 2005). Regarding the experimental uncertainties, it should be noted that the DMPS system is operated according to the GAW standards (Hatakka *et al.*, 2003) and the DMPS measurements are continuously verified against a reference instrument. Two condensation particle counters were used to measure total particle number concentration, CPC (Airmodus A20) connected to total air, and CPC (TSI 3010) connected to PM 2.5  $\mu\text{m}$  inlet.

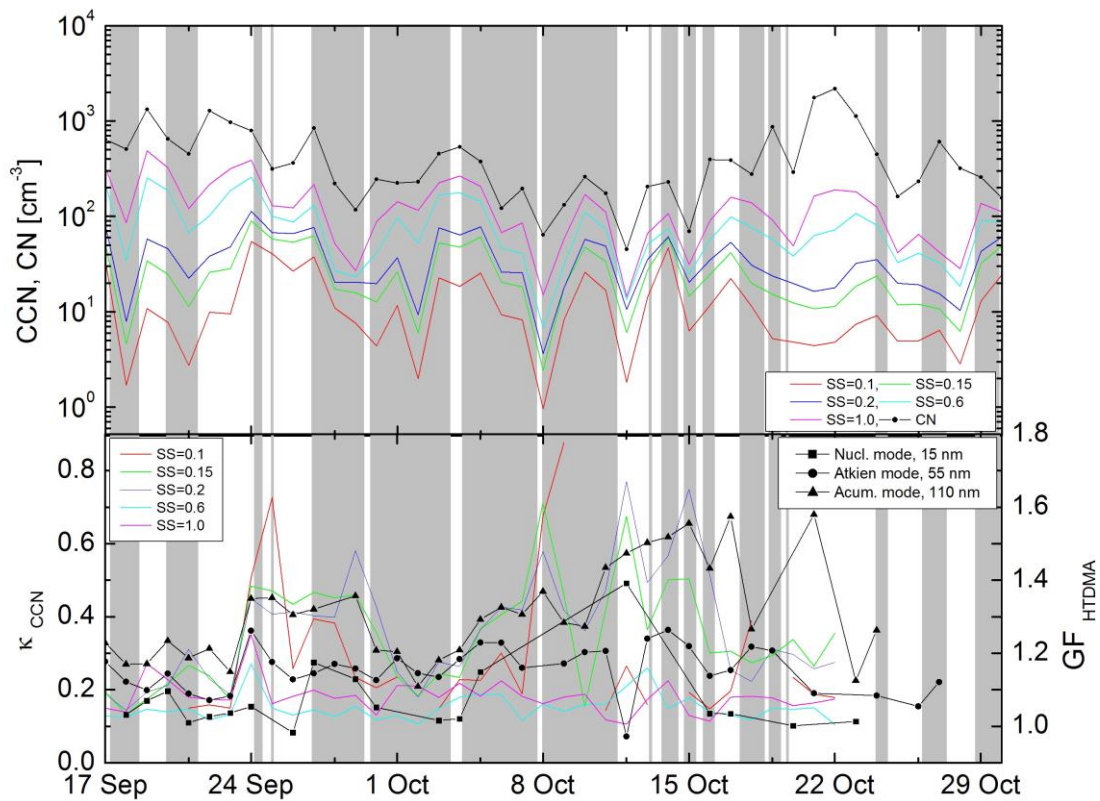


Figure 1. Total CN and CCN concentrations at five supersaturation levels 0.1, 0.2, 0.3 0.6 and 1.0 (upper panel) together with  $\kappa$  and GF values obtained with CCNC and HTDMA respectively (lower panel). Grey areas represent cloud events determined from visibility measurements

Cloud droplet number size distributions (3–47  $\mu\text{m}$ ) were measured with a Forward Scattering Spectrometer Probe (FSSP, Particle Measuring Systems Inc, USA, model SPP-100) with upgraded electronics (DMT). The FSSP was placed onto a rotating platform, so that the inlet was always against the wind with average airspeed of approximately 12 m/s. The Cloud, Aerosol and Precipitation Spectrometer (CAPS, DMT) which includes three instruments: the Cloud Imaging Probe (CIP, 12.5  $\mu\text{m}$ –1.55 mm), the Cloud and Aerosol Spectrometer (CAS-DPOL, 0.51–50  $\mu\text{m}$ ) with depolarization feature, and the Hotwire Liquid Water Content Sensor (Hotwire LWC, 0–3  $\text{g m}^{-3}$ ). The CAPS probe was equipped with tailored inhalator to make it suitable for ground-based measurements. The average airspeed in the system was approximately 30 m/s. The growth dynamics of the nano-size aerosol measured with DMPS to cloud particles ( $\sim 1$  mm) measured with CAPS probe can be seen in Fig. 2.

Absorption of aerosol particles was measured from total air inlet with the Aethalometer (model AE 31, Magee Scientific) and the Single Particle Soot Photometer (SP2, DMT) which directly measures also mixing state. The Multi-Angle Absorption Photometer (MAAP, Thermo Scientific) was connected to PM 2.5  $\mu\text{m}$  inlet. Scattering of aerosol particles was measured only from PM 2.5  $\mu\text{m}$  inlet with integrating Nephelometer (model 3563, TSI).

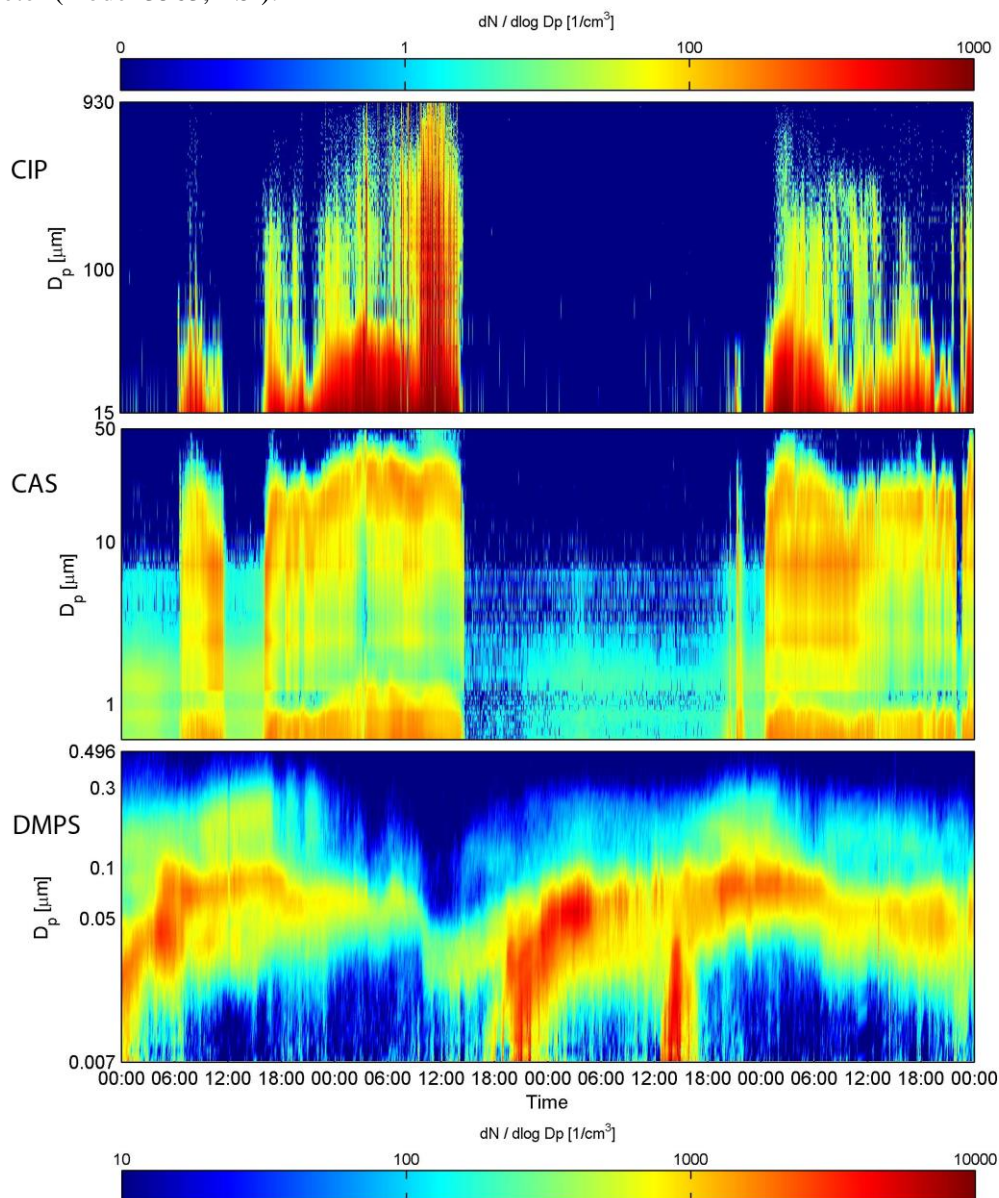


Figure 2. Aerosol dynamics from new particle formation to cloud droplet activation and rain drops (from lower to upper panel). Three instruments (DMPS, CAS-DPOL and CIP) cover together size distribution from 7 nm to 0.93 mm.

Mass and chemical composition of non-refractory submicron particulate matter was characterized with Aerosol Chemical Speciation Monitor (ACSM, Aerodyne) in real time. Under ambient conditions, mass concentrations of particulate organics, sulfate, nitrate, ammonium, and chloride are obtained with a detection limit  $<0.2 \mu\text{g}/\text{m}^3$  within 60 minute averaging time (Ng *et al.*, 2011). In subarctic background environment, where mass concentrations are low, hourly signal averaging was justified. An online ion chromatograph for Measuring AeRosols and Gases (MARGA 2S ADI 2080, Metrohm Applikon Analytical BV) that is able to detect 5 gases from the gas phase ( $\text{HCl}$ ,  $\text{HNO}_3$ ,  $\text{HONO}$ ,  $\text{NH}_3$ ,  $\text{SO}_2$ ) and 8 major inorganic species from aerosol phase ( $\text{Cl}^-$ ,  $\text{NO}_3^-$ ,  $\text{SO}_4^{2-}$ ,  $\text{NH}_4^+$ ,  $\text{Na}^+$ ,  $\text{K}^+$ ,  $\text{Mg}^{2+}$ ,  $\text{Ca}^{2+}$ ) has been also

used with one hour averaging time (Makkonen *et al.*, 2012). Both, the ACSM and MARGA were connected to total inlet air.

Trajectory analysis was done with NOAA HYSPLIT model using GDAS meteorological data at three heights (100, 500, 1000 m a.g.l.). The air mass source regions were divided into five categories: Arctic, Eastern, Southern, Western and Local, (Fig. 3.). Based on weighted fractions of air masses over the source regions, for each trajectory the region of the highest weight was considered to represent this air mass type.

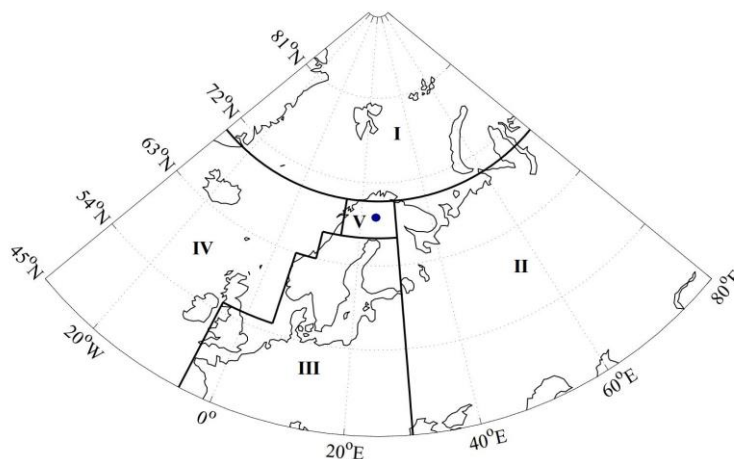


Figure 3. Map of air mass sectors: I (Arctic), II (East), III (South), IV (West) and V (Local). Table summarizes statistics over each sector for all three heights.

Aerosol composition determined from ACSM and MARGA measurements divided according to sectors of air mass origin (at 500 m a.g.l.) can be seen in Fig 4.

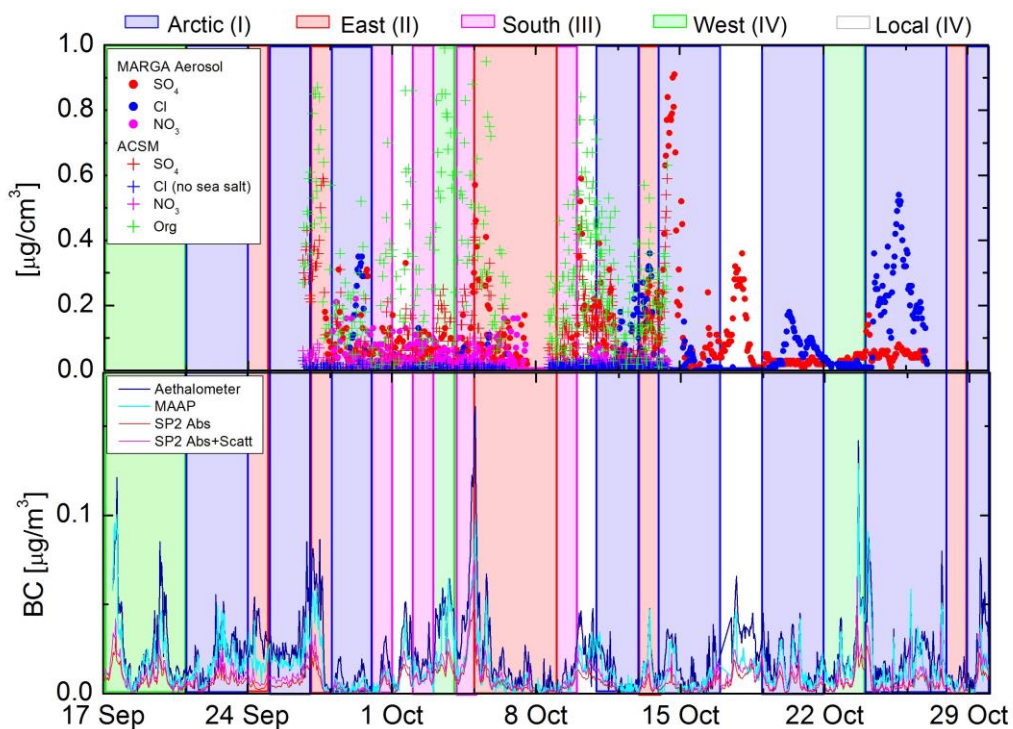


Figure 4. Aerosol chemistry according to air mass sectors of origin, upper panel: ACSM and MARGA, lower panel black carbon (BC) concentration measured by Aethalometer, MAAP and SP2 (absorbing and mixed particles separately).

## ACKNOWLEDGEMENTS

Authors would like to acknowledge financial support provided by Academy of Finland Centre of Excellence program (project no. 1118615).

## REFERENCES

- Vavrus, S. (2004), *J. Climate*, **17**, 603-615
- Komppula, M., H. Lihavainen, V.-M. Kerminen, M. Kulmala, and Y. Viisanen, (2005), *J. Geophys. Res.*, **110**, D06204.
- Lihavainen, H., V.-M. Kerminen, M. Komppula, A.-P. Hyvärinen, J. Laakia., S. Saarikoski, U. Makkonen, N. Kivekäs, R. Hillamo, M. Kulmala, and Y. Viisanen (2008), *Atmos. Chem. Phys.*, **8**, 6925-6938, doi:10.5194/acp-8-6925-2008.
- Hatakka, J., T. Aalto, V. Aaltonen, M. Aurela, H. Hakola, M. Komppula, T. Laurila, H. Lihavainen, J. Paatero, K. Salminen and Y. Viisanen, (2003), *Boreal Environ. Res.*, **8**, 365–384.
- Anttila, T., P. Vaattovaara, M. Komppula, A.-P. Hyvärinen, H. Lihavainen, V.-M Kerminen and A. Laaksonen (2009), *Atmos. Chem. Phys.*, **9**, 4841–4854, doi:10.5194/acp-9-4841-2009.
- Kivekas, N., V.-M. Kerminen, T. Raatikainen, P. Vaattovaara, and H. Lihavainen (2009), *Boreal. Environ. Res.*, **14**, 515–526.
- Anttila, T., D. Brus, A. Jaatinen, A.-P. Hyvärinen, N. Kivekäs, S. Romakkaniemi, M. Komppula, and H. Lihavainen (2012), *Atmos. Chem. Phys.*, **12**, 11435-11450, doi:10.5194/acp-12-11435-2012.
- Ng, N. L., S. C. Herndon, A. Trimborn, M. R. Canagaratna, P. L. Croteau, T. B. Onasch, D. Sueper, D. R. Worsnop, Q. Zhang, Y. L. Sun, and J. T. Jayne (2011), *Aerosol Science and Technology*, **45**:7, 780-794
- Makkonen, U., A. Virkkula, J. Mäntykenttä, H. Hakola, P. Keronen, V. Vakkari and P.P. Aalto (2012), *Atmos. Chem. Phys.*, **12**, 5617-5631, doi:10.5194/acp-12-5617-2012.

# DETECTION OF TRACE METALS WITH THE SOOT-PARTICLE AEROSOL MASS SPECTROMETER

S. CARBONE<sup>1</sup>, S. SAARIKOSKI<sup>1</sup>, D.R. WORSNOP<sup>2,3</sup> and R. HILLAMO<sup>1</sup>

<sup>1</sup> Air Quality Research, Finnish Meteorological Institute, P.O. Box 503, FI-00101 Helsinki, Finland

<sup>2</sup> Aerodyne Research, Inc. 45 Manning Road, Billerica, MA 01821-3976, USA

<sup>3</sup> Department of Physics, University of Helsinki, P.O. Box 64, FI-00014 University of Helsinki, Finland

Keywords: trace metals, SP-AMS

## INTRODUCTION

Trace elements found in atmospheric fine aerosol particles originate from traffic emissions and industrial sources and are related to adverse health effects. For example, Cr, Mn and Ni are among the hazardous air pollutants listed by EPA (EPA 2005). There are several applications where the detection and quantification of trace elements are relevant. For example, during biomass burning episodes potassium (K) has been used as a tracer to identify this source. Conversely, iron, vanadium and nickel were used to identify ship emissions and aluminum and iron to smelters, (Andreae *et al.*, 1988, Healy *et al.*, 2009, Boullemant, 2011).

Online measurements of trace metals using the Aerosol Time-of-Flight Mass Spectrometer (TSI ATOFMS) were reported by Liu *et al.* (1997), however, because the detection method is based on individual particles the quantification of those is rather limited. The first online and quantified measurements of trace metals were obtained in the Mexico City using the Aerodyne Aerosol Mass Spectrometer (Salcedo *et al.*, 2012). The authors reported the detection of Cu, Zn, As, Se, Sn and Sb. However, the temperature of the vaporizer, 600 °C, enables only elements with low boiling and melting points to be measured. For this reason, the AMS was equipped with a laser vaporizer, which allows refractory material, like soot, to be vaporized and measured (Onasch *et al.*, 2012). The elevated temperature achieved by the laser vaporizer enables also the vaporization of trace elements such as Ca and Mg, which were measured from the emission of a marine ship engine with the new Soot-Particle Aerosol Mass Spectrometer (Cross *et al.*, 2013). Although those trace metals were identified, their properties were not investigated and therefore their quantification was not feasible. For these reasons, the purpose of this study is to investigate different trace metals and obtain their ionization efficiencies relative to ammonium nitrate.

## METHODS

The online chemical composition of submicron particles was measured by using a Soot-Particle Aerosol Mass Spectrometer (SP-AMS, Aerodyne Research Inc., USA; Onasch *et al.*, 2012). SP-AMS is a combination of two well-characterized instruments: the Aerodyne high resolution time-of-flight aerosol mass spectrometer (HR-ToF-AMS; Aerodyne Research Inc. MA, USA; DeCarlo *et al.*, 2006) and the single particle soot photometer (SP2; Droplet Measurement Technologies, CO, USA). In the SP-AMS an intracavity Nd:YAG laser vaporizer (1064 nm), based on the design used in the SP2 instrument, was incorporated into the HR-ToF-AMS. The addition of laser enables to vaporize refractory particles, specifically laser-light absorbing refractory black carbon (rBC) particles that are not detected in the standard AMS. The time resolution for the SP-AMS was set to 30 seconds. Half of the time the SP-AMS measured PToF (size distribution) and the other half mass spectra (mass concentration without particle size information).

In this study, aerosol particles containing the trace metals Al, Cr, Rb, Sr and Ba in solution with regal black and deionized water were generated through an atomizer (TSI model 3076). After generation the aerosol particles were size selected, 300 nm (electrical mobility diameter,  $D_m$ ), by a differential mobility analyzer (TSI model 3080) and counted by a condensation particle counter (TSI model 3772).

Standard solutions of Al, Cr, Rb, Sr and Ba were used to make a solution of metals ( $1 \times 10^{-2}$  g/L). This solution was added to another solution containing regal black and deionized water (0.24 g/L) in order to generate the aerosol particles. Regal black is typically used because its mass spectrum is very similar to soot and is here called refractory black carbon, rBC (Onasch *et al.*, 2012).

## RESULTS

The metals solution was added to the rBC solution, one mL per time, i.e.  $1 \times 10^{-5}$  g of each metal per time. The addition of each mL of metals solution results in an increase of the signal of the metals measured by the SP-AMS, Figure 1. Al, Cr, Rb, Sr and Ba correspond to the mass-to-charge ratios ( $m/z$ ) 26.981, 49.946, 84.911, 87.905 and 137.905 respectively and due to the large negative mass defect can easily be identified and measured by the SP-AMS. In addition, the size distribution of those metals in unit mass resolution can be obtained, Figure 2. The 300 nm ( $D_m$ ) monodisperse aerosol particles are measured by the SP-AMS at 230 nm in vacuum aerodynamic diameter ( $D_{va}$ ) as consequence of rBC density and shape factor.

In order to determine the ionization efficiency of each metal the signal obtained by the SP-AMS is compared to the mass calculated on the basis of number concentration measured with the CPC. Assuming that the particles generated by the atomizer present a constant size distribution, the mass ratio between the metals and the rBC in the solution is the same as in the particle phase. Therefore, the mass of metals in the particles is calculated based on the mass ratio and the total number of particles, equation 1,

$$m_M = Z \times m_{rBC} \quad (1)$$

where  $m_M$  is the mass in  $\mu\text{g m}^{-3}$  of each metal obtained by the CPC,  $Z$  is the ratio between the mass of each metal added to the solution and rBC and  $m_{rBC}$  is the mass of rBC obtained with the CPC in  $\mu\text{g m}^{-3}$ . The  $m_{rBC}$  is calculated based on the rBC density, particles diameter and total number of particles obtained by the CPC.  $Z$  is zero when no metal solution is added to the rBC solution and it increases to  $4 \times 10^{-4}$ ,  $8 \times 10^{-4}$ ,  $1.2 \times 10^{-3}$ ,  $1.6 \times 10^{-3}$  and  $2 \times 10^{-3}$  when 1, 2, 3, 4 and 5 mL of metal solution is added to the rBC solution, respectively. The slope obtained between the SP-AMS signal for each metal and the CPC mass corresponds to the ionization efficiency (IE). Because the SP-AMS quantification method is based on the ammonium nitrate (AN) calibration, the ionization efficiency of the metals is then divided by the AN IE, which result in a relative ionization efficiency (RIE) for each metal. The RIEs obtained for the metals analyzed in this study are 3.8, 0.8, 168.9, 19.1 and 25.1. When compared to the literature (Nelson 1976, Vainshtein *et al.*, 1972), all metals, except Cr, present higher ionization efficiencies. The explanation for that is related to surface ionization. Elements that require less energy to be ionized are likely to be thermally ionized. This is the case of the alkali and alkaline earth metals such as Rb, Sr and Ba.

## CONCLUSIONS

This study investigated the detection and quantification of trace metals by the SP-AMS. The results indicate that the measured signal for each metal by SP-AMS is proportional to the amount of metals added to the solution. For the quantification the proposed method works, however further investigation is required to obtain the RIEs for each metal. Moreover, different metals should be used.

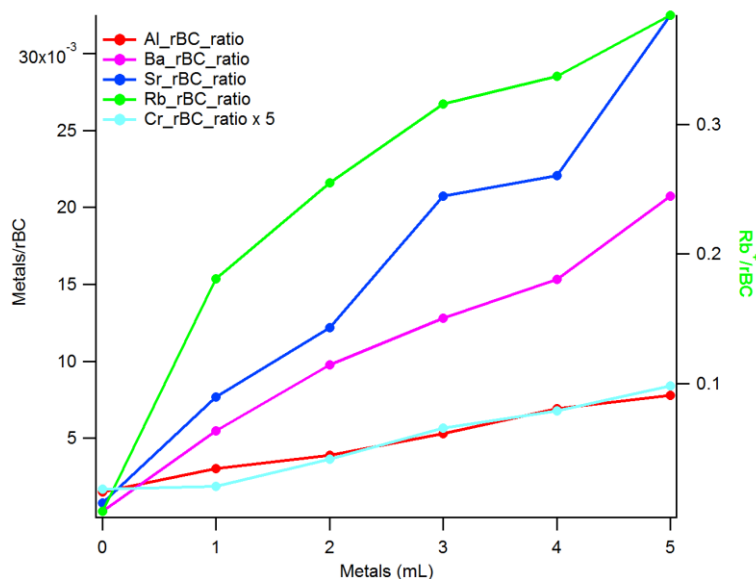


Figure 1. Ratio between the trace metals Al, Cr, Rb, Sr and Ba to rBC as a function of the addition of metals solution to the rBC solution.

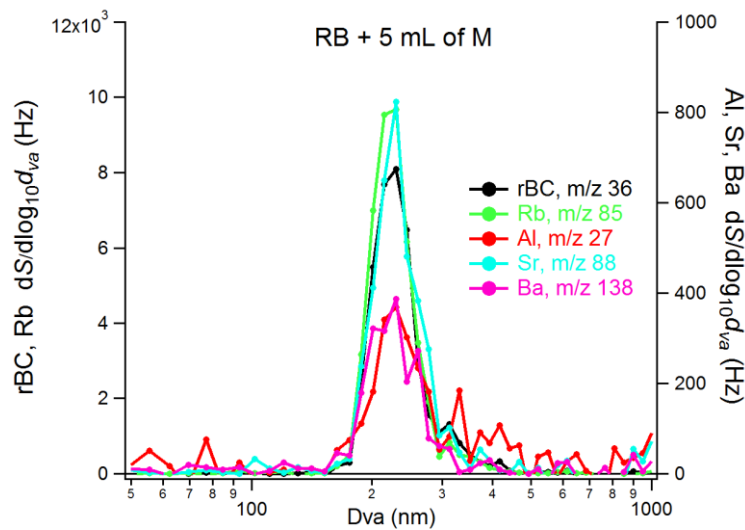


Figure 2. Size distributions, in Hertz, of the trace metals Al, Rb, Sr and Ba and rBC, here represented by m/z 36 only, in vacuum aerodynamic diameter (Dva).

#### ACKNOWLEDGEMENTS

Financial support from the Graduate School in Physics, Chemistry, Biology and Meteorology of Atmospheric Composition and Climate Change (University of Helsinki) is gratefully acknowledged.

## REFERENCES

- Andreae, M. O., Browell, E.V., Garstang, M., Gregory, G.L., Harriss, R.C., Hill, G.F., Jacob, D.J., Pereira, M.C., Sachse, G.W., Setzer, A.W., Silva Dias, P.L., Talbot, R.W., Torres, A.L. and Wofsy, S.C. (1988) Biomass Burning Emissions and Associated Haze Layers over Amazonia, *J. Geophys. Res.*, **93D2**, 1509–1527.
- Boullemant, A. (2011) PM<sub>2.5</sub> Emissions from Aluminum Smelters: Coefficients and Environmental Impact, *J. Air & Waste Manage. Assoc.* **61**, 311-318.
- DeCarlo, P.F., Kimmel, J.R., Trimborn, A., Northway, M.J., Jayne, J.T., Aiken, A.C., Gonin, M., Fuhrer, K., Horvath, T., Docherty, K.S., Worsnop, D.R. and Jimenez, J.L. (2006) Field-deployable, high-resolution, time-of-flight mass spectrometer, *Anal. Chem.* **78**, 8281–8289.
- Healy, R.M., O'Connor, I.P., Hellebust, S., Allan, A., Sodeau, J.R. and Wenger, J.C. (2009) Characterisation of single particles from in-port ship emissions, *Atmospheric Environment*. **43**, 6408-6414.
- Nelson, A. N. (1976) Electron Impact Ionization Cross Sections of gold, chromium and iron. Massachusetts Institute of Technology, USA.
- Onasch, T.B. Trimborn, A., Fortner, E.C., Jayne, J.T., Kok, G.L., Williams, L.R., Davidovits, P. and Worsnop, D.R. (2012) Soot Particle Aerosol Mass Spectrometer: Development, Validation, and Initial Application, *Aerosol Sci. Technol.* **46**, 804-817.
- Schnaiter, M., Horvath, H., Möhler, O., Naumann, K.-H., Saathoff, H. and Schöck, O.W. (2003) UV-VIS-NIR spectral optical properties of soot and soot-containing aerosols, *J. Aerosol Sci.* **34**, 1421–1444.
- Vainshtein, L.A., Ochur, V.I., Rakhovskii, V.I. and Stepanov, A.M. (1972). Absolute values of electron impact ionization cross sections for Magnesium, Calcium, Strontium and Barium, *Sov. Phys. JETP*, **34**, 271-275.
- EPA, List of Air Toxics in the 2005 NATA Assessment, <http://www.epa.gov/ttnatw01/188polls.html>

# SEASONAL DYNAMICS OF STEM CO<sub>2</sub> EFFLUX AND STEM DIAMETER GROWTH

T. CHAN, T. HÖLTTÄ, F. BERNINGER, E. NIKINMAA

University of Helsinki, Department of Forest Sciences  
P.O.Box 27, FIN-00014 University of Helsinki, Finland

Keywords: STEM CO<sub>2</sub> EFFLUX, STEM DIAMETER CHANGE,  
GROWTH EFFICIENCY, SCOTS PINE.

## INTRODUCTION

Stem CO<sub>2</sub> efflux plays a large role in the carbon balance of trees and forests. There are two functional components to which CO<sub>2</sub> efflux (or respiration) may be separated into: maintenance- and growth-associated components. Maintenance respiration provides the energy required for the turnover of protein and the maintenance of ion and metabolite gradients (De Vries, 1975; Roux *et al.*, 2001). Moreover, maintenance respiration is correlated to the amount of living biomass and temperature, which the latter increases exponentially (Ryan, 1995). Growth respiration, on the other hand, refers to CO<sub>2</sub> production from the processes of energy generation for the synthesis of tree dry matter (De Vries, 1975; Ryan, 1987).

Studies in variations of stem CO<sub>2</sub> efflux during the growing season have been well studied and documented (Sprugel & Benecke, 1991; Lavigne & Ryan, 1997; Gruber *et al.*, 2009). However, phenological control of how stem CO<sub>2</sub> efflux varies during the growing seasonal lacks proper understanding. Therefore, a study using stem diameter measurements (from which the cambial growth rate can be derived from) and stem CO<sub>2</sub> efflux rates are important to shed more light into these processes.

The purpose of this study was to identify the seasonal dynamics between stem CO<sub>2</sub> efflux and stem diameter growth of *Pinus sylvestris* L. Microcore samples were used to separate stem diameter measurements into cell growth stages, and a hydraulic model was used to separate growth from stem diameter change – with the aim of achieving a clear relationship between stem growth and growth-related respiration throughout the season. In addition, calculation of stem growth efficiency would be supplemental to the study, independent from radial stem growth to show similar intra-annual dynamics.

## METHODS

Measurements were conducted in an even-aged 50-year-old homogenous Scots pine forest (*Pinus sylvestris* L.), belonging to the southern boreal zone, at Helsinki University SMEAR II field measurement station in Hyytiälä, (61°51'N, 24°17'E, 181 m a.s.l). Continuously measured field data, including air temperature, precipitation, stem CO<sub>2</sub> efflux and stem diameter changes were analyzed from April 1–October 5 for years 2007–2009 to fully capture the beginning and the end of the growing season. Air temperature was measured with pt-100-type resistance thermometer sensors at a height of 8.4 m, while precipitation data was collected using a rain gauge (AGR-100, Environmental Measurements Ltd., Sunderland U.K.). Changes in radial stem diameter was analyzed using two linear variable displacement transducers (LVDT; model AX/5.0/S, Solartron Inc. West Sussex, U.K.) at a height of 15 m., and affixed using a rectangular stainless steel frame (Sandvik 1802 Steel, Sandvik, Sandviken, Sweden). Stem CO<sub>2</sub> efflux was extrapolated using an automated chamber system, comprising of two acrylic chambers (height 20 cm and width 3.5 cm) attached to the bark of the tree (Kolari *et al.*, 2009). A continuous flow of 1 l min<sup>-1</sup> was applied through the system and the efflux was measured as the difference between the CO<sub>2</sub> concentration of the ambient air into the system and the CO<sub>2</sub> concentration flowing out from the system.

Two distinct stem diameter signals were extracted from the data: xylem ( $d_x$ ) and whole stem diameter. The  $d_x$  signal was attained by inserting a small screw roughly 3 cm into the tree and placing the sensor on the head of the screw. Whole stem diameter was measured by incising the thick outer bark, exposing the fleshy phloem tissue, and placing the sensor on top. Refer to Sevanto *et al.* (2005) for a more detailed description of the dendrometer instrument installation. To determine measured inner-bark diameter ( $d_b$ ),  $d_x$  was subtracted from whole stem diameter.

Inner-bark diameter variations arise due to two processes: an irreversible cambial growth-driven change and a reversible water pressure-driven change (Sevanto *et al.*, 2003; Daudet *et al.*, 2005). Following Hooke's Law, where changes in  $d_x$  reflect changes in xylem water pressure (Perämäki *et al.*, 2001), a transpiration-driven hydraulic model adapted from Mencuccini *et al.* (2013) was used to separate the reversible hydraulic-influenced changes ( $d_b$ ) to reveal solely irreversible cambial growth-driven and inner-bark osmotic concentration-driven change. Assuming osmotic potential is constant, no growth is occurring and as the inner-bark tends towards equilibrium with the xylem, the change in  $d_b$  can be predicted from xylem dynamics (Mencuccini *et al.*, 2013):

$$\frac{\Delta d_b}{\Delta t} = \alpha(\beta \Delta d_x - \Delta d_b) \quad (1)$$

where  $\Delta t$  is the change in time,  $\alpha$  reflects the radial hydraulic conductance between the xylem and inner-bark,  $\beta$  represents the ratio of the change in  $d_x$  to the change in  $d_b$  for a given change in pressure and  $\Delta d_x$  and  $\Delta d_b$  reflect the changes in  $d_x$  and  $d_b$  from their values at a reference state, respectively. These changes are calculated quantities between two measuring points separated by a time interval (i.e. at the beginning of the measurement period).

From Eq. 1, the inner-bark change which is affected exclusively by hydraulic influences from the xylem ( $\Delta d_p$ ) can be predicted at  $t+\Delta t$  (the next measuring point) from  $\Delta d_b$  and  $\Delta d_x$  at time  $t$ :

$$\Delta d_p(t + \Delta t) = \Delta d_b(t) + \alpha(\beta \Delta d_x(t) - \Delta d_b(t))\Delta t \quad (2)$$

The change in  $d_b$  due to changes in solely osmotic concentration and cambial growth ( $\Delta P_M$ ) is then determined as the difference between the measured change of the inner-bark diameter ( $\Delta d_b$ ) and the inner-bark diameter change predicted from xylem dynamics:

$$\Delta P_M = \Delta d_b - \Delta d_p \quad (3)$$

Parameterization of daily  $\beta$  was calculated as the daily ratio of change between  $d_b$  and  $d_x$ :

$$\beta = \frac{d_{bMAX} - d_{bMIN}}{d_{xMAX} - d_{xMIN}} \quad (4)$$

where  $d_{bMAX}$  and  $d_{bMIN}$  refer to the trend-corrected daily maximum and daily minimum of  $d_b$ , respectively. On the other hand,  $d_{xMAX}$  and  $d_{xMIN}$  correspond to the daily maximum and daily minimum of  $d_x$ , respectively. Daily  $\alpha$  was then estimated using Eq. 1 using the values of calculated daily  $\beta$  from Eq. (4). The regression model minimized the daily sum of squared residuals, and was iterated 100 times to optimize daily  $\alpha$  values (Excel Solver, SPSS), and outliers were removed using inter-quartile ranges. As daily  $\alpha$  and  $\beta$  changed during the course of the measurement period, a linear equation of statistically estimated daily  $\alpha$  and  $\beta$  was employed to Eq. 1. Parameterization of the daily values of  $\alpha$  and  $\beta$  were collected from midnight to midnight as a function of  $\Delta d_b$  and  $\Delta d_x$ .

In order to capture stem CO<sub>2</sub> efflux ( $E_s$ ) from the point of measurement, daily night-time measurements were used for this study (22:00-05:00) in order to capture solely CO<sub>2</sub> effluxes which had not been affected by axial convection of respired CO<sub>2</sub> along with xylem sap flow. Hölttä and Kolari (2009) demonstrated that the sap flow rate was affecting both the actual sap flow rate and  $E_s$  rate at the study site. Days with incidences of precipitation have been retained in the study, as the hydraulic cambial growth model removed water-related changes from stem diameter measurements.

To separate growth respiration ( $R_g$ ) and maintenance respiration ( $R_m$ ) from  $E_s$ , the temperature coefficient of  $E_s$  ( $Q_{10}$ ) was calculated.  $Q_{10}$  was determined by examining respiration and temperature rates over an interval of two consecutive weeks during non-growth activity (typically before Julian day 130 and after day 240). These periods would assume that  $E_s$  rates would be solely due to the maintenance component, and that variations due to temperature would also reflect similar changes during the growing period.  $Q_{10}$  was calculated using the equation:

$$Q_{10} = \left( \frac{R_2}{R_1} \right)^{\frac{10}{T_2 - T_1}} \quad (5)$$

where  $R_1$  and  $R_2$  are  $E_s$  rates of a certain interval, and  $T_1$  and  $T_2$  are the temperatures at the respective  $E_s$  rate.  $R_m$  values were extrapolated by introducing  $Q_{10}$  values to measured seasonal changes of  $E_s$  and temperature using the exponential equation:

$$R_m = R_f Q_{10}^{(T - T_f)/10} \quad (6)$$

where  $R_m$  is the calculated respiration rate at temperature  $T$ ,  $R_f$  is the measured respiration at the reference temperature  $T_f$  and  $Q_{10}$  is the temperature coefficient of respiration.  $R_f$  was calculated within the same two-week interval as  $Q_{10}$  and  $R_g$  was determined as the difference between  $E_s$  and  $R_m$ .

The growth efficiency or yield ( $Y$ ) is a dimensionless coefficient defined as the ratio at which sugar is transformed into new dry mass ( $\Delta W$ ) to the total amount of assimilates required for this transformation to occur, which consists of the sum of the total accumulated seasonal growth respiration and  $\Delta W$  (Roux *et al.*, 2001):

$$Y = \frac{\Delta W}{(\Delta W + R_g)} \quad (7)$$

$\Delta W$  is observed as the amount of carbon content-per-wood volume ( $\rho_{\frac{\text{carbon\_content}}{\text{wood\_volume}}}$ ) within a certain change in volume of stem ( $\Delta V$ ):

$$\Delta W = \rho_{\frac{\text{carbon\_content}}{\text{wood\_volume}}} \Delta V \quad (8)$$

For Scots pine, it is estimated that  $\rho_{\frac{\text{carbon\_content}}{\text{wood\_volume}}}$  is roughly 220 kg m<sup>-3</sup>.  $\Delta V$  can further be expressed as:

$$\Delta V \approx 2\pi r \Delta d \approx \pi d \Delta d \quad (9)$$

where  $d$  is the diameter of the tree and  $\Delta d$  is the growth during the growing season. From this equation, equation 8 can be rewritten to express the change in volume as the change in inner-bark diameter (for 1 m length of stem):

$$\Delta W = \rho_{\frac{\text{carbon\_content}}{\text{wood\_volume}}} \pi d \Delta d . \quad (10)$$

For this study, field-collected stem diameter measurements and  $\Delta P_M$  were offset to zero on April 1 of each year, and any increment in  $\Delta P_M$  following this date was considered growth. This was due to limitations of dendrometer measurements, where growth cannot be verified by visual observation. Formation of tree wood growth is a continual seasonal three-step process that begins with cell division in the spring, cell radial expansion from the beginning of summer, and cell wall thickening in the late summer (Cuny *et al.*, 2013). This study separated  $\Delta P_M$  into these three distinct periods with the use of measured radial increment and microcores. To identify the beginning of the cell expansion phase, field-collected microcores were observed and noted when the initial tracheid development occurred. The beginning of the cell wall thickening period was recorded when 95% of total seasonal radial stem growth has been attained.

All microclimate, stem diameter and stem CO<sub>2</sub> efflux sensors were taken from continuously-measured data loggers (Campbell Scientific Ltd., Leics., UK), with the current study using 30-minute interval values. For some analyses, daily values of temperature ( $T_m$ ) and growth respiration was used. In addition, the daily  $\Delta P_M$  values ( $G_m$ ) were calculated along with the daily rate of growth ( $G_c$ ) – the difference between  $G_m$  to the previous day's  $G_m$ .  $G_c$  was compared against daily growth respiration by Pearson product-moment correlation coefficient for analysis.

## RESULTS AND CONCLUSIONS

Results showed that during cell division, the relationship between the rate of change in stem diameter growth and stem growth respiration is little/low, but increases greatly during the cell expansion phase (see Figure 1.). In addition, a one day time lag of growth respiration to daily growth rate was observed.

An examination of growth efficiency during these phases showed that during the cell expansion phase, the efficiency was similarly for all three years (see Table 1.). Meanwhile, the efficiency decreased up to a half during the cell thickening phase.

Together, the calculated growth efficiencies and relationship between growth respiration and daily rate of stem diameter change demonstrated the physiological changes which trees undergo on a seasonal scale. This finding is important to understand greater how respiration and newly created biomass share a more unique relationship than previously thought.

This study demonstrated that there were clear changes in growth respiration during the growing season. While little to none was recorded during the early spring, the greatest was associated during the cell expansion period (where much of diameter growth occurred), before decreasing during the thickening phase. These findings correlated well with estimated growth efficiency, based on living biomass and stem CO<sub>2</sub> efflux – a result independent from radial stem growth.

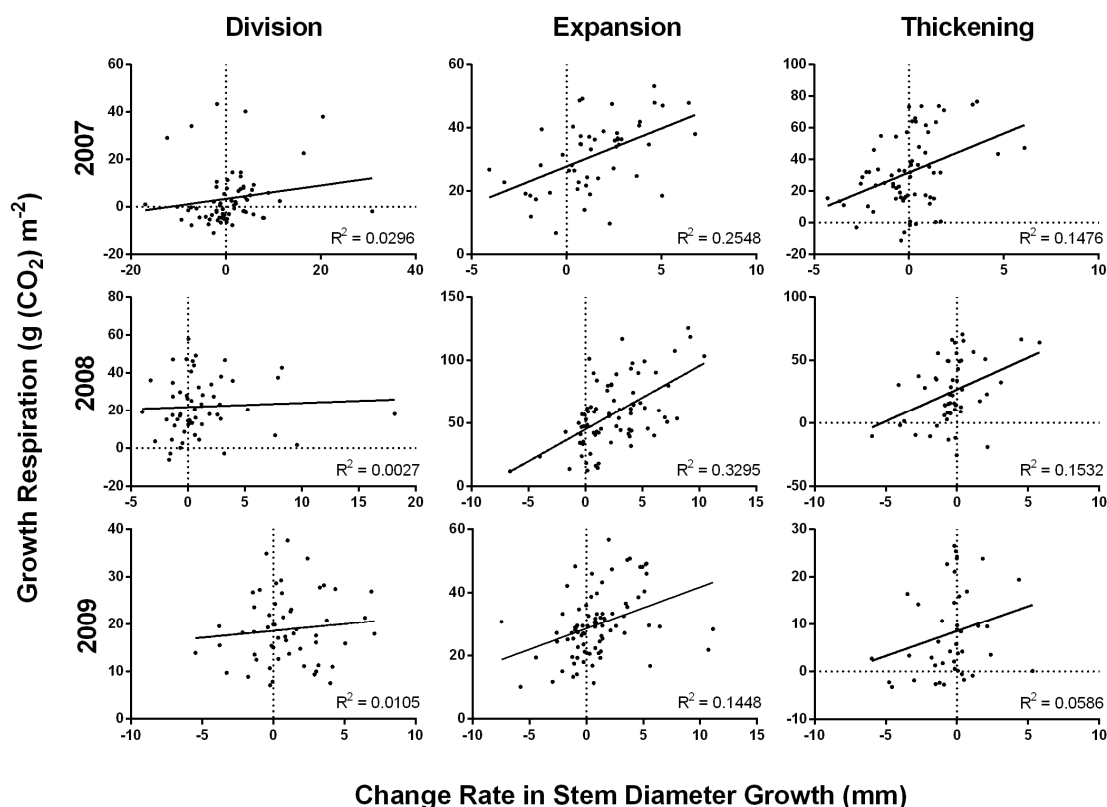


Figure 1. Relationship between stem CO<sub>2</sub> growth respiration and rate of change in stem diameter growth (mm) during each phase in stem diameter expansion from 2007–2009. Dotted line denotes zero-intercept point of their respective x- and y-axis.

Year	Division	Expansion	Thickening	Year
2007	-	0.78	0.47	0.78
2008	-	0.79	0.35	0.78
2009	-	0.75	0.49	0.78

Table. 1. Calculated growth efficiency for years 2007-2009 during cell expansion, cell thickening and overall year.

#### ACKNOWLEDGEMENTS

This paper was funded by the Finnish Centre of Excellence as part of the Decade project (Finnish academy project #140781).

#### REFERENCES

Cuny HE, Rathgeber CBK, Kiessé TS, Hartmann FP, Barbeito I, Fournier M. 2013. Generalized additive models reveal the intrinsic complexity of wood formation dynamics. *Journal of Experimental Botany* **64**(7): 1983-1994.

- Daudet F-A, Améglio T, Cochard H, Archilla O, Lacointe A. 2005.** Experimental analysis of the role of water and carbon in tree stem diameter variations. *Journal of Experimental Botany* **56**(409): 135-144.
- De Vries FP. 1975.** The cost of maintenance processes in plant cells. *Annals of Botany* **39**(1): 77-92.
- Gruber A, Wieser G, Oberhuber W. 2009.** Intra-annual dynamics of stem CO<sub>2</sub> efflux in relation to cambial activity and xylem development in *Pinus cembra*. *Tree Physiology* **29**(5): 641-649.
- Hölttä T, Kolari P. 2009.** Interpretation of stem CO<sub>2</sub> efflux measurements. *Tree Physiology* **29**(11): 1447-1456.
- Kolari P, Kulmala L, Pumpanen J, Launiainen S, Ilvesniemi H, Hari P, Nikinmaa E. 2009.** CO<sub>2</sub> exchange and component CO<sub>2</sub> fluxes of a boreal Scots pine forest. *Boreal Environment Research* **14**: 761-783.
- Lavigne M, Ryan M. 1997.** Growth and maintenance respiration rates of aspen, black spruce and jack pine stems at northern and southern BOREAS sites. *Tree Physiology* **17**(8-9): 543-551.
- Mencuccini M, Hölttä T, Sevanto S, Nikinmaa E. 2013.** Concurrent measurements of change in the bark and xylem diameters of trees reveal a phloem-generated turgor signal. *New Phytologist*.
- Perämäki M, Nikinmaa E, Sevanto S, Ilvesniemi H, Siivola E, Hari P, Vesala T. 2001.** Tree stem diameter variations and transpiration in Scots pine: an analysis using a dynamic sap flow model. *Tree Physiology* **21**(12-13): 889-897.
- Roux XL, Lacointe A, Escobar-Gutiérrez A, Dizès SL. 2001.** Carbon-based models of individual tree growth: A critical appraisal. *Ann. For. Sci.* **58**(5): 469-506.
- Ryan M. 1987.** Growth efficiency, leaf area and sapwood volume in subalpine conifers. *Symposium proceedings, Management of Subalpine Forests: Building on 50 Years of Research. USDA Forest Service, General Technical Report(RM-149)*: 5.
- Ryan M. 1995.** Foliar maintenance respiration of subalpine and boreal trees and shrubs in relation to nitrogen content. *Plant, Cell & Environment* **18**(7): 765-772.
- Sevanto S, Hölttä T, Markkanen T, Perämäki M, Nikinmaa E, Vesala T. 2005.** Relationships between diurnal xylem diameter variation and environmental factors in Scots pine. *Boreal Environment Research* **10**(5): 447-458.
- Sevanto S, Vesala T, Perämäki M, Nikinmaa E. 2003.** Sugar transport together with environmental conditions controls time lags between xylem and stem diameter changes. *Plant, Cell & Environment* **26**(8): 1257-1265.
- Sprugel D, Benecke U. 1991.** Measuring woody-tissue respiration and photosynthesis. *Techniques and approaches in forest tree ecophysiology* **1**: 329-355.

# VARIATIONS IN ION CONCENTRATIONS AND THE POSSIBLE EFFECT OF LIGHTNING AND OZONE

X. CHEN<sup>1</sup>, H. E. MANNINEN<sup>1,2</sup>, A. FRANCHIN<sup>1</sup>, P. AALTO<sup>1</sup>, P. KERONEN<sup>1</sup>, A. MÄKELÄ<sup>3</sup>, T. PETÄJÄ<sup>1</sup>, M. KULMALA<sup>1</sup>

<sup>1</sup>Department of Physics, University of Helsinki, Finland

<sup>2</sup>Institute of Physics, University of Tartu, Estonia

<sup>3</sup>Finnish Meteorological Institute, Helsinki, Finland

Keywords: ion, new particle formation, lightning, particle growth

## INTRODUCTION

Atmospheric ions, or air ions, refer to a large variety of charge carriers present in the atmosphere. They could have distinct features in chemical composition, mass, size as well as number of carried charge. Tammet classified them into small or cluster ions, intermediate ions, and large ions, according to their mobility ( $Z$ ) in air ( $Z > 0.5 \text{ cm}^2\text{V}^{-1}\text{s}^{-1}$ ,  $0.5 \text{ cm}^2\text{V}^{-1}\text{s}^{-1} \geq Z \geq 0.03 \text{ cm}^2\text{V}^{-1}\text{s}^{-1}$  and  $Z < 0.03 \text{ cm}^2\text{V}^{-1}\text{s}^{-1}$ , respectively) (Tammet, 1998). The corresponding mobility diameter ranges are ca. 0.8 – 1.7 nm, 1.7 – 7 nm and 7 – 42 nm in the case of NAIS (Neutral cluster and Air Ion Spectrometer) measurement.

Ions in the atmosphere are initially formed via the ionisation of gas molecules (mainly  $\text{N}_2$  and  $\text{O}_2$  in the air) by radon decay and external radiation, i.e.  $\gamma$ -ray and cosmic radiation (Hirsikko, 2011), which are known as primary ions. On collisions with other molecules present in the air, depending on the proton or electron affinity of these trace molecules, the triggered chemical reactions will involve either positive or negative primary ions. Further with going through phase transition processes, also known as nucleation, small particles bearing charge or not are produced within less than a second (Hirsikko et al., 2011). This process is also termed as ion-induced nucleation (Seinfeld & Pandis, 2006). Although ion-induced nucleation is thermodynamically more favorable over the neutral pathway, the ions have been observed with minor contribution to the overall nucleation rate (Kulmala et al., 2010; Kulmala et al., 2007).

Atmospheric ions are also involved in new particle formation (NPF) via ion-mediated processes, namely ion-ion recombination and ion-neutral attachment, with the former one possibly generating neutral particles and the latter one charged particles (atmospheric ions). The total ion concentration is dominated by cluster ions and typically there are very few ions in the intermediate and large sizes. Increase in the intermediate ion concentration can be observed when there is a NPF event or processes involving the growth in ion size, such as the late afternoon growth and rain effect, which will be discussed in more detail later in the text.

Atmospheric ions possess complicated chemical properties originated from the various possible combinations of gaseous species for their composition. These gaseous substances could comprise both inorganic and organic compounds. The negative ions consist of mainly inorganic acids and their clusters (Junninen et al., 2010). Ehn et al. (2010) found that the APi-TOF (Atmospheric Pressure Interface Time-of-Flight Mass Spectrometer) spectra of negative polarity measured in Hyytiälä are dominated by bisulphate ions ( $\text{HSO}_4^-$ ) and related clusters. Sulphuric acid has an important role in the nucleation (Nieminen et al., 2009; Sipilä et al., 2010). Due to its relatively stronger acidity among the species present in the atmosphere, it tends to lose hydrogen and become negatively charged as  $\text{HSO}_4^-$ , which will subsequently cluster or react with other gas-phase molecules forming small ions. Besides, Ehn et al. (2010) also reported the observation of organosulphates and the presence of ammonia with sulphuric acid tetramer. The positive ions, on the other hand, are composed of substances with basic property, such as alkyl pyridines and amines (Ehn et al., 2010; Junninen et al., 2010). The night-time pattern of the ion spectrum was suggested to have contribution of highly oxidized organics by Ehn et al. (2010).

This abstract will present results from the NAIS data analysis, together with the BSMA (Balanced Scanning Mobility Analyzer) (Tammet, 2006) as a comparison for the annual variation study over the period of 2009 – 2012. Also case studies about the late afternoon growth and the lighting effect on the ion

concentration will be investigated, together with the trace gases for the speculation of the possible reasons for the observations. Results are presented in Finnish winter time (UTC+2).

## METHODS

The NAIS has a diameter range of 0.8 – 42 nm for ions and 2 – 42 nm for neutral particles with an inlet flow rate of 60 lpm. It is capable measuring both atmospheric ions and neutral particles. It can be operated in 3 modes: offset mode, ion mode and particle mode. The offset mode measures the background signal of the electrometers in the analyser by discharging and pre-filtering out the ions. When measuring the ions, the chargers and filters are turned off and the naturally charged particles are size-segregated in two cylindrical DMAs (Differential Mobility Analyzer) according to their polarity, each of which has 21 individual electrometer rings receiving the current the ions produce. In particle mode, the total number concentration including both charged and uncharged particles is measured and only the main chargers and filters are in use (Manninen et al., 2009; Mirme & Mirme, 2013).

The BSMA differs from the NAIS primarily in analyzer type, flow rate and measured mobility range. It consists of two plate DMAs and a balanced capacitance bridge. The signals from both polarities are analyzed by a common electrometer system (Tammet, 2006). This design can prevent the variations in electrometer readings between the two polarities which might be problematic in the multichannel instrument (Tammet, Hörrak, & Kulmala, 2009). The BSMA measures only atmospheric ions and has a diameter range of 0.8 – 8 nm. The inlet flow rate of the BSMA is 2400 lpm.

The trace gas data of O<sub>3</sub> and H<sub>2</sub>O are collected from the Hyytiälä mast measurement. O<sub>3</sub> is measured with the ultraviolet light absorption analyzers (TEI 49C) with detection limit of 1 ppb and the relative accuracy of  $\pm 3\%$ . The H<sub>2</sub>O data are obtained with the infrared light absorption analyzers (URAS 4 H<sub>2</sub>O till Sept. 2011 and LI-840 from Sept. 2011 onwards), which can measure down to 0.5 mmol/mol and 0.2 mmol/mol respectively with relative accuracy of  $\pm 2\%$ . The measurements were carried out at different heights: 4.2 m, 8.4 m, 16.8 m, 33.6 m, 50.4 m and 67.2 m above the mast base. Precipitation data are acquired with a Vaisala FD12P Weather sensor, which is situated above the forest at 18 m high. More detailed description of Hyytiälä mast instrumentation can be found in Kulmala et al. (2001). The lightning location data is acquired from the Nordic lightning location system (NORDLIS) consisting of about 30 ground-based sensors in Finland, Sweden, Norway, and Estonia (Mäkelä, Tuomi, & Haapalainen, 2010).

## RESULTS AND DISCUSSION

### ANNUAL VARIATION

Higher ion concentrations are obtained with the BSMA, compared with the NAIS, especially in the cluster size range (Figure 1). Concentrations of positive cluster ions are higher than that of the negative polarity throughout the year measured by the NAIS. This is due to the earth electrode effect (Hirsikko et al., 2011). The earth is slightly negatively charged and therefore it attracts positive ions towards it and negative ions are drifting away under the weak repelling force. Both polarities show similar annual profile. More positive cluster ions are also observed in the BSMA measurement, except in summer. The negative polarity of the BSMA annual pattern follows a similar trend to that of the ionization rate derived from the external radiation (Franchin, 2009). A possible reason for this observation could be that the BSMA, due to its higher sample flow rate (2400 lpm), is able to detect the primary ions, the formation of which is largely dependent on the external radiation. The discrepancy between the two instruments is reduced significantly for the intermediate ions. The highest ion concentrations in the different size ranges appear generally in summer. However, more negative ions in the intermediate range are detected by both the NAIS and the BSMA. This phenomenon could be resulted from the fact that NPF happens more frequently in the spring time and the negative ions are more favored in this process. For the full measurable size range of the BSMA, the annual cycles preserve the features in the cluster ions and this indicates that the number concentration of ions is dominated by cluster ions.

Diurnal pattern can be seen in spring and summer time as well as slightly in autumn in both positive and negative ion concentrations (Figure 2). However, no clear trend can be found in winter. Concentration drop during noon can be observed in cluster ions, which could be related to the NPF and growth, as correspondingly, the number concentration of larger-size ions increases

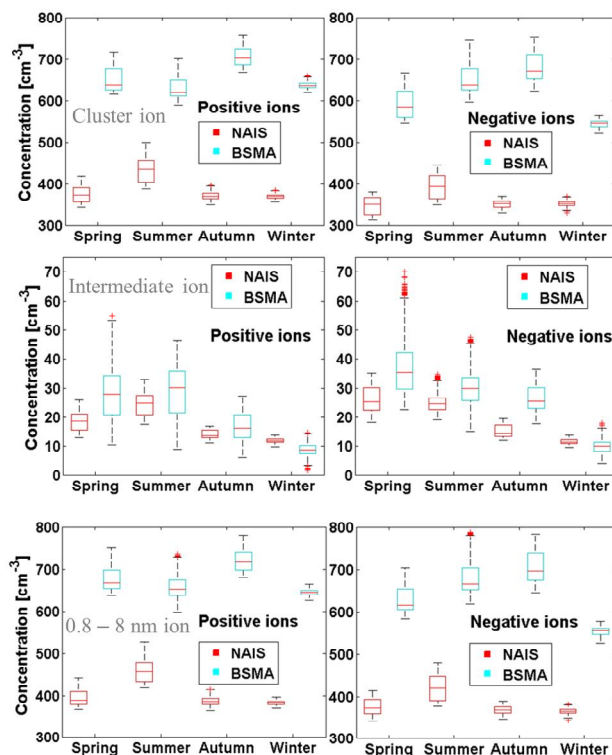


Figure 1: Annual variation of ion concentration measured by NAIS and BSMA based on Hyytiälä measurement in the period of 2009 – 2012. Cluster ion (0.8 – 1.7 nm) in the upper panel, intermediate ion (1.7 – 7 nm) in the middle and 0.8 – 8 nm ion (full BSMA size range) in the lower.

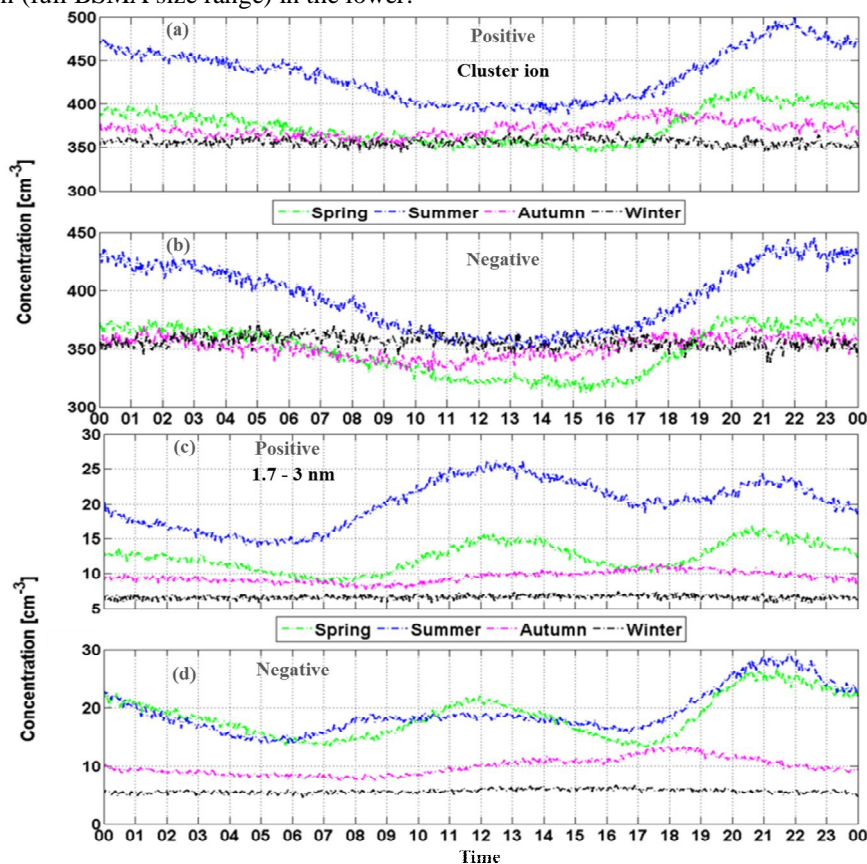


Figure 2: Diurnal cycle of seasonal median concentration calculated from the Hyytiälä NAIS data (2009 - 2012) for cluster size (0.8 – 1.7 nm) in (a) & (b) and 1.7 – 3 nm in (c) & (d). Positive polarity is shown in the upper panel and negative in the lower. Spring in green, summer in blue, autumn in pink and winter in black.

## LATE AFTERNOON GROWTH

In Figure 2, also the concentration increase at late afternoon can be observed. This is anti-correlated with  $O_3$  concentration: when there is a rise in intermediate ion concentration,  $O_3$  concentration declines. Figure 3 shows an example of the correlation between ion and  $O_3$  concentration, with correlation coefficient ( $R$ ) being -0.59.

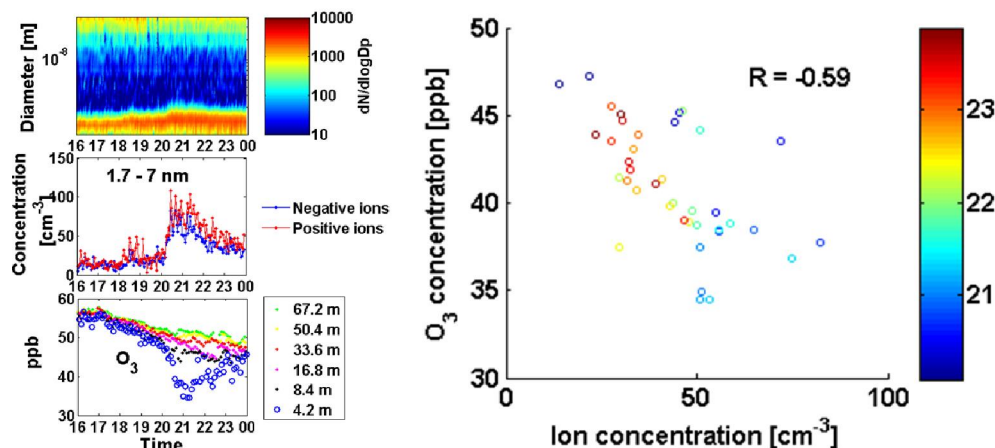


Figure 3: Correlation between ion concentration (1.7 – 7 nm) and  $O_3$  concentration on May 15, 2012, in Hyytiälä. The color represents the time of the day in hours. Time series of ion and  $O_3$  concentration and contour plot on the left panel. Ion concentration was obtained from the NAIS measurement.

This observation could be linked with  $O_3$  oxidation of some VOCs, which differ from the ones emitted during morning or early afternoon in composition, relatively rapidly producing less volatile organic vapors. And this process could be contributed by the low wind speed below canopy occurred around 8 p.m. on this day, which results in less mixing and accumulation of emitted VOCs at ground level. The oxidation products then get involved in nucleation or condense on existing particles leading to particle growth. This phenomenon could also be the onset of the nocturnal event, which however, is limited by some factors that terminate the suitable conditions for the continuous growth. Lehtipalo et al. (2011) has proposed similar growth mechanism with the participation of  $O_3$  for the nocturnal event. Ehn et al. (2010) studied ambient ions with APi-TOF (Atmospheric Pressure interface Time of Flight Mass Spectrometer) and he found that the night-time spectrum was mainly composed of substances falling in the mass to charge ratio range of 300-400 Th. Based on the negative spectrum, they proposed chemical formulae for two dominant peaks at 308 and 340 Th, being  $C_{10}H_{14}NO_{10}^-$  and  $C_{10}H_{14}NO_{12}^-$ .

## LIGHTNING AND RAIN EFFECT

The rain tends to produce negative ions mainly, known as Lenard effect or balloelectric effect (Laakso et al., 2007; Tammet et al., 2009), which can be supported by our observation in Figure 4b and 4c on May 17, 2011. The lighting occurred on this day at 13:46 and rain at 13:56. The rises in cluster ion concentrations were at 13:52 and 13:48 for the negative and the positive polarities respectively. For the increase in intermediate ion concentration, it was observed at around 13:52. The ion concentration increase happened after the lightning and before the rain. Right after the lightning, the concentration increase in the positive polarity could be clearly observed.

The  $O_3$  concentration started to decrease after the lightning, in coincidence with the rise in water concentration, with the minimum and maximum reached after the rain episode, at approximately the same time as the ion concentration dropped back to the ground level. This could imply that the  $\cdot OH$  radical production from  $O_3$  pathway is disturbed by lightning and there is something else that consumes  $O_3$  and possibly causing the NPF. The VOCs (Volatile Organic Compounds) could be speculated responsible for the sink of  $O_3$  in this circumstance and contribute to nucleation. However, further investigation is needed to reveal the truth. The positive intermediate ions produced during the lightning event are seemingly able to grow to larger sizes, as shown in Figure 4. The concentration ratio of ions to neutral particles, in the intermediate size range of 2.5 – 7 nm, rises up to almost 0.8 in the positive polarity and 0.4 in the negative from the background level of less than 0.05, right after the lightning.

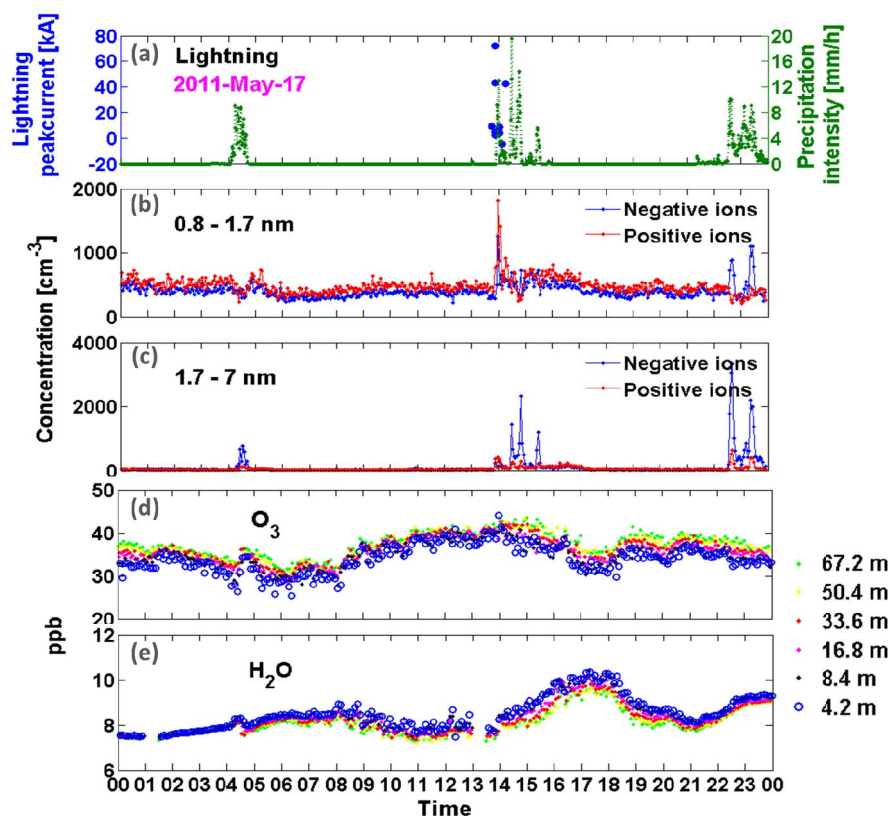


Figure 4: Lightning and rain effects on ion and trace gas concentrations (May 17, 2011) in Hyytiälä. Time-series of lightning peakcurrent and precipitation intensity in (a), cluster ion concentration in (b), intermediate ion concentration in (c), ozone and water concentration in (d) and (e). Lightning occurred within 10 km distance from Hyytiälä on this day.

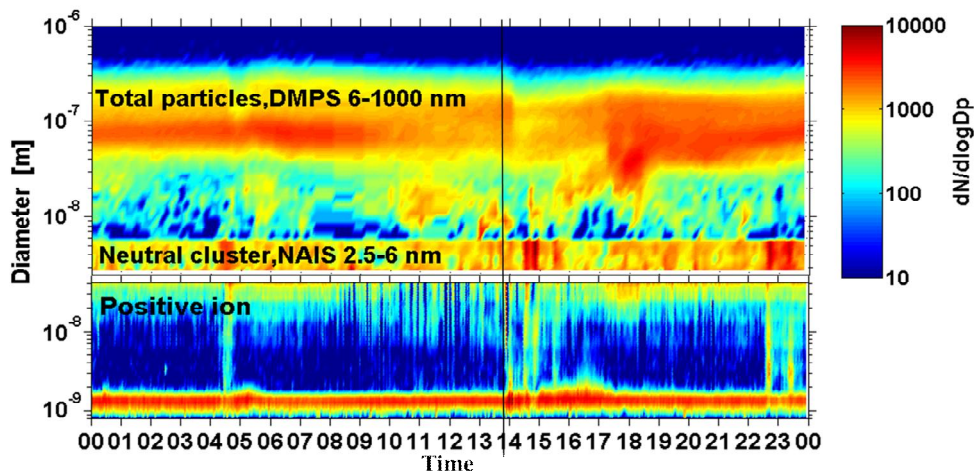


Figure 5: Contour plot of the ions and the total particles at Hyytiälä on May, 17, 2011. Upper panel: combined particle surface plot of NAIS (2.5 – 6 nm) and DMPS (6 – 1000 nm). DMPS measures dry particle size. Lower panel: surface of plot of positive ions measured with NAIS. Black line represents that beginning of the lightning episode.

## CONCLUSION

Due to the earth electrode effect, more positive cluster ions are observed close to the ground surface where our measurements are located. The concentration levels in the cluster size measured by the NAIS and the BSMA have some disagreement with each other and this could be the consequence of the different instrumental design. The BSMA may be capable of detecting the primary atmospheric ions. Decrease in the concentration of cluster ions in spring, summer and autumn could be ascribed to the NPF events. The late afternoon growth is possibly caused by  $O_3$  oxidation of the VOCs and could be the onset of the disrupted nocturnal event. The rain contributes to the rise in the number concentration of negative ions

whereas lightning could have effect on both polarities, generating relatively more positive ions compared with negative ions. The formation of  $\cdot\text{OH}$  radical through  $\text{O}_3$  photolysis and subsequent reaction with  $\text{H}_2\text{O}$  could be diminished by the lightning. The VOCs might be responsible for the consumption of  $\text{O}_3$  and evoking the growth.

#### ACKNOWLEDGEMENTS

This research was supported by Finnish Cultural Foundation. The support by the Academy of Finland Centre of Excellence program (project no. 1118615) is also gratefully acknowledged.

#### REFERENCES

- Ehn, M., Junninen, H., Petäjä, T., Kurtén, T., Kerminen, V. M., Schobesberger, S., . . . Worsnop, D. R. (2010). Composition and temporal behavior of ambient ions in the boreal forest. *Atmospheric Chemistry and Physics*, 10(17), 8513-8530. doi: 10.5194/acp-10-8513-2010
- Franchin, A. (2009). Relation Between  $222\text{Rn}$  Concentration And Ion Production Rate In Boreal. In Markku Kulmala, Jaana Bäck, Tuomo Nieminen & A. Lauri (Eds.), *Proceedings of the Finnish Center of Excellence and Graduate School in "Physics, Chemistry, Biology and Meteorology of Atmospheric Composition and Climate Change" Annual Workshop 27.-29.4.2009* (pp. 105-108).
- Hirsikko, A. (2011). On formation, growth and concentrations of air ions *Report Series in Aerosol Science* (Vol. 125). Helsinki, Finland: University of Helsinki.
- Hirsikko, A., Nieminen, T., Gagné, S., Lehtipalo, K., Manninen, H. E., Ehn, M., . . . Kulmala, M. (2011). Atmospheric ions and nucleation: a review of observations. *Atmospheric Chemistry and Physics*, 11(2), 767-798. doi: 10.5194/acp-11-767-2011
- Junninen, H., Ehn, M., Petäjä, T., Luosujärvi, L., Kotiaho, T., Kostianen, R., . . . Worsnop, D. R. (2010). A high-resolution mass spectrometer to measure atmospheric ion composition. *Atmospheric Measurement Techniques*, 3(4), 1039-1053. doi: 10.5194/amt-3-1039-2010
- Kulmala, M., Hämeri, K., Aalto, P. P., Mäkelä, J., Pirjola, L., Nilsson, E. D., . . . O'dowd, C. D. (2001). Overview of the international project on biogenic aerosol formation in the boreal forest (BIOFOR). *Tellus*, 53B, 324-343.
- Kulmala, M., Riipinen, I., Nieminen, T., Hultkonen, M., Sogacheva, L., Manninen, H. E., . . . Kerminen, V.-M. (2010). Atmospheric data over a solar cycle: no connection between galactic cosmic rays and new particle formation. *Atmos. Chem. Phys.*, 10, 1885 - 1898.
- Kulmala, M., Riipinen, I., Sipila, M., Manninen, H. E., Petaja, T., Junninen, H., . . . Kerminen, V. M. (2007). Toward direct measurement of atmospheric nucleation. *Science*, 318(5847), 89-92. doi: 10.1126/science.1144124
- Laakso, L., Hirsikko, A., Grönholm, T., Kulmala, M., Luts, A., & Parts, T.-E. (2007). Waterfalls as sources of small charged aerosol particles. *Atmos. Chem. Phys.*, 7, 2271-2275.
- Lehtipalo, K., Sipilä, M., Junninen, H., Ehn, M., Berndt, T., Kajos, M. K., . . . Kulmala, M. (2011). Observations of Nano-CN in the Nocturnal Boreal Forest. *Aerosol Science and Technology*, 45(4), 499-509. doi: 10.1080/02786826.2010.547537
- Manninen, H. E., Petäjä, T., Asmi, E., Riipinen, I., Nieminen, T., Mikkilä, J., . . . Kulmala, M. (2009). Long-time filed measurements of charged and neutral clusters using Neutral cluster and Air Ion Spectrometer (NAIS) *Boreal Environment Reseach*, 14, 591-605.
- Mirme, S., & Mirme, A. (2013). The mathematical principles and design of the NAIS – a spectrometer for the measurement of cluster ion and nanometer aerosol size distributions. *Atmospheric Measurement Techniques*, 6(4), 1061-1071. doi: 10.5194/amt-6-1061-2013
- Mäkelä, A., Tuomi, T. J., & Haapalainen, J. (2010). A decade of high-latitude lightning location: Effects of the evolving location network in Finland. *Journal of Geophysical Research*, 115(D21). doi: 10.1029/2009jd012183
- Nieminen, T., Manninen, H. E., Sihto, S. L., Yli-Juuti, T., Mauldin, I. R. L., Petäjä, T., . . . Kulmala, M. (2009). Connection of Sulfuric Acid to Atmospheric Nucleation in Boreal Forest. *Environmental Science & Technology*, 43(13), 4715-4721. doi: 10.1021/es803152j
- Seinfeld, J. H., & Pandis, S. N. (2006). *Atmospheric Chemistry and Physics From Air Pollution to Climate Change* (2 ed.). United States: John Wiley & Sons, Inc.
- Sipila, M., Berndt, T., Petaja, T., Brus, D., Vanhanen, J., Stratmann, F., . . . Kulmala, M. (2010). The role of sulfuric acid in atmospheric nucleation. *Science*, 327(5970), 1243-1246. doi: 10.1126/science.1180315
- Tammet, H. (1998). Air ions *CRC Handbook of hemistry and Physics* (79 ed., Vol. 14, pp. 32-34 ). Boca Raton, Ann Arbor, London, Tokyo CRC Press.
- Tammet, H. (2006). Continuous scanning of the mobility and size distribution of charged clusters and nanometer particles in atmospheric air and the Balanced Scanning Mobility Analyzer BSMA. *Atmospheric Research*, 82(3-4), 523-535. doi: 10.1016/j.atmosres.2006.02.009
- Tammet, H., Hörrak, U., & Kulmala, M. (2009). Negatively charged nanoparticles produced by splashing of water. *Atmos. Chem. Phys.*, 9, 357-367.

# EFFECT OF IONS ON SULPHURIC ACID-WATER BINARY NUCLEATION: EXPERIMENTAL DATA AND COMPARISON WITH IMPROVED CLASSICAL NUCLEATION THEORY

J. DUPLISSY<sup>1,2</sup>, J. MERIKANTO<sup>2</sup>, D. WIMMER<sup>2,3</sup>, L. RONDO<sup>3</sup>, H. VUOLLEKOSKI<sup>2</sup>,  
S. SCHOBESBERGER<sup>2</sup>, A. FRANCHIN<sup>2</sup>, K. LEHTIPALO<sup>2</sup>, A. KUERTEN<sup>3</sup>, G. TSAGKOGEOORGAS<sup>4</sup>,  
F. RICCOBONO<sup>5</sup>, F. BIANCHI<sup>5</sup>, A. PRAPLAN<sup>2,5</sup>, G. STEINER<sup>2</sup>, J. KANGASLUOMA<sup>2</sup>,  
H. JUNNINEN<sup>2</sup>, T. NIEMINEN<sup>1,2</sup>, M. BREITENLECHNER<sup>9</sup>, D., S. EHRHART<sup>3</sup>, R. SITALS<sup>3</sup>,  
A. AMORIN<sup>6</sup>, A. TOME<sup>6</sup>, A. MÄÄTTÄNEN<sup>7,8</sup>, A. KUPC<sup>10</sup>, H. VEHKAMÄKI<sup>2</sup>, M. KULMALA<sup>2</sup> AND  
CLOUD COLLABORATION

<sup>1</sup>Helsinki Institute of Physics, University of Helsinki, Finland

<sup>2</sup>Division of Atmospheric Sciences, University of Helsinki, Finland

<sup>3</sup>Goethe-University of Frankfurt, Institute for Atmospheric and Environmental Sciences, Frankfurt am  
Main, Germany

<sup>4</sup>Leibniz Institute for Tropospheric Research, Leipzig, Germany

<sup>5</sup>Paul Scherrer Institute, Laboratory of Atmospheric Chemistry, Villigen, Switzerland

<sup>6</sup>SIM, University of Lisbon and University of Beira Interior, Lisbon, Portugal

<sup>7</sup>Université Versailles St Quentin, LATMOS-IPSL, 11 boulevard d'Alembert, 78280 Guyancourt, France

<sup>8</sup>Centre National de la Recherche Scientifique (CNRS), LATMOS-IPSL, France

<sup>9</sup>Institute of Ion Physics and Applied Physics, University of Innsbruck, Innsbruck, Austria

<sup>10</sup>University of Vienna, Faculty of Physics Boltzmanngasse 5, 1090 Vienna, Austria.

Keywords: BINARY NUCLEATION, IONS-INDUCED NUCLEATION, SULPHURIC ACID, CLOUD  
chamber, GALACTIC COSMIC RAYS.

## INTRODUCTION

Sulphuric acid is thought to be the main nucleating species in the atmosphere due to its low vapour pressure. Recent finding shows that other compounds, like NH<sub>3</sub>, organics or DMA could have an important contribution in the nucleation processes in the troposphere. In the troposphere, low concentration, such as few ppt, of these species can have a key role in determining the nucleation rate, although sulphuric acid is also needed. However, in the free troposphere, where these trace gases are not present and where the temperature is colder, pure binary nucleation of sulphuric acid and water could be the main processes of nucleation. But this “simple” pure binary nucleation is not yet well understood, with predictions being order of magnitude off from experimental data. In this presentation, we investigate the neutral and charged binary nucleation processes of sulphuric acid and water for in both theoretical and experimental way.

## METHODS

Experimental data: We use the CLOUD chamber at CERN to study binary nucleation of sulphuric acid and water with the dependency to relative humidity, temperature and ions concentration. Technical input for the CLOUD design was obtained in a pilot experiment in 2006. The chamber is a 3m-diameter electro-polished stainless-steel cylinder (26.1 m<sup>3</sup>). A field cage is installed inside the chamber to allow the removal of ions, when required. The contents of the chamber is irradiated by UV light in the range 250-400 nm and mixed by two fans. Experimental runs can be performed at stable temperatures between 40°C and -65°C. The chamber is exposed to a 3.5 GeV/c secondary pion beam from the CERN PS, corresponding to the characteristic energies and ionization densities of cosmic ray muons in the lower troposphere. The beam intensity can be adjusted to cover the natural ion range concentration from ground level to the stratosphere. Ultra-pure air is obtained from the evaporation of cryogenic liquid N<sub>2</sub> and liquid

O<sub>2</sub>. The air is humidified with a Nafion humidifier. Trace gases such as SO<sub>2</sub> are added from gas cylinders containing pressurised N<sub>2</sub> as the carrier. The chamber instrumentation includes PTRMS, CIMS, Nano-SMPS, CPC battery, PSM, API-ToF, NAIS, Gerdien, LOPAP, dew point sensor, SO<sub>2</sub> and O<sub>3</sub> analyser, as well as T, P and UV sensors. Sulphuric acid was generated by means of UV light, SO<sub>2</sub> and water. From the API-tof data, pure binary nucleation of sulphuric acid and water can be clearly identified and unwanted nucleation processes including other species than water and sulphuric acid have been excluded from this study.

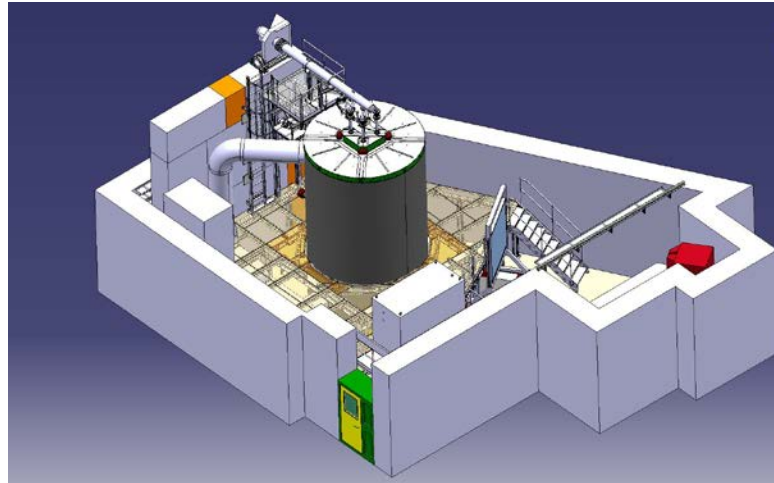


Figure 1: An illustration of CLOUD chamber in the T11 experimental zone at the CERN PS. The de-focused particle beam exits a dipole magnet (right), crosses the hodoscope counter (middle) and then traverses the 3m-diameter CLOUD chamber (Duplissy et al. 2010, Kirkby et al. 2011, Kupc et al. 2011, Voigtlander et al. 2012).

The variables range used in this binary nucleation study, such as temperature, sulphuric acid concentration, relative humidity, and ions concentration are summarized in Table 1.

Table 1: Variables range investigated during the CLOUD experiment.

Variables	Range of study
Temperature [K]	208-295
Relative Humidity [%]	12-50
Ions [cm <sup>-3</sup> ]	0-4000
Sulfuric acid [cm <sup>-3</sup> ]	1e6-1e9

Theory: An improved classical nucleation theory including the charged effect on nucleation and hydrate has been developed and will be presented, together with an inter-comparison between theory and data.

## CONCLUSIONS

The key success of this experiment is the very well controlled cleanness of the CLOUD chamber, associated to the possibility to look at the cluster composition. With this complete set of instrumentation, truly binary nucleation has been studied, excluding other nucleation processes. In addition, the improved

nucleation theory has been fully implemented and compared with the CLOUD data set. To finalise this study, further lab work would be needed to complete the data set of variable values used in the theory such as temperature dependency of surface tension of sulphuric acid-water mixture.

## ACKNOWLEDGEMENTS

We would like to thank CERN for supporting CLOUD with important technical and financial resources, and for providing a particle beam from the CERN Proton Synchrotron. This research has received funding from the EC Seventh Framework Programme (Marie Curie Initial Training Network "CLOUD-ITN" no. 215072, MC-ITN "CLOUD-TRAIN" no. 316662, and ERC Advanced "ATMNUCLE" grant no. 227463), the German Federal Ministry of Education and Research (project nos. 01LK0902A and 01LK1222A), the Swiss National Science Foundation (project nos. 200020 135307 and 206620 130527), the Academy of Finland (Center of Excellence project no. 1118615), the Academy of Finland (135054, 133872, 251427, 139656, 139995, 137749, 141217, 141451), the Finnish Funding Agency for Technology and Innovation, the Nessling Foundation, the Austrian Science Fund (FWF; project no. P19546 and L593), the Portuguese Foundation for Science and Technology (project no. CERN/FP/116387/2010), the Swedish Research Council, Vetenskapsrådet (grant 2011-5120), the Presidium of the Russian Academy of Sciences and Russian Foundation for Basic Research (grants 08-02-91006-CERN and 12-02-91522-CERN), and the U.S. National Science Foundation (grants AGS1136479 and CHE1012293).

## REFERENCES

Duplissy, J., Enghoff, M. B., Aplin, K. L., Arnold, F., Aufmhoff, H., Avngaard, M., Baltensperger, U., Bondo, T., Bingham, R., Carslaw, K., Curtius, J., David, A., Fastrup, B., Gagne, S., Hahn, F., Harrison, R. G., Kellett, B., Kirkby, J., Kulmala, M., Laakso, L., Laaksonen, A., Lillestol, E., Lockwood, M., Makela, J., Makhmutov, V., Marsh, N. D., Nieminen, T., Onnela, A., Pedersen, E., Pedersen, J. O. P., Polny, J., Reichl, U., Seinfeld, J. H., Sipila, M., Stozhkov, Y., Stratmann, F., Svensmark, H., Svensmark, J., Veenhof, R., Verheggen, B., Viisanen, Y., Wagner, P. E., Wehrle, G., Weingartner, E., Wex, H., Wilhelmsson, M., and Winkler, P. M.: Results from the CERN pilot CLOUD experiment, *ATMOSPHERIC CHEMISTRY AND PHYSICS*, 10, 1635-1647, 2010.

Kirkby, J., Curtius, J., Almeida, J., Dunne, E., Duplissy, J., Ehrhart, S., Franchin, A., Gagne, S., Ickes, L., Kurten, A., Kupc, A., Metzger, A., Riccobono, F., Rondo, L., Schobesberger, S., Tsagkogeorgas, G., Wimmer, D., Amorim, A., Bianchi, F., Breitenlechner, M., David, A., Dommen, J., Downard, A., Ehn, M., Flagan, R. C., Haider, S., Hansel, A., Hauser, D., Jud, W., Junninen, H., Kreissl, F., Kvashin, A., Laaksonen, A., Lehtipalo, K., Lima, J., Lovejoy, E. R., Makhmutov, V., Mathot, S., Mikkila, J., Minginette, P., Mogo, S., Nieminen, T., Onnela, A., Pereira, P., Petaja, T., Schnitzhofer, R., Seinfeld, J. H., Sipila, M., Stozhkov, Y., Stratmann, F., Tome, A., Vanhanen, J., Viisanen, Y., Vrtala, A., Wagner, P. E., Walther, H., Weingartner, E., Wex, H., Winkler, P. M., Carslaw, K. S., Worsnop, D. R., Baltensperger, U., and Kulmala, M.: Role of sulphuric acid, ammonia and galactic cosmic rays in atmospheric aerosol nucleation, *Nature*, 476, 429-U477, 10.1038/nature10343, 2011.

Kupc, A., Amorim, A., Curtius, J., Danielczok, A., Duplissy, J., Ehrhart, S., Walther, H., Ickes, L., Kirkby, J., Kurten, A., Lima, J. M., Mathot, S., Minginette, P., Onnela, A., Rondo, L., and Wagner, P. E.: A fibre-optic UV system for H<sub>2</sub>SO<sub>4</sub> production in aerosol chambers causing minimal thermal effects, *Journal of Aerosol Science*, 42, 532-543, 10.1016/j.jaerosci.2011.05.001, 2011.

Voigtlander, J., Duplissy, J., Rondo, L., Kurten, A., and Stratmann, F.: Numerical simulations of mixing conditions and aerosol dynamics in the CERN CLOUD chamber, *ATMOSPHERIC CHEMISTRY AND PHYSICS*, 12, 2205-2214, 10.5194/acp-12-2205-2012, 2012.

# IMPROVING THE SIZE RESOLUTION OF AIR ION MEASUREMENTS IN THE [1-6] nm RANGE

A. FRANCHIN<sup>1</sup>, J. KANGASLUOMA<sup>1</sup>, T. NIEMINEN<sup>1</sup>, K. LEHTIPALO<sup>1</sup>, A. DOWNARD<sup>2</sup>, J. DUPLISSY, THE CLOUD COLLABORATION, T. PETÄJÄ<sup>1</sup>, R. FLAGAN<sup>2</sup>, AND M. KULMALA<sup>1</sup>.

<sup>1</sup> Department of Physics, University of Helsinki, P.O. Box 64, FI-00014, Helsinki, Finland

<sup>2</sup>Department of Chemical Engineering, California Institute of Technology, 391 South Holliston Avenue, Pasadena, California 91125, USA

Keywords: AIR IONS, NANO RADIAL DMA, PARTICLE SIZE MAGNIFIER, CLOUD CHAMBER.

## INTRODUCTION

Measuring air ions is important for two main reasons, first because, under certain conditions, ions can enhance secondary aerosol production. They can act as seeds and lower the activation energy and start a gas to aerosol transition. If there is enough vapour to grow them to large enough sizes (50 to 90 nm) they can act as cloud condensation nuclei, modify properties of clouds and, therefore, influence the climate (Kirkby *et al.*, 2011). The second reason is that measuring, and more importantly improving ion measurements is the first step towards measuring neutral clusters and aerosol nano particles, once determined which charging mechanism is most suitable it is possible to transfer the technique to the neutral cluster measurements. The challenge in measuring air ions consists in maximizing the size resolution, possibly the time resolution as well, keeping the transmission efficiency high and proportional to the real concentrations (avoiding false counts or unknown size-dependent effects in the transmission efficiency). An instrument that measures ion size distributions at high size resolution in the range 1 to 6 nm would be complementary to the present commercial instrumentation e.g. Air Ion Spectrometer, AIS (Kulmala *et al.*, 2007) and Atmospheric Pressure interface Time of Flight Mass Spectrometer, APiTOF (Junninen *et al.* (2010)) adding valuable information about the link between formation and growth of atmospheric cluster ions, moreover it could be used as well for neutrals with a suitable inlet charger design.

## METHODS

In this study we used an instrumental setup consisting of a nano Radial DMA, nRDMA (Brunelli *et al.*, 2009) equipped with a new high transmission inlet and a Particle Size Magnifier, PSM Airmodus 09, (Vanhanen *et al.*, 2011) used as a counter.

We characterized the whole setup carrying out a set of experiments in the laboratory, in order to determine the transmission efficiency and the transfer functions of the DMA we used mobility standards and ammonium sulfate. We also determined the resolving power of the DMA calculating the full width at half maximum of mono-disperse aerosol at 1.5, 1.8, 2.3, 3.1 and 4 nm mobility equivalent diameter.

We also carried out measurement at the CLOUD chamber at CERN during the CLOUD7 campaign, using the new setup equipped with a cooling system for the sheath air to keep it at the same temperature as the chamber (5 °C) to avoid evaporation of the sample in the DMA

## RESULTS

We built and tested a new instrumental setup consisting of a PSM, a nRDMA and new high transmission inlet. The implementation of the high transmission inlet was essential to be able to measure concentrations of a few hundred ions per cc distributed in the size range [1.3 - 6] nm. We determined the transfer functions of this setup. The transmission efficiency at 1.5 nm is about 6% and the size resolution is about 7. We measured ion size distributions in the CLOUD7 campaign and we were able to retrieve grow rates that are of nice complement, connecting molecular sized ion cluster measured with the APiTOF and aerosol particles measured with an SMPS confirming the NAIS measurements in ion mode and providing additional information on the size development of the new born ion clusters and charged particles.

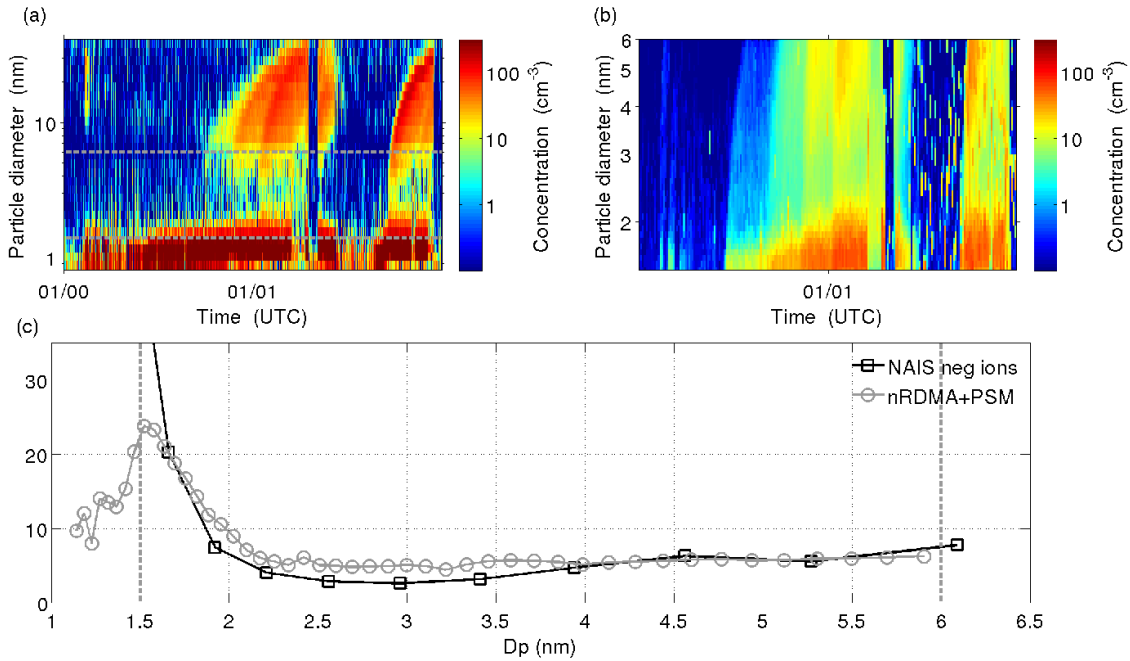


Figure 1: Comparison between measurements taken with the NAIS, panel (a), and our setup, panel (b), during the CLOUD7 campaign, note that where the concentration is dropping abruptly to zero, an electric field inside the chamber was turned on and the ions were swept away. In panel (a) the horizontal dashed lines delimit the size range overlapping with the size range measured using the nRDMA and PSM setup. In panel (b) is shown the corresponding number size distribution for the same time interval as in panel (a) and (b) plotted in linear scale.

## ACKNOWLEDGEMENTS

This research was supported by the Academy of Finland Center of Excellence program (project number 1118615). We would like to thank CERN for supporting CLOUD with important technical and financial resources, and for providing a particle beam from the CERN Proton Synchrotron. This research has received funding from the EC Seventh Framework Programme (Marie Curie Initial Training Network "CLOUD-ITN" grant n°. 215072, and ERC-Advanced "ATM-NUCLE" grant no. 227463), the German Federal Ministry of Education and Research (project n°. 01LK0902A), the Swiss National Science Foundation (project n°. 206621-125025 and 206620-130527), the Academy of Finland Center of Excellence program (project no. 1118615), the Austrian Science Fund (project n°. P19546 and L593), the Portuguese Foundation for Science and Technol-

ogy (project no. CERN/FP/116387/2010), and the Russian Foundation for Basic Research (grant N08-02-91006-CERN).

## REFERENCES

- N. A. Brunelli, R. C. Flagan, K. P. Giapis, *Aerosol Sci. Technol.* **43**, 53–59 (2009)
- H. Junninen, M. Ehn, T. Petäjä, L. Luosujärvi, T. Kotiaho, R. Kostianen, U. Rohner, M. Gonin, K. Fuhrer, M. Kulmala, and D. R. Worsnop, *Atmos. Meas. Tech.* **3**(4), 039–1053 (2010)
- Kirkby, J. and Curtius, J., Almeida, J., Dunne, E., Duplissy, J., Ehrhart, S., Franchin, A., Gagne, S., Ickes, L., Kurten, A., Kupc, A., Metzger, A., Riccobono, F., Rondo, L., Schobesberger, S., Tsagkogeorgas, G., Wimmer, D., Amorim, A., Bianchi, F., Breitenlechner, M., David, A., Dommen, J., Downard, A., Ehn, M., Flagan, R. C., Haider, S., Hansel, A., Hauser, D., Jud, W., Junninen, H., Kreissl, F., Kvashin, A., Laaksonen, Ari, Lehtipalo, Katrianne, Lima, Jorge, Lovejoy, Edward R., Makhmutov, Vladimir, Mathot, Serge, Mikkilä, J., Minginette, P., Mogo, S., Nieminen, T., Onnela, A., Pereira, P., Petäjä, T., Schnitzhofer, R., Seinfeld, J. H., Sipilä, M., Stozhkov, Y., Stratmann, F., Tome, A., Vanhanen, J., Viisanen, Yrjo, Vrtala, Aron, Wagner, Paul E., Walther, Hansueli, Weingartner, Ernest, Wex, Heike, Winkler, Paul M., Carslaw, K. S., Worsnop, D. R., Baltensperger, U., Kulmala, M., (2011). Role of sulphuric acid, ammonia, galactic cosmic rays in atmospheric aerosol nucleation. *Nature* **476**, 429–433.
- Kulmala, M., Riipinen, I., Sipilä, M., Manninen H. E., Petäjä, T., Junninen, H., Dal Maso, M., Mordas, G., Mirme, A., Vana, M., Hirsikko, H., Laakso, L., Harrison, R. M., Hanson, I., Leung, C., Lehtinen, K. E. J. and Kerminen, V-M. (2007). Toward Direct Measurement of Atmospheric Nucleation. *Science*, **318**, 89-92.
- J. Vanhanen, J. Mikkilä, M. Sipilä, T. Berndt and M. Kulmala, *Aerosol Sci. Technol.* **45**, 533–542 (2011)

# YEAR-ROUND MODELLING STUDY ON PARTICLE FORMATION ON A SOUTH AFRICAN SAVANNAH

R. GIERENS<sup>1</sup>, D. MOGENSEN<sup>1</sup>, L. ZHOU<sup>1</sup>, V. VAKKARI<sup>1</sup>, L. LAAKSO<sup>2,3</sup>, J.P. BEUKES<sup>3</sup>,  
P.G. VAN ZYL<sup>3</sup> and M. BOY

Department of Physics, Division of Atmospheric Sciences, University of Helsinki,  
Helsinki, 00014, Finland.

<sup>2</sup>Finnish Meteorological Institute, Research and Development, P.O. BOX 503, FI-00101, Finland.

<sup>3</sup>School of Physical and Chemical Sciences, North-West University, Potchefstroom, South Africa.

Keywords: AEROSOL MODELLING, PARTICLE FORMATION AND GROWTH, BOUNDARY LAYER, SOUTH AFRICAN SAVANNAH.

## INTRODUCTION

Africa is one of the less studied continents with regard to atmospheric aerosols both from a measurement and a modelling point of view. Savannahs are complex dynamic systems sensitive to climate and land-use changes, but the interaction with the atmosphere is not well understood. Atmospheric particles affect the climate on regional and global scale, and are an important factor in air quality. In this study measurements from a savannah environment in South Africa were used to model new particle formation and growth for a full year. There are already some combined long-term measurements of trace gas concentrations together with aerosol and meteorological variables available (Vakkari *et al.*, 2013), and we aim to utilize these for detailed simulations that include all the main processes relevant to particle formation. In the first part of the work a case study with 6 days was done, and in the second part the simulation was done for a full year.

## METHODS

In the first part of the work we did a case study, for which we selected 6 days during the local spring. The model used, Malte, is a column model that includes boundary layer meteorology, aerosol dynamical and chemical processes, as well as emissions from the canopy (Gierens *et al.*, 2013). The measurements were performed in South-Africa, at the Botsalano game reserve. The location is characterized with relatively low pollutant concentrations with occasional polluted air masses. New particle formation at the site has been found to take place during most of the sunny days – 69% of the days showing clear nucleation with additional 14 % of the days with non-growing nucleation mode (Vakkari *et al.*, 2013).

In the second part of the work we did a simulation for a full year. For this the model SOSAA (Model to Simulate the concentrations of Organic vapours, Sulphuric Acid and Aerosols) was used. It is a one-dimensional model, which includes modules for boundary layer meteorology, emissions from the canopy and chemical processes (Boy *et al.*, 2011). For this work a further developed version of the model was used, which also includes aerosol dynamics simulated with UHMA (University of Helsinki Multicomponent aerosol model). SOSAA has the advantage compared to Malte, that it is written in parallel enabling longer simulation times. UHMA focuses on new particle formation and growth (Korhonen *et al.*, 2004), and thereby SOSAA is well suited to study these phenomena. Boundary layer meteorology and plant-atmosphere interactions are solved by SCADIS (Scalar Distribution). The emissions of monoterpenes and other organic vapours from the canopy are calculated with MEGAN (Model of Emissions of Gases and Aerosols from Nature). The chemistry is calculated using the Kinetic PreProcessor (KPP), and chemical reaction equations are from the Master Chemical Mechanism (<http://mcm.leeds.ac.uk/MCM/>).

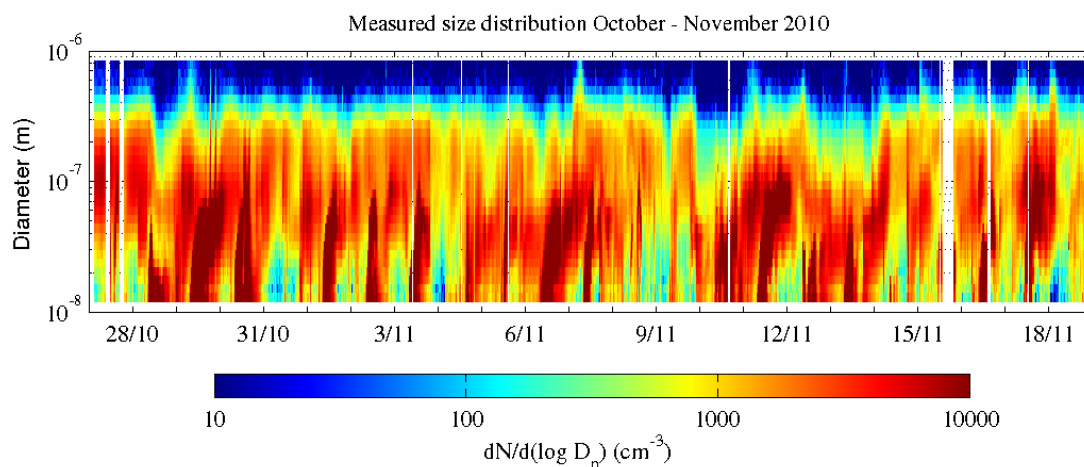


Figure 1. Observed size distribution in Welgegund, South Africa, during 23 days in October and November 2010.

The measurements utilized in the second part of the study were done at the Welgegund measurement station, a savannah site in northern South Africa, approximately 100 km west of Johannesburg. The site has very few local pollutant sources, but pollutant plumes from metropolitan and industrial areas are observed frequently, as well as clean air advected from areas with little anthropogenic sources. Figure 1 shows the measured size distribution for 23 days in October/November in 2010, which also shows the high frequency of nucleation events. More information about the station can be found at <http://www.welgegund.org/>.

The measurements include meteorological variables (temperature, relative humidity, wind speed and direction, precipitation, vertical temperature gradient, and radiation), trace gas concentrations ( $\text{SO}_2$ ,  $\text{NO}_x$ ,  $\text{CO}$ , and  $\text{O}_3$ ), flux measurements ( $\text{H}_2\text{O}$ ,  $\text{CO}_2$ , and sensible heat), soil measurements (moisture and heat at different depths), aerosol number size distribution, and concentrations of volatile organic compounds (VOC). Additionally, sensible and latent heat fluxes as well as soil temperature measurements from Welgegund were included in the second part of the study. The observational data was used for input and comparisons with the simulations.

The aim of simulating a full year is to be able to study the different air masses on the site as well as seasonal variations in particle formation. Knowledge from the case studies can be utilized in setting up the simulations. The data is processed for the model and the runs will be performed soon.

#### ACKNOWLEDGEMENTS

This work was supported by the Academy of Finland Center of Excellence (project no 1118615), and for computational resources CSC – IT Center for Science Ltd is gratefully acknowledged.

#### REFERENCES

- Boy, M., Sogachev, A., Lauros, J., Zhou, L., Guenther, A. and Smolander, S. (2011) SOSA - a new model to simulate the concentrations of organic vapours and sulphuric acid inside the ABL - Part I: Model description and initial evaluation, *Atmos. Chem. Phys.* **11**, 43.
- Gierens, R., Laakso, L., Mogensen, D., Vakkari, V., Beukes, P., van Zyl, P., Hakola, H., Guenther, A., Pienaar, J.J., Boy, M. Modelling new particle formation events in South African savannah, *South African Journal of Science*, under revision

- Korhonen, H., Lehtinen, K. E. J., and Kulmala, M. (2004) Multicomponent aerosol dynamics model UHMA: model development and validation, *Atmos. Chem. Phys.* **4**, 471.
- V. Vakkari, J. P. Beukes, H. Laakso, D. Mabaso, J. J. Pienaar, M. Kulmala, and L. Laakso (2013). Long-term observations of aerosol size distributions in semi-clean and polluted savannah in South Africa, *Atmos. Chem. Phys.* **13**, 1751.

# HYGROSCOPICITY OF SUB-6 NM SODIUM CHLORIDE AND AMMONIUM BISULFATE PARTICLES

J. HAKALA<sup>1</sup>, J. KANGASLUOMA<sup>1</sup> AND T. PETÄJÄ<sup>1</sup>

<sup>1</sup>Division of Atmospheric Sciences, Department of Physics, University of Helsinki, 00014 University of Helsinki, Finland.

Keywords: HYGROSCOPICITY, HTDMA.

## INTRODUCTION

Some studies suggest that the hygroscopic growth of water soluble salt particles may not follow the Köhler theory with particles below the diameter of 8 nm (Hakala *et al.*, 2013; Biskos *et al.*, 2006a). So far the hygroscopic growth of salt particles has not been studied below the mobility diameter of 6 nm (Biskos *et al.*, 2006a; Biskos *et al.*, 2006b; Hämeri *et al.*, 2001; Hämeri *et al.*, 2000). In this study we present our investigations in hygroscopic growth of sodium chloride (NaCl) and ammonium bisulfate (NH<sub>4</sub>HSO<sub>4</sub>) measured with a specially made nano Hygroscopicity Tandem Differential Mobility Analyzer (nHTDMA) from mobility diameter of 2.5 nm to 6 nm and in relative humidities from 10% to 95%.

## METHODS

The nHTDMA is consisted of a high resolution Herrmann Differential Mobility Analyzer (HDMA) for selecting the initial mobility diameter, a humidifier, and a TSI nano Differential Mobility Analyzer (nDMA, TSI DMA 3085) for measuring the mobility diameter after the humidifying. The nDMA was used in a closed loop arrangement and the particles were detected with a Condensation Particle Couter (CPC, TSI 3776). This way the humidifying is easy to achieve and keep stable with just one humidifier. The particles were produced in a tube furnace by vaporization-condensation method in ultrapure nitrogen carrier gas flow (Kangasluoma *et al.*, 2013). To convert the agglomerates produced by this method (Krämer *et al.*, 2000) into cubical crystals, the sample aerosol flow was humidified with an additional humidifier and cooled to 2°C. The aerosol experienced supersaturated conditions inside the cooling unit undergoing a phase transition into solute droplets. After drying in a silica gel diffusion dryer the NaCl particles were assumed to be cubical crystals. When producing NH<sub>4</sub>HSO<sub>4</sub> particles, the humidifier and cooling unit were bypassed as the NH<sub>4</sub>HSO<sub>4</sub> particles are almost spherical crystals. In Fig. 1 is the schematic of the measurement setup.

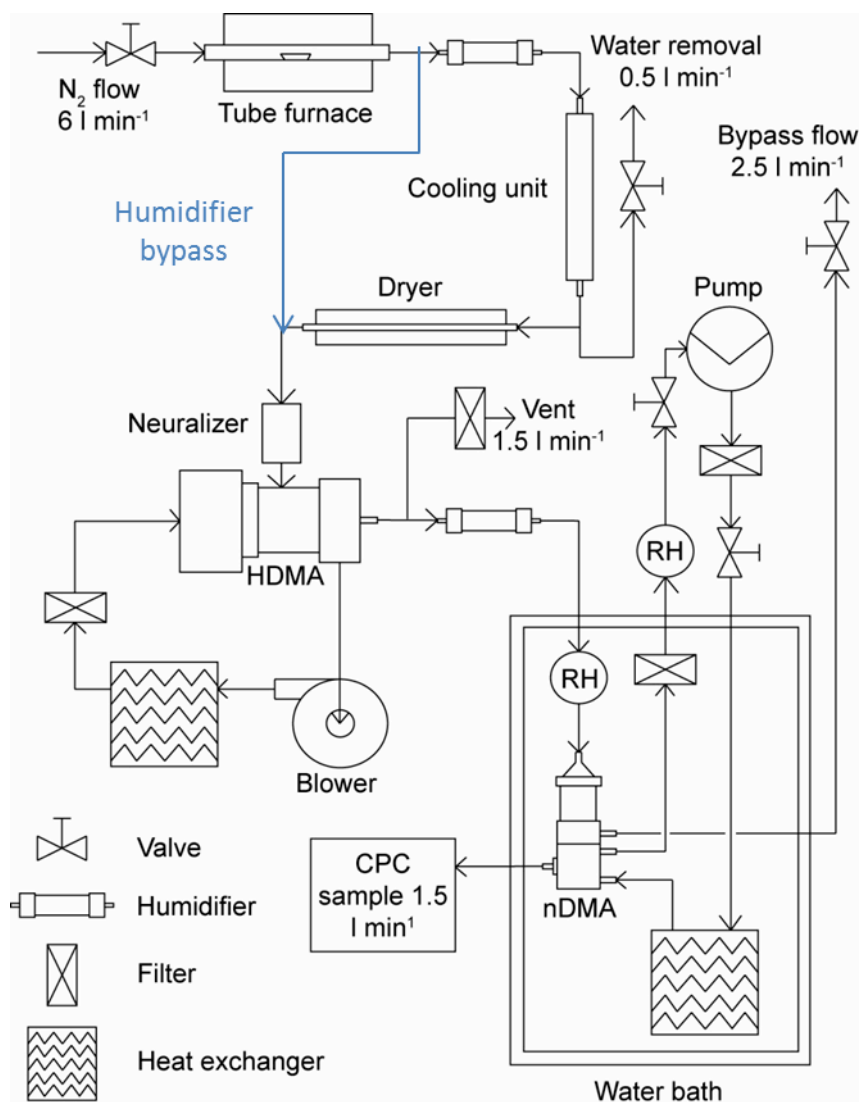


Figure 1. The measurement setup.

## RESULTS AND DISCUSSION

The Hygroscopic Growth Factors (HGF=diameter of humidified particle/diameter of dry particle) in different RH conditions were measured for NaCl and  $\text{NH}_4\text{HSO}_4$  particles with mobility diameters of 2.5 nm, 3 nm, 4 nm, 5 nm and 6 nm. The results are presented in Fig. 2 and Fig. 3, respectively. The Köhler effect can be clearly seen in diminishing HGF when moving to a smaller particle size. While comparing the theoretical prediction with the measured results, it is evident that the Köhler theory overestimates the growth in both cases. The Deliquescence Relative Humidities (DRH) were also determined for 4 nm, 5 nm and 6 nm NaCl particles. The DRH was higher the smaller the particle was. Particles below the mobility diameter of 4 nm had higher DRH than 95%. The DRHs for NaCl are collected in Table 1. The DRHs for  $\text{NH}_4\text{HSO}_4$  couldn't be determined.

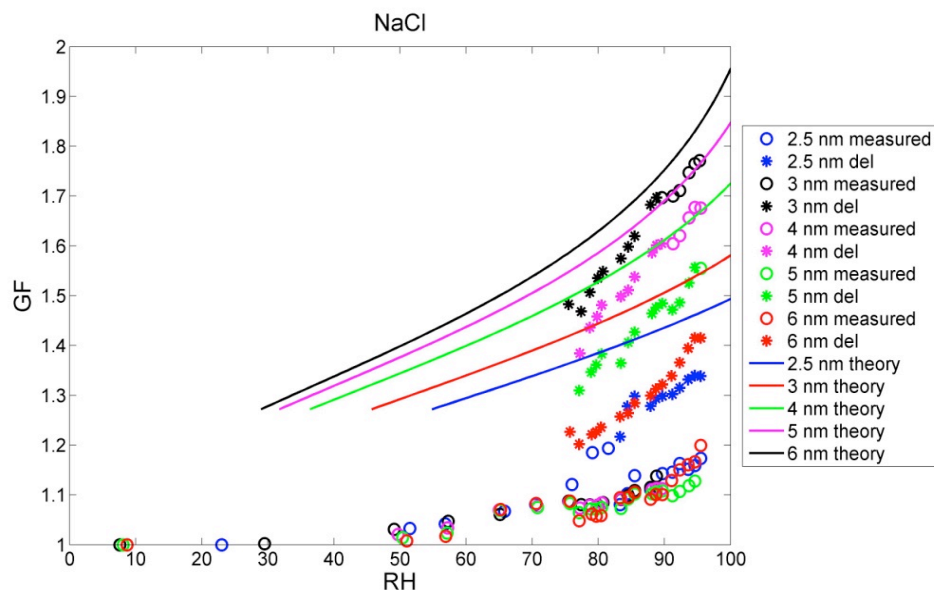


Figure 2. Theoretical and measured hygroscopic growth factors of NaCl particles. The asterisks represent particles that have experienced RH above the deliquescence RH, but are measured below deliquescence RH. Thus, the deliquescence RH is at the RH where asterisks turn into open circles.

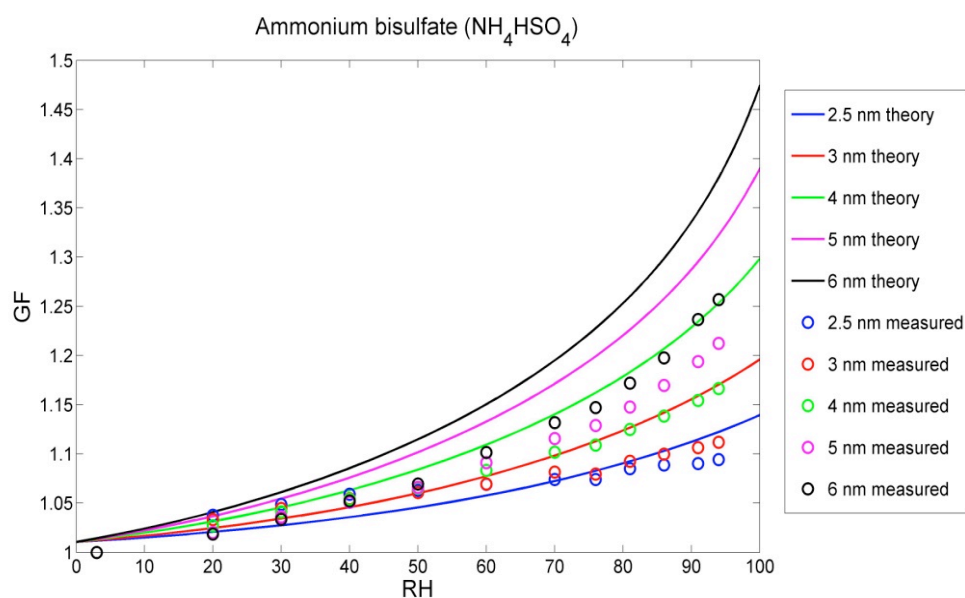


Figure 3. Theoretical and measured hygroscopic growth factors of  $\text{NH}_4\text{HSO}_4$  particles.

Particle diameter [nm]	Deliquescence RH [%]	Reference value [%]
2.5	-	-
3	-	-
4	95	-
5	91	-
6	90	87 (Biskos <i>et al.</i> , 2006b)

Table 1. Measured deliquescence RHs for NaCl particles.

## ACKNOWLEDGEMENTS

This research was supported by Academy of Finland (project 139656) and Academy of Finland Center of Excellence (project no 1118615).

## REFERENCES

- Biskos, G., L. M. Russell, P. R. Buseck, and S. T. Martin (2006a). Nanosize effect on the hygroscopic growth factor of aerosol particles. *Geophys. Res. Lett.*, **33**, L07801.
- Biskos, G., A. Malinowski, L. M. Russell, P. R. Buseck, and S. T. Martin (2006b). Nanosize effect on the deliquescence and the efflorescence of sodium chloride particles. *Aerosol Sci. Technol.* **40**, 97-106.
- Hakala, J., H. E. Manninen, T. Petäjä and M. Sipilä (2013). Counting efficiency of TSI environmental particle counter monitor model 3783. *Aerosol Sci. Technol.* **47**, 482-487.
- Hämeri, K., M. Väkevä, H-C Hansson and A. Laaksonen (2000). Hygroscopic growth of ultrafine ammonium sulfate measured with ultrafine tandem differential mobility analyzer. *J. Geophys. Res.*, **105**, 22231-22242.
- Hämeri, K., A. Laaksonen, M. Väkevä and T. Suni (2001). Hygroscopic growth of ultrafine sodium chloride particles. *J. Geophys. Res.*, **106**, 20749-20757.
- Kangsluoma, J., H. Junninen, K. Lehtipalo, J. Mikkilä, J. Vanhanen, M. Attoui, M. Sipilä, D. Worsnop, M. Kulmala, and T. Petäjä (2013). Remarks on ion generation for CPC detection efficiency studies on sub-3-nm size range. *Aerosol Sci. Technol.*, **47**, 566-563.
- Krämer, L., U. Pöschl, and R. Niessner (2000). Microstructurel reanrrangement of sodium chloride condensation aerosol particles on interaction with water vapor. *J. Aerosol Sci.*, **31**, 673–685.

# OBSERVATION OF ATMOSPHERIC ORGANIC NITRATE AEROSOLS AND APPLICATION IN CLOUDS BY AEROSOL MASS SPECTROMETRY

L.Q. HAO<sup>1</sup>, S. ROMAkkANIEMI<sup>1</sup>, A. KORTelAINEN<sup>1</sup>, A. JAATINEN<sup>1</sup>, H. PORTIN<sup>1,2</sup>, P. MIETTINEN<sup>1</sup>, M. KOMPPULA<sup>2</sup>, A. LESKINEN<sup>2</sup>, J.N. SMITH<sup>1,4</sup>, D. SUEPER<sup>4</sup>, D.R. WORSNOP<sup>1,3,5</sup>, K. LEHINEN<sup>1,2</sup>, A. LAAKSONEN<sup>1,3</sup> and A. VIRTANEN<sup>1</sup>

<sup>1</sup>Department of Applied Physics, University of Eastern Finland, Kuopio, P.O. Box 1627, Finland

<sup>2</sup>Finnish Meteorological Institute, Kuopio Unit, Kuopio, P.O. Box 1627, Finland

<sup>3</sup>Finnish Meteorological Institute, Research and Development, Helsinki, P.O. Box 503, Finland

<sup>4</sup>National Centre for Atmospheric Research, Boulder, CO, P.O. Box 3000, USA

<sup>5</sup>Department of Physics, University of Helsinki, Helsinki, P.O. Box 64, Finland

Keywords: CLOUD, CHEMICAL COMPOSITION, ORGANIC NITRATE AEROSOL, AMS.

## INTRODUCTION

Boreal forests emit large amounts of biogenic volatile organic compounds (VOCs). The photochemical or nocturnal oxidation reactions of these VOCs can produce large, multifunctional organic nitrates with vapor pressure potentially low enough to condense and form secondary organic aerosol (SOA). This process contributes 0.5%-8% of the total SOA mass loading in a global scale (Fry et al., 2009; Hao et al., 2013a). Despite the potential importance of organic nitrate aerosol, it remains a nearly unexplored aspect of atmospheric chemistry. The mechanism behind organic nitrate production are poorly understood and generally ignored in model due in part to a lack of measurement approaches.

The traditional off-line analysis of organic nitrate aerosols by Fourier Transform Infrared Spectroscopy and the on-line detection by thermal dissociation-laser induced fluorescence are subject to contamination interference, detection limit and time resolution, limiting their wide implication. Recently developed Aerodyne High Resolution Time-of-Flight Aerosol Mass Spectrometer (HR-ToF-AMS) has been widely used by the aerosol research community by the advantage of its fast data acquisition, low detection limit, and specially the ability of separation of ions with the same nominal mass but different elemental composition that were previously obscured among ions in the unit resolution spectra and facilitates the better identification of aerosol components (e.g. N-containing compounds) (Farmer et al., 2010). This provides the possible solution of measurement of ambient organic nitrates.

The paper focuses on the application the HR-ToF-AMS in the detection of chemical composition in the real atmospheric clouds. The aim is to investigate the role of organic nitrate aerosol in cloud formation.

## METHODS

The observation of cloud events was carried during Sep. 21-Oct. 27, 2010 in Puijo Cloud Experiment 2010 campaign (PuCE2010). (Hao et al., 2013b). The observation station is located on the top of Puijo tower in Kuopio. An Aerodyne high resolution aerosol time-of-flight mass spectrometer (TOF-AMS) was used to measure the chemical composition of cloud particles (DeCarlo et al., 2006). During cloud events, samples from the cloud were introduced into the instruments through two parallel sampling lines. The first one is a PM<sub>tot</sub> sampling line. It took particles with a typical cut-off size of 40 µm. The inlet was heated (to 40 °C) in order to dry the cloud droplets. From this inlet line we obtained the total particle size distribution (TOT) including both cloud interstitial particles (INT) and cloud droplet residuals (RES). The other is a PM<sub>1.0</sub> sampling line. Samples from this line provided the chemical information of cloud interstitial particles. In order to separate contributions of organic nitrate and inorganic nitrate to aerosol chemical composition during the cloud event, we also performed positive matrix factorization (PMF) analysis on the high

resolution mass spectra (Ulbrich et al., 2009). Supporting measurements on the aerosol, gas and meteorological parameters were also made.

## RESULTS AND DISCUSSION

The weather conditions during the study were characterized with relatively low temperature (-4-12°C) and high RH (40-100%). The wind speed was at  $8.4 \pm 3.2 \text{ m s}^{-1}$  with an average high speed. Its directions were predominantly from southern, southwestern and northwest, accounting for 16.5%, 28.5% and 26.6% of wind arriving at the station, respectively. Other directions from north and west contributed to 15.1% of the wind while wind from eastern direction was rarely blown to the measurement site in this campaign.

The masses of individual chemical species, chemical composition, and total mass concentration from ASM measurements showed dramatic variations. Multiday episodes of fine particle plumes were interleaved with clean periods following the arrival of clear air mass from northern direction and rainfall events. Occasionally we have observed few spikes in the time series of sulfate, nitrate and organic species during Sep. 27- 28. Generally, the total aerosol mass concentrations by AMS compare well with the collocated measurement via DMPS, demonstrating a linear correlation to each other with the Person coefficient  $R^2=0.92$ . The statistics of the mass concentrations of each species are summarized in table 1. A broad range of PM1 total mass concentration between 0.19-12.9  $\mu\text{g m}^{-3}$  was observed with mean mass concentration of 2.27  $\mu\text{g m}^{-3}$ . All the individual species varied very largely alike the total mass. Organic frequently comprises the largest fraction of PM1 with the contributions of more than 50% for ~ 63% of the time, while sulfate is the second one (Fig 2e). On average, organic and sulfate accounted for 52.7 % and 31.2 % of PM1 mass, respectively, with the rest being ammonium (10.0 %), nitrate (5.4 %) and chloride (0.7 %).

Table 1 Summarization of mass concentrations of PM1 species during the campaign

( $\mu\text{g m}^{-3}$ )	Total	Organics	Sulfate	Nitrate	Ammonium	Chloride
Mean	2.27	1.19	0.71	0.12	0.23	0.02
1 $\sigma$	2.28	1.17	0.83	0.14	0.30	0.02
Median	1.40	0.75	0.37	0.08	0.10	0.01
Minimum	0.19	0.08	0.07	0.01	0.01	< D.L.
Maximum	12.9	6.57	7.49	2.12	2.94	0.22

PMF analysis of the high-resolution mass matrix of organic species together with NO and NO<sub>2</sub> ions identified four aerosol types. They were categorized to three organic components: hydrocarbon-like organic aerosol (HOA), semi-volatile oxygenated OA (SVOOA), low-volatile oxygenated OA (LVOOA), and one inorganic factor: nitrate inorganic aerosol (NIA). The components are determined by their mass spectra signatures, the correlation of their time series with tracers and optimized in the PMF evaluation tool (Ulbrich et al., 2009). Figure 1 shows the mass spectra profiles of the four factors, their time series of mass concentrations and comparison to the co-located measurement of tracers. The four factors account for 98.9% of the total fitted aerosol masses. Of which, 50.5% of the aerosol masses is from SVOOA, 33.4% from LVOOA, 8.2% from HOA, and the rest (6.8%) is attributed to the contribution from NIA component. For the NIA factor, it is the mixture of organic and inorganic signals. The mass spectrum signature is dominated by the inorganic NO and NO<sub>2</sub> ions, composing of 86% of the mass of this factor with the rest species from organic fragments. On average, the organic ions constitute 94.1% of the fitted aerosol species, in contract to 5.9% for inorganic ions.

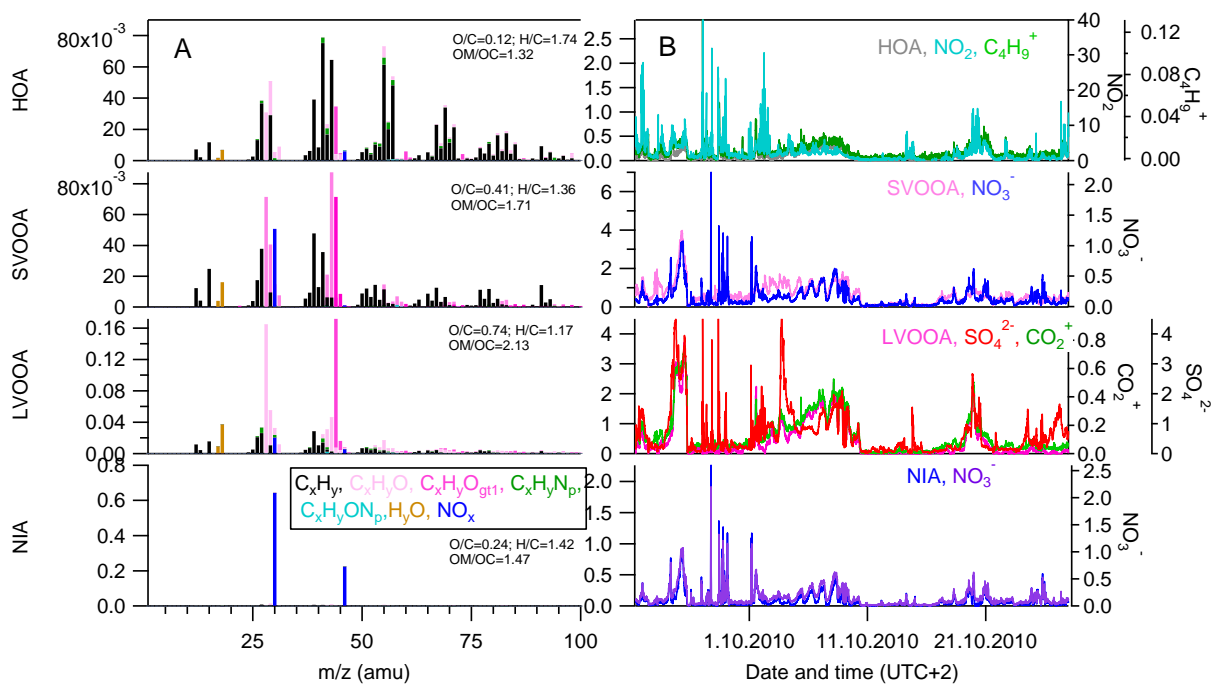


Figure 1 Time series and mass profiles identified by PMF solutions and correlations with tracers.

The signal of nitrate in AMS was dominated by  $\text{NO}^+$  and  $\text{NO}_2^+$  ions, the sum of which accounted for 96% of the total nitrate mass in this study. Previous studies have reported the strong dependence of the ratio  $\text{NO}^+/\text{NO}_2^+$  on nitrate compounds. PMF results showed that the majority of  $\text{NO}^+$  and  $\text{NO}_2^+$  ions were extracted as the  $\text{NH}_4\text{NO}_3$  factor while the rest were distributed in the organic factors. The sum of  $\text{NO}^+$  and  $\text{NO}_2^+$  ions in each organic factor enables the derivation of total organic nitrate ( $\text{NO}_3^-_{\text{org}}$ ) and inorganic nitrate ( $\text{NO}_3^-_{\text{inorg}}$ ) in a similar way:

$$\text{NO}_3^-_{\text{org}} = (\text{NO}^+_{\text{org}} + \text{NO}_2^+_{\text{org}}) / 0.96 \quad (2)$$

$$\text{NO}_3^-_{\text{inorg}} = (\text{NO}^+_{\text{inorg}} + \text{NO}_2^+_{\text{inorg}}) / 0.96 \quad (3)$$

where  $\text{NO}^+_{\text{org}}$  and  $\text{NO}_2^+_{\text{org}}$  are the sum of mass concentrations of  $\text{NO}^+$  and  $\text{NO}_2^+$  ions in each organic factor, respectively and  $\text{NO}^+_{\text{inorg}}$  and  $\text{NO}_2^+_{\text{inorg}}$  are the mass concentrations of  $\text{NO}^+$  and  $\text{NO}_2^+$  ions in the  $\text{NH}_4\text{NO}_3$  factor. The factor 0.96 is the mass fraction of  $\text{NO}^+$  and  $\text{NO}_2^+$  ions accounting for the entire nitrate mass.  $\text{NO}_3^-_{\text{inorg}}$  refers to inorganic nitrate in the form of  $\text{NH}_4\text{NO}_3$  from the PMF.

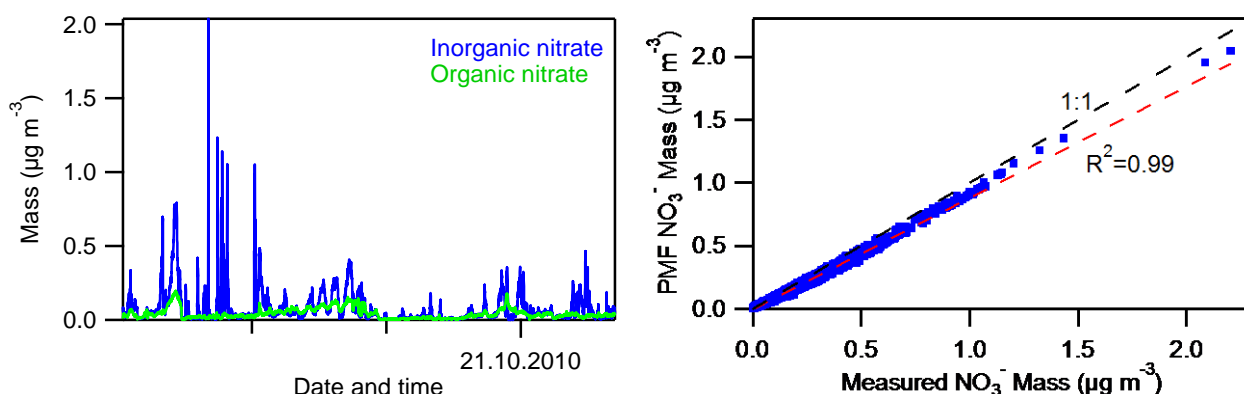


Figure 2 The determined time series of organic nitrate aerosols in the campaign.

The determined time series of organic nitrate aerosols in the campaign is shown in Figure 2. The nitrate mass concentrations are tabulated in the middle columns of Table 2. For the INT particles organic nitrate accounted for 51% of the total nitrate and the rest of nitrate was in the form of  $\text{NH}_4\text{NO}_3$ . In contrast, the mass

fraction of organic nitrate in the RES particles was only 26%, only half of the percentage of the INT particles. Organic nitrate contributed 36% to the total nitrates during the no-cloud period.

As a supplementary verification of PMF fitting results, a box model was also developed to estimate the masses of inorganic and organic nitrates. The model assumes that nitrates exist only in the forms of organic nitrate and  $\text{NH}_4\text{NO}_3$  in this study. Because the measurement site is surrounded by boreal forests where monoterpenes dominate the emitted volatile organic compounds, we took the ratios of  $\text{NO}^+/\text{NO}_2^+$  as 10 for organic nitrate according to the reactions of monoterpenes with  $\text{NO}_3$  radicals. From the mass balances of  $\text{NO}^+$  and  $\text{NO}_2^+$  ions, we have

$$\text{NO}_{\text{org}}^+ + \text{NO}_{\text{inorg}}^+ = \text{NO}_{\text{tot}}^+ \quad (4)$$

$$\text{NO}_{2,\text{org}}^+ + \text{NO}_{2,\text{inorg}}^+ = \text{NO}_{2,\text{tot}}^+ \quad (5)$$

$$\text{NO}_{\text{org}}^+ / \text{NO}_{2,\text{org}}^+ = 10 \quad (6)$$

$$\text{NO}_{\text{inorg}}^+ / \text{NO}_{2,\text{inorg}}^+ = 2.8 \quad (7)$$

where  $\text{NO}_{\text{tot}}^+$  and  $\text{NO}_{2,\text{tot}}^+$  are ion concentrations from direct AMS measurements, the values for which are well known. The factor of 2.8 is the ratio of  $\text{NO}^+/\text{NO}_2^+$  for  $\text{NH}_4\text{NO}_3$  in this study.  $\text{NO}_{\text{org}}^+$ ,  $\text{NO}_{\text{inorg}}^+$ ,  $\text{NO}_{2,\text{org}}^+$  and  $\text{NO}_{2,\text{inorg}}^+$  are four unknown variables, for which we seek a solution.

Table 2. Distributions of organic nitrate and inorganic nitrate during the cloud events.

Mass concentration ( $\mu\text{g m}^{-3}$ )	AMS measurements			PMF fitting			Calculations***		
	TOT	INT	RES**	TOT	INT	RES**	TOT	INT	RES**
$\text{NO}_3^-, \text{org}$	-	-	-	$0.11 \pm 0.011$	$0.050 \pm 0.017$	0.060	$0.099 \pm 0.022$	$0.042 \pm 0.013$	0.057
$\text{NO}_3^-, \text{inorg}^*$	-	-	-	$0.22 \pm 0.039$	$0.048 \pm 0.028$	0.172	$0.21 \pm 0.030$	$0.051 \pm 0.029$	0.16
$\text{NO}_3^-, \text{total}$	$0.31 \pm 0.037$	$0.094 \pm 0.043$	0.22	$0.33 \pm 0.040$	$0.098 \pm 0.045$	0.23	$0.31 \pm 0.034$	$0.094 \pm 0.041$	0.22
Fra. $\text{NO}_3^-, \text{org}$ (%)	-	-	-	$34 \pm 5$	$51 \pm 7$	26	$32 \pm 6$	$45 \pm 8$	26
Fra. $\text{NO}_3^-, \text{inorg}$ (%)	-	-	-	$66 \pm 5$	$49 \pm 7$	74	$68 \pm 6$	$55 \pm 8$	74

\* refers to nitrate in form of  $\text{NH}_4\text{NO}_3$

\*\* RES = TOT-INT

\*\*\* based on the equations (2)-(7)

By substituting the above solution for the four ions into Eqs.(2) and (3), we are able to calculate the masses of organic and inorganic nitrate, listed in the right side columns in Table 1. A nice correspondence between the calculation and PMF fitting gives us confidence that the calculation assumption is valid.

## CONCLUSIONS

This work demonstrates the distinct difference in the chemical compositions between the cloud interstitial particles and cloud droplet residuals from the HR-ToF-AMS measurements. We have observed much higher mass fractions of organic nitrate and less oxidized organic compounds in the cloud interstitial particles than in the cloud droplet residuals. The chemical difference can be attributed to the activation ability of aerosol particles into cloud droplets and to subsequent occurred gas-particle partitioning mechanisms in and out of the cloud as well as particle size effects. The results will have potential implications in facilitating the aerosol-cloud modeling study and in advancing our understanding of the cloud formation and global climate change.

## ACKNOWLEDGEMENTS

This work was supported by Academy and Finland Centre of Excellence of Programme (project no 1118615), UEF Postdoc Research Foundation (No. 930275) and the strategic funding of the University of Eastern Finland.

## REFERENCES

- DeCarlo, P.F., Kimmel, J.R., Trimborn, A., Northway, M.J., Jayne, J.T., Aiken, A.C., Gonin, M., Fuhrer, K., Horvath, T., Docherty, K., Worsnop, D.R., Jimenez, J.L (2006). Field-Deployable, High-Resolution, Time-of-Flight Aerosol Mass Spectrometer. *Anal. Chem.* **78**, 8281.
- Farmer, D. K., Matsunaga, A.,Docherty, K. S., Surratt, J. D., Seinfeld, J. H.,Ziemann, P. J., Jimenez, J. L. (2010). Response of an aerosol mass spectrometer to organonitrates and organosulfates and implications for atmospheric chemistry. *Proc. Natl. Acad. Sci. U. S. A.* **107**, 6670.
- Fry, J. L., Kiendler-Scharr, A., Rollins, A. W., Wooldridge, P. J., Brown, S. S., Fuchs, H., Dubé, W., Mensah, A., dal Maso, M., Tillmann, R., Dorn, H.-P., Brauers, T., and Cohen, R. C. (2009). Organic nitrate and secondary organic aerosol yield from NO<sub>3</sub> oxidation of  $\beta$ -pinene evaluated using a gas-phase kinetics/aerosol partitioning model. *Atmos. Chem. Phys.*, **9**, 1431.
- Hao, L. Q., et al., (2013a). Chemical Characterization and Organic Nitrate of Atmospheric Aerosols by Aerosol Mass Spectrometry in the Forestland-Urban Interface, *in preparation*.
- Hao, L. Q., Romakkaniemi, S., Kortelainen, A., Jaatinen, A., Portin, H., Miettinen, P., Leskinen, A., Virtanen, A., Super, D., Smith, J.N., Worsnop, D.R., Lehtinen K.E.J. and Laaksonen, A. (2013b). Aerosol Chemical Composition in Cloud Event by High Resolution Time-of-flight Aerosol Mass Spectrometer, *Environ. Sci. Technol.*, **47**, 2645.
- Ulbrich, I.M., Canagaratna M.R., Zhang Q., Worsnop, D.R., Jimenez, J.L (2009). Interpretation of Organic Components from Positive Matrix Factorization of Aerosol Mass Spectrometric Data. *Atmos. Chem. Phys.* **9**, 2891.
- Zhang, Q., Jimenez, J.L., Worsnop, D.R., Canagaratna, M. (2007). A case study of urban particle acidity and its influence on secondary organic aerosol. *Environ. Sci. Technol.* 2007, **41**, 3213.

# FOREST SOIL AMINES: ECTOMYCORRHIZAL FUNGI IS SIGNIFICANT RESERVOIR BUT IS IT ALSO A SOURCE OF VOLATILE AMINES?

J. HEINONSALO<sup>1</sup>, A.-J. KIELOAHO<sup>1</sup>, K. BÄCKLUND<sup>1</sup>, M. KULMALA<sup>2</sup>, M. PIHLATIE<sup>2</sup>, J. PUMPANEN<sup>3</sup>, M.-L. RIEKKOLA<sup>4</sup>, T. VESALA<sup>2</sup> and J. PARSHINTSEV<sup>4</sup>

<sup>1</sup>Department of Food and Environmental Sciences,  
P.O. BOX 56, FIN-00014 University of Helsinki, Finland

<sup>2</sup>Department of Physics, Division of Atmospheric Sciences,  
P.O. BOX 48, FIN-00014 University of Helsinki, Finland

<sup>3</sup>Department of Forest Sciences,  
P.O. Box 27, FIN-00014 University of Helsinki, Finland

<sup>4</sup>Department of Chemistry, Laboratory of Analytical Chemistry  
P.O. Box 55, FIN-00014 University of Helsinki, Finland

Keywords: FOREST SOIL, FUNGI, AMINES.

## INTRODUCTION

The major part of nitrogen (N) in boreal forest soil is in organic form (Soil Organic Nitrogen, SON) and largely in forms not directly available for plants or microbes (Knicker, 2011). One of the main pathways for amine production is amino acid decarboxylation where amino acids react with specific decarboxylase enzymes which transform them to amines. Therefore, amino acid production by protease enzymes might be the critical step for amine production and release from forest soil.

The aim of the study was to determine forest soil amine pools and investigate what is the role of forest soil fungi as amine storage, and in transformations and release of volatile forms into the atmosphere.

## METHODS

Several experiments were performed to investigate the pools and sources of amines in boreal forest soil: In the first trial (1), forest soil was collected from SMEAR II research site in Hyytiälä and the amine concentrations from the soil extract was analysed. From the same soil, fungal hyphal biomass was collected using microscope and fine forcips. Amines in fungal biomass, and soil from the same site were compared (Figure 1).

In the second experiment (2), biomass from 25 different fungal strain from four different functional groups were analysed for their amine content to investigate are there any species-specific differences in fungal amine content.

In the third experiment (3), after identifying *Piloderma croceum* as the most amine containing fungal species of the studied ones, the occurrence of *Piloderma* species in Hyytiälä over one growth season was studied. Additionally, protease enzyme activity of *Piloderma* pure culture strains was investigated.

In the fourth and last experiment (4), *Piloderma croceum* was cultivated in axenic laboratory conditions on three different growth media: one containing mainly  $\text{NH}_4^+$  and  $\text{NO}_3^-$  as N source, one containing amino acids and one containing proteins as main N source. From the cultures, the release of volatile amines, amines excreted into the media and amines bound to fungal biomass were measured.

From all the experiments, amines were measured by high performance liquid chromatography-triple quadrupole mass spectrometry (HPLC-QQQ, Agilent) after extraction and derivatization with dansyl chloride. Liquid samples were directly derivatized while solid samples were extracted by dynamic

sonication assisted extraction prior derivatization. Multiple reaction monitoring of dansylated fragments was chosen in order to increase sensitivity and selectivity of the method.

## CONCLUSIONS

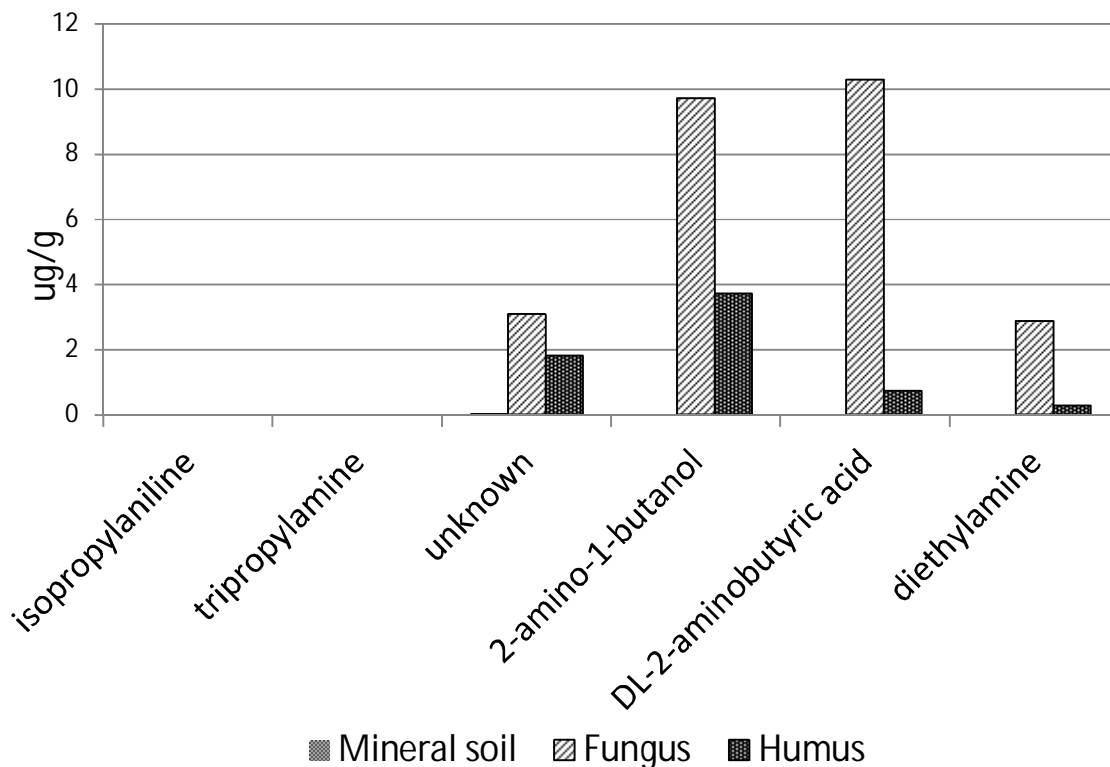


Figure 1. Amine concentrations in humus and fungal biomass at SMEAR II station in Hyytiälä.

The series of experiments revealed that fungal biomass may explain high amine concentrations in soil. One of the most common ectomycorrhizal fungal species in soil at SMEAR II station, *Piloderma croceum*, seem to contain large quantities of amines and as having the ability to produce high protease activities, may play a key role in soil organic N transformations and amine synthesis. The potential significance of soil as a source of volatile amines and its seasonality needs further investigations.

## ACKNOWLEDGEMENTS

This work was supported by Academy of Finland Research grants 263858, 259217, 218094 and Academy of Finland Centre of Excellence program (project no 1118615) and the Nordic Centers of Excellence CRAICC and DEFROST.

## REFERENCES

Knicker, H. (2011) Soil organic N – An under-rated player for C sequestration in soils? *Soil Biol. Biochem.* **43**, 1118-1129.

# INSIGHTS INTO THE IMPACT OF HYDRATION ON SULPHURIC ACID/BASE MEDIATED PARTICLE FORMATION

H. HENSCHER<sup>1</sup>, O. KUPIAINEN-MÄÄTTÄ<sup>1</sup>, T. OLENIUS<sup>1</sup>, I. K. ORTEGA<sup>1</sup>, T. KURTÉN<sup>2</sup> and H. VEHKAMÄKI<sup>2</sup>

<sup>1</sup>Division of Atmospheric Sciences, Department of Physics, P.O. Box 64,  
00014 University of Helsinki, Finland.

<sup>2</sup>Laboratory of Physical Chemistry, Department of Chemistry, P.O. Box 55,  
00014 University of Helsinki, Finland.

Keywords: PARTICLE FORMATION, SULPHURIC ACID, WATER, COMPUTATIONAL CHEMISTRY.

## INTRODUCTION

The formation of new particles in the atmosphere through condensation from gas phase is generally agreed to involve sulphuric acid and water. It is, however, known that these compounds alone are insufficient in order to explain the observed particle formation rates (Kulmala *et al.* 2004). Thus, several contributions increasing the nucleation rate have been discussed. Amongst others, involvement of ions, ammonia or organic compounds has been suggested. One component that is generally accepted to be able to augment sulphuric acid-water nucleation is ammonia, though its effect is known to be too small to explain observed nucleation rates. Other important candidates for explanation of elevated nucleation rates are amines. It has been shown that several different amines bind much more strongly to sulphuric acid than ammonia – to an extent that they are potentially able to enhance particle formation more than ammonia (Kurtén *et al.* 2008). While the hydration of pure sulphuric acid clusters has been examined in a number of studies – certainly small systems containing less than three acid molecules have been thoroughly studied, studies also including the hydrates of ammonia-, or dimethylamine-containing systems are less abundant. Additionally, the use of different methodologies in different studies makes the results impossible to compare directly. We have now studied the hydration of the most relevant clusters containing up to four sulphuric acid molecules and up to three ammonia or two dimethylamine molecules.

## METHODS

Electronic structure calculations were performed using a multi step approach (Ortega *et al.* 2012). For each cluster composition a series of geometries was optimized using the Gaussian 09 program package (Frisch *et al.* 2009) with the B3LYP functional (Becke 1993) and CBSB7 basis set. Single point calculations were then performed on several clusters within approximately 3 kcal/mol of the lowest Gibbs free energy at B3LYP/CBSB7 level for each composition. Single point energy calculations were performed using the Turbomole program package (TURBOMOLE 2011) for the RICC2 method (Christiansen *et al.* 2011) with a aug-cc-pV(T+d)Z basis set for sulphur, and aug-cc-pVTZ for all other atoms. From the obtained formation Gibbs free energies, relative concentrations of the hydrated clusters were calculated at several values for the relative humidity, assuming chemical equilibrium under standard conditions. Individual hydrate concentrations were also converted into average number of water molecules bound per cluster of respective type.

## RESULTS AND DISCUSSION

The obtained average hydration numbers for pure sulphuric acid clusters are illustrated in Fig 1a. While clusters with up to three molecules of sulphuric acid show a similar general behaviour with hydration

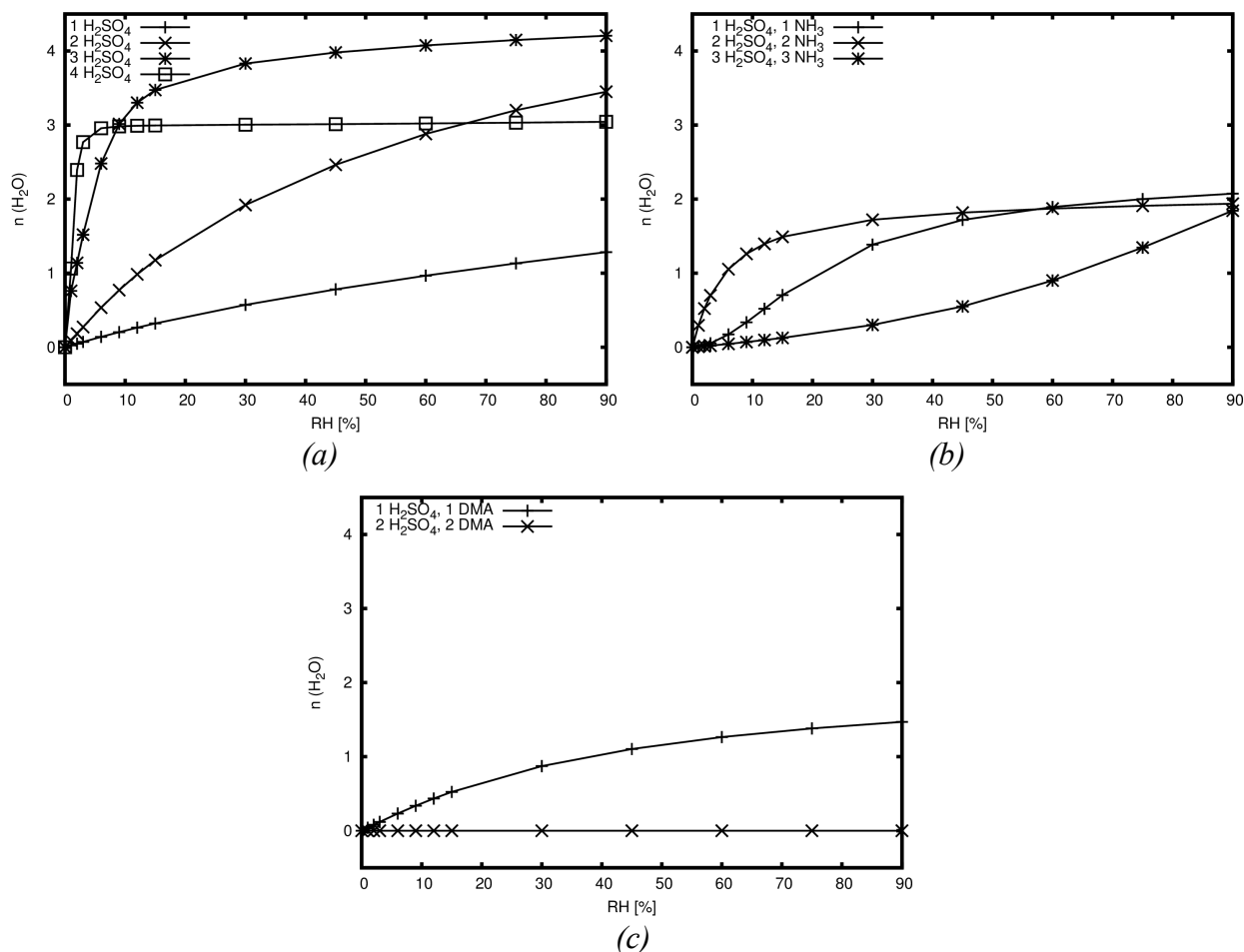


Figure 1. Average hydration numbers of sulphuric acid and neutralized clusters.

numbers being correlated to the number of acid molecules, the sulphuric acid tetramer, exhibits a different behaviour with the hydration number rising to close to three already at very low relative humidities, and then being close to constant. In Fig 1 b and c the hydration of the studied neutralised clusters are depicted. Clusters with only one sulphuric acid molecules are hydrated similarly to the free sulphuric acid molecule, despite the presence of a base molecule. In the larger clusters the base presence lowers the hydration numbers considerably – in case of the two acid/two dimethylamine cluster even close to zero. As these average hydration numbers give a measure of the added size of the clusters due to hydration, they can be

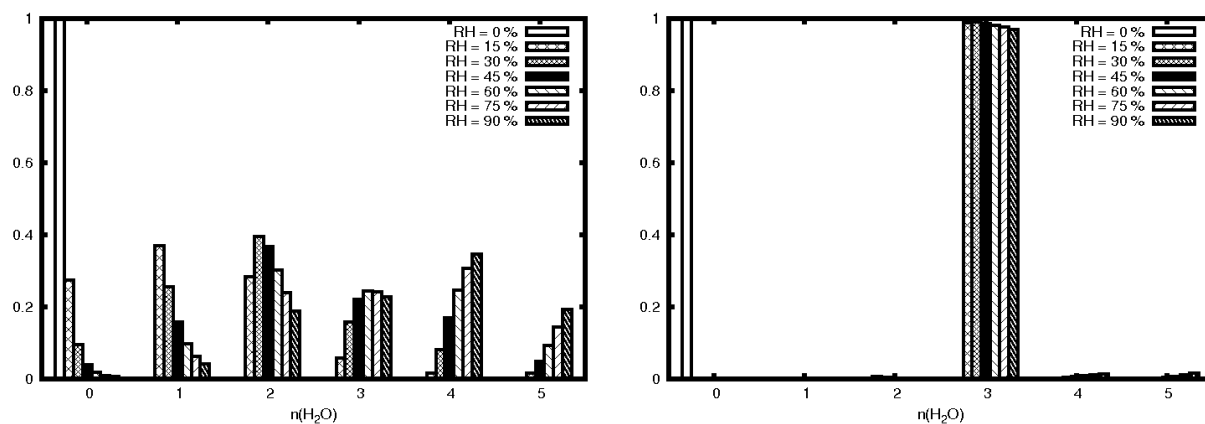


Figure 2. Population profiles of the sulphuric acid dimer and tetramer.

easily translated into the changes to collision coefficients of the respective clusters. These effects on collision coefficients is, however, relatively small, ranging of up to 20 %.

Evaporation coefficients, however, cannot be derived directly from the average hydrations shown above, as they depend on the exact evaporation pathways enabled or hindered by the individual hydrate populations. Two such hydrate population profiles are exemplified in Fig 2. The sulphuric acid dimer shows a smooth transition from low to higher hydration numbers. The opposite behaviour is exemplified by the acid tetramer, which at very low humidities populates the trihydrate, and does not show any significant change at higher relative humidities. These different profiles have direct implications for the evaporation coefficients of the involved systems – at high relative humidities the preferred hydrates of the sulphuric acid dimer cannot be formed by evaporation from the tetramer, making this specific process less probable at elevated humidities. Similar effects can be found for many of the possible evaporation processes. These changes of evaporation rates can range up to three orders of magnitude.

## CONCLUSIONS

The observed differences in energies and hydration ratios have consequences for rates particle formation in the different systems. While formation rates of clusters in general rise directly with hydration numbers of the colliding clusters/monomers, the effect of hydration of evaporation rates can not be predicted as easily. In some situations, if a cluster can evaporate into two particularly stable subunits, evaporation can be enhanced. In other situations, if a certain cluster is more stabilized by the water molecules than its possible evaporation products, evaporation rates are lower than for the water-free system. Also, while effects on collision rates are relative small, evaporation rates can vary with several orders of magnitude. The net effect on particle formation can therefore be expected to depend on the relevance of evaporation processes for a given system. Thus, the overall effect on the sulphuric acid/dimethylamine system can be expected to be negligible, while for sulphuric acid/ammonia a significant effect can be expected.

## ACKNOWLEDGEMENTS

We thank the CSC–IT Center for Science in Espoo, Finland, for computing time, and ERC StG 257360 MOCAPAF, and the Academy of Finland (Center of Excellence program project #1118615, LASTU program project #135054) for funding.

## REFERENCES

- Becke, A. D. (1993). Density-functional thermochemistry. III. The role of exact exchange, *J. Chem. Phys.* **98**, 5648.
- Christiansen, O., H. Koch, and P. Jørgensen (1995). The second-order approximate coupled cluster singles and doubles model CC, *Chem. Phys. Lett.* **243**, 409.
- Frisch, M. J. *et al.* (2009). Gaussian 09 Revision C.1, Gaussian Inc. Wallingford CT.
- Kulmala, M., H. Vehkamäki, T. Petäjä, M. D. Maso, A. Lauri, V.-M. Kerminen, W. Birmili, and P. McMurry (2004). Formation and growth rates of ultrafine atmospheric particles: a review of observations, *J. Aerosol Sci.* **35**, 143.
- Kurtén, T., V. Loukonen, H. Vehkamäki, and M. Kulmala (2008). Amines are likely to enhance neutral and ion-induced sulfuric acid-water nucleation in the atmosphere more effectively than ammonia, *Atmos. Chem. Phys.* **8**, 4095.
- Ortega, I. K., O. Kupiainen, T. Kurtén, T. Olenius, O. Wilkman, M. J. McGrath, V. Loukonen, and H. Vehkamäki (2012). From quantum chemical formation free energies to evaporation rates, *Atmos. Chem. Phys.* **12**, 225.
- TURBOMOLE V6.3 (2011), a development of University of Karlsruhe and Forschungszentrum Karlsruhe GmbH, 1989-2007, TURBOMOLE GmbH, since 2007; available from <http://www.turbomole.com>.

# A WHOLE TREE LEVEL APPROACH TO EXPLAIN STOMATAL CONTROL OF TRANSPIRATION AND PHOTOSYNTHESIS

T. HÖLTTÄ<sup>1</sup> and E. NIKINMAA<sup>1</sup>

<sup>1</sup>Department of Forest Sciences, University of Helsinki, P.O. Box 27, 00014 University of Helsinki, Finland

Keywords: phloem transport, photosynthesis, source-sink relations, stomatal control, xylem transport

## INTRODUCTION

Pressure driven transport in trees means that gas exchange, material transport, growth and structural development are linked processes with clear feedbacks although the time constants of these different processes are very different (Fig. 1). Proper matching of the gas exchange, current structural growth and accumulated structure with the environmental conditions is crucial to the success and survival of trees (Brodridg 2009), particularly in the rapidly changing climate. This determines both the competitive capacity and resistivity to extreme conditions of trees.

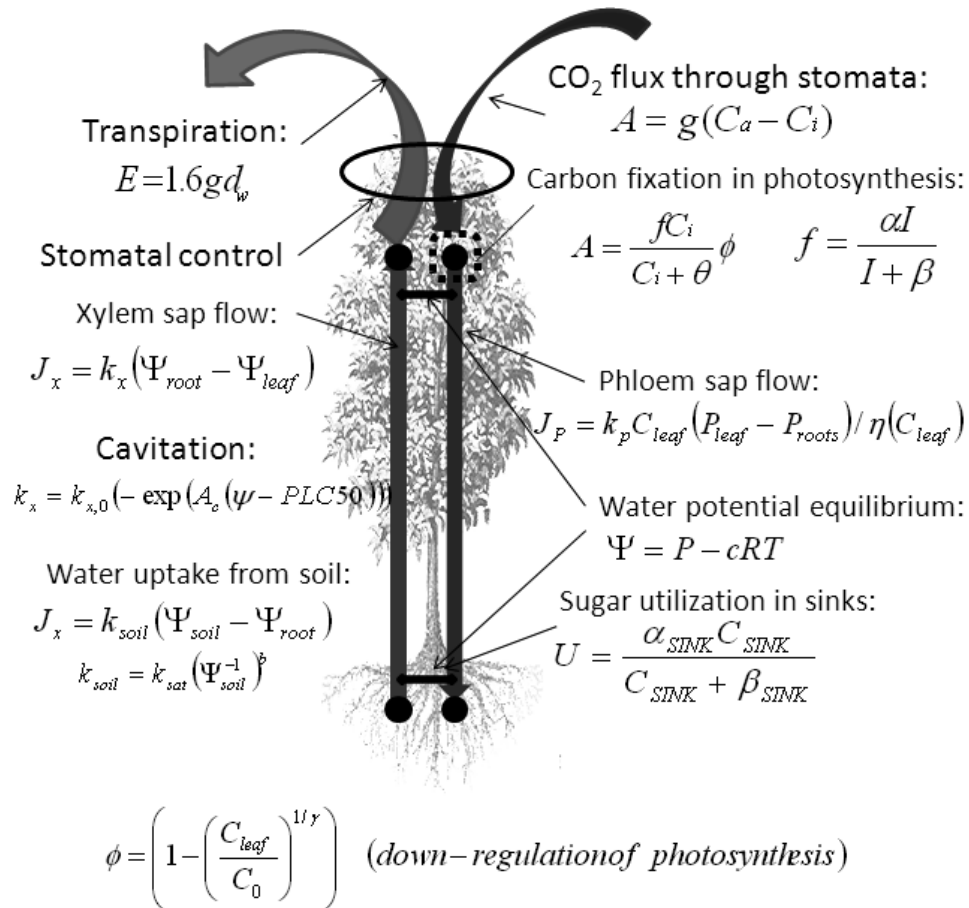


Fig. 1. Xylem and phloem transport, stomatal conductance and photosynthesis, and sink relations are interrelated.  $E$  is transpiration rate,  $J_x$  is xylem sap flow rate,  $k_x$  is xylem conductance ( $10^{-12} \text{ m}^3 \text{ Pa}^{-1} \text{ s}^{-1}$ ),  $k_{x,0}$  is xylem conductance in absence of cavitation,  $PLC 50$  is the  $\Psi$  at which half of xylem conductance is lost (2 MPa),  $A_c$  is the slope of the xylem vulnerability curve ( $2 \cdot 10^{-6} \text{ Pa}^{-1}$ ),  $\Psi_{leaf}$  and  $\Psi_{root}$  are leaf and root

water potential,  $g$  is stomatal conductance,  $dw$  is vapor pressure deficit (VPD) ( $0.03 \text{ mol mol}^{-1}$ ),  $\psi_{soil}$  is soil water potential,  $b$  is an empirical coefficient (3),  $K_{soil}$  is soil-to-root hydraulic conductance,  $K_{sat}$  is  $K_{soil}$  of saturated soil ( $2.5 \cdot 10^{-7} \text{ m}^3 \text{ Pa}^{-1} \text{ s}^{-1}$ ),  $A$  is CO<sub>2</sub> assimilation rate,  $C_{leaf}$  and  $C_{sink}$  is leaf and sink sugar concentration,  $k_p$  is phloem conductance ( $0.1 \cdot 10^{-12} \text{ m}^3 \text{ Pa}^{-1} \text{ s}^{-1}$ ),  $P_{leaf}$  and  $P_{root}$  is leaf and root turgor pressure,  $J_p$  is phloem sap flow rate,  $C_a$  and  $C_i$  is ambient (400ppm) and leaf internal CO<sub>2</sub> concentration,  $R$  is a physical constant,  $T$  is temperature (300 K),  $f$  is the dependency CO<sub>2</sub> assimilation on light intensity,  $I$  is light intensity (PAR) ( $300 \mu\text{mol m}^{-2} \text{ s}^{-1}$ ),  $\Theta$  is a parameter describing saturation of the A-C<sub>i</sub> relation (200 ppm),  $\alpha$  and  $\beta$  are photosynthetic parameters ( $0.04$  and  $400 \mu\text{mol m}^{-2} \text{ s}^{-1}$ ),  $\alpha_{sink}$  and  $\beta_{sink}$  are sink parameters ( $5 \cdot 10^{-5} \text{ mol s}^{-1}$  and  $500 \text{ mol m}^{-3}$ ),  $\phi$  is the relative down-regulation of photosynthesis,  $Co$  is  $C_{leaf}$  at which photosynthesis goes to zero ( $3000 \text{ mol m}^{-3}$ ),  $\gamma$  is the slope of the relation of photosynthetic down-regulation (4).

Water and carbon exchange occur in opposing directions in a tightly controlled manner at the vegetation-atmosphere interphase through stomatal openings in the leaves. The loss of water to atmosphere in leaves is replaced with flow from soil through the xylem, while the assimilated carbohydrates are transported in the phloem from leaves to sites of consumption such as roots (see Fig. 1). Water pressure gradients drive both the xylem and phloem transport. It has been well established that the efficiency and safety of xylem transport is crucial for tree productivity, growth and overall performance (Bond & Kavanagh 1997). In the xylem, water is in a metastable state under negative (hydrostatic) pressure and thus vulnerable to phase transition by cavitation, which threatens xylem transport capacity if leaf transpiration rate exceeds the transport capacity of the xylem (Tyree and Sperry 1989). In phloem, water is under positive pressure maintained by osmotic forces. The rate of phloem transport is limited by phloem conductivity, but also by high sugar concentrations and low temperatures that can slow phloem transport due to elevated viscosity (Hölttä et al. 2006). Xylem and phloem transport thus impose upper limits to leaf gas exchange which can be sustained in steady state at the whole tree level. With growth in tree height, the transport distance within the tree increases, and the transport of water (e.g. Koch et al. 2004), and perhaps even that of the assimilate products (e.g. Thompson 2006, Hölttä et al. 2009), become increasingly limiting for tree performance and growth. Interaction between the negative pressure in the xylem and the osmotically created positive water pressure in the phloem set strong physical boundary condition for tree functioning throughout the tree structure.

Phloem osmotic pressure and turgor depend mostly on xylem water status, and on the phloem loading and unloading dynamics as they determine the sugar concentration in phloem. Phloem loading is linked to photosynthesis especially tightly in trees where the sugars diffuse from the mesophyll cells to phloem sieve tubes passively along a concentration gradient (e.g. Turgeon 2010). Accumulation of assimilated sugars in the leaf may decrease photosynthesis due to stomatal and non-stomatal factors, e.g. due to down-regulation of photosynthetic machinery and decreases in mesophyll conductance (e.g. Flexas and Medrano 2002, Chaves et al. 2003). The phloem unloading dynamics is linked to sugar utilization for growth, respiration and root exudates. The growth of new tissues also requires high carbohydrate availability and positive water pressure in the different phases of growth including cell division, enlargement, and cell wall synthesis (Hölttä et al. 2010, Pantin 2012). The positive water (turgor) pressure results from the interplay between the negative water pressure in xylem and sufficient sugar concentration in the living cambium to maintain positive pressure osmotically.

Adjustment of the stomatal opening controls leaf gas exchange in response to various environmental and internal signals. This topic has long been under rigorous study, but is still far from being understood (Buckley 2005). Present understanding is based mainly on leaf level relations (Ball et al. 1987). Stomata appear to respond to VPD and light and seem to optimize water loss per carbon gain in a given leaf environment (e.g. Hari and Mäkelä 2003, Medlyn et al. 2011). However, responses to factors that are not directly connected to leaves such as soil water availability, changes in xylem hydraulic conductivity, and the utilization of photosynthates in sugar sinks have been considered only a little (eg. Tuzet et al. 2003).

Here we consider whole tree level interactions and constraints to leaf exchange, and present a model framework to demonstrate how stomatal gas exchange is constrained by xylem and phloem transport, soil water status and sink dynamics, in addition to the leaf level environmental conditions. We employ a numerical model to demonstrate that the typically observed stomatal behaviour of trees can be qualitatively understood in terms of maximizing the rate of photosynthetic production, with the additional condition that the assimilated sugars can be transported in steady state from the leaves to the sugar sinks. The model employed is described in Hölttä and Nikinmaa (2013), and is a steady state simplification of the dynamic model used in Nikinmaa et al. (2013), where we demonstrated that the stomatal behaviour of trees could be predicted by maximizing the instantaneous phloem mass transport rate.

## METHODS

The interconnections and the underlying mathematical formulation used amongst transpiration, photosynthesis, xylem and phloem transport, soil water status, and sink sugar status depicted in Fig. 1 are solved using a numerical model. The equations presented form a closed-form solution. The model predicts stomatal conductance which maximized the photosynthetic production rate ( $A$ ). The solution is dependent on leaf level environmental conditions (VPD and light), the photosynthetic efficiency in relation to leaf internal CO<sub>2</sub> concentration and leaf sugar concentration, tree structural properties, xylem and phloem hydraulic conductance, soil water potential and the sink strength for growth, respiration, and exudation of sugars to the soil. Note that in the steady state formulation the photosynthesis rate equals the phloem transport rate ( $J_p$ )

## RESULTS AND DISCUSSION

Fig. 2 shows the stomatal conductance which maximizes the steady state photosynthesis rate as a function of environmental drivers and structural parameters. The drivers and parameter were varied one by one while keeping the others at their base case values, which are given in the Figure caption 1. The stomatal conductance calculated so reproduces the qualitative trends of stomatal behaviour known from the literature, e.g. the increase in stomatal conductance with increasing PAR (photosynthetically active radiation), xylem hydraulic conductance, and sink strength, and with decreasing VPD, soil water potential, and ambient CO<sub>2</sub> concentration.

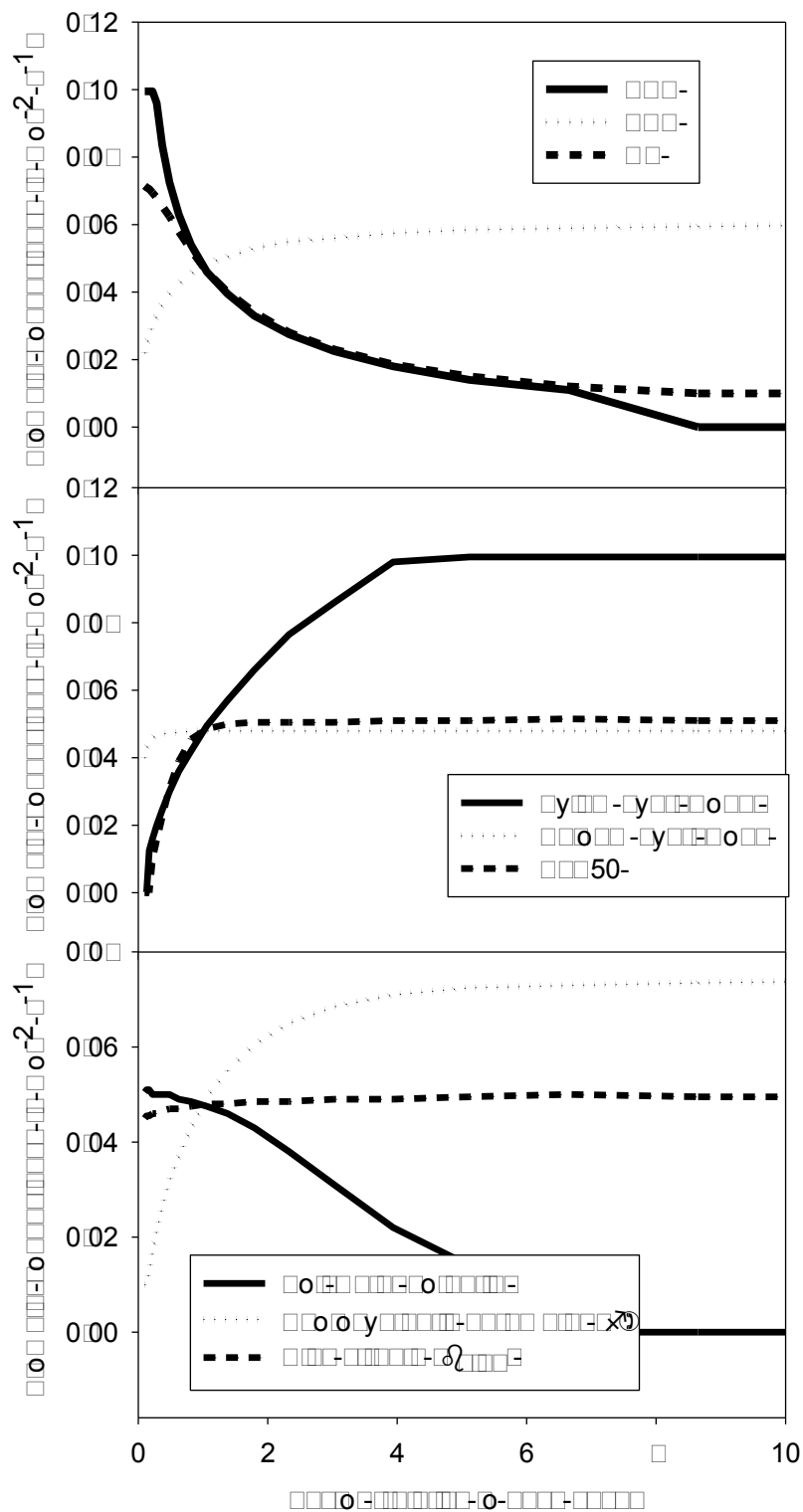


Fig. 2. Stomatal conductance predicted by the model as a function of VPD, light level (PAR), ambient  $\text{CO}_2$  concentration ( $\text{CO}_{2,a}$ ) (A), xylem hydraulic conductance ( $k_x$ ), phloem hydraulic conductance ( $k_p$ ), and PLC50 (B), soil water potential, leaf sugar concentration at which photosynthesis goes to zero ( $\text{Co}$ ), sink strength parameter  $\beta_{\text{sink}}$  (C). Each parameter was varied independently while the others were kept at their base case values. The stomatal conductance was restricted to values below  $0.1 \text{ mol m}^{-2} \text{s}^{-1}$  in this simulation.

## CONCLUSIONS

Our formulation is an improvement from previous theories of stomatal behaviour since our new approach gives a single well-defined criterion for optimization of stomatal behaviour, whereas previous models describe stomatal action differently under different conditions of e.g. maximizing water use efficiency, conserving water, sink related function or avoiding excessive cavitation.

## ACKNOWLEDGEMENTS

Study was supported by the Academy of Finland Center of Excellence (project no 1118615) and the Nordic Centers of Excellence CRAICC or DEFROST, and by Academy of Finland projects #1132561 and # 140781.

## REFERENCES

- Bond B. and Kavanagh K. (1997). Stomatal behavior of four woody species in relation to leaf-specific hydraulic conductance and threshold water potential. *Tree Physiology* **19**, 503-510.
- Brodribb, T.J. (2009). Xylem hydraulic physiology: the functional backbone of terrestrial plant productivity. *Plant Science* **177**, 245-251.
- Buckley, T.N. (2005). The control of stomata by water balance. *New Phytol.* **168**:275–292.
- Chaves, M.M., Maroco, J.P. and Pereira J.S. (2003). Understanding plant response to drought: from genes to the whole plant. *Functional Plant Biology* **30**, 239–264.
- Flexas, J. and Medrano H. (2002). Drought-inhibition of Photosynthesis in C3 Plants: Stomatal and Non-stomatal Limitations Revisited. *Annals of Botany* **89**, 183-189.
- Hari, P. and Mäkelä, A. (2003). Annual pattern of photosynthesis in Scots pine in the boreal zone. *Tree Physiol* **23**, 145-155.
- Hölttä T, Vesala T, Sevanto S, Perämäki M and Nikinmaa E. (2006). Modeling xylem and phloem water flows in trees according to cohesion theory and Münch hypothesis. *Trees* **20**, 67-78.
- Hölttä, T., Mencuccini, M. and Nikinmaa, E. (2009). Linking phloem function to structure: analysis with a coupled xylem–phloem transport model. *J. Theor. Biol.* **259**, 325–337.
- Hölttä, T., Mäkinen, H., Nöjd, P., Mäkelä, A. and Nikinmaa, E. (2010). A physiological model of softwood cambial growth. *Tree Physiol* **30**, 1235-1252.
- Hölttä, T. and Nikinmaa, E. (2013). Modelling the Effect of Xylem and Phloem Transport on Leaf Gas Exchange. IX International Workshop on Sap Flow 991.
- Koch, G.W., Sillett, S.C., Jennings, G.M. and Davis, S.D. (2004). The limits to tree height. *Nature* **428**, 851–854.
- Medlyn, B.E., Duursma, R.A., Eamus D., Ellsworth, D.S., Prentice, I.C., Barton, C.V.M., Crous, K.Y., De Angelis, P., Freeman, M. and Wingate, L.. (2011). Reconciling the optimal and empirical approaches to modelling stomatal conductance. *Global Change Biol.* **17**, 2134–2144.
- Nikinmaa, E., Hölttä, T., Hari, P., Kolari, P., Mäkelä, A., Sevanto, S. and Vesala, T. (2013). Assimilate transport in phloem sets conditions for leaf gas exchange. *Plant Cell Environ* **36**, 655-669.

- Pantin, F., Simonneau, T., and Muller, B. (2012). Coming of leaf age: control of growth by hydraulics and metabolics during leaf ontogeny. *New Phytol* **196**, 349–366.
- Thompson, M. (2006). Phloem: the long and the short of it. *Trends in Plant Science* **11**, 26–32.
- Turgeon R. (2010). The role of phloem loading reconsidered. *Plant Physiology* **152**, 1817-1823.
- Tuzet A., Perrier A., & Leuning R. 2003. A coupled model of stomatal conductance, photosynthesis and transpiration. *Plant Cell Environ* **26**, 1097-1116.
- Tyree, M.T and Sperry, J.S. (1989). Vulnerability of xylem to cavitation and embolism. *Annu. Rev. Plant Physiol. Plant Mol. Biol.* **40**, 19-38.

# HYGROSCOPIC, CCN AND VOLATILITY PROPERTIES OF SUBMICRON ATMOSPHERIC AEROSOL IN A BOREAL FOREST ENVIRONMENT DURING THE SUMMER OF 2010

J. HONG<sup>1</sup>, S. A. K. HÄKKINEN<sup>1</sup>, M. ÄIJALA<sup>1</sup>, J. HALKALA<sup>1</sup>, J. MIKKILÄ<sup>1</sup>, M. PARAMONOV<sup>1</sup>  
AND T. PETÄJÄ<sup>1</sup>, M. KULMALA<sup>1</sup>

<sup>1</sup>Division of Atmospheric Science, Department of Physics, University of Helsinki,  
Gustaf Hållströmin katu 2, 00014, Helsinki, Finland

Keywords: HYGROSCOPICITY, CCN ACTIVITY, VOLATILITY, GROWTH FACTOR

## INTRODUCTION

Hygroscopic properties of atmospheric aerosol particles describe the interaction between the particles with ambient water molecules at both sub and supersaturated conditions in the atmosphere. Although the size of the particle is dominant factor (Dusek et al. 2006) determining whether a particle is a potential cloud condensation nuclei (CCN), hygroscopicity plays a role at the size close to the limit of activation (e.g. Roberts et al. 2002). For example atmospheric oxidation of particles can modify the hygroscopicity of the particles making them CCN active (Petäjä et al. 2006, Massoli et al. 2010, and Chang et al. 2010). Furthermore, hygroscopicity can give essential information on particle composition (Swietlicki et al. 2008).

## RESULTS

A Volatility Hygroscopicity Tandem Differential Mobility Analyzer (VHTDMA) was used to measure the hygroscopicity and volatility of the ambient aerosols from 24 July to 07 August 2010 in Hyytiälä, Finland as a part of the HUMPPA-COPEC 2010 campaign. Several particle sizes were investigated, 50, 75 and 110 nm in more detail. In general the bigger the particle was the more hygroscopic it was. Black carbon had a little influence on hygroscopicity of aerosols of this study. The competition between the mass fraction of organics and  $\text{SO}_4^{2-}$  is probably the major contributor to the fluctuation of the hygroscopicity.

The CCNc-derived  $\kappa$  was slightly higher than the ones from HTDMA. This discrepancy has been observed before and it has to do with the fact that particulate organics have different solubilities in sub and supersaturated conditions, shown in Fig. 1. HTDMA measurements for larger particles should be performed to obtain better agreement between HTDMA-derived  $\kappa$  and the predicted  $\kappa$  (0.17) based on ZSR mixing rule.

The volatility properties obtained from the VHTDMA were compared with aerosol volatility behavior investigated using (VDMPS) during the studied period in Hyytiälä and during earlier years (Häkkinen et al., 2012), and they showed a good agreement with each other. Small particles evaporated more compared with large particles when heated. At temperatures above 200 °C, 80% of the aerosol material (by volume) was evaporated from the particles. However, there was still a significant amount of aerosol volume left at these high temperatures, see Fig. 2.

We studied the hygroscopicity of the particles after heating up to different temperatures. Particle hygroscopicity increased first when the heating temperature was increased to around 150 °C and decreased after 150 °C for 110 nm particles. This indicates that when heated up to 150 °C, the less hygroscopic aerosol material evaporated at lower temperatures than the more hygroscopic compounds. For 50 nm particles, the increasing and decreasing trends are not obvious. On the other hand, particles (50, 75 and 110 nm) were observed to have some hygroscopic material in them at all different heating temperatures. Comparing the hygroscopic growth factors from VHTDMA using V-mode and VH-mode, we could see that even at the highest heating temperature (280 °C) there was some hygroscopic material left, see Fig. 3. Since black carbon is hydrophobic this result supports recent studies that have found very low-volatile

non-BC aerosol material in submicron ambient particles. This material can be e.g. organic salts or organic polymers from aerosol aging. We estimated the hygroscopicity of this “non-volatile” non-BC aerosol material for the three different sized particles. Due to simplicity of our approach the estimation gave too high hygroscopicities for the 50 nm and 75 nm particles. However, for the largest particles we obtained reasonable hygroscopic growth factor of 1.17. In the future it would be important to obtain information about the hygroscopic properties of different low-volatile organics e.g. organic salts. This would help us to further interpret the VH-TDMA results we got and to understand better the chemical properties of submicron aerosol particles, most importantly particulate organics.

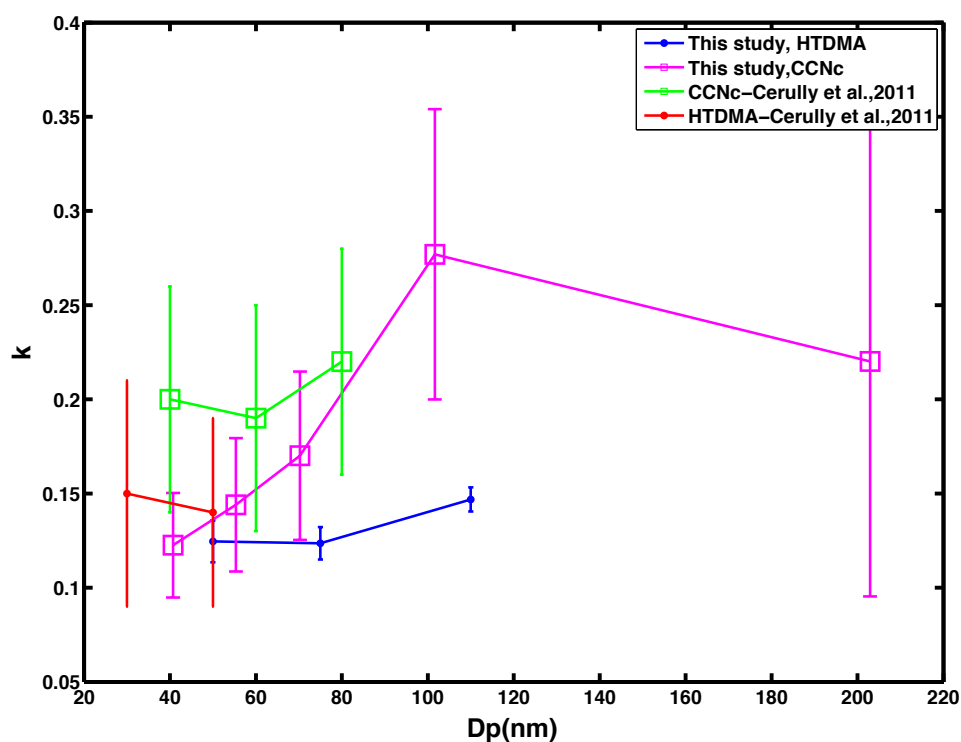


Figure 1: Calculated  $\kappa$  values ( $\kappa_{\text{HTDMA}}$  and  $\kappa_{\text{CCN}}$ ) as a function of particle diameter using HTDMA measurements and CCNc measurements from this study and from study by Cerully et al. (2011).

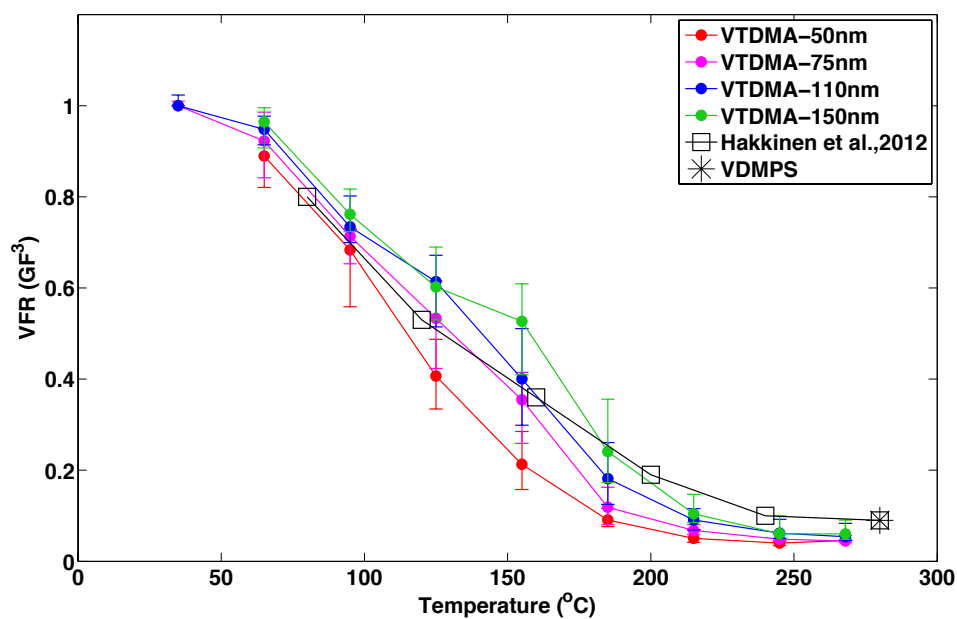


Figure 2: Volume remaining fraction calculated from volatile growth factor ( $GF_V$ ) obtained from the VTDMA measurements as a function of heating temperature for four different particle sizes.

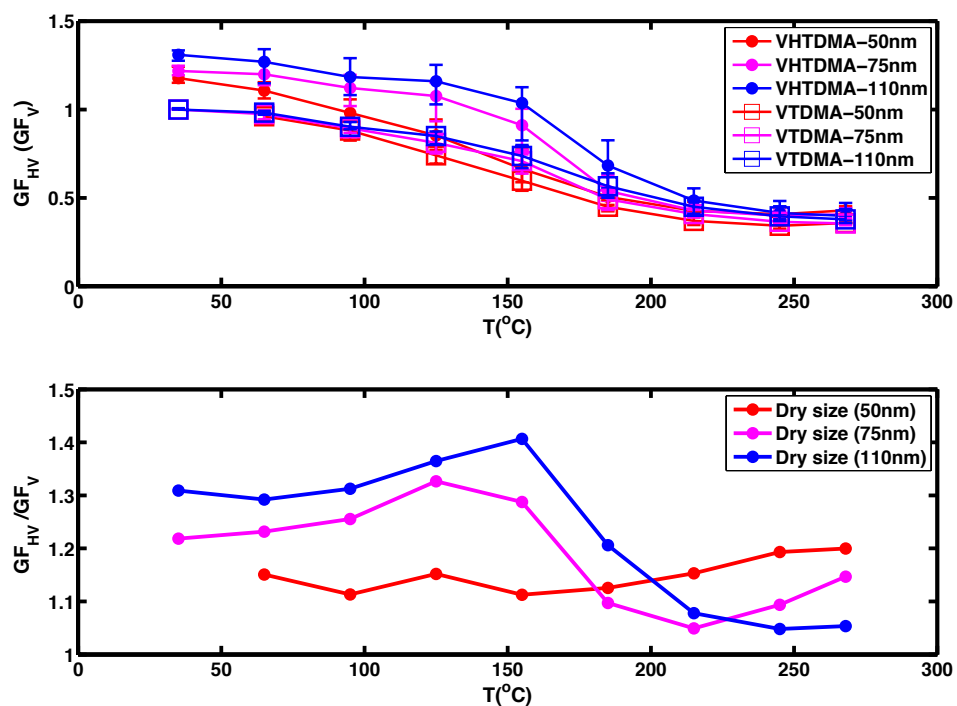


Figure 3: Hygroscopic and volatile growth factors as a function of heating temperature obtained from the VHTDMA and the VTDMA of this study for 50 nm, 75 nm and 110 nm particles.

## REFERENCES

Cerully et al (2011). Aerosol hygroscopicity and CCN activation kinetics in a boreal forest environment during the 2007 EUCAARI campaign. *Atmo.Chem. Phys. Discuss* 11, 15029-15074.

Desuk et al (2011). Size Matters More Than Chemistry for Cloud-Nucleating Ability of Aerosol Particles. *Sciences* 312(5778), 1375-1378.

Ehn et al (2007). Hygroscopic properties of ultrafine aerosol particles in the boreal forest: diurnal variation, solubility and the influence of sulphuric acid. *Atmos. Chem. Phys* 7, 211-222.

Gysel M., McFiggans G. B., Coe H. (2009). Inversion of tandem differential mobility analyser (TDMA) measurements. *Aerosol Science* 40, 134-151, 2009.

Hari P. and Kulmala M. (2005). Station for Measuring Ecosystem-Atmosphere Relations (SMEAR II). *Boreal Environment Research* 10, 315-322.

Hakala J., Mikkilä J., Ehn M., Siivola E., Kulmala M., and Petäjä T. (2010) Indirect aerosol chemical composition measurements with a VH-TDMA, Proceedings of the Finnish Centre of Excellence in Physics, Chemistry, Biology and Meteorology of Atmospheric Composition and Climate Change, Annual Workshop in Kuopio, May 17-19, 2010.

Häkkinen S., Äijälä M., Lehtipalo K., Junninen H., Backman J., Virkkula A., Nieminen T., Vestenius M., Hakola H., Ehn M., Worsnop D. R., Kulmala M., Petäjä T., and Riipinen I. (2012). Long-term volatility measurements of submicron atmospheric aerosol in Hyytiälä, Finland. *Atmos. Chem. Phys. Discuss* 12, 11201-11244, doi:10.5194/acpd-12-11201-2012, 2012.

Massoli et al (2010). Relationship between aerosol oxidation level and hygroscopic properties of laboratory generated secondary organic aerosol (SOA) particles. *Geo. Res. Lett* 37, L24801.

Petäjä et al (2006). Sub-micron atmospheric aerosol in the surroundings of Marseille and Athens: physical characterization and new particle formation. *Atmos. Chem. Phys. Discuss* 6, 8605-8647.

Petters, M. D. and Kreidenweis, S. M (2007). A single parameter representation of hygroscopic growth and cloud condensation nucleus activity. *Atmos. Chem. Phys* 7, 1961-1971.

Roberts G. C. and Nenes A (2005). A Continuous-Flow Streamwise Thermal-Gradient CCN Chamber for Atmospheric Measurements. *Aerosol Science and Technology* 39, 206-221.

Rose et al (2010). Cloud condensation nuclei in polluted air and biomass burning smoke near the megacity Guangzhou, China-Part 1: Size-resolved measurements and implications for the modelling of aerosol particle hygroscopicity and CCN activity. *Atmos.Chem. Phys* 10, 3365-3383.

Riipinen et al (2011). Organic condensation: a vital link connecting aerosol formation to cloud condensation nuclei (CCN) concentrations. *Atmos. Chem. Phys* 11, 3865-3878.

Swietlicki et al (2008). Hygroscopic properties of submicrometer atmospheric aerosol particles measured with H-TDMA instruments in various environments-a review. *Tellus* 60B, 432-469.

Sihto et al (2010). Seasonal variation of CCN concentrations and aerosol activation properties in boreal forest. *Atmos. Chem. Phys. Discuss* 10, 28231-28272.

Williams et al (2011). The summertime Boreal forest field measurement intensive (HUMPPA-COPEC-2010): an overview of meteorological and chemical influences. *Atmos. Chem. Phys. Discuss* 11, 15921-15973.

# THE EVAPORATION OF AMMONIUM NITRATE IN THE DMT-CCN COUNTER

A. JAATINEN<sup>1</sup>, S. ROMAkkANIEMI<sup>1</sup>, A. LAAKSONEN<sup>1,2</sup>, and A. VIRTANEN<sup>1</sup>

<sup>1</sup>Department of Applied Physics, University of Eastern Finland, Kuopio, P.O. Box 1627, Finland

<sup>2</sup>Finnish Meteorological Institute, Climate Change, Helsinki, P.O. Box 503, Finland

Keywords: AMMONIUM NITRATE, CCN, CCN COUNTER.

## INTRODUCTION

Atmospheric aerosol particles are composed of large variety of chemical compounds. Some of these can be considered to be nonvolatile meaning their vapor pressure is so low that in practice they are always found from the particle phase. Other group of compounds found from particles is semivolatile. Depending on the conditions, like temperature and relative humidity, these compounds may exist in the gas, liquid or solid particle phase. In the case of aqueous droplets, the partitioning between phases depends on the effective Henry's law coefficient that can be determined from liquid phase thermodynamics.

Behaviour of semivolatile compounds causes problems for both modellers and experimentalists. Beyond the condition dependent partitioning between the gas and particles, also the partitioning between particles of different size and composition needs be taken into account to fully address the effect of semivolatiles in direct and indirect aerosol forcing.

Measuring the hygroscopicity of aerosol that is even partly semivolatile is not a straightforward task. For example it has been noticed in several publications that in the HTDMA measurements the hygroscopicity can be underestimated (e.g. Hu *et al.*, 2011). In the measurements ambient aerosol is first dried before it is size selected in the first DMA, and depending on the conditions, some of the semivolatiles might evaporate, and part of them might stay in the dry aerosol during water evaporation. After that aerosol is wetted, and depending on the relative humidity some semivolatiles might condense back to aerosol or they might condense on the walls of the instrument depending on the design of humidifier. Thus the hygroscopicity measured might be different than the actual hygroscopicity in the ambient air. Similar might happen also in the CCN-counter, and in this work we are studying how a semivolatile compound, ammonium nitrate, behaves in the Cloud Condensation Nuclei counter (CCNc). In the case of particle evaporation, we found that ammonium nitrate is partly evaporating before maximum supersaturation is reached in the CCN counter, thus causing underestimation of CCN activity. The effect of evaporation is clearly visible in all supersaturation, leading to underestimation of critical dry diameter.

## METHODS

Our experimental setup consisted of atomizer (TSI 3076), diffusion drier, Vienna type DMA and DMT-CCNc, which operation principle is presented in Roberts and Nenes (2005). In the experiments particles were generated by atomizer and dried. Before entering the CCN counter particles were size selected using DMA with 10l/min sheath and excess flows. To avoid evaporation of dried particles, the distance between DMA and CCN counter was kept as short as possible. Critical dry size in different supersaturations was determined by changing the particle size with DMA and keeping the supersaturation constant in the CCN-column. Activation curves were corrected to take into account multiple charging in the DMA, and the critical dry size was determined as a size where 50% of particles activated.

## RESULTS

In the performed laboratory experiments ammonium nitrate particles were created and their critical diameters were measured as a function of supersaturation. In Figure 1 we show the activation curves for both ammonium sulphate and ammonium nitrate in different supersaturations. What we can see is that the activation behavior is quite similar, and the shapes of the activation curves are similar for both compounds. This shows that all particles go through the same conditions in the CCNc's measurement column. However, the measurements show that the CCN-activity of ammonium nitrate particles is lower than ammonium sulphate particles, although it should be more hygroscopic (the hygroscopicity parameter  $\kappa$  for ammonium nitrate is 0.67 and for ammonium sulphate 0.61 (Petters and Kreidenweis, 2007)). The CCN-activities become closer to each other for larger particles (lower supersaturations) because ammonium sulphate dissociates more perfectly due to lower Kelvin effect.

Table 1 shows the experimental and theoretical critical particle diameter as a function of supersaturation for pure ammonium nitrate particles. The measurement results show that the evaporation in the CCN-column is visible in all supersaturations, but the effect is relatively stronger in higher supersaturation where particle size is smaller. This happens mainly because small particles are able to follow their equilibrium size more closely than the larger ones, and thus they are losing ammonia and nitrate more quickly.

SS (%)	Measured critical diameter (nm)	Theoretical critical diameter (nm)
0.12	121	112
0.23	84	74
0.31	70	60
0.42	63	51

Table 1. Measured and theoretical critical diameter for four different supersaturation (SS) values.

In future we will expand the laboratory work to see if the measurement setup can be used also to quantify the enhancing effect of semivolatile gases on cloud droplet formation (Kulmala *et al.*, 1993, Laaksonen *et al.*, 1998).

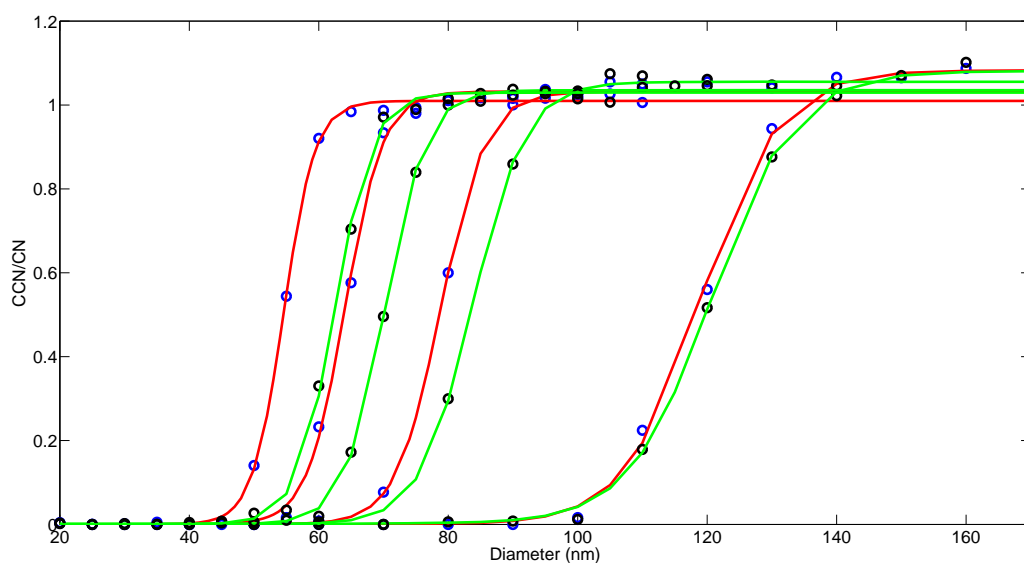


Figure 1. Measured activation curves for ammonium sulphate (red) and ammonium nitrate (green) for SS=0.12, 0.23, 0.31 and 0.41%

## ACKNOWLEDGEMENTS

This study has been supported by the Academy of Finland Center of Excellence program (project number 1118615) and by the strategic funding of the University of Eastern Finland. A. Jaatinen was supported by the KONE foundation.

## REFERENCES

- Hu, D., Chen, J., Ye, X., Li, L., and Yang, X.: Hygroscopicity and evaporation of ammonium chloride and ammonium nitrate: Relative humidity and size effects on the growth factor, *Atmos. Environ.*, 45, 14, 2349–2355, <http://dx.doi.org/10.1016/j.atmosenv.2011.02.024>, 2011.
- Kulmala, M., A. Laaksonen, P. Korhonen, T. Vesala, T. Ahonen, J.C. Barrett: The effect of atmospheric nitric acid vapor on CCN activation. *Journal of Geophysical Research (Atmospheres)* 98, 22949–22958, 1993.
- Laaksonen, A., P. Korhonen, M. Kulmala, R.J. Charlson: Modification of the Köhler equation to include soluble trace gases and slightly soluble substances. *Journal of the Atmospheric Sciences* 55, 853–862, 1998.
- Petters, M. D., and S. M. Kreidenweis, S. M.: A single parameter representation of hygroscopic growth and cloud condensation nucleus activity *Atmos. Chem. Phys.*, 7, 1961–1971, 2007.
- Roberts, G. C. and Nenes, A.: A Continuous-Flow Streamwise Thermal-Gradient CCN Chamber for Atmospheric Measurements, *Aerosol Sci. Tech.*, 39, 206–221, doi:10.1080/027868290913988, 2005.

# MODELLING OF SURFACE ENERGY AND WATER BALANCE IN HIGH LATITUDE CITIES – IMPACT OF SNOW

L. JÄRVI<sup>1</sup>, C.S.B. GRIMMOND<sup>2,3</sup>, A. NORDBO<sup>1</sup>, I. STRACHAN<sup>4</sup>, M. TAKA<sup>5</sup> and H. SETÄLÄ<sup>6</sup>

<sup>1</sup>Department of Physics, University of Helsinki, P.O.Box 48, Helsinki, Finland

<sup>2</sup>Department of Meteorology, University of Reading, Reading, United Kingdom

<sup>3</sup>Department of Geography, King's College London, London, United Kingdom

<sup>4</sup>Department of Natural Resource Sciences, Ste. Anne de Bellevue, QC, Canada

<sup>5</sup>Department of Geography, University of Helsinki, Helsinki, Finland

<sup>6</sup>Department of Environmental Sciences, University of Helsinki, Helsinki, Finland

Keywords: RUNOFF, SNOW, TURBULENT FLUX, URBAN.

## INTRODUCTION

The surface energy and water balance in urban areas have major consequences on our quality of life as they determine the forcing between the surface and the atmosphere in weather prediction and climate models and impact pollutant mixing. Also, they directly affect urban dwellers via increased heat stress, decreased evaporation and increased risk for flooding. Despite their importance, the energy and water cycles at high-latitude cities are understudied. Particularly the impact of snow on both balances is important as springtime snowmelt can cause floods in cities as well as in natural environments. In this study the Surface Urban Energy and Water Balance Scheme (SUEWS; Järvi et al. 2012) will be developed to take snow into account.

## METHODS

SUEWS simulates the energy and water balance components through the use of commonly measured meteorological variables (Table 1) and information on the surface cover. Rates of evaporation-interception for a single layer with multiple surface types (paved, buildings, coniferous trees/shrubs, deciduous trees/shrubs, irrigated grass, non-irrigated grass and water) are calculated. Below each surface type, except water, there is a single soil layer. At each time step (5 min to 1 h) the moisture state of each surface and soil type are calculated. The model allows for a continuous treatment of surface resistance for the transition between wet and dry surfaces. Horizontal water movements at the surface and in the soil are incorporated. Latent heat flux is calculated with a modified Penman-Monteith equation and sensible heat flux as a residual from the available energy minus the latent heat. The model contains several sub-models for e.g. net all-wave radiation (NARP, Offerle et al. 2003), storage heat (Grimmond et al. 1991), anthropogenic heat flux, and external irrigation. In this study an additional snow module is developed to improve SUEWS performance in simulating snow and its impact. In the module, the accumulation of snow is allowed in below zero temperatures and its melting is calculated using the degree-day-method using net all-wave radiation and air temperature. Also the impact of snow on the surface energy balance via albedo is improved (Table 1). The model is developed and tested using observations from two cities Helsinki and Montreal.

### *Helsinki*

The turbulent fluxes of sensible and latent heat ( $Q_H$  and  $Q_E$ , respectively) and meteorological data used to force the model are measured at the semi-urban measurements station SMEAR III - Kumpula (Järvi et al. 2009). The turbulent fluxes using the eddy covariance (EC) technique are measured on top of a 31 meters high lattice tower (60°12.17'N, 24°57.671'E, 26 m above sea level) situated at the university campus five kilometers north-east from downtown Helsinki. According to the prevailing wind direction, the measurement surroundings can be divided into three surface areas: built (Ku1), road (Ku2) and vegetation (Ku3) (Järvi et al. 2012; Vesala et al. 2008). The built area is covered with university campus buildings

and Finnish Meteorological Institute in the vicinity of the measurement tower, and a single family house area behind. A heavily trafficked road with 44 000 vehicles per workday passes the road surface area with the closest distance between the road and the tower being 150 m. The area between the road and the tower is covered with forest, and the area behind the road is covered with a combined mix of residential and commercial buildings. In the vegetation area, the fraction of vegetation is high as the University Botanical Garden and City Allotment Garden are located in the area.

The EC setup consists of an ultrasonic anemometer (USA-1, Metek GmbH, Germany) to measure all three wind speed components and sonic temperature, and open- and closed-path infrared gas analyzers (LI-7500 and LI-7000, respectively, LI-COR, USA) to measure water density and mixing ratio, respectively. Data is recorded with 10 Hz and the 60-minute fluxes are calculated using commonly accepted methods (Nordbo *et al.* 2012). Data from the closed path analyzer is used as a main source for  $Q_E$ , but if the outdoor relative humidity is above 85%, data from the open-path analyzer is used. Additional measurements in the same tower cover the short-wave and long-wave radiation components of the net all-wave radiation  $Q^*$  (CNR1, Kipp&Zonen, Netherlands), air temperature (platinum resistant thermometer, Pt-100) and wind speed (Thies Clima 2.1x, Germany). Rest of the meteorological variables used to force the model are measured on the roof of a nearby building. These include relative humidity (HMP243, Vaisala Oyj, Finland), air pressure (DPA500, Vaisala Oyj) and precipitation (rain gauge, Pluvio2, Ott Messtechnik GmbH, Germany). Also snow depth measured by the Finnish Meteorological Institute is used to evaluate the model performance.

<i>Input</i>	Variable	Units
Downward shortwave radiation	$K\downarrow$	$\text{W m}^{-2}$
Precipitation	$P$	$\text{mm h}^{-1}$
Air temperature	$T_a$	$^{\circ}\text{C}$
Wind speed	$u$	$\text{m s}^{-1}$
Air pressure	$Pres$	kPa
Relative humidity	$RH$	%
<i>Output – original</i>		
Net all-wave radiation	$Q^*$	$\text{W m}^{-2}$
Sensible heat flux	$Q_H$	$\text{W m}^{-2}$
Latent heat flux	$Q_E$	$\text{W m}^{-2}$
Storage heat flux	$\Delta Q_S$	$\text{W m}^{-2}$
Anthropogenic heat flux	$Q_F$	$\text{W m}^{-2}$
Surface temperature	$T_S$	$^{\circ}\text{C}$
Leaf area index	LAI	$\text{m}^2 \text{m}^{-2}$
Irrigation	$I_e$	$\text{mm h}^{-1}$
Evaporation	$E$	$\text{mm h}^{-1}$
Runoff	$R$	$\text{mm h}^{-1}$
Soil moisture deficit	$\Delta\theta$	mm
Surface state	$C$	mm
<i>Output – new</i>		
Snow water equivalent	$S_{WE}$	mm
Snow depth	$d_s$	cm
Snow density	$\rho_s$	$\text{kg m}^{-3}$
Snow albedo	$\alpha_n$	-
Snow melt	$M$	$\text{mm h}^{-1}$
Fraction of snow	$f_s$	-
Transport of snow	$T_R$	$\text{mm h}^{-1}$
Heat release by rain	$Q_P$	$\text{W m}^{-2}$
Melt/freezing related energy	$Q_m$	$\text{W m}^{-2}$

Table 1. Meteorological variables needed to run SUEWS and the main output variables.

Surface runoff is monitored in two catchments (Pa and Pi) located one and 3.8 kilometres from the SMEAR III – Kumpula. The two sites represent different land use management and can be divided to high-intensity and medium-intensity catchments, respectively. At both sites, runoff is monitored at the catchment area discharge point with one minute interval using a constant flow meter (OCM Pro CF, Nivus GmbH, Germany).

### Montreal

In Montreal, the  $Q_H$  and  $Q_E$  used in the model development and testing are observed from urban (RL) and suburban areas (PR). At both sites, the measurements are made at 25 meters using a telescopic triangular lattice tower with a sonic anemometer (CSAT3, Campbell Scientific, Canada) and an open-path infrared gas analyser (LI-7500). Similarly, the 20 Hz data is saved for post-processing using commonly accepted quality controlling procedures (Bergeron and Strachan 2010). At both sites, air temperature (HMP45C-212 in urban, HMP45C in suburban, Campbell Scientific) and radiation balance components (CNR1) and relative humidity (HMP45C) are measured at the same tower at the height of 25 meters. Precipitation data is obtained from a rural area 35 km southwest from the urban EC site with missing data and snowfall from the Pierre Elliot Trudeau Airport 7 km south-east from the suburban and 16 km from the urban sites (National Climate Data and Information Archive of Canada, 2013). Snow depths are monitored in the backyard of the suburban site and on the roof of the urban site using snow ranging sensors (SR5, Campbell Scientific). In addition, snow density and albedo observed from four snow cover types weekly in 2007 – 2008 and bi-weekly in 2008 – 2009 are used in the model development and testing.

Variable	Helsinki			Montreal			
	Ku1	Ku2	Ku3	Pa	Pi	RL	PR
Lat (°)		60.203 N		60.199	60.238	45.501 N	45.457 N
Lon (°)		24.961 E		24.940	25.014	73.811 W	73.592 W
$\lambda_{pav}$	0.42	0.39	0.30	0.42	0.33	0.37	0.44
$\lambda_{blg}$	0.20	0.15	0.11	0.20	0.12	0.12	0.27
$\lambda_{veg}$	0.38	0.46	0.59	0.38	0.55	0.51	0.29
$A$ (ha)	44.7	78.2	78.2	23.8	44.8	314.2	314.2
$z$ (m)		31		-	-	25	25
$z_h$ (m)	8.4	9.9	8.5	15.2	10.8	6.4	7.9
$p$ (# ha <sup>-1</sup> )	31	37	44	42	55	24	84

Table 2. Measurement site characteristics used in the model development and testing.

### Model runs

In total, the model is run at five sites each of them representing different urban surface cover with varying fraction of vegetation and impervious surfaces (Table 2). To take the complexity of the SMEAR III - Kumpula site into account, SUEWS is run separately for the three surface cover areas and the final model output to be compared with the observations is combined from these according to the prevailing wind direction. For Kumpula, the model is run for 2010 – 2012 with the first six months being used as a spin-up time for the model, the next 18 months to develop the model and the final 12 months as independent evaluation of the model. From the two catchments, observations from Pa are used in the model development and observations from Pi, for independent model testing. At both catchments, SUEWS is run for Jan 2010 – April 2011 and the first six months is used for model spin-up. In Montreal, data from the suburban site is used in model development whereas data from the urban site is used as independent testing for the model runs. At both sites, the model is run for December 2007 – September 2009 and the first month is used as a spin-up time

## CONCLUSIONS

The impact of snow aging on snow albedo and snow density is examined using the observations from Montreal suburban site. With correct adjusting of the aging time constants, the snow aging equations are found to give reasonable estimates for both snow albedo and density. The snow density varies between 100 and 400 kg m<sup>-3</sup>, which is a typical range observed in urban areas (Lemonsu *et al.* 2010). Snow albedo ranges between 0.18 and 0.8, which again is a typical range for urban snow. The modelled albedo gives reasonable values also for the reflected shortwave radiation at both cities, which supports its correct estimation. Differences between the observed and simulated net all-wave radiation ( $Q^*$ ) at both sites are mostly related to the parameterization of the downward longwave radiation that uses only air temperature and relative humidity (Loridan *et al.* 2011). Despite this, good correlation between the observed and modelled ( $Q^*$ ) is obtained both in the cold snow and melting snow periods (Figure 1). Here cold snow period is defined when the air temperatures are below zero degrees and melting snow conditions when the air temperature is above zero degrees.

The amount of snowmelt parameterized using degree day method is adjusted using observations from the high-intensity catchment in Helsinki. For this site, the modelled cumulative runoff for winter 2010 – 2011 is 83 mm, which is 3 mm less than the observed runoff. At the medium-intensity catchment, the modelled runoff is 86, which is 2 mm more than the observed value. The model underestimated slightly the cold snow period runoff and overestimates the runoff during the melting period. When simulating the turbulent fluxes, SUEWS performs well at both sites. In Figure 1, the diurnal behaviour of modelled and observed  $Q^*$ ,  $Q_H$  and  $Q_E$  are plotted in Helsinki with the year 2012 data. Largest problems of SUEWS are related the patchiness of the snow, which creates differences particularly between the observed and modelled  $Q^*$ .

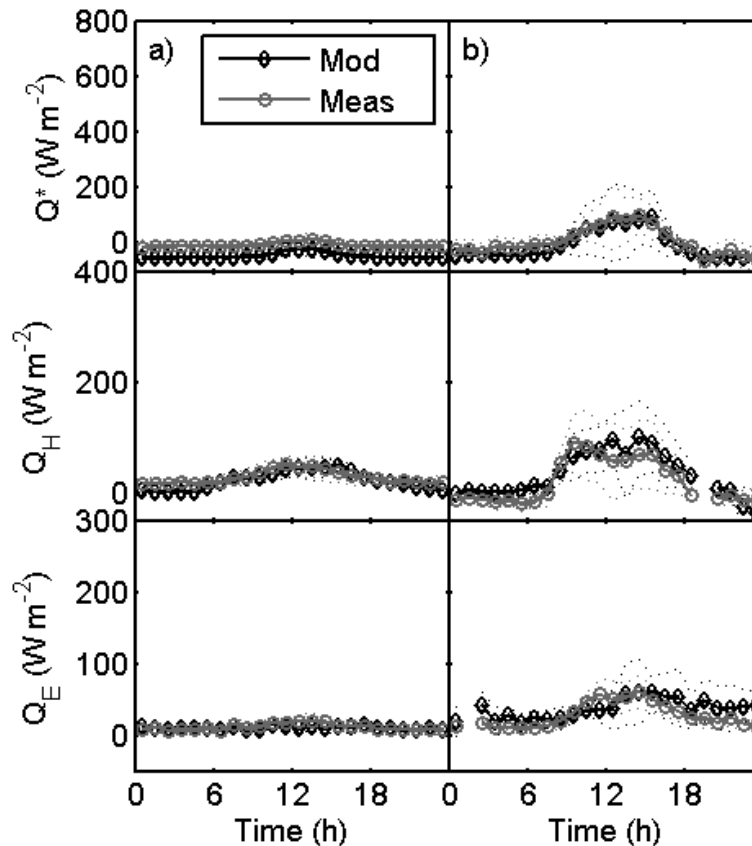


Figure 2. Diurnal behaviour of the net all-wave radiation ( $Q^*$ ), sensible ( $Q_H$ ) and latent heat ( $Q_E$ ) fluxes for cold and melting snow periods in Kumpula, Helsinki, in 2012.

## ACKNOWLEDGEMENTS

This work was supported by the Academy of Finland (Project numbers 138328 and ICOS-Finland, 263149), and the EU-funded-project BRIDGE. We thank Erkki Siivola and Petri Keronen for the instrument maintenance of the eddy covariance setups in Helsinki.

## REFERENCES

- Bergeron, O. and I.B. Strachan (2010). Wintertime radiation and energy budget along an urbanisation gradient in Montreal, Canada. *Int. J. Climatology*. doi:10.1002/joc.2246.
- Grimmond C.S.B., H.A. Cleugh and T.R. Oke (1991). An objective urban heat storage model and its comparison with other schemes. *Atmos. Env.* 25B, 311 – 174.
- Järvi L., H.Hannuniemi, T.Hussein, H.Junninen, P. P. Aalto, R. Hillamo, T. Mäkelä, P. Keronen, E. Siivola, T. Vesala and M. Kulmala (2009). The urban measurement station SMEAR III: Continuous monitoring of air pollution and surface-atmosphere interactions in Helsinki, Finland, *Boreal Env. Res.* 14 (Suppl. A), 86-109.
- Järvi L., C.S.B. Grimmond and A. Christen (2011). The surface urban energy and water balance scheme (SUEWS): Evaluation in Los Angeles and Vancouver, *J. Hydrol.* 411, 219 – 237.
- Lemonsu A., Bélair S., Mailhot J. and Leroyer S. (2010). Evaluation of the Town Ebergy Balance Model in Cold and Snowy Conditions during the Montreal Urban Snow Experiment 2005. *J. Appl. Meteorol. Climatol.* 49, 346 – 362.
- Loridan T., Grimmond C. S. B., Offerle B. D., Young D. T., Smith T., Järvi L. and Lindberg F. (2011). Local-scale Urban Meteorological Parameterization Scheme (LUMPS): Longwave radiation parameterization and seasonality related developments. *J. Appl. Meteorol. Climatol.*, DOI: 10.1175/2010JAMC2474.1.
- Nordbo A., L. Järvi and T. Vesala (2012). Revised eddy covariance flux calculation methodologies – effect on urban energy balance. *Tellus B* 48, 18184, <http://dx.doi.org/10.3402/tellusb.v64i0.18184>.
- Offerle B., C.S.B. Grimmond and T.R. Oke (2003). Parameterization of net all-wave radiation for urban areas. *J. Appl. Meteorol.* 42, 1157 – 1173.
- Semadeni-Davies A., A. Lundberg and L. Bengtsson (2001). Radiation balance of urban snow: a water management perspective. *Cold Reg. Sci. Technol.* 33, 59 – 76.

## THE EFFECT OF NITROGEN FERTILIZATION ON SHOOT NO FLUXES

J. JOENSUU<sup>1</sup>, A.-J. KIELOAHO<sup>2</sup>, M. RAIVONEN<sup>1,2</sup>, N. ALTIMIR<sup>1</sup>, P. KOLARI<sup>1,2</sup>, T. SARJALA<sup>3</sup>, J. BÄCK<sup>1</sup>, P. KERONEN<sup>2</sup>, T. VESALA<sup>2</sup> and E. NIKINMAA<sup>1</sup>

<sup>1</sup>Department of Forest Sciences, University of Helsinki,  
PO Box 27, 00014 University of Helsinki, Finland.

<sup>2</sup>Division of Atmospheric Sciences, Department of Physics, University of Helsinki,  
PO Box 64, 00014 University of Helsinki, Finland.

<sup>3</sup>The Finnish Forest Research Institute,  
Kaironiementie 15, 39700 Parkano, Finland.

Keywords: nitrogen oxides, shoot emissions, chamber measurements, nitrogen fertilization.

### INTRODUCTION

Nitrogen oxides (NO<sub>x</sub>, here NO and NO<sub>2</sub>) are reactive trace gases that have an important role in tropospheric air chemistry. Both are taken up by plants through plant stomata, but the possibility of emissions at ambient concentrations below a certain level (known as compensation point) is still under discussion (e.g. Breuninger *et al.*, 2012). NO deposition is small compared to NO<sub>2</sub> (Rondón *et al.*, 1993, Hereid and Monson, 2001).

In plants, NO is involved in the regulation of physiological processes such as stomatal closure, germination and defence responses (Baudoin, 2011). For these purposes, production of NO from nitrite is catalyzed by a nitrate reductase enzyme (NR); another proposed pathway is production from arginine by a nitric oxide synthase (NOS) (see Fröhlic and Durner (2011) or Gupta *et al.* (2011) for discussion). Excess NO created in the NR-nitrite process could result in NO emission. However, NR strongly prefers NO<sub>3</sub><sup>-</sup> to NO<sub>2</sub><sup>-</sup> as substrate (Rockel *et al.*, 2002). NO and NO<sub>2</sub> emission has been observed from plants treated with a herbicide that blocks nitrite reduction (Klepper, 1979) and also from plants lacking the enzyme nitrite reductase (NiR) (Morot-Gaudry-Talarmain *et al.*, 2002). Reactions between accumulated nitrite and plant metabolites are a possible explanation to these observations.

The nitrogen present in soil as ammonium (NH<sub>4</sub><sup>+</sup>) or nitrate (NO<sub>3</sub><sup>-</sup>) is easily available to plants, but for use in synthesis of e.g. amino acids, nitrate is first reduced to ammonium. In Finnish forest soils nitrogen is usually scarce, and plants readily take up all available nitrogen. Ammonium is in natural conditions present in higher concentrations than nitrate in the soil. Nitrogen deposition from the atmosphere creates a man-made addition of both nitrate and ammonium – this “fertilization” amounts in Hyytiälä annually to approximately 340 mg N m<sup>-2</sup> (Lindroos *et al.*, 2000). Nitrogen deposition may therefore change the natural ratios of ammonium and nitrate ions in forest soil.

Pine trees preferably reduce nitrate already in their roots (Pietiläinen and Lähdesmäki 1988), and nitrogen transportation within the tree therefore mostly happens in other chemical forms. However, when this process is slow because of low soil temperature, nitrate is transported to the foliage before reduction (Huffaker 1982). It is possible that transportation takes place also when nitrate ions are abundant in the soil. Nitrate reaching the needles induces NaR activity (Huffaker 1982). Accumulating nitrite could then serve as a secondary substrate for NR, leading to NO production and possibly emission from the needles.

Such emission has been observed in laboratory conditions: Wildt *et al.* (1997) observed clear NO emission from different species of plants, including Norway spruce (*Picea abies* L.), when given nitrogen as nitrate

only, but not when fertilized with an ammonium-fertilizer. If a similar phenomenon exists in nature, it could affect plant-atmosphere interactions in a significant way.

The aim of this study was to find out if the form of nitrogen available to a plant has a measurable effect on the NO flux of a shoot or the concentration of nitrite in the needles in field conditions.

## METHODS

This experiment was conducted in July 2012 at the SMEAR II station in Hyytiälä (Hari and Kulmala 2005), outdoors atop the forest canopy, on a 20 m measuring tower. The plant material consisted of 15 grafted Scots pine (*P. sylvestris* L.) seedlings, grown for 5 years in the field and transplanted into 10 l plastic pots before the fertilization treatments were started. The seedlings were transported into the tower two weeks before the first flux measurements to allow them to recover from transportation stress and adjust to the environment.

The seedlings received three different fertilization treatments: fertilization with ammonium (ammonium sulphate,  $(\text{NH}_4)_2\text{SO}_4$ ), fertilization with nitrate (potassium nitrate,  $\text{KNO}_3$ ) or no nitrogen fertilization. To compensate for the effect of potassium in the nitrate fertilizer, the ammonium and control treatments received the same amount of potassium as potassium sulphate ( $\text{K}_2\text{SO}_4$ ). The treatments were applied as an aqueous solution in three doses, the first one in early June and the last one on the day before the last round of measurements for each seedling. For both nitrogen treatments, the total fertilizer dose was equivalent to  $20 \text{ g N m}^{-2}$ , approximately 60 times the annual nitrogen deposition in the area (Lindroos *et al.*, 2000).

We measured the shoot-level gas fluxes ( $\text{NO}$ ,  $\text{NO}_2$ ,  $\text{O}_3$ ,  $\text{CO}_2$  and  $\text{H}_2\text{O}$ ) using four box-shaped chambers with a volume of  $1 \text{ dm}^3$ . The chambers were made of plexiglass teflonized on the inside, with an UV-transparent quartz glass roof. The measurement system is described in detail in Raivonen *et al.* (2003).  $\text{NO}$  and  $\text{NO}_2$  concentrations were measured with a chemiluminescence analyzer (TEI 42CTL, Thermo Environmental Instruments, Franklin, MA, USA) equipped with a photolytic converter.

Three chambers enclosed a first-year pine shoot each, and the fourth was measured empty for reference. Each shoot was measured for 24 hours (from 6 p.m. to 6 p.m.). On each day, one seedling was measured from each treatment in randomized order and combination. After all seedlings were measured once, the chambers were cleaned. The three chambers were rotated between treatments for each of the three measurement rounds.

Each measured shoot was cut from the tree and photographed. Projected shoot area was estimated from the photograph using the ImageJ software. The needles were weighed and dried at  $70^\circ\text{C}$  for 48 hours to obtain dry weight.

To compare the  $\text{NO}$  fluxes in an empty chamber, the four chambers were measured empty for two days in the end of the experiment. As a short test of the effect of shoot age, two second-year shoots (debudded in May to prevent new growth) from each treatment were included in the last round of measurements.

The seedlings were sampled for needles and soil before the treatments and in the end of the experiment. From soil samples,  $\text{pH}_{\text{H}_2\text{O}}$  and gravimetric soil water content were determined and the rest of the sample was extracted with 1 M potassium chloride for exchangeable nitrate, nitrate and ammonium. The needle samples were frozen in liquid nitrogen immediately after sampling, ground at  $-196^\circ\text{C}$  and kept deep-frozen until extraction. The extraction method for needles was a modification of the method introduced by Sarjala (1991). Needle extractions for nitrate, nitrate and ammonium analysis were stored in  $-20^\circ\text{C}$  until analysis.

## FIRST RESULTS

The weather was exceptionally rainy for the duration of the experiment. The current-year needles were not fully developed at the time of the measurements because of the slowly progressing growth period in 2012.

We observed no evident differences in shoot NO or NO<sub>2</sub> flux between the treatments for either first-year or second-year needles (Figure 1). Also the nighttime fluxes (not shown) were very similar. The temperature response of NO emission in the different fertilization treatments is shown in Figure 2. Again, the response is very similar in all three treatments, and temperature has no measurable effect on the shoot NO flux.

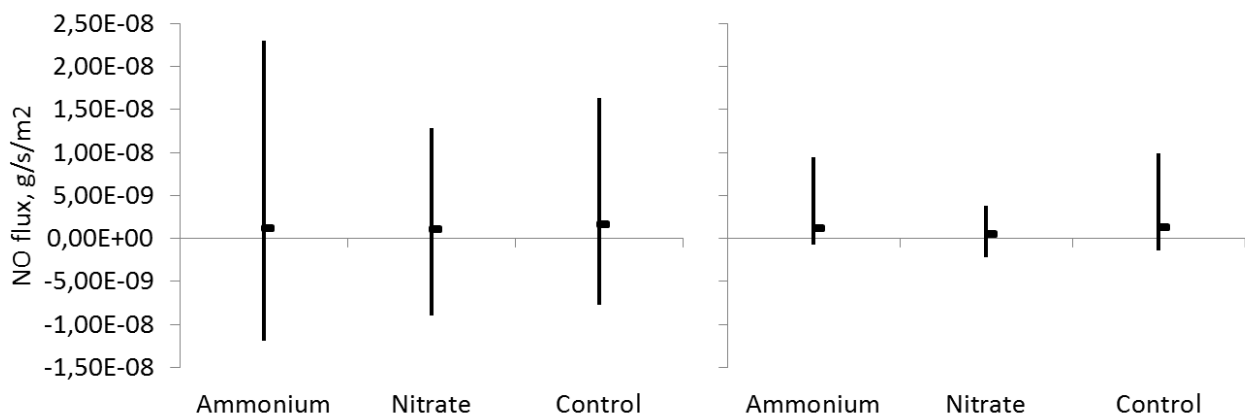


Figure 1. Average, minimum and maximum values of daytime shoot-level NO and NO<sub>2</sub> fluxes in the different fertilization treatments after correcting for the flux in the empty chamber. Left: current-year shoots, right: one-year old shoots. Positive sign indicates emission.

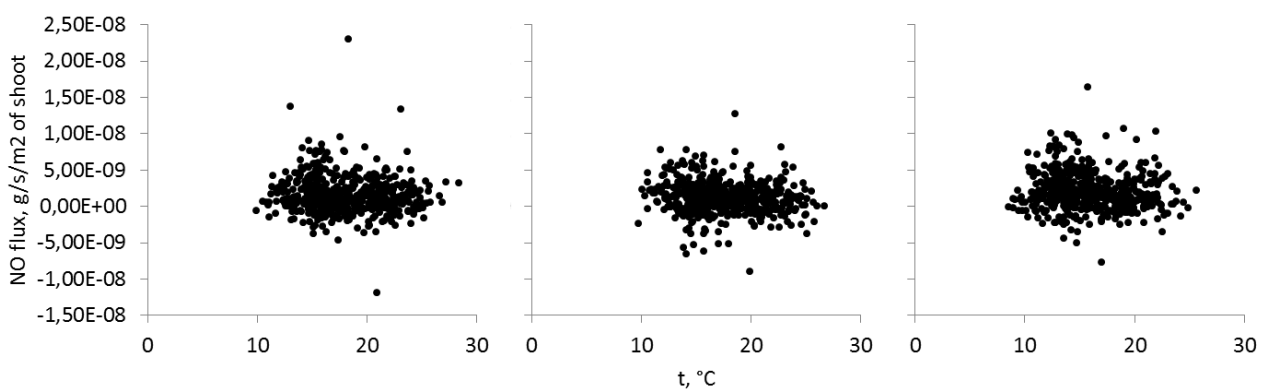


Figure 2. Temperature response of NO emission in the different fertilization treatments (current-year shoots). Left: ammonium fertilization, middle: nitrate fertilization, right: no nitrogen fertilization. Positive sign indicates NO emission.

The nutrient analysis did not reveal any clear differences in nitrite or nitrate concentrations of the needles (Figure 3). Total nitrogen content, however, was slightly higher in the trees that had received nitrogen

Figure 1 consists of four scatter plots arranged in a 2x2 grid, showing nitrogen concentrations in water and sediment for three treatments: NH<sub>4</sub>, NO<sub>3</sub>, and Control. The y-axis for all plots represents concentration in g N/g.

- Top Left Plot:** Water  $\text{NO}_2^-$  concentration (g N/g). The y-axis ranges from 0 to 2.0. Data points are clustered around 1.0-1.5 for NH<sub>4</sub> and NO<sub>3</sub>, and higher (1.0-1.8) for Control.
- Top Right Plot:** Water  $\text{NO}_3^-$  concentration (g N/g). The y-axis ranges from 0 to 25. Data points are clustered around 13-14 for NH<sub>4</sub> and NO<sub>3</sub>, and higher (12-18) for Control.
- Bottom Left Plot:** Sediment Total N concentration (g N/g). The y-axis ranges from 0 to 900. Data points are clustered around 380-580 for NH<sub>4</sub> and NO<sub>3</sub>, and higher (320-530) for Control.
- Bottom Right Plot:** Sediment  $\text{NO}_3^-$  concentration (g N/g). The y-axis ranges from 0 to 25. Data points are clustered around 12-14 for NH<sub>4</sub> and NO<sub>3</sub>, and higher (12-18) for Control.

Based on these results, it seems unlikely that additional nitrate in the soil could cause measurable NO emission in field conditions, possibly because of complex soil chemistry that affects the real nutrient conditions the tree roots experience.

## ACKNOWLEDGEMENTS

This work was supported by the Maj and Thor Nessling Foundation, the Ella and Georg Ehnrooth Foundation and by the Academy of Finland Center of Excellence program (project number 1118615). The authors thank Kaisa Rissanen for her assistance during the measurements and Finnish Forest Research Institute (Metla) Haapastensyrjä Unit for the plant material.

## REFERENCES

- Baudoin, E. (2011). The language of nitric oxide signalling. *Plant Biology* **13**, 233–242.
- Breuninger, C., Meixner, F. X. and Kesselmeier, J. (2012). Field investigations of nitrogen dioxide (NO<sub>2</sub>) exchange between plants and the atmosphere. *Atmos. Chem. Phys. Discuss.* **12**, 18163–18206.
- Fröhlich, A. and Durner, J. (2011). The hunt for a plant nitric oxide synthase (NOS): Is one really needed? *Plant Science* **181**: 401–404.
- Gupta, K. J., Fernie, A. R., Kaiser, W. M. and van Dongen, J. T. (2011). On the origins of nitric oxide. *Trends in Plant Science* **16**, 160–168.
- Hari, P. and Kulmala, M. (2005). Station for Measuring Ecosystem-Atmosphere Relations (SMEAR II). *Boreal Environment Research* **10**, 315–322.
- Hereid, D. P. and Monson, R. K. (2001). Nitrogen oxide fluxes between corn (*Zea mays* L.) and the atmosphere. *Atmospheric Environment* **35**, 975–983.
- Huffaker, R.C. (1982). Biochemistry and physiology of leaf proteins. In: Parthier, B. & Boulter, D.(eds.). Encyclopedia of plant physiology, new series 14A, 370–400. Springer-Verlag, New York.
- Klepper, L. (1979). Nitric oxide (NO) and nitrogen dioxide (NO<sub>2</sub>) emissions from herbicide-treated soybean plants. *Atmospheric Environment* **13**, 537–542.
- Lindroos, A.-J., Derome, J., Derome, K. and Niska, K. (2002). Deposition on the forests and forest floor in 2000. In: Rautjärvi, H., Ukonmaanaho, L. and Raitio, H. (eds.). Forest condition monitoring in Finland. National report 2001. *Metsäntutkimuslaitoksen tiedonantoja - The Finnish Forest Research Institute, Research Papers* **879**, 63–69.
- Morot-Gaudry-Talarmain, Y., Rockel, P., Moureaux, T., Quilleré, I., Leydecker, M. T., Kaiser, W. M. and Morot-Gaudry, J. F. (2002). Nitrite accumulation and nitric oxide emission in relation to cellular signaling in nitrite reductase antisense tobacco. *Planta* **215**, 708–715.
- Pietiläinen, P. and Lähdesmäki, P. (1988). Effect of various concentrations of potassium nitrate and ammonium sulphate on nitrate reductase activity in the roots and needles of Scots pine seedlings in N Finland. *Ann. Botanici Fennici* **25**, 201–206.
- Raivonen, M., Keronen, P., Vesala, T., Kulmala, M. and Hari, P. (2003). Measuring shoot-level NO<sub>x</sub> flux in field conditions: the role of blank chambers. *Boreal Environment Research* **8**, 445–455.
- Rockel, P., Strube, F., Rockel, A., Wildt, J. and Kaiser, W. M. (2002). Regulation of nitric oxide (NO) production by plant nitrate reductase in vivo and in vitro. *J of Experimental Botany* **53**, 103–110.
- Rondón, A., Johansson, C., Granat, L. (1993). Dry deposition of nitrogen dioxide and ozone to coniferous forests. *J of Geophysical Research* **98**, 5159–5172.
- Sarjala, T. (1991). Effect of mycorrhiza and nitrate nutrition on nitrate reductase activity in Scots pine seedlings. *Physiologia Plantarum* **81**, 89–94.
- Wildt, J., Kley, D., Rockel, A., Rockel, P. and Segschneider, H. J. (1997). Emission of NO from several higher plant species. *J of Geophysical research* **102**, 5919–5927.

# OXIDATION PRODUCT STUDY FROM THREE DIFFERENT MONOTERPENES

T. JOKINEN<sup>1,2</sup>, T. BERNDT<sup>1</sup>, M. SIPILÄ<sup>2</sup>, M. EHN<sup>2</sup>, H. JUNNINEN<sup>2</sup>, H. HERRMANN<sup>1</sup> and  
M. KULMALA<sup>2</sup>,

<sup>1</sup>Department of Chemistry, Leibniz Institute for Tropospheric Research, Leipzig, 04318, Germany

<sup>2</sup>Department of Physics, University of Helsinki, Helsinki, 00014, Finland

Keywords: monoterpenes, oxidation, mass spectrometry

## INTRODUCTION

Volatile organic compounds (VOC) are emitted in the atmosphere by several biological sources and can have effects on both human health and the climate. One of the largest groups of biogenic VOCs is monoterpenes (C<sub>10</sub>H<sub>16</sub>). Monoterpenes, such as  $\alpha$ -pinene and limonene, are previously recognized as potential aerosol number sources (Metzger *et al.*, 2010). Oxidation of terpenes is also able to produce stabilized Criegee Intermediates (sCI) that are very recently suggested to function as important new oxidants in the atmosphere (Mauldin *et al.*, 2012). The reactions of monoterpenes with O<sub>3</sub>, OH radical and other oxidants remove monoterpenes from the atmosphere in rapid oxidation reactions and produces secondary organic aerosols (Presto *et al.*, 2005). The importance of these oxidized organic compounds in atmospheric nucleation and growth still is unclear even though the oxidation of terpenes is widely studied (e.g. Bonn & Moortgat 2002). Recently Riipinen *et al.* 2012 studied the connections between VOC emissions, nanoparticle growth and climate. Their results indicated that at sizes around 5 nm more than half of the aerosol mass fraction is organic. The exact nature of these organic vapours condensing on nanoparticles is unknown. Ehn *et al.* (2012) studied naturally charged ions and published a study about  $\alpha$ -pinene oxidation products both in the laboratory and in the Hyytiälä boreal forest site (SMEAR II). They found very high O:C ratios in oxidized organics-nitrate ion clusters and concluded that these oxidation products can have an important role in aerosol particle early growth because of the very low vapor pressures, relatively high molecular masses and concentrations similar to sulphuric acid. This study is continuing the work of Ehn *et al.* and concentrates on finding differences in oxidation product yields and properties of three different structured monoterpenes, limonene,  $\alpha$ -pinene and myrcene during ozonolysis and/or OH oxidation.

## METHODS

The experiments were conducted in a laminar flow tube (lft-Ift, Institute for Tropospheric Research – Laminar Flow Tube, i.d. 8 cm; length 505 cm) at Leibniz-Institute in Germany. The flow tube was always operated at constant temperature (293  $\pm$  0.5 K) and relative humidity (25 %) and in atmospheric pressure using purified synthetic air as the carrier gas (Berndt *et al.*, 2005). The humidified main carrier-gas stream was introduced at the top of the flow tube containing the selected monoterpene and an OH radical scavenger if needed. Ozone diluted in the carrier gas was added through an inlet and rapidly mixed with the main stream using nozzles. The monoterpene concentration was detected by means of proton transfer reaction mass spectrometry (Ionicon, high sensitivity PTR-MS) (Lindinger *et al.*, 1998).

All oxidation products were detected with a high resolution mass spectrometer with a chemical ionization inlet, CI-API-TOF (Jokinen *et al.*, 2012). This instrument utilizes NO<sub>3</sub><sup>-</sup> ions for chemical ionization of the neutral compounds in the sample air. Organic compounds were detected as clusters with the charger ion. The advantage of this ionization method is that it uses similar ionization method as detected in the

atmosphere and it is also conducted in atmospheric pressure. The inlet is designed in a way that the sample air never gets contact with the walls so the wall losses can be minimized.

All data analysis was done using tofTools (version 567), a Matlab based toolbox (Junninen *et al.* 2010) that allows fast processing of high resolution mass spectrometry data.

## CONCLUSIONS

The first result is shown in figure 1 that presents a mass defect plot after the reaction with limonene in the presence of ozone and OH radical. Limonene (and  $\alpha$ -pinene) oxidation produces similar reaction products in the mass ranges of 300-400 Th ( $C_{10}$  compounds) and 450-600 Th ( $C_{20}$  compounds) as in the previous study by Ehn *et al.*. These compounds are referred here as extremely low volatility compounds (ELVOC) according to their high O:C (Donahue *et al.* 2012). Myrcene with a linear carbon skeleton also produces  $C_{10}$  based ELVOC but from a different mechanism than cyclic limonene and  $\alpha$ -pinene. During the experiments we also used OH scavengers (propane or  $H_2$ ) to study pure ozonolysis with all the selected monoterpenes. We were able to demonstrate that unsaturated cyclic monoterpenes efficiently produce ELVOC from reaction with ozone alone while the reaction initiated by OH is significantly larger in initiating the ELVOC formation from an unsaturated non-cyclic monoterpene like myrcene. Ozonolysis of limonene and  $\alpha$ -pinene yields two thirds higher are approximately of those from myrcene OH oxidation. These results are preliminary and will be further analyzed in the near future.

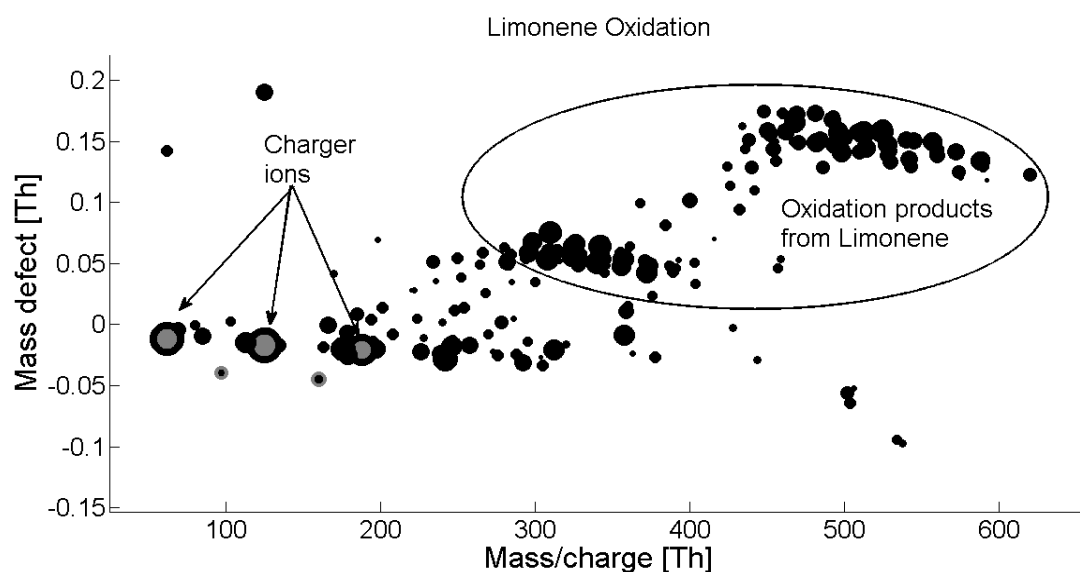


Figure 1. Mass defect plot of reaction products from limonene oxidation in the presence of OH radical and  $O_3$ . The first “band” of peak at 300-400 Th is identified as highly oxygenated  $C_{10}$  compounds and the second “band” correspond to highly oxygenated  $C_{20}$  compounds. All compounds are detected as nitrate clusters.

## ACKNOWLEDGEMENTS

The Academy of Finland Center of Excellence program (project no. 1118615), Academy of Finland Project (139656), the Nordic Centers of Excellence CRAICC and PEGASOS project funded by the European Commission under the Framework Programme 7 (FP7-ENV-2010-265148). We would also like to thank R.Gräfe and K. Pielok for technical assistance during IfT flow tube experiments.

## REFERENCES

- Bonn, B. and Moorgat, G. K. (2002): New particle formation during  $\alpha$ - and  $\beta$ -pinene oxidation by  $O_3$ , OH and  $NO_3$ , and the influence of water vapour: particle size distribution studies, *Atmos. Chem. Phys.*, 2, 183-196, doi:10.5194/acp-2-183-2002.
- Donahue, N. M., Kroll, J. H., Pandis, S. N., and Robinson, A. L. (2012): A two-dimensional volatility basis set – Part 2: Diagnostics of organic-aerosol evolution, *Atmos. Chem. Phys.*, 12, 615-634, doi:10.5194/acp-12-615-2012.
- Ehn, M., Kleist, E., Junninen, H., Petäjä, T., Lönn, G., Schobesberger, S., Dal Maso, M., Trimborn, A., Kulmala, M., Worsnop, D. R., Wahner, A., Wildt, J., Mentel, Th. F. (2012), *Atmos. Chem. Phys.*, 12, 5113-5127, doi:10.5194/acp-12-5113-2012.
- Jokinen, T., Sipilä, M., Junninen, H., Ehn, M., Lönn, G., Hakala, J., Petäjä, T., Mauldin III, R. L., Kulmala, M., and Worsnop, D. R., (2012), *Atmos. Chem. Phys.*, 12, 4117-4125, doi:10.5194/acp-12-4117-2012.
- Junninen, H., Ehn, M., Petäjä, T., Luosujärvi, L., Kotiaho, T., Kostianinen, R., Rohner, U., Gonin, M., Fuhrer, K., Kulmala, M. and Worsnop, D.R. (2010): API-ToFMS: a tool to analyze composition of ambient small ions. *Atmos. Meas. Technol.*, 3, pp. 1039-1053.
- Lindinger W., Hansel A., Jordan A. (1998): On-line monitoring of volatile organic compounds at pptv levels by means of proton-transfer-reaction mass spectrometry (PTR-MS) medical applications, food control and environmental research, *International Journal of Mass Spectrometry and Ion Processes*, 173, 3,191-241, ISSN 0168-1176, [http://dx.doi.org/10.1016/S0168-1176\(97\)00281-4](http://dx.doi.org/10.1016/S0168-1176(97)00281-4).
- Mauldin (III) R. L., Berndt T., Sipilä M., Paasonen P., Petäjä T., Kim S.,Kürten T., Stratmann F., Kerminen V.-M., Kulmala M., (2012), *Nature*, 488, 193–196, doi:10.1038/nature11278
- Metzger, A., Verheggen B., Dommen J., Duplissy J., Prevot A. Weingartner E., Riipinen I., Kulmala M., Spracklen D. V., Carslaw K. S., Baltensperger U., (2010), *Proceedings of the National Academy of Sciences* doi:10.1073/pnas.0911330107.
- Presto A. A., Huff Hartz K. E., and Donahue N. M., (2005), *Environ. Sci. Technol.*, 39 (18), pp 7046 7054, doi: 10.1021/es050400s
- Riipinen, I., Yli-Juuti, T., Pierce, J.R., Petäjä, T., Worsnop, D.R., Kulmala, M. and Donahue, N.M. (2011): The contribution of organics to atmospheric nanoparticle growth, *Nat. Geo. Sci.* 5, 453 458, doi: 10.1038/ngeo1499.

# NOVEL VIEWPOINTS FOR THE TRANSACTIONS OF FORESTS AND ATMOSPHERE -ART/SCIENCE RESIDENCE AT HYYTIÄLÄ 2013-2014

E. JUUROLA<sup>1,2</sup>, J.F. KORHONEN<sup>1</sup>, U. TAIPALE<sup>3</sup> AND J. LEVULA<sup>4</sup>

<sup>1</sup>Department of Physics, PL 48, FIN-00014, University of Helsinki, Finland.

<sup>2</sup>Department of Forest Sciences, University of Helsinki, Finland.

<sup>3</sup>Aalto University, School of Arts, Design and Architecture, Aalto Biofilia -Base for Biological Arts, Finland.

<sup>4</sup>Hyytiälä Forestry Field Station, Finland

Keywords: Art and Life Sciences

## BACKGROUND

The SMEAR II station, Finnish flagship station for measuring the relationships of atmosphere and forest in boreal climate zone, is a unique place, where in addition to top quality research, also important scientific design and innovations are made. It is important that these unique achievements reach also audience outside the scientific community.

A project 'Novel viewpoints for the transactions of forests and atmosphere' was started officially in the beginning of year 2013. The objective of the project is to use novel methods at the intersection of arts and eco-physiological research for transmission of the complex and multilevel research, carried out at SMEAR II station at Hyytiälä Forestry Field Station in South Finland, for a wider audience.

Initiating discussions and collaboration between scientists and artists may not be an easy task. In this kind of art residence there could be a high risk of failure for example due to the lack of common language, or shortage of time. In this project, importantly, this risk is overcome by allocating resources for appointing a dedicated mentor who will introduce the artist in the world of measurements and equipment.

## THE PROJECT

In the beginning of 2013 a call for shortlisted artists was organized. The artists were asked to write a proposal for art-residency in the Hyytiälä Forestry Field Station, including the development of a project related with the station's research areas, more specifically with the research related with the interaction between forests and the atmosphere, and furthermore, a plan for an art&science workshop in 2014 around this particular topic.

Based on the proposals, a German media artist Agnes Meyer-Brandis was invited to Hyytiälä for two to three months residency to do her own artistic work, linked to the investigations at the SMEAR II research station. In her work, Meyer-Brandis interweaves trans-disciplinary research and thought together with insightful use of technology, creating remarkable art that always includes fantastic elements. In recent years she has explored, for example, the formation of the water droplets during scientific weightlessness flights by German Space Agency, trailed along the migration routes of the mysterious Moon Geese and designed an apparatus that enhance cloud formation.

During her residency, Meyer-Brandis is investigating research and the phenomena of the nature in Hyytiälä. The work is centred around trees and the communication between men and trees. An important part of her work is to exchange ideas and knowledge with researchers and other people in Hyytiälä. The visit will lead to a piece of contemporary art, which will be unveiled in 2014.



**Figure.** The TreeTable with Agnes Meyer-Brandis at Hyytiälä Forestry Field Station in August 2013. Picture by Jens Brand.

The art-residency will be followed by an art&science workshop in fall 2014, led by Meyer-Brandis. The idea is to invite participants – students, researchers and artists – to share visions and ideas. More information about Agnes Meyer-Brandis can be found at <http://www.ffur.de/>

The residency is carried out in collaboration between the Institute of Atmospheric Research and Earth System Science and Department of Forest Sciences in Helsinki University, and Aalto Biofilia. It is funded by Kone Foundation.

## CONCLUSIONS

Although the project is still on going, the experiences on the art residence are encouraging. The keys to the success of the project seem to be e.g. an efficient and professional call to attract interesting artists, and the ability to have a dedicated mentor involved in the project. We have managed to involve an internationally renowned artist for the first residence, artist who has an enthusiastic attitude towards science and research, and the research community in Hyytiälä.

The workshop that will be organised in 2014 will be a new experience, but surely most thought-provoking and educative. It will be a challenge to get together scientists, students and artists, in such a way that it will create a fruitful and productive atmosphere where everybody feels they can contribute in a meaningful way. However, active presence of Mayer-Brandis has already initiated inspired discussions and activities in Hyytiälä.

Finally, it is utmost important to collect the experiences from the first art residence, both from the people working at the Hyytiälä and SMEAR II station, as well as from the residential artist. The aim is to continue the interactions between art and science and include the art residence as a regular activity of the research group.

## ACKNOWLEDGEMENTS

The financial support by Kone Foundation, the Academy of Finland Centre of Excellence program (project no 1118615) and the Academy project “ICOS” (project no 17352) are gratefully acknowledged.

# FORMATION OF CROWN STRUCTURE IN SCOTS PINE TREES

K. KABIRI KOUPAEI, E. NIKINMAA and P. HARI

Department of Forest Sciences, PO Box 27, 00014 University of Helsinki, Finland

Keywords: Carbon balance, nitrogen allocation, SMEAR II, MicroForest, structural regularities

## INTRODUCTION

Scots pine forms a whorl of branches each year at the top of the tree. Thereafter the branches grow annually, new needles are formed and the length and diameter of the branches increase. The growth is strong in a young branch, it slows down and finally the branch dies. The needles in the branch are, however, unable to photosynthesize without water that is taken up by roots and transported in the woody structures from roots to needles. At the same time proteins are needed for photosynthesis since pigment complexes, enzymes and membrane pumps carry out the synthesis of sugar. The high nitrogen concentration of proteins (15 – 17%) explains the crucial role of nitrogen in the metabolism of trees where carbon and nitrogen uptake are connected with each other

We consider that whorls are the functional units of Scots pine trees; the needles, water transport system and fine roots for water and nitrogen uptake form the whorl. The sugars synthesized in the needles and the nitrogen taken up from the soil and obtained from the senescent needles are used for the growth and maintenance of the whorl and for the growth of the treetop. The sugars are used mainly for the synthesis of cellulose, lignin, lipids and starch while the nitrogen is crucial for the synthesis of proteins.

The allocation of sugars and nitrogen for needles, water pipes and fine roots is a very demanding task for the biochemical regulation system of the tree. We assume that the regulation system is powerful and it is able to utilize the resources in an efficient way. There must exist a balance between the transpiration from needles and the water transport capacity in the branches, stem and in transport roots. The commonly observed linear relationship between needle mass and sap wood area (Hari *et al.*, 1986, Nikinmaa, 1992 and Perttunen *et al.*, 1996) is a result of the action of the biochemical regulation system and it makes the balance between the transpiration from needles and water transport in the stem.

The relationship between the sapwood area and needle mass determines the amount of new water pipes needed for a gram of needle growth in a whorl. Thus we can obtain the amount of sugars used for water pipes from the needle growth in the whorl. The tissues have characteristic nitrogen concentrations, high in needles and fine roots and low in woody structures. The amount of fine roots must be such that the fine roots can provide the nitrogen needed for the synthesis of proteins in the needles, fine roots and water pipes. We formulate the above ideas as carbon and nitrogen balance equations. We assume that the action of the biochemical regulation system produces such structures that they fulfil the carbon and nitrogen balance equations.

The carbon and nitrogen balance equations include two unknowns; needle and fine root growth. We solve these unknowns and thereafter we determine the growth of the woody structures. We obtain branch elongation from the requirement that needle density is constant. The whorls form the crown of a pine tree and we obtain the crown development from the growth of the whorls in the tree.

The ecosystem model MicroForest (Hari *et al.*, 2008; Hari *et al.*, 2013) describes the development of trees, ground vegetation and forest soil in a Scots pine stand. Here, we introduce MicroForest as an ecosystem model which can predict the development of stand from an early initial state of stand establishment. Our aim is to present a theoretical framework for structural regularities in crown development in Scots pine and test it. The crown development is based on carbon and nitrogen balance both as a function of needle mass. Thus we can simulate the crown development with MicroForest from an

initial state. Then the reduction of photosynthesis per needle mass caused by shading is introduced into the simulations through stand development.

## METHODS

We selected the Scots pine stand around SMEAR II measuring station in Finland to test the behaviour of our crown model. We cut two trees in the 50 years old Scots pine stand, one from the dominant (in thinned stand) and one from intermediate (in un-thinned stand) size class. The annual length growth of all branches along the main axis of the branches and the needle mass were measured for both trees. There would be eight more trees to be cut during the summer and autumn 2013 to cover all size classes for better understanding of the structural regularities and testing the model.

## CONCLUSIONS

The needle growth in a branch has a clear pattern, first rapid growth following a stabilization phase and finally a slow decline (Fig.1a and 1b). The pattern of branch elongation is also clear as a saturating function where a slow declining trend is dominating (Fig.2a and 2b).

The results for the prediction of needle biomass profile for both trees in thinned (Fig.1) and un-thinned (Fig.2) stands are rather off comparing the measurements but have the same pattern. This means that there is some tuning required for getting a prediction close to the reality.

However, the results for branch elongation seem to be promising and the pattern is clear as a saturating function following a slow declining trend in both trees in thinned (Fig.3) and un-thinned stand (Fig.4). Thus, evidently our novel measurements provide valuable information for the development of the model.

Based on the simulated needle mass profile and branch elongation model we are able to predict crown size development for Scots pine trees. We will test the simulations with measurements done in the summer 2013.

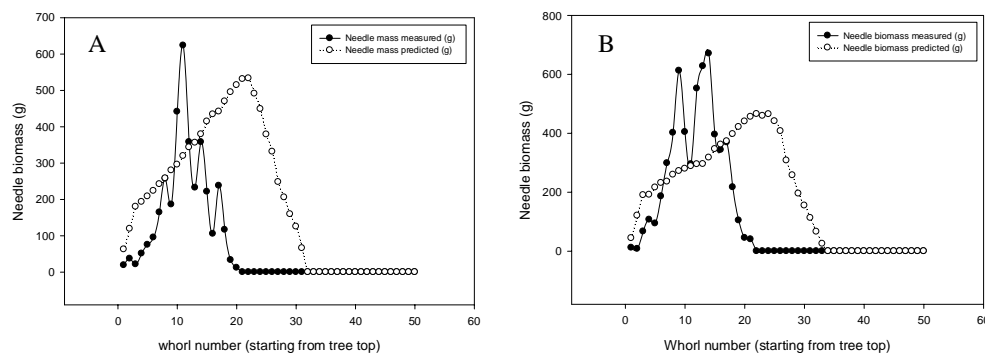


Fig 1. Measured and predicted needle biomass in a dominant tree in un-thinned stand (A) and an intermediate tree in thinned stand (B) of Scots pine in SMEAR II station in southern Finland.

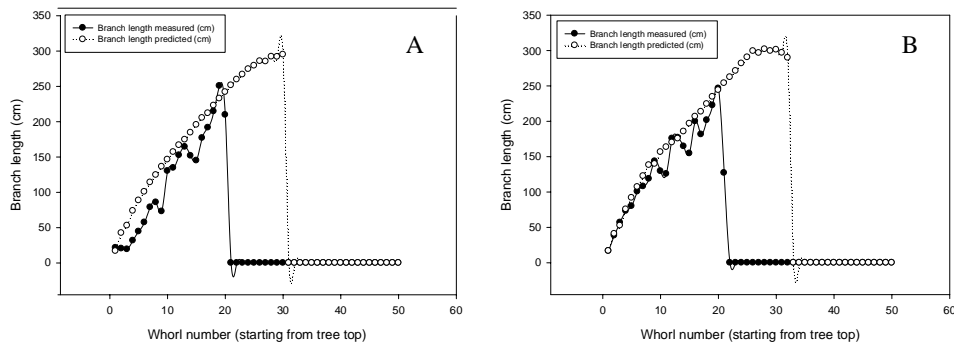


Fig 2. Measured and predicted branch length in a dominant tree in un-thinned stand (A) and an intermediate tree in thinned stand (B) of Scots pine in SMEAR II station in southern Finland.

## ACKNOWLEDGEMENTS

This work was supported by the Academy of Finland project no. 1118615.

## REFERENCES

- Hari, P., Heikinheimo, P., Mäkelä, A., Kaipiainen, L., Korpilahti, E. and Salmela, J. 1986. Trees as water transport system. *Silva Fennica*. 20: 205-210.
- Hari, P., Kulmala, M., 2005. Station for measuring ecosystem–atmosphere relations (SMEAR II). *Boreal Environment Research*. 10: 315–322.
- Hari, P., Salkinoja-Salonen, M. S., Liski, J., Simojoki, A., Kolari, P., Pumpanen, J., Kähkönen, M., Aakala, T., Havimo, M., Kivekäs, R. and Nikinmaa, E. 2008. Growth and development of forest Ecosystems: : the MicroForest model. In: *Boreal forest and climate change*. Hari, P. & Kulmala, L. (editors.) Springer s. 433-461. 29 (Advances in global change research; 34).
- Hari, P., Havimo, M., Kabiri Koupei, K., Jögiste, K., Kangur, A., Salkinoja-Salonen, M., Aakala, T., Aalto, J., Schiesl-Aalto, P., Liski, J. and Nikinmaa, E. 2013. Dynamics of carbon and nitrogen fluxes and pools in forest ecosystem. In: *Physical and physiological forest ecology*. Hari, P., Heliövaara, K. & Kulmala, L. (editors.) Springer s. 346-396.
- Nikinmaa, E. 1992. Analyses of the growth of Scots Pine: matching structure with function. *Acta Forestalia Fennica*. 235.
- Perttunen, J., Sievänen, R., Nikinmaa, E., Salminen, H., Saarenmaa, H. and Väkevä, J. 1996. LIGNUM: a tree model based on simple structural units. *Annals of Botany* 77: 87-98.

# CONCENTRATIONS OF OXIDIZED VOCs AND AROMATIC VOCs AT A BOREAL FOREST

M.K. KAJOS<sup>1</sup>, M. HILL<sup>2</sup>, H. HELLÉN<sup>3</sup>, P. RANTALA<sup>1</sup>, J. PATOKOSKI<sup>1</sup>, R. TAIPALE<sup>1</sup>, C. C. HOERGER<sup>2</sup>, S. REIMANN<sup>2</sup>, H. HAKOLA<sup>3</sup>, T. PETÄJÄ<sup>1</sup> AND T.M. RUUSKANEN<sup>1</sup>

<sup>1</sup> Department of Physics, University of Helsinki, P.O.Box 64, 00014 University of Helsinki, Finland.

<sup>2</sup> Empa, Laboratory for Air Pollution/ Environmental Technology, Ueberlandstr. 129, 8600 Duebendorf, Switzerland

<sup>3</sup> Finnish Meteorological Institute, P.O.Box 503, 00101 Helsinki, Finland

Keywords: OVOCs, aromatic VOCs, PTR-MS, GC-MS, boreal forest.

## INTRODUCTION

Oxidized volatile organic compounds (OVOCs) such as acetaldehyde and acetone and aromatic VOCs such as benzene and toluene originate from various anthropogenic and biogenic sources. These compounds have relatively long lifetimes, varying from a few days in the summer to hundreds of days in the winter. Thus they are effectively transported for long distances. In this study, we wanted to investigate the concentrations of acetaldehyde, acetone, benzene and toluene at rural background site located in a boreal forest. The measurements were done with two different methods; Gas Chromatography-Mass Spectrometry (GC-MS) and Proton Transfer Reaction-Mass Spectrometry (PTR-MS). The aim of our study was to compare the performance of two different methods for measuring the concentrations of aromatic and oxidized VOCs in the ambient air of a boreal forest.

## METHODS

The concentrations were measured with two GC-MSs and two PTR-MSs (Ionicon Analytik, Austria) at the SMEAR II site (Station for Measuring Forest Ecosystem-Atmosphere Relations, 61°51'N, 24°17'E, 181 m a.s.l.) in Hyytiälä, Southern Finland in April-May 2012. The site is located in a rural boreal forest, which is dominated by Scots pine but there are also some Norway spruces, European aspens and birches. Continuous measurements of trace gas concentrations, aerosol particle size distributions as well as meteorological parameters are performed at the site (Hari and Kulmala, 2005). The nearest municipality (Korkeakoski) is about 10 km and the nearest big city (Tampere) is about 50 km from the site. OVOCs and aromatic hydrocarbons arrive to SMEAR II station from both regional and long range sources (Patokoski et al., 2014).

GC-MS is a well-established and old method (the development of GC-MS started in the 1950s) to measure VOCs with a low, often one hour, time resolution. However it is rather labor intensive method and often used in short term campaigns. The other method, proton-transfer-reaction mass spectrometry, is a relatively new technique (Lindinger et al., 1998; de Gouw and Warneke, 2007) to measure VOCs in-situ. PTR-MS has a sub-minute time resolution and it is suitable for long term continuous measurements. The disadvantage of the PTR-MS is that the identification of the compounds is solely based on mass, thus compounds with the same nominal mass cannot be distinguished. Both of these methods are widely used for atmospheric measurements around the world.

The two GC-MSs and one of the PTR-MSs were using the same c.a. 20 m long inlet line (Teflon PTFE, 8mm id), which was sampling from 10 m height. The inlet of the other PTR-MS, which is part of the

permanent measurement set up of the SMEAR II, was located about 20 m away from the common inlet of the other instruments.

## RESULTS

The results, which will be presented in the FCoE meeting, show promising agreement between the instruments.

## ACKNOWLEDGEMENTS

We thank the Aerosols, Clouds and Trace gases Research InfraStructure (ACTRIS) Network for financial support. The financial support by the Academy of Finland Centre of Excellence program (project no 1118615) is gratefully acknowledged.

## REFERENCES

- de Gouw, J., Warneke, C., (2007). Measurements of volatile organic compounds in the earth's atmosphere using proton-transfer-reaction mass spectrometry. *Mass Spectrometry Reviews* 26, 223-257.
- P. Hari and M. Kulmala (2005), Station for measuring Ecosystem-Atmosphere Relations, *Boreal Environmental Research* 10, 315-322.
- Lindinger, W., Hansel, A., Jordan, A., (1998). On-line monitoring of volatile organic compounds at pptv levels by means of Proton- Transfer-Reaction Mass Spectrometry (PTR-MS) Medical applications, food control and environmental research. *International Journal of Mass Spectrometry and Ion Processes* 173, 191–241.
- Patokoski, J., Ruuskanen, T. M., Hellén, H., Taipale, R., Grönholm, T., Kajos, M. K., Petäjä, T., Hakola, H., Kulmala, M. & Rinne, J. (2014): Winter to spring transition and diurnal variation of VOCs in Finland at an urban background site and a rural site. *Boreal Environmental Research* 19. In press.

# MODELING LATENT HEAT EXCHANGE IN BOREAL AND ARCTIC BIOMES

V., KASURINEN<sup>1,2</sup>, P., KOLARI<sup>1</sup>, K., ALFREDSEN<sup>2</sup>, I., MAMMARELLA<sup>3</sup>, P.,  
ALEKSEYCHICK<sup>3</sup>, T., VESALA<sup>3</sup>, F., BERNINGER<sup>2</sup>

<sup>1</sup>University of Helsinki, Department of Forest Sciences,

<sup>2</sup>Norwegian University of Science and Technology, Department of Hydraulic and Environmental Engineering

<sup>3</sup>University of Helsinki, Department of Physics

Keywords: LATENT HEAT FLUX, EDDY COVARIANCE, PENMAN-MONTEITH, STOMATAL RESISTANCE, AERODYNAMIC RESISTANCE

## ABSTRACT

Boreal and arctic ecosystems cover almost 25% of the surface area of the globe and are sensitive to the potential effects of the climate change. The most of the intensive work concerning the eddy covariance tower network during the past decades has concentrated to study the fluxes of carbon dioxide while only few large scale intensive latent heat flux and evapotranspiration studies have been done. Evapotranspiration from the vegetation surfaces is, in most cases, largely regulated by the stomata of the forest trees or other vegetation.

The Penman-Monteith equation (PM) is probably the most used approach that has been used in the estimation of crop evapotranspiration (Penman 1948, Allen 1998). In the simplest approaches the component of aerodynamic resistance is expected to be constant (mean wind speed  $2 \text{ m s}^{-1}$ ) and many studies have used successfully different simplified formulations of PM. However, in biological systems the annual biological dynamics of the system will determine the rates of evapotranspiration.

In this study we introduce a new approach that is taking into account the delayed stomatal spring recovery that has been observed in studies concerning the photosynthesis (Gea et al 2010, Mäkelä et al 2004). We modeled latent heat flux parameters based on the data that is collected from the boreal and arctic eddy covariance stations. The calibration of the model was done in order to produce site-specific parameters and also for different ecosystem types. This information is valuable for estimating how vegetation specific latent heat flux might change in the warming climate.

## METHODS

Site data for the model calibration were collected from the different Fluxnet database (European Fluxes Database Cluster <http://gaia.agraria.unitus.it>, Fluxnet Canada [http://fluxnet.ornl.gov/site\\_list/Country/CA](http://fluxnet.ornl.gov/site_list/Country/CA), Ameriflux <http://ameriflux.ornl.gov>, and Asiaflux <http://www.asiaflux.net>). The selected eddy covariance (EC) sites were representative for hemi-boreal, boreal and arctic conditions and covered the most common ecosystem types. Agricultural ecosystems were excluded from the analysis. The sites were grouped based on the dominant plant type and time since disturbance into 9 different categories. These were: cut or burnt areas temporary void of trees (C), Douglas fir forests (D), pine forests (P), spruce or fir dominated forests (S), deciduous forests (Le), larch forests (La), wetlands (W) and tundra (T). We attempted to select all sites in the boreal and hemi-boreal region but we finally rejected sites with short time series, with measurements only during summer and with large gaps in the data. We acknowledge that this rejection process was partly subjective. Our quality requirements were stricter for ecosystem types

that are well represented in the database while we had less stringent requirements for vegetation types that were not often measured.



Figure 1. Site location and distribution of eddy covariance sites used in the modeling.

## DATA QUALITY CONTROL AND GAP-FILLING

Over 400 EC years were pre-checked and quality controlled concerning the meteorological variables and latent heat flux ( $\lambda E$ ) required for the estimation. We required rather complete time series of eight meteorological variables: air temperature ( $T_a$ ), wind speed (WS), global radiation ( $R_g$ ), net radiation ( $R_n$ ) and air pressure (Pa) and water vapor deficit. Relative humidity (RH) was used to calculate saturation vapor pressure (VPD) if it was not provided in the original data.

The model parameter estimation used (sometimes but rarely gap-filled) meteorological variables provided by the data owners were used. However, parameter estimation was always using non-gap-filled measured  $\lambda E$  fluxes. Small gaps (a few hours) in recorded air temperature data were linearly interpolated. For some stations longer gaps in air temperature and VPD were calculated from data recorded at the nearest weather station

## LATENT HEAT FLUX MODEL

We estimated evapotranspiration using the Penman-Monteith equation (as presented by Monteith 1948):

$$1) \lambda E = \frac{R_n + \rho_a c_p \delta_e r_a^{-1}}{\Delta + \gamma (r_s + r_a) r_s^{-1}}$$

Where,  $\lambda E$  is the latent heat flux ( $\text{W m}^{-2}$ ),  $R_n$  is the net radiation ( $\text{W m}^{-2}$ ),  $\rho_a$  the dry air density ( $\text{kg m}^{-3}$ ),  $c_p$  the specific heat capacity of air ( $\text{J kg}^{-1} \text{K}^{-1}$ ),  $\delta_e$  is vapor pressure deficit (Pa),  $\Delta$  is the rate of change of saturation specific humidity with air temperature ( $\text{Pa K}^{-1}$ ) and  $\gamma$  is psychrometric constant ( $\gamma \approx 66 \text{ Pa K}^{-1}$ ),  $r_s$  is the stomatal resistance ( $\text{s m}^{-1}$ ) (referred also as surface resistance). Atmospheric resistance  $r_a$  ( $\text{s m}^{-1}$ ) (referred also as aerodynamic resistance) was calculate from the EC data according to

$$2) r_a = \frac{U}{u_*^2} + \frac{kB^{-1}}{ku_*}$$

, where  $U$  is wind speed ( $\text{m s}^{-1}$ ),  $u$  is friction velocity ( $\text{m s}^{-1}$ ),  $k$  is the von Karman constant (dimensionless). The excess resistance parameter  $B^{-1}$  was set to the value of 2 (dimensionless) in order to estimate the aerodynamic resistance in a similar way for all sites. The used value is suggested to be representative for forest (Launiainen 2010, Verma 1989) and has been used also for other vegetation types.  $kB^{-1}$  might vary between vegetation types as well as seasonally (Kustas et al 1989). However, in simulations the effect of this element in relation to total aerodynamic resistance is small and we assume that used parameterization does not have a significant role in the calculations related to  $r_a$ .

The stomatal resistance was estimated using a multiplicative model.

$$3) r_s = f(P) f(\delta_e) f(R_D)$$

Based on the works of Mäkelä et al. (2004) and Gea-Izquierdo et al. (2010), we assume that there is a change in stomatal resistance ( $S(t)$ ) within the year as a function temperature, with the following functions:

$$4) S(t) = \min\left(\frac{\int_{t-\tau}^t T(t)dt}{\tau\theta}, 1\right)$$

where,  $T$  is air temperature,  $\theta$  is the average temperature below which there is slow/delayed response of stomatal resistance to temperature,  $\tau$  is the delay of stomatal response in days.

The phenological development of stomatal resistance  $f(P)$  was described as:

$$5) f(P) = r_{sMax} - 2(r_{sMax} - r_{sMin})\left(1 - \frac{1}{1+S}\right)$$

where,  $r_{sMax}$  and  $r_{sMin}$  are the modeled maximum and minimum stomatal resistance ( $\text{s m}^{-1}$ ),  $k_r$  is stomatal response to global radiation ( $\text{W m}^{-2}$ ) and  $k_{vpd}$  is the stomatal sensitivity to VPD slope (Pa).

We estimated the stomatal resistance based on ideas of Wong et al. (1979) and Leuning (1995) that assume a linear relationship between stomatal conductance and the rate of photosynthesis.:

$$6) f(R_g) = \frac{k_R + R_g}{(R_g + 5)}$$

Where  $k_R$  is a parameter and  $R_g$  the global radiation

and

$$7) f(\delta_e) = \left(1 + \frac{\delta_e}{k_{vpd}}\right)$$

## STATISTICAL ANALYSIS

The modeling was implemented in R software (R-core team 2013) by using non-linear least squares regression (the `nls`-function of the `stat` library using the `nl2sol` algorithm)). The parameter  $\theta$

and  $\tau$ , linked to the phenology of transpiration, were estimated, however, iteratively using a grid with a density of 1 days ( $\tau$ ) and 1 degree Celsius ( $\theta$ ). For rare cases where the use of the phenology model improved the fit of the model by less than 2%,  $\theta$  and  $\tau$  were set as constants ( $\theta=5$  degrees C and  $\tau=2$  days).

Parameter estimation was done using half hourly values. We provide two different parameter estimates. Firstly we estimated parameter values for each site separately and secondly we pooled our data for each functional type and estimated the parameters for each ecosystem type. We use a pseudo  $R^2$  (also called proportion of explained variance here after considered as  $PR^2$ ) often called proportion of explained variance to measure the goodness of fit of our models. It is defined as:

$$8) PR = 1 - \frac{\sum(y-y_2)^2}{\sum(y-y_3)^2}$$

where,  $y$  is the measured value of the variable in question  $y_2$  is its predicted value and  $y_3$  its measured values.  $PR^2$  is the pseudo  $R^2$ . For a linear regression this would give the same values as the traditional  $R^2$ .

## RESULTS & DISCUSSION

The annual average air temperature (as calculated from the climatological data) was lowest for Tundra sites and highest for Douglas fir varying almost 20 C from -10 to + 8 C. Extremely continental sites, Yakutsk Larch & Pine sites (RU-Ylr & RU-Ypf) had also very low annual mean temperatures (-10 C (data not shown)).

Concerning the  $S$  and  $\tau$  factors the mean air temperature threshold to reach minimum stomatal resistances were lower for wet- and tundra-type sites and the values of  $\tau$  smaller than for forested sites. For forests the threshold temperature varied from 10 to 13 C and  $\tau$  from 15 to 25 days (Fig 2 a & b). The longest adaptation period and highest saturation temperature were observed for grass-type vegetation. Douglas fir did not show any seasonal phenological pattern for stomatal conductance and there were no clear values for  $\tau$ .

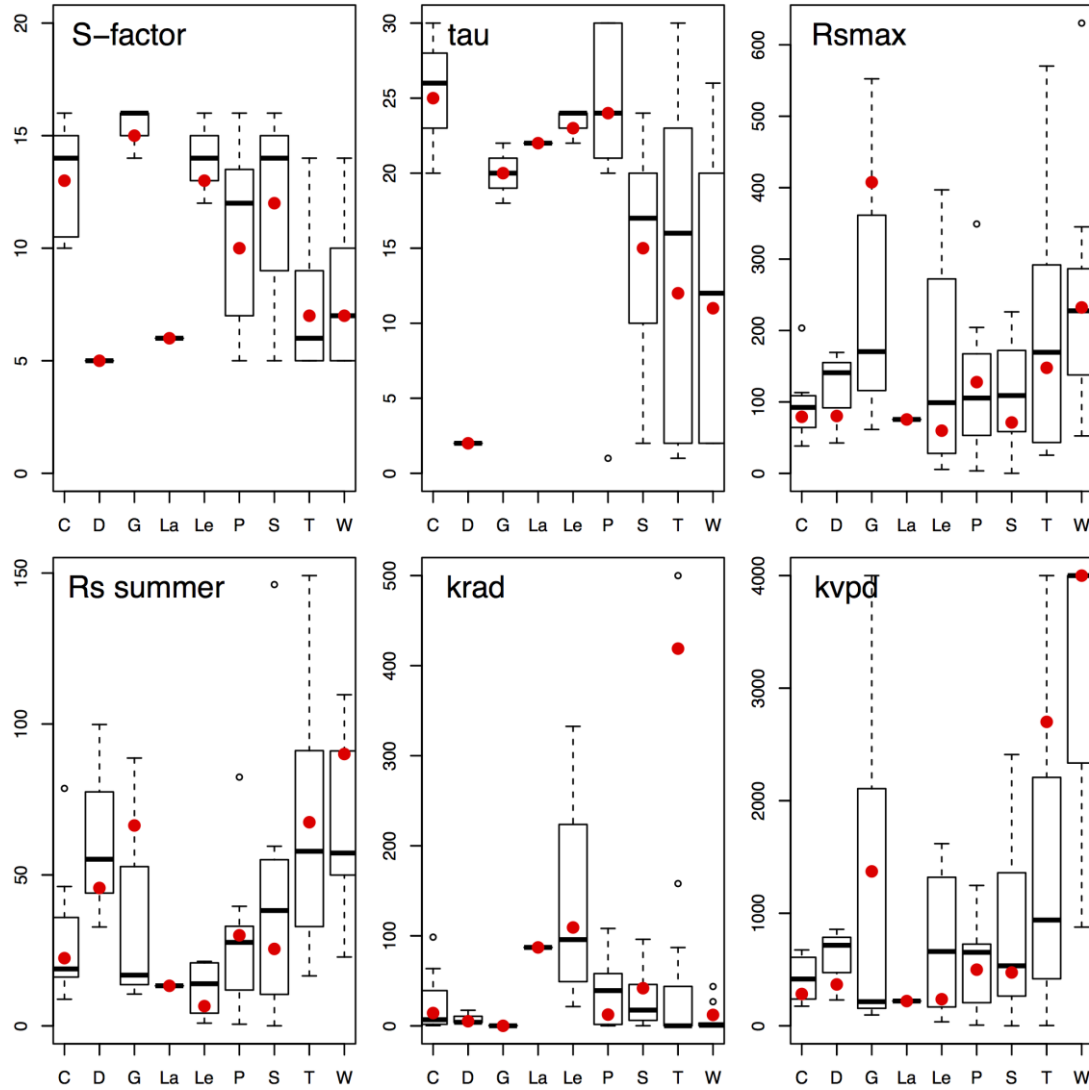


Figure 2. Distribution of model parameters  $r_{sMax}$  (a),  $r_s$  summer (b)  $k_{rd}$  (c) and  $k_{vpd}$  (d). Results are presented according to biome types: C: cut / open / burned originally forested sites, D: Douglas Fir, G: Grassland, La: Larch, Le: Deciduous Broadleaf forest, P: Pine, S: Spruce, T: Tundra, W: wetland. Red points are model parameters that are calibrated against the all ecosystem-specific data and represents universal values that can be used in the modeling.

### FIT OF THE MODEL

Squared pseudo correlation  $PR^2$  values for half hourly data varied from 0.4 to 0.84. The mean  $PR^2$  value was  $0.65 (\pm 0.1)$  (mean  $\pm$  sd). When we estimated the model for average daily evapotranspiration values the  $PR^2$  varied from 0.48 to 0.92 with a mean of  $0.77 (\pm 0.1)$  (RU-Cok, CA-NS5) and for monthly evapotranspiration estimates  $PR^2$  values varied between 0.58 to 0.99 with a mean  $0.90 (\pm 0.07)$  (RU-Cok, RU-Ha1) (Figure 3).

When all data from each land cover types were pooled and estimated together, biome specific  $PR^2$  was slightly lower for all vegetation types for 0.5 h data than the arithmetic mean based on site-wise estimation. However, for daily and monthly time span, the biome specific  $PR^2$  were slightly higher

than the mean of site-wise calculated estimated data, except for tundra sites (Figure 3). Estimated and measured daily means for  $\lambda E$  exchange were highly correlated and  $PR^2$  varied from 0.84 to 0.98 (Fig 3).

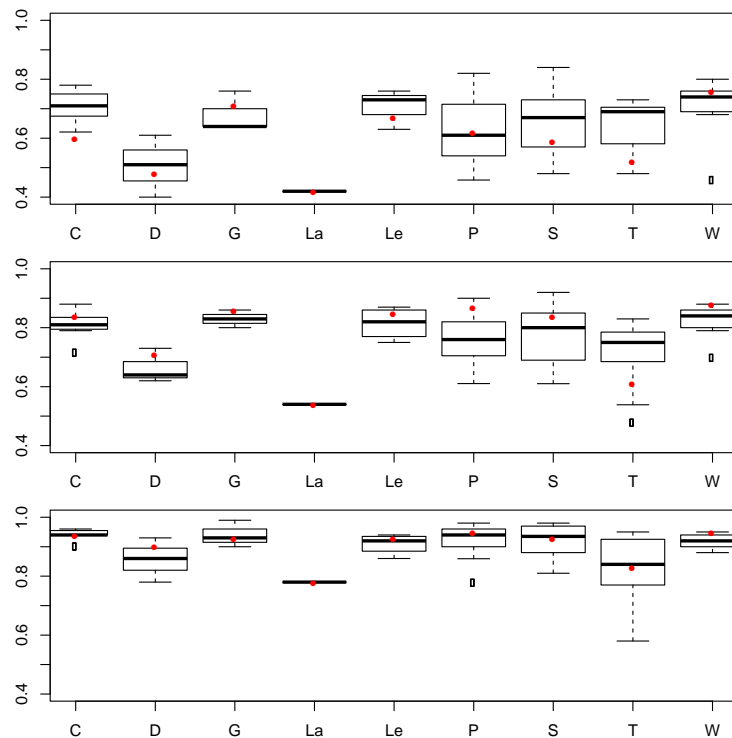


Figure 3. Pseudo correlation coefficients for 0.5 h (A), daily (B) and monthly (C) model fits. Results are presented according to vegetation types: C: cutted / open canopy, D: Douglas Fir, G: Grassland, La: Larch, Le: Leaf, P: Pine, S: Spruce, T: Tundra, W: wetland. Red points are correlation coefficients for the pooled data.

### VEGETATION DIFFERENCES IN $\lambda E$

In order to investigate differences between vegetation type,  $\lambda E$  flux for different land cover types were modeled based on meteorological data and ecosystem calibrated model parameters in daily scale. Predicted  $\lambda E$  flux for daytime (from 9:00 to 17:00) where highest for deciduous broadleaf forest and lowest for tundra and Douglas fir. We did not observe any major differences between daily and annual  $\lambda E$  flux behavior (Fig 4 & 5) when simulations were done based on the meteorological data of Hyytiälä (FI-Hyy 2011).

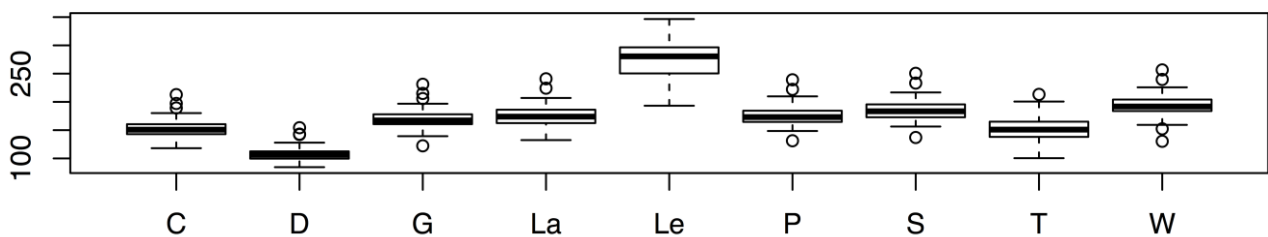


Figure 4. Predicted  $\lambda E$  flux based on bulk meteorological variables recorded at Smear II station (FI-Hyy) 29.6.2011.  $\lambda E$  flux is calculated for the daytime from am 9:00 to 17:00 pm.

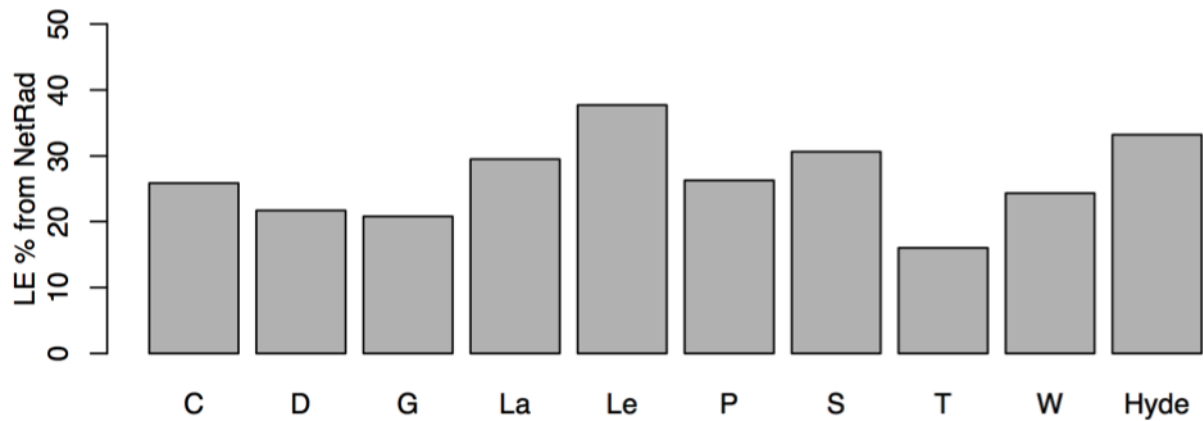


Figure 5. Proportion of  $\lambda E$  (%) from the annual net radiation (NetRad) based on the universal vegetation specific model parameters.

The  $\lambda E$  flux from the vegetated surfaces is regulated by the aerodynamic and stomatal resistance. Based on the simulation with bulk meteorological data (fig 4 & 5) shows that  $\lambda E$  values under identical meteorological conditions differ depending on the vegetation type. One reason for these differences is that the proportion of stomatal resistance of the canopy resistance varies (Fig 6). These results suggest that stomatal control is mainly controlling the  $\lambda E$  in Larch, Leaf, Pine and Spruce while in some other ecosystems the role of  $r_a$  can be significant.

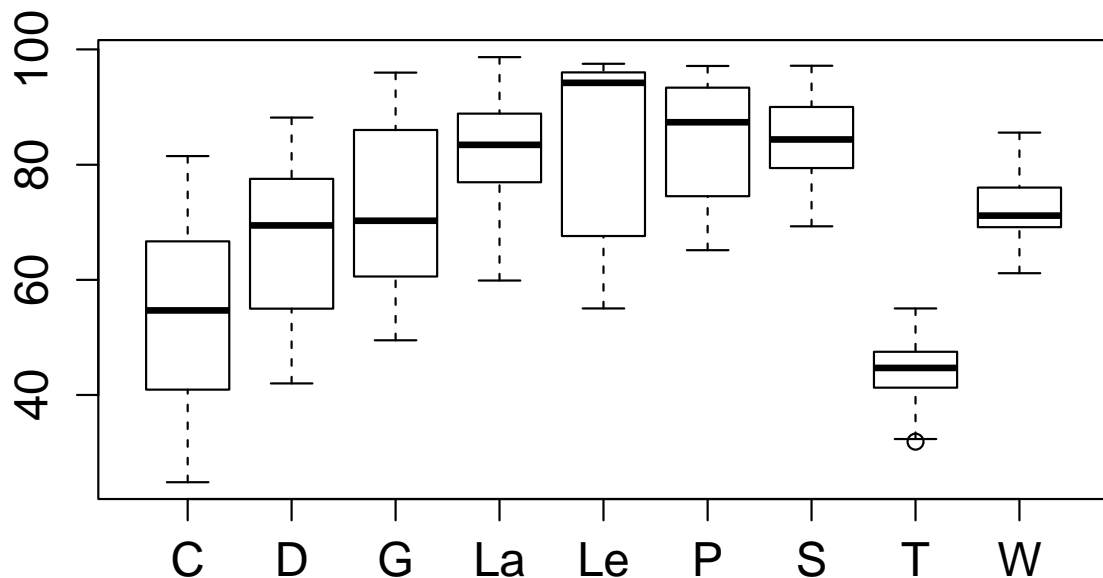


Figure 6. The proportion of stomatal resistance from the total canopy resistance ( $R_s/(R_a+R_s)*100$ ). Bars represent the variation range and proportion (%) of  $r_s$  from  $r_c$  based on daily pooled data.

## CONCLUSIONS

The key findings of this study are the seasonal behavior of stomatal conductance and the differences of phenology between ecosystem types govern the land surface in the boreal and arctic biomes. In general the site-specific fits were good and for most sites and ecosystem types the universal parameterization of the model introduced fair estimates related to  $\lambda E$  flux between land surface and atmosphere. The fit of the generalized parameterization was lower than for the other ecosystem types that might be caused by the fact that the model does not take into account ground heat flux or the energy that is used to melt the frozen surface layer in arctic stations. Further on, the over estimation of the flux for some sites might be caused by the drought and limited water availability.

Our results could be used in later in the research topics related to Earth system and hydrological modeling.

## ACKNOWLEDGEMENTS

This research was funded by the Nordic Center of Excellence CRAICC (Cryosphere-atmosphere interactions in a changing Arctic climate). We also thank the Academy of Finland Center of Excellence (project number 1118615).

## REFERENCES

- Allen, R. G. (1998). Crop Evapotranspiration (guidelines for computing crop water requirements). *FAO Irrigation and Drainage Paper*, (56), 1–296.
- Chapin, F. S., Mcguire, A. D., Randerson, J., & Pielke, S. R., Baldocchi, D., Hobbie, E., Roulet, N., Eugesten, W., Kasichke, E., Rastetter, E. B., Zimov, S. A., Running, S. W. (2000). Arctic and boreal ecosystems of western North America as components of the climate system. *Global Change Biology*, 6, 211–223.
- Gea-Izquierdo, G., Mäkelä, A., Margolis, H., Bergeron, Y., Black, T. A., Dunn, A., Hadley, J., et al. (2010). Modeling acclimation of photosynthesis to temperature in evergreen conifer forests. *The New phytologist*, 188(1), 175–86. doi:10.1111/j.1469-8137.2010.03367.x
- Kolari, P., Lappalainen, H. K., Hänninen, H., & Hari, P. (2007). Relationship between temperature and the seasonal course of photosynthesis in Scots pine at northern timberline and in southern boreal zone. *Tellus B*, 59(3), 542–552. doi:10.1111/j.1600-0889.2007.00262.x
- Kustas, W. P., Choudhury, B. J., Moran, M. S., Reginato, R. J., Jackson, R. D., Gay, L. W., Weaver, H. L. (1989). Determination of sensible heat flux over sparse canopy using thermal infrared data. *Agricultural and Forest Meteorology*, 44, 197–216.
- Langer, M., Westermann, S., Muster, S., Piel, K., & Boike, J. (2011). The surface energy balance of a polygonal tundra site in northern Siberia – Part 2 : Winter. *The Cryosphere*, 5, 509–524. doi:10.5194/tc-5-509-2011
- Launiainen, S. (2010). Seasonal and inter-annual variability of energy exchange above a boreal Scots pine forest. *Biogeosciences Discussions*, 7(12), 3921–3940. doi:10.5194/bg-7-3921-2010

Mäkelä, A., Pulkkinen, M., Kolari, P., Lagergren, F., Berbigier, P., Lindroth, A., Loustau, D., et al. (2007). Developing an empirical model of stand GPP with the LUE approach: analysis of eddy covariance data at five contrasting conifer sites in Europe. *Global Change Biology*, 071124112207003–??? doi:10.1111/j.1365-2486.2007.01463.x

Mäkelä, A., Hari, P., Berninger, F., Hänninen, H., & Nikinmaa, E. (2004). Acclimation of photosynthetic capacity in Scots pine to the annual cycle of temperature. *Tree physiology*, 24(4), 369–76. Retrieved from <http://www.ncbi.nlm.nih.gov/pubmed/14757576>

Penman, H.L., 1948. Natural evaporation from open water, bare soil and grass. *Proceedings of the Royal Society London Academy*, 193, 120–146. doi: 10.1098/rspa.1948.0037

R Core Team (2013). R: A language and environment for statistical computing. R Foundation for Statistical Computing, Vienna, Austria. ISBN 3-900051-07-0, URL <http://www.R-project.org/>.

Richardson, A. D., Keenan, T. F., Migliavacca, M., Ryu, Y., Sonnentag, O., & Toomey, M. (2013). Climate change, phenology, and phenological control of vegetation feedbacks to the climate system. *Agricultural and Forest Meteorology*, 169, 156–173. doi:10.1016/j.agrformet.2012.09.012

Suni, T., Berninger, F., Vesala, T., Markkanen, T., Hari, P., Makela, A., Ilvesniemi, H., et al. (2003). Air temperature triggers the recovery of evergreen boreal forest photosynthesis in spring. *Global Change Biology*, 9(10), 1410–1426. doi:10.1046/j.1365-2486.2003.00597.x

Verma, S. B.: Aerodynamic resistances for transfer of mass, heat and momentum, in: Estimation of Aerial Evapotranspiration (Proceedings of a workshop held at Vancouver, B.C. Canada, August 1987), IAHS Publ. no. 177, 1989.

Vesala, T. (2005). Effect of thinning on surface fluxes in a boreal forest. *Global Biogeochemical Cycles*, 19(2), 1–12. doi:10.1029/2004GB002316

Wang, K., & Dickinson, R. E. (2012). A REVIEW OF GLOBAL TERRESTRIAL EVAPOTRANSPIRATION : OBSERVATION ,. *Reviews of Geophysics*, (2011), 1–54. doi:10.1029/2011RG000373.1.INTRODUCTION

# HYGROSCOPIC PROPERTIES OF NUCLEATED NANOPARTICLES IN THE PRESENCE OF SULFURIC ACID AND ORGANICS DURING CLOUD 7

J. KIM<sup>1</sup>, H. KESKINEN<sup>1</sup>, P. VAATTOVAARA<sup>1</sup>, P. MIETTINEN<sup>1</sup>, J. JOUTSENSAARI<sup>1</sup>, A. VIRTANEN<sup>1</sup>, and CLOUD COLLABORATION

<sup>1</sup>Department of Applied physics, University of Eastern Finland, P.O. Box 1627, FIN-70211 Kuopio, Finland.

Keywords: CLOUD, NANOPARTICLES, HYGROSCOPICITY, NANO-TDMA.

## INTRODUCTION

The aim of this study is to estimate chemical composition in nucleated nanoparticles. We focus on hygroscopic properties of nucleated nanoparticles in the presence of sulfuric acid and organics generated by oxidation of dimethylamine and  $\alpha$ -pinene. Particles were produced inside CLOUD (Cosmic Leaving Outdoor Droplets) during CLOUD 7 experiments.

## METHODS

A nano-tandem differential mobility analyser (nano-TDMA) was applied to measure hygroscopicity of nanoparticles in the presence of sulfuric acid and organics during CLOUD 7 experiment. The nano-TDMA consisted of two nano-DMAs (TSI 3085), a condensation particle counter (CPC; TSI 3785), and humidifiers. Generated particles inside CLOUD chamber were dried and then particles having certain size (10, 15, and 20 nm) were selected with DMA according to electrical mobility of particles. The selected particles were introduced into aerosol humidifier. Relative humidity in the humidifier was around 90%. Size distributions of humidified particles were observed with another DMA and CPC.

In this way, we can determine hygroscopic growth factor (HGF) that is the ratio of geometric mean diameter (GMD) of size dependent nanoparticles at humidified condition to that at dry condition. From measured HGF values, the single hygroscopicity parameter ( $\kappa$ ) can be calculated using semi-empirical model introduced by Petters and Kreidenweis, 2007:

$$\kappa = (HGF^3 - 1) \cdot \left[ \frac{1}{S} \cdot \exp\left( \frac{4\sigma_w M_w}{RT\rho_w d_{dry} HGF} \right) - 1 \right]$$

where  $M_w$  is the molecular weight of water,  $\sigma_{sol}$  is the surface tension of the solution,  $R$  is the ideal gas constant,  $T$  is the temperature,  $\rho_w$  is the density of water, and  $d_p$  is the diameter after humidification ( $d_p = d_{dry} \times HGF$ ). Here, we assumed that  $\sigma_{sol}$  is same with the surface tension of water.

In addition, the organic volume fraction ( $\varepsilon_o$ ) in the nucleated nanoparticles was calculated assuming two compounds consisting of organic and inorganic sulphates (Keskinen et al., 2013)

$$\varepsilon_{org} = \frac{\kappa - \kappa_{inorg}}{\kappa_{org} - \kappa_{inorg}}$$

where  $\kappa$  is a result derived from nano-HTDMA measurements,  $\kappa_{org}$  and  $\kappa_{inorg}$  are hygroscopicity parameter for organic and inorganic sulfate, respectively. We assumed that O:C ratio is from 0.1 to 0.5, corresponding the hygroscopicities of 0.05 and 0.14 (Massoli et al., 2010). The hygroscopicity of pure sulfuric acid and ammonium sulfate are 0.7 (Sullivan et al., 201) and 0.47 (Topping et al., 2005) at 90% relative humidity, respectively. In this study, averaged organic volume fraction estimated by sulfuric acid with organic and ammonium sulfate with organic compounds is used.

## CONCLUSIONS

The hygroscopicity of nucleated nanoparticles (10 and 15 nm) in the presence of sulfuric acid and organics without OH radicals was smaller than those with OH radicals in the chamber regardless of experimental conditions, as can be seen in Figure 1. It suggests that hygroscopicity of nucleated nanoparticles is enhanced by OH radicals.

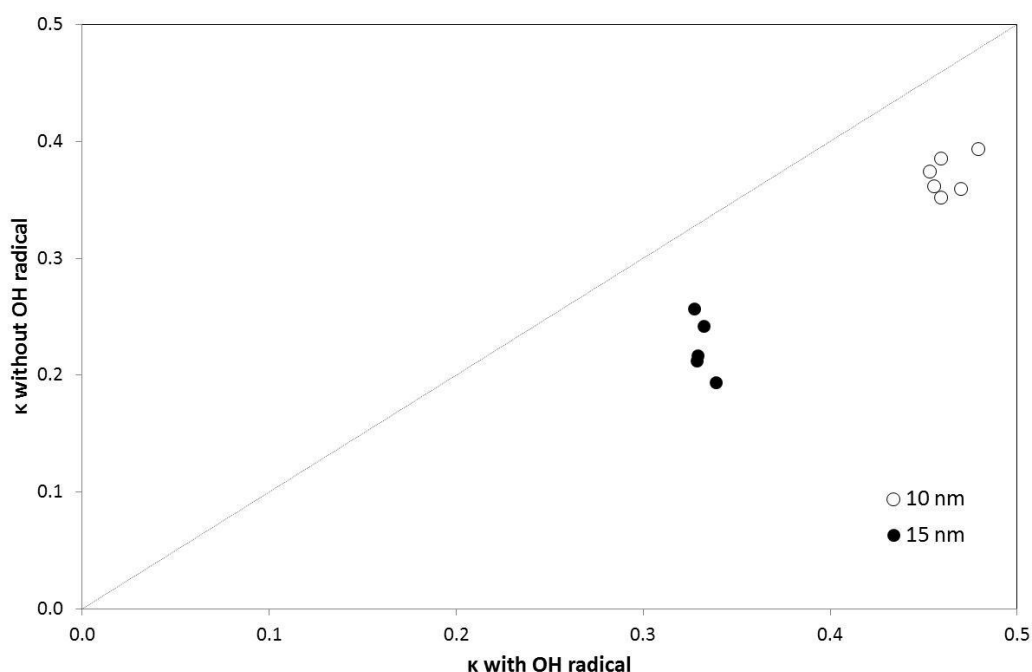


Figure 1. Comparison of  $\kappa$  values for nucleated nanoparticles in the presence of sulfuric acid, DMA, and organics derived from oxidation of  $\alpha$ -pinene with and without OH radicals.

## ACKNOWLEDGEMENTS

We would like to thank CERN for supporting CLOUD with important technical and financial resources, and for providing a particle beam from the CERN Proton Synchrotron. This research has received funding from the EC Seventh Framework Programme (Marie Curie Initial Training Network "CLOUD-ITN" no. 215072, MC-ITN "CLOUD-TRAIN" no. 316662, and ERC-Advanced "ATMNUCLE" grant no. 227463), the German Federal Ministry of Education and Research (project nos. 01LK0902A and 01LK1222A), the Swiss National Science Foundation (project nos. 200020\_135307 and 206620\_130527), the Academy of Finland Center of Excellence (project no. 1118615) the Nordic Centers of Excellence CRAICC or DEFROST, the Academy of Finland (135054, 133872, 138951, 251427, 139656, 139995, 137749, 141217, 141451), the Finnish Funding Agency for Technology and Innovation, the Nessling Foundation, the Austrian Science Fund (FWF; project no. P19546 and L593), the Portuguese Foundation for Science and Technology (project no. CERN/FP/116387/ 2010), the Swedish Research Council, Vetenskapsrådet

(grant 2011-5120), the Presidium of the Russian Academy of Sciences and Russian Foundation for Basic Research (grants 08-02-91006-CERN and 12-02-91522-CERN), and the U.S. National Science Foundation (grants AGS1136479 and CHE1012293).

## REFERENCES

- Petters, M.D. and Kreidenweis, S.M.(2007). A single parameter representation of hygroscopic growth and cloud condensation nucleus activity, *Atmos. Chem. Phys* 7, 1961-1971.
- Keskinen, H., Virtanen, A., Joutsensaari, J., Tsagkogeorgas, G., Duplissy, J., Schobesberger, S., Gysel, M., Riccobono, F., Slowik, J.G., Bianchi, F., Yli-Juuti, T., Lehtipalo, K., Rondo, L., Breitenlechner, M., Kupc, A., Almeida, J., Amorim, A., Dunne, E.M., Downard, A.J., Ehrhart, S., Franchin, A., Kajos, M.K., Kirkby, J., Kürten, A., Nieminen, T., Makhmurov, V., Mathot, S., Miettinen, P., Onnela, A., Petäjä, T., Praplan, A., Santos, F.D., Schallhart, S., Sipilä, M., Stozhkov, Y., Tomé, A., Vaattovaara, P., Wimmer, D., Prevot, A., Dommen, J., Donahue, N.M., Flagan, R.C., Weingartner, E., Viisanen, Y., Riipinen, I., Hanse, A., Curtius, J., Kulmala, M., Worsnop, D.R., Baltensperger, U., Wex, H., Stratmann, F. and Laaksonen, A. (2013). Evolution of particle composition in CLOUD nucleation experiments, *Atmos. Chem. Phys.* 13, 5587–5600.
- Massoli, P., Lambe, A.T., Ahern, A.T., Williams, L.R., Ehn, M., Mikkilä, J., Canagaratna, M.R., Brune, W.H., Onasch, T.B., Jayne, J.T., Petäjä, T., Kulmala, M., Laaksonen, A., Kolb, C.E., Davidovits, P., and Worsnop, D.R. (2010). Relationship between aerosol oxidation level and hygroscopic properties of laboratory generated secondary organic aerosol (SOA) particles, *Geophys. Res. Lett.*, 24, L24801.
- Sullivan, R.C., Petters, M.D., DeMott, P.J., Kreidenweis, S.M., Wex, H., Niedermeier, D., Hartmann, S., Clauss, T., Stratmann, F., Reitz, P., Schneider, J. and Sierau, B. (2010). *Atmos. Chem. Phys.* 10, 11471-11487.
- Topping, D.O., McFiggans, G.B., and Coe, H. (2005). A curved multicomponent aerosol hygroscopicity model framework: Part1 – Inorganic compounds, *Atmos. Chem. Phys.*, 5, 1205–1222.

# FLAMO - FLEXIBLE ATMOSPHERIC MODEL: A NEW HIGH-RESOLUTION 3D REGIONAL MODEL TO STUDY ATMOSPHERIC PROCESSES IN THE PLANETARY BOUNDARY LAYER

G.V. KOKKATIL<sup>1</sup>, H.VUOLLEKOSKI<sup>1</sup>, V.SINCLAIR<sup>1</sup>, A.HELLSTEN<sup>2</sup>, M. KULMALA<sup>1</sup> and M.BOY<sup>1</sup>

<sup>1</sup> University of Helsinki, Department of Physical Sciences, P.O. Box 48,00014 Helsinki, Finland

<sup>2</sup> Finnish Meteorological Institute, P.O. Box 503, 00560 Helsinki, Finland

Keywords: Atmospheric-Chemistry, Modelling, CTM (Chemical Transport model), Aerosols

## INTRODUCTION

Nucleation is one of the key atmospheric processes that have large uncertainties. The occurrences of extremely complex processes in the atmosphere contribute to the hardships in understanding the topic of new particle formation. Effect of aerosols on climate needs further understanding and so does the regional feedback mechanisms. Regional models are a useful tool to attain high enough resolution to provide targeted impact assessment and for various type of resource management. High-resolution regional models can help in understanding the topography and the changes in the atmospheric circulations and also the sources of anthropogenic emissions of certain Volatile Organic Compounds (VOC's). Regional models are capable of reproducing or predicting the entire atmosphere up to a certain degree of accuracy. In order to attain these scientific goals we have developed a high-resolution three-dimensional model FLAMO (Flexible Atmospheric Model) that tries to reconstruct the atmosphere. This means FLAMO is capable of simulating the emissions, transport, chemistry and aerosol processes within the atmospheric boundary layer. FLAMO would be a very useful and essential tool for further applications in environmental research.

## MODEL DESCRIPTION

FLAMO can be defined as an interface between modules having different functionalities and thus can be of potential use in various fields of atmospheric research. Its inter-operability and flexibility allows the user the freedom to assimilate modules from various fields and to run these codes in parallel in multi-core clusters. The prime objective of FLAMO is to allow the user the degree of freedom to use the model as a box model, a 1D model or a 3D model depending on the scientific requirement and computational resources. FLAMO is ideally designed to be a high-resolution atmospheric model that is capable of reproducing the chemical and physical processes in the atmosphere. This requires an offline or an online meteorological module, a transport scheme that emulates the transport mechanism in the atmosphere, an emission module, a chemical reaction module and an aerosol module.

### Meteorology:

FLAMO in its current form couples meteorological data obtained from WRF (Weather and Research Forecasting Model) or referred to as ARW (Advanced Research WRF). WRF is used extensively across the world for weather predictions and for research related studies.

### Transport Scheme:

FLAMO has its own advection and diffusion schemes implemented so as to enable transport mechanism within the 3-dimensional grid. Fifth order spatial discretization scheme and a third order Runge-Kutta scheme has been implemented in to FLAMO. The time- splitting advection scheme is based on the method adopted by Wicker and Skamarock, 2001. The sharp discontinuities and gradients in scalars cause

dispersion and diffusion. With an aim to minimise this effect along with maintaining the stability and efficiency of the scheme a positive definite flux limiter was used along with the advection scheme. Positive definiteness helps in maintaining the positive value for all scalar-mixing ratios. A second order diffusion scheme is implemented in to solving the advection-diffusion equation.

#### Emission:

Emissions from the canopy are simulated using the Model of Emissions of Gases and Aerosols from Nature (MEGAN). This is a system for estimating the net emissions of gases and aerosols from terrestrial ecosystems in to the atmosphere. Megan was set up with a base resolution of about  $\sim 1\text{km}$  (Guenther et.al, 2006).

#### Chemistry:

The chemistry, which accounts for most of the simulation time is taken from the Master Chemical Mechanism (MCM). MCM is a near explicit chemical mechanism that describes the degradation of hundreds of volatile organic compounds (VOC). This mechanism is implemented into Fortran 90 using KPP (The Kinetic Pre-Processor).

#### Aerosols:

The University of Helsinki Multicomponent Aerosol model (UHMA) for aerosol dynamics will be included later in to the code. The main objective of this module is to study new particle formation under clear sky condition in the troposphere.

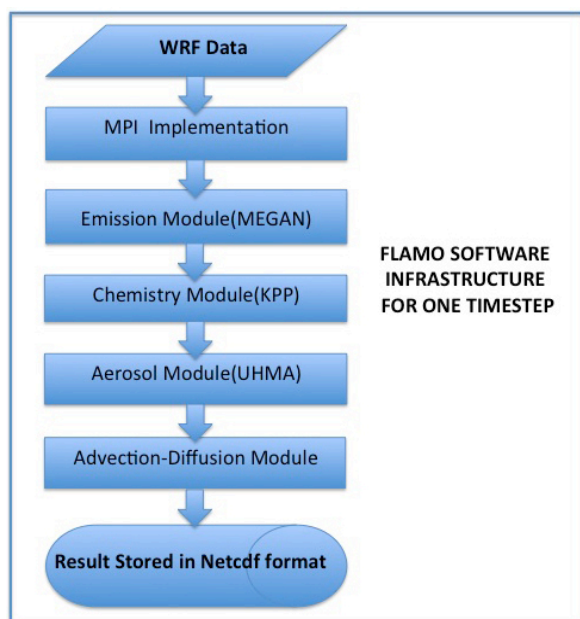


Fig 1: Flow-chart for a single time step in FLAMO.

We have coupled the emission module in the code with the meteorology and the advection schemes. The next step is to implement the Chemistry module already used in SOSA (Boy et al., 2011). This will enable us to investigate the impact of various local sources of organic compounds (e.g. Tampere) on the measured concentrations of volatile organic compounds measured at the SMEAR II station in Hyytiälä.

Further step will be to implement the aerosol module and study various nucleation theories (e.g. binary nucleation of sulphuric acid and water) in and above the ABL for the SMEAR II in Hyytiälä, Finland. Further we will study the chemical processes and feedback mechanisms crucial for aerosol formation and nucleation processes.

## ACKNOWLEDGEMENTS

We acknowledge the financial support by Maj ja Tor Nessling Foundation and the Academy of Finland Center of Excellence program (project number 1118615).

## REFERENCES

- Boy, M., Sogachev, A., Lauros, J., Zhou, L., Guenther, A. and Smolander, S. (2011) *SOSA – a new model to simulate the concentrations of organic vapours and sulphuric acid inside the ABL – Part 1: Model description and initial evaluation* Atmos. Chem. Phys., 11, 43–51, 2011  
[www.atmos-chem-phys.net/11/43/2011/](http://www.atmos-chem-phys.net/11/43/2011/) doi:10.5194/acp-11-43-2011
- Guenther, A., Karl, T., Harley, P., Wiedinmyer, C., Palmer, P.I. and Geron, C. (2006) *Estimates of global terrestrial isoprene emissions using MEGAN (Model of Emissions of Gases and Aerosols from Nature)* Atmos. Chem. Phys., 6, 3181–3210, 2006
- Wicker, L.J. and Skamarock, W.C. (2001). *Time-Splitting Methods for Elastic Models Using Forward Time Schemes* Mon. Wea. Rev., 130.

## PHOTOSYNTHESIS AND NITROGEN IN DIFFERENT NEEDLE AGE CLASSES IN SCOTS PINE

P. KOLARI<sup>1,2</sup>, M. DOMINGUEZ<sup>2</sup>, E. JUUROLA<sup>1,2</sup>, S. JUNTILA<sup>2</sup>, J. BÄCK<sup>2</sup> and E. NIKINMAA<sup>2</sup>

<sup>1</sup>Department of Physics, P.O. Box 48, 00014 University of Helsinki

<sup>2</sup>Department of Forest Sciences, P.O. Box 27, 00014 University of Helsinki

Keywords: Scots pine, photosynthetic capacity, nitrogen content, nitrogen partitioning

### INTRODUCTION

Photosynthetic capacity of plant leaves is known to change with leaf aging (Freeland, 1952, Warren, 2006). It typically increases with leaf development, levels off soon after leaf maturation and decline with leaf aging (e.g. Radoglou and Teskey, 1997, Warren, 2006).

A considerable proportion of photosynthetic production in the crowns of evergreen conifers takes place in leaves developed during previous growing seasons. We studied how photosynthetic capacity and responses of photosynthesis to the environment vary with needle age in Scots pine (*Pinus sylvestris* L.) in order to evaluate the significance of changing photosynthetic parameters on modelling of whole-tree photosynthesis. We also studied how changes in photosynthesis are linked with changes in the functional compartments of nitrogen in the needles.

### MATERIAL AND METHODS

The sample trees are growing at SMEAR II station in Hyytiälä, Southern Finland. Randomly selected branches from upper half of the crowns were cut in the morning and kept well watered and protected from direct sunlight. The gas exchange measurements were done with a portable gas exchange fluorescence system (Walz GFS-3000, Heinz Walz, Germany). For each needle age class in the branch, four fascicles, totalling eight needles were placed in the Walz measuring cuvette. The age classes were measured in random order to avoid bias due to gas exchange parameters changing during storage. Total of 17 branches were measured between 11 July and 9 August 2011.

Light response of CO<sub>2</sub> exchange was determined at T=22°C and CO<sub>2</sub>=400 ppm, CO<sub>2</sub> response at T=22°C and PPFD=1000 µmol m<sup>-2</sup> s<sup>-1</sup>. RH in the cuvette was set to 50%. After the measurements, the needles inside the cuvette were photographed and their projected area calculated. The needles were then collected to measure their fresh weight and total (all-sided) needle area, and dried at 105°C for 24 hours to obtain the dry weight. Immediately after the measurements the needles for nitrogen measurements were sampled and frozen with liquid nitrogen and later stored at -80°C.

We determined the maximum light-saturated photosynthetic rate ( $P_{\max}$ ) from the light response measurements using the simple nonrectangular hyperbola

$$P = \frac{P_{\max} I}{I + K} \quad (1)$$

where  $I$  is the intensity of photosynthetically active radiation (PAR) and  $K$  curvature parameter.

We measured the nitrogen partitioning in needles following the method introduced by Takashima *et al.* (2004) and Harrison *et al.* (2009), by determining the protein content in two fractions: water-soluble and detergent-soluble. Water-soluble proteins appear in stroma and cytosol and are related to photosynthetic dark reactions, and detergent-soluble are membrane-associated proteins related to photosynthetic light reactions. The water-soluble and detergent-soluble proteins were extracted in two different buffers.

Needles were homogenized using nitrogen liquid in a ball mechanical grinder (2000-230 Geno / Grinder, Spex SamplePred, USA) and after that lyophilized in a freeze dryer (Christ Gamma 2-16 LSC Freezer dryer, SciQuip Ltd, Merrington, UK). Approximately 20 mg of freeze-dried and grinded needle material was transferred to test tubes, and 1,5 ml of 100 mM Na-phosphate buffer (pH 7,5) with 0,4 M sorbitol, 2 mM MgCl<sub>2</sub>, 10 mM NaCl, 5 mM iodo acetate, 1% polyvinylpyrrolidone, 5 mM dithiothreitol was added into the tube.

The sample was shaken on ice for 30 min and centrifuged at 4°C and 4000 rpm. The supernatants were separated in new falcon tubes. The process was repeated one more time with 1,5 ml of Na-phosphate buffer and the supernatant collected all together. This was regarded as the water-soluble fraction.

1 ml of 100mM Na-phosphate buffer with 3% SDS was added to the pellet. The sample was homogenized, heated at 90°C for 5 min and centrifuged at 4000 rpm for 10 min. The supernatant was separated into new falcon tubes. The process was repeated four times and the supernatant collected was considered SDS-soluble proteins, detergent-soluble fraction.

Water-soluble and SDS-soluble proteins were measured with Bradford method in a micro-volume spectrophotometer (Thermo Scientific NanoDrop 2000), and the nitrogen content was calculated assuming that the nitrogen percentage in the cell proteins is 16%.

Finally, total nitrogen content in dried and homogenized needle sample was measured with a CHN analyzer (Vario Max).

## RESULTS

Light-saturated photosynthesis per unit needle area was similar in all needle age classes. On average the youngest needles were most efficient but the differences between the age classes were not statistically significant. Specific leaf area (SLA), i.e. the ratio of needle surface area to dry mass, was significantly higher in the current year's needles than in the 1-year-old needles (Table 1). Also the fresh weight to dry weight ratio was highest in the current year's needles. There was no significant difference in SLA between 1-year-old and 2-year-old needles. The decreasing needle surface area to mass ratio most probably results from thickening and lignification of cell wall during the maturation of the needles. The high SLA in the young needles resulted in them being considerably more efficient in photosynthetic rate per unit needle mass. The results are in line with other studies (e.g. Radoglou and Teskey, 1997; Warren, 2006).

The proportion of functional nitrogen, allocated to dark reactions (N1%) and light reactions (N2%) in the needles was consistent with the decrease in specific leaf area with needle aging (Fig. 1a). However, no changes were observed in the total nitrogen mass fraction in relation to needle age (Fig. 1b). This indicates that the structural nitrogen continues increasing gradually after needles have already reached full size and photosynthetic capacity (Warren and Adams, 2001; Harrison *et al.*, 2009).

Needle age (years)	$P_{\max}$ ( $\mu\text{mol m}^{-2} \text{s}^{-1}$ )	Projected SLA ( $\text{m}^{-2} \text{kg}^{-1}$ )	$P_{\max}$ ( $\mu\text{mol kg}^{-1} \text{s}^{-1}$ )
0	19.6 (4.7)	4.05	79.4 (19.0)
1	18.3 (4.4)	3.23	59.0 (14.2)
2	17.1 (4.0)	3.11	53.1 (12.4)

**Table 1.** Light-saturated photosynthetic rate ( $P_{\max}$ ), mean and standard deviation, and specific leaf area in the different needle age classes in Scots pine.  $P_{\max}$  is expressed as unit  $\text{CO}_2$  per unit needle area and per unit needle mass.

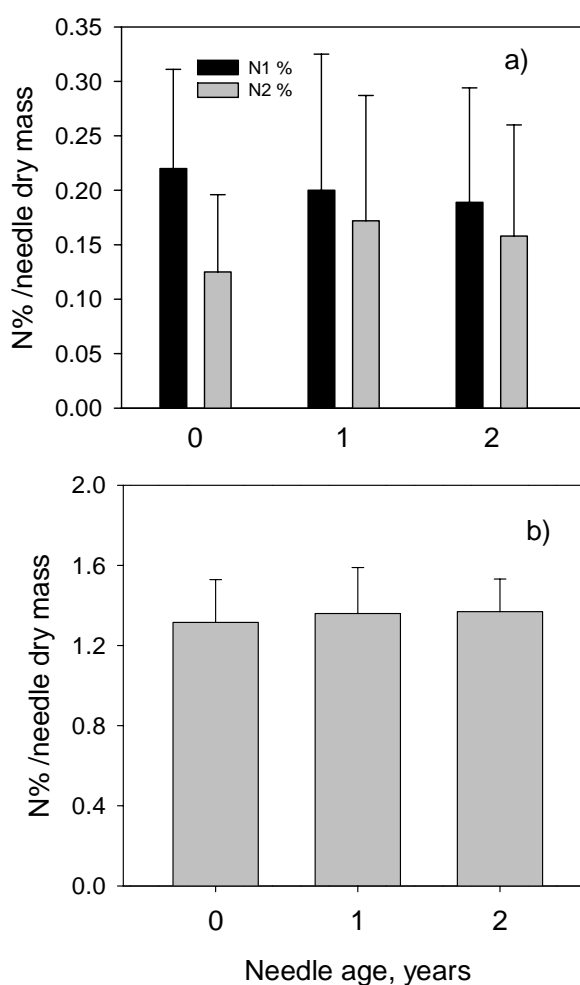


**Figure 1.** Concentration of functional nitrogen in Scots pine needles of different age, allocated in photosynthetic dark reactions (N1%) and in photosynthetic light reactions (N2%) a) and corresponding total nitrogen concentration needles b). Values are mean  $\pm$  standard deviation.

When considering whole-tree or stand photosynthetic production, the bias resulting from omitting the change in photosynthesis parameters with needle age is insignificant. However, if the sampling of needle

cohorts is based on dry mass while photosynthesis is estimated on area basis assuming constant SLA, crown photosynthesis will be underestimated by as much as 10%.

#### ACKNOWLEDGEMENTS

This study was supported by Academy of Finland Center of Excellence (project no 1118615).

#### REFERENCES

- Freeland, R. (1952). Effect of age leaves upon the rate of photosynthesis in some conifers. *Plant Physiology* **27**, 685–690.
- Harrison M. T., E. J. Edwards, G. D. Farquhar, A. B. Nicotricha and J.R. Evans (2009). Nitrogen in cell walls of sclerophyllous leaves accounts for little of the variation in photosynthetic nitrogen-use efficiency. *Plant, Cell and Environment* **32**, 259–270
- Radoglou, K. and R. Teskey (1997). Changes in rates of photosynthesis and respiration during needle development of loblolly pine. *Tree Physiology* **17**, 485–488.
- Takashima T., K. Hikosaka and T. Hirose (2004). Photosynthesis of persistence: nitrogen allocation in leaves of evergreen and deciduous *Quercus* species. *Plant, Cell and Environment* **27**, 1047–1054.
- Warren, C.R. (2006). Why does photosynthesis decrease with needle age in *Pinus pinaster*? *Trees* **20**, 157–164.
- Warren, C.R. and M. Adams (2001). Distribution of N, Rubisco and photosynthesis in *Pinus pinaster* and acclimation to light. *Plant Cell Environment* **24**, 597–609.

# OBSERVATIONS OF SUB 3-NM ATMOSPHERIC CLUSTERS AND PARTICLES IN DIFFERENT ENVIRONMENTS

J. KONTKANEN<sup>1</sup>, K. LEHTIPALO<sup>1,2</sup>, J. KANGASLUOMA<sup>1</sup>, H. E. MANNINEN<sup>1</sup>, E. JÄRVINEN<sup>3</sup>, J. HAKALA<sup>1</sup>, A. HAMAD<sup>4</sup>, A. LAAKSONEN<sup>4</sup>, C. ROSE<sup>5</sup>, K. SELLEGRI<sup>5</sup>, E. ASMI<sup>6</sup>, T. PETÄJÄ<sup>1</sup>, and M. KULMALA<sup>1</sup>

<sup>1</sup> Department of Physics, University of Helsinki, Helsinki, Finland,

<sup>2</sup> Airmodus Oy, Helsinki, Finland,

<sup>3</sup> Institute for Meteorology and Climate Research, Karlsruhe Institute of Technology, Karlsruhe, Germany

<sup>4</sup> Department of Applied Physics, University of Eastern Finland, Finland,

<sup>5</sup> Laboratoire de Météorologie Physique CNRS UMR6016, Université Blaise Pascal, France

<sup>6</sup> Finnish Meteorological Institute, Helsinki, Finland

Keywords: CLUSTERS, NANOPARTICLES, NEW PARTICLE FORMATION

## INTRODUCTION

Atmospheric new particle formation includes the formation of nanometer-sized clusters and their subsequent growth to larger particles (Kulmala *et al.*, 2004). Therefore, to estimate the importance of new particle formation for the climate effects of aerosol particles, it is essential to have knowledge of the concentrations of atmospheric clusters. The direct measurements of atmospheric clusters and particles in the sub-2nm size range have, however, become possible only recently. Kulmala *et al.* (2013) observed a large population of atmospheric clusters at a boreal forest site in Finland during spring 2011. This population was dominated by electrically neutral clusters whose activation was suggested to be the dominant nucleation mechanism (Kulmala *et al.*, 2013). Still, the measurements conducted in Hyytiälä may not reveal the whole picture as the concentrations of atmospheric clusters and their role in new particle formation may not be similar in different environments. Thus, in this work, we compare the measurements of sub-3 nm clusters and particles performed at four different measurement sites. In this way, we aim to understand better how the concentrations of atmospheric clusters and their significance for new particle formation vary depending on the environmental conditions.

## MEASUREMENTS

The summary of the measurements used in this study is presented in Table 1. The measurements were performed at four different measurement sites: Hyytiälä, San Pietro Capofiume, Puy de Dôme, and Centreville. Hyytiälä is a boreal forest site in Central Finland, San Pietro Capofiume is a rural site located in polluted Po Valley in Northern Italy, Puy de Dôme is a mountain site (1465 m a. s. l.) in Central France, and Centreville is a rural site located in Alabama in the Southeastern United States. The measurements in Hyytiälä took place during spring 2011 (2 months), spring 2012 (6 weeks), and summer 2013 (4 months). In San Pietro Capofiume the measurements were conducted during summer 2012 (4 weeks), in Puy de Dôme during winter 2012 (3 weeks), and in Centreville during summer 2013 (6 weeks).

Table 1. The summary of the measurements used in this study.

Measurement site	Instruments	Measurement period	Size range
Hyytiälä (HTL11)	PSMA09, DMPS	13.3–10.5.2011	1.1–3 nm
Hyytiälä (HTL12)	PSMA09, DMPS	27.3–11.5.2012	1.1–3 nm
Hyytiälä (HTL13)	PSMA10, DMPS	29.4–31.8.2013	1.0–3 nm
San Pietro Capofiume (SPC)	PSMA09, DMPS	9.6–9.7.2012	1.5–3 nm
Puy de Dôme (PDD)	PSMA09	23.1–15.2.2012	1.3–2.5 nm
Centreville (CTR)	PSMA10	31.5–16.7.2013	1.1–2.7 nm

At all measurement sites the total concentration of clusters in the 1–2 nm size range was measured with the Airmodus Particle Size Magnifier (PSM), which is a mixing type condensation particle counter (Vanhanen *et al.*, 2011). The measured size range was not exactly the same in different measurement campaigns due to differences in the lowest and highest cut-off sizes of the PSM. In Hyytiälä and San Pietro Capofiume Differential Mobility Particle Sizer (DMPS) was also used to measure the concentration of larger aerosol particles. Thus, at those sites, the concentration of clusters and particles between the highest cut-off size of the PSM ( $\sim 2$  nm) and the lowest cut-off size of the DMPS (3 nm) was also obtained by subtracting the concentration measured with the DMPS from the concentration measured with the PSM.

## RESULTS

Figure 1 shows the concentrations of sub-3nm clusters and particles at different measurement sites. The highest sub-3nm concentrations were observed in San Pietro Capofiume where the median concentration was  $8300 \text{ cm}^{-3}$ . The high concentration is in agreement with the high frequency of new particle formation events observed at the site in the summertime (Manninen *et al.*, 2010). In Hyytiälä the median concentration was  $2700 \text{ cm}^{-3}$  during spring 2011 and spring 2012, and  $1400 \text{ cm}^{-3}$  during summer 2013. Thus, it seems that in Hyytiälä the sub-3nm concentrations are higher in spring than in summer. This is consistent with the fact that in Hyytiälä new particle formation events are more frequent during spring (Dal Maso *et al.*, 2005). In Puy de Dôme the median sub-3nm concentration was clearly lower than in Hyytiälä and San Pietro Capofiume,  $100 \text{ cm}^{-3}$ , which results from the very different conditions at these sites. During the measurement campaign in Puy de Dôme the site was often in the free troposphere where cluster concentrations are low, especially when there is no new particle formation taking place (Rose *et al.*, 2013). In Centreville the median sub-3nm concentration was also low,  $200 \text{ cm}^{-3}$ .

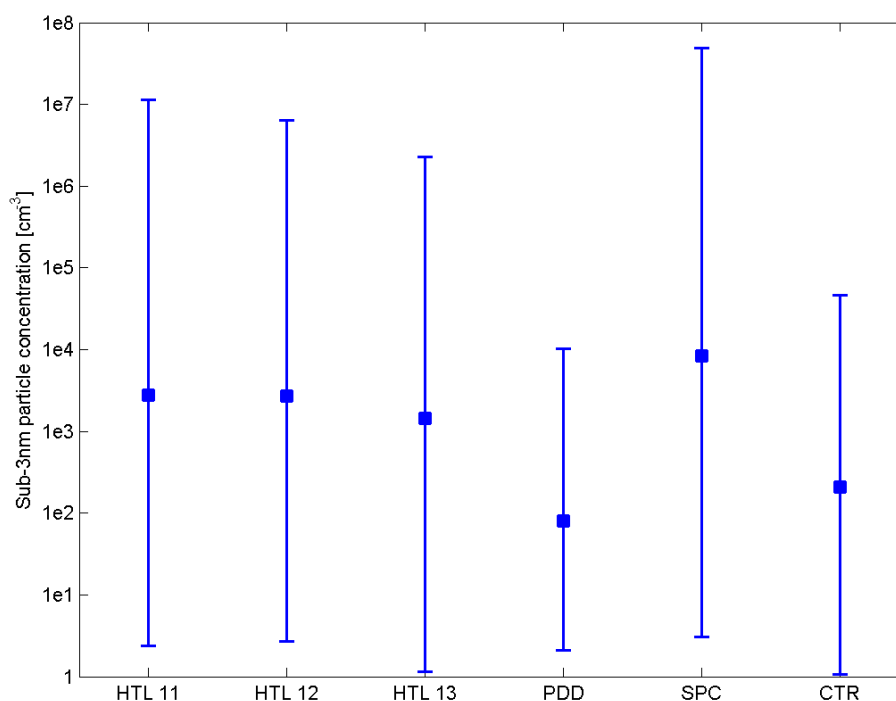


Figure 1. The median concentrations of sub-3 nm clusters and particles at different measurement sites. The errorbars show 25th and 75th percentiles. The explanations for the abbreviations and the measured size ranges are presented in Table 1.

Figure 2 illustrates the median diurnal variation of sub-3nm cluster and particle concentrations at different measurements sites. In San Pietro Capofiume the concentration was high during the whole day, reaching the maximum around noon due to new particle formation. In Hyytiälä the sub-3nm concentration had also a daytime maximum related to new particle formation during spring 2011 and spring 2012. However, in summer 2013 the concentration did not have as distinct diurnal cycle. This difference may result from new particle formation events being more infrequent and weaker in summer compared to spring. In Puy de Dôme the sub-3nm concentration also increased during daytime at the same time when new particle formation was observed to take place at the site (Rose *et al.*, 2013). In Centreville the sub-3nm concentration stayed low during the whole day. This is expected as no clear new particle formation events were observed at the site during the measurement period.

## CONCLUSIONS

In this work the measurements of sub-3nm atmospheric clusters and particles conducted at four different measurement sites were compared. At these sites the median sub-3nm concentration varied from  $100 \text{ cm}^{-3}$  to  $8000 \text{ cm}^{-3}$ . The diurnal variation of the concentration was observed to be linked to the occurrence of new particle formation events. However, at all measurement sites a certain number of clusters was observed to be present all the time, also at night. This indicates that clusters are formed in the atmosphere continuously, and only some of them are connected to new particle formation.

## ACKNOWLEDGEMENTS

This work was supported by Finnish Centre of Excellence (FCoE; project no 1118615), Nordic Center of Excellence Cryosphere-Atmosphere Interactions in a Changing Arctic Climate (CRAICC), and European Research Council (ERC).

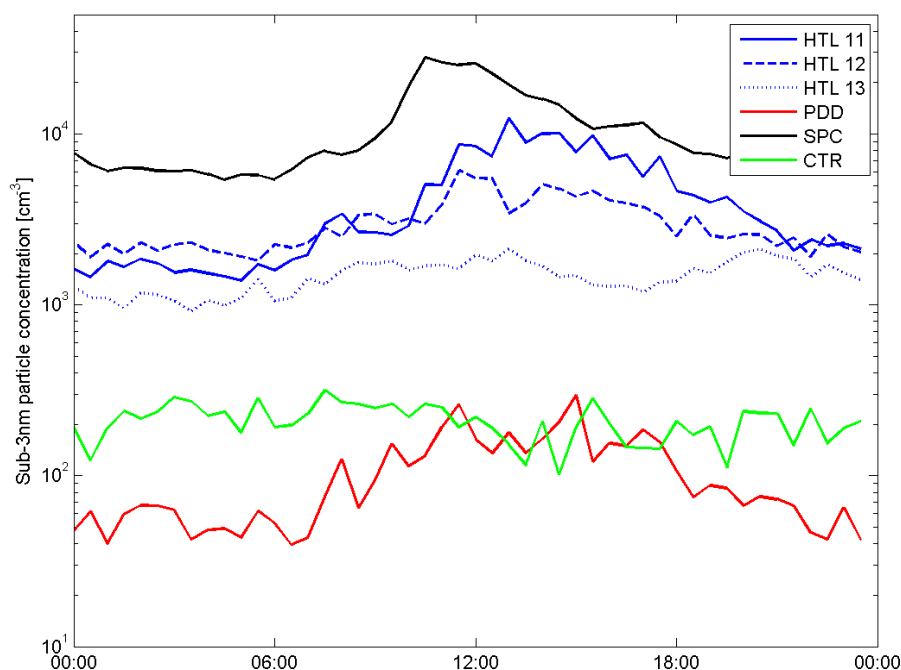


Figure 2. The median diurnal variation of sub-3nm cluster and particle concentration at different measurement sites. The explanations for the abbreviations and the measured size ranges are presented in Table 1.

## REFERENCES

- Dal Maso, M., Kulmala, M., Riipinen, I., Wagner, R., Hussein, T., Aalto, P. P., and Lehtinen, K. E. J. (2005). Formation and growth of fresh atmospheric aerosols: eight years of aerosol size distribution data from SMEAR II, Hyytiälä, Finland, *Boreal Environ. Res.*, **10**, 323–336.
- Kulmala, M., Vehkamäki, H., Petäjä, T., Dal Maso, M., Lauri, A., Kerminen, V.-M., Birmili, W., and McMurry, P. H. (2004). Formation and growth rates of ultrafine atmospheric particles: A review of observations, *J. Aerosol Sci.*, **35**, 143–176.
- Kulmala, M., Kontkanen, J., Junninen, H., Lehtipalo, K., Manninen, H. E., Nieminen, T., Petäjä, T., Sipilä, M., Schobesberger, S., Rantala, P., Franchin, A., Jokinen, T., Järvinen, E., Äijälä, M., Kangasluoma, J., Hakala, J., Aalto, P., Paasonen, P., Mikkilä, J., Vanhanen, J., Aalto, J., Hakola, H., Makkonen, U., Ruuskanen, T., Mauldin III, R. L., Duplissy, J., Vehkamäki, H., Bäck, J., Kortelainen, A., Riipinen, I., Kürten, T., Johnston, M. V., Smith, J. N., Ehn, M., Mentel, T. F., Lehtinen, K. E. J., Laaksonen, A., Kerminen, V.-M., and Worsnop, D. R. (2013). Direct observations of atmospheric aerosol nucleation, *Science*, **339**, 943–946.
- Manninen, H. E., Nieminen, T., Asmi, E., Gagne, S., Häkkinen, S., Lehtipalo, K., Aalto, P., Vana, M., Mirme, A., Mirme, S., Hörrak, U., Plass-Dülmer, C., Stange, G., Kiss, G., Hoffer, A., Toro, N., Moerman, M., Henzing, B., de Leeuw, G., Brinkenberg, M., Kouvarakis, G. N., Bougiatioti, A., Mihalopoulos, N., O'Dowd, C., Ceburnis, D., Arneth, A., Svenningsson, B., Swietlicki, E., Tarozzi, L., Decesari, S., Facchini, M.C., Birmili, W., Sonntag, A., Wiedensohler, A., Boulon, J., Sellegri, K., Laj, P., Gysel, M., Bukowiecki, N., Weingartner, E., Wehrle, G., Laaksonen, A., Hamed, A., Joutsensaari, J., Petäjä, T., Kerminen, V.-M., and Kulmala, M. (2010). EUCAARI ion spectrometer measurements at 12 European sites – analysis of new-particle formation events, *Atmos. Chem. Phys.*, **10**, 7907–7927.
- Rose *et al.* (2013), manuscript in preparation.
- Vanhanen, J., Mikkilä, J., Lehtipalo, K., Sipilä, M., Manninen, H. E., Siivola, E., Petäjä, T., and Kulmala, M. (2011). Particle size magnifier for nano-CN detection, *Aerosol Sci. Tech.*, **45**, 533–542.

# COMPARISON OF CLOUD DROPLET ACTIVATION BETWEEN SECTIONAL AND MODAL AEROSOL MODELS

T.KORHOLA<sup>1</sup>, H.KOKKOLA<sup>2</sup>, H.KORHONEN<sup>2</sup>, S.ROMAKKANIEMI<sup>1</sup>

<sup>1</sup>Department of Applied Physics, University of Eastern Finland, P.O. Box 1627, 70211 Kuopio, Finland

<sup>2</sup>Finnish Meteorological Institute, Kuopio Unit, P.O. Box 1627, 70211 Kuopio, Finland

Keywords: Modeling, Sectional model, Modal model, Aerosol activation.

## INTRODUCTION

High resolution sectional aerosol models are capable of simulating aerosol dynamics more accurately compared to modal models. However, in global scale applications the sectional models have to be used with low particle size resolution to achieve feasible computational times. Modal aerosol models are inherently faster but the simplicity of the distribution representation may affect the accuracy of the model. So far there has not been a robust comparison between these two modelling approaches. Here we present preliminary results from a comparison between the models in respect to their ability to predict cloud droplet number concentration (CDNC) during a nucleation event followed by particle growth. Since aerosol particles affect climate strongly through cloud formation we chose to first focus on the CDNC. For a reference in the comparison we chose a high resolution sectional model. Instead of comparing models in global environment, a box model setup is chosen to facilitate the control of physical, numerical and statistical phenomena effectively in addition to having reasonable runtimes.

## METHODS AND RESULTS

Both the sectional and modal models included nucleation, condensation, coagulation, water uptake and cloud droplet activation parameterization by Nenes and Seinfeld (Nenes & Seinfeld 2005). To be able to compare the ability of the models to predict CDNC accurately we set identical starting conditions with bi-modal initial distribution with number concentrations of  $500 \text{ cm}^{-3}$  and  $200 \text{ cm}^{-3}$  particles in Aitken and accumulation modes with mean diameters of 30 nm and 200 nm respectively. The standard deviation was 1.59. All three models had same injection rate of sulphuric acid into the system to produce nucleation and condensational growth. The results here are from a 15 hours simulation with updraft velocity of  $0.5 \text{ ms}^{-1}$ . To minimize external differences between the models we used the same sectional version of the cloud droplet activation parameterization for the modal model as well, by transforming the modal distribution to sectional one with high resolution. The transform causes negligible effect to the results.

Number-size distribution plots show clearly the differences between the models (Figure 1). The modal model distribution deviates strongly from the sectional and reference models due to the reallocation routine used in the model. Effects of the reallocation routine are described in detail in Korhola et al. (2013). The differences in the distributions consecutively cause noticeable differences in the CDNC (Figure 2). The sectional model agrees well with the reference model during the first six hours, after which it overestimates the cloud droplet number concentration. The overestimation seems to be caused by the coarse size resolution where inclusion of even one more section in to the activation viable particles can potentially increase the number of cloud droplets significantly. We are also using a shape assumption in the sectional model by using a linear fit between the middle points on the top of each section (Kokkola et al 2008). This is done to compensate the effects of low size resolution. Eventhough the same bimodal initial distribution was used, there was an offset in CDNC in the beginning of the simulation between the

sectional and the modal model. This is because the coarse sectional model is not able to follow exactly the same distribution shape as the reference model.

In this experiment the modal model shows clearly smaller increase in the CDNC compared to the reference model. With the fixed mode width and rather low growth rate of the Aitken mode the modal model is unable to noticeably increase the number of particles exceeding the critical activation diameter. The difference can be seen in the Figure 1, middle and rightmost panels. In the reference model the Aitken mode narrows during the simulation and the peak value of the mode increases, with the critical dry diameter varying around 80 nm the Aitken mode particles begin to contribute to the CDNC. With the fixed mode width similar growth of the smaller particles in the Aitken mode to activation size is not occurring. Since the particles in the nucleation mode remain small their coagulation losses are significantly larger compared to the sectional or reference model, where the particles are allowed to grow freely. This also partly explains the small number of activated particles.

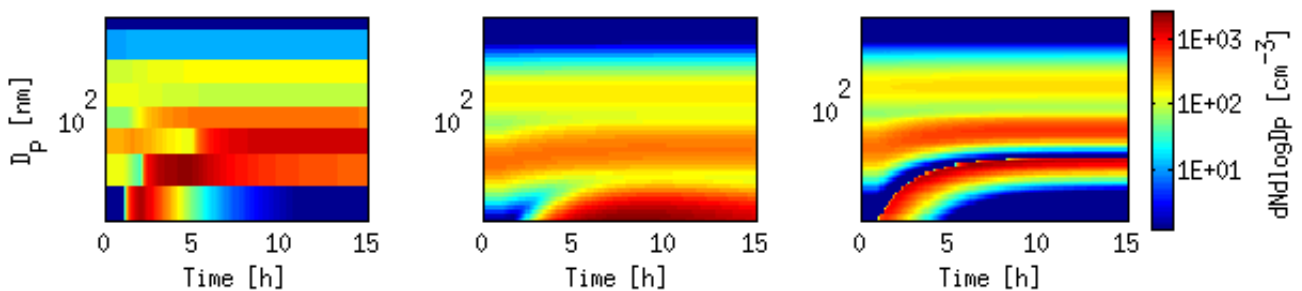


Figure 1. Number size distribution by sectional model, modal model and the reference model.

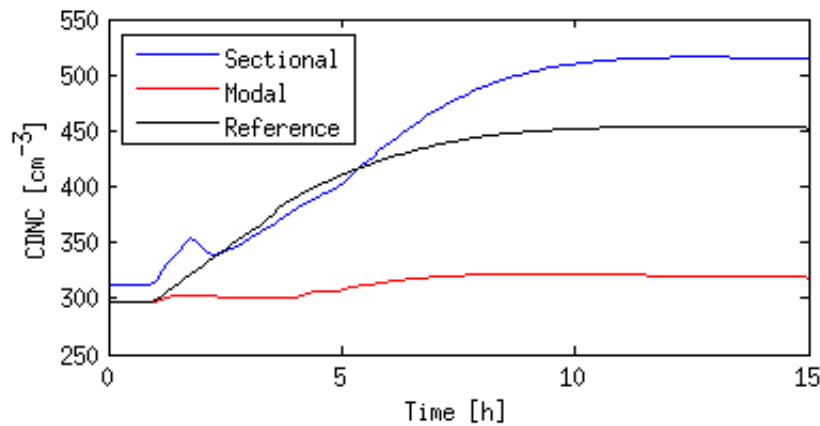


Figure 2. Cloud droplet number concentrations during the simulations for the sectional, modal and reference models.

## CONCLUSIONS

Here we presented the preliminary results from a comparison of sectional and modal aerosol models. With a high resolution sectional model as a reference we used a box model setup to compare cloud droplet number concentrations during a new particle formation event. The results show better agreement between the sectional and reference model compared to the modal and reference model.

Next we are going to expand the experiment with an ensemble of different initial distributions, wide range of updraft velocities and varying concentrations of sulphuric acid. The goal is also to develop the sectional

model further by making it computationally lighter while retaining or even improving its accuracy. One of the promising new methods is so called Random Forest approximation error correction approach (Lipponen et al. 2013) in addition to reducing the number of size section even further

#### ACKNOWLEDGEMENTS

The research has been supported by the strategic funding of the University of Eastern Finland, and by the Academy of Finland Centre of Excellence Program (project no 1118615).

#### REFERENCES

- Nenes, A., and Seinfeld J.H. (2003) Parameterization of cloud droplet formation in global climate models, *J. Geophys. Res.*, 108 (D14), 4415, doi:10.1029/2002JD002911.
- Korhola, T., Kokkola, H., Korhonen, H., Partanen, A.-I., Laaksonen, A., Lehtinen, K. E. J., Romakkaniemi, S., (2013) Reallocation in modal aerosol models: impacts on predicting aerosol radiative effects. *Geosci. Model Dev. Discuss.*, 6, 4207-4242
- Kokkola, H., Korhonen, H., Lehtinen, K. E. J., Makkonen, R., Asmi, A., Järvenoja, S., Anttila, T., Partanen, A.-I., Kulmala, M., Järvinen, H., Laaksonen, A., and Kerminen, V.-M. (2008) SALSA – a Sectional Aerosol module for Large Scale Applications, *Atmos. Chem. Phys.*, 8, 2469-2483, doi:10.5194/acp-8-2469-2008
- Lipponen, A., Kolehmainen, V., Romakkaniemi, S., Kokkola, H. (2013) Correction of approximation errors with Random Forests applied to modelling of aerosol first indirect effect. *Geosci. Model Dev. Discuss.*, 6, 2551-2583

# A NEW WAY TO ASSESS THE SYSTEMATIC ERRORS IN STATIC CHAMBER MEASUREMENTS

J.F.J. KORHONEN<sup>1</sup>, J. PUMPANEN<sup>2</sup> and M. PIHLATIE<sup>1</sup>

<sup>1</sup>Division of Atmospheric Sciences, Department of Physics, University of Helsinki  
P.O. Box 48, FI-00014, University of Helsinki, Finland

<sup>2</sup>Department of Forest Sciences, P.O. Box 27, FI-00014, University of Helsinki

Keywords: GAS EXCHANGE, SOIL EFFLUX, GAS STORAGE, TRANSPORT COEFFICIENT

## INTRODUCTION

Chamber method is a useful tool to quantify gas exchange (gas flux / gas efflux) between ecosystems and the atmosphere. Chamber measurement is especially suitable for process-studies, in which it is important to quantify fluxes from individual ecosystem components, such as soil, instead of the ecosystem net flux. In addition to the quantity of the gas flux, raw data of the chamber measurement includes useful information about the measurement system. This information could be used for decreasing the uncertainty of gas flux estimations, and this is the aim of this study.

Static chambers are commonly used in measuring carbon dioxide (CO<sub>2</sub>) methane (CH<sub>4</sub>) and nitrous oxide (N<sub>2</sub>O) emissions from soil. However, static chamber measurements include systematic errors (Pumpanen et al., 2004; Pihlatie et al., 2013), which are different in different environments and with different chamber designs. It has been proposed, that researchers should use similar design for chambers for different ecosystems. However, due to combination effect of the chamber design and the ecosystem, different chambers are related to different systematic errors in different ecosystems. Therefore, only guidelines for chamber design can currently be provided (Pihlatie et al., 2013).

Closing the chamber causes disturbances to the measurement (Christiansen et al., 2011). Therefore, the first measurement points during the chamber closure are not reliable. Unfortunately, to estimate the flux, the first points are the most important ones. One issue that is potentially causing severe systematic errors in static chamber measurements, is the change in storage of the gas concentration under the chamber during the measurement. This can cause either over- or underestimation to the flux (Lai et al., 2012). The gas concentration under the chamber may change rapidly when the chamber is closed, because of pressure effects, or because of the change in wind velocity inside the chamber. According to our knowledge, so far there are no suggestions how to correct this problem in data analysis.

In the abstract we present a method to study the problem in laboratory, and solve it when additional data is available. We hope that after laboratory experiments planned for year 2014, this correction could be applied to actual field measurements.

## THEORY

During enclosure of a static chamber, gas concentration inside the chamber changes in time (Fig. 1). Theoretically, the change is linear in the beginning, but the gas concentration development saturates with time. Different equations are fitted in the data and the fitting parameters are used to calculate the flux. It has been suggested that an exponential function should be used (Kutzbach et al., 2007; Kroon et al., 2008). Nevertheless, a linear is robust and provides the smallest random error, whereas exponential functions

provide smaller systematic error when signal-to-noise ratio is good and there are enough data points per closure (Korhonen et al., 2010). The systematic error of linear (and probably also exponential) function depends on how fast the concentration difference in the soil and in the chamber headspace decreases. This depends on transport coefficient ( $k$ ):

$$J = k (c_s - c_c) , \quad (1)$$

where  $J$  is the concentration change in time in chamber (ppm/min), and  $C_s$  and  $C_c$  are concentrations in the soil and in the chamber headspace, respectively. Usually it is assumed that the transport in soil occurs via diffusion, which in turn depends mainly on gas diffusivity and transport distance. When using the concept of transport coefficient it is assumed that the source (or sink) of the gas is at a specific depth.

An ideal gas concentration development in a chamber headspace, and fit exponential function is shown in Fig. 1. The flux is linearly dependent on the rate of change in gas concentration with time, and thus flux decreases in time in Fig 1. In the beginning of the measurement the slope represents undisturbed flux, which is the variable that the whole measurement aims at estimating. The exponential function is fitted to the whole enclosure, and then rate of change is calculated for the undisturbed flux at the beginning of the measurement. This is represented as line in Fig 1. During this moment, the gas concentration within the chamber headspace should equal to ambient concentration.

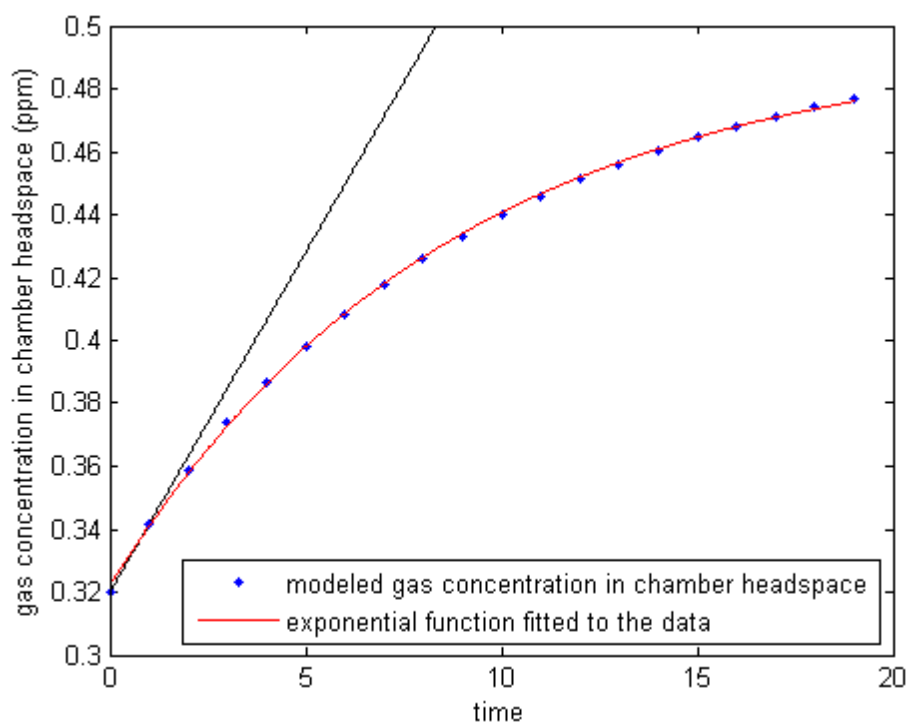


Figure 1. Simulated chamber gas concentration during a chamber enclosure, including disturbance in the beginning. An exponential function is fitted to data. The flux estimation is linearly dependent of the rate of change of gas concentration in time. In the beginning of the measurement the slope (black line) represents undisturbed flux, which is the variable that the whole measurement aims at estimating.

Theoretically, exponential function works usually fine. However, if there are disturbances in the beginning of the enclosure, the use of an exponential function may be problematic. Unfortunately, these disturbances may be difficult to recognize.

When  $C_s$  and  $C_c$  are known (or estimated), the value for  $k$  can be calculated during the enclosure (Fig 2) by writing Eq 1. in form

$$k = J \frac{J}{C_s - C_c} . \quad (2)$$

Because the changes in soil physical properties and temperature during an enclosure lasting for maximum an hour are negligible, it is reasonable to assume that the transport coefficient ( $k$ ) is constant during one enclosure. If this is not true, there is something wrong with the measurement. Analyzing trends in  $k$  in time can reveal the problematic periods during the enclosure. These data points, are assumed to often occur in the beginning of the enclosure, should be removed from the analysis. However, when using an exponential function, this means that the function must be extrapolated to the beginning of the enclosure to calculate the flux. This may lead to very large errors in flux estimation.

Here we propose a method to calculate the flux even after removing the bad data points, detected by  $k$  filtering. After removing the data points that are associated with a trend in  $k$ , undisturbed flux can be calculated by using Eq. 1, using  $C_s$  as the measured gas concentration in the soil, and  $C_c$  as the ambient gas concentration.

## MATERIALS AND METHODS

Gas concentration change in chamber ( $C_c$ ) was simulated with a very simple dynamic model, based on Eq 1. A constant gas concentration in soil ( $C_s = 0.5$  ppm) and a constant but arbitrary gas transport coefficient ( $k = 0.1$  / min) were used. Two simulations were performed. Normal simulation was performed as described. In storage simulation  $J$  was increased 10%, 5%, 2.5% and 1.25% for the 1<sup>st</sup>, 2<sup>nd</sup>, 3<sup>rd</sup> and 4<sup>th</sup> minute, respectively. The purpose of this increase was to simulate a disturbance in the beginning of the enclosure. Both simulations were run for 20 minutes using one minute time-step. Linear ( $y = ax + b$ ) and exponential functions ( $y = ax^{-bx} + c$ ) were fitted to the two simulated data sets.

## RESULTS AND DISCUSSION

Our disturbed simulation resulted in 8% higher flux estimation than the ideal measurement. In this simple simulation the change in soil gas concentration is not taken into account, and thus there was no random uncertainty involved in the estimated flux estimates. Because exponential fit is quite sensitive and unstable, it is expected that by extrapolating the data to the beginning of the enclosure with noisy data would cause relatively large uncertainty in the flux estimation.

In field conditions, in case of disturbance in the beginning of an enclosure, the gas concentration in soil would probably decrease in the beginning, and increase in the end of the enclosure. This would cause even stronger bias to the flux estimate calculated based on exponential fit. However, in this case change in soil gas concentration was not taken into account. Ideally soil gas concentration would be monitored during the measurement, to further improve the method.

The method proposed should be tested with real measurements. A chamber calibration campaign to quantify and assess errors in chamber measurements planned for 2014 will be a good opportunity to test this method. We hope that this method could be useful for analysing static chamber field measurements, in conjunction with soil gas concentration (profile) measurements. Looking at the changes in transport

coefficient during the enclosure during laboratory experiments could help in understanding the systematic errors in static chamber measurements.

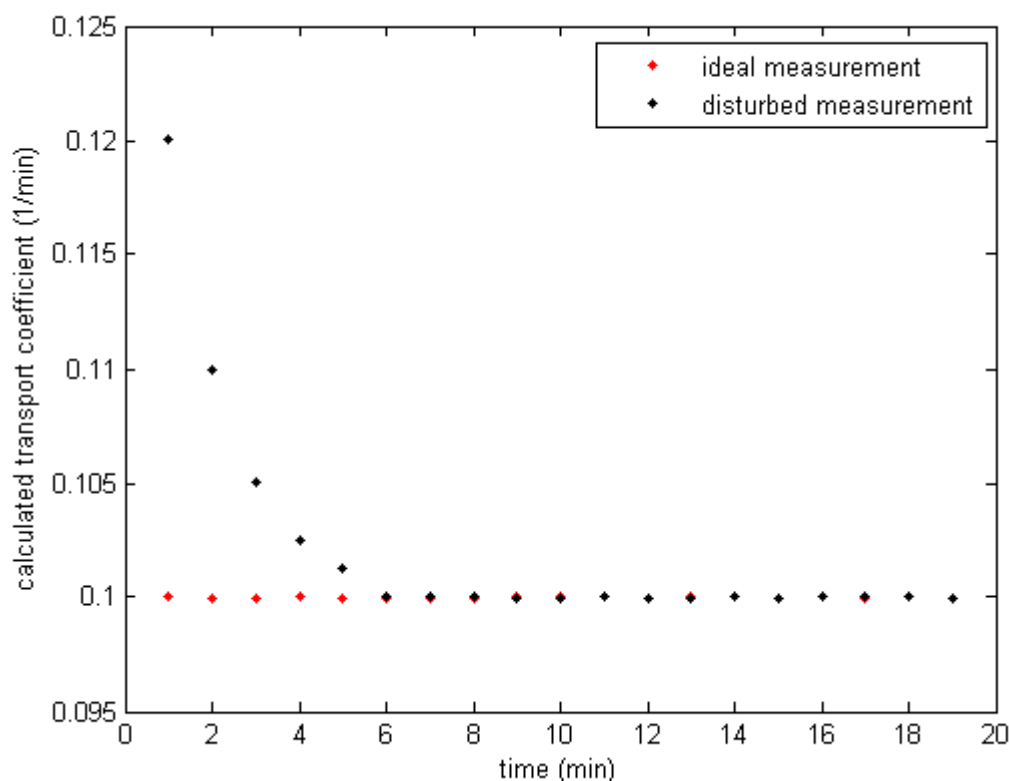


Figure 2. Calculated transport coefficient from the modeled chamber headspace concentration data. The black dots show that something is wrong in the data, because transport coefficient should be constant during the measurement.

## CONCLUSIONS

Disturbances in static chamber measurements can cause systematic bias in flux estimates. This bias can be difficult to detect. Here we propose a method to detect disturbances, and a method to calculate the fluxes with smaller bias, in case disturbances are detected. This method could be used in laboratory experiments to detect potentially biases related to static chamber measurements. Furthermore, the applicability of the method should be tested in laboratory, and in the field.

## ACKNOWLEDGEMENTS

We would like to thank InGos, Academy of Finland Center of Excellence (project no 1118615) and the Nordic Centers of Excellence DEFROST.

## REFERENCES

Christiansen, J. R., Korhonen, J. F. J., Juszczak, R., Giebels, M., and Pihlatie, M.: Assessing the effects of chamber placement, manual sampling and headspace mixing on CH<sub>4</sub> fluxes in a laboratory experiment, *Plant and Soil*, 343, 171-185, DOI 10.1007/s11104-010-0701-y, 2011.

- Korhonen J.F.J., Nordbo A., Kieloaho A.-J., Vesala T. and Pihlatie M.K. A method to decrease random and systematic errors in static chamber flux calculations. Annual meeting of Finnish Center of Excellence in Physics, Chemistry, Biology and Meteorology of Atmospheric Composition and Climate Change, May 17<sup>th</sup> - 19<sup>th</sup> 2010, Kuopio, Finland. Abstract: Report Series in Aerosol Science, 109, 2010.
- Kroon, P. S., Hensen, A., van den Bulk, W. C. M., Jongejan, P. A. C., and Vermeulen, A. T.: The importance of reducing the systematic error due to non-linearity in N<sub>2</sub>O flux measurements by static chambers, *Nutr Cycl Agroecosys*, 82, 175-186, DOI 10.1007/s10705-008-9179-x, 2008.
- Kutzbach, L., Schneider, J., Sachs, T., Giebels, M., Nykanen, H., Shurpali, N. J., Martikainen, P. J., Alm, J., and Wilmking, M.: CO<sub>2</sub> flux determination by closed-chamber methods can be seriously biased by inappropriate application of linear regression, *Biogeosciences*, 4, 1005-1025, 2007.
- Lai, D. Y. F., Roulet, N. T., Humphreys, E. R., Moore, T. R., and Dalva, M.: The effect of atmospheric turbulence and chamber deployment period on autochamber CO<sub>2</sub> and CH<sub>4</sub> flux measurements in an ombrotrophic peatland, *Biogeosciences*, 9, 3305-3322, DOI 10.5194/bg-9-3305-2012, 2012.
- Pihlatie, M. K., Christiansen, J. R., Aaltonen, H., Korhonen, J. F. J., Nordbo, A., Rasilo, T., Benanti, G., Giebels, M., Helmy, M., Sheehy, J., Jones, S., Juszczak, R., Klefoth, R., Lobo-do-Vale, R., Rosa, A. P., Schreiber, P., Serca, D., Vicca, S., Wolf, B., and Pumpanen, J.: Comparison of static chambers to measure CH<sub>4</sub> emissions from soils, *Agricultural and Forest Meteorology*, 171, 124-136, DOI 10.1016/j.agrformet.2012.11.008, 2013.
- Pumpanen, J., Kolari, P., Ilvesniemi, H., Minkkinen, K., Vesala, T., Niinisto, S., Lohila, A., Larmola, T., Morero, M., Pihlatie, M., Janssens, I., Yuste, J. C., Grunzweig, J. M., Reth, S., Subke, J. A., Savage, K., Kutsch, W., Ostreng, G., Ziegler, W., Anthoni, P., Lindroth, A., and Hari, P.: Comparison of different chamber techniques for measuring soil CO<sub>2</sub> efflux, *Agricultural and Forest Meteorology*, 123, 159-176, DOI 10.1016/j.agrformet.2003.12.001, 2004.

# HR-TOF-AMS MEASUREMENTS OF PARTICULATE EMISSIONS FROM WOODCHIP COMBUSTION

A. KORTELAINE<sup>1</sup>, J. JOUTSENSAARI<sup>1</sup>, P. TIITTA<sup>2</sup>, A. JAATINEN<sup>1</sup>, P. MIETTINEN<sup>1</sup>, L. HAO<sup>1</sup>, J. LESKINEN<sup>2</sup>, O. SIPPULA<sup>2</sup>, T. TORVELA<sup>2</sup>, J. TISSARI<sup>2</sup>, J. JOKINIEMI<sup>2,5</sup>, D. R. WORSNOP<sup>1,3,4</sup>, A. LAAKSONEN<sup>1,3</sup> and A. VIRTANEN<sup>1</sup>

<sup>1</sup>Department of Applied physics, University of Eastern Finland, Kuopio, 70211, Finland.

<sup>2</sup>Department of Environmental Science, University of Eastern Finland, Kuopio, 70211, Finland.

<sup>3</sup>Finnish Meteorological Institute, Climate change, Helsinki, 00101, Finland.

<sup>4</sup>Aerodyne Research Inc., Billerica, MA, 01821, USA.

<sup>5</sup>VTT Technical Research Centre of Finland, Fine Particles, P.O. Box 1000, FI-02044 VTT, Espoo, Finland.

Keywords: combustion, aerosol, aerosol mass spectrometry, chemical composition.

## INTRODUCTION

Fine particle emissions have both adverse health and environmental effects. Current levels of thoracic (PM<sub>10</sub>; D<sub>a</sub> < 10 µm) and fine particles (PM<sub>2.5</sub>; D<sub>a</sub> < 2.5 µm) in Europe are associated with about 350 000 premature annual deaths, increased hospital admission, and restricted activity in tens of millions of children and people with chronic cardiovascular and pulmonary disease ((EU/CAFÉ) WHO 2003, U.S. EPA 2004). Residential wood combustion (RWC) produces high amounts of gaseous and particulate emissions into the atmosphere. The main components of particulate emissions in wood combustion are ash (inorganic species), soot (elemental carbon) and organic matter (Tissari, 2008). The particulate organic matter formed in wood combustion is a complex mixture including compound groups such as anhydrosugars (e.g. levoglucosan), methoxyphenols, PAHs, organic acids, sterols and alkanes (Hays, 2011; Orasche, 2013a). Combustion conditions and fuel quality have an important effect on aerosol chemical composition, particle size and concentration (Sippula, 2007; Orasche, 2013b). The composition of particles is in key role, when either the health effects or atmospheric effects of the emissions are considered. Therefore, it is important to understand how chemical composition of particulate emissions varies during different burning processes and conditions.

## METHODS

The measurements were carried out as a part of Biohealth project at in University of Eastern-Finland in Kuopio during Oct-Nov.2010. The experiments were performed by burning wood chips (mixture of spruce and deciduous wood) in a moving step-grate burner (Arterm Multijet, 40 kW) under different combustion conditions, and measuring the emission products. The wood chips were added into the heater periodically. In every 20 minutes the grate elements were moving automatically in order to enhance removing of the ash from the grate. The experiments were divided into efficient, intermediate and smouldering combustion conditions by the emission rates of CO (low, elevated and high, respectively). According to carbon monoxide, efficient combustion represents combustion in modern pellet boiler, smouldering conventional batch combustion conditions and intermediate partly both conditions or malfunction in the continuously working burner (Tissari, 2008; Lamberg, 2011).

HR-ToF-AMS (High Resolution Time-Of-Flight Aerosol Mass Spectrometer) (DeCarlo, 2006; Jayne, 2000) was used to quantify organic and inorganic species, and for the first time, employed the positive matrix factorization (PMF) (Paatero and Tapper, 1994; Paatero, 1997 ;Ulbrich, 2006) method to analyse organics data from the combustion source to gain the detailed information on temporal changes in chemical composition of organic aerosol (OA), and further how different burning phases and conditions affect the composition of the particle emitted.

## CONCLUSIONS

Total mass loading of emissions elevated from efficient to smouldering combustion according to AMS measurements. In efficient combustion the main constituents were ultrafine inorganic salt particles whilst in intermediate and smouldering combustion main constituents were organic carbon (OC) and elemental carbon (EC). Furthermore, the size of the emitted particles was markedly larger in smouldering combustion conditions. OC as well as organic mass (OM), and also particulate PAH emissions increased from intermediate to smouldering combustion.

Particles were not detected in AMS at efficient combustion conditions for two reasons 1) small size, 2) inorganic material that was not vaporizing in the AMS heater at 600 °C. In intermediate combustion conditions main constituents analyzed by AMS were organics, sulfate (SO<sub>4</sub>), chloride (Chl) and small amount of nitrate (NO<sub>3</sub>). In smouldering combustion organics and particularly PAH were the dominating groups and in addition to them, also small amounts of chloride and nitrate were detected. The nitrate, mainly composed of NO fragment, was originated mainly from inorganic salts and in addition organic compounds including NO ion fragments.

The organic subgroups were specified by their formation mechanisms for instance oxidation, and according to the combustion conditions that were related to combustion efficiency. Organics detected by AMS were split by PMF into a formerly reported factor HOA (Hydrocarbon-like Organic Aerosol) (Zhang, 2006) and new factors named “C-OOA” (Combustion-Oxidized Organic Aerosol), “PAH” and “Aromatics”.

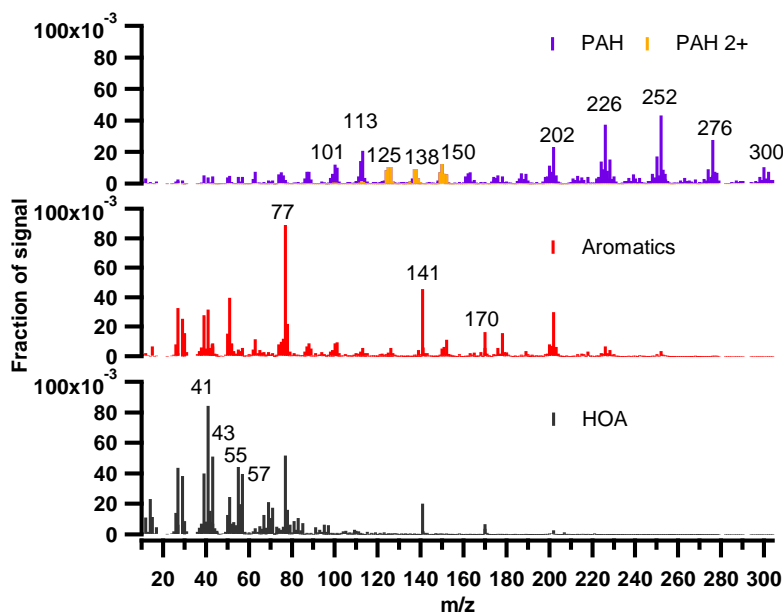


Figure 1: Mass spectra of PMF derived organic compounds “PAH”, “Aromatics” and HOA.

C-OOA found in combustion experiments is representing the highly oxidized organic aerosol that is quite similar with LV-OOA, which is typical highly aged aerosol in atmospheric measurements. The highest peaks were  $\text{CO}_2^+$  and  $\text{CO}^+$  and O:C ratio was 0.56 (see Fig. 1). These markers are typical for the LV-OOA factor. The C-OOA was increasing during the momentary CO-peaks, when the oxidation level of the OM increased. C-OOA could be related carboxylic acids, which are generally known to be abundant in wood smoke (Hays, 2011; Orasche 2013a).

HOA (Hydrocarbon-like Organic Aerosol) is typical combustion emission product and it was found also in this work from intermediate and smouldering combustion conditions. In the mass spectrum of HOA, highest peaks were  $\text{C}_3\text{H}_5$  ( $m/z$  41),  $\text{C}_2\text{H}_3\text{O}$  (43),  $\text{C}_4\text{H}_7$  (55),  $\text{C}_4\text{H}_9$  (57) (See Fig. 1). The HOA mass spectra also included hydrocarbon series of  $\text{C}_n\text{H}_{2n+1}$  with low O/C ratio ap. 0.1. HOA was found to be correlating with the gaseous hydrocarbons detected by FTIR, which might indicate that gaseous hydrocarbons (i.e. alkanes, alkenes) are condensing and/or adsorbing onto the particle surface or that they are formed at the same time with the hydrocarbon-like organic aerosol particles.

The species containing aromatic ring organics split into two factors. The species containing one ring belonged to Aromatic factor and species containing several rings belonged to “PAH” factor. Aromatic factor was mainly composed aromatic ring containing ion fragments from which three notable peaks of  $\text{C}_6\text{H}_5$  ( $m/z$  77),  $\text{C}_6\text{H}_5\text{SO}_2$  (141) and  $\text{C}_7\text{H}_8\text{NO}_2\text{S}$  (170) (see Fig. 1) were likely formed from decomposition of n-butyl benzosulfoamide compound ( $\text{C}_6\text{H}_5\text{SO}_2\text{NH}_2$ ). The Aromatics factor was the only organic factor that was higher in the stable combustion conditions than during the momentary CO-peaks indicating that the compounds in the Aromatic factor were mainly formed during the stable combustion conditions (see Table 1). PAH compounds were formed during the momentary CO-peaks in smouldering combustion (see Table 1.). With AMS PAHs wasn’t found in intermediate combustion. The explanation according to the gas chromatography mass spectrometer (GC-MS) analyses was that they comprised mainly of small PAHs (2-3 aromatic rings) and due to the high dilution ratio they were mainly present in gas phase. On the other hand in smouldering combustion large share of PAHs were containing several aromatic rings (>4 rings) and therefore they are found in the particulate phase in AMS.

In addition it was observed that sulphate was likely originated from organosulphates that was forming during stable conditions. Results show that particulate emissions from wood combustion can be varied significantly when combustion conditions are changed, even for short periods. The results indicate that PAHs formation can be reduced efficiently when keeping combustion conditions stable.

Compound	during peak (%)	outside of peak ( $\mu\text{g}/\text{m}^3$ )
HOA	6.4 (3.01 $\text{mg}/\text{m}^3$ )	30.9 (4.90 $\text{mg}/\text{m}^3$ )
C-OOA	27.3 (12.86 $\text{mg}/\text{m}^3$ )	4.2 (0.67 $\text{mg}/\text{m}^3$ )
“Aromatics”	0.6 (0.30 $\text{mg}/\text{m}^3$ )	47.1 (7.46 $\text{mg}/\text{m}^3$ )
“PAH”	29.9 (14.04 $\text{mg}/\text{m}^3$ )	0.1 (0.02 $\text{mg}/\text{m}^3$ )
PAH	30.1 (14.18 $\text{mg}/\text{m}^3$ )	8.2 (1.30 $\text{mg}/\text{m}^3$ )
$\text{SO}_4$	1.7 (0.80 $\text{mg}/\text{m}^3$ )	3.1 (0.48 $\text{mg}/\text{m}^3$ )
Chl	3.2 (1.49 $\text{mg}/\text{m}^3$ )	6.2 (0.98 $\text{mg}/\text{m}^3$ )
$\text{NO}_3$	0.8 (0.38 $\text{mg}/\text{m}^3$ )	0.2 (0.04 $\text{mg}/\text{m}^3$ )
Total mass ( $\text{mg}/\text{m}^3$ )	47 $\pm$ 7	16 $\pm$ 3

Table 1: Relative abundance of compounds, average mass concentrations and total mass concentration ( $\pm$  standard deviation) during and outside of CO peaks in smouldering combustion.

#### ACKNOWLEDGEMENTS

The financial support by the Academy of Finland Centre of Excellence program (project no 1118615) and ERA-NET Bioenergy BioHealth project (grant agreement n° 40392/09, dnro 1262/31/09) is gratefully acknowledged. Hao, L. acknowledges the financial support of UEF Postdoc Research Foundation (No. 930275).

## REFERENCES

- DeCarlo, P.F., J.R. Kimmel, A. Trimborn, M.J. Northway, J.T. Jayne, A.C. Aiken, M. Gonin, K. Fuhrer, T. Horvath, K. Docherty, D.R. Worsnop, and J.L. Jimenez, Field-Deployable, High-Resolution, Time-of-Flight Aerosol Mass Spectrometer, *Analytical Chemistry*, 78:8281-8289, 2006.
- Hays, M. D., Gullett, B., King, C. and Robinson, J. Characterization of carbonaceous aerosols emitted from outdoor wood boilers, *Energy & Fuels*, 25 (11), 5632-5638, 2011.
- Jayne, J. T., Leard, D. C., Zhang, X., Davidovits, P., Smith, K. A., Kolb C. E. & Worsnop, D. R., Development of an aerosol mass spectrometer for size and composition. Analysis of submicron particles, *Aerosol Science and Technology*, 33, 49-70, 2000.
- Lamberg, H., Sippula, O., Tissari, J. and Jokiniemi, J., Effects of air staging and load on fine-particle and gaseous emissions from a small-scale pellet boiler. *Energy & Fuels*, 25(11):4952-4960, 2011.
- Orasche, J., Seidel, T., Hartmann, H., Schnelle-Kreis, J., Chow, J. C., Ruppert, H. and Zimmermann, R. Comparison of emissions from wood combustion. Part 1: Emission factors and characteristics from different small-scale residential heating appliances considering particulate matter and polycyclic aromatic hydrocarbon (PAH) – related toxicological potential of particle-bound organic species, *Energy & Fuels*, 26 (11), 6695-6704, 2013a.
- Orasche, J., Schnelle-Kreis, J., Schön, C., Hartmann, H., Ruppert, H., Arteaga-Salas, J. M. and Zimmermann, R. Comparison of emissions from wood combustion. Part 2: Impact of combustion conditions on emission factors and characteristics of particle-bound organic species and polycyclic aromatic hydrocarbon (PAH) – related toxicological potential, *Energy & Fuels*, 27 (3), 1482-1491, 2013b.
- Paatero, P. and Tapper, U.: Positive Matrix Factorization: a nonnegative factor model with optimal utilization of error estimates of data values, *Environmetrics*, 5, 111–126, 1994.
- Paatero, P.: Least squares formulation of robust non-negative factor analysis, *Chemometrics and Intelligent Laboratory Systems*, 37, 23–35, 1997.
- Sippula, O., Hytönen, K., Tissari, J., Raunemaa, T. and Jokiniemi, J. Effect of wood fuel on the emissions from a top-feed pellet stove, *Energy & fuels*, 21 (2), 1151-1160, 2007.
- Tissari, J., Lyyränen, J. Hytönen, K., Sippula, O., Tapper, U., Frey, A., Saarnio, K., Pennanen, A. S., Hillamo, R., Salonen, R. O., Hirvonen, M. –R. and Jokiniemi, J. Fine Particle and gaseous emissions from normal and smouldering wood combustion in a conventional masonry heater, *Atmospheric Environment*, 42, 7862-7873, 2008.
- Ulbrich, I.M. , Canagaratna, M.R., Zhang, Q., Worsnop, D.R., and Jimenez J.L. Interpretation of Organic Components from Positive Matrix Factorization of Aerosol Mass Spectrometric Data. *Atmospheric Chemistry and Physics*, 9(9), 2891-2918, 2009.
- Zhang, Q., Alfarra, R., Worsnop, D. R., Allan, J. D., Coe, H., Canaratagna, M. R. ja Jimenez, J. L. Deconvolution and quantification of hydrocarbon-like and oxygenated organic aerosols based on aerosol mass spectrometry. *Environmental science and technology*, 39:4938–4952, 2005.

# CHANGES IN SOIL ENZYME ACTIVITIES AND LITTER DECOMPOSITION ACROSS THE CHRONOSEQUENCE OF FOREST FIRES IN VÄRRIO STRICT NATURE RESERV, EASTERN LAPLAND.

K. KÖSTER<sup>1,2</sup>, J. HEINOSALO<sup>3</sup>, J. PUMPANEN<sup>1</sup>, E. KOSTER<sup>1</sup>, F. BERNINGER<sup>1</sup>

<sup>1</sup>Department of Forest Sciences, University of Helsinki, Finland.

<sup>2</sup>Institute of Forestry and Rural Engineering, Estonian University of Life Sciences, Estonia.

<sup>3</sup>Department of Food and Environmental Sciences, University of Helsinki

Keywords: SOIL CARBON, FIRE CHRONOSEQUENCE, SOIL CO<sub>2</sub> EFFLUX, DECOMPOSITION, EXTRACELLULAR ENZYMES

## INTRODUCTION

Boreal forests are a crucial part of the climate system since they contain about 60% of the carbon bound in global forest biomes. The temperature changes predicted for the future climate will be the most pronounced in boreal region (Kasischke, 2000). With increasing temperature there will be also changes in the disturbance regimes (intervals, intensity, severity). Fire is one of the most important natural disturbances in the boreal forest influencing strongly the structure, composition and functioning of the forests (Franklin et al., 2002). Fire is the primary process which organizes the physical and biological attributes of the boreal biome and influences energy flows and biogeochemical cycles, particularly the carbon (C) and nitrogen (N) cycle. It is expected, that with future climate change the fire frequencies in boreal forests will increase as a result of long drought events (Yakov, 2010). In boreal ecosystems, fungi and bacteria are important drivers of soil C loss, as they produce extracellular enzymes required to degrade litter inputs of the plant species (Högberg et al., 2007; Allison et al., 2009; Allison et al., 2010). Soil organic and litter compounds such as cellulose, lignin and chitin are degraded enzymatically and fire induced changes in the soil microbial community could influence the production and activity of such enzymes (Rietl and Jackson, 2012).

The aim of this study was to investigate the effect of fire on the soil enzyme activities. We assessed the changes occurring in soil C dynamics (CO<sub>2</sub> efflux, soil C content, soil C turnover times), enzyme activity and litter decomposition along a chronosequence of fires.

## METHODS

The measurements were conducted in Värriö Nature Park (67°46' N, 29°35' E), which is located close to the Russian border in Lapland (Finland), in the northern boreal or subarctic coniferous forests. The sites are situated north of the Arctic Circle, near to the northern timberline at an average of 300 m altitude. Lowlands in the area are covered by taiga, where the main tree species is Scots pine (*Pinus sylvestris* L.). The soil in the area is moraine (with plenty of stones). Typical herbaceous plants: *Vaccinium myrtillus*, *Vaccinium vitis-idaea*, *Empetrum nigrum*, indicates also rather poor soil conditions. Treeline is around 470 m a.s.l. Annual mean precipitation in the area is about 600 mm and average annual mean temperature at Värriö research station (altitude 380 m) is around -1 °C. The climate in the area is subcontinental and the soil has no underlying permafrost. The snow covers the ground for around 200–225 days per year, and the length of the growing season is 105–120 days. The growing season in the area (mean monthly temperature more than 5 °C) lasts for 4 months and the average temperature during that period (from June to August) in the area is around 12 °C.

We have established 10 sample areas (with two replicate plots in each) in a chronosequence of 5 age classes (2 to 150 years since the last fire) during the summer 2011. The chronosequence consisted of four types of areas: (i) old areas, fire more than 150 years ago, (ii) fire around 60 years ago, (iii) fire around 40 years ago, (iv) fire 2 years ago. To characterize the stands we have established circular sample plots on areas with a radius of 11.28 m, where different tree characteristics were measured (diameter at 1.3 m height, height of a tree, crown height, crown diameter, stand age, etc.).

To characterize the soil carbon (C) and nitrogen (N) content, and fine root biomass at the sites, we have taken 10 soil cores (0.1 m long and 0.05 m in diameter) from every sample plot. The soil cores were divided according to morphological soil horizons to litter and humus layers and the mineral layers to eluvial and illuvial horizons and sieved. Fine roots were separated from the soil. The soil C and N content was measured with elemental analyser (varioMAX CN elemental analyser, Elementar Analysensysteme GmbH, Germany) after drying the samples in an oven at 105 °C for 24 hours.

Five litter bags with Scots pine needles have been installed to each plot under the humus layer together with iButton temperature sensors (Maxim Integrated Products Ltd.) for soil organic matter (SOM) decomposition measurements. Litterbags were deployed at the end of May 2011 for one year in the field (Scots pine litter was collected in year 2011 from Hyytiälä. Litter was air-dried to constant mass and placed into litter bags (7 cm x 10cm) consisting of 0.2 mm nylon mesh. Each litterbag received 5g of air-dried litter). After a year of decomposition, litterbags were harvested and frozen at -24°C following collection. For mass loss measurements the samples were later oven-dried at 50°C to constant mass. Mass loss percentage was determined as the difference between initial and final dry weight of the litter. For extracellular enzyme activity measurements the subsamples from the frozen litter bags were used. We performed three 0.2 - 0.3 g (wet weight) subsamples from the litter bags, all together 132 subsamples. We studied the activities of seven extracellular enzymes involved in C and nutrient cycling.

## RESULTS AND CONCLUSIONS

The overall/total C and N contents in the first 10 cm of the topsoil (all soil layers taken into consideration) were highest on old areas (fire more than 152 years ago) and lowest on newly burned areas (fire 2-40 years ago). The highest C pools were measured on old areas from top soil horizons (consisting of decomposing litter). The area where the fire was 2 years ago had the lowest total C pools. These results are also correlating to the soil respiration measurements, where we had the lowest values in areas where the fire was 2 years ago and highest values were measured in old areas, where the fire was more than 152 years ago.

The mass loss of Scots pine litter increased significantly with the time since the last fire disturbance. The litter decomposition in old areas lost around 10% more mass than litter decomposition at recently burned areas. The differences in decomposition can be explained also with the moisture content (wet mass compared to dry mass) of litter inside the litter bag - it was much higher in older areas (fire 60 and 152 years ago) compared with younger areas (fire 2 and 40 years ago).

The measured enzymes where  $\beta$ -xylosidase (XYL), glucuronidase (GLR), cellobiohydrolase (CEL),  $\alpha$ -glucosidase (GLS), laccase (LAC), chitinase (NAG) and phosphatase (PHO). Extracellular enzyme activities varied significantly with time since fire for each enzyme type. In general, across all enzyme types we measured, fire reduced the enzymatic activity. For all measured enzymes the enzymatic activity was lowest on the areas where the fire was two years ago. Carbon targeting enzymes (XYL, GLR, CEL, GLS, LAC), nitrogen targeting (NAG) and phosphorus targeting enzymes (PHO) showed similar responses to the fire. When we summed up the enzymes that have main function in C-compound decomposition (carbon targeting enzymes - XYL, GLR, CEL, GLS, LAC) and assessed their relationship

to soil respiration, soil C content and mass loss of litter, it showed high positive correlation. With higher amount of enzymes we have higher soil respiration rates, higher mass loss rates, etc.

Our preliminary results show that forest fire has a substantial effect on the C and N pool in top soil layer, but not in the humus layer and in mineral soil layers. The values for soil respiration, litter decomposition (mass loss) and for extracellular enzyme activity were lowest straight after fire.

#### ACKNOWLEDGEMENTS

This work was supported by the Academy of Finland projects number 138575, 255576 and European Social Fund and Estonian Science Foundation “Mobilitas” grant MJD94.

#### REFERENCES

- Allison, S.D., LeBauer, D.S., Ofrecio, M.R., Reyes, R., Ta, A.-M., Tran, T.M. (2009). Low levels of nitrogen addition stimulate decomposition by boreal forest fungi. *Soil Biology and Biochemistry* 41, 293-302.
- Allison, S.D., McGuire, K.L., Treseder, K.K. (2010). Resistance of microbial and soil properties to warming treatment seven years after boreal fire. *Soil Biology and Biochemistry* 42, 1872-1878.
- Franklin, J.F., Spies, T.A., Pelt, R.V., Carey, A.B., Thornburgh, D.A., Berg, D.R., Lindenmayer, D.B., Harmon, M.E., Keeton, W.S., Shaw, D.C., Bible, K., Chen, J. (2002). Disturbances and structural development of natural forest ecosystems with silvicultural implications, using Douglas-fir forests as an example. *Forest Ecology and Management* 155, 399-423.
- Högberg, M., Högberg, P., Myrold, D. (2007). Is microbial community composition in boreal forest soils determined by pH, C-to-N ratio, the trees, or all three? *Oecologia* 150, 590-601.
- Kasischke, E.S. (2000). Boreal ecosystems in the global carbon cycle. In: Kasischke, E.S., Stocks, B.J. (Eds.), *Fire, Climate Change, and Carbon Cycling in the Boreal Forests*. Springer, New York, 461 p., pp. 19-31.
- Rietl, A.J., Jackson, C.R. (2012). Effects of the ecological restoration practices of prescribed burning and mechanical thinning on soil microbial enzyme activities and leaf litter decomposition. *Soil Biology and Biochemistry* 50, 47-57.
- Yakov, K. (2010). Priming effects: Interactions between living and dead organic matter. *Soil Biology and Biochemistry* 42, 1363-1371.

# BLACK CARBON IN GLOBAL CLIMATE MODELLING

T. KÜHN<sup>1</sup>, H. KOKKOLA<sup>2</sup>, S. ROMAkkANIEMI<sup>1</sup>, and A. LAAKSONEN<sup>1,3</sup>

<sup>1</sup> Department of Applied Physics, University of Eastern Finland, Kuopio, Finland

<sup>2</sup> Finnish Meteorological Institute, Kuopio, Finland

<sup>3</sup> Finnish Meteorological Institute, Helsinki, Finland

Keywords: black carbon, aerosol, climate, modelling.

## INTRODUCTION

Anthropogenic aerosols significantly contribute to the global radiation budget. As aerosols reflect sun light back to space (direct aerosol effect), but also increase cloud albedo (first indirect effect) and cloud lifetime (second indirect effect), this contribution is mostly negative, thereby counter-acting global warming (Forster et al., 2007). However, aerosols also have warming effects on the atmosphere like, for instance, through absorption of radiation (Ramanathan and Carmichael, 2008) and by changing snow, glacier and sea ice albedo through deposition (McConnell et al., 2007). Black carbon (BC) makes a major warming contribution to the global radiation budget, which has even been suggested to only be second to that of carbon dioxide (Jacobson, 2001; Ramanathan and Carmichael, 2008).

Among the current major global aerosol models, the estimated BC radiative forcing (RF) varies between  $0.05 \text{ W/m}^2$  and  $0.37 \text{ W/m}^2$  (Myhre et al., 2013), emphasizing the need for a better description of BC in the models.

## METHODS

In this study we use the general circulation model ECHAM6 (Roeckner et al., 2003; Roeckner et al., 2006) which is extended by the microphysical aerosol model HAM2 (Stier et al., 2005). Within HAM2, aerosol distributions can either be represented by a superposition of seven log-normal modes (Vignati et al., 2004) or using the fairly recently developed sectional model SALSA (Bergman et al., 2012). In SALSA the width of the size bins and the internal mixing vary with the particle size, thereby lifting the limitations introduced by modal models without introducing too much additional computational cost.

In general, the computed RF caused by anthropogenic BC, varies considerably between currently employed aerosol models, with results produced by ECHAM5, the predecessor of the model used here, agreeing well with average results. The origin of this spread among models is manifold, including differences in BC vertical distributions, optical properties, and deposition and in the treatment of clouds (Samset et al., 2013).

As part of the ACRONYM project (Aerosols and Climate: reduction of the uncertainty of the models), this study aims to optimize the realization of SALSA for ECHAM6 with emphasis on developing a more reliable treatment of BC in the atmosphere. Measurement data for model evaluation and for characterization of the global distribution of BC is taken from (AeroNet) and (Calipso).

## CONCLUSIONS

Black carbon (BC) is one of the main contributors to anthropogenic global warming. Due to big differences in the treatment of BC in global aerosol models, the uncertainty in the estimated radiative forcing it produces are large. This work in progress aims to refine the treatment of BC in ECHAM6 with careful evaluation against measured data.

## ACKNOWLEDGEMENTS

The research is supported by the strategic funding of the University of Eastern Finland, the Academy of Finland Center of Excellence (project no. 1118615), and the Finnish Center for Scientific Computing (project no. uel1593).

## REFERENCES

- Bergman, T., Kerminen, V.-M., Korhonen, H., Lehtinen, K. J., Makkonen, R., Arola, A., Mielonen, T., Romakkaniemi, S., Kulmala, M., and Kokkola, H. (2012). Evaluation of the sectional aerosol microphysics module salsa implementation in echam5-ham aerosol-climate model. *Geoscientific Model Development*, 5(3):845–868.
- Forster, P., Ramaswamy, V., Artaxo, P., Berntsen, T., Betts, R., Fahey, D. W., Haywood, J., Lean, J., Lowe, D. C., Myhre, G., Nganga, J., Prinn, R., Raga, G., Schulz, M., , and Van Dorland, R. (2007). *Changes in Atmospheric Constituents and in Radiative Forcing, In: Climate Change 2007: The Physical Science Basis. Contribution of Working Group I to the Fourth Assessment Report of the Intergovernmental Panel on Climate Change*. Cambridge Univ. Press, Cambridge, United Kingdom and New York, NY, USA.
- Jacobson, M. Z. (2001). Strong radiative heating due to the mixing state of black carbon in atmospheric aerosols. *Nature*, 409(6821):695–697.
- McConnell, J. R., Edwards, R., Kok, G. L., Flanner, M. G., Zender, C. S., Saltzman, E. S., Banta, J. R., Pasteris, D. R., Carter, M. M., and Kahl, J. D. (2007). 20th-century industrial black carbon emissions altered arctic climate forcing. *Science*, 317(5843):1381–1384.
- Myhre, G., Samset, B. H., Schulz, M., Balkanski, Y., Bauer, S., Berntsen, T. K., Bian, H., Bellouin, N., Chin, M., Diehl, T., Easter, R. C., Feichter, J., Ghan, S. J., Hauglustaine, D., Iversen, T., Kinne, S., Kirkevåg, A., Lamarque, J.-F., Lin, G., Liu, X., Lund, M. T., Luo, G., Ma, X., van Noije, T., Penner, J. E., Rasch, P. J., Ruiz, A., Seland, Ø., Skeie, R. B., Stier, P., Takemura, T., Tsigaridis, K., Wang, P., Wang, Z., Xu, L., Yu, H., Yu, F., Yoon, J.-H., Zhang, K., Zhang, H., and Zhou, C. (2013). Radiative forcing of the direct aerosol effect from aerocom phase ii simulations. *Atmospheric Chemistry and Physics*, 13(4):1853–1877.
- Ramanathan, V. and Carmichael, G. (2008). Global and regional climate changes due to black carbon. *Nature geoscience*, 1(4):221–227.
- Roeckner, E., Baeuml, G., Bonventura, L., Brokopf, R., Esch, M., Giorgetta, M., Hagemann, S., Kirchner, I., Kornblueh, L., Manzini, E., Rhodin, A., Schlese, U., Schulzweida, U., and A., T. (2003). The atmospheric general circulation model echam5, part i: Model description. *Report 349, Max Planck Institute for Meteorology, Hamburg, Germany*.
- Roeckner, E., Brokopf, R., Esch, M., Giorgetta, M., Hagemann, S., Koernblueh, L., Manzini, E., Schlese, U., and Schulzweida, U. (2006). Sensitivity of simulated climate to horizontal and vertical resolution in the echam5 atmosphere model. *J. Climate*, (19):3771–3791.

- Samset, B. H., Myhre, G., Schulz, M., Balkanski, Y., Bauer, S., Berntsen, T. K., Bian, H., Bellouin, N., Diehl, T., Easter, R. C., Ghan, S. J., Iversen, T., Kinne, S., Kirkevåg, A., Lamarque, J.-F., Lin, G., Liu, X., Penner, J. E., Seland, Ø., Skeie, R. B., Stier, P., Takemura, T., Tsigaridis, K., and Zhang, K. (2013). Black carbon vertical profiles strongly affect its radiative forcing uncertainty. *Atmos. Chem. Phys.*, 13(5):2423–2434.
- Stier, P., Feichter, J., Kinne, S., Kloster, S., Vignati, E., Wilson, J., Ganzeveld, L., Tegen, I., Werner, M., Balkanski, Y., Schulz, M., Boucher, O., Minikin, A., , and Petzold, A. (2005). The aerosolclimate model echam5-ham. *Atmos. Chem. Phys.*, 5:1125 –1156.
- Vignati, E., Wilson, J., and Stier, P. (2004). M7: An efficient size-resolved aerosol microphysics module for large-scale aerosol transport models. *Journal of Geophysical Research: Atmospheres (1984–2012)*, 109(D22).
- Cloud-Aerosol Lidar and Infrared Pathfinder Satellite Observations (Calipso), see [http://aeronet.gsfc.nasa.gov/new\\_web/index.html](http://aeronet.gsfc.nasa.gov/new_web/index.html).
- Aerosol Robotic Network (AeroNet), see [https://eosweb.larc.nasa.gov/project/calipso/calipso\\_table](https://eosweb.larc.nasa.gov/project/calipso/calipso_table).

# PHYSIOLOGICAL GROWTH MODEL CASSIA PREDICTS CARBON ALLOCATION AND WOOD FORMATION OF SCOTS PINE

L. KULMALA<sup>1</sup>, P. SCHIESTL-AALTO<sup>2</sup>, H. MÄKINEN<sup>1</sup>, A. MÄKELÄ<sup>2</sup>

<sup>1</sup>Finnish Forest Research Institute, P.O.Box 18, 01301 Vantaa, Finland

<sup>2</sup>Department of Forest Sciences, University of Helsinki, Finland

Keywords: dynamic modelling, *Pinus sylvestris* L, sink-source interaction

## INTRODUCTION

The conifer trees of the Boreal forests regulate and control their biological activity, such as growth, due to the annual changes in the environment. In the boreal region, especially temperature is in a key role in the annual cycle of Scots pine (*Pinus sylvestris* L.). In spring, the increase in temperature precedes the recovery of photosynthesis (Hänninen & Hari, 2002) as well as the beginning of growth (Rossi *et al.* 2008).

Photosynthesis is the source of carbon compounds that are used for the vital functions and accumulation of biomass. The source and sinks of carbon vary independently and thus, there is not a clear relationship between the photosynthesis and growth (Promnitz, 1975). The carbon storages play a key role in balancing the under- and oversupply of carbon. The storages are usually starch and short chain sugars, such as fructose and glucose (Kibe & Masuzawa, 1992; Fischer & Höll, 1991).

Most of the process-based growth models can be divided into two classes: sink- and source-driven approaches. In the source-driven models, the photosynthetic production is usually allocated according to the fixed share to the vital functions and the different growing sections. In the sink-driven models, the allocation of sugars is determined by the sink strength. In reality, the growth varies from sink-driven to source-driven depending on the environmental circumstances and phase of annual cycle. The availability of carbon, on the other hand, affects the emergence of sinks (Sievänen *et al.* 2000).

We aim to study the sink-source relationship using a novel dynamic model called Carbon Allocation Sink-Source Interaction Analysis (CASSIA). The model uses thermal time, i.e. the accumulation of temperature (temperature sum), as proxy for the tree's internal phase of annual cycle. The sink strength due to growth follows the thermal time and prevailing temperature. The photosynthetic production and carbon storages of the tree determine whether the sink demand can be fulfilled or not.

## THE MODEL

In the model, the state variables are the storages of short chain sugars (labile sugars such as sucrose), long chain sugars (starch), and the biomasses of needles, primary and secondary wood and fine roots (Fig. 1). The cambial growth is further divided to enlarging, wall forming and mature tracheids. The model works during the growing season on a daily time step.

The daily change in the pool of sugars ( $dS/dt$ , g C day<sup>-1</sup>), without the exchange between sucrose and starch storages, depends on photosynthesis,  $P(t)$ , and maintenance respiration,  $R^M(t)$ , growth,  $G^{tot}(t)$ , and growth respiration,  $R^G(t)$ :

$$\frac{dW}{dt} = P(t) - R^M(t) - G(t) - R^G(t), \quad (1)$$

The photosynthesis,  $P(t)$ , is derived from the Eddy Covariance measurements (Vesala *et al.* 2005; Kolari *et al.* 2009). The maintenance respiration,  $R^M(t)$ , is set to depend on biomass and ambient temperature that is the air temperature for the aboveground parts and soil temperature for the roots. The empirical temperature dependence of each tree part is obtained from the measurements at the SMEAR II station. The growth respiration,  $R^G(t)$ , is linearly dependent on growth according to Running and Coughlan (1988).

The potential growth, i.e., the growth sink, is based on the environment of the tree. The most influential environmental factor for the above-ground growth is the air temperature whereas soil temperature and moisture determine the potential growth of roots. The potential growth follows the annual cycle of thermal time, which is calculated as an accumulation of a sigmoid function of daily mean temperature (Hänninen, 1990; Hänninen & Kramer, 2007). The active growth period begins and ends when the thermal time reaches certain threshold values. The rate of growth proceeds with the thermal time as a sine function for shoots, needles and roots, whereas the cambial growth follows a square root function of the thermal time.

The potential growth is achieved when carbon is not a limiting factor, i.e., the sink strengths of different tree parts regulate their growth. If photosynthetic input exceeds the sinks, the sugars are converted and stored as starch. If the carbon bound in photosynthesis is insufficient for entirely covering the sink needs, the carbon storages are used to supplement the growth. If the carbon storage is low, the growth becomes source-limited and it is lower than the potential growth.

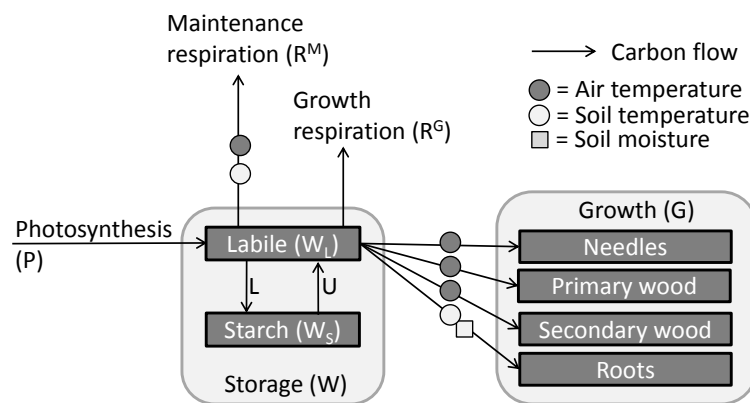


Figure 1. A schematic presentation of the model. The photosynthesis is the source of carbon whereas the growth and respiration act as carbon sinks. The arrows represent carbon flows and the circles and squares stand for the effects of environmental factors.

## MEASUREMENTS

The shoot lengths were measured using a calliper three to five times a week from the beginning of May in the years 2002–2009 and thereafter from photograph images. The branch closest to the crown apex and at three to four heights along the crown were chosen. The growth of one needle of each measured shoot was measured in the same manner as the shoot growth. The tracheid formation in the stem was measured from the microcores taken from four trees twice a week in spring and early summer, and once a week in late summer and autumn in the years 2007–2010. The measurements are explained in detail in Kulmala *et al.* (2013, this proceeding).

We estimated the model parameters separately for the shoots, needles and stem, assuming that the source did not limit the growth. The parameters for shoot growth were estimated using the daily averages of the measured shoot lengths in 2008. The parameters for the needle length increment and tracheid formation were estimated using the data of the year 2009.

The annual variation in ring width was determined from the increment cores taken at breast height from 14 Scots pines with breast height diameter between 19 and 25 cm in May 2012. The annual height increment was measured as an average of two felled sample trees.

## RESULTS

Early in the growing season, the increase in photosynthesis also increased the carbon storages before the acceleration of respiration and growth (Figure 2A). In the late season, the carbon storages increased again because the photosynthesis continued after the cessation of growth (Figure 2B).

The onset of shoot elongation took place between the end of April and late May. Thereafter, the needle, root and diameter growth started approximately at the same time. The growth of needles was the first one to be completed, whereas the secondary cell wall formation and lignification of tracheids in the stem was the last one to cease in the late autumn.

Using the parameters estimated from the measurements of one year, the model succeeded in predicting the intra-annual phases of needle growth in different years (Fig. 3). The daily needle growth was slow in the beginning and the end of the growing season, as well as during the cold spells. The model also managed to predict the intra-annual course of the shoot and stem growth.

The model predicted large inter-annual differences in the final length of needles, whereas differences in the predicted shoot length and the widths of the annual rings were small (Fig. 4). The measured annual variations in the needle length were similar with the predicted ones, except for the rainy and cold year 2008 (Fig. 4A). The predicted annual variations of the shoot length growth coincided with the measured shoot increment (Fig. 4C), especially after a thinning in 2002, but the magnitude of the annual variation was lower (8% vs. 41% in the predicted and measured increments, respectively). The simulated annual ring width was thinner and more stable than measured from the core samples (Fig. 4B).

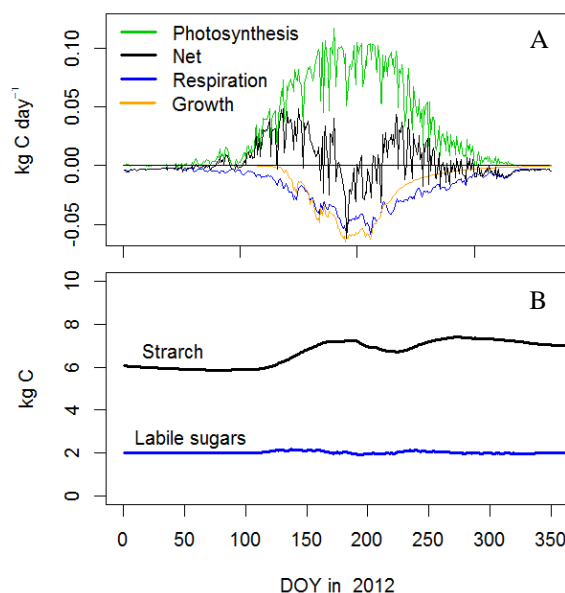


Figure 2. (A) The daily rates of photosynthesis, respiration and growth ( $\text{kg C}$ ) per tree and the net carbon balance, (B) the daily pool of carbon storages of a tree in the year 2012. In the upper panel, positive values mean carbon gain whereas negative values indicate carbon losses.

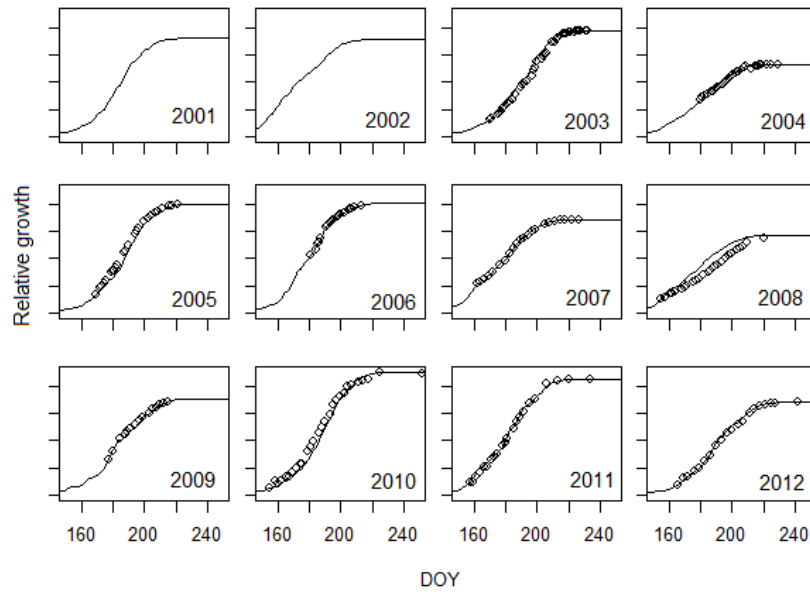


Figure 3. Averages of predicted (line) and measured (dots) needle growth in the years 2001–2012. The yearly simulation is scaled to the measurements using first and last measurement.

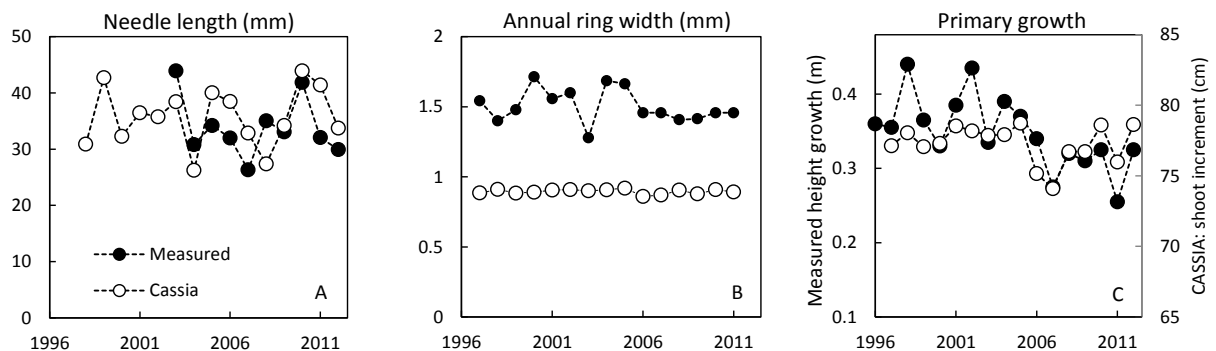


Figure 4. (A) Measured and predicted annual final needle length, (B) measured and predicted annual ring width and (C) measured height increment together with predicted mean shoot increment during 1997–2012.

## CONCLUSIONS

The model using the thermal time as proxy for the internal stage of the tree, prevailing temperature and the carbon balance of the tree succeeded in predicting the intra-annual growth dynamics and the inter-annual changes in needle and height growth. In the future, we will develop the model by refining the description of uptake, allocation and transport processes of sugars and water within a tree to improve understanding about stress responses, especially the effects of prolonged drought on tree growth.

## ACKNOWLEDGEMENTS

We acknowledge Kourosh Kabiri for the annual height increments and Janne Levula for the annual ring width data. We thank Juho Aalto and Janne Korhonen for the help in needle and shoot length

measurements. Pasi Kolari is acknowledged for the analysis of Eddy Covariance data. The financial support by the Academy of Finland Centre of Excellence program (project no 1118615) and project ‘Multi-scale modelling of tree growth, forest ecosystems, and their environmental control’ (257641) are gratefully acknowledged.

## REFERENCES

- Fischer C, Höll W (1992) Food reserves of scots pine (*Pinus sylvestris* L.) II. Seasonal changes and radial distribution of carbohydrate and fat reserves in pine wood. *Trees* **6**: 147-155
- Hänninen H, Hari P. (2002) Recovery of photosynthesis of boreal conifers during spring: A comparison of two models. *Forest Ecology and Management* **169**: 53-64
- Hänninen H, Kramer K. (2007) A framework for modelling the annual cycle of trees in boreal and temperate regions. *Silva fennica* **41**: 167-205
- Hänninen H. (1990) Modeling dormancy release in trees from cool and temperate regions. In: Dixon, R.K., Meldahl, R.S., Ruark, G.A. & Warren, W.G. (eds.). Process modeling of forest growth responses to environmental stress. Timber Press, Portland p. 159-165
- Kibe T, Masuzawa T (1992) Seasonal changes in the amount of carbohydrates and photosynthetic activity of *Pinus pumila* Regel on alpine in central Japan. *Proceedings of the NIPR Symposium on Polar Biology* **5**: 118-124
- Kolari P, Kulmala L, Pumpanen J, Launiainen S, Ilvesniemi H, Hari P, Nikinmaa E (2009) CO<sub>2</sub> exchange and component CO<sub>2</sub> fluxes of a boreal Scots pine forest. *Boreal Environment Research* **14**: 761–783.
- Kulmala, L, Aalto, J, Helmisääri, H-S., Kabiri, K, Kolari, P, Korhonen JFJ, Levula, J, Leppälampi-Kujansuu, J, Mäkinen, H, Schiestl-Aalto, P, Hari, P, Bäck, J, Mäkelä, A, Nikinmaa, E (2013) Tree growth measurements at SMEAR II. *This proceedings*.
- Promnitz LC (1975) A photosynthate allocation model for tree growth. *Photosynthetica* **9**: 1-15
- Rossi S, Deslauriers A, Gricar J, Seo J-W, Rathgeber C, Anfodillo T, Morin H, Levanic T, Oven P, Jalkanen R (2008) Critical temperatures for xylogenesis in conifers of cold climates. *Global Ecology and Biogeography* **17**: 696-707
- Running SW, Coughlan JC. (1988) A general model of forest ecosystem processes for regional applications I. Hydrologic balance, canopy gas exchange and primary production processes. *Ecological Modelling* **42**: 125-154
- Sievänen R, Nikinmaa E, Nygren P, Ozier-Lafontaine H, Pettunen J, Hakula H (2000) Components of functional-structural tree models. *Annals of Forest Science* **57**: 399-412
- Vesala T, Suni T, Rannik Ü, Keronen P, Markkanen T, and co-authors (2005) Effect of thinning on surface fluxes in a boreal forest. *Global Biogeochem. Cycles* **19**, GB2001, doi:10.1029/2004GB002316

## TREE GROWTH MEASUREMENTS AT SMEAR II

L. KULMALA<sup>1</sup>, J. AALTO<sup>2</sup>, H.-S. HELMISAARI<sup>2</sup>, K. KABIRI<sup>2</sup>, P. KOLARI<sup>2,3</sup>, J.F.J. KORHONEN<sup>3</sup>, J. LEVULA<sup>3</sup>, J. LEPPÄLAMMI-KUJANSUU<sup>2</sup>, H. MÄKINEN<sup>1</sup>, P. SCHIESTL-AALTO<sup>2</sup>, P. HARI<sup>2</sup>, J. BÄCK<sup>2</sup>, A.MÄKELÄ<sup>2</sup>, E.NIKINMAA<sup>2</sup>

<sup>1</sup>Finnish Forest Research Institute, P.O. Box 18, 01301 Vantaa, Finland

<sup>2</sup>Department of Forest Sciences, University of Helsinki, Finland

<sup>3</sup>Department of Physics, University of Helsinki, Finland

Keywords: microcores, minirhizotrones, *Pinus sylvestris* L, biomass sampling

### INTRODUCTION

The gross primary production (GPP) of a stand varies yearly depending on the weather conditions during the growing season. However, net primary production (NPP) i.e. the tree growth, that is more closely linked to long term carbon storage, does not necessarily directly follow the variation in GPP. At SMEARII, we have measured the intra-annual shoot length, needle and root growth and tracheid formation in stems during several growing seasons and inter-annual variation in annual ring width and tree height increment. Here, we introduce the numerous measurements and show preliminary results on the growth variation together with GPP to illustrate the annual variation in carbon allocation.

### MEASUREMENTS

#### 1) Manual intra-annual measurements of shoot and needle length

We measured the shoot length manually during the years 2002–2009. Measured trees, the number of shoots, the position in the crown and the predominant compass direction varied slightly from year to year but, in principle, the branches closest to the stem apex and at three to four heights along the crown were evenly chosen from three to five trees. The branches were in the same compass direction in a tree but the direction varied between the trees, depending on the access from the measurement tower. From these branches, the length of the terminal shoot of the main axis, as well as the length of one side branch, were measured using a calliper or a ruler. The shoot length was measured three to five times a week from the beginning of May. Schiestl-Aalto *et al.* (2013) presented a detailed description of the measurements and results on the growth differences between a crown position and different years.

The length growth of one needle of each measured shoot was measured in the same manner as the shoot growth. The needles were selected systematically in different positions of a shoot (0%, 25%, 50%, 75% and 100% of the length of the shoot). The direction of the needles in a shoot was random.

#### 2) Photographs for the determination of intra-annual shoot and needle length

Since 2010, the shoot and needle length have been measured with the help of digital photographs (Fig. 1) taken at a distance of at least two meters. The photographs have been taken so that the growing shoot fills the picture; in this composition the 35-mm equivalent focal length is close to or higher than 200 mm; together with the minimum distance of 2 meters this substantially reduces the distortion-originated errors in photographs. The elongation has been determined using the ImageAnalyzer software. Theoretical accuracy of the measurement method is 0.065 mm and practical repeatability is less than 1 mm. The number of the monitored shoots has annually varied from 6 to 12 and they have grown in three heights: in the highest, middle and lowest parts of the crown.

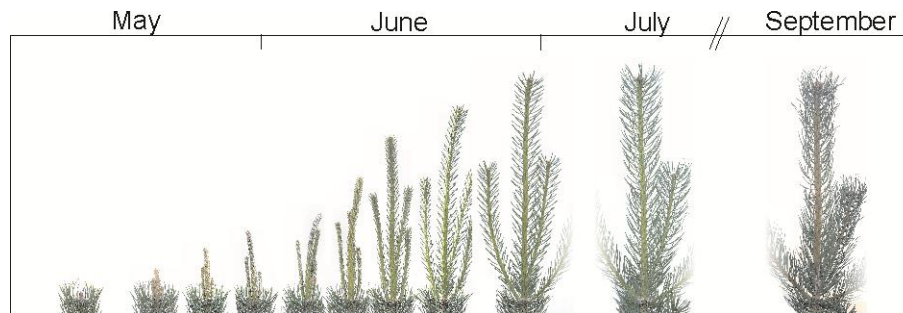


Figure 1: Samples of shoot images during a growing season. Redrawn from Hari *et al.* (2013).

### 3) Microcore samples of intra-annual wood formation

The phases of tracheid formation in the stem were monitored throughout the growing season by repeatedly collecting microcores at breast height. In years the 2007–2012, microcores were taken from four randomly selected dominant trees twice a week in spring and early summer, and once a week in late summer and autumn. The first samples are taken between early April and mid-May and the sampling continued to mid-September. In 2007, microcores were collected with medical cannulas ( $2.0 \times 50$  mm). In 2008–2012, microcores were extracted using a tool designed for microcoring (Rossi *et al.* 2006). After the rough outer bark was removed, the tool was inserted about 15 mm into the stem. Three parallel microcores were extracted in a zigzag pattern from each sample tree. From the images taken of the current-annual ring samples, the number and diameters of tracheids in different cell formation phases were measured along one representative cell row in each microcore (Figure 2). The details of the sampling and the laboratory analyses are described by Kalliokoski *et al.* (2012).

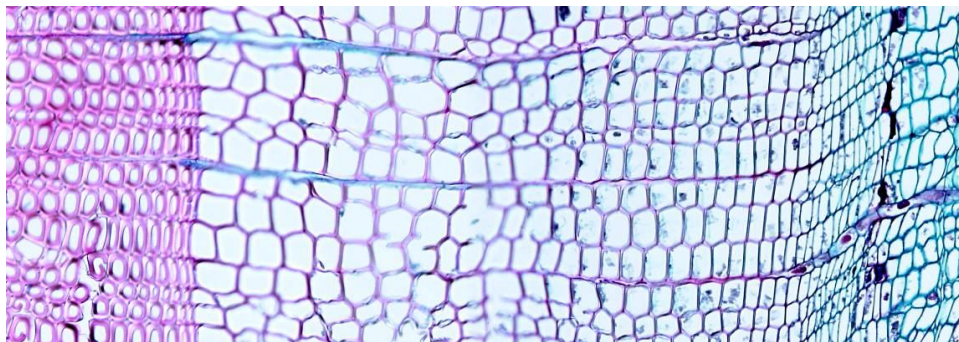


Figure 2: An image of a microcore sample. The latewood cells of the previous annual ring on the left, mature, cell wall thickening and enlarging tracheids in the middle, and cambium and phloem on the right.

### 4) Simultaneous xylem and stem diameter measurements

Simultaneous xylem and stem diameter measurements have been conducted since 2003. The diameter variation measurement system consists of two pen-like diameter variation sensors (LVDT; Solartron AX/5.0/S, Solartron Inc., West Sussex, UK) attached next to each other to a rectangular metal frame mounted around the stem. In addition, we have measured the temperature of the stem (1 cm depth) and the metal frame using copper–constantan thermocouples and corrected the data for the effects of thermal expansion of wood and the frame (see Sevanto *et al.* 2005). The data have been collected with frequency  $\text{min}^{-1}$ . The inner bark diameter change was simply calculated to be the whole stem diameter change (excluding the bark) minus the xylem diameter change.

The high frequency diameter variation includes reversible changes driven by variation in the stem water potential and irreversible growth. Water potential changes follow a diurnal pattern due to transpiration and both diurnal and more long-term variation in the osmotic concentration of the living cells. The diurnal variation of water potential can be cleared from the bark thickness changes using the xylem measurements

that reflect the transpiration related changes only (Mencuccini *et al.* 2013). This way modelled bark thickness variation reflects the thickness growth and long term osmotic changes in the bark where the former dominates. This allows us to get the daily values of thickness growth that has not been previously possible due to large variation in the stem hydraulics (Chan *et al*, manuscript).

#### 5) *Intra-annual fine root growth and turnover rate*

Fine-root growth and longevity at the site is studied with minirhizotrones (MR). Five transparent acrylic tubes were installed vertically in the soil of the three replicate plots in June 2011. A 20 cm long section of the tubes extends above the soil surface, and this part was painted first black (to inhibit light) and then white (to protect against possible warming by sunlight) before installation.

The first image collection took place in September 2011, and is still going on in 2013, at eight weeks intervals during the growing seasons. Images are taken on two sides of each tube as a continuous image column with an MR camera (Bartz Technology Inc., CA). Due to the high stoniness of the site, we use MR –tubes of two different lengths, and thus the length of the image column varies between the tubes (12-27.5 cm).

Later on, the length and mean diameter of each fine root born during the study period will be analyzed by manual tracing on the digital images using the image analysis software (WinRHIZO Tron MF, Regent, Quebec, Canada). The date when a root is first observed and the date of its death or disappearance will be recorded separately for tree and understory fine roots. The data files produced by WinRhizo Tron are in ASCII text format, which are converted into Excel format, each column having a defined file.

The median longevity of the fine roots will be estimated by a parametric regression model with Weibull error distribution using the SurvReg function in the R program (R 2.13.0).

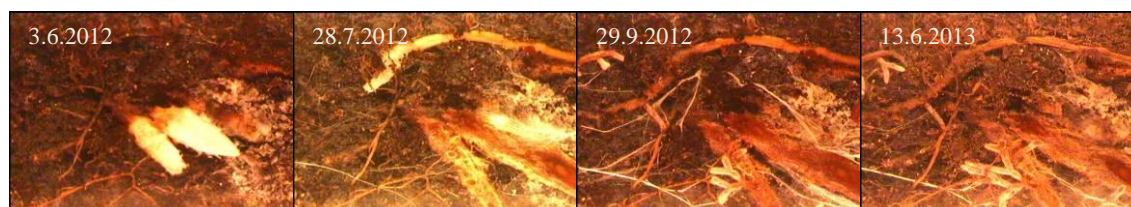


Figure 3: Example images (image size 1.1 x 2.0 mm) of fine roots during one year. Scots pine dicotomous mycorrhizal short roots are visible in the two last images next to decomposing understorey roots which grew in June 2012 but had already died and were decomposing in the July image. Thin white threads are mycorrhizal hyphae rhizomorphs, most abundant in the September image.

#### 6) *Inter-annual variation in tree ring width*

In 2012, we measured the annual variation in ring width during the years 1981–2011 from increment cores taken at breast height. The annual ring widths of each tree core were determined in the laboratory, using an Addo tree ring analyser (Parker Instruments).

In 2007, we fell 12 Scots pines with ages from 41 to 57 years. Half of the trees grew on thinned area and half on unthinned area. From these trees, the height and crown area together with the annual ring widths were measured on discs taken at the heights of stump, breast height, crown base, 0.2% of height and 0.33% and 0.66% of crown height. The collected sample disks were stored in a freezer before further analysis at Finnish Forest Research Institute.

### 7) *Biomass measurement and sampling*

Currently, we are measuring five Scots pines from five size classes in detail. From these trees, annual height growth, crown length and diameter at crown base are measured after felling the tree. One disc from the inter-whorl is also taken for the measurement of the ring widths development and stem analysis including measurement of the sapwood and heartwood proportion for each disc. The time series of the annual length growths of all branches in each whorl are measured as well as the sapwood area at the branch base. For each branch, its orientation, the branch angle with the main stem (in 5° intervals) and the vertical and horizontal projection of the branch tip are measured in the field. After cutting the branches the needle and wood biomass for each branch are measured. In addition, for one branch from each whorl the needle biomass of all needle age-classes is separated and measured to determine their proportion. Fresh needle samples are also taken from the branch tips of the current year growth to determine the specific leaf mass and leaf area index for the stand. The measurements will be finished in the spring 2014.

### *Gross primary production*

The ecosystem CO<sub>2</sub> net exchange was measured with a closed-path eddy-covariance measuring system. The anemometer and the sample air intake were installed above the stand at a height of 23 m. The net exchange was corrected for half-hourly changes in the CO<sub>2</sub> storage below the measuring height. The net exchange was partitioned into gross primary production (GPP) and ecosystem respiration, which was modelled using an exponential equation with soil temperature as the explanatory factor. The instrumentation is documented in detail in Vesala *et al.* (2005) and the data processing in Kolari *et al.* (2009).

### *Data-analysis*

Annual averages were calculated for the final length of the needles and shoots. We also present the annual height growth from two trees. The average tree ring widths were calculated from the core samples of trees that had breast height diameter between 19 and 25 cm.

## RESULTS

Even if some similarities existed, the different tree parts (shoots, needles, height and diameter) did not have similar year-to-year growth pattern during 1997–2012 (Figure 4A). The relative shoot and needle growth greatly varied while the radial growth (annual ring width) was the most stable one, especially after 2005. The height and diameter growth showed slowly decreasing trends due to the maturing of the stand.

The year-to-year growth changes did not coincide with the changes in the mean air temperature or GPP (Figure 4B). Nevertheless, the growth contained some interesting periods compared with these changes in the environment between the years 1997 and 2012:

- 1) 2002–2003. Summer 2002 was very warm with a local peak in GPP whereas the temperature and GPP were clearly lower in following summer 2003. The diameter and height growth followed the same pattern with the temperature and GPP whereas the shoot and needle growth were the all-time highest in 2003.
- 2) 2006–2007. Summer 2006 was warm but the prolonged drought in the mid and late summer decreased annual GPP. In 2006, the annual ring width had a local minimum with more or less average height, shoot and needle growth. The latter ones were, however, close to the smallest record in 2007, while the radial growth slightly increased.
- 3) 2008–2010. Year 2008 was cold and rainy, whereas the year 2010 was warm and dry. Year 2009 had temperature in between resulting in a high annual GPP. These differences in temperature and GPP, however, did not cause major differences in the relative radial and height growth, whereas the needle and shoot length growth were similar in 2008 and 2009. In 2010, however, the needle growth was almost at maximum whereas the shoot growth was the all-time minimum.

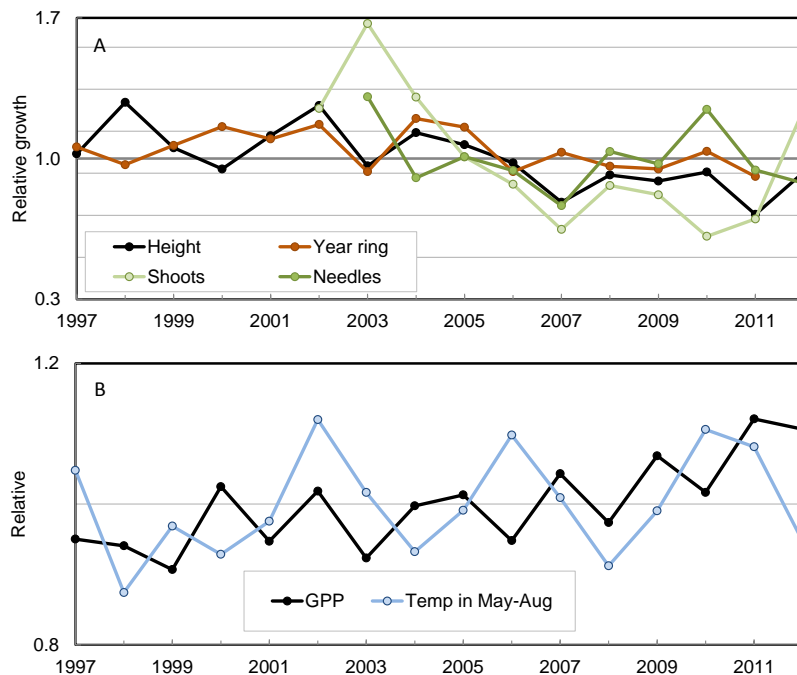


Figure 4. Year-to-year changes in (A) relative height increment, maximum shoot and average needle length, and annual ring width and in (B) annual GPP and mean air temperature in May-August at SMEAR II station in 1997–2012. The values below and above one indicate lower and higher growth than the average during the study period.

## DISCUSSION AND CONCLUSIONS

Various types of data are required for coherent analysis and understanding of environment – tree growth interaction processes. The versatile measurements at SMEAR II open a new possibility to combine different metabolic phenomena in forest ecosystems. The good-quality measurements of the intra-annual growth dynamics of shoots and needles exist for over 10 years, in addition to intra-annual wood formation and root growth during several years.

The results illustrated that the different tree parts (needles, roots, primary and secondary wood) have their own growing periods. The averages of temperature and GPP calculated over the entire growing season were not closely related to the annual growth variation and there was a different timing of responses in different tree parts to environment. Secondary growth is tightly linked to tree water and carbon status as water pressure is needed to expand the growing cells (Hölttä *et al.* 2010) and it is no surprising that the diameter growth was the closest in following GPP. On the other hand, we have observed that new shoot extension growth depends on the previous year's growing conditions (Schiestl-Aalto *et al.* 2013) and thus there is a time lag between GPP and shoot growth.

In the future studies, we will quantify the relationship between the intra-annual climatic variation and tree growth in detail. These studies are interesting as they will help us to understand the causal variation between weather and tree growth. This type of understanding is crucial in predicting how forests will react to the changing climate as opposing trends will follow. On one hand, the average growing conditions will improve which will enhance the growth but on the other hand, extreme drought years will become more severe and more frequent. Now the overall forest growth depends on how long the carry-over effects of extreme years last and are they strong enough to decrease the growth enhancement of milder average climate. At the moment, the growth measurements are used to study the role of carbon and water balance in the allocation of photosynthates using the CASSIA model (Kulmala *et al.* 2013, this proceeding) but the

growth studies are also linked to our other observations of transport and metabolism in trees also to understand the impact of varying weather on other aspects of metabolism, such as VOC-production.

## ACKNOWLEDGEMENTS

The financial support by the Academy of Finland Centre of Excellence program (project no 1118615) and projects 'Multi-scale modelling of tree growth, forest ecosystems, and their environmental control' (257641) and 'Decadal climate prediction in adaptation to climate change' (140781) are gratefully acknowledged.

## REFERENCES

- Chan T, Hölttä T, Berninger F, Nikinmaa E (manuscript). Removing hydraulic influences reveals daily variation of cambial growth.
- Hari P, Heliövaara K, Kulmala L (eds.) (2013) Physical and Physiological Forest Ecology. Springer Science+Business Media. 534 p.
- Hölttä T, Mäkinen H, Nöjd P, Kolari P, Mäkelä A & E. Nikinmaa (2010) A Physiological model of softwood cambial growth. *Tree Physiology* **10**: 1235-1252.
- Kalliokoski T, Reza M, Jyske T, Mäkinen H, Nöjd P (2012) Intra-annual tracheid formation of Norway spruce provenances in southern Finland. *Trees: Structure and Function*. **26**: 543-555.
- Kolari P, Kulmala L, Pumpanen J, Launiainen S, Ilvesniemi H, Hari P, Nikinmaa E (2009) CO<sub>2</sub> exchange and component CO<sub>2</sub> fluxes of a boreal Scots pine forest. *Boreal Environment Research* **14**: 761–783.
- Kulmala, L, Schiestl-Aalto, P, Mäkinen H, Mäkelä, A (2013) Physiological growth model CASSIA predicts carbon allocation and wood formation of Scots pine. *This Proceedings*.
- Mencuccini M, Hölttä T, Sevanto S, Nikinmaa, E (2013). Concurrent measurements of change in the bark and xylem diameters of trees reveal a phloem-generated turgor signal. *New Phytologist* **198**: 1143-1154.
- Rossi S, Anfodillo T, Menardi R (2006) Trephor: a new tool for sampling microcores from tree stems. *IWA J* **27**: 89–97
- Schiestl-Aalto P, Nikinmaa E, Mäkelä A (2013) Duration of shoot elongation in Scots pine varies within the crown and between years. *Annals of Botany*
- Vesala T, Suni T, Rannik Ü, Keronen P, Markkanen T, Sevanto S, Grönholm T, Smolander S, Kulmala M, Ilvesniemi H, Ojansuu R, Uotila A, Levula J, Mäkelä A, Pumpanen J, Kolari P, Kulmala L, Altimir N, Berninger F, Nikinmaa E, Hari P (2005) Effect of thinning on surface fluxes in a boreal forest. *Global Biogeochem. Cycles* **19**, GB2001, doi:10.1029/2004GB002316

# ASSESSING THE VALIDITY OF THE NUCLEATION THEOREM FOR MEASURED DATA

O. KUPIAINEN-MÄÄTTÄ<sup>1</sup>, T. OLENIUS<sup>1</sup> and H. VEHKAMÄKI<sup>1</sup>

<sup>1</sup> University of Helsinki, Department of Physics, Division of Atmospheric Sciences P.O. Box 64, FI-00014 Helsinki, Finland

Keywords: Nucleation theorem, molecular clusters, modeling, data analysis.

## INTRODUCTION

Numerous field studies have shown a link between atmospheric new-particle formation and the gas-phase sulfuric acid concentration. More specifically, most studies report a dependence of the functional form  $J \propto [\text{H}_2\text{SO}_4]^2$  (Kuang *et al.*, 2008). On the other hand, recent laboratory experiments studying sulfuric acid nucleation have yielded power law dependencies  $J \propto [\text{H}_2\text{SO}_4]^x$  with the exponent  $x$  ranging from 1.3 to 8 (Zollner *et al.*, 2012). Also the value of the new-particle formation rate has varied by several orders of magnitude between field measurements and laboratory experiments, as well as between laboratory experiments using a different setup.

Nucleation measurements are often interpreted using the nucleation theorem

$$\left( \frac{\partial \log J}{\partial \log C_i} \right)_{C_{j \neq i}} = n_i^* + \delta_i,$$

where  $J$  is the nucleation rate,  $C_i$  are precursor vapor concentrations,  $n_i^*$  is the number of molecules of type  $i$  in the critical cluster, and  $\delta_i$  is a small correction term. The nucleation theorem is derived using the following assumptions: 1) the  $\Delta G$  surface has one energy barrier located at the critical cluster size, 2) there are no external losses, 3) all other conditions are kept constant while taking the derivative, and 4) the nucleation rate is determined at steady state. When these conditions are fulfilled, the nucleation rate can be used to determine the critical cluster size by fitting a line to a set of nucleation measurement data presented on a log-log scale.

## SIMULATIONS

The formation of electrically neutral sulfuric acid-dimethylamine (DMA) and sulfuric acid-ammonia clusters was simulated using the Atmospheric Cluster Dynamics Code (ACDC) (McGrath *et al.*, 2012). The cluster formation free energies used in the simulations were calculated using quantum chemistry (Ortega *et al.*, 2012; Olenius *et al.*, 2013). The derivative  $(\partial(\log J)/\partial(\log C_i))_{C_{j \neq i}}$  was computed from simulated particle formation rates, and compared to the critical cluster size determined directly from the cluster energies and cluster formation pathways.

## RESULTS

The formation free energy surface of the sulfuric acid-ammonia system has three local maxima along the cluster formation pathway:  $(\text{H}_2\text{SO}_4)_2$ ,  $(\text{H}_2\text{SO}_4)_3 \cdot \text{NH}_3$  and  $(\text{H}_2\text{SO}_4)_5 \cdot (\text{NH}_3)_3$ . The heights of these energy barriers vary with the precursor concentrations, and each of them is the critical cluster at some conditions. Accordingly, the slope of the formation rate plot changes with sulfuric acid

concentration as seen in Figure 1. The slope follows the number of sulfuric acid molecules in the critical cluster,  $n_{\text{acid}}^*$ , as predicted by the nucleation theorem, except that the discreet jumps in  $n_{\text{acid}}^*$  are smoothed out.

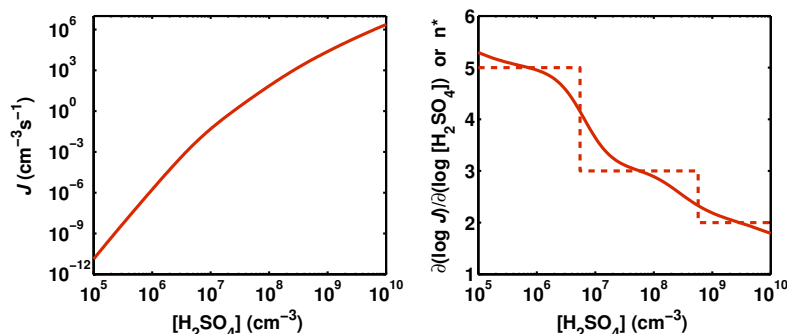


Figure 1: Left panel: Particle formation rate vs. sulfuric acid monomer concentration at  $T = 278$  K and  $[\text{NH}_3] = 10$  ppt. Right panel: Logarithmic partial derivative of the particle formation rate with respect to the sulfuric acid concentration (solid line), and the number of sulfuric acid molecules in the critical cluster (dashed line).

In the case of sulfuric acid-DMA clusters, each step of the cluster formation process is energetically favorable, and there is no critical cluster. Even the first cluster on the formation pathway,  $\text{H}_2\text{SO}_4 \cdot \text{DMA}$ , is very stable, and its concentration can be comparable to or even higher than that of the  $\text{H}_2\text{SO}_4$  monomer. As the Chemical Ionization Mass Spectrometer (CIMS) used for measuring gas-phase sulfuric acid probably also measures the  $\text{H}_2\text{SO}_4 \cdot \text{DMA}$  clusters as sulfuric acid, the measured sulfuric acid concentration does not correspond to the precursor monomer concentration appearing in the nucleation theorem. This can lead to an erroneous assignment of the critical cluster, if the total measured sulfuric acid concentration is used in place of the monomer concentration (Fig. 2).

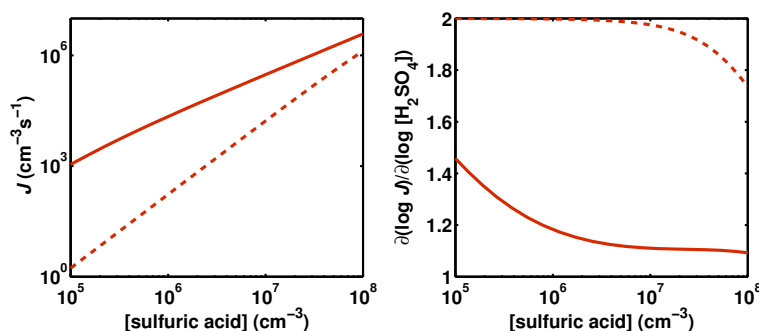


Figure 2: Left panel: Particle formation rate vs. sulfuric acid concentration, defined either as monomer concentration (solid line) or total measurable sulfuric acid concentration (dashed line), at  $T = 278$  K and  $[\text{DMA}] = 10$  ppt. Right panel: Logarithmic partial derivative of the particle formation rate with respect to the sulfuric acid monomer concentration (solid line) or the total measurable sulfuric acid concentration (dashed line).

In atmospheric new-particle formation as well as in laboratory experiments, some fraction of the clusters are lost by coagulation to larger particles or deposition to surfaces before they are large enough to be measured. The effect of external losses is strongest when the initial growth of clusters to the detection threshold is slow. If the same compounds are responsible both for formation of the

clusters and their growth to detectable sizes, the effect of loss terms on the formation rate varies with precursor concentration, and the derivative  $(\partial (\log J) / \partial (\log C_i))_{C_{j \neq i}}$  is altered by the losses.

## CONCLUSIONS

The nucleation theorem should definitely not be used if there are external losses or if the precursor monomer concentration cannot be measured, and in any case one should be careful when using it. However, having several local maxima on the formation pathway is not a major problem as long as the slope is not fitted over a very wide range of precursor concentrations.

## ACKNOWLEDGEMENTS

This work was supported by FP7-ATMNUCLE project No 227463 (ERC Advanced Grant), FP7-MOCAPAF project No 257360 (ERC Starting grant), Väisälä Foundation, Academy of Finland Center of Excellence (project No 1118615), Academy of Finland LASTU program (project No 135054), and Nordic Center of Excellence CRAICC.

## REFERENCES

- Kuang, C., P.H. McMurry, A.V. McCormick, and F.L. Eisele. (2008). Dependence of nucleation rates on sulfuric acid vapor concentration in diverse atmospheric locations. *J. Geophys. Res.*, **113**, D10209.
- McGrath, M.J., T. Olenius, I.K. Ortega, V. Loukonen, P. Paasonen, T. Kurtén, M. Kulmala, and H. Vehkamäki. (2012). Atmospheric Cluster Dynamics Code: A flexible method for solution of the birth-death equations. *Atmos. Chem. Phys.*, **12**, 2345.
- Olenius, T., O. Kupiainen-Määttä, I.K. Ortega, T. Kurtén, and H. Vehkamäki. (2013). Free energy barrier in the growth of sulfuric acid-ammonia and sulfuric acid-dimethylamine clusters. *J. Chem. Phys.*, **139**, 084312.
- Ortega, I.K., O. Kupiainen, T. Kurtén, T. Olenius, O. Wilkman, M.J. McGrath, V. Loukonen, and H. Vehkamäki. (2012). From quantum chemical formation free energies to evaporation rates. *Atmos. Chem. Phys.*, **12**, 225.
- Zollner, J.H., W.A. Glasoe, B. Panta, K.K. Carlson, P. H. McMurry, and D.R. Hanson. (2012). Sulfuric acid nucleation: Power dependencies, variation with relative humidity, and effect of bases. *Atmos. Chem. Phys.*, **12**, 4399.

# ESTIMATING THE EFFECT OF STAND AGE ON FOREST ALBEDO

N. KUUSINEN<sup>1</sup>, E. TOMPPONEN<sup>2</sup>, F. BERNINGER<sup>1</sup>

<sup>1</sup>Department of Forest Sciences, P.O. Box 27, 00014 University of Helsinki, Finland

<sup>2</sup>The Finnish Forest Research Institute, P.O. Box 18, 01301 Vantaa, Finland

Keywords: albedo, forest, remote sensing

Surface albedo is defined as the fraction of incident solar radiation reflected from the surface. Albedo of a forest stand can vary as a function of, for example, tree species, understory composition, snow cover and canopy structure. In managed even aged forests, all of these factors may change as the forest ages, as the amount of deciduous trees and the contribution of the understory on the whole stand reflectance often decreases with stand age.

We estimated the influence of stand age on forest albedo using the linear unmixing approach combined with a non-linear regression. As dependent variables, we used the MODIS (MCD43A3) composited albedos and as the predictors the forest resource estimates produced in the Finnish NFI. Exponential functions were used to describe the albedo decline as a function of forest age for coniferous species in summer and spring and for broadleaved species in winter. In addition, we estimated average albedos (independent of age) for all species and used the resulted albedo functions to predict albedo values for a test data set.

In summer and spring, the initial seedling stand albedo was always higher and the saturated albedo lower for spruce than for pine. In winter, the albedo decay as a function of forest age was rather similar for all species, although the saturated albedo of spruce was lower than that of pine or of broadleaved species. The overall range in forest albedo as a function of age was clearly higher in winter than in the snow free time. However, no difference between the seedling stand albedos could be estimated in winter. When both the species specific mean albedos as well as the albedo-age functions were applied to the test data set, we noticed that the prediction of the test data set albedos was only slightly more accurate when the albedo-age functions were used.

A clear non-linear dependency of forest albedo on stand age, saturating approximately at the time of the canopy closure, was detected. However, the main determinant of forest albedo in a heterogeneous landscape seemed to be the tree species composition. The results indicated that the tendency of the regression towards the mean somewhat smoothed the estimated albedo-age functions, and the highest and lowest forest albedos could not be predicted by the models. The spatial mismatch between the MODIS grid cells and the forest resource information used could have contributed to this.

## ACKNOWLEDGEMENTS

The study was funded by the Helsinki University Centre for Environment (HENVI) and the Center of Excellence in Physics, Chemistry, Biology and Meteorology of Atmospheric Composition and Climate Change of the Academy of Finland.

# LONG-TERM AEROSOL AND TRACE GAS MEASUREMENTS IN EASTERN LAPLAND, FINLAND: THE IMPACT OF KOLA AIR POLLUTION TO NEW PARTICLE FORMATION AND POTENTIAL CCN

E.-M. KYRÖ<sup>1</sup>, R. VÄÄNÄNEN<sup>1</sup>, V.-M. KERMINEN<sup>1</sup>, A. VIRKKULA<sup>2</sup>, A. ASMI<sup>1</sup>, T. NIEMINEN<sup>1</sup>, M. DAL MASO<sup>3</sup>, T. PETÄJÄ<sup>1</sup>, P. KERONEN<sup>1</sup>, P. P. AALTO<sup>1</sup>, I. RIIPINEN<sup>4</sup>, K. LEHTIPALLO<sup>1</sup>, P. HARI<sup>5</sup> and M. KULMALA<sup>1</sup>

<sup>1</sup> Department of Physics, University of Helsinki, Helsinki, Finland

<sup>2</sup>Department of Physics, Tampere University of Technology, Tampere, Finland

<sup>3</sup>Air Quality Research, Finnish Meteorological Institute, Helsinki, Finland

<sup>4</sup>Department of Applied Environmental Science and Bert Bolin Centre for Climate research, Stockholm University, Stockholm, Sweden

<sup>5</sup>Department of Forest Sciences, University of Helsinki, Helsinki, Finland

Keywords: new particle formation, long-term measurements, air pollution.

## INTRODUCTION

Sulphur and primary emissions are decreasing largely all over Europe, resulting in improved air quality and decreased direct radiation forcing by aerosols. Changes in indirect radiative forcing however, are not well known since the decrease in CCN (cloud condensing nuclei) due to the decrease in primary production can be at least to certain extent compensated by secondary CCN production (Hamed *et al.*, 2010; Makkonen *et al.*, 2012) as well as climate warming (Makkonen *et al.*, 2012; Paasonen *et al.*, 2013).

The smelter industry in Kola Peninsula is - depending on the definition of the Arctic - the most or second most important source of anthropogenic  $SO_2$  within the Arctic domain. During the past couple of decades the sulphur emissions have been decreasing, even though they still exceed the emissions of entire Finland (Paatero *et al.*, 2008; Prank, 2010). SMEAR I station (Station for Measuring Ecosystem-Atmosphere Relations) (Hari *et al.*, 1994), located only 6km from the Russian boarder, was established in 1991 in order to measure the impact of Kola Peninsula sulphur dioxide emissions to the forests in Eastern Lapland. In general, the station is a clean background station but during airmass transport over Kola, the sulphur dioxide concentration increases drastically (Ruuskanen *et al.*, 2003). The highest values of  $SO_2$  are observed in late winter and early spring (Ruuskanen *et al.*, 2003).

New particle formation (NPF) is closely linked with  $SO_2$  since in the atmosphere it is oxidised into  $H_2SO_4$  which in turn is known to be the key chemical component in atmospheric NPF (Sipilä *et al.*, 2010; Kerminen *et al.*, 2012). Via this pathway  $SO_2$  has an effect on the condensation sink ( $CS$ ), which is determined by the amount of pre-existing particles. Low  $CS$  favours NPF but on the other hand low  $H_2SO_4$  disfavours NPF. We will investigate which of these counteracting effects is more important in Eastern Lapland and what kind of trends there are seen in  $SO_2$  as well as aerosol and NPF related properties. We will later connect the Kola emissions to the NPF observed at SMEAR I. In the analyses, we used data from 1998 – 2011, since particle size distributions were available from 1998 onwards.

## METHODS

SMEAR I station is located on top of Kotovaara hill, 390 m.a.s.l. and surrounded by 60 years old Scots pine (*Pinus sylvestris*) forest. The infrastructure includes a small hut for the aerosol- and trace gas analysers and a 16m high mast with instruments for meteorological, irradiance and eddy-covariance measurements. Also, some instruments have housings outside the hut and continuous chamber measurements from the Scots pines are conducted. We will use measurements of aerosol size distributions,  $SO_2$  concentration as well as meteorological variables to investigate the long-term trends and the effect of Kola Peninsula smelter industry to NPF. Aerosol size distributions are measured with a Differential Mobility Particle Sizer (DMPS) (Aalto *et al.*, 2001) and  $SO_2$  is measured with a pulsed fluorescence analyser (Ruuskanen *et al.*, 2003).

The days were classified into event, non-event and undefined days by visual inspection of the daily aerosol size distributions. A day was classified into an event day when there was a new, growing mode appearing below 25nm (Dal Maso *et al.*, 2005; Kulmala *et al.*, 2012). The event days were further classified into Class I and Class II so that from Class I it is possible to calculate both growth and formation rate ( $GR$  and  $J_8$  or  $J_3$ , respectively) whereas for Class II event this is not possible due to strong fluctuations in the mode concentration or diameter. During an undefined day, a new sub-25nm mode is appearing but the mode doesn't grow. Particle formation rate was calculated by taking into account the time evolution of 3 – 25 – nm (8 – 25 – nm) sized particles and coagulation and the particle growth rate was obtained by following the nucleation mode mean diameter. We also calculated sulphuric acid proxy using two existing parametrizations: a simple linear function including only measurements of  $SO_2$ ,  $CS$  and Global radiation (Petäjä *et al.*, 2009) as well as a non-linear parametrization including also  $RH$ , temperature and pressure (Mikkonen *et al.*, 2011).

We made trend-analysis to various parameters in least-squares sense fitting to logarithms of the data. This data was then fitted to data model with a logarithmic trend component (relative trend) and 4-component stationary sinusoidal seasonal signal. In practice, the least squares fitting was obtained with Matlab routine `lscov` (MathWorks, Inc, 2010).

## RESULTS AND CONCLUSIONS

On average there are 54 new particle formation days in a year, out of which from 20 Class I events. The events peak in spring with another minor peak in the autumn. However, the Class I events have been decreasing dramatically (Table 1) from about 40 to less than 10 Class I events in a year. Although the mean value of Class I events per year is clearly higher than in Western Lapland, Pallas (Asmi *et al.*, 2011), the recent years the NPF events have levelled to the same values as in Pallas (Asmi *et al.*, 2011). The number of events has been decreasing especially during spring and autumn in such a way that the autumn peak has disappeared. At the same time, the number of undefined days has increased during spring and the non-event days during summer and autumn.

The linear trends [%/year] of various measured and calculated parameters are shown in Table 1. The greatest decreases are obtained in  $SO_2$ , Condensation sink ( $CS$ ), Sulphuric acid proxy and Event class I days. All particle concentrations have been decreasing except for nucleation mode concentration. Also, the formation rate of 3 – nm particles has been increasing but on the other hand the apparent formation rate of 8 – nm particles has been decreasing at the same time. These results suggest that cleaning of the air from industrial  $SO_2$  and primary emissions has decreased the  $CS$  leading to higher  $J_3$  and thus higher nucleation mode concentration but this is not reflected to the  $CCN$ -sized (cloud condensing nuclei) particles due to decreases in the primary production and on the other hand less condensable vapours (namely  $H_2SO_4$ ) that could form new particles. This is especially true in spring when the forest is still covered by snow and the organic emissions from the trees are very small and thus not contributing to the condensational growth as much as

during summertime. It also seems that the current temperature increase is not yet sufficient enough to compensate the loss of primary particles but it is expected that the concentrations of potential *CCN* would increase with increasing temperature (Paasonen *et al.*, 2013).

Parameter	Trend 1998 – 2011 [%/year]	Median value
Nucleation mode concentration	+4.3	$34 \text{ cm}^{-3}$
Total concentration	−2.5	$549 \text{ cm}^{-3}$
Condensation sink	−7.7	$9.2 \cdot 10^{-4} \text{ s}^{-1}$
$CN \geq 50\text{nm}$	−3.9	$298 \text{ cm}^{-3}$
$CN \geq 80\text{nm}$	−4.1	$197 \text{ cm}^{-3}$
$CN \geq 100\text{nm}$	−3.9	$165 \text{ cm}^{-3}$
$CN \geq 150\text{nm}$	−3.2	$103 \text{ cm}^{-3}$
$SO_2$ (1998-2011)	−10.9	$0.2 \text{ ppb}$
$SO_2$ (1992-1997)	−5.7	$0.3 \text{ ppb}$
$H_2SO_4$ proxy (Petäjä <i>et al.</i> )	−5.2	$1.1 \cdot 10^6 \text{ molec.cm}^{-3}$
$H_2SO_4$ proxy (Mikkonen <i>et al.</i> )	−8.0	$1.5 \cdot 10^6 \text{ molec.cm}^{-3}$
Event class I days	−9.8	$20 \text{ /year}$
Non-event days	+3.2	$179 \text{ /year}$
$J_3$ (2005-2011)	+23	$0.08 \text{ cm}^{-3}\text{s}^{-1}$
Temperature	+1.5 °C/decade	−0.6 °C

Table 1: Trends and median values of selected measured variables and calculated parameters.

Sulphur species have a big impact on both the formation and growth at SMEAR I.  $H_2SO_4$  explains approximately 20 – 50% of the condensational growth and there is large seasonal variation with highest values obtained during spring (50%) and autumn (30%). These values are higher than e.g. at Pallas, in Western Lapland (Asmi *et al.*, 2011). Using the obtained *GR* we calculated the estimated time at which 1.5 – nm clusters were formed assuming constant growth rate below the cut-off size of DMPS. We observed that

- particles form earlier during spring due to high concentrations of  $SO_2$  and  $H_2SO_4$  as well as sufficient amount of radiation,
- several events have occurred during in the absence of light and they are connected to especially high concentrations of  $SO_2$  and,
- high  $SO_2$  concentrations can advance the onset of nucleation by several hours, especially in the presence of high global radiation.

Finally, we calculated the fraction of time that trajectories arrive over Kola in general and during event days only. The relative difference between these two was greatest during spring and autumn: during these times airmasses pass over Kola more frequently during NPF days than in general.

All in all, these results show that the sulphur emissions from Kola peninsula smelters have a large impact on the NPF observed in Eastern Lapland. It seems, however, that the NPF frequency has now levelled near the natural background level when the extra sulphur boost from Kola has decreased distinctively.

## ACKNOWLEDGEMENTS

This work was financed by the Academy of Finland Centre of Excellence program (project no. 1118615) and the Nordic Centre of Excellence CRAICC (Cryosphere-atmosphere interactions in a changing Arctic climate).

## REFERENCES

- Aalto, P., *et al.* (2001), Physical characterization of aerosol particles during nucleation events. *Tellus*, **53B**, 344-358
- Asmi, E., *et al.* (2011), Secondary new particle formation in Northern Finland Pallas site between the years 2000 and 2010. *Atmos. Chem. Phys.*, **11**, 12959-12972.
- Dal Maso, M., *et al.* (2005). Formation and growth of fresh atmospheric aerosols: eight years of aerosol size distribution data from SMEAR II, Hyytiälä, Finland. *Boreal Environ. Res.*, **10**, 323-336.
- Hamed, A., *et al.* (2010). Changes in the production rate of secondary aerosol particles in Central Europe in view of decreasing  $SO_2$  emissions between 1996 and 2006. *Atmos. Chem. Phys.*, **10**, 1071-1091.
- Hari, P., *et al.* (1994). Air Pollution in Eastern Lapland: Challenge for an Environmental Measurement Station. *Silva Fennica*, **28**(1), 29-39.
- Kerminen, V.-M., *et al.* (2012). Cloud condensation nuclei production associated with atmospheric nucleation: a synthesis based on existing literature and new results. *Atmos. Chem. Phys.*, **12**, 12037-12059.
- Kulmala, M., *et al.* (2012). Measurement of the nucleation of atmospheric aerosol particles. *Nat. Protoc.*, **7**, 1651-1667.
- Makkonen, R., *et al.* (2012). BVOC-aerosol-climate interactions in the global aerosol-climate model ECHAM5.5-HAM2. *Atmos. Chem. Phys.*, **12**, 10077-10096.
- MathWorks, Inc. (2010) Matlab user manual for R2010a.
- Mikkonen, S., *et al.* (2011). A statistical proxy for sulphuric acid concentration. *Atmos. Chem. Phys.*, **11**, 11319-11334.
- Paasonen, P., *et al.* (2013). Warming-induced increase in aerosol number concentration likely to moderate climate change. *Nature Geosci.*, **6**, 438-442.
- Paatero, J., *et al.* (2008). Effects of Kola air pollution on the environment in the Western part of the Kola peninsula and Finnish Lapland - Final report. *Finnish Meteorological Institute Reports*, **6**, 1-26.
- Petäjä, T., *et al.* (2009). Sulfuric acid and OH concentrations in a boreal forest site. *Atmos. Chem. Phys.*, **9**, 7434-7448.
- Prank, M., M. *et al.* (2010). A refinement of the emission data for Kola Peninsula based on inverse dispersion modelling. *Atmos. Chem. Phys.*, **10**, 10849-10865.
- Ruuskanen, T., *et al.* (2003). Atmospheric trace gas and aerosol particle concentration measurements in Eastern Lapland, Finland 1992-2001. *Boreal Env. Res.*, **8**, 335-349.
- Sipilä, M., *et al.* (2010). The role of sulfuric acid in atmospheric nucleation. *Science*, **327**, 1243-1246.

# INVESTIGATIONS ON THE SPATIOTEMPORAL PROPERTIES OF NEW PARTICLE FORMATION EVENTS IN A BOREAL FOREST ENVIRONMENT

J. LAMPILAHTI<sup>1</sup>, H.E. MANNINEN<sup>1,2</sup>, T. NIEMINEN<sup>1,3</sup>, S. MIRME<sup>2</sup>, I. PULLINEN<sup>4</sup>, T. YLI-JUUTI<sup>1</sup>, S. SCHOBESBERGER<sup>1</sup>, J. KANGASLUOMA<sup>1</sup>, K. LEHTIPALO<sup>1,5</sup>, T.F. MENTEL<sup>6</sup>, T. PETÄJÄ<sup>1</sup> and M. KULMALA<sup>1</sup>

<sup>1</sup>Department of Physics, University of Helsinki, Finland

<sup>2</sup>Institute of Physics, University of Tartu, Estonia

<sup>3</sup>Helsinki Institute of Physics, Helsinki, Finland

<sup>4</sup>Forschungszentrum Jülich, IBG-2, 52425 Jülich, Germany

<sup>5</sup>Airmodus Oy, Helsinki, Finland

<sup>6</sup>Forschungszentrum Jülich, IEK-8, 52425 Jülich, Germany

Keywords: new particle formation, airborne measurements, boreal forest

## INTRODUCTION

Aerosol particles are an important component of the atmosphere affecting health, atmospheric chemistry and climate (e.g. Myhre et al., 2013; Pope III and Dockery, 2006; Kolb and Worsnop, 2012). The formation of new aerosol particles in the atmosphere (NPF) is an important contributor to the atmosphere's aerosol budget (Spracklen et al., 2006). It involves the formation of molecular clusters from precursor gases by nucleation, their growth by condensation, clumping together by coagulation and removal by deposition (e.g. Seinfeld and Pandis, 1997; Kulmala et al., 2013). It is still unclear where NPF begins and how it develops spatially. Knowing this could help to understand the mechanisms behind NPF and also make climate models more accurate. Previous measurements are scarce and do not deliver a consistent picture.

Balloon measurements performed in Germany near Leipzig suggest that NPF begins near the entrainment zone and the freshly formed particles mix into the growing mixed layer (ML) homogeneously, continuing their growth there. This suggests that turbulence and mixing play an important role in the initiation of NPF (Startmann et al., 2003; Siebert et al., 2004; Wehner et al., 2007). Laakso et al. (2007) measured vertical profiles of aerosol particles with a hot-air balloon up to about 2 km on NPF event days in Hyytiälä, southern Finland. They observed homogeneous NPF inside the ML. By modeling the development of the planetary boundary layer (PBL) it was concluded that the particles formed either homogeneously inside the ML or near the surface. O'Dowd et al. (2009) measured nucleation mode particle concentrations over boreal forest in southern Finland with an airplane during NPF events and concluded that the particles were forming right above canopy. Concentrations were highest over forest areas suggesting that the organic molecules released by the forest are the main contributor to NPF. Wehner et al. (2010) observed high ultrafine particle concentrations in turbulent places of the residual layer (RL) during helicopter measurements conducted in Cabauw, Holland. The freshly formed particles were mixed into the ML as it reached them. The results suggest that NPF may begin in turbulent places of the RL. Schobesberger et al. (2013) measured nucleation mode particle concentrations over southern Finland using an airplane and observed NPF inside the ML. Particle number concentration changed spatially and small particles were observed in larger numbers near the top of the ML. The authors explained

the inhomogeneity by PBL dynamics and by changes in NPF intensity.

We analyzed the Zeppelin measurements conducted in spring 2013 over the boreal forest in Hyytiälä, southern Finland during the PEGASOS (Pan-European Gas-Aerosol-Climate Interaction Study) campaign. Zeppelin measured vertical and horizontal profiles of particle and ion number size distributions during NPF events. The surface layer measurements were provided by SMEAR II station located in Hyytiälä. The Zeppelin had done similar measurements during the summer 2012 in Po Valley, Italy. There NPF was observed to begin in the surface layer from where the particles mixed into ML homogeneously. NPF coincided with the onset of mixing. High concentrations of sulfuric acid, known to be beneficial for NPF, were also measured near the entrainment zone (Manninen et al., 2013).

## METHODS

The Zeppelin conducted measurements in southern Finland during 4.5.2013-10.6.2013. It was fitted with different instrument layouts on different flight days. NPF was specifically measured by the nucleation layout and it was used on a total of six flights. NPF events were scarce that spring however one clear and interesting NPF event was observed on 8.5.2013 and it is the case analyzed here. The analysis is based on meteorological and aerosol measurements from SMEAR II station and the Zeppelin.

Surface layer conditions were measured on SMEAR II station (61.85 °N, 24.29 °E, 181 m above sea level) located in a boreal forest environment (Hari and Kulmala, 2005). In this analysis data was used from the station's NAIS (Neutral cluster and Air Ion Spectrometer, AIREL Ltd.), that continuously measures the ambient particle number size distribution in the size range 2-42 nm and ion number size distribution in the size range 0.8-42 nm with a 3-5 minute time resolution (Mirme and Mirme, 2011). The data was checked against the station's DMPS (Differential Mobility Particle Spectrometer) that measures the particle number size distribution in the size range 3-1000 nm with a 10 minute time resolution (Aalto et al., 2001). In addition temperature, relative humidity (RH) and wind data from the SMEAR II mast were used (height 16.8 m). The data was available at 30 min time resolution from Smart-SMEAR service (Junninen et al., 2009).

The platform for airborne measurements was a Zeppelin NT class airship. It was stored in the Jämsijärvi airfield (61.778611 °N, 27.16111 °E, 154 m, above sea level, ICAO: EFJM). A Zeppelin is ideal for airborne aerosol measurements since it has an excellent maneuverability and can house multiple instruments inside the cabin. Data was used from NAIS which was part of the nucleation package and has the same specifications as the one in SMEAR II station. RH, temperature and wind parameters were measured at one second time resolution from the end of a boom attached to the front of the cabin. Coordinates and height above ground were obtained from a GPS unit at a one second time resolution. On 8.5.2013 height measurements are missing around the peak altitudes from the first three profiles.

The Zeppelin took off early in the morning in order to get measurements from both sides of the growing PBL. In Hyytiälä the Zeppelin flew profiles that vertically fell inside approximately 100-1000 m and horizontally inside an area of 4-5 km in diameter. The average airspeed during profiles was approximately 70 km/h, ascend speed 30 m/min and descend speed 90 m/min. The first profiles covered the mixed layer, entrainment zone and the residual layer. The PBL quickly exceeded the vertical measurement area, after which measurements were only from inside the ML. The onset of NPF was determined from an increase in 1.7-3 nm ion concentration (small ions). PBL height was estimated from the minimum vertical gradient of RH measured onboard Zeppelin (Seidel et al., 2009).

Particle concentration changed sharply in a periodic fashion during the NPF event that day. This

was due to a plume of growing particles moving across the area, a robust method that operated time step at a time was needed to estimate particle growth rates (GR). The chosen method consists of finding a representative particle size  $\bar{D}_p(t)$  as a function of time for the growing mode by weighing the particle sizes with concentrations according to equation (1).

$$\bar{D}_p(t) = 10^{N_{tot}(t)^{-1} \times \sum_i (dN_i(t) \times \log_{10} D_{p,i})}, \quad (1)$$

where  $dN(t)$  is the time dependent particle concentration in a size interval that's geometric mean size is  $D_p$ ,  $i$  numbers the size intervals in the growing mode and they are estimated from the number size distribution and  $N_{tot}(t) = \sum_i dN_i(t)$  is the total particle concentration in the chosen size intervals. We chose points on the plume to represent the plume and points clearly not on the plume to represent the background. Linear least-squares fit was performed on the points to get the GR of plume and background as the slope of the fit. The altitude dependence of the plume's particle number size distribution was estimated by taking the median number size distribution observed at each height. Estimations for the locations where the plume was observed were obtained visually from the number size distribution plotted as a function of time. Backward trajectories of airmasses ending at the chosen plume locations were calculated from HYSPLIT (HYbrid Single Particle Lagrangian Integrated Trajectory) model (Draxler and Rolph, 2013). Only locations observed near full hour were used because the time resolution of the model is one hour. Using the plume GRs from SMEAR II and Zeppelin along with the representative size  $\bar{D}_p$  at each plume location we calculated the time it took for the particles to grow from 1.5 nm (approximately the birth size of the particles) to the representative size. By going back this time along the trajectory we estimated where the particles were born.

## RESULTS AND CONCLUSIONS

The findings are summarized in Figures 1-4. In Figure 1 we see that NPF seems to begin almost simultaneously and homogeneously inside the ML. Very few small ions were observed in the RL. The estimated times of onset at SMEAR II and the Zeppelin were 08:42 and 08:54 respectively. The event seems to begin at SMEAR II about 12 minutes earlier, but since the Zeppelin was above the ML during this time we can not say that the event started earlier in the surface layer. It also seems that the onset is not connected to the break-up of nocturnal inversion and onset of mixing, which happened at least 1.5-2 hours before we see the increase in small ions.

In Figure 2 we see that the Zeppelin repeatedly entered a narrow high concentration plume of particles, which can be seen as stripes on the number size distribution plotted as a function of time. The plume moved over the measurement area from west to east. A similar change in wind direction was observed. Particle number size distribution in the plume seems to be vertically homogeneous.

In Figure 3 we see a similar background NPF event happening at SMEAR II and the Zeppelin, suggesting a regional event as well. The GRs for the plume at Zeppelin, plume at SMEAR II, background at Zeppelin and background at SMEAR II were 2.2 nm/h, 2.3 nm/h, 1.9 nm/h and 1.9 nm/h respectively. Small particle size, compatibility with the background event, and the observed growth suggest that the plume is of atmospheric origin. The wind conditions and plume movement along with the observation of growth and vertical homogeneity suggest that the particles were formed throughout the height of a long and narrow strip of air. The birth places of plume particles, estimated from backward trajectories seem to fall on a narrow strip of air north-west from SMEAR II station. More work needs to be done to further characterize the spatiotemporal properties of NPF events.

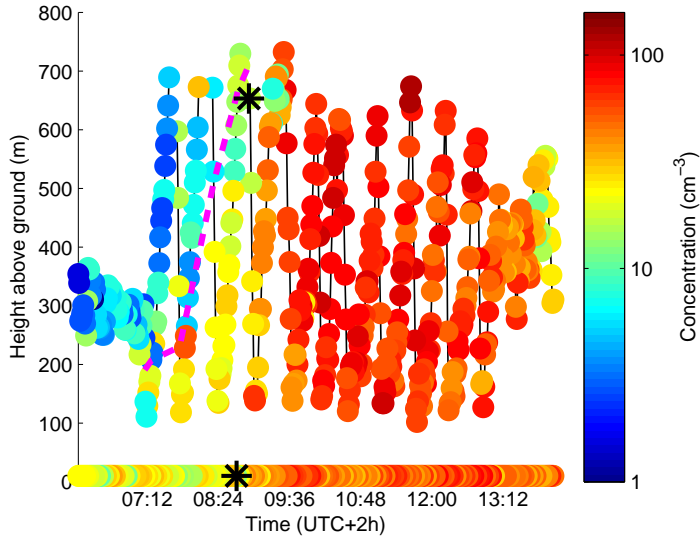


Figure 1: 1.7-3 nm negative ion concentrations on 8.5.2013 as a function of time and height above ground from the Zeppelin's NAIS. The concentration on ground level is from the SMEAR II station's NAIS. The black asterisk marks the beginning of NPF (SMEAR II: 08:42 and Zeppelin: 08:54). The magenta colored dashed line is the PBL height estimated from RH.

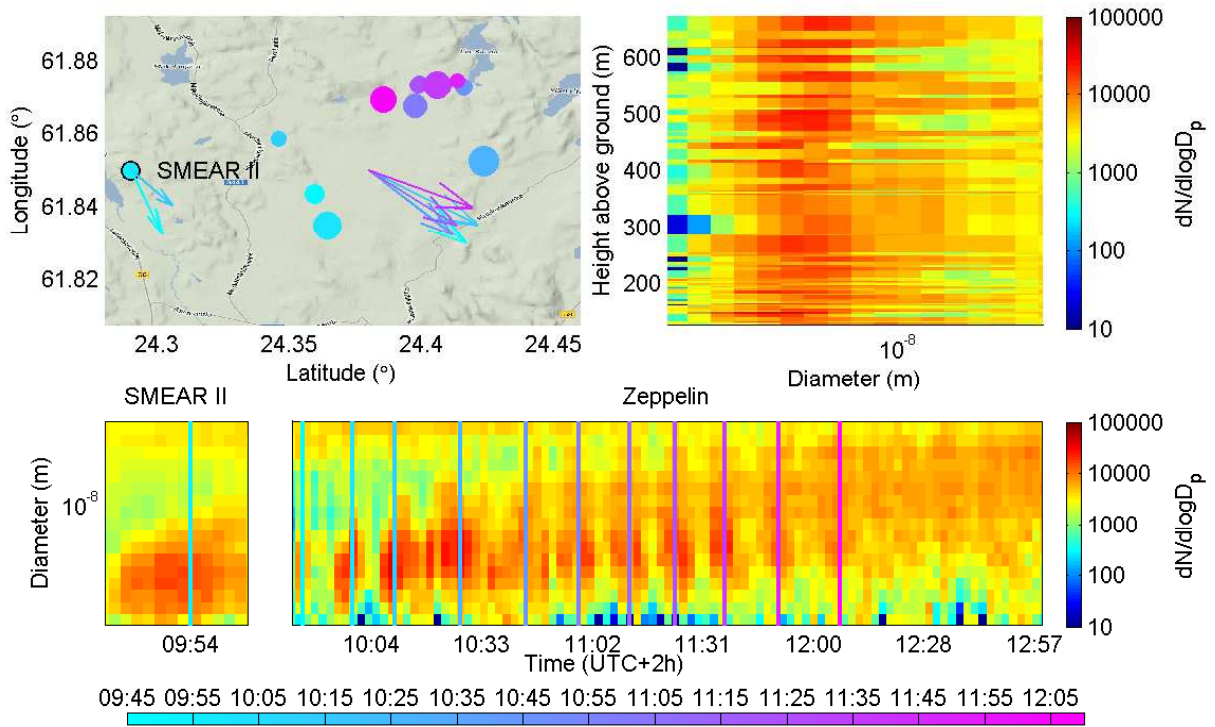


Figure 2: Upper left corner: plume location as a function of time. Wind vectors using 30 min averaging from SMEAR II and Zeppelin are plotted as well. The size of the dot is proportional to height above ground (except for SMEAR II) and the color tells the time. Upper right corner: particle number size distribution of the plume as a function of height. Below these are particle number size distributions measured by NAIS as a function of time from SMEAR II and Zeppelin. The estimations for plume locations are marked by the vertical lines that are also color coded with the color representing time. The date of measurements is 8.5.2013.

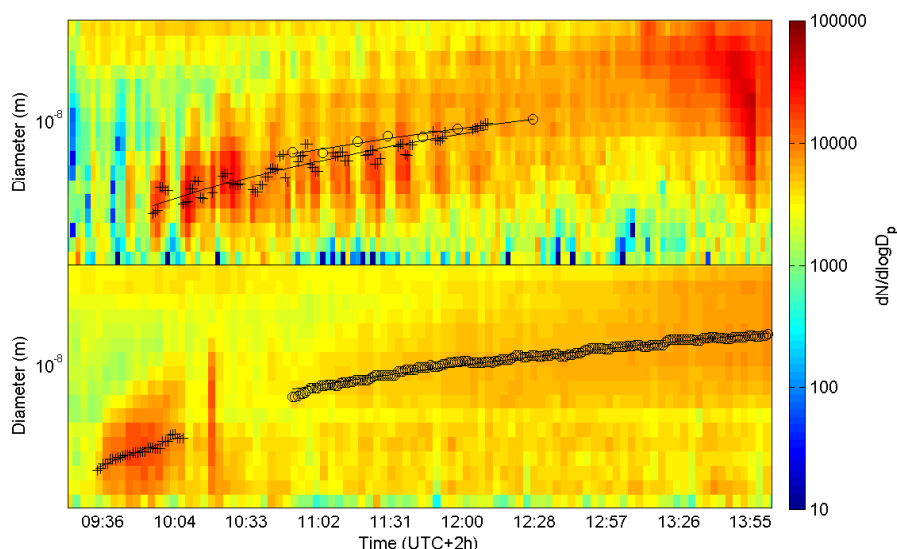


Figure 3: Number size distribution of the NPF event as a function of time on 8.5.2013 from NAIS. Above: Zeppelin and below: SMEAR II. The points on the plot mark the representative particle sizes of the growing mode. Plus represents the plume, circle represent the background. The lines are linear least-square fits to the points.

## ACKNOWLEDGEMENTS

This research is supported by European Commission under the Framework Programme 7 (FP7-ENV-2010-265148). The support by the Academy of Finland Centre of Excellence program (project no. 1118615) and Finnish Cultural Foundation is also gratefully acknowledged. The Zeppelin is accompanied by an international team of scientists and technicians. They are all warmly acknowledged.

## REFERENCES

- Aalto, P., Hämeri, K., Becker, E., et al. (2001). Physical characterization of aerosol particles during nucleation events. *Tellus*, 53B:344–358.
- Draxler, R. and Rolph, G. (2013). *HYSPLIT (HYbrid Single-Particle Lagrangian Integrated Trajectory)*. NOAA Air Resources Laboratory, College Park, MD. URL: <http://www.arl.noaa.gov/HYSPLIT.php>.
- Hari, P. and Kulmala, M. (2005). Station for Measuring Ecosystem–Atmosphere Relations (SMEAR II). *Boreal Environment Research*, 10:315–322.
- Junninen, H., Lauri, A., Keronen, P., et al. (2009). Smart-SMEAR: on-line data exploration and visualization tool for SMEAR stations. *Boreal Environment Research*, 14:447–457.
- Kolb, C. and Worsnop, D. (2012). Chemistry and composition of atmospheric aerosol particles. *Annual Review of Physical Chemistry*, 63:471–491.
- Kulmala, M., Kontkanen, J., Junninen, H., et al. (2013). Direct observations of atmospheric aerosol nucleation. *Science*, 339:943–947.
- Laakso, L., Grönholm, T., Kulmala, L., et al. (2007). Hot-air balloon as a platform for boundary layer profile measurements during particle formation. *Boreal Environment Research*, 12:279–294.
- Manninen, H., Mirme, S., Ehn, M., et al. (2013). Does the onset of new particle formation occur in the planetary boundary layer? *AIP Conference Proceedings*, 1527:567–570.

- Mirme, S. and Mirme, A. (2011). The mathematical principles and design of the NAIS – a spectrometer for the measurement of cluster ion and nanometer aerosol size distributions. *Atmospheric Measurement Techniques*, 4:7405–7434.
- Myhre, G., C. E. L., Myhre, B. H. S., and Storelvmo, T. (2013). Aerosols and their relation to global climate and climate sensitivity. *Nature Education Knowledge*, 4(5):7.
- O’Dowd, C., Yoon, Y., Junkermann, W., et al. (2009). Airborne measurements of nucleation mode particles II: boreal forest nucleation events. *Atmospheric Chemistry and Physics*, 9:937–944.
- Pope III, C. and Dockery, D. (2006). Health effects of fine particulate air pollution: lines that connect. *Journal of the Air and Waste Management Association*, 56:709–742.
- Schobesberger, S., Väänänen, R., Leino, K., et al. (2013). Airborne measurements over the boreal forest of southern finland during new particle formation events in 2009 and 2010. *Boreal Environment Research*, 18:145–163.
- Seidel, D., Chi, O., and Li, K. (2009). Estimating climatological planetary boundary layer heights from radiosonde observations: Comparison of methods and uncertainty analysis. *Journal of Geophysical Research*, 115:D16113.
- Seinfeld, J. and Pandis, S. (1997). *Atmospheric chemistry and physics - from air pollution to climate change*. (John Wiley and Sons Inc., NY, USA).
- Siebert, H., Stratmann, F., and Wehner, B. (2004). First observations of increased ultrafine particle number concentrations near the inversion of a continental planetary boundary layer and its relation to ground-based measurements. *Geophysical Research Letters*, 31:L09102.
- Spracklen, D., Carslaw, K., Kulmala, M., et al. (2006). The contribution of boundary layer nucleation events to total particle concentrations on regional and global scales. *Atmospheric Chemistry and Physics*, 6:5631–5648.
- Startmann, F., Siebert, H., Spindler, G., et al. (2003). New-particle formation events in a continental boundary layer: first results from the SATURN experiment. *Atmospheric Chemistry and Physics*, 3:1445–1459.
- Wehner, B., Siebert, H., Ansmann, A., et al. (2010). Observations of turbulence-induced new particle formation in the residual layer. *Atmospheric Chemistry and Physics*, 10:4319–4330.
- Wehner, B., Siebert, H., Stratmann, F., et al. (2007). Horizontal homogeneity and vertical extent of new particle formation events. *Tellus*, 59B:362–371.

# A10 PSM: A NEW VERSION OF THE PARTICLE SIZE MAGNIFIER FOR DETECTION OF ATMOSPHERIC CLUSTERS AND PARTICLES AS SMALL AS 1 NM

K. LEHTIPALO<sup>1,2</sup>, A. FRANCHIN<sup>1,2</sup>, J. KONTKANEN<sup>1</sup>, J. MIKKILÄ<sup>2</sup>, J. VANHANEN<sup>2</sup>, J. KANGASLUOMA<sup>1</sup>, T. PETÄJÄ<sup>1</sup>, AND M. KULMALA<sup>1</sup>

<sup>1</sup>Department of Physics, University of Helsinki, Helsinki, Finland

<sup>2</sup>Airmodus Oy, Helsinki, Finland

Keywords: condensation particle counters, nucleation, nano-particles

## INTRODUCTION

There has been a growing demand on measuring atmospheric clusters and recently formed particles as small as 1 nm in diameter. For example, the new particle formation and growth processes are not yet completely understood on a molecular level, mainly due to the lack of suitable instruments to detect the recently formed clusters and particles. A new generation of condensation particle counters have emerged in recent years (*e.g.* Vanhanen *et al.*, 2011, Jiang *et al.*, 2011, Wimmer *et al.*, 2013), which mainly use diethylene glycol for activating the smallest particles (Iida *et al.*, 2009). These particle counters allow deriving parameters describing the new particle formation process, *e.g.* the formation and growth rates, directly from measurements also in the size range below 2 nm (Kirkby *et al.*, 2011; Kulmala *et al.*, 2013).

## METHODS

The Airmodus Particle Size Magnifier (PSM; Vanhanen *et al.*, 2011) can be used to resolve the size distribution of particles below about 3 nm by varying the cut-off size of the instrument. This is done by changing the mixing ratio of saturator and aerosol flow and thus changing the supersaturation created inside the particle mixing region and growth tube. Schematics of the instrument are presented in Fig. 1.

A new version of the Particle Size Magnifier, A10, was developed during 2012-2013. It includes modifications especially in the air and liquid flow design. A special care has been taken in making the instrument stable in varying operating conditions, which is critical for long-term field measurements.

The A10 PSM was tested and calibrated at the University of Helsinki laboratory facilities using size-selected negatively charged ammonium sulphate clusters and particles. In spring 2013, the A10 PSM was used for measuring the size distribution of particles between 1 – 3 nm at the Hyytiälä SMEAR II measurement station in southern Finland during the PEGASOS campaign. The measurements have been going on continuously since then. One example of the size distribution measured with the A10 PSM and the NAIS ion spectrometer is presented in figure 2.

## CONCLUSIONS

In the laboratory calibrations the new PSM was found to activate ammonium sulphate clusters consisting of just a few molecules, and it was able to detect even single large molecules, for example tetra-alkyl ammonium halides (Ude and Fernandez de la Mora, 2005). Clusters and particles of different composition activate at slightly different flow rates, indicating that there is a composition dependency. The effect of composition and conditions to the activation efficiency is further studied in Kangasluoma *et al.*, (2013).

The A10 proved to be a reliable tool for field measurements. By combining data from the PSM, ion spectrometers and the new mass spectrometric methods (*e.g.* Jokinen *et al.*, 2012) it is possible to cover the whole size range from molecules to clusters and to aerosol particles.

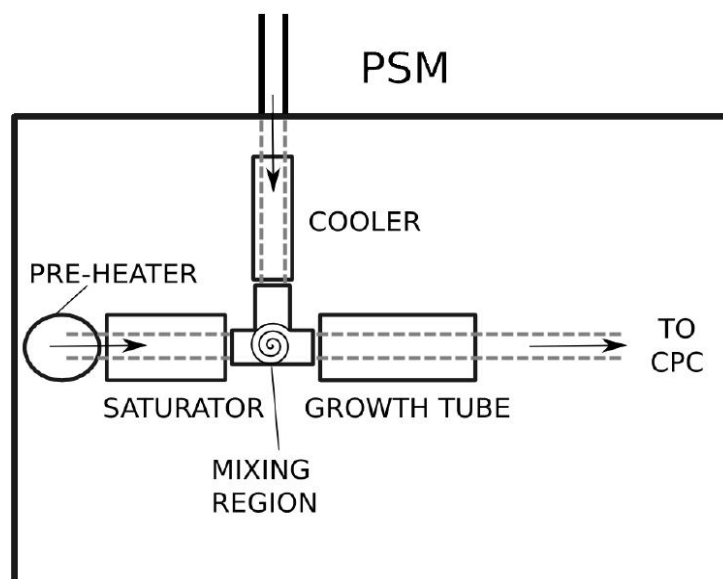


Figure 1. Schematics of the Particle Size Magnifier. Sample air is going from the inlet through a cooler before being mixed with saturated clean air in the mixing region. Particles grow to about 90 nm in the growth tube before they are directed to a counter CPC.

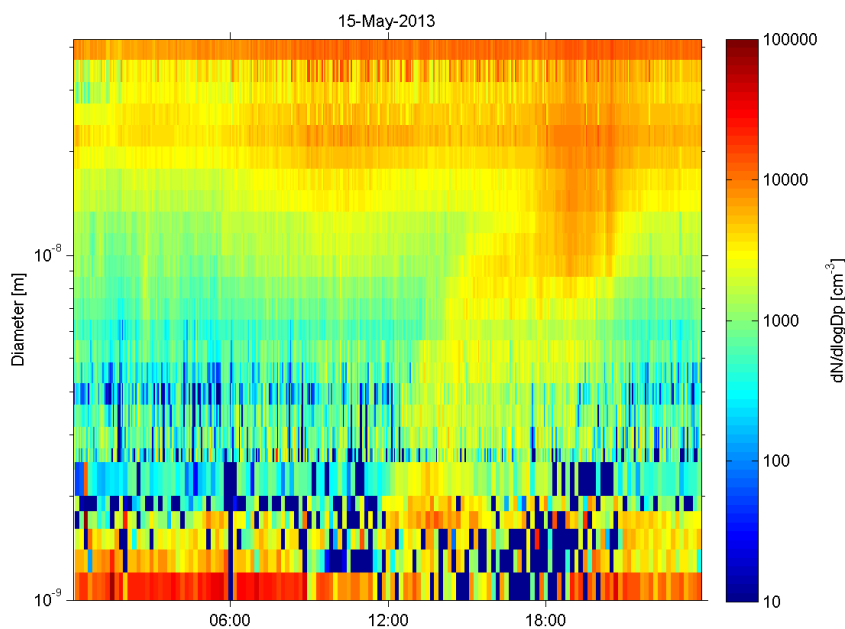


Figure 2. The size distribution of 1-40 nm particles measured at Hyytiälä SMEAR II station at 15.5.2013. The size range 1-3 nm is measured with the A10 PSM and 3-40 nm with the NAIS ion spectrometer.

## ACKNOWLEDGEMENTS

This research has been funded by the ERC-Advanced "ATMNUCLE" grant no. 227463), the Academy of Finland (Center of Excellence project no. 1118615), and the Eurostars Programme under contract no. E!6911

## REFERENCES

- Iida, K., Stolzenburg, M.R., and McMurry, P.H.: Effect of working fluid on sub-2nm particle detection with a laminar flow ultrafine condensation particle counter. *Aerosol Sci. Technol.* **43**, 81-96, 2009.
- Jiang, J., Zhao, J., Chen, M., Eisele, F.L., Scheckman, J., Williams, B.J., Kuang, C., and McMurry, P.H.: First measurements of neutral atmospheric cluster and 1-2nm particle number size distributions during nucleation events. *Aerosol Sci. Technol.*, 45, 2-4, 2011.
- Jokinen, T., Sipilä, M., Junninen, H., Ehn, M., Lönn, G., Hakala, J., Petäjä, T., Mauldin III, R. L., Kulmala, M., and Worsnop, D. R.: Atmospheric sulphuric acid and neutral cluster measurements using CI-API-TOF, *Atmos. Chem. Phys.*, 12, 4117-4125, doi:10.5194/acp-12-4117-2012, 2012.
- Kangasluoma, J., Junninen, H., Lehtipalo, K., Mikkilä, J., Vanhanen, J., Attoui, M., Sipilä, M., Worsnop, D., Kulmala, M. and Petäjä, T.: Remarks on ion generation for CPC detection efficiency studies in sub 3 nm size range. *Aerosol Sci. Technol.*, 5, 556- 563, 2013.
- Kirkby, J., Curtius, J., Almeida, J., Dunne, E., Duplissy, J., Erhart, S., Franchin, A., Gagné, S., Ickes, L., Kürten, A., Kupc, A., Metzger, A., Riccobono, F., Rondo, L., Schobesberger, S., Tsagkogeorgas, G., Wimmer, D., Amorim, A., Bianchi, F., Breitenlechner, M., David, A., Dommen, J., Downard, A., Ehn, M., Flagan, R.C., Haider, S., Hansel, A., Hauser, D., Jud, W., Junninen, H., Kazil, J., Kreissl, F., Kvashin, A., Laaksonen, A., Lehtipalo, K., Lima, J., Lovejoy, E.R., Makhmutov, V., Mathot, S., Mikkilä, J., Minginette, P., Mogo, S., Nieminen, T., Onnela, A., Pereira, P., Petäjä, T., Schnitzhofer, R., Seinfeld, J.H., Sipilä, M., Stozhkov, Y., Stratmann, F., Tome, A., Vanhanen, J., Viisanen, Y., Vrtala, A., Wagner, P.E., Walther, H., Weingartner, E., Wex, H., Winkler, P.M., Carslaw, K.S., Worsnop, D.R., Baltensperger, U., and Kulmala, M.: The role of sulphuric acid, ammonia and galactic cosmic rays in atmospheric aerosol nucleation, *Nature*, 476, 429-433, 2011.
- Kulmala, M., Kontkanen, J., Junninen, H., Lehtipalo, K., Manninen, H.E., Nieminen, T., Petäjä, T., Sipilä, M., Schobesberger, S., Rantala, P., Franchin, A., Jokinen, T., Järvinen, E., Äijälä, M., Kangasluoma, J., Hakala, J., Aalto, P.P., Paasonen, P., Mikkilä, J., Vanhanen, J., Aalto, J., Hakola, H., Makkonen, U., Ruuskanen, T., Mauldin, R.L., Duplissy, J., Vehkamäki, H., Bäck, J., Kortelainen, A., Riipinen, I., Kürten, T., Johnston, M.V. Smith, J.N., Ehn, M., Mentel, T.F., Lehtinen, K.E.J., Laaksonen, A., Keminen, V.-M., and Worsnop, D.: Direct observations of atmospheric aerosol nucleation. *Science*, 22, 911-912, 2013.
- Manninen, H. E., Petäjä, T., Asmi, E., Riipinen, I., Nieminen, T., Mikkilä, J., Hörrak, U., Mirme, A., Mirme, S. Laakso, L., Kerminen, V.-M., and Kulmala, M.: Long-term field measurements of charged and neutral clusters using Neutral cluster and Air Ion Spectrometer (NAIS). *Boreal Env. Res.*, **14**, 591–605, 2009.
- Ude S., and Fernandez de la Mora, J.: Molecular monodisperse mobility and mass standards from electrosprays of tetra-alkyl ammonium halides, *J. Aerosol Sci.*, **36**, 1224–1237, 2005.
- Vanhanen, J., Mikkilä, J., Lehtipalo, K., Sipilä, M., Manninen, H. E., Siivola, E., Petäjä, T., Kulmala, M.: Particle Size Magnifier for Nano-CN Detection. *Aerosol Sci. Tech.*, **45**, 4, 533-42, 2011.
- Wimmer, D., Lehtipalo, K., Franchin, A., Kangasluoma, J., Kreissl, F., Kürten, A., Kupc, A., Metzger, A., Mikkilä, J., Petäjä, T., Riccobono, F., Vanhanen, J., Kulmala, M., and Curtius, J.: Performance of diethylene glycol-based particle counters in the sub-3 nm size range, *Atmos. Meas. Tech.*, 6, 1793-1804, doi:10.5194/amt-6-1793-2013, 2013.

## OBSERVATIONS OF RUSSIAN WILD FIRE SMOKE IN FINLAND IN SUMMER 2010

K. LEINO<sup>1</sup>, T. NIEMINEN<sup>1,3</sup>, L. RIUTTANEN<sup>1</sup>, R. VÄÄNÄNEN<sup>1</sup>, T. PETÄJÄ<sup>1</sup>, L. JÄRVI<sup>1</sup>, P. KERONEN<sup>1</sup>, A. VIRKKULA<sup>1,2</sup>, T. POHJA<sup>1</sup>, P.P. AALTO<sup>1</sup>, and M. KULMALA<sup>1</sup>

<sup>1</sup> Department of Physics, University of Helsinki, PO Box 48, FIN-00014 Helsinki, Finland.

<sup>2</sup> Finnish Meteorological Institute, Erik Palmenin aukio, FIN-00560 Helsinki, Finland.

<sup>3</sup> Helsinki Institute of Physics, P.O. Box 64, FIN-00014 Helsinki, Finland.

Keywords: BIOMASS BURNING, AEROSOL, GREENHOUSE GAS.

### INTRODUCTION

Biomass burning originated emissions have impacts on many parts of life. Aerosol particles, black carbon, as well as e.g. carbon monoxide (CO) and different greenhouse gases have both local and global effects on the environment. Greenhouse gases, soot particles and organic aerosols have effect on radiative balance of the Earth (IPCC, 2007), while the emitted fine particles are injurious to human health (WHO, 2006). Burning emissions can be originated on air from wild fires. Russian forest and peat bog fires occur almost every summer over large areas in the Russian boreal forests due to long rainless and heat periods at summertime (Konovalov *et al.*, 2011). The long range transport of biomass burning emissions; aerosol particles and different gases (CO, CO<sub>2</sub>, NO<sub>x</sub>, O<sub>3</sub>, SO<sub>2</sub>) in air can be observed, even up to distances of several thousand of kilometres in far away from burning areas (Bertschi and Jaffe, 2005). During the Russian forest fires in the summer of 2010 we observed for instance the elevated concentrations of carbon monoxide (CO) and black carbon (BC) at SMEAR II field measurement station in Hyytiälä, Southern Finland on certain days. During these days and past few days the wind direction had been from fire areas to Finland.

### METHODS

In our study we investigate and compare different gas and particle concentrations measured in different parts of Finland during Russian wild fire episodes in the late summer of 2010. For the comparison we have several years extensive aerosol and different gas data sets obtained from ground based measurements at three SMEAR (Station for Measuring Forest Ecosystem – Atmosphere Relations) stations round in Finland which can be used as reference on investigation. For the ensuring the source of the detected emissions we determine backward air mass trajectories and fire locations by HYSPLIT4 model (Draxler, 1999) and Aqua and Terra satellite data by MODIS (Moderate Resolution Imaging Spectroradiometer) to getting information about air mass origin and movements.

### RESULTS

On Table 1 we have mean (max) gas concentrations, particle concentrations and mean particle sizes measured at the all three SMEAR stations in Finland during two remarkable smoke days in the summer of 2010 (27.7.2010 and 8.8.2010) and several year mean concentrations for these days of summertime as reference. The most significant ratios are bold.

	Epi. 29.7.2010	Ref. 29.7.	Ratio	Epi. 8.8.2010	Ref. 8.8.	Ratio
<b>Hyytiälä</b>						
CO [ppb]	262 (450)	110	<b>2.39</b>	276 (416)	123	<b>2.24</b>
CO <sub>2</sub> [ppm]	396 (422)	369	1.07	405 (436)	370	1.10
SO <sub>2</sub> [ppb]	1.34 (3.26)	0.12	<b>11.51</b>	0.35 (0.79)	0.11	<b>2.84</b>
O <sub>3</sub> [ppb]	55.7 (70.1)	29.6	<b>1.88</b>	42.0 (64.9)	31.0	1.35
NO <sub>x</sub> [ppb]	0.41 (1.49)	0.42	0.98	0.55 (1.06)	0.65	0.86
BC [µgm <sup>-3</sup> ]	1054 (1798)	159	<b>6.61</b>	1270 (1715)	335	<b>3.79</b>
D <sub>p</sub> [µm]	0.14	0.11	1.26	0.19	0.14	1.34
N <sub>tot</sub> [cm <sup>-3</sup> ]	3496	2095	<b>1.67</b>	1806	1881	0.96
CS [s <sup>-1</sup> ]	0.012 (0.020)	0.003	<b>3.70</b>	0.011 (0.015)	0.004	<b>2.71</b>
<b>Helsinki</b>						
CO [ppb]	251 (534)	169	1.49	433 (584)	169	<b>2.56</b>
SO <sub>2</sub> [ppb]	1.03 (2.67)	0.74	1.40	0.86 (1.90)	0.70	1.23
O <sub>3</sub> [ppb]	45.9 (59.3)	29.1	1.58	41.3 (60.1)	27.2	1.51
NO <sub>x</sub> [ppb]	9.84 (18.68)	7.57	1.30	7.87 (15.67)	8.14	0.97
D <sub>p</sub> [µm]	0.089	0.082	1.09	0.109	0.072	<b>1.51</b>
N <sub>tot</sub> [cm <sup>-3</sup> ]	6999	9212	0.76	6041	8564	0.71
CS [s <sup>-1</sup> ]	0.014	0.008	<b>1.78</b>	0.018	0.010	<b>1.86</b>
<b>Värriö</b>						
NO <sub>x</sub> [ug/m <sup>3</sup> ]	0.13 (0.25)	0.40	<b>0.33</b>	1.32 (3.60)	0.37	<b>3.58</b>
O <sub>3</sub> [ug/m <sup>3</sup> ]	43.2 (47.5)	53.2	0.81	46.5 (71.0)	54.9	0.85
N <sub>tot</sub> [cm <sup>-3</sup> ]	1003 (2048)	1252	0.80	1766 (5455, but 12 770 by DMPS)	1127	1.57
D <sub>p</sub> [µm]	0.16	0.13	1.21	0.05	0.14	<b>0.39</b>
CS [s <sup>-1</sup> ]	0.010 (0.018)	0.002	<b>4.50</b>	0.0004 (0.002)	0.002	<b>0.18</b>

Table 1. Mean (max) gas concentrations, particle concentrations, condensation sinks (CS) and mean particle size at three SMEAR stations in Finland during two smoke days (27.7.2010 and 8.8.2010) and several years mean concentrations for these days as reference.

During the two most remarkable smoke days in Finland in the summer of 2010 (selected on the basis of observations by Mielonen *et al.*, 2011 and concentration – time series measured at SMEAR stations) the most clearly observed biomass burning parameters thinking of the long-range transport originated from the fire areas were carbon dioxide (CO) and black carbon (BC) compared to several mean concentrations. Also SO<sub>2</sub> concentration has been elevated on 29 July in Hyytiälä, but the sulphur dioxide is generally speaking that kind of parameter that the peaks can due to industrial nearby as well. In the case of the Värriö station it is mentioned that the 8 of August has been NPF (new particle formation) event day which explain the particle results there at the time. The condensation sink (CS) is the parameter, which characterizes the maximum rate of condensation of surrounding vapour to particle surfaces (Kulmala *et*

al., 2001). Also the condensation sink values have been elevated at all three stations during both fire days, except for 8 of August in Värriö.

## CONCLUSIONS

In conclusion it can be said that the Russian wild fire emissions can be detected also in Finland if the wind direction is from fire areas to Finland. The best long-range transport fire emission indicators are black carbon, carbon monoxide and particle concentration. To get more information about fire emissions transported to Finland we have to investigate for instance carbon monoxide and other gases or particle data correlations to resolve which of the parameters correlate with each other. In this method the reference period can be the shorter smokeless period during the same summer.

## ACKNOWLEDGEMENTS

The financial support by the Academy of Finland Centre of Excellence program (project no 1118615) is gratefully acknowledged.

## REFERENCES

Bertschi, I. T. and Jaffe, D. A. (2005). Long-range transport of ozone, carbon monoxide, and aerosols to the NE Pacific troposphere during the summer of 2003: Observations of smoke plumes from Asian boreal fires. *J. Geophys. Res.*, **110**, D05303, doi:10.1029/2004JD005135.

Draxler, R.R. (1999). HYSPLIT4 user's guide. NOAA Tech. Memo. ERL ARL-230.

IPCC (the Intergovernmental Panel on Climate Change) (2007). Climate Change 2007: The Physical Science Basis. Summary for Policymakers. Contribution of Working Group I to the Fourth Assessment Report of the Intergovernmental Panel on Climate Change [Solomon, S., D. Qin, M. Manning, Z. Chen, M. Marquis, K.B. Averyt, M. Tignor and H.L. Miller (eds.)]. Cambridge University Press, Cambridge, United Kingdom and New York, NY, USA. Available online at [http://www.ipcc.ch/publications\\_and\\_data/ar4/wg1/en/spm.html](http://www.ipcc.ch/publications_and_data/ar4/wg1/en/spm.html).

Konovalov, I. B. et al., (2011). Atmospheric impacts of the 2010 Russian wildfires: integrating modelling and measurements of an extreme air pollution episode in the Moscow region. *Atmos. Chem. Phys.*, **11**, 10031–10056.

Kulmala, M., et al., (2001). On the formation, growth and composition of nucleation mode particles, *Tellus B*, **53**, 479–490.

Mielonen, T., et al., (2011). Biomass burning aerosols observed in Eastern Finland during the Russian wildfires in summer 2010 – Part 2: Remote sensing. *Atmos. Env.*, **1–9**.

WHO (2006): Health Risks of Particulate Matter from Long-range Transboundary Air Pollution. Joint WHO/Convention Task Force on the Health Aspects of Air Pollution., WHO Regional Office for Europe, Copenhagen.

# TEMPERATURE INFLUENCE ON NATURAL AEROSOL PRODUCTION POTENTIALS OVER BOREAL FORESTS

L. LIAO<sup>1</sup>, V. M. KERMINEN<sup>1</sup>, M. BOY<sup>1</sup>, M. KULMALA<sup>1</sup> and M. D. MASO<sup>1</sup>

<sup>1</sup>Division of Atmospheric Sciences, Department of Physics, University of Helsinki, P.O.Box 48, 00014, Helsinki, Finland

Keywords: aerosol, temperature, BVOCs.

## INTRODUCTION

Atmospheric aerosol has climatic influence, and affects air quality and human health. The source of atmospheric aerosols includes both natural and anthropogenic origins. Secondary aerosol formed via the oxidation of biogenic volatile organic compounds accounts for the most significant fraction among the global aerosol budget. The boreal forest emitted VOCs, in particular terpenes, have shown to be one of the important aerosol precursor sources linking to the secondary aerosol production in northern hemisphere (Tunved et al., 2006). The emission of biogenic VOCs is temperature dependent, thus it may influence the secondary aerosol production as well as the CCN loading (Tunved et al., 2008), which further forms the vegetation, aerosol and climate interaction system (Kulmala et al., 2004).

In this work, we investigate the potential and the order of magnitude of the temperature influence on the natural aerosol budgets; we discuss the natural aerosol growth at different size ranges in different temperature bins from back trajectory analysis.

## METHODS

The research and data analysis were based on the measurements at two Finnish SMEAR (Station for Measuring Ecosystem-Atmosphere Relations) stations: SMEAR I (67°46' N, 29°35' E, 400 m asl) in Värriö, and SMEAR II (61°51' N, 24°17' E, 170 m asl) in Hyytiälä, Finland. 13 year dataset from 1998 to 2010 at SMEAR I and 15 year dataset between 1996 and 2010 at SMEAR II have been used, including continuously DMPS measurements, temperature and backward trajectory data. The DMPS particle size spectrums were divided into three size modes: the nucleation mode in the particle size range of 3--25 nm, Aitken mode (25--100 nm), and accumulation mode (100--1000 nm). Particle number concentrations at each mode were calculated every one hour. Hourly particle volume concentrations were integrated from the DMPS size distribution assuming spherical particles. The hourly 96 hour backward trajectories arriving at 100 m a.g.l over both stations were calculated from the HYSPLIT4 model (Draxler et al., 1997).

Trajectories transporting 90% of time in one 180° transport sector 0°N-180°S relative Värriö, and travelled only above 60° North at the SMEAR I station, and one 180° transport sector 90°W-90°E relative Hyytiälä at the SMEAR II station, (seen in Figure 1), were extracted from the whole dataset. The travelling time over land for each trajectory was estimated from topographical data. The temperature along each trajectory was equally separated to 5 bins from 0 to 20 Celsius degrees.

## CONCLUSIONS

The preliminary results suggest that temperature plays a strong role on controlling the growth of aerosol particles (see. E.g. Figure 2). First, temperature controls the precursor emissions of secondary aerosols, which will directly link to the volume and mass growth of aerosol particles. Second, temperature influences the gas/particle partitioning mechanisms. However, temperature has various influences on aerosol particles at different mode

## ACKNOWLEDGEMENTS

The Authors wish to thank the Maj and Tor Nessling foundation for financial support (grant No 2009362), as well as the Academy of Finland Center of Excellence program (project number 1118615).

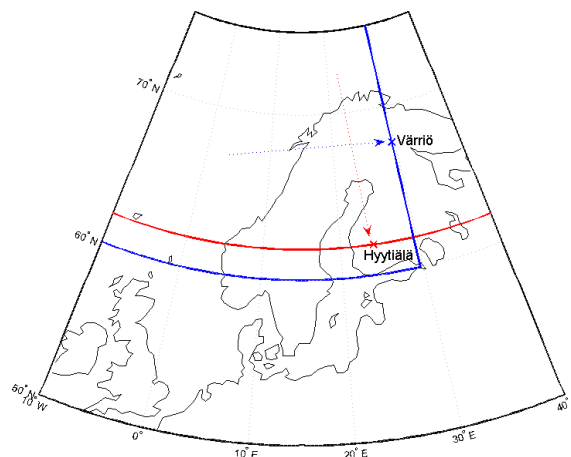


Figure 1. The transport sectors of back trajectories at the two stations. Area above red line is the travelling zone of selected trajectories arriving at Hyttiälä station. The blue sector covers the transport area of trajectories arriving at Värriö station. At both stations, each trajectory should spend at least 90% of travelling time inside the transport sectors.

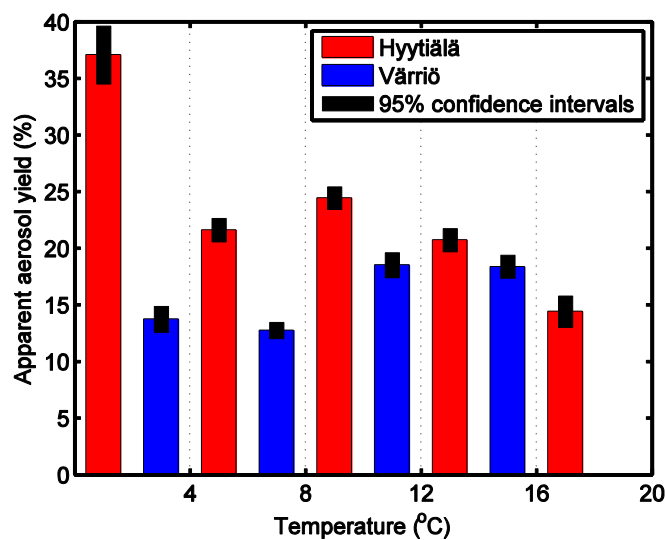


Figure 2. Estimated aerosol yield (i.e. the direct fitting slope between aerosol mass and total monoterpene emission) in five temperature bins both at the SMEAR I station (blue bars) and the SMEAR II station (red bars). The black bars indicate 95% confidence intervals from the fitting slopes at both stations.

## REFERENCES

Draxler, R. R. & G. D. Hess (1997) Description of the Hysplit\_4 modelling system. *NOAA Tech Memorandum*, ERL ARL-224.

- Tunved, P., H. C. Hansson, V. M. Kerminen, J. Strom, M. Dal Maso, H. Lihavainen, Y. Viisanen, P. P. Aalto, M. Komppula & M. Kulmala (2006) High natural aerosol loading over boreal forests. *Science*, 312, 261-263.
- Tunved, P., J. Stroem, M. Kulmala, V. M. Kerminen, M. Dal Maso, B. Svenningsson, C. Lunder & H. C. Hansson (2008) The natural aerosol over Northern Europe and its relation to anthropogenic emissions - implications of important climate feedbacks. *Tellus Series B-Chemical and Physical Meteorology*, 60, 473-484.
- Kulmala, M., T. Suni, K. E. J. Lehtinen, M. Dal Maso, M. Boy, A. Reissell, U. Rannik, P. Aalto, P. Keronen, H. Hakola, J. B. Back, T. Hoffmann, T. Vesala & P. Hari (2004) A new feedback mechanism linking forests, aerosols, and climate. *Atmospheric Chemistry and Physics*, 4, 557-562.

# **FREEZING ASSOCIATED DEPRESSION OF PHOTOSYNTHESIS OF SCOTS PINE SEEDLINGS**

L. LINDFORS<sup>1,2</sup>, T. HÖLTTÄ<sup>1</sup>, A. LINTUNEN<sup>1</sup>, A. PORCAR-CASTELL<sup>1</sup>, E. NIKINMAA<sup>1</sup>, E. JUUROLA<sup>1,2</sup>.

<sup>1</sup>Department of Forest Sciences, University of Helsinki, P.O. BOX 27, FI-00014 University of Helsinki, Finland

<sup>2</sup>Department of Physics, University of Helsinki, P.O. BOX 64, FI-00014 University of Helsinki, Finland

Keywords: Photosynthesis, freezing, water potential, diameter change

## **INTRODUCTION**

The ability to photosynthesize by plants can be restricted by low temperatures in the winter. This has been recently studied in the field (Strand et al. 2002, Schwarz, Fahey & Dawson 1997, Schaberg et al. 1995) and in controlled freezing experiments (Gaumont-Guay et al. 2003, Strand, Öquist 1985). Conifers are able to avoid freezing to some extent by supercooling i.e. by preventing ice nucleation in xylem and extracellular spaces (Burke et al. 1976). When freezing eventually occurs, conifers freeze extracellularly to hinder lethal intracellular freezing (Burke et al. 1976). The exact freezing temperature can be identified based on the exothermic reaction.

In response to ice masses formed in extracellular space following a freezing, a steep water potential gradient develops between living cells and the ice due to the low water potential of ice and the living cells lose water to the apoplast and dehydrate, shrink and their water potential decrease. Both xylem and living bark diameter change due to changes in the water content of these tissues (Sevanto et al. 2011). Diameter change measurements of the xylem (Irvine, Grace 1997) and living bark (Mencuccini et al. 2013) have been used to study the water status of the xylem and phloem, respectively.

Several different factors may contribute to the depression of photosynthesis during freezing. The depression may result from (A) decreased mesophyll conductance, (B) biochemical limitations in the Calvin cycle or (C) decreased stomatal conductance. Mesophyll cells also experience freezing associated water stress that can result to factors A and B. The stomatal closure (C) typically occurs to limit transpiration, and the further decrease of water potential in the plant. Our aim was to investigate the importance and coordination of freezing associated dehydration of living and the importance of the different factors contributing to the depression of photosynthesis.

## **METHODS**

Measurements were carried out with 4 year old *Pinus sylvestris* seedlings in 8 runs of freeze-thaw treatment inside a climate chamber under 150  $\mu\text{mol m}^{-2} \text{s}^{-1}$  illumination. During the runs leaf gas exchange, chlorophyll fluorescence and xylem and living bark diameter changes and temperature in various parts of the plants were followed.

## **RESULTS & DISCUSSION**

Our measurement revealed perhaps for the first time a rapid decline in leaf gas exchange following a freezing in xylem and parallel shrinking in xylem and living bark diameters (see figure 1). The shrinking of the diameters can be explained with water relation changes in the tissues following dehydration of living cells due to extracellular freezing. While our measurements involve only the xylem and living bark, all living cells including mesophyll cells are likely to experience a similar dehydration driven by the low water potential of ice.

The freezing and the decrease in photosynthesis was followed by an increase in intercellular CO<sub>2</sub> concentration (ci). Similar increase in ci has been observed also in previous investigations (Strand et al. 2002, Gaumont-Guay et al. 2003, Strand, Öquist 1985).

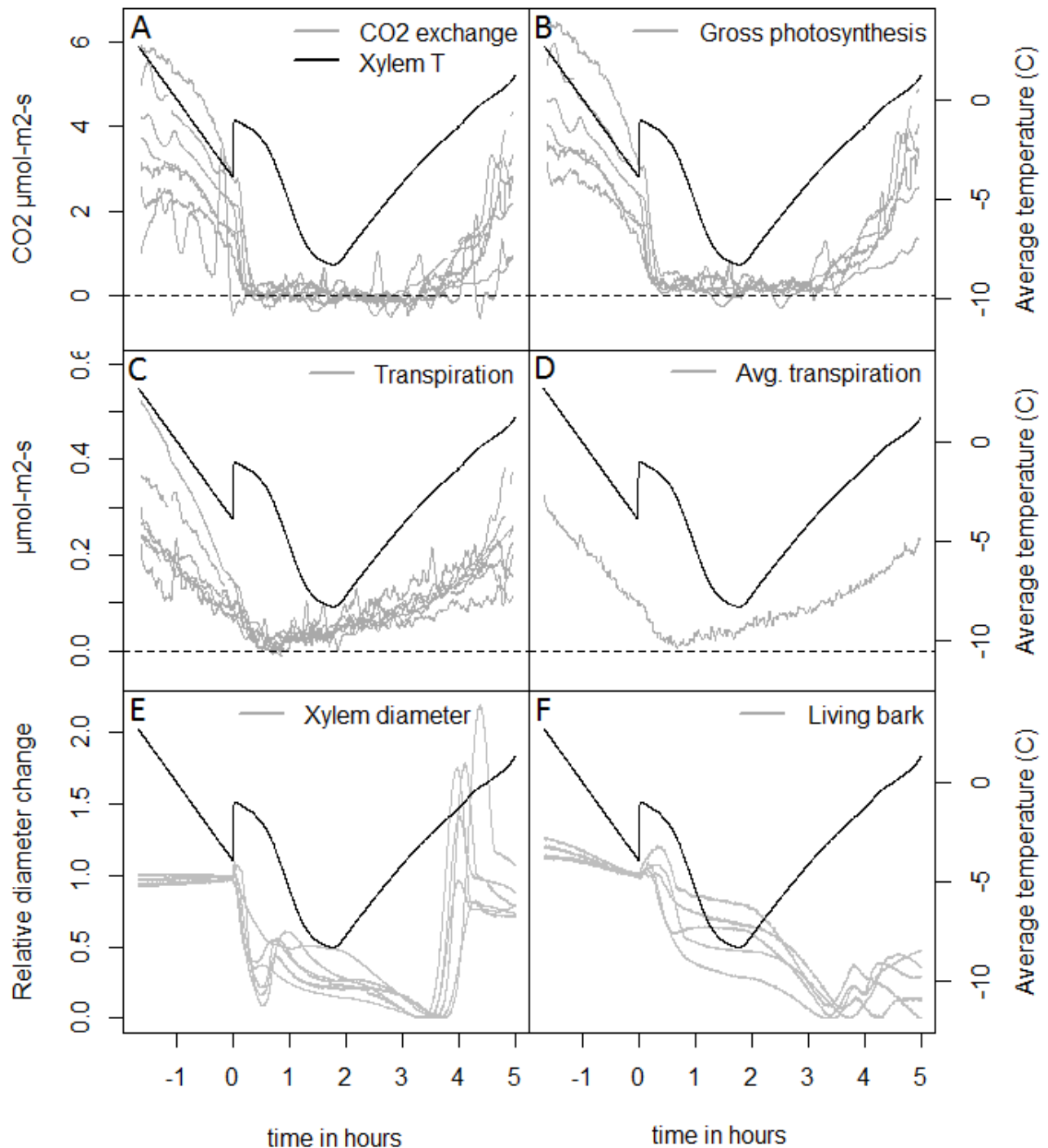


**Figure 1.** Dynamics in gas exchange and diameter changes during freeze-thaw treatments. The zero in the time x-axis refers to beginning time of freezing in the xylem. The xylem temperature and the average transpiration (box D) are the averages of 7 discrete runs. Gas exchange data is averaged temporally by 15 points in boxes A, B and C and by 5 points in box D. N for gas exchange in boxes A-D is 7, for xylem diameter change 6 and for living bark 5. Value 1 in the y-axis of the relative diameter change refers to a diameter at the beginning time of freezing and 0 refers to the minimum diameter during a run.

## ACKNOWLEDGEMENTS

This study was supported by the Academy of Finland Finnish Centre of Excellence in Physics, Chemistry, Biology and Meteorology of Atmospheric Composition and Climate Change.

## REFERENCES

- Burke, M.J., Gusta, L.V., Quamme, H.A., Weiser, C.J. & Li, P.H. 1976, "Freezing and Injury in Plants", *Annual Review of Plant Physiology and Plant Molecular Biology*, vol. 27, pp. 507-528.
- Gaumont-Guay, D., Margolis, H.A., Bigras, F.J. & Raulier, F. 2003, "Characterizing the frost sensitivity of black spruce photosynthesis during cold acclimation", *Tree physiology*, vol. 23, no. 5, pp. 301-311.
- Irvine, J. & Grace, J. 1997, "Continuous measurements of water tensions in the xylem of trees based on the elastic properties of wood", *Planta*, vol. 202, no. 4, pp. 455-461.
- Mencuccini, M., Holtta, T., Sevanto, S. & Nikinmaa, E. 2013, "Concurrent measurements of change in the bark and xylem diameters of trees reveal a phloem-generated turgor signal", *New Phytologist*, vol. 198, no. 4, pp. 1143-1154.
- Schaberg, P.G., Wilkinson, R.C., Shane, J.B., Donnelly, J.R. & Cali, P.F. 1995, "Winter Photosynthesis of Red Spruce from 3 Vermont Seed Sources", *Tree physiology*, vol. 15, no. 5, pp. 345-350.
- Schwarz, P.A., Fahey, T.J. & Dawson, T.E. 1997, "Seasonal air and soil temperature effects on photosynthesis in red spruce (*Picea rubens*) saplings", *Tree physiology*, vol. 17, no. 3, pp. 187-194.
- Strand, M., Lundmark, T., Soderbergh, I. & Mellander, P.E. 2002, "Impacts of seasonal air and soil temperatures on photosynthesis in Scots pine trees", *Tree physiology*, vol. 22, no. 12, pp. 839-847.
- Strand, M. & Öquist, G. 1985, "Inhibition of Photosynthesis by Freezing Temperatures and High Light Levels in Cold-Acclimated Seedlings of Scots Pine (*Pinus-Sylvestris*) .1. Effects on the Light-Limited and Light-Saturated Rates of Co<sub>2</sub> Assimilation", *Physiologia Plantarum*, vol. 64, no. 4, pp. 425-430.

# THE IMPACT OF POSSIBLE PRIMING EFFECT ON DIFFERENT CO<sub>2</sub> BALANCE IN TWO FORESTRY-DRAINED PEAT SOILS

M. LINKOSALMI<sup>1</sup>, C. BIASI<sup>2</sup>, J. PUMPANEN<sup>3</sup>, J. HEINONSALO<sup>4</sup>, A. LINDEN<sup>3</sup> AND A. LOHILA<sup>1</sup>

<sup>1</sup>Climate Change Research, Finnish Meteorological Institute, Helsinki, Finland

<sup>2</sup>Department of Environmental Science, University of Kuopio, Finland

<sup>3</sup>Department of Forest Sciences, University of Helsinki, Finland

<sup>4</sup>Department of Food and Environmental Sciences, University of Helsinki, Finland

Keywords: Carbon balance, forestry-drained peatlands, priming effect, isotopes.

## INTRODUCTION

Natural peatlands are globally a major carbon (C) store. Soil C has been accumulating to peatlands over thousands of years in humid conditions. Land-use changes cause significant shifts in the C balance, for example draining a peatland for forestry or agricultural use changes the hydrology and increases the decomposition of old C (Laiho 2006). Managed peatlands can be a source of C to the atmosphere depending on the use, in forestry-drained peatlands this can also be the opposite. About third of the land area in Finland has originally been covered by peatlands, but nowadays approximately half of this area has been drained, mostly for forestry use (Vasander et al. 1996). The soil carbon pools can be divided into soil organic matter (SOM) originating from dead plant residues and to organic substrates that are released by living roots via exudation and leaching (Kuzyakov 2006). Microorganisms produce CO<sub>2</sub> from these pools through decomposition via the heterotrophic respiration pathway. In addition, also plant roots contribute significantly to CO<sub>2</sub> emissions from soils through autotrophic respiration. Separating these different respiration fluxes is crucial for determining CO<sub>2</sub> losses from soils and thus evaluating the various components of CO<sub>2</sub> balance of ecosystems. Isotopic methods using intact soil-root systems to separate the root and rhizosphere respiration are increasingly applied (e.g. Hanson *et al.* 2000). These methods are based on the different isotopic signature between the soil respiration and root and plant derived respiration. The C cycle of two forestry-drained peatlands in Southern Finland has been studied by eddy covariance method for many years. The peatlands are located close to each other and both were drained about 40 years ago. The difference between these two sites is the nutrient status; the nutrient-rich site was originally fen and the the nutrient-poor site was a bog. According to the eddy covariance measurements the nutrient-rich site, Lettosuo, is a source of C to the atmosphere (Lohila *et al.* 2010), whereas the nutrient-poor site, Kalevansuo, is a strong C sink (Lohila *et al.* 2011). We hypothesize that the differences in C balance between these two sites could be explained by the peat nutrient status and in particular by the differences in priming effect between the sites. Priming effect stands for a change in old C decomposition when fresh C is added to soil. To test this we conducted two laboratory-scale C isotope experiments.

## METHODS

We studied the priming effect in two separate experiments: 1) at the natural abundance level (<sup>14</sup>C) by planting Scots pine (*Pinus sylvestris*) seedlings to peat and 2) by adding <sup>13</sup>C-labelled glucose to bare peat samples, thus simulating root exudation. In the Experiment 1 we used microcosm systems (Pumpanen *et al.* 2009) to simulate plant-soil conditions and utilized the natural difference in <sup>14</sup>C (age) between peat and plants. The Scots pine seedlings were planted to deep (old) and surface (young) peat. Photosynthesis and respiration were measured altogether four times every 1–2 months during the six month study period. In the end of the experiment <sup>14</sup>CO<sub>2</sub> respired from the peat was collected with molecular sieves. The <sup>14</sup>C samples were prepared and analyzed by the Radiocarbon Dating Laboratory in the University of Helsinki. The <sup>14</sup>CO<sub>2</sub> dating was done only for the deep peat samples to see the difference between the old (old peat) and the fresh (seedling) C more clearly, which is needed to reliably apply the isotopic mixing models for

source partitioning. In the Experiment 2 the excretion of recent photosynthates was simulated by adding  $^{13}\text{C}$ -labelled glucose to peat samples. In this experiment only surface peat was used for 120 peat samples. Half of these samples were labelled with  $^{13}\text{C}$ -glucose and also nutrients were added to 30 labelled and 30 non-labelled samples. Respiration was measured during three weeks and the gas samples of  $^{13}\text{CO}_2$  were taken regularly. The  $\text{CO}_2$  of soil respiration was analyzed with the gas chromatograph (Hewlett Packard 5890 Series II) and the  $^{13}\text{CO}_2$  samples with the isotope ratio mass spectrometer (Thermo Fisher Finnigan Delta Plus).

## CONCLUSIONS

In these experiments we observed negative priming or no priming at all, at both study sites. This indicates that the fresh plant-derived carbon or labelled sugar did not increase the decomposition of the old peat. Additionally, we showed that the nutrient status does not play a crucial role in plant-mediated impacts on the peat decomposition. However, the results of the labelling experiment showed that the basal respiration rate of the fresh nutrient-rich peat is much higher than that of nutrient-poor, which can at least partly explain the observed differences in the ecosystem  $\text{CO}_2$  balances. In the natural abundance experiment the difference was not so clear. This might be due to the longer incubation time in this experiment: most of the easily available C has probably been used already during the incubation period. We can conclude that the *in situ* respiration was higher in the nutrient-rich site, Lettosuo, but the difference between the sites disappeared quickly in the laboratory conditions. High soil respiration rates *per se* could explain the net C loss at the nutrient-rich site, observed earlier, even though the tree growth is much greater there. The overall differences in the C balances between the two sites under examination cannot be explained by different activation/deactivation of peat decomposition in the presence of plants (priming effect).

## ACKNOWLEDGEMENTS

This work was supported by the Maj and Tor Nessling foundation, Academy of Finland Center of Excellence program (project number 1118615), and EU-project GHG Europe (244122).

## REFERENCES

- Hanson, P.J., Edwards, N.T., Garten, C.T. & Andrews, J.A. 2000. Separating root and soil microbial contributions to soil respiration: A review of methods and observations. *Biogeochemistry*, 48, 115-46.
- Kuzyakov, Y. 2006. Sources of  $\text{CO}_2$  efflux from soil and review of partitioning methods. *Soil Biology and Biochemistry*, 38, 425-48.
- Laiho, R. 2006. Decomposition in peatlands: Reconciling seemingly contrasting results on the impacts of lowered water levels. *Soil Biology and Biochemistry*, 38, 2011-24.
- Lohila, A., Aurela, M., Hatakka, J., Tuovinen, J.-P., Penttilä, T., Ojanen, P., Laurila, T. 2011. *Biogeosciences*, 8, pp. 3203-3218.
- Pumpanen, J. S., Heinonsalo, J., Rasilo, T., Hurme, K.-R., Ilvesniemi, H. 2009. Trees-Structure and Function 23, pp.611-621.
- Vasander, H., Korhonen, R., Aapala, K., Laine, J., Myllys, M., Ruuhijärvi, R. & Sopo, R. 1996. Suomen suot (Peatlands in Finland).

# GAS BURSTS DURING FREEZING HELP TREES TO AVOID WINTER EMBOLISM

A. LINTUNEN, L. LINDFORS, P. KOLARI, E. NIKINMAA, E. JUUROLA and T. HÖLTÄ

Department of Forest Sciences, University of Helsinki,  
P.O. BOX 27, FI-00014 University of Helsinki, Finland

Keywords: freeze-thaw embolism, *Picea abies*, *Pinus sylvestris*, stem CO<sub>2</sub>-flux

## INTRODUCTION

Winter embolism is an important factor for tree survival and growth in all regions where sub-zero temperatures occur. Winter embolism is caused by formation of gas bubbles during freezing and subsequent expansion during thawing (e.g. Sucoff, 1969; Pittermann and Sperry, 2003, 2006). Gases are not soluble in ice and are thus forced to form bubbles when the xylem sap freezes. The fate of gas bubbles during thawing, i.e. whether they will collapse or expand to embolise xylem conduits, is dependent on the size of the gas bubbles and the pressure of the surrounding xylem sap according to the LaPlace law (Pittermann and Sperry, 2006). It has been empirically shown in several studies that the pressure causing winter cavitation is dependent on the diameter of the conduit (e.g. Davis *et al.*, 1999; Sperry and Robson, 2001). This dependency has been theorized to be related to larger volume of dissolved gases in larger conduits leading to formation of larger bubbles at freezing (Pittermann and Sperry, 2006).

One major assumption made in connection with the theory of the dependence of winter embolism on conduit size is that all the gas is trapped inside the conduits upon freezing. We will test this assumption here. Ice proceeds inside trees rather fast (e.g. Kitaura, 1967; Pramsohler *et al.*, 2012), concentrating the dissolved gases in front of the moving ice front (Sevanto *et al.*, 2012), and a large concentration difference between the gas inside the conduits and the inter-conduit spaces and further outside air is created. This concentration difference can be expected to accelerate the diffusion of gases out from the stem, at least as long as the stem is not completely frozen.

## METHODS

We conducted laboratory measurements with three Scots pine and three Norway spruce seedlings by measuring the CO<sub>2</sub> efflux out of the stem during freezing, and evaluated the fraction of the CO<sub>2</sub> bursting out from the xylem during freezing. We also analyze additional measurements of CO<sub>2</sub> efflux from an adult Scots pine tree during freezing and thawing conducted in field conditions in years 2006-2009.

## RESULTS

Both laboratory experiments and field measurements showed clear bursts in CO<sub>2</sub> efflux upon freezing (Figs. 1, 2). In laboratory experiments, the size of the burst relative to the CO<sub>2</sub> content within xylem was on average 47% if respiration was assumed to drop down at the moment of freezing and 16% if respiration was assumed to follow temperature with the same relationship while frozen as it did in warm temperatures (Fig. 1). In the field, 24 clear CO<sub>2</sub> efflux bursts were analyzed and the relative size of the burst was from 26% to 51% (Fig. 2) depending on the assumed CO<sub>2</sub> concentration within stem on scale 2 to 4% (Hari *et al.*, 1991).

The burst started on average 4.8 min after the freezing exotherm and continued on average 37 minutes in the laboratory measurements, which is more or less the length of the freezing exotherm. In field, the duration of the burst was on average 9 hours.

## DISCUSSION

We showed here empirically that all gases dissolved in liquid water upon freezing are not trapped inside the ice in the stem as previously assumed. In terms of the prevailing theories of winter embolism, our results give new insight to the proportionality between water volume within a conduit and the size of the gas bubbles forming upon freezing. Results of this study imply that in addition to conduit size that determines the initial gaseous volume within the conduit, the efficiency of extraction of gases from the conduit upon freezing could be a crucial factor affecting the risk of embolism upon thawing.

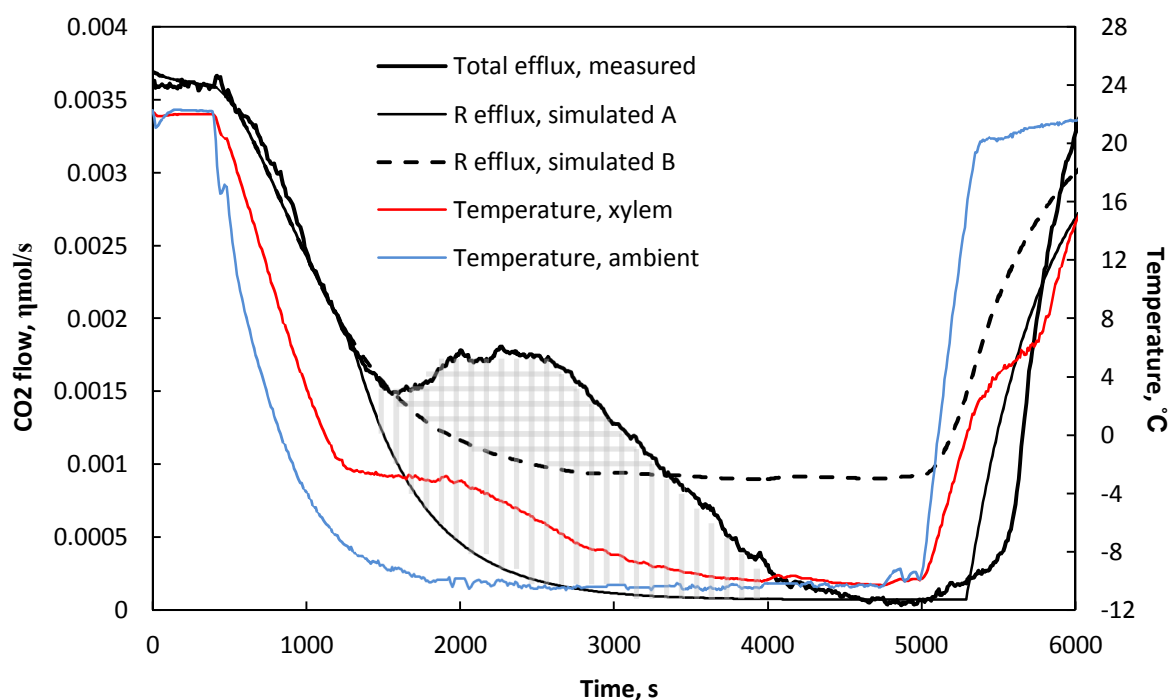


Figure 1. An example of a freezing experiment conducted in a climate chamber for a pine sapling. Measured total CO<sub>2</sub> efflux during the freezing experiment is shown together with two different assumptions of stem respiration efflux and temperatures measured from the xylem and from the climate chamber. In approach A, respiration rate was dropped after the freezing exotherm down to the level measured after the burst has settled, and in approach B, respiration was extrapolated to temperatures while frozen using the same relation which was obtained for the respiration rate before freezing. The integral between the measured CO<sub>2</sub> total efflux and simulated respiration efflux represents the burst of CO<sub>2</sub> out of the stem due to freezing, which is shown for both approaches with grey area.

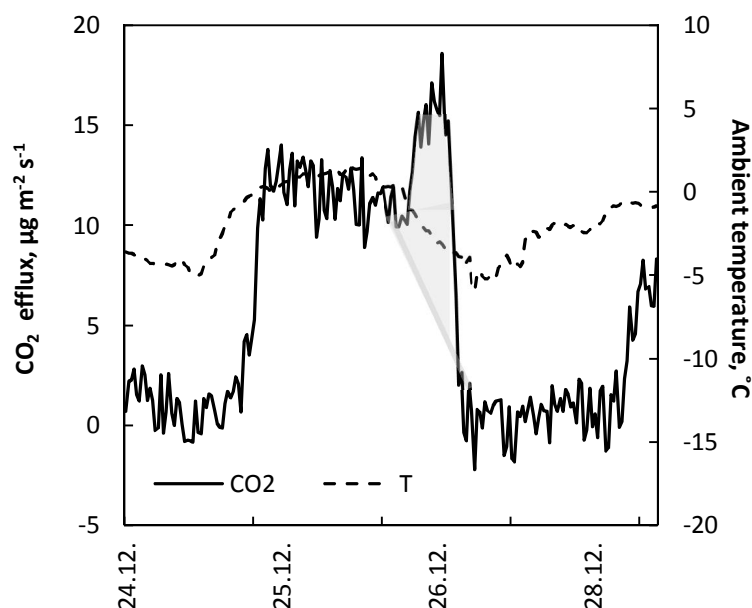


Figure 2. Selected time series of CO<sub>2</sub> efflux measured from pine stem on field in year 2008. CO<sub>2</sub> burst is marked with grey circles. The ambient temperature was measured near the top of the tree.

Results obtained regarding the relative size of the burst were of same magnitude in the laboratory and on field. Also the difference in the temporal length of the burst between laboratory and field measurements was of similar magnitude relative to the difference in stem size. Length of the freezing process is in terms of heat diffusion dependent on the volume of the stem and stem surface area.

In addition to CO<sub>2</sub>, xylem sap consists of other dissolved gases, namely N<sub>2</sub> and O<sub>2</sub>. The proportions of these three different gases dissolved in the xylem sap are 0.94 moles of N<sub>2</sub> and 0.53 moles of O<sub>2</sub> per mole of CO<sub>2</sub>. The diffusion coefficients of N<sub>2</sub> and O<sub>2</sub> are 2.5 and 1.7 times higher than that of CO<sub>2</sub>. This means that CO<sub>2</sub> is the slowest gas to diffuse out from the liquid phase to the air phase inside the stem. However, only a minor proportion of N<sub>2</sub> and O<sub>2</sub> are expected to diffuse out from the stem to ambient air due to the small diffusion gradient compared to CO<sub>2</sub>, but the dissolution of N<sub>2</sub> to the air phase inside the stem would raise the pressure inside the stem, thus creating pressure driven mass flow of air from the stem to the ambient air, which is much faster than diffusion.

## REFERENCES

- Davis, S.D., J.S. Sperry JS and U.G. Hacke (1999). The relationship between xylem conduit diameter and cavitation caused by freezing. *American Journal of Botany* 86: 1367–1372.
- Hari, P, P. Nygren and E. Korpilahti (1991). Internal circulation of carbon within a tree. *Can. Journal of Forest Research* 21: 514–515.
- Kitaura, K. (1967). Supercooling and ice formation in mulberry trees. In: Asahina E, ed. *Cellular injury and resistance in freezing organisms: international conference on low temperature science* vol. 2. Hokkaido, Hokkaido University. 143–156.
- Pittermann, J. and J.S. Sperry (2003). Tracheid diameter is the key trait determining the extent of freezing-induced embolism in conifers. *Tree Physiology* 23: 907–914.
- Pittermann, J. and J.S. Sperry (2006). Analysis of freeze–thaw embolism in conifers. The interaction between cavitation pressure and tracheid size. *Plant Physiology* 140: 374–382.
- Pramsohler, M., J. Hacker and G. Neuner (2012). Freezing pattern and frost-killing temperature of apple (*Malus domestica*) wood under controlled conditions and in nature. *Tree Physiology* 00, 1–10.
- Sevanto, S., N.M. Holbrook and M. Ball (2012). Freeze/thaw-induced embolism: probability of critical bubble formation depends on speed of ice formation. *Frontiers in Plant Science* 3, 107.
- Sperry, J.S. and D.J. Robson (2001). Xylem cavitation and freezing in conifers. In: Bigras FJ, Colombo SJ, eds. *Conifer cold hardiness*. Dordrecht, the Netherlands: Kluwer Academic Publishers, 121–136.
- Suuff, E. (1969). Freezing of conifer xylem and the cohesion–tension theory. *Physiologia Plantarum* 22: 424–431.

# CH<sub>4</sub> AND N<sub>2</sub>O FLUXES IN A SPRUCE FOREST IN NORTHERN FINLAND

A. LOHILA<sup>1</sup>, T. PENTTILÄ<sup>2</sup> and T. LAURILA<sup>1</sup>

<sup>1</sup>Finnish Meteorological Institute, Climate Change Research, PO Box 503, FI-00101 Helsinki, Finland.

<sup>2</sup>Finnish Forest Research Institute, Vantaa Research Unit, PO Box 18, FI-01301 Vantaa, Finland

Keywords: ECOSYSTEM-ATMOSPHERE INTERACTION, GREENHOUSE GASES, FLUX MEASUREMENTS, BOREAL FOREST.

## INTRODUCTION

Forest soils are considered as an important sink of atmospheric methane (CH<sub>4</sub>) (e.g. Steudler *et al.*, 1989; Jang *et al.*, 2006). Uptake of CH<sub>4</sub> occurs due to the microbial methane oxidation in the soil surface, the rate of which is enhanced in dry soils (Billings *et al.*, 2000), in soils with thin organic layer (Borken and Beese, 2006), and at sites with low atmospheric N deposition (Butterbach-Bahl *et al.*, 2002). Forest soils are, on the other hand, typically sources of nitrous oxide (N<sub>2</sub>O) (Pilegaard *et al.*, 2006). Although soil moisture (Davidson *et al.*, 2000) and C/N ratio (Pilegaard *et al.*, 2006) has been shown to be important, the factors controlling the production of N<sub>2</sub>O in upland forest soils are not understood as well as the exchange of CH<sub>4</sub>. Fluxes of both CH<sub>4</sub> and N<sub>2</sub>O can vary much both spatially and temporally (Christiansen *et al.*, 2012). For example, there can be wet CH<sub>4</sub>-emitting microsites in forest where rest of the soil area is acting as a CH<sub>4</sub> sink, or there can be periods of soil inundation during which the forest soil turn into a CH<sub>4</sub> source (Savage *et al.*, 1997).

Recently there has been debate on the correct method to calculate the chamber fluxes (e.g., Pihlatie *et al.* 2012; Levy *et al.*, 2011). The main concern in this debate is related to the underestimation of the flux if using a linear fit when calculating the flux from the consecutive concentration measurements in the closed chamber. Some papers have suggested that using a non-linear fit reduces this error, while others have stated that non-linear and linear fit give equally high fluxes, or even that the method of non-linear fit is prone to uncertainties or errors, as the small concentration differences during the first seconds of chamber closure may introduce a serious bias on the flux estimate (Pihlatie *et al.*, 2012; Koskinen *et al.*, 2013).

Here we present initial results of the measurements of CH<sub>4</sub> and N<sub>2</sub>O exchange conducted with a static chamber and snow gradient method in a spruce forest in northern Finland between October 2010 and December 2012. The specific objectives are to 1) find out the best flux calculation method and 2) to quantify the seasonal dynamics of these two greenhouse gases.

## METHODS

The measurement site, Kenttäröva spruce forest (67°59.3'N, 24°14.4'E, 347 m asl), is located on the top of a moderate hill in Kittilä municipality, northern Finland. It is part of the Pallaslompola catchment, which is an intensive monitoring area of e.g. GHG and energy fluxes, hydrology, water chemistry, ecology, and meteorology. The waters from the western side of the hill drain into the lake Pallasjärvi through the Lompolaänkkä fen, both of which have the facilities to measure GHG fluxes. At Kenttäröva forest, CO<sub>2</sub>, H<sub>2</sub>O and sensible heat fluxes between the ecosystem and atmosphere have been measured since 2003 with the eddy covariance method. There is also an official weather station of Finnish Meteorological Institute at the site. Main tree species is Norway spruce (*Picea abies*), the ground floor being dominated by *Vaccinium myrtillus*, *Empetrum nigrum*, *Vaccinium vitis-idaea* and forest mosses. The

soil type at the site is moraine, in which the proportion of the fine material ( $< 63 \mu\text{m}$ ) at 20-40 cm depth is about 23 % (Derome *et al.*, 2001).

In fall 2010 we started sampling the soil  $\text{CH}_4$  and  $\text{N}_2\text{O}$  fluxes using a static chamber method. We installed 7 steel collars (60 cm x 60 cm) carefully into the soil at depth of ca. 5 cm. Every 2-3 weeks each collar was covered with a steel chamber (height 30 cm), which was installed, prior to the measurements, on the shallow groove covered with foam to prevent excess leakage of the gas out from the chamber. There was a battery powered fan in the chamber. Four 20 ml samples were drawn with a syringe from the chamber during the 35-min closure and transferred into glass vials, which were sent to laboratory and analyzed using the gas chromatography. Fluxes were calculated based on the concentration change in the chamber. In winter time, when the snow cover exceeded 30 cm, flux was determined by taking samples from the snowpack and just above it. The flux was calculated based on the concentration difference between the soil and snow surfaces and the diffusivity of the gas in the snow. The porosity of snow, which is needed to calculate the diffusion rate, was determined by weighing a known volume of snow at the same time with the concentration measurements.

### THE EFFECT OF CALCULATION METHOD ON THE FLUXES

We tested different methods for the calculation of fluxes. In a situation of  $\text{CH}_4$  uptake, the concentration decrease in the closed chamber was typically either linear, or the slope was slightly reducing along the time. To test how consistent the reduction of the uptake rate during the chamber closure was, we show in Table 1 the ratio of fluxes calculated using first 2, 3 or 4 points (first we calculated for each single measurement the ratio of slopes calculated using either 3 or 4 (and 2 or 4) points, and then took the mean of these ratios). The higher the ratio, the higher the underestimation of the flux due to the linear fitting. As Table 1 indicates, the fluxes were underestimated by 7.7% if calculated using a linear fit for all 4 points, as compared to using only first 2 points. Similarly, fluxes were underestimated on average 5.2 %, if calculated using a linear fit of 4 points instead of 3. However, the uncertainty gets larger when using fewer points for flux calculation. Here, in the further analysis we decided to use the fluxes calculated using the linear fit of the first 3 points, as the resulting flux is on average only slightly smaller as compared to two-point-fit, but the error in the estimate is remarkably lower (Table 1).

Flux calculation method	Ratio $\pm$ SE [-]
Ratio of slopes with 3/4 points	$1.052 \pm 0.019$
Ratio of slopes with 2/4 points	$1.077 \pm 0.048$

Table 1. Ratio of fluxes calculated using 3 or 4 points (and 2 or 4 points) in the linear fit of  $\text{CH}_4$  concentration measured in the chamber.

### SEASONAL AND ANNUAL DYNAMICS IN $\text{CH}_4$ AND $\text{N}_2\text{O}$ FLUXES

The forest soil acted as a small  $\text{CH}_4$  sink from September 2010 to August 8, 2011, the flux rate varying from  $-2.6 (\pm 1.3)$  to  $-0.23 (\pm 0.55) \text{ mg CH}_4 \text{ m}^{-2} \text{ d}^{-1}$ , with lowest and highest uptake occurring in winter and summer, respectively (mean  $\pm$  stdev is given, minus sign indicates flux from the atmosphere to soil). In mid-August 2011, the forest soil turned into a  $\text{CH}_4$  source of  $88 (\pm 23) \text{ mg CH}_4 \text{ m}^{-2} \text{ d}^{-1}$ , the source persisting most of the time until the next January (Fig. 1). During summer and fall 2012, the soil sink was recovered to the level observed in previous summer. The switch from a sink to source was probably due to the wet conditions in fall 2011, which have not only reduced the diffusion rate of  $\text{CH}_4$  into the soil, but also resulted in deficiency of  $\text{O}_2$  in the soil, enabling the microbial production of  $\text{CH}_4$ . The observed flux rates outside this exceptionally wet autumn were typical for forest soils. For example, Jang *et al.* (2006) estimated, based on a literature review, that the mean methane uptake rate in forest soils was  $1.9 \text{ mg m}^{-2} \text{ d}^{-1}$ , higher uptake being observed at deciduous as compared to coniferous forests. Also, the switch of an

upland forest soil from a CH<sub>4</sub> sink to a source during wet conditions has been reported earlier (e.g., Savage *et al.*, 1997).

For N<sub>2</sub>O, the soil was a continuous source during the study period of over 2 years, the flux rate varying between 0 and 0.4 mg m<sup>-2</sup> d<sup>-1</sup>. The N<sub>2</sub>O emissions were smaller during the snow gradient measurements, which raises a question on the reliability of the estimation of the diffusion rate in the snowpack.

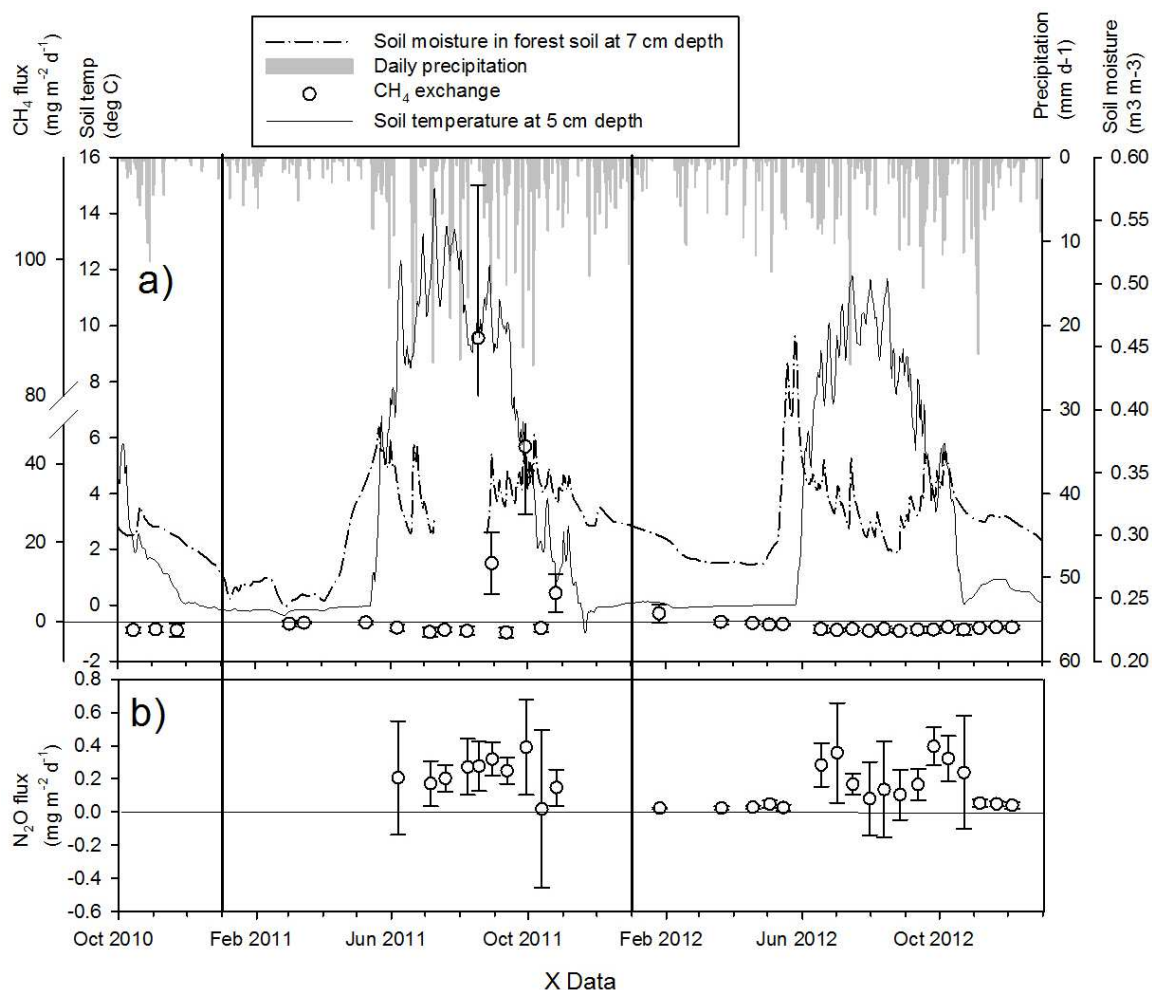


Figure 1. a) Soil CH<sub>4</sub> exchange, soil moisture, precipitation and soil temperature and b) N<sub>2</sub>O efflux at the Kenttäröva spruce forest in October 2010 – December 2012. Horizontal lines show the zero level of fluxes and bold vertical lines indicate the start of the year.

During the growing season, methane uptake was related to soil temperature, higher uptake occurring with higher temperatures. This may be related to soil moisture, as the moisture and temperature are likely to correlate inversely. For N<sub>2</sub>O, the relationship was of same direction but less evident (results not shown). Fluxes of both gases showed a relationship with soil moisture: with increasing moisture, the CH<sub>4</sub> uptake was reduced and N<sub>2</sub>O emission increased (Fig. 3). For methane, this correlation was evident only for the measurements taken during the snow-free season and outside the episodic CH<sub>4</sub> emission peak in fall 2011.

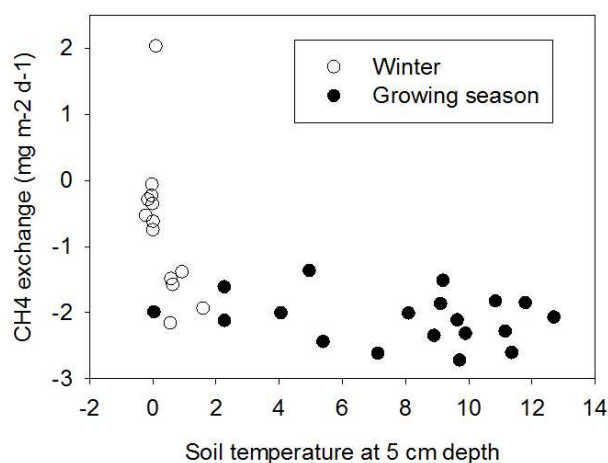


Figure 2. Methane exchange plotted against soil temperature. Fluxes measured during the wet soil period in fall 2011 are excluded.

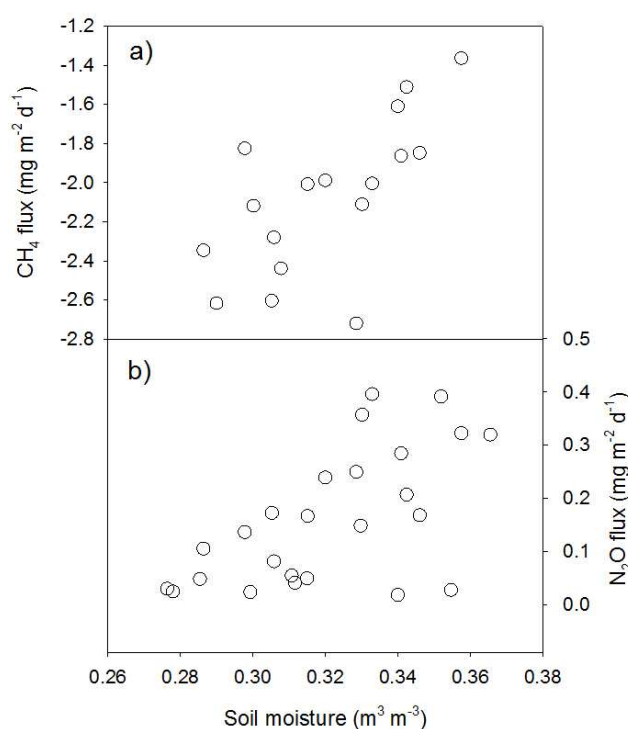


Figure 3. a) Methane and b) nitrous oxide exchange plotted against soil moisture. In a) only data with  $\text{CH}_4$  exchange rate  $< -1 \text{ mg m}^{-2} \text{ d}^{-1}$  (i.e., the black dots in Fig. 2) has been plotted.

## CONCLUSIONS

For our data set, the most appropriate flux calculation method appeared to be the linear fit using first three measurements points. This is a compromise between the flux underestimation and flux reliability. The fluxes of  $\text{CH}_4$  varied more temporally than spatially. Most of the time, even in winter, the soil acted as a  $\text{CH}_4$  sink, however in very wet autumn 2011 the soil turned to a large  $\text{CH}_4$  source in many occasions. Regarding  $\text{N}_2\text{O}$ , the spruce forest acted as a source during the whole study period. During the non-winter

period when the soil was not excessively wet, the CH<sub>4</sub> and N<sub>2</sub>O fluxes show a correlation with soil moisture and temperature, with higher N<sub>2</sub>O emission and lower CH<sub>4</sub> uptake during wetter and cooler periods. It is still unclear, which one is a more important control for these fluxes, soil moisture or temperature.

## ACKNOWLEDGEMENTS

We are grateful for the Academy of Finland Center of Excellence (project no 1118615) and the Nordic Center of Excellence DEFROST.

## REFERENCES

- Billings, S.A., D.D. Richter and J. Yarie (2000). Sensitivity of soil methane fluxes to reduced precipitation on boreal forest soils, *Soil Biol. Biochem.* **32**, 1431–1441.
- Borken, W. and F. Beese (2006). Methane and nitrous oxide fluxes of soils in pure and mixed stands of European beech and Norway spruce, *European J. Soil Sci.* **57**, 617–625.
- Butterbach-Bahl, K., L. Breuer, R. Gasche, G. Willibald and H. Papen (2002). Exchange of trace gases between soils and the atmosphere in Scots pine forest ecosystems of the northeastern German lowlands 1. Fluxes of N<sub>2</sub>O, NO/NO<sub>2</sub> and CH<sub>4</sub> at forest sites with different N-deposition, *Forest Ecol. Managem.* **167**, 123–134.
- Christiansen, J.R., L. Vesterdal and P. Gundersen (2012). Nitrous oxide and methane exchange in two small temperate forest catchments – effects of hydrological gradients and implications for global warming potential of forest soils, *Biogeochem.* **107**, 437–454.
- Derome, J., A.-J. Lindroos and M. Lindgren (2001). Soil acidity parameters and defoliation degree in six Norway spruce stands in Finland, *Water, Air, and Soil Pollution: Focus* **1**: 169–186.
- Jang, I., S. Lee, J.-H. Hong and H. Kang (2006). Methane oxidation rates in forest soils and their controlling variables: a review and a case study in Korea, *Ecol. Res.* **21**, 849–854.
- Koskinen, M., K. Minkkinen, P. Ojanen, M. Kämäräinen, T. Laurila, A. Lohila (2013). Measurements of CO<sub>2</sub> exchange with an automated chamber system throughout the year: challenges in measuring nighttime respiration on porous peat soil, *Biogeosciences Discuss.*, **10**, 14195–14238.
- Levy, P.E., A. Gray, S.R. Leeson, J. Gaiawyn, M.P.C. Kelly, M.D.A. Cooper, *et al.* (2011). Quantification of uncertainty in trace gas fluxes measured by the static chamber method, *European J. Soil Sci.* **62**, 811–821.
- Pihlatie, M., J.R. Christiansen, H. Aaltonen, J.F.J. Korhonen, A. Nordbo, T. Rasilo, *et al.* (2013). Comparison of static chambers to measure CH<sub>4</sub> emissions from soils, *Agric. For. Meteorol.* **171–172**, 124–136.
- Pilegaard, K., U. Skiba, P. Ambus, C. Beier, N. Brüggemann, K. Butterbach-Bahl, *et al.* (2006). Factors controlling regional differences in forest soil emission of nitrogen oxides (NO and N<sub>2</sub>O), *Biogeosci.* **3**, 651–661.
- Savage, K., T.R. Moore and P.M. Crill (1997). Methane and carbon dioxide exchanges between the atmosphere and northern boreal forest soils, *J. Geophys. Res.* **102**, D24, 29279–29288.
- Steudler, P.A., R.D. Bowden, J.M. Melillo and J.D. Aber (1989). Influence of nitrogen fertilization on methane uptake in temperate forest soils, *Nature*, **341**, 314–316.

# INSIGHTS INTO ATMOSPHERICALLY RELEVANT MOLECULAR COLLISIONS FROM FIRST-PRINCIPLES MOLECULAR DYNAMICS

V. LOUKONEN, N. BORK and H. VEHKAMÄKI

Division of Atmospheric Sciences, Department of Physics, University of Helsinki, Helsinki,  
P.O. Box 64, FI-00014 University of Helsinki, Finland.

Keywords: ATMOSPHERIC CLUSTERS, MOLECULAR DYNAMICS, MOLECULAR COLLISIONS, SULFURIC ACID.

## FIRST-PRINCIPLES MOLECULAR DYNAMICS AND THE ATMOSPHERE

First-principles molecular dynamics (FPMD) simulation is a modern, versatile and powerful computational method. In FPMD one typically integrates the classical equations of motion of the system of interest to obtain the dynamics of the system. As one of the most important unsolved problems in Earth sciences is the formation and growth of atmospheric aerosol particles (Kulmala et al., 2011), we shall concentrate here on atmospherically relevant molecular systems. In practice, to integrate the equations of motions, one needs to obtain the forces driving the dynamics. In FPMD simulations the forces are obtained by solving the electronic Schrödinger equation of the system in question. The remaining necessary boundary conditions are set by defining the system to be studied: the identities and the initial positions and velocities of the atomic nuclei of the molecular cluster to be investigated. In other words, one is free to specify any desired atmospherically interesting system, and the FPMD simulation show how the system evolves under the fundamental laws of nature – FPMD simulation is as close as one can get to performing “computer experiments”. For example, FPMD simulations can be used to study the stability, energetics and dynamical structural properties of various sulfuric acid clusters (Loukonen et al., 2013a). In addition, the method enables the investigation of molecular collision processes. For example, FPMD collision simulations can be used to obtain insight into the possible reaction pathways in SO<sub>2</sub> oxidation or into the formation dynamics of sulfuric acid nanoclusters. We shall discuss these examples in the next section.

## INSIGHTS

The oxidation process of SO<sub>2</sub> is the most important source of sulfuric acid in the atmosphere. The bottleneck in the oxidation is the step from SO<sub>2</sub> to SO<sub>3</sub> (Morokuma and Muguruma, 1994). Besides the dominant oxidation routes via OH or Criegee radicals, also atmospheric ions, such as O<sub>3</sub><sup>−</sup>, might provide an oxidation pathway via SO<sub>2</sub> + O<sub>3</sub><sup>−</sup>(H<sub>2</sub>O)<sub>n</sub> → SO<sub>3</sub><sup>−</sup>(H<sub>2</sub>O)<sub>n</sub> + O<sub>2</sub> followed by SO<sub>3</sub><sup>−</sup>(H<sub>2</sub>O)<sub>n</sub> + O<sub>3</sub> → O<sub>3</sub><sup>−</sup>(H<sub>2</sub>O)<sub>n</sub> + SO<sub>3</sub>. We used FPMD collision simulations to investigate the first step of such an oxidation pathway: the collisions between SO<sub>2</sub> and O<sub>3</sub><sup>−</sup>(H<sub>2</sub>O)<sub>5</sub>. The FPMD collision simulations are particularly suitable method for this problem, as the collisions may lead to several different reactions, not necessarily only to SO<sub>3</sub><sup>−</sup>(H<sub>2</sub>O)<sub>5</sub> + O<sub>2</sub> (Bork et al., 2013).

We performed 24 collisions with two different configurations of the target cluster O<sub>3</sub><sup>−</sup>(H<sub>2</sub>O)<sub>5</sub>. The collisions resulted in three different outcomes: (a) the incoming SO<sub>2</sub> collided with the target cluster, but no reaction took place and the SO<sub>2</sub> drifted away from the cluster, (b) SO<sub>2</sub> resulted in a sticking collision, but no reaction took place, and, (c) SO<sub>2</sub> collision induced a reaction with an outcome of SO<sub>3</sub><sup>−</sup>(H<sub>2</sub>O)<sub>5</sub> + O<sub>2</sub>. One representative collision with an outcome (c) is illustrated in Figure 1. In conclusions, the simulations suggest that only the outcome of SO<sub>3</sub><sup>−</sup>(H<sub>2</sub>O)<sub>n</sub> + O<sub>2</sub> is likely to form in

atmospheric conditions in the collisions between  $\text{SO}_2$  and  $\text{O}_3^-(\text{H}_2\text{O})_5$ . From the statistics obtained in the simulations, we were able to estimate that the reaction rate for this reaction is roughly  $3/4$  of the collision rate (Bork et al., 2013).

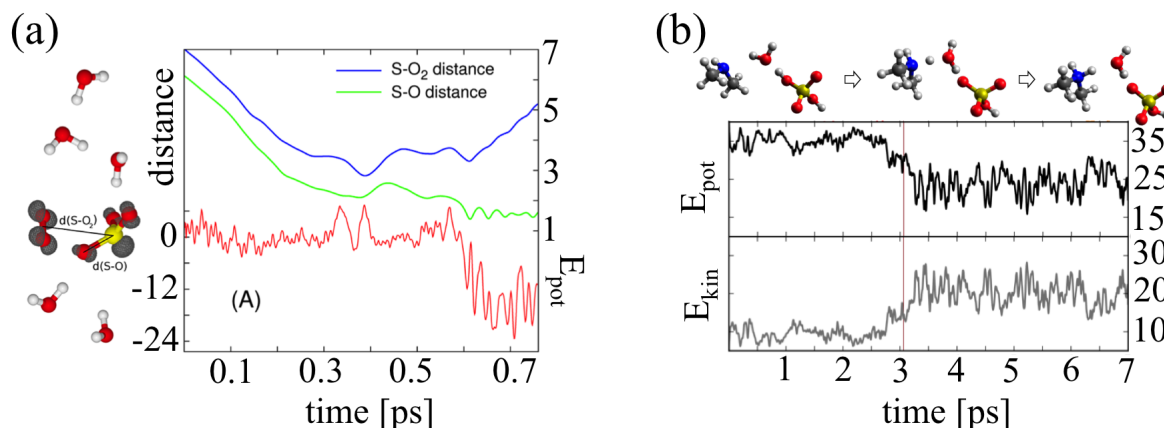


Figure 1: (a) Collision leading to  $\text{SO}_3^-(\text{H}_2\text{O})_n + \text{O}_2$ . Two descriptive distance (blue and green curves; in Å) and the potential energy (red curve; in kcal/mol) are shown as a function of time (in ps). The gray shading shows the spin density. (b) Collision leading to (sulfuric acid)<sub>1</sub>(dimethylamine)<sub>1</sub>(water)<sub>1</sub>. The time evolution of the potential energy (black curve; in kcal/mol) and the kinetic energy (gray curve; in kcal/mol) clearly show the proton transfer (marked with vertical bar). On top of the graph the proton bridge mechanism is depicted.

Besides probing the possible reaction paths, FPMD collision simulations provide ideal means to investigate the very first steps of sulfuric acid nanocluster formation dynamics. Recently, the involvement of various amine compounds, such as dimethylamine, in sulfuric acid driven particle formation has attracted some attention. In this scheme the formation of (sulfuric acid)<sub>1</sub>(dimethylamine)<sub>1</sub> cluster is of utmost importance (Olenius et al., 2013). We used FPMD collision simulations to shed light into the formation details of the cluster. Straightforward collisional approach allowed us to address the important questions regarding the sticking factor, proton transfer and the ion pair dynamics of the newly-formed cluster. Furthermore, as in atmospheric conditions sulfuric acid is typically hydrated by at least one water molecule, we also studied the collision of (sulfuric acid)<sub>1</sub>(water)<sub>1</sub> + (dimethylamine).

We performed twelve head-on collisions with different initial collision geometries for both the unhydrated and the hydrated case. The simulations revealed that the sticking factor in these head-on collisions is always unity. This is due (a) to the proton transfer reaction which takes place in every collision, and, (b) to the ample amount of degrees of freedom which are able to allocate some of the released energy (Loukonen et al., 2013b). In some of the hydrated simulations the water molecule mediated the proton transfer by acting as a proton bridge, one example is shown in Figure 1. The newly-formed clusters also showed very pronounced ion pair dynamics, clearly differing from equilibrium FPMD simulations. Interestingly, the existence of the water molecule was able to notably stabilize the ion pair structure.

## FUTURE AVENUES

We have demonstrated the applicability of first-principles molecular dynamics simulations to investigate atmospherically relevant molecular collision processes. In future, we will seek to uncover

the details of cluster relaxation via carrier gas collisions. Collision and equilibrium FPMD simulations combined with a metadynamics approach open up new possibilities to study cluster formation mechanisms and the entropic contributions to the formation free energies.

## ACKNOWLEDGEMENTS

This work has been supported by the Maj and Tor Nessling Foundation (project #2011200), the Academy of Finland (Center of Excellence program, project #1118615 and LASTU program, project #135054), the European Research Council (project #257360 MOCAPAF), the Villum Foundation and the Nordic Center of Excellence CRAICC. We also cordially acknowledge the CSC – IT Center for Science Ltd. and the University of Helsinki for providing computational resources.

## REFERENCES

- Bork, N, Loukonen, V., and H. Vehkamäki (2013). Reactions and Reaction Rate of Atmospheric  $\text{SO}_2$  and  $\text{O}_3^-(\text{H}_2\text{O})_n$  Collisions via Molecular Dynamics Simulations. *J. Phys. Chem. A*, **117**, 3143.
- Kulmala, M., Asmi, A., Lappalainen, H. K., Baltensperger, U., Brenguier, J.-L., Facchini, M. C., Hansson, H.-C., Hov, Ø., O’Dowd, C. D., Pöschl, U., Wiedensohler, A., Boers, R., Boucher, O., de Leeuw, G., Denier van der Gon, H. A. C., Feichter, J., Krejci, R., Laj, P., Lihavainen, H., Lohmann, U., McFiggans, G., Mentel, T., Pilinis, C., Riipinen, I., Schulz, M., Stohl, A., Swietlicki, E., Vignati, E., Alves, C., Amann, M., Ammann, M., Arabas, S., Artaxo, P., Baars, H., Beddows, D. C. S., Bergström, R., Beukes, J. P., Bilde, M., Burkhardt, J. F., Canonaco, F., Clegg, S. L., Coe, H., Crumeyrolle, S., D’Anna, B., Decesari, S., Gilardoni, S., Fischer, M., Fjaeraa, A. M., Fountoukis, C., George, C., Gomes, L., Halloran, P., Hamburger, T., Harrison, R. M., Herrmann, H., Hoffmann, T., Hoose, C., Hu, M., Hyvärinen, A., Hörrak, U., Iinuma, Y., Iversen, T., Josipovic, M., Kanakidou, M., Kiendler-Scharr, A., Kirkevåg, A., Kiss, G., Klimont, Z., Kolmonen, P., Komppula, M., Kristjánsson, J.-E., Laakso, L., Laaksonen, A., Labonnote, L., Lanz, V. A., Lehtinen, K. E. J., Rizzo, L. V., Makkonen, R., Manninen, H. E., McMeeking, G., Merikanto, J., Minikin, A., Mirme, S., Morgan, W. T., Nemitz, E., O’Donnell, D., Panwar, T. S., Pawlowska, H., Petzold, A., Pienaar, J. J., Pio, C., Plass-Duelmer, C., Prévôt, A. S. H., Pryor, S., Reddington, C. L., Roberts, G., Rosenfeld, D., Schwarz, J., Seland, Ø., Sellegri, K., Shen, X. J., Shiraiwa, M., Siebert, H., Sierau, B., Simpson, D., Sun, J. Y., Topping, D., Tunved, P., Vaattovaara, P., Vakkari, V., Veefkind, J. P., Visschedijk, A., Vuollekoski, H., Vuolo, R., Wehner, B., Wildt, J., Woodward, S., Worsnop, D. R., van Zadelhoff, G.-J., Zardini, A. A., Zhang, K., van Zyl, P. G., Kerminen, V.-M., S Carslaw, K., and Pandis, S. N. (2011). General overview: European Integrated project on Aerosol Cloud Climate and Air Quality interactions (EUCAARI) - integrating aerosol research from nano to global scales. *Atmos. Chem. Phys.*, **11**, 13061.
- Loukonen, V., Kuo, I-F. W., McGrath, M. J., and H. Vehkamäki (2013a). On the Stability and Dynamics of (sulfuric acid)(ammonia) and (sulfuric acid)(dimethylamine) clusters: a first-principles molecular dynamics investigation. Submitted to *Physical Chemistry Chemical Physics*.
- Loukonen, V., Bork, N., and Vehkamäki, H. (2013b). From collisions to clusters: first steps of sulfuric acid nanocluster dynamics. Submitted to *Physical Review A*.
- Morokuma, K., Muguruma, C. (1994). Ab Initio Molecular Orbital Study of the Mechanism of the Gas Phase Reaction  $\text{SO}_3 + \text{H}_2\text{O}$ : Importance of the Second Water Molecule. *J. Am. Chem. Soc.*, **116**, 10316.

Olenius, T., Kupiainen, O., Ortega, I. K., Kurtén, T., and Vehkamäki, H. (2013). Free energy barrier in the growth of sulfuric acid-ammonia and sulfuric acid-dimethylamine clusters. *Accepted for publication in Journal of Chemical Physics*.

# CLOUD RESOLVING MODEL SIMULATIONS OF MARINE STRATOCUMULUS CLOUD BY SEA SALT INJECTIONS

Z. MAALICK<sup>1</sup>, H. KORHONEN<sup>2</sup>, H. KOKKOLA<sup>2</sup>, A. LAAKSONEN<sup>1,3</sup> and S. ROMAkkANIEMI<sup>1</sup>

<sup>1</sup>Department of Applied Physics, University of Eastern Finland, Kuopio, 70211, Finland.

<sup>2</sup>Finnish Meteorological Institute, Kuopio Unit, Kuopio, 70211, Finland.

<sup>3</sup>Finnish Meteorological Institute, P.O.Box 503, Helsinki, 00101, Finland.

Keywords: STRATOCUMULUS CLOUDS, SEA SPRAY, AEROSOLS, CDNC.

## INTRODUCTION

Increase in the anthropogenic green house emissions, followed by increase in the concentrations, is considered as a main reason for global warming. Need for an emission cut has been acknowledged, but there is no visible change in the emission trends. Thus, researchers are trying to develop some geo-engineering methods to control the climate conditions in order to reduce or counteract the effect of the greenhouse gas emissions. Many different methods of geo-engineering has been proposed so far but increasing the brightness of stratocumulus marine clouds and mimicking of volcano eruptions by adding aerosol particles to stratosphere are considered to be the quickest ways to counteract the warming caused by anthropogenic GHG emissions. It has been suggested that the albedo of marine boundary layer clouds can be increased enough to counteract warming from up to quadrupled CO<sub>2</sub> concentrations by injecting high concentration of sea-salt particles in the air that will increase the number of cloud droplets (*Latham 1990*).

Studies has shown that marine stratocumulus geo-engineering is a potential candidate to counteract global warming but most of the studies has been conducted by using global climate models and without discussion of the detailed aerosol-cloud microphysical issues. Recent calculations using global models with size- resolved aerosol representations indicate that previously proposed sea spray producing vessel designs and emission fluxes are unlikely to lead to uniform cloud fields with high enough drop concentrations for cooling (*Korhonen et al. 2010, Partanen et al. 2011*). This may have important implications on the size of the spray vessel fleet required to achieve desired effect. Also the study by *Wang et al. (2011)*, using the cloud resolving model, shown that this kind of geoengineering is efficient only in the cases where drizzle formation is suppressed by the increased number of cloud droplets and thus the cloud thickness is increased. They also concluded that this method is less effective in polluted and water-vapor-limited regimes. However, this study did not consider radiative effect of injected CCN particles, and also the representation of aerosol particles in the model was quite simple. Recently *Jenkins et al (2013a, 2013b)* perform LES simulations with more realistic aerosol size distribution representation and found that aerosols injection are more efficient in night time. Further, it was concluded that by taking into account the water, that might partly evaporate from sea-spray causing cooling and negative buoyancy, cause delay in aerosol transport to boundary layer. The cooling due to latent heat was found to be 0.3K at maximum, and the evaporation of water was found to take place in less than 2 seconds after injection.

## METHODS

In this study we have used large eddy model UCLALES (Stevens and Seifert 2007) with the aerosol module SALSA (Kokkola et al 2007) to study aerosol-cloud interactions in a cloud resolving scale. UCLALES model has been designed to study the marine stratocumulus clouds, and

in this study we have coupled it with aerosol module to study aerosol-cloud-aerosol interaction at micro-physical level. With SALSA we are able to represent realistic aerosol size distribution found in marine environment. The number concentration of cloud droplet formed is parameterized as a function of updraft velocity in the cloud base and the aerosol size distribution present in the air parcel forming the cloud. With the model we are able to study aerosol cloud interactions in realistic conditions with artificial sea salt injections. In the study we will use typical profiles for potential temperature and moisture content as well as surface fluxes to produce boundary layer dynamics with UCLALES.

The model simulations of marine stratocumulus geoengineering are performed by assuming the vessel emits sea spray particles with a prescribed flux. Initial surface air temperature is 288K and the wind speed is 5 m/s in east-west direction. Sea-spray vessel moves with the speed of 2 m/s in south-north direction i.e. perpendicular to the wind direction. The aim is to see how well particles disperse in boundary layer before they enter the cloud and how big fraction of them is removed through sedimentation before they become cloud droplets.

We have used domain size of 4.8x8.4x1.5 km with 50m horizontal and 10m vertical resolution. In the simulations we assume continuous boundary conditions in the horizontal direction. The post injected analysis were restricted to 5 hours because we are mainly interested in the aerosol microphysics and dispersion taking place soon after emission. We have performed a 24 hours baseline simulation and performed geoengineering simulations at three different times of the day i.e. 04:00, 07:00 and 13:00. The amount of injected seawater was 15 kg/s. Different test cases were simulated at these three times i.e. inclusion and exclusion of water with injected aerosols, with and without the effect of microphysical processes like coagulation and dry deposition. All the simulations had been made on three different horizontal resolutions i.e. 300m, 150m and 50m.

## RESULTS

Example of the simulation is presented in figure 1a where particle number concentration at the emission level of 15m is shown. Emissions start at 7:00 am in the morning and lasts for 40 minutes. Here, particles are dispersing in wind direction (east-west). In the simulation the relative humidity of the emission level was around 77%, and that led to partial evaporation of water from emitted seaspray. This can be seen as a cooling in Figure 1b. The maximum cooling is around 1.7 K right after emission.

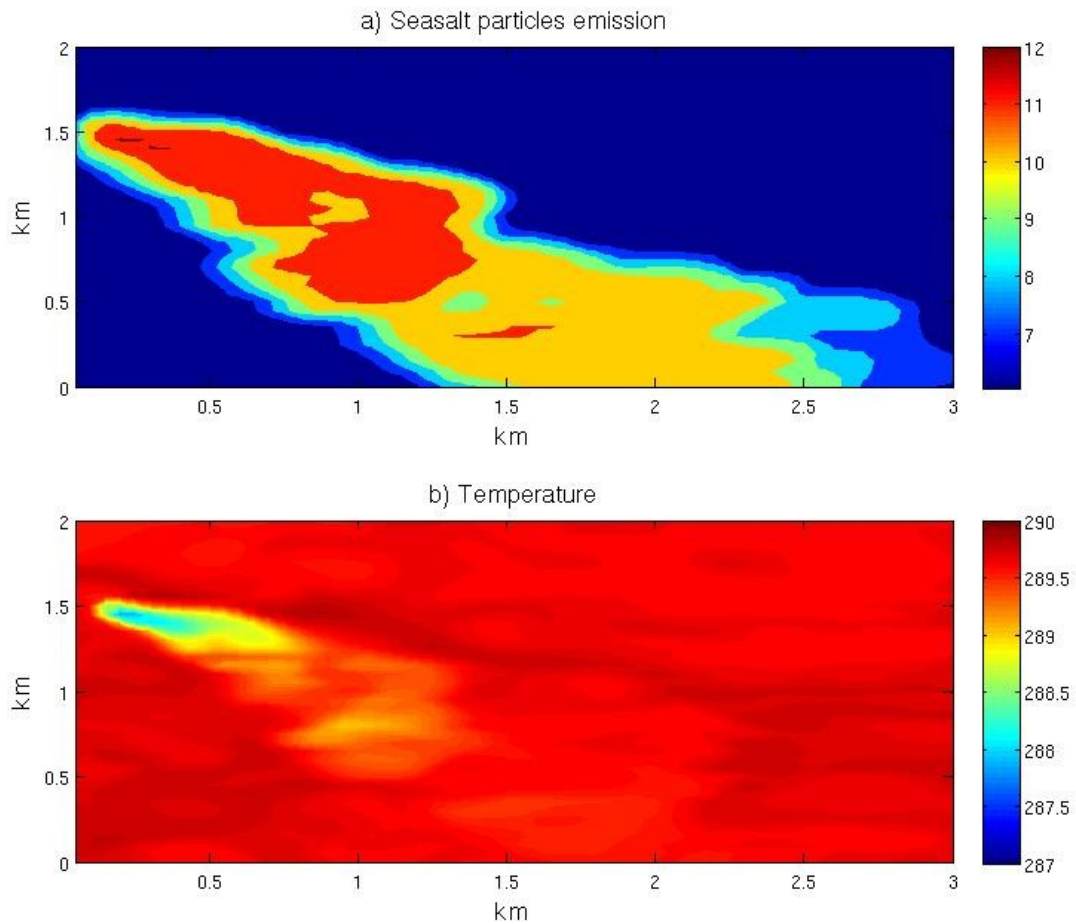


Figure 1. a) Particles number concentration at the emission altitude. Colour is 10 base logarithm of the aerosol number concentration. Size of the simulation area is  $2 \times 3 \text{ km}^2$ , and the wind is from left to right. b) Potential temperature at the emission level.

Figure 2a shows the comparison of particles emission with (WET) and without (DRY) the inclusion of water over the whole domain i.e.  $4.8 \times 8.4 \text{ Km}^2$ . Particles subtracted out over the whole domain with almost same rate. Figure 2b shows the number concentration of particles in the cloud layer. In WET case particles reaches cloud layer with a little delay. This is caused by latent heat released from evaporating sea salt particles, which will cause negative buoyancy forming a pool of cold air close to the surface. Potentially this could increase the deposition on the surface. However, as can be seen by comparing Figure 2a and 2b, later the difference cannot be seen as clearly. However, the change is small, and actually it seems like the inaccuracy in the calculation of aerosol advection is more important for aerosol concentration than the removal through sedimentation. Also it is more important to take into account the coagulation right after emission as then aerosol concentration is high leading to quick decrease in total concentration (Stuart et al 2013)

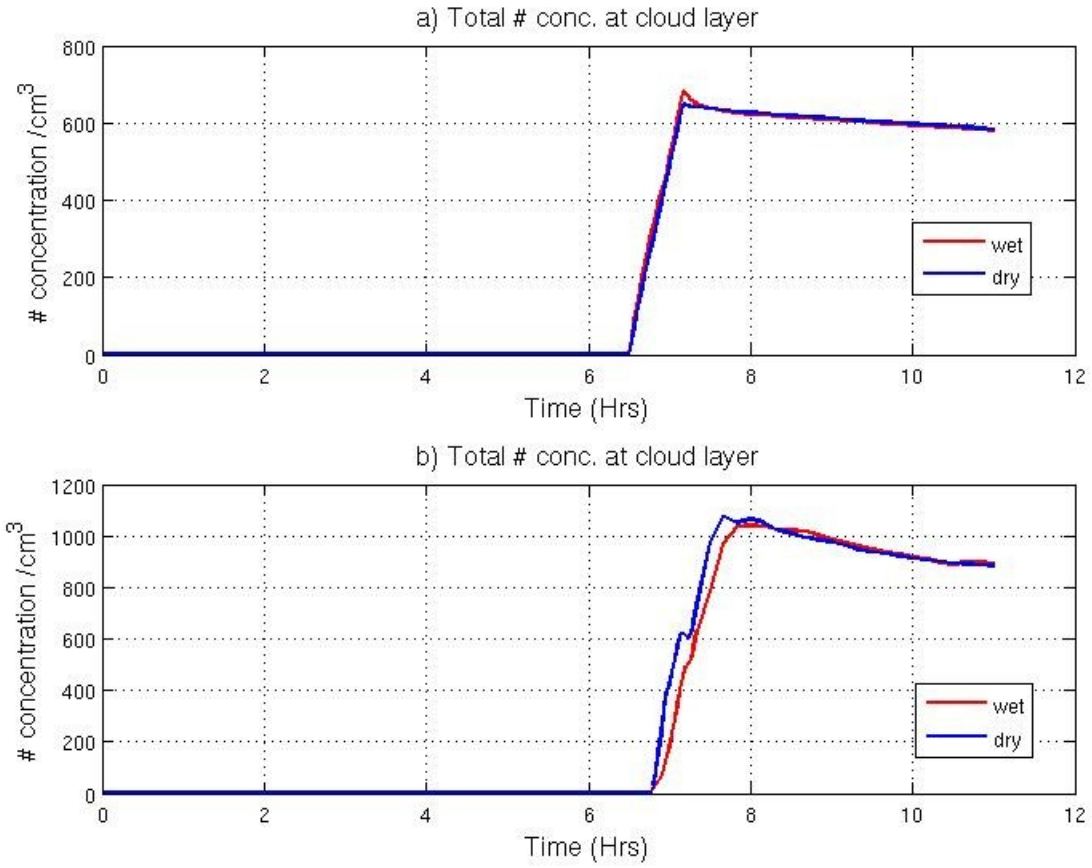


Figure 2. a) shows comparison of, WET and DRY simulation, of particle number concentration over the whole domain. b) shows number concentration of particles in cloud layer

#### ACKNOWLEDGEMENTS

This study has been supported by the Academy of Finland (project number 140907 and Center of Excellence program with project number 1118615) and by the strategic funding of the University of Eastern Finland.

## REFERENCES

- Latham, J., P. Rasch, C. Chen, L. Kettles, A. Gadian, A. Gettelman, H. Morrison, K. Bower and T. Choulaton (2008) “*Global temperature stabilization via controlled albedo enhancement of low-level maritime clouds*”, Phil. Trans. R. Soc. A 366, 3969-3987
- Wang, H., P. J. Rasch, and G. Feingold (2011) “*Manipulating marine stratocumulus cloud amount and albedo: a process-modelling study of aerosol cloud-precipitation interactions in response to injection of cloud condensation nuclei*”, Atmos. Chem. Phys., 11, 885-916
- Korhonen, H., K.S. Carslow. And S. Romakkaniemi (2010) “*Enhancement of marine cloud albedo via controlled sea spray injections: a global model study of the influence of emission rates, micro-physics and transport*”, Atmos. Chem. Phys., 10, 4133-4143
- Partanen, A.-I., H. Kokkola, S. Romakkaniemi, V. Kerminen, K. Lehtinen, T. Bergman, A. Arola and H. Korhonen (2012) “*Direct and indirect effects of sea spray geoengineering and the role of injected particle size*”. J. Geophysical research 117, 0148-0227
- Kokkola, H., H. Korhonen, K. Lehtinen, M. Kulmala, A. Partanen and A. Laaksonen (2008) “*SALSA- a sectional aerosol module for large scale application*”. Atmos. Chem. Phys., 8, 2469-2483
- Stevens B. and A. Seifert (2008) “*Understanding macrophysical outcomes of microphysical choices in simulations of shallow cumulus convection*”, J. Met.Soc. Japan , 86A , 143\_162
- Jenkins AKL, Forster PM, Jackson LS. (2013). “*The effects of timing and rate of marine cloud brightening aerosol injection on albedo changes during the diurnal cycle of marine stratocumulus clouds*”. 13: 1659–1673
- Jenkins AKL, Forster PM. (2013). “*The inclusion of water with the injected aerosols reduces the simulated effectiveness of marine cloud brightening*”. Atmospheric Science Letters 14:164–169(2013)
- Stuart GS, Stevens RG, Partanen AI, Jenkins AKL, Korhonen H, Forster PM, Sparcklen DV, Pierce JR (2013) “*Reduced efficacy of marine cloud brightening geoengineering due to in-plume aerosol coagulation: parameterization and global implications*”. Atmospheric Chemistry and Physics 13- 18679-18711

## CAN PINE TREES ACT AS SOURCES FOR NITROUS OXIDE (N<sub>2</sub>O) AND METHANE (CH<sub>4</sub>)?

KATEŘINA MACHÁČOVÁ<sup>1</sup>, MARI PIHLATIE<sup>3</sup>, ANNI VANHATALO<sup>4</sup>,  
ELISA HALMEENMÄKI<sup>3</sup>, HERMANNI AALTONEN<sup>4</sup>, PASI KOLARI<sup>3,4</sup>, JUHO AALTO<sup>4</sup>,  
JUKKA PUMPANEN<sup>4</sup>, MARIAN PAVELKA<sup>2</sup>, MANUEL ACOSTA<sup>2</sup>, OTMAR URBAN<sup>1</sup>,  
JAANA BÄCK<sup>3,4</sup>

<sup>1</sup>Laboratory of Plant Ecological Physiology, Global Change Research Centre, Academy of Sciences of the Czech Republic, Bělidla 4a, 603 00 Brno, Czech Republic

<sup>2</sup>Department of Substance and Energy Fluxes, Global Change Research Centre, Academy of Sciences of the Czech Republic, Bělidla 4a, 603 00 Brno, Czech Republic

<sup>3</sup>Department of Physics, University of Helsinki, P.O. Box 48,  
FI-00014 University of Helsinki, Finland

<sup>4</sup>Department of Forest Sciences, University of Helsinki, P.O. Box 27,  
FI-00014 University of Helsinki, Finland

Keywords: METHANE, NITROUS OXIDE, SCOTS PINE, TRANSPORT

### INTRODUCTION

Nitrous oxide (N<sub>2</sub>O) and methane (CH<sub>4</sub>) are important greenhouse gases contributing to global climate change. Both gases can be emitted from the surfaces of plants, especially from plants possessing an aerenchyma system. CH<sub>4</sub> and N<sub>2</sub>O emitted from aboveground plant surfaces can be produced by soil microorganisms followed by diffusion into roots, transport within the plant and emission into the atmosphere. The plant transport is thought to proceed via intercellular spaces and the aerenchyma system, and/or through the xylem via the transpiration stream. The release into the atmosphere can run via lenticels and/or stomata (e.g. Butterbach-Bahl *et al.*, 1997; Rusch and Rennenberg, 1998). In addition, both gases may be formed by microorganisms living inside the plant and/or by the plant itself. However, the contribution of these two sources to global emissions appears to be low.

Over the last decades, N<sub>2</sub>O and CH<sub>4</sub> emissions from plants into the atmosphere were almost exclusively studied on herbaceous species possessing an aerenchyma system (mainly rice). If trees were investigated, studies focused on species naturally living in riparian forests, which are usually well adapted to flooding (e.g. aerenchyma formation) (e.g. Rusch and Rennenberg, 1998; McBain *et al.*, 2004; Terazawa *et al.*, 2007; Gauci *et al.*, 2010; Rice *et al.*, 2010; Macháčová 2012; Machacova *et al.*, 2013). However, to our knowledge, N<sub>2</sub>O and CH<sub>4</sub> emissions have never been studied on coniferous tree species under field conditions.

The main objective of the presented study was the characterisation and quantification of CH<sub>4</sub> and N<sub>2</sub>O emissions from stems and shoots of Scots pine (*Pinus sylvestris*), as affected by soil moisture. The gas fluxes were investigated on mature trees under natural field conditions.

We hypothesised that: i) mature *P. sylvestris* can emit measurable quantities of N<sub>2</sub>O and CH<sub>4</sub> from its aboveground tissues, ii) N<sub>2</sub>O and CH<sub>4</sub> emissions from tree stems are lower compared to forest floor emissions, and iii) trees growing under higher soil moisture exhibit higher emission rates of both gases than trees growing under lower mean soil humidity.

### METHODS

The main task was to determine whether and to which extent mature *P. sylvestris* (50 years old) emits N<sub>2</sub>O and CH<sub>4</sub> from stems and shoots under field conditions. The experiments were performed at the SMEAR II measuring station in Hyytiälä, Southern Finland, from May to July 2013. Two

experimental plots with different soil moisture were selected (mean soil volumetric water content: wet (W) site  $0.75 \text{ m}^3 \text{ m}^{-3}$ , dry (D) site  $0.33 \text{ m}^3 \text{ m}^{-3}$ ). On each plot, 6 trees were chosen for stem flux measurements. Shoot emissions were measured in crowns of 3 trees at the dry site parallel to stem emissions. Forest floor emissions of both trace gases were determined parallel to tree emissions.  $\text{N}_2\text{O}$  and  $\text{CH}_4$  emissions from bottom part of stems, top level shoots, and from forest floor were measured manually using static chamber systems (Fig.1). The closure times of chambers were ca. 5.5 hours for shoot and stem chambers and ca. 40 min for soil chambers. Six gas samples were taken from each closed chamber in regular intervals, stored in glass vials (Labco Exetainer) at  $+4^\circ\text{C}$  and analysed by a gas chromatograph for  $\text{N}_2\text{O}$  and  $\text{CH}_4$  (Pihlatie *et al.*, 2013). The emission rates of both gases were calculated by using linear least square fits of time series of the gas concentration (Macháčová 2012). A temperature correction was applied.

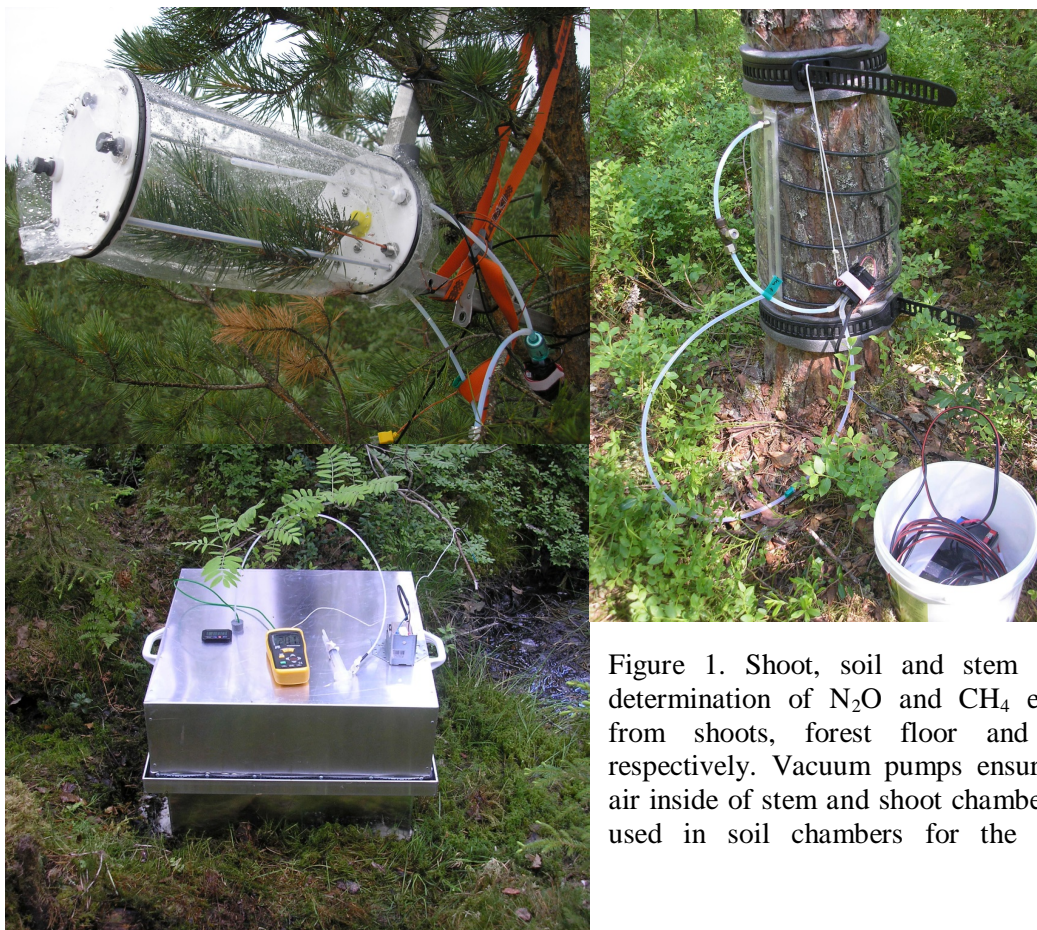


Figure 1. Shoot, soil and stem chambers for determination of  $\text{N}_2\text{O}$  and  $\text{CH}_4$  emission rates from shoots, forest floor and tree stems, respectively. Vacuum pumps ensured mixing of air inside of stem and shoot chambers. A fan was used in soil chambers for the same reason.

## RESULTS AND DISCUSSION

*P. sylvestris* emitted measurable quantities of  $\text{CH}_4$  and  $\text{N}_2\text{O}$  from its aboveground surfaces (Fig. 2, 3), which is in accordance with our first hypothesis. The stem emission rates of  $\text{CH}_4$  were significantly higher from trees growing on a wet site compared to trees at the dry site, as supposed in the third hypothesis (Fig. 2). Similar significant trend was detected in  $\text{CH}_4$  emissions from forest floor (Fig. 4). These findings are in accordance with literature (e.g. Rusch and Rennenberg, 1998; Machacova *et al.*, 2013). Forest floor emission rates of  $\text{CH}_4$  exceeded the stem emission rates on the wet site, as assumed in the second hypothesis, whereas in case of the dry site, the stems emitted small amounts of  $\text{CH}_4$  while the forest floor showed  $\text{CH}_4$  deposition. This suggests that  $\text{CH}_4$  emission from dry experimental plot seems to occur predominantly via *P. sylvestris*, as demonstrated e.g. by *Alnus glutinosa* and *Fagus sylvatica* (both Machacova *et al.*, 2013), or rice plants (e.g. Butterbach-Bahl *et al.*, 1997). This could be explained by the presence of an aerobic soil surface layer with a high  $\text{CH}_4$  consumption rate. Surprisingly, the total emission rates of  $\text{CH}_4$  from shoots of trees growing on the dry site were non-

significantly higher than emissions from stems, especially by tree n. 6 (Fig. 3). In comparison, Rusch and Rennenberg (1998) and Terazawa *et al.* (2007) demonstrated a strong decline of CH<sub>4</sub> and N<sub>2</sub>O emissions with increasing stem height by broad leaved trees, thus suggesting bottom part of stems as main release area of both gases.

Fig. 2

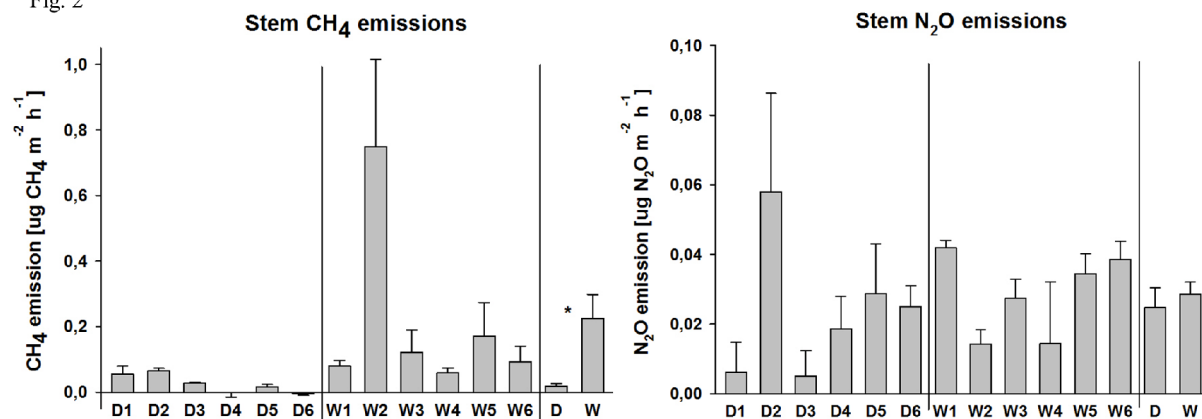


Figure 2. Stem CH<sub>4</sub> and N<sub>2</sub>O emissions as affected by soil moisture. Emissions were determined by 6 trees from dry site (tree n. D1–D6, mean of 3 to 6 replicates per tree  $\pm$  s.e.) and 6 trees from wet site (tree n. W1–W6, mean of 3 to 6 replicates per tree  $\pm$  s.e.). Bars D and W show the mean emission rates from all trees from dry (D) or wet (W) site, respectively. The emission rates from stems are related to m<sup>2</sup> of stem surface area. Statistically significant differences at  $p < 0.05$  (Mann-Whitney-U-test) between total emission rates from dry and wet site are indicated by asterisk.

Fig. 3

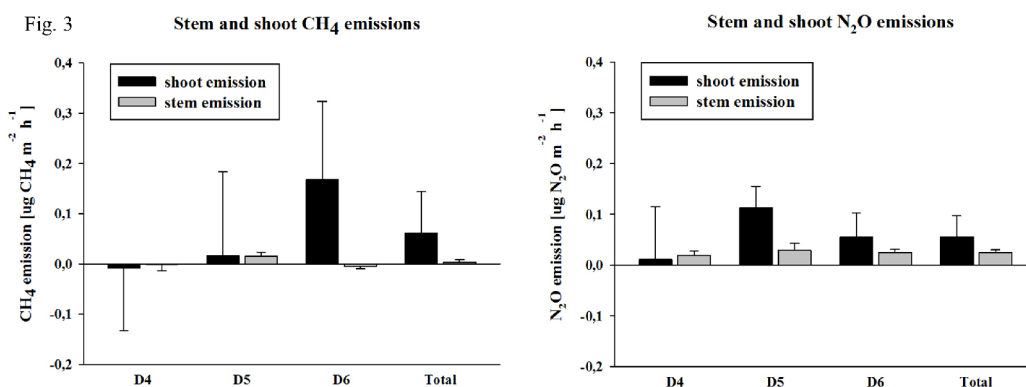


Figure 3. Shoot and stem CH<sub>4</sub> and N<sub>2</sub>O emissions parallel detected from 3 trees from dry site (tree n. D4–D6). Mean of 4 to 5 replicates  $\pm$  s.e. per tree are presented. Bars „Total“ show the mean emission rates from all 3 trees. The emission rates from stems and shoots are related to m<sup>2</sup> of stem and shoot (both needles and wooden parts) surface area, resp. No statistically significant differences at  $p < 0.05$  (Mann-Whitney-U-test) between shoot and stem emission rates were detected.

N<sub>2</sub>O emission rates from stems and shoots were in similar range as CH<sub>4</sub> emission rates. However, no statistical significant differences between wet and dry site were detected. The shoot emission rates of N<sub>2</sub>O were non-significantly higher compared to the stem emissions underlining that shoots are not-negligible sources of N<sub>2</sub>O. This fact could be explained by preferable plant transport pathway for N<sub>2</sub>O via transpiration stream and stomata by *P. sylvestris*, and/or by internal N<sub>2</sub>O production in needles. Forest floor emissions of N<sub>2</sub>O exceeded the emission rates of N<sub>2</sub>O from aboveground tree surfaces, as expected.

Fig. 4

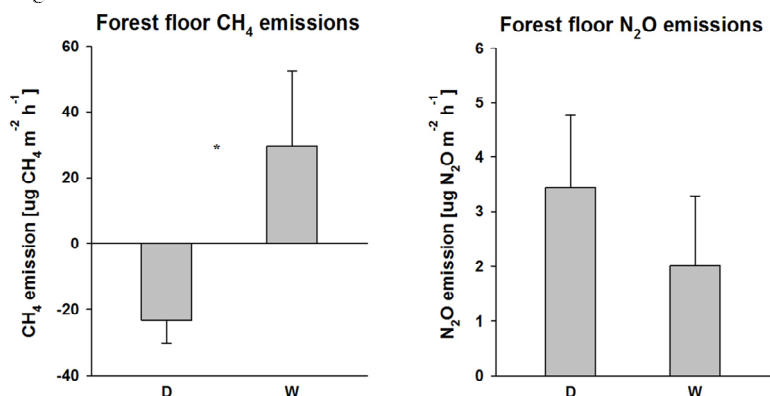


Figure 4. Forest floor CH<sub>4</sub> and N<sub>2</sub>O emissions as affected by soil moisture. Bars D and W illustrate the total emission rates (mean ± s.e.) from 3 soil chambers on dry site (D; 9 replicates per each chamber) and from 2 soil chambers on wet site (W; 6 replicates per each chamber). The emission rates from forest floor are related to m<sup>2</sup> of soil surface area. Statistically significant difference at p=0.053 (Mann-Whitney-U-test) is indicated by asterisk.

## CONCLUSIONS

The results demonstrate for the first time that mature *P. sylvestris* can emit small amounts of CH<sub>4</sub> and N<sub>2</sub>O not only from stems but also from shoots under field conditions. To our knowledge this is the first study investigating both stem and shoot emissions of CH<sub>4</sub> and N<sub>2</sub>O. N<sub>2</sub>O and CH<sub>4</sub> emissions from tree stems are lower compared to forest floor emissions with exception of CH<sub>4</sub> emissions on the dry site, where the stems emitted small amounts of CH<sub>4</sub> while the forest floor showed CH<sub>4</sub> deposition. The CH<sub>4</sub> emissions from stems of *P. sylvestris* are significantly positively affected by soil moisture.

## ACKNOWLEDGEMENTS

This research was financially supported by the ExpeER project (Experimentation in Ecosystem Research), project CzechGlobe (CZ.1.05/1.1.00/02.0073), The Academy of Finland Centre of Excellence (project 1118615) and Helsinki University Centre for Environment, HENVI.

## REFERENCES

- Butterbach-Bahl K., H. Papen and H. Rennenberg (1997). Impact of gas transport through rice cultivars on methane emission from rice paddy fields, *Plant, Cell and Environment* **20**, 1175.
- Gauci V., D.J.G. Gowing, E.R.C. Hornibrook, J.M. Davis, and N.B. Dise (2010). Woody stem methane emission in mature wetland alder trees, *Atmospheric Environment*, **44**, 2157.
- Machacova K., H. Papen, J. Kreuzwieser, and H. Rennenberg (2013). Inundation strongly stimulates nitrous oxide emissions from stems of the upland tree *Fagus sylvatica* and the riparian tree *Alnus glutinosa*, *Plant and Soil*, **364**, 287.
- Macháčová K. (2012). Nitrous oxide (N<sub>2</sub>O) and methane (CH<sub>4</sub>) emissions from stems of different tree species. Doctoral thesis, Albert-Ludwigs-Universität Freiburg, Germany.
- McBain M.C., J.S. Warland, R.A. McBride, and C. Wagner-Riddle (2004). Laboratory-scale measurements of N<sub>2</sub>O and CH<sub>4</sub> emissions from hybrid poplars (*Populus deltoids* x *Populus nigra*), *Waste Management & Research*, **22**, 454.
- Pihlatie M.K., J.R. Christiansen, H. Aaltonen, J.F.J. Korhonen, A. Nordbo, T. Rasilo, G. Benanti, M. Giebel, M. Helmy, J. Sheehy, S. Jones, R. Juszczak, R. Klefoth, R. Lobo do Vale, A.P. Rosa, P. Schreiber, D. Serca, S. Vicca, B. Wolf, and J. Pumpanen (2013). Comparison of static chambers to measure CH<sub>4</sub> emissions from soils, *Agricultural and Forest Meteorology*, **171–172**, 124.

- Rice A.L., C.L. Butenhoff, M.J. Shearer, D. Teama, T.N. Rosenstiel, and M.A.K. Khalil (2010). Emissions of anaerobically produced methane by trees, *Geophysical Research Letters*, **37**, 1.
- Rusch H. and H. Rennenberg (1998). Black alder (*Alnus glutinosa* (L.) Gaertn.) trees mediate methane and nitrous oxide emission from the soil to the atmosphere, *Plant and Soil*, **201**, 1.
- Terazawa K., S. Ishizuka, T. Sakata, K. Yamada, and M. Takahashi (2007). Methane emissions from stems of *Fraxinus mandshurica* var. *japonica* trees in a floodplain forest, *Soil Biology and Biochemistry*, **39**, 2689.

# SECONDARY AEROSOL FORMATION IN A CHANGING ENVIRONMENT

R. MAKKONEN<sup>1, 2</sup>, Ø. SELAND<sup>3</sup>, A. KIRKEVÅG<sup>3</sup>, T. IVERSEN<sup>1,3</sup> AND J.E. KRISTJÁNSSON<sup>1</sup>

<sup>1</sup> Department of Geosciences, University of Oslo, Norway.

<sup>1</sup> Department of Physics, University of Helsinki, Finland.

<sup>3</sup>Norwegian Meteorological Institute, Oslo, Norway.

Keywords: ESM, NUCLEATION, BVOC, CLIMATE FEEDBACK.

## INTRODUCTION

Several components of the Earth System will respond to a climate change. Climate feedbacks can either counteract (negative feedback) or facilitate (positive feedback) the original perturbation. One example of a negative feedback is the lapse rate: in a warmer climate the vertical temperature gradient will likely be less steep, resulting in relatively more emitted longwave radiation from Earth's atmosphere. Cryosphere provides the Earth System with a positive feedback: increasing global temperatures act to decrease the amount of sea-ice, which leads to decreased albedo and more absorption of solar radiation.

There are also several feedbacks connected to emissions and processing of atmospheric aerosols (Carslaw et al., 2010). Climate change can modify emissions from e.g. deserts, wildfires, biosphere and oceans. The most studied aerosol-related climate feedback is the CLAW hypothesis, which connects rising ocean temperatures to increased phytoplankton growth, DMS emissions and aerosol formation, eventually forming a negative feedback cycle (Charlson et al., 1987). A similar negative feedback can be found from continental biosphere, where increasing temperatures and photosynthesis could increase the emission of biogenic volatile organic compounds (BVOCs) resulting in an increase of aerosol mass and number (Kulmala et al., 2004). To study these biosphere-atmosphere interactions with Earth System Models, the models need to be equipped with detailed microphysical models describing secondary aerosol formation.

In this study, we improve the Norwegian Earth System Model NorESM (Iversen et al., 2013; Bentsen et al., 2013) in terms of nucleation, particle growth and secondary organic aerosol (SOA) formation. The model is used to study the climate effects of secondary aerosol formation in different climate and emission environments.

## NUCLEATION IN NORESM

The aerosol model in NorESM1-M (Kirkevåg et al., 2013) does not include a mechanism for atmospheric nucleation, but instead, all excess sulfuric acid after condensation is assumed to form new particles of 23.8 nm in diameter. In this work, we have removed this assumption from the NorESM and introduced several nucleation mechanisms to the model. The implemented parameterizations include binary homogeneous nucleation (BHN) by sulfuric acid and water, activation-type nucleation, kinetic-type nucleation and nucleation by organic vapors. NorESM does not include ammonia, hence ternary sulfuric acid-ammonia-water nucleation is not available at the moment.

BHN is implemented throughout the atmosphere (Vehkamäki et al., 2002). The parameterization produces a high number of particles in the upper troposphere and lower stratosphere (UTLS) but

very low nucleation rates in the boundary layer. Since BHN has been shown to be inadequate for reproducing observed nucleation rates and particle concentrations in the boundary layer, we have complemented the NorESM nucleation module with several optional boundary layer nucleation mechanisms. Activation-type nucleation (Kulmala et al., 2006) assumes that the formation of new particles is linearly proportional to sulfuric acid gas concentration,  $J_{2nm} = A[H_2SO_4]$ . The activation-type nucleation coefficient  $A$  should take into account factors other than sulfuric acid concentration. Naturally, these factors are not constant in time or space. Sulfuric acid concentration measurements are not abundant, and detailed information from nucleation is only available from campaigns. Paasonen et al. (2010) studied formation rates of 2 nm particles in four sites in Europe and found median  $A$  coefficient ranging from  $6.0 \cdot 10^{-7}$  to  $19 \cdot 10^{-7} s^{-1}$ . We have applied the median value of  $1.7 \cdot 10^{-6} s^{-1}$  (Paasonen et al., 2010) as a global activation coefficient in NorESM.

Although sulfuric acid is likely to be the main driver for atmospheric nucleation (Sipilä et al., 2010), amines, ammonia low-volatile organic vapors could play a role in the early steps of new particle formation. To account for the effect of organics on nucleation rate, we have included a parameterization which combines sulfuric acid and organics,  $J_2 = A_{S1}[H_2SO_4] + A_{S2}[ORG]$  (Paasonen et al., 2010). In this parameterization the coefficient  $A_{S1}$  is smaller than the coefficient  $A$  in pure sulfuric acid nucleation, and the nucleation rate is affected by the availability of low-volatility organic vapors. In the simulations, organic nucleation is expected to increase the natural background number concentration and decrease the anthropogenic influence, compared to activation-type nucleation.

## SOA FORMATION AND PARTICLE GROWTH

Nucleated particles of 1-2 nm size are rather irrelevant for climate as such. Further growth is needed in order to affect e.g. cloud properties. Even if the initial nucleated particle would consist mainly of sulfuric acid, organic vapors play an important role for the subsequent growth (Riipinen et al., 2011). In recent CLOUD experiments in CERN, the organic volume fraction was shown to increase from 0.4 to 0.9 when particles grew from 2 to 63 nm (Keskinen et al., 2013).

In order to improve the simulated effect of SOA formation on aerosol number, we have further developed the SOA model in NorESM. Original NorESM1-M (Kirkevåg et al., 2013) introduces SOA as a "primary" emission of OC from monthly average precursor fields. The SOA is assumed to have a diameter similar to other OC emissions. We have introduced two precursor tracers for monoterpene and isoprene. The emissions of these BVOCs are taken either from monthly prescribed MEGAN2 (Guenther et al., 2006) emissions or the interactive vegetation model CLM, which is implemented in NorESM. At the moment, only monoterpene is assumed to form SOA with a 15 % yield. Compared to the original mechanism, SOA formation in the modified version can occur also above the surface level of the model.

In NorESM, we have taken into account the growth by both sulfuric acid and organics in the size range 1-24 nm. The formation of nucleation mode particles ( $J_x$ ) is estimated from the nucleation rate  $J_{nuc}$  as (Lehtinen et al., 2007)

$$J_x = J_{nuc} \exp \left( -\gamma \cdot d_{nuc} \frac{CoagS(d_{nuc})}{GR} \right), \quad (1)$$

where the coagulation sink  $CoagS$  is calculated from the NorESM particle population and particle growth rate  $GR$  from sulfuric acid and low-volatility organic vapor concentration. We assume that 50 % of the monoterpene ozonolysis products are enough low-volatile that they can partition to the nucleated particles (below 24 nm). Currently, the information of SOA mass from new particle formation is lost, since OC mass is not transported in the nucleated mode. Improving the microphysical module to take into account SOA mass fraction is under work.

## ROLE OF NUCLEATION IN SIMULATED PARTICLE CONCENTRATIONS

Fig. 1 shows the observed and simulated aerosol number concentrations at Arctic stations Värriö and Zeppelin, and high altitude sites Moussala and South Pole. The simulated results are shown from experiments with and without nucleation. In Värriö, simulations without nucleation are clearly unable to reproduce observed concentrations outside winter months. Including nucleation in the model improves the simulated seasonal cycle, although summer concentrations are overestimated. Using organic nucleation increases summer maximum even further. The observed concentrations at Zeppelin station are almost a magnitude lower than those in Värriö, and the station is less influenced by continental biogenic emissions. All simulations capture the concentration variability rather well, although with some overestimation during October-January. In the high altitude site Moussala the observed concentrations are well reproduced by the model with nucleation included, however, the results are rather insensitive to the selected nucleation rate parameterization (activation-type or organic nucleation). The extremely low winter concentrations in South Pole are somewhat overestimated, but the overall intra-annual variation is well captured. Nucleation has very little effect in the Antarctic aerosol number concentrations, which are simulated extremely well by all experiments.

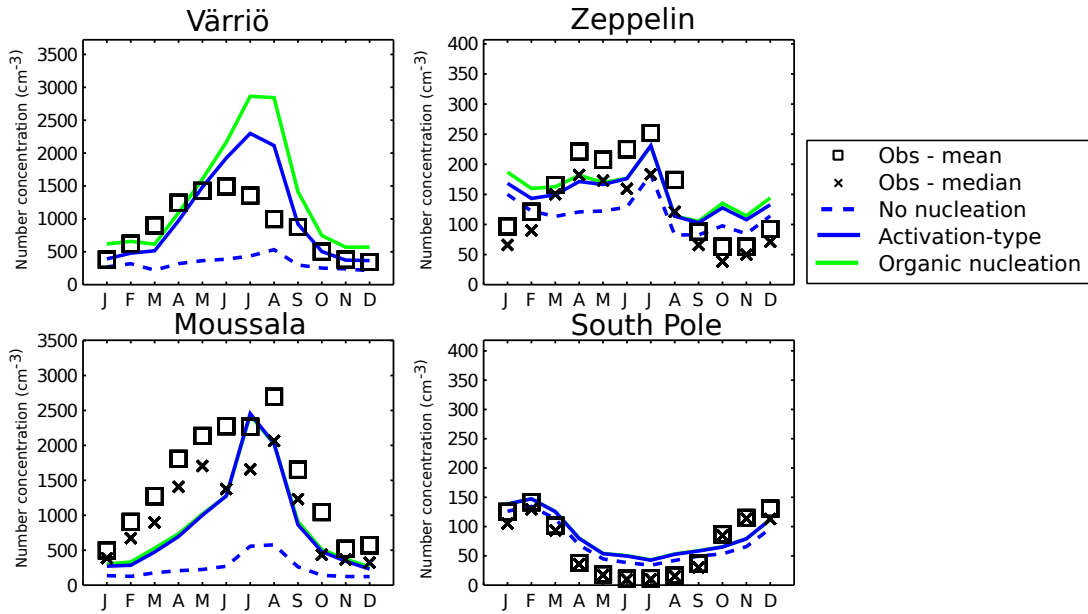


Figure 1: Simulated and observed total aerosol number concentrations ( $\text{cm}^{-3}$ ) in Värriö, Zeppeli, Moussala and South Pole. Three simulations are shown: without any nucleation (blue dashed line), activation-type nucleation (blue) and nucleation including organic vapors (green). The pie charts represent the fractional contribution of aerosol components to number concentration: SS=sea salt, SO<sub>4</sub>=sulfate, OM=organic matter, DST=dust, BC=black carbon.

In Makkonen et al. (2013), the aerosol number concentrations of NorESM are evaluated against 60 stations and 12 vertical profiles from flight observations. Altogether 10 sensitivity experiments are used to study the effects of SOA formation, black carbon size distribution and nucleation on aerosol number concentration. Including nucleation in the simulations improves the simulated concentrations in terms of aerosol number bias and seasonal cycle (Makkonen et al., 2013).

## EFFECT OF NUCLEATION ON CLOUD PROPERTIES

While nucleation plays an important role for the total number concentration of aerosols, the effect on larger particles is dampened by particle losses during growth from nanometer size to e.g. CCN sizes. Fig. 2 shows the simulated increase in cloud droplet number concentration (CDNC) due to nucleation. It should be noted that in the reference simulation without nucleation, the sulfuric acid can still condense on existing particles, providing also growth towards CCN sizes. With less competition on condensing vapors in the case of no nucleation, certain particles might reach CCN size more easily. Generally over Northern Hemispheric continents, nucleation increases CDNC by more than 10 %. In North America and central Eurasia, the effect can exceed even 50 %. The CDNC increment due to nucleation is highest during summer months, partly due to photochemistry and availability of biogenic organic vapors.

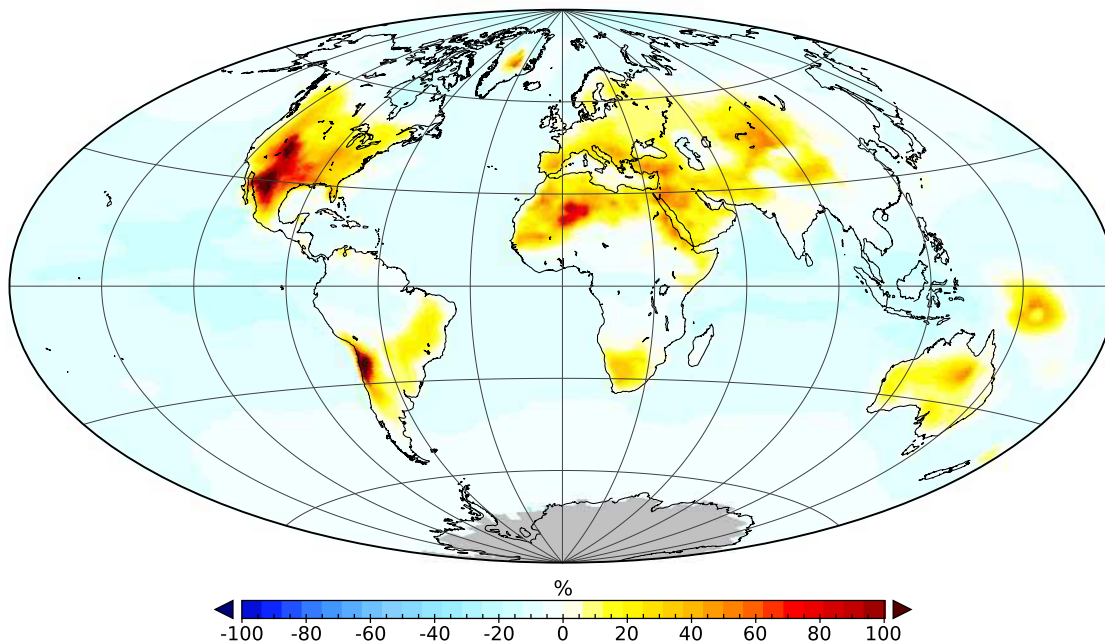


Figure 2: Relative change in cloud droplet number concentration burden due to nucleation.

## ENVIRONMENTAL CHANGES MODIFYING NEW PARTICLE FORMATION

As nucleation is sensitive to sulfuric acid concentration, it is affected by both natural (e.g. DMS, volcanoes, wildfires) and anthropogenic sources ( $\text{SO}_2$  from e.g. industry, traffic). The climate effect of nucleation is highly dependent on availability of vapours for particle growth, where biogenic VOC emissions could play an important role. The strength of certain natural sources could be changing as a response to climate change or anthropogenic influence. The aerosol and precursor emissions from anthropogenic sources have generally been increasing from pre-industrial to 1970-1980, when emission regulations became effective in many regions. Possible future decreases in anthropogenic emissions can induce large changes in the aerosol cooling effects (Makkonen et al., 2012).

We have used the NorESM to study both the effect of anthropogenic emissions and natural responses on new particle formation. Fig. 3a shows the evolution of simulated particle number concentration between years 1950 and 2000, when only changes in anthropogenic emissions are considered

(Lamarque et al., 2010).  $\text{SO}_2$  emissions and aerosol number concentration in Asia have increased rather steadily in the simulations, while number concentrations in Europe and North America have been declining since the 1980s. In the applied emission inventory the peak in  $\text{SO}_2$  emission was in the 1970s in both Europe and North America, but the modeled number concentrations are also sensitive to emissions of fossil fuel BC, which peaked in the 1980s. We are currently studying the effect of co-changing BVOC emissions on particle number since 1950s.

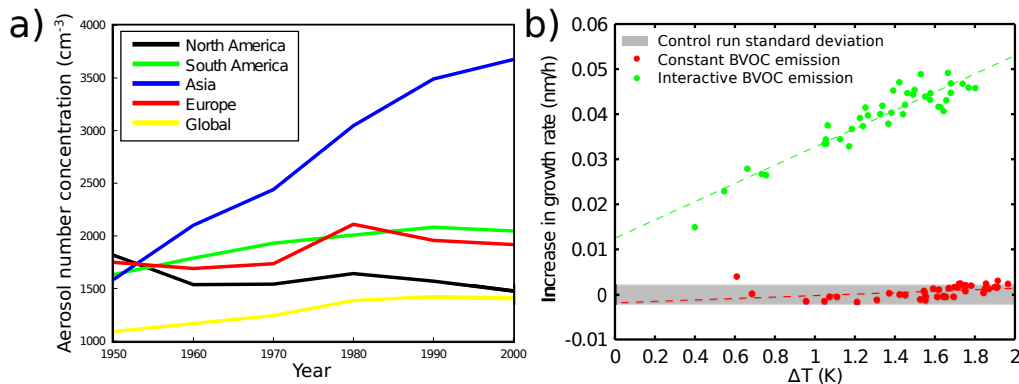


Figure 3: Evolution of total aerosol number concentration ( $\text{cm}^{-3}$ ) from the year 1950 to year 2000 (a) and the response of aerosol growth rate to 2-m temperature change (b). Each point in (b) represents one simulated year.

The NorESM provides an excellent framework to study interactions between Earth System components. We have used the model built in this work to study the negative BVOC-aerosol-climate feedback: increasing temperatures (and photosynthesis) would act to increase BVOC emissions, which in turn would increase aerosol concentrations and cause more aerosol cooling (Kulmala et al., 2004). We have run a set of 4 simulations: control simulations with and without interactive BVOC emission, and two climate change simulations perturbed with  $2\times\text{CO}_2$  concentration. Fig. 3b shows the response of aerosol growth rate (GR in Eq.1) to the changing climate. With constant BVOC emissions (prescribed monthly emission, red dots), the growth rate changes only slightly with changing climate. However, there is a clear signal to the aerosol growth rate when BVOC emissions can respond to the climate change. The growth rate increase due to 1.5-1.8 K temperature change is  $\sim 20\%$ . The increase in aerosol mass, aerosol growth rates and survival of nucleated particles can cause a significant additional aerosol cooling to counteract the initial climate change.

## ACKNOWLEDGEMENTS

R.M. acknowledges CRAICC for financial support. The authors wish to thank NOTUR for computational resources. We are grateful to NCAR and the development teams for CCSM4 and CESM1 for access to their model code. The Academy of Finland Center of Excellence (project no 1118615) is acknowledged.

## REFERENCES

- Bentsen, M., Bethke, I., Debernard, J. B., Iversen, T., Kirkevåg, A., Seland, Ø., Drange, H., Roelandt, C., Seierstad, I. A., Hoose, C., and Kristjánsson, J. E. (2013). The Norwegian Earth System Model, NorESM1-M — Part 1: Description and basic evaluation of the physical climate. *Geosci. Model Devel.*, 6(3):687–720.

- Carslaw, K. S., Boucher, O., Spracklen, D. V., Mann, G. W., Rae, J. G. L., Woodward, S., and Kulmala, M. (2010). A review of natural aerosol interactions and feedbacks within the earth system. *Atmos. Chem. Phys.*, 10(4):1701–1737.
- Charlson, R. J., Lovelock, J. E., Andreas, M. D., and Warren, S. G. (1987). Oceanic phytoplankton, atmospheric sulphur, cloud albedo and climate. *Nature*, 326:655–661.
- Guenther, A., Karl, T., Harley, P., Wiedinmyer, C., Palmer, P. I., and Geron, C. (2006). Estimates of global terrestrial isoprene emissions using megan (model of emissions of gases and aerosols from nature). *Atmos. Chem. Phys.*, 6(11):3181–3210.
- Iversen, T., Bentsen, M., Bethke, I., Debernard, J. B., Kirkevåg, A., Seland, Ø., Drange, H., Kristjansson, J. E., Medhaug, I., Sand, M., and Seierstad, I. A. (2013). The Norwegian Earth System Model, NorESM1-M — Part 2: Climate response and scenario projections. *Geosci. Model Devel.*, 6(2):389–415.
- Keskinen, H., Virtanen, A., Joutsensaari, J., Tsagkogeorgas, G., Duplissy, J., Schobesberger, S., Gysel, M., Riccobono, F., Slowik, J. G., Bianchi, F., Yli-Juuti, T., Lehtipalo, K., Rondo, L., Breitenlechner, M., Kupc, A., Almeida, J., Amorim, A., Dunne, E. M., Downard, A. J., Ehrhart, S., Franchin, A., Kajos, M., Kirkby, J., Kürten, A., Nieminen, T., Makhmutov, V., Mathot, S., Miettinen, P., Onnela, A., Petäjä, T., Praplan, A., Santos, F. D., Schallhart, S., Sipilä, M., Stozhkov, Y., Tomé, A., Vaattovaara, P., Wimmer, D., Prevot, A., Dommen, J., Donahue, N. M., Flagan, R., Weingartner, E., Viisanen, Y., Riipinen, I., Hansel, A., Curtius, J., Kulmala, M., Worsnop, D. R., Baltensperger, U., Wex, H., Stratmann, F., and Laaksonen, A. (2013). Evolution of particle composition in cloud nucleation experiments. *Atmos. Chem. Phys.*, 13(11):5587–5600.
- Kirkevåg, A., Iversen, T., Seland, Ø., Hoose, C., Kristjánsson, J. E., Struthers, H., Ekman, A. M. L., Ghan, S., Griesfeller, J., Nilsson, E. D., and Schulz, M. (2013). Aerosol-climate interactions in the Norwegian Earth System Model - NorESM1-M. *Geosci. Model. Dev.*, 6(1):207–244.
- Kulmala, M., Lehtinen, K. E. J., and Laaksonen, A. (2006). Cluster activation theory as an explanation of the linear dependence between formation rate of 3 nm particles and sulphuric acid concentration. *Atmos. Chem. Phys.*, 6:787–793.
- Kulmala, M., Suni, T., Lehtinen, K. E. J., Dal Maso, M., Boy, M., Reissell, A., Rannik, U., Aalto, P., Keronen, P., Hakola, H., Bäck, J., Hoffmann, T., Vesala, T., and P., H. (2004). A new feedback mechanism linking forests, aerosols, and climate. *Atmos. Chem. Phys.*, 4:557–562.
- Lamarque, J.-F., Bond, T. C., Eyring, V., Granier, C., Heil, A., Klimont, Z., Lee, D., Lioussé, C., Mieville, A., Owen, B., Schultz, M. G., Shindell, D., Smith, S. J., Stehfest, E., Van Aardenne, J., Cooper, O. R., Kainuma, M., Mahowald, N., McConnell, J. R., Naik, V., Riahi, K., and van Vuuren, D. P. (2010). Historical (1850–2000) gridded anthropogenic and biomass burning emissions of reactive gases and aerosols: methodology and application. *Atmos. Chem. Phys.*, 10(15):7017–7039.
- Lehtinen, K., Dal Maso, M., Kulmala, M., and Kerminen, V.-M. (2007). Estimating nucleation rates from apparent particle formation rates and vice versa: Revised formulation of the kerminen-kulmala equation. *Journal of Aerosol Science*, 38(9):988–994.
- Makkonen, R., Asmi, A., Kerminen, V.-M., Boy, M., Arneth, A., Hari, P., and Kulmala, M. (2012). Air pollution control and decreasing new particle formation lead to strong climate warming. *Atmos. Chem. Phys.*, 12(3):1515–1524.

- Makkonen, R., Seland., O., Kirkevåg, A., Iversen, T., and Kristjánsson, J. (2013). Evaluation of aerosol number concentrations simulated by NorESM. *Manuscript in preparation*.
- Paasonen, P., Nieminen, T., Asmi, E., Manninen, H. E., Petäjä, T., Plass-Dülmer, C., Flentje, H., Birmili, W., Wiedensohler, A., Hõrrak, U., Metzger, A., Hamed, A., Laaksonen, A., Facchini, M. C., Kerminen, V.-M., and Kulmala, M. (2010). On the roles of sulphuric acid and low-volatility organic vapours in the initial steps of atmospheric new particle formation. *Atmos. Chem. Phys.*, 10(22):11223–11242.
- Riipinen, I., Pierce, J. R., Yli-Juuti, T., Nieminen, T., Häkkinen, S., Ehn, M., Junninen, H., Lehtipalo, K., Petäjä, T., Slowik, J., Chang, R., Shantz, N. C., Abbatt, J., Leaitch, W. R., Kerminen, V.-M., Worsnop, D. R., Pandis, S. N., Donahue, N. M., and Kulmala, M. (2011). Organic condensation: a vital link connecting aerosol formation to cloud condensation nuclei (CCN) concentrations. *Atmos. Chem. Phys.*, 11(8):3865–3878.
- Sipilä, M., Berndt, T., Petäjä, T., Brus, D., Vanhanen, J., Stratmann, F., Patokoski, J., Mauldin, R. L., Hyvärinen, A.-P., Lihavainen, H., and Kulmala, M. (2010). The Role of Sulfuric Acid in Atmospheric Nucleation. *Science*, 327(5970):1243–1246.
- Vehkamäki, H., Kulmala, M., Napari, I., Lehtinen, K. E. J., Timmreck, C., Noppel, M., and Laaksonen, A. (2002). An improved parameterization for sulfuric acid/water nucleation rates for tropospheric and stratospheric conditions. *J. Geophys. Res.*, 107:4622–4631.

# NH<sub>3</sub>–HNO<sub>3</sub> AND HONO DIURNAL CYCLES IN THE SUMMER OF 2010 AND 2012

U. MAKKONEN<sup>1</sup> and A. VIRKKULA<sup>1,2</sup>

<sup>1</sup>Finnish Meteorological Institute, FI-00560 Helsinki, Finland

<sup>2</sup>University of Helsinki, Department of Physics FI-00017, Helsinki, Finland

Keywords: ammonia, nitric acid, nitrous acid, diurnal cycles

## INTRODUCTION

Concentrations of inorganic gases and ions in PM<sub>10</sub> and PM<sub>2.5</sub> particles have been measured with an on-line ion chromatograph MARGA 2S at Hyytiälä SMEAR II station, since 21 June 2010. Here we discuss the diurnal behaviour of the nitrogen-containing gases (HNO<sub>3</sub>, HONO, NH<sub>3</sub>) in the summer of 2010 and 2012. Ammonia is the most abundant base in the atmosphere with an important role in neutralizing acids. Furthermore, it is one of the precursor gases in the formation of new particles (Kirkby et al., 2011; Kulmala et al., 2000). Nitrogen compounds participate in both the production and loss of the most important day-time atmospheric oxidant, the hydroxyl radical (OH). The dissociation of HONO contributes to the production of OH radicals (Kulmala and Petäjä, 2011). In daytime, OH radicals are consumed to form nitric acid in the reaction: NO<sub>2</sub> + OH + M → HNO<sub>3</sub> + M (Finlayson-Pitts and Pitts, 2000).

## METHODS

The MARGA 2S ADI 2080 (Applikon Analytical BV, Netherlands) has two sample boxes. Ambient air was drawn through a PM<sub>10</sub>-inlet (Teflon coated) and divided into two flows, one going to the PM<sub>10</sub> sample box while the other was directed through a PM<sub>2.5</sub> cyclone (Teflon coated) into the PM<sub>2.5</sub> sample box. In both compartments, the air was led through a Wet Rotating Denuder (WRD) where water-soluble gases diffuse to the absorption solution (10 ppm hydrogen peroxide). Subsequently the ambient particles were collected in a Steam Jet Aerosol Collector (SJAC). Hourly samples were analysed with a Metrohm anion and cation chromatograph using LiBr as an internal standard. There was more uncertainty in the HNO<sub>3</sub> results in 2010, although the HNO<sub>3</sub> blank of the instrument, caused by the HNO<sub>3</sub> cation eluent slightly leaking to the anion side, was subtracted from the results. In August 2010, the HNO<sub>3</sub> eluent was replaced by MSA which gave an improved nitrate baseline.

## RESULTS AND DISCUSSION

The average concentrations of all nitrogen-containing gases were higher in summer 2010 than in summer 2012. Ammonia decreased from 0.47 ppb to 0.26 ppb and HNO<sub>3</sub> from 0.10 ppb to 0.04 ppb. Furthermore, HONO concentrations were slightly lower in 2012 (average 0.08 ppb) compared to 2010 (0.10 ppb). One reason for the high ammonia concentrations in 2010 was the very dry and warm weather. The results of 2010 were found to increase with the prevailing temperature according to the equation:

$$\text{NH}_3(\text{RH}, t) = \left( 0.000739 \frac{\text{ppb}}{\%} \text{RH} + 0.00891 \text{ppb} \right) \exp \left( \left( -0.00118 \frac{\text{RH}}{^\circ\text{C}\%} + 0.164 \frac{1}{^\circ\text{C}} \right) t \right)$$

There was a clear diurnal cycle for HNO<sub>3</sub>, with its maximum in the afternoon in both 2010 and 2012. This was expected, since OH-radicals producing HNO<sub>3</sub> from NO<sub>2</sub> had their highest concentrations at noon. The

diurnal cycle of HONO was the opposite: concentrations were highest at night and low during daytime, because in sunlight, HONO is dissociated by solar radiation:  $\text{HONO} + h\nu \rightarrow \text{OH}^\cdot + \text{NO}$ .

In the summer of 2010, the diurnal variation of ammonium was large, with the highest values in the afternoon. At the same time, there was no diel cycle for particulate ammonium. Therefore, the summertime diurnal cycle of ammonia cannot be explained by dissociation of  $\text{NH}_4\text{NO}_3$ . In the summer of 2012, the ammonia maximum was already at 10 – 12 (Fig. 1). The diurnal cycle suggests that ammonia absorbed on the leaf surfaces of trees and vegetation during night-time may be re-emitted as the temperature of the leaves rises again during warm summer days. In addition, the decomposition of leaves and the processes within the forest soil release ammonia.

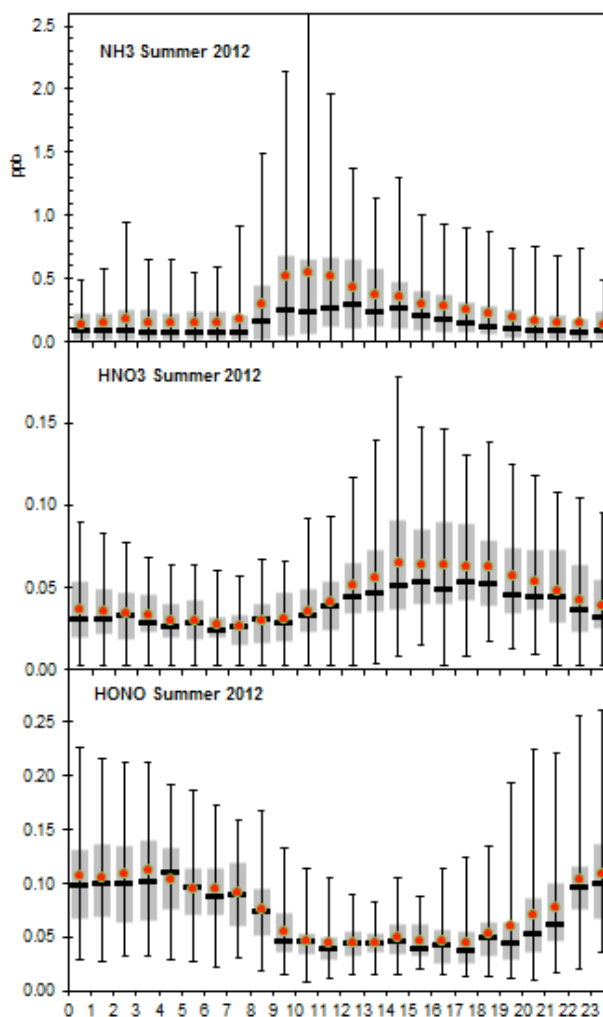


Figure 1. Diurnal cycles of  $\text{NH}_3$ ,  $\text{HNO}_3$  and HONO (ppb) in the summer of 2012 (17 July - 20 August).

#### ACKNOWLEDGEMENTS

This work was supported by the Academy of Finland as part of the Centre of Excellence program (project no 1118615).

## REFERENCES

- Finlayson-Pitts, B. J., and Pitts, J. N.: Chemistry of the upper and lower atmosphere: theory, experiments and application, Academic Press, San Diego, CA (ISBN 0-12-257060-x), 2000.
- Kirkby, J., Curtius, J., Almeida, J., Dunne, E., Duplissy, J., Ehrhart, S., Franchin, A., Gagné, S., Ickes, L., Kürten A., Kupc, A., Metzger, A., Riccobono, F., Rondo, L., Schobesberger, S., Tsagkogeorgas, G., Wimmer, D., Amorim, A., Bianchi, F., Breitenlechner, M., David, A., Dommen, J., Downard, A., Ehn, M., Flagan, R. C., Haider, S., Hansel, A., Hauser, D., Jud, W., Junninen, H., Kreissl, F., Kvashin, A., Laaksonen, A., Lehtipalo, K., Lima, J., Lovejoy, E. R., Makhmutov, V., Mathot, S., Mikkilä, J., Minginette, P., Mogo, S., Nieminen, T., Onnela, A., Pereira, P., Petäjä, T., Schnitzhofer, R., Seinfeld, J. H., Sipilä, M., Stozhkov, Y., Stratmann, F., Tomé A., Vanhanen, J., Viisanen, Y., Vrtala, A., Wagner, P. E., Walther, H., Weingartner, E., Wex, H., Winkler, P. M., Carslaw, K. S., Worsnop, D. R., Baltensperger, U., and Kulmala, M.: Role of sulphuric acid, ammonia and galactic cosmic rays in atmospheric aerosol nucleation, *Nature*, 476, 429–433, [doi:10.1038/nature10343](https://doi.org/10.1038/nature10343), 2011.
- Kulmala, M., Pirjola L., and Mäkelä J. M.: Stable sulphate clusters as a source of new atmospheric particles, *Nature* 404, 66-69, [doi:10.1038/35003550](https://doi.org/10.1038/35003550), 2000.
- Kulmala, M. and Petäjä, T.: Soil nitrites influence atmospheric chemistry, *Science* 333, 1586-1587, 2011.

# ESTIMATING THE VISCOSITY RANGE OF SECONDARY ORGANIC MATERIAL FROM PARTICLE COALESCENCE TIMES

J. MALILA<sup>1</sup>, A. PAJUNOJA<sup>1</sup>, L.Q. HAO<sup>1</sup>, J. JOUTSENSAARI<sup>1</sup>, A. LAAKSONEN<sup>1,2</sup>, K.E.J. LEHTINEN<sup>1,3</sup> and A. VIRTANEN<sup>1</sup>

<sup>1</sup> Department of Applied Physics, University of Eastern Finland–Kuopio

<sup>2</sup> Finnish Meteorological Institute, Climate Change, Helsinki

<sup>3</sup> Finnish Meteorological Institute, Kuopio Unit

Keywords: SOA, amorphous, glass, viscosity

## INTRODUCTION

Condensation and reactive uptake of organic vapours by atmospheric nanoparticles is a significant source of cloud condensation nuclei, thus affecting both global climate and the hydrological cycle via changes in cloud properties. During recent years it has been established that

- the phase of secondary organic material in aerosol particles can significantly affect both organic and water vapour uptake (Riipinen *et al.*, 2012), and
- particles derived from the oxidation of monoterpenes—typical plant volatiles e.g. from conifers—have mechanically solid or semi-solid character while being thermodynamically distinct from crystalline solids even at low relative humidity (RH) (Kannosto *et al.*, 2013; Renbaum-Wolff *et al.*, 2013; Virtanen *et al.*, 2010).

The second point implies that the particles have high viscosity that effectively increases the thermodynamic equilibration time scale of particles far beyond their atmospheric life times, contrary to the assumptions applied in current models presenting aerosols in regional and global simulations. Here we discuss on a new method presented by Pajunoja *et al.* (2013) for the estimation of particle viscosity, and compare the obtained results with those recently reported by other groups.

## METHODS

All secondary organic aerosol (SOA) particles were formed in the Kuopio Aerosol Chamber: Full experimental details are given by Hao *et al.* (2009), Virtanen *et al.* (2010) and Kannosto *et al.* (2013), with a detailed overview by Pajunoja *et al.* (2013). Briefly, two systems were studied:

- ozonolysis products of  $\alpha$ -pinene, and
- reaction products of natural volatile organic compounds emitted by live Scots pine (*Pinus sylvestris* L.) seedlings with OH in the presence of trace amounts of SO<sub>2</sub> in the gas phase.

Size distribution and chemical composition of the particles were monitored by scanning mobility particle sizer (SMPS) and Aerodyne Aerosol Mass Spectrometer (AMS), and particle samples were collected on electron microscopy grids. Degree of primary particle coalescence was then determined using visual analysis of scanning electron microscope (SEM) graphs after keeping grid plates in dark, dry (RH < 20%) environment for two months prior the analysis (Pajunoja *et al.*, 2013). Electron

diffraction analysis was done on selected particles to test whether particles were crystalline—they were not. All the experiments were done at room temperature and pressure.

After evaluation of particle sizes and the degree of coalescence from SEM samples (and SMPS measurements), characteristic time of coalescence  $\tau$ , either less or more than two months, was deduced. This was used to give an order-of-magnitude estimate of the viscosity of particles  $\eta$ , as

$$\tau \approx \frac{\eta d_p}{\sigma}, \quad (1)$$

where  $d_p$  is the diameter of a primary particle and  $\sigma$  surface tension (Frenkel, 1945).

## RESULTS AND DISCUSSION

Based on the method described in the previous paragraph,  $\eta$  was estimated using  $\sigma = 35$  mN/m, corresponding *cis*-pinonic acid, an oxidation product of  $\alpha$ -pinene with the same O:C-ratio (0.3) as determined by AMS for studied particles. Results are depicted in Fig. 1 together with recent results from other groups (Abramson *et al.*, 2013; Koop *et al.*, 2011; Renbaum-Wolff *et al.*, 2013), and two possible natural analogues of secondary organic matter—rosin and (tar) pitch.

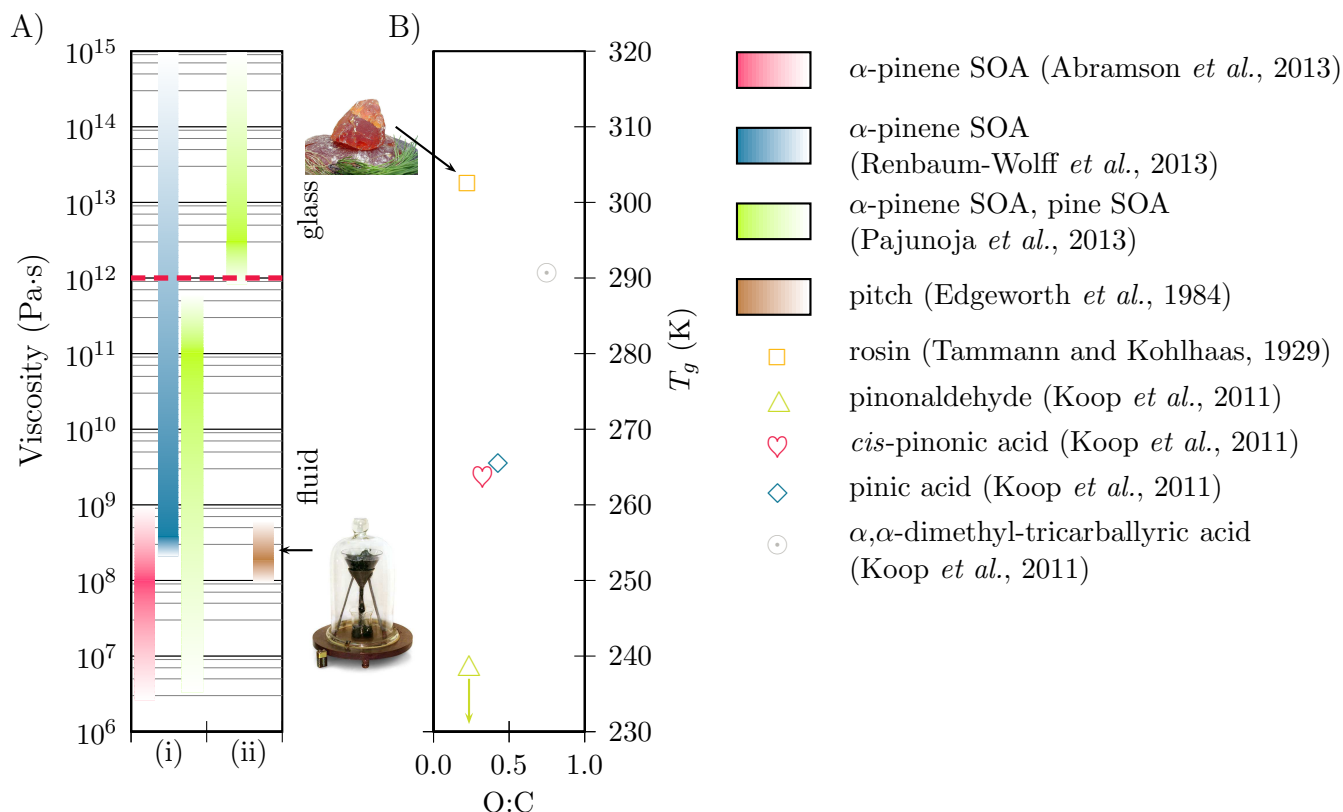


Figure 1: Estimated A) viscosities of secondary organic material from  $\alpha$ -pinene ozonolysis (i) and true pine emissions in presence of OH and SO<sub>2</sub> (ii) from this work with comparison to other studies and pitch, and B) glass transition temperatures  $T_g$  of selected  $\alpha$ -pinene ozonolysis products and natural rosins from *Pinus* spp. Images of *P. pinaster* rosin and the pitch drop experiment at the University of Queensland are taken from Wikimedia Commons under GFDL.

From Fig. 1 A) we can see that our results for SOA from  $\alpha$ -pinene ozonolysis [case (i)] agree within assumed uncertainties to the results of Renbaum-Wolff *et al.* (2013), who also relied on

relaxation time scale analysis similar to our method in their work. We can conclude that the viscosity of secondary organic material from  $\alpha$ -pinene ozonolysis is most likely between  $10^8$  and  $10^{11}$  Pa·s at room temperature and dry conditions. Result of Abramson *et al.* (2013) agrees with the lower limit of this range. However, Abramson *et al.* (2013) measured diffusion of aromatic species inside SOA particle, and then applied Stokes–Einstein relation to convert measured diffusivities into viscosity values. Organic molecules making up secondary organic material are likely to be fragile glass formers, which means that the Stokes–Einstein relation cannot be assumed in the vicinity of the glass transition (Berthier and Biroli, 2011), increasing the uncertainty of the viscosity estimate of Abramson *et al.* (2013). It should be noted that with viscosities around  $10^8$  Pa·s or more, secondary organic material from  $\alpha$ -pinene ozonolysis—although technically being fluid—shows bounce behaviour similar to undeniably glassy particles from the oxidation of living pine emissions (Kannosto *et al.*, 2013).

We can also make some civilized guesses on the molecular structure of secondary organic material when combining viscosity and O:C-ratio measurements with estimates of glass transition temperatures by Koop *et al.* (2011) [Fig. 1 B)]. For  $\alpha$ -pinene ozonolysis, first generation oxidation products and possibly their dimers can explain the observations. These conclusions are in line with other related studies (Abramson *et al.*, 2013; Koop *et al.*, 2011) as well as direct mass spectrometric measurements of SOA composition (Hall and Johnston, 2012; Nizkorodov *et al.*, 2011). Instead, the secondary organic material from the oxidation of volatile organic compounds emitted by pine seedlings is characterised by higher  $T_g$  with respect to the O:C-ratio that can be expected from monoterpene oxidation products: In fact, the secondary organic material is similar to diterpenes, main components of natural rosins, in this regard. Possible explanation for this is that these particles consist mainly of oligomers of monoterpene oxidation products; the presence of catalysing sulfuric acid from SO<sub>2</sub> oxidation can explain the higher amount of oligomers when compared to  $\alpha$ -pinene ozonolysis products.

## CONCLUSIONS

We have studied the viscosity of SOA particles produced from  $\alpha$ -pinene and living pine emission oxidation. SOA particles from the ozonolysis of  $\alpha$ -pinene can be characterised as semi-solid, whereas SOA particles from living pine emissions in the presence of OH and SO<sub>2</sub> are glassy. Further work is needed to get more quantitative estimate of particle viscosity  $\eta$  and its relation to the diffusion coefficient at secondary organic material in various atmospherically relevant conditions.

## ACKNOWLEDGEMENTS

Financial support from the Academy of Finland through the Centre-of-Excellence programme (decision no 1118615) and projects 259005, 252908 and 264989, ACCC graduate school, and from the strategic funding of the University of Eastern Finland are acknowledged.

## REFERENCES

- Abramson, E., D. Imre, J. Beránek, J. Wilson and A. Zelenyuk (2013). Experimental determination of chemical diffusion within secondary organic aerosol particles. *Phys. Chem. Chem. Phys.*, **15**, 2983.
- Berthier, L. and G. Biroli (2011). Theoretical perspective on the glass transition and amorphous materials. *Rev. Mod. Phys.*, **83**, 587.
- Edgeworth, R., B.J. Dalton and T. Parnell (1984). The pitch drop experiment. *Eur. J. Phys.*, **5**, 198.

- Frenkel, J. (1945). Viscous flow of crystalline bodies under the action of surface tension. *J. Phys.* (Moscow), **9**, 385.
- Hall, W.A. and M.V. Johnston (2012). Oligomer formation pathways in secondary organic aerosol from MS and MS/MS measurements with high mass accuracy and resolving power. *J. Am. Soc. Mass Spectrom.*, **23**, 1097.
- Hao, L.Q., P. Yli-Pirilä, P. Tiitta, S. Romakkaniemi, P. Vaattovaara, M.K. Kajos, J. Rinne, J. Heijari, A. Kortelainen, P. Miettinen, J.H. Kroll, J.K. Holopainen, J.N. Smith, J. Joutsensaari, M. Kulmala, D.R. Worsnop and A. Laaksonen (2009). New particle formation from the oxidation of direct emissions of pine seedlings. *Atmos. Chem. Phys.*, **9**, 8121.
- Kannosto, J., P. Yli-Pirilä, L.Q. Hao, J. Leskinen, J. Jokiniemi, J.M. Mäkelä, J. Joutsensaari, A. Laaksonen, D.R. Worsnop, J. Keskinen and A. Virtanen (2013). Bounce characteristics of  $\alpha$ -pinene-derived SOA particles with implications to physical phase. *Boreal Env. Res.*, **18**, 329.
- Koop, T., J. Bookhold, M. Shiraiwa and U. Pöschl (2011). Glass transition and phase state of organic compounds: dependency on molecular properties and implications for secondary organic aerosols in the atmosphere. *Phys. Chem. Chem. Phys.*, **13**, 19238.
- Nizkorodov, S.A., J. Laskin and A. Laskin (2011). Molecular chemistry of organic aerosols through the application of high resolution mass spectrometry. *Phys. Chem. Chem. Phys.*, **13**, 3612.
- Pajunoja, A., J. Malila, L. Hao, J. Joutsensaari, K.E.J. Lehtinen and A. Virtanen (2013). Estimating the viscosity range of SOA particles based on their coalescence time. *Aerosol Sci. Tech.*, revised version submitted.
- Renbaum-Wolff, L., J.W. Grayson, A.P. Bateman, M. Kuwata, M. Sellier, B.J. Murray, J.E. Schilling, S.T. Martin and A.K. Bertram (2013). Viscosity of  $\alpha$ -pinene secondary organic material and implications for particle growth and reactivity. *Proc. Natl. Acad. Sci. U.S.A.*, **110**, 8014.
- Riipinen, I., T. Yli-Juuti, J.R. Pierce, T. Petäjä, D.R. Worsnop, M. Kulmala and N.M. Donahue (2012). The contribution of organics to atmospheric nanoparticle growth. *Nat. Geosci.*, **5**, 453.
- Tammann, G. and A. Kohlhaas (1929). Die Begrenzung des Erweichungsintervalles der Gläser und die abnorme Änderung der spezifischen Wärme und des Volumens im Erweichungsgebiet. *Z. Anorg. Allgem. Chem.*, **182**, 49.
- Virtanen, A., J. Joutsensaari, T. Koop, J. Kannosto, P. Yli-Pirilä, J. Leskinen, J.M. Mäkelä, J.K. Holopainen, U. Pöschl, M. Kulmala, D.R. Worsnop and A. Laaksonen (2010). An amorphous solid state of biogenic secondary organic aerosol particles. *Nature*, **467**, 824.

# LONG TERM MEASUREMENTS OF CARBON DIOXIDE AND METHANE FLUXES OVER A SMALL BOREAL LAKE IN SOUTHERN FINLAND

I. MAMMARELLA<sup>1</sup>, K.-M. ERKKILÄ<sup>1</sup>, S. HAAPANALA<sup>1</sup>, J. HEISKANEN<sup>1,2</sup>, A. OJALA<sup>2</sup>, T. VESALA<sup>1</sup>

<sup>1</sup> Department of Physics, University of Helsinki, Finland

<sup>2</sup> Department of Environmental Sciences, University of Helsinki, Finland

Keywords: EDDY COVARIANCE, LAKE-ATMOSPHERE EXCHANGE, CH<sub>4</sub> FLUX, CO<sub>2</sub> FLUX

## INTRODUCTION

Fresh water ecosystems (lakes, rivers, ponds, reservoirs) are able to process large amounts of organic carbon and their importance in terrestrial carbon cycle and climate change issues is well recognised (Battin et al., 2009). Nevertheless, the amount of carbon dioxide and methane released into the atmosphere is largely uncertain (Alsdorf et al., 2007; Bastviken et al., 2011). Standard methods for estimating lake-atmosphere gas exchange are based on non-continuous and indirect techniques, e.g. gas concentration gradient (Cole and Caraco 1998) and floating chamber techniques (Duchemin et al., 1999). The major source of uncertainty of the former approach is related to the parameterization used for the physical rate of exchange between the water and the air, usually expressed as a piston velocity (Cole and Caraco 1998), while with the latter disturbances of air-water interface may cause a bias in the flux measurements (Vachon et al., 2010). The eddy covariance (EC) technique is widely used for continuous and long-term monitoring of energy and gas exchange between land ecosystems (forest, wetland, crop) and atmosphere (Baldocchi et al., 2003). The method has been applied only recently to inland aquatic ecosystems, and at moment a comprehensive network of EC long term sites covering different latitude and climatic zones, and lake characteristics does not exist. Most of the previous studies focused on water-atmosphere energy exchange, and only few studies reported direct measurements of carbon dioxide and methane fluxes by eddy covariance technique (see Vesala et al., 2012).

The aims of this study are: i) to provide new insights on EC methodologies applied to lake ecosystems, based on long term flux measurements; ii) to determine the seasonal and interannual variations of CO<sub>2</sub> and CH<sub>4</sub> fluxes; iii) to assess the relative contribution of shear and buoyancy-induced water turbulence on air-water gas exchange.

## METHODS

Energy and CO<sub>2</sub> exchange has been monitored in Lake Kuivajärvi, located close to the Hyytiälä Forest Field Station, since 2009. Lake Kuivajärvi is a small humic boreal lake extending about 2.6 km in North/West-South/East direction and it is a few hundred meters wide (Fig. 1). The measurement platform is located approximately 1.8 km and 0.8 km from the Northern and Southern shorelines, respectively. The lake has a maximum depth of 13.2 m, and the depth at the location of the platform is 12.5 m.

The eddy covariance system on the platform includes an ultrasonic anemometer (Metek USA-1, GmbH, Germany) to measure the three wind velocity components and sonic temperature, and the enclosed-path infrared gas analyser Licor 7200 (LiCor Inc., Lincoln, NE, US) that measures CO<sub>2</sub> and H<sub>2</sub>O concentrations. Starting from June 2012, the CH<sub>4</sub> turbulent fluctuations are also measured by using the fast response gas analyser G1301-f (Picarro Inc., USA). All data were sampled at 10 Hz and the gas inlets were located at 1.5 m above the water surface close to the sonic anemometer.

The eddy covariance fluxes were calculated as 30 min block averaged co-variances between the scalars (or horizontal wind speed) and vertical wind velocity according to commonly accepted procedures (Aubinet et al., 2000). Fluxes were corrected for high frequency loss, due to the limited frequency response of the EC

system. In this study we used the theoretical approach (Aubinet et al., 2000), for correcting the momentum and buoyancy fluxes. Instead, the CO<sub>2</sub> and H<sub>2</sub>O fluxes were corrected by using experimentally estimated co-spectral transfer functions, as described in Mammarella et al. (2009).

Auxiliary data are continuously measured in proximity of the platform (5 sec sampling frequency), and they are water CO<sub>2</sub> and temperature profiles, radiation components, air temperature and relative humidity. Additionally, manual samples of CO<sub>2</sub>, CH<sub>4</sub> and N<sub>2</sub>O water concentrations at different depths are performed weekly.

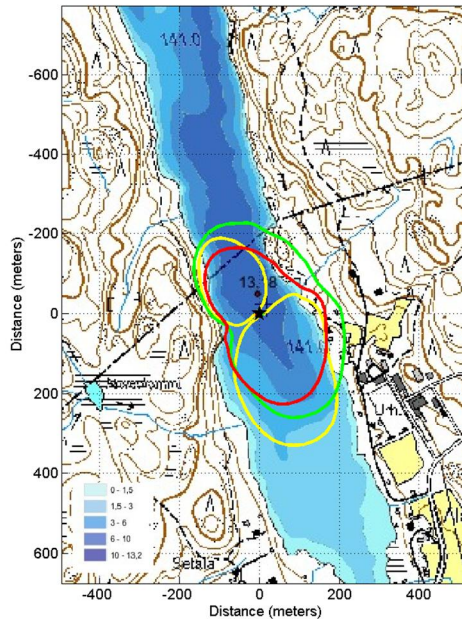


Fig 1. Bathymetric map of the lake. The location of the raft is indicated by a star. Contour lines represent the 80% flux footprint for different atmospheric stability and all wind direction. Red line ( $z/L < -0.0625$ ), green line ( $-0.0625 < z/L < 0$ ) and yellow line ( $0 < z/L < 0.03$ ), where  $z$  is the measurement height and  $L$  is the Obukhov length.

## RESULTS AND DISCUSSIONS

Daily mean values of wind speed ranged between 1 and 5 m s<sup>-1</sup>, with an average value of about 2 m s<sup>-1</sup> during all the years. The wind is mainly blowing along the lake, and the prevailing wind direction is thus from south-east and north-west (not shown). The distributions are very similar for each year, meaning that lake-induced local effect (channelling effect) is the main reason. For all years the lake is thermally stratified during summer and a thermocline, which develop in early June, deepens through the summer months, reaching a depth of 8 m at the beginning of September. After the middle of September, the upper layers of water start to cool down, and the lake turns over. The lake surface is typically ice covered between December and April. Flux footprint distribution functions were estimated by using the Kormann and Meixner (2001) model. Figure 1 shows that the averaged source area contributing to 80% of the flux ranges from 100 m (in slightly unstable conditions) up to about 300 m (in near-neutral conditions). All wind directions have been included in the analysis. Such simple model clearly overestimates the footprint, because it does not account for the landscape heterogeneity and the extra turbulence generated by the surrounding forest, which would result in a smaller source area (Vesala et al, 2006). On the other hand, this result give us confidence that, selecting only periods when the wind is blowing along the lake, the measured fluxes represent the net exchange of energy and matter between water and air.

### Carbon dioxide fluxes

Figure 2 shows the CO<sub>2</sub> flux timeseries as 30 min values (grey dots) and daily means (red dots) for one year period (June 2012 – June 2013). Turbulent fluxes are higher during open water periods than during winter months. On average the lake acts as a small CO<sub>2</sub> source during the analysed periods, and the daily mean values range between 0.5 and 2  $\mu\text{mol m}^{-2} \text{s}^{-1}$  in the summer and early autumn, and stay below 0.5  $\mu\text{mol m}^{-2} \text{s}^{-1}$  in the late autumn and winter. The maximum efflux of CO<sub>2</sub> was measured after the ice melt at begin of May 2013. No clear diurnal variation was found. The mean annual CO<sub>2</sub> emission was 9.67 mol m<sup>-2</sup>y<sup>-1</sup> (about 116 gC m<sup>-2</sup>), which is larger than the value (77 gC m<sup>-2</sup>) measured in another small boreal lake in Southern Finland (Huotari et al., 2011). Finally, we found that shear (wind) induced water turbulence was driving the CO<sub>2</sub> diffusive fluxes especially during daytime, instead CO<sub>2</sub> exchange rates were highly correlated with the water surface layer buoyancy fluxes during night-time cooling of the lake, when the turbulent mixing in the water was generated by penetrative convection (Eugster et al., 2003).

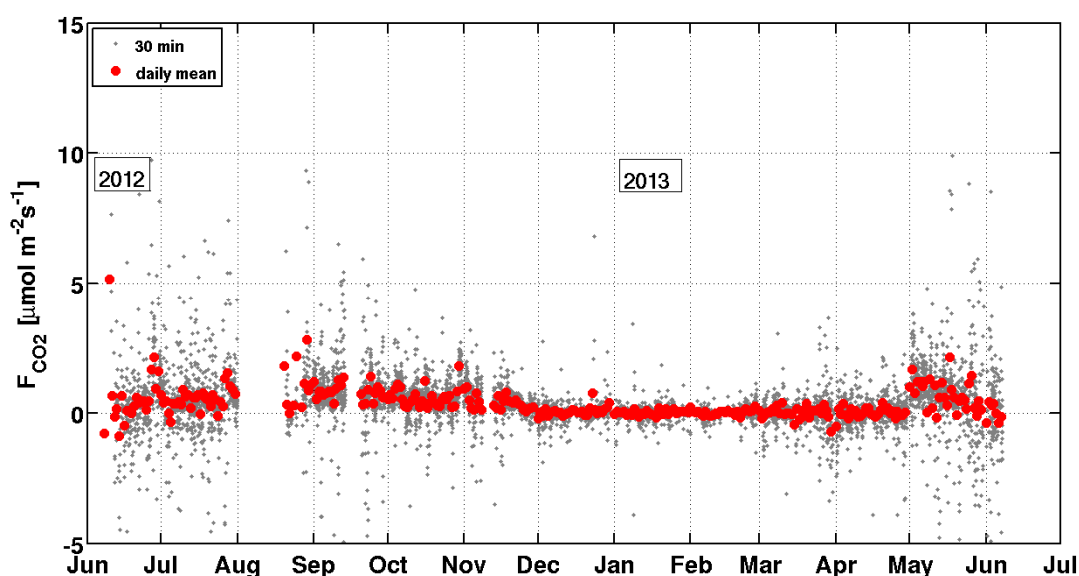


Fig.2. Fluxes of CO<sub>2</sub> measured between June 2012 and June 2013. The grey dots are 30 min values and the red dots are daily mean values.

### Methane fluxes

Preliminary results shows that methane fluxes are very low (Figure 3), especially during winter months, when the fluxes are below the detection limit of the EC system (estimated mean value equal 0.5 nmol m<sup>-2</sup> s<sup>-1</sup>). The mean annual CH<sub>4</sub> efflux was about 0.2 gC m<sup>-2</sup>, which is much smaller than the value estimated (by chamber and gradient methods) in another small boreal lake in Southern Finland (Kankaala et al., 2006). Maximum CH<sub>4</sub> efflux to the atmosphere was measured during 1<sup>st</sup> - 5<sup>th</sup> of May 2013, just after the ice cover melted, when the daily mean rates ranged between 1 and 6 nmol m<sup>-2</sup> s<sup>-1</sup>. Furthermore, we hypothesized that this spring time flux peak originates from outside of the lake, because the bottom water of Lake Kuivajärvi remained oxic throughout the winter and no excess CH<sub>4</sub> was built-up under ice. No significant differences in CH<sub>4</sub> effluxes was found between summer stratification and fall lake turnover periods, and although the measured fluxes (mean values = 1.2 nmol m<sup>-2</sup> s<sup>-1</sup>) are above the EC detection limit, they are one order of magnitude lower than those reported in other lake studies (Kankaala et al.,

2006, Schubert et al., 2012). Our results suggest that most of CH<sub>4</sub> accumulated in the hypolimnion is oxidized (most probably at oxic-anoxic interfaces) before being released to the atmosphere. Further analysis of methanotrophic activity and measured CH<sub>4</sub> concentration profiles in the water column is needed in order to verify this hypothesis.

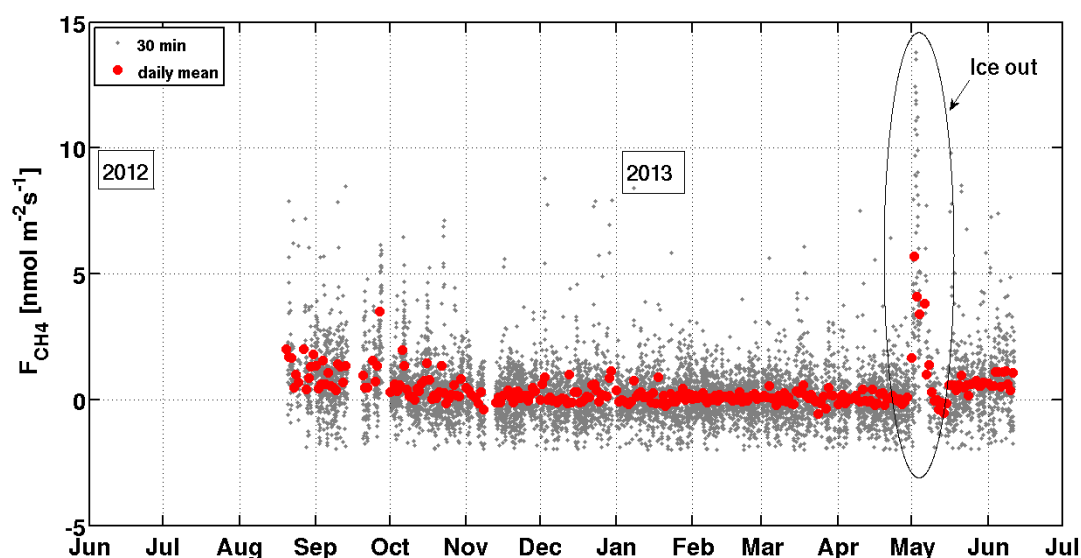


Fig.3. Fluxes of CH<sub>4</sub> measured between June 2012 and June 2013. The grey dots are 30 min values and the red dots are daily mean values.

## ACKNOWLEDGEMENTS

The financial supports by the Academy of Finland Centre of Excellence program (project no 1118615), Nordic Centre of Excellence DEFROST, and EU projects ICOS and GHG-Europe are gratefully acknowledged.

## REFERENCES

- Aubinet, M., A. Grelle, A. Ibrom, U. Rannik, J. Moncrieff, T. Foken, A. S. Kowalski, P. H. Martin, P. Berbigier, C. Bernhofer, R. Clement, J. Elbers, A. Granier, T. Grünwald, K. Morgenstern, K. Pilegaard, C. Rebmann, W. Snijders, R. Valentini, and T. Vesala (2000). Estimates of the annual net carbon and water exchange of forests: The EUROFLUX methodology, *Adv. Ecol. Res.*, 30, 113–175.
- Baldocchi. (2003), Assessing the eddy covariance technique for evaluating carbon dioxide exchange rates of ecosystems: past, present and future. *Global Change Biology*, 9: 479–492. doi: 10.1046/j.1365-2486.2003.00629.x
- Bastviken, D., L. Tranvik, J. Downing, P. Crill, and A. Enrich-Prast (2011), Freshwater Methane Emissions Offset the Continental Carbon Sink, *Science*, 331(6013), 50-50, doi:10.1126/science.1196808.
- Battin, T.J., S. Luyssaert, L.A. Kaplan, A.K. Aufdenkampe, A. Richter L.J. and Tranvik (2009). The boundless carbon cycle. *Nature Geoscience*, 2, 598-600.
- Cole, J. J. & Caraco, N. F. (1998). Atmospheric exchange of carbon dioxide in a low-wind oligotrophic lake measured by the addition of SF<sub>6</sub>. *Limnol. Oceanogr.* 43: 647-656

- Duchemin, E., M. Lucotte, and R. Canuel, (1999). Comparison of static chamber and thin boundary layer equation methods for measuring greenhouse gas emissions from large water bodies, *Environ. Sci. Technol.*, 33, 350-357.
- Eugster, W. *et al.* (2003). CO<sub>2</sub> exchange between air and water in an Arctic Alaskan and midlatitude Swiss lake: Importance of convective mixing. *J. Geophys. Res.* 108, doi:10.1029/2002JD002653.
- Finkelstein, P. and P. Sims, (2001): Sampling error in eddy correlation flux measurements. *Journal of Geophysical Research-Atmospheres*, 106(D4), 3503-3509.
- Foken, T., and B. Wichura (1996), Tools for quality assessment of surface based flux measurements, *Agric. For. Meteorol.*, 78, 83–105,
- Kaimal, J. C. and J. J. Finnigan, (1994): *Atmospheric boundary layer flows : their structure and measurement*. Oxford University Press, New York. ISBN 0-19-506239-6 (sid.).
- Kankaala, P., J. Huotari, E., Peltoma, T. Saloranta and A. Ojala (2006). Methanotrophic activity in relation to methane efflux and total heterotrophic bacterial production in a stratified, humic, boreal lake. *Limnol. Oceanogr.*, 51(2), 1195-1204.
- Mammarella I., S. Launiainen, T. Gronholm, P. Keronen, J. Pumpanen, Ü. Rannik and T. Vesala (2009). Relative humidity effect on the high frequency attenuation of water vapour flux measured by a closed-path eddy covariance system, *Journal of Atmospheric and Oceanic Technology*, 26(9), 1856-1866.
- Schubert, C.J., T. Diem, and W. Eugster (2012). Methane emissions from a small wind shielded lake determined by eddy covariance, flux chambers, anchored funnels, and boundary model calculations: a comparison. *Environ. Sci. Technol.* 46(8), 4515-4522.
- Vachon, D., Y. T. Prairie, and J. J. Cole, (2010). The relationship between near-surface turbulence and gas transfer velocity in freshwater systems and its implications for floating chamber measurements of gas exchange. *Limnol. Oceanogr.* 55: 1723-1732
- Vesala, T., J. Huotari, , Ü. Rannik, ,T. Suni, S. Smolander, A. Sogachev, S. Launiainen, and A. Ojala, (2006). Eddy covariance measurements of carbon exchange and latent and sensible heat fluxes over a boreal lake for a full open-water period. *J. Geophys. Res.* vol 111, D11101, doi:10.1029/2005JD006365
- Vesala, T., W. Eugster, and A. Ojala, (2012). Eddy covariance measurements over lakes. in *Eddy Covariance. A practical Guide to Measurement and Data Analysis*, 1<sup>st</sup> ed (eds Aubinet *et al.*), 365-376 (Springer Atmospheric Sciences).
- Vickers, D., and L. Mahrt (1997), Quality control and flux sampling problems for tower and aircraft data, *J. Atmos. Oceanic Technol.*, 14, 512–526,

# ASSESSING REGIONAL FORCING FOR LAND SURFACE SCHEMES IN CARBON CYCLE STUDIES

T. MARKKANEN, T. THUM, J. SUSILUOTO, J. KAUROLA and T. AALTO

Finnish Meteorological Institute, Helsinki, Finland

Keywords: REGIONAL CLIMATE MODELING, METEOROLOGICAL FORCING

## INTRODUCTION

Global land surface schemes (LSS) of both weather prediction models (NWP) and Earth system models (ESM), as well as their regional counterparts, are under intense development. They include increasing number of processes impacting the energy and matter exchange between the atmosphere and surface. An important regulator of energy balance is stomatal control of land vegetation. As stomata are the pathway for carbon dioxide into the plant, a proper description of their functioning in the model is a precondition for inclusion of photosynthesis. While, in ESMs the full carbon cycle, including photosynthesis, soil processes and ocean carbon cycles, is indispensable, LSSs of many of the advanced NWPs include it also.

The LSSs of these models are fully coupled to the circulation model, which means that any change in the state of one part has an instant effect to the other. Eco-physiological models, in turn, aim at producing the responses of ecosystems, or even selected eco-physiological processes, to climatic conditions. They are typically driven with prescribed meteorological data. Time-steps of the required forcing data vary from sub-daily to decadal and there is no implicit feedback to the atmosphere. Prescribed forcing is frequently applied with the LSSs of NWPs and ESMs as well, especially when their surface processes are under development or when the LSS is applied for a limited region whose feedback to the atmosphere is local and of no global importance in the time scale of interest. The main benefit of prescribed forcing is its low computational cost compared to a fully coupled run, which facilitates various sensitivity studies with a single prescribed meteorological data set.

We assess the applicability of the air temperature from a regional climate model, as prescribed forcing for LSS testing and development as well as for forcing eco-physiological models. Specifically we explore whether the lowest resolved level air temperature or the parameterized 2 m air temperature is more appropriate for land surface model simulations in daily and sub-daily timescales. Our focus is on the impact of the selection of the temperature forcing on the modeled land surface carbon balance .

## METHODS

REMO (Jacob, 2001; Jacob and Podzun, 1997) is a regional climate model that derives from the operational weather forecast model of the German weather service, and thus it has been thoroughly evaluated for its capability to predict the synoptic scale meteorological phenomena. Surface characteristics constant in time are topography, surface roughness length, land-sea mask and soil field capacity. Monthly varying parameters are surface background albedo, vegetation fraction and leaf area index (LAI). REMO has a fractional surface coverage, i.e., each grid box can contain land, water and sea ice fractions. The above mentioned surface parameter values are allocated according

to the surface cover class that gives areal information about the prominent vegetation type or, in the absence of vegetation, other characterization of land surface cover, such as desert or city, or a characterization of water surface, such as lake or ocean. In standard model versions the surface cover data is adopted from a global 1 km resolution land cover dataset by Hagemann (2002). In the simulations used in this study the original land cover data is replaced with Corine land cover data. Detailed description of its implementation is given in Gao *et al* (2013).

In the vertical, the resolved variables (air temperature, specific humidity, wind speed, etc.) are represented by a hybrid vertical coordinate system (Simmons and Burridge, 1981). In addition to the resolved variables, the model produces 2 m air temperature and dew point temperature, as well as 10-meter wind velocity for comparison with standard weather observations.

In this study REMO was run for a domain covering Fennoscandia with a resolution of  $0.167^\circ$ . ERA-Interim, the latest global atmospheric re-analysis produced by the European Centre for Medium-Range Weather Forecasts (ECMWF) (Dee *et al*, 2011), was used as lateral boundary data for the large scale atmospheric variables and surface variables such as soil temperature, soil wetness and snow depth. The forward run covered the period from 1979 to 2011. An additional 10 year spin-up period was applied before the forward run to equilibrate slowly changing variables such as deep soil temperatures.

## RESULTS

From the 31 year dataset we selected the years 1999-2011 to represent the present climate. We concentrate on a rectangular area enclosing Finland. We present seasonal probability density functions (PDF) of daily averages, maximum and minimum air Temperatures from the Lowest resolved Level (TLL) and from 2 m (T2m). Inspection of daily minimum and maximum temperatures gives insight for selecting appropriate input for models requiring sub-daily prescribed forcing.

In winter the PDFs of the daily average as well as daily minimum T2m and TLL (Fig. 1) deviate from each other especially in below zero values. The deviations derive from potentially deep temperature inversions that are typical especially for the northern part of Finland and lead to cold bias of T2m as the surface gets cooler than the air above under conditions of poor vertical mixing. In winter most of the important processes from the carbon balance point of view, such as melting of snow, take place close to  $0^\circ\text{C}$ . Thus, this difference in forcing does not have direct effect on the carbon balance. However, indirect effects, for instance via the impact on snow pack and soil temperatures may take place.

In spring the PDFs of the daily average and minimum T2m and TLL (Fig. 2) show similar behaviour of the deviations in below zero temperatures as in winter (Fig. 1). The maximum T2m and TLL deviate from each other close to  $0^\circ\text{C}$  that is crucial temperature for snow accumulation, snow melting and the startup of photosynthesis. Both snow melting and recovery of plants benefit from higher temperatures that are more frequent in maximum T2m.

In summer, while the PDFs of the daily average T2m and TLL (Fig. 3) are very similar, the minimum and maximum values deviate showing more extreme values of T2m implying higher daily range of T2m than that of TLL. This may lead to differences in simulations of processes having nonlinear dependence on the air temperature. Especially, processes described with threshold temperature values, may manifest themselves differently under the extreme conditions.

In autumn the differences between T2m and TLL PDFs are very small (Fig. 4). However, the deviation close to  $0^\circ\text{C}$  may effect soil temperatures and leaf senescence. Indirectly the deviations effect, for instance, snow accumulation and the startup of photosynthesis in the following year.

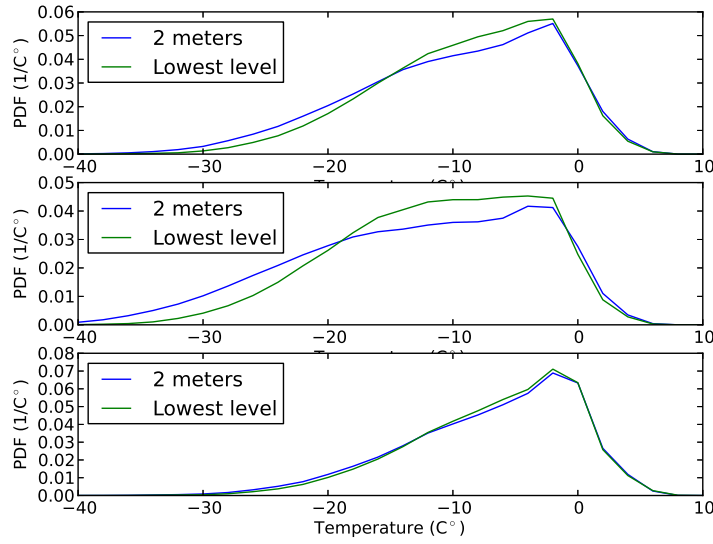


Figure 1: Probability densities of daily average (top), maximum (middle) and minimum (bottom) air temperatures of winter (December, January and February).

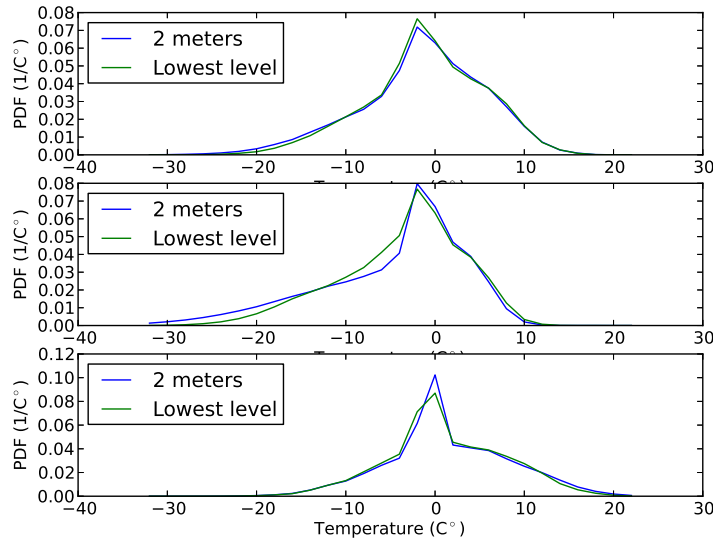


Figure 2: Probability densities of daily average (top), maximum (middle) and minimum (bottom) air temperatures of spring (March, April and May).

## CONCLUSIONS

The seasonal deviations of T2m and TLL PDFs are generally relatively small. However, when the small differences manifest themselves during the crucial time periods from the ecosystem point of view, they may influence the carbon balance. Moreover, other important controls of ecosystem processes include precipitation, radiation and air humidity. To fully assess the impact of the air temperature forcing, its time and spatial correlations with the other controlling variables have to be studied. The PDFs of daily average T2m and TLL deviate very little during most of the seasons,

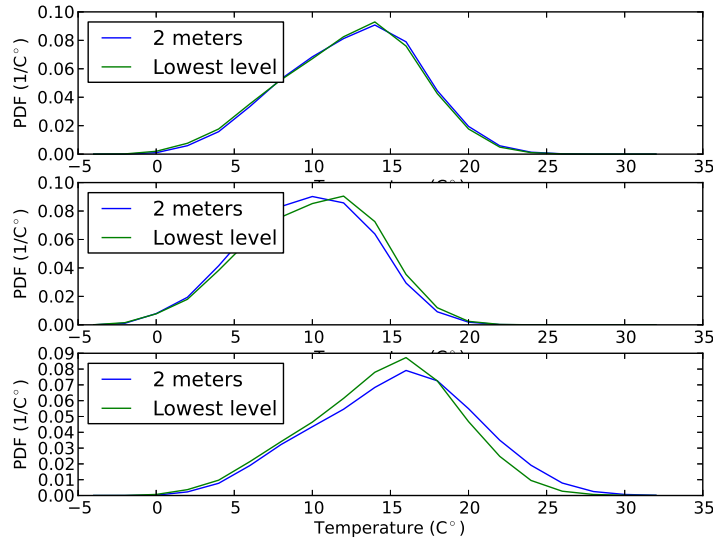


Figure 3: Probability densities of daily average (top), maximum (middle) and minimum (bottom) air temperatures of summer (June, July and August).

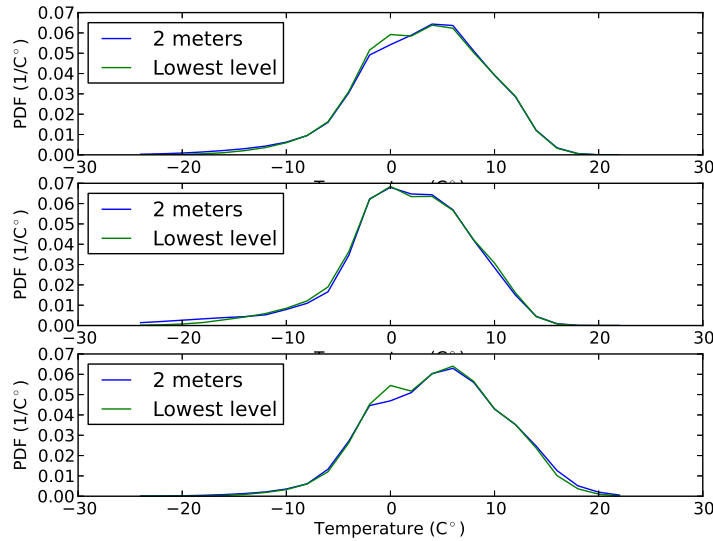


Figure 4: Probability densities of daily average (top), maximum (middle) and minimum (bottom) air temperatures of autumn (September, October and November).

implying that the selection of model level is not as important with daily time-step as with sub-daily time-step.

#### ACKNOWLEDGEMENTS

The authors acknowledge LIFE+ project SnowCarbo (LIFE07 ENV/FIN/000133). This work was supported by the Academy of Finland Center of Excellence (project no 1118615) and the Nordic Centers of Excellence CRAICC and DEFROST.

## REFERENCES

- Dee, D. P., Uppala, S. M., Simmons, A. J., Berrisford, P., Poli, P., Kobayashi, S., Andrae, U., Balmaseda, M. A., Balsamo, G., Bauer, P., Bechtold, P., Beljaars, A. C. M., van de Berg, L., Bidlot, J., Bormann, N., Delsol, C., Dragani, R., Fuentes, M., Geer, A. J., Haimberger, L., Healy, S. B., Hersbach, H., Hólm, E. V., Isaksen, I., Kållberg, P., Köhler, M., Matricardi, M., McNally, A. P., Monge-Sanz, B. M., Morcrette, J.-J., Park, B.-K., Peubey, C., de Rosnay, P., Tavolato, C., Thépaut, J.-N. and Vitart, F. (2011). The ERA-Interim reanalysis: configuration and performance of the data assimilation system. *Q.J.R. Meteorol. Soc.*, **137**, 553-597. doi: 10.1002/qj.828.
- Gao, Y., Weiher, S., Markkanen, T., Pietikäinen, J-P., Gregow, H., Henttonen, H.M., Jacob, D. and Laaksonen, A., Implementation of the CORINE land use classification in the regional climate model REMO. Submitted to Bor. Env. Res.
- Hagemann, S. (2002). An improved land surface parameter data set for global and regional climate models. Max-Planck-Institute for Meteorology, Report No. 336, Hamburg, Germany.
- Jacob, D. (2001). A note to the simulation of the annual and interannual variability of the water budget over the Baltic Sea drainage basin. *Meteorol Atmos Phys*, **77**, 61-73.
- Jacob, D. and R. Podzun (1997). Sensitivity studies with the regional climate model REMO. *Meteorol Atmos Phys*, **63**, 119-129.
- Simmons, A. J. and D. M. Burridge (1981). An energy and angular-momentum conserving vertical finite-difference scheme and hybrid vertical coordinate. *Monthly Weather Review*, **109**, 758-766.

# CHARGED AND NEUTRAL NUCLEATION OF SULFURIC ACID AND WATER: FROM EXPERIMENTS TO THEORY AND TO ATMOSPHERIC MODELING

J. MERIKANTO<sup>1</sup>, J. DUPLISSY<sup>1,2</sup>, A. MÄÄTTÄNEN<sup>3,4</sup>, H. VEHKAMÄKI<sup>1</sup>, AND M. KULMALA<sup>1</sup>

<sup>1</sup>Division of Atmospheric Sciences, Department of Physics, University of Helsinki, Finland.

<sup>2</sup>CERN, PH Department, Geneva, Switzerland.

<sup>3</sup> Université Versailles St Quentin, LATMOS-IPSL, 11 boulevard d'Alembert, 78280 Guyancourt, France

<sup>4</sup> Centre National de la Recherche Scientifique (CNRS), LATMOS-IPSL, France

Keywords: CLOUD experiments, nucleation theory, atmospheric modeling.

## INTRODUCTION

Homogeneous nucleation of sulphuric acid and water is widely modeled in global aerosol and climate models, and this mechanism contributes significantly to global cloud condensation nuclei (CCN). The representation of this mechanism varies from simple mass-based parameterizations to more complex theory-based parameterizations. These parameterizations can lead to different CCN production rates from atmospheric nucleation, which compromises the reliability of the model results. Partly the reason for this is the lack of theoretical understanding of the mechanism itself.

While sulfuric acid is long considered to be involved in most of atmospheric nucleation phenomena, the role of other components, such as ions produced by cosmic rays, has remained unclear. Global models predict that approximately half of all global cloud condensation nuclei (CCN) originate from atmospheric nucleation (Merikanto et al., 2010). To better understand the role of humans in historical and future evolution of cloud albedo and lifetime, we need to understand the anthropogenic and natural influences to nucleation rates and subsequent CCN production rates. This research is impeded by the lack of high quality laboratory measurements of nucleation rates at atmospheric conditions. Such measurements have now been produced at the CLOUD chamber in CERN for both homogeneous and ion-induced nucleation of sulphuric acid and water. We have derived a theoretical model that can predict the outcome of these experiments accurately. The model is based on reaction coefficients for the sulfuric acid hydration obtained from quantum chemistry computations applied together with the improved Classical Nucleation Theory (CNT). Here we discuss the importance of quantum chemical coefficients to the nucleation rates, and use the new theoretical model in a global aerosol model GLOMAP.

## METHODS

### CLOUD experiments

High quality experiments on neutral and ion induced nucleation of sulphuric acid and water were performed in the CERN CLOUD chamber during the CLOUD3 and CLOUD5 campaigns. The chamber is a 3m-diameter electro-polished 316L stainless-steel cylinder (26.1 m<sup>3</sup>). In the experiments, highly purified air of N<sub>2</sub> and O<sub>2</sub> with a mixing ratio of 79:21, clean de-ionized water, and trace amounts of SO<sub>2</sub> are lead to the chamber. The adjustable UV irradiation stimulates the oxidation of SO<sub>2</sub> to H<sub>2</sub>SO<sub>4</sub>. By varying the light intensity, the H<sub>2</sub>SO<sub>4</sub> production can be adjusted as required.

Since the chamber is not shielded, it is continuously exposed to galactic cosmic rays. In addition to galactic cosmic rays, the chamber can be exposed to a 3.5 GeV/c secondary pion beam. This corresponds to the characteristic energies and ionization rates of cosmic ray muons in the lower troposphere. In the experiments with the beam turned on, the beam intensity was adjusted to produce the natural range of

equilibrium ion-pair (i.p.) concentrations at the ground level ( $200 \text{ i.p cm}^{-3}$ ). The ion-pair concentration can also be reduced down to near zero using the clearing field inside the chamber. Experimental runs were performed at temperatures between 208 K and 293 K. The CLOUD chamber is described in detail in the supplementary material of [Kirkby et al. \(2011\)](#).

The experiments produced us a large set of data points where neutral and ion induced nucleation rates were obtained for 1.7 nm clusters.

### Nucleation theory

For the theoretical calculations we apply an improved form of Classical Nucleation Theory (CNT) following the work of Vehkamäki et al. (2002) presented for neutral sulphuric acid-water nucleation. We have generalized the approach of Vehkamäki et al. (2002) for the ion-induced case. We will not discuss the full theoretical model here, but focus on the one key aspect in our improved approach: the use of quantum chemical reaction coefficient in the theoretical model.

It is widely known that the liquid drop model applied by CNT is not accurate for the prediction of the free energies of small molecular clusters. In the approach by Vehkamäki et al. (2002) the total nucleation free energy barrier is calculated as the sum of the free energy between vapor phase and a sulfuric acid dihydrate (used as a reference cluster), and the CNT prediction for the free energy difference between sulfuric acid dihydrate and the critical cluster. Vehkamäki et al. (2002) used experimentally extrapolated results for the dihydrate free energy, whereas in here we use direct quantum chemical computations. In the ion induced case the quantum chemical hydrate model is also applied, but the reference cluster is the free ion.

The activity of the sulfuric acid vapor depends on the concentration of free sulfuric acid monomers and temperature. To obtain an accurate monomer concentration, all relevant hydrates or other clusters need to be accounted for.

We tested two different sets of quantum chemistry calculations for the sulfuric acid hydrate free energies. The first set was computed using B3LYP/CBSB7 for geometries and frequencies and RI-CC2/aug-cc-pV(T+d)Z for electronic energies (Kupiainen et al., 2012), and included clusters up to five sulfuric acid molecules and five water molecules, together with various clusters containing up to five ammonia molecules. Tests with this set showed that only clusters containing up to four water molecules affect the sulfuric acid activity over a sulfuric acid-water droplet, and ammonia concentrations of some ppt do not significantly affect the sulfuric acid monomer concentrations or lead to significant clusterization. Therefore, possible small trace amounts of ammonia contamination in the experimental set up are unlikely to affect the results.

For the second set we used the results from Kurten et al. (2007) using the MP2/aug-cc-pV(D + d)Z quantum chemical method, with higher-order corrections computed at the MP2/aug-cc-pV(T + d)Z and MP4/aug-cc-pV(D + d)Z levels, including clusters with one sulfuric acid molecule and up to four water molecules. The free energies obtained with the two sets are very similar besides the anharmonic correction, that is taken into account only in the second set. The anharmonic correction turns out to be significant for the calculation of the nucleation rate (Figure 1).

The theoretical model that includes the second set of quantum chemical coefficients predicts the measured nucleation rates typically within a factor of two both for neutral and ion induced nucleation.

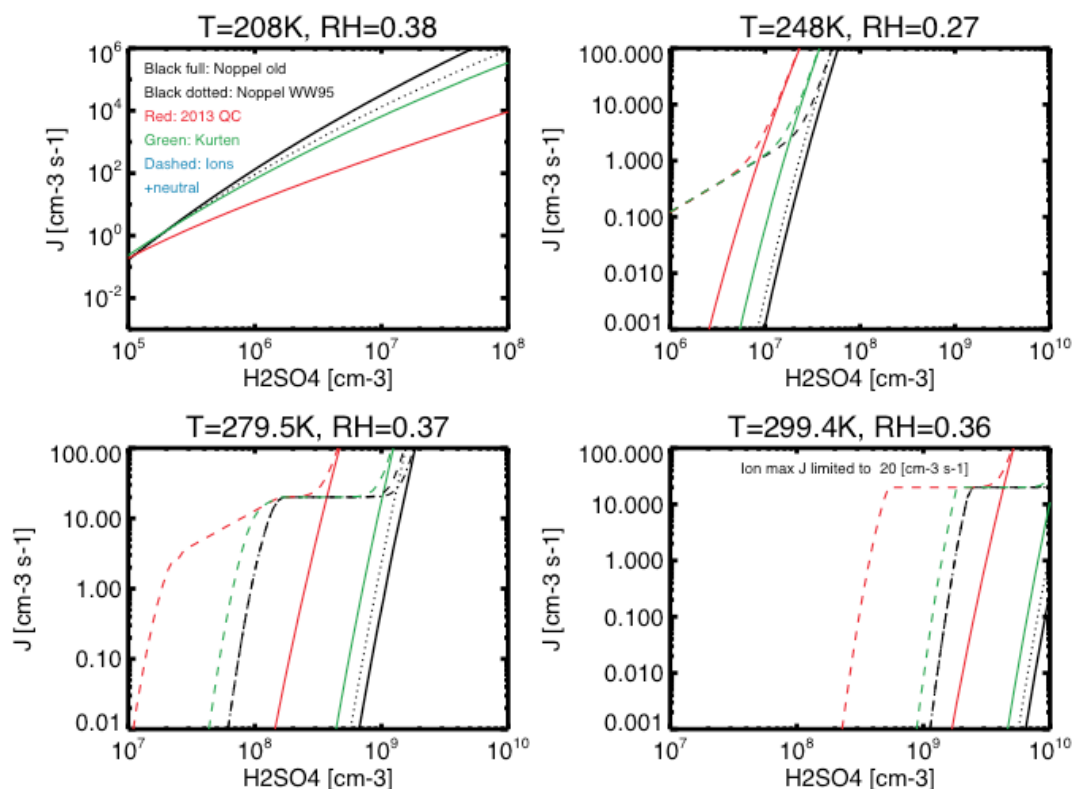


Figure 1: Theoretical nucleation rates (y-axis) against sulphuric acid concentrations (x-axis). The red lines correspond to the first set of quantum chemical reaction coefficients, while the green lines correspond to the second set of coefficients. Various other sets are also shown. The dashed lines include ion induced nucleation at the maximum ion production rate of  $20 \text{ cm}^{-3} \text{ s}^{-1}$ . Notice that the two sets have a very different temperature dependency for the nucleation rate, and that the absolute magnitudes of the rates can vary by several orders of magnitude.

### Atmospheric modelling

We apply the theoretical model for the neutral and ion induced nucleation in a global aerosol model GLOMAP. In the model the atmospheric ionization takes into account both the ion production from galactic cosmic rays and from radon decay. We will test the strength of both nucleation mechanisms in different parts of the atmosphere, and their subsequent CCN production capacity. The model is currently being run, and the results will be presented in the conference.

## CONCLUSIONS

The CLOUD measurements of neutral and ion induced nucleation of sulphuric acid and water have for the first time provided accurate enough data that can be reliably used to test the theoretical calculations. We have build a theoretical model that applies quantum chemistry computations for sulfate hydration together with CNT, and is capable of reproducing measured nucleation rates typically within a factor of two. We have implemented the theoretical model to a global aerosol model GLOMAP to study the strength of both nucleation mechanisms in different parts of the atmosphere, and their subsequent CCN production capacity.

## ACKNOWLEDGEMENTS

This work was supported by the National Council for Aerosol Research under grant A1/001.

## REFERENCES

- Kirkby, J., et al. (2011). Role of sulphuric acid, ammonia and galactic cosmic rays in atmospheric aerosol nucleation, *Nature* **476**, 429-433.
- Kupiainen, O., Ortega, I. K., Kurtén, T., and Vehkamäki, H.: Amine substitution into sulfuric acid – ammonia clusters. *Atmospheric Chemistry and Physics*, Vol 12, pp 3591-3599, 2012.
- Kurtén, T., Noppel, M., Vehkamäki, H., Salonen, M., and Kulmala, M. Quantum chemical studies of hydrate formation of H<sub>2</sub>SO<sub>4</sub> and HSO<sub>4</sub><sup>-</sup>. *Boreal Environmental Research*, Vol 12, 421-430, 2007.
- Merikanto, J., Spracklen, D. V., Mann, G. W., Pickering, S. J. & Carslaw, K. S. (2009). Impact of nucleation on global CCN. *Atmos. Chem. Phys.* **9**, 8601–8616
- Vehkamäki, H., M. Kulmala, I. Napari, K. E. J. Lehtinen, C. Timmreck, M. Noppel, and A. Laaksonen (2002), An improved parameterization for sulfuric acid–water nucleation rates for tropospheric and stratospheric conditions, *J. Geophys. Res.*, 107, 4622, doi:10.1029/2002JD002184.

# VERTICAL PARTICLE FLUX AT LAKE PYHÄSELKÄ

P. MIETTINEN<sup>1</sup>, A. JAATINEN<sup>1</sup> and A. LAAKSONEN<sup>2</sup>

<sup>1</sup>Department of Applied Physics, University of Eastern Finland,  
Kuopio, PL1627, Finland.

<sup>2</sup>Finnish Meteorological Institute, Helsinki, Finland.

Keywords: PARTICLE FLUX, LAKE INDUCED, PARTICLE SINK.

## INTRODUCTION

Aerosol particles have significant role in atmosphere as many phenomena like cloud formation are heavily impacted by presence and properties of aerosol particles. The estimation of the vertical particle flux is important method for evaluating the contribution of different mechanisms removing and sourcing atmospheric particles. Direct methods for measuring vertical aerosol fluxes include Eddy Covariance method (EC). In this experiment we used EC method for estimating vertical particle flux over lake Pyhäselkä in Joensuu.

## METHODS

The experiment site is located in Finland near Joensuu at lake Pyhäselkä Lat: 62° 32' 45" N Long: 29° 40' 6" E, elevation of lake surface is 80m ASL and area of Pyhäselkä is 361 km<sup>2</sup>. Anemometer tower was standing on little plain rock island about 200 m<sup>2</sup> of size. Lake area around experiment site includes open lake area with nearest shore at 1km to North-West while there is open lake area of near 20km to the South of the experiment site. Nearest urban areas lie in Joensuu 3km to North-East while other directions consists of rural areas. Experiment was carried out during year 2010 from 1<sup>st</sup> September 27<sup>th</sup> October. At the experiment site the Finnish Meteorological Institute maintains automated weather station acquiring temperature, humidity and wind speed and directional data, all instrument run off grid power including battery, wind and solar power.

Measurement system included Metek USA-1 3D sonic anemometer, TSI 3007 condensation particle counter (CPC) and data logging system. Anemometer can measure wind speed components of -50 m/s to 50m/s with resolution of 0.01m/s, sonic temperature can be determined between -30C and 50C while resolution is 0.001K. Anemometer sampling rate can be set from 0.004 to 50 Hz with averaging interval of 1 to 65535 samples. Sound path length in this anemometer is 175mm. TSI 3007 CPC can detect particle sizes between 10nm and 1000nm, maximum detectable concentration is 100 000 particles/cc. Total inlet sampling flow is 700cc/min while aerosol volume going through detector is 100 cc/min. In this CPC isopropanol is used as condensing agent and we modified CPC to allow continuous operation rather than running normal set up which requires filling the CPC every 6 hours. CPC was modified also to gain access to detector pulses which were saved by data logging system. Data logging system consists of LabView program running on PC based computer. System recorded 3 dimensional wind component speeds, sonic temperatures and CPC pulse counts.

The EC data was corrected for anemometer tilt correction and particle signal delay which grow out of particle sampling line with 125cc of volume and internal flow delays inside the CPC. Anemometer data was used to determine if turbulent conditions existed to assure presumptions of EC method. Long term

meteorological data from FMI will be used to evaluate whether prevailing weather represented typical conditions at the experiment site and hence making conclusions more universal.

## RESULTS

Maximum wind speed detected during experiment resulted 12.9 m/s with average wind speed of 5.6 m/s. Southern wind directions dominated during this experiment while strongest winds came from the North. Day time particle flux data does not indicate strong dependence of wind speed thus suggesting that wave breaking and subsequent spray generation is likely minor when compared to ocean sea spray generation as well absence of sea salt diminishes the ability to form aerosol when droplets evaporate.

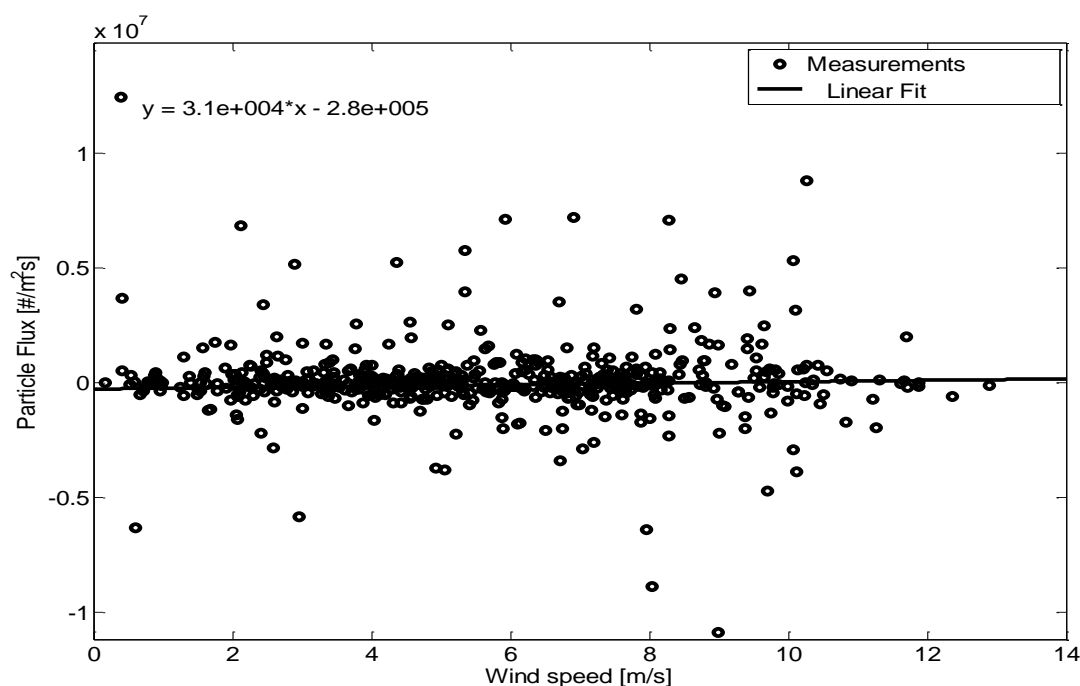


Figure 1. Particle day time vertical flux as function of wind speed.

## ACKNOWLEDGEMENTS

This work was supported by Academy of Finland Center of Excellence (project no 1118615) the Nordic Centers of Excellence CRAICC

## REFERENCES

X. Lee, W. Massman and B. Law (2004). *Handbook of micrometeorology: A guide for surface flux measurements and analysis* (Springer-Verlag, New York, LCC).

## THE LESSER STUDIED ISOPRENOIDS IN HYYTIÄLÄ

D. MOGENSEN<sup>1</sup>, M. K. KAJOS<sup>1</sup>, J. AALTO<sup>2</sup>, J. BÄCK<sup>2</sup>, M. KULMALA<sup>1</sup>,  
S. SCHALLHART<sup>1</sup>, S. SMOLANDER<sup>1</sup>, R. TAIPALE<sup>1</sup>, L. ZHOU<sup>1</sup>, and M. BOY<sup>1</sup>

<sup>1</sup>Department of Physics, University of Helsinki, P.O. Box 48, FIN-00014.

<sup>2</sup>Department of Forest Sciences, University of Helsinki, P.O. Box 27, FIN-00014.

Keywords: ATMOSPHERIC MODELLING, BVOCs, PTR-TOF-MS

### INTRODUCTION

With its definite potential for influencing everyone's life, global warming has drawn the World's attention and so has boreal forests, since it is one of the areas that is expected to heat most during the future climate warming (2 - 10°C predicted by IPCC 2006). Boreal forests are a great source of a vast amount of different volatile organic compounds (VOCs) – emitted both from the forest soil and litter, tree trunks, but mostly from the tree crown. These VOCs are various in their formation and in their chemical and physical properties. In this study, we focus on the ambient concentration of the lesser studied isoprenoids in the Eurasian taiga: isoprene and the sesquiterpenes. Though isoprene is the biogenic VOC that dominates the global BVOC emission, it has not been paid much attention in Hyytiälä due to its small ambient abundance (Rinne *et al.*, 2009). Concentration measurements of isoprene are usually done by PTR-MS and/or GC-MS. However, the measured signal can be polluted by 2-methyl-3-buten-2-ol (232MBO, molecular mass: 86.13 g/mol) that dehydrates inside the instrument and shows up on the same signal as isoprene (molecular mass: 68.10 g/mol). The occurrence of this dehydration depends on e.g. temperature and humidity (Kaser *et al.*, 2013). Sesquiterpenes are very reactive which results in a short life time (in the order of a few seconds-minutes) and they therefore become hard to measure. In Hyytiälä only one published study exists; Hakola *et al.* (2012) measured ambient sesquiterpene concentrations with GC-MS during a whole year for the less reactive, but not most abundant, sesquiterpenes. Reaction products from both isoprene and sesquiterpenes have potential to participate in aerosol growth and thereby affect climate (e.g. Lee *et al.*, 2006). In order to understand climate change we need to simulate the globe – including the boreal forests - in a perturbed environment. However, in order to do that, we firstly need to understand the processes that occur in the current state of the boreal forests.

### METHODS

We present results from SMEAR II (Station for Measuring Ecosystem-Atmosphere Relations), Hyytiälä, Southern Finland (Hari and Kulmala, 2005) for three time periods: 1) the HUMPPA-COPEC-10 campaign, 12 July – 12 August 2010 (Williams *et al.*, 2011), 2) October 2010–October 2011, which is the same period as Hakola *et al.* (2012) measured ambient sesquiterpene concentrations in Hyytiälä, and 3) June 2012 – September 2013, which is the complete period that the PTR-TOF-MS has been operating at SMEAR II. We consider GCMSD measurements of: m/z69 (only suppose to be isoprene), PTR-MS ColdTrap measurements of: m/z69 (isoprene + 232MBO), PTR-MS measurements of: m/z69 (isoprene + 232MBO) and m/z87 (232MBO + ?), PTR-TOF-MS measurements of: m/z69.0699 (isoprene), m/z69.0699 and m/z87.0805 (both 232MBO), and m/z205.3549 (sesquiterpenes), together with measured temperature and humidity. We also simulate the ambient air concentration of isoprene, 232MBO and the individual sesquiterpenes using the 1D vertical chemistry transport model SOSA (Model to Simulate the concentrations of Organic vapors and Sulfuric Acid, Boy *et al.*, 2011). This model includes modules for meteorology (SCADIS), emissions (MEGAN) (Guenther *et al.*, 2006), and chemistry (MCM version 3.2 and KPP) (Damian *et al.*, 2002). In the model we assume a 100 % homogeneous Scots pine (*Pinus sylvestris*) forest with standard emission potential values for isoprene of 100 ng/g(dw)·h<sup>-1</sup>, for 232MBO of 12-78 ng/g(dw)·h<sup>-1</sup>, for beta-caryophyllene of 0-120 ng/g(dw)·h<sup>-1</sup>, for alpha-farnesene of 0-30 ng/g(dw)·h<sup>-1</sup> and for 'other sesquiterpenes' of 0-12 ng/g(dw)·h<sup>-1</sup> (with a maximum in July for all the sesquiterpenes). A

molecule light-dependent emission factor is also included. This factor is for isoprene and 232MBO 0.9999 and for the sesquiterpenes 0.5. If this factor  $\rightarrow 1$ , then the emission of the compound is very light-dependent. If the value is zero, the emission of the compound is completely light independent.

## RESULTS & DISCUSSION

For this preliminary study we will only show results for a shorter time period, however the aim is to look at longer periods (as mentioned in the method section) and analyse the seasonal dependencies.

### ***What hides behind PTR-MS signal m/z69?***

Kaser *et al.* (2013) writes that 232MBO has a characteristic fragmentation pattern in PTR-(TOF)-MS. On m/z 87(.0805) a typical abundance of 13-25 % of the total MBO signal is found, while the corresponding fragment-ion (water loss) is found at m/z 69(.0699). This fragmentation depends on the humidity and temperature. During the HUMPPA campaign GCMSD measurements of m/z69 was made. Only isoprene is suppose to be measured on this signal. If we assume that everything measured at PTR-MS m/z87 is 232MBO and calculate how much is 232MBO on m/z69 using the GCMSD data, we can calculate the fraction of 232MBO that is suppose to be measured at m/z69 and 87. We find that ~53 % of the total 232MBO signal is found on m/z69 and ~47 % on m/z87, which is very different from the literature (e.g. Kaser *et al.*, 2013). If we use the GCMSD measurements and assume that 75 % of the total 232MBO signal is found on m/z87, then there are ~3.6 times more 'other than 232MBO' found on m/z87 than actual 232MBO. According to theory more 232MBO converts to isoprene at lower RH and at higher temperature. During the HUMPPA period we do observe a slight increase in the (m/z69)/(m/z87) ratio with increasing temperature. However we see no effect from RH. One reason for this is that we most probably never reach low enough RH. If we compare our simulated isoprene concentrations with the GCMSD measured m/z69 concentration, we underestimate the isoprene concentration by a factor of up to 4. The simulated [isoprene]/[232MBO] ratio is ~2-3. In our poster we will present short term PTR-TOF-MS data in order to separate the PTR-MS m/z69 signal into isoprene and 232MBO. The long term aim is to analyse a full year of PTR-TOF-MS data, make the signal separation and apply it to the long time series of several years of PTR-MS data for Hyytiälä.

### ***Ambient sesquiterpene concentration***

The concentration of beta-caryophyllene and alpha-farnesene, which are suppose to be the most abundant sesquiterpenes in Hyytiälä (based on the emission measurements), have never been measured there due to their high reactivity. Instead Hakola *et al.* (2012) measured the less reactive isolongifolene, longifolene, a-humulene and aromadendrene with a total concentration of up to ~2 ppt = ~5E7 #/cm<sup>3</sup>. We simulate sesquiterpene concentrations as high as ~4E7 #/cm<sup>3</sup>, which consists of ~77% beta-caryophyllene, ~16% alpha-farnesene and ~7% other sesquiterpenes. During daytime we simulate the highest [sum of sesquiterpenes]/[sum of monoterpenes] ratio to ~0.2%. Also, according to our simulations, we have a higher concentration of sesquiterpenes than isoprene during night time. In Fig. 1 the average daily pattern of the vertical concentration of the three individual modelled sesquiterpenes and the sum of the sesquiterpenes during the HUMPPA time period is illustrated. This shows a daytime peak in the sesquiterpene concentration, which is the opposite conclusion from Hakola *et al.* (2012), where they see a similar diurnal variability as observed in the case of monoterpenes with lower daytime concentrations. If the light-dependent emission factor (model value) for the sesquiterpenes is decreased, then the daily pattern would look differently than showed here. It is uncertain how much of the sesquiterpene emission originates from biosynthesis and how much from storage pool emissions. Our daily pattern correspond to the measured pattern for beta-caryophyllene in Manitou, Colorado, USA (Boy *et al.*, 2008) however Manitou is a mountain station, located in a valley, with completely different meteorology.

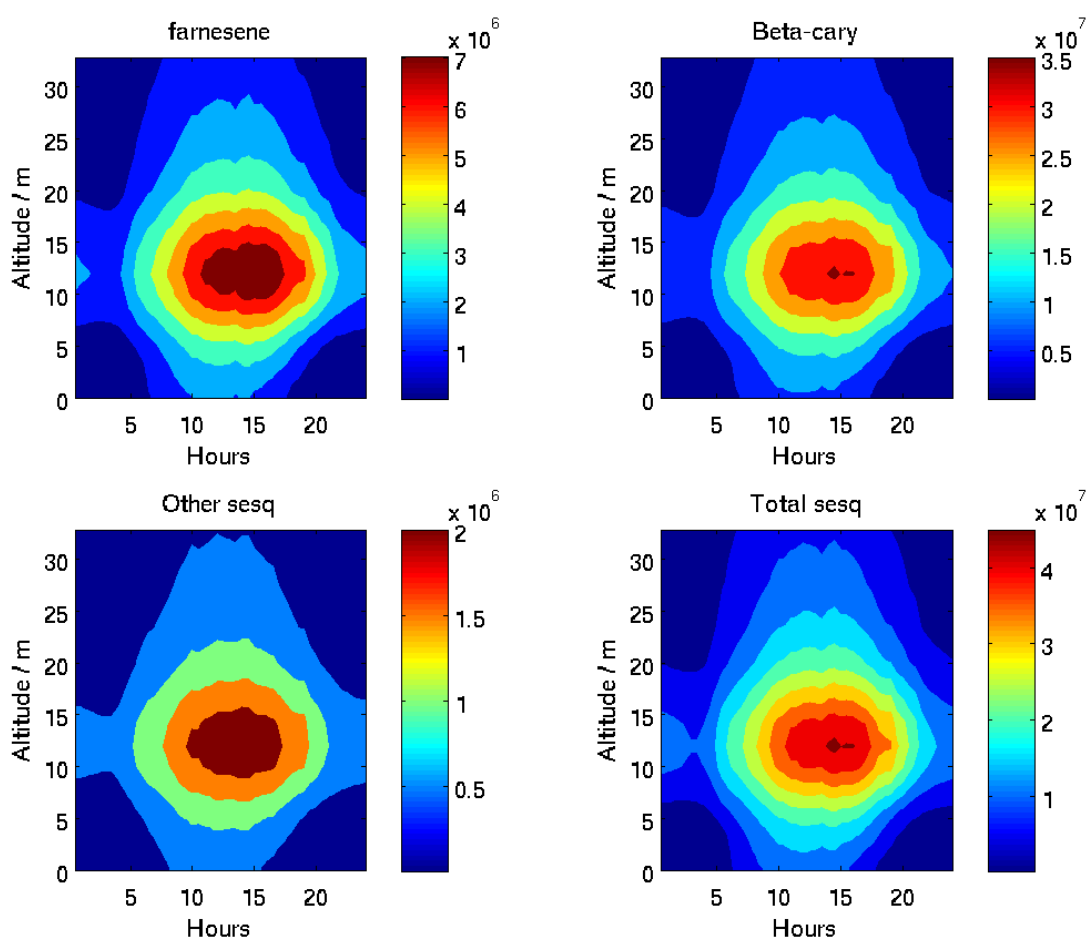


Figure 1. Average daily pattern of the vertical concentration gradient of the three individual modelled sesquiterpenes and the sum of the sesquiterpenes during the HUMPPA period. The unit is  $\text{#}/\text{cm}^3$ . Be aware that the scale of the four individual plots are different.

#### ACKNOWLEDGEMENTS

This work was financially supported by the Academy of Finland Center of Excellence (project no 1118615), the Nordic Center of Excellence CRAICC, the Helsinki University Centre for Environment (HENVI) and the doctoral program ACCC (Atmospheric Composition and Climate Change).

#### REFERENCES

- Boy, M., T. Karl, A. Turnipseed, R. L. Mauldin, E. Kosciuch, J. Greenberg, J. Rathbone, J. Smith, A. Held, K. Barsanti, B. Wehner, S. Bauer, A. Wiedensohler, B. Bonn, M. Kulmala and A. Guenther (2008). New particle formation in the Front Range of the Colorado Rocky Mountains, *Atmos. Chem. Phys.*, **8**, 1577.
- Boy, M., A. Sogachev, J. Lauros, L. Zhou, A. Guenther and S. Smolander (2011). SOSA - a new model to simulate the concentrations of organic vapours and sulphuric acid inside the ABL - Part I: Model description and initial evaluation, *Atmos. Chem. Phys.*, **11**, 43.
- Damian, V., A. Sandu, M. Damian, F. Potra and G. R. Carmichael (2002). The kinetic preprocessor KPP - a software environment for solving chemical kinetics, *Comput. Chem. Eng.*, **26**, 1567.
- Guenther, A., T. Karl, P. Harley, C. Wiedinmyer, P. I. Palmer and C. Geron (2006). Estimates of global terrestrial isoprene emissions using MEGAN (Model of Emissions of Gases and Aerosols from Nature), *Atmos. Chem. Phys.*, **6**, 3181.

- Hakola, H., H. Hellén, M. Hemmilä, J. Rinne and M. Kulmala (2012). In situ measurements of volatile organic compounds in a boreal forest, *Atmos. Chem. Phys.* **12**, 11665.
- Hari, P. and M. Kulmala. (2005). Station for measuring ecosystem-atmosphere relations (SMEAR II), *Boreal Env. Res.*, **10**, 315.
- Kaser, L., T. Karl, R. Schnitzhofer, M. Graus, I. S. Herdinger-Blatt, J. P. DiGangi, B. Sive, A. Turnipseed, R. S. Hornbrook, W. Zheng, F. M. Flocke, A. Guenther, F. N. Keutsch, E. Apel and A. Hansel (2013). Comparison of different real time VOC measurement techniques in a ponderosa pine forest, *Atmos. Chem. Phys.* **13**, 2893.
- Lee, A., A. H. Goldstein, J. H. Kroll, N. L. Ng, V. Varutbangkul, R. C. Flagan and J. H. Seinfeld (2006). Gas-phase products and secondary aerosol yields from the photooxidation of 16 different terpenes, *J. Geophys. Res.*, **11**, D17305.
- Rinne, J., J. Bäck and H. Hakola (2009). Biogenic volatile organic compound emissions from the Eurasian taiga: current knowledge and future directions, *Boreal Environ. Res.* **14**, 807.
- Williams, J., J. Crowley, H. Fischer, H. Harder, M. Martinez, T. Petäjä, J. Rinne, J. Bäck, M. Boy, M. Dal Maso, J. Hakala, M. Kajos, P. Keronen, P. Rantala, J. Aalto, H. Aaltonen, J. Paatero, T. Vesala, H. Hakola, J. Levula, T. Pohja, F. Herrmann, J. Auld, E. Mesarchaki, W. Song, N. Yassaa, A. Nölscher, A. M. Johnson, T. Custer, V. Sinha, J. Thieser, N. Pouvesle, D., Taraborrelli, M. J. Tang, H. Bozem, Z. Hosaynali-Beygi, R. Axinte, R. Oswald, A. Novelli, D. Kubistin, K. Hens, U. Javed, K. Trawny, C. Breitenberger, P. J. Hidalgo, C. J. Ebben, F. M. Geiger, A. L. Corrigan, L. M. Russell, H. G. Ouwersloot, J. Vila-Guerau de Arellano, L. Ganzeveld, A. Vogel, M. Beck, A. Bayerle, C. J. Kampf, M. Bertelmann, F. Köllner, T. Hoffmann, J. Valverde, D. Gonzalez, M.-L. Riekkola, M. Kulmala and L. Lelieveld (2011). The summertime boreal forest field measurement intensive (HUMPPA-COPEC-2010): an overview of meteorological and chemical influences, *Atmos. Chem. Phys.*, **11**, 10599.

# EVALUATION OF THE MULTI-COMPARTMENT SIZE-RESOLVED INDOOR AEROSOL MODEL

B. MØLGAARD<sup>1</sup>, J. ONDRÁČEK<sup>2</sup>, P. ŠT'ÁVOVÁ<sup>3</sup>, L. DŽUMBOVÁ<sup>2</sup>, M. BARTÁK<sup>4</sup>, T. HUSSEIN<sup>1,5</sup>,  
and J. SMOLÍK<sup>5</sup>

<sup>1</sup>Department of Physics, University of Helsinki, PL48, FI-0014 University of Helsinki, Finland

<sup>2</sup>Department of Aerosol and Laser Studies, Institute of Chemical Process Fundamentals, Rozvojova 135, Prague 6, 165 02, Czech Republic

<sup>3</sup>Czech Green Building Council, Drtinova 10, Prague 5, 150 00, Czech Republic

<sup>4</sup>Department of Environmental Engineering, Technická 4, Czech Technical University in Prague, Prague 6, 166 07, Czech Republic

<sup>5</sup>Department of Physics, The University of Jordan, Amman-11942, Jordan.

Keywords: AIRFLOW RATES, TRACER AEROSOL, TRACER GAS.

## INTRODUCTION

Indoor aerosol models have been used for decades in studies of indoor air pollution. Models range in complexity from simple one-box models to models involving several aerosol dynamical processes and computational fluid dynamics. When using advanced models detailed knowledge of the indoor environment is required. Such knowledge is often missing, especially in the case of natural ventilation. The Multi-Compartment Size-resolved Indoor Aerosol Model (MC-SIAM, Hussein *et al.*, 2005) assumes a number indoor zones (each having well-mixed air) and includes several aerosol dynamical processes. As input parameters it requires among others air flows, penetration factors, and friction velocities. The latter are needed for the incorporated deposition model. Because at least some of these parameters are usually unknown, the model has previously been used together with aerosol measurements to estimate the values of these input parameters. We have investigated the reliability of such input parameter estimates, by comparing air flow estimates with measured values.

## METHODS

Measurements were performed in a small naturally ventilated apartment in Prague. The apartment comprised a kitchen, a corridor, and a living room. This apartment was divided into two zones. There was no door between the corridor and the kitchen, so these were considered as one zone. We used four different setups for the windows and the internal door; in one setup the door and both windows were closed, and in the three other setups either the door or a window was partially open. Aerosols were sampled in turns from the each of these zones and from the outdoors, and particle number size distributions were measured with a Differential Mobility Particle Sizer and an Optical Particle Sizer. To make the estimation of air flows possible, a tracer aerosol was injected to either the kitchen or the living room 21 times. Each of these times, two different tracer gases were also injected, one to each room. These tracer gas concentrations were monitored and reference values for the air flows were obtained based on these measurements. For each zone  $k$  the MC-SIAM simulates the number concentration  $N_k$  in each size section based on the equation

$$\frac{dN_k}{dt} = \frac{1}{V_k} (Q_{0k} P_k N_0 - Q_{k0} N_k + Q_{jk} N_j - Q_{kj} N_k) + S - \beta N_k + J_{coag},$$

where  $Q_{jk}$  is the airflow from zone  $j$  to  $k$ ,  $j$  represents the other zone, and zone 0 is the outdoors,  $P_k$  is the penetration factor,  $S$  is a source rate,  $\beta$  is the deposition rate, and  $J_{coag}$  is the change rate due to coagulation. So the first terms give the change rate due to air exchange with the outdoors and the other zone. Using the MC-SIAM and outdoor particle number size distributions we simulated the indoor particle number size distributions. While comparing simulations with measurements we iterated the input parameters (air flows, penetration factors, and friction velocities), and we chose the input parameters which gave the best agreement between simulations and measurements.

## RESULTS AND DISCUSSION

We succeeded in simulating the indoor particle size distribution for part of the time during each of these four setups. For some periods it was, however, impossible to obtain good simulations. Most probably the difficulties were caused by changes in the flows, which are expected for natural ventilation. Based the successful simulations we estimated the air flows and compared estimations to estimations based analysis of tracer gases (Table 1). For most of the air flows the estimates obtained with the two methods are consistent with each other. The main difference is seen for the two internal flows, where the estimates based on tracer gases are somewhat higher. The reason for this difference is most likely that the MC-SIAM assumes that all particles penetrate through when the air moves from one room to the other.

For more information see Mølgaard *et al.* (2013).

Setup	Method	$Q_{01}$	$Q_{10}$	$Q_{02}$	$Q_{20}$	$Q_{12}$	$Q_{21}$
All Closed	MC-SIAM	2.9–14	1.3–13	1.3–2.5	1.0–3.4	0–2.2	0–1.7
	Tracer gas	10–11.5	9.4–10.5	0–1.1	0.6–1.5	1.3–2.5	0.3–1.8
Door open	MC-SIAM	3.1	1.3	1.5	3.3	11.0	9.3
	Tracer gas	1.9–2.3	1.0–5.0	0.7–1.4	0–2.4	7.6–15.4	10.3–14.4
Living room window open	MC-SIAM	6.6–7.5	5.7–6.4	33–43	34–44	0.9–5.3	0–4.2
	Tracer gas	4.5–13	8–19	29–30	24–26	3.5–5.9	9.5–9.6
Kitchen window open	MC-SIAM	75–92	75–96	2.2–4.3	0.3–1.6	0.3–0.4	0.9–4.4
	Tracer gas	70–75	68–75	0–2.4	1.0–2.2	0.7–2.2	0.4–0.8

Table 1: Comparison of air flow estimates obtained with the MC-SIAM and the reference tracer gas method.

## CONCLUSIONS

As expected, the airflow estimates obtained with the MC-SIAM are generally good. This result confirms the reliability past studies which used this method.

## REFERENCES

- Hussein T., H. Korhonen, E. Herrmann, K. Hämeri, K.E.J. Lehtinen and M. Kulmala (2005) Emission Rates Due to Indoor Activities: Indoor Aerosol Model Development, Evaluation, and Applications, *Aerosol Sci. Technol.* **39**, 1111–1127.
- Mølgaard, B., J. Ondráček, P. Šťávoř, L. Džumbová, M. Barták, T. Hussein and J. Smolík (2013) Migration of Aerosol Particles within a Two-Zone Apartment with Natural Ventilation: a Multi-Zone Validation of the MC-SIAM, *Indoor Built Environ.* In Press.

# URBAN PARTICLE NUMBER CONCENTRATION FORECAST MODEL EVALUATION

B. MØLGAARD<sup>1</sup>, W. BIRMILI<sup>2</sup>, SAM CLIFFORD<sup>3</sup>, ANDREAS MASSLING<sup>4</sup>, K. ELEFThERIADIS<sup>5</sup>, M. NORMAN<sup>6</sup>, S. VRATOLIS<sup>5</sup>, B. WEHNER<sup>2</sup>, J. CORANDER<sup>7</sup>, K. HÄMERI<sup>1</sup>, and T. HUSSEIN<sup>1,8</sup>

<sup>1</sup>Department of Physics, P.O. Box 48, FI-00014, University of Helsinki, Finland.

<sup>2</sup>Leibniz Institute for Tropospheric Research, 04303 Leipzig, Germany.

<sup>3</sup>School of Chemistry, Physics and Mechanical Engineering, Queensland University of Technology, 2 George St, Brisbane 4001, Australia.

<sup>4</sup>Department of Environmental Science, Aarhus University, DK-4000 Roskilde, Denmark.

<sup>5</sup>Institute of Nuclear Technology and Radiation Protection, N.C.S.R. Demokritos, 15310 Ag. Paraskevi, Attiki, Greece

<sup>6</sup>Environment and Health administration, City of Stockholm, 104 20 Stockholm, Sweden

<sup>7</sup>Department of Mathematics and Statistics, P.O. Box 68, FI-00014, University of Helsinki, Finland

<sup>8</sup>Department of Physics, The University of Jordan, Amman 11942, Jordan

Keywords: URBAN AIR, AIR POLLUTION, STATISTICAL MODEL.

## INTRODUCTION

Because of the high population density, the density of pollution sources is high in cities. Among the sources are vehicular traffic, combustion for domestic heating, industry, power plants, harbours, and airports. The concentrations of many pollutants are elevated in cities due to these sources and they pose a threat to the health of the urban population. In addition to the strength of the sources, also the weather conditions affect the pollutant concentrations. For many gaseous pollutant and for particle mass concentrations several forecast models exist, but urban particle number concentrations have not been modelled as extensively. We recently published a model which to our knowledge is the first urban particle number concentration forecast model (Mølgaard *et al.*, 2012). During the development of this model we used sub-urban background particle number concentrations measured in Helsinki (2005-2008). The model performed well for this data set. However, to know whether this model performs well for urban background locations in general, a test with data sets from other locations was needed. Therefore, we have tested this model with data from Stockholm, Copenhagen, Leipzig, and Athens in addition to the Helsinki data we already used.

## METHODS

Our model (Mølgaard *et al.*, 2012) is a statistical model which relates particle number concentrations to meteorological parameters (wind, temperature, relative humidity), traffic intensity and time of day, week, and year. It is a regression model with an autoregressive structure for the error term, and it contains 78 parameters. For each data set we used the first year as learning data only, and the forecast model was implemented in a sequential manner which allowed the model to benefit

from the growing learning data set as it moved forward in time. We used two data sets from Stockholm. These both contained particle number concentration measurements, and one data set was from an urban background station (Rosenlundsgatan), while the other one was from a street canyon (Hornsgatan). Although the latter data set did not come from an urban background station, it was included to investigate how the model works under heavy traffic influence. The data from the other cities included particle number size distributions, and based on those we calculated the particle number concentrations for ultrafine particles (diameter  $< 100$  nm) and for the accumulation mode (diameter  $> 100$  nm). We chose a time resolution of one hour.

## RESULTS

The performance of the forecast model was evaluated by comparing the forecasts with measurements. To quantify this comparison we calculated the  $R^2$  and the Index of Agreement ( $IA$ ), which are listed in Table 1. Based on these model performance metrics we see that the model performed best for Helsinki and Stockholm, while the performance was poor for the Leipzig data. In (Mølgaard *et al.*, 2013) we have investigated the reasons for this and found that the model works best for locations in which local emission dominate the aerosol, and in locations with clear seasonal variation of the aerosol.

Site	$R^2$	$IA$	$n_{data}$
Helsinki UFP	0.596	0.858	21514
Helsinki Acc	0.513	0.801	19142
Hornsgatan	0.696	0.899	3653
Rosenlundsgatan	0.518	0.814	2435
Copenhagen UFP	0.396	0.746	9451
Copenhagen Acc	0.475	0.776	9694
Leipzig UFP	0.389	0.725	8923
Leipzig Acc	0.259	0.663	9426
Athens UFP	0.492	0.806	5902
Athens Acc	0.428	0.775	5797

Table 1: Model performance metrics and the number of data points used in the calculation of the model performance metrics.

## REFERENCES

- Mølgaard, B., T. Hussein, J. Corander and K. Hämeri (2012). Forecasting size-fractionated particle number concentrations in the urban atmosphere, *Atmos. Environ.*, **46**, 155–163.
- Mølgaard, B., W. Birmili, S. Clifford, A. Massling, K. Eleftheriadis, M. Norman, S. Vratolis, B. Wehner, J. Corander, K. Hämeri, T. Hussein (2013). Evaluation of a statistical forecast model for size-fractionated urban particle number concentrations using data from five European cities *J. Aerosol Science*, In press.

# CLEAN AIR DELIVERY RATE TEST OF FIVE PORTABLE AIR CLEANERS

B. MØLGAARD<sup>1</sup>, A.J. KOIVISTO<sup>2</sup>, T. HUSSEIN<sup>1,3</sup> and K. HÄMERI<sup>1</sup>

<sup>1</sup>University of Helsinki, Department of Physics, P.O. Box 48, FI-00014 Helsinki, Finland

<sup>2</sup>Finnish Institute of Occupational Health, Nanosafety Research Centre, Topeliuksenkatu 41 a A, FI-00250 Helsinki

<sup>3</sup>Department of Physics, Faculty of Science, The University of Jordan, Amman, 11942 Jordan

Keywords: AIR QUALITY, INDOOR AEROSOL

## INTRODUCTION

People in the western world generally spend most of the time indoors, so indoor air quality is important for our health and well-being. Pollutants in the indoor air originate either from indoor sources or from the outdoors. Common indoor sources are cooking, heating, electronics, building materials, furniture, and cleaning agents. The air quality can be improved by removing the pollution sources. Ventilation is also important from removal of pollutants, but if the outdoor air is polluted, ventilation is not enough for ensuring good indoor air quality. Moreover, ventilation may be costly if the outdoor air is cold. Portable air cleaners can supplement the ventilation in obtaining good air quality. No air cleaner can remove all pollutants, but many can remove both particles and a wide range of gaseous pollutants. We have tested the ability of five air cleaners to remove particles.

## METHODS

We tested the air cleaners in a room sized chamber with well-mixed air. It had a constant ventilation rate ( $0.6 \text{ h}^{-1}$ ), and the air was sampled both from inside the chamber and from where the incoming air entered the room. The incoming air was cleaned and part of the time aerosol generators injected particles into the ventilation duct of the incoming air. We measured particle number size distributions of the sampled air masses using a scanning mobility particle sizer and an optical particle sizer. For each air cleaner we conducted an experiment which lasted 24 hours, and consisted of three periods. In the beginning of the experiment, the air cleaner was off and the aerosol generators were on. Then after 160 minutes, the air cleaner was turned on, and the concentration of particles in the chamber first decreased and then reached a steady state. Finally, three hours before the end of the experiment the aerosol generators were turned off, and the concentration decreased again. The time derivative of the concentration  $N_i$  of particles in size section  $i$  is given by the balance equation:

$$\frac{dN_i}{dt} = \lambda N_{\text{vent},i} - (\lambda + \beta_i + \gamma_i) N_i + J_{\text{coag},i},$$

where  $\lambda$  is the ventilation rate,  $N_{\text{vent},i}$  is the concentration of same sized particles in the incoming air,  $\beta_i$  is the deposition rate,  $\gamma_i$  is the cleaning rate, and  $J_{\text{coag},i}$  is the change rate due to coagulation. The three unknowns that we needed to estimate from the data were the ventilation rate, deposition rate, and cleaning rate. These were assumed to be constant throughout the experiment. During the beginning of the experiment the cleaning rate was zero (because the air cleaner was off), and in the end of the experiment  $N_{\text{vent},i}$  was zero. Based on this information and simple derivations from the equation above, we estimated  $\lambda$ ,  $\beta$ , and  $\gamma$  from the data. By multiplying the cleaning rate  $\gamma$  with the volume of the chamber we obtained the Clean Air Delivery Rate (CADR), which is a standard measure of the air cleaner performance.

## RESULTS AND DISCUSSION

The obtained CADR for the five air cleaners are seen in Figure 1. We also performed an identical experiment with no air cleaner and obtained CADR close to zero, as expected. This experiment served as a simple test of our method. The best CADR were obtained for IQAir, Electrolux, and Plymovent. These all used fans to blow or suck the air through filters. Elixair differed by using an electrostatic precipitator for the cleaning. The air cleaner from LightAir was an ion generator. The CADR for this device was poor for particles larger than 100 nm, but it performed better for ultrafine particles. All the other devices had options for the user to increase the CADR by increasing the fan speed at the cost of higher electricity consumption and more noise. When considering CADR and electricity consumption, the air cleaner from Electrolux performed best.

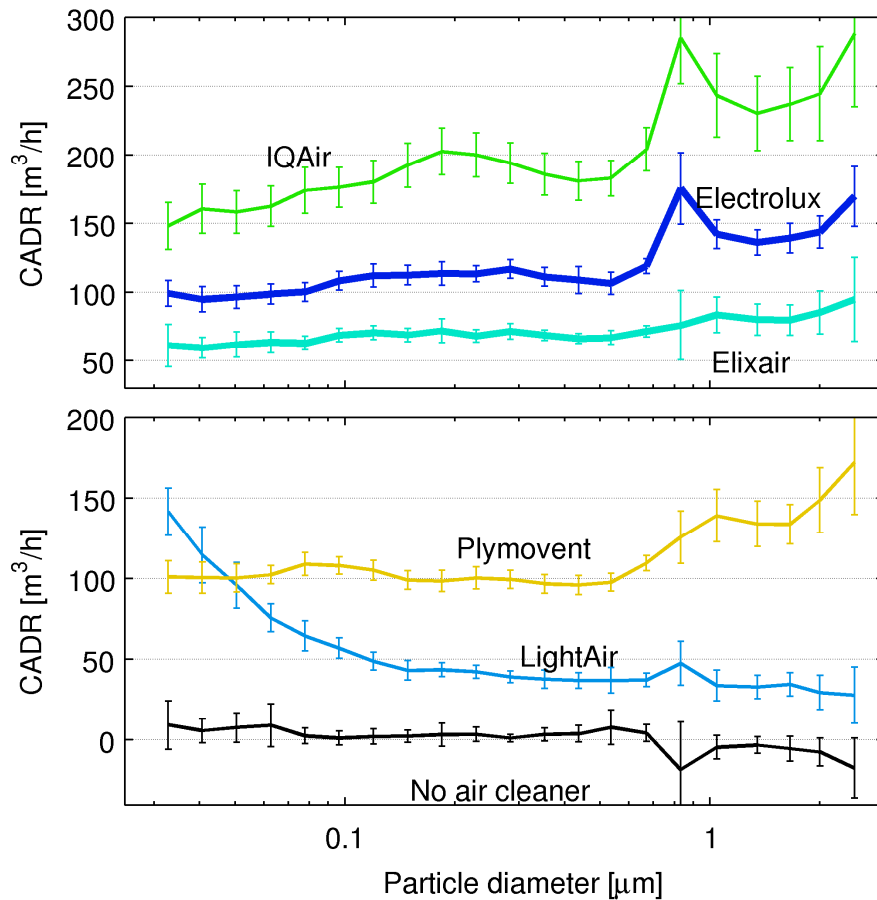


Figure 1: Size resolved Clean Air Delivery Rates for the five air cleaners, and for an experiment with no air cleaner. The air cleaners are denoted by the names of the manufacturers.

# SULPHURIC ACID MONOMER VS. TOTAL SULPHATE IN NUCLEATION STUDIES

K. NEITOLA<sup>1</sup>, D. BRUS<sup>1</sup>, U. MAKKONEN<sup>1</sup>, M. SIPILÄ<sup>2</sup>, T. JOKINEN<sup>2</sup>, K. KYLLÖNEN<sup>1</sup>, H. LIHAVAINEN<sup>1</sup> and M. KULMALA<sup>2</sup>

<sup>1</sup>Finnish Meteorological Institute, Erik Palménin aukio, P.O. Box 503, FI-00101 Helsinki, Finland

<sup>2</sup>Department of Atmospheric Sciences, University of Helsinki, Gustaf Hållströmin katu 2, FI-00560 Helsinki, Finland

Keywords: nucleation, sulphuric acid, total sulphate

## INTRODUCTION

Sulphuric acid is known to be key component in atmospheric nucleation (Kulmala *et al.*, 2006) but the exact mechanism of the first steps of nucleation are not yet known. Recent numerous laboratory experiments on the role of sulphuric acid in nucleation have been conducted using mass spectrometry analysis to quantify the sulphuric acid concentration and it's relation to the observed nucleation rate (Benson *et al.*, 2008; Sipilä *et al.*, 2010; Kirkby *et al.*, 2011; Zollner *et al.*, 2012). In our study, we found a discrepancy of one to two orders of magnitude between sulphuric acid monomer concentration and total sulphate concentration measured with two independent methods from the same source of sulphuric acid vapour.

## METHODS

Sulphuric acid vapour was produced by saturating purified, dry, particle free carrier gas in a thermally controlled saturator half filled with pure (97% w.t. baker analysed) sulphuric acid. The flow from the saturator was mixed with humidified clean air in the mixing unit. The output of the saturator was tested with two independent methods of detecting sulphuric acid. The measured output was compared to theoretical prediction from vapour pressure of sulphuric acid (Kulmala and Laaksonen, 1990). After the output test, a nucleation study of sulphuric acid water system was conducted using a laminar flow tube. The measurement setup is presented in figure 1.

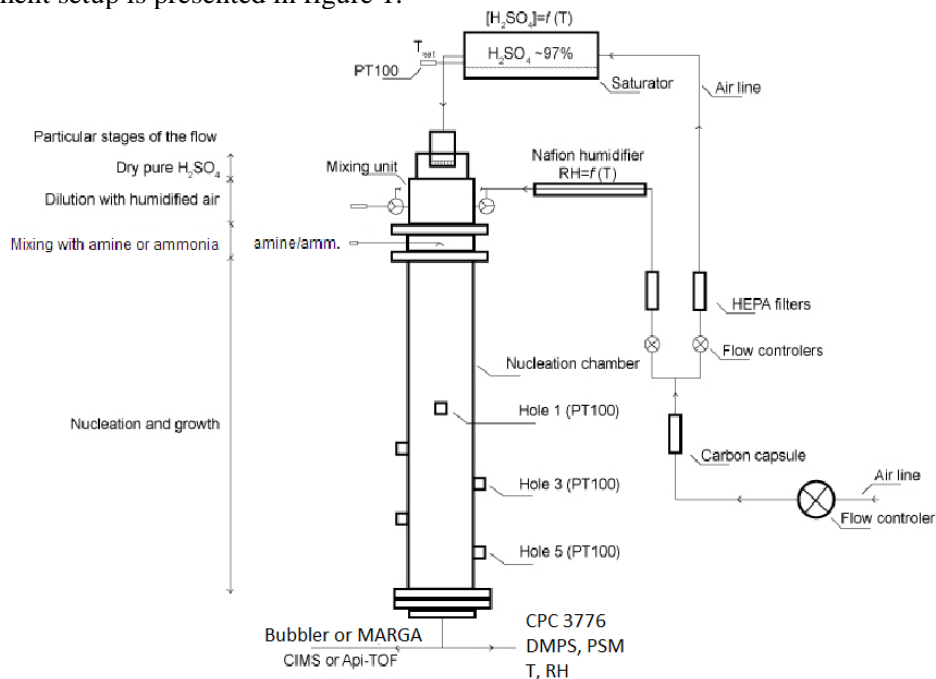


Figure 1. Schematic illustration of the setup.

Particle concentration was monitored with CPCs; Particle Size Magnifier (PSM, Vanhanen *et al.*, 2011), TSI model 3776 or 3025A. The size distribution of the particles was measured in the range of approximately 3-250 nm using a Differential Mobility Particle Sizer (DMPS) system. It consisted of radioactive neutralizer ( $^{63}\text{Ni}$ ), HAUKE-type Differential Mobility Analyzer (DMA) and a CPC 3025A.

Sulphuric acid monomer concentration was measured with mass spectrometers; Chemical Ionization Mass Spectrometer (CIMS, Eisele & Tanner, 1993; Mauldin *et al.*, 1998; Petäjä *et al.*, 2009) and Chemical Ionization Atmospheric pressure interface Time of Flight mass spectrometer (CI-API-ToF, ToFwerk AG, Thun, Switzerland and Aerodyne Research Inc., USA, Junninen *et al.*, 2010; Jokinen *et al.*, 2012). These instruments used a similar chemical ionization inlet, where sulphuric acid molecules are ionized using nitrate ions ( $\text{NO}_3^-$ ) produced from nitric acid using radioactive charger ( $^{241}\text{Am}$ ). For more details see above mentioned references.

An instrument for Measuring AeRosols and Gases (MARGA, Metrohm Applikon Analytical BV, Netherlands, ten Brink *et al.*, 2007) was used to monitor total sulphate concentration. MARGA is an online ion chromatograph that is able to measure concentrations of several different gas phase and particulate phase substances, including sulphate. The main difference between the methods is that mass spectrometers measure the gas phase sulphuric acid monomer concentration compared to MARGA which measures total sulphate concentration including particle phase.

First the output of the saturator was tested changing the sulphuric acid concentration by changing the temperature of the saturator in 5 degree centigrade steps from 273K to approximately 305K. The flow through the saturator was kept constant. Also a flow rate tests were conducted, by keeping the temperature constant and increasing the saturator flow rate from 0.25 lpm to 2 lpm to define the range of flow which would get saturated within the saturator. Three different carrier gases were used in flow rate tests to estimate the effect of carrier gas impurity. After the tests, a nucleation experiment using the laminar flow tube was conducted to measure nucleation rates of water-sulphuric acid system. The results of the nucleation experiment were compared to our previous results, where a furnace was used to produce the sulphuric acid vapour and bubblers were used to measure total sulphate concentration. Bubbler is similar ion chromatography method as MARGA instrument, the main difference being that bubbler is offline method as MARGA is online.

## RESULTS

The measured output of the saturator is presented in figure 2 as a function of predicted concentration calculated from the vapour pressure using equation (33) from Kulmala & Laaksonen (1990). Total sulphate concentration measured with MARGA lies on top of the one-to-one line. Output was measured with mass spectrometers using several flow rates through the saturator and with two inlet flow rates. Dry and two humid conditions were used. Experiment with 1 meter tubing after the saturator was done to investigate the magnitude of the inlet losses after the saturator. Results from mass spectrometers lies from one to two orders of magnitude lower than the one-to-one line. RH and inlet flow rates do not influence the results. The flow rate through the saturator affects the results if it is too low as seen in the figure with flow rate of 0.05 and 0.2 lpm. Extended inlet has very little or no effect on the results.

Figure 3 presents the nucleation rates of sulphuric acid-water nucleation as a function of sulphuric acid monomer or total sulphate concentration, obtained in this study and from our previous studies, for comparison. The conditions in these measurements are exactly the same ( $T = 298\text{K}$ ,  $\text{RH} \sim 30\%$ ,  $\tau = 30\text{s}$ ), which is evident from the nucleation rates. Data points measured using CIMS (squares, on the left) are done by using several CPC's. The green squares are measured using CPC 3776, which might be undercounting at low sulphuric acid concentration due to small sizes of the particles. This is supported by the results as the slope of the points is bending at lower sulphuric acid concentration. The black points in the figure represents measurements, where sulphuric acid was produced using furnace method (Brus, *et al.*, 2010). The production method does not have any effect as the results lie in same space with both

production methods. The stars present results measured with ion chromatography methods, bubbler or MARGA. See Brus et al., (2010) for details of bubbler method. Main finding here is the one to two orders of magnitude difference between sulphuric acid monomer vs. total sulphate concentrations with similar nucleation rates.

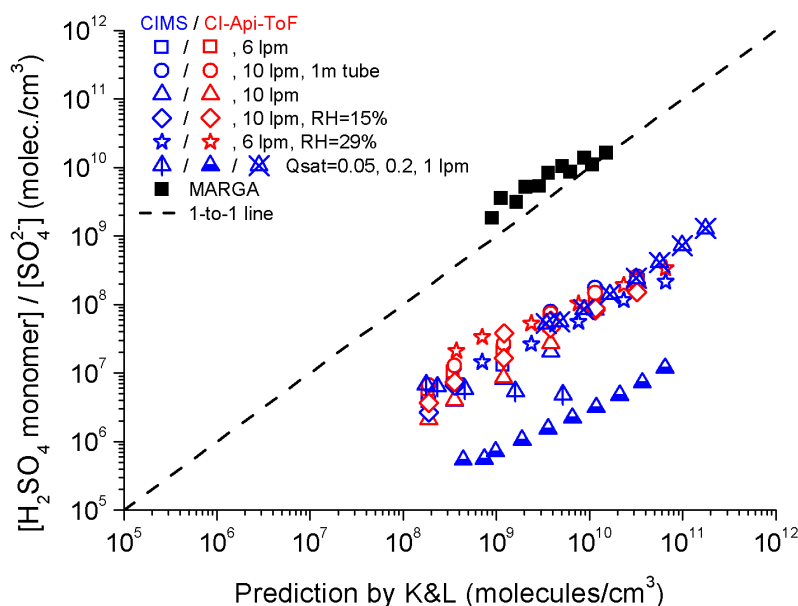


Figure 2. Output of the saturator as a function of prediction by Kulmala & Laaksonen (1990) measured with MARGA and mass spectrometers. Several saturator and two inlet flow rates were used with three (dry, RH 15% and RH 29%) humidity conditions.

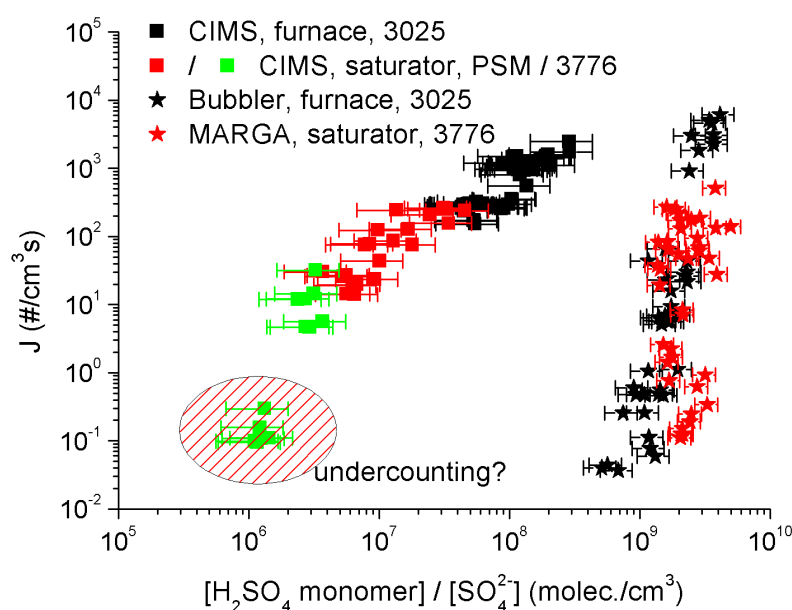


Figure 3.  $\text{H}_2\text{SO}_4\text{-H}_2\text{O}$  nucleation rates as a function of residual sulphuric acid monomer or total sulphate concentration. Black points are from our previous studies using furnace method.

Figure 4 shows the results of flow rate tests conducted with three different carrier gases ( $\text{N}_2$  grades 6.0 and 5.0, and pressurized air) between 0.25 lpm and 2 lpm with constant saturator temperature (283K). As seen

from figure 4, the data points are on top of each other so the effect of carrier gas purity and the amount of contaminants is not an issue here.

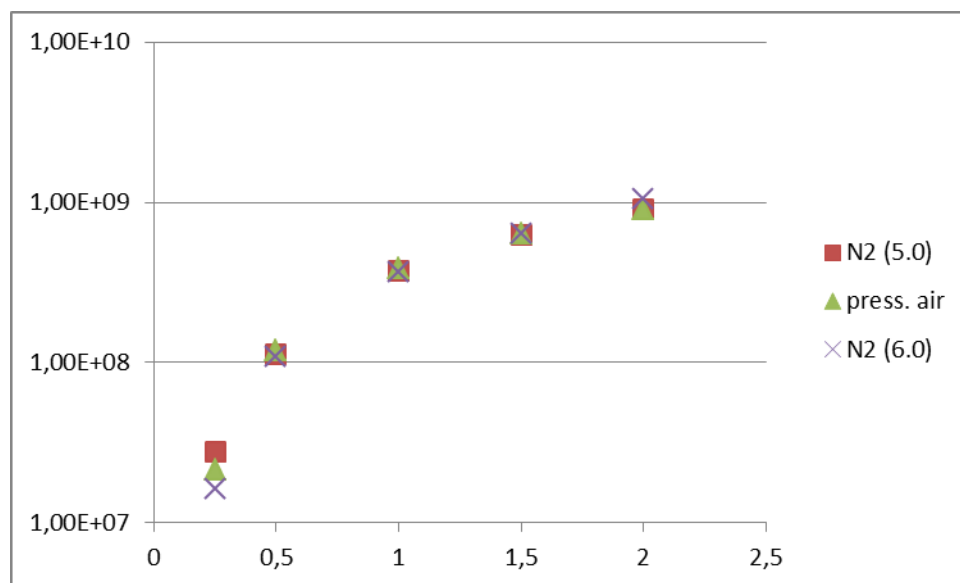


Figure 4. CI-API-TOF measured sulphuric acid monomer concentration as a function of saturator flow rate using three different carrier gases (N<sub>2</sub> grades 6.0 and 5.0, and pressurized air) with constant saturator temperature (283K).

## CONCLUSIONS

The saturator method for producing sulphuric acid vapour is determined to perform well when comparing to the previous method of furnace. It produces constant sulphuric acid concentration with reproducible nucleation results. Total sulphate concentrations measured with MARGA agree very well with prediction as the mass spectrometers measured monomer concentration is one to two orders lower than prediction. This difference between total sulphate and monomer concentration cannot be explained by formation of larger clusters (dimer, trimer, etc.) as the dimer concentration was always less than 1% of monomer, with decreasing trend when moving towards larger clusters. The nucleation rates also agree well when using similar instruments for sulphuric acid detection. When comparing similar nucleation rates between monomer and total sulphate concentration the difference in sulphuric acid concentration is from one to two orders of magnitude.

The flow rate tests show that the contaminants of carrier gas is not resulting to the loss of sulphuric acid as all the carrier gases tested produces exactly similar results. Sulphuric acid lost to the particulate phase contributes only for less than 10% of the total sulphate, so the sulphuric acid is not hidden there either.

From these results it is evident that most (90-99%) of the sulphuric acid is distributed to clusters not containing solely sulphuric acid. These clusters might be very important in the nucleation mechanism. The results also raises questions like, what is the contribution of total sulphate to the growth of the particles in the early stages of nucleation?

## ACKNOWLEDGEMENTS

This research was supported by the Academy of Finland Center of Excellence program (project number 1118615).

## REFERENCES

- Benson, D. R., L.-H. Young, F. R. Kameel and S.-H. Lee (2008). Laboratory-measured nucleation rates of sulfuric acid and water binary homogeneous nucleation from the  $\text{SO}_2 + \text{OH}$  reaction, *Geophys. Res. Lett.*, 35, 11.
- Brus, D., Hyvärinen, A.-P., Viisanen, Y., Kulmala, M. and Lihavainen H. (2010). Homogeneous nucleation of sulfuric acid and water mixture: experimental setup and first results, *Atmos. Chem. Phys.*, 10, 2631–2641.
- Eisele, F. and D. Tanner. (1993). Measurement of the gas phase concentration of  $\text{H}_2\text{SO}_4$  and methane sulfonic acid and estimates of  $\text{H}_2\text{SO}_4$  production and loss in the atmosphere, *J. Geophys. Res.*, 98, D5, 9001–9010.
- Jokinen, T., Sipilä, M., Junninen, H., Ehn, M., Lönn, G., Hakala, J., Petäjä, T., Mauldin III, R. L., Kulmala, M., and D. R. Worsnop, D. R. (2012). Atmospheric sulphuric acid and neutral cluster measurements using CI-API-TOF. *Atmos. Chem. Phys.*, 12, 4117–4125.
- Junninen, H., Ehn, M., Petäjä, T., Luosujärvi, L., Kotiaho, T., R. Kostianen, R., Rohner, U., Gonin, M., Fuhrer, K., Kulmala, M. and Worsnop, D. (2010). A high-resolution mass spectrometer to measure atmospheric ion composition, *Atmos. Meas. Tech.*, 3, 1039–1053.
- Kirkby, J., Curtius, J., Almeida, J., Dunne, E., Duplissy, J., Ehrhart, S., Franchin, A., Gagné, S., Ickes, L., Kürten, A., Kupc, A., Metzger, A., Riccobono, F., Rondo, L., Schobesberger, S., Tsagkogeorgas, G., Wimmer, D., Amorim, A., Bianchi, F., Breitenlechner, M., David, A., Dommen, J., Downard, A., Ehn, M., Flagan, R., Haider, S., Hansel, A., Hauser, D., Jud, W., Junninen, H., Kreissl, F., Kvashin, A., Laaksonen, A., Lehtipalo, K., Lima, J., Lovejoy, E., Makhmutov, V., Mathot, S., Mikkilä, J., Minginette, P., Mogo, S., Nieminen, T., Onnela, A., Pereira, P., Petäjä, T., Schnitzhofer, R., Seinfeld, J., Sipilä, M., Stozhkov, Y., Stratmann, F., Tomé, A., Vanhanen, J., Viisanen, Y., Aron Vrtala, A., Wagner, P., Walther, H., Weingartner, E., Wex, H., Winkler, P., Carslaw, K., Worsnop, D., Baltensperger, U. & Kulmala, M. (2011). Role of sulphuric acid, ammonia and galactic cosmic rays in atmospheric aerosol nucleation, *Nature*, 476, 429–433.
- Kulmala M. & Laaksonen, A. (1990). Binary nucleation of water-sulfuric acid system: Comparison of classical theories with different  $\text{H}_2\text{SO}_4$  saturation vapor pressures, *J. Chem. Phys.*, 93 (1). 1.
- Kulmala, M., K. E. J. Lehtinen and A. Laaksonen (2006). Cluster activation theory as an explanation of the linear dependence between formation rate of 3 nm particles and sulphuric acid concentration, *Atmos. Chem. Phys.*, 6, 787–793.
- Mauldin III, R. L., Frost, G., Chen, G., Tanner, D., Prevot, A., Davis, D., and Eisele, F. (1998). OH measurements during the First Aerosol Characterization Experiment (ACE 1): Observations and model comparisons, *J. Geophys. Res.*, 103, 16713–16729.
- Ortega, K., O. Kupiainen, T. Kurtén, T. Olenius, O. Wilkman, M. J. McGrath, V. Loukonen and H. Vehkamäki (2012). From quantum chemical formation free energies to evaporation rates. *Atmos. Chem. Phys.*, 12, 225–235.
- Petäjä, T., Mauldin, III, R., Kosciuch, E., McGrath, J., Nieminen, T., Paasonen, P., Boy, M., Adamov, A., Kotiaho, T. and Kulmala M. (2009). Sulfuric acid and OH concentrations in a boreal forest site, *Atmos. Chem. Phys.*, 9, 7435–7448.
- Sipilä, M., Berndt, T., Petäjä, T., Brus, D., Vanhanen, J., Stratmann, F., Patokoski, J., Mauldin III, R. L., Hyvärinen, A.-P., Lihavainen, H. and Kulmala, M. (2010). The Role of Sulfuric Acid in Atmospheric Nucleation, *Science*, 327 (5970): 1243–1246.
- ten Brink, H., Otjes, R., Jongejan, P. and Slanina S. (2007). An instrument for semi-continuous monitoring of the size-distribution of nitrate, ammonium, sulphate and chloride in aerosol, *Atmos. Env.*, 41, 13, 2768–2779.
- Vanhanen, J., J. Mikkilä, K. Lehtipalo, M. Sipilä, H. E. Manninen, E. Siivola, T. Petäjä and M. Kulmala, (2011). Particle Size Magnifier for Nano-CN Detection. *Aerosol Sci. & Tech.*, 45, 4.
- Zollner, J. H., Glasoe, W. A., Panta, B., Carlson, K. K., McMurry, P. H. and Hanson, D. R. (2012). Sulfuric acid nucleation: power dependencies, variation with relative humidity, and effect of bases, *Atmos. Chem. Phys.*, 12, 4399–4411.

# FORECASTING NPF EVENTS DURING PEGASOS-ZEPPELIN NORTHERN MISSION 2013 IN HYYTIÄLÄ, FINLAND

T. NIEMINEN<sup>1,2</sup>, T. YLI-JUUTI<sup>1</sup>, H. E. MANNINEN<sup>1,3</sup>, V.-M. KERMINEN<sup>1</sup> and M. KULMALA<sup>1</sup>

<sup>1</sup>Department of Physics, University of Helsinki, P. O. Box 64, FI-00014, University of Helsinki, Finland

<sup>2</sup>Helsinki Institute of Physics, P. O. Box 64, FI-00014, University of Helsinki, Finland

<sup>3</sup>Institute of Physics, University of Tartu, Ülikooli 18, EE-50090 Tartu, Estonia

Keywords: new particle formation and growth, forecasts.

## INTRODUCTION

Atmospheric new particle formation (NPF) events have been observed in numerous locations and in different environments in the planetary boundary layer (Kulmala et al., 2004). Most of these observations are based on stationary ground-level measurements. In order to obtain information on the spatial extent of NPF events both in the vertical and horizontal directions, measurements using aircrafts are needed. As part of the 4 year-long EU funded PEGASOS (Pan-European Gas-Aerosol-Climate Interaction Study) project, a Zeppelin NT airship was performing aerosol, trace gas and photochemistry measurement flights in Central Finland during May–June 2013. In order to most efficiently utilize the flight hours of the airship, it was necessary to prepare forecasts on the probability of NPF events in the coming days.

Most of the Zeppelin measurement flights were directed to vicinity of the University of Helsinki SMEAR II measurement station in Hyytiälä (Hari and Kulmala, 2005). Measurements of aerosol number size-distributions, various trace gas concentrations and basic meteorological data were started at the SMEAR II station in January 1996. These long time-series records have been used to extensively characterize the conditions in which NPF occurs (or does not occur) in this boreal forest environment, both based on the local atmospheric conditions as well as the synoptic situation and airmass origins (Lyubovtseva et al., 2005; Dal Maso et al., 2007; Sogacheva et al., 2008).

Field observations, laboratory experiments and theoretical considerations have shown that sulphuric acid is one of the key components in atmospheric NPF events, but in addition also trace amounts of other vapors such as ammonia, amines or oxidized organics are needed (e.g. Kulmala et al., 2013). Proxies for the concentrations of these trace gases have been developed based on campaign-wise measurements (Petäjä et al., 2009). Based on the concentrations and emissions of these trace gases, several parametrizations have been developed to describe the occurrence and intensity of NPF (e.g. Bonn et al., 2008; Paasonen et al., 2010).

## METHODS

The main objective of the NPF forecasts was to predict whether during the next 3 days NPF events are likely to occur at the SMEAR II station area. A time period of 3 days was chosen to have long enough time for preparing the measurement instruments needed on different flights while still maintaining reliability of the input data used in making the NPF forecasts. The final NPF forecast was always given for the next day, as the Zeppelin measurement flights were typically planned one day in advance.

Forecasts for concentrations of trace gases SO<sub>2</sub>, O<sub>3</sub>, NO<sub>x</sub>, CO and OH as well as particulate matter (PM<sub>10</sub>) and relative humidity were obtained from the Finnish Meteorological Institute SILAM (System for

Integrated modelLing of Atmospheric coMposition) air quality model. This model provides predictions for the next 5 days at several levels above ground. All SILAM forecast data is freely accesible via internet (<http://silam.fmi.fi/>), and the forecast is updated once per day. For the purposes of the current NPF event forecasts, we used predictions for the ground level during next 3 days from the model grid point nearest to Hyytiälä SMEAR II station.

Air mass arrival directions and source areas were forecasted for 96 hours prior to their arrival at Hyytiälä using the HYSPLIT model developed by NOAA (<http://www.arl.noaa.gov/HYSPLIT.php>). As input we used the US National Weather Service's Global Forecasting System (GFS) weather forecast data. As supporting data we also used several “traditional” weather forecasts available on the internet (including Finnish Meteorological Institute and Foreca), mainly to evaluate the probabilities of cloudiness and rain.

In a data-mining study of the SMEAR II station long-time series records, Hyvönen et al. (2005) found that condensation sink (describing the pre-existing aerosol surface area) and relative humidity were the two parameters most effectively separating NPF days from non-NPF days, NPF occurring only on days with low CS and RH. On the other hand, photochemical production of sulphuric acid and oxidation products of organics is faster in clear-sky conditions with high UV radiation intensity. Thus, our main criteria in forecasting NPF to occur was clear sky conditions, low condensation sink (in practise low PM10 concentration) and low relative humidity. We also developed several “nucleation parameters” to forecast the intensity of NPF. The parameters that worked best were either related to only the proxy concentration of sulphuric acid, or to proxies for both sulphuric acid and oxidation products of monoterpenes. The monoterpene concentrations were predicted on the basis of temperature (Lappalainen et al., 2009), and OH radical and ozone concentrations were used to calculate the proxy concentrations of their oxidation products. Also the air mass source area and transport route to Hyytiälä were considered when making the NPF forecasts, as the occurrence of NPF in Hyytiälä has been observed to be highly favorable in air masses arriving from the Arctic Ocean and Northern Atlantic over Scandinavia (Dal Maso et al., 2007).

## RESULTS AND CONCLUSIONS

The PEGASOS-Zeppelin Northern mission took place between 3.5. and 11.6.2013. Figure 1 shows the particle number size-distributions during this time along with the forecasted NPF occurrence. In the beginning of the campaign several strong NPF bursts occurred, and our forecasts were able to capture these as well as the days of no particle formation. During this time air masses were originating mainly from the Atlantic and arriving to Hyytiälä over Scandinavia. On some days the air was remarkably clean, characterized by very low SO<sub>2</sub> concentration (below 0.1 ppb), resulting in low sulphuric acid concentration and weak or no NPF even on clear-sky conditions.

After mid-May until early June the airmasses arrived to Hyytiälä mainly from east, either spending several days over continental Russia or in some cases more directly from the Arctic Ocean via northwest Russia. This is rather unusual airmass transport pattern to Hyytiälä, and also made the NPF forecasting more challenging. During this time there were situations when the polluted airmasses resulted in high condensation sink preventing NPF occurrence. Also SILAM forecasts for SO<sub>2</sub> and PM10 concentrations were less accurate during the easterly airmasses compared to when airmasses came from west or south. This might be related to less accurate emission data for these species over the Russian area.

During the 40 day campaign we forecasted NPF to occur on 8 days, and during 7 of these an NPF event occurring over several hours was observed. On the other hand, on none of the days forecasted to be non-NPF days was there appearance and growth of new nucleation mode particles. The main challenges in making the NPF forecasts were to obtain as reliable as possible input data from SILAM, HYSPLIT and weather forecasts. The methods utilized here are most likely also applicable to other locations where there is sufficiently long datasets available characterizing the occurrence of particle formation.

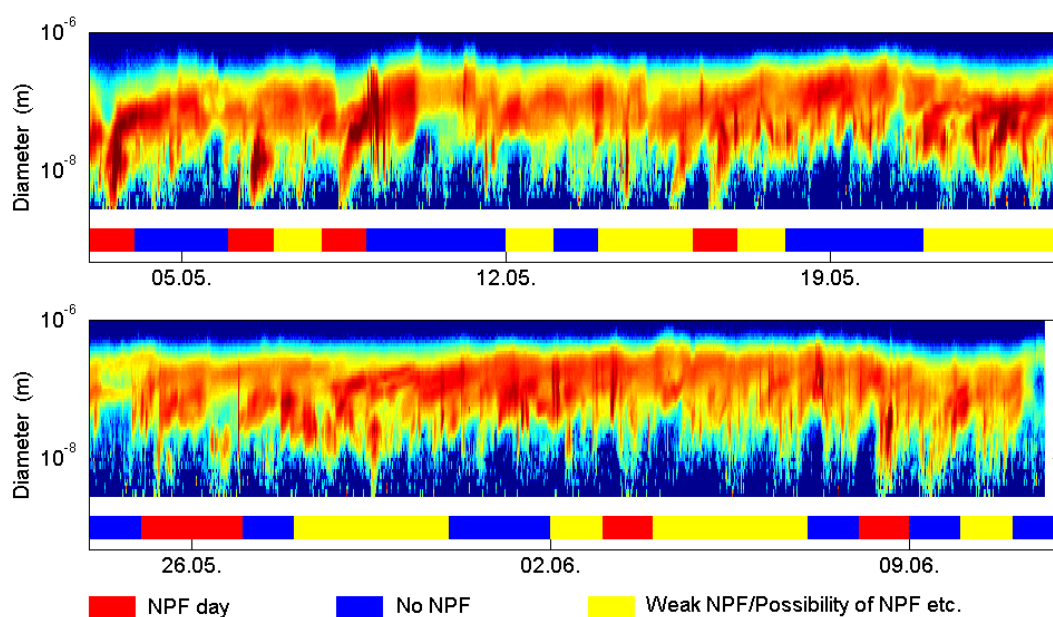


Figure 1. Time series of 3–1000 nm particle number size distributions during the PEGASOS-Zeppelin campaign 3.5.–11.6.2013 in Hyytiälä. The color bar indicates which days were forecasted to be NPF days (red), non-NPF days (blue) or to possibly have NPF occurring (yellow).

## ACKNOWLEDGEMENTS

This research is supported by European Commission under the Framework Programme 7 (FP7-ENV-2010-265148). The support by the Academy of Finland Centre of Excellence program (project no. 1118615) and Finnish Cultural Foundation is also gratefully acknowledged. The Zeppelin NT was accompanied by an international team of scientists and technicians who are all warmly acknowledged.

## REFERENCES

- Bonn B., Boy M., Kulmala M., Groth A., Trawny K., Borchert S. and Jacobi S. (2008). A new parametrization for ambient particle formation over coniferous forests and its potential implications for the future. *Atmos. Chem. Phys.* **9**, 8079–8090.
- Dal Maso M., Sogacheva L., Aalto P. P., Riipinen I., Komppula M., Tunved P., Korhonen L., Suur-Uski V., Hirsikko A., Kurtén T., Kerminen V.-M., Lihavainen H., Viisanen Y., Hansson H.-C. and Kulmala M. (2007). Aerosol size distribution measurements at four Nordic field stations: identification, analysis and trajectory analysis of new particle formation bursts. *Tellus* **59B**, 350–361.
- Hari P. and Kulmala M. (2005). Station for Measuring Ecosystem–Atmosphere Relations (SMEAR II). *Boreal Env. Res.* **10**, 315–322.
- Hyvönen, S., Junninen, H., Laakso, L., Dal Maso, M., Grönholm, T., Bonn, B., Keronen, P., Aalto, P., Hiltunen, V., Pohja, T., Launiainen, S., Hari, P., Mannila, H. and Kulmala M. (2005). A look at aerosol formation using data mining techniques. *Atmos. Chem. Phys.* **5**, 3345–3356.
- Kulmala M., Vehkamäki H., Petäjä T., Dal Maso M., Lauri A., Kerminen V.-M., Birmili W. and McMurry, P. H. (2004). Formation and growth rates of ultrafine atmospheric particles: a review of observations. *Journal of Aerosol Science* **35**, 143–176.
- Kulmala M., Kontkanen J., Junninen H., Lehtipalo K., Manninen H. E., Nieminen T., Petäjä T., Sipilä M., Schobesberger S., Rantala P., Franchin A., Jokinen T., Järvinen E., Äijälä M., Kangasluoma J.,

- Hakala J., Aalto P. P., Paasonen P., Mikkilä J., Vanhanen J., Aalto J., Hakola H., Makkonen U., Ruuskanen T., Mauldin R. L., Duplissy J., Vehkamäki H., Bäck J., Kortelainen A., Riipinen I., Kurtén T., Johnston M. V., Smith J. N., Ehn M., Mentel T. F., Lehtinen K. E. J., Laaksonen A., Kerminen V.-M. and Worsnop D. R. (2013). Direct observations of atmospheric aerosol nucleation. *Science* **339**, 943–946.
- Lappalainen H. K., Sevanto S., Bäck J., Ruuskanen T. M., Kolari P., Taipale R., Rinne J., Kulmala M. and Hari P. (2009). Day-time concentrations of biogenic volatile organic compounds in a boreal forest canopy and their relation to environmental and biological factors. *Atmos. Chem. Phys.* **9**, 5447–5459.
- Lyubovtseva Y. S., Sogacheva L., Dal Maso M., Bonn B., Keronen P. and Kulmala M. (2005). Seasonal variations of trace gases, meteorological parameters, and formation of aerosols in boreal forests. *Boreal Env. Res.* **10**, 493–510.
- Paasonen P., Nieminen T., Asmi E., Manninen H. E., Petäjä T., Plass-Dülmer C., Flentje H., Birmili W., Wiedensohler A., Hörrak U., Metzger A., Hamed A., Laaksonen A., Facchini M. C., Kerminen V.-M. and Kulmala, M. (2010). On the roles of sulphuric acid and low-volatility organic vapours in the initial steps of atmospheric new particle formation. *Atmos. Chem. Phys.* **10**, 11223–11242.
- Petäjä T., Mauldin R. L., Kosciuch E., McGrath J., Nieminen T., Paasonen P., Boy M., Adamov A., Kotiaho T. and Kulmala M. (2009). Sulfuric acid and OH concentrations in a boreal forest site. *Atmos. Chem. Phys.* **9**, 7435–7448.
- Sogacheva L., Saukkonen L., Nilsson E. D., Dal Maso M., Schultz D. M., De Leeuw G. and Kulmala M. (2008). New aerosol particle formation in different synoptic situations at Hyytiälä, Southern Finland. *Tellus* **60B**, 485–494.

# CLIMATE FEEDBACKS LINKING ATMOSPHERIC CO<sub>2</sub> CONCENTRATION, BVOC EMISSIONS AND AEROSOLS IN FOREST ECOSYSTEMS DERIVED FROM SATELLITE DATA

A. NIKANDROVA, A-M. SUNDSTRÖM, V-M. KERMINEN and M. KULMALA

<sup>1</sup>University of Helsinki, Department of Physical Sciences, P.O. Box 64, FIN-00014, University of Helsinki, Finland

Keywords: SATELLITE REMOTE SENSING, AOD, GPP, BVOC.

## INTRODUCTION

Trace gases, Biogenic Volatile Organic Compounds (BVOC) and aerosol particles are tightly linked by various chemical and physical processes taking place in the atmosphere and biosphere (Arneth et al. 2010, Carslaw et al. 2010). However, there are a lot of feedback mechanisms in the earth system that are poorly understood and not yet quantified. Kulmala et al (2013) suggested a framework that couples several feedback mechanisms. A study, based on ground measurements from a boreal forest site, proves the existence of the loop. The aim of this work is to investigate the possibility of using satellite borne products for analyzing this feedback loop.

## METHODS AND DATA

Figure 1 illustrates the proposed feedback mechanism between increasing CO<sub>2</sub>, processes in forest ecosystems, aerosols and radiation. A rise in the atmospheric CO<sub>2</sub> concentration enhances photosynthesis and thus gross primary production (GPP), i.e. the rate at which ecosystems generate their biomass from chemical energy. This relation initiates the whole feedback loop. The first step demonstrates a rise in BVOC emissions caused by increase in terrestrial vegetation. The next step shows that higher BVOC emissions intensify new particles formation, expressed as aerosol optical depth (AOD), which is a measure of absorbed or scattered light by aerosols. The atmospheric aerosol loading influences significantly the diffuse fraction of radiation, which can be seen at step 3. The feedback loop is completed with the positive connection between increased diffuse radiation and GPP.

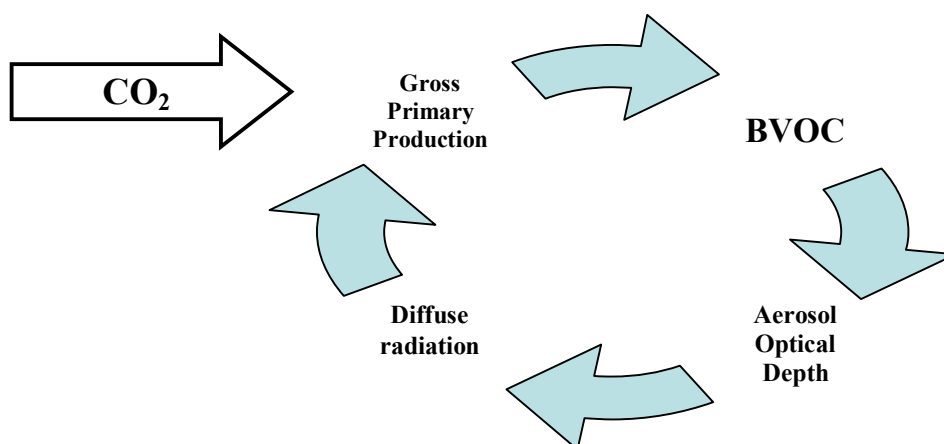


Figure 1. The feedback loop associated with CO<sub>2</sub> increase.

The data used in this study includes various satellite based observations. The Moderate imaging spectroradiometer (MODIS) onboard Aqua platform was used to get AOD and GPP. The radiation fluxes were obtained from Clouds and Earth's Radiant Energy System (CERES) level 3 data calculated using diurnal data from geostationary satellites. CO<sub>2</sub> concentration is retrieved by Atmospheric Infrared Sounder (AIRS), while formaldehyde (HCHO) is derived from the Ozone Monitoring Instrument (OMI)

measurements. All data points were co-located with the SMEAR II station in Hyytiälä, southern Finland (61° 51' N, 24° 17' E, 181 meters above sea level), corresponding to typical boreal coniferous forest.

## RESULTS AND CONCLUSIONS

The satellite-derived parameters were analyzed to show the causal relation between each step. The time period from 2006 to 2009 was chosen according to the availability of data from all instruments that were used. Only summer was considered as photosynthesis is inhibited during winter and thus all the related processes cease.

All steps of the loop showed a statistically significant positive correlation. As an example of one of the steps, Figure 2 demonstrates the last step of the loop: the relation between fraction of diffuse radiation and GPP. The data points are averages of 8 days of measurements during the months May-August in 2009. The solid line shows the linear least squares fit and the correlation coefficient is 0.78.

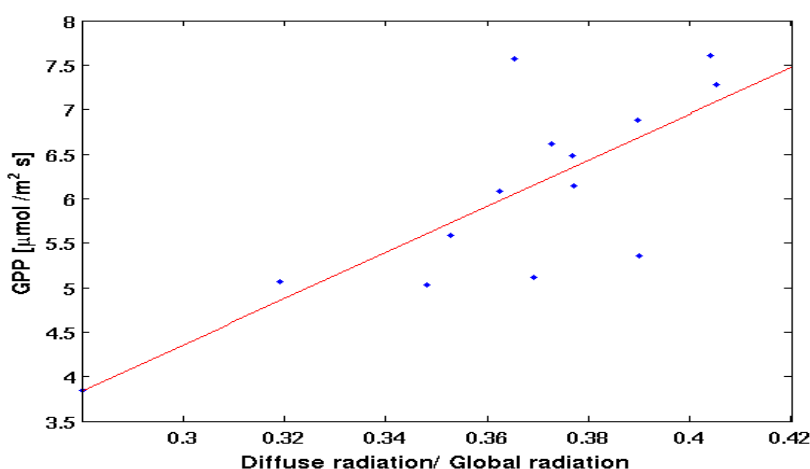


Figure 2. Gross primary production as a function of the diffuse radiation fraction. The linear least squares fit to the data is shown with the solid line.

The results show that boreal forest serves as a sink of CO<sub>2</sub> as well as a source for aerosol particles. These both mechanisms lead to the mitigation of climate warming as long as there is an increase in forest growth. Our future plans include working with other types of terrestrial ecosystems and quantifying the strength of this feedback. Satellite data provide a good tool for this purpose in places where there are no long datasets of ground-based measurements available.

## ACKNOWLEDGEMENTS

This work was supported by the Academy of Finland Centre of Excellence program ( project no 1118615).

## REFERENCES

- Arneth, A., Unger, N., Kulmala, M., and Andreae M. O. (2009): Clean the air, heat the planet, *Science*, **326**: 672-673.
- Carslaw, K. S., Boucher, O., Spracklen, D. V., Mann, G. W., Rae, J. G. L., Woodward, S., and Kulmala, M. (2010): A review of natural aerosol interactions and feedbacks within the Earth system, *Atmos. Chem. Phys.*, **10**, 1701.
- Kulmala, M et al (2013). Climate feedback linking the increasing atmospheric CO<sub>2</sub> concentration, BVOC emissions, aerosols and clouds in forest ecosystems (in preparation).

# **SIMULATED INTERACTION BETWEEN TREE STRUCTURE AND XYLEM AND PHLOEM TRANSPORT IN 3D TREE CROWNS USING MODEL LIGNUM**

E. NIKINMAA<sup>1</sup>, R. SIEVÄNEN<sup>2</sup> AND T. HÖLTTÄ<sup>1</sup>

<sup>1</sup>Department of Forest Sciences, PO Box 27, 00014 University of Helsinki, Finland, <sup>2</sup>Vantaa Res. Ctr, Finnish Forest Research Institute, PO Box 18, 01301 Vantaa, Finland

Keywords: phloem translocation, sap flow, photosynthesis, transpiration, tree architecture

## **INTRODUCTION**

Traditionally leaf and canopy gas exchange of CO<sub>2</sub> and H<sub>2</sub>O are estimated based on intercepted radiation, micrometeorological variables and leaf and canopy conductances (Landsberg 1986, Ball et al. 1987, Leuning 1995). These approaches work well for a given canopy structure, provided that they are parameterized accordingly (e.g. Hari and Mäkelä 2003). However, situation changes as for example trees grow in size. Hydraulic limitation of photosynthesis has been suggested as one reason for maximal tree size (Ryan and Yoder 1997). With increasing tree size, water transport resistance from soil to transpiring leaves increases per unit leaf area. This signifies that similar transpiration rate from leaf surface, i.e. leaf-atmosphere conductance for water vapor, would result into higher tension gradient that lifts water up, in the xylem tissue of taller trees. This is problematic as increasing tension increases the probability of gas bubble formation in the transport stream that would hinder further water transport in that part of tissue (Sperry et al. 2002). By decreasing the stomatal conductance such cavitation risk would be avoided but that would simultaneously mean that also CO<sub>2</sub> intake would be compromised. It has been argued that such situation need not to rise as trees are structurally formed in such a way that transport resistance per unit length decreases with increasing tree height (West et al. 1999). If the structural compensation was perfect, the gas exchange would not be influenced by tree height. However, there are limitations to the compensation due to xylem cell properties or the required xylem investment per unit leaf area. Bigger proportion of the photosynthetic production needs to be invested into wood formation that decreases leaf growth and eventually limits productivity.

Similarly as the xylem's ability to transport water up the stem may limit the stomatal conductance also the photosynthesized sugars need to be transported away from the leaf or the photosynthesis becomes down-regulated. Recently Nikinmaa et al. (2013) demonstrated that it may actually be phloem transport that is determining the leaf gas exchange. Phloem transport is driven osmotically from high turgor pressure at the source, that loading of solutes to phloem cause, to a low turgor pressure at the sink where the solutes are unloaded. Photosynthesized sugars that are used for growth at the sinks are major substance driving the flow. The flow rate results from the interplay between the negative hydrostatic pressure in xylem and osmotic gradient of the phloem that makes up the positive turgor pressure (Hölttä et al. 2006). However, exactly the same properties determine how the new secondary tissue in xylem and phloem grow (Hölttä et al. 2010). Growth, on the other hand, determines the xylem and phloem permeabilities which, as shown above, determine the rates of xylem and phloem transport and the leaf-atmosphere gas exchange.

The global atmospheric change has already changed the water CO<sub>2</sub> exchange rate at the leaf surface. Presumably this change is also influencing pressure gradients in xylem and phloem and also the vertical growth trends in trees. With increasing atmospheric CO<sub>2</sub> concentration it becomes easier to maintain both xylem and phloem transport rates, which should reflect both on the gas exchange of particularly large trees and also their growth. To be able to truly appreciate the potential significance of these changes on forest-atmosphere interaction and also tree growth we need to make models that consider the above processes. Our aim is to develop a mechanistic tree model where gas-exchange, transport and growth are explicitly modeled and where the tree performance and development results as their interplay over time. Here we combined an assimilation and transpiration model (Mäkelä et al. 2006), xylem and phloem transport model (Hölttä et al. 2006) with 3D tree model LIGNUM (Sievänen et al. 2008). The aim in this first phase of model development is to study how widely realistic 3D tree structure, transport and leaf gas exchange can vary.

## MATERIAL AND METHODS

### The model

LIGNUM trees consist of rows of connected internodes with their own dimensions (Fig. 1). The gas exchange with atmosphere takes place in internodes with needles that are represented as a cylinder surrounding the woody axis. Xylem and phloem transport was implemented as differential equations for water pressure in xylem ( $P_x$ ) and in phloem ( $P_p$ ), and amount of sugar solute in phloem ( $N_p$ ) in each internode as:

$$\begin{aligned}\frac{dP_x}{dt} &= a_x (Q_{x,ax,in} - Q_{x,ax,out}) - E_{xp} - S_x \\ \frac{dP_p}{dt} &= a_p (Q_{p,ax,in} - Q_{p,ax,out}) + E_{xp} \\ \frac{dN_p}{dt} &= a_n (Q_{p,ax,in} - Q_{p,ax,out}) \frac{N_p}{V_p} + L + U\end{aligned}$$

where  $Q_{i,ax,in}$ ,  $Q_{i,ax,out}$  are axial inflow and outflow of water in xylem ( $i=x$ ) and phloem ( $i=p$ ),  $E_{xp}$  is flow of water from xylem to phloem,  $S_x$  is transpiration sink,  $a_x$ ,  $a_p$ ,  $a_n$  are coefficients,  $V_p$  is volume of phloem in the internode, and  $L$  and  $U$  are rates of loading and unloading of sugars.

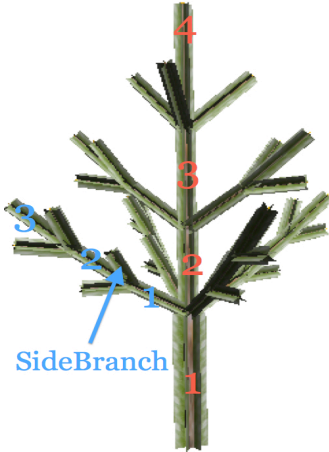


Figure 1. Tree (grown by LIGNUM) used in simulations; data for numbered internodes in stem and branch are displayed in the Figure 3

We solve the equations using the Runge-Kutta method with time step of order of seconds and follow daily patterns of environmental drivers (radiation, temperature and water vapor deficit). Radiation interception in tree crown is evaluated by LIGNUM and photosynthesis and transpiration are modeled on the basis of radiation interception and the other environmental drivers. Loading ( $L$ ) is proportional to photosynthetic rate and unloading ( $U$ ) is:

$$U = \max[U_0(N_p - N_0), 0]$$

where  $U_0$  and  $N_0$  are parameters.

### The simulations

The parameter values of the transport model were as in Hölttä et al. (2006). Phloem thickness was set at 2 mm. We ran the model for the tree of Fig. 1 in low radiation ( $100 \mu\text{mol(PAR)}/\text{m}^2/\text{s}$ ), temperature was  $20^\circ \text{C}$ , VPD was  $0.4 \text{ mol(H}_2\text{O)}/\text{m}^3$ . Soil was dry: xylem water pressure in roots was  $-0.25 \text{ Mpa}$  and roots had a high assimilate sink (=boundary conditions). Rates of photosynthesis and transpiration in internodes varied

between  $0.7 - 5.6 \mu\text{mol}(\text{CO}_2)/\text{s}$  and  $3 - 200 \mu\text{mol}(\text{H}_2\text{O})/\text{s}$ . The simulations were repeated varying the xylem permeability between  $1.3 \cdot 10^{-13} - 3.0 \cdot 10^{-13} \text{ ms}^{-1}$  and phloem permeability  $0.5 \cdot 10^{-16} - 6 \cdot 10^{-16} \text{ ms}^{-1}$ .

## RESULTS AND DISCUSSION

The simulations showed that the hypotheses concerning the xylem and phloem transport can be successfully implemented within the 3D structural framework of a tree. The first results show logic model behavior. The initial state of the model was unrealistic but realistic pressure gradients in xylem and phloem developed as the model was allowed to run for sufficiently long time. Transpiration from leaves created a decreasing pressure from base to the leaves almost immediately but phloem gradient developed more slowly with gradual development of correct sugar concentrations. Initially also the phloem pressure dropped to negative but with time the phloem pressure became positive with higher pressure in the photosynthesizing leaves vs. the base of the stem. Reaching a steady state was very slow even for the small simulated tree (Fig 2).

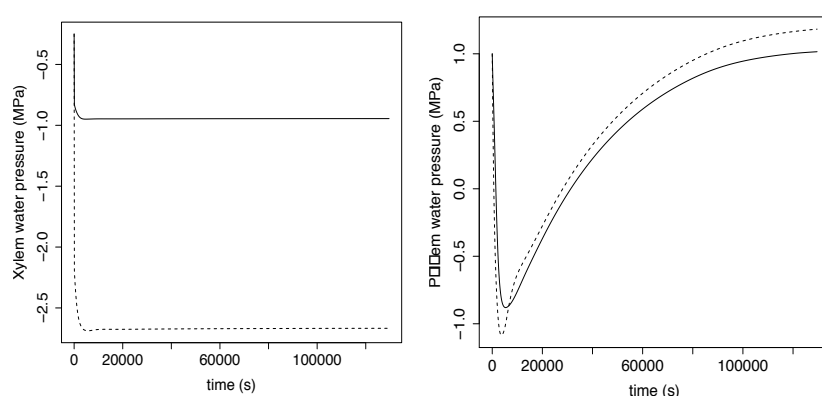


Figure 2. Time dynamics of a) xylem and b) phloem pressure at the top (dotted line) and base (continuous line) internodes.

In simulations the leaf gas exchange was assumed to be driven by external conditions only according to Mäkelä et al. (2006). These transpiration rates lead into very low xylem pressures ( $-4 \text{ MPa}$ ) in the shoots that forked most strongly from the main axis while that of the main axis was only about ( $-2 \text{ MPa}$ ). This result as such indicates that the combination of gas exchange from each internode and the hydraulic properties of the conducting xylem pathway were not very realistic and that they are strongly interlinked in real trees i.e. low water potential gives a feedback for stomatal control to decrease. In Scots pine normal measured minimal water potential is close to  $-2 \text{ MPa}$ .

Variation in the xylem and phloem conductivity reflect as variation both as pressure and concentration levels and their within tree gradients (Figure 3). Xylem permeability changes reflected almost equally on the xylem and pressures in the main axis. Lower permeability lead to decreasing negative water pressures in the xylem and that, in turn, to decreased phloem turgor pressure. However the phloem turgor pressure gradient was not influenced by xylem permeability changes, indicating that it resulted from the modeled differences in sugar loading and unloading rates in sources and sink, as Münch pressure flow hypothesis suggests. Tree architecture influenced results and the branch xylem pressure was much more sensitive to the change than that of the main axis. Interestingly, that was not the case for phloem pressure in branches, but it behaved more or less equally to the main stem. This clearly indicates the important role of the source processes in the maintaining the phloem pressure. It is interesting that altered phloem unloading rate caused qualitatively similar changes in phloem pressure than the changes in xylem permeability, demonstrating the tight linking between the transport and source- sink process.

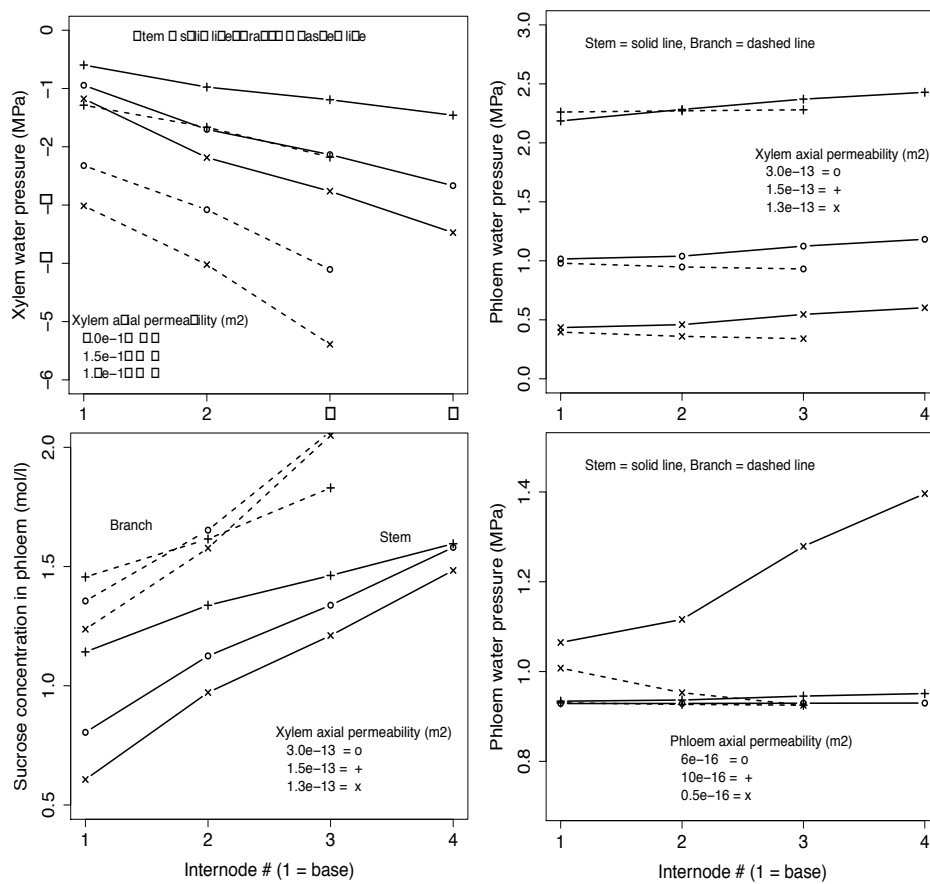


Figure 3. Xylem (a) and phloem (b) pressure and phloem sugar concentration (c) with varied xylem conductivity, and phloem pressure with varied phloem conductivity (d) in stem (solid line) and branch (dotted line).

## CONCLUSIONS

The model shows promise for studying whole tree level variation of a range of processes such as growth, stomatal conductance, photosynthesis and cavitation after their feedbacks with local pressure and solute concentrations are implemented. It is clear that these processes are much more tightly connected than previously considered. Even the quite limited simulation study of this exercise showed that quantitative analysis of flows within 3D tree structure bring out quite powerfully unrealistic combinations of structures and processes. This type of modeling capacity is needed as the interactions within 3D tree structures are extremely complex but simultaneously it is them that determine how trees will respond to changing climate.

## ACKNOWLEDGEMENTS

Study was supported by the Academy of Finland projects #1132561 and # 140781, the Finnish Centre of Excellence "Physics, chemistry, biology and meteorology of atmospheric composition and climate change and Nordic centre of excellencies CRAICC and DEFROST

## LITERATURE CITED

Hölttä, T., Vesala, T., Sevanto, S., Perämäki, M., Nikinmaa, E. 2006. Modeling xylem and phloem water flows in trees according to cohesion theory and Münch hypothesis. *Trees* 20, 67–78.

- Hölttä, T., Mäkinen, H., Nöjd, P., Kolari, P., Mäkelä, A. & E. Nikinmaa 2010. A Physiological model of softwood cambial growth. *Tree Physiology*.
- Mäkelä, A., Kolari, P., Karimäki, J., Nikinmaa, E., Perämäki, M., Hari, P. 2006. Modelling five years of weather-driven variation of GPP in a boreal forest. *Agricultural and Forest Meteorology* 139: 382-398.
- Nikinmaa, E., Hölttä T., Hari P., Kolari P., Mäkelä A., Sevanto S. & Vesala T. 2012. Assimilate transport in phloem sets conditions for leaf gas exchange. *Plant Cell and Environment* First published online : 11 OCT 2012, DOI: 10.1111/pce
- Ryan M.G. & Yoder B.J. (1997) Hydraulic limits to tree height and tree growth. *Bioscience* **47**, 235–242.
- Sievänen, R., Perttunen, J., Nikinmaa, E. & Kaitaniemi, P. 2008. Toward extension of a single tree functional structural model of Scots pine to stand level: effect of the canopy of randomly distributed, identical trees on development of tree structure. *Functional Plant Biology* 35(9/10): 964-975.
- West G., Brown J., Enquist B. (1999*a*). A general model for the structure and allometry of plant vascular systems. *Nature* 400: 664–667.

# URBAN SURFACE COVER DETERMINED USING AIRBORNE LIDAR IN HELSINKI

A. NORDBO and L. JÄRVI

Division of atmospheric sciences, Department of Physics, University of Helsinki, 00014-University of Helsinki, Finland.

Keywords: lidar scanning, surface cover, urban land cover.

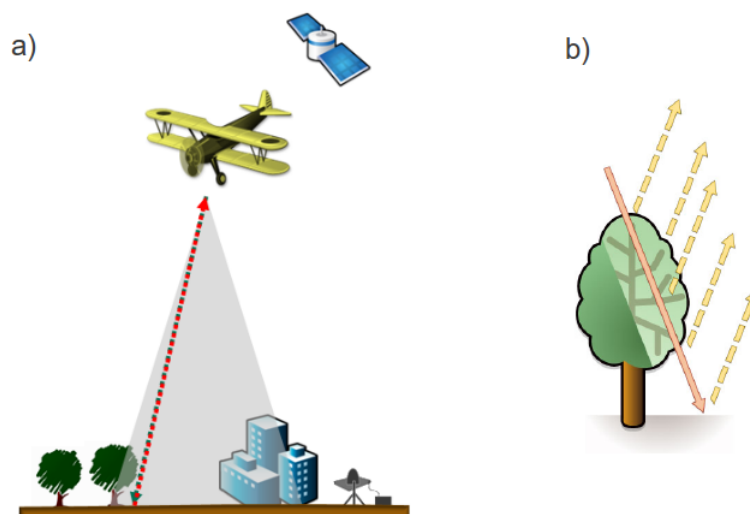
## INTRODUCTION

Knowledge on urban morphology and surface cover are crucial for the interpretation of eddy-covariance flux measurements (Nordbo et al., 2012a) and as an input in energy and water balance modeling (Grimmond et al., 2011). Unfortunately, the horizontal resolution of surface cover data is often too coarse to resolve the fluxes properly (Moilanen, 2012). For instance, street-canyon trees are not resolved at this resolution which leads to errors in CO<sub>2</sub> and water budget estimations.

Recently, airborne lidar scanning data have been used for the determination of urban topography (Lindberg and Grimmond, 2011) and even surface cover (Goodwin et al., 2009; Matikainen and Karila, 2011). Airborne lidar measurements are based on the emittance and receipt of NIR light pulses that are emitted at a very high pulse frequency (e.g. 50 kHz, FIG. 1 a). Each sent pulse may have up to five return pulses which each contain the information of the height and the return intensity of the object they hit (FIG. 1 b). Different return intensities are caused by the variation in NIR reflectance by different surface types. Topography is easier to determine since only height information is needed, whereas surface cover classification requires also information on the return intensity, which is harder to calibrate (Ahokas et al., 2006).

The aim of this study is to use airborne lidar scanning data to calculate the surface cover of central Helsinki, in addition to height mapping. Decision trees, a machine learning algorithm, is used for classification into six surface cover classes: built, impervious, grass, low vegetation and high vegetation. The mapping is done at a 2 m resolution and the study area will cover three eddy-covariance stations in Helsinki (Järvi et al., 2009; Nordbo et al., 2012b).

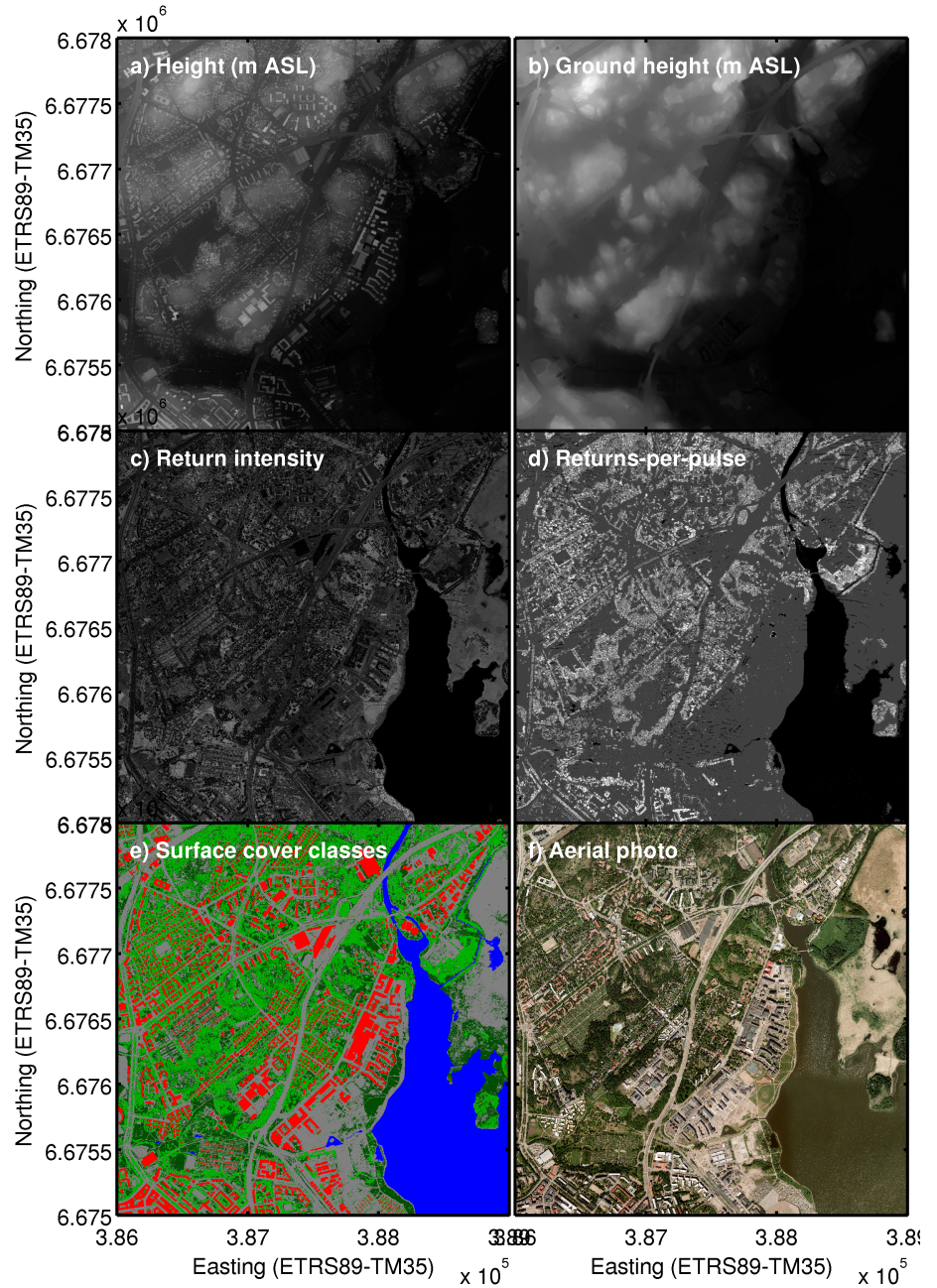
Figure 1: a) A schematic of the basic idea of airborne lidar scanning. b) The concept of multiple returns per sent pulse. Source: resources.arcgis.com.



## METHODS

The data included in this study cover an area of 6 km by 9 km, consisting of six 3 km by 3 km tiles, and covering central Helsinki. The lidar data were collected with an Optech ATLM GEMINI lidar on four flights occurring on three days in 2008 (National Land Survey of Finland, 2011). The data are part of an open database that aims at a nationwide lidar scanning coverage for the determination of a new elevation map. The data set includes the coordinates of each return (ETRS-TM35FIN), height (m a.s.l.), pulse number, return per pulse (RPP) and return intensity. All together there are over 40 million data points in the six-tile data set. In addition to the lidar data, geographical information on the coastline and building edges were used (HSY, 2008).

Figure 2: Example maps of one of the six tiles that includes the Kumpula campus (3 km by 3 km area): a) height above sea level, b) ground height above sea level, c) return intensity, d) returns-per-pulse, e) surface cover classes (see FIG. 3 for color explanations) and f) aerial photograph.



The lidar data post-processing tool FUSION (McGaughey, 2009) was used to create a Digital Elevation Map (DEM, FIG. 2 a) and filter outliers from lidar data. Second, ground points were extracted, excluding building points based on building polygons, and a ground height map was created (FIG. 2 b). The return intensity values were corrected for spherical loss using 1900 m as the reference height, but no incidence angle or atmospheric correction was done since data were divided according to flights and decision trees were used for each flight separately. An example of an intensity map is given in FIG. 2 c, where the reflectance difference between grass and a paved road is evident.

RPP is also an indication of the surface cover type. Multiple RPPs indicates a patchy object, such as a tree or a building with a gridded or glass roof. Edges of buildings also often have two returns: one from the roof and one from the ground. To remove such effects a filtering of linear structures was done (Goodwin et al., 2009). The resulting map distinguishes forest quite well (FIG. 2 d).

The actual surface cover classification was done at lidar point level, rather than at pixel level. For each flight, a training dataset with over 10 000 data points, for which the surface cover was known, was created. The training data sets included only first returns and the information on height above ground, return intensity, returns-per-pulse and height difference between the first and last return. Half of the training data were used for training the decision tree (MathWorks Inc., 2012) and half were used for validation. Buildings were required to have a height above 2 m and low vegetation between 0.5 m and 2 m, but otherwise the decision tree algorithm was allowed to do the classification.

When the tree was developed, it was used for predicting the classes of the rest of the data. The data were then converted to a matrix using modes and further fine-tuned. Pixels with  $RPP > 1$  were designated as forest, a building and sea mask was used, bridges were removed with a linear filter and rivers were flood-filled.

## CONCLUSIONS

The performance of the tree classification algorithm was evaluated with the second half of the training data. The success percentage for high vegetation and buildings was generally above 90%, whereas for grass and impervious the value was mainly below 90%. This is because impervious and grass surface cannot be clearly distinguished by the number of returns or the height, since the classification is mainly based on the intensity value. The errors in buildings and high vegetation were due to confusion between them and the same applies for grass and impervious surfaces. The fraction of data points for which the prediction probability is  $< 0.6$  was always under 4%. Height above ground was always the most important classifier, followed by intensity, RPP and height difference between the first and the last return.

The surface cover of the whole study domain is given in FIG. 3. Under 0.5% of the area remains unclassified due to a lack of data. Impervious is the most common land cover type, followed by tall vegetation and buildings. Qualitatively, the classification also seems successful when compared with an orthoimage (FIG. 2 e and f). The largest remaining problems are high, non-building objects that are classified as buildings, for instance power lines and cranes. Dry grass can also be classified as impervious. Nevertheless, their contribution to the final surface cover fractions is minimal.

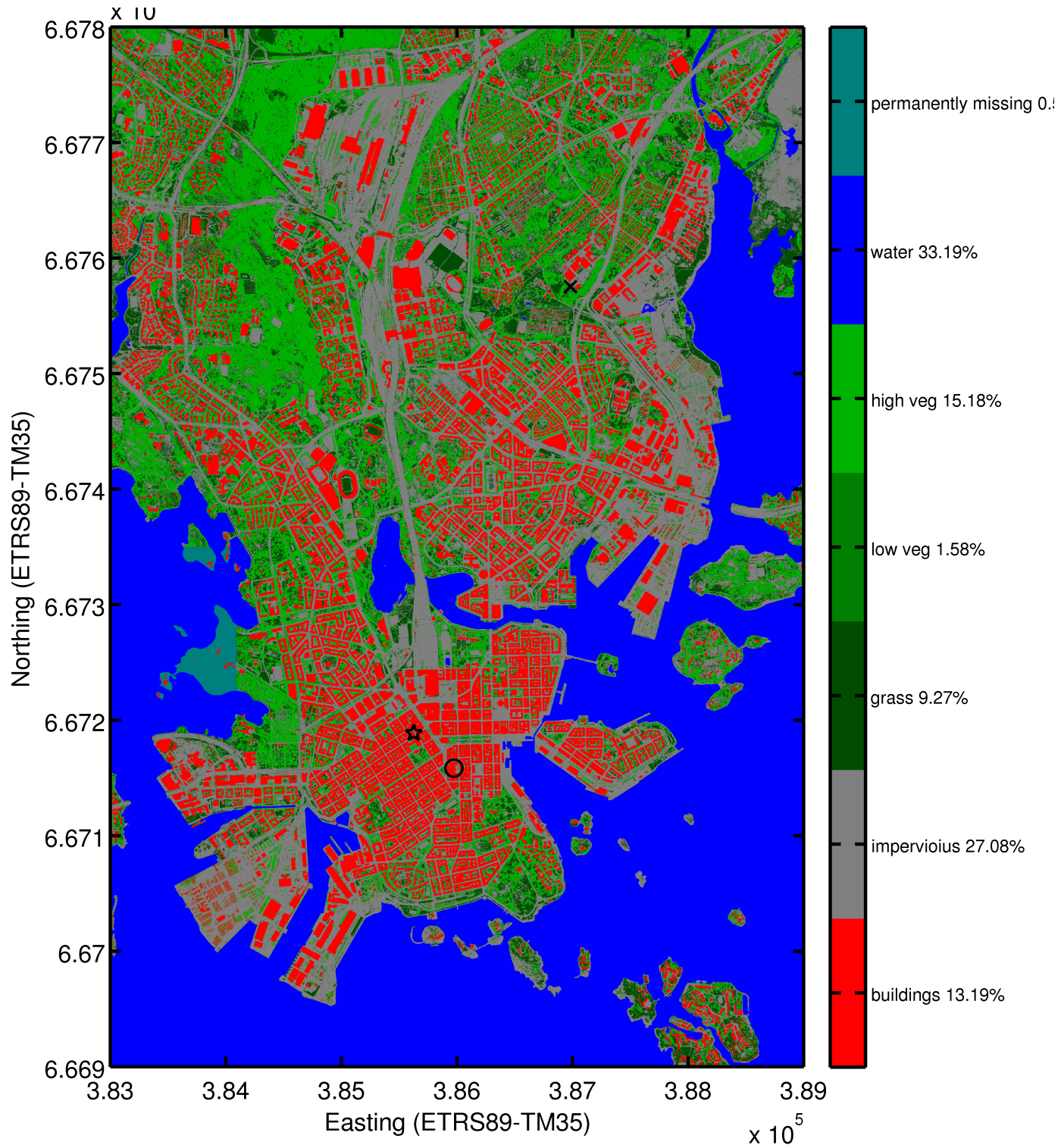
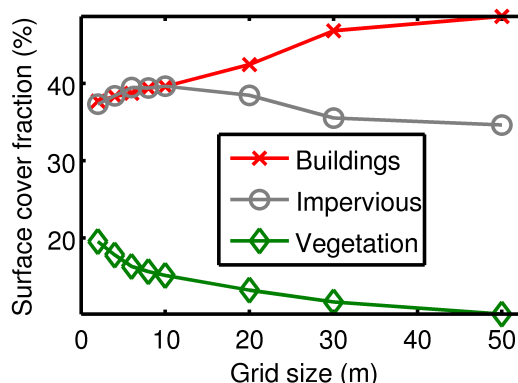


Figure 3: Surface cover in Helsinki in a 6 by 9 km area. Surface cover classes and their fraction (in %) are given in the colorbar. Three eddy-covariance measurement stations are marked: SMEAR III Kumpula (cross), Fire Station (circle) and Hotel Torni (pentagram).

Figure 4: Surface cover fractions as a function of surface cover data grid size. Data are from around the Hotel Tornı eddy-covariance flux measurement station, with a 1000 m radius. Vegetation includes low and high trees and grass.



The 2-m-resolution surface cover maps can be aggregated to a coarser resolution to simulate the effect of a map with worse resolution. FIG. 4 shows how the fraction of vegetation falls fast near the Hotel Tornı flux measurement station when the resolution is dropped down from 2 m. In fact, the fraction of vegetation falls from about 20% at 2-m-resolution to 0% when the resolution is 50 m, which is still not the coarsest resolution commonly used in urban energy and water balance modeling. The implications to energy, water and CO<sub>2</sub> balance modeling are evident.

The created surface cover map will be used for modeling the energy and water balance of Helsinki using the SUEWS model (Järvi et al., 2011). Runs with different map resolutions will be made in order to estimate the aggregation effect shown in FIG. 4. The DEM will be used as an input for Large eddy simulation of the flow field of Helsinki near the Hotel Tornı eddy-covariance flux station. The final output of the Large eddy simulation will be flux footprints (source areas) for measured fluxes.

#### ACKNOWLEDGEMENTS

This work was supported by the Academy of Finland Centre of Excellence in "Atmospheric Science – From Molecular and Biological Processes to the Global Climate". For general advice, A. Nordbo is also grateful to Juha Hyypä and Leena Matikainen from the Finnish Geodetic Institute, Fredrik Lindberg from King's College London and Juha Kareinen and Annamaija Krannila from the National Land Survey of Finland.

#### REFERENCES

- Ahokas, E., Kaasalainen, S., Hyypä, J., and Suomalainen, J. (2006). Calibration of the Optech ALTEM 3100 laser scanner intensity data using brightness targets. *ISPRS*.
- Goodwin, N. R., Coops, N. C., Tooke, T. R., Christen, A., and Voogt, J. A. (2009). Characterizing urban surface cover and structure with airborne lidar technology. *Canadian Journal of Remote Sensing*, 35(3):297–309.
- Grimmond, C. S. B., Blackett, M., Best, M. J., Baik, J. J., Belcher, S. E., Beringer, J., Bohnenstengel, S. I., Calmet, I., Chen, F., Coutts, A., Dandou, A., Fortuniak, K., Gouvea, M. L., Hamdi, R., Hendry, M., Kanda, M., Kawai, T., Kawamoto, Y., Kondo, H., Krayenhoff, E. S., Lee, S. H., Loridan, T., Martilli, A., Masson, V., Miao, S., Oleson, K., Ooka, R., Pigeon, G., Porson, A., Ryu, Y. H., Salamanca, F., Steeneveld, G. J., Tombrou, M., Voogt, J. A., Young, D. T., and Zhang, N. (2011). Initial results from phase 2 of the international urban energy balance model comparison. *International Journal of Climatology*, 31(2):244–272.

- HSY (2008). Seutu CD - a dataset by the Helsinki region environmental services authority.
- Järvi, L., Grimmond, C. S. B., and Christen, A. (2011). The surface urban energy and water balance scheme (SUEWS): Evaluation in Los Angeles and Vancouver. *Journal of Hydrology*, 411(3-4):219–237.
- Järvi, L., Hannuniemi, H., Hussein, T., Junninen, H., Aalto, P. P., Hillamo, R., Mäkelä, T., Keronen, P., Siivola, E., Vesala, T., and Kulmala, M. (2009). The urban measurement station SMEAR III: Continuous monitoring of air pollution and surface-atmosphere interactions in Helsinki, Finland. *Boreal Environment Research*, 14:86–109.
- Lindberg, F. and Grimmond, C. S. B. (2011). Nature of vegetation and building morphology characteristics across a city: Influence on shadow patterns and mean radiant temperatures in London. *Urban Ecosystems*, 14(4):617–634.
- MathWorks Inc. (2012). Matlab, version 2012a.
- Matikainen, L. and Karila, K. (2011). Segment-based land cover mapping of a suburban area-comparison of high-resolution remotely sensed datasets using classification trees and test field points. *Remote Sensing*, 3(8):1777–1804.
- McGaughey, R. J. (2009). Fusion/LDV: Software for lidar data analysis and visualization. United States. *Department of Agriculture, Seattle*.
- Moilanen, J. (2012). MSc thesis: Energiatasapaino Helsingin keskustassa.
- National Land Survey of Finland (2011). National laser scanning database.
- Nordbo, A., Jarvi, L., Haapanala, S., Wood, C. R., and Vesala, T. (2012a). Fraction of natural area as main predictor of net CO<sub>2</sub> emissions from cities. *Geophysical Research Letters*, 39:L20802.
- Nordbo, A., Järvi, L., and Vesala, T. (2012b). Revised eddy covariance flux calculation methodologies - effect on urban energy balance. *Tellus Series B-Chemical and Physical Meteorology*, 64:18184.

# EVIDENCE OF LATERAL TRANSPORT OF CARBON GASES OF TERRESTRIAL ORIGIN IN BOREAL AQUATIC ECOSYSTEMS

A. OJALA<sup>1</sup>, J. PUMPANEN<sup>2</sup>, T. RASILO<sup>2\*</sup>, H. MIETTINEN<sup>3</sup>, M. RANTAKARI<sup>3</sup>, J. HEISKANEN<sup>6</sup>, I. MAMMARELLA<sup>6</sup>, J. HUOTARI<sup>1\*\*</sup>, P. KANKAALA<sup>4</sup>, J. LEVULA<sup>5</sup>, J. BÄCK<sup>2</sup>, P. HARI<sup>2</sup> and T. VESALA<sup>6</sup>

<sup>1</sup>Department of Environmental Sciences, University of Helsinki, Lahti, Finland

<sup>2</sup>Department of Forest Sciences, University of Helsinki, Finland

<sup>3</sup>Department of Environmental Sciences, University of Helsinki, Finland

<sup>4</sup>Department of Biology, University of Eastern Finland, Joensuu, Finland

<sup>5</sup>Hyytiälä Forestry Field Station, University of Helsinki, Finland

<sup>6</sup>Department of Physics, Division of Atmospheric Sciences, University of Helsinki, Finland

\*Present address: Université du Québec à Montréal, Département des Sciences Biologiques, C.P 8888 succursale Centre-Ville, Montréal H3C 3P8, Canada

\*\*Present address: Lammi Biological Station, University of Helsinki, Finland

Keywords: carbon cycling, extreme events, riparian zone, hydrology

## INTRODUCTION

In the boreal zone with numerous lakes, streams and rivers, the freshwater ecosystems are a significant component of carbon cycling at the landscape level. Thus, e.g. total organic carbon (TOC) loads of terrestrial origin have been extensively studied with the notice that the export of TOC is strongly related to the abundance of coniferous forests in the catchment area (Humborg *et al.*, 2004; Mattson *et al.* 2003) and especially to the coverage of peatlands (Kortelainen, 1993, Kortelainen *et al.*, 2006). Therefore, e.g. in Finland freshwater ecosystems receive high loads of carbon of terrestrial origin and about 60 % of lakes in southern Finland have dissolved organic carbon (DOC) concentrations > 10 mg L<sup>-1</sup> (Kortelainen, 1993). Especially the riparian as well as littoral zones around the water bodies are important to lateral transport of carbon. However, contrary to organic carbon the transport of inorganic carbon is little studied, partly because the lateral signals of e.g. CO<sub>2</sub> can be difficult to detect. Here we used different approaches in several lakes and running waters over several years altogether to verify the phenomenon, especially during extreme weather events such as spells of heavy rains. Besides CO<sub>2</sub>, we studied CH<sub>4</sub> which due to its strictly anaerobic origin outcompetes CO<sub>2</sub> as a tracer of lateral influence.

## METHODS

We installed automatic continuous measurement systems with NDIR CO<sub>2</sub> sensors (Vaisala) in the riparian zone soil matrix around a small pristine headwater lake Valkea-Kotinen (surface area 4.1 ha), in

the lake itself, and in the outflowing stream and followed up the seasonal variation in CO<sub>2</sub> concentration as well as rain event-driven changes in concentrations (Rasilo *et al.*, 2012). We also used the sensors in a second-order stream draining to Lake Kuivajärvi and discharging a catchment of managed forest. In this study the focus was also on high flow events (Dinsmore *et al.*, 2013). The more conventional weekly sampling protocol throughout the open water periods on water column CO<sub>2</sub> and CH<sub>4</sub> concentrations as well as gas fluxes was applied in lakes Pääjärvi (area 13.4 km<sup>2</sup>), Ormajärvi (area 6.53 km<sup>2</sup>) (Ojala *et al.*, 2011) and Kuivajärvi (area 63.8 ha) surrounded by managed forests and some crop land but having different size. The lakes also differ in terms of water quality since lakes Valkea-Kotinen, Pääjärvi and Kuivajärvi are strongly stratifying humic lakes whereas Lake Ormajärvi is a clear water lake with a less stable water column. Lakes Pääjärvi and Kuivajärvi can be regarded as mesoeutrophic lakes whereas lakes Valkea-Kotinen and Ormajärvi are more productive. In lakes Pääjärvi and Kuivajärvi less frequent sampling on gas concentrations was also carried out under ice in winter. Besides the general seasonal pattern of lacustrine carbon gases, these studies were also used to reveal the importance of high summer time precipitation in large lakes since the summer of the study year was exceptionally rainy. In the conventional studies gas concentrations were determined using headspace technique and gas chromatography. As an example of ultimate lateral transport route we finally had a measuring campaign of 40 days on CO<sub>2</sub> concentrations (Vaisala sensor) and fluxes in River Kymijoki which is the largest river in southern Finland draining to Gulf of Finland in Baltic Sea. The campaign extended from early to mid-summer and the fluxes were determined with the micrometeorological eddy covariance technique. During the campaign the river discharge fluctuated from ca. 200 to 300 m<sup>3</sup> s<sup>-1</sup> with a slightly decreasing trend.

## RESULTS AND DISCUSSION

All the studies revealed the importance of hydrological events such as high spring discharge after snow melt and extreme rain events in summer to riverine as well as lacustrine carbon gas dynamics. In lakes Ormajärvi and Pääjärvi the most drastic changes in gas concentrations as well as fluxes occurred not in spring after snow melt but during or just after the heavy summer rains. As a consequence of the high precipitation the clear water lake changed from a small carbon sink to carbon source whereas in the humic lake almost half of the CO<sub>2</sub> and CH<sub>4</sub> fluxes took place during or just after the rainy period. Analysis of gas concentrations in the water columns revealed that the high surface water concentrations resulting in peak fluxes were not due to transport from hypolimnia rich in gases but were due to soil processes and lateral export from the flooded catchments (Lopez Bellido *et al.*, 2012). In Lake Kuivajärvi the seasonal peak fluxes took place just after ice out but again this was not a result of carbon gases accumulated under the ice but gases originated from the surrounding catchment. In this lake almost one third of the annual CO<sub>2</sub> flux occurred in May and > 10 % of CH<sub>4</sub> was emitted during one single week in May. In general, when appearing as a surface water maximum in thermally stratified lakes, CH<sub>4</sub> proved to be a good tracer for lateral transport (Lopez Bellido *et al.*, 2012). The importance of spring for lacustrine carbon gas fluxes has also been shown e.g. by Michmerhuizen *et al.* (1996), Riera *et al.* (1999) and Lopez Bellido *et al.* (2009).

In the soil-lake-stream continuum around Lake Valkea-Kotinen seasonal variation in CO<sub>2</sub> was greatest and concentrations highest deep in the soil and in the lake itself, but also in the stream, especially further down from the lake. In the stream, the influence of the riparian zone superseded that of the lake at less than 150 m distance, which resulted in wider variation and higher concentrations of CO<sub>2</sub>. After a spell of heavy rain, the CO<sub>2</sub> concentration in the soil increased and supposedly, a considerable amount of CO<sub>2</sub> of terrestrial origin entered the lake annually. However, since the rain event was combined with exceptionally high winds mixing the water column, the riparian CO<sub>2</sub> load was diluted and could not be properly tracked down. Although we could not resolve the exact routes of water flow in and from the riparian zone, we estimated that a considerable amount of CO<sub>2</sub> of terrestrial origin entered the lake annually, i.e. the flow of terrestrial DIC into the aquatic part of the catchment was up to 13% of NEP (Rasilo *et al.*, 2012).

The second-order stream draining a lake of 30 ha had a fairly unresponsive catchment with high base flow contribution and the low flow was important for the total annual CO<sub>2</sub> export (Dinsmore *et al.*, 2013). In general, CO<sub>2</sub> export was controlled by runoff. There was no concentration-discharge relationship which was different from four other catchments across Canada, UK and Sweden. The only exception was snowmelt event in spring when CO<sub>2</sub> concentrations were high. This high concentration could be tracked down in the downstream lake. This is in accordance with Dyson *et al.* (2010) stating that spring snowmelt can be responsible for 37–45% of annual runoff of different carbon species. In River Kymijoki the CO<sub>2</sub> flux increased slightly in the course of the measuring period while discharge decreased. The increase in flux was associated with the increase in concentration of dissolved CO<sub>2</sub> which is consistent with the findings that river water concentration of DIC or CO<sub>2</sub> is negatively correlated with discharge (Finlay, 2003; Lynch *et al.*, 2010).

In conclusion, knowledge of lateral transport of carbon also in gaseous form and the effects of hydrological events on it is still limited, but important since climate change will increase the frequency of extreme weather events such as heavy rains. High frequency measurements are the best way to catch the short but significant hydrological events, otherwise the role of the aquatic ecosystems as a pathway for terrestrial carbon loss could be underestimated.

#### ACKNOWLEDGEMENTS

This work was supported by the Academy of Finland projects No. 1118615 (Centre of Excellence), 1116347, 130984 and 213093 as well as the Nordic Centre of Excellence CRAICC. We are grateful for the staff of Lammi Biological Station and Hyytiälä Forestry Field Station.

#### REFERENCES

- Dinsmore, K. J., Wallin, M. B., Johnson, M. S., Billett, M. F., Bishop, K., Pumpanen, J. and A. Ojala (2013) Contrasting streamflow CO<sub>2</sub> dynamics in headwater streams: a multicatchment comparison, *J. Geophys. Res. Biogeosciences*, **118**: 1-17, doi: 10.1002/jgrg.20047, 2013.
- Dyson, K.E., Billett, M.F., Dinsmore, K.J., Harvey, F., Thomson, A.M., Piirainen, S. and Kortelainen, P. (2010) Release of aquatic carbon from two peatland catchments in E. Finland during the spring snowmelt period. *Biogeochem.*, **103**, 125–142, doi:10.1007/s10533-010-9452-3.
- Finlay, J. C. (2003) Controls of streamwater dissolved inorganic carbon dynamics in a forested watershed, *Biogeochem.*, **62**, 231-252.
- Humborg, C., Smedberg, E., Blomqvist, S., Mörtz, C.M., Brink, J., Rahm, L., Danielsson, A. and J. Sahlberg (2004) Nutrient variations in boreal and subarctic Swedish rivers: landscape control of land-sea fluxes, *Limnol. Oceanogr.*, **49**, 1871-1883.
- Kortelainen, P. (1993) Content of total organic carbon in Finnish lakes and its relationship to catchment characteristics, *Can. J. Fish. Aquat. Sci.*, **50**, 1477-1483. doi:10.1139/f93-168.
- Kortelainen, P., Rantakari, M., Huttunen, J.T., Mattson, T., Alm, J., Juutinen, S., Larmola, T., Silvola, J. and P. J. Martikainen (2006) Sediment respiration and lake trophic state are important predictors of large CO<sub>2</sub> evasion from small boreal lakes, *Global Change Biol.*, **12**, 1554-1567. doi:10.1111/j.1365-2486.2006.01167.
- Lopez Bellido, J., Tulonen, T., Kankaala, P. and A. Ojala (2009) CO<sub>2</sub> and CH<sub>4</sub> fluxes during spring and autumn mixing periods in a boreal lake, *J. Geophys. Res.*, **114**, G04007, doi: 10.1029/2009JG000923, 2009.
- Lopez Bellido, J., Tulonen, T., Kankaala, P. and A. Ojala (2012) Concentrations of CO<sub>2</sub> and CH<sub>4</sub> in water column of two stratified boreal lakes during a year of atypical summer precipitation, *Biogeochemistry*, DOI 10.1007/s10533-012-9792-2.

- Lynch, J. K., Beatty, C. M., Seidel, M. P., Jungst, L. J. and M. D. DeGrandpre (2010) Controls of riverine CO<sub>2</sub> over an annual cycle determined using direct, high temporal resolution *p*CO<sub>2</sub> measurements, *J. Geophys. Res.*, **115**, G03016, doi:10.1029/2009JG001132.
- Mattsson, T., Finér, L., Kortelainen, P. and T. Sallantausta (2003) Brook water quality and background leaching from unmanaged forested catchments in Finland, *Water, Air, Soil Pollut.* **147**, 275-297.
- Michmerhuizen, C.M. and R.G. Striegl (1996) Potential methane emission from north-temperate lakes following ice melt, *Limnol. Oceanogr.*, **41**, 985-991.
- Ojala, A., Lopez Bellido, J., Tulonen, T., Kankaala, P. and J. Huotari (2011) Carbon gas fluxes from a brown-water and a clear-water lake in the boreal zone during summer with extreme rain events, *Limnol. Oceanogr.*, **51**, 61-76.
- Rasilo, T., Huotari, J., Ojala, A. and J. Pumpanen (2012) Rain induced changes in CO<sub>2</sub> concentrations in the soil – lake – brook –continuum of a boreal forested catchment. *Vadoze Zone Journal*, doi: 10.2136/vzj2011.0039.
- Riera, J. L., Schindler, J. E. and T. K. Kratz (1999) Seasonal dynamics of carbon dioxide and methane in two clear-water lakes and two bog lakes in northern Wisconsin, U.S.A., *Can. J. Fish. Aquat. Sci.*, **56**, 265-274.

# THE RELATIONSHIP BETWEEN FLUORESCENCE YIELD AND PHOTOCHEMICAL YIELD IN THE PRESENCE OF PHOTOINHIBITION OF REACTION CENTRES

B. OLASCOAGA and A. PORCAR-CASTELL

Department of Forest Sciences, University of Helsinki, Latokartanonkaari 7 PO-Box 27, 00014 Helsinki, Finland.

Keywords: PAM FLUORESCENCE, SCOTS PINE (*PINUS SYLVESTRIS* L.)

## INTRODUCTION

Photosynthesis estimation at a global scale is a crucial goal to achieve for climate change research and political decision making. For this purpose chlorophyll fluorescence, and optical phenomenon intimately related to photosynthesis, has been proposed as a potential tool. However, chlorophyll fluorescence competes with photochemistry and thermal dissipation on the utilization of the absorbed energy. Therefore, an increase in the efficiency of photochemistry will decrease the efficiency of chlorophyll fluorescence. This phenomenon is termed photochemical quenching of fluorescence, or PQ. Accordingly, the fluorescence yield ( $\Phi_F$ ) and the photochemical yield ( $\Phi_P$ ) are inversely correlated in response to PQ. Yet, green leaves often absorb more energy than the amount they can use (e.g. a green pine needle during winter), exposing the photochemical apparatus to damage (Melis, 1999). Under excessive energy conditions, plants activate dynamic regulatory mechanisms that increase the fraction of the absorbed energy that is thermally dissipated. As the efficiency of thermal dissipation affects the efficiency of chlorophyll fluorescence, the phenomenon has been termed non-photochemical quenching of fluorescence, or NPQ. Accordingly, since NPQ competes both with fluorescence and photochemistry,  $\Phi_F$  and  $\Phi_P$  are positively correlated in response to NPQ. Thus, PQ and NPQ affect inversely the relation between both yields.

At the leaf-level, the pulse amplitude modulated (PAM) fluorescence technique in conjunction with saturating light pulses, solves the non-triviality on the relation between  $\Phi_F$  and  $\Phi_P$ . As the saturating light pulses momentarily block the photochemical process, the technique allows estimating  $\Phi_P$  from variations in fluorescence regardless NPQ (Maxwell and Johnson, 2000). However, the latter technique is not valid for scales larger than the leaf-level. Recently, estimating the sun-induced chlorophyll fluorescence (SIF) (Meroni *et al.*, 2009) emission from vegetation at a global scale has been achieved (Frankenberg *et al.*, 2011; Joiner *et al.*, 2011). As SIF is a good proxy of the product between  $\Phi_F$  and the fraction of the photosynthetically active radiation (PAR) absorbed by vegetation, the possibility to infer global scale photosynthesis from SIF is high. Still, as the technique does not assess the effect of PQ and NPQ on the estimated chlorophyll fluorescence, the relation between  $\Phi_F$  and  $\Phi_P$  cannot be concluded, and the estimation of photosynthesis at a global scale still awaits to find alternative ways to link  $\Phi_F$  and  $\Phi_P$ .

At a diurnal scale, variations in chlorophyll fluorescence at the leaf-level reveal that the relation between  $\Phi_F$  and  $\Phi_P$  is dominated by the PQ-phase under low light, progressing to an NPQ-phase with increasing light (Fig. 1a). As future SIF satellite missions (e.g. FLEX) are expected to measure around noon time, when NPQ dominates over PQ, a positive relation between  $\Phi_F$  and  $\Phi_P$  has been proposed to facilitate the interpretation of SIF data. Nevertheless, at the seasonal scale the vegetation also

undergoes acclimation processes of the photosynthetic apparatus to optimize energy absorption and minimize photodamage (Öquist and Huner, 2006). Thus, seasonal changes in the contribution of the reversible and sustained forms of NPQ (Porcar-Castell *et al.*, 2008; Porcar-Castell, 2011), or in the extension of photoinhibition of reactions centres associated to photosynthesis could alter the relation between  $\Phi_F$  and  $\Phi_P$  and have implications on the interpretation of SIF. The aim of our study was to evaluate the relation between  $\Phi_F$  and  $\Phi_P$  on a seasonal scale under conditions of photoinhibition of the reaction centres.

## MATERIAL AND METHODS

Fluorescence of current-year old needles of a boreal Scots pine tree growing in the field was recorded during a year by a monitoring-PAM multichannel chlorophyll fluorometer (Porcar-Castell, 2011), and noon time fluorescence values were used to calculate  $\Phi_P$  and  $\Phi_F$ .

We also transferred eight boreal Scots pine saplings acclimated to summer conditions to a weather chamber to study the dynamics of fluorescence in response to 40 min treatment of light under different temperatures. Current-year old needles of each of the saplings were attached to four measuring heads of the PAM-fluorometer, and each sapling was dark-acclimated to a temperature ranging from -5°C to 30°C. The light treatments used in the experiments ranged from 45  $\mu\text{mol photons m}^{-2} \text{s}^{-1}$  to 1300  $\mu\text{mol photons m}^{-2} \text{s}^{-1}$  actinic light. The data were used to estimate PQ, NPQ,  $\Phi_P$ , and  $\Phi_F$  according to Porcar-Castell (2011).

## RESULTS AND DISCUSSION

At a diurnal scale (Fig. 1a)  $\Phi_P$  and  $\Phi_F$  tend to correlate negatively under low light intensities as almost all the absorbed energy is used into photochemistry. In this phase PQ dominates over NPQ. However, as the light intensity increases, the importance of thermal dissipation of the absorbed energy increases until a certain point in which NPQ equals PQ. Under stronger light intensities, NPQ overrates PQ thus making the correlation between  $\Phi_P$  and  $\Phi_F$  to become positive.

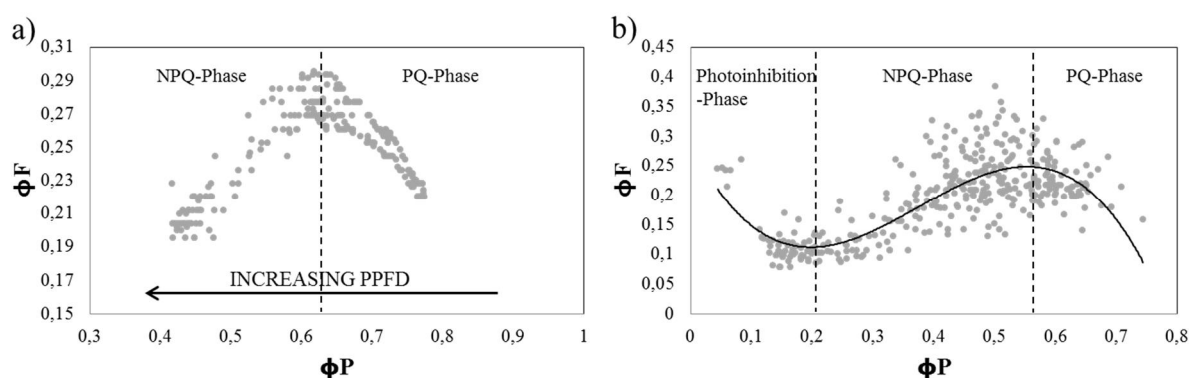


Figure 1. Relation between the photochemical yield ( $\Phi_P$ ) and the fluorescence yield ( $\Phi_F$ ) under a diurnal scale (a), and a seasonal scale (b) for current-year old needles of a boreal Scots pine (*Pinus sylvestris* L.) tree growing in the field.

At the seasonal scale (Fig. 1b), the relation between  $\Phi_P$  and  $\Phi_F$  shows an additional phase to the previously detected PQ and NPQ phases. The new phase is characterized by a positive relation between  $\Phi_P$  and  $\Phi_F$ . The new positive relation between both yields is representative of a photoinhibitory phase in which thermal dissipation is not sufficient to cope with the excessive excitation energy, which damages the reactions centres of the photosynthetic apparatus and produces an increase in  $\Phi_F$ .

Laboratory studies reveal that this photoinhibitory-phase becomes relevant under low temperatures and strong light (Fig. 2), as the rate of photodamage to the reaction centres exceeds the rate of repair by the reducing enzymatic activity. The same phenomenon is detectable in the field during sunny days of winter (Fig. 1b)

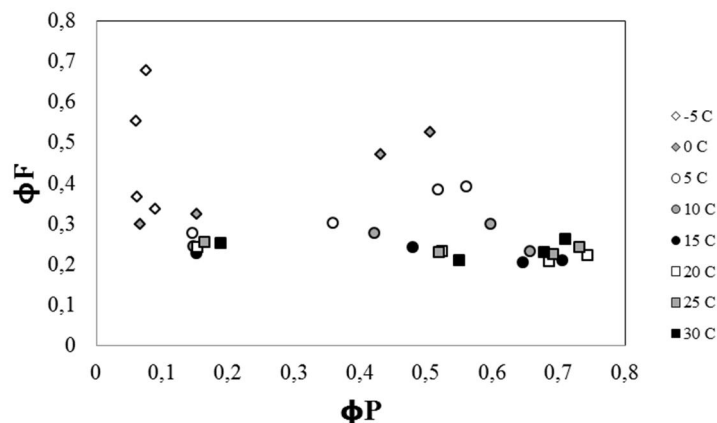


Figure 2. Relation between the photochemical yield ( $\Phi_P$ ) and the fluorescence yield ( $\Phi_F$ ) under different temperatures (from -5°C to 30°C), after 40 min light treatment (from 45  $\mu\text{mol photons m}^{-2} \text{s}^{-1}$  to 1300  $\mu\text{mol photons m}^{-2} \text{s}^{-1}$  actinic light) in current-year old needles of Scots pine (*Pinus sylvestris* L.) saplings acclimated to boreal summer conditions. The light intensities within each temperature are not presented.

In this study we characterized the seasonal relation between  $\Phi_P$  and  $\Phi_F$ , and identify a new phase linked to the process of photoinhibition of the reaction centres. This new phase, together with the presence of sustained forms of NPQ, has important implications on the interpretation of seasonal changes in remotely sensed SIF, since both the photoinhibitory-phase and the NPQ-phase are present under high light. We conclude that seasonal changes in SIF cannot be solely interpreted in terms of variations in NPQ, and other processes need to be considered. Developing mathematical models that capture the effect of photoinhibition and sustained NPQ from chlorophyll fluorescence data (see Abstract by Porcar-Castell *et al.*) will certainly help us to advance towards the interpretation of remotely sensed SIF and the estimation of photosynthesis at a global scale.

#### ACKNOWLEDGEMENTS

This study was supported by the Academy of Finland (projects #1118615 and #138884), and the University of Helsinki (project #490116)

#### REFERENCES

- Frankenberg C., J. Fisher, J. Worden, G. Badgley, S. Saatchi, J.-E. Lee, G.C. Toon, A. Butz, M. Jung, A. Kuze and T. Yokota (2011) New global observations of the terrestrial carbon cycle from GOSAT: Patterns of plant fluorescence with gross primary productivity. *Geophys. Res. Lett.* **38**(17), L17706.
- Joiner J., Y. Yoshida, A.P. Vasilkov, Y. Yosida, L.A. Corp and E.M. Middleton (2011) First observations of global and seasonal terrestrial chlorophyll fluorescence from space. *Biogeosciences* **8**(3), 637-651.
- Maxwell K. and G.N. Johnson (2000) Chlorophyll fluorescence— a practical guide. *J. Exp. Bot.* **51**(345), 659-668.

- Melis A (1999) Photosystem-II damage and repair cycle in chloroplasts: what modulates the rate of photodamage *in vivo*? *Trends Plant Sci.* **4**(4), 130-135.
- Meroni M., M. Rossini, L. Guanter, L. Alonso, U. Rascher, R. Colombo and J. Moreno (2009) Remote sensing of solar-induced chlorophyll fluorescence: Review of methods and applications. *Remote Sens. Environ.* **113**, 2037-2051.
- Öquist G. and N.P.A. Huner (2003) Photosynthesis of overwintering evergreen plants. *Annu. Rev. Plant Biol.* **54**, 329-355.
- Porcar-Castell A., E. Juurola, E. Nikinmaa, F. Berninger, I. Ensminger and P. Hari (2008) Seasonal acclimation of photosystem II in *Pinus sylvestris*. I. Estimating the rate constants of sustained thermal energy dissipation and photochemistry. *Tree Physiol.* **8**, 1475-1482.
- Porcar-Castell, A. (2011) A high-resolution portrait of the annual dynamics of photochemical and non-photochemical quenching in needles of *Pinus sylvestris*. *Physiol. Plantarum* **143**, 139-153.

# CAN HIGHLY OXIDIZED ORGANICS CONTRIBUTE TO NEW PARTICLE FORMATION?

I.K. ORTEGA<sup>1</sup>, N.M. DONAHUE<sup>2</sup> AND H. VEHKAMÄKI<sup>1</sup>

<sup>1</sup> Department of Physics, University of Helsinki, Post Office Box 64, FI-00014, Helsinki, Finland.

<sup>2</sup> Center for Atmospheric Particle Studies, Carnegie Mellon University, Pittsburgh PA, USA.

Keywords: HIGHLY OXIDIZED ORGANICS, CLUSTER FORMATION, QUANTUM CHEMISTRY.

## INTRODUCTION

Atmospheric new particle is an important source of aerosols and cloud condensation nuclei (Merikanto et al. 2009). Sulfuric acid plays a key role in new particle formation (Sipilä et al. 2010). On the other hand, atmospheric concentrations of sulfuric acid can not explain the new particle formation rates observed in atmospheric measurements. This indicates that some additional compounds should be involved, together with sulfuric acid, in atmospheric new particle formation.

The identity of these stabilizing compounds has been the subject of several studies during the recent years. Ammonia has been one of the most studied candidates to stabilize sulfuric acid clusters. Ternary new-particle formation involving base molecules has been one the most studied alternatives to sulfuric acid-water binary mechanism (Weber et al. 1996, Benson et al. 2011). Organic acids produced by oxidation of volatile organic compounds (VOCs) have been proposed as key compounds in new-particle formation as well. However, while some studies conclude that these oxidized VOC are just involved in particle growth (Laaksonen et al. 2008) other studies state that they are involved in the very first steps of new-particle formation (Zhang et al. 2009).

In the present work we have used quantum chemical methods to study the stability of heterodimers formed by one sulfuric acid molecule and on molecule of an oxidized organic compound (OxdOrg). We have chosen seven oxidation products of alpha-pinene with increasing O:C ratio (Figure 1), namely pinanendiol (PD), pinonic acid (PA), 7-hydroxy-pinonic acid (HPA), pinic acid (PiA), pinonic peroxide (Pper), di-keto pinic acid (DKPi) and 3-methyl-1,2,3-butane-tricarboxylic acid (MBTCA).

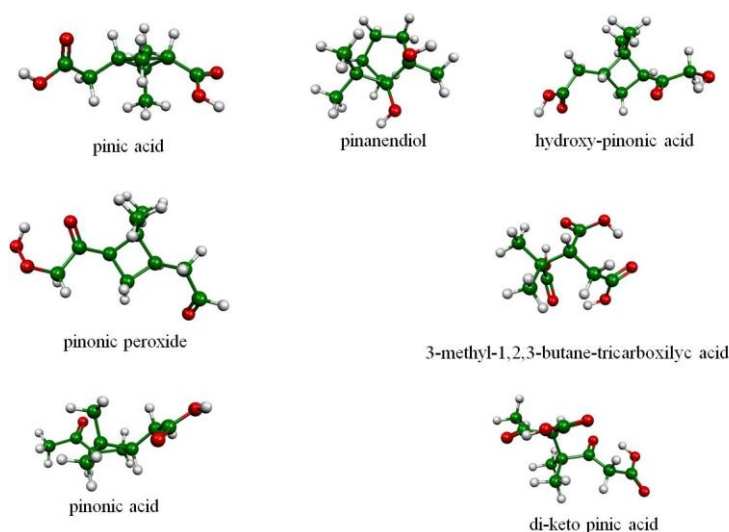


Figure 1. Organic compounds studied in this work. Green spheres represent carbon atoms, white spheres hydrogen atoms and red spheres oxygen atoms.

## METHODS

We used a multi-step method developed by our group (Ortega et al. 2012). The geometry optimizations and frequency calculations were performed with the Gaussian09 program (Frisch et al. 2009) using the B3LYP hybrid functional combined with a CBSB7 basis set, and a single-point electronic energy was then calculated with the TURBOMOLE program (Ahlich, et al. 1989) using the RI-CC2 method and an aug-cc-pV(T+d)Z basis set.

## RESULTS

We have calculated the formation free energy of clusters formed by one sulfuric acid molecule and one organic compound. Figure 2 shows the formation free energy of the hetero-dimer ( $\text{H}_2\text{SO}_4\text{-OxdOrg}$ ) versus O:C ratio of the organic compound forming the dimer. Formation free energy of the pure sulfuric acid dimer is shown as a reference.

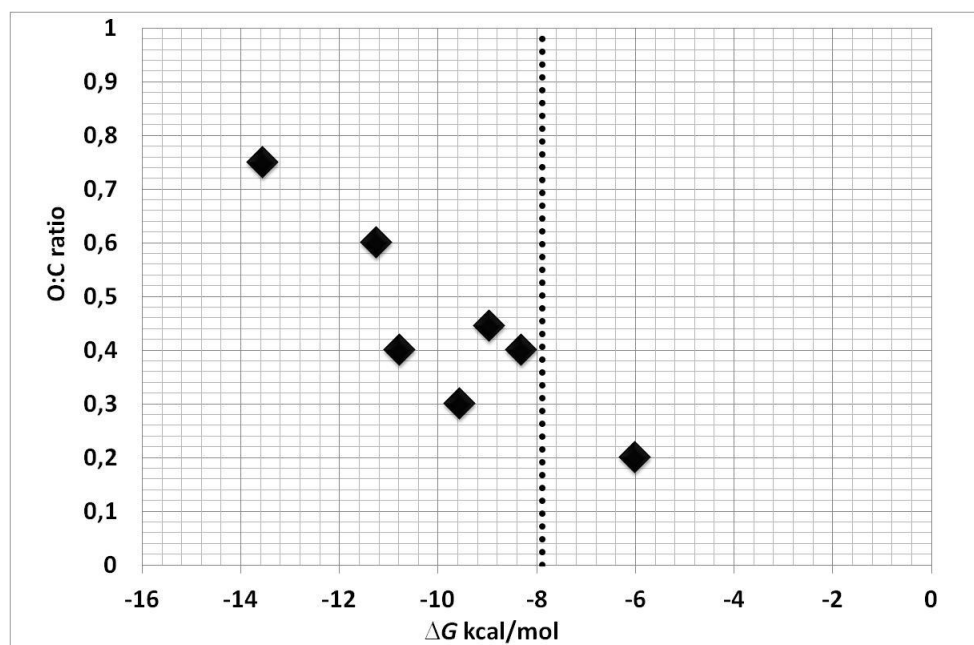


Figure 2. O:C ratio versus formation free energy at 298.15K of heterodimers, dotted line represent the formation free energy of sulfuric acid dimer (-7.89 kcal/mol) .

In general when the O:C ratio of the organic compound increases, the formation of the heterodimer is favoured. PD heterodimer is the only one that is less stable than the sulfuric acid dimer. This is not surprising since PD only have two  $-\text{OH}$  groups, and the hydrogen bond formed with the sulfuric acid is weak. In this study we have included two compounds with the same O:C, HPA and Pper. Comparing the heterodimer formation free energies of those two compounds we found that Pper can form more stable clusters than HPA ( $\sim 2.5$  kcal/mol). The reason for that difference is the number of hydrogen bonds formed in the heterodimer. While HPA forms two hydrogen bonds with the sulfuric acid molecule, Pper is able to form three, leading to a more stable cluster. Figure 3 shows how the number of H-bonds formed in the heterodimers is related to its formation free energy.

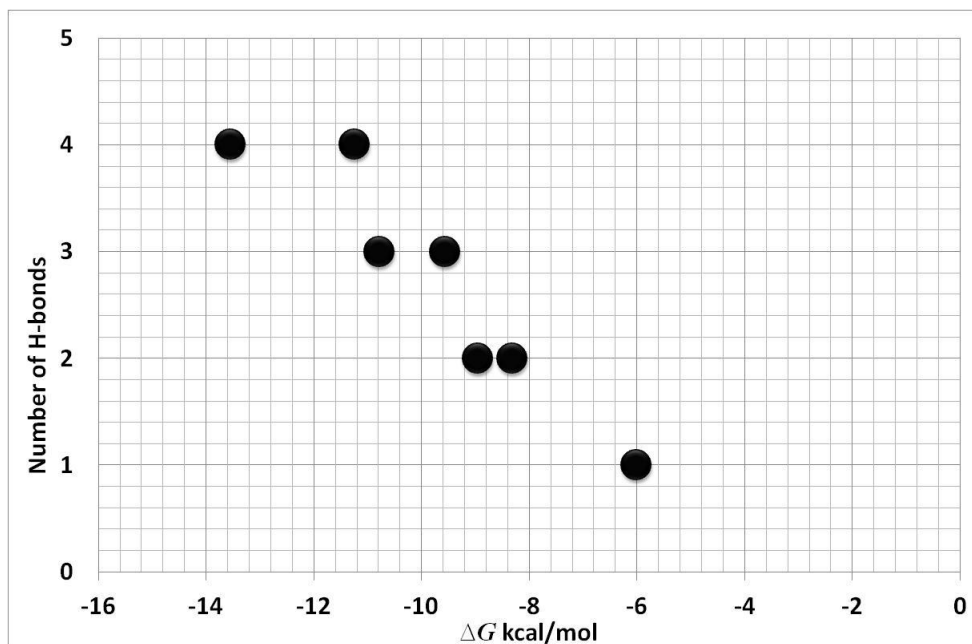


Figure 3. Number of hydrogen bonds versus formation free energy at 298.15K of heterodimers

In this case MBTCA and DKPi heterodimers four hydrogen bonds are formed, but MBTCA heterodimer is 2.3 kcal/mol more stable than the DKPi heterodimer. The reason for this difference is different hydrogen bond formed (Figure 4). Both compounds form 3 hydrogen bonds with the sulfuric acid molecule. The extra hydrogen bond is an internal hydrogen formed by the free carboxylic acid group (COOH), in the case of MBTCA COOH group binds to a third COOH existing in the molecules, while in the case of DKPi the internal hydrogen bond is between the COOH group and one carbonyl group (C=O).

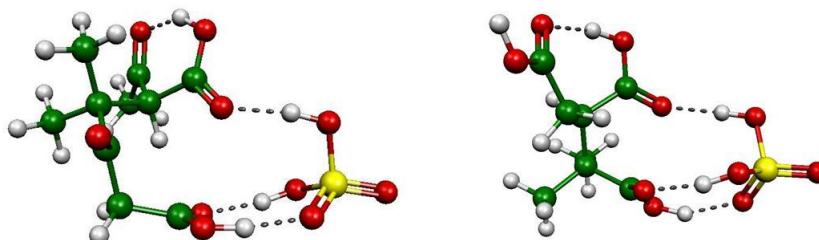


Figure 4. Most stable heterodimers of DKPi (left) and MBTCA (right). Green spheres represent carbon atoms, white spheres represents hydrogen atoms, yellow spheres represents sulfur atoms and red spheres represents oxygen atoms.

## CONCLUSIONS

We have shown that oxidized organic compounds with a high O:C ratio are able to form stable clusters with sulfuric acid. This implies that they can be involved in new particle formation. The presence of carboxylic acid groups favours the formation of the heterodimer. Indeed the most stable heterodimer is formed with MBTCA a tri-carboxylic acid. There is a clear correlation between the number of hydrogen bonds formed and the stability of the clusters. To confirm the possible participation of oxidized organic in new particle formation in the future we will extend the calculations to larger clusters.

## ACKNOWLEDGEMENTS

We acknowledge the Academy of Finland (CoE Project No. 1118615, LASTU Project No. 135054), the Nessling Foundation, ERC Project Nos. 257360- MOCAPAF and 27463-ATMNUCLE for funding. We

thank the CSC Centre for Scientific Computing in Espoo, Finland for computer time, and the CLOUD team for helpful discussions.

#### REFERENCES

- Merikanto, J., Spracklen, D.V., Mann, G.W., Pickering, S.J. and Carslaw, K.S. (2009). Impact of nucleation on global CCN. *Atmos.Chem.Phys.* **9**, 8601.
- Sipilä, M., Berndt, T., Petäjä, T. Brus, D., Vanhanen, J., Stratmann, F.; Patokoski, J., Mauldin III, R. L., Hyvärinen, A-P., Lihavainen H., and Kulmala, K. (2010). The Role of Sulfuric Acid in Atmospheric Nucleation. *Science*, **327**, 1243.
- Weber, R. J., Marti, J. J., McMurray, P. H., Eisele, F. L., Tanner, D. J., and Jefferson, A. (1996). Measured atmospheric new particle formation rates: Implications for nucleation mechanisms *Chem. Eng. Commun.* **151**, 53.
- Benson, D., Markovich, A. , and Lee, S-H., (2011). Ternary homogeneous nucleation of H<sub>2</sub>SO<sub>4</sub>, NH<sub>3</sub>, and H<sub>2</sub>O under conditions relevant to the lower troposphere. *Atmos. Chem. Phys.* **11**, 4755.
- Laaksonen, A. et al. (2008). The role of VOC oxidation products in continental new particle formation, *Atmos. Chem. Phys.* **8**, 2657.
- Zhang, R.; et al. (2009). Formation of nanoparticles of blue haze enhanced by anthropogenic pollution *Proc. Natl. Acad. Sci.* **106**, 17650.
- Ortega, I.K., et al. (2012). Formation of nanoparticles of blue haze enhanced by anthropogenic pollution *Atmos. Chem. Phys.* **12**, 225.
- M.J. Frisch et al. Gaussian 09, Revision A.01, (2009).
- Ahlrichs, R., Bär, M., Häser, Horn, J.H., and Kölmel, C.(1989). Electronic structure calculations on workstation computers: the program system TURBOMOLE. *Chem. Phys. Lett.* **162**, 165

# ESTIMATING THE NUMBER AND SIZES OF PARTICLES FROM ANTHROPOGENIC EMISSIONS – NOW AND IN FUTURE

P. PAASONEN<sup>1,2</sup>, K. KUPIAINEN<sup>2,3</sup>, M. AMANN<sup>2</sup> and M. KULMALA<sup>1</sup>

<sup>1</sup>Division of Atmospheric Sciences, Department of Physics, University of Helsinki,  
PL 64, 00014 University of Helsinki, Finland.

<sup>2</sup>International Institute for Applied Systems Analysis (IIASA), Schlossplatz 1, A-2361 Laxenburg, Austria.

<sup>3</sup>Finnish Environment Institute (SYKE), PL 140, 00251 Helsinki, Finland

Keywords: Anthropogenic emissions, particle number, size distribution.

## INTRODUCTION

The health and climate effects of aerosol particles are strongly affected by the size and number of particles. Ultrafine particles with diameters below 100 nm can enter through the lungs to human cardiovascular system and cause adverse health effects which differ from those of larger particles (WHO, 2013). On the other hand, particles with diameters close to or over 100 nm can be activated as cloud droplets, thus cooling the climate (Forster *et al.*, 2010). During the last year we have implemented particle number emission factors with size distributions to GAINS (Greenhouse gas and Air pollution Interactions and Synergies) model. By applying these emission factors with the existing country-specific information in GAINS (the consumption of different fuels in varying source sectors, currently applied emission abatement technologies and future political scenarios with varying environmental ambition levels) we can study the sources of the current anthropogenic aerosol emissions and estimate their impacts. Moreover, the estimating the future development of the emissions under different political scenarios is necessary for the decision making bodies. In this presentation the anthropogenic particle number emission estimates in Europe are described from 2010 to 2025 under three different policy scenarios.

## METHODS

GAINS (Greenhouse gas and Air pollution Interactions and Synergies) model is an integrated assessment model, managed by Mitigation of Air pollution and Greenhouse gases (MAG) group at the International Institute for Applied Systems Analysis (IIASA). GAINS brings together several levels of information on the sources of various air pollutants and greenhouse gases – emission levels, health and environmental impacts, control potentials and the costs of these controls. The political scenarios in GAINS allow for researchers and modellers to study the future global emissions and their spatial distribution and for decision makers to compare the costs and outcomes of regulations and investments on new technologies. The variety of pollutants (SO<sub>2</sub>, NO<sub>x</sub>, PM mass (PM<sub>10</sub>, PM<sub>2.5</sub>, PM<sub>1</sub>, PM<sub>BC</sub> and PM<sub>OC</sub>), NMVOC, NH<sub>3</sub>, CO<sub>2</sub>, CH<sub>4</sub>, N<sub>2</sub>O, F-gases) makes it possible to optimize the abatement strategies for various pollutants. The annual emissions  $E$  in a country or a region  $i$  are calculated with

$$E_i = \sum_{jkm} E_{ijkm} = \sum_{jkm} A_{ijkm} X_{ijkm} EF_{ijkm}, \quad (1)$$

where the indices and symbols refer to

$j$  Source sector (e.g. domestic single house heating boilers)  
 $k$  Fuel (e.g. firewood, coal)

$m$	Abatement technology (e.g. pellet boilers, boilers with electrostatic precipitator)
$A$	Volume of annual activity (typically annual energy consumption in sector $j$ with fuel $k$ )
$X$	Share of abatement technology of the activity $m$ (so that $\sum_m X_m = 1$ )
EF	Emission factors for each sector-fuel-technology –combination (emissions per activity unit)

Lately we have introduced aerosol particle number emission factors (PNEF) with corresponding particle (number) size distributions (PSD) to GAINS (Paasonen *et al.*, 2013). For road transport PNEFs and PSDs are based on the latest version of TRANSPHORM database (Vouitsis *et al.*, 2013), whereas other sources are covered with emission factors from the literature and from the emission inventory by TNO (Denier van der Gon *et al.*, 2009; Kulmala *et al.*, 2011).

The implemented emission factors and size distributions represent the aerosol emissions after cooling and initial dilution to the surrounding air. The emission factors include particle number emissions in size range 3-1000 nm, including emissions of both primary and secondary particles. In the online downloadable data of GAINS the emissions will be given in two size categories, particles with mobility diameters below and above 100 nm, named as ultrafine particle number (PN<sub>UFP</sub>) and non-ultrafine particle number (PN<sub>nonUFP</sub>, in this presentation PN<sub>>100</sub>), respectively. Emissions of PN<sub>>100</sub> can be taken as a rough estimate for direct cloud condensation nuclei (CCN) emissions. More detailed size distribution of emissions, distribution to 15 size bins, will be available for modelling purposes and upon request. The aerosol number emissions are anticipated to be online during year 2013.

## RESULTS

Particle number emissions are determined mainly with ultrafine particle (UFP) emissions, which form 88 % of the emissions. Thus, in the following results the total emissions PN<sub>tot</sub> are shown together with non-UFP emissions, the previous can be interpreted roughly as UFP emissions.

In year 2010 the particle number emissions in EU28 were clearly dominated by road transport emissions, which were estimated to contribute over 60 % to the total emissions PN<sub>tot</sub> (Figure 1). The second largest contributions were those of national shipping and domestic combustion of firewood and coal, 14 % and 13%, respectively. These shares are in stark contrast with the mass emissions of particles with diameters below 1 µm (PM<sub>1</sub>), for which domestic combustion contributes 56 % and road transport and shipping only 12 % and 1 %, respectively.

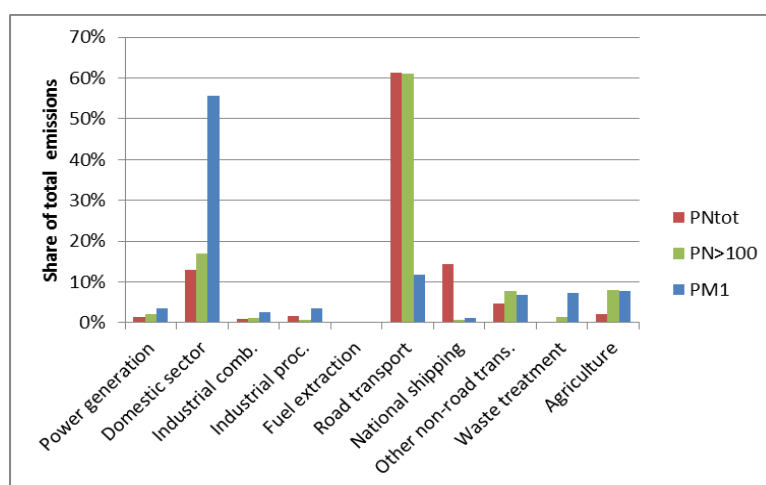


Figure 1. The distribution of number emissions PN<sub>tot</sub> and PN<sub>>100</sub> and mass emissions PM<sub>1</sub> in different source sectors in EU28 for year 2010.

Current legislation gives strict limitations to the mass emissions of particulate matter from road transport. According to the TRANSPHORM-database (Vouitsis et al., 2013), where the emission factors for road vehicles are derived from, especially EURO V and VI technologies decrease efficiently also the number emissions from diesel engines, at least in EU where the sulphur content of the fuel is very low. Replacement of the old vehicles by new ones is estimated to decrease PN emissions from road transport until 2025 by 88 %. Under the current legislation (CLE) scenario the emissions from national shipping are not estimated to change significantly and domestic combustion emissions are estimated to decrease 17 %. Consequently, the emissions from the latter two source sectors are anticipated to exceed road transport emissions by 2025 (Figure 2.). In the more ambitious policy scenarios, A5 and MTFR (central policy- and maximum technologically feasible reductions –scenarios, Amann et al., 2013), in which the transport sector is similar to CLE, the decrease in domestic sector emissions is 20 % and 32 %, respectively.

The estimated decrease in total emissions from 2010 to 2025 according to CLE, A5 and MTFR-scenarios, is 59 %, 64 % and 66 %, respectively. The corresponding decreases for  $PN_{>100}$  are somewhat larger, 61 %, 75 % and 78 %. For comparison, the corresponding values for  $PM_{10}$  mass emissions are 27 %, 54 % and 66 %.

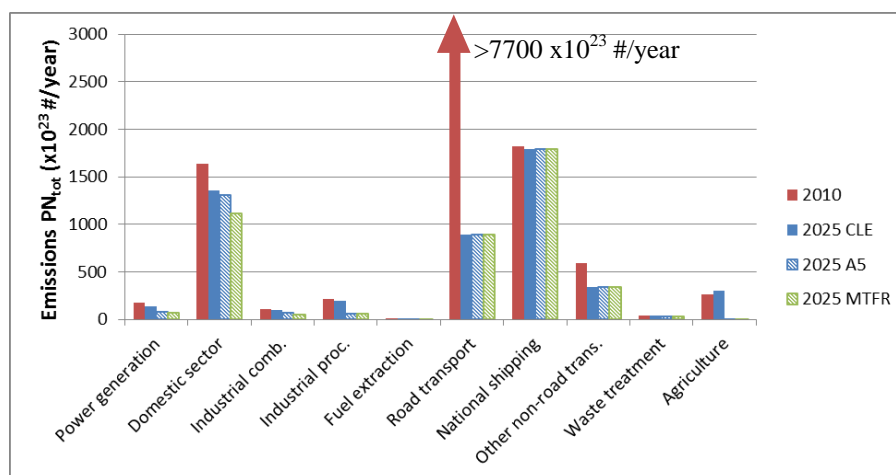


Figure 2. Annual emissions in EU28 from different source sectors in 2010 and in 2025 under CLE, A5 and MTFR scenarios. Note that road transport emissions in 2010 exceed the y-axis scale.

More detailed size distributions of the particle emissions in EU28 for the main source sectors are presented in Figure 3. Note that the upper and lower panels have different scales on y-axis. The drastic difference between CLE and the more ambitious scenarios in Figure 3d is due to banning of open burning of agricultural residues in A5 and MTFR scenarios.

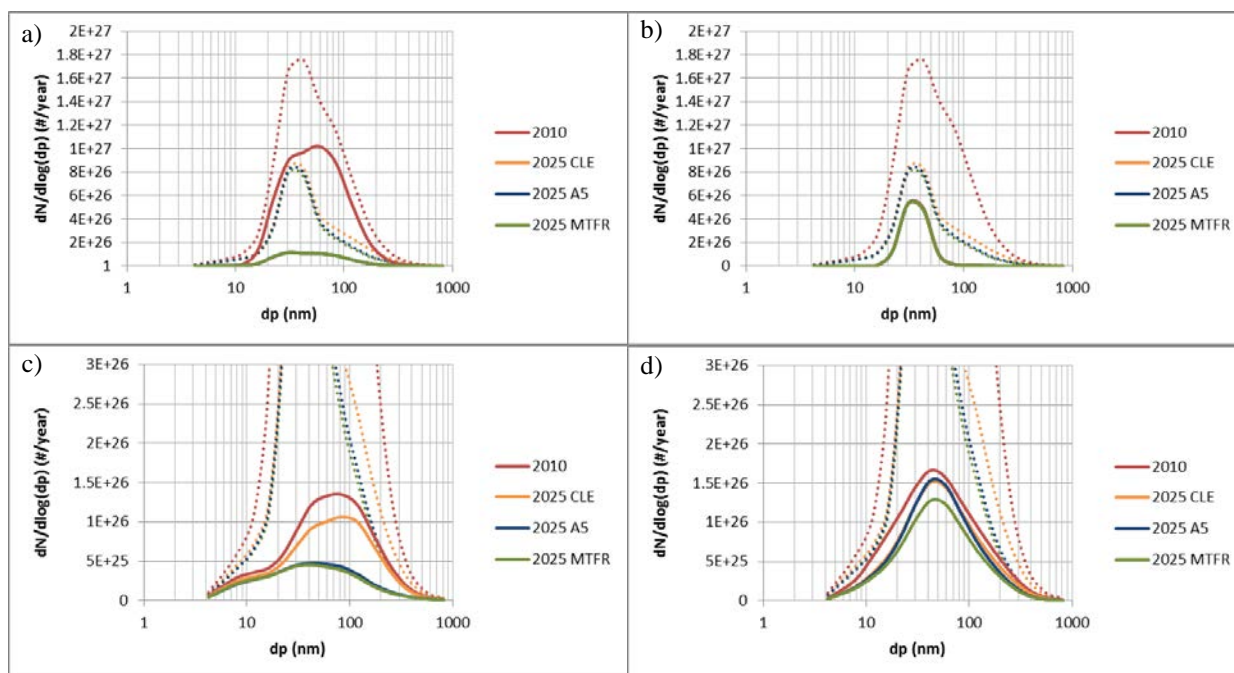


Figure 3. Size resolved PN emissions in EU28 under the studied scenarios. Total emissions are shown with dotted lines in all panels, whereas the solid lines indicate PN emissions from (a) road transport, (b) shipping, (c) domestic combustion and (d) other source sectors. Note the order of magnitude difference in scales between upper and lower panels.

## CONCLUSIONS

Estimation of particle number emissions, including the information on their size distribution, was performed for the first time with the GAINS model. The first results show that currently in EU28 countries the dominating source in terms of particle numbers is road transport, covering 60 % of all emissions. However, the emission abatement strategies applied in road transport sector in order to meet the strict limitations on particle mass emissions decrease efficiently also the number emissions. It is anticipated that this decrease is enough to bring the European traffic emissions to lower level than either of the currently next largest sources, national shipping and domestic combustion, by 2025.

It is to be noted that the first results presented here are subject to significant uncertainties, mainly due to scarcity of published information on the particle number emission factors and size distributions in several source sectors. However, introducing the particle number emissions to GAINS model provides new information on the changes in anthropogenic PN emissions required in modelling the future climate, as well as helps building the basis for possible future limitations on particle number emissions.

## ACKNOWLEDGEMENTS

This work was funded by the Academy of Finland Center of Excellence (project no 1118615), European Commission seventh Framework program (PEGASOS, contract no 265148) and Otto A. Malm foundation.

## REFERENCES

- Amann, M., et al. (2013). Policy Scenarios for the Revision of the Thematic Strategy on Air Pollution. TSAP Report #10. International Institute for Applied Systems Analysis, Laxenburg, Austria.
- Denier van der Gon, H. et al. (2009). Size-resolved Pan European Anthropogenic Particle Number Inventory, EUCAARI Deliverable 141.
- Forster, P., et al. (2007) in: *Climate Change 2007: The Physical Science Basis. Contribution of Working Group I to the Fourth Assessment Report of the Intergovernmental Panel on Climate Change*. Eds. Solomon, S., et al. (Cambridge University Press, United Kingdom and New York, NY, USA).
- Kulmala, M. et al. (2011). General overview: European Integrated project on Aerosol Cloud Climate and Air Quality interactions (EUCAARI) - integrating aerosol research from nano to global scales. *Atmos. Chem. Phys.* **11**, 13061–13143.
- Paasonen et al. (2013). Aerosol particle number emissions and size distributions: Implementation in the GAINS model and initial results. IIASA Interim Report.
- Vouitsis, I., Ntziachristos, L., Han, Z. (2013). Methodology for the quantification of road transport PM emissions, using emission factors or profiles. TRANSPHORM Deliverable D1.1.2.
- WHO (2013). Review of evidence on health aspects of air pollution – REVIHAAP [WWW Document]. URL [http://www.euro.who.int/\\_\\_data/assets/pdf\\_file/0020/182432/e96762-final.pdf](http://www.euro.who.int/__data/assets/pdf_file/0020/182432/e96762-final.pdf) (accessed 3.27.13).

# INVESTIGATION OF THE EFFECTS OF CHEMICAL AND PHYSICAL FACTORS ON THE PHASE STATE OF SOA PARTICLES

A. PAJUNOJA<sup>1</sup>, M. R. ALFARRA<sup>2,3</sup>, A. BUCHHOLZ<sup>2</sup>, W.T. HESSON<sup>2</sup>, G.B. MCFIGGANS<sup>2</sup>, A. VIRTANEN<sup>1</sup>

<sup>1</sup>Department of Applied Physics, University of Eastern Finland, Kuopio, FI-70210, Finland

<sup>2</sup>Centre for Atmospheric Science, The University of Manchester, Manchester, M13 9PL, UK

<sup>3</sup>National Centre for Atmospheric Science, The University of Manchester, Manchester, M13 9PL, UK

Keywords: SOA, phase state, viscosity, VOC.

## INTRODUCTION

Secondary organic aerosol (SOA) formed from partitioning of oxidation products of volatile organic compounds (VOC) accounts for a significant portion of atmospheric particulate matter. Important fraction of Secondary Organic Aerosol (SOA) particles in the atmosphere may be composed of amorphous (glassy) material (Virtanen et al., 2010; Koop et al., 2011) and behaviour of SOA particles in the atmosphere is affected by the phase of particles; not heeding these effects can result in remarkable errors when the atmospheric implications of SOA particles are predicted. The phase of SOA particles affects their ability to uptake organic compounds to grow into cloud condensation nuclei (CCN), and their water uptake and activation into cloud droplets (Riipinen et al., 2012; Pöschl, 2011). Phase change of the particles can be induced e.g. by temperature change, absorption of water, or other solvent, or by chemical aging.

## METHODS

The phase state of SOA particles cannot be measured directly. Present studies show that particle bounce correlates with the phase state of particles (Virtanen et al. (2010), Saukko et al. (2012a), Saukko et al. (2012b)). A similar but modified method was employed in this study. The schematic of the new measurement system is shown in Figure 1. The system consists of a size classification DMA (selected sizes 70-150 nm), humidity control unit, a single MOUDI-type impactor stage (cut-off size 67 nm) and two CPCs. Upstream and downstream pressures of the impactor stage were stabilized to 0.85 bar and 0.7 bar.

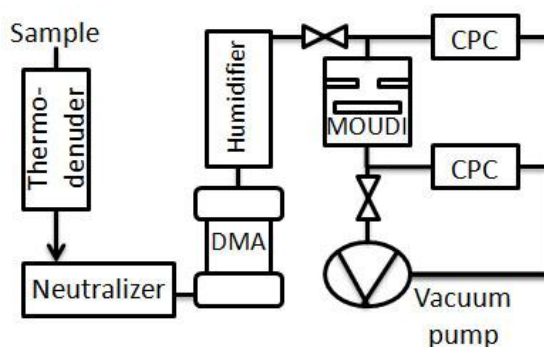


Figure 1: Schematic representation of the Aerosol Bounce Instrument (ABI) measurement system.

The chamber experiments were performed in the Manchester Photochemical Aerosol Chamber (Alfarra et al., 2012). In these experiments both biogenic and anthropogenic precursors were used ( $\alpha$ -pinene, 1,3,5-trimethylbenzene,  $\beta$ -caryophyllene, limonene and n-heptadecane). The measurement schedule for different VOC mixtures is shown in Table 1. Mixtures of one to three precursors were investigated with and without the presence of ammonium sulphate seeds.

Table 1. Chamber experiment schedule for four VOCs and specific NO<sub>x</sub> and O<sub>3</sub>-levels (ppb). X means the existence of ammonium sulphate seeds or usage of UV filter.

1	2	3	NO <sub>x</sub>	O <sub>3</sub>	seed	filter
α-pin.	TMB		20	40		X
α-pin.	TMB		20	40		
α-pin.	TMB		115	40		X
α-pin.	TMB		20	40	X	X
α-pin.	β-car.		20	40		X
α-pin.	β-car.		20	40	X	X
limon.			20	40		X
α-pin.	β-car.		20	40		
α-pin.	TMB	β-car.	20	40		
α-pin.	TMB	β-car.	20	40	X	X
α-pin.	TMB	β-car.	20	40		X
α-pin.	limon.		20	40		X
β-car.	limon.		20	40		X
α-pin.	β-car.	limon.	20	40		X
n-hept			50	80		

The oxidation conditions in the chamber were altered, namely the NO<sub>x</sub>-level (20-115 ppb) and the UV exposure (filter on/off) while the O<sub>3</sub> level and relative humidity (RH) in the chamber were constantly 40 ppb and 60%, respectively. The exposure to light (visible and UV) varied between 0 and 5 hours. The particle bounce was investigated for RH between 5 and 85% in the impactor. These RH scans were conducted for several thermodenuder temperatures (25 - 75°C).

## CONCLUSION

In this paper, results of the particle bounce measurements will be compared to findings from measurements of particle composition and sub- and super-saturated water uptake determined by high resolution AMS, HTDMA and CCNc, respectively. Clear effects of chemical composition and aging, hygroscopicity and relative humidity on the phase state of the SOA particles were observed. In addition differences between the bounce fractions in the SOA-coated seed experiments with different temperatures and aging times were found.

## ACKNOWLEDGEMENTS

Financial support from the Academy of Finland through the Center-of-Excellence programme (decision no: 259005 & 264989) and from the strategic funding of the University of Eastern Finland are acknowledged.

## REFERENCES

- Alfarra, R. et al. (2012), *Atmos. Chem. Phys.*, 12, 6417-6436.  
Koop, T. et al. (2011) *Phys. Chem. Chem. Phys.* 13:19238–19255  
Kroll, J. et al. (2010) *Nat. Chem.* 948:1-7  
Pöschl, U. (2011), *Atmos. Res.* 101:562–573.  
Riipinen, I. et al. (2012) *Nat. Geosci.* 5:453–458.  
Saukko, E. et al. (2012a) *Atmos. Meas. Tech.* 5:259-265  
Saukko, E. et al. (2012b) *Atmos. Chem. Phys.* 12:7517-7529  
Virtanen, A. et al. (2010) *Nat.* 467:824-827  
Zhang, X. et al. (2013) *Atmos. Chem. Phys.*, 13, 5907–5926

# LONG-TERM SIZE-SEGREGATED CLOUD CONDENSATION NUCLEI COUNTER (CCNC) MEASUREMENTS IN A BOREAL ENVIRONMENT AND ITS IMPLICATIONS FOR AEROSOL-CLOUD INTERACTIONS

M. PARAMONOV<sup>1</sup>, M. ÄIJÄLÄ<sup>1</sup>, P.P. AALTO<sup>1</sup>, A. ASMI<sup>1</sup>, N. PRISLE<sup>1</sup>, T. NIEMINEN<sup>1</sup>, U. MAKKONEN<sup>2</sup>, H. HAKOLA<sup>2</sup>, M. KAJOS<sup>1</sup>, J. PATOKOSKI<sup>1</sup>, R. TAIPALE<sup>1</sup>, T. RUUSKANEN<sup>1</sup>, J. RINNE<sup>1</sup>, V.-M. KERMINEN<sup>1</sup>, M. KULMALA<sup>1</sup> and T. PETÄJÄ<sup>1</sup>

<sup>1</sup>Department of Physics, University of Helsinki, P.O. Box 64, FI-00014, Helsinki, Finland.

<sup>2</sup>Finnish Meteorological Institute, P.O. Box 503, 00101, Helsinki, Finland.

Keywords: CCNC, aerosol, cloud, critical diameter, hygroscopicity.

## INTRODUCTION

Aerosol particles are omnipresent in the atmosphere, and besides directly influencing the radiative balance of the Earth, they play a crucial role in cloud formation (Stevens and Feingold, 2009). Through a variety of microphysical processes aerosol particles influence the albedo, lifetime and precipitation patterns of clouds in what is known as indirect effects of aerosols on climate (Forster *et al.*, 2007). The ability of aerosol particles to act as cloud condensation nuclei (CCN) is strongly linked to their physical and chemical properties, with the most important parameters being CCN number concentration, aerosol critical diameter  $D_c$  and hygroscopicity parameter  $\kappa$  (Seinfeld and Pandis, 2006).

## METHODS

Size-segregated CCNC measurements have been conducted continuously since February 2009 at the SMEAR II (Station for Measuring Ecosystem-Atmosphere Relations) in Hyytiälä Forestry Field Station in Finland (61° 50' 50.685"N, 24° 17' 41.206"E, 179 m a.m.s.l.) (Hari and Kulmala, 2005). The CCNC in question is a diffusion-type CCN counter, including a differential mobility analyzer (DMA), condensation particle counter (CPC), optical particle counter (OPC) and a saturator unit. CCN concentrations are measured across 30 size channels, with particle diameters ranging from 20 to 300 nm for five supersaturation  $S_{\text{eff}}$  levels ranging between 0.1% and 1%. Data were analysed up to April 2012, and, following processing and filtering, a total of 29 non-consecutive months of CCNC data are presented.

Critical diameter  $D_c$  was calculated for each activation spectrum as a mid-point of the fitted sigmoid curve, i.e. 50% of particles activated (Rose *et al.*, 2008). For each pair of  $D_c$  and  $S_{\text{eff}}$ ,  $\kappa$  was calculated according to the EH1 Köhler model using Eq. A30 in Rose *et al.* (2008). The surface tension of pure water of 0.072 J m<sup>-2</sup> was assumed. No normalisation of activation spectra took place prior to the curve fitting; therefore, discussion below concerns only the CCN-active fraction of the ambient aerosol.

## RESULTS

The median critical diameter  $D_c$  for the whole dataset in this study is reported at 75 nm, with the quartiles indicating a range from 57 nm to 105 nm. The median hygroscopicity parameter  $\kappa$  for the whole dataset in this study is reported at 0.22, with quartiles indicating a range from 0.15 to 0.36. The median  $\kappa$  shows that aerosol in the boreal environment of Southern Finland is less hygroscopic than the global continental and European continental averages, as presented by (Pringle *et al.*, 2010). The lower  $\kappa$  is likely explained by the presence of a larger aerosol organic fraction within the aerosol. Agreeing with Birmili *et al.* (2009), particle hygroscopicity was found to be size-dependent. Comparing  $\kappa$  values from several studies, which utilized a similar measurement setup, reveals that ambient aerosol in the boreal environment is more

hygroscopic than in the Amazon rainforest (Gunthe *et al.*, 2009), high alpine (Jurányi *et al.*, 2011) or mountainous forest environments (Levin *et al.*, 2012) (Fig. 1). This comparison amongst sites also reveals that the rate of change of aerosol hygroscopicity with size in Hyytiälä is higher than in three other locations, indicating differences in the species of condensing material and the oxidation and aging processes.

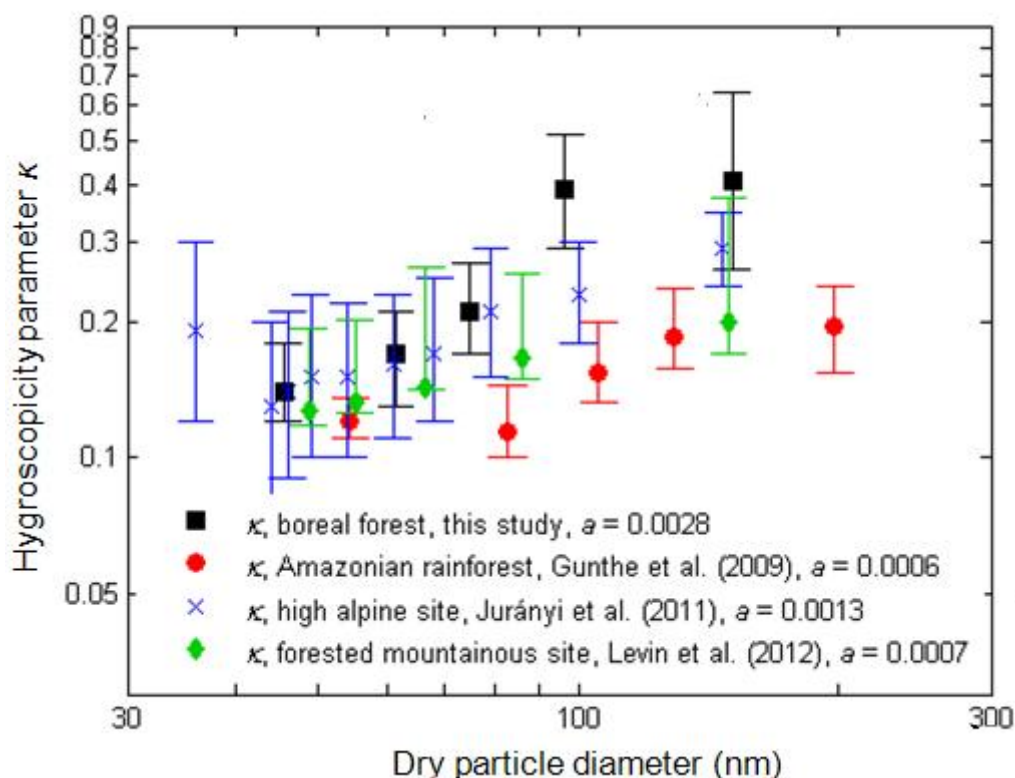


Figure 1. Relationship between particle dry size (taken as  $D_c$ ) and hygroscopicity parameter  $\kappa$  for four different sites. Both panels show the median values with error bars being 25<sup>th</sup> and 75<sup>th</sup> percentiles (for Gunthe *et al.*, 2009 percentiles estimated from the original publication). Legend entries also indicate the slope of the linear regression  $y = ax + b$  fit.

For each level of  $S_{\text{eff}}$ , it was discovered that the distributions of  $\kappa$  are log-normal, and these distributions exhibit different shapes between levels of  $S_{\text{eff}}$ . These size-dependent differences in the  $\kappa$  distributions do not support the use of a single  $\kappa$  value, mean or median, to describe the hygroscopicity of the whole aerosol population.

The biogenic emissions in the boreal environment of Southern Finland make ambient aerosol of  $>100$  nm in diameter less hygroscopic in the spring and summer time, compared to other seasons – the seasonal variation of  $D_c$  needed for CCN activation is important to remember when estimating CCN concentrations from aerosol particle number measurements. The participation of biogenic emissions in photochemical reactions is responsible for introducing a diurnal pattern in the behaviour of aerosol hygroscopicity in the spring and summer for particles  $\sim 50$  nm in diameter. The diminished photochemistry, temperature and biogenic activity in autumn and winter result both in the highest seasonal hygroscopicity of larger ambient aerosol and in the absence of the diurnal trend of  $D_c$  and  $\kappa$  for particles of any size.

A subset of CCNC data measured in the spring and summer was used to determine the possible effect of atmospheric new particle formation (NPF) on the diurnal behaviour of CCN activation properties, as described by the  $D_c$ . In the overall seasonal analysis, during spring and summer  $D_c$  at  $S_{\text{eff}}$  of 1.0% exhibited a minimum around noon for reasons stated above, similar to what can be seen for the days with no NPF (Fig. 2). During the NPF days the variation of  $D_c$  is larger, and the diurnal pattern is clearer (Fig.

2). By the time the newly formed particles are expected to grow to 50 nm in diameter (around midnight), there is no difference in  $D_c$  between NPF and non-NPF days. It seems as though the hygroscopicity of aerosol ~50 nm in diameter is more dictated by meteorological, photochemical and emission parameters, rather than by NPF.

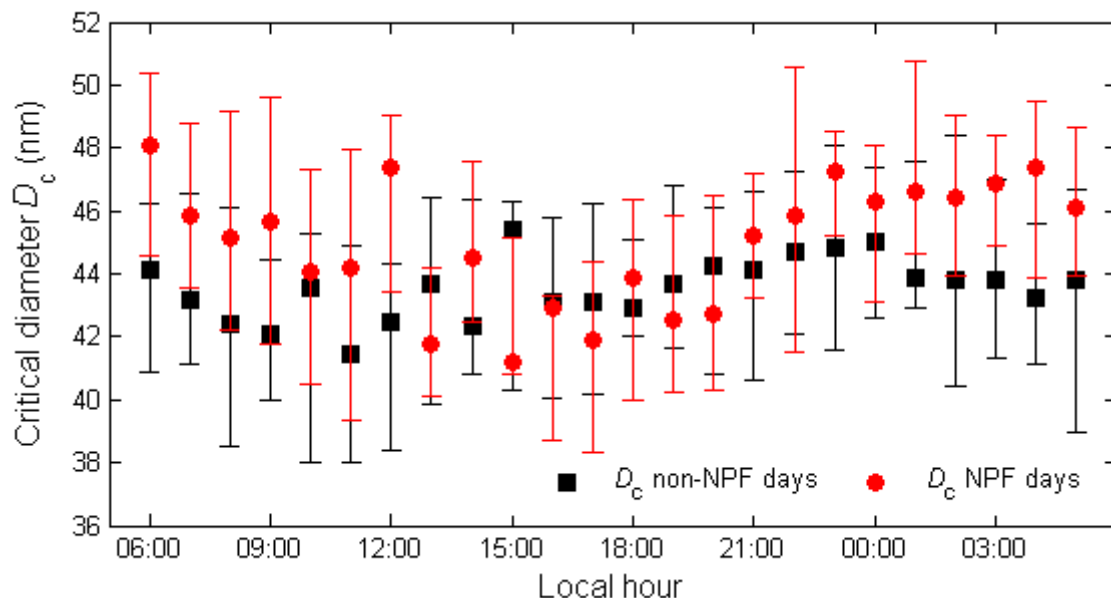


Figure 2. Diurnal variation of median critical diameter  $D_c$  on 29 spring Type I event (red) and 53 spring non-event (black) days. Shown from 06:00 of the day in question until 05:00 of the following day for  $S_{eff}$  of 1.0%. Error bars are 25<sup>th</sup> and 75<sup>th</sup> percentiles.

To get an insight into the chemistry of CCN, the dataset was analyzed in parallel with long-term measurements and proxies of various atmospheric constituents in both gas and particle phase. The sulphuric acid proxy (Petäjä *et al.*, 2009) and sulphate measurements by the aerosol mass spectrometer (AMS) both correlated positively with  $\kappa$ , pointing out the hygroscopic nature of atmospheric sulphur compounds. It was also found that organic mass fraction and concentrations of monoterpenes and isoprene decrease the  $\kappa$  of aerosol. Some seasonal differences were discovered in the effects of abovementioned parameters on  $\kappa$ ; however, the effect of these constituents on aerosol hygroscopicity is larger and more important for particles over 100 nm in diameter. Atmospheric nitric acid and nitrate mass fraction were found to decrease  $\kappa$ ; the correlations, however, were poor and inconclusive. It is suspected that the reduced  $\kappa$  at elevated nitrate and nitric acid concentrations may be related either to the fact that nitrate may be present in the organic form, or to the features of airmasses.

#### ACKNOWLEDGEMENTS

This work was supported by the Maj and Tor Nessling Foundation projects nr. 2010143, 2012443 and 2013325 "The effects of anthropogenic air pollution and natural aerosol loading to cloud formation". The authors are thankful to Dr. Ezra Levin and Anthony Prenni for a timely provision of some complimentary data. Prof. Miikka Dal Maso and MSc Juan Hong are gratefully acknowledged for their help with computations.

#### REFERENCES

Birmili, W., K. Schwirn, A. Nowak, T. Petäjä, J. Joutsensaari, D. Rose, A. Wiedensohler, K. Hämeri, P. Aalto, M. Kulmala and M. Boy (2009). Measurements of humidified particle number size distributions in a Finnish boreal forest: derivation of hygroscopic particle growth factors. *Boreal*

- Environ. Res.*, **14**, 458–480.
- Forster, P., V. Ramaswamy, P. Artaxo, T. Berntsen, R. Betts, D.W. Fahey, J. Haywood, J. Lean, D.C. Lowe, G. Myhre, J. Nganga, R. Prinn, G. Raga, M. Schulz and R. Van Dorland (2007): Changes in Atmospheric Constituents and in Radiative Forcing. *In: Climate Change 2007: The Physical Science Basis. Contribution of Working Group I to the Fourth Assessment Report of the Intergovernmental Panel on Climate Change* [Solomon, S., D. Qin, M. Manning, Z. Chen, M. Marquis, K.B. Averyt, M. Tignor and H.L. Miller (eds.)]. Cambridge University Press, Cambridge, United Kingdom and New York, NY, USA.
- Gunthe, S. S., S. M. King, D. Rose, Q. Chen, P. Roldin, D. K. Farmer, J. L. Jimenez, P. Artaxo, M. O. Andreae, S. T. Martin and U. Pöschl (2009). Cloud condensation nuclei in pristine tropical rainforest air of Amazonia: size-resolved measurements and modeling of atmospheric aerosol composition and CCN activity, *Atmos. Chem. Phys.*, **9**, 7551–7575.
- Hari, P. and M. Kulmala (2005). Station for measuring ecosystem-atmosphere relations. *Boreal Env. Res.* **10**, 315–322.
- Jurányi, Z., M. Gysel, E. Weingartner, N. Bukowiecki, L. Kammermann and U. Baltensperger (2011). A 17 month climatology of the cloud condensation nuclei number concentration at the high alpine site Jungfraujoch, *J. Geophys. Res.*, **116**, D10204.
- Levin, E. J. T., A. J. Prenni, M. D. Petters, S. M. Kreidenweis, R. C. Sullivan, S. A. Atwood, J. Ortega, P. J. DeMott and J. N. Smith (2012). An annual cycle of size-resolved aerosol hygroscopicity at a forested site in Colorado, *J. Geophys. Res.*, **117**, D06201.
- Petäjä, T., R.L. Mauldin III, E. Kosciuch, J. McGrath, T. Nieminen, P. Paasonen, M. Boy, A. Adamov, T. Kotiaho and M. Kulmala (2009). Sulfuric acid and OH concentrations in a boreal forest site. *Atmos. Chem. Phys. Discuss.* **9**, 7435–7448.
- Pringle, K.J., H. Tost, A. Pozzer, U. Pöschl and J. Lelieveld (2010). Global distribution of the effective aerosol hygroscopicity parameter for CCN activation. *Atmos. Chem. Phys. Discuss.* **10**, 6301–6339.
- Rose, D., S.S. Gunthe, E. Mikhailov, G.P. Frank, U. Dusek, M.O. Andreae and U. Pöschl (2008). Calibration and measurement uncertainties of a continuous-flow cloud condensation nuclei counter (DMT-CCNC): CCN activation of ammonium sulfate and sodium chloride aerosol particles in theory and experiment. *Atmos. Chem. Phys.* **8**, 1153–1179.
- Seinfeld, J.H. and S.N. Pandis (2006). *Atmospheric Chemistry and Physics. from air pollution to climate change* (2<sup>nd</sup> edition). (John Wiley & Sons, New York, USA).
- Stevens, B. and G. Feingold (2009). Untangling aerosol effects on clouds and precipitation in a buffered system. *Nature* **461**, 607–613.

# LONG-TERM SOURCE ANALYSIS OF VOCS IN BOREAL FOREST DURING YEARS 2006-2011

J. PATOKOSKI<sup>1</sup>, T.M. RUUSKANEN<sup>1</sup>, M.K. KAJOS<sup>1</sup>, R. TAIPALE<sup>1</sup>, P. RANTALA<sup>1</sup>, J. AALTO<sup>1</sup>, H. HAKOLA<sup>2</sup> and J. RINNE<sup>1</sup>

<sup>1</sup>Division of Atmospheric Sciences, Department of Physics, University of Helsinki, P.O. Box 64, 00014 University of Helsinki, Finland.

<sup>2</sup>Finnish Meteorological Institute, P.O. Box 503, FI-00101 Helsinki, Finland

Keywords: VOLATILE ORGANIC COMPOUNDS, TRAJECTORY ANALYSIS, LONG-TERM MEASUREMENTS

## INTRODUCTION

Volatile organic compounds (VOCs) have several sources, both biogenic and anthropogenic. Emissions of biogenic VOCs in a global scale are estimated to be an order of magnitude higher than anthropogenic ones (Guenther et al., 1995). However there can be seen stationary or local anthropogenic hotspots due to, for example heavy industry or wild forest fires. The aim of this study was to clarify potential source areas of VOCs, which were investigated with trajectory analysis and Unmix (Norris et al., 2007) multivariate receptor model. The volume mixing ratios (VMRs) of VOCs were measured with a proton-transfer-reaction mass spectrometer (PTR-MS, Ionicon Analytik) at SMEAR II (Station for Measuring Ecosystem - Atmosphere Relations, Hari and Kulmala, 2005), in Hyytiälä, Finland.

## METHODS

SMEAR II is a rural site located in Hyytiälä in Southern Finland ((61°51'N, 24°17'E, 180 m a.s.l.) 220 km North-West from Helsinki. Tampere is the largest city near SMEAR II and its population is about 200 000. There are continuous long-term measurements of trace gases, aerosol particles and micrometeorology (Hari and Kulmala, 2005). Volatile organic compounds (VOCs) were measured with PTR-MS (de Gouw and Warneke, 2007) from mid June 2006 to end of year 2011. The measurement set up, calibration procedure and volume mixing ratio calculations are presented in detail in Taipale et al. (2008). In addition to VOC measurements there are also other trace gas measurements such as CO, NO<sub>x</sub> and SO<sub>2</sub>. In this study a set of selected VOCs (methanol (M33), acetonitrile (M42), acetaldehyde (M45), acetone (M59), isoprene (M69), benzene (M79), toluene (M93) and monoterpenes (M137) are discussed. These VOCs, excluding monoterpenes and isoprene, had long life time and they were investigated with trajectory analysis. Monoterpenes and isoprene were included to multivariate analysis. For Unmix analysis data was divided to three sectors according to source areas found from trajectory analysis. Sectors were: North (0°-5° and 300°-360°), Urbanized continental (5°-210°) and Urban mixed with harbours and sea (210°-300°).

## RESULTS AND DISCUSSION

VOCs source areas seem to vary between years and seasons. During the measurement periods two different forest fire episodes happened in Russia. There were several fire hotspots in Russia. Forest fires which showed up in these measurements were in 2006 near the border of Finland in Vyborg area and 2010 in Moscow area. They can be seen very well in trajectory analysis of benzene, toluene and methanol and also CO and NO<sub>x</sub>. Anthropogenic influenced source areas can be seen in Eastern and Central Europe, harbours and Kola Peninsula. Interesting biogenic VOC source may be algae from Baltic Sea. However VMR levels of VOCs originating from algae are low compared to anthropogenic sources.

Receptor model gave three sources for every sector in which North sector was the most biogenic influenced compared to those two other anthropogenic influenced sectors.

#### ACKNOWLEDGEMENTS

The financial support by the Academy of Finland Centre of Excellence program (project no 1118615) is gratefully acknowledged.

#### REFERENCES

- de Gouw, J. and Warneke, C., (2007). Measurements of volatile organic compounds in the earth's atmosphere using proton-transfer-reaction mass spectrometry. *Mass Spectrom. Rev.* **26**:223-257.
- Guenther, A., Hewitt, C. N., Erickson, D., Fall, R., Geron, C., Graedel, T., Harley, P., Klinger, L., Lerdau, M., McKay, W. A., Pierce, T., Scholes, B., Steinbrecher, R., Tallamraju, R., Taylor, J., Zimmerman, P., (1995). A global model of natural volatile organic compound emissions. *J Geophys Res*, **100**, 8873-8892.
- Hari, P., and Kulmala, M. (2005). Station for Measuring Ecosystem–Atmosphere Relations(SMEAR II), *Boreal Environ. Res.*, **10**, 315–322.
- Norris G. Vedenham R. & Duvall R. (2007). *EPA Unmix 6.0 fundamentals & user guide*. U.S. Environmental Protection Agency, Office of Research and Development, Washington, DC.
- Taipale, R., Ruuskanen, T. M., Rinne, J., Kajos, M. K., Hakola, H., Pohja, T., and Kulmala, M.: (2008). Technical Note: Quantitative long-term measurements of VOC concentrations by PTR-MS-measurement, calibration and volume mixing ratio calculation methods, *ACP*, **8**, 6681-6698.

# MEASUREMENTS OF METHANE EMISSIONS ON MULTIPLE SCALES IN AN AGRICULTURAL LANDSCAPE

O. PELTOLA<sup>1</sup>, A. HENSEN<sup>2</sup>, C. HELFTER<sup>3</sup>, L. BELELLI MARCHESINI<sup>4</sup>, S. HAAPANALA<sup>1</sup>,  
F. BOSVELD<sup>5</sup>, W. C. M. VAN DEN BULK<sup>2</sup>, T. RÖCKMANN<sup>6</sup>, T. LAURILA<sup>7</sup>, A.  
VERMEULEN<sup>2</sup>, E. NEMITZ<sup>3</sup> and I. MAMMARELLA<sup>1</sup>

<sup>1</sup> University of Helsinki, Helsinki, Finland

<sup>2</sup> ECN, Petten, the Netherlands

<sup>3</sup> CEH, Edinburgh, UK

<sup>4</sup> VU, Amsterdam, the Netherlands

<sup>5</sup> KNMI, De Bilt, the Netherlands

<sup>6</sup> IMAU, Utrecht, the Netherlands

<sup>7</sup> FMI, Helsinki, Finland

Keywords: eddy covariance, methane, spatial variability.

## INTRODUCTION

Eddy covariance (EC) method is nowadays widely used in measuring surface-atmosphere exchange in various different ecosystems and conditions. The method is a non-intrusive measurement method which provides estimates for the fluxes on a continuous basis. It integrates the surface fluxes over a larger area called footprint, which is usually on the order of 1 ha. Thus the measured fluxes can be thought to represent ecosystem scale fluxes. Traditionally the method has been used to study ecosystem scale CO<sub>2</sub> exchange, however during recent years also CH<sub>4</sub> EC flux studies have become more common, due to development of new CH<sub>4</sub> instruments which are usable for EC measurements (Peltola *et al.*, 2013).

In this study variability in CH<sub>4</sub>-fluxes in an agricultural landscape is assessed. The common notion that EC fluxes measured at one location represent the flux at a homogeneous surrounding landscape is tested. Moreover CH<sub>4</sub> fluxes measured at several heights are compared in order to study the flux variability with height and how the differences in the fluxes correspond to different footprints. EC fluxes are often upscaled to landscape and continental scales and thus by investigating the flux variability in space, the possible errors in this upscaling procedure can be assessed.

## METHODS

The measurement campaign was held between 1st and 30th of July 2012 in Cabauw (51°58'12.00"N, 4°55'34.48"E, -0.7 m a.s.l), the Netherlands. Agricultural activities are carried out intensively in the surrounding area. This includes grazing ruminants such as sheep and cows. The ruminants are a strong source of methane, however CH<sub>4</sub> is emitted also from the peaty soil in the area and the ditches between the fields. Anoxic conditions in the soil and the ditches provide favorable conditions for methanogenic bacteria to produce CH<sub>4</sub>. From a micrometeorological perspective the site is ideal: flat with no pronounced slope and the vegetation is generally low (few tens of centimeters).

Methane fluxes were measured at three locations which are from now on called as Farm, Depot and Cabauw (see Fig. 1 for the locations). At Cabauw,  $\text{CH}_4$  flux measurements were made at three heights: 6 m, 20 m and 60 m. At the other two sites the fluxes were measured only at 6 m height. At the Farm site a laser based gas analyzer FMA (Los Gatos Research, USA) was used to measure  $\text{CH}_4$  concentrations, LI-7000 (LI-COR Inc., USA) was used to measure  $\text{CO}_2$  and  $\text{H}_2\text{O}$  and sonic anemometer/thermometer (USA-1, METEK, Germany) was used to acquire the three wind components and air temperature. At the Depot site DLT-100 (Los Gatos Research, USA) was measuring  $\text{CH}_4$ , in addition to sonic anemometer WindMaster Pro (Gill Instruments Ltd, UK) which provided the high frequency wind and temperature data. At Cabauw 6 m height gas analyzer G2311-f (Picarro Inc., USA) and a sonic anemometer USA-1 (METEK, Germany) were used, at 20 m height analyzers FMA (Los Gatos Research, USA) and G1301-f (Picarro Inc., USA) were used, in addition to sonic anemometer WindMaster Pro (Gill Instruments Ltd, UK) and at 60 m height gas analyzer FGGA (Los Gatos Research, USA) and sonic anemometer R3 (Gill Instruments Ltd, UK) were used to acquire the high frequency data.  $\text{CH}_4$  fluxes were measured at all three levels.

All the eddy covariance measurements were recorded at 10 Hz frequency in order to capture turbulent flux at all relevant eddy sizes. 30-min averaging time was used and the commonly accepted data post-processing methods were applied (Aubinet *et al.*, 2000). Data post-processing was done with eddy covariance data post-processing software EddyUH. The software is freely distributed at [http://www.atm.helsinki.fi/Eddy\\_Covariance/EddyUHsoftware.php](http://www.atm.helsinki.fi/Eddy_Covariance/EddyUHsoftware.php). Footprints were calculated with simple analytical model based on Kormann and Meixner (2001).

## RESULTS

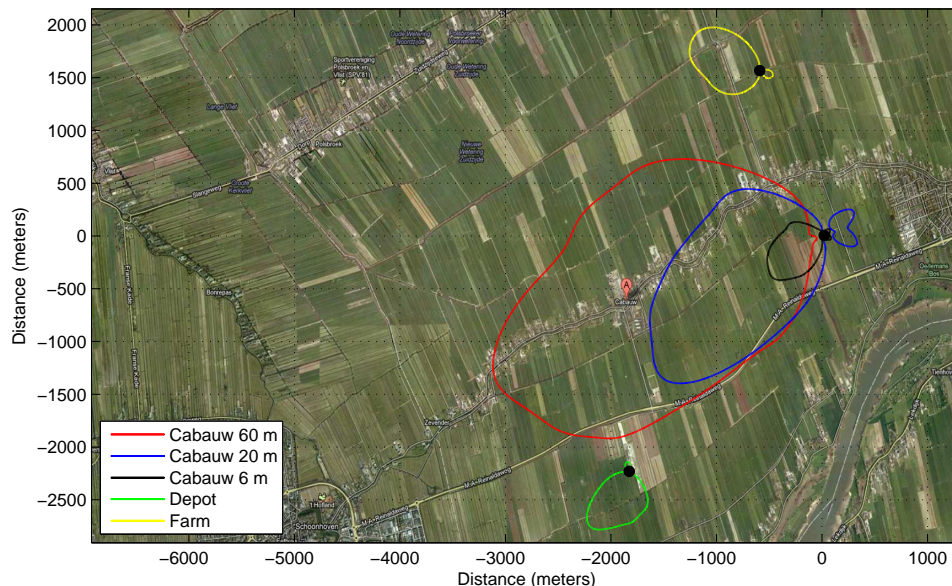


Figure 1: Cumulative footprints, i.e. source areas, for different flux measurements locations. An 80th percentile curve is shown, meaning that 80th percent of the measured signal originated from within the shown area. Black dots show the tower locations. Map: Google, Aerodata International Surveys.

Cumulative footprints during the measurement campaign are shown in Fig. 1. The curves in Fig. 1 show 80th percentiles, so 80 % percent of the measured signal at each site originated from within the shown areas. Most of the CH<sub>4</sub> fluxes measured at the short towers originated closer than 500 meters away from the tower, for 20 m height measurements the source area was approximately 2000 m long and for 60 m height measurements the area was on average 3400 m long. Thus the fluxes measured at different heights correspond to surface fluxes at different spatial scales.

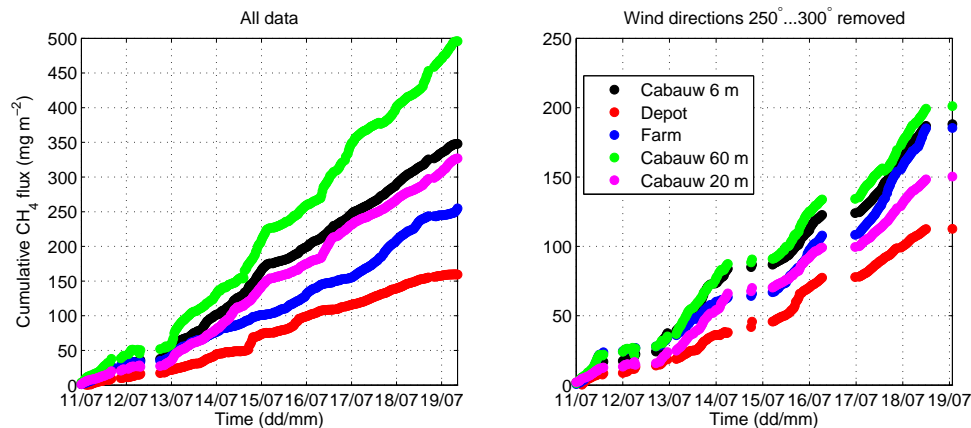


Figure 2: Cumulative CH<sub>4</sub> fluxes during a part of the campaign. Plot on the left show all the data and plot on the right show otherwise the same data, except wind directions 250°...300° are removed.

CH<sub>4</sub> fluxes were significantly different from each other measured at the three 6 m high towers (Fig. 2). Fluxes at the Depot site were on average half of the CH<sub>4</sub> fluxes measured at the 6 m high tower at the Cabauw site and the Farm site was between these two. Although part of these differences can be possibly explained with differences between the used instruments, it cannot explain the differences completely. Thus if Cabauw 6 m CH<sub>4</sub> fluxes are thought to represent the methane fluxes in this landscape, two times larger emission estimates are obtained in contrast of using Depot site measurements. Locations of cows and sheep in the area was not monitored and this complicates the comparison of different sites and flux time series, since the ruminants are strong sources methane and they will affect the measured CH<sub>4</sub> fluxes significantly if they are within the flux footprint.

Due to the spatial variation of CH<sub>4</sub> flux discussed above, one might be tempted to measure fluxes at higher levels since then the source area is larger (Fig. 1) and thus the spatial variation is averaged out leaving only the mean flux within the large source area. Therefore these fluxes could be upscaled to landscape scale more rigorously. The cumulative CH<sub>4</sub> flux measured at Cabauw 20 m height is slightly smaller than what was measured at Cabauw 6 m height, however cumulative methane flux measured at 60 m height is approximately 1.4 times the cumulative flux at 6 m height (Fig. 2 left plot). This means that the CH<sub>4</sub> fluxes at 60 m height were on average 1.4 times the fluxes at 6 m height. The source areas for 20 m and 60 m flux measurements contain also part of the residential area where farms with several cowhouses are located (Fig. 1). It was observed that fluxes from wind directions 250°...300°, where most of the farms are located, were approximately twice as large as CH<sub>4</sub> fluxes from other wind directions. If measurements from these wind directions were omitted, the cumulative CH<sub>4</sub> flux at 60 m height agrees relatively well with the cumulative flux from 6 m height at the Cabauw site, whereas cumulative emission measured at 20 m height is slightly smaller (Fig. 2, right plot).

## CONCLUSIONS

Methane fluxes were measured with eddy covariance technique at three locations approximately 2...3 kilometers away from each other and at three heights (6 m, 20 m and 60 m) at one location. The fluxes were different from each other at the three locations and the measurements at higher measurement levels did not average out this spatial variability of the fluxes, possibly because all the measurement locations did not fall within the source area of the measurements done at the higher level (20 m and 60 m). Fluxes measured at 60 m height were greatly affected by hotspot emissions originating from cowhouses. These hotspots had a lesser impact on 20 m height measurements and almost negligible effect on 6 m measurements. This study highlights the fact that the high methane flux spatial variability cannot be captured with only one short flux tower and moreover short tower and tall tower flux measurements complement each other providing a better overall picture of the CH<sub>4</sub> emission dynamics at the studied landscape.

## ACKNOWLEDGEMENTS

The research leading to these results has received funding from the European Community's Seventh Framework Programme (FP7/2007-2013) in the InGOS project under grant agreement n° 284274. Also support from Magnus Ehrnrooth Foundation and by the Academy of Finland Centre of Excellence program (project no 1118615) are greatly acknowledged.

## REFERENCES

- Aubinet, M., A. Grelle, A. Ibrom, Ü Rannik, J. Moncrieff, T. Foken, A.S. Kowalski, P.H. Martin, P. Berbigier, C. Bernhofer, R. Clement, J. Elbers, A. Granier, T. Grunwald, K. Morgenstern, K. Pilegaard, C. Rebmann, W. Snijders, R. Valentini and T. Vesala (2000) Estimates of the annual net carbon and water exchange of forests: The EUROFLUX methodology *Advances in Ecological Research*, **30**, 113.
- Peltola, O., I. Mammarella, S. Haapanala, G. Burba and T. Vesala (2013) Field intercomparison of four methane gas analyzers suitable for eddy covariance flux measurements *Biogeosciences*, **10**, 3749.
- Kormann, R. and F.X. Meixner (2001) An analytical footprint model for nonneutral stratification *Boundary-Layer Meteorology*, **99**, 207.

# OXIDATION CAPACITY AND RATE OF MONOTERPENES OVER A BOREAL FOREST: TEMPORAL VARIATION AND CONNECTION TO NEW PARTICLE FORMATION EVENTS

O. PERÄKYLÄ<sup>1</sup>, M. VOGT<sup>1</sup>, T. PETÄJÄ<sup>1</sup>, J. AALTO<sup>2</sup>, M.K. KAJOS<sup>1</sup>, P.A. RANTALA<sup>1</sup>, H. AALTONEN<sup>2</sup>, T. NIEMINEN<sup>1</sup>, R. TAIPALE<sup>1</sup>, P. KOLARI<sup>2</sup>, P. KERONEN<sup>1</sup>, H.K. LAPPALAINEN<sup>1</sup>, T.M. RUUSKANEN<sup>1</sup>, J. RINNE<sup>1</sup>, V.-M. KERMINEN<sup>1</sup>, T. VESALA<sup>1</sup>, I. MAMMARELLA<sup>1</sup>, M. KULMALA<sup>1</sup>, J. BÄCK<sup>2</sup>

<sup>1</sup> University of Helsinki, Department of Physics, 00014 University of Helsinki, Finland

<sup>2</sup> University of Helsinki, Department of Forest Sciences, 00014 University of Helsinki, Finland

Keywords: New particle formation, NO<sub>3</sub>, OH, O<sub>3</sub>.

## INTRODUCTION

Volatile organic compounds, especially monoterpenes, are emitted in large quantities by boreal forests (Rinne et al., 2009). These compounds are then removed from the atmosphere by oxidation reactions with ozone, or with radicals such as OH and NO<sub>3</sub>. These reactions lead to the formation of less volatile species, and to potential condensation. In this way volatile organic compounds can affect the formation and growth of aerosol particles. In this study, the variation of oxidation capacity and rate of monoterpenes over a boreal forest in Finland and its connection to new particle formation was studied.

## METHODS

The rate of loss of monoterpenes (MT) through oxidation reactions, or the oxidation rate, in the atmosphere can be defined as the sum of the reaction rates of monoterpenes with different oxidants. Each of these can be calculated if the concentrations of the monoterpenes and the oxidant are known, along with the corresponding reaction rate coefficient. This is shown in equation (1).

$$\text{Oxidation rate of monoterpenes} = [MT] \times (k_{OH/MT} \times [OH] + k_{O_3/MT} \times [O_3] + k_{NO_3/MT} \times [NO_3]) \quad (1)$$

The oxidation capacity of the atmosphere with respect to monoterpenes is then the oxidation rate divided by the monoterpene concentration, as is shown in equation (2).

$$\text{Oxidation capacity of monoterpenes} = k_{OH/MT} \times [OH] + k_{O_3/MT} \times [O_3] + k_{NO_3/MT} \times [NO_3] \quad (2)$$

In a steady state between the production and destruction of monoterpenes, the oxidation capacity also becomes the inverse of the turnover time and mean lifetime of monoterpenes.

The oxidation capacity and rate of monoterpenes was calculated for a time period from 2006 to 2011 using data measured in the Hyytiälä field station (Hari and Kulmala, 2005). The ozone concentration was measured directly, but the OH and NO<sub>3</sub> concentrations were calculated from

proxies. For the OH concentration, a UVB-radiation based proxy adapted from Petäjä et al. (2009) was used.

For the  $\text{NO}_3$ , the production rate was calculated from measured  $\text{NO}_2$  and  $\text{O}_3$  concentrations. The turnover time,  $\tau$ , of  $\text{NO}_3$  was calculated from various sinks during the night as suggested by Allan et al. (2000). The sinks used included the uptake into aerosols and hydrolysis of gas-phase  $\text{N}_2\text{O}_5$ , which is produced in an equilibrium reaction between  $\text{NO}_3$  and  $\text{NO}_2$ , and reaction of  $\text{NO}_3$  with monoterpenes and isoprene. In sunlight, the nitrate radical is rapidly photolysed, and the turnover time was assumed to be 5 seconds during the day (Geyer et al., 2001; Vrekoussis et al., 2004). Using a steady-state assumption, the concentration of  $\text{NO}_3$  was then calculated by multiplying the production rate of  $\text{NO}_3$  by  $\tau$ .

The relation of the concentration, oxidation capacity and -rate of monoterpenes to particle growth during NPF days was then investigated.

## CONCLUSIONS

The oxidation capacity of monoterpenes is for most of the year higher during the night, explained by high  $\text{NO}_3$  concentrations.  $\text{NO}_3$  also accounts for the bulk of the night-time oxidation capacity for most of the year, while  $\text{O}_3$  dominates daytime oxidation. However, from around April to September, the night-time oxidation is dominated by ozone and daytime oxidation by OH. Curiously, this also coincides with the period of highest new particle formation activity.

Investigating the relation of monoterpenes to nanoparticle growth, the highest correlation ( $r=0.72$  on a log-log scale) was found between the median concentration of monoterpenes during the night preceding a NPF event with the growth rate (GR) of 7-20 nm particles during the event. Of the oxidation rates by different species, the preceding night median oxidation rate of monoterpenes by ozone shows the highest correlation with the GR, with a correlation coefficient only marginally lower than that of the monoterpene concentration ( $r=0.72$  on a log-log scale).

The oxidation capacity itself, however, does not show any clear correlation to the growth rate. This is likely due to the fact that oxidation capacity is on average quite high, corresponding to the turnover times of monoterpenes of the order of hours. In any timescale much longer than this, the oxidation rate of monoterpenes is not limited by the availability of oxidants, but rather the emission rate of monoterpenes.

## ACKNOWLEDGEMENTS

This research was supported by the Academy of Finland (Center of Excellence program, project number 127534), and by the Nordic Top-level Research Initiative (TRI) Cryosphere-Atmosphere Interactions in a Changing Arctic Climate (CRAICC).

## References

- Allan, B., McFiggans, G., Plane, J., Coe, H., and McFadyen, G. (2000). The nitrate radical in the remote marine boundary layer. *JOURNAL OF GEOPHYSICAL RESEARCH-ATMOSPHERES*, 105(D19):24191–24204.
- Geyer, A., Ackermann, R., Dubois, R., Lohrmann, B., Muller, T., and Platt, U. (2001). Long-term observation of nitrate radicals in the continental boundary layer near Berlin. *Atmospheric Environment*, 35(21):3619–3631.
- Hari, P. and Kulmala, M. (2005). Station for measuring ecosystem-atmosphere relations (SMEAR II). *Boreal Environment Research*, 10(5):315–322.

- Petäjä, T., Mauldin, III, R. L., Kosciuch, E., McGrath, J., Nieminen, T., Paasonen, P., Boy, M., Adamov, A., Kotiaho, T., and Kulmala, M. (2009). Sulfuric acid and OH concentrations in a boreal forest site. *Atmospheric Chemistry and Physics*, 9(19):7435–7448.
- Rinne, J., Back, J., and Hakola, H. (2009). Biogenic volatile organic compound emissions from the Eurasian taiga: current knowledge and future directions. *Boreal Environment Research*, 14(4):807–826.
- Vrekoussis, M., Kanakidou, M., Mihalopoulos, N., Crutzen, P., Lelieveld, J., Perner, D., Berresheim, H., and Baboukas, E. (2004). Role of the NO<sub>3</sub> radicals in oxidation processes in the eastern Mediterranean troposphere during the MINOS campaign. *Atmospheric Chemistry and Physics*, 4:169–182.

# INTERPRETATION OF TEMPORAL DYNAMICS IN LEAF-LEVEL CHLOROPHYLL FLUORESCENCE: A MECHANISTIC MODEL

A. PORCAR-CASTELL<sup>1</sup>, B. OLASCOAGA<sup>1</sup>, J. ATHERTON<sup>1</sup>, F. BERNINGER<sup>1</sup> and P. KOLARI<sup>1,2</sup>

<sup>1</sup>Department of Forest Sciences, University of Helsinki, PO Box. 27, 00014 Finland

<sup>2</sup>Department of Physics, University of Helsinki, PO Box 64, 00014 Finland

Keywords: PHOTOSYNTHESIS, REMOTE SENSING, EVERGREENS, LIGHT USE EFFICIENCY

## INTRODUCTION

Photosynthesis has an important role in global biogeochemistry and atmospheric chemistry. Photosynthesis is the engine that regulates the global carbon cycle (assimilation of atmospheric carbon dioxide into ecosystems), plays a role in the water cycle through transpiration (water flux from soil to atmosphere via plants), and controls to some extent the emission of a number of volatile organic compounds (VOCs) that in turn have an impact on atmospheric chemistry (see Abstract by J. Aalto et al.). No doubt, resolving the spatial and temporal dynamics of photosynthesis at the global scale would be very useful, a challenge that falls in the domain of remote sensing.

Photosynthesis starts with the absorption of electromagnetic radiation by chlorophyll pigments in leaves. The energy of the absorbed quanta is rapidly partitioned into three main competing processes: photosynthesis, thermal energy dissipation, and re-emission of fluorescence quanta. Clearly, the efficiency of the fluorescence emission will depend on the performance of photosynthesis, the more photosynthesis the less fluorescence and *vice versa*. Nevertheless, plants do also regulate the efficiency of thermal energy dissipation or NPQ (Non-Photochemical Quenching of fluorescence). NPQ is a regulatory mechanism that operates under conditions in which photosynthesis cannot utilize all absorbed energy. When NPQ kicks in, both photosynthesis and fluorescence quantum efficiencies decrease concomitantly (Müller et al. 2001). In addition, seasonal processes such as the photoinhibition of reaction centres also affect the fluorescence intensity. The result is a complex relationship between quantum yield of fluorescence and that of photosynthesis (see Abstract by B. Olascoaga & Porcar-Castell).

At the leaf-level, a pulse of saturating light can be supplied to the leaf in order to momentarily shut down photochemistry. This technique is used to estimate the quantum yield of photochemistry by comparing the relative increase in fluorescence levels independently of the presence of NPQ (Bolhar-Nordenkamp et al. 1989). Yet, this technique cannot be implemented to large distances. Instead, the solar induced fluorescence (SIF) signal emanating from vegetation can be estimated using different techniques (Meroni et al. 2009). In fact, global maps of terrestrial SIF have been recently presented (Frankenberg et al. 2011, Joiner et al. 2011) and quality and quantity of remotely sensed fluorescence data is expected to increase in the near future. In addition to satellite measurements, SIF can be measured from towers, aircrafts or Unmanned Aerial Vehicles (UAVs), areas that are under intensive research.

Despite these technical advances, there are to date no modelling tools capable of interpreting the temporal dynamics in the resulting SIF signal in terms of photosynthesis. In this abstract we present our recent work on the modelling of the temporal dynamics in leaf-level fluorescence. Our goal is to generate a process-based dynamic model, based on the model by Porcar-Castell et al. (2006) that incorporates the effect of seasonal acclimation mechanisms.

## METHODOLOGY

The model by Porcar-Castell et al. (2006) was used as the basis for developing the structure of the seasonal model (Fig. 1), namely, the effect of temperature and the photoinhibition of reaction centres are added. Model development, parameterization and validation are conducted in two phases. On a first phase a laboratory experiment was conducted to parameterize the dynamics of NPQ and photoinhibition in response to variations in light and temperature. The dynamics of the fluorescence signal were studied from needles of Scots pine seedlings inside a weather chamber. Temperatures ranging from  $-5^{\circ}\text{C}$  to  $40^{\circ}\text{C}$  and light intensities from PPFD=0 to PPFD=1300 were used. The data was used to parameterize the light and temperature dependencies of the processes and to obtain parameterization functions. On a second phase, annual time series of fluorescence data obtained in SMEAR-II using a fluorescence Monitoring PAM system (Porcar-Castell 2011) will be used to test and validate the structure of the model in a real-case scenario.

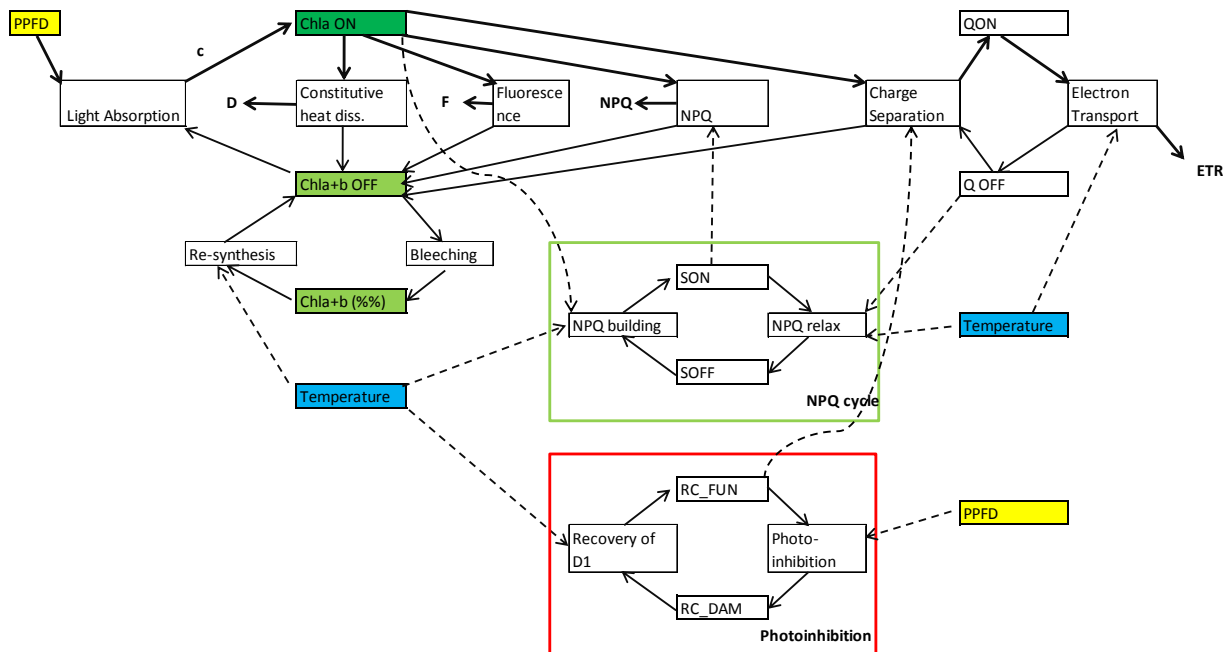


Fig. 1. Model Structure. Upon light absorption, chlorophyll molecules pass from a relaxed state (Chla+b OFF) into an excited state (Chla ON). Excitation energy can be lost in four different pathways: thermal energy dissipation (both constitutive, D, and regulated NPQ), charge separation (photochemistry), or emission of fluorescence (F). Each process is associated with a first-order rate constant. The dynamics of NPQ and the fraction of functional reaction centres able to perform charge separation are estimated separately using light and temperature dependent parameters.

## FINAL REMARKS

The present model facilitates the interpretation of seasonal changes in leaf-level fluorescence data and opens up a number of possibilities to study seasonal processes. In the near future, the model will be coupled to a leaf and canopy radiative transfer model to facilitate its implementation to the interpretation of tower, UAV, aircraft, and eventually satellite data.

## ACKNOWLEDGEMENTS

This work was supported by the Academy of Finland (Projects 1138884 and 1118615), and the University of Helsinki (Project 490116).

## REFERENCES

- Bolh  r-Nordenkamp, H.R., S.P. Long, N.R. Baker, G.   quist, U. Schreiber and E.G. Lechner (1989) Chlorophyll fluorescence as a probe of the photosynthetic competence of leaves in the field: a review of current instrumentation. *Functional Ecology* **3**, 497-514.
- Frankenberg, C., J.B. Fisher, J. Worden, G. Badgley, S.S. Saatchi, J.-E. Lee, G.C. Toon, A. Butz, M. Jung, A. Kuze and T. Yokota (2011) New global observations of the terrestrial carbon cycle from GOSAT: Patterns of plant fluorescence with gross primary productivity. *Geophysical Research Letters* **38**, L17706.
- Joiner, J., Y. Yoshida, A.P. Vasilkov, Y. Yoshida, L.A. Corp and E.M. Middleton (2011) First observations of global and seasonal terrestrial chlorophyll fluorescence from space. *Biogeosciences* **8**, 637-651.
- Meroni, M., M. Rossini, L. Guanter, L. Alonso, U. Rascher, R. Colombo and J. Moreno (2009) Remote sensing of solar-induced chlorophyll fluorescence: Review of methods and applications. *Remote Sensing of Environment* **113**, 2037-2051.
- M  ller, P., X.-P. Li and K.K. Niyogi (2001) Non-photochemical quenching. A response to excess light. *Plant Physiology* **125**, 1558-1566.
- Porcar-Castell, A., J. B  ck, E. Juurola and P. Hari (2006) Dynamics of the energy flow through photosystem II under changing light conditions: a model approach. *Functional Plant Biology* **33**, 229-239.
- Porcar-Castell, A. (2011) A high-resolution portrait of the annual dynamics of photochemical and non-photochemical quenching in needles of *Pinus sylvestris*. *Physiologia Plantarum* **143**, 139-153.

# EFFECT OF LOCAL POLLUTANT SOURCES ON AEROSOL-CLOUD INTERACTIONS AT PUIJO TOWER MEASUREMENT STATION

H. PORTIN<sup>1,2</sup>, A. LESKINEN<sup>1</sup>, L. HAO<sup>2</sup>, A. KORTELAJINEN<sup>2</sup>, P. MIETTINEN<sup>2</sup>, A. JAATINEN<sup>2</sup>, S. ROMAKKANIEMI<sup>2</sup>, A. LAAKSONEN<sup>2,3</sup>, K.E.J. LEHTINEN<sup>1,2</sup> and M. KOMPPULA<sup>1</sup>

<sup>1</sup>Finnish Meteorological Institute, Kuopio Unit, P.O.Box 1627, FI-70211, Kuopio, Finland

<sup>2</sup>University of Eastern Finland, Department of Applied Physics, P.O.Box 1627, FI-70211, Kuopio, Finland

<sup>3</sup>Finnish Meteorological Institute, Research and Development, P.O.Box 503, FI-00101 Helsinki, Finland

Keywords: atmospheric aerosols, cloud droplet activation, aerosol-cloud interactions, chemical composition.

## INTRODUCTION

The connection between various properties of condensation nuclei and cloud droplet activation has been studied in several field and lab experiments (e.g. Dusek *et al.* 2006, Hudson, 2007). It is known that weather conditions, particle size and number concentration are the main factors influencing cloud droplet activation. Chemical composition is known to have an effect as well but although some research has already been done (Drewnick *et al.* 2007, Hao *et al.* 2013), its role remains somewhat unclear.

Puijo measurement station has provided continuous data on aerosol-cloud interactions since June 2006 (Leskinen *et al.* 2009). The station is located on top of the Puijo observation tower (306 m a.s.l, 224 m above the surrounding lake level) near the town of Kuopio, Finland. The station has been observed to be covered by cloud about 15 % of the time, offering perfect conditions for aerosol-cloud interaction studies. The station is occasionally under the influence of various local pollutant sources, located within 10 km from the tower. Puijo frequently encounters also clean air masses.

## METHODS

With a twin-inlet setup (total and interstitial inlets) activated and non-activated particles can be measured separately. Continuous twin-inlet measurements include aerosol size distribution (twin-DMPS, 7-800 nm), light scattering and absorption. Other continuous measurements include cloud droplet number and size distribution, weather parameters and some gas species (O<sub>3</sub>, NO<sub>x</sub>, SO<sub>2</sub>, CO<sub>2</sub>, CH<sub>4</sub>).

We also arrange intensive measurement campaigns every autumn (Puijo Cloud Experiment, PuCE) when the occurrence of clouds is the highest. During these campaigns, extra measurement devices have included aerosol mass spectrometer (AMS), cloud condensation nuclei counter and Hygroscopic Tandem Differential Mobility Analyzer. The AMS has been connected to the twin-inlet system, providing data about the chemical composition of activated and non-activated particles (Hao *et al.* 2013).

In our current work, we have been analyzing results from PuCE 2010 and 2011 campaigns. During these campaigns, a total of 39 cloud events took place, with a total of 156 hours of in-cloud data. The aim of the research has been the identification of the possible effect of local pollutant sources on aerosol-cloud interactions. The tower is surrounded by residential areas and traffic routes in north, east and south, whereas in west and northwest there aren't any significant sources. Also, two important point sources exist within a few kilometres from the tower, a paper mill and a heating plant.

## RESULTS

An example of a cloud event, during which it was possible to pinpoint the effect of local sources, took place on 22.-23.10., 2011. There were several periods with different particle population properties, which

period	$N_{\text{tot}}$ ( $\text{cm}^{-3}$ )	$N_{\text{acc}}$ ( $\text{cm}^{-3}$ )	$\text{GF}_{100}$	$N_{\text{drop}}$ ( $\text{cm}^{-3}$ )	$D_{\text{drop}}$ ( $\mu\text{m}$ )
Fresh&rainy	2200	149	1.25	219	9.2
Clean	451	62	1.42	138	12.2
Paper mill	357	139	1.37	240	10.9
Heating plant	1130	169	1.36	n.a.	n.a.

Table 1. Total particle concentration ( $N_{\text{tot}}$ ), accumulation mode particle concentration (diameter  $> 100$  nm,  $N_{\text{acc}}$ ), hygroscopic growth factor of 100 nm particles ( $\text{GF}_{100}$ ) and cloud droplet concentration + diameter ( $N_{\text{drop}}$ ,  $D_{\text{drop}}$ ) for the periods during the cloud event on 22.-23.10.2011.

also affected the cloud properties to some extent. Here, four of these periods are chosen for a closer inspection (Table 1).

The cloud event started with a period characterized by southerly wind, some rain and high particle number concentration (fresh&rainy, 22.10. 9:00-12:00). The aerosol is most probably externally mixed, with fresh, organic, less hygroscopic particles from local traffic and domestic wood combustion. The maximum activated fraction of the particles for this period is low (Figure 1b). Some of the less hygroscopic particles may not form droplets even though they are large enough. Other explanation is that rain drops remove cloud droplets, leading to underestimation of the amount of activated particles by our twin-inlet system.

During the clean period (22.10. 22:00-23.10. 5:45), wind direction was from north and northwest with low total particle and accumulation mode concentrations (Figure 1a). The aerosol was aged and internally mixed with relatively high hygroscopicity. Between 5:45-6:15 on 23.10. wind direction was from northeast where the paper mill is located. Total particle concentration was still low but a pronounced accumulation mode was present. Particle chemical composition during this period was dominated by  $\text{SO}_4$  and  $\text{NH}_4$ . When wind direction shifted to south (23.10. 9:45-13:00), a plume from the heating plant hit the tower. Elevated particle concentration was observed, with a distinguishable accumulation mode, consisting almost entirely of  $\text{SO}_4$ .

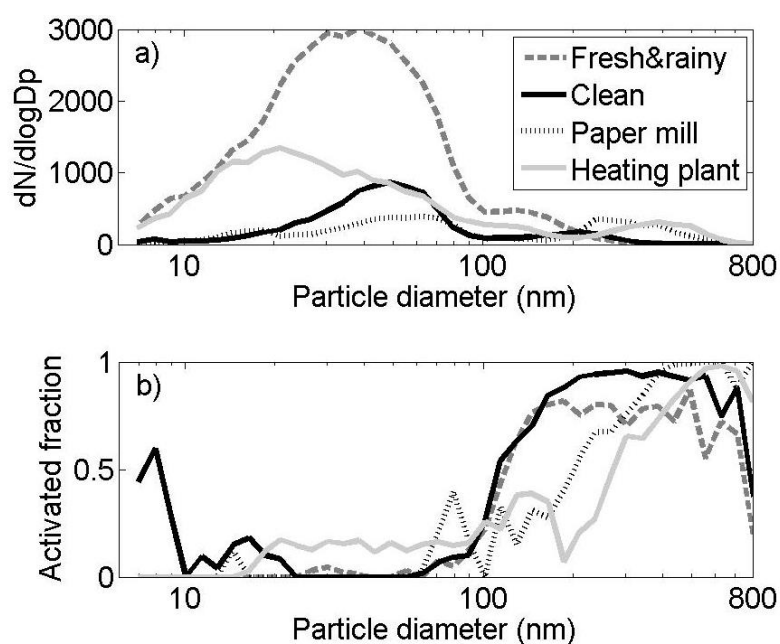


Figure 1. a) Aerosol number size distributions and b) activated fractions for the four subperiods of the cloud event observed on 22.-23.10.2011.

During the pollutant episodes, the size of activated particles was larger when compared to the clean period (fig. 1b). In clean conditions, as small as 100 nm particles activated, whereas during the polluted periods the average diameter for activation was larger. During the paper mill plume, droplet concentration was higher with a smaller average droplet diameter when compared to the clean period (Table 1). Unfortunately the cloud droplet probe was frozen during the heating plant plume.

As a conclusion, it is evident that local pollutant sources affect aerosol-cloud interactions. However, it is too early to say if this is only caused by the elevated number concentrations or if the different chemical composition also plays a role. Also, how often these periods take place requires more research and data from forthcoming campaigns.

## REFERENCES

- Drewnick, F., Schneider, J., Hings, S.S., Hock, N., Noone, K., Targino, A., Weimer, S., Borrmann, S., 2007. Measurement of ambient, interstitial, and residual aerosol particles on a mountaintop site in central Sweden using an aerosol mass spectrometer and a CVI. *J. Atmos. Chem.* **56**, 1-20.
- Dusek, U., Frank, G.P., Hildebrandt, L., Curtius, J., Schneider, J., Walter, S., Chand, D., Drewnick, F., Hings, S., Jung, D., Borrmann, S., Andreae, M.O., 2006. Size matters more than chemistry for cloud-nucleating ability of aerosol particles. *Science* **312**, 1375-1378.
- Hao, L., S. Romakkaniemi, A. Kortelainen, A. Jaatinen, H. Portin, P. Miettinen, M. Komppula, A. Leskinen, A. Virtanen, J. Smith, D. Sueper, D. Worsnop, K.E.J. Lehtinen and A. Laaksonen (2013). Aerosol Chemical Composition in Cloud Events by High Resolution Time-of-Flight Aerosol Mass Spectrometry, *Environ. Sci. Technol.* **47**, 2645-2653.
- Hudson, J.G., 2007. Variability of the relationship between particle size and cloud-nucleating ability. *GRL* **34**, L08801, doi:10.1029/2006GL028850.
- Leskinen, A., H. Portin, M. Komppula, P. Miettinen, A. Arola, H. Lihavainen, J. Hatakka, A. Laaksonen and K.E.J. Lehtinen (2009). Overview of the research activities and results at Puijo semi-urban measurement station, *Boreal Env. Res.* **14**, 576-590.

## SURFACTANTS IN MICROSCOPIC DROPLETS

N.L. PRISLE<sup>1</sup>, J. KOSKINEN<sup>2</sup>, B. MOLGAARD<sup>1</sup>, T. RAATIKAINEN<sup>2</sup>, T.B KRISTENSEN<sup>3</sup>, T. YLI-JUUTI<sup>1</sup>, and A.-P. HYVÄRINEN<sup>2</sup>

<sup>1</sup>Division of Atmospheric Science, Department of Physics, University of Helsinki,  
PO BOX 48, Helsinki, 00014, Finland.

<sup>2</sup>Finnish Meteorological Institute, Helsinki, Finland.

<sup>3</sup>University of Copenhagen, Copenhagen, Denmark.

Keywords: SURFACTANTS, ORGANIC AEROSOL, SURFACE TENSION, CCN.

### INTRODUCTION

Equilibrium Köhler theory predicts that aqueous droplet surface tension can significantly impact cloud condensation nuclei (CCN) activation, as reduced surface tension will dampen the curvature enhancement of water vapour pressure over a sub-micron droplet (Shulman *et al.*, 1996). Surface active molecules, or surfactants, preferentially concentrate in the surface of a solution upon dissolution and may thereby reduce aqueous surface tension from the pure water value. Surfactants like straight-chain fatty acids and humic-like substances (HULIS) have been found in organic aerosol samples from many different types of environment and can significantly reduce aqueous surface tension (Mochida *et al.*, 2002; Dinar *et al.*, 2006, Kiss *et al.*, 2005). Facchini *et al.* (1999) measured surface tension reductions up to about 30% from the value for pure water, for aqueous solutions of atmospheric aerosol samples at concentrations relevant for activating cloud droplets. They estimated that such a reduction in droplet surface tension would lead to a 20% increase in cloud droplet numbers from enhancement of aerosol CCN activity and that, on a global scale, this increase in droplet numbers would in turn lead to a cooling effect of the order of 1 W/m<sup>2</sup> from the aerosol indirect climate forcing.

Li *et al.* (1998) and Sorjamaa *et al.* (2004) then showed, for the model surfactant sodium dodecyl sulphate, how surface activity leads to significant bulk-surface partitioning in sub-micron droplets and this way may affect droplet activation thermodynamics through the solute effect (Raoult effect), in addition to the curvature effect (Kelvin effect) on water vapour pressure. In order to further quantify and constrain surfactant effects on atmospheric aerosol CCN activity, a number of studies, including the present work, have studied the impact of atmospheric organics on aqueous surface tension. There is, however, currently no available technique with which to measure surface tensions of sub-micron droplets directly and these surface tensions then have to be obtained from measurements on macroscopic samples containing atmospheric surfactants. In this work, we take a closer look at the considerations necessary for obtaining well-constrained estimates of surface tension in aqueous droplets from measurement performed on corresponding macroscopic samples. We wish to more firmly establish the effect of surface active organic aerosol on cloud activation in the atmosphere.

### METHODS

We have measured surface tensions of aqueous solutions comprising different organic surfactants, using either a pendant drop or Wilhelmy plate tensiometer. Surfactants studied were a series of straight-chain fatty acid sodium salts, with 8-12 carbon atoms in the hydrocarbon chain, and the reference substance Nordic Aquatic Fulvic Acid (NAFA). The latter is not found immediately in atmospheric samples, but is extracted from aquatic sources, and nevertheless believed to resemble atmospheric HULIS, in particular

with respect to surfactant properties. NAFA is an unresolved mixture of complex organic molecules that is commercially available and has been obtained according to standardized procedures. Examples of measured surface tensions are shown in Figure 1 for aqueous mixtures of NAFA and sodium chloride (NaCl) in different mixing ratios and at different concentrations.

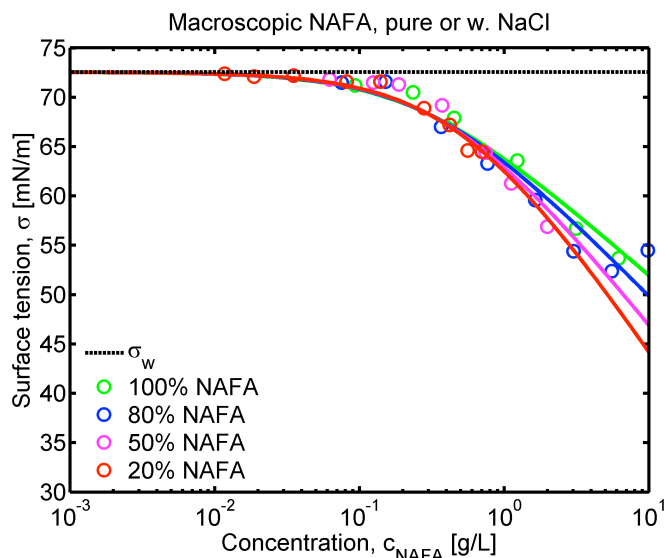


Figure 1. Surface tensions measured for macroscopic aqueous solutions of NAFA mixed with NaCl in different mass ratios. The surface tension of pure water ( $\sigma_w$ ) is indicated at about 72 mN/m.

From the measured surface tensions for macroscopic solutions, we have made ternary parametrizations of variations in aqueous surface tension with respect to independent variations in concentrations of the different organic and inorganic solutes. We then apply the parameterized surface tensions in Köhler theory, to evaluate equilibrium droplet growth and the critical point of droplet activation for particles comprising the same organic and inorganic compounds. Figure 2 shows the concentrations of solutes calculated in activating droplets formed on mixed NAFA (solid curves) and NaCl (dashed curves) particles with different relative compositions and each with a spherical dry diameter of 50 nm. We see that, due to bulk-surface partitioning of NAFA, the bulk-phase concentrations of NAFA, which govern the equilibrium aqueous surface tensions in the activating droplets, are much lower (blue curve) than would be predicted if NAFA depletion was not considered (pink curve).

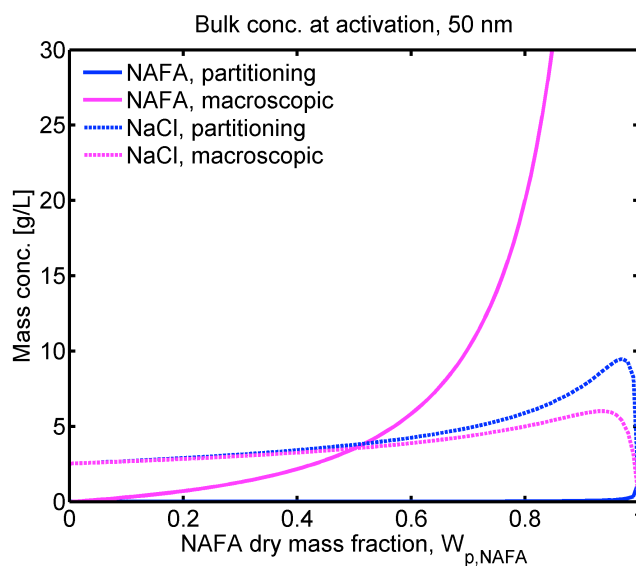


Figure 2. Calculated bulk-phase mass concentrations of activating droplets formed on 50 nm dry particles comprising NAFA mixed with NaCl, when droplets are treated as macroscopic solutions, and when NAFA surface partitioning is considered, respectively.

The consequence of bulk-phase depletion of surfactant, for droplet surface tension, is seen in Figure 3. With the very low NAFA concentrations remaining in the droplet bulk-phase, the surface tensions of activating droplets are only for particles with the highest fractions of NAFA even modestly reduced from the value for pure water (pink line). There is a large difference between surface tensions predicted, when considering activating droplets equivalent to macroscopic solutions (green curve), and when taking NAFA surface partitioning into account (blue curve), respectively. The implications of these differences in surface tension, for predicted CCN activity of NAFA particles, are significant.

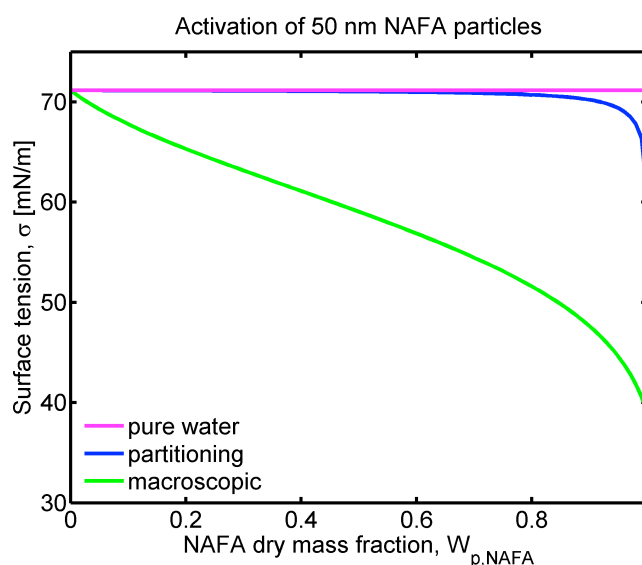


Figure 3. Calculated surface tensions for activating aqueous droplets formed on 50 nm dry particles comprising NAFA mixed with NaCl, when droplets are treated as macroscopic solutions, and when NAFA surface partitioning is considered, respectively.

An important consequence of bulk-surface partitioning and bulk-phase depletion of surfactants in microscopic droplets is that the relative mixing ratio of inorganic (non-partitioning) and surface active organic (partitioning) solutes changes from the original dry particle compositions. Figure 4 shows measured surface tensions (circles) for aqueous solutions containing 20, 50, 80, and 100% by mass of sodium octanoate surfactant mixed with NaCl, and a ternary parametrization made from fitting the data as a function of sodium octanoate and NaCl concentrations to a Szyszkowski-type surface tension expression. In the same figure is also indicated predicted concentrations and surface tensions (stars) for activating droplets formed on 50 nm dry particles with the same relative sodium octanoate and NaCl compositions as the solutions measured. The calculated surface tensions for activating droplets all fall in the top left corner of the plot. It is clear that the measurements on macroscopic solutions do not constrain or sufficiently resolve the variation in conditions predicted at the point of droplet activation.

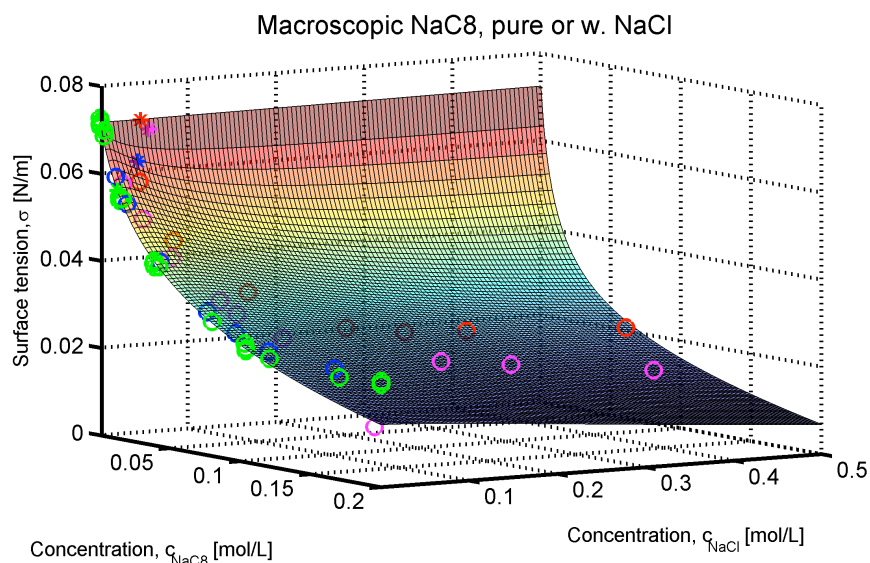


Figure 4. Measurements (circles) and ternary parametrization of surface tension for aqueous sodium octanoate and NaCl mixtures containing 20, 50, 80 and 100% by mass of sodium octanoate, together with concentrations and surface tensions calculated for activating aqueous droplets formed on 50 nm dry particles comprising sodium octanoate mixed with NaCl, with consideration of sodium octanoate surface partitioning (stars).

## CONCLUSIONS

We have measured surface tensions of macroscopic aqueous solutions of atmospherically relevant surfactants mixed with sodium chloride and used a ternary parametrization based on these measurements to predict concentrations of surfactants in microscopic activating droplets from equilibrium Köhler theory. Due to bulk-phase depletion by surface partitioning, predicted surfactant concentrations in droplets are very low at the point of activation, and the surface tension of the droplets is only modestly reduced from the pure water value. The significant increase in CCN activity expected from the measured surface tension reduction in macroscopic atmospheric samples is therefore unlikely to occur. Furthermore, surfactant partitioning changes the relative mixing state of organic and inorganic solutes in the droplets, compared to macroscopic solutions, as well as to the original dry particle compositions. This must be taken into consideration when performing surface tension measurements intended to constrain the properties of activating cloud droplets.

## ACKNOWLEDGEMENTS

This work was supported by the Academy of Finland Center of Excellence (project no 1118615) and the Nordic Center of Excellence CRAICC.

## REFERENCES

- Dinar, E., *et al.* (2006). *Atmos. Chem. Phys.*, **6**, 2465-2481.
- Facchini, M.C., *et al.* (1999). *Nature*, **401**, 257-259.
- Kiss, G., *et al.* (2005). *J. Atmos. Chem.*, **50**, 279-294.
- Li, Z., *et al.* (1998), *J. Atmos. Sci.*, **55**, 1859-1866.
- Mochida, M., *et al.* (2002). *J. Geophys. Res.*, **107**, D17S4325.
- Shulman, M., *et al.* (1996). *Geophys. Res. Lett.*, **23**, 277-280.
- Sorjamaa, R., *et al.* (2004). *Atmos. Chem. Phys.*, **4**, 2107-2117.

# BLACK CARBON CONCENTRATIONS AND COATING THICKNESS AT PALLAS, FINLAND

T. RAATIKAINEN<sup>1</sup>, D. BRUS<sup>1</sup>, A.-P. HYVÄRINEN<sup>1</sup>, J. SVENSSON<sup>1</sup> and H. LIHAVAINEN<sup>1</sup>

<sup>1</sup>Finnish Meteorological Institute, Helsinki, Finland

Keywords: Black carbon, Soot, SP2.

## INTRODUCTION

Absorbing aerosol such as black carbon has a warming effect on the global climate (Bond et al., 2013). In addition to directly absorbing solar radiation, black carbon deposition on snow and ice changes the surface albedo. This enhances snow and ice melting which further increases the albedo. Black carbon has also an effect on aerosol-cloud interactions. The water insoluble black carbon itself is a poor cloud condensation nuclei (CCN), but this can make it a better ice nuclei. For practical modelling, it is important to know both soot particle size distribution and coating thickness distribution (Bond et al., 2013; Zhang et al., 2008). Initially soot particles or agglomerates can be composed of almost pure carbon, but will be coated in a few hours. One of the few instruments that can measure both soot particle size distribution and coating thickness is Single Particle Soot Photometer (Stephens *et al.*, 2003; Gao *et al.*, 2007; Moteki and Kondo, 2007) manufactured by the Droplet Measurement Technologies. Single Particle Soot Photometer (SP2) was used to measure soot particle size distributions and coating thickness in a remote site at the Finnish Lapland.

## METHODS

Black carbon concentrations were measured at the Pallas GAW station located at a hilltop in Northern Finland. The station is equipped with several other aerosol instruments such as DMPS (Differential Mobility Particle Sizer) for measuring aerosol size distributions, CCN counter for hygroscopicity and MAAP (Multi-Angle Aerosol Photometer) for aerosol absorption. SP2 is a single particle instrument capable of detecting both BC-containing and purely scattering particles. Aerosol sample flow goes through a high power intra-cavity laser beam. Absorbing particles are quickly heated to their boiling point and at the same time they emit thermal radiation. Soot particles have a high boiling point (>4000 K) so they emit at the visible wave lengths, thus the method is called Laser Induced Incandescence (LII). The incandescence signal is recorded from 400 to 800 nm wavelengths, and the maximum value is proportional to the particle BC mass. Therefore, the SP2 black carbon is often referred as refractory BC or rBC. The instrument has also detectors for the laser wavelength (1064 nm) which record the light scattered from the particles. For purely scattering particles the peak signal is proportional to the particle size. Mixed particles are more problematic, because volatile material evaporates when the non-volatile soot warms up. This means that the incandescence signal is unperturbed, but the maximum scattering signal is only a fraction of that what it would be without evaporation. Only the first part of the scattering signal before significant heating is representative of the original particle size, and this can be used in reconstructing the unperturbed signal. In practise, also the laser beam position and width are needed to reconstruct the signal. The beam width can be obtained from those of purely scattering particles, but an additional detector (split detector) is needed for the position information (Gao *et al.*, 2007). Two methods called Leading Edge Optimization (Gao *et al.*, 2007) and Normalized Derivative Method (Moteki and Kondo, 2008) were applied to the current data set. The Normalized Derivative Method is computationally heavy and fully valid for cases where the laser beam parameters are constants. Because the laser beam parameters changed considerably during the Pallas measurement campaign, the Leading Edge Optimization (LEO) was used to reconstruct scattering signals. The LEO method was also able to account for some of the variations of the laser parameters. When both scattering and incandescence (BC core) sizes have been derived for all particles, the data analysis is relatively simple statistics.

## RESULTS

Figure 1 shows time series of total observed BC mass concentration, number fraction of BC-containing particles (for 200-250 nm diameter range) and the average relative coating thickness ( $D_{\text{scat}}/D_{\text{core}}$ ) for core sizes from 150 to 200 nm. The average mass concentration is just  $0.025 \mu\text{g}/\text{m}^3$ , which a relatively low value, but not uncommon for remote locations. The average fraction of BC-containing particles is 7% and the average relative coating thickness is  $1.50 \pm 0.11$ , but both time series have clear peaks. The origin of these peaks is not yet known, but they resemble plumes of fresh thinly coated BC. Diurnal cycles were also calculated, but the variations were within noise.

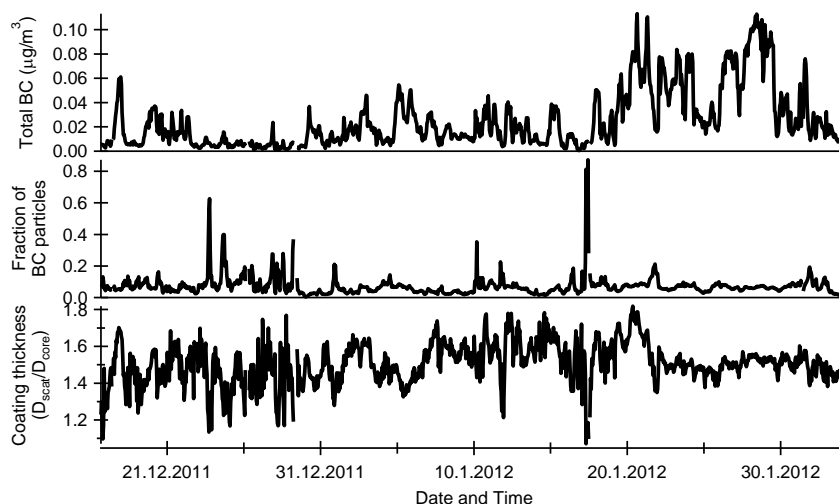


Figure 1. Total BC concentration, number fraction of the coated particles (200-250 nm size range) and the average relative coating thickness for 150-200 nm soot cores.

Figure 2 shows a comparison of SP2 and DMPS number size distributions. SP2 scattering size detection limit is 180 nm and at this point the SP2 seem to detect about half of the scattering particles. It was not possible to calculate coating thickness for the smallest soot particles (SP2 BC without scattering size), which the scattering size would be below the detection limit. Therefore, it is likely that the smallest soot particles are actually coated and that these particles are a part of the main mode where the other BC-containing particles were observed. In general, SP2 and DMPS size distributions are in good agreement.

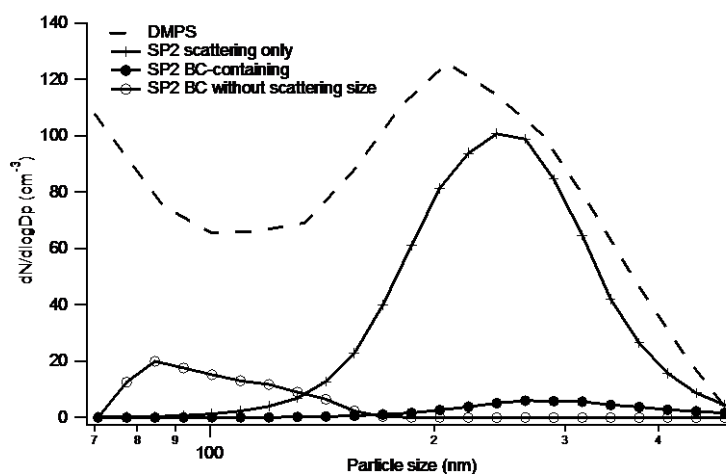


Figure 2. Average number size distributions from SP2 and DMPS for 21.12.2011 04:00-18:00 (UTC). The “SP2 BC without scattering size” is shown as a function of soot diameter.

Figure 3 shows a comparison between MAAP and SP2 black carbon concentrations. On the average, MAAP measures five times higher BC concentrations than those detected by the SP2. One possible reason for this is that the SP2 has a limited particle size detection range, but the MAAP detects the sub-10  $\mu\text{m}$  soot mass. In addition, SP2 detects only the refractory BC, which is the light absorbing carbon (and sometimes also mineral dust) that is not evaporated before the incandescence, but MAAP detects also the volatile absorbing material such as brown carbon.

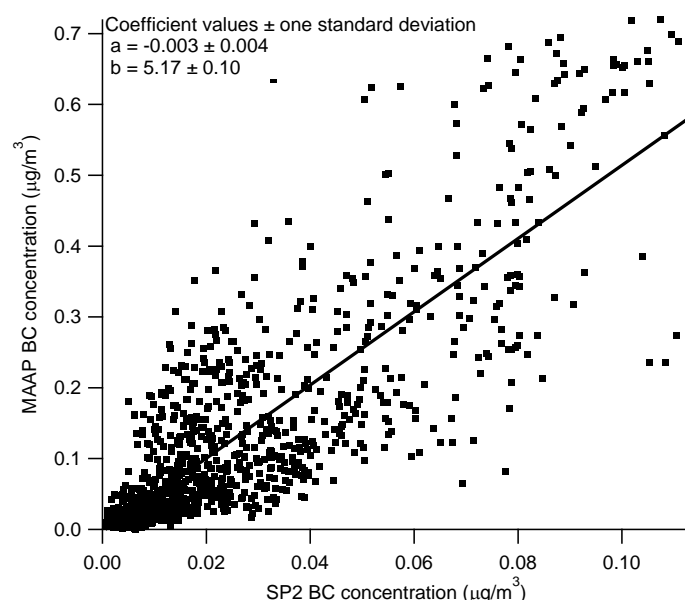


Figure 3: Correlation between MAAP and SP2 black carbon concentrations.

## CONCLUSIONS

Black carbon aerosol concentrations and size and coating thickness distributions were measured by an SP2 at Pallas in Northern Finland. The black carbon concentration is just  $0.025 \mu\text{g}/\text{m}^3$ , but relatively large fraction (7%) of the particles contains BC. There were some clear peaks in the coating thickness and BC number fraction, but consistent diurnal variations were not observed possibly due to lack of solar radiation. The average relative coating thickness (particle diameter divided by the core diameter) was  $1.50 \pm 0.11$  for 150-200 nm BC cores.

## ACKNOWLEDGEMENTS

The work is supported by the EU LIFE+ project MACEB (project no. LIFE09 ENV/FI/000572), the Academy of Finland through the FCoE in Physics, Chemistry, Biology and Meteorology of Atmospheric Composition and Climate Change (program no. 1118615), black and brown carbon influence on climate and climate change in India – from local to regional scale (project no. 264242), Arctic Absorbing Aerosols and Albedo of Snow (project no. 3162) and the Nordic research and innovation initiative CRAICC.

## REFERENCES

Bond, T.C., S.J. Doherty, D.W. Fahey, P.M. Forster, T. Berntsen, B.J. DeAngelo, M.G. Flanner, S. Ghan, B. Kärcher, D. Koch, S. Kinne, Y. Kondo, P.K. Quinn, M.C. Sarofim, M.G. Schultz, M. Schulz, C. Venkataraman, H. Zhang, S. Zhang, N. Bellouin, S.K. Guttikunda, P.K. Hopke, M.Z. Jacobson, J.W. Kaiser, Z. Klimont, U. Lohmann, J.P. Schwarz, D. Shindell, T. Storelvmo, S.G. Warren and C.S. Zender (2013). Bounding the role of black carbon in the climate system: A scientific assessment, *J. Geophys. Res.* **118**, 5380.

- Moteki, N. and Y. Kondo (2007). Effects of Mixing State on Black Carbon Measurements by Laser-Induced Incandescence, *Aerosol, Sci. Technol.* **41**, 398.
- Moteki, N and Y. Kondo (2008). Method to measure time-dependent scattering cross sections of particles evaporating in a laser beam, *Aerosol Science* **39**, 348.
- Gao, R.S. , J.P. Schwarz , K.K. Kelly, D.W. Fahey, L.A. Watt, T.L. Thompson and J.R. Spackman (2007). A Novel Method for Estimating Light-Scattering Properties of Soot Aerosols Using a Modified Single-Particle Soot Photometer, *Aerosol Sci. Technol.* **41**, 125
- Stephens, M., N. Turner and J. Sandberg (2003). Particle identification by laser-induced incandescence in a solid-state laser cavity, *Applied Optics* **42**, 3726
- Zhang, R., A.F. Khalizov, J. Pagels, D. Zhang, H. Xue and P.H. McMurry (2008). Variability in morphology, hygroscopicity, and optical properties of soot aerosols during atmospheric processing, *Proc. Natl. Acad. Sci, USA* **15**, 10291.

## A MODEL OF METHANE EMISSIONS FROM BOREAL PEATLANDS

M. RAIVONEN<sup>1</sup>, S. SMOLANDER<sup>1</sup>, M. TOMASIC<sup>1</sup>, T. HÖLTTÄ<sup>2</sup>, J. SUSILUOTO<sup>3</sup>, T. AALTO<sup>3</sup>, E.-S. TUUTTILA<sup>2,4</sup>, J. RINNE<sup>1</sup>, S. HAAPANALA<sup>1</sup>, A. VALDEBENITO<sup>5</sup>, R.J. SCHULDT<sup>6</sup>, V. BROVKIN<sup>6</sup>, C. REICK<sup>6</sup>, T. KLEINEN<sup>6</sup> and T. VESALA<sup>1</sup>

<sup>1</sup>Division of Atmospheric Sciences, Department of Physics, University of Helsinki, Finland

<sup>2</sup>Department of Forest Sciences, University of Helsinki, Finland

<sup>3</sup>Finnish Meteorological Institute, Helsinki, Finland

<sup>4</sup>School of Forest Sciences, University of Eastern Finland, Joensuu, Finland

<sup>5</sup>Norwegian Meteorological Institute, Oslo, Norway

<sup>6</sup>Land in the Earth System, Max-Planck-Institute for Meteorology, Hamburg, Germany

Keywords: METHANE, PEATLANDS, GLOBAL MODELLING

### INTRODUCTION

Methane (CH<sub>4</sub>) is the second most important greenhouse gas after carbon dioxide (CO<sub>2</sub>) and it has produced current radiative forcing of ~30% of that of CO<sub>2</sub>. Although the total CH<sub>4</sub> emissions in the atmosphere are known relatively well, the contributions and trends of different sources are not. Most CH<sub>4</sub> (over 70%) is released from biogenic sources like rice cultivation, livestock and, above all, natural wetlands that are the largest single source of CH<sub>4</sub> in the atmosphere (Denman *et al.*, 2007).

In wetlands, conditions in the soil are anoxic because of the high water table. This slows down the decomposition of soil organic matter, consequently, carbon starts to accumulate as peat. In addition, the microbial action of the anoxic decomposition produces CH<sub>4</sub>. Root exudates, extracted from plants, seem to be essential organic material for methanogenesis; they are recent photosynthates, and a clear connection between net primary production and CH<sub>4</sub> emissions has been found (Bridgman *et al.* 2013, Whiting & Chanton 1993).

After being produced, a CH<sub>4</sub> molecule can have different fates. It can be transported to the atmosphere through the soil by diffusion in water- and air-filled soil pores. It can form gas bubbles with other molecules and be released to the atmosphere in ebullition. It can be transported via plants: in stems and roots of flood-tolerant plant species there are air spaces (*aerenchyma*) that enable atmospheric oxygen to move down to the roots, and this route allows also CH<sub>4</sub> to move upwards. The molecule can also be destroyed: in the oxic parts of the soil there are methanotrophic bacteria that oxidize CH<sub>4</sub> to CO<sub>2</sub>. This CH<sub>4</sub>-removal process is quite effective: in field studies, up to 80% of potential CH<sub>4</sub> emissions have been estimated to be oxidized before they occurred (Whalen, 2005). At least via the plant roots and possibly in ebullition, CH<sub>4</sub> can bypass the oxidation.

As CH<sub>4</sub> source and carbon sink, wetlands play an important role in the climate system, and dynamic wetland models are being developed for the Earth System Models (Melton *et al.* 2012). We have been working on a process model of CH<sub>4</sub> transport and oxidation in wetlands, starting from boreal peatlands. The model is aiming to be a part of the CBALANCE carbon tool of the JSBACH (Jena Scheme for Biosphere-Atmosphere Coupling in Hamburg), the land surface model of the MPI (Max Planck Institute) Earth System Model. The peatland model has been done in co-operation with the MPI-Hamburg. They developed the model of peat accumulation and decomposition (Schuldt *et al.*, 2013) while our part is its sub-model that simulates production of CH<sub>4</sub> as a proportion of anoxic soil respiration, transport of CH<sub>4</sub> and oxygen between the soil and the atmosphere via diffusion in aerenchymatous plants and peat, CH<sub>4</sub> ebullition, and oxidation of CH<sub>4</sub>. The model is largely based on the CH<sub>4</sub> emission model of Wania *et al.* (2010); however, we have modified several parts.

## MODEL DESCRIPTION

In the peatland model, the soil carbon pool is divided into two parts: catotelm that is always inundated and thus anoxic, and acrotelm that can be partly or completely above water and thus is partly or completely oxic. Water table depth (WTD) determines how much of the acrotelm carbon is decomposing in anoxic conditions. In short, the methane model calculates how much of the decomposition becomes  $\text{CH}_4$  emission (Fig. 1).

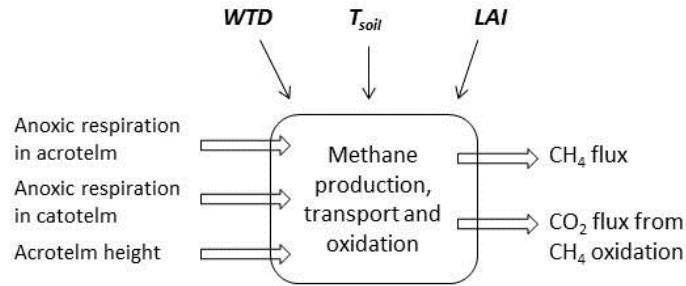


Figure 1. Input, forcing data and essential output of the  $\text{CH}_4$  module. WTD stands for water table depth,  $T_{\text{soil}}$  is soil temperature profile and LAI is the leaf area index of the plants that transport gases and produce root exudates.

The methane module has a more detailed vertical geometry than the other parts of the peatland model: peat is divided into layers, thicknesses of which grow from the top to the bottom. The total layer depth is adjustable but it is currently set to 1.96 m. The layering has been designed so that it fits the soil layer system of JSBACH. Our layers are seven sublayers of 3.25 JSBACH layers. Our layer thicknesses starting from the top are: 0.06, 0.13, 0.13, 0.23, 0.23, 0.46 and 0.72 m. All these layers have  $\text{CH}_4$  and  $\text{O}_2$  concentrations that change when different processes consume or produce  $\text{CH}_4$  or  $\text{O}_2$  in the layer.

WTD governs how many layers are filled with water. We always fill full layers, hence the WTD is rounded to the nearest layer. We have assumed that all the soil pores below the water table are filled with water and all the pores above the WTD are filled with air. This is a simplification. In reality, there probably are water-filled soil pores above the WTD and air-filled pores below it.

Biomass of the roots of the gas-transporting plants also is vertically distributed. It decreases exponentially with depth, the longest roots reaching the 1.96 meters depth. We use the root decay function given by Wania *et al.* (2010).

### *Methane production*

The  $\text{CH}_4$  module gets as input the anoxic respiration, separately for acrotelm and catotelm. This is distributed vertically in the layers according to the root decay function.  $\text{CH}_4$  production is set to be a fixed percentage of the anoxic respiration. At the moment, we use 20%.

### *Oxidation of $\text{CH}_4$*

Rate of  $\text{CH}_4$  oxidation depends on the  $\text{O}_2$  concentration in the soil layer. We adopted the model presented by Arah & Stephen (1998), where the oxidation follows Michaelis-Menten kinetics.

### *Molecular diffusion of $\text{CH}_4$ and $\text{O}_2$*

Diffusion of  $\text{CH}_4$  and  $\text{O}_2$  through the peat layer and between the soil and the atmosphere is calculated with Fick's law. In the soil layers below the WTD, the process is assumed to happen in water, above the WTD in dry peat. For the latter, we use the diffusivity of porous soil calculated with the Millington-Quirk model (Millington and Quirk, 1961).

### *Plant transport*

For plant-mediated transport of CH<sub>4</sub> and O<sub>2</sub> between atmosphere and different depths of the peat column, a formulation by Stephen *et al.* (1998) is adopted. The vertical distribution of roots (see above) determines the cross-sectional area of roots that end in each layer. This is the cross-sectional area of "root tubes" that is available for the plant-mediated transport between the layer and the atmosphere. We get as input the current LAI and maximum LAI (LAI<sub>max</sub>) of the gas-transporting plants. The root area available for transport is thus scaled with the relation LAI/LAI<sub>max</sub>. The resistance depends of the length (depth) and the diffusion coefficient in air, as the aerenchyma inside roots is filled with air.

### *Ebullition*

The ebullition model is essentially the same as in Wania *et al.* (2010). The principle is to calculate for each soil layer whether there is so much CH<sub>4</sub> that it cannot dissolve anymore, and whether also the gas-phase CH<sub>4</sub> exceeds certain limit of volumetric gas content (value of this parameter is set to 15%). If this condition is fulfilled, methane bubbles escape from the layer, and the volumetric gas content of CH<sub>4</sub> drops to a lower limit (14.5%). If ebullition occurs, the bubbles go directly to the atmosphere – unless the top soil temperature is below the freezing temperature and the bubbled CH<sub>4</sub> remains in the soil below frozen layers.

## CURRENT STATUS

Standalone version of the model is more or less ready. We have performed tests on the general functionality of the model, however, validation against field observations has not been started yet.

## ACKNOWLEDGEMENTS

This research was supported by the Academy of Finland Center of Excellence program (project number 1118615) and the Nordic Center of Excellence DEFROST.

## REFERENCES

- Arah, J. R. M. and K. D. Stephen (1998). A model of the processes leading to methane emission from peatland. *Atmospheric Environment* 32(19), 3257-3264.
- Bridgman, S. D., H. Cadillo-Quiroz, J. K. Keller and Q. Zhuang (2013). Methane emissions from wetlands: biogeochemical, microbial, and modeling perspectives from local to global scales. *Global Change Biology*, 19, 1325-1346.
- Denman, K. L., G. Brasseur, A. Chidthaisong, P. Ciais, P. Cox, R.E. Dickinson, D. Hauglustaine, C. Heinze, E. Holland, D. Jacob, U. Lohmann, S. Ramachandran, P.L. da Silva Dias, S.C. Wofsy, and X. Zhang (2007). Chapter 7: Couplings between changes in the climate system and biogeochemistry, in: *Climate Change 2007: The Physical Science Basis. Contribution of Working Group I to the Fourth Assessment Report of the Intergovernmental Panel on Climate Change*, edited by: Solomon, S., Qin, D., Manning, M., Chen, Z., Marquis, M., Averyt, K., Tignor, M., and Miller, H., Cambridge University Press, UK and New York, NY, USA, 2007.
- Melton, J. R. et al. (2012). Present state of global wetland extent and wetland methane modelling: conclusions from a model intercomparison project (WETCHIMP). *Biogeosciences Discussions* 9, 11577-11654.
- Millington, R. J., and J. P. Quirk (1961). Permeability of porous solids. *Trans Faraday Soc.* 57, 1200-1207.
- Schuldt, R. J., V. Brovkin, T. Kleinen and J. Winderlich (2013). Modelling Holocene carbon accumulation and methane emissions of boreal wetlands – an Earth system model approach. *Biogeosciences* 10, 1659-1674.

- Stephen, K.D., J.R.M. Arah, W. Daulat and R.S. Clymo (1998). Root-mediated gas transport in peat determined by argon diffusion. *Soil Biology and Biochemistry*, 30(4), 501–508.
- Wania, R., I. Ross and I.C. Prentice (2012). Implementation and evaluation of a new methane model within a dynamic global vegetation model: LPJ-WHyMe v1.3.1. *Geoscientific Model Development* 3: 565-584.
- Whalen, S. C. (2005). Biogeochemistry of methane exchange between natural wetlands and the atmosphere. *Environmental Engineering Science* 22, 73-94.
- Whiting, G. J. and J. P. Chanton (1993). Primary production control of methane emission from wetlands. *Nature* 364, 794-795.

# VOC MEASUREMENTS WITH PTR-MS AT URBAN BACKGROUND SITE IN HELSINKI

P. RANTALA<sup>1</sup>, S. HAAPANALA<sup>1</sup>, M.K. KAJOS<sup>1</sup>, J. PATOKOSKI<sup>1</sup>, L. JÄRVI<sup>1</sup>, R. TAIPALE<sup>1</sup>, J. RINNE<sup>1</sup> and T.M. RUUSKANEN<sup>1</sup>

<sup>1</sup> Division of Atmospheric Sciences, Department of Physics, University of Helsinki, Finland.

Keywords: Volatile organic compounds, PTR-MS, Urban site, Helsinki.

## INTRODUCTION

Volatile organic compounds (VOCs) are mostly emitted into the atmosphere from natural sources (Guenther *et al.*, 1995). However, approximately 10 % of the total emissions is caused by a human activity, such as traffic and industry. These anthropogenic VOCs effect to the atmospheric chemistry especially at urban areas (i.e. near the sources) and long-lived compounds have also a contribution to VOC concentrations at rural areas, especially outside the growing season when a biological activity tends to be only minimal (Patokoski *et al.*, 2014, in press).

Since November 2012 we have measured several VOCs using the proton transfer reaction mass spectrometer (PTR-MS, Lindinger *et al.*, 1998) at the SMEAR III which is an urban background station in Helsinki (60° 12' N, 24° 58' E, for a detailed description see Järvi *et al.*, 2009). Our aim is to study the importance of VOC sources (both biogenic and anthropogenic) in Helsinki by performing flux measurements. It has been already shown (Hellén *et al.*, 2012; Patokoski *et al.*, 2014, in press) that surroundings of the measurement site are a clear source for many VOCs, however, VOC emissions have not been measured directly before and in this abstract we give an overview of our measurements and research goals.

## METHODS

The PTR-MS is a highly sensitive instrument for real-time measurements of VOCs. It uses hydronium ions ( $\text{H}_3\text{O}^+$ ) to ionize target compounds via proton transfer reaction and quadrupole technique as a mass analyzer. PTR-MS measures with 1 amu (atomic mass unit) resolution, thus isobaric compounds cannot be identified. The PTR technique is still one of the most applicable methods to investigate a major part of common VOCs, such as methanol, acetone, isoprene and monoterpenes.

We measured the VOC fluxes using the disjunct eddy covariance -technique (DEC) which is a conventional method to do direct flux measurements (see Rinne *et al.*, 2007). Ambient concentrations of 27 compounds and fluxes of 11 compounds were measured, by turns, every second hour. The flux, calibration and volume mixing ratio calculation procedures for the PTR-MS are explained elsewhere (Taipale, 2011; Taipale *et al.*, 2008)

## RESULTS AND CONCLUSIONS

According to our preliminary results for spring 2013 (January–April), clear emissions of M33 (methanol) and M47 (ethanol) were detected. We observed also emissions for M31 (formaldehyde), M42 (acetonitrile), M59 (acetone), M79 (benzene), M93 (toluene) and M107 (o-xylene) but clear cross covariance peaks (indicates how significant a measured flux value is) occurred only occasionally.

However, these measurements have been done mostly during winter when the micrometeorological conditions are usually challenging for flux measurements.

As an example, Figure 1 shows the diurnal cycles of M33 and M93 emissions and the traffic intensity from a highway near the site. The graphs demonstrate well how vehicles might be one important source of the anthropogenic VOCs and in future, our aim is to have better understanding which other processes are producing VOCs in Helsinki and how large are the total emissions in the different seasons.

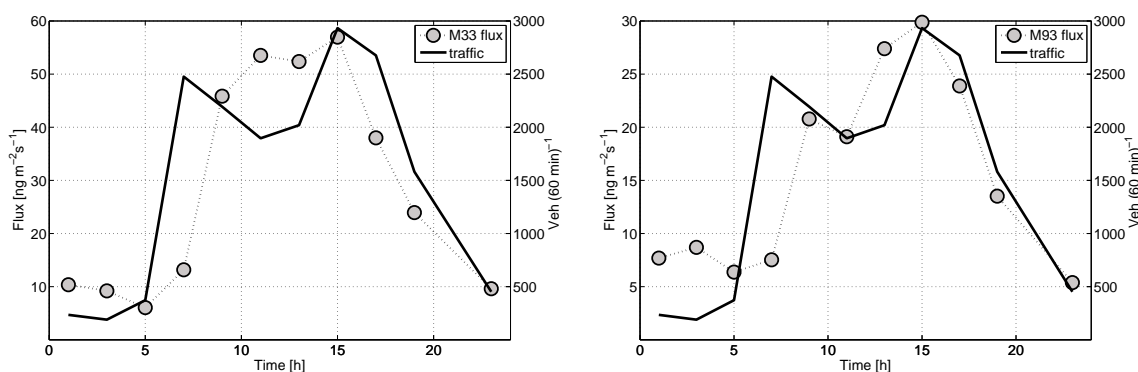


Figure 1: The lefthandside figure describes the median diurnal cycle of M33 flux and the traffic intensity (measured during January–April 2013) and the righthandside figure shows the same for M93.

## ACKNOWLEDGEMENTS

This research was supported by the Academy of Finland Center of Excellence program (project number 1118615).

## REFERENCES

- Guenther, A., C. N. Hewitt, D. Erickson, R. Fall, C. Geron, T. G. P. Harley, L. Klinger, M. Lerdau, W. A. McKay, T. Pierce, B. Scholes, R. S. R. Tallamraju, J. Taylor and P. Zimmerman (1995). A global model of natural volatile organic compound emissions. *Journal of Geophysical Research*, **100**, 8873–8892.
- Hellén, H., Tykkä, T. and H. Hakola (2012). Importance of monoterpenes and isoprene in urban air in northern Europe. *Atmospheric Environment*, **59**, 59–66.
- Järvi, L., Hannuniemi, H., Hussein, T., Junninen, H., Aalto, P. P., Hillamo, R., Mäkelä, T., Keronen, P., Siivola, E., Vesala, T., and M. Kulmala (2009). The urban measurement station SMEAR III: Continuous monitoring of air pollution and surface-atmosphere interactions in Helsinki, Finland. *Boreal environment research*, **14**, 86–109.
- Lindinger, W., A. Hansel and A. Jordan (1998). On-line monitoring of volatile organic compounds at pptv levels by means of Proton-Transfer-Reaction Mass Spectrometry (PTR-MS)—Medical applications, food control and environmental research. *Int. J. Mass Spectrom.*, **173**, 191–241.
- Patokoski, J., Ruuskanen, T. M., Hellén, H., Taipale, R., Grönholm, T., Kajos, M. K., Petäjä, T., Hakola, H., Kulmala, M. and Rinne, J. (2014) Winter to spring transition and diurnal

variation of VOCs in Finland at an urban background site and a rural site. *Boreal environment research*, **19**, *In press*.

Rinne, J., R. Taipale and T. Markkanen and T. M. Ruuskanen, H. Hellen, M. Kajos, T. Vesala and M. Kulmala (2007). Hydrocarbon fluxes above a Scots pine forest canopy : measurements and modeling. *Atmospheric Chemistry and Physics*, **7**, 3361–3372.

Taipale, R., T. M. Ruuskanen, J. Rinne, M. K. Kajos, H. Hakola, T. Pohja and M. Kulmala (2008). Technical note : quantitative long-term measurements of VOC concentrations by PTR-MS - measurement, calibration, and volume mixing ratio calculation methods. *Atmospheric Chemistry and Physics*, **8**, 6681–6698.

Taipale, R. (2011). *Disjunct eddy covariance measurements of volatile organic compound fluxes using proton transfer reaction mass spectrometry*. Academic Dissertation, University of Helsinki.

# SENSITIVITY OF RADIATIVE FORCING TO CHANGES IN UPPER TROPOSPHERIC HUMIDITY ASSOCIATED WITH AEROSOLS

L. RIUTTANEN<sup>1</sup>, A.-M. SUNDSTRÖM<sup>1</sup>, J. RÄISÄNEN<sup>1</sup> and M. BISTER<sup>1</sup>

<sup>1</sup> Department of Physics, University of Helsinki, Finland.

Keywords: aerosol-cloud-climate interactions, radiative forcing, upper tropospheric humidity.

## INTRODUCTION

Theory of aerosol effect on upper tropospheric humidity was presented by Bister and Kulmala (2011). They stated that aerosol effects on microphysics of deep convective clouds could increase upper tropospheric humidity in convectively active regions. Water vapor is known as the most important greenhouse gas that absorbs thermal radiation and thus reduces the outgoing longwave radiation. In this work the sensitivity of outgoing longwave radiation to perturbations in upper tropospheric humidity in tropical regions was tested.

## METHODS

Dunion (2011) constructed a set of reference soundings for tropical atmosphere by averaging soundings over July-October from eight years over the Caribbean Sea. Using a more extensive data set and air mass analysis they were able to improve the well-known tropical reference sounding of Jordan (1958) by dividing the soundings into three groups: moist tropical (MT) air masses from Saharan air layers (SAL) and mid-latitude dry air intrusions (MLD).

To test the sensitivity of tropical air to perturbations in the upper tropospheric humidity we added 1, 2, 5 and 10 percentage units of relative humidity to a layer of 500-200 hPa in Dunion (2011) reference soundings of moist tropical (MT) and mid-latitude dry (MLD) air and calculated the radiative transfer.

The radiative transfer simulations were carried out using libRadtran radiative transfer code (Mayer and Kylling, 2005). The outgoing longwave flux at the top of the atmosphere was integrated over 3.7-70 micron wavelength band using the correlated k-method by Fu and Liou (1992). In the lowest 2 km atmospheric layer maritime aerosols (Shettle 2005) were assumed with optical thickness of 0.15 (at 0.55 microns wavelength, other wavelengths were scaled accordingly).

## RESULTS

Increased humidity in upper troposphere decreases the outgoing longwave radiation (Table 1). Decreased OLR causes local instantaneous positive longwave radiative forcing of same magnitude.

## DISCUSSION

It is to be noted that relatively small perturbations in water vapor at high levels cause climatically significant forcings. For example 2 %-units increase in the upper tropospheric humidity for moist tropical air causes a local positive forcing of 0.52 W/m<sup>2</sup> (0.82 W/m<sup>2</sup> for dry air), comparable to the total anthropogenic aerosol direct effect that was globally estimated to be -0.5 W/m<sup>2</sup> (-0.9 to

	MT		MLD	
	OLR (W/m <sup>2</sup> )	forcing (W/m <sup>2</sup> )	OLR (W/m <sup>2</sup> )	forcing (W/m <sup>2</sup> )
Dunion (2011)	276.96	0	289.40	0
+1 RH	276.69	0.26	288.99	0.41
+2 RH	276.43	0.52	288.59	0.82
+5 RH	275.67	1.29	287.44	1.96
+10 RH	274.47	2.49	285.70	3.70

Table 1: Outgoing longwave radiation (OLR) and forcing caused by decrease in OLR when relative humidity in upper troposphere (500-200 hPa) is increased by 1, 2, 5, and 10 percentage units to moist tropical (MT) and mid-latitude dry air (MLD) reference soundings of Dunion (2011).

-0.1 W/m<sup>2</sup>) in IPCC AR4 report (2007). This is almost one third of the global effect of the CO<sub>2</sub> increase since preindustrial times that was estimated to be 1.66 W/m<sup>2</sup> (1.49 to 1.83 W/m<sup>2</sup>, IPCC 2007). In dry air (MLD) the effect of 2%-units increase in relative humidity is as much as half of that of global CO<sub>2</sub> increase. However, it is important to note that these IPCC values correspond to global radiative forcing and we have studied only certain local atmospheric situations and no global forcings can be derived.

These forcings are calculated only for the longwave region, as the shortwave effect is estimated to be minor. No stratospheric adjustment is taken into account, in contrast to radiative forcing values reported e.g. by the IPCC.

## CONCLUSIONS

Reductions of outgoing longwave radiation (OLR) by 0.26 to 2.49 W/m<sup>2</sup> in moist tropical air were produced by the libRadtran model when upper tropospheric humidity in the 500-200 hPa layer was increased by 1 to 10 percentage units. Corresponding reductions in mid-latitude dry air were 0.41-3.70 W/m<sup>2</sup>. We conclude that the radiative balance is highly sensitive to changes in upper tropospheric humidity. Therefore even small changes in upper tropospheric humidity due to aerosol modification of deep convection would be significant to climate.

## ACKNOWLEDGEMENTS

This work was supported by the Academy of Finland Center of Excellence program (project number 1118615).

## REFERENCES

- Bister, M. and Kulmala, M. (2011) Anthropogenic aerosols may have increased upper tropospheric humidity in the 20th century. *Atm. Chem. Phys.*, vol. 11, no. 9, pp. 4577-4586.
- Dunion, J. P. (2011) Rewriting the Climatology of the Tropical North Atlantic and Caribbean Sea Atmosphere. *J. Climate*, **24**, 893-908.
- Fu, Q. and Liou, K. (1992) On the correlated k-distribution method for radiative transfer in nonhomogeneous atmospheres. *J. Atmos. Sci.*, **49**, 2139-2156.
- Solomon, S., D. Qin, M. Manning, Z. Chen, M. Marquis, K.B. Averyt, M. Tignor and H.L. Miller (eds.) (2007) *Contribution of Working Group I to the Fourth Assessment Report of the Intergovernmental Panel on Climate Change*. Cambridge University Press, Cambridge, United Kingdom and New York, NY, USA.

Jordan, C. L. (1958) Mean soundings for the West Indies area. *J. Atmos. Sci.*, **15**, 91-97.

Mayer, B. and Kylling, A. (2005) Technical note: The libRadtran software package for radiative transfer calculations - description and examples of use. *Atmos. Chem. Phys.*, **5**, 1855-1877, doi:10.5194/acp-5-1855-2005.

Shettle, E. (1989) Models of aerosols, clouds and precipitation for atmospheric propagation studies. in: Atmospheric propagation in the uv, visible, ir and mm-region and related system aspects, no. 454 in AGARD Conference Proceedings.

# MULTICOMPONENT AEROSOL MODELLING WITH SPECIFIC CHEMICAL SPECIES

A. RUSANEN<sup>1</sup>, M. BOY<sup>1</sup>, S. SMOLANDER<sup>1</sup>, D. MOGENSEN<sup>1,2</sup>, P. ROLDIN<sup>3,4</sup> and E. HERMANSSON<sup>3,4</sup>

<sup>1</sup> Department of Physics, University of Helsinki, Helsinki, P.O. Box 48 FI-00014, Finland

<sup>2</sup> Helsinki University Centre for Environment, University of Helsinki, Helsinki, P.O. Box 27 FI-00014, Finland

<sup>3</sup> Division of Nuclear Physics, Department of Physics, Lund university, P.O. Box 118 SE-221 00, Lund, Sweden

<sup>4</sup> Centre for Environmental and Climate Research, Lund university, P.O. Box 118 SE-221 00, Lund, Sweden

Keywords: AEROSOL DYNAMICS, ORGANIC AEROSOLS, AEROSOL MODELLING.

## INTRODUCTION

Organic compounds are an important constituent of atmospheric aerosols. Their role is complex and intensely studied. A recent overview is presented for example in Riipinen et al. (2012).

One way to represent organic species in models is the two-dimensional volatility basis set (VBS, Donahue et al., 2011), which uses saturation mass concentration of organic compounds and the oxygen content to describe volatility, mixing thermodynamics, and chemical evolution of organic aerosols. When using the VBS explicit knowledge of the condensing organic species and their thermodynamic properties is not required. However, depending on the set of different reaction rates in the code it tends to over- or underestimate the simulated SOA mass. Another way is summing compounds into groups and estimating average physical properties for these groups as done for example in Boy et al. (2006). The problem is that values for these group properties are not well defined.

We used the model MALTE-BOX to simulate the incorporation of organic vapours into aerosols. The model was setup with values for an average day in spring at the SMEAR II station in Hyytiälä. In this preliminary run we simulated the complete reaction paths for isoprene, 2-methyl-3-buten-2-ol,  $\alpha$ -pinene,  $\beta$ -pinene, limonene,  $\beta$ -caryophyllene, methanol, acetone, acetaldehyde, formaldehyde, methane and relevant inorganic reactions together with first order reactions between OH, O<sub>3</sub> and NO<sub>3</sub> and other measured VOCs, for which we do not have full chemistry.

## METHODS

MALTE-BOX is an improved zero-dimensional version of the Model to predict new Aerosol formation in the Lower TropospherE described by Boy et al. (2006). It combines several models to simulate chemistry, emissions and aerosol dynamics.

Emissions were calculated with the model MEGAN, Model of Emissions of Gases and Aerosols from Nature (Guenther et al., 2006). After emissions gas-phase chemistry was calculated. Equations for chemistry are mostly acquired from MCM, Master Chemical Mechanism v3.2 (Jenkin et al., 1997; Saunders et al., 2003), and calculated with KPP, the Kinetic PreProcessor (Damian et al., 2002).

The calculated chemical concentrations were used to calculate aerosol dynamics. Aerosol dynamics were simulated with University of Helsinki Multicomponent Aerosol model, UHMA, described in Korhonen et al. (2004) to simulate the growth of the particle distribution. The initial distribution of particles was acquired from Differential Mobility Particle Sizer data. Since we were only interested in the compound specific condensation in these preliminary runs, other aerosol dynamical processes were not considered.

Simulating aerosol dynamics requires various properties of the condensing vapours to be known. Measurements of these are not always available. The properties can be estimated by different methods from the molecular structure (Poling et al., 2001). We used the method described in Nannoolal et al. (2008) to estimate the saturation vapour pressures of the vapours and the method described in Fuller et al. (1966) to estimate their diffusion volumes. The method described in Girolami (1994) was used to predict the liquid phase density of the compounds.

## RESULTS

We made one run for 23 hours with environmental properties of an average spring day in Hyytiälä. The resulting aerosol volumes are shown in Figure 1 and 2. Both figures are from the same simulation and show compounds that have an contribution over  $1 \mu\text{m}^3/\text{m}^3$  to the total aerosol volume concentration.

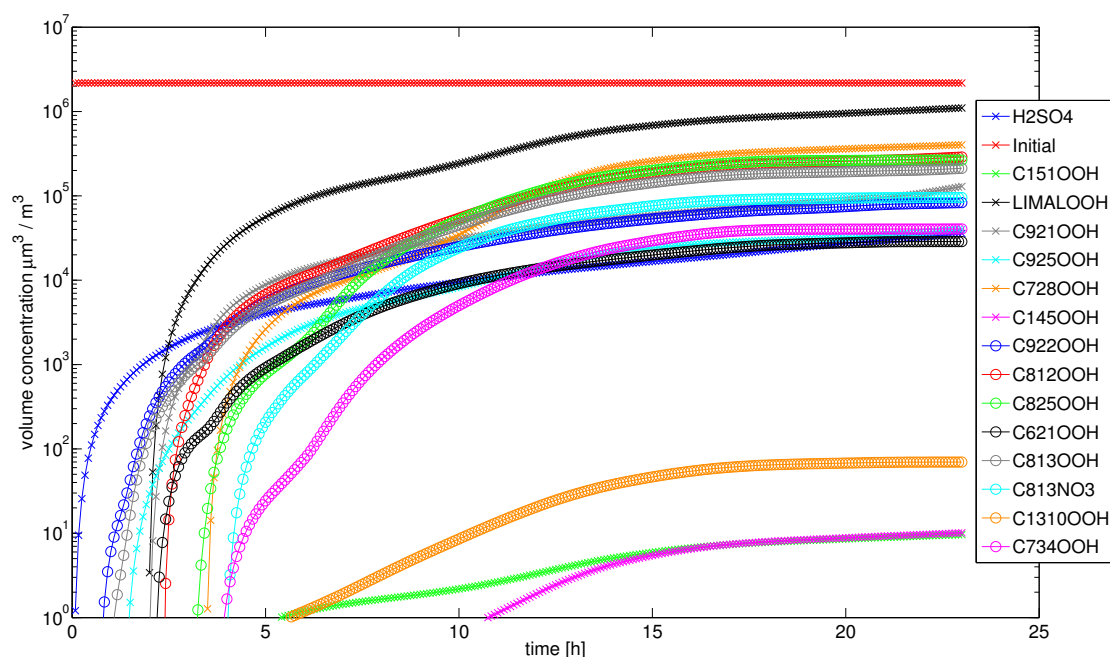


Figure 1: The total aerosol volume concentrations of compounds as a function of time. The constant red line labeled initial represents the initial aerosol volume, which is considered to be nonvolatile. The only aerosol dynamical processes included in the run were condensation and evaporation. The compound names are from MCM.

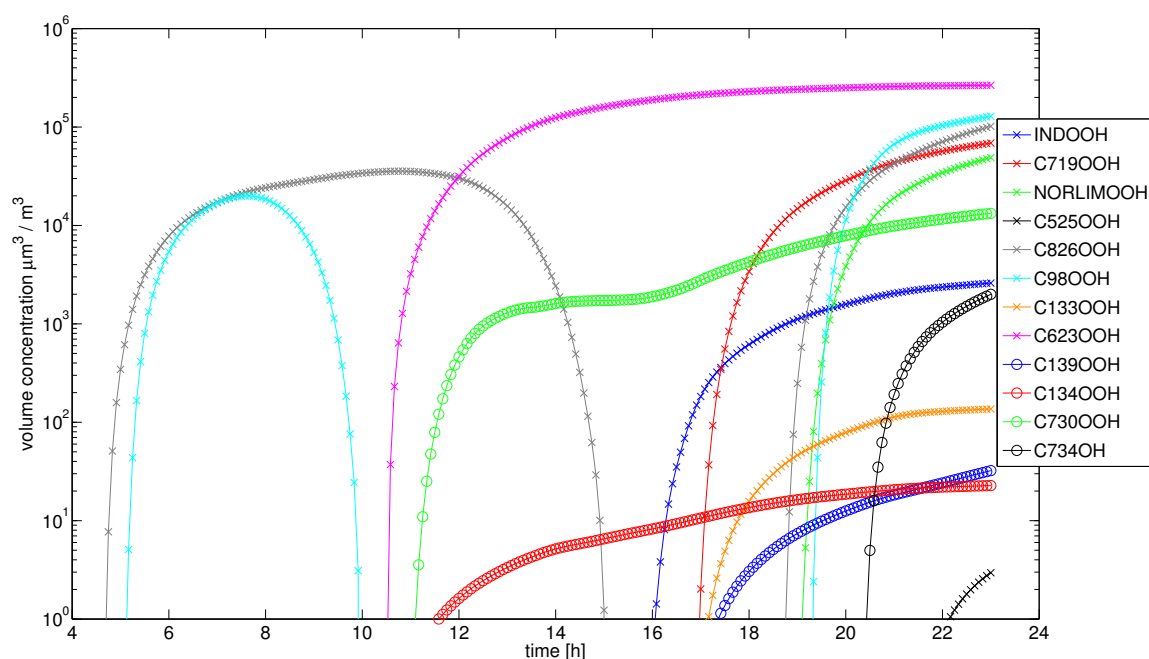


Figure 2: The total aerosol volume concentrations of compounds as a function of time. These compounds differ from the ones in Figure 1 by evaporating, having a delayed onset of condensation or being connected to photochemistry. The only aerosol dynamical processes included in the run were condensation and evaporation. The compound names are from MCM.

## CONCLUSIONS

As Figures 1 and 2 show individual reaction products are present in sufficient amounts to condense on the particles, given their estimated physical properties. There are also compounds that experience evaporation during the daytime. This could improve the description of aerosols in MALTE-BOX, since it previously considered organics in limited groups of various oxidation products.

Since the preliminary run was limited and used average data, comparing it to measurements was not done at this time. In the future we will expand the model to include the processes of coagulation, deposition and nucleation in the runs. Particle phase chemistry is also likely to influence how the compounds stay in the particles, but MALTE-BOX does not consider it at the moment.

## ACKNOWLEDGEMENTS

This research was supported by the Academy of Finland Center of Excellence program (project number 1118615). This research was supported by the Nordic Center of Excellence CRAICC. The python scripts used to calculate the saturation vapour pressures were acquired from professor Gordon McFiggans' group at the University of Manchester.

## REFERENCES

Boy, M., et al. (2006). MALTE-model to predict new aerosol formation in the lower troposphere *Atmos. Chem. Phys.*, **6**, 4499-4517

- Damian, V., et al. (2002). The kinetic preprocessor KPP-a software environment for solving chemical kinetics. *Comput. Chem. Eng.*, **26**, 1567-1579.
- E.N. Fuller, P.D. Schettler, and J.C. Giddings (1966). New Method For Prediction Of Binary Gas-Phase Diffusion Coefficients *Industrial And Engineering Chemistry*, 58,(5):19
- Guenther, A., et al. (2006). Estimates of global terrestrial isoprene emissions using MEGAN (Model of Emissions of Gases and Aerosols from Nature). *Atmos. Chem. Phys.* , **6**, 3181-3210.
- Girolami, G. (1994) A Simple “Back of the Envelope” Method for Estimating the Densities and Molecular Volumes of Liquids and Solids *Journal of Chemical Education*, Vol. 71, Issue 11, 962
- Riipinen, I., Yli-Juuti, T., Pierce, J. R., Petäjä, T., Worsnop, D. R., Kulmala, M., and Donahue, N. M. (2012) The contribution of organics to atmospheric nanoparticle growth *Nature Geoscience*, **5** (7), 453-458.
- Jenkin, M. E., et al. (1997). The tropospheric degradation of volatile organic compounds: A protocol for mechanism development. *Atmos. Environ.* , **31**,81-104.
- Korhonen, H., Lehtinen, K.E.J. and Kulmala, M. (2004). Multicomponent aerosol dynamics model UHMA: model development and validation *Atmos. Chem. Phys.*, **4**, 757-771
- Nannoolal, Y., Rarey, J. and Ramjugernath, D. (2008). Estimation of pure component properties- Part 3. Estimation of the vapor pressure of non-electrolyte organic compounds via group contributions and group interactions *Fluid Phase Equilibria*, **269**, 117-133
- Poling, B.E., Prauznitz, J.M. and O’Connel J.P. (2001). *The properties of gases and liquids 5th ed.* (McGraw-Hill, New York)
- Saunders, S. M., et al. (2003) Protocol for the development of the Master Chemical Mechanism, MCM v3 (Part A): tropospheric degradation of non-aromatic volatile organic compounds. *Atmos. Chem. Phys.* , **3**, 161-180

# THE CHARGING PROPERTIES OF PROTONATED ACETONE AND ACETONE CLUSTERS

K. RUUSUVUORI<sup>1</sup>, P. HIETALA<sup>1</sup>, O. KUPIAINEN<sup>1</sup>, T. KURTÉN<sup>2</sup> AND H. VEHKAMÄKI<sup>1</sup>

<sup>1</sup>Division of Atmospheric Sciences, Department of Physics, P.O. Box 64,  
FI-00014, University of Helsinki, Finland.

<sup>2</sup>Laboratory of Physical Chemistry, Department of Chemistry, P.O. Box 55,  
FI-00014, University of Helsinki, Finland.

Keywords: Computational, Nucleation, Amines, CIMS.

## INTRODUCTION

Understanding atmospheric new particle formation is vital to understanding the role atmospheric aerosol particles play in e.g. climate change and human health. While the initial steps of atmospheric new particle formation generally require sulphuric acid (Sipilä *et al.*, 2010), sulphuric acid does not form aerosol particles by itself in typical atmospheric conditions. Thus, other condensing vapours are needed to explain observations. During recent years, amines have become a subject of interest, as studies have suggested that they may play an important role in new particle formation, at least in the lower atmosphere (Kirkby *et al.*, 2011; Petäjä *et al.*, 2011). However, confirming the role of amines by direct observation of the initial steps of new particle formation is a very difficult task. We can try to go around these difficulties using computational methods, such as quantum chemical simulations, to model reactions which may take place in the beginning of new particle formation. Such simulations have been shown to be a valuable tool for gaining insight into the initial steps of new particle formation (see e.g. Kurtén *et al.*, 2007). The information gained from computational studies can also help in the development and testing of experimental methods suitable for amine measurements.

Our aim is to employ a combination of quantum chemical calculations and a cluster kinetics code to study the ability of protonated acetone dimers to charge amine clusters with and without sulphuric acid. Understanding the possible reaction pathways will give us important insight on amine measurements performed using an acetone based Chemical Ionization Atmospheric Pressure interface Time-Of-Flight mass spectrometer (CI-APi-TOF).

## METHODS

Geometries, enthalpies, structures, evaporation rates and dipole moments were obtained as described in Ortega *et al.* (2012), but the methods will be briefly mentioned here. Quantum chemical calculations were performed using a multi-step method: structures and frequencies were calculated at the B3LYP/CBSB7 level using Gaussian 09 and single point energies were calculated at the RI-CC2/aug-cc-pVTZ level using Turbomole 6.3.1. Values obtained from these calculations were then used as input for the cluster kinetics code ACDC (see e.g. Olenius *et al.*, 2013), which was used to obtain concentrations before, during and after CI. The concentration of sulfuric acid in the ACDC runs was set to 0 cm<sup>-3</sup>, 10<sup>6</sup> cm<sup>-3</sup> or 10<sup>8</sup> cm<sup>-3</sup>, while the concentration of dimethylamine was set to 0.01 ppt, 1 ppt or 100 ppt

## CONCLUSIONS

Initial results imply that protonated acetone could be a viable alternative for a CI reagent. The used sulfuric acid concentrations seem to have little effect on the cluster distributions. However, further work is still needed to test the sensitivity of the result with respect to various simulation parameters (such as assumed wall losses).

## ACKNOWLEDGEMENTS

We thank the CSC – IT Center for Science Ltd. For computer time and technical assistance. We also thank Dr. Mikael Ehn for his assistance. The financial support by the Academy of Finland (Centre of Excellence program Project No. 1118615 and LASTU program project number 135054) and ERC StG 257360-MOCAPAF is gratefully acknowledged.

## REFERENCES

- Kirkby, J., Curtius, J., Almeida, J., Dunne, E., Duplissy, J., Ehrhart, S., Franchin, A., Gagné, S., Ickes, L., Kürten, A., Kupc, A., Metzger, A., Riccobono, F., Rondo, L., Schobesberger, S., Tsagkogeorgas, G., Wimmer, D., Amorim, A., Bianchi, F., Breitenlechner, M., David, A., Dommen, J., Downard, A., Ehn, M., Flagan, R. C., Haider, S., Hansel, A., Hauser, D., Jud, W., Junninen, H., Kreissl, F., Kvashin, A., Laaksonen, A., Lehtipalo, K., Lima, J., Lovejoy, E. R., Makhmutov, V., Mathot, S., Mikkilä, J., Minginette, P., Mogo, S., Nieminen, T., Onnela, A., Pereira, P., Petäjä, T., Schnitzhofer, R., Seinfeld, J. H., Sipilä, M., Stozhkov, Y., Stratmann, F., Tome, A., Vanhanen, J., Viisanen, Y., Vrtala, A., Wagner, P. E., Walther, H., Weingartner, E., Wex, H., Winkler, P. M., Carslaw, K. S., Worsnop, D. R., Baltensperger, U., and Kulmala, M. (2011). Role of sulphuric acid, ammonia and galactic cosmic rays in atmospheric aerosol nucleation, *Nature* **476**, 429–433.
- Kurtén, T., Torpo, L., Sundberg, M. R., Kerminen, V.-M., Vehkamäki, H., and Kulmala, M. (2007). Estimating the  $\text{NH}_3\text{:H}_2\text{SO}_4$  ratio of nucleating clusters in atmospheric conditions using quantum chemical methods, *Atmos. Chem. Phys.* **7**, 2765–2773.
- Olenius, T., Schobesberger, S., Kupiainen, O., Franchin, A., Junninen, H., Ortega, I. K., Kurtén, T., Loukonen, V., Worsnop, D., Kulmala, M., and Vehkamäki, H. (2013). Comparing simulated and experimental molecular cluster distributions, *Faraday Discuss.*, doi: 10.1039/C3FD00031A
- Ortega, I. K., Kupiainen, O., Kurtén, T., Olenius, T., Wilkman, O., McGrath, M. J., Loukonen, V., and Vehkamäki, H. (2012). From quantum chemical formation free energies to evaporation rates, *Atmos. Chem. Phys.* **12**, 225–235.
- Petäjä, T., Sipilä, M., Paasonen, P., Nieminen, T., Kurtén, T., Ortega, I. K., Stratmann, F., Vehkamäki, H., Berndt, T., and Kulmala, M. (2011). Experimental Observation of Strongly Bound Dimers of Sulfuric Acid: Application to Nucleation in the Atmosphere, *Phys. Rev. Lett.* **106**, 228302.
- Sipilä, M., Berndt, T., Petäjä, T., Brus, D., Vanhanen, J., Stratmann, F., Patokoski, J., Mauldin III, R. L., Hyvärinen, A.-P., Lihavainen, H., and Kulmala, M. (2010). The Role of Sulfuric Acid in Atmospheric Nucleation, *Science* **327**, 1243–1246 .

# **THE INTERACTIONS BETWEEN SOIL FUNGAL COMMUNITIES AND SOIL ORGANIC NITROGEN (SON) TRANSFORMATION IN BOREAL FORESTS – THE EFFECTS OF SEASON, GEOGRAPHICAL LOCATION AND NATURAL DISTURBANCES**

M. SANTALAHTI<sup>1</sup>, H. SUN<sup>1,2</sup>, A.-J. KIELOAHO<sup>1</sup>, F. ASIEGBU<sup>2</sup>, F. BERNINGER<sup>2</sup>,  
K. KOSTER<sup>2</sup>, J. PUMPANEN<sup>2</sup> AND J. HEINONSALO<sup>1</sup>

<sup>1</sup>Department of Food and Environmental Sciences, Division of Microbiology and Biotechnology, P.O. Box 56, FI-00014 University of Helsinki, Finland.

<sup>2</sup> Department of Forest Sciences, P.O. Box 27, FI-00014 University of Helsinki, Finland.

Keywords: BOREAL FOREST, CLIMATE CHANGE, C AND N CYCLING, PYROSEQUENCING

## **INTRODUCTION**

Biosphere-atmosphere interactions have been actively and successfully studied in Finland for few decades, the oldest continuous monitoring site has been in function since 1991 in north-eastern Lapland in Värriö. Despite many advances made in gas flux measurements, the functioning of forest soil is still not properly understood. In addition to the methodological challenges that are intimate part of soil science, relatively little research effort has been put in understanding soil and microbial processes and their effects on ecosystem-level responses.

The main aim of this project is to identify for the first time the fungal community structure and some of their functions in three main ecosystem stations in Finland. We will connect pyrosequence data to organic nitrogen decomposition from several aspects: spatio-temporal dynamics and disturbances in forest ecosystem (fire and reindeer husbandry). The recently developed, extremely powerful sequencing technology (pyrosequencing) allows detailed community analysis with relatively low labour costs. In one sequence analysis, almost one million sequences are amplified that can be later divided into treatments, replicates and different sites using state-of-the-art bioinformatics tools. The project is therefore unique in Finland: microbial community structure and their functions, and field monitoring data have never before been combined in a large scale study.

The aim of the research project is to investigate soil fungal community structure in three different field sites in Finland in a South-North transect. Further, the aim is to compare the fungal community structures to soil organic nitrogen (SON) decomposition rates and enzyme activities. The field sites have different local treatments and research focuses: in southern Finland (Hyytiälä SMEAR II site), community structure in different soil horizons will be monitored over the whole growth season to be able to detect spatial and seasonal variation linked to soil protease activities. In northern Finland (Sodankylä and Värriö sites), the effect of reindeer farming (alteration in ground vegetation) and in north-eastern Finland (Värriö site SMEAR I site) the effect of forest fire chronosequence is studied and linked to soil N transformations.

## **METHODS**

### **METHOD 1: LITTER BAGS**

Between the humus and mineral soil horizons, litter bags with different mesh sizes are buried for 2 years in Hyytiälä, Sodankylä and Värriö control sites. Using different mesh size, three types of treatments are formed: mesh size 1.6 mm do not limit fine root and hyphal in-growth, 42 µm mesh excludes roots but not fungal hyphae and 2 µm excludes also fungal penetration (Wallander et al. 2001). The bags are filled with

killed and dried fungal biomass that has approximately five times higher organic N content than normal litter. The analysis of mass loss, N forms as well as  $\delta^{15}\text{N}$ -value of the litter (Method 2), before and after the incubation makes it possible to estimate organic N removal from the litter. From the litter bags, soil proteolytic activities are also measured (Method 3).

## METHOD 2: NITROGEN CHEMISTRY

Total N,  $\text{NH}_4^+$ ,  $\text{NO}_3^-$ , amino acids, total organic N (total N subtracted by inorganic N), microbial biomass N (and C) and dissolved organic N (DON) are analyzed using standard protocols (Sparks et al. 2005). In addition, a fraction called 'extractable proteinaceous material' will be measured (material that is recovered after phosphorus buffer solution-phenol extraction and subsequent MeOH- $\text{NH}_4$ -acetate precipitation; Benndorf et al. 2007; Chen et al. 2009, Kanerva et al. unpublished). Isotope ratios for  $^{15}\text{N}$  are measured in an isotope ratio mass spectrometer (DeltaPlusAdvantage, Thermo Scientific, Bremen, Germany) connected on-line via an interface (ConFlo III, Thermo Scientific, Bremen, Germany) to an elemental analyzer NC 2500 (CE Instruments, Milan, Italy).

## METHOD 3: ENZYME ACTIVITY ANALYSIS

From each litter bag, soil solution is extracted (Heinonsalo et al. 2012) for total proteolytic (PF0100 Protease Fluorescent Detection Kit, Sigma Aldrich, St. Louis, USA) and leucine aminopeptidase (Courtney et al. 2005, with modifications) enzyme activity measurements.

## METHOD 4: PYROSEQUENCING

Pyrosequencing is the most powerful community-level sequencing technique available today. In one analysis that can be divided into numerous samples or treatments, approximately one million sequences can be obtained allowing very detailed and profound analysis of the diversity of DNA templates in the samples. Fungal community structure will be analyzed from all three locations using pyrosequencing (Method 4) from humus soil core samples and community data will be analyzed in correlation with N decomposition (Method 2) and proteolytic enzyme activities (Method 3). The seasonal and spatial changes in fungal community structure are identified and compared to available proteolytic enzyme activity data. The pyrosequencing method is described in more detail below.

From the soil samples DNA is extracted from 0.25 g (fresh weight) of soil with Mobio Power Soil DNA Isolation Kit (Mobio, Carlsbad, USA) according to manufactures instructions. Bead beating step is done with Fast-Prep®-24 machine (MP Biomedicals, Illkirch, France) for 30 seconds at speed 4  $\text{m s}^{-1}$ . DNA concentrations are measured with NanoDrop ND-1000 and DNA extractions are diluted in 10  $\text{ng } \mu\text{l}^{-1}$  concentrations.

Fungal ITS 2 regions are amplified by PCR with fungal specific primers gITS7 (Ihrmark et al. 2012) and ITS4 (White et al. 1990) with pyrosequencing A- and B-adapters for 454 GS FLX Titanium Sequencing Platform (454 Life Sciences, Roche Diagnostic, CT, USA) and 6 bp identification tags for each sample. All PCR reactions are done in 25  $\mu\text{l}$  volume and reaction mix include 0.2 mM of dNTP Mix (Thermo Fischer, Vantaa, Finland), 0.5 mM of both primers, 1 U of Phusion DNA Polymerase (Thermo Fischer, Vantaa, Finland), 1x Phusion HF Buffer (Thermo Fischer, Vantaa, Finland), nuclease free water and 30 ng of template DNA. All PCR reactions are done in three replicates. PCR program include initial denaturation at 98 °C for 30 seconds, 22 cycles of 98 °C for 10 seconds, 56 °C for 30 seconds, 72 °C for 20 seconds and final elongation at 72 °C for 5 minutes. DNA is visualized on 1 % agar gel with ethidium bromide under UV-light. All three replicates from each sample are pooled together. Pyrosequencing is done in the Institute of Biotechnology at the University of Helsinki.

All sequence data is processed using mothur v.1.31.2 (Schloss et al. 2009) software package. Sequence data is trimmed, screened and aligned with mothur so that only high quality sequences are obtained.

Fungal ITS sequences are aligned using a pairwise alignment. Sequences are submitted to EMBL and/or UNITE database (EMBL [www.embl.de/](http://www.embl.de/) and UNITE database <http://unite.ut.ee/>) and species identification obtained through Blast search (<http://blast.ncbi.nlm.nih.gov/Blast.cgi>).

The ratio of saprotrophic and ECM and ERM mycorrhizal biomass is estimated as follows: ergosterol from soil is analyzed as total fungal biomass estimate. From the Blast-identified sequences, those with more than 2 % of the total number of reads are divided to ECM, ERM and other fungi. The ratio of ECM, ERM vs. other fungi is used as an estimate for the proportion of mycorrhizal and saprotrophic fungal biomass, derived from ergosterol data.

Pyrosequencing of fungal community from different sampling locations are ongoing. The fire chronosequence dataset from Värriö is currently under analysis. As preliminary results of pyrosequencing Värriö samples, we have got 312 954 sequences from where 54 893 are unique after trimming and chimera checking of the sequences with mothur v.1.31.2 (Schloss et al. 2009). Pyrosequencing data-analysis from Hyytiälä samples will be started shortly. DNA extractions and PCR is in progress from the reindeer grazing area samples from Sodankylä and Värriö.

## CONCLUSIONS

This project will deepen the understanding of the impact of soil fungal communities and soil organic N (SON) cycle in the boreal forest ecosystem. Currently, it is not known whether soil C and N storages will increase or decrease due to climate change, and how will soil disturbances affect SON transformations. Due to positive effect of potentially increasing N availability on net primary production (NPP), the quantification of SON decomposition and mechanisms affecting it are of major importance in order to improve ecosystem level models and their ability to predict the effects of climate change. The indirect societal impacts are therefore significant. The novelty of the project is to combine soil organic N transformations, the micro-organisms responsible for the processes and compounds responsible for the reactions (enzyme analyses). These parameters can be compared to extensive environmental data from the ecosystem stations, including greenhouse gas fluxes.

## ACKNOWLEDGEMENTS

This work is supported by Academy of Finland Research grants 263858, 259217, 218094, Academy of Finland Centre of Excellence program (project no 1118615), University of Helsinki Three-year research grant (PYROFUNGI-project), and the Nordic Centers of Excellence CRAICC and DEFROST.

## REFERENCES

- Benndorf, D., Balcke, G., Harms, H. and Bergen, M. (2007) *The ISME Journal*, 1: 224–234.
- Chen, S., Rillig, M.C. and Wang, W. (2009) *Proteomics* 9, 4970–4973.
- Courty, P.-E., Pritsch, K., Schlöter, M., Hartmann, A. and Garbaye, J. (2005) *New Phytol* 167:309–319.
- Heinonsalo, J., Kabiersch, G., Niemi, R.M. et al. (2012) *Fungal Ecology* 5(2):261–269.
- Ihrmark, K., Bödeker, I.T.M., Cruz-Martinez, K., Friberg, H., Kubartova, A., Schenck, J., Strid, Y., Stenlid, J., Brandström-Durling, M., Clemmensen K.E. and Lindahl, B.D. (2012). *FEMS Microbiol Ecol* 82:666–677.
- Schloss, P.D., Westcott, S.L., Ryabin T., Hall, J.R., Hartmann, M., Hollister, E.B., Lesniewski, R.A., Oakley, B.B., Parks D.H., Robinson, C.J., Sahl, J.W., Stres, B., Thallinger, G.G., Van Horn, D.J. and Weber, C.F. (2009). *Appl Environ Microbiol* 75(23):7537–41.
- Sparks, D.L., Page, A.L., Helmke, P.A., et. al. Eds. (2005) *Methods of Soil Analysis. Part 3. Chemical Methods*. SSSA Book Series 5. Soil Science Society of America Inc., 1996. Reprinted in 2005.
- Wallander, H., Nilsson, L.O., Hagerberg, D. and Bååth, E. (2001) *New Phytol* 151:753–76.
- White, T.J., Bruns, T., Lee, S. and Taylor, J. (1990) *PCR Protocols: A Guide to Methods and Applications* (Innis MA, Gelfand DH, Sninsky JJ & White TJ, eds), pp. 315–322. Academic Press, San Diego, CA.

## VOC EXCHANGE MEASUREMENTS AT BOSCO FONTANA (IT) AND HYYTIÄLÄ (FI)

S. SCHALLHART<sup>1</sup>, P. RANTALA<sup>1</sup>, R. TAIPALE<sup>1</sup>, E. NEMITZ<sup>2</sup>, R. TILLMANN<sup>3</sup>, T.F. MENTEL<sup>3</sup>,  
T. RUUSKANEN<sup>1</sup> and J. RINNE<sup>1</sup>

<sup>1</sup>Department of Physics, University of Helsinki, Finland.

<sup>2</sup>Centre of Ecology & Hydrology (CEH), Penicuik, United Kingdom.

<sup>3</sup>Forschungszentrum Juelich GmbH, Germany

Keywords: FLUXES, VOCS, ECLAIRE.

### INTRODUCTION

Hydroxyl (OH) radicals, nitrate (NO<sub>3</sub>) radicals and ozone (O<sub>3</sub>) play a key role in the chemistry of the lower troposphere. The ozone formation and removal mechanisms in the troposphere depend on the abundance of NO<sub>x</sub> and volatile organic compounds (VOCs). VOCs are emitted by anthropogenic processes (e.g. combustion, biomass burning), but the major part is coming from biogenic emissions. The aim of the ECLAIRE programme is to model how climate change alters the threat of air pollution on European land ecosystems including soils. The first measurement campaign was done in Bosco Fontana, where the effect of in-canopy processes on net biosphere/atmosphere exchange fluxes was investigated.

### METHODS

A six week intensive campaign was carried out in the Nature Reserve “Bosco della Fontana” in the Po valley, Italy. This 198 ha forest is dominated by *Quercus robur* (English oak), *Quercus cerris* (Turkey oak) and *Carpinus betulus* (hornbeam) trees. The air was sampled from 32 m height through a PDFA tube (1/2” o.d) to the instruments, which were placed inside an air conditioned container.

The fluxes were measured with a Proton transfer reaction- time of flight mass spectrometer (PTR-TOF; Ionicon Analytik, Austria) using the PTR-TOF Data Analyzer (Mueller et al. 2013) and the eddy covariance method. The instrument is capable of measuring full spectra of VOCs (up to a mass of 300 amu) in real-time with a resolution of 10 Hz. The vertical wind was measured with a 3D Anemometer (Gill HS 50), which was placed next to the inlet.

The results will be compared to the emissions (calculated using the disjunct eddy covariance method) measured from a *Pinus sylvestris* (Scots Pine) dominated forest in Hyytiälä, Finland (Taipale et al. 2011). The two ecosystems show different emission profiles, as the Bosco Fontana forest emits more isoprene, while the in Hyytiälä monoterpenes dominate the terpenoid emissions. Furthermore Bosco Fontana has higher emissions and the monoterpenes fluxes correlate better with the radiation than they do in Hyytiälä.

### CONCLUSIONS

The radiation dependent emissions in Bosco Fontana suggest, that monoterpenes are released right after they are produced (de novo). In Hyytiälä the emissions are a mixture of storage and de novo emissions and they are temperature and light depended. This is due to the large monoterpenes storages of pines, which are emitted during high temperatures. The cuvette measurements, done by Ghirardo et al. (2010), show similar results.

## ACKNOWLEDGEMENTS

This research received funding from the EC Seventh Framework Programme (Collaborative project "ECLAIRE" grant no. 282910) and by the Academy of Finland Center of Excellence program (project number 1118615).

## REFERENCES

- Ghirardo, A., Koch, K., Taipale, R., Zimmer, I., Schnitzler, J-P. and Rinne, J. *Determination of de novo and pool emissions of terpenes from four common boreal/alpine trees by  $^{13}\text{CO}_2$  labelling and PTR-MS analysis*. Plant, Cell & Environment, 33, 5, 781-792, 2010.
- Mueller, M., Mikoviny, T., Jud, W., D'Anna, B. and Wisthaler, A. *A new software tool for the analysis of high resolution PTR-TOF mass spectra*. Chemometrics and Intelligent Laboratory Systems, 127, 158-165, 2013.
- Taipale, R., Kajos, M.K., Patokoski, J., Rantala, P., Ruuskanen, T.M. and Rinne, J. *Role of de novo biosynthesis in ecosystem scale monoterpene emissions from a boreal Scots pine forest*. Biogeosciences, 8, 8, 2247-2255, 2011.

# MEASUREMENTS OF CLUSTER COMPOSITION IN NEW PARTICLE FORMATION FROM SULPHURIC ACID, SMALL BASES, AND OXIDISED ORGANICS

S. SCHOBESBERGER<sup>1</sup>, H. JUNNINEN<sup>1</sup>, A. FRANCHIN<sup>1</sup>, F. BIANCHI<sup>2</sup>, J. DOMMEN<sup>2</sup>, N.M. DONAHUE<sup>3</sup>, J. DUPLISSY<sup>1</sup>, M. EHN<sup>1</sup>, K. LEHTIPALO<sup>1</sup>, G. LÖNN<sup>1</sup>, T. NIEMINEN<sup>1</sup>, I.K. ORTEGA<sup>1</sup>, M. SIPILÄ<sup>1</sup>, THE CLOUD COLLABORATION, T. PETÄJÄ<sup>1</sup>, M. KULMALA<sup>1</sup> and D.R. WORSNOP<sup>1,4</sup>

<sup>1</sup>Department of Physics, University of Helsinki, Helsinki, 00014, Finland

<sup>2</sup>Laboratory of Atmospheric Chemistry, Paul Scherrer Institut, Villigen, 5232, Switzerland

<sup>3</sup>Department of Chemical Engineering, Carnegie Mellon University, Pittsburgh, PA 15213-3890, USA

<sup>4</sup>Aerodyne Research, Inc., MA 01821-3976, USA

Keywords: ION CLUSTERS, NUCLEATION, ORGANICS, MASS SPECTROMETRY.

## INTRODUCTION

Atmospheric aerosol affects both health and climate. The climatic effects are due to direct interactions with solar radiation, as well as indirect effects by acting as seeds for cloud condensation nuclei. Up to half of global cloud condensation nuclei may be produced by the formation of new particles from gaseous precursors (Merikanto *et al.*, 2009). It is widely accepted that sulphuric acid (H<sub>2</sub>SO<sub>4</sub>) plays a major role (Riipinen *et al.*, 2007), but it is clear that H<sub>2</sub>SO<sub>4</sub> is not abundant enough to account, together with the ubiquitous water vapour, for new particle formation in the planetary boundary layer, where most new particle formation has been observed (Kulmala *et al.*, 2004). Instead, H<sub>2</sub>SO<sub>4</sub> needs to be stabilised to form initial molecular clusters. Proposed stabilisers are electric charge, water, ammonia (NH<sub>3</sub>), amines, and various oxidised organic molecules, such as organic acids. Electric charge, water and NH<sub>3</sub> were all shown to be indeed able to stabilise H<sub>2</sub>SO<sub>4</sub> clusters, but not effectively enough to explain particle formation rates in typical boundary layer conditions (Kirkby *et al.*, 2011). However, clusters of H<sub>2</sub>SO<sub>4</sub> with NH<sub>3</sub>, amines or both are observed in boundary layer particle formation events in the boreal forest. These observations suggest that small bases such as NH<sub>3</sub> do play a role in initially stabilising H<sub>2</sub>SO<sub>4</sub> clusters, but other compounds, such as oxidised organics, have to be involved from an early stage onward as well (Kulmala *et al.*, 2013).

The CLOUD (Clouds Leaving Outdoor Droplets) experiment at CERN aims at elucidating the first steps of atmospheric particle formation and growth. It is centred on a 26 m<sup>3</sup> stainless-steel aerosol chamber and built to highest standards to provide exceptionally low concentrations of contaminants and well-controlled conditions. A pion beam provided by CERN's Proton Synchrotron is available to increase the ionisation rate inside the chamber on demand. A suite of state-of-the-art instruments continuously samples the chamber's contents to investigate the particle formation in the chamber. So far, experiments were performed during six intensive campaigns to investigate particle formation from the systems of H<sub>2</sub>SO<sub>4</sub> plus NH<sub>3</sub>, dimethylamine (C<sub>2</sub>H<sub>7</sub>N), and/or oxidised organics derived from either pinanediol (C<sub>10</sub>H<sub>18</sub>O<sub>2</sub>) or  $\alpha$ -pinene (C<sub>10</sub>H<sub>16</sub>).

## METHODS

During the particle formation experiments, one or two atmospheric pressure interface time-of-flight mass spectrometers (APi-TOF) were deployed at the CLOUD chamber. The APi-TOF measures the exact mass of ions at a high resolving power (5300 Th/Th) and accuracy (< 10 ppm) (Junninen *et al.*, 2010). Vacuum inside the instrument draws the sample into the instrument's interface via a critical orifice, and ions are

then focused and guided to the mass spectrometer. The sampling method attempts to minimise fragmentation of ion clusters. No ionisation of the sample is performed, and only ions charged in the CLOUD chamber are detected. At CLOUD, one APi-TOF was either switched between measuring negatively and positively charged ions, or two APi-TOFs measured ions of each polarity simultaneously. The data were analysed using latest versions tofTools, a software package based on MATLAB, under development mainly at the University of Helsinki (Ehn *et al.*, 2012). Elemental compositions of most ions and ion clusters could be determined based mainly on their exact mass, and time series of ion counts could be established at an effective time resolution of 30 to 60 s. The identification of ion compositions was particularly successful if compared to ambient measurements, mainly due to the chamber's cleanliness, as well as due to the high ion number concentrations available when the pion beam on. Ion mass spectra obtained from the APi-TOFs can be presented as mass defect diagrams, where the mass defect (i.e. the deviation from the nominal, integer mass) of each ion is plotted against its exact mass. Each ion or ion cluster shows up as a circle, with its area scaled by ion count rate. The benefit of this diagram is that each elemental composition shows up at a unique location.

## RESULTS AND DISCUSSION

Initial particle formation experiments at CLOUD investigated particle formation and growth in the binary system of water + H<sub>2</sub>SO<sub>4</sub> and the ternary system of water + H<sub>2</sub>SO<sub>4</sub> + NH<sub>3</sub>. Water was usually too weakly bound to H<sub>2</sub>SO<sub>4</sub>-clusters to prevail long enough in the APi-TOF's vacuum to be observed. But the APi-TOF measurements showed that ion clusters grow by the step-wise addition of H<sub>2</sub>SO<sub>4</sub> and NH<sub>3</sub> molecules, (Kirkby *et al.*, 2011). The amount of NH<sub>3</sub> and H<sub>2</sub>SO<sub>4</sub> respectively adding to the growing clusters depends on the exact mix of vapours in the CLOUD chamber (e.g. Fig. 1).

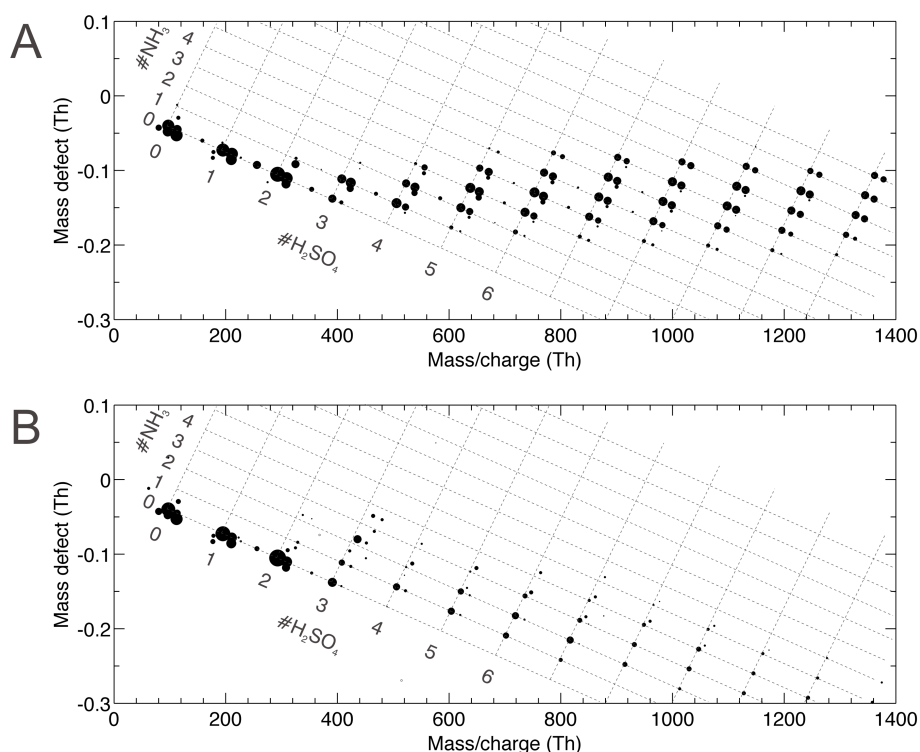


Figure 1. Anion mass spectra for two similar yet different experiments. A: Ion clusters forming during new particle formation from H<sub>2</sub>SO<sub>4</sub> and NH<sub>3</sub>. They are mostly of the type (NH<sub>3</sub>)<sub>m</sub>(H<sub>2</sub>SO<sub>4</sub>)<sub>n</sub>HSO<sub>4</sub><sup>-</sup>, marked by the dashed grid, and (NH<sub>3</sub>)<sub>m</sub>(H<sub>2</sub>SO<sub>4</sub>)<sub>n</sub>HSO<sub>5</sub><sup>-</sup>, offset from the grid to the lower right due to the extra mass and the negative mass defect of the extra oxygen atom. B: Ion clusters forming in almost the same conditions, except for a much lower concentration of NH<sub>3</sub>. They are again mostly of the type (NH<sub>3</sub>)<sub>m</sub>(H<sub>2</sub>SO<sub>4</sub>)<sub>n</sub>HSO<sub>4</sub><sup>-</sup>, marked by the dashed grid, but contain a smaller number of NH<sub>3</sub> molecules.

In subsequent experiments, dimethylamine, pinanediol and  $\alpha$ -pinene were added to the mix in the chamber as well. The rates of formation of particles, their rates of growth, as well as the composition of growing ion clusters were found to always react on the specific composition of the vapours present in the CLOUD chamber. Ions then included mixed clusters of sulphuric acid and dimethylamine and/or oxidised organic compounds arising from the oxidation of either pinanediol or  $\alpha$ -pinene. Some of these oxidised organics are surprisingly highly oxidised, and in part similar to those observed in earlier laboratory experiments (Ehn *et al.*, 2012). In particular the clusters containing such oxidised organics are believed to be relevant to the first steps of new particle formation in events observed in the boreal forest (Kulmala *et al.*, 2013).

We observe a very wide range of oxidised organic compounds, complicating the attribution of elemental compositions to peaks in the ion mass spectra, with many peaks containing signal from more than one elemental composition (e.g. Fig. 2). However, the ion mass spectra still typically contain a smaller variety of compounds than those from ambient measurements, and feature a superior signal-to-noise ratio. Therefore, using tofTools, a large part of the spectra can be de-convoluted and most ions up to about 500 Th identified, providing valuable insights on which and how oxidised organics participate in the first steps of new particle formation, together with sulphuric acid and small bases such as  $\text{NH}_3$  and amines.

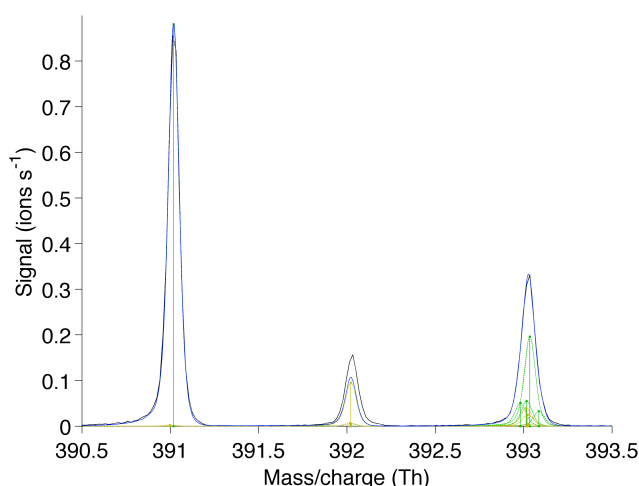


Figure 2. Part of an anion mass spectrum during new particle formation from  $\text{H}_2\text{SO}_4$  and organics obtained from the oxidation of pinanediol. All peaks here are from ions mainly consisting of oxidised organics. The peak at 391 Th only contains signal from a single elemental composition, and most of the peak at 392 Th is attributed to its main isotope (yellow). Most of the peak at 393 Th, however, can only be explained by a mix of elemental compositions, but again mostly consisting of oxidised organic compounds (green).

## ACKNOWLEDGEMENTS

CERN's support of CLOUD with important technical and financial resources and provision of a particle beam from the Proton Synchrotron is gratefully acknowledged. This research was funded by the EC 7th Framework Programme (Marie Curie Initial Training Network "CLOUD-ITN", grant no. 215072), the ERC Advanced Grant "ATMNUCLE" (no. 227463), the Academy of Finland via the Centre of Excellence programme (project no. 1118615) and grant no. 1133872, the German Federal Ministry of Education and Research (project no. 01LK0902A), the Swiss National Science Foundation (project nos. 206621\_125025 & 206620\_130527), the Austrian Science Fund (project nos. P19546 & L593), the Portuguese Foundation for Science and Technology (project no. CERN/FP/116387/2010), the Russian Foundation for Basic Research (grant N08-02-91006-CERN), the Davidow Foundation, and the U.S. National Science Foundation (grants AGS1136479 and CHE1012293).

## REFERENCES

- Ehn, M., E. Kleist, H. Junninen, T. Petäjä, G. Lönn, S. Schobesberger, M. Dal Maso, A. Trimborn, M. Kulmala, D.R. Worsnop, A. Wahner, J. Wildt, and Th.F. Mentel (2012). Gas phase formation of extremely oxidized pinene reaction products in chamber and ambient air, *Atmos. Chem. Phys.* **12**, 5113-5127.
- Junninen, H., M. Ehn, T. Petäjä, L. Luosujärvi, T. Kotiaho, R. Kostianen, U. Rohner, M. Gonin, K. Fuhrer, M. Kulmala and D.R. Worsnop (2010). A high-resolution mass spectrometer to measure atmospheric ion composition, *Atmos. Meas. Tech.* **3**, 1039–1053.
- Kirkby, J., J. Curtius, J. Almeida, E. Dunne, J. Duplissy, S. Ehrhart, A. Franchin, S. Gagné, L. Ickes, A. Kürten, A. Kupc, A. Metzger, F. Riccobono, L. Rondo, S. Schobesberger, G. Tsagkogeorgas, D. Wimmer, A. Amorim, F. Bianchi, M. Breitenlechner, A. David, J. Dommen, A. Downard, M. Ehn, R.C. Flagan, S. Haider, A. Hansel, D. Hauser, W. Jud, H. Junninen, F. Kreissl, A. Kvashin, A. Laaksonen, K. Lehtipalo, J. Lima, E.R. Lovejoy, V. Makhmutov, S. Mathot, J. Mikkilä, P. Minginette, S. Mogo, T. Nieminen, A. Onnela, P. Pereira, T. Petäjä, R. Schnitzhofer, J.H. Seinfeld, M. Sipilä, Y. Stozhkov, F. Stratmann, A. Tomé, J. Vanhanen, Y. Viisanen, A. Vrtala, P.E. Wagner, H. Walther, E. Weingartner, H. Wex, P.M. Winkler, K.S. Carslaw, D.R. Worsnop, U. Baltensperger and M. Kulmala (2011). Role of sulphuric acid, ammonia and galactic cosmic rays in atmospheric aerosol nucleation, *Nature* **476**, 429-433.
- Kulmala, M., H. Vehkamäki, T. Petäjä, M. Dal Maso, A. Lauri, V.-M. Kerminen, W. Birmili and P.H. McMurry (2004). Formation and growth rates of ultrafine atmospheric particles: a review of observations. *J. Aerosol Sci.* **35**, 143-176.
- Kulmala, M., J. Kontkanen, H. Junninen, K. Lehtipalo, H.E. Manninen, T. Nieminen, T. Petäjä, M. Sipilä, S. Schobesberger, P. Rantala, A. Franchin, T. Jokinen, E. Järvinen, M. Äijälä, J. Kangasluoma, J. Hakala, P.P. Aalto, P. Paasonen, J. Mikkilä, J. Vanhanen, J. Aalto, H. Hakola, U. Makkonen, T. Ruuskanen, R.L. Mauldin, J. Duplissy, H. Vehkamäki, J. Bäck, A. Kortelainen, I. Riipinen, T. Kurtén, M.V. Johnston, J.N. Smith, M. Ehn, T.F. Mentel, K.E.J. Lehtinen, A. Laaksonen, V.-M. Kerminen and D.R. Worsnop (2013). Direct observations of atmospheric aerosol nucleation. *Science* **339**, 943-946.
- Merikanto, J., D.V. Spracklen, G.W. Mann, S.J. Pickering and K.S. Carslaw (2009). Impact of nucleation on global CCN. *Atmos. Chem. Phys.* **9**, 8601-8616.
- Riipinen, I., S.-L. Sihto, M. Kulmala, F. Arnold, M. Dal Maso, W. Birmili, K. Saarnio, K. Teinilä, V.-M. Kerminen, A. Laaksonen and K.E.J. Lehtinen (2007). Connections between atmospheric sulphuric acid and new particle formation during QUEST III–IV campaigns in Heidelberg and Hyytiälä, *Atmos. Chem. Phys.* **7**, 1899–1914.

## NEW TOOL FOR CO<sub>2</sub> FLUX GAP-FILLING AND FLUX SEPARATION

L. ŠIGUT<sup>1,2</sup>, I. MAMMARELLA<sup>3</sup>, P. KOLARI<sup>3</sup> AND P. SEDLÁK<sup>2,4</sup>

<sup>1</sup>Department of Physics, Faculty of Science, Ostrava University, 30. dubna 22, CZ-701 03 Ostrava 1, Czech Republic.

<sup>2</sup>CzechGlobe – Global Change Research Centre AS CR, v.v.i., Bělidla 986/4a CZ-603 00 Brno, Czech Republic.

<sup>3</sup>University of Helsinki, Gustaf Hållströmin Katu 2, FIN-00014 Helsinki, Finland.

<sup>4</sup>Institute of Atmospheric Physics AS CR, v.v.i., Boční II 1401, CZ-141 31 Praha 4, Czech Republic.

**Keywords:** EDDY COVARIANCE, CARBON BALANCE, ECOSYSTEM RESPIRATION, GROSS PRIMARY PRODUCTION.

### INTRODUCTION

Eddy covariance method (EC) is one of the most accurate and direct approaches for measurements of fluxes of matter and energy on the level of whole ecosystem. CO<sub>2</sub> fluxes data acquired using the global network of EC flux towers help us to better understand the impacts of natural and anthropogenic phenomena on the global carbon balance. Comparisons among different sites are usually performed on annual sums of net ecosystem exchange (NEE). However, the average data coverage during a year is only 65% due to system failures or data rejection (Falge et al., 2001). Therefore robust and consistent gap-filling methods for the global network were created mainly within project CarboEurope-IP (Lasslop et al., 2010, Reichstein et al., 2005). Nowadays, the EC is also used in complex terrains on the edge of its applicability (e.g. hills, cities) such as mountain forest site at Bílý Kříž, Czech Republic [basic general information about the complicated air flow in topographically complex terrain can be found e.g. in Foken (2008)]. This requires revisiting of generally applied algorithms for computation of annual sums of NEE. The aim of this study is assessment of performance and correctness of the new tool for CO<sub>2</sub> flux gap-filling and flux separation in comparison with standard algorithms. It also presents the first step before the attempt to estimate defensible annual sums of NEE for complex terrain site with help of auxiliary biomass inventory and soil chamber measurements.

### METHODS

The proposed R software script uses gap-filling method based on parameterisation of “functional models” which at the same time serve for flux separation of NEE to gross primary productivity (GPP) and ecosystem respiration ( $R_{eco}$ ). For  $R_{eco}$  there is an exponential response to temperature well expressed by Arrhenius type  $R_{eco}$  function (Johnson a Thornley, 1985, Hikosaka, 1997):

$$R_{eco} = R_{10} \cdot Q_{10}^{\frac{T-T_{10}}{10}},$$

where  $R_{10}$  is the  $R_{eco}$  at reference temperature 10 °C ( $T_{10}$ ) and  $Q_{10}$  determines change in respiration rate resulting from a 10 °C increase in temperature  $T$ . Light response curve, i.e. response of GPP to photosynthetic active radiation, is described by logistic sigmoid function (Moffat, 2010):

$$NEE = 2 \cdot GPP_{\max} \cdot \left( 0.5 - \frac{1}{1 + \exp\left(\frac{-2 \cdot \alpha \cdot PAR}{GPP_{\max}}\right)} \right) + R_{eco},$$

where  $\alpha$  is apparent quantum yield at low irradiances,  $GPP_{\max}$  is the asymptotic maximum assimilation rate or optimum gross primary production under high light level.  $R_{eco}$  parameterisation is performed using night-time NEE only as photosynthesis is not present during night. Directly measured NEE can be in this way separated to  $R_{eco}$  and GPP. The code was designed with the emphasis on visualisation of the whole procedure and on its modularity. It means that the whole process can be controlled and parts of the script switched on/off. Additional modules can be also added later. Also disturbance days were introduced which allow to mark dates when the state of ecosystem changed abruptly typically due to tillage or harvesting. Gap-filling would be then performed separately for homogenous subperiods. Part of the procedure is also determining whether photosynthesis is occurring during particular day. It relies on soil and air temperature thresholds derived for each individual site and statistical testing. Storage addition and ustar filtering is included but the determination of ustar threshold is not part of the script.

## CONCLUSIONS

The computed annual and monthly sums of NEE, GPP and  $R_{eco}$  for different sites and years will be compared with estimates produced by standard algorithms [Menzer, O. (2011-2012)]. This way overall assessment of the here proposed method will be obtained and we will be able to address and analyse the biggest differences. Potential strengths or weaknesses of this approach will be discussed. We expect that this algorithm will become another alternative to perform gap-filling and flux separation and it will also serve as a backbone for complex sites solution.

## ACKNOWLEDGEMENTS

This work was supported by OU SGS20/PřF/2013, CZ.1.05/1.1.00/02.0073 and CZ.1.07/2.4.00/31.0056 grants.

## REFERENCES

- Falge, E., Baldocchi, D., Olson, R. et al. (2001). Gap filling strategies for defensible annual sums of net ecosystem exchange, *Agricultural and Forest Meteorology* **107**, 43–69.
- Reichstein, M., Falge, E., Baldocchi, D. et al. (2005). On the separation of net ecosystem exchange into assimilation and ecosystem respiration: review and improved algorithm. *Global Change Biology* **11**, 1424–1439.
- Lasslop, G., Reichstein, M., Papale, D. et al. (2010). Separation of net ecosystem exchange into assimilation and respiration using a light response curve approach: critical issues and global evaluation. *Global Change Biology* **16**(1), 187–208.
- Johnson, I.R. and Thornley, J.H.M. (1985). Temperature dependence of plant and crop processes. *Annals of Botany* **55**, 1–24.
- Hikosaka, K. (1997). Modelling optimal temperature acclimation of the photosynthetic apparatus in C3 plants with respect to nitrogen use. *Annals of Botany* **80**, 721–730.
- Moffat, A.M. (2010). *A new methodology to interpret high resolution measurements of net carbon fluxes between the terrestrial ecosystems and the atmosphere*, (Ph.D. thesis, Friedrich Schiller University, Jena).
- Menzer, O. (2011-2012). Eddy covariance gap-filling & flux-partitioning tool. *Max Planck Institute for Biogeochemistry*, [cit. 2013-09-04], Web. Avail. from: <http://www.bgc-jena.mpg.de/~MDIwork/eddyproc/>

# GLOBAL VEGETATION SIMULATIONS WITH ISOPRENE AND MONOTERPENES EMISSIONS FOR PAST 8000 YEARS

S. SMOLANDER<sup>1</sup>, A. ARNETH<sup>2</sup> and T. VESALA<sup>1</sup>

<sup>1</sup>Department of Physics, University of Helsinki, Finland.

<sup>2</sup>Institute of Meteorology and Climate Research, Karlsruhe Institute of Technology,  
Garmisch-Partenkirchen, Germany.

Keywords: BVOC, ISOPRENE, MONOTERPENES, DYNAMIC VEGETATION MODEL.

## INTRODUCTION

Past atmospheric concentrations of biogenic volatile organic compounds (BVOCs) have contributed both to the formation of secondary organic aerosols (SOAs) in past atmospheres, and the oxidative capacity of the atmosphere. The hydroxyl radical (OH) acts as the main atmospheric sink for methane, and BVOCs and methane compete for being oxidized by OH. We have run global dynamic vegetation simulations for the past 8000 years to estimate past levels of isoprene and monoterpenes emissions for both pre-industrial and pre-agriculture times. We used two different scenarios of the extent of past human land use to provide a high and a low estimate of the effect.

## METHODS

LPJ-GUESS (Smith et al. 2001, Sitch et al. 2003, Gerten et al. 2004, Hickler et al. 2006) is a process-based dynamic vegetation model. Using a daily time step, physical drivers (temperature, precipitation, sunlight, ambient CO<sub>2</sub> concentration, soil type) are used to simulate ecosystem processes (photosynthesis, evapotranspiration, vegetation and soil respiration, decomposition in the soil, and also BVOC emissions). Soil carbon dynamics is modelled with 3 pools: litter, fast soil carbon, slow soil carbon. Some processes (allocation of accumulated carbon to vegetation growth, mortality, fire disturbances) are accounted for yearly. Vegetation is represented with different plant function types (PFTs), which differ in physiological, morphological and life history characteristics and bioclimatic limits. Our simulation use 11 PFTs (see Table 1). Each gridcell will grow a combination PFTs, depending on climate, competition, succession and disturbances.

Plant Functional Type	$E_{Isoprene}$	$E_{Monoterpenes}$	Monoterpenes storage?
Boreal needleleaved evergreen tree	8	4.8	50%
Boreal needleleaved evergreen tree	8	4.8	50%
Boreal needleleaved summergreen tree	8	4.8	50%
Shade-tolerant temperate broadleaved summergreen tree	45	1.6	no
Shade-intolerant broadleaved summergreen tree	45	1.6	no
Temperate broadleaved evergreen tree	24	1.6	no
Tropical broadleaved evergreen tree	24	0.8	no
Tropical broadleaved evergreen tree	24	0.8	no
Tropical broadleaved raingreen tree	45	2.4	no
Cool (C3) grass	16	1.6	50%
Warm (C4) grass	8	2.4	50%

Table 1. Emission factors, in  $\mu\text{g}(\text{C in emissions}) \text{ g}(\text{C in biomass})^{-1} \text{ h}^{-1}$ , for the 11 Plant Functional Types

The BVOC emission module (based on Niinemets et al. 1999 and Arneth et al. 2007 for isoprene emissions and on Niinemets et al. 2002 and Schurgers et al. 2009 for monoterpene emissions) links the BVOC production to the electron transfer rate, as calculated by the photosynthesis model. The emission rates for different PFTs are scaled so that in standard conditions (reference light, temperature and ambient CO<sub>2</sub>) the emissions per unit dry leaf biomass are as in Table 1.

We used two different estimates of the spatial distribution of human land use during the last 8000 years: one by Kaplan et al. (2010), here labeled KK10, and one by Klein Goldewijk et al. (2011), here labeled HYDE 3.1. Although based on very similar estimate on the human population sizes (see Fig. 1 in Kaplan et al. 2010), the two reconstructions arrive at quite different estimates of area under human land use before modern times (Fig. 1). Kaplan et al. (2010) have assumed that humans start to use land more intensively, and thus the land area required per capita decreases, as population density increases, whereas per capita need for land is assumed both much smaller, and less variable, by Klein Goldewijk et al. (2011) (see Fig. 2 in Kaplan et al. 2010).

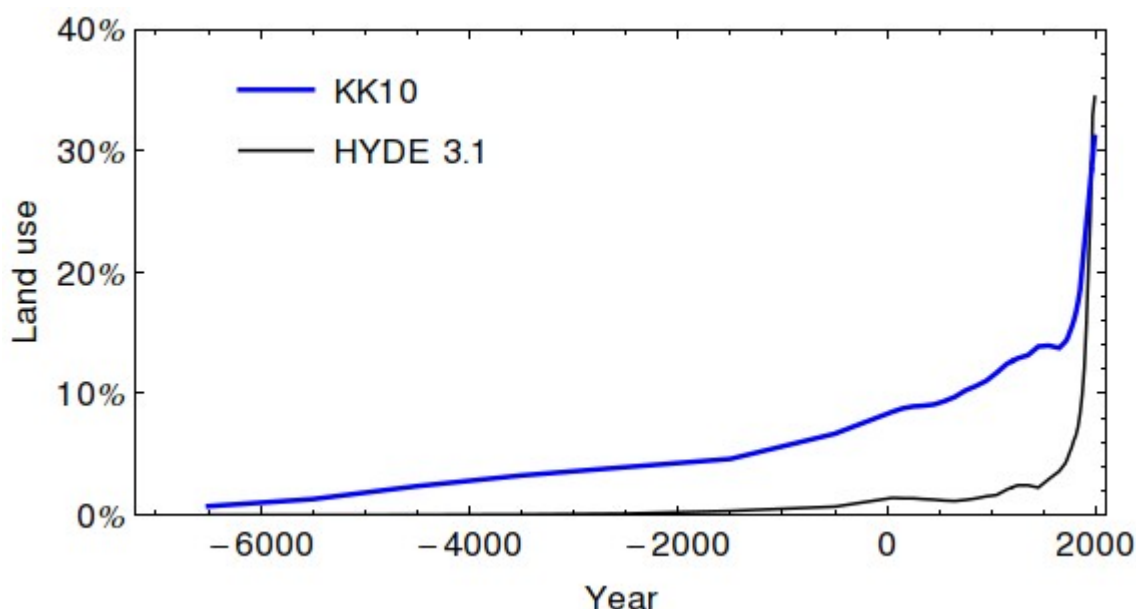


Figure 1. Fraction of total land area under human land use in the two scenarios, KK10 and HYDE 3.10.

## RESULTS

The KK10 land use scenario starts a larger extent of human land use in much earlier times than the HYDE 3.10 land use scenario. Coming to modern times, they finally converge to very similar extent of human land use. The usual pattern is that forested areas, with broadleaved or coniferous trees with high emission factors (see Table 1) are being replaced with agricultural land, modelled as C3 or C3 grass, which have lower emission factors (Figs. 2 and 3). Especially in areas where human agricultural land use has started early, like Middle-East, Europe and East and South Asia, also the emissions have decreased in tandem.

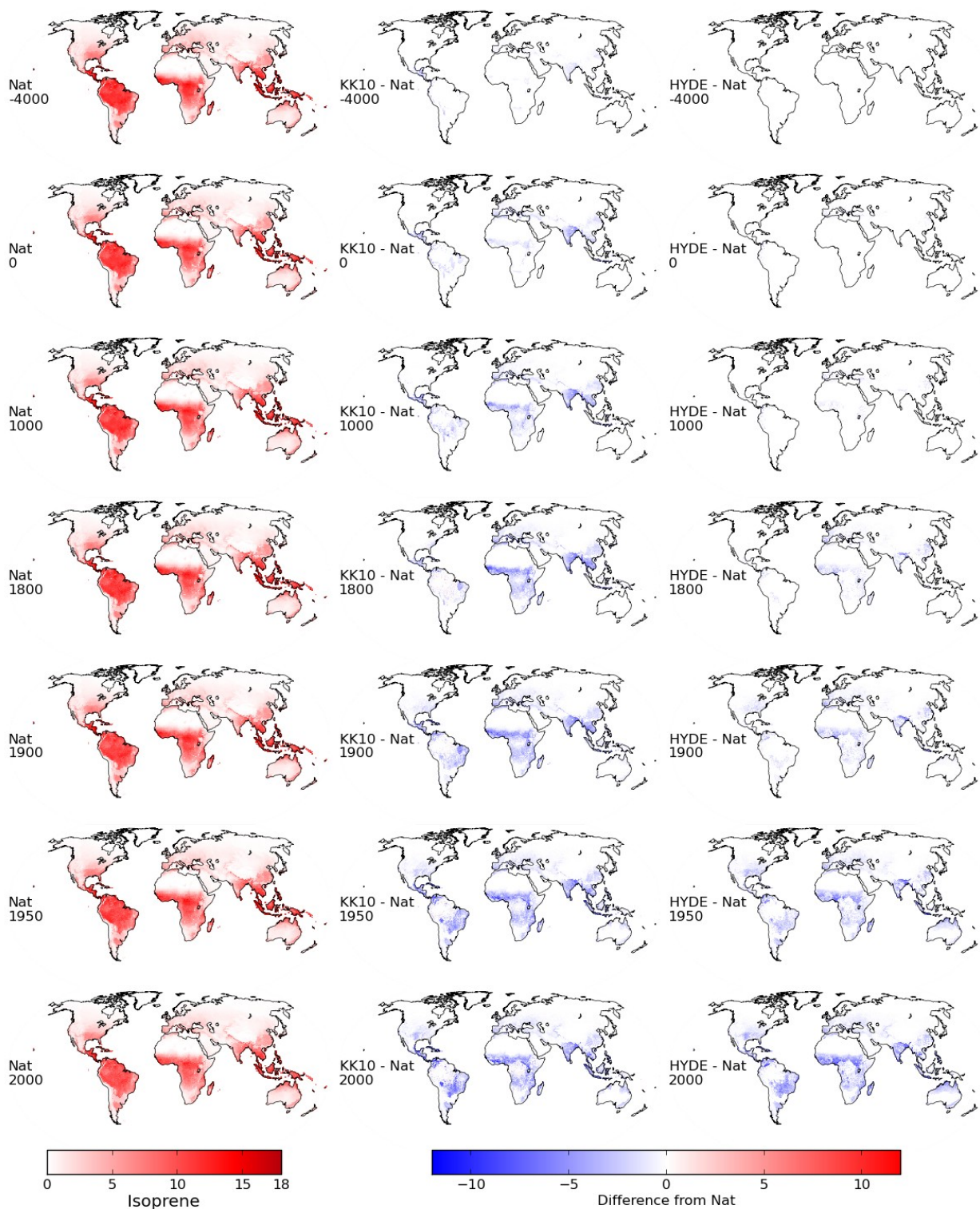


Figure 2. Isoprene emissions ( $\text{gC m}^{-2} \text{a}^{-1}$ ) at selected timepoints for the natural (no human landuse) scenario, and how the KK10 and HYDE 3.1 scenario emissions differ from that.

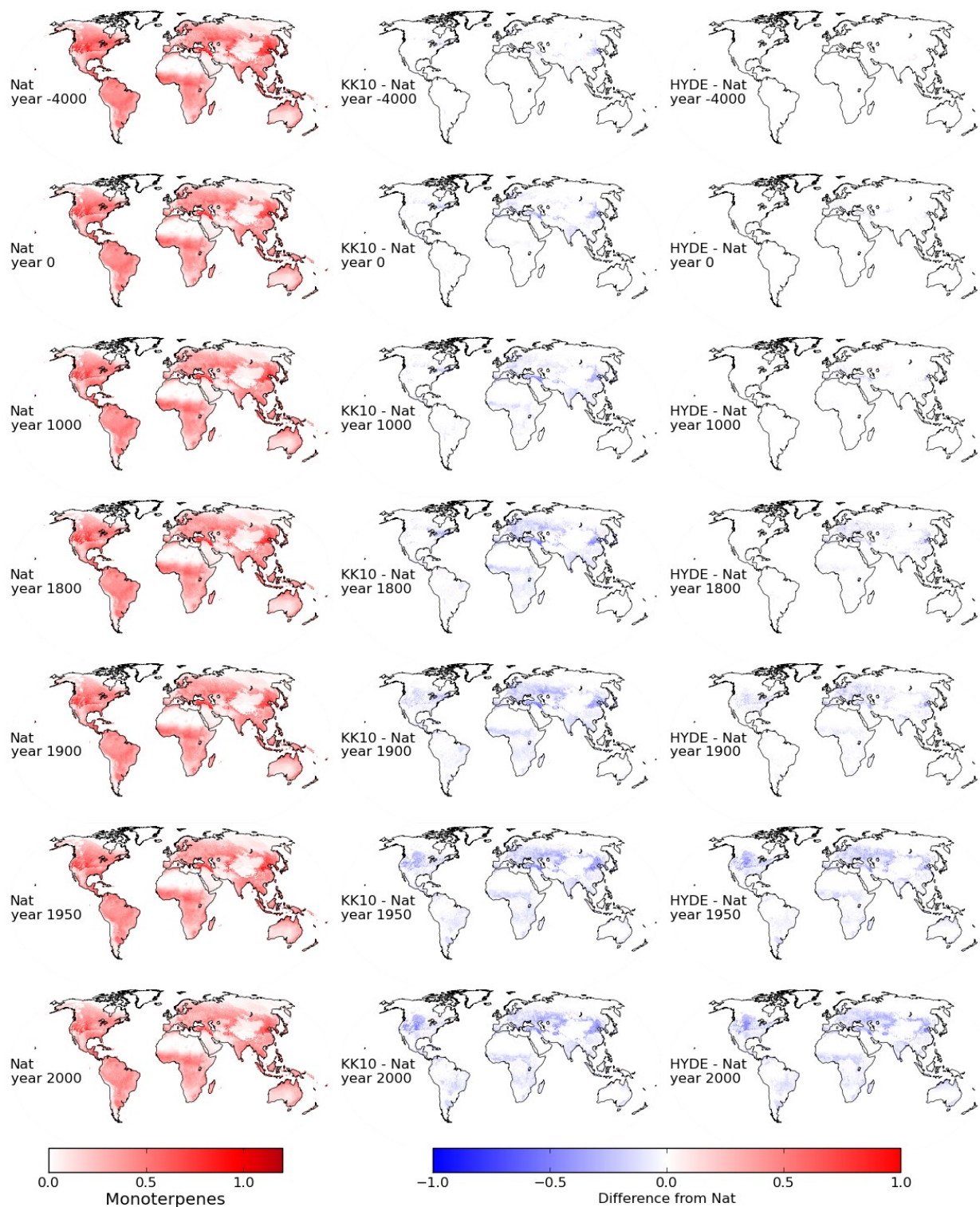


Figure 3. Monoterpenes emissions (gC m<sup>-2</sup> a<sup>-1</sup>) at selected timepoints for the natural (no human landuse) scenario, and how the KK10 and HYDE 3.1 scenario emissions differ from that.

## ACKNOWLEDGEMENTS

Financial support from the Academy of Finland (132100) and computational resources from CSC – IT Center for Science Ltd. are all gratefully acknowledged.

## REFERENCES

- Arneth, A., Niinemets, Ü., Pressley, S., Bäck, J., Hari, P., Karl, T., Noe, S., Prentice, I. C., Serça, D., Hickler, T., Wolf, A. and Smith, B. (2007). Process-based estimates of terrestrial ecosystem isoprene emissions: incorporating the effects of a direct CO<sub>2</sub> isoprene interaction. *Atmos. Chem. Phys.*, 7: 31-53.
- Gerten D, Schaphoff S, Haberlandt U, Lucht W, Sitch S (2004). Terrestrial vegetation and water balance —hydrological evaluation of a dynamic global vegetation model. *J Hydrol* 286:249– 270
- Hickler T, Prentice IC, Smith B, Sykes MT, Zaehle S (2006). Implementing plant hydraulic architecture within the LPJ Dynamic Global Vegetation Model. *Global Ecol Biogeogr* 15:567–577
- Kaplan, J. O., Krumhardt, K. M., Ellis, E. C., Ruddiman, W. F., Lemmen, C., & Goldewijk, K. K. (2011). Holocene carbon emissions as a result of anthropogenic land cover change. *The Holocene*, 21(5), 775-791.
- Klein Goldewijk, K., Beusen, A., Van Drecht, G., & De Vos, M. (2011). The HYDE 3.1 spatially explicit database of human-induced global land-use change over the past 12,000 years. *Global Ecology and Biogeography*, 20(1), 73-86.
- Niinemets, U., Tenhunen, J. D., Harley, P. C., and Steinbrecher, R. (1999). A model of isoprene emission based on energetic requirements for isoprene synthesis and leaf photosynthetic properties for *Liquidambar* and *Quercus*. *Plant, Cell, Environ.*, 22, 1319–1335.
- Niinemets, Ü., Seufert, G., Steinbrecher, R. and Tenhunen, J. D. (2002). A model coupling foliar monoterpene emissions to leaf photosynthetic characteristics in Mediterranean evergreen *Quercus* species. *New Phytol.*, 153:257–275.
- Schurgers, G., Arneth, A., Holzinger, R., & Goldstein, A. H. (2009). Process-based modelling of biogenic monoterpene emissions combining production and release from storage. *Atmos. Chem. Phys.*, 9(10), 3409-3423.
- Sitch, S., Smith, B., Prentice, I. C., Arneth, A., Bondeau, A., Cramer, W., Kaplan, J. O., Levis, S., Lucht, W., Sykes, M. T., Thonicke, K., and Venevsky, S. (2003). Evaluation of ecosystem dynamics, plant geography and terrestrial carbon cycling in the LPJ dynamic global vegetation model, *Global Change Biol.*, 9, 161– 185.
- Smith, B., Prentice, I. C., and Sykes, M. T. (2001). Representation of vegetation dynamics in the modelling of terrestrial ecosystems: comparing two contrasting approaches within European climate space, *Glob. Ecol. Biogeosci.*, 10, 621–637.

## A PORTABLE CLUSTER CALIBRATION UNIT

G.STEINER<sup>1,2</sup>, M. BREITENLECHNER<sup>2</sup>, A. HANSEL<sup>2</sup>, T. PETÄJÄ<sup>1</sup>, M. KULMALA<sup>1</sup>

<sup>1</sup>Division of Atmospheric Sciences, Department of Physics, University of Helsinki, Finland

<sup>2</sup>Institute of Ion Physics and Applied Physics, University of Innsbruck, Austria

Keywords: DMA, electrical mobility, molecular clusters, calibration

### INTRODUCTION

Recent breakthroughs in the investigation of New Particle Formation (NPF) – a process strongly contributing to Earth's radiative balance and playing a key role in climate change – were achieved by using newly developed instrumentation. The new instruments comprise Atmospheric Pressure interface Time-Of-Flight (APi-TOF) mass spectrometers for the detection of charged and neutral clusters, but also condensation particle counters that are able to access the particle size range below 3 nm. Despite their sophisticated technique, the new instruments are facing a major problem: their performance is highly sensitive to different operating conditions and settings. Accordingly, each setting requires a thorough calibration. Unfortunately, the necessary instrumentation is currently only available to a very limited number of research groups and requires a laboratory based operation.

Here we present a solution to the problem: a field portable ion cluster calibration unit, based on high resolution ion mobility spectrometry, to perform the necessary instrumental calibration on-site during the measurement campaign.

### METHODS

A crucial prerequisite for using all the newly developed mass spectrometers for quantitative cluster ion measurements is the knowledge of the total transmission efficiency of cluster ions at given  $m/z$ . Without the knowledge of the transmission efficiency over the whole mass range, the actual ionic cluster concentration cannot be determined quantitatively. Since the transmission curve is strongly dependent on the voltage settings of the time-of-flight mass spectrometer, as well as of the atmospheric interface parts, every new voltage setting requires a completely new calibration of the cluster transmission curve of the instrument. Accordingly, for a versatile use of the newly developed mass spectrometers, a field portable cluster calibration unit is of great benefit.

It is important to mention that not only mass spectrometric devices but virtually all instrumentation (e.g. recent developments of Condensation Particle Counters (CPCs, Iida et al., 2009; Vanhanen et al., 2011) which is aimed to measure molecular cluster and small nanoparticles at atmospheric conditions require a proper calibration.

High Resolution Electrical Mobility Spectrometry (HR-EMS) is a measurement technique, where particles and clusters are classified according to their electrical mobility at ambient pressure. The idea of mobility classification goes back to John Zeleny and his work at the Cavendish laboratories in England around 1898 as thoroughly summarized by Flagan in his overview of the history of electrical aerosol measurements (Flagan, 1998). Pioneering work was done by Knutson and Whitby (1975a, 1975b) making the EMS method a standard technique in the field of aerosol science by improving the theory as well as the classifying instrumentation.

The core component for electrostatic mobility measurements is the so called Differential Mobility Analyzer (DMA). Most commonly, DMAs are designed as cylindrical capacitors. Nevertheless, there exist

designs with a rectangular flow channel in a planar plate design (Fernández de la Mora, 1999) and radial designs (Zhang et al. 1995) which are also very successful for rather specific applications.

One remarkable feature of the DMA is the possibility to use it as an analyzing device as well as a classifying device. That said, together with an appropriate aerosol generator, it can be used to classify one specific mobility band out of a broad particle distribution to serve as a source of monodispersed particles.

As the behaviour of nanometer sized particles down to molecular clusters has become of special interest in the last years (e.g. Winkler et al. 2008, Kulmala et al. 2013), several authors have reported improved DMA designs. Recent developments of High Resolution Differential Mobility Analyzers (HR-DMA; Rossell-Llompart et al. 1996; Rosser and Fernández de la Mora 2005; Brunelli et al. 2009, Steiner et al. 2010, Fernández de la Mora and Kozłowski 2013) are capable of accessing the size range below 3 nm and are also optimized for high resolution mobility measurements of molecular clusters.

The core components of the portable cluster calibration unit consist of a HR-DMA and an electrospray ion source. The HR-DMA that was used in the current work is called UDMA (Steiner et al. 2010). This device was developed at the University of Vienna and is based on the well-known Vienna-DMA type design (Winklmayr et al., 1991). At optimal operating conditions, the UDMA has a resolution power of  $R=40$  at a cluster diameter of 1.4 nm. Because of the high resolution power, the UDMA can be used as source of highly monodisperse test clusters or test aerosols by combination with a suitable ion source.

Since the discovery of electrospray ionization by John Fenn (Nobel laureate in chemistry in 2002) and coworkers in 1989 (Fenn et al., 1989), the electrospray method is widely used for the generation of well-defined nanometer sized particles and molecular clusters for various scientific fields. Its applications are ranging from the use as ionization source for mass spectrometric investigations to the production of ion beams in a vacuum for electrical propulsion in space (e.g. Romero-Sanz et al., 2005). Basically, a liquid sample – that is meant to be atomized – is raised to a high voltage potential and exposed to a strong electric field. The electric field induces a surface charge on the liquid that forces the surface of the liquid into a conical shape (due to the balance between surface tension and electrical forces), called Taylor cone (Taylor, 1964). The electrical forces further cause a jet of droplets emanating from the tip of the Taylor cone and dispersing into a fine spray of highly charged droplets (see Fig. 1).

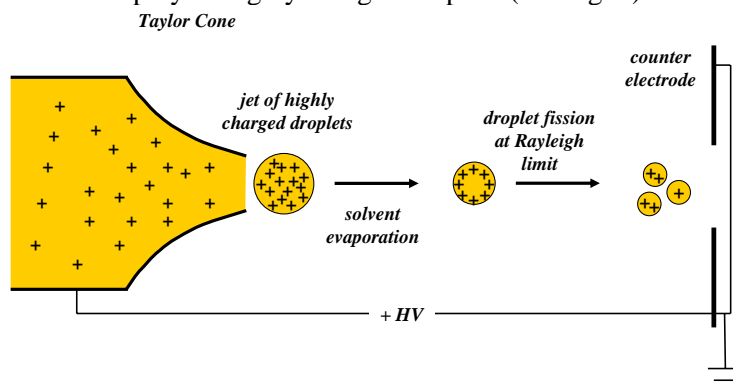


Fig. 1 : Operating principle of an electrospray generator in positive ion mode (negative mode is also possible).

Subsequently, the solvent liquid evaporates resulting in a coulombic fission of the droplets when Rayleigh's charge limit is exceeded (e.g. Hinds, 1999). This process finally leads to (in the ideal case) singly charged ultrafine particles or clusters. Electrosprayed nanodroplets of tetra-alkyl halide salts dissolved in alcohol as reviewed by Ude & Fernández de la Mora (2005) have been found to be well qualified molecular mass- and mobility standards for HR-DMA and mass spectrometer calibration purposes. Their mobility distribution yields to unique patterns of several distinctively separated peaks, associated with stable cluster species of the form  $A^{+/-}(AB)_n$  where "A" denotes in the positive mode the tetra-alkyl ammonium ion (monomer) and in the negative mode the halide anion. "AB" stands for the neutral tetra-alkyl ammonium halide molecule. As an example, a typical mobility spectrum of tetra-heptyl

ammonium bromide in positive mode (0.05 mMol/L solution in spectroscopy grade methanol) is shown in Fig. 2.

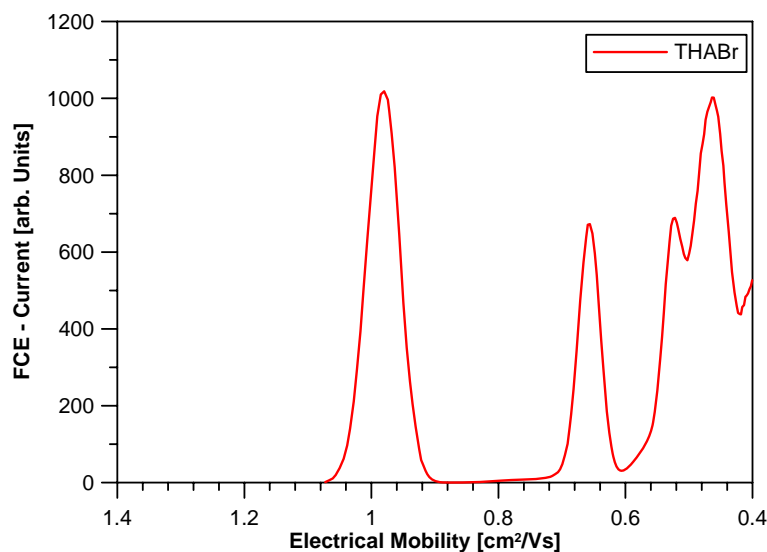


Fig. 2 Electrical mobility spectrum of tetra-heptyl ammonium bromide. The peak at  $Z=0.97 \text{ cm}^2/\text{Vs}$  corresponds to the  $A^+$  cluster (tetra-heptyl ammonium ion; monomer) and the peak at  $Z=0.65 \text{ cm}^2/\text{Vs}$  to the  $A^+(AB)_1$  cluster (dimer). The trimer cluster  $A^+(AB)_2$  is found at  $Z=0.53 \text{ cm}^2/\text{Vs}$  but overlapping with the signal of larger, multiply charged clusters.

The UDMA can be used to classify one of those peaks (one cluster species) and feed it to the inlet of an atmospheric pressure interface mass spectrometer (e.g. APi-TOF, CI-API-TOF) or any other instrumentation that requires a stable concentration of certain sized charged clusters. The corresponding setup for atmospheric pressure interface mass spectrometer is shown in Fig. 3.

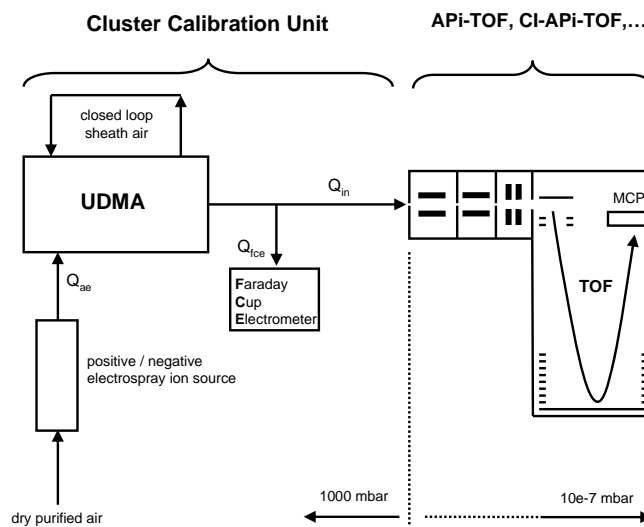


Fig. 3 : Filtered pressurized air is used as carrier gas for an electrospray ion source. The ions are separated with respect to their electrical mobility by the high resolution UDMA and subsequently enter the TOF mass spectrometer. Simultaneously, a Faraday-Cup electrometer measures the current of the ions exiting the UDMA, thereby monitoring the concentration of ions at the inlet of the TOF mass spectrometer.

## CONCLUSIONS

We have set up a robust field portable cluster calibration unit as source of highly monodispersed charged mobility and mass standards for both polarities in the size range below 2nm. The unit can be used as versatile tool for the mobile, on-site calibration of any instrumentation that requires a stable cluster/particle source operating at atmospheric pressure.

## ACKNOWLEDGEMENTS

This study was supported by the Finish Centre of Excellence and the University of Innsbruck.

## REFERENCES

- Brunelli, N.A., Flagan, R.C., Giapis, K.P., (2009) Radial Differential Mobility Analyzer for One Nanometer Particle Classification. *Aerosol Sci. Technol.*, 43, 1, 53-59
- Fenn, J. B., Mann, M., Meng, C. K., Wong, S. K., and Whitehouse, C. (1989) Electrospray ionization for mass spectrometry of large biomolecules. *Science* 246, 64–71.
- Fernández de la Mora, J. (1999) Method and apparatus for separation of ions in a gas for mass spectrometry. *United States Patent* 5,869,831.
- Fernández de la Mora, J., Kozlowski, J. (2013) Hand-held differential mobility analyzers of high resolution for 1-30nm particles: design and fabrication considerations. *J. Aerosol Sci.*, 57, 45-53
- Flagan, R.C. (1998) History of Electrical Aerosol Measurements. *Aerosol Sci. Technol.*, 28:4, 301-380
- Hinds, W. (1999) Aerosol Technology: Properties, behaviour, and measurement of airborne particles. 2nd edition, Wiley and Sons, New York.
- Iida, K., Stolzenburg, M.R., McMurry, P.H. (2009) Effect of Working Fluid on Sub-2nm Particle Detection with a Laminar Flow Ultrafine Condensation Particle Counter. *Aerosol Sci. Technol.*, 43:1, 81-96
- Knutson, E.O. and Whitby, K.T. (1975a) Aerosol Classification by Electric Mobility: Apparatus, Theory and Applications. *J. Aerosol Sci.*, 6, 443
- Knutson, E.O. and Whitby, K.T. (1975b) Accurate Measurement of Aerosol Electric Mobility Moments. *J. Aerosol Sci.*, 6, 453
- Kulmala, M., Kontkanen, J., Junninen, H., Lehtipalo, K., Manninen, H.E., Nieminen T., Petäjä, T., Sipilä, M., Schobesberger, S., Rantala, P., Franchin, A., Jokinen, T., Järvinen, E., Äijälä, M., Kangasluoma, J., Hakala, J., Aalto, P.P., Paasonen, P., Mikkilä, J., Vanhanen, J., Aalto, J., Hakola, H., Makkonen, U., Ruuskanen T., Mauldin III, R.L., Duplissy, J., Vehkamäki, H., Bäck, J., Kortelainen, A., Riipinen I., Kurtén, T., Johnston, M.V., Smith, J. N., Kerminen, V-M., Worsnop, D.R. (2013) Direct Observations of Atmospheric Aerosol Nucleation. *Science*, 339, 943
- Romero-Sanz, I., Aguirre-de-Carcer, I. and Fernández de la Mora, J. (2005) Ionic propulsion based on heated Taylor cones of ionic liquids, *J. Prop. and Power*, 21, No. 2, 239-24
- Rosell-Llompart, J., Loscertales, I.G., Bingham, D. and Fernández de la Mora, J. (1996) Sizing nanoparticles and ions with a short differential mobility analyzer. *J. Aerosol Sci.*, 27, 695–719
- Rosser, S., and Fernández de la Mora, J. (2005) Vienna type DMA of high Resolution and high flow rate. *Aerosol Sci. Technol.*, 39,12, 1191-1200
- Steiner, G., Attoui, M., Wimmer, D. and Reischl, G.P. (2010) A Medium Flow, High Resolution Vienna DMA running in Recirculating Mode. *Aerosol Sci. Technol.*, 44: 4, 308 – 315
- Taylor, G (1964) Disintegration of Water Drops in an Electric Field. *Proc. R. Soc. Lond. A* July 28, 1964 280:383-397
- Ude, S. and Fernández de la Mora, J. (2005) Molecular monodisperse mobility and mass standards from electrosprays of tetra-alkyl ammonium halides. *J. Aerosol Sci.*, 36, 1224-1237
- Vanhanen, J., Mikkilä, J., Lehtipalo, K., Sipilä, M., Manninen, E., Siivola, E., Petäjä, T. and Kulmala, M. (2011) Particle Size Magnifier for Nano-CN Detection. *Aerosol Sci. Technol.*, 45:4, 533-542

- Winkler, P.M., Steiner, G., Vrtala, A., Vehkamäki, H., Noppel, M., Lehtinen, K.E.J., Reischl, G.P., Wagner, P.E. and Kulmala, M. (2008) Heterogeneous nucleation experiments bridging the scale from molecular ion clusters to nanoparticles. *Science*, 319, 5868, 1374-1377
- Winklmayr, W., Reischl, G.P., Lindner, A.O. and Berner A. (1991). A New Electromobility Spectrometer for the Measurement of Aerosol Size Distribution in the Size Range from 1 to 1000 nm. *J. Aerosol Sci.*, 22, 289
- Zhang, S. H., Akutsu, Y., Russell, L.M., Flagan, R.C. and Seinfeld, J.H. (1995). Radial Differential Mobility Analyzer. *Aerosol Sci. Technol.*, 23, 357

# ON THE USE OF SATELLITE REMOTE SENSING BASED APPROACH TO DETERMINE AEROSOL DIRECT RADIATIVE EFFECT OVER LAND

A.-M. SUNDSTRÖM<sup>1</sup>, A. AROLA<sup>2</sup>, P. KOLMONEN<sup>3</sup>, AND G. DE LEEUW<sup>3,1</sup>

<sup>1</sup> Department of Physics, University of Helsinki,  
Helsinki, Finland.

<sup>2</sup> Finnish Meteorological Institute, Kuopio, Finland.

<sup>3</sup> Finnish Meteorological Institute, Helsinki, Finland.

Keywords: Aerosol direct radiative effect, remote sensing, China.

## INTRODUCTION

Aerosols influence the radiative budget of the Earth-atmosphere system directly by scattering and absorbing solar and thermal infrared radiation, and indirectly by modifying the microphysical, and hence the radiative properties and lifetimes of clouds. However, the quantification of aerosol radiative effects is complex and large uncertainties still exist, mainly due to the high spatial and temporal variation of the aerosol concentration and mass as well as their relatively short lifetime in the atmosphere (e.g. IPCC 2007, Hatzianastassiou *et al.*, 2007). The clear-sky direct aerosol radiative effect at the top of the atmosphere in the short wave (SW) region ( $ADRE_{TOA}$ ) is defined as the difference between the outgoing SW fluxes without ( $F_{0,TOA}$ ) and with ( $F_{aer, TOA}$ ) aerosols. The negative values of  $ADRE_{TOA}$  correspond to increased outgoing SW radiation and planetary cooling, whereas positive values correspond to decreased outgoing SW radiation at the TOA and increased atmospheric warming. Several studies show that globally  $ADRE_{TOA}$  is negative (e.g. Yu *et al.*, 2006 and references therein) and hence aerosols tend to cool the atmosphere, but locally also positive values can be observed if e.g. highly absorbing aerosols are transported over bright surfaces such as snow.

Majority of the  $ADRE_{TOA}$  estimates introduced in the literature are based on models. During the past decade an increasing number of observation based studies of aerosol radiative effect have been carried out where remote sensing from space play an important role. In this work we studied the multi-sensor satellite based approach where coincident broadband flux observations from Clouds and the Earth's Radiant Energy System (CERES) and aerosol optical depth (AOD) from Moderate Imaging Spectroradiometer (MODIS) were used to derive  $ADRE_{TOA}$ . This approach has been previously used e.g. by Zhang *et al.* (2005) for defining SW aerosol radiative effect over cloud-free oceans as well as Patadia *et al.* (2008) and Sena *et al.* (2013) for studying biomass burning effects over Amazon. In the previous studies the satellite based method has been described but not studied in detail, which was the focus in this work. Our goal was to investigate how applicable this approach is for determining  $ADRE_{TOA}$  over land in highly variable aerosol conditions. The study area was Eastern China (20-45 N, 100-125 E), where the aerosol loading and type as well as surface type vary from highly polluted urban and industrial areas to rural deserts.

## METHODS

The direct aerosol radiative effect  $ADRE_{TOA}$  for cloud-free sky is defined as the difference between the SW fluxes in the absence and presence of aerosols;

$$ADRE_{TOA} = F_{0,TOA}^{\uparrow} - F_{aer,TOA}^{\uparrow}$$

For a cloud-free pixel, the CERES measurement represents the instantaneous value of  $F_{aer, TOA}$ . Since aerosols are always present in the atmosphere, it is not possible to obtain the value for  $F_{0,TOA}$  directly

from the satellite measurements. In this approach  $F_{0,TOA}$  is estimated using collocated SW flux and  $AOD$  retrievals from CERES and MODIS instruments (CERES SSF product). It is assumed that over a month in one grid cell ( $0.5 \times 0.5$  deg.) the aerosol mixture and surface properties do not vary significantly, and the changes in  $F_{aer, TOA}$  are mainly caused by changes in the aerosol loading ( $AOD$ ). When the aerosol loading is not extremely high ( $< 2.0$ ), the relationship between  $F_{aer, TOA}$  and  $AOD$  is close to linear. Hence, for each grid cell linear regression between the  $AOD$  and  $F_{aer, TOA}$  observations is defined, and the value for  $F_{0,TOA}$  is obtained as the y-intercept of the regression line ( $AOD = 0$ ). For a successful regression there are several criteria, e.g. that the number of observations in a grid cell over a month must be at least 10 and the absolute value of correlation coefficient must be 0.2 or greater.

However, there are also other factors affecting the observed  $F_{aer, TOA}$  than the aerosol loading.  $F_{aer, TOA}$  depends also on the solar zenith angle, amount of precipitable water, day of year and surface brightness. Variation of these parameters over one month in a grid cell causes scatter to the  $F_{aer, TOA}$  values which is not connected to aerosols. Excluding the effect of possible surface brightness variation which is assumed to be small, a normalization scheme for the CERES fluxes was introduced to reduce the noise of observed fluxes before the actual linear fitting against  $AOD$ :

$$F_{TOA, norm}^{CER} = F_{TOA, obs}^{CER} \cdot \frac{F_{TOA, normSZA}^{mod} \cdot F_{TOA, normWV}^{mod} \cdot F_{TOA, normDOY}^{mod}}{(F_{obs}^{mod})^3}$$

where the superscript "CER" refers to a CERES observation, "mod" to a modelled TOA flux, and "obs" to observed flux. The subscript "norm" refers to the fixed values of SZA, water vapour content (WV) and day of year (DOY), respectively, to which the observed CERES fluxes are normalized. The reference fluxes were modelled using Libradtran radiative transfer code (Mayer *et al.*, 2005). After the normalization of the CERES fluxes, the linear regression with the MODIS  $AOD$  was established, and  $F_{0,TOA}$  as well as instantaneous  $ADRE_{TOA}$  were defined.

## RESULTS AND DISCUSSION

The instantaneous direct aerosol radiative effect was defined using coincident CERES and MODIS data on a monthly basis from March to November 2009 over Eastern China. Since measurements of aerosol-free TOA fluxes do not exist, a dataset of modelled  $F_{0,TOA}$  values for each month was also created using Libradtran. Before defining  $ADRE_{TOA}$ , the normalization of observed CERES fluxes was carried out as explained. Results showed that in the majority of the cases normalization of the fluxes reduced the noise in the linear fitting, and increased the correlation between CERES SW fluxes and MODIS AODs (Fig. 1). In addition, the normalization somewhat changed the slope, and decreased the value of estimated  $F_{0,TOA}$  reducing the difference to the corresponding modelled  $F_{0,TOA}$  values.

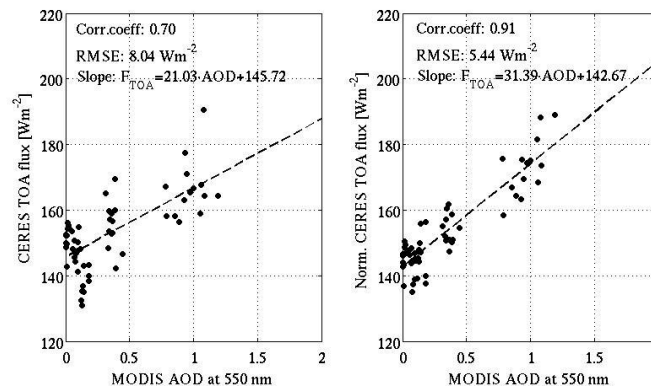


Figure 1. An example of the effect of the normalization of the CERES fluxes and the linear regression with MODIS AOD. On the left panel the linear regression is carried out in a grid cell without the

normalization, resulting in correlation of 0.70. On the right panel the same linear fitting is carried out after applying the normalization procedure, resulting in an increased correlation with of 0.90.

The key question when assessing the applicability of satellite based approach to determine  $ADRE_{TOA}$  is how well the method produces  $F_{0,TOA}$ . Comparison of the modelled and satellite based values of  $F_{0,TOA}$  showed that qualitatively both methods produce similar pattern over Eastern China. In 58% of all cases the difference between the aerosol-free fluxes from model and satellite fitting was  $\leq 10\text{Wm}^{-2}$ . Overall, the satellite based method produced slightly higher  $F_{0,TOA}$  than the model with the exception of bright desert surfaces where the value from satellite approach was systematically lower.

Figure 2. shows an example of instantaneous monthly  $ADRE_{TOA}$  over Eastern China and the mean of the AODs that has been used in the fitting. In general  $ADRE_{TOA}$  was negative and in majority of the cases high aerosol loading corresponds to stronger negative effect. Especially during summer months local positive values of  $ADRE_{TOA}$  were observed. However, the positive values of  $ADRE_{TOA}$  were mainly observed over dark surfaces, where the aerosol effect was expected to be negative even with absorbing aerosols. This was most probably a method artefact, related to either subvisual cirrus contamination, systematic change of aerosol type or both.

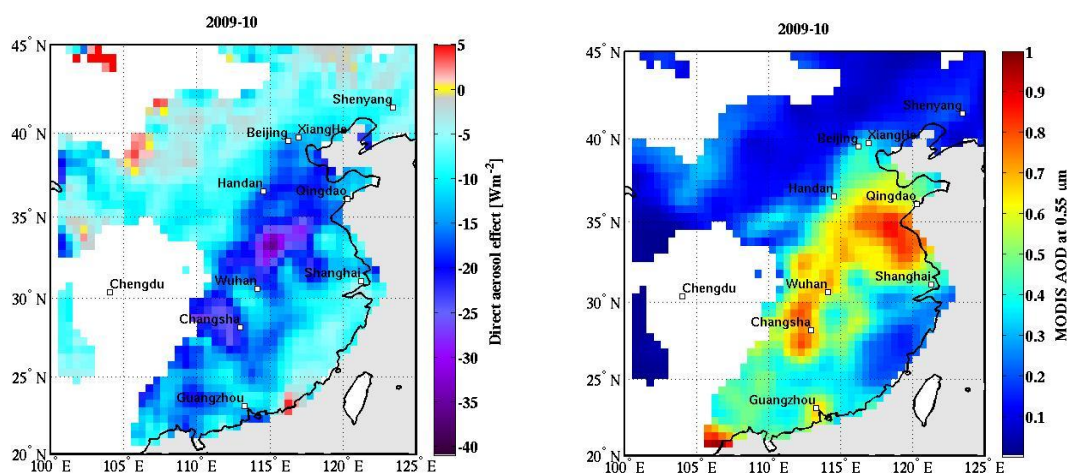


Figure 2. The instantaneous  $ADRE_{TOA}$  (left panel) obtained with the satellite based approach for October 2009, and mean AOD at 550 nm (right panel) calculated from the values included in the linear regression. White areas denote areas where successful regression was not obtained.

#### ACKNOWLEDGEMENTS

This research was supported by the Academy of Finland Center of Excellence program (project number 1118615).

#### REFERENCES

- Hatzianastassiou, N., C. Matsoukas, E. Drakakis, P.W. Stackhouse Jr., P. Koepke, A. Fotiadis, K.G. Pavlakis and I. Vardavas. (2007). The direct effect of aerosols on solar radiation based on satellite observations, reanalysis datasets, and spectral aerosol optical properties from Global Aerosol Data Set (GADS). *Atmos. Chem. Phys.*, **7**, 2585-2599.
- IPCC, Intergovernmental Panel on Climate Change, Fourth Assessment Report: Climate Change 2007. Cambridge University Press, Cambridge, United Kingdom and New York, NY, USA, 2007.
- Mayer, B., and A. Kylling (2005). Technical note: The libRadtran software package for radiative transfer calculations – description and examples of use. *Atmos. Chem. Phys.*, **5**, 1855–1877.

Patadia, F., P. Gupta, S.A. Christopher, and J.S. Reid (2008). A Multisensor satellite-based assesment of biomass burning aerosol radiative impact over Amazonia. *J. Geophys. Res.*, **113**, D12214.

Sena, E.T., Artaxao, P., and Correia, A-L. (2013). Spatial variability of the direct radiative forcing of biomass burning aerosols and the effects of land use change in Amazonia. *Atmos. Chem. Phys*, **13**, 1261-1275.

Yu, H., Kaufman, Y. J., Chin, M., Feingold, G., Remer, L.A., Anderson, T.A., Balkanski, Y., Bellouin, N., Boucher, O., Christopher, S., DeCola, P., Kahn, R., Koch, D., Loeb, N., Reddy, M.S., Schulz, M., Takemura, T., and M. Zhou (2006). A review of measurement-based assessments of the aerosol direct radiative effect and forcing. *Atmos. Chem. Phys*, **6**, 613–666.

Zhang J. and S. A. Christopher(2005). Shortwave aerosol radiative forcing over cloud-free oceans from Terra: Seasonal and global distributions. *J. Geophys. Res.*, **110**, D10S24.

# ESTIMATING THE CONCENTRATION OF NUCLEATION MODE PARTICLES OVER SOUTH AFRICA USING SATELLITE REMOTE SENSING MEASUREMENTS

A.-M. SUNDSTRÖM<sup>1</sup>, A. NIKANDROVA<sup>1</sup>, K. ATLASKINA<sup>1</sup>, T. NIEMINEN<sup>1</sup>, V. VAKKARI<sup>1</sup>, L. LAAKSO<sup>2,3</sup>, J.P. BEUKES<sup>3</sup>, P.G. VAN ZYL<sup>3</sup>, M. JOSIPOVIC<sup>3</sup>, A.D. VENTER<sup>3</sup>, K. JAARS<sup>3</sup>, J.J. PIENAAR<sup>3</sup>, S. PIKETH<sup>3</sup>, A. WIEDENSOHLER<sup>4</sup>, E.K. CHILOANE<sup>3,5</sup>, G. DE LEEUW<sup>2,1</sup> AND M. KULMALA<sup>1</sup>

<sup>1</sup> Department of Physics, University of Helsinki,  
Helsinki, Finland.

<sup>2</sup> Finnish Meteorological Institute, Helsinki, Finland.

<sup>3</sup> North-West University, Potchefstroom, South Africa.

<sup>4</sup> Leibniz Institute for Tropospheric Research, Leipzig, Germany.

<sup>5</sup> Eskom Holdings SOC Ltd, Sustainability Division, South Africa.

Keywords: Nucleation mode aerosol particles, satellite remote sensing.

## INTRODUCTION

Nucleation and the growth of nucleated aerosol particles are one of the key phenomena associated with the atmospheric aerosol system. Nucleation mode particles are smaller than 25–30 nm in diameter, and are formed either via primary emissions or gas-to-particle conversion. A number of *in situ* based studies (e.g. Kulmala and Kerminen 2008) have shown that nucleation occurs frequently in the continental boundary layer and free troposphere. Over South Africa the frequency of the nucleation event days is among highest currently reported in the literature (Laakso *et al.*, 2008, Vakkari *et al.*, 2011 and Hirsikko *et al.*, 2012).

Several remote sensing instruments provide information about the spatial distribution of atmospheric composition with adequate resolution and coverage from regional to global scales. The remote sensing of aerosol particles is mainly based on measurements carried out in the visible and near infrared regions ( $\lambda \sim 500\text{--}2000$  nm), and the detectable aerosol sizes are limited to particles diameter greater than about 100 nm. Hence, the nucleation mode particles cannot be detected directly with the satellite instruments and therefore remote sensing instruments have not much been utilized for studying atmospheric nucleation. However, the satellite based observations can be used to estimate the concentrations of nucleated particles using parametrizations, i.e. proxies, first introduced by Kulmala *et al.* (2011). The proxies obtained from satellite observations are based on studies carried out using ground based measurements (e.g. Petäjä *et al.*, 2009). The aims of this study were to investigate in more detail the proxies obtained from satellite measurements over South Africa using improved satellite products, compare them to proxies calculated from the *in situ* data and to study the possible effects of different meteorological factors.

## METHODS

Regional scale nucleation is associated with photochemistry, and typically has spatial scale of hundreds of kilometres (Kulmala *et al.*, (2011) and references therein). The number concentration of nucleation mode particles on a regional scale can be estimated as a ratio of source term proportional to UV-radiation and sulphur dioxide concentration and a sink term, expressed as

$$N_{nuc,regional} = \frac{UV [SO_2]}{AOD^2}$$

and for primary emissions,

$$N_{nuc,prim.} = \frac{[NO_2]}{AOD}, N_{nuc,prim.} = \frac{[SO_2]}{AOD}$$

where UV is the UV-B irradiance at the surface at local noon, SO<sub>2</sub> and NO<sub>2</sub> the total atmospheric column values obtained from satellite, and AOD the aerosol optical depth which describes quantitatively the column-integrated extinction (scattering+absorption) of solar light caused by atmospheric aerosols in the optically-active size range. In this work the satellite data is obtained from NASA's Afternoon-train constellation, which consists of 7 different satellites providing near simultaneous observations of various atmospheric constituents having equatorial overpass time about 1:30 pm local time. The Ozone Monitoring Instrument (OMI) was used to get the total column of NO<sub>2</sub> and SO<sub>2</sub> (PBL product), and the amount of UV-B radiation. AOD was obtained from The Moderate Imaging Spectroradiometer (MODIS) onboard NASA's Aqua platform, and The Cloud-Aerosol Lidar and Infrared Pathfinder Satellite Observation (CALIPSO) was used for the vertical profiles of aerosol extinction. The *in situ* data were collected at four different stations in South Africa: Elandsfontein, Marikana, Botsalano and Welgegund. All the stations are located in north eastern part of the country. More detailed description of the *in situ* measurements and sites can be found in e.g. Beukes et al. (2013), Hirsikko et al., 2012, Venter et al. (2012), Vakkari et al., (2011). and Laakso et al. (2012).

## RESULTS AND DISCUSSION

The major difference between the satellite and *in situ* based proxies is the sink term, where AOD is used as a satellite based estimate to the condensation sink (CS), which describes the rate of loss of vapor molecules. Both parameters are roughly proportional to the particle surface area, but there are differences related to theoretical definitions of the parameters, measurement technique (CS), and the vertical distribution of aerosols. Hence, CS was compared with ground based nephelometer data (scattering), and column integrated AODs from both ground based sunphotometer as well as satellite to estimate which factor might affect most to the AOD-CS relation. High correlation (0.84) was obtained between ground based nephelometer and CS data indicating that even the theoretical differences exist, correlation between the parameters is significant at the same atmospheric level. On the other hand, the comparison of CS and column integrated AOD revealed that elevated aerosol layers contribute frequently to AOD, and the correlation of columnar aerosol extinction and CS decreased significantly to a value of about 0.3.

Each of the satellite based parameter was analyzed for three years (Jan. 2007- Dec. 2009). The clear sky noon UV irradiance depends on the season and hence had namely only small latitudinal variation during the year. Figure 1. shows the three year averages of SO<sub>2</sub> and NO<sub>2</sub> column densities obtained from the OMI measurements, as well as AOD at 550 nm from MODIS Aqua. As Fig. 1 shows the spatial pattern for NO<sub>2</sub> and SO<sub>2</sub> column densities were very similar, highest values being observed over the Highveld Mpumalanga industrial area. AOD had somewhat of a different spatial pattern than NO<sub>2</sub> and SO<sub>2</sub>. Highest AOD averages were observed in the northern part of the study area, and were most likely connected to the dust outbreaks and field fires. Overall AOD was relatively low if compared to other international industrialized areas having comparable emissions of NO<sub>2</sub> e.g. certain areas in China. This might be due to the fact that de-SO<sub>x</sub> and de-NO<sub>x</sub> technologies are not applied at most of the large point sources in South Africa (Lourens et al., 2011). However, most of these large point sources have effective particle abatement technology installed.

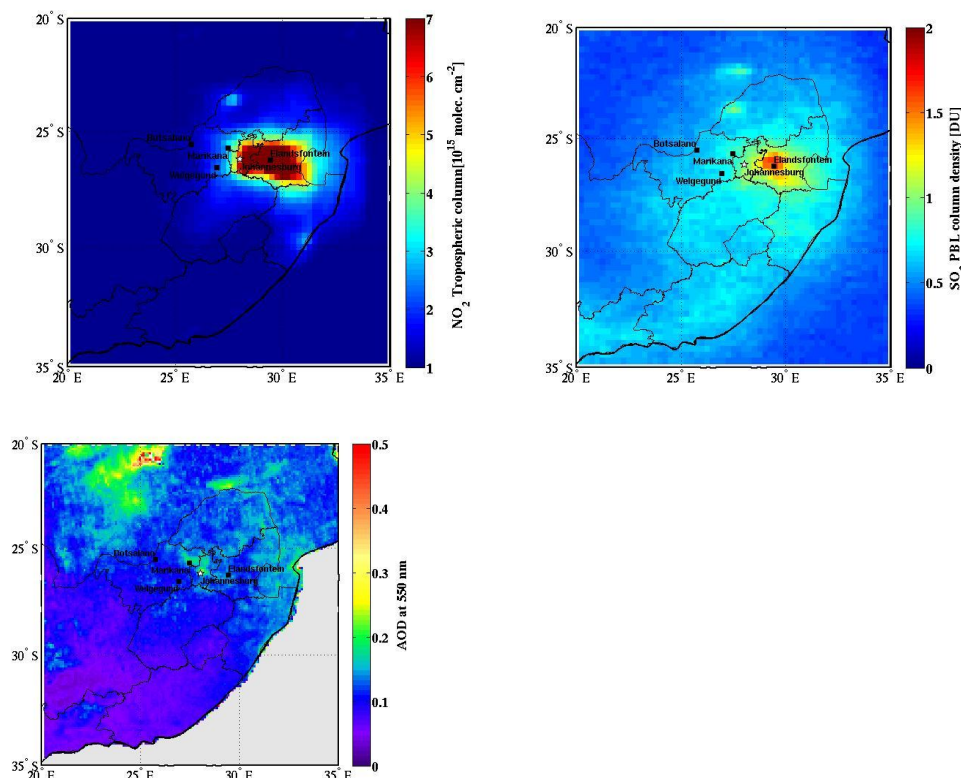


Figure 1. The three year averages of column densities of NO<sub>2</sub> (up left) and SO<sub>2</sub> (up right) from the OMI instrument and AOD at 550 nm (low left) from the MODIS Aqua over South Africa.

The proxies for primary emissions and regional nucleation were defined for each season between 2007 and 2009. Figure 2. shows an example of winter (JJA) average of both satellite based proxies. Over Mpumalanga Highveld area both regional scale nucleation and primary emission proxies showed high values, but some differences can be seen over the Johannesburg-Pretoria megacity. The proxy for primary emissions showed high values over Johannesburg-Pretoria, but the proxy for regional scale showed lower values comparable to the remote background areas.

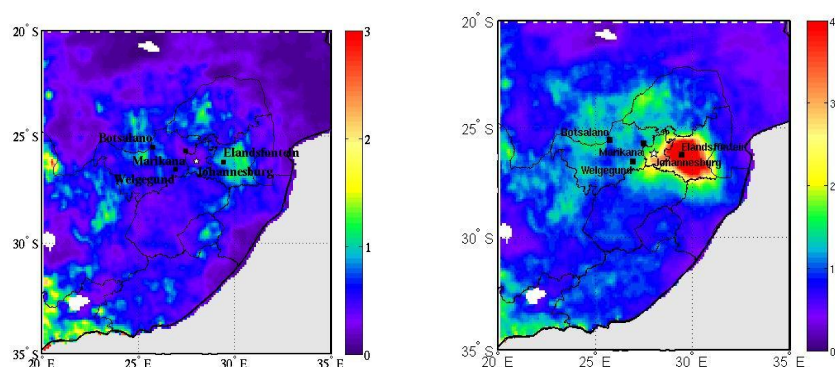


Figure 2. An example of the satellite based proxies for regional scale nucleation (left) and primary emissions (NO<sub>2</sub>/AOD) (right) for winter (JJA). The UVB/AOD<sup>2</sup> ratio in the regional scale proxy is normalized by a factor of 10<sup>4</sup>.

The overall challenge in determining the satellite based proxies over South Africa is that over major part of the study area the satellite AOD is very close to the lowest detection limit and the uncertainty is high. This might cause some artefact features in the proxy patterns, especially to the regional proxy,

which is assumed to be proportional to the inverse of  $AOD^2$ . However, in this study the spatial pattern for the proxies improved, because upgraded satellite data was used. First, the AOD data was obtained at 10 times finer spatial resolution than in Kulmala *et al.* (2011), which seems to be important in locations such as South Africa where the overall AOD is low. Coarse spatial resolution can effectively smooth out small scale variation. On the other hand also new, recently upgraded  $SO_2$  PBL product used in this study described better anthropogenic emissions, and hence improved the results.

More studies in different type of locations and environments are needed to improve the understanding of the relation between AOD and CS, and possibly to develop another type of satellite parameter that estimates better the condensation sink. In the future, the proxy approach will be studied in China and India, where in addition to the elevated  $NO_2$  and  $SO_2$  column densities aerosol signal is also strong.

## ACKNOWLEDGEMENTS

This research was supported by the Academy of Finland Center of Excellence program (project number 1118615). European Research Council (ATMNUCLE) and The European Integrated project on Aerosol Cloud Climate and Air Quality Interactions (EUCAARI). Eskom and Sasol supplied logistical support for measurements at Elandsfontein, while the town council of Rustenburg supplied support to the measurement at Marikana.

## REFERENCES

- Beukes, J.P., Vakkari, V., van Zyl, P.G., Venter, A.D., Josipovic, M., Jaars, K., Tiitta, P., Kulmala, M., Worsnop, D., Pienaar, J.J., Järvinen, E., Chellapermal, R., Ignatius, K., Maalick, Z., Cesnulyte, V., Ripamonti, G., Laban, T. L., Skrabalova, L., du Toit, M., Virkkula, A., and Laakso, L. (2013). *In preparation to be submitted to Atmos. Chem. Phys. Discuss.*
- Hirsikko, A., Vakkari, V., Tiitta, P., Hatakka, J., Kerminen, V.-M., Sundström, A.-M., Beukes, J.P., Manninen, H.E., Kulmala, M., and Laakso, L. (2013). Multiple daytime nucleation events in semi-clean savannah and industrial environments in South Africa: analysis based on observations. *Atmos. Chem. Phys.*, **13**, 5523-5532.
- Kulmala, M., and Kerminen, V.-M.: On the formation and growth of atmospheric nanoparticles (2008). *Atm. Res.*, **90**, 132-150.
- Kulmala, M., Arola, A., Riuttanen, L., Sogacheva, L., de Leeuw, G., Kerminen, V.-M. and Lehtinen, K.E.J. (2011): The first estimates of global nucleation mode aerosol concentrations based on satellite measurements. *Atmos. Chem. Phys.* **11**, 10791-10801.
- Laakso, L., Laakso, H., Aalto, P.P., Keronen, P., Nieminen, T., Pohja, T., Siivola, E., Kulmala, M., Kgabi, N., Molefe, M., Mabaso, D., Phalatse, D., Pienaar, K., and Kerminen, V.-M. (2008). Basic characteristics of atmospheric particles, trace gases and meteorology in a relatively clean Southern African Savannah environment, *Atmos. Chem. Phys.*, **8**, 4823-4839.
- Lourens, A. S. M., Beukes, J. P., Van Zyl, P. G., Fourie, G. D., Burger, J. W., Pienaar, J. J., Read, C. E., and Jordaan, J. H. (2011): Spatial and Temporal assessment of gaseous pollutants in the Highveld of South Africa, *S. Afr. J. Sci.*, 107, 8 pp.
- Petäjä, T., Maudin III, R.L., Kosciuch, E., McGrath, J., Nieminen, T., Paasonen, P., Boy, M., Adamov, A., Kotiaho, T., and Kulmala, M. (2009). Sulfuric acid and OH concentrations in a boreal forest site. *Atmos. Chem. Phys.*, **9**, 7435-7448.
- Vakkari, V., Laakso, H., Kulmala, M., Laaksonen, A., Mabaso, D., Molefe, M., Kgabi, N., and Laakso, L. (2011): New particle formation events in semi-clean South African savannah. *Atmos. Chem. Phys.*, **11**, 3333-3346.

Venter, A.D. , Vakkari, V., Beukes, J.P., van Zyl, P.G., Laakso, H., Mabaso, D., Tiitta, P., Josipovic, M., Kulmala, M., Pienaar, J.J., and L. Laakso (2012). *S. Afr. J. Sci.*, **108**(9/10).

# A NEW INSTRUMENT FOR MEASURING ATMOSPHERIC CONCENTRATIONS OF NON-OH OXIDANTS OF SO<sub>2</sub>

R. TAIPALE<sup>1</sup>, N. SARNELA<sup>1</sup>, M. RISSANEN<sup>1</sup>, H. JUNNINEN<sup>1</sup>, F. KORHONEN<sup>1</sup>, E. SIIVOLA<sup>1</sup>,  
M. KULMALA<sup>1</sup>, R. L. MAULDIN III<sup>1,2</sup>, T. PETÄJÄ<sup>1</sup> and M. SIPILÄ<sup>1</sup>

<sup>1</sup>Division of Atmospheric Sciences, Department of Physics, University of Helsinki, PO Box 64,  
00014 University of Helsinki, Finland

<sup>2</sup>Department of Atmospheric and Oceanic Sciences, University of Colorado at Boulder, Boulder,  
Colorado 80309, USA

Keywords: chemical ionisation, mass spectrometry, sulphuric acid, volatile organic compounds

## INTRODUCTION

Gaseous sulphuric acid is one of the major initiators of atmospheric new particle formation and thus relevant to global climate and air quality (e.g. Sipilä et al., 2010). Oxidation of sulphur dioxide (SO<sub>2</sub>) by the hydroxyl radical (OH) is considered the main source of sulphuric acid (H<sub>2</sub>SO<sub>4</sub>). However, recent studies suggest that also non-OH oxidants can have a substantial role in the H<sub>2</sub>SO<sub>4</sub> production (e.g. Mauldin III et al., 2012; Boy et al., 2013). Some of these oxidants are probably stabilized Criegee intermediates which are produced in the ozonolysis of alkenes. Novel instruments are needed to measure atmospheric concentrations of non-OH oxidants of SO<sub>2</sub> in different ecosystems. This paper presents a new technique combining a Flow Tube with a Chemical Ionisation Atmospheric Pressure interface Time Of Flight mass spectrometer, or FT-CI-APi-TOF.

## METHODS

The FT-CI-APi-TOF instrument measures the total concentration of all non-OH oxidants (termed X hereafter) which react with SO<sub>2</sub> at a reasonable rate. It consists of a flow tube (FT) and a chemical ionisation atmospheric pressure interface time of flight mass spectrometer (CI-APi-TOF). Ambient air is pumped through the flow tube continuously and X present in the sample is converted into H<sub>2</sub><sup>34</sup>SO<sub>4</sub> by injecting an excess of <sup>34</sup>SO<sub>2</sub> through injectors at different positions along the tube axis. The H<sub>2</sub><sup>34</sup>SO<sub>4</sub> concentration is measured with the CI-APi-TOF following the methods presented by Jokinen et al. (2012). Carbon monoxide (CO) is used as an OH scavenger.

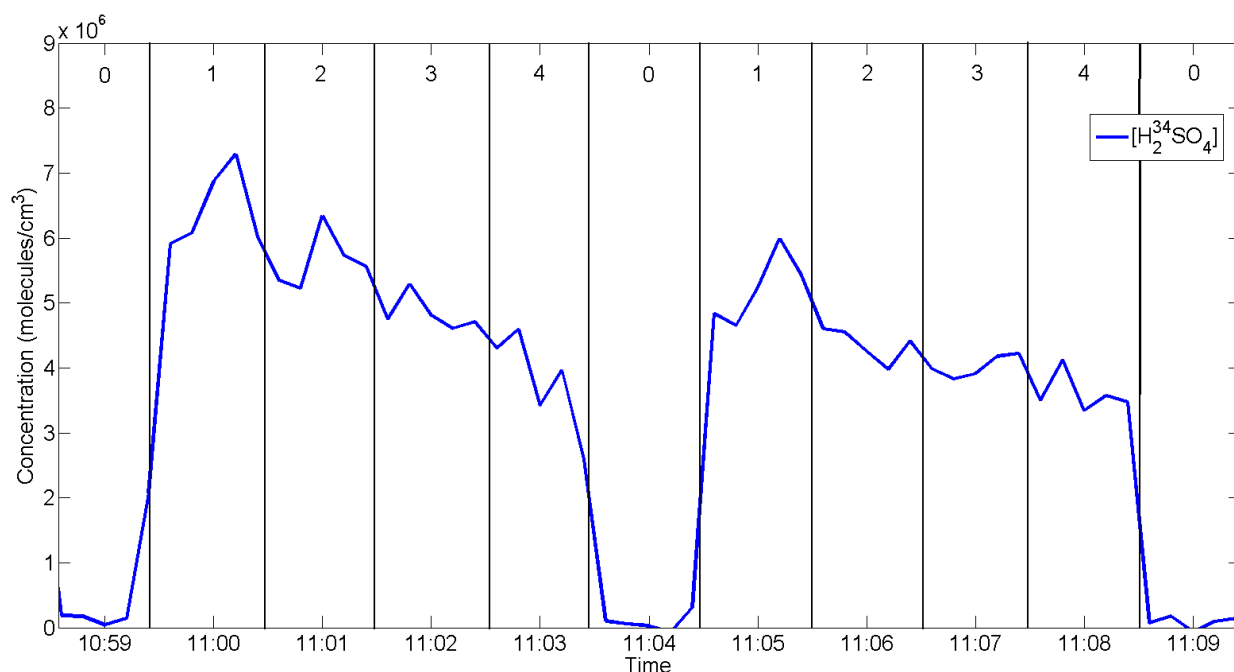
The H<sub>2</sub><sup>34</sup>SO<sub>4</sub> concentration is represented by  $[H_2^{34}SO_4] = [X]_{ss} + X_{pr}t_r$  where  $[X]_{ss}$  is the steady state concentration of X and  $X_{pr}$  is the production rate of X (e.g. Berndt et al., 2012). The reaction time  $t_r$  depends on the position of the <sup>34</sup>SO<sub>2</sub> injection and the sample flow. During a measurement cycle, the reaction time is changed by switching between the different <sup>34</sup>SO<sub>2</sub> injectors. This gives the H<sub>2</sub><sup>34</sup>SO<sub>4</sub> concentration as a function of the reaction time. Fitting a linear regression to these data yields the steady state concentration (intercept) and the production rate (slope). An estimate of the average lifetime of X is given by  $t_{lt} = [X]_{ss}/X_{pr}$  (for details, see e.g. Berndt et al., 2012).

The first field measurements with the FT-CI-APi-TOF were conducted at the SMEAR II station in Southern Finland in August 2013. The flow tube (length 798 mm, OD/ID 19.05/16.30 mm, flow 7 l min<sup>-1</sup>) was connected directly to the ion source of the CI-APi-TOF. It contained five pairs of injectors (length 29 mm, OD/ID 0.46/0.25 mm) installed at 30, 100, 250, 350 and 450 mm from the inlet of the tube. The first injectors were used continuously for injecting 300 ml min<sup>-1</sup> of CO (purity 99.997 %) to scavenge OH. The

other injectors were used sequentially for injecting  $100 \text{ ml min}^{-1}$  of  $^{34}\text{SO}_2$  (0.3–0.5 % in  $\text{N}_2$ ) and  $40 \text{ ml min}^{-1}$  of  $\text{N}_2$  (purity 99.999 %). One measurement cycle consisted of five one-minute steps. First  $^{34}\text{SO}_2$  and  $\text{N}_2$  were injected through the four different injector pairs, starting from the one corresponding to the longest reaction time. Then  $^{34}\text{SO}_2$  and  $\text{N}_2$  were fed to an exhaust line to determine the instrumental background signal of  $\text{H}_2^{34}\text{SO}_4$ .

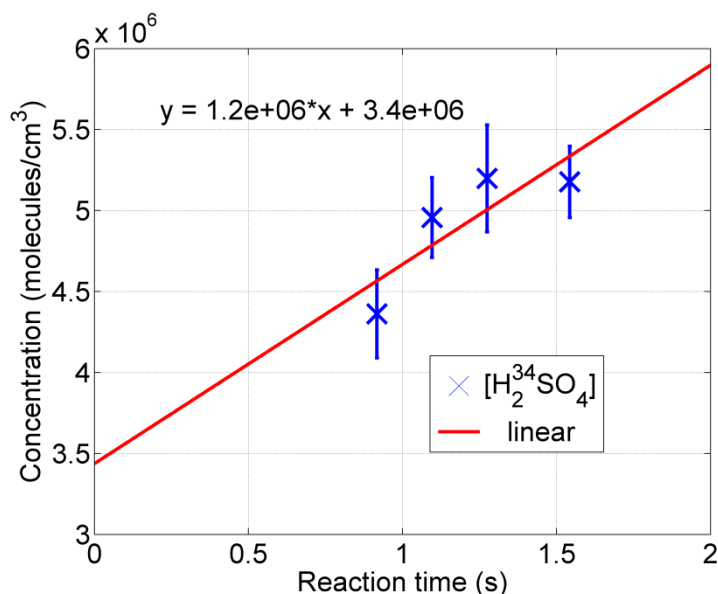
## RESULTS

Figure 1 illustrates the measurement cycle. The  $\text{H}_2^{34}\text{SO}_4$  concentration decreased when the reaction time was shortened by switching the position of the  $^{34}\text{SO}_2$  injection (steps 1–4). The background signal (step 0) was very low and stable during the measurements, indicating the fast response time of the FT-CI-APi-TOF and the minor importance of memory effects.



**Fig. 1.** Measurement cycle in the FT-CI-APi-TOF measurements of non-OH oxidants of  $\text{SO}_2$  (8 August 2013). Isotopically labelled  $^{34}\text{SO}_2$  was injected sequentially through four pairs of injectors in one-minute steps (1–4). One step (0) was allocated for background measurements when no  $^{34}\text{SO}_2$  was fed into the flow tube.

Figure 2 shows the  $\text{H}_2^{34}\text{SO}_4$  concentration as a function of the reaction time for a 30-minute averaging period. The linear least squares fit yielded a production rate of  $1.2 \times 10^6 \text{ molecules cm}^{-3} \text{ s}^{-1}$  (slope) and a steady state concentration of  $3.4 \times 10^6 \text{ molecules cm}^{-3}$  (intercept). Other averaging periods indicated similar daytime steady state concentrations of X. Thus it seems that the total concentration of all non-OH oxidants can be comparable with (or even higher than) daytime OH concentrations at the same site (Petäjä et al., 2009). Based on the steady state concentrations and production rates, the average daytime lifetime of X was around 2–4 s.



**Fig. 2.** Concentration of non-OH oxidants of SO<sub>2</sub> as a function of the reaction time. The measurements were performed at a boreal coniferous forest (8 August 2013 11:19–11:49 LT). The blue crosses represent 30-minute medians and the red line shows the linear least squares fit. The intercept gives the steady state concentration and the slope gives the production rate. The error bars show the standard deviations.

## CONCLUSIONS

The FT-CI-APi-TOF instrument is capable of measuring atmospheric concentrations of non-OH oxidants of SO<sub>2</sub>. The first measurements at a boreal coniferous forest indicated that daytime concentrations of these oxidants can be around  $3\text{--}5 \times 10^6$  molecules cm<sup>-3</sup>, i.e. comparable with daytime OH concentrations. Due to the indirect detection method, the non-OH oxidants cannot be identified by this instrument. However, since the instrument is calibrated for H<sub>2</sub>SO<sub>4</sub>, it produces quantitative estimates of the total concentration of all non-OH oxidants reacting with SO<sub>2</sub> at a reasonable rate. Although the results presented here are preliminary and a more detailed characterisation of detection limits and uncertainty estimates is still needed, the FT-CI-APi-TOF instrument seems suitable for quantitative online measurements with a time resolution of around 30 min.

## ACKNOWLEDGEMENTS

This work was supported by the Centre of Excellence program of the Academy of Finland (project 1118615) and the Advanced Grant program of the European Research Council (project 227463).

## REFERENCES

- Berndt, T., T. Jokinen, R. L. Mauldin III, T. Petäjä, H. Herrmann, H. Junninen, P. Paasonen, D. R. Worsnop and M. Sipilä (2012). Gas-phase ozonolysis of selected olefins: the yield of stabilized Criegee intermediate and the reactivity toward SO<sub>2</sub>, *J. Phys. Chem. Lett.* **3**, 2892–2896.
- Boy, M., D. Mogensen, S. Smolander, L. Zhou, T. Nieminen, P. Paasonen, C. Plass-Dülmer, M. Sipilä, T. Petäjä, L. Mauldin, H. Berresheim and M. Kulmala (2013). Oxidation of SO<sub>2</sub> by stabilized Criegee intermediate (sCI) radicals as a crucial source for atmospheric sulphuric acid concentrations, *Atmos. Chem. Phys.* **13**, 3865–3879.

- Jokinen, T., M. Sipilä, H. Junninen, M. Ehn, G. Lönn, J. Hakala, T. Petäjä, R. L. Mauldin III, M. Kulmala and D. R. Worsnop (2012). Atmospheric sulphuric acid and neutral cluster measurements using CI-API-TOF, *Atmos. Chem. Phys.* **12**, 4117–4125.
- Mauldin III, R. L., T. Berndt, M. Sipilä, P. Paasonen, T. Petäjä, S. Kim, T. Kurtén, F. Stratmann, V.-M. Kerminen and M. Kulmala (2012). A new atmospherically relevant oxidant of sulphur dioxide, *Nature* **488**, 193–197.
- Petäjä, T., R. L. Mauldin III, E. Kosciuch, J. McGrath, T. Nieminen, P. Paasonen, M. Boy, A. Adamov, T. Kotiaho and M. Kulmala (2009). Sulfuric acid and OH concentrations in a boreal forest site, *Atmos. Chem. Phys.* **9**, 7435–7448.
- Sipilä, M., T. Berndt, T. Petäjä, D. Brus, J. Vanhanen, F. Stratmann, J. Patokoski, R. L. Mauldin III, A.-P. Hyvärinen, H. Lihavainen and M. Kulmala (2010). The role of sulfuric acid in atmospheric nucleation, *Science* **327**, 1243–1246.

# THE EFFECT OF TEMPERATURE AND PRECIPITATION ON CARBON BALANCES IN FINLAND ACCORDING TO THE JSBACH MODEL

T. THUM<sup>1</sup>, T. MARKKANEN<sup>1</sup>, T. AALTO<sup>1</sup>, T. LAURILA<sup>1</sup>, N. CARVALHAIS<sup>2</sup>, S. ZAEHLE<sup>2</sup>,  
C. REICK<sup>3</sup>, M. TÖRMÄ<sup>4</sup> and S. HAGEMANN<sup>3</sup>

<sup>1</sup>Finnish Meteorological Institute, Climate Change Research, P.O. Box 503, 00101 Helsinki, Finland

<sup>2</sup>Max Planck Institute for Biogeochemistry, P.O. Box 10 01 64, 07701 Jena, Germany

<sup>3</sup>Max Planck Institute for Meteorology, Bundesstraße 53, 20146 Hamburg, Germany

<sup>4</sup>Finnish Environment Institute, P.O. Box 140, 00251 Helsinki, Finland

Keywords: REGIONAL MODELLING, GPP, RESPIRATION

## INTRODUCTION

The climate change is predicted to have large effect on the conditions in the boreal region. The carbon cycle of the boreal region is highly dependent on climate with its strong seasonal cycle. Changes in the climate of the “shoulder” seasons, spring and autumn, will likely influence the carbon cycle and the carbon stored in the biosphere, vegetation and soil.

The exchange of carbon between vegetation and atmosphere occurs in two directions simultaneously. The plants uptake carbon by photosynthesis. Carbon is released by the plants via autotrophic respiration and additional carbon from the biosphere originates from soil decomposition by microbes via heterotrophic respiration. The carbon uptake of an ecosystem is called Gross Primary Production (GPP) and the release of carbon by the ecosystem is Total Ecosystem Respiration (TER) consisting of both the autotrophic and heterotrophic respiration. Together GPP and TER determine the net carbon balance of the ecosystem.

Earlier spring start-up might have influence on the summertime peak values of photosynthesis (Buermann *et al.*, 2013) and the warmer autumn temperatures might lead to the longer respiration time (Piao *et al.*, 2008). Both of these phenomena and similar ones will have influence on the carbon balances of the vegetation.

In the present study we used process-based biosphere model JSBACH to assess the carbon balance of Finland in years 2001-2008. We studied how the modelled carbon fluxes responded to the climate variability during different years. This will reveal characteristics about the model behaviour and possible impacts the climate change will have on the Finnish carbon balance.

## MODEL DESCRIPTION AND SET-UP

We used the biosphere model JSBACH (Raddatz *et al.*, 2007) that is part of the MPI Earth System Model where the atmosphere is simulated by the ECHAM6 model. In addition, JSBACH can be applied at regional and site scales. JSBACH has been developed in the Max Planck Institute for Meteorology and the Max Planck Institute for Biogeochemistry. The JSBACH model is modelling the exchanges of carbon, water and energy between the land surface and atmosphere.

The photosynthesis is described by the Farquhar *et al.* (1980) model for the C3 plants and the stomatal conductance is based on Ball *et al.* (1987). The photosynthesis is controlled by the air temperature, radiation, air humidity and CO<sub>2</sub> concentration. The photosynthesis is coupled with the stomatal conductance and there is an additional constraint to stomatal conductance when the soil water content is low. The radiation scheme is calculated to four canopy layers using the two stream approximation (Dickinson, 1983; Sellers, 1985).

The biomass is divided into three different pools: wood, leaves and carbohydrates. The soil carbon is modelled by the CBALANCE model that has two litter pools (non-lignified and wood) and slow carbon pool (Goll *et al.*, 2012). The heterotrophic respiration is controlled by the soil temperature and moisture. The autotrophic respiration consists of growth and maintenance respiration. The growth respiration is a constant per cent of the fixed carbon and the maintenance respiration is a function of temperature and the magnitude of the biomass pools.

The physical processes mainly follow the physics package of ECHAM4 (Roeckner *et al.* 1996). This comprises the separation of rainfall and snow melt into surface runoff and infiltration and the calculation of lateral drainage following the Arno scheme (Dümenil and Todini 1992). Soil moisture is represented by a single-layer (“bucket scheme”) whose maximum depth is spatially varying and taken from the LSP2 (Land Surface Parameter Vs. 2) dataset (Hagemann, 2002). This maximum water depth corresponds to the root zone soil moisture and no water below it is considered.

The vegetation in JSBACH is described by Plant Functional Types (PFTs). Different PFTs have specific physiological properties, such as photosynthetic capacity, and physical properties, such as albedo of canopy. Each grid cell can contain up four different PFTs and in our simulation we had 13 different PFTs for vegetation. The most common PFT in Finland is boreal coniferous forest. The current JSBACH version does not include wetlands.

The photosynthesis of the coniferous forest in the model during shoulder seasons is mostly controlled by the temperature sensitivity of the photosynthesis and not by phenology. The phenology of other PFTs is dependent on predefined calendar dates, temperature, soil moisture and NPP (Raddatz *et al.*, 2007).

In our model set-up we obtained the climatic forcing from a regional climate model REMO and did not perform a coupled run with the atmospheric model. REMO was run with hourly time-step with the boundary conditions obtained from the ERA Interim re-analysis for the Finnish region. REMO was restarted with the boundary conditions each day, thus the conditions were forced to remain close to the observations. The spatial resolution of REMO was 0.17 degrees, i.e., about 18 km. The land cover data for the REMO and JSBACH runs were obtained from the national CORINE. The same spatial and temporal resolutions were used for the JSBACH run.

For the initialization of JSBACH we run the soil water into steady state by recycling the climatic forcing for 30 years. The biomass and soil carbon pools were run into steady state with the input of soil moisture and temperature, NPP and litter flux. The spin-up run for the soil carbon lasted over 1000 years. The model simulation was performed for the years 2000-2009. We had a closer look at years 2001-2008 with Finland divided into three parts: south, middle and north. The division was done so that each part would be approximately one third of the latitudinal extent of Finland, the latitudes separating the different parts were around 63.5 and 65.5 degrees of northern latitude.

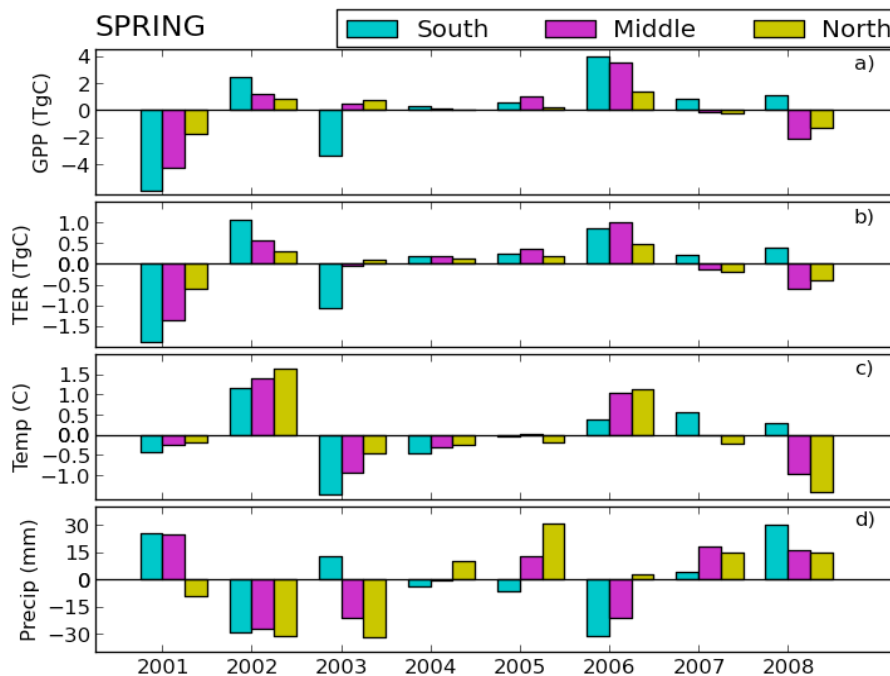


Figure 1. The anomalies of GPP (a), TER (b), air temperature (c) and precipitation (d) during spring in 2001-2008 in southern, mid- and northern Finland.

## RESULTS

We investigated how the simulated carbon fluxes and two meteorological variables air temperature and precipitation differ from their mean seasonal values during the years. Each season included three months. Spring consisted of March, April and May, summer of June, July and August, autumn of September, October and November and winter of December, January and February. The sums of the GPP and TER fluxes were calculated for each of the three regions and the anomaly was the divergence from the averaged sum over the years. Positive anomaly indicated above average flux and negative anomaly below average flux. For the temperature the averages instead of sums were calculated.

The anomalies of different variables in spring, summer and autumn are shown in Figures 1-3, respectively. The GPP and TER generally have similar magnitudes, but the GPP has larger deviations during spring and summer (Fig. 1-3a) whereas TER is having larger anomalies during autumn (Fig. 1-3b). This might be caused by the lack of radiation during autumn that might limit the photosynthesis.

Generally the carbon flux anomalies have the same direction in differing regions in spring and summer (Fig. 1-2a, b). The biggest negative anomaly in the carbon fluxes during spring occurs in 2001 (Fig. 1a, b) when there is a drop in temperature (Fig. 1c). However, in spring 2004 similar temperature anomaly takes place (Fig. 1c) but does not have a pronounced effect on the carbon

fluxes (Fig. 1a, b). In 2008 there is difference between the southern Finland and the other parts (Fig. 1c) in the temperature anomaly. The flux anomalies show similar behaviour region-wise in that spring (Fig. 1a, b). The largest positive anomalies in spring happen in 2002 and 2006 that

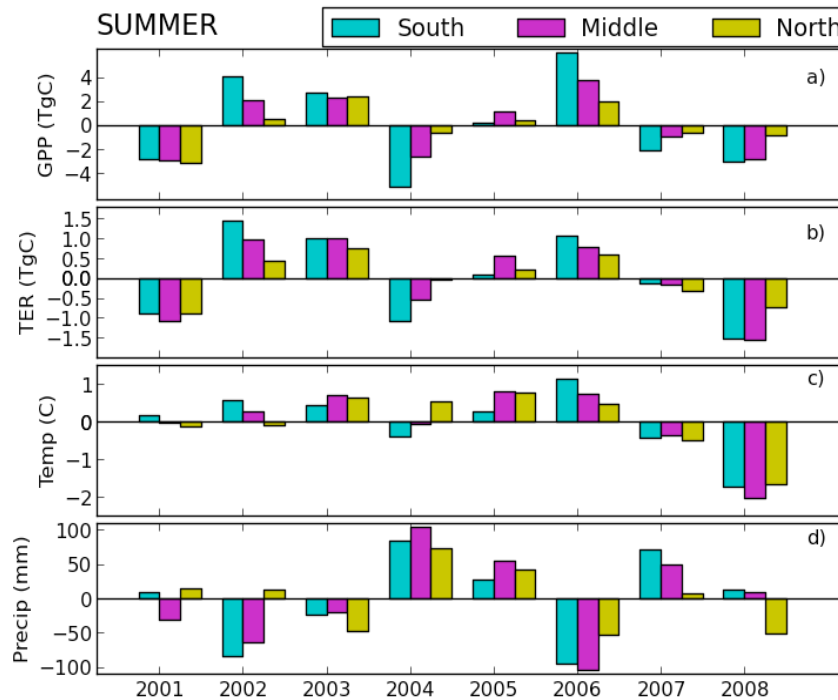


Figure 2. The anomalies of GPP (a), TER (b), air temperature (c) and precipitation (d) during summer in 2001-2008 in southern, mid- and northern Finland.

are both connected to positive temperature anomalies. The negative springtime precipitation anomalies have no effect on the fluxes in those years (Fig. 1).

In summers 2001 and 2004 negative flux anomalies occur without pronounced changes in temperature (Fig. 2a, b, c). The precipitation does not clearly limit the carbon fluxes although both modeled fluxes have a potential soil moisture limitation. In 2006 both of the carbon fluxes increase with warmer temperatures, even though the precipitation has its highest negative anomaly (Fig. 2).

In autumn the most striking feature in the time series is the continual increase of the temperature (Fig. 3c). This change is also visible in the carbon fluxes. In the autumn the carbon fluxes are influenced by the temperature, but the variation in GPP is small and even has opposite direction in 2006 than the temperature (Fig. 3a, b, c).

Overall, the air temperature had a profound effect on the carbon fluxes whereas the precipitation did not have large influence. Even during the driest cases there were not prominent decreases in the carbon fluxes in this time scale.

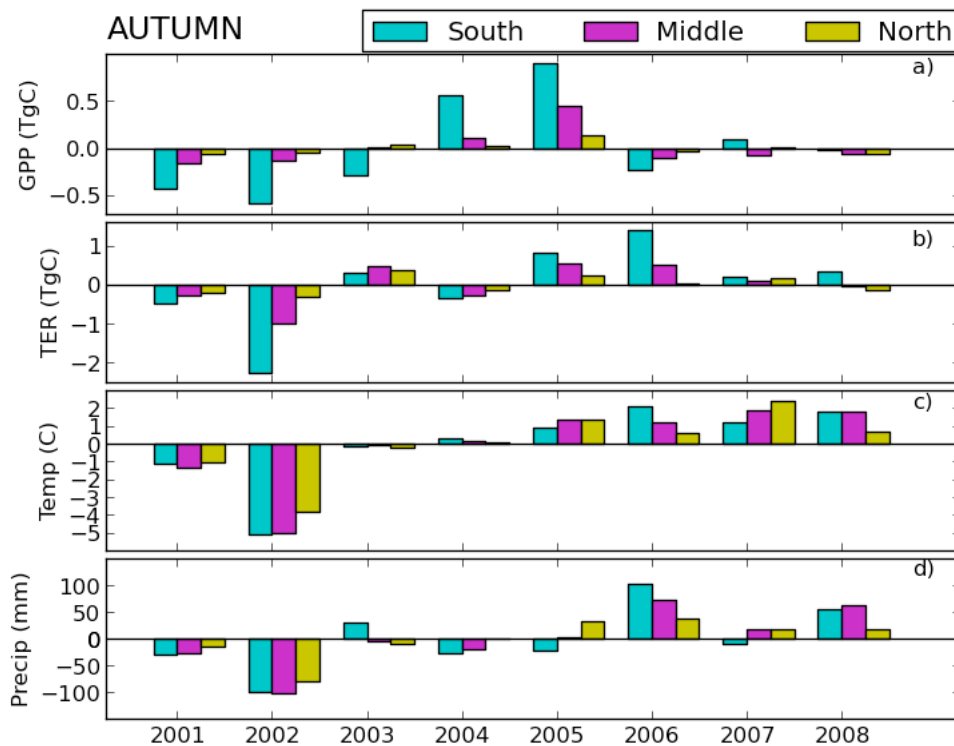


Figure 3. The anomalies of GPP (a), TER (b), air temperature (c) and precipitation (d) during autumn in 2001-2008 in southern, mid- and northern Finland.

## CONCLUSIONS

We assessed how the modelled regional carbon fluxes vary inter-annually during different seasons in Finland. The variability of the GPP was more pronounced in spring and summer whereas the TER had larger anomalies in autumn. Air temperature had large effect on the carbon fluxes but times of lower precipitation did not lead to reduced fluxes. The micrometeorological flux measurements can be used further to calibrate the model to Finnish conditions. Additionally, a simulation with a different land cover map will be performed to assess the significance of the different PFTs for the Finnish carbon balance.

Our study has some limitations, as we did not include the anthropogenic carbon sources or land-use change. Also, the nitrogen availability might impose some constraints on the carbon fluxes, but we were not using the nitrogen cycle version of JSBACH. However, in our study we can assess the different responses of the vegetation to climate and draw some conclusions about the consequences this will have in the light of climate change. If the temperatures are to increase in autumn, we expect to have larger respiration annually that will likely affect the carbon balances. On the other hand, the biosphere is very complicated system with the amount of litter fall influencing the magnitude of respiration. Therefore it is important to do studies with models of higher complexity so that several feedback mechanisms can be included and taken into account.

## ACKNOWLEDGEMENTS

We wish to thank the financial support from the Finnish Academy Center of Excellence (project no 111865) and SnowCarbo project (EU Life+ project, LIFE07 ENV/FIN/000133).

## REFERENCES

- Ball, J.T., I.E. Woodrow and J.A. Berry (1987). A model predicting stomatal conductance and its contribution to the control of photosynthesis under different environmental condition, in *Progress in Photosynthesis Research*, **Vol. IV** (ed. I. Biggins), 221–224. Martinus-Nijhoff Publishers, Dordrecht, The Netherlands.
- Buermann, W., P. R. Bikas, M. Jung, D. H. Burn and M. Reichstein (2013). Earlier springs decrease peak summer productivity in North American boreal forests. *Environmental Research Letters* **8**, 024027.
- Dickinson, R.E. (1983). Land surface processes and climate — Surface albedos and energy balance. *Advances in Geophysics* **25** 305-353.
- Dümenil, L. and E. Todini (1992). A rainfall-runoff scheme for use in the Hamburg climate model. Ed.: J.P. Kane: *Advances in Theoretical Hydrology - a Tribute to James Dooge*, Elsevier Science Publishers, 129-157.
- Farquhar, G.D., S. von Caemmerer and J.A. Berry (1980). A biogeochemical model of photosynthesis in leaves of C<sub>3</sub> species. *Planta* **149**, 78-90.
- Goll, D. S., V. Brovkin, B. R., Parida, C. H., Reick, J., Kattge, , P. B. Reich, P. M., van Bodegom and Ü. Niinemets (2012). Nutrient limitation reduces land carbon uptake in simulations with a model of combined carbon, nitrogen and phosphorus cycling. *Biogeosciences* **9**, 3547-3569.
- Hagemann, S. (2002) An improved land surface parameter dataset for global and regional climate models; MPI Report 336, Max Planck Institute for Meteorology, Hamburg, Germany [Report available electronically from <http://www.mpimet.mpg.de/en/wissenschaft/publikationen.html>].
- Piao, P., P. Ciais, P. Friedlingstein, P. Peylin, M. Reichstein, S. Luyssaert, H. Margolis, J. Fang, A.- Barr, A. Chen, A. Grelle, D.Y. Hollinger, T. Laurila, A. Lindroth, A.D. Richardson and T. Vesala (2008). Net carbon dioxide losses of northern ecosystems in response to autumn warming. *Nature* **451**, 49-52.
- Raddatz, T., C. Reick, W. Knorr, J. Kattge, E. Roeckner, R. Schnur, K.-G. Schnitzler, P. Wetzel and J. Junglaus (2007). Will the tropical land biosphere dominate the climate-carbon cycle feedback during the twenty-first century? *Clim. Dyn.* **29**, 565-574.
- Roeckner, E., G. Bäuml, L. Bonaventura, R. Brokopf, M. Esch, M. Giorgetta, S. Hagemann, I. Kirchner, L. Kornbluh, E. Manzini, A. Rhodin, U. Schlese, U. Schulzweida, and A. Tompkins (2003), The atmospheric general circulation model ECHAM5. Part I: Model description, Max Planck Institute for Meteor. Rep., 349, 127 pp. [available from MPI for Meteorology, Bundesstr. 53, 20146 Hamburg, Germany].
- Sellers, P.J. (1985). Canopy reflectance, photosynthesis and transpiration, *Int. J. Remote Sensing* **6**, 1335-1372.

# COMPUTATIONAL STUDIES OF ION-INDUCED OXIDATION OF SO<sub>2</sub>

N.T. TSONA<sup>1</sup>, N. BORK<sup>1,2</sup> and H. VEHKAMÄKI<sup>1</sup>

<sup>1</sup>Division of Atmospheric Sciences, Department of Physics, University of Helsinki, Helsinki, 00014, Finland.

<sup>2</sup>Department of Chemistry, University of Copenhagen, Copenhagen, 2100, Denmark.

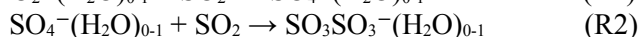
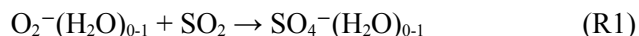
Keywords: SULFURIC ACID, MOLECULAR CLUSTERS, ION-INDUCED NUCLEATION.

## INTRODUCTION

Aerosol particles are important in human life as they affect the climate and human health. They are either emitted directly to the atmosphere or they are produced by nucleation of gas-phase species. In order to predict climate it is fundamental to understand the formation of aerosols.

Sulphuric acid (H<sub>2</sub>SO<sub>4</sub>) is well known to be an important precursor for nucleation in the gas-phase (Kulmala *et al.* 2006). By strongly interacting with bases, water, and various organics in the atmosphere, it forms stable molecular clusters that may grow to a size relevant to new particle formation. Understanding the formation of H<sub>2</sub>SO<sub>4</sub> is therefore important to predict the nucleation rate. H<sub>2</sub>SO<sub>4</sub> is mostly formed in the gas phase from SO<sub>2</sub> oxidation by OH radical, catalysed by UV light but a new synthesis mechanism involving ions was found recently (Enghoff *et al.* 2008).

From experiments SO<sub>2</sub> was also found to react rapidly with atmospheric ions (e.g. O<sub>2</sub><sup>-</sup>, O<sub>3</sub><sup>-</sup>, and CO<sub>3</sub><sup>-</sup>) (Möhler *et al.* 1992). Berndt *et al.* (2008) showed that other SO<sub>2</sub> oxidation products may trigger the formation of new particles in the atmosphere. This means that SO<sub>2</sub> is important in aerosol formation and it is therefore necessary to explore all the relevant SO<sub>2</sub> oxidation reactions. We have investigated the oxidation reaction of SO<sub>2</sub> by two different ions: O<sub>2</sub><sup>-</sup> and SO<sub>4</sub><sup>-</sup>.



The former ion is readily produced when galactic cosmic rays enter the atmosphere and collide with e.g. N<sub>2</sub> and O<sub>2</sub>, realising free electrons and cations. The latter was detected in the atmosphere at relatively high concentration by Ehn *et al.* (2010). To examine the effect of hydration, one water molecule was included in both reactions.

## METHODS

We used ab initio calculations to determine structures and formation energies of relevant species. The structures and vibrational frequencies were calculated using the DFT based on the CAM-B3LYP method and the aug-cc-pVDZ basis set, while single point energy calculations were performed using the CCSD(T) coupled cluster theory with the same basis set. The formation energy  $\Delta E$  of a cluster is calculated as the difference between the energy of the cluster and the sum of energies of the separate reactants.

$$\Delta E = E_{\text{cluster}} - \sum E_{\text{reactant}} \quad (1)$$

The reaction rates were determined using the transition state theory and all the calculations were performed at T=298.15 K and p= 1atm.

## RESULTS

The immediate product of reaction (R1) is  $\text{O}_2\text{SO}_2^-$  and may oxidise to  $\text{SO}_4^-$  by crossing an energy barrier. Concerning reaction (R2),  $\text{SO}_2\text{SO}_4^-$  is formed upon  $\text{SO}_2$  and  $\text{SO}_4^-$  collision and the immediate product also oxidises further to  $\text{SO}_3\text{SO}_3^-$ . The formation of  $\text{SO}_3\text{SO}_3^-$  from separate reactants occurs with ca.  $\Delta G = -8$  kcal/mol, meaning that the reaction (R2) is a likely process in the atmosphere although there is an energy barrier separating the reactant complex ( $\text{SO}_2\text{SO}_4^-$ ) and the final product. The Gibbs free energy surface of reaction (R1) is shown in Figure 1.

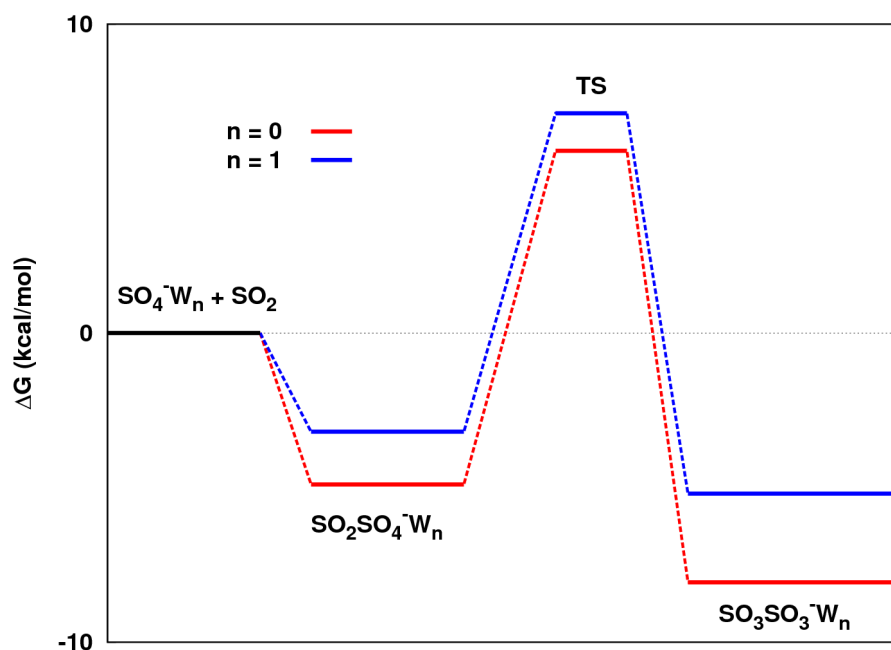


Figure 1. Gibbs free energy surface of the most relevant intermediates in  $\text{SO}_2$  and  $\text{SO}_4^-\text{W}_n$  collision. The energy values are plotted relative to  $\text{SO}_2 + \text{SO}_4^-\text{W}_n$  energy. “W” is the shorthand notation for water and “TS” stands for transition state.

Using the transition state theory, the fraction of collisions leading to oxidation are determined for reactions (R1) and (R2). We find that a small fraction (ca. 5%) of oxidation will occur in both reactions at standard conditions. This suggests that most of the collisions would lead to different end products than oxidation products, most likely the re-evaporation of  $\text{O}_2$  for reaction (R1) and of  $\text{SO}_2$  for reaction (R2). Water is seen to have an inhibiting effect on oxidation. Meanwhile, the chemical fate of  $\text{SO}_3\text{SO}_3^-$  was investigated, mostly by reaction with  $\text{O}_3$ . The reaction



is atmospherically important since it is distinctly exothermic ( $\Delta G = -37$  kcal/mol) and produces  $\text{SO}_3$  which is an important reactant in the formation of  $\text{H}_2\text{SO}_4$  (Larson *et al.*, 2000).

## CONCLUSIONS

The reaction mechanisms of  $\text{SO}_2$  oxidation by  $\text{O}_2^-$  and  $\text{SO}_4^-$  were investigated. The main products at standard conditions are not the oxidation products. Most important is the  $\text{SO}_3\text{SO}_3^-$  decomposition by  $\text{O}_3$ ,

leading to the regeneration of  $\text{SO}_4^-$  and the formation of  $\text{SO}_3$  which is an important source of sulphuric acid in the atmosphere.

## ACKNOWLEDGEMENTS

This work was supported by Academy of Finland (LASTU Project No. 135054) and ERC Project No. 257360-MOCAPAF. We acknowledge the CSC IT Centre for Science in Espoo, Finland for computer time.

## REFERENCES

- Kulmala, M., Lehtinen, K.E.J. and Laaksonen, A. (2006). Cluster activation theory as an explanation of the linear dependance between formation rate of 3 nm particles and sulphuric acid concentration, *Atmos. Chem. Phys.* **6**, 787.
- Enghoff, M.B. and Svensmark, H. (2008). The role of atmospheric ions in aerosol nucleation – a review, *Atmos. Chem. Phys.* **8**, 4911.
- Möhler, O., Reiner, T. and Arnold, F. (1992). The formation of  $\text{SO}_5^-$  by gas phase ion-molecule reactions, *J. Chem. Phys.* **97**, 8233.
- Berndt, T., Stratmann, F., Bräsel, S., Heintzenberg, J., Laaksonen, A. and Kulmala, M. (2008).  $\text{SO}_2$  oxidation products other than  $\text{H}_2\text{SO}_4$  as a trigger of new particle formation. Part1: Laboratory investigations, *Atm. Chem. Phys.* **8**, 6365.
- Ehn, M., Junninen, H., Petäjä, T., Kurtén, T., Kerminen, V.-M., Schobesberger, S., Manninen, H.E., Ortega, I.K., Vehkamäki, H., Kulmala M. and Worsnop, D.R. (2010). Composition and temporal behavior of ambient ions in the boreal forest, *Atmos. Chem. Phys.* **10**, 8513.
- Larson, L.J., Kuno, M. and Tao, F.-M. (2000). Hydrolysis of sulfur trioxide to form sulfuric acid in small clusters, *J. Chem. Phys.* **112**, 8830.

# LARGE EDDY SIMULATIONS FOR FOREST CANOPY

S. M. TU<sup>1</sup>, A. NORDBO<sup>1</sup>, A. HELLSTEN<sup>2</sup>, J. RINNE<sup>1</sup> and T. VESALA<sup>1</sup>

<sup>1</sup>Department of Physics, University of Helsinki, Helsinki, Finland.

<sup>2</sup>Finnish Meteorological Institute, Helsinki, Finland.

Keywords: LARGE EDDY SIMULATION, FOREST CANOPY.

## INTRODUCTION

Source/sink heterogeneity of a surface is a critical issue for micrometeorological measurement methods of turbulent surface fluxes because the surface is heterogeneous in nature which violates the assumption of horizontal homogeneity, a prerequisite for most methods. This affects methods such as the eddy-covariance technique where fluxes are measured in situ from a mast and the source area (i.e. footprint, Vesala et al., 2008) of the measurements lies upwind from the mast. If the horizontal scale of the heterogeneity is very small compared to the measurement height, effects of surface heterogeneity will be averaged out above a blending height, which would be below the measurement height. Moreover, if the spatial scale of the surface patches is so large compared to the measurement height that the turbulent flux footprint of the measurements will cover only one patch, the area within the footprint will be homogeneous.

Because surface heterogeneities have an important influence on the atmospheric flow above a vegetation surface, forest edges have become an essential topic for both experimental and numerical studies. Due to the pressure gradient induced by the presence of the canopy, the flow starts to decelerate slightly upwind from the edge and an internal boundary layer starts to grow from the edge (Dupont et al., 2010). Internal boundary layer height (IBL, reviewed by Garratt 1990) is essential for studying measurements in broad areas such as pasture land and forests. The flux measured above the canopy often deviates from the source strength underlying the measurements due to the consequence of limited fetch. Hence, in order to improve data quality of EC and to provide a judicious interpretation of flux measurements over patchy forests, deviation analyses are strongly required, especially in the region adjacent to a forest edge (Sogachev et al., 2008).

The goal of the present study is to analyse flux data in detail in the case of forest canopy for the preparation of the mutual cooperation of measurements and large-eddy simulations in the future. In the end goal, we want to evaluate the impact of the scale of horizontal homogeneity on the turbulent flux for varying measurement heights in order to prepare next steps for understanding the influence of blending height to measurement data qualities.

## METHODS

To obtain detailed turbulence information in the atmospheric boundary layer, large eddy simulations with the latest canopy model (LES, Raasch and Schröter, 2011) are applied here. In addition, a Lagrangian stochastic (LS) model is applied for particle simulations in order to interpret source areas. Neutral and cyclic boundary conditions are set for the LES model. Simulations are based on an ideal “one stripe” surface with alternating surface exchange: particles are released from alternating squares as the canopy location and the source height is close to the surface (0.75 m). Particles will be released from the LS

model only when the flow reaches steady state. The horizontal domain is 768 m times 192 m with 2 meter resolution. The domain height is 128 m with 1 m resolution. Rayleigh damping height is 70 meter. The total simulation time is 6 hours and the integration time for all statistics was chosen as 30 min. A 15 m high canopy is located from 300 m to 616 m streamwise direction and the value for drag coefficient is 0.2. The clearing length is set to 20 times canopy height in order to limit the effect of the upwind forest on the edge flow. A beta distribution function will be applied for leaf area density (LAD) calculation within the canopy: leaf area index (LAI) value is 2, alpha value is 5 and beta value is 2. Each simulated surface has a different, but homogeneous, roughness.

## DISCUSSION

Since the momentum flux adjusts to new surface conditions from the open area to canopy terrain, the flow disturbances caused by the forest edge are complex. The streamwise wind velocity decreases as the flow meets the resistance created by the canopy aerodynamic drag when the flow reaches the frontal edge. From Fig. 1, the streamwise flow splits into upper and lower flows due to the effect of foliage in the upper region of the crown: the flow is mostly deflected over the forest and a smaller part penetrates into the trunk zone, but it slows down soon after. Small eddies with a diameter twice the canopy height are seen within and above the canopy. When the flow reaches the back edge of the forest it subsidises rapidly. The vertical deflection before and after the canopy are also clearly visible in the vertical wind speed (Fig. 2). The flow patterns presented in Figs. 1 and 2 are classic and were reproduced by previous numerical studies (Li et al., 1990, Wilson and Flesch, 1999, Park and Paw U, 2006, Sogachev et al., 2008).

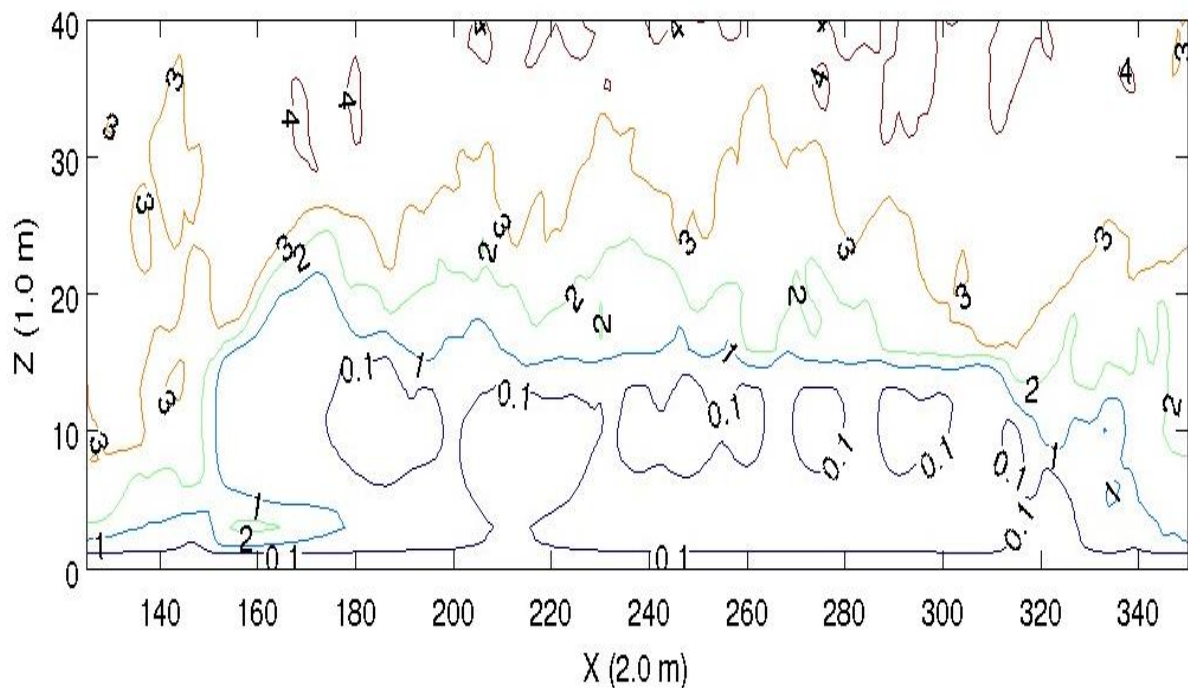


Figure 1. The vertical cross-section of the averaged streamwise wind component of flow at time 21600 s with unit m/s in the vicinity of the leading forest edge. X is the streamwise distance and Z is height. The forest spans from X = 150 to X = 308.

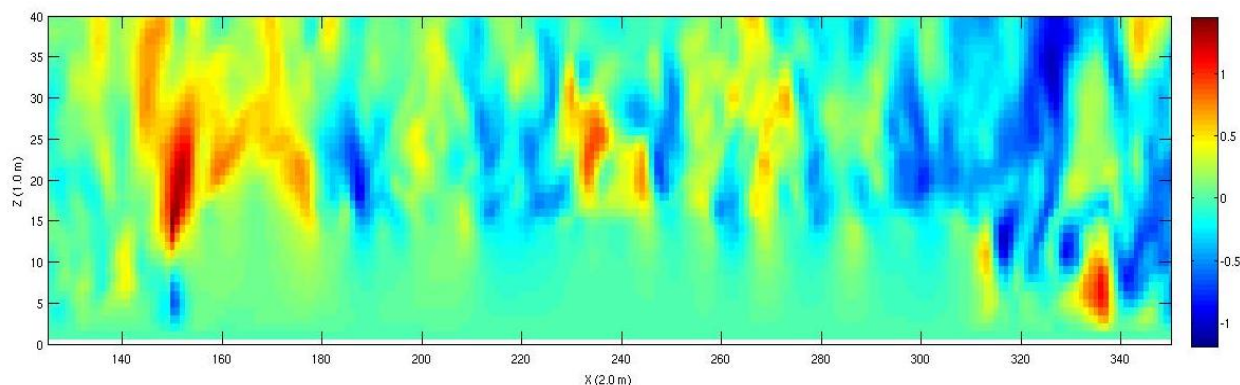


Figure 2. The vertical cross-section of averaged vertical wind component of flow at time 21600 s with unit m/s in the vicinity of the leading forest edge.

This study reveals important information on the relationship between atmospheric flow and horizontal homogeneity of the surface based on canopy terrain with a one stripe pattern. The results of the study can be used in the design of future flux measurement systems, and in the interpretation of results from the existing systems.

#### ACKNOWLEDGEMENTS

This work was supported by the Academy of Finland Center of Excellence (project no 1118615) the Nordic Centers of Excellence CRAICC or DEFROST and CSC in Finland.

#### REFERENCES

- Dupont S, Bonnefond JM, Irvine M, Lamaud E, Brunet Y. (2011). Long-distance edge effects in a pine forest with a deep and sparse trunk space: in situ and numerical experiments. *Agric. For. Meteorol.* 151:328–44.
- Garratt, J. R. (1990). ‘The Internal Boundary Layer – A Review’, *Boundary-Layer Meteorol.* 47, 17–40.
- Li, Z. J., Lin, J. D. and Miller, D. R. (1990). Air flow over and through a forest edge: a steady-state numerical simulation. *Boundary-Layer Meteorology*, 51, 179-197.
- Park, Y. –S. and Paw U K. T. (2006). Flow simulation of turbulent and mean advective velocity and scalar fields across a canopy edge. Preprints of 17<sup>th</sup> Symposium on Boundary Layers and Turbulence and 27<sup>th</sup> Conference on Agricultural and Forest Meteorology. San Diego, California, USA.
- Raasch, S. and Schröter, M. (2001). PALM – A large eddy simulation model performing on massively parallel computers, *Z. Meteorol.* 10, 363–372.
- Sogachev, A., Leclerc, M.Y., Zhang, G., Rannik, and Vesala, U. T. (2008). CO<sub>2</sub> fluxes near a forest edge: A numerical study, *Ecol. Appl.*, 18 (6) pp. 1454–1469.

- Vesala, T., Kljun, N., Rannik, U., Rinne, J., Sogachev, A., Markkanen, T., Sabelfeld, K., Foken, Th., and Leclerc, M. Y. (2008). Flux and concentration footprint modelling: State of the art. *Environ. Poll.*, 152, 653–666.
- Wilson, J. D. and Flesch T. K. (1999). Wind and remanat tree sway in forest openings III. A windflow model to diagnose spatial variation. *Agricultural and Forest Meteorology*, 93, 1197-1205.

# CH<sub>4</sub> AND N<sub>2</sub>O FLUXES OF BOREAL FOREST MIRE TRANSITIONS

B. ĽUPEK<sup>1a</sup>, K. MINKKINEN<sup>1a</sup>, T. VESALA<sup>1b</sup>, and E. NIKINMAA<sup>1a</sup>

<sup>1a</sup>Department of Forest Sciences, P.O. Box 27, 00014 University of Helsinki, Finland.

<sup>1b</sup>Department of Physics, P.O. Box 48, 00014 University of Helsinki, Finland.

Keywords: Methane, Nitrous oxide, Soil moisture gradient.

## INTRODUCTION

Boreal landscape is highly heterogeneous mosaic of forests and peatlands associated with variation in soil conditions and carbon storage (Weishampel et al. 2009). Drier hills are connected with wetter depressions by transitional zone. The forest/mire transition typically connects well drained upland forests and poorly drained peatlands. The transition between forests and peatlands is an ecological switch, where vegetation of forests and soils of peatlands coincide and frequently undergo fluctuations in water level position (Hartshorn et al. 2003).

Trace gas fluxes such as CH<sub>4</sub>, and N<sub>2</sub>O of upland and peatland soils change especially along the wide range of moisture conditions (Solondz et al. 2008, Pihlatie et al. 2004). The CH<sub>4</sub>, and N<sub>2</sub>O dynamics of forest/mire transition may be expected to differ from typical forests and peatlands.

The aim of our study was to evaluate variation of soil CH<sub>4</sub>, and N<sub>2</sub>O fluxes of forest/mire transitions in a wide range of water table fluctuations during years with exceptionally wet, dry and intermediate weather .

## MATERIAL AND METHODS

The forest and mire transitions form a gradient in vegetation distribution, soil moisture and nutrient conditions in Central Finland (61° 47', 24° 19'). The forest types range between the site on the margin with well-drained upland forests (OMT+), trough paludified spruce forest (KgK), to the site close to the poorly-drained sparsely forested mires (KR). Catena of soils is formed between intermediately drained histic and gleyic-histic podzols in forest/mire transitions on the toe of the slope.

The micrometeorological and gas exchange measurements of forest mire transitions were taken weekly during summers of 2004 (July-November), 2005 (May-November), 2006 (May-September), and occasionally during winters. The measurements of the forest floor soil temperatures in 5 cm depth (T<sub>5</sub>), the volumetric soil water content in 10 cm depth, the depth of water level followed the same procedure as described by Ľupek *et al.* (2008).

The field gas sampling was conducted weekly during 2004 and 2005 season and bi-weekly during 2006 season. The occasion of the gas sampling was at the same day  $\pm$  one day as the occasion of the micrometeorological measurements. The samples were taken from 3 opaque, vented, closed, static chambers ( $\varnothing$  315 mm, h 295 mm) placed on collars air tightly. For each measuring occasion one ambient gas and four 15 ml samples were drawn in syringes from each of three chambers at intervals of 5, 10, 15, 20 min totalling into 13 samples for each site. Chamber temperature was monitored during the sampling. After the sampling event, the gas samples were stored in coolers +4°C and analysed within 36 hours in laboratory by using gas chromatograph. Gas chromatograph (Hewlett-Packard, USA) was fitted with a flame ionisation detector (FID) for CH<sub>4</sub> and an electron capture detector (ECD) for N<sub>2</sub>O detection. The CH<sub>4</sub> (mgm<sup>-2</sup> h<sup>-1</sup>) and N<sub>2</sub>O ( $\mu$ gm<sup>-2</sup> h<sup>-1</sup>) fluxes were calculated from the slope of linear regression between the set of 4 gas concentrations and chamber closure time. Fluxes were calculated with the script developed

by Dept. of Physics (University of Helsinki) and verified against the standard and ambient gas concentration adopting criteria as used in Alm et al. (2007). The quantification limit of gas chromatograph was calculated based on standard deviation of 10 subsequently analysed samples of reference gas of known CH<sub>4</sub> and N<sub>2</sub>O concentration as in Pihlatie et al. (2013).

## PRELIMINARY RESULTS

The monthly medians of forest/mire types CH<sub>4</sub> dynamics was in the forest/mire transitions balanced between small consumption and small production (Figure 1). Evaluation of CH<sub>4</sub> production/consumption in the forest/mire transitions showed weak linear increase in CH<sub>4</sub> consumption with lowering ground water levels.

The N<sub>2</sub>O fluxes were at the detection limit for each site. Although, the median values showed weak N<sub>2</sub>O production along the forest/mire ecotone (Figure 1). The monthly medians of N<sub>2</sub>O fluxes in the forest/mire transitions showed small differences between intermediate and dry years. The N<sub>2</sub>O fluxes were larger during water table levels closer to the surface in 2005, whereas in drier conditions in 2006 fluxes were close to zero.

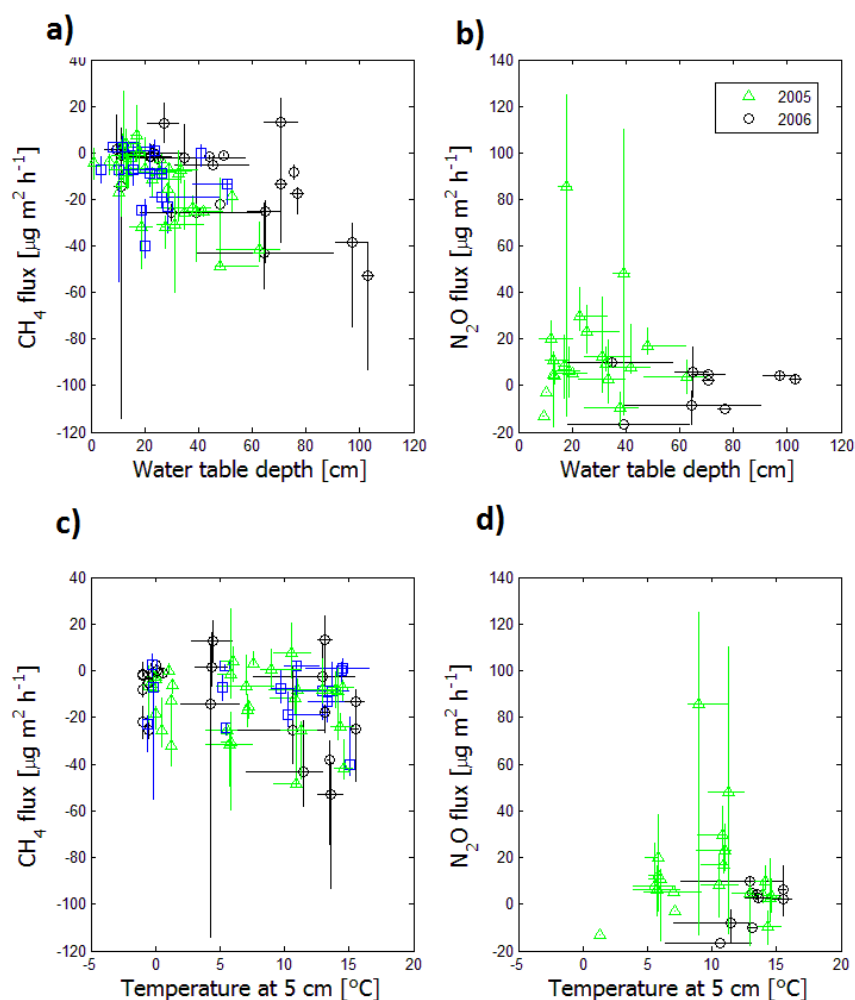


Figure 1. The panels show water level and soil temperature relation to monthly medians of the forest/mire transitions (OMT+ - *Oxalis-Myrtillus* Paludified, KgK - *Myrtillus* Spruce Forest Paludified, KR - Spruce Pine Swamp). The panels show: a) methane flux in relation to water table depth, b) nitrous oxide flux in relation to water table depth, c) methane flux in relation to soil temperature, d) nitrous oxide in relation to

soil temperature during wet 2004 (blue symbols), intermediate 2005 (green symbols), and dry year 2006 (black symbols). The error bars represent 25th and 75th percentile.

## ACKNOWLEDGEMENTS

This work was supported by Finnish Centre of Excellence in Physics, Chemistry, Biology and Meteorology of Atmospheric Composition and Climate Change (FCoE), Academy of Finland Center of Excellence program (project number 1118615), and through Nordic Centre of Excellence (project DEFROST).

## REFERENCES

- Alm, J., Shurpali, N. J., Tuittila, E., Laurila, T., Maljanen, M., Saarnio, S., et al. (2007). Methods for determining emission factors for the use of peat and peatlands - flux measurements and modelling. *Boreal Environment Research*, **12**(2), 85-100.
- Hartshorn, A. S., Southard, R. J., and Bledsoe, C. S. (2003). Structure and function of peatland-forest ecotones in southeastern alaska.. *Soil Sci Soc Am J*, **67**, 1572-1581.
- Pihlatie, M., Syväsalö, E., Simojoki, A., Esala, M., & Regina, K. (2004). In (Ed.), Contribution of nitrification and denitrification to N<sub>2</sub>O production in peat, clay and loamy sand soils under different soil moisture conditions ( Trans.). Springer Netherlands.  
doi:10.1023/B:FRES.0000048475.81211.3c
- Pihlatie, M., Riis Christiansen, J., Aaltonen, H., Korhonen, J., Nordbo, A., Rasilo, T., et al. (2013). Comparison of static chambers to measure CH<sub>4</sub> emissions from soils. *Agricultural and Forest Meteorology*. **5**,124-136.
- Solondz, D. S., Petrone, R. M., and Devito, K. J. (2008). Forest floor carbon dioxide fluxes within an upland-peatland complex in the Western Boreal Plain, Canada. *Ecohydrology*, **1**(4), 361-376.  
doi:10.1002/eco.30
- Ťupek, B., Minkkinen, K., Kolari, P., Starr, M., Chan, T., Alm, J., Vesala, T., Laine, J. and Nikinmaa, E. (2008), Forest floor versus ecosystem CO<sub>2</sub> exchange along boreal ecotone between upland forest and lowland mire. *Tellus B*, **60**: 153–166.
- Weishampel, P., Kolka, R., and King, J. Y. (2009). Carbon pools and productivity in a 1-km(2) heterogeneous forest and peatland mosaic in minnesota, USA. *Forest Ecology and Management*, **257**(2), 747-754. doi:10.1016/j.foreco.2008.10.008

## AIRBORNE AEROSOL MEASUREMENTS PERFORMED DURING THE PEGASSOS SPRING 2013 CAMPAIGN

R. VÄÄNÄNEN<sup>1</sup>, R. KREJCI<sup>2,1</sup>, P.P. AALTO<sup>1</sup>, T. POHJA<sup>1</sup>, L. ZHOU<sup>1</sup>, V. HEMMILÄ<sup>1</sup>, H. MANNINEN<sup>1</sup>, T. YLIJUUTI<sup>1</sup>, T. NIEMINEN<sup>1</sup>, T. PETÄJÄ<sup>1</sup>, M. KULMALA<sup>1</sup>

<sup>1</sup>Division of Atmospheric Sciences, Department of Physics, University of Helsinki, Finland.

<sup>2</sup>Department of Applied Environmental Science (ITM), Atmospheric Science Unit, Stockholm University, Sweden

Keywords: airborne measurements, aerosols, Pegassos campaign

### INTRODUCTION

Airborne measurements using a small Cessna 172 aircraft were carried out between 23<sup>rd</sup> of April and 15<sup>th</sup> of July as a part of the Pegassos measurement campaign. The Pegassos campaign was an intensive multi-platform campaign performed between April and June in 2013. Other parts of it included airborne measurements performed by Zeppelin and an extensive on-ground measurements performed in SMEAR (Station for measuring Ecosystem-Atmosphere Relations, Hari and Kulmala, 2005) II research station in Hyytiälä. Some measurements were performed also by Skyvan (Asmi et al, 2013), an aircraft hosted by Finnish Meteorological Office, and by a Sniffer car (Pirjola et al, 2004) which is a van specially equipped for mobile aerosol measurements.

The Cessna flights supported the Zeppelin flights and when possible, both aircrafts operated above same area to ensure the comparability of the datasets. Cessna could cover a higher altitude span and its flight patterns covered horizontally larger areas. Zeppelin on its turn could carry more payloads and thus was more extensively equipped.

### METHODS

The flying measurement platform we used was a Cessna 172 aircraft. It was equipped with aerosol, gas and meteorological instruments. The measurement flights were performed from Tampere-Pirkkala airport (EFTP) mainly either towards the area near of SMEAR II station, or towards Jämi airport (EFJM) area during the days when Zeppelin was operating there. The length of one measurement flight was up to 3 hours and the altitude span was from 200 m up to 3.5 km above the ground. A typical flight pattern included an ascending up to the free troposphere to obtain the height and overview structure of the boundary layer, and several parallel flight legs at different altitudes above and inside the boundary layer. The flight legs at a certain altitude typically were 30 km wide. The flights provided information of time evolution of the structure of the boundary layer, as well as the spatial variability of the aerosols. A big fraction of the flights were performed towards Hyytiälä station on same time of the day during mornings, and they offer a time series of one and half month.

Most of the instruments were installed into a rack located inside the un-pressurized cabin. The aerosol instruments included an ultrafine condensation particle counter (uCPC) TSI 3776 (Mordas et al. 2008) with an aerosol cut-off size diameter of 3 nm, a Scanning mobility particle meter (SMPS, Wang and Flagan, 1990) with a size range of 10-320 nm, and a Particle size magnifier (PSM, Vanhanen et al, 2011) with a cut-off size of 1.5-2 nm with a condensational particle counter (CPC) TSI 3772. Also a gas analyzer LiCor Li-840 for H<sub>2</sub>O and CO<sub>2</sub> as well as a pressure sensor were located inside the cabin. The

temperature and relative humidity sensors were mounted under a wing. Also an isokinetic inlet was located under the wing out from the turbine flow. The flight track was recorded by a GPS receiver, and the payload included also computers for data accumulation and batteries for power.

## PRELIMINARY RESULTS AND CONCLUSIONS

The Cessna measurement flights performed during the Pegassos spring 2013 campaign provided an interesting one-and-half month time-series of airborne aerosols above Southern Finland. Results offer information of temporal and spatial variability of particle concentration and size distribution between particle diameters of 1.5-350 nm.

A careful analysis of the results will offer insights to several atmospheric phenomena. They include the altitude and spatial variability of the onset of new particle formation in lower troposphere. Preliminary results gave indications that nucleation in some conditions takes place at the top of the boundary layer. They also indicated that new particle formation could be a relatively local phenomenon also in the boreal forest.

## ACKNOWLEDGEMENTS

The financial support by the Academy of Finland Centre of Excellence program (project no 1118615) and the Nordic Centre of Excellence CRAICC (CRyosphere–Atmosphere Interactions in Changing Climate) are gratefully acknowledged.

## REFERENCES

- Asmi, E., D. Brus, S. Carbone, R. Hillamo, J. Hatakka, T. Laurila, H. Lihavainen, E. Rouhe, S. Saarikoski and Y. Viisanen (2013). Airborne measurements of aerosol particle physical, optical and chemical properties in Finland, in Proc. European Aerosol Conference 2013, Prague.
- Hari, P. and Kulmala, M. (2005). Station for measuring ecosystem-atmosphere relations (SMEAR II), *Boreal Env. Res.* 10, 5, 315-322.
- Mordas, G. et al. (2008). 'On Operation of the Ultra-Fine Water-Based CPC TSI 3786 and Comparison with Other TSI Models (TSI 3776, TSI 3772, TSI 3025, TSI 3010, TSI 3007)', *Aerosol Science and Technology*, 42:2, 152 – 158.
- Pirjola, L., H. Parviainen, T. Hussein, A. Valli, K. Hämeri, P. Aalto, A. Virtanen, J. Keskinen, T.A. Pakkanen, T. Mäkelä, R.E. Hillamo (2004), "Sniffer"—a novel tool for chasing vehicles and measuring traffic pollutants, *Atmospheric Environment*, **38**, 22, 3625-3635.
- Vanhanen, J., J. Mikkilä, K. Lehtipalo, M. Sipilä, H. E. Manninen, E. Siivola, T. Petäjä and M. Kulmala (2011), Particle Size Magnifier for Nano-CN Detection, *Aerosol Science and Technology*, **45**, 4, 533-542
- Wang, S.C. and Flagan, R.C. (1990). Scanning electrical mobility spectrometer, *Aerosol Science and Technology*, 13:2, 230-240.

# SIGNIFICANT INCREASE IN CCN YIELD IN FRESH BIOMASS BURNING PLUMES IN SOUTHERN AFRICA

V. VAKKARI<sup>1,2</sup>, V.-M. KERMINEN<sup>1</sup>, J.P. BEUKES<sup>3</sup>, P. TIITTA<sup>3,4</sup>, P.G. VAN ZYL<sup>3</sup>, M. JOSIPOVIC<sup>3</sup>, A.D. VENTER<sup>3</sup>, K. JAARS<sup>3</sup>, M. KULMALA<sup>1</sup> and L. LAAKSO<sup>2,3</sup>

<sup>1</sup>University of Helsinki, Department of Physics, FI-00014 Helsinki, Finland

<sup>2</sup>Finnish Meteorological Institute, Research and Development, FI-00101 Helsinki, Finland

<sup>3</sup>North-West University, Environmental Sciences and Management, ZA-2520 Potchefstroom, South Africa

<sup>4</sup>University of Eastern Finland, Department of Environmental Science, FI-70211 Kuopio, Finland

Keywords: biomass burning, wild fires, savannah, secondary aerosol formation.

## INTRODUCTION

Biomass burning (wild fires) is one of the largest sources of carbonaceous aerosol particles and trace gases into the atmosphere (e.g. Andreae and Merlet, 2001). However, biomass burning emissions are also among the parameters that create the largest uncertainties in the Cloud Condensation Nuclei (CCN) budgets in current global climate models (e.g. Spracklen *et al.*, 2011). This is partly because of uncertainties on the size distribution at the emission (Spracklen *et al.*, 2011), but also because of plume evolution in size scales below the resolution of current global climate models (Hennigan *et al.*, 2012).

We present here observations of biomass burning plumes from southern Africa and show that under favourable conditions the aerosol particle size distribution evolves quickly during the transport of the plume, which results in a significant increase in the CCN-sized particle yield from the fire.

## METHODS

Measurements were carried out from May 2010 to April 2012 at Welgegund measurement station (www.welgegund.org), 100 km south-west of Johannesburg, South Africa. Here we utilise the aerosol number size distributions from 12 to 840 nm measured with a differential mobility particle sizer (DMPS) (Hoppel, 1978), black carbon (BC) concentration from a Thermo model 5012 MAAP, carbon monoxide (CO) concentration from a Horiba APMA-360 analyser and basic meteorological quantities including solar radiation and local wind speed and direction.

The biomass burning plumes were identified in the measurements based on simultaneous increase in CO, BC and aerosol particle concentrations. The plumes were included in this study only if the MODIS burned area product (Roy *et al.*, 2008) indicated burned areas upwind of the measurement site. Only cases when fire generated aerosol (denoted with  $\Delta$ ) could be clearly separated from the pre-existing aerosol were used. The dilution of the plume during the transport is accounted for by presenting extensive properties as emission ratios with respect to  $\Delta\text{CO}$ , for instance the BC emission ratio is calculated as  $\Delta\text{BC}/\Delta\text{CO}$ .

During the dry season fires are widely spread over southern Africa (Swap *et al.*, 2003) and therefore there are often several potential fires where the detected plume could originate and thus the exact origin could not be determined for all plumes. However, when the location of the fire could be reliably determined the distance from the fire to the measurement station and the measured local wind speed were used to estimate the time the fire emissions had travelled in the atmosphere, i.e. the age of the plume.

## RESULTS

From May 20<sup>th</sup> 2010 to April 15<sup>th</sup> 2012 altogether 60 biomass burning plumes were observed at Welgegund. New particle formation and growth was observed in daytime plumes, as seen in Figure 1, but not in the plumes that had been transported in dark. This is reflected also in the growth rate of the plume count mean diameter (CMD). In the daytime plumes the CMD growth rate was 24 nm h<sup>-1</sup> during the first five hours, but in the night-time plumes the CMD growth rate was only 8 nm h<sup>-1</sup>.

A clear difference between day- and night-time plumes was also observed in the time evolution of particles larger than 100 nm (N100), i.e. in the CCN-sized particles. In the daytime plumes the N100 emission ratio ( $\Delta N_{100}/\Delta CO$ ) increased in nearly all cases, but no night-time plumes showed increase in the N100 emission ratio.

In the daytime plumes the increase in N100 emission ratio was dependant on the fraction of smouldering combustion in the fire. A high fraction of smouldering combustion, indicated by a low BC emission ratio (Yokelson *et al.*, 2009), led up to a factor of 5.1 increase in the N100 emission ratio after the first two hours of plume transport in daylight conditions. Conversely, in the daytime plumes that originated in mainly flaming combustion (indicated by a high BC emission ratio) the N100 emission ratio increased by only 20 %.

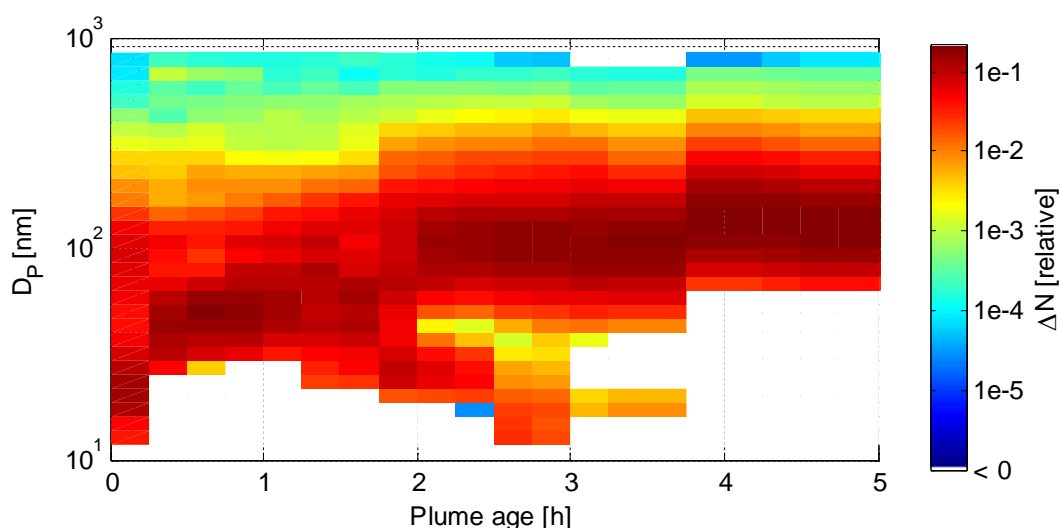


Figure 1. The time evolution of the submicron aerosol particle size distribution in daytime biomass burning plumes. The size distribution is plotted as a 45 minute running mean with 15 minute time step.

## CONCLUSIONS

Secondary aerosol formation was found to increase significantly the CCN-sized particle yield in southern African biomass burning plumes during the first few hours of plume ageing. However, photochemical reactions appear to be critical for secondary aerosol formation in the plumes as no aerosol formation was observed in plumes that were transported in dark. The formation of secondary aerosol was more pronounced if the plume originated in a fire with a higher fraction of smouldering combustion, which is reasonable considering that volatile organic compounds, which are important precursor compounds for secondary aerosol formation in the plume (e.g. Hennigan *et al.*, 2012), are emitted mainly in the smouldering phase of combustion (e.g. Yokelson *et al.*, 2009).

## ACKNOWLEDGEMENTS

This research was supported by the Academy of Finland under the projects Air pollution in Southern Africa (APSA) (project number 117505) and Atmospheric monitoring capacity building in Southern Africa (project number 132640), by the North-West University and by the Academy of Finland Center of Excellence program (project number 1118615).

## REFERENCES

- Andreae, M.O. and P. Merlet (2001). Emission of trace gases and aerosols from biomass burning, *Global Biogeochem. Cycles* **15**, 955–966.
- Hennigan, C.J., D.M. Westervelt, I. Riipinen, G.J. Engelhart, T. Lee, J.L. Collett Jr, S.N. Pandis, P.J. Adams and A.L. Robinson (2012). New particle formation and growth in biomass burning plumes: An important source of cloud condensation nuclei, *Geophys. Res. Lett.*, **39**, L0985, doi:10.1029/2012GL050930.
- Hoppel, W. A. (1978). Determination of the aerosol size distribution from the mobility distribution of the charged fraction of aerosols, *J. Aerosol Sci.*, **9**, 41–54.
- Roy, D.P., L. Boschetti, C.O. Justice and J. Ju (2008). The Collection 5 MODIS Burned Area Product – Global Evaluation by Comparison with the MODIS Active Fire Product, *Remote Sens. Environ.*, **112**, 3690–3707.
- Spracklen, D.V., K.S. Carslaw, U. Pöschl, A. Rap and P.M. Forster (2011). Global cloud condensation nuclei influenced by carbonaceous combustion aerosol, *Atmos. Chem. Phys.*, **11**, 9067–9087.
- Swap, R.J., H.J. Annegarn, J.T. Suttles, M.D. King, S. Platnick, J.L. Privette, and R.J. Scholes (2003). Africa burning: A thematic analysis of the Southern African Regional Science Initiative (SAFARI 2000), *J. Geophys. Res.*, **108**, 8465.
- Yokelson, R.J., J.D. Crounse, P.F. DeCarlo, T. Karl, S. Urbanski, E. Atlas, T. Campos, Y. Shinozuka, V. Kapustin, A.D. Clarke, A. Weinheimer, D.J. Knapp, D.D. Montzka, J. Holloway, P. Weibring, F. Flocke, W. Zheng, D. Toohey, P.O. Wennberg, C. Wiedinmyer, L. Mauldin, A. Fried, D. Richter, J. Walega, J.L. Jimenez, K. Adachi, P.R. Buseck, S.R. Hall and R. Shetter (2009). Emissions from biomass burning in the Yucatan, *Atmos. Chem. Phys.*, **9**, 5785–5812.

## DYNAMIC RELATIONSHIP BETWEEN THE VOC EMISSIONS FROM A SCOTS PINE STEM AND THE TREE WATER RELATIONS

A. VANHATALO<sup>1</sup>, T. CHAN<sup>1</sup>, J. AALTO<sup>1</sup>, J. KORHONEN<sup>1,2</sup>, P. KOLARI<sup>1,2</sup>,  
K. RISSANEN<sup>1</sup>, H. HAKOLA<sup>3</sup>, T. HÖLTTÄ<sup>1</sup>, E. NIKINMAA<sup>1</sup> and J. BÄCK<sup>1,2</sup>

<sup>1</sup>Department of Forest Sciences, University of Helsinki, Finland.

<sup>2</sup>Department of Physics, University of Helsinki, Finland.

<sup>3</sup>Finnish Meteorological Institute, Finland.

Keywords: VOC, WATER TRANSPORT, SCOTS PINE, SPRING RECOVERY.

### INTRODUCTION

The stems of coniferous trees contain huge storages of oleoresin, a viscous mixture of mono- and sesquiterpenes and resin acids. The composition of oleoresin depends on e.g. tree species, age, provenance, health status and environmental conditions. Oleoresin is constantly under pressure within the extensive network of resin ducts in wood, bark and needles. It flows out from a mechanically damaged site to protect the tree by sealing the wounded area. Once it is in contact with outside air, volatile parts of oleoresin evaporate and the residual compounds harden to make a solid protective seal over damaged tissues. Not only tree damage does oleoresin cause to flow out, but it commonly forms small drops onto buds and immature cones. Eller *et al.* (2013) has suggested that this kind of exposed resin might make a remarkable contribution to total ecosystem emissions.

VOC (volatile organic compound) emissions from pine oleoresin are dominated by monoterpenes, but also sesquiterpenes occur in the volatile blend. VOC emissions from pine foliage have been studied to some extent (e.g. Komenda and Koppmann, 2002; Räisänen *et al.*, 2008; Bäck *et al.*, 2012), but the emissions from woody plant parts are poorly known; not only in the case of pine but also other tree species.

Stem water transport is linked to canopy processes, such as stomatal conductance and soil water availability. Generally, water and solute transport in tree stems cease during the cold winter period, but as temperature rises in the early spring, the transport capacity of the stem recovers, resulting in the xylem conduits (in which air bubbles have formed during the winter) replenishing with water. The dehardening process in the spring involves biochemical changes affecting membrane transport properties, e.g. changes in their lipid composition (e.g. Pukacki and Kaminska-Rozek, 2013; Martz *et al.*, 2006). These changes are also linked to pressure changes over the membranes.

We set up an experiment to measure emissions of isoprene and monoterpenes as well as two oxygenated VOCs, methanol and acetone, from a Scots pine (*Pinus sylvestris*) stem and branches. To analyse the springtime dynamics of VOC emissions and their relationships with tree stem water transport capacity, we compared a wide set of measured emissions, diameter changes reflecting the pressure changes inside stem tissues, sap flow and transpiration data indicating the refilling of stem water storages after winter dehydration (the ratio of sap flow at the stem base to water loss by foliage) and many environmental factors. We hypothesize that the changes in membrane properties during springtime dehardening induce release of VOCs from the lipid storage pools, and that this can also be seen in the diameter changes at the time when the tree water transport capacity is recovered as a consequence of improved membrane permeability.

## METHODS

All the field measurements were conducted at the SMEAR II station during springtime. The measurements were started in early April when thick snow cover still laid on the ground and continued until mid-June, 2012. Pine shoots, thick branches and parts of the stem were enclosed in airtight chambers to observe their gas exchange. Chambers were connected with FEP lines to the H<sub>2</sub>O and CO<sub>2</sub> analysers and a quadrupole proton transfer reaction mass spectrometer (Q-PTR-MS). Simultaneously with gas exchange measurements, stem diameter changes were detected with pin-type sensors installed on either xylem or phloem of the stem. The sap flow between roots and stem was followed with Granier-type sensors.

During spring recovery, trees might have slightly different rhythms with their physical processes. This is why we here refer only to the data collected from a single tree having a breast height diameter of 20 cm and a height of 18,6 m.

## RESULTS AND CONCLUSIONS

The results show that already very early in the spring, significant VOC emissions from the pine stem can be detected (Fig. 1. upper panel), and that they exhibit a diurnal cycle similar to that of ambient

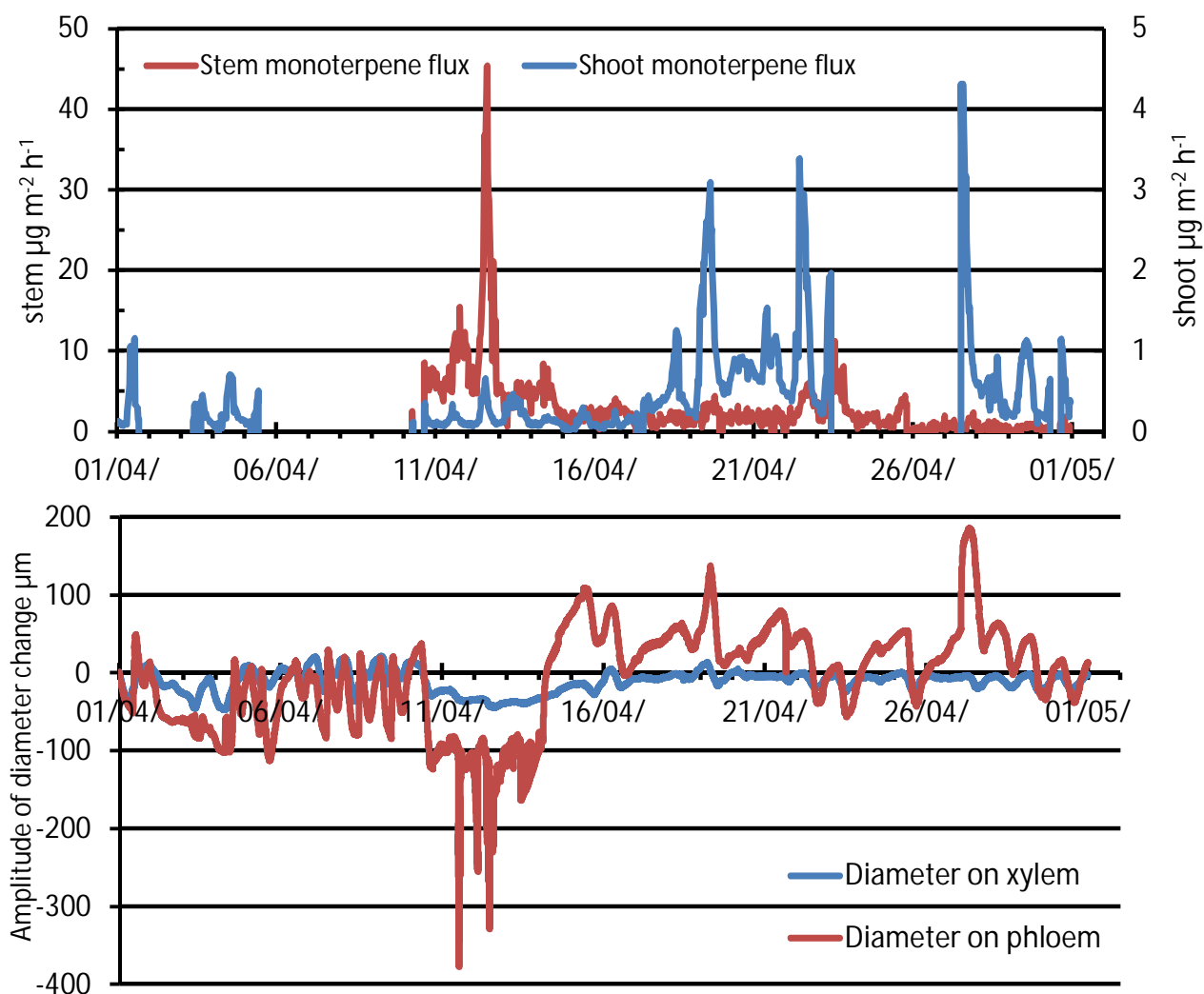


Figure 1. Monoterpene emissions from stem and shoot (upper panel) and stem diameter changes (lower panel) of a Scots pine in April 2012.

temperature. During the highest emission period a sudden decrease in the stem diameter was observed (Fig 1. lower panel), which we hypothesize could either indicate a decrease in the pressure of living cells in connection with stem VOC emissions, or result mechanically from the exudation of oleoresin from the stem. We also found that the stem water stores and xylem water transport capacity increased during periods of VOC emissions, which indicates xylem embolism refilling during the times of VOC emissions.

By taking samples for gas chromatographic analysis, a qualitative difference was found between VOC emissions from the pine stem, thick branches and shoots.  $\alpha$ -pinene and  $\delta$ -3-carene together formed always over 80% of the emissions, but the samples from the branch had a bigger proportion of  $\delta$ -3-carene and a smaller proportion of  $\alpha$ -pinene compared with the samples from the stem. Terpinolene was found only in the samples from the branch, and there it formed 10% of the emissions.

We measured only one single tree, but similar changes are visible also at the ecosystem level. The coinciding ecosystem flux measurements of  $\text{CO}_2$  reveal that during the same days the forest ecosystem turns from a  $\text{CO}_2$  source to a clear  $\text{CO}_2$  sink (Figure 2.). Likely there are differences between tree individuals when their photosynthesis capacity recovers after winter, but on average it seems to happen at the same time as in the case of our measured tree.

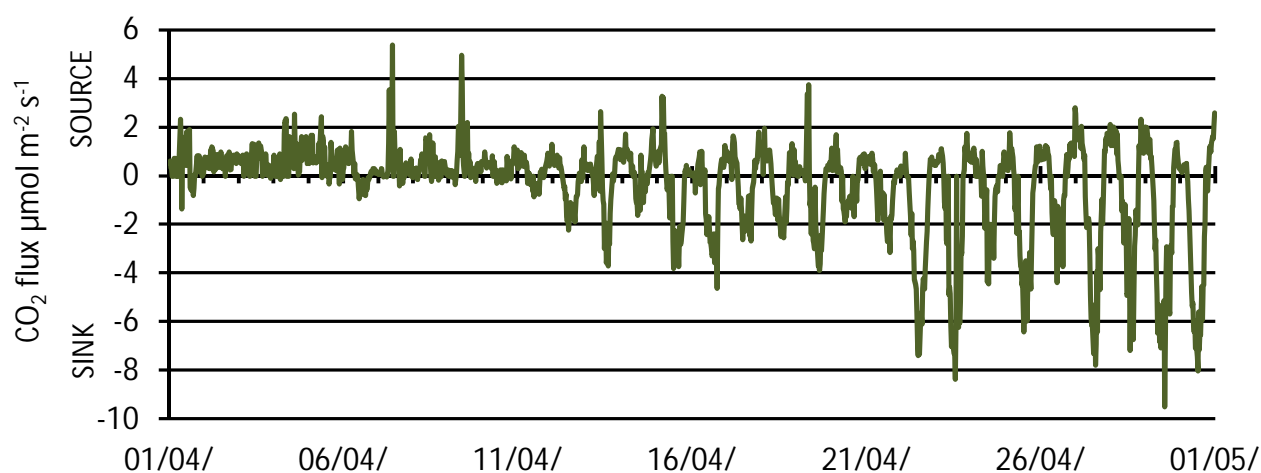


Figure 2.  $\text{CO}_2$  flux from the forest ecosystem in April 2012. Flux was measured with an eddy covariance system nearby the intensively monitored pine.

Our results show that emissions from tree stems are connected to the tree water relations at least at the beginning of the growing period. In addition, as most of the tree biomass is in the lower part of the stem, monoterpene emissions from tree stems are important during the period when the foliage still is rather inactive.

In conclusion, the springtime processes where a tree shifts from winter dormancy to active growing period state include changes in both tree physiology and chemistry. In boreal forests, these changes occur early in the spring, already before snow melt. Thus, the common impression that nothing happens in tree physiology before bud burst is flawed.

## ACKNOWLEDGEMENTS

This work was supported by the Finnish Center of Excellence ‘Physics, Chemistry, Biology and Meteorology of Atmospheric Composition and Climate Change’ (project 1118615) and Helsinki University Centre for Environment HENVI.

## REFERENCES

- Bäck, J., J. Aalto, M. Henriksson, H. Hakola, Q. He and M. Boy (2012). Chemodiversity of a Scots pine stand and implications for terpene air concentrations, *Biogeosciences* **9**, 689.
- Eller, A.S.D., P. Harley, and R.K. Monson (2013). Potential contribution of exposed resin to ecosystem emissions of monoterpenes, *Atm Env* **77**, 440.
- Komenda, M. and R. Koppmann (2002). Monoterpene emissions from Scots pine (*Pinus sylvestris*): Field studies of emissions rate variabilities, *J Geophys Res* **107**, D13.
- Martz, F., M.-L. Sutinen, S. Kiviniemi and J.P. Palta (2006). Changes in freezing tolerance, plasma membrane H<sup>+</sup>-ATPase activity and fatty acid composition in *Pinus resinosa* needles during cold acclimation and de-acclimation, *Tree Phys* **26**, 783.
- Pukacki, P.M. and E. Kaminska-Rozek (2013). Differential effects of spring reacclimation and deacclimation on cell membranes of Norway spruce seedlings, *Acta Societatis Botanicorum Poloniae* **82**, 77.
- Räisänen, T., A. Ryyppö and S. Kellomäki (2008). Effects of elevated CO<sub>2</sub> and temperature on monoterpene emission of Scots pine (*Pinus sylvestris* L.), *Atm Env* **42**, 4160.

# SUB3-NM GROWTH RATES IN THE CLOUD EXPERIMENT

D. WIMMER<sup>1,2</sup>, K. LEHTIPALO<sup>2, 3</sup>, T. PETÄJÄ<sup>2</sup>, M. KULMALA<sup>2</sup>, J. CURTIUS<sup>1</sup> and the CLOUD collaboration.

<sup>1</sup> Goethe Universität, Frankfurt am Main, Altenhöferallee 1, 60438 Frankfurt am Main, Germany.

<sup>2</sup>Department of Physics, University of Helsinki, Gustaf Hallströmin katu 2a, 00550, Helsinki, Finland.

Keywords: growth rate, sub-3nm, CLOUD.

## INTRODUCTION

As the mechanisms and the exact amount and composition of atmospheric trace gases leading to atmospheric new particle formation are still not fully understood. To study the initial processes and also the effect of galactic cosmic rays underlying new particle formation the CLOUD experiment at CERN was designed (Duplissy, 2010; Kirkby, 2011). The CLOUD facility comprises state of the art instruments measuring the concentration of trace gases (CIMS, PTR-ToF, LoPap,...), aerosol size distributions and concentrations (SMPS, CPC battery, PSMs, LDT,...) covering the size range from 1 nm up to CCN sizes. The work presented here will mostly deal with the measurements of particle concentrations and formation rates in the sub-3 nm size range. When calculating growth rates in the small sizes, using total particle counters there is no standard method developed so far. The CLOUD facility gives the opportunity to study the effects of small clusters (i. e. <1.7 nm) on the direct measurements of the particle growth rates. As we have the opportunity to have a variety of particle counters in CLOUD, the growth rates can be determined from instruments using different methods to measure the size distributions independently.

## METHODS

The growth rates in the sub-3 nm size range have been evaluated for two different CLOUD campaigns focussing on two different topics. The results shown here, were determined for the CLOUD 4 and 5 campaign. In the CLOUD 4 campaign the goal was to study the nucleation processes of clusters under very clean conditions (e.g. well controlled composition of the clusters). In CLOUD 4 ammonia and dimethylamine were added in various concentrations to the chamber. The main focus of the CLOUD 5 campaign was to study the nucleation processes under conditions typical for the upper troposphere, which was achieved by varying the temperature in the chamber between 208 and 270 K.

The instruments used for analysing the sub-3nm growth rates include a particle size magnifier (PSM), two laminar flow Diethylene glycol based Condensation Particle Counters (DEG CPCs) and a commercial butanol based TSI CPC (model Nr 3776). In CLOUD 4 the PSM was set to scanning mode where the supersaturations are constantly changed to achieve cut-offs between 1 and 2nm where the two DEG CPCs were measuring at two fixed cut-off diameters (1.7 and 2 nm for negative sodium chloride clusters). The settings of the commercial butanol CPC are the standard settings, resulting in a cut-off of 2.9 nm for tungsten oxide particles. In CLOUD 5 all the configurations were the same, except that two PSMs were used at two different fixed cut-offs.

The growth rates for the PSMs were determined according to the method presented in (Lehtipalo, 2013).

For the laminar flow CPCs on the other hand, a slightly modified method was applied. The times when the particles reach 50 % of the maximum concentrations were determined. The difference in the d50 was assumed to be 1.2 nm (d50 of 1.7 for the DEG CPC and 2.9 for the commercial ultrafine CPC.)

As lab studies have shown (Wimmer, 2013) the behaviour of the laminar flow DEG CPCs depends rather strongly on the particle composition. Therefore it is not so straight forward to calculate the growth rates using these instruments. To get an idea of how far the growth rate analysis using the 50 % method is influenced by the different composition of the clusters, the growth rates have been analysed using the two laminar flow DEG CPC and the TSI 3776 and compared to the growth rates, evaluated using the PSMs.

The same procedure has been applied for the CLOUD 5 data. As in CLOUD 5 the temperatures inside the CLOUD chamber were varied it might also affect the growth rates determined using the laminar flow CPCs. A set of calibration measurements was performed using the CLOUD chamber as aerosol generator and a Grimm nano-DMA to classify the aerosol at the end of the CLOUD 5 campaign. Due to time restrictions and a non-optimum set-up, no valuable results could be achieved.

## CONCLUSIONS

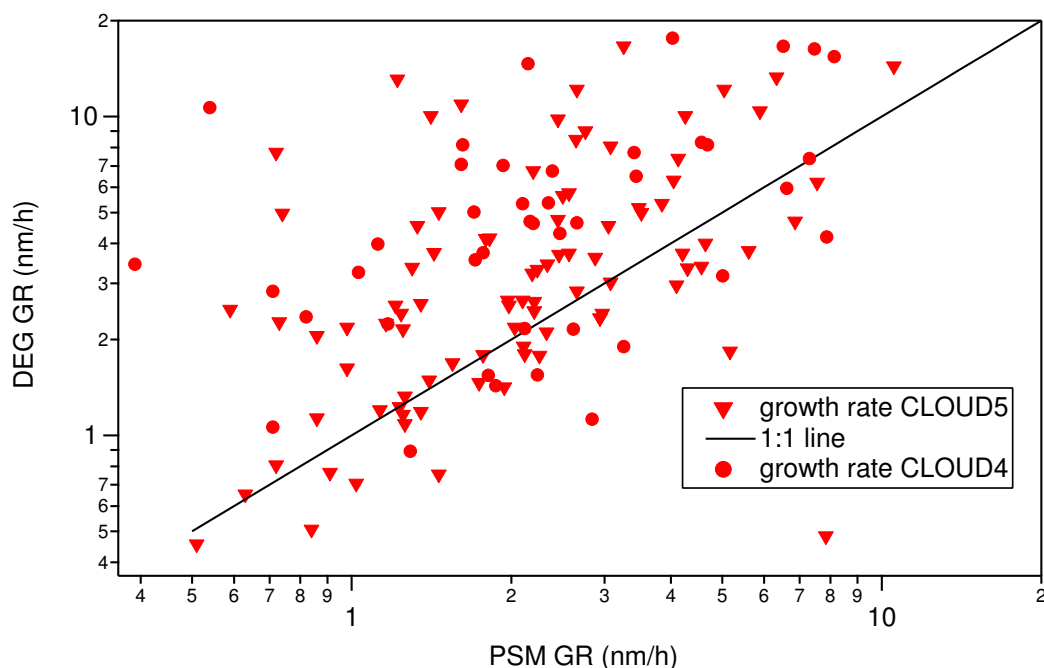


Figure 1: Scatter plot of the growth rates in nm/h determined using the PSM on the y-axis and the laminar flow CPCs on the x-axis. Circles represent CLOUD 4 data, triangles CLOUD5. The black line shows the 1:1 line. The scatter might be explained by the different response of the laminar flow CPCs to the different cluster composition. Also the different conditions in the chamber might have an influence on the response of the CPCs.

More in-depth analysis is necessary to get a deeper insight in the response of the laminar flow DEG CPCs to various cluster compositions. The first step analysis shows that there is some relation in the growth rates determined from the PSMs as well as from the laminar flow CPCs. There appears to be a lot of scatter in the data too, which is not clear yet, why. The reasons can be due to

the different response of the laminar flow CPCs due to different cluster composition, but it is also very likely that it is due to the different conditions in the chamber (RH, temperature, background contamination,...). The next step will be to have a closer look at the different conditions and how they affect the response of the laminar flow CPCs. It could be considered to think about a set of calibration measurements using the CLOUD chamber by using a different measurement set-up in the near future.

## ACKNOWLEDGEMENTS

We would like to thank CERN for supporting CLOUD with important technical and financial resources, and for providing a particle beam from the CERN Proton Synchrotron. This research has received funding from the EC Seventh Framework Programme (Marie Curie Initial Training Network “CLOUD-ITN” grant no. 215072, and ERC-Advanced “ATMNUCLE” grant no. 227463), the German Federal Ministry of Education and Research (project no. 01LK0902A), the Academy of Finland Center of Excellence program (project no. 1118615).

## REFERENCES

- Duplissy, J., Enghoff, M. B., Aplin, K. L., Arnold, F., Aufmhoff, H., Avngaard, M., Baltensperger, U., Bondo, T., Bingham, R., Carslaw, K., Curtius, J., David, A., Fastrup, B., Gagne, S., Hahn, F., Harrison, R. G., Kellet, B., Kirkby, J., Kulmala, M., Laakso, L., Laaksonen, A., Lillestol, E., Lockwood, M., Mäkelä, J., Makhmutov, V., Marsh, N. D., Nieminen, T., Onnela, A., Pedersen, E., Pedersen, J. O. P., Polny, J., Reichl, U., Seinfeld, J. H., Sipilä, M., Stozhkov, Y., Stratmann, F., Svensmark, H., Svensmark, J., Verheggen, B., Viisanen, Y., Wagner, P. E. Wehrle, G., Weingartner, E., Wex, H., Wilhelmsson, M., Winkler, P. M. (2010). Results from the CERN pilot CLOUD experiment. *Atmos Chem Phys*, **10**, 1635-1647.
- Kirkby J., Curtius J., Almeida J., Dunne E., Duplissy J., Ehrhart S., Franchin A., Gagne S., Ickes L., Kürten A., Kupc A., Metzger A., Riccobono F., Rondo L., Schobesberger S., Tsagkogeorgas G., Wimmer D., Amorim A., Bianchi F., Breitenlechner M., David A., Dommen J., Downard A., Ehn M., Flagan R., Haider S., Hansel A., Hauser D., Jud W., Junninen H., Kreissl F., Kvashin A., Laaksonen A., Lehtipalo K., Lima J., Lovejoy, Makhmutov A., Mathot S., Mikkilä J., Minginette P., Mogo S., Nieminen T., Onnela A., Pereira, Petäjä T., Schnitzhofer R., Seinfeld J., Sipilä M., Stozhkov J., Stratmann F., Tome A., Vanhanen J., Viisanen, Vrtala A., Wagner P., Walther H., Weingartner E., Wex H., Winkler P., Carslaw K., Worsnop D., Baltensperger U., and Kulmala M. (2011). Role of sulphuric acid, ammonia and galactic cosmic rays in atmospheric aerosol nucleation, *Nature*, **476**, 429–433.
- Lehtipalo K., Rondo L., Schobesberger S., Jokinen T., Sarnela N., Franchin A., Nieminen T., Sipilä M., Kürten A., Riccobono F., Ehrhart S., Yli-Juuti T., Kontkanen J., Adamov A., Almeida J., Amorim A., Bianchi F., Breitenlechner M., Dommen J., Downard A. J., Dunne E. M., Duplissy J., Flagan R. C., Guida R., Hakala J., Hansel A., Jud W., Kangasluoma J., Keskinen H., Kim J., Kupc A., Laaksonen A., Mathot S., Ortega I. K., Onnela A., Praplan A., Rissanen M. P., Ruuskanen T., Santos D. F., Schallhart S., Schnitzhofer R., Smith J. N., Tröstl J., Tsagkogeorgas G., Tome A., Vaattovaara P., Vrtala A. E., Wagner P. E., Williamson C., Wimmer D., Winkler P. M., Virtanen A., Donahue N. M., Carslaw K. S., Baltensperger U., Kirkby J., Riipinen I., Curtius J., Kulmala M. and Worsnop D. R. (2013). Hidden sulphuric acid leads to rapid growth of freshly nucleated nanoparticles under atmospheric conditions *submitted to Science*, 2013
- Wimmer D., Lehtipalo K., Franchin A., Kangasluoma J., Kreissl F., Kürten A., Kupc A., Metzger

A., Mikkiä J., Petäjä T., Riccobono F., Vanhanen J., Kulmala M., Curtius J. (2013). Performance of Diethylene glycol-based particle counters in the sub-3 nm size range *Atmos. Meas. Tech.*, **6**, 1793–1804.

## EXPERIMENTAL STUDIES ON THE EFFECTS OF BLACK CARBON ON SNOW ALBEDO

A.VIRKKULA<sup>1,2</sup>, A.AARVA<sup>1</sup>, O.JÄRVINEN<sup>2</sup>, J.SVENSSON<sup>1</sup>, N.KIVEKÄS<sup>1</sup>, O.MEINANDER<sup>1</sup>,  
A.HYVÄRINEN<sup>1</sup>, K.NEITOLA<sup>1</sup>, H.LIHAVAINEN<sup>1</sup>, H.-R.HANNULA<sup>3</sup>, A.KONTU<sup>3</sup>,  
K. ANTTILA<sup>1,4</sup>, J. PELTONIEMI<sup>4</sup>, M. GRITSEVICH<sup>4</sup>, T. HAKALA<sup>1,4</sup>,  
H. KAARTINEN<sup>4</sup>, P. LAHTINEN<sup>1</sup>, A. RAATEROVA<sup>3</sup>, R.VÄÄNÄNEN<sup>2</sup>,  
P. DAGSSON-WALDHAUSEROVA<sup>5</sup>, R.E. BICHELL<sup>2</sup> and G.DE LEEUW<sup>1,2</sup>

<sup>1</sup>Finnish Meteorological Institute, 00560 Helsinki, Finland

<sup>2</sup>Department of Physics, FI-00014 University of Helsinki.

<sup>3</sup>Finnish Meteorological Institute, Sodankylä Observatory, FI-99600 Sodankylä, Finland

<sup>4</sup>Finnish Geodetic Institute, Finnish Geodetic Institute, FI-02431 Masala, Finland

<sup>5</sup>Agricultural University of Iceland, Hvanneyri, 311 Borgarnes, Iceland

Keywords: BLACK CARBON, SNOW, ALBEDO

### INTRODUCTION

Soot particles contain black carbon (BC) and organics. When soot particles get deposited on snow the BC and also some of the organics will absorb solar radiation. This leads to a decrease of the snowpack albedo, heating of the snow and acceleration of its melting (e.g., Warren and Wiscombe, 1980; Clarke and Noone, 1985; Flanner *et al.*, 2007; Quinn *et al.*, 2008). These effects may be responsible for as much as a quarter of the observed global warming (Hansen and Nazarenko, 2004).

The above-mentioned effects have been investigated in the Soot-on-Snow project. It consists of a series of experiments aimed for studying the effects of soot on snow, for example the effect on albedo, snow grain size, and melting. Experiments have so far been conducted during three consequent late winters / springs. The first one of the series was conducted in spring 2011, the second in winter/spring 2012 and the latest one in spring 2013 (e.g., Meinander *et al.*, 2013). The experiments were organized by the Finnish Meteorological Institute in cooperation with University of Helsinki Physics department, Finnish Geodetic Institute, and Agricultural University of Iceland.

### METHODS

In all experiments soot was deposited on snow but with different methods. In the first campaign in 2011 soot particles were produced by burning various organic materials in a wood-burning stove. The smoke was lead through a pipe, cooled by snow surrounding the pipe, and lead into a rectangular chamber on top of the snow. In 2012 the soot was first acquired from a chimney-sweeping company in Helsinki. The chimneys the company had cleaned were in residential buildings with small-scale wood burning. The soot was blown into a cylindrical (diameter 4 m) chamber laying on snow of a farming field.

The blowing system consisted of a blower, a tube blowing air into a barrel filled with the soot, and a cyclone that removed largest particles. In 2013 the blowing system was modified so that the amount of soot blown could be controlled. The soot was from the same source as in the 2012 experiment, i.e., from small-scale wood-burning chimneys but also from chimneys from buildings with an oil burner and from a peat-burning power plant.

In addition, in the 2013 experiment, Icelandic volcanic sand and glaciogenic silt were blown over the snow. The volcanic sand was a near black mixture of the volcanic ash of glaciofluvial nature, originating from under the Myrdalsjokull glacier, which may be mixed with the ash of the Eyjafjallajokull eruption in 2010 and the Grimsvotn eruption in 2011. The glaciogenic silt was lighter in colour than sand, from light-brown to slightly yellowish colour consisting mainly of silt and some coarse clay sized particles, capable

of being transported and deposited on the local glaciers as well as several hundreds of kilometres towards the Europe (Arnalds *et al.*, 2013).

After depositing the soot, pyranometers were set up over the soot and reference fields to measure incoming global radiation and reflected radiation. From the ratio the albedo was calculated. Snow samples were taken and analyzed for elemental and organic carbon with a Sunset Labs EC/OC analyzer. Snowpack thickness was measured, and a physical characterization of snow stratigraphy was done, including thickness, density, hardness, grain size and shape, and temperature. In addition, the spectral reflected and transmitted irradiance was measured for some spots.

The first experiment was conducted at a private farming field in Nurmijärvi, southern Finland in March – April 2011. The second experiment was conducted at the FMI observatory in Jokioinen, southern Finland in February – March 2012. The third experiment was conducted at the Sodankylä airfield near the FMI Sodankylä observatory, Finnish Lapland in April – May 2013.

## RESULTS AND DISCUSSION

The experiment demonstrated very clearly the effects of soot on snow: the albedo decreased, the snow grain size, the whole stratigraphy, temperature profile, and melting rate in the snow pack changed compared with the reference site. The albedo of the snowpack decreased logarithmically as a function of elemental carbon concentrations (Figure 1). The data are in a fairly good agreement with the laboratory experiments and modeled data of Hadley and Kirchstetter (2012).

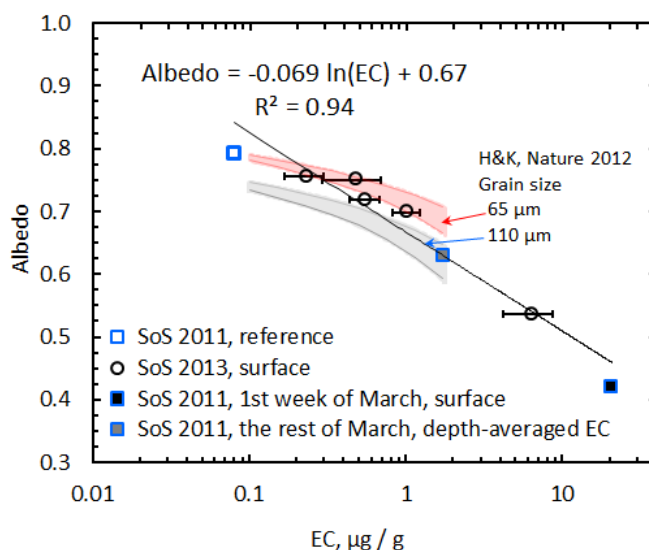


Figure 1. Albedo of snow at solar noon as a function of Elemental Carbon concentration in snow.

## ACKNOWLEDGEMENTS

This work was supported by the Nordic Centre of Excellence CRAICC (Cryosphere-atmosphere interactions in a changing Arctic climate), the Academy of Finland (Arctic Absorbing Aerosols and Albedo of Snow (A4), project number 3162), the Maj and Tor Nessling foundation, the Finnish Centre of Excellence in Physics, Chemistry, Biology and Meteorology of Atmospheric Composition and Climate Change (program number 1118615), and the EU Life+ project Mitigation of Arctic warming by controlling European black carbon emissions (MACEB).

## REFERENCES

- Arnalds, O., E.F. Thorarinsdottir, J. Thorsson, P. Dagsson-Waldhauserova, A.M. Agustsdottir (2013). An extreme wind erosion event of the fresh Eyjafjallajökull volcanic ash. *Nature*, Scientific Reports 3, 1257.
- Clarke, A. D. and Noone, K. J. (1985). Soot in the Arctic snowpack: a cause for perturbations in radiative transfer, *Atmos. Environ.*, **19**, 2045–2053.
- Flanner, M. G., C. S. Zender, J. T. Randerson, and P. J. Rasch (2007). Present-day climate forcing and response from black carbon in snow, *J. Geophys. Res.*, 112, D11202, doi:10.1029/2006JD008003.
- Hadley, O.L. and Kirchstetter, T.W.: Black-carbon reduction of snow albedo, *Nature Climate Change*, **2** (3), <http://dx.doi.org/10.1038/nclimate1433M3>, 2012.
- Hansen, J. and Nazarenko, L. (2004). Soot climate forcing via snow and ice albedos, *Proc. Nat. Acad. Sci.*, 101, 423–428, 2004.
- Meinander, O., A. Virkkula, J. Svensson, N. Kivekäs, H. Lihavainen, P. Dagsson-Waldhauserova, O. Arnalds, H.-R. Hannula, A. Kontu, K. Anttila, J. Peltoniemi, M. Gritsevich, T. Hakala, H. Kaartinen, P. Lahtinen, O. Järvinen, A. Aarva, Neitola K., A. Raaterova, R.E. Bichell and G. De Leeuw (2013) Snow reflectance affected by soot, volcanic sand, and glaciogenic silt deposited on snow (sos-2013 experiment), This issue.
- Quinn, P. K., Bates, T. S., Baum, E., Doubleday, N., Fiore, A. M., Flanner, M., Fridlind, A., Garrett, T. J., Koch, D., Menon, S., Shindell, D., Stohl, A., and Warren, S. G. (2008). Short-lived pollutants in the Arctic: their climate impact and possible mitigation strategies, *Atmos. Chem. Phys.*, 8, 1723–1735, doi:10.5194/acp-8-1723-2008.
- Warren, S., and W. Wiscombe (1980). A model for the spectral albedo of snow. II: Snow containing atmospheric aerosols, *J. Atmos. Sci.*, 37, 2734–2745.

# EFFECTIVE PARTICLE SIZE ESTIMATED FROM TOTAL SCATTERING COEFFICIENT AND TOTAL NUMBER CONCENTRATION

A.VIRKKULA<sup>1,2</sup>

<sup>1</sup>Finnish Meteorological Institute, 00560 Helsinki, Finland

<sup>2</sup>Department of Physics, FI-00014 University of Helsinki.

Keywords: SCATTERING COEFFICIENT, NUMBER CONCENTRATION, PARTICLE SIZE

## INTRODUCTION

Particle size distribution and chemical composition determine the optical properties of aerosols. In an ideal setup for studying the direct radiative effects and the contributing species there should be instrumentation for measuring particle size distributions, scattering and absorption, and size-dependent chemical composition. With such a setup it is possible to calculate the degree of closure using modeling, for example to evaluate uncertainties and the contributions of the constituents to the aerosol radiative properties (e.g., Ogren, 1995; Huebert et al., 2003). A simpler measurement setup where scattering coefficients and aerosol mass concentration are measured simultaneously yield the mass scattering efficiencies. This type of measurements have been conducted for decades (e.g., Charlson et al., 1968; Waggoner and Weiss, 1980) and they are useful in for instance air quality monitoring (Malm and Hand, 2007).

However, in both field and laboratory work there are sometimes situations when only a nephelometer and a condensation particle counter are available without proper information on size distributions. For instance, University of Helsinki Department of Physics operated a Radiance Research nephelometer that measures total scattering coefficient at  $\lambda = 545$  nm simultaneously with a condensation particle counter in a research aircraft without full particle size distribution measurements during several flights in the years 2009 and 2010 (Schobesberger et al., 2013). The same setup was used also during airborne measurements as part of the prescribed burning of a boreal forest in Hyytiälä, Finland in June 2009 (Virkkula et al., 2013) and in the Arctic Ocean during the fifth Chinese National Arctic Expedition (CHINARE 5) onboard the Chinese polar research vessel Xue Long in late summer and autumn of 2012 (Virkkula et al., 2012).

The purpose of this paper is to show what is the information that can and cannot be obtained from the simultaneous measurements of total light scattering at one wavelength and total number concentration without additional size distribution information in typical atmospheric conditions. The principle will be presented and applied to data obtained from the SMEAR II field station in Finland (Hari and Kulmala, 2005). The data set is the same that was presented by Virkkula et al. (2011).

## THEORY

For a monodisperse particle size distribution light scattering coefficient  $\sigma_{sp}$  is calculated from

$$\sigma_{sp} = N A_p Q_s \equiv N C_{sca} \quad (1)$$

where  $N$  is the particle number concentration,  $A_p$  is the geometric cross section of the particles,  $Q_s$  is the particle scattering efficiency, and  $C_{sca}$  is the scattering cross section of the particles.  $C_{sca}$  is a hypothetical area by which the particle scatters light and depending on the scattering efficiency  $Q_s$  it may be either larger or smaller than  $A_p$ . If it is assumed that the particles are spherical, the diameter of the scattering cross section can be calculated from

$$D_{C_{sca}} = \sqrt{\frac{4}{\pi} C_s} = \sqrt{\frac{4}{\pi} \frac{\sigma_{sp}}{N}} \quad (2)$$

However, in the real atmosphere size distributions are not monodisperse. Therefore the diameter obtained from (2) may be called the effective scattering cross section diameter.

To evaluate the ability of  $D_{\text{Cscs}}$  to describe particle sizes it should be compared with some real data from a site where also particle number size distributions are measured. Two weighted diameters are typically calculated for describing the effective size: the count mean diameter

$$CMD = \frac{\sum D_{p,i} N_i}{\sum N_i} \quad (3)$$

and the geometric mean diameter

$$D_g = \exp\left(\frac{\sum N_i \ln(D_{p,i})}{\sum N_i}\right) \quad (4)$$

where  $N_i$  is the number of particles with diameter  $D_{p,i}$ . Below these two weighted diameters will be compared with the effective scattering cross section diameter  $D_{\text{Cscs}}$ . In addition to analyzing real measurement data, simulated lognormal functions can be used for evaluating the relationships of  $D_{\text{Cscs}}$ , CMD, and  $D_g$ . I generated monomodal size distributions by varying the geometric standard deviation  $\sigma_g$  and  $D_g$  and for each of these I calculated the total scattering coefficient from

$$\sigma_{sp}(\lambda) = \int Q_s(\lambda, D_p, m) \frac{\pi D_p^2}{4} n_i dD_p \quad (5)$$

where  $Q_s(\lambda, D_p, m)$  is the scattering efficiency of particles with diameter  $D_p$  and  $m$  the complex refractive index. For simplicity I only used the refractive index of ammonium sulfate ( $m = 1.521 + 0i$ ) which is very close to the average refractive index obtained by an iterative procedure (Virkkula et al., 2011). The scattering efficiencies were calculated using the Mie code by Barber and Hill (1990). Then I calculated  $D_{\text{Cscs}}$  for these simulations from (2).

I also compared  $D_{\text{Cscs}}$  with two intensive aerosol optical properties that are known to be related to the size distributions. The Ångström exponent of scattering  $\alpha_{sp}$  describes the wavelength dependency of scattering. In general it is assumed that large values ( $\alpha_{sp} > 2$ ) indicate the dominance of small particles and small values ( $\alpha_{sp} < 1$ ) the dominance of large particles. The backscatter fraction  $b$  is a measure related to the angular distribution of light scattered by aerosol particles. In general, larger particles scatter less light backwards than small particles so the size relationship of  $b$  is qualitatively similar to that of  $\alpha_{sp}$ .

## MEASUREMENT DATA

The measurements were conducted at the Station for Measuring Ecosystem–Atmosphere Relations (SMEAR II) station in Hyytiälä, Finland, from October 2006 to May 2009. The measurements used for the present work were discussed in detail by Virkkula et al. (2011), here just a brief description is given. Total scattering coefficients ( $\sigma_{sp}$ ) and backscattering coefficients ( $\sigma_{bsp}$ ) were measured with a TSI model 3963 nephelometer at  $\lambda = 450$  nm, 550 nm, and 700 nm and corrected for truncation. Particle number size distributions were measured with a custom-made Twin-DMPS (TDMPS) system in the size range 3 – 1000 nm (Aalto *et al.*, 2001) and a TSI aerodynamic particle sizer APS in the aerodynamic diameter size range 0.53 – 20  $\mu\text{m}$ . In the overlapping range of the TDMPS and the APS the number concentrations from the TDMPS were used up to 700 nm. The data presented here were averaged over 60 minutes. Only those data were used that were measured when the relative humidity within the nephelometer was  $< 50\%$ .

## RESULTS AND DISCUSSION

The effective scattering cross section diameter ( $D_{\text{Cscs}}$ ) is positively correlated with both weighted mean diameters but better ( $R^2 = 0.77$ ) with the count mean diameter (CMD) than with the geometric mean diameter ( $D_g$ ) ( $R^2 = 0.61$ ) (Figure 1). The relationship is not unambiguous, however.  $D_{\text{Cscs}}$  in the range of

about 70 – 200 nm corresponds to a wide range of both weighted mean diameters: there is almost an order of magnitude range of geometric mean diameters that can correspond to each  $D_{Cscs}$ . For larger values, especially in the range  $> 300$  nm  $D_{Cscs}$  predicts both weighted mean diameters much better. This is even more evident when the relationships are presented as the ratios of the weighted mean diameters to  $D_{Cscs}$  (Figure 2). I also classified the data into  $D_{Cscs}$  bins so that there were 5 logarithmically evenly-spaced bins in decade and calculated simple descriptive statistics in each bin: average, median, and the 2.5<sup>th</sup>, 25<sup>th</sup>, 75<sup>th</sup>, and the 97.5<sup>th</sup> percentiles. The scatter plot of ratio (Figure 2) shows, like the regression, that CMD can be better predicted with  $D_{Cscs}$  than  $D_g$ .

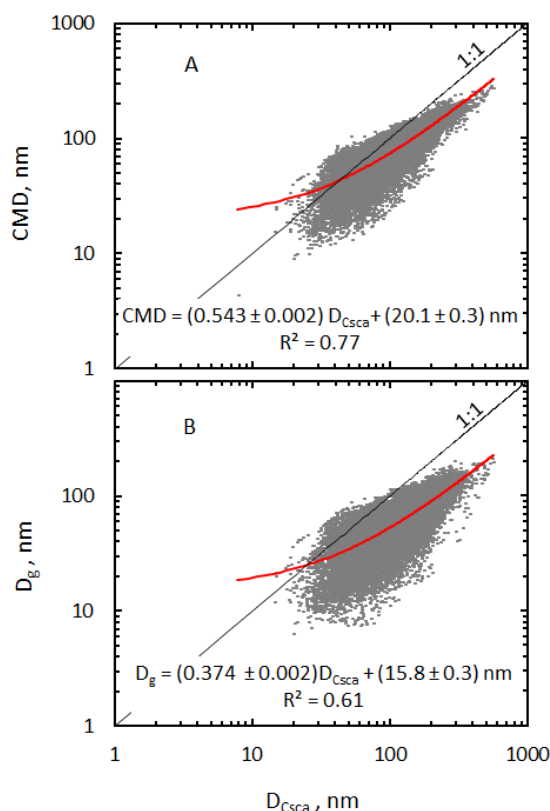


Figure 1. Count mean diameter (CMD) and geometric mean diameter ( $D_g$ ) as a function of the effective scattering cross section diameter ( $D_{Cscs}$ ) at SMEAR II from October 2006 to May 2009. The equations show slope and offset and the respective standard errors obtained from linear regressions shown in the red line.

I simulated simple monomodal size distributions by varying the geometric standard deviation  $\sigma_g$ . For narrow size distributions ( $\sigma_g < 1.6$ ) both the  $D_g$ -to- $D_{Cscs}$  ratio and the CMD-to- $D_{Cscs}$  ratios would be clearly larger than any of the observed ratios (Figure 2). Monomodal size distributions would explain some of the observations if  $\sigma_g > 1.6$  but even with  $\sigma_g = 2.4$  a large fraction of the observed ratios were smaller than for the simulation (Figure 2). The explanation is that in the real size distributions there are typically more modes – for instance in a size distribution there may simultaneously exist a nucleation, an Aitken, an accumulation and a coarse particle mode. The particles in the larger modes contribute most to scattering. This is probably the case in the size distributions where  $D_{Cscs}$  is in the range of about 70 – 200 nm and  $D_g$  is almost an order of magnitude lower (Figure 2). These probably correspond to such new particle formation events during which also large particles were present. When  $D_{Cscs}$  was in the size range of less than about 40 nm the median  $D_g$ -to- $D_{Cscs}$  ratio was  $\sim 0.73$  and the median CMD-to- $D_{Cscs}$  ratio  $\sim 0.96$ , suggesting that the nephelometer – particle counter combination can also to some extent indicate the dominance of nucleation mode particles.

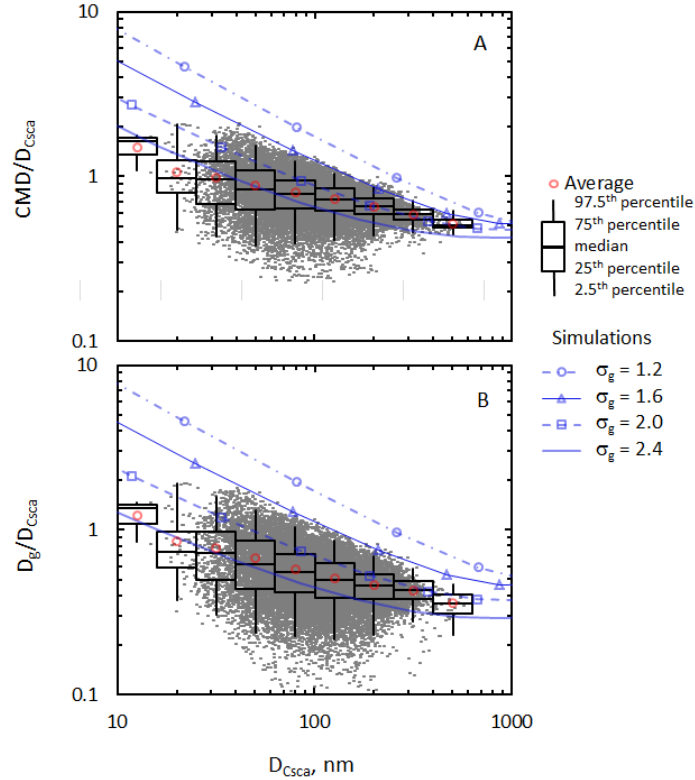


Figure 2. The ratios of A) count mean diameter (CMD) and B) geometric mean diameter ( $D_g$ ) to the effective scattering cross section diameter ( $D_{Csca}$ ) as a function of  $D_{Csca}$  at SMEAR II from October 2006 to May 2009. The boxes show the 25<sup>th</sup> to 75<sup>th</sup> percentile ranges and the whiskers the 2.5<sup>th</sup> to 97.5<sup>th</sup> percentile ranges in logarithmically evenly-spaced bins of  $D_{Csca}$ . The lines show the respective ratios in simulated monomodal size distributions with four different geometric standard deviations ( $\sigma_g$ ).

The intensive aerosol optical properties Ångström exponent and backscatter fraction are plotted as a function of  $D_{Csca}$  in Figure 3. For  $\alpha_{sp}$  there was no correlation with  $D_{Csca}$ . On the other hand, the backscatter fraction clearly follows the expected inverse relationship – the larger particle size the smaller  $b$  – in the size range  $D_{Csca} > 100$  nm, even if the uncertainty range is large.

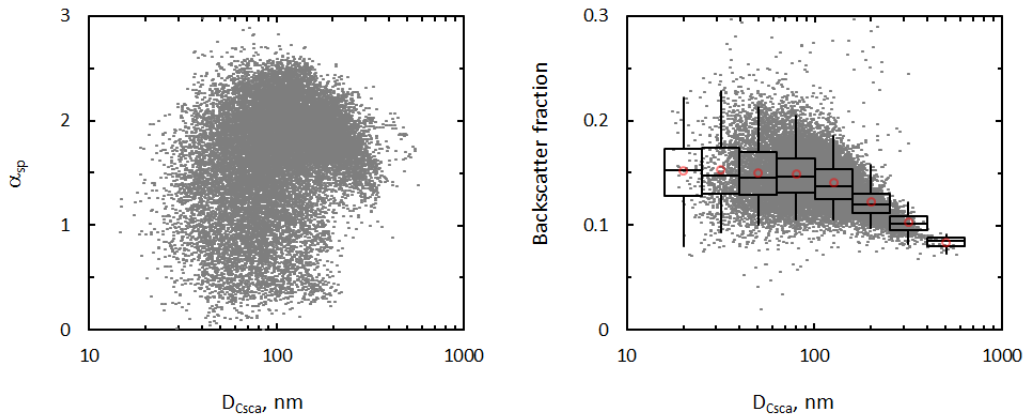


Figure 3. Ångström exponent of scattering ( $\alpha_{sp}$ ) and backscatter fraction as a function of effective scattering cross section diameter ( $D_{Csca}$ ). The boxes show the 25<sup>th</sup> to 75<sup>th</sup> percentile ranges and the whiskers the 2.5<sup>th</sup> to 97.5<sup>th</sup> percentile ranges and the red circles the averages in logarithmically evenly-spaced bins of  $D_{Csca}$ .

## CONCLUSIONS

The goal of this paper was to estimate what is the size-distribution-related information that can be obtained if only a single-wavelength nephelometer measuring total scattering coefficient and a condensation particle counter are available for measuring atmospheric aerosols. The analysis of three years' measurement data from SMEAR II shows that this combination does indeed give some size-related information: the effective scattering cross section diameter ( $D_{\text{Cscs}}$ ) was clearly positively correlated with both the count mean diameter (CMD) and the geometric mean diameter ( $D_g$ ). The ability of  $D_{\text{Cscs}}$  to predict the other two size descriptors was good even in the size range  $D_{\text{Cscs}} < 40$  nm. The worst was the  $D_{\text{Cscs}}$  range of about 70 – 200 nm. When  $D_{\text{Cscs}}$  was in this range  $D_g$  was in some cases even an order of magnitude lower. Simulations showed that the bad agreement is due to multimodal size distributions. In the  $D_{\text{Cscs}}$  range  $> 300$  nm the theoretical uncertainty was the lowest and  $D_{\text{Cscs}}$  predicted well both  $D_g$  and CMD. The obtained  $D_g$ -to- $D_{\text{Cscs}}$  and CMD-to- $D_{\text{Cscs}}$  ratios can be used for estimating some more commonly used descriptors of size distribution, if the total scattering is measured at the wavelength of 550 nm and total number concentration in the size range  $> 3$  nm.

The analysis also showed that  $D_{\text{Cscs}}$  cannot be used for estimating the Ångström exponent of scattering. However, there was a clear negative relationship between  $D_{\text{Cscs}}$  and the backscatter fraction in the size range  $D_{\text{Cscs}} > 100$  nm, which is consistent with the theory.

## ACKNOWLEDGEMENTS

This work was supported by the Nordic Centre of Excellence CRAICC (Cryosphere-atmosphere interactions in a changing Arctic climate), the Finnish Centre of Excellence in Physics, Chemistry, Biology and Meteorology of Atmospheric Composition and Climate Change (program number 1118615), European Union Seventh Framework Programme (FP7/2007–2013) under grant agreement no. 262254 (ACTRIS) and the EU FP6 project European Supersites for Atmospheric Aerosol Research (EUSAAR)

## REFERENCES

- Aalto, P., Hämeri, K., Becker, E., Weber, R., Salm, J., Mäkelä, J.M., Hoell, C., O'Dowd, C.D., Karlsson, H., Hansson, H.-C., Väkevä, M., Koponen, I.K., Buzorius, G., and Kulmala, M.: Physical characterization of aerosol particles during nucleation events, *Tellus*, 53B, 344–358, 2001.
- Anderson, T. L., Covert, D. S., Marshall, S. F., Laucks, M. L., Charlson, R. J., Waggoner, A. P., Ogren, J. A., Caldow, R., Holm, R. L., Quant, F. R., Sem, G. J., Wiedensohler, A., Ahlquist, N. A., and Bates, T. S.: Performance characteristics of a high-sensitivity, three-wavelength total scatter/backscatter nephelometer, *J. Atmos. Ocean. Tech.*, 13, 967–986, 1996.
- Barber, P.W. and Hill, S.C.: Light scattering by particles: Computational methods. *World Scientific Publishing*, Singapore, 1990.
- Charlson, R. J., Ahlquist, N. C., and Horvath, H. : On the generality of correlation of atmospheric aerosol mass concentration and light scatter, *Atmospheric Environment*, 2, 455-464., 1968.
- Hari, P. and Kulmala, M.: Station for measuring ecosystem-atmosphere relations (SMEAR II), *Boreal Env. Res.* 10, 5, 315-322, 2005.
- Huebert, B. J., T. Bates, P. B. Russell, G. Shi, Y. J. Kim, K. Kawamura, G. Carmichael, and T. Nakajima, An overview of ACE-Asia: Strategies for quantifying the relationships between Asian aerosols and their climatic impacts, *J. Geophys. Res.*, 108(D23), 8633, doi:10.1029/2003JD003550, 2003.
- Malm, W.C. and Hand, J.L.: An examination of the physical and optical properties of aerosols collected in the IMPROVE program, *Atm. Env.* 41, 3407 – 3427, 2007.
- Ogren, J.A.: In Situ observations of aerosol properties. In: Charlson, R.J., Heintzenberg, J. (Eds.), *Aerosol Forcing of Climate*. Wiley, Chichester, pp. 215-226, 1995

- Schobesberger, S., Vaananen, R., Leino, K., Virkkula, A., Backman, J., Pohja, T., Siivola, E., Franchin, A., Mikkila, J., Paramonov, M., Aalto, P. P., Krejci, R., Petaja, T. and Kulmala, M.: Airborne measurements over the boreal forest of southern Finland during new particle formation events in 2009 and 2010, *Boreal Environment Research*, 18.2, 145-163, 2013.
- Virkkula, A., Väänänen, R., Jónsdóttir, I., Hakala, J., Petäjä, T., Järvinen, O., Svensson, J., Backman, J., Aalto, P. P., Lei, R., and Kulmala, M. In situ aerosol measurements and snow sampling during CHINARE 5 cruise through the Arctic sea, *Report Series in Aerosol Science*, **134**, 646 - 648, 2012, <http://www.atm.helsinki.fi/FAAR/reportseries/rs-134.pdf>.
- Virkkula, A., Levula, J., Pohja, T., Aalto, P. P., Keronen, P., Schobesberger, S., Clements, C. B., Pirjola, L., Kieloaho, A.-J., Kulmala, L., Aaltonen, H., Patokoski, J., Pumpanen, J., Rinne, J., Ruuskanen, T., Pihlatie, M., Manninen, H. E., Aaltonen, V., Junninen, H., Petäjä, T., Backman, J., Dal Maso, M., Nieminen, T., Olsson, T., Grönholm, T., Kerminen, V.-M., Schultz, D. M., Kukkonen, J., Sofiev, M., de Leeuw, G., Bäck, J., Hari, P., and Kulmala, M.: Overview of a prescribed burning experiment within a boreal forest in Finland, *Atmos. Chem. Phys. Discuss.*, 13, 21703-21763, doi:10.5194/acpd-13-21703-2013, 2013.
- Waggoner, A.P. and Weiss, R.E.: Comparison of fine particle mass concentration and light scattering extinction in ambient aerosol, *Atmospheric Environment*, 14, 623-626, 1980.

## SURFACES FOR WATERHARVESTING

M. VOGT<sup>1</sup>, H. VUOLLEKOSKI<sup>1</sup>, T. PETÄJÄ<sup>1</sup>, M. SIPILÄ<sup>1</sup>, H. LAPPALAINEN<sup>1</sup>, J. AHOKAS<sup>2</sup>, A. KORPELA<sup>3</sup>, H. MIKKOLA<sup>2</sup> and M. KULMALA<sup>1</sup>

<sup>1</sup> Department of Agricultural Sciences, Agrotechnology University of Helsinki, Finland.

<sup>2</sup> Division of Atmospheric Sciences, Department of Physics, University of Helsinki Finland.

<sup>3</sup> VTT Technical Research Centre of Finland, Finland

Keywords: DEW, FOG, WATER-HARVESTING

### INTRODUCTION

Availability of water is one of the most severe developmental challenges of the world. Water scarcity already affects every continent and more than 40% of the people on the Earth. By 2025, approximately 1.8 billion people will be living in countries or regions with absolute water scarcity, and two thirds of the worlds population could be living under water stressed conditions (FAO, 2007). In this project, the aim is to provide practical solutions to water shortages in developing countries in arid and semi-arid environments ,by investigating the usability of dew collectors as harvesters of water vapor directly from the atmosphere under (semi-)arid climate conditions. The hypothesis is that utilizing cost-effective and environmentally safe modern materials as a substrate to collect dew will initiate development and production of dew collectors not only among Finnish industry but also among local industry in the developing countries.

### METHODS and MATERIALS

According to Nilsson et al., (1994) a ” *dew collector material should display a high emittance (or equivalently a high absorption) in the infrared wavelength range, in order to experience a high thermal power loss leading to a low temperature at the surface. In addition the solar reflectance should be high in order to collect dew for some period after sunrise and to prevent evaporation of the collected water from the surface.*” Following these design specifications, dew will condensate on such a surface if the temperature sinks below the dew point of the surrounding air mass. The key advantage of such an approach is the passive nature of the collector, which relies only on the creation of a local temperature gradient through emission spectrum bands of included pigments.

#### Surface matrix

For the surface matrix two possible polymers will be tested. The first one is polyethylene (PE), which is a thermoplastic polymer consisting of long hydrocarbon chains. PE is the cheapest polymer and has excellent chemical resistance, meaning that it is not attacked by strong acids or strong bases. It is also resistant to gentle oxidants and reducing agents in the atmosphere.

The second polymer is polylactide (PLA), which is a thermoplastic aliphatic polyester derived from renewable resources, such as corn starch, tapioca roots, or sugarcane. In addition to the origin from renewable resources the material is also biodegradable.

## Pigments

For the embedded pigments in the surface matrix we have decided on four compounds which alone or on combination with each other have a high solar reflectance in the UV/Vis and a high absorption in the IR (wavelengths 8-13  $\mu\text{m}$ ).

### *ZnS*

Zinc sulfide is an inorganic compound with the chemical formula of ZnS. Zinc sulfide is a good infrared optical material, transmitting from visible wavelengths to just over 12 micrometers (Cotton, Wilkinson and Gaus, 1995).

### *CaCO<sub>3</sub>*

Calcium carbonate is a chemical compound with the formula  $\text{CaCO}_3$ . Calcium Carbonate has several absorption peaks in the atmospheric window and has the additional advantage of being very cheap (Cotton, Wilkinson and Gaus, 1995).

### *BaSO<sub>4</sub>*

Barium sulfate is an inorganic compound with the chemical formula  $\text{BaSO}_4$ . In addition to its high reflectance in the UV/Vis it is used as polymer filler due to its effect of increasing acid and alkali resistance and opacity (Cotton, Wilkinson and Gaus, 1995).

### *TiO<sub>2</sub>*

Titanium dioxide, is the naturally occurring oxide of titanium, chemical formula is  $\text{TiO}_2$ . Titanium dioxide is known for its brightness and very high refractive index. Used as a pigment it provides whiteness and opacity (Cotton, Wilkinson and Gaus, 1995).

## OUTOOK

With the above mentioned parameters, we intend to design polymer foils which are able to harvest water vapour from the atmosphere. The foils will be tested and evaluated in the lab on their performances. A device which mimics the night sky is used to determine the radiative cooling power of each foil. The amount of condensed water vapour is determined using gravimetry.

## ACKNOWLEDGEMENTS

This research was supported by the Academy of Finland (Center of Excellence program, project number 127534), and by the Nordic Top-level Research Initiative (TRI) Cryosphere-Atmosphere Interactions in a Changing Arctic Climate (CRAICC).

## REFERENCES

- Cotton, Wilkinson and Gaus, (1995). *Basic Inorganic Chemistry*. John Wiley and Sons Inc, New York, U.S.
- FAO, 2007. Coping with water scarcity. FAO Newsroom.
- Niisson, (1994). *Optical Scattering Properties of Pigmented Foils for Radiative Cooling and Water Condensation: Theory and Experiment*. Thesis, Chalmers University of Technology, Göteborg, Sweden.

## CLIMATE AND BIOFUELS IN BRAZIL

H. VUOLLEKOSKI<sup>1</sup>, R. MAKKONEN<sup>1,2</sup>, A. ASMI<sup>1</sup>, R. HILLAMO<sup>2</sup>, T. PETÄJÄ<sup>1</sup> and M. KULMALA<sup>1</sup>

<sup>1</sup>Division of Atmospheric Sciences, Department of Physics, University of Helsinki,  
Helsinki, 00014, Finland

<sup>2</sup>Department of Geosciences, University of Oslo, Oslo, 0371, Norway

<sup>3</sup>Finnish Meteorological Institute, Helsinki, 00560, Finland.

Keywords: BIOFUELS, CLIMATE, MODELING.

### INTRODUCTION

Biofuels provide a source of renewable energy that may help increase the energy independence and economic well being of nations, as well as cause a reduction in the net greenhouse gas emissions. These are some of the reasons why the usage of biofuels especially in transport is increasing rapidly. However, while this replacement of fossil fuels may decrease the net carbon dioxide emissions, the growing demand of biofuels may have consequences related to e.g. human health, agriculture and climate.

Brazil is one fine example of such nation, and has had a pro-biofuel regulatory environment already since 1975, and is the current world-leader in terms of vehicles running on sugarcane ethanol. If Brazil manages to replace all its consumption of fossil fuels by biofuels in the near future, what kind of climatic implications could this conversion potentially have? The transition would require significant agricultural changes to enhance sugarcane production, and these plantations would likely spread over currently forested regions. The usual methods of harvesting sugarcane involve burning, which causes serious air pollution in certain regions (Lara et al., 2005). Additionally, the primary emissions caused by combustion of ethanol fuel differ from those of traditional gasoline. The scope of our research is limited to the aforementioned effects, although a more realistic scenario would likely include some socio-economic side effects.

The land area of Brazil accounts for less than 6% of the global land surface. With this in mind, we try to identify some potential global climatic effects of the Brazilian transition to biofuels. We approach this question with global climate modeling.

### METHODS

All modeling in this study has been performed with the ECHAM5.5-HAM2 (Zhang et al., 2012), which is a general circulation model that includes parameterizations for the effects of aerosols on climate. The sensitivity studies implemented so far have been executed by replacing the characteristic size of emissions due to fossil fuel combustion, according to current estimates (Stier et al., 2005), in a region covering Brazil, while leaving rest of the world as it was. This change in size (approximated by a change in mean diameter from 60 nm to 30 nm) of the emitted particles is based on experimental laboratory studies on car engines.

### RESULTS

Our first sensitivity study consisted of a 5-year (+6 months for meteorology spin-off) control run and an otherwise identical run but with emissions in smaller size over Brazil. The results indicate significant increase in Aitken mode particles on surface level over Brazil, but this is likely due to the mass-based emission scenario, see Figure 1. There is also a slight increase in the concentration of cloud condensation nuclei, but this and other effects may be attributed to noise.

We then modified our sensitivity run to account for a smaller number of particulate emissions in the same smaller size. This modification made most of the aforementioned differences disappear, but nevertheless, some patterns remain visible, see Figure 2. However, the mean relative change in the concentration of cloud condensation nuclei that activate at a super saturation of 1% is insignificant: 0.0005. Note that the concentrations over polar regions are so low that even relatively large changes over them are small in absolute number. There is also some seasonal fluctuation in the concentrations, as can be seen in Figure 3, but these are also small.

In order to get some perspective, we run the same sensitivity run with a global change. The resulting relative change in the concentration of cloud condensation nuclei that activate at a super saturation of 1% is visualized in Figure 4. Its mean value is still very low, 0.006, in spite of the now significant change in global emissions. However, these exhibit greater seasonal and regional variability, which requires further investigation.

Relative change in number mixing ratio – aerosol mode Aitken soluble (surface level)

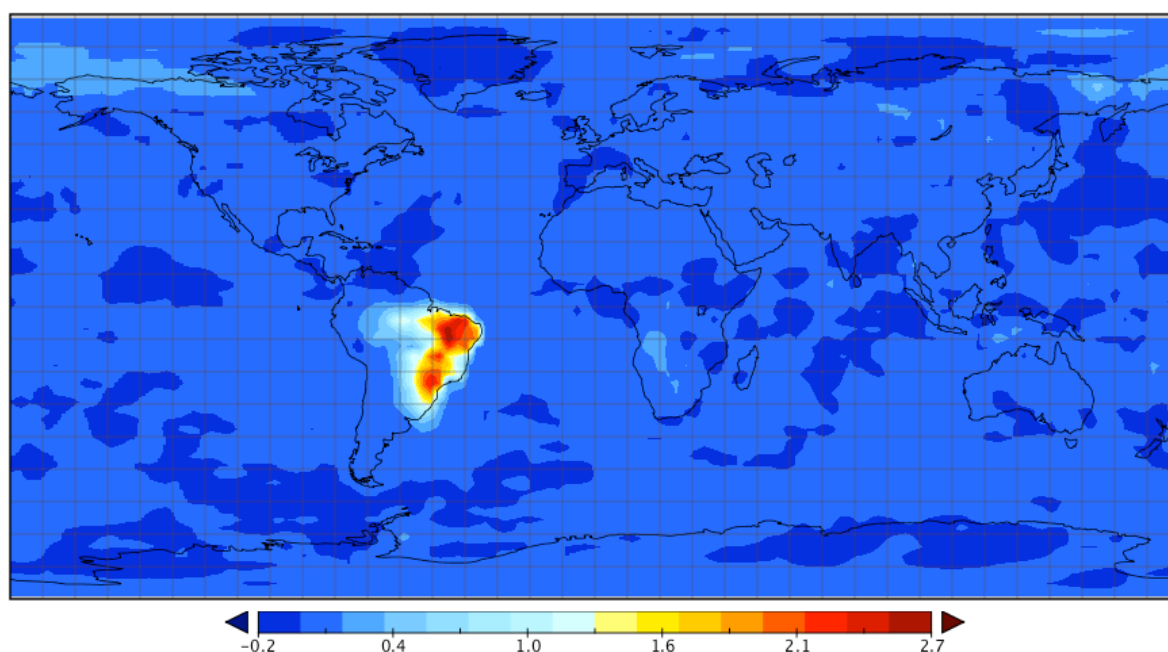


**Figure 1: The relative change in number mixing ratio of Aitken mode particles, when only the size of fossil fuel emissions over Brazil is modified.**

## CONCLUSIONS

The climatic effects of bioethanol adoption were studied from both Brazilian and global perspectives. So far our investigation has involved only changing some parameters in the fossil fuel based emission scenarios, namely the mean size of emitted particles has been halved, and the number concentration has been reduced by 75%. In spite of these relatively big modifications in scenarios covering both Brazilian and global emissions, neither show any significant climatic effects. However, there appears to be some seasonal and regional fluctuation, which requires deeper insight and statistical analysis. The side effects of large-scale bioethanol adoption, such as changes in agriculture and its related emissions also require further consideration. We also intend to run sensitivity tests with other emission scenarios besides the currently used AEROCOM.

Relative change in Cloud Condensation Nuclei at S=CCN 1.000 %

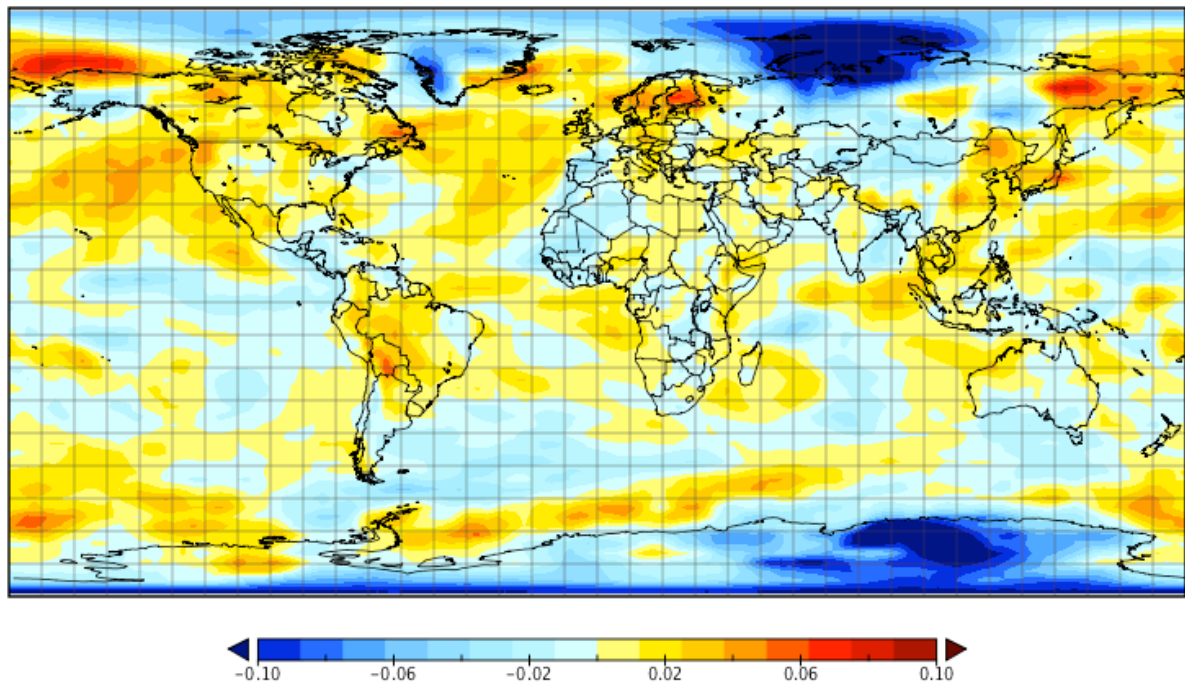


Figure 2: The relative change in CCN at S=1% in boundary layer. Fossil fuel emissions over Brazil have been modified.

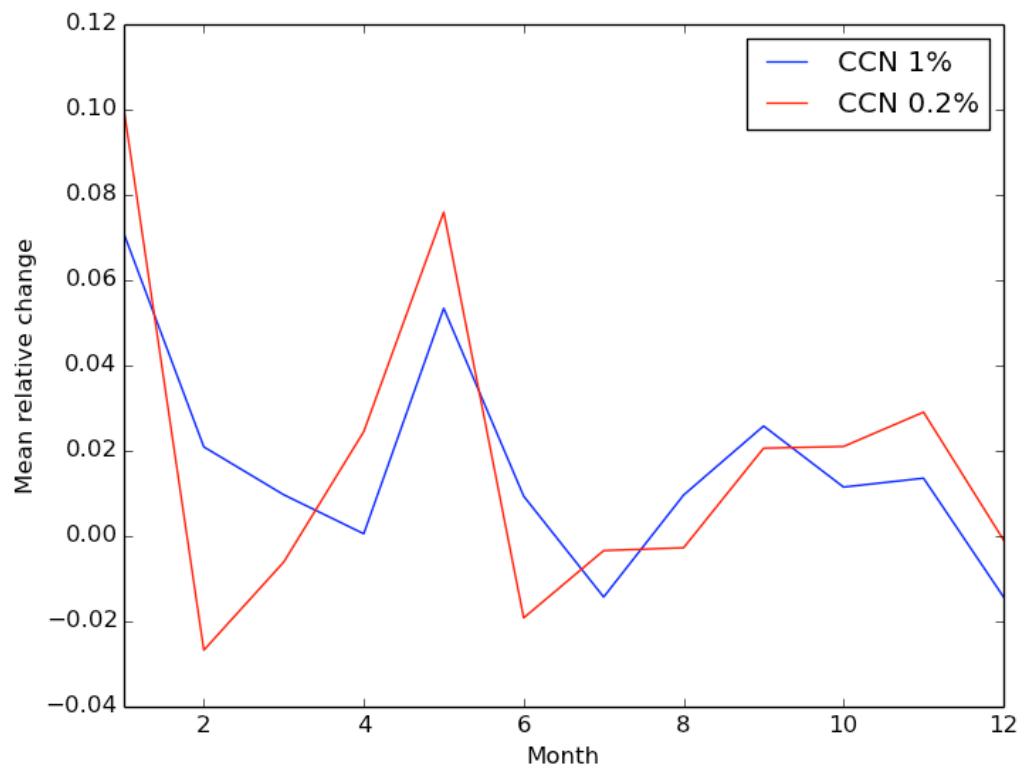


Figure 3: The mean relative changes in the activated concentrations of CCN in Brazilian boundary layer, scenario as in Figure 2.

Relative change in Cloud Condensation Nuclei at S=CCN 1.000 %

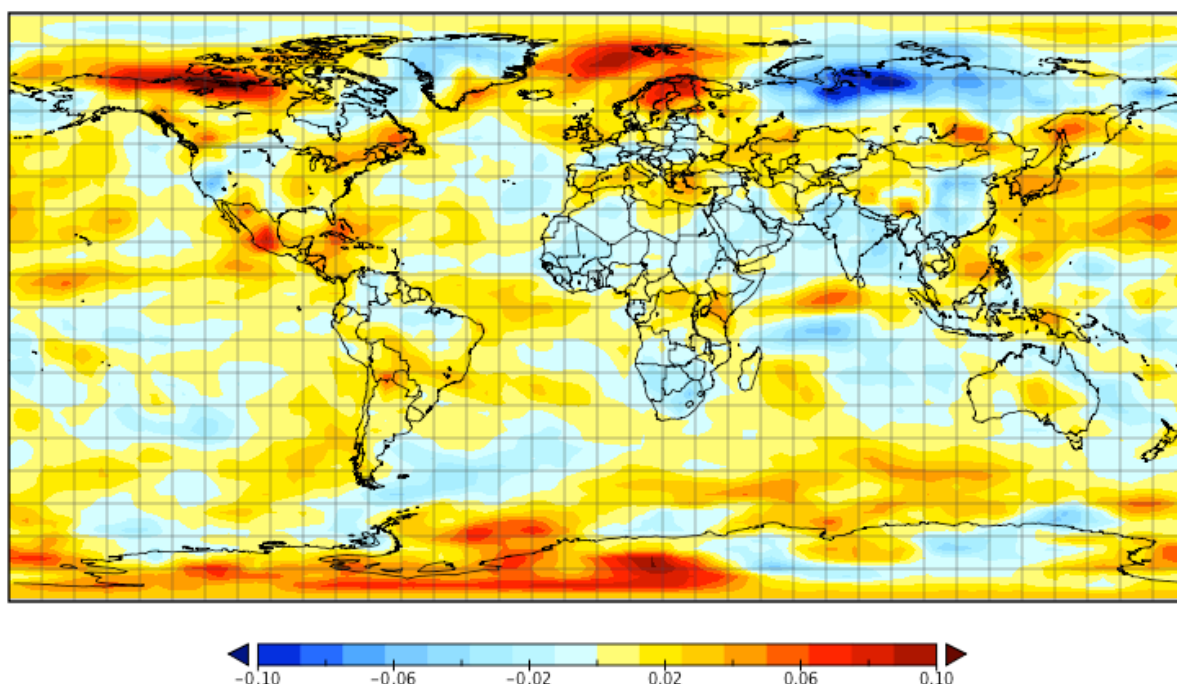


Figure 4: The relative change in CCN at S=1%, where fossil fuel emissions have been modified globally.

## ACKNOWLEDGEMENTS

We acknowledge funding from “The effects of intensive bio-fuel production and use on regional air quality and global climate, BIOFUSE” (Academy of Finland, project 133603).

We thank Dr. Topi Rönkkö from Tampere University of Technology for technical consultation.

Risto Makkonen acknowledges funding from the CRAICC project.

This research was supported by the Academy of Finland Center of Excellence program (project number 1118615).

## REFERENCES

- Lara, L., Artaxo, P., Martinelli, L., et al. (2005). Properties of aerosols from sugar-cane burning emissions in Southeastern Brazil, *Atmos. Env.*, **39** (26), 4627–4637.
- Zhang, K., O’Donnell, D., Kazil, J., et al. (2012). The global aerosol-climate model ECHAM-HAM, version 2: sensitivity to improvements in process representations, *Atmos. Chem. Phys.*, **12** (19), 8911–8949.
- Stier, P., Feichter, J., Kinne, S., et al. (2005). The aerosol-climate model ECHAM5-HAM, *Atmos. Chem. Phys.*, **5**, 1125–1156.

## A BRIEF GLANCE AT PUMA: PYTHONIC UNIFIED MODEL OF AEROSOLS

H. VUOLLEKOSKI, A. RUSANEN and M. KULMALA

Division of Atmospheric Sciences, Department of Physics, University of Helsinki,  
00014 Helsinki, Finland.

Keywords: MODELING, AEROSOLS.

### INTRODUCTION

Admittedly, many computer models for solving basic microphysical processes concerning aerosols already exist. However, the level of detail in their implementation varies, and they tend to focus on modeling only a limited set of features accurately: number concentration, mass, new particle formation, particle growth, ions, clusters, chemistry etc. To our knowledge no model does them all, and adding new functionality to existing program architecture often calls for tricks that decrease code readability, i.e. increase the risk of errors, and make it more difficult to debug.

Trying to solve these problems was the starting point of design of our new Pythonic Unified Model of Aerosols (PUMA). It combines a modern, popular, high-level programming language, Python, with numerically efficient NumPy (Oliphant, 2007) and ODEPACK (Hindmarsh, 1983) libraries, as well as takes advantage of both object-oriented and functional programming paradigms. Our goal is to create an attractive platform for a wide range of box-model studies related to aerosol science, with support for various numerical and physical representations, and built-in tools for visualization and common methods of analysis. PUMA should be easily included in automatized batch script run sets, run independently or interactively from iPython shell (Pérez and Granger, 2007) or even through a graphical user-interface within a web browser. The program code itself will be published in public domain.

### MODEL DESCRIPTION

Although offering a limited set of features at the moment, the technical model structure of PUMA is starting to settle. A conceptual schematic of it is presented in Figure 1. Starting from the top, the user-interface can be an interactive shell, a graphical user-interface or another model (e.g. a regional advection model). Following the object-oriented programming paradigm, the user instantiates a “simulation” class, which then provides all the necessary functionality outside of the model: public settings, variables and methods for controlling the simulation, and routines for reading and writing files on computer disk. The user may even have several instances running in parallel, and compare them in real-time.

As the user requests iterations from the model, ordinary differential equations are fed into an ODE solver. Because the model state is stored in objects, the actual equations that are called can be made *ad hoc* methods for the simulated scenario; for example, particle modes are governed by a different set of equations as compared to clusters, and the model automatically chooses the appropriate functionality for each representation. Class inheritance decreases the amount of code repetition as well as facilitates maintenance; for example, ions inherit the behavior of (neutral) particles in addition to their own special properties. The representation classes, including their behavior, may be added and combined freely, as long as they fulfill the interface requirements set by the abstract base class standard. A similar analogue is applied with the modeled vapors (e.g. condensing vapors form a subset of all vapors) as well as the environment (e.g. chamber, boreal forest etc.)

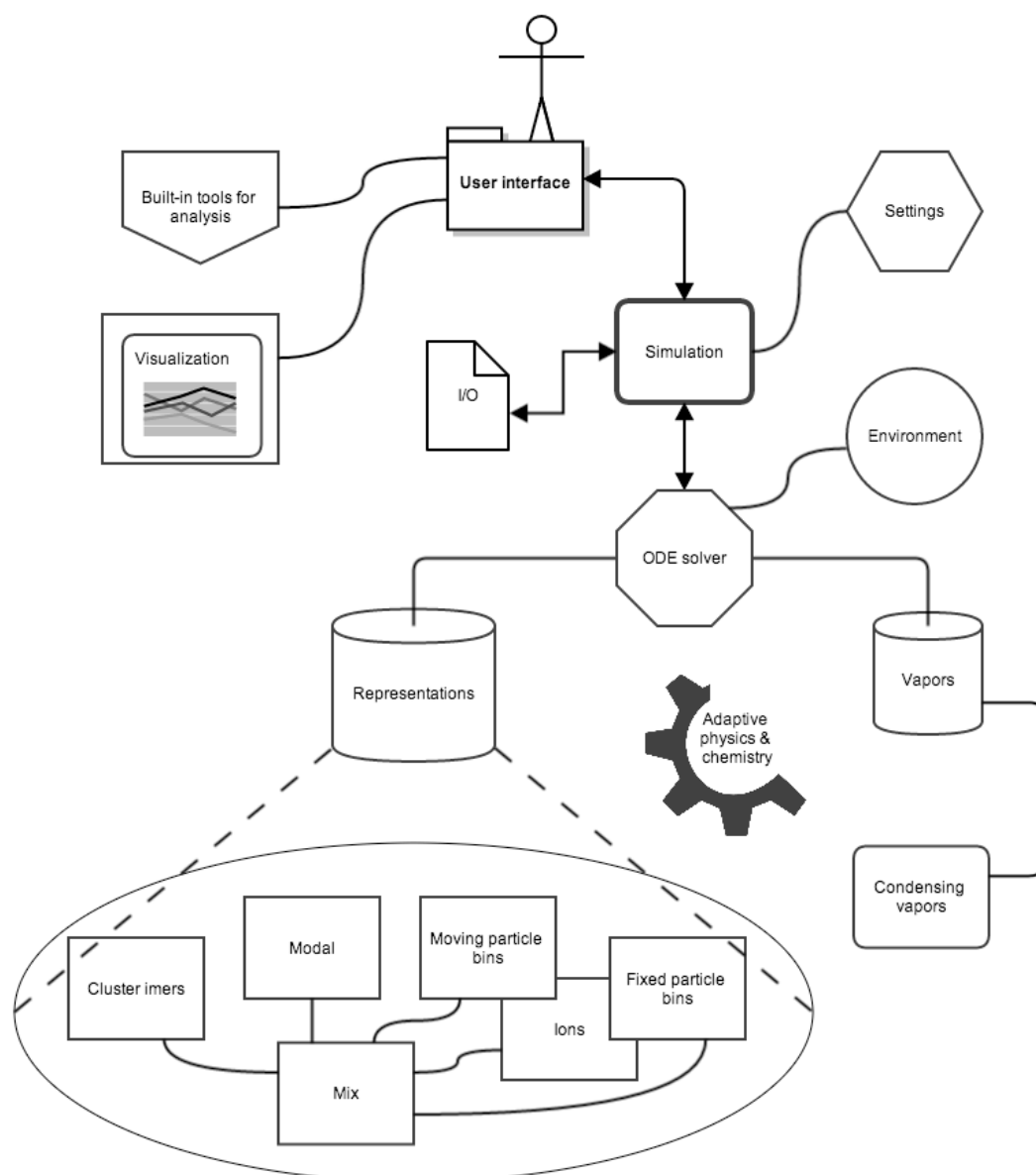


**Figure 1: A schematic of conceptual model design.**

Although having e.g. a list of particle bin objects representing the particle number-size distribution is practical and intuitive, it is computationally quite inefficient. For this reason PUMA, at the time of main class instantiation, reserves two large arrays in computer memory: one for storing the values of important model variables, such as particle concentrations and diameters, the other is for communication within the solver and includes the rates of change for each of the values in the first array. These big arrays are split into subarrays that represent meaningful quantities and permit efficient linear algebra operations. Elements of these arrays are then linked with the attributes of individual model objects, such as particle bins, see Figure 2.

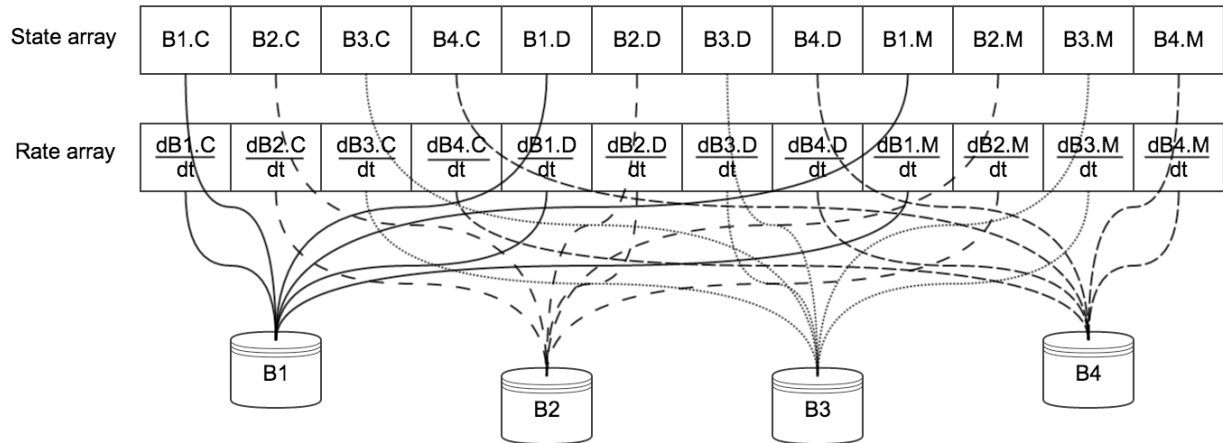


**Figure 2: A schematic of how PUMA links instance attributes to arrays in contiguous memory.**

## CONCLUSIONS

A new multi-purpose aerosol model is being developed. Flexible extensibility, applicability and minimizing potential sources of programming errors have been the guiding principles in designing of PUMA, which should prove to be a valuable tool in combining features from existing models. Being an integrated platform with many built-in features it should also work as a practical ground to facilitate conceptual and implementation tests for large-scale applications. As the list of intended model features is extensive, we welcome suggestions and other input from potential users.

## ACKNOWLEDGEMENTS

This research was supported by the Academy of Finland Center of Excellence program (project number 1118615).

Support from the Nordic Center of Excellence CRAICC is acknowledged.

## REFERENCES

- T. E. Oliphant (2007). Python for Scientific Computing, *Comput. Sci. Eng.* **9**, 10.
- A. C. Hindmarsh (1983). *ODEPACK, A Systematized Collection of ODE Solvers*, in: *Scientific Computing* (North-Holland, Amsterdam, Netherlands).
- F. Pérez and B. E. Granger (2007). IPython: A System for Interactive Scientific Computing, *Comput. Sci. Eng.*, **9**, 3.

# NANOPARTICLE GROWTH AND PARTICLE PHASE ACID-BASE CHEMISTRY – A MODELING STUDY

T. YLI-JUUTI<sup>1</sup>, K. BARSANTI<sup>2</sup>, L. HILDEBRANT RUIZ<sup>3,4</sup>, A.-J. KIELOAHO<sup>1</sup>, U. MAKKONEN<sup>5</sup>,  
T. PETÄJÄ<sup>1</sup>, T. RUUSKANEN<sup>1</sup>, M. KULMALA<sup>1</sup> and I. RIIPINEN<sup>6</sup>

<sup>1</sup>Department of Physics, University of Helsinki, Helsinki, Finland.

<sup>2</sup>Department of Civil & Environmental Engineering, Portland State University, Portland, OR, USA.

<sup>3</sup>Atmospheric Chemistry Division, National Center for Atmospheric Research, Boulder, CO, USA.

<sup>4</sup>Now at: McKetta Department of Chemical Engineering, The University of Texas at Austin, Austin, TX, USA.

<sup>5</sup>Finnish Meteorological Institute, Helsinki, Finland

<sup>6</sup>Department of Applied Environmental Science and Bert Bolin Center for Climate Research, Stockholm University, Stockholm, Sweden.

Keywords: NEW PARTICLE FORMATION, CONDENSATIONAL GROWTH, AEROSOL CHEMISTRY, ORGANIC AEROSOL.

## INTRODUCTION

Atmospheric new particle formation produces nanometer sized particles from atmospheric trace gases through phase change. These nanoparticles need to grow tens of nanometers in order to affect the climate. During the growth the nanoparticles are subject to coagulation losses and the growth rate of particles largely determines how large fraction of the formed nanoparticles reach climatically significant sizes.

In many environments, condensation of organic vapors is accounting for significant fraction of the particle growth. However, considerable uncertainties are related to this organic contribution to nanoparticle growth. The exact identification of the condensing organic compounds and their thermodynamic properties is currently lacking, and the role of particle phase processes in the condensation of vapors on the nanoparticles is not fully known (Riipinen et al., 2012).

In order to contribute to the growth of nanoparticles significantly, the vapors need to either be low-volatile or transfer into low-volatile substances through particle phase processes after uptake into nanoparticles. One of such particle phase processes is salt formation. Detection of semi-volatile organic acids and amines in atmospheric nanoparticles has suggested that particle phase salt formation may play an important role in nanoparticle growth (Smith et al., 2010).

In this study, we have developed a nanoparticle growth model MABNAG, which takes into account particle phase acid base chemistry. The model is applied for boreal forest environment in order to study the role of salt formation in nanoparticle growth. The focus is on the enhancement of uptake of organic acids on nanoparticles due to salt formation and on the relative roles of ammonia and amines in the salt formation.

## METHODS

MABNAG (Model for Acid-Base chemistry in NAnoparticle Growth; Yli-Juuti et al., 2013) is a particle growth model where the dynamics of condensation are coupled with particle phase acid-base chemistry. The model is currently set for monodisperse population of aqueous solution particles. The acid-base chemistry, i.e. dissociation of acids and protonation of bases, in MABNAG is based on bulk thermodynamics and the model uses Extended Aerosol Inorganic Model (E-AIM; Clegg et al., 1992; Clegg and Seinfeld, 2006) for this.

The inputs for the model are initial particle size and composition and concentrations of condensing vapors. Based on these the model predicts the time evolution of particle size and composition. In addition to water, the condensing vapors can include inorganic and organic compounds, both acids and bases. In this study, the modeled system consisted from two acids, two bases and water. The acids were sulfuric acid and an organic acid and the bases were ammonia and an amine. For the organic acid the thermodynamic properties of malonic acid, but with varied saturation vapor pressure, were assumed and for the amine the properties of dimethylamine were assumed.

Salt formation affects the nanoparticle growth through the equilibrium vapor pressures of condensing vapors. In MABNAG, both the composition and size dependence of equilibrium vapor pressures are taken into account.

## RESULTS

In this study, MABNAG was applied for ambient conditions of boreal forest based in measurements at Hyytiälä, Southern Finland, to study the growth of sub-20 nm particles. At typical conditions, most of the particle growth was predicted to be due to the condensation of the organic acid and the mass fraction of the organic acid increased with increasing particle size (Figure 1). The mass fractions of sulfuric acid and the two bases decreased along the particle growth.

At typical ambient conditions, MABNAG predicted only a small fraction of the organic acid to dissociate. Therefore the effect of salt formation was predicted to be small for the condensation of the organic acid. However, at elevated concentrations of the bases (amine conc.  $> 10^9 \text{ cm}^{-3}$  / ammonia conc.  $> 10^{10} \text{ cm}^{-3}$ ) the salt formation was predicted to enhance the condensation of the organic acid significantly.

The relative roles of the two bases, ammonia and the amine, depended largely on their gas phase concentrations. However, the relative roles of the two bases were rather similar across the size range between 3-20 nm. In all cases, all ammonia and amine were predicted to be protonated in the particle phase, which indicates the importance of salt formation for the uptake of the bases on nanoparticles.

MABNAG, which is based on bulk thermodynamics of acid-base chemistry, was compared to a nanoparticle growth model where salt formation was included conceptually based on quantum chemistry calculations on stabilities of clusters that contained ammonia or dimethylamine. The comparison showed a difference between the two approaches in predictions of condensation of amines. Thus, further study is needed on the applicability of bulk thermodynamics, which are used in MABNAG, in the nanoparticle size range.

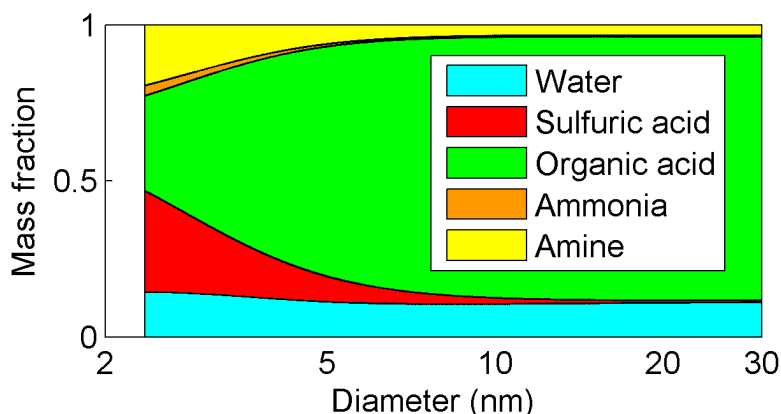


Figure 1. Predicted mass fractions at typical ambient conditions at boreal forest site Hyytiälä.

## CONCLUSIONS

The model predicted only a small enhancement of the uptake of the organic acid on the nanoparticles due to salt formation. This might suggest that other factors than salt formation are affecting the existence of the semi-volatile organic acids in nanoparticles. On the other hand, due to the small size-scale of the nanoparticles, it is possible that the current bulk-based thermodynamics may not capture the behavior of the real nanoparticles correctly.

Due to the important role of acid-base chemistry in the condensation of sulfuric acid and the bases, salt formation does play a significant role in the particle growth. Since the contribution of the organic acid was predicted to increase with increasing particle size, the contribution on salts on the particle mass was largest for the smallest particles.

## ACKNOWLEDGEMENTS

This research was supported by the Academy of Finland Center of Excellence program (project No. 1118615), ACCC Doctoral Programme (project No. 129663), Vetenskapsrådet (project No. 2011-5120), European Research Council Grant ATMOGAIN (No. 278277), and US DOE Grant (No. DE-SC0006861).

## REFERENCES

- Clegg, S. L., K. S. Pitzer, and P. Brimblecombe (1992). Thermodynamics of multicomponent, miscible, ionic solutions. II. Mixtures including unsymmetrical electrolytes. *J. Phys. Chem.* **96**, 9470.
- Clegg, S. L. and J. H. Seinfeld (2006). Thermodynamic models of aqueous solutions containing inorganic electrolytes and dicarboxylic acids at 298.15 K. I. The acids as non-dissociating components. *J. Phys. Chem. A* **110**, 5692.
- Riipinen, I., T. Yli-Juuti, J. R. Pierce, T. Petäjä, D. R. Worsnop, M. Kulmala, and N. M. Donahue (2012). The contribution of organics to atmospheric nanoparticle growth. *Nature Geoscience* **5**, 453.
- Smith, J. N., K. C. Barsanti, H. R. Friedli, M. Ehn, M. Kulmala, D. R. Collins, J. H. Scheckman, B. J. Williams, and P. H. McMurry (2010). Observations of aminium salts in atmospheric nanoparticles and possible climatic implications. *PNAS* **107**, 6634.
- Yli-Juuti, T., K. Barsanti, L. Hildebrandt Ruiz, A.-J. Kielloaho, U. Makkonen, T. Petäjä, T. Ruuskanen, M. Kulmala, and I. Riipinen (2013). Model for acid-base chemistry in nanoparticle growth (MABNAG). *Atmos. Chem. Phys. Discuss.* **13**, 7175.

# LONG TERM MODELLING OF NEW PARTICLE FORMATION EVENT IN A BOREAL FOREST

L. ZHOU<sup>1</sup>, M. BOY<sup>1</sup>, T. NIEMINEN<sup>1</sup>, D. MOGENSEN<sup>1</sup>, S. SMOLANDER<sup>1</sup> and M. KULMALA<sup>1</sup>

<sup>1</sup>Division of Atmospheric Sciences, Department of Physics, University of Helsinki, Finland.

<sup>2</sup>Wind Energy Division, Risø National Laboratory for Sustainable Energy, Technical University of Denmark, Denmark

Keywords: Nucleation, particle growth, PBL, Atmospheric Modelling

## INTRODUCTION

Natural and anthropogenic aerosols may have a great impact on climate as they can directly interact with solar radiation and indirectly affect the Earth's radiation balance and precipitation by modifying clouds. In order to quantify the direct and indirect effect, it is essential to understand the complex processes that connect an aerosol particle to a cloud droplet. However, while modern measurement techniques are able to detect particle sizes down to nanometre all the way from ground up to the stratosphere, the data does not serve for all of our needs for understanding the processes. Hence we will demonstrate a modelling approach to investigate the complex processes of aerosols in the planetary boundary layer (PBL).

## METHODS

SOSAA (model to Simulate the concentration of Organic vapours, Sulphuric Acid, and Aerosols) is a 1D chemical-transport model with detailed aerosol dynamics. It was constructed to study the emissions, transport, chemistry, as well as aerosol dynamic processes in the PBL in and above a canopy [Boy et al., 2011].

As a first application of the model after the aerosol dynamics module was implemented, we tested different nucleation theories by simulating the new particle formation events in year 2010 at SMEAR II station, Finland. Since there has been numerous evidence that condensable organic vapours are the dominant contributors to the aerosol particle growth particularly in regions where biogenic volatile organic compound emissions are high, we also simulated the concentrations of a set of organic compounds and their first reaction products from oxidation [e.g. Kerminen et al. (2000); Sellegri et al. (2005); Boy et al. (2005); Allan et al. (2006); Laaksonen et al. (2008)].

## CONCLUSIONS

The results have showed the ability of SOSAA to reconstruct the general behaviour of atmospheric trace gases and new particle formation in a boreal forest environment with reasonable uncertainties. The underestimation in H<sub>2</sub>SO<sub>4</sub> concentration supports the view that other production mechanisms of H<sub>2</sub>SO<sub>4</sub> exist. The simulations about particle nucleation emphasize the complexity of the phenomenon since there is no single nucleation theory that works all the time. We also verified the importance of organic vapours in particle growth.

## ACKNOWLEDGEMENTS

We thank Helsinki University Centre for Environment (HENVI), the Academy of Finland Centre of Excellence program (project no. 1118615), the European Commission 6<sup>th</sup> Framework program project

EUCAARI, the Pan-European Gas-Aerosol-climate interaction Study (project no. 400798) and the Nordic Centers of Excellence CRAICC for their financial support. We thank CSC – IT Center for Science for providing computing facilities.

## REFERENCES

- Allan, J. D., M. R. Alfarra, K. N. Bower, H. Coe, J. T. Jayne, D. R. Worsnop, P. P. Aalto, M. Kulmala, T. Hyötyläinen, F. Cavalli, and A. Laaksonen (2006). Size and composition measurements of background aerosol and new particle growth in a Finnish forest during QUEST 2 using an Aerodyne Aerosol Mass Spectrometer, *Atmos. Chem. Phys.* 6, 315 - 327.
- Boy, M., M. Kulmala, T. M. Ruuskanen, M. Pihlatie, A. Reissell, P. P. Aalto, P. Keronen, M. Dal Maso, H. Hellen, H. Hakola, R. Jansson, M. Hanke, and F. Arnold (2005). Sulphuric acid closure and contribution to nucleation mode particle growth, *Atmos. Chem. Phys.* 5, 863 - 878.
- Boy, M., A. Sogachev, J. Lauros, L. Zhou, A. Guenther, and S. Smolander (2011). SOSA - a new model to simulate the concentrations of organic vapours and sulphuric acid inside the ABL - Part1: Model description and initial evaluation, *Atmos. Chem. Phys.* 11, 43 - 51.
- Kerminen, V.-M., A. Virkkula, R. Hillamo, A. S. Wexler, and M. Kulmala (2000). Secondary organics and atmospheric CCN production, *J. Geophys. Res.* 105, 9255 - 9264.
- Laaksonen, A., M. Kulmala, C. D. O'Dowd, J. Joutsensaari, P. Vaattovaara, S. Mikkonen, K. E. J. Lehtinen, L. Sogacheva, M. Dal Maso, P. Aalto, T. Petäjä, A. Sogachev, Y. J. Yoon, H. Lihavainen, D. Nilsson, M. C. Facchini, F. Cavalli, S. Fuzzi, T. Homann, F. Arnold, M. Hanke, . Sellegri, K., B. Umann, W. Joukermann, H. Coe, J. D. Allan, M. R. Alfarra, D. R. Worsnop, M.-L. Riekkola, T. Hyytiäinen, and Y. Viisanen (2008). The role of VOC oxidation products in continental new particle formation, *Atmos. Chem. Phys.* 8, 2657 - 2665.
- Sellegri, K., B. Umann, F. Arnold, and M. Kulmala (2005). Measurements of organic gases during aerosol formation events in the boreal forest atmosphere during quest, *Atmos. Chem. Phys.* 5, 373 - 384.

# LARGE-EDDY SIMULATION OF CANOPY EFFECTS ON SPATIAL DISTRIBUTION OF CHEMICALS AND AEROSOLS

P. ZHOU<sup>1</sup>, M. BOY<sup>1</sup>, S. SMOLANDER<sup>1</sup>, K. OSWALD<sup>2</sup> and Ü. RANNIK<sup>1</sup>

<sup>1</sup> Division of Atmospheric Sciences, Department of Physics, University of Helsinki, Helsinki, Finland

<sup>2</sup> Leibniz Institute for Tropospheric Research (TROPOS), Leipzig, Germany

Keywords: Large-Eddy Simulation, Forest canopy, Turbulence, Planetary boundary layer.

## INTRODUCTION

In boreal forests, the emission and spatial distribution of precursor gases (Bäck et al., 2012), the conversion of these gases to aerosol particles (Riipinen et al., 2011), the transportation and turbulent mixing of them (Lauros et al., 2011), and the influence of the turbulence on chemical and physical processes are all key issues in studying aerosol dynamics (Kulmala et al., 2001, 2011). Here the precursor gases mainly refer to volatile organic compounds (VOCs, e.g., isoprene, monoterpenes and sesquiterpenes) and semi-volatile organic compounds (SVOCs) (Ehn et al., 2012).

In boreal forest regions the canopy plays a crucial role in these issues in the planetary boundary layer (PBL). First, the forest canopy emits a large amount of VOCs (Hakola et al., 2003; Tarvainen et al., 2005; Bäck et al., 2012). Some of the VOCs can react with other compounds in the air and are then oxidized to SVOCs (Kavouras et al., 1999; Riipinen et al., 2011). Moreover, some SVOCs are released directly from the vegetations (Ieda et al., 2006). These SVOCs are less volatile and may participate in atmospheric new particle formation (Riipinen et al., 2012). This process increases the concentration of aerosol particles inside and above the canopy and thus alters the spatial distribution of the aerosol particles in the whole PBL (Bonn et al., 2008). On the other hand, canopy drag can change wind profiles and also produce turbulence within and above the forest canopy, which significantly influences the advection and convection of chemicals and aerosol particles in the PBL. Besides, the diurnal variation of heat fluxes from the canopy also has significant impacts on the energy balance and even the chemical reaction rates near the ground.

Therefore, it is of great interest to study the canopy effects on the emission, chemical reactions, aerosol dynamics and spatial distribution of chemicals and aerosol particles in the PBL.

## METHODS

In this project we plan to implement new modules into a 3-dimensional (3D) Large-Eddy Simulation (LES) model ASAM (All Scale Atmospheric Model) to simulate and investigate all the processes mentioned above.

Previous numerical models have shown many valuable results of the canopy effects in the PBL. However, they did not combine chemical processes and aerosol dynamics directly with 3D turbulent transport, canopy drag and heat fluxes from canopy. For example, SOSA (model to simulate the concentration of organic vapours and sulphuric acid) was used to research the emission, reactions and transportation of the chemicals in Hyytiälä (Boy et al., 2011). However, it is a 1-dimensional (1D) model and cannot simulate the details of turbulent transport. While some meteorological

models only concerned the turbulent flow and they did not implement explicit chemistry or aerosol part (Aumond et al., 2013)

The LES model is mainly used for simulating turbulence in fluid. It only directly simulates the large eddies while parameterizing eddies smaller than the filter size. Many studies have applied LES models in their research of turbulence structure within and above the forest canopy in the PBL (e.g., Shaw and Shumann, 1992; Shen and Leclerc, 1997). Therefore, it is used here to investigate the inhomogeneous spatial distribution of chemicals and aerosol particles under the effects of turbulent mixing.

In this project we use ASAM as the LES model. ASAM is a developing research code developed and maintained by TROPOS (Leibniz Institute for Tropospheric Research, Leipzig, Germany). It has several optional modules to manipulate different physical and chemical processes. Researchers at TROPOS have tested many benchmarks for ASAM, which ensures that it is reliable and appropriate for our research (Hinneburg and Knoth, 2005; Horn, 2012). The model was installed at the IT Center for Science (CSC) in Espoo, Finland in spring 2012. Thus parallel computation is available for our simulation cases.

On the basis of that, we have implemented a canopy module into ASAM. Some subroutines are directly from MEGAN (Model of Emissions of Gases and Aerosols from Nature). In general, the current ASAM contains four parts, the dynamics part, the energy balance, the emissions from canopy and the chemistry part. (Fig. 1). The aerosol part will be implemented in future. The dynamics, mainly referring to the wind field, is calculated by dynamic modules and the canopy drag is computed simultaneously for a given LAD (Leaf Area Density) profile. In the energy balance part the solar radiation and long wave radiation are considered, as well as the heat fluxes from both canopy and soil. The emissions from canopy are obtained from MEGAN subroutines and the list of chemical reactions are mainly from SOSA.

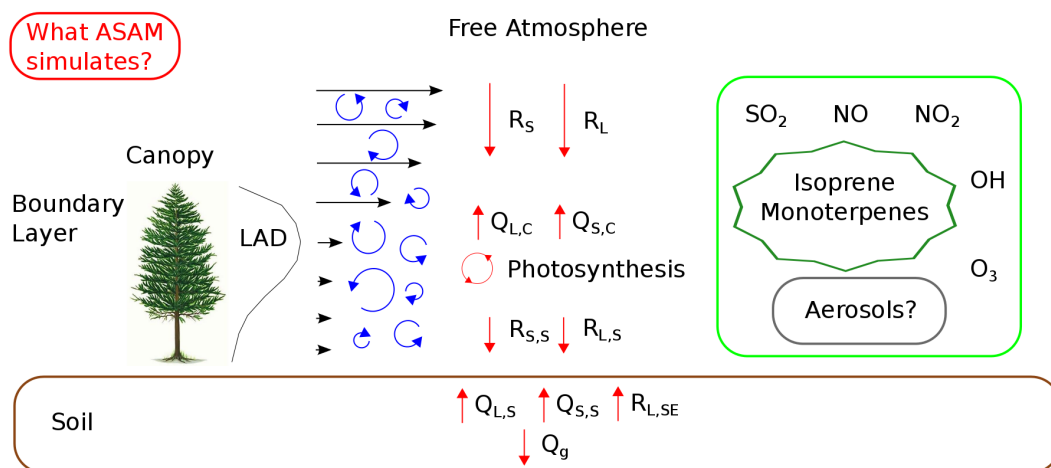


**Figure 1:** Diagram for different parts of ASAM.

## RESULTS

Fig 2 shows a sample of transient temperature pattern in a simulation case. More details of the figure can be found in the caption. From the figure we can clearly see the turbulence within and above the canopy. Moreover, in average the temperature decreases with height, but it nearly keeps constant from about 5m to 90m due to turbulent mixing. It is worth noting that the temperature near the ground is 1K to 2K lower than that above. This realistic result was obtained because we considered the penetration rate of sunshine between different canopy layers. So the lower the leaves

stand, the less solar radiation they receive. Certainly, the cooler leaves also cool the air around. As a result, the temperature of the air is much lower near the ground surface.

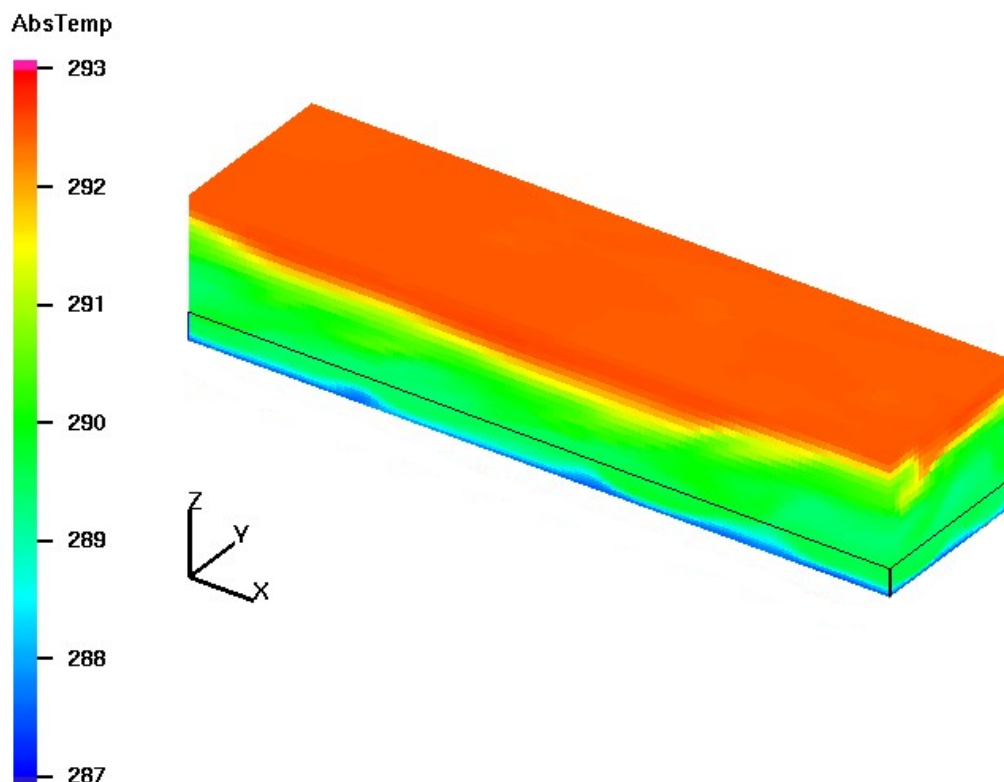


**Figure 2:** The 3D pattern of the absolute temperature. This box ( $500\text{m} \times 125\text{m} \times 100\text{m}$ ) is the lowest part of the whole simulation domain ( $500\text{m} \times 250\text{m} \times 2405\text{m}$ ). The horizontal black lines around the box are the top of the canopy (20 meters high). The colorbar is shown on the left side and the coordinates are also shown.

This is just a verification case for the new model. More processes, especially the ones related to the chemicals and aerosol particles, will be simulated in future.

## References

- Aumond, P., Masson, V., Lac, C., Gauvreau, B., Dupont, S., and Berengier, M. (2013). Including the drag effects of canopies: real case Large-Eddy Simulation studies. *Boundary-Layer Meteorol.*, 146:65–80.
- Bonn, B., Kulmala, M., Riipinen, I., Sihto, S.-L., and Ruuskanen, T. M. (2008). How biogenic terpenes govern the correlation between sulfuric acid concentrations and new particle formation. *J. Geophys. Res.*, 113:D12209, doi:10.1029/2007JD009327.
- Boy, M., Sogachev, A., Lauros, J., Zhou, L., Guenther, A., and Smolander, S. (2011). SOSA—a new model to simulate the concentrations of organic vapours and sulphuric acid inside the ABL – Part 1: Model description and initial evaluation. *Atmos. Chem. Phys.*, 11:43–51.
- Bäck, J., Aalto, J., Henriksson, M., Hakola, H., He, Q., and Boy, M. (2012). Chemodiversity of a Scots pine stand and implications for terpene air concentrations. *Biogeosciences*, 9:689–702.
- Ehn, M., Kleist, E., Junninen, H., Petäjä, T., Lönn, G., Schobesberger, S., Dal Maso, M., Trimborn, A., Kulmala, M., Worsnop, D. R., Wahner, A., Wildt, J., and Mentel, T. F. (2012). Gas phase

- formation of extremely oxidized pinene reaction products in chamber and ambient air. *Atmos. Chem. Phys.*, 12:5113–5127.
- Hakola, H., Tarvainen, V., Laurila, T., Hiltunen, V., Hellén, H., and Keronen, P. (2003). Seasonal variation of VOC concentrations above a boreal coniferous forest. *Atmos. Env.*, 37:1623–1634.
- Hinneburg, D. and Knoth, O. (2005). Non-dissipative cloud transport in Eulerian grid models by the volume-of-fluid (VOF) method. *Atmospheric Environment*, 39:4321–4330.
- Horn, S. (2012). ASAMgpu V1.0—a moist fully compressible atmospheric model using graphics processing units (GPUs). *Geosci. Model Dev.*, 5:345–353.
- Ieda, T., Kitamori, Y., Mochida, M., Hirata, R., Hirano, T., Inukai, K., Fujinuma, Y., and Kawamura, K. (2006). Diurnal variations and vertical gradients of biogenic volatile and semi-volatile organic compounds at the Tomakomai larch forest station in Japan. *Tellus*, 59B:177–186.
- Kavouras, I. G., Mihalopoulos, N., and Stephanou, E. G. (1999). Formation and gas/particle partitioning of monoterpenes photo-oxidation products over forests. *Geophysical Research Letters*, 26(1):55–58.
- Kulmala, M., Asmi, A., Lappalainen, H. K., Baltensperger, U., Brenguier, J.-L., Facchini, M. C., Hansson, H.-C., Hov, Ø., O’Dowd, C. D., Pöschl, U., Wiedensohler, A., Boers, R., Boucher, O., de Leeuw, G., Denier van der Gon, H. A. C., Feichter, J., Krejci, R., Laj, P., Lihavainen, H., Lohmann, U., McFiggans, G., Mentel, T., Pilinis, C., Riipinen, I., Schulz, M., Stohl, A., Swietlicki, E., Vignati, E., Alves, C., Amann, M., Ammann, M., S.; A., Artaxo, P., Baars, H., Beddows, D. C. S., Bergström, R., Beukes, J. P., Bilde, M., Burkhardt, J. F., Canonaco, F., Clegg, S. L., Coe, H., Crumeyrolle, S., D’Anna, B., Decesari, S., Gilardoni, S., Fischer, M., Fjaeraa, A. M., Fountoukis, C., George, C., Gomes, L., Halloran, P., Hamburger, T., Harrison, R. M., Herrmann, H., Hoffmann, T., Hoose, C., Hu, M., Hyvärinen, A., Hörrak, U., Inuma, Y., Iversen, T., Josipovic, M., Kanakidou, M., Kiendler-Scharr, A., Kirkevåg, A., Kiss, G., Klimont, Z., Kolmonen, P., Komppula, M., Kristjánsson, J.-E., Laakso, L., Laaksonen, A., Labonnote, L., Lanz, V. A., Lehtinen, K. E. J., Rizzo, L. V., Makkonen, R., Manninen, H. E., McMeeking, G., Merikanto, J., Minikin, A., Mirme, S., Morgan, W. T., Nemitz, E., O’Donnell, D., Panwar, T. S., Pawlowska, H., Petzold, A., Pienaar, J. J., Pio, C., Plass-Duelmer, C., Prévôt, A. S. H., Pryor, S., Reddington, C. L., Roberts, G., Rosenfeld, D., Schwarz, J., Seland, Ø., Sellegri, K., Shen, X. J., Shiraiwa, M., Siebert, H., Sierau, B., Simpson, D., Sun, J. Y., Topping, D., Tunved, P., Vaattovaara, P., Vakkari, V., Veeckind, J. P., Visschedijk, A., Vuollekoski, H., Vuolo, R., Wehner, B., Wildt, J., Woodward, S., Worsnop, D. R., van Zadelhoff, G.-J., Zardini, A. A., Zhang, K., van Zyl, P. G., Kerminen, V.-M., S Carslaw, K., and Pandi, S. N. (2011). General overview: European Integrated project on Aerosol Cloud Climate and Air Quality interactions (EUCAARI) – integrating aerosol research from nano to global scales. *Atmos. Chem. Phys.*, 11:13061–13143.
- Kulmala, M., Hämeri, K., Aalto, P. P., Mäkelä, J. M., Pirjola, L., Nilsson, D. E., Buzorius, G., Rannik, Ü., Dal Maso, M., Seidl, W., Hoffman, T., Janson, R., Hansson, H.-C., Viisanen, Y., Laaksonen, A., and O’Dowd, C. D. (2001). Overview of the international project on biogenic aerosol formation in the boreal forest (BIOFOR). *Tellus*, 53B:324–343.
- Lauros, J., Sogachev, A., Smolander, S., Vuollekoski, H., Sihto, S.-L., Mammarella, I., Laakso, L., Rannik, Ü., and Boy, M. (2011). Particle concentration and flux dynamics in the atmospheric boundary layer as the indicator of formation mechanism. *Atmos. Chem. Phys.*, 11:5591–5601.
- Riipinen, I., Pierce, J. R., Yli-Juuti, T., Nieminen, T., Häkkinen, S. A. K., Ehn, M., Junninen, H., Lehtipalo, K., Petäjä, T., Slowik, J., Chang, R., Shantz, N. C., Abbatt, J., Leaitch, W. R.,

- Kerminen, V.-M., Worsnop, D. R., Pandis, S. N., Donahue, N. M., and Kulmala, M. (2011). Organic condensation: a vital link connecting aerosol formation to cloud condensation nuclei (CCN) concentrations. *Atmos. Chem. Phys.*, 11:3865–3878.
- Riipinen, I., Yli-Juuti, T., Pierce, J. R., Petäjä, T., Worsnop, D. R., Kulmala, M., and Donahue, N. M. (2012). The contribution of organics to atmospheric nanoparticle growth. *Nature Geoscience*, 5:453–458.
- Shaw, R. H. and Shumann, U. (1992). Large-eddy simulation of turbulent flow above and within a forest. *Boundary-Layer Meteorol.*, 61:47–64.
- Shen, S. and Leclerc, M. (1997). Modelling the turbulence structure in the canopy layer. *Agric. For. Meteorol.*, 87(1):3–25.
- Tarvainen, V., Hakola, H., Hellén, H., Bäck, J., Hari, P., and Kulmala, M. (2005). Temperature and light dependence of the VOC emissions of Scots pine. *Atmos. Chem. Phys.*, 5:989–998.

# IDENTIFYING THE CHEMICAL FINGERPRINTS OF AEROSOL SOURCES AT A RURAL BACKGROUND SITE

M. ÄIJÄLÄ<sup>1</sup>, H. JUNNINEN<sup>1</sup>, M. EHN<sup>1</sup>, T. PETÄJÄ<sup>1</sup>, M. KAJOS<sup>1</sup>,  
R. VÄÄNÄNEN<sup>1</sup>, F. CANONACO<sup>2</sup>, J. SLOWIK<sup>2</sup>, A. PRÉVÔT<sup>2</sup>, P. AALTO<sup>1</sup>,  
M. KULMALA<sup>1</sup> and D. WORSNOP<sup>1,3</sup>

<sup>1</sup>Department of Physics, University of Helsinki, P.O. Box 64, FI-00014 Helsinki, Finland  
<sup>2</sup>Laboratory of Atmospheric Chemistry, Paul Scherrer Institut, 5232 Villigen PSI, Switzerland  
<sup>3</sup>Aerodyne Research Inc, Billerica, MA 01821, USA

Keywords: RURAL AEROSOL, SOURCE APPOINTMENT, ME-2

## INTRODUCTION

The aerosols' effects on climate, human health and visibility are dependent not only on their size but to a large extent also by their chemical properties. Particle mass loadings in various size classes are routinely and widely monitored, but less attention is generally paid to the particles' chemistry. However, the developments in measurement instrumentation and analysis methods, in the past ten years or so, have made possible direct online measurement of aerosol chemical composition and a detailed source analysis of the results using factor analysis. In this study an application of the new analysis methods to mass spectrometric measurement datasets from a boreal forest research site is presented.

## METHODS

The SMEAR II atmospheric research site (Hari & Kulmala, 2005) at Hyytiälä, Southern Finland is a well-known example of a rural background measurement station, influenced often by clean air masses from sparsely populated areas of Northern Scandinavia and the Arctic Ocean, but also experiencing pollution episodes when the incoming air masses originate from continental Europe or the industrial regions of Russia. Also aerosols from the local and regional pollution sources, such as sawmills, heating and traffic from nearby large cities are frequently observed. The aerosol loadings and their chemical composition are therefore extremely event-driven and very dependent on wind directions and trajectories. From the perspective of characterizing the various aerosol types, the SMEAR II aerosol datasets are an intriguing opportunity to test out the functionality of some of the new mass spectrometric data analysis methods.

Available measurement data consist of 3 one month long measurement campaigns in 2008-2009, in connection to the EUCAARI project (European integrated project on aerosol cloud climate air quality interactions. The main focus of this study is on the Aerosol Mass Spectrometer (C-ToF AMS, Drewnick et al., 2005) data, but there is also a variety of aerosol chemical properties, meteorological, radiation, VOC and trace gas data available for the measurement periods. The analysis of the datasets will utilize application of the positive matrix factorization (PMF) method and its constrained variation, ME-2 (Multilinear Engine 2; Paatero, 1999), that gives the user more freedom to incorporate available knowledge of the known aerosol properties.

The main scientific aim of this study is to identify the “chemical fingerprints” of various anthropogenic aerosol sources, that we expect to show less chemical variation over time, and to use them as an input for resolving the more subtle biogenic aerosol components and their expected seasonal variation. We further aim to utilize trajectory clustering to solve the geographical source areas for the different aerosol types.

## CONCLUSIONS

Although the analysis is still ongoing, several distinct aerosol types have already been identified. Common recurrent anthropogenic pollution events include e.g. local sawmill emissions, pollution from biomass burning, traffic emissions, long and medium range transported pollution from Southern Finland and Western Russia respectively. due to the pollution event driven nature of aerosol environment in Hyytiälä, it is possible to isolate specific emission signatures from the total mass spectra using PMF techniques. The evaluation and selection of PMF results is much eased in cases where a factor emerges and disappears without much of an effect on the long-time “background aerosol” factor(s) (Figures 1 and 2). After characterizing the emission signatures of these (mostly local and regional) sources, the obtained characteristic mass spectra can be used as an input for ME-2 analysis to resolve first the long and medium range transported pollution spectra and finally the more elusive biogenic aerosol mass spectra. Applying PMF and ME-2 analysis to AMs datasets from the Hyytiälä measurement station shows great promise in unambiguously identifying several distinct aerosol types related to specific emission sources.

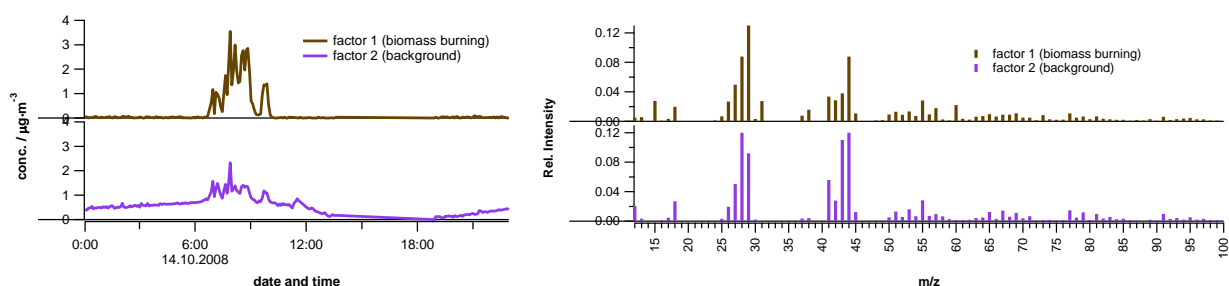


Figure 1. An example of a biomass burning event time series (left) and mass spectra (right), resolved via 2-factor PMF analysis. The solution is supported by the clear plume-like time series of the event as well as the pronounced signals at  $m/z$  60 and 73 in the biomass burning factor, relating to the common biomass burning marker compound, levoglucosan.

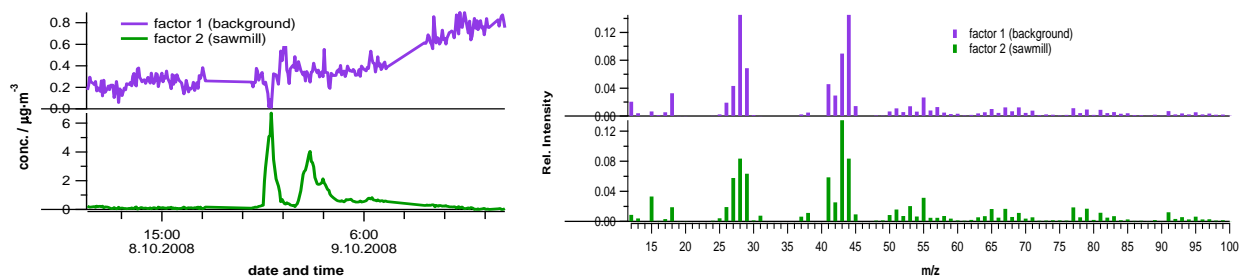


Figure 2. A pollution event caused by emission from a nearby sawmill. A time series for a 2-factor PMF solution is displayed on the left panel and the corresponding mass spectra on the right. The time series are well separated but for understandable reasons the mass spectra from the sawmill (i.e. cutting trees) resembles the background (SOA from natural emissions from the forests). Still the sawmill aerosol is much fresher than the background aerosol, indicated by the higher  $m/z$  43 to  $m/z$  44 ratio. There are also distinct differences in some masses (e.g.  $m/z$  15 Th).

## REFERENCES

- Drewnick F., et al. (2005). A new time – of – flight aerosol mass spectrometer (TOF-AMS) - Instrument description and first field deployment, *Aerosol Sci. Technol.*, 39:7:637-658.
- Hari P. and M. Kulmala (2005). Station for Measuring Ecosystem–Atmosphere Relations (SMEAR II), *Boreal Env. Res.*, 10:315–322.
- Paatero P. (1999). The multilinear engine - a table-driven, least squares program for solving multilinear problems, including the n-way parallel factor analysis model, *J Comput Graph Stat*, 8: 854-888.